







Colloids and Surfaces A: Physicochemical and Engineering Aspects

Volume 657, Part B, 20 January 2023, 130561

Facile approach to fabricate a high-performance superhydrophobic PS/OTS modified SS mesh for oil-water separation

Rajaram S. Sutar^a, Sanjay S. Latthe^b  , Nilam B. Gharge^a, Pradip P. Gaikwad^a, Akshay R. Jundle^a, Sagar S. Ingole^a, Rutuja A. Ekunde^a, Saravanan Nagappan^c, Kang Hyun Park^c, **Appasaheb K. Bhosale^a**, Shanhu Liu^d  

Show more 

 Share  Cite

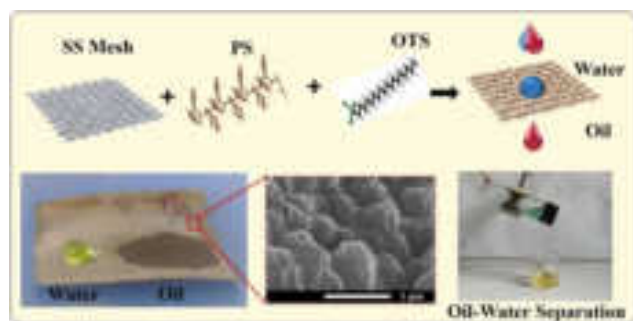
<https://doi.org/10.1016/j.colsurfa.2022.130561> 

[Get rights and content](#) 

Abstract

Special wetting materials have been used for the oil and water separation due to their different interfacial attraction of oil and water. Herein, we successfully fabricated superhydrophobic coatings on stainless steel (SS) mesh by depositing successive layers of polystyrene (PS) and octadecyltrichlorosilane (OTS) through the dip-coating method. The as-prepared coating showed a water contact angle (WCA) of $157.5 \pm 2^\circ$, a rolling angle of $6 \pm 2^\circ$ and an oil contact angle (OCA) of around 0° . The surface microstructure analysis of the coating revealed a regular pattern of microscale bumps with nanoscale folds on it, both of which improve the overall superhydrophobicity of the surface. The capacity of coatings to separate oil and water was examined by employing a variety of mixtures of oil and water, including petrol, diesel, kerosene, vegetable oil, and coconut oil. In case of low viscosity oil, the coated mesh demonstrated separation effectiveness of more than 97% and on the other hand, high viscosity oil demonstrated just 89% efficiency. Low viscosity oils showed a greater permeation flux through the mesh than extremely viscous oil. The mechanical strength of the coating was examined using bending, twisting, adhesive tape testing, sandpaper abrasion tests, and the findings indicated that coated mesh had exceptional mechanical resilience. In addition, the developed superhydrophobic mesh demonstrated excellent thermal stability and self-cleaning properties. Therefore, this superhydrophobic/superoleophilic mesh has a significant deal of application potential in practical.

Graphical Abstract



[Download : Download high-res image \(229KB\)](#)

[Download : Download full-size image](#)

Introduction

Oil spills and industrial effluents inflict significant harm to the ecosystems of the seas, human health, and the surrounding environment [1], [2]. The safe and responsible disposal of wastewater containing oil has been shown to be a challenging problem on a global scale. Many approaches have been used for the treatment of oil-water pollution, including oil skimmers, filtration, oil-absorbing materials, magnetic separations, centrifugal machine, flotation technologies, and combustion [3], [4], [5]. Traditional methods have various drawbacks, including limited separation efficiency, time consumption, cost-effectiveness, and the generation of secondary pollutants [6], [7], [8]. Therefore, cutting-edge technologies are an absolute necessity for the disposal of oily wastewater and the protection of the environment. Many efforts have been reported in the fabrication of separation membranes with controlled surface wetting property [9], [10]. The utilization of bio-inspired superhydrophobic materials in oil-water separation processes is a popular area of study due to its high water repellency and ability to allow oil to enter in it [4], [11], [12]. Therefore, superhydrophobic materials have been added to commercially available cotton textiles, 3D porous materials, different polymer membranes, filter papers, and metal meshes for considerable oil-water separation [13], [14]. Chemical etching [15], [16], spray deposition [17], [18], dip coating [19], hydrothermal method [20], sol-gel processing [21], [22], chemical vapor deposition [23], electrospinning [24], [25], and layer by layer [26] methods have been used for modification of porous surfaces. Among these, dip-coating is a quick and effective method of producing bulky, intricately formed products [27]. Metal meshes have sparked a lot of attention since they are long-lasting, reusable, and may be used in industry [2], [23]. Porous materials can absorb or filter liquids, and when their surface structure is adjusted with a specific wettability material, they can help separate oil or water from oil-water mixtures [28], [29]. Numerous types of porous metal meshes, including those constructed of nickel, copper, and stainless steel (SS), among other materials were used for oil-water separation [30], [31], [32], [33]. Among them, SS meshes have found widespread use for oil-water separation owing to their high electrical and electrothermal capabilities as well as their superior resistance to thermal shock [33].

OTS has been used to tune the surface wettability of porous substrates so that oil and water can be effectively separated. The OTS has low surface energy, hence it improves the hydrophobicity of the rough surface and also shows high oil absorption capacity [35], [36]. Li et al. [34] recently made superhydrophobic SS mesh by spraying it with a mixture of OTS-modified SiO₂ nanoparticles and waterborne PU. This superhydrophobic mesh was able to separate a mixture of kerosene and water at a rate of 98.3%. Latthe et al. [27] created a superhydrophobic surface by varying the concentration of OTS in PS solution and the number of dipping cycles. At first, they prepared a homogenous solution containing PS and OTS using tetrahydrofuran (THF) as a solvent. The pre-cleaned glass substrate was dip-coated (4 times) on the homogenous solution and air-dried to get a superhydrophobic surface with a contact angle of $154 \pm 2^\circ$. Ke et al. [37] have built a superhydrophobic and superoleophilic sponge by immersing it in OTS solution. This kind of sponge has shown an absorption capacity of 42–68 times more than the mass of the sponge for toluene, light oil, and

methyl silicone oil. Even after being put through 50 separation cycles, this adsorption capacity remained the same. Liang et al. [38] modified a polyurethane sponge by immersing in an OTS solution for oil-water separation. Cheng et al. [24] used coaxial electrospinning with PVDF solution as a lumen solution and reactive silicon-containing monomers as the outer solution to generate superhydrophobic nanofiber membranes with hierarchical micro nano-scale morphology. The outstanding separation efficiency of 99.6% is achieved with the as-prepared asymmetric composite membrane, which has an extremely rapid permeation flux. They show a water-in-n-octane permeation flux of 17331 L/(m²h) and retain 88% of their original permeance after 20 cycles of operation [24]. Rasouli et al. [13] briefly reviewed the various aspects of fabrication of superhydrophobic/superoleophilic membranes having mesh, films, and porous substrates for efficient oil-water separation applications. In order to modify the surface energy of superhydrophobic/superoleophilic membranes, it is usual practice to use low surface energy chemicals such as fatty acids, thiols, silanes, polymers based on polyethylene, and carbon nanotubes [13]. These membranes have >99% oil separation efficiency in oil-water combinations.

In this research work, a layer of PS was first applied on SS mesh using a dip coating process, followed by an OTS dip layer to achieve superhydrophobicity. The dip coating cycles were consequently carried out by dip and dry in both PS in THF and OTS in hexane. The surface structure of a red rose petal was obtained on SS mesh. SEM and EDS were used to describe the surface morphology and chemical composition, respectively. The gravity-driven oil-water separation technique was used to determine the oil-water separation efficiency and permeation flux using a custom-made setup. The mechanical durability of superhydrophobic mesh was evaluated using adhesive tape tests, sandpaper abrasion tests, bending, twisting, and folding tests. We have achieved the contact angles of 157.5±2° for OPS-2 as well as 154±2° for OPS-3 in superhydrophobic range and a comparable contact angle of 148.5±2° for OPS-1. The stable and robust self-cleaning coating was produced by this method as compared with the reported methods.

Section snippets

Materials

Polystyrene (PS) having average molecular weight ~ 280,000 and octadecyltrichlorosilane (OTS) were obtained from Sigma Aldrich, St. Louis, MO, USA. Tetrahydrofuran (THF) and hexane were purchased from Spectrochem, Mumbai, India. Stainless steel (SS) mesh with pore sizes of about 50µm was obtained from Shanghai Titan Technology Co. Ltd. China. The petrol, diesel, kerosene (from Bharat Petroleum Corporation Limited, India), vegetable oil (from Garud, India), and coconut oil (from Parachute...

Surface morphology and chemical composition

Fig. 2(a-f) depicts the surface morphology of meshes after being treated with varying doses of OTS. At low OTS concentrations, ten successive coating layers of PS and OTS create a rougher surface with nanoscale folds, as seen in Fig. 2(a). The enlarged view shows that there is a regular micro and nanoscale rough texture, which is essential for improving hydrophobicity and can be observed in Fig. 2(d). Surprisingly, regular shaped bumps emerged after raising the OTS concentration by twofold, as...

Conclusions

In conclusion, we have successfully fabricated superhydrophobic and superoleophilic SS mesh by depositing consecutive layers of polystyrene (PS) and octadecyltrichlorosilane (OTS) using an easy and inexpensive dip coating method. This allowed us to create a superhydrophobic and superoleophilic surface on the SS mesh. The WCA of 157.5 ±

2°, the OCA of about 0°, and the rolling angle of $6 \pm 2^\circ$ were all attained by adjusting the concentration of OTS in successive layered deposition. The...

CRedit authorship contribution statement

Rajaram S. Sutar: Conceptualization, Methodology, Investigation, Writing – original draft, Writing – review & editing, **Sanjay S. Latthe:** Supervision, Writing – review & editing, Visualization, **Nilam B. Gharge:** Methodology, **Pradip P. Gaikwad:** Methodology, Investigation, **Akshay R. Jundle:** Methodology, Investigation, **Sagar S. Ingole:** Methodology, Investigation, **Rutuja A. Ekunde:** Methodology, **Saravanan Nagappan:** Formal analysis, Writing – review & editing, **Kang Hyun Park:** Validation, Investigation, ...

Declaration of Competing Interest

The authors declare that they have no known competing financial interests or personal relationships that could have appeared to influence the work reported in this paper....

Acknowledgement

This work is financially supported by DST – INSPIRE Faculty Scheme, Department of Science and Technology (DST), Govt. of India. [DST/INSPIRE/04/2015/000281]....

[Recommended articles](#)

References (54)

Y. Liu *et al.*

[Bioinspired structured superhydrophobic and superoleophilic stainless steel mesh for efficient oil-water separation](#)

Colloids Surf. A: Physicochem. Eng. Asp. (2016)

M. Bennett *et al.*

[Monitoring the operation of an oil/water separator using impedance tomography](#)

Miner. Eng. (2004)

Y. Deng *et al.*

[Recent development of super-wettable materials and their applications in oil-water separation](#)

J. Clean. Prod. (2020)

S.S. Latthe *et al.*

[Superhydrophobic surfaces for oil-water separation, in](#)

[Superhydrophobic Polymer Coatings](#)(2019)

S. Rasouli *et al.*

[Superhydrophobic and superoleophilic membranes for oil-water separation application: a comprehensive review](#)

Mater. Des. (2021)

Y. Liu *et al.*

[On-demand oil/water separation of 3D Fe foam by controllable wettability](#)

Chem. Eng. J. (2018)

R. Liao *et al.*

[Fabrication of superhydrophobic surface on aluminum by continuous chemical etching and its anti-icing property](#)

Appl. Surf. Sci. (2014)

W. Ma *et al.*

[Lightweight, elastic and superhydrophobic multifunctional nanofibrous aerogel for self-cleaning, oil/water separation and pressure sensing](#)

Chem. Eng. J. (2022)

Y. Wan *et al.*

[The research on preparation of superhydrophobic surfaces of pure copper by hydrothermal method and its corrosion resistance](#)

Electrochim. Acta (2018)

Y. Xiu *et al.*

[UV and thermally stable superhydrophobic coatings from sol-gel processing](#)

J. Colloid Interface Sci. (2008)



[View more references](#)

Cited by (19)

[Oil/water separation copper membranes modified by laser induced ZnO nanowires growth with enhanced catalytic function](#)

2024, Colloids and Surfaces A: Physicochemical and Engineering Aspects

[Show abstract](#)

[Magnetic superhydrophobic sponge with 3D interpenetrating network structure coating for multimodal driven oil/water separation](#)

2024, Progress in Organic Coatings

[Show abstract](#)

[Multifunctional carbonized Zn-MOF coatings for cotton fabric: Unveiling synergistic effects of superhydrophobic, oil-water separation, self-cleaning, and UV protection features](#)

2023, Surface and Coatings Technology

[Show abstract](#)

[Ecofriendly superhydrophobic fabrics for ultra-fast oil/water separation by self-assembly](#)

2023, Surface and Coatings Technology

[Show abstract](#)

Efficient separation of oil-water emulsions: Competent design of superwetting materials for practical applications

2023, Journal of Environmental Chemical Engineering

[Show abstract](#) 

Sustainable approach to oil recovery from oil spills through superhydrophobic jute fabric

2023, Marine Pollution Bulletin

[Show abstract](#) 

[>](#) [View all citing articles on Scopus](#) 

[View full text](#)

© 2022 Elsevier B.V. All rights reserved.



All content on this site: Copyright © 2024 Elsevier B.V., its licensors, and contributors. All rights are reserved, including those for text and data mining, AI training, and similar technologies. For all open access content, the Creative Commons licensing terms apply.



ISBN-978-81-927211-3-7

Bhakti Movement in India
भारतातील भक्ती चळवळ

Editor

Dr. Archana Shriram Jadhav

Assistant Professor & Head,
Department of History,
Shikshanmaharshi Dr. Bapuji Salunkhe College, Miraj

Publishers

Dr. Udaysinh Manepatil

Principal,

Shikshanmaharshi Dr. Bapuji Salunkhe College,

Miraj

and

Prarup Publication, Kolhapur

Bhakti Movement in India
भक्त्यात्मक चळवळीचा इतिहास

Sponsored:
Indian Council of Historical Research (ICHR), New Delhi

Editor:
Dr. Archana Shriram Jadhav

Publisher:
Dr. Udaysinh Manepatil
Principal,
Shikshamaharshi Dr. Bapuji Salunkhe College, Miraj
and
Prarup Publication, Kolhapur

© Principal, Shikshamaharshi Dr. Bapuji Salunkhe College, Miraj
& Prarup Publication, Kolhapur.
All rights reserved. This book or any part thereof may not be reproduce in any form
without the written permission of the publisher.

Printed by:
Pdmashri Printers,
Mangalwar Peth, Miraj

Disclaimer:
The views expressed by the authors in their articles, reviews etc. insight issue are
their own. The editor and publisher are not responsible for them. All disputes concerning
the proceeding book shall in the court at Miraj, Maharashtra.

ISBN-978-81-927211-3-7

INDEX

Invited Talks			
1.	Prof. Dr. Arun Bhosale	Inaugural Speech- भारतीय भक्ति परंपरा: एक दृष्टिकोण	1-3
2.	Dr. Abadualgani Inaratwale	Impact of Bhakti and Sufi Movements on Indian Society	4-7
3.	Prof. Madhao Patil	Valedictory address- Bhakti Movement: Its relevance today	8-9
Research Papers			
Sr. No	Name	Title of the Paper	Page No.
1.	Dr. Prabhavati A. Patil	Swami Vivekananda on Bhakti Yoga a Way of Liberation	10-12
2.	Dr. S. R. Kattimani	Bhakti Movement in Medieval India- Impact and Importance	13-15
3.	Dr. Arati B. Nadgouda	Bhakti Movement with special reference to Shankaracharya	16-19
4.	Dr. C. M. Naik	Bhakti Movement in North India with Special Reference to Gurunanak	20-23
5.	Dr. Jayant Anant Kulkarni	Bhakti Movement: A Means of Social Welfare	24-27
6.	Dr. Nalini Avinash Waghmare	Bhakti Movement in Karnataka with special reference to Virasaivism	28-31
7.	Mr. Gulab Bagwan Dr. Bandu J. Kadam	Bhakti Movement in Maharashtra	32-36
8.	Jayashri D. Janganure	Indian Bhakti Tradition Through Foreign Perspective : A Study of Journey to Ithaca	37-45
9.	Sou. Arundhati Sanjay Mali	Swami Vivekanand: Apostle of Modern India	46-49
10.	Dr. S. B. Bhambar	Prakash Deshpande-Kejkar's Baradana: A Study in Indian Bhakti Tradition	50-52
11.	Mr. Rahul Subhash Chougale Mrs. Vidya Rahul Kamane	Impact of Information Technology on Bhakti Movement	53-54
12.	डा. सुधाकर डाडी	भक्ति आंदोलन एवं सामाजिक सुधार के अग्रदूत सात कबीर	55-58
13.	डा. शैलजा टिळे	भक्ति आंदोलन के परिप्रेष्य में कबीर के सामाजिक संस्कार	59-62

14.	प्रा. सी. आशादाजी आसगावामी सावळे	हिंदीसंगुण भक्ति धारा के सूरज - गोस्वामी तुलसीदास	63-66
15.	श्री. विश्वनाथ बालचंद्र सुतार	भारत में भक्ति आंदोलन का उद्भव और विकास	67-71
16.	डॉ. मजूमदार शिवाजीराव घोरपडे	भारतातील भक्ती चळवळीचा उदय आणि महात्त्व	72-76
17.	श्री. सुजाता सचिन देशमुख	भक्ती चळवळीचा उदय: एक ऐतिहासिक दृष्टिक्षेप	77-80
18.	शिवाजी आनंदा परीट	भारतातील मुक्ती संप्रदाय आणि त्याचे इतर पंथांवर झालेले परिणाम	81-84
19.	डॉ. ज्योती चटकर - खरात	भक्ती संप्रदाय : महाराष्ट्राचा सांस्कृतिक वारसा	85-88
20.	डॉ. विलास वरावत पगडूम	महाराष्ट्रातील भक्ती संप्रदाय	89-94
21.	उज्वला अर्जुनराव देसाई	महाराष्ट्रातील वारकरी संप्रदायाचे ऐतिहासिक कार्य	95-98
22.	श्री. राजाजी माळेकर	भक्तिमार्ग व वारकरी संप्रदाय	99-103
23.	डॉ. मंगेश एम. कोळसेकर	वारकरी संप्रदायातील प्रमुख फुड	104-106
24.	प्रा. पी. वाय पाटील	वारकरी संप्रदाय आणि साहित्य	107-109
25.	डॉ. श्री. श्री. पांडवकर	'महाराष्ट्रातील वारकरी संप्रदायाचे योगदान' एक दृष्टिक्षेप	110-113
26.	प्रा. चौधरी पुंडलिक जयपाल	समाजसुधारणेत वारकरी संप्रदायाचे योगदान	114-119
27.	डॉ. अर्चना श्रीराम जाधव	भक्ती संप्रदाय आणि राष्ट्रीय एकतामता: विशेष संदर्भ मराठी सत्तेचा उदय	120-123
28.	प्रा. सचिन सुभाष बोलाईकर	मध्ययुगीन समाजातील समन्वयक: दत्त संप्रदाय	124-128
29.	आनंद व. पवार	महाराष्ट्रातील दत्त संप्रदाय	129-131
30.	डॉ. तानाजी रामचंद्र इबलदार	भारतातील नाथ संप्रदाय: उदय आणि विकास	132-134
31.	प्रा. उमाकांत इत्तीकट	भक्ती चळवळीतील नाथ संप्रदायाचे योगदान	135-136
32.	प्रा. कं. आर. गावडे	भक्ती चळवळ आणि सामाजिक सुधारणा	137-139
33.	डॉ. मृगणा प्रकाश पाटील	धर्म, सतसहित्य आणि समाज प्रबोधन	140-143
34.	प्रा. रेखा काशिनाथ पसाळे	परिवर्तनाच्या चळवळीत महाराष्ट्रातील भक्ती संप्रदायाचे योगदान	144-146

समाजसुधारणेत वारकरी संप्रदायाचे योगदान

वैश्वी पुंडलिक जयपाल
महा. प्राध्यापक,
इतिहास विभाग,
राजे रामराव महाविद्यालय, जत.

प्रस्ताविक:

मध्ययुगीन काळखंडात सामाजिक आणि धार्मिक सुधारणा घडवून आणण्यासाठी झालेल्या भक्ती चळवळीत वारकरी संप्रदायाने केलेले कार्य महत्त्वपूर्ण आहे. या काळात धार्मिकता लयाला जाऊन समाजामध्ये अंधश्रद्धा, कर्मबंद, वर्णव्यवस्था, उच्च-निचपणा इत्यादी गोष्टींनी माणसा-माणसात भेद करून असमानता निर्माण झालेली होती. मध्ययुगीन काळखंडात संपूर्ण समाजरचनेत स्वातंत्र्य, समता, बंधुभाव राहिलेला नव्हता. प्राचीन काळपासून चालत आलेल्या अविष्ट प्रथा, परंपरा, रुढी इत्यादींनी या काळात उण्याक पाडलेला होता. ही सर्व व्यवस्था परंपरेने समाजमानावर रुजलेली होती. गुलामांना गुलामीची जाणीव राहिलेली नव्हती, अशा कठीण परिस्थितीमध्ये वारकरी संप्रदायातील संतांनी समाजात जागृती निर्माण करून धार्मिक सुधारणेबरोबरच समाजसुधारणा घडवून आणण्यासाठी कार्य केले. त्यामध्ये संत ज्ञानेश्वर, संत तुकाराम, संत नामदेव, संत एकनाथ, संत मुक्ताबाई, संत जनाबाई, संत चोखामेळ इत्यादी संतांनी अविष्ट प्रथा, परंपरा, कर्मकांडाच्या विरोधात मध्ययुगीन काळात आंदोलन करण्याचे कार्य केले. या समाजसुधारणेचा आधार धार्मिक होता. ईश्वर भक्तीच्या सहाय्याने विश्वबंधुत्वाची भावना समाजात निर्माण करण्यासाठी प्रयत्न केले. ईश्वराबरोबर प्रभेदप्राप्तीचा मानवतावाद, करुणा, सत्यनिष्ठा, प्रेम, विवेकबोध, निष्ठा, धार्मिकसंगनता, नैतिकता इत्यादी मूल्यांचे अविष्टान निर्माण करण्याचे कार्य केले. मध्ययुगीन काळात निर्माण झालेल्या समाजव्यवस्थेच्या विरोधात कार्य करणे म्हणजे एक प्रकारचा गुनहास मानला जाई. त्यामुळे या कार्यामध्ये अनेक संतांचा बळीही समाजव्यवस्थेने घेतलेला दिसून येतो. तरीही वारकरी संप्रदायातील संतांनी समाजाला प्रेरित करण्याचे कार्य केले. वारकरी संप्रदायाची ही चळवळ महाराष्ट्रापुरती सिमित नव्हती तर उत्तर भारताचाही त्यामध्ये समावेश होता. उत्तर भारतात निर्माण झालेल्या भक्ती चळवळीचा प्रारंभकर्ता संत ज्ञानेश्वरच होता. ज्याने बाराव्या व्या शतकापासून भक्ती चळवळीचा प्रारंभ केला व त्याचा वारसा संत नामदेवाने चालविला. त्यामुळे उत्तर भारतातील भक्ती चळवळ चालविण्याचे श्रेय वारकरी संप्रदायातील संत ज्ञानेश्वरानाच जाते.

वारकरी संप्रदायाचा उदय:

मध्ययुगीन काळखंडात महाराष्ट्रात जी भक्ती चळवळ चालविली गेली ती सर्वसाधारण माणसे, सिद्धा, सर्व जातींच्या लोकपर्यंत पोहचविण्याचे कार्य वारकरी संप्रदायाने केले. जाती-पातीची बंधने तोडून भक्तीमार्ग सर्वांसाठी खुला करण्याचे कार्य या संप्रदायाने केले. "उत्तरे आंदोलन को पंढरपूर आंदोलन कहा जाता है।" वारकरी संप्रदायाचा पाया घालण्याचे कार्य संत ज्ञानेश्वरानी केले. त्यास निवृत्तीमाथानी (जेष्ठ वंधु) सहाकार्य केले. ही एक धर्म सुधार आणि सामाजिक परिवर्तन घडवून आणण्यासाठी चालविली गेलेली चळवळ होती. वारकरी संप्रदायाने चालविलेली भक्ती चळवळ १२ व्या शतकापासून ते १७ व्या शतकाच्या अखेरपर्यंत महाराष्ट्रात लोकप्रिय झालेली दिसून येते. या चळवळीचे प्रतिनिधीत्व संत ज्ञानेश्वरानंतर संत नामदेव, संत एकनाथ, संत तुकाराम, संत रामदास, संत जनाबाई, संत मुक्ताबाई इत्यादी संतांनी केले. मध्ययुगीन काळात धर्मसुधारणेबरोबरच समाजसुधारणा करून जनताला प्रेरित केले. ईश्वर भक्तीचा मार्ग सिद्धा व सर्व जातींच्या लोकांसाठी खुला करण्यामागचा उद्देश समाजसुधारणा घडवून आणणे हाच होता. त्यासाठी सर्व संतांनी अथक परिश्रम केले.

भक्ती चळवळीतील तात्वज्ञान:

भारतात प्राचीन काळापासूनच भक्ती चळवळ सुरू होती. भक्ती चळवळीचे मूळ आपल्याला वेदांमध्ये असतांना दिसून येते. "वेदांमध्ये काही ऋचा देवी सामर्थ्यांमोर नतमस्तक होणा-या आहेत, आणि या देवी सामर्थ्यांभी अनुभूती गुडवादी मार्गाने मिळविणे भक्तीमध्ये अभिप्रेत आहे." उग्रनिषदांमध्येही याच भावना व्यक्त झालेल्या दिसून येतात. प्राचीन ऋषींनी स्वतःच्या अतिअतिश्यात असलेल्या शक्तींनी प्राचीन करण्यासाठी विहित करण्यात आलेल्या तप्यातून अतर्गत शक्तींची अनुभूती मानवात्म होवू लागली. निःसर्गांमध्ये मानवी हित साधू शकले अशी कोणातीतरी शक्ती आहे याची ओळख मानवात्म झाली. त्या शक्तीला ईश्वर, परमेश्वर या नावाने ओळखले जावू लागले. प्रेम, भक्तीच्या जोरावर आपण त्या शक्तीला प्राप्त करू शकतो हा दृष्टिकोन मानवात्म निर्माण झाला. त्यातून ईश्वरगंध्या कुपेने त्या शक्तीशी अद्वैत साधण्यावर भक्ती चळवळीने भर दिले.

भक्ती संबंधी दोन वेगवेगळे प्रवाह आहेत. एका प्रवाहानुसार भक्तीचा मार्ग ईश्वरगंध्या सेवेवर अवलंबून आहे. यामध्ये भक्त पूर्णतः ईश्वरगंध्या दयेवर अवलंबून असतो. ईश्वरपुत्री स्वतःला पूर्णतः समर्पित करून घेते. त्याला प्रपत्ती किंवा समर्पनाचा मार्ग म्हणतात. तर दुसरा 'भक्त' मधील मूळ शब्द 'भाग' असा आहे त्यामुळे 'भक्त' या शब्दिक अर्थ 'ज्याला भाग मिळतो तो' असा होतो. मुळांमध्ये भक्त हा शब्द आपल्या घालण्याच्या संघर्षाच्या हिंसा मिळविणा-या सेवकाला लावला जात होता. त्यामुळे पुढे हा शब्द 'ईश्वरगंध्या सेवक या अर्थाने वापरला जावू लागला.'^१

भक्तीचा दुसरा प्रकार केंवळ शुध्द, निःसीम प्रेमाच्या बंधनावर आधारित आहे. हा मार्ग सेवेवर अवलंबून नसून समानतेवर आधारित होता. त्यात मुक्ती ऐवजी देवी जीवनात सहभाग हे उद्दिष्ट होते. विष्णुपुराणातील प्रल्हादाच्या कथेमध्ये प्रल्हाद ईश्वरगंध्या असा आशीर्वाद मागतो की, आपण कुठेही जन्मले तरी आपल्याला ईश्वरगंध्या अर्जळ भक्तीचे बरदान मिळवे. भक्तीच्या या दुस-या प्रकारानुसार जातीव्यवस्था, वर्णव्यवस्था, उन्न-निच या गोष्टींचा भक्ती चळवळीत कोणातीही स्थान नव्हते. निचा प्रसार-प्रसार व-यात प्रमाणात संतांनी लोकप्रिय कोला दक्षिणेतील नयनार आणि अजय्यार सातानी शैव व वैष्णव पंथांची स्थापना केली. त्यामध्ये ब्राम्हणाप्रमाणेच निम्न जातीतील अनेक संतांचा समावेश होता. त्यात अर्जळ नावाची र्मी संत होती. संतांचे वर्तन व व्यक्तीमत्त्व अतिशय सर्वसमावेशक होते. जातीपातीला कुठेही स्थान देण्यात आलेले नव्हते.

जाती व्यवस्थेचा विरोध:

कारकी संप्रदायातील सर्व संतांचा दृष्टीकोन सर्वसमावेशक व मानवतावादी होता. भक्ती मार्गात सर्व जाती, धर्म, पंथांच्या लोकांचे स्वागत करण्यात संतांनी प्राधान्य दिले होते. त्यामुळे त्यांनी जाती व्यवस्थेचा विरोध करण्याचे कार्य केले. ईश्वरगंध्या भक्ती कारण विशिष्ट वर्गांची किंवा जातीची मक्तेदारी नाही, तर ती भक्ती सर्वांसाठी खुली आहे, असे कारकी संप्रदायातील संत समाजाला समजवून सांगत असत. उत्तरेच्या भागात ज्याप्रमाणे भक्ती चळवळीने जातीव्यवस्थेचा विरोध केलेला होता, सर्व मानवाच्या प्रेमावर भर दिलेला होता व सर्व धर्मांना समान अधिकार देण्याचे कार्य केलेले होते. त्या संबंधाने गेहिलास यांभार म्हणतो, "माझी जात निच, माझी कार्ये निच आणि माझ व्यवसायही निच आहे. या निच परिस्थितीतून ईश्वराने मला वर उचलले." त्याप्रमाणे संतांनी विविध जातीतील लोकांना मुक्तीच्या मार्गासाठी नाही तर ईश्वराने भक्त म्हणून प्रत्येक जातीतील व्यक्तीला सामावून घेतले हे कार्य महाराष्ट्रांमध्ये कारकी संप्रदायाने केले. "गुकराम महाराजांनी पदरीला सर्व लोकांचे मूळ मानले. परंतु पदरपूरमध्ये जात, वर्ण, उन्न-निच हे प्रकारचे साक्षरित भेदभाव नाहीत. विद्वत्काला भेटण्याचा सर्वांना अधिकार आहे." असे ते म्हणत असत. कारण यज्ञापूर्वीच कालखंडात ईश्वरभक्ती करणाऱ्या अधिकार फक्त उन्न जातीतील लोकांना दिलेला होता. त्याचा परिणाम समाज जीवनावर पडलेला होता. वर्ण व्यवस्थेने त्यांवर जातीव्यवस्थेवर झालेले होते व खालच्या वर्णातील लोकांना सर्व अधिकार नकारलेले होते.

हे अधिकार सर्वांना मिळवून देण्यासाठी वारकरी संप्रदायातील संतानी ईश्वरभक्तीचा साहाय्य घेवून जातीव्यवस्था संपविण्याचा प्रयत्न केला. डॉ. अर. सी. मुजुमदार यांच्या मते, "ज्यावेळी धार्मिक कल्पना शुष्क, निर्जीव व सुष्क होण्याच्या मार्गावर होत्या आणि धर्म विधी व समारंभांनी आध्यात्मिक साक्षात्काराचे स्थान पटक्याविले होते, त्यावेळी संतांच्या शिकवणीने बहुजन समाजात धार्मिक जनजागृतीचे अमृत पाजले." धार्मिक जीवनात बहुजनना उच्च वर्णांच्याबरोबर सामावून घेतल्यामुळे आपोआपच समाजात समानता निर्माण होण्यास प्रारंभ झाला. जाती व्यवस्थेमुळे जी बंधने समाजमनावर पातलेली होती ती बंधने दूर करण्यास भक्ती चळवळीने महत्त्वपूर्ण कार्य केले व बहुजन समाजाला ईश्वर भक्तीबरोबर जातीव्यवस्थे विरुद्ध मत तयार करण्यास योगदान दिले. त्यातून पहिल्यांदा संतांमध्ये अनेक जातीव्यवस्थे विरुद्ध मत तयार करण्यास योगदान दिले. त्यातून पहिल्यांदा संतांमध्ये अनेक जाती पंचाचे लोक सामावलेले दिसून येतात. हे कार्य महाराष्ट्रात वारकरी संप्रदायाने केलेल्यामुळे विविध जातीतील संत वारकरी संप्रदायात आहेत. त्यांच्यात कोणताही उच्च-निचता आपल्याला दिसून येत नाही. त्यानंतर हळूहळू संपूर्ण समाजात सामाजिक जागृती निर्माण झालेली दिसून येते. उच्च वर्णाने प्राचीन काळापासून चालत आलेले आपले हितसंबंध अपून देण्यासाठी बहुजन समाजावर प्रथा, परंपरा, कर्मकांड लादून गुलामीचे जीवन जगण्यास बन्वता मानणारी व्यवस्था निर्माण केलेली होती. जातीपरिवर्तन तर दूरच, परंतु व्यवस्था परिवर्तन करणेसुध्दा कठीण केले होते. वडीलांचा व्यवसाय मुलाने केलाच पाहिजे अशी व्यवस्था निर्माण केली होती. ईश्वरभक्ती किंवा पूजा करण्याचा अधिकार बहुजननांसाठी घालण्याची नाकारलेला होता. तो अधिकार बहुजनना मिळवून देण्याचे कार्य वारकरी संप्रदायानी केले. त्यामुळे बहुजन समाजाचा विकास होण्यास मदत झाली. भक्ती मार्गातील जातीय भेदभाव समाप्त झाला. त्यामुळे बहुजन जातीतील व-याच संतानी समाजात आदर प्राप्त केला. त्यात संत तुकाराम, संत नामदेव, संत चोखामेढळ, संत गेहिदास, संत गोरा कुभार इत्यादी बहुजन समाजातील संतानी समाज व्यवस्थेत परिवर्तन घडवून आणण्यासाठी कार्य केले व महाराष्ट्राला वारकरी संप्रदायाच्या चळवळीमध्ये ज्या चळवळीची सुरुवात ज्ञानेश्वरानी केलेली होती आणि धर्मसुधारणेबरोबर समाज सुधारणेसाठी कार्य केले. त्या कार्याला पुढे नेण्याचे कार्य बहुजन समाजातील संतानी केले. वारकरी संतानी जातीव्यवस्थेचा विरोध करीत असताना व बहुजन समाजाला ईश्वरभक्तीचा अधिकार मिळवा म्हणून धार्मिक विधीतील अंधश्रद्धा व कर्मकांडाची समाप्ती करण्याचे कार्य केले. "अब विरवाजा या शारवों के प्रणयन की आवश्यकता नही रह गई। मोक्ष प्राप करने के लिए गृह त्याग की आवश्यकता नहीं थी।" त्यामुळे सर्वसामान्यांना भक्तीमार्ग सुकर झाला. पूर्वाप्रमाणे शास्त्रांचा अभ्यास करणा-यांना ईश्वरभक्ती करण्याचा अधिकार भक्ती चळवळीने समाप्त केला व हा मार्ग सर्व सामान्यांसाठी खुला केला. त्याचबरोबर गृहत्याग करण्याच्या आवश्यकतेला तिलाजली देवून घरातील सर्व कामे करून, प्रपंच नीट करून ईश्वरभक्ती करू शकतो असा मार्ग समाजाला दाखविण्याचे कार्य केले. त्यामुळे समाजातील सर्व सामान्य माणूसही भक्ती मार्ग पत्करू लागला. त्या भक्तीतून सामाजिक एकतेचा संदेश जनतेला संतानी दिला. समाजातील जातीव्यवस्थेला नाकारण्याचे कार्य केले. जाती ईश्वराने निर्माण केलेल्या असून मानसामानसात भेदभाव निर्माण करण्यासाठी उच्च वर्णांच्यांनी निर्माण केलेल्या, हे जनतेला समजावून सांगितले.

स्त्रियांचा सहभाग:

स्त्रियांच्या जीवनात सुधारणा घडवून आणणे हा समाज सुधारणेचा महत्त्वाचा भाग असतो. मध्ययुगीन काळात स्त्रियांची स्थिती अतिशय दयनीय होती. स्त्रीला 'बुल आणि मूढ' यापुढेच सिमित ठेवण्यात आलेले होते. शिक्षण घेण्याचा अधिकार नाकारण्यात आलेला होता. स्त्रीला समाजात पुण्याच्या बरोबरीने वावरण्याचा अधिकार नव्हता. सतीप्रथा, विधवांना पुनर्विवाह करण्याचा अधिकार नाकारण्यात आलेला होता. त्यामुळे स्त्रियांची स्थिती अतिशय दयनीय झालेली होती. अशा स्थितीत स्त्रियांना समानतेचा दर्जा देण्याचे कार्य भक्ती मार्गातील संतानी केलेले होते. त्यामुळे भक्ती मार्गात मिरबाई, जनाबाई, मुक्ताबाई इत्यादी स्त्रीया संतांच्या बरोबरीने असताना दिसतात. 'एक तुलसीदास मोडले तर मध्ययुगात

मीराबाई इतके हृदय देलावून टाकण्याने सामर्थ्य अन्य कोणा कधीला लाभले नाही" ती उत्तम संत कविपती होती. कृष्ण भक्तीत तल्लीन होवून अनेक कविता मीराबाईंनी निर्माण केल्या होत्या. त्या रवी असल्यामुळे ब्राह्मणी व्यवस्थेने तिच्या या भक्ती कार्याचा विरोध केला होता. सुरुवातीला मीराबाईंला लोकसहभागसुद्धा मिळत नव्हता. परंतु संत मंडळींचा सहभाग जसा-जसा तिला प्राप्त झाला, तसे तिच्या कार्याचे महत्त्व जनसामान्यांमध्ये वाढत गेले. मुक्ताबाई ज्ञानेश्वर, निवृत्तीनाथ, सोपानदेव यांची लहान बहिण होती, तरी भावांचा सहवास लाभल्यामुळे कुठेही कमी पडली नाही. ज्ञानेश्वरप्रमाणेच मुक्ताबाईंसुद्धा अर्भगाची रचना केली. संत जनाबाई संत नामदेवाची भक्ती पाहून तीही विदुल भक्ती करू लागली. तीला नामदेवाने भक्ती चळवळीत सामावून घेतले. संत गोखामेळाची पत्नी सोयराबाई व बहिण निर्मळ्य यांनी संतांची संगत मिळवली. संत बहिणाबाई ह्या संत तुकारामाच्या शिष्य होत्या. संत तुकारामांनी एका स्त्रीला भक्ती चळवळीत शिष्यत्व देवून स्त्रीयांसमोर एक आदर्श निर्माण करण्याचे कार्य केले. त्यामुळे या भक्ती मार्गात अनेक स्त्रिया संतांच्या बरोबरीने सहभागी झालेल्या आपल्याला दिसून येतात व पुरुष संतांबरोबरच समाजजागृती करण्याचे कार्य यांनी केलेले होते. संतांनी आपल्या घरच्या स्त्रियांना संत चळवळीत अगोदर सामावून घेवून स्त्रियांना सामाजिक स्वातंत्र्य देण्यासाठी कृती केलेली दिसून येते. त्यामुळेच उच्च कुळातील स्त्रियांचाच नाही तर निम्न कुळातील स्त्रियांनीसुद्धा भक्ती मार्गात प्रवेश केला होता.

व्यावहारिक धर्म:

वारकरी संप्रदायातील सर्वसामान्य लोकांना भक्तीच्या मार्गाने कठीण ज्ञान न घेता ईश्वर प्राप्त करता येतो असा व्यावहारिक धर्म दिला. परंपरागत भक्तीच्या मार्गात आत्मक्लेशावर भर देण्यात आलेला होता. हा व्यक्तीवादी मार्ग होता. सर्व सामान्यांना त्याचे पालन करणे शक्य नव्हते. त्यासाठी ईश्वर भक्तीचा सोपा मार्ग वारकरी संप्रदायाने समाजाला दाखवून दिला. तसेच आत्मक्लेशावर ईश्वरप्राप्तीच्या तत्वावर आधारित मार्गात सर्वच जाती-जमाती, वर्ण इत्यादींना स्थान देण्यात आलेले नव्हते. उच्च वर्णांपुरताच हा मार्ग सिमित होता. बहुजन समाज त्यापासून कोसे दूर होता. तो ईश्वरभक्तीचा अधिकार प्राप्त करून देण्याचे कार्य महाराष्ट्रात वारकरी संप्रदायाने केले. वास्तवात उत्तर "हिंदुस्थानातील भक्ती चळवळीची सुरुवात प्रथम महाराष्ट्रातच झाली. संत ज्ञानेश्वरांनी ज्ञानेश्वरी हे भगवद्गीतेवरील भाष्य लिहिले. त्यामध्ये ज्ञान, कर्म व भक्ती यावर सारखाच भर देण्यात आला होता." ईश्वरप्राप्तीसाठी आत्मक्लेशाचा मार्ग नाकारून माणसाच्या चांगल्या गोष्टी व ईश्वर भक्ती या दोन्ही गोष्टींना समान महत्त्व भक्ती मार्गात देण्यात आलेले होते. या ठिकाणी कोणत्याही वर्गाची किंवा व्यक्तीची मक्तेदारी राहिलेली नव्हती. भक्ती मार्ग एक व्यावहारिक धर्म बनलेला होता की ज्यामध्ये सर्वसमावेशक तत्त्व अभिप्रेत होते. असा मार्ग समाजाला दाखविण्याचे कार्य वारकरी संप्रदायाने केले.

समानतेचा विचार:

मध्ययुगातील भक्तीमार्ग हा सामाजिक व धार्मिक जीवनातील सर्वांसाठी खुला असलेला समानतेचा विचार होता. त्यात भेदभावाला कुठलाही आधार देण्यात आलेल्या नव्हता तर फक्त चांगल्या तत्वाच्या माध्यमाने ईश्वरभक्ती बरोबर सर्व लोकांचे समान कल्याण घडवून आणणारी समाज व्यवस्था निर्माण करणे हा दृष्टिकोण त्यामध्ये होता. म्हणूनच संतांनी भक्तीचा संदेश सर्वसामान्य जनतेपर्यंत पोहचविला व सर्वांना ईश्वर भक्तीचा मार्ग खुला केला. "ज्ञानेश्वरप्रमाणेच नामदेवाचा दृष्टिकोनही तितकाच सर्वसमावेशक होता" त्यांनी भारतातील प्रदेशांचा प्रवास केला व लोकांसमोर किर्तनाच्या माध्यमाने भक्ती मार्गातील समानतेचा विचार त्यांनी मांडला व आपल्या भक्तीची सल्लयना चारही वर्णांच्या जातीच्या लोकांना शिकविले. स्त्रियांनासुद्धा भक्ती चळवळीत सामावून घेतले. त्यामुळे अनेक महिला संत निर्माण होऊ शकल्या. समाजात सुधारणा घडवून आणायची असेल तर भक्ती चळवळीच्या तत्वात समानतेच्या तत्वाची आवश्यकता आहे. हे वारकरी संप्रदायातील संताना माहिती होते. म्हणून ज्यांनी समानतेचा विचाराने भर दिला व भक्ती चळवळीत सर्वांना

Bhakti Movement in India

सामाज्य वेण्याचे कार्य केले. त्यामुळे वारकरी संप्रदायात ब्राह्मण, क्षत्रीय, वैश्य, शूद्र या वारगी वर्णातील संत एकत्र कार्य करित असताना दिसून येतात व हे सामाजिक समतेची कार्य सर्वसामान्य लोकांमध्ये केलेले दिसते. त्यातून समाजातील विषमता दूर करण्यास भक्ती संप्रदाय प्रयत्नशील असताना दिसते. वारकरी संप्रदायाची मीहिम मुरिलिम संतांनी बस परिवर्तन घडवून आणून मुरिलिम बनविण्याचे कार्य जे चालविले होते त्याला बांधवापणे असेल तर महात्मागातील शीर्षीत, पिढीत वर्गाल समाजात समान दर्जा देण्याची आवश्यकता होती. समाजात एका निर्माण करण्यासाठी संतांनी समानतेचा विचार समाजासमोर मांडला.

सर्वसमावेशक दृष्टिकोन:

वारकरी संप्रदायाने जात, धर्म, वर्ण, लिंग इत्यादी समाजामध्ये असलेला भेदभाव समाप्त करून सर्वांना एकत्र आणण्याचे कार्य केले. समाजामध्ये मानवतेचा, तत्त्वाचा प्रभाव समाजावर पाडला व सर्वांनी एकत्र राहून गुण्यागेविदाने जगण्याचा मार्ग दाखविला. त्यातून समाजात सर्वसमावेशक दृष्टिकोन निर्माण करण्याचे कार्य केले. भक्ती आंदोलनाने हिंदू आणि मुसलमानांना जवळ आणण्याचे कार्य केले. त्यामुळे मध्ययुगात हिंदू-मुसलमानांमध्ये ऐक्योक्तविषयी तिरस्काराची जी भावना अस्तित्वात होती ती समाप्त करण्याचे कार्य वारकरी संप्रदायाने केले. त्याचबरोबर मध्ययुगात असलेली धर्मांतर करण्याची प्रक्रिया समाप्त झाली. ज्याच्यातून खरा भेदभाव हिंदू-मुसलमानांमध्ये निर्माण झालेला होता, तो समाप्त करण्यात या चळवळीला यश आले. बहुजन समाजातील सामाजिक व धार्मिक संकुचितपणा संपविण्यात वारकरी संप्रदाय यशस्वी ठरला. भक्ती चळवळीत बहुजन समाजाचा समावेश झाल्यामुळे स्वधर्म रक्षणासाठी बहुजन समाज पुढे सरसावला व स्वधर्म टिकवून ठेवणे किती महत्त्वाचे आहे हे सर्व समाजाला सांगण्याचे कार्य केले. त्याच्या मनातील संकुचित वृत्ती समूळ नष्ट झाली. ईश्वरभक्ती करण्याचा अधिकार हा उच्च वर्गीयानाच नाही तर सर्वांना आहे याची जाणीव बहुजन समाजाला झाली. त्यातून निम्न जातींचा विकास घडून आला व हिंदू समाजामध्ये सुधारणा घडून आली. जाती-पातीला महत्त्व राहिले नाही. स्त्रियांनाही भक्ती करण्याचा अधिकार प्राप्त झाला. हिंदू-मुसलमानांमध्ये ऐक्याची भावना निर्माण झाली. असा आधुनिक समाज निर्माण करण्याची प्रक्रिया मध्ययुगीन काळातील वारकरी संप्रदायातील संतांनी केले. त्यांनी चालविलेल्या चळवळीचे अंतिम फळ आधुनिक काळात मानवाला मिळाले. परंतु समाजसुधारणा घडवून आणण्यासाठी चळवळ प्रारंभ करण्याचे श्रेय मात्र मध्ययुगीन काळातील संतांना द्यावे लागेल.

मूल्यमापन:

मध्ययुगीन काळाखंडात उत्तर भारतातील भक्ती चळवळ प्रारंभ करण्याचे श्रेय वारकरी संप्रदायाला द्यावे लागेल. १२ व्या शतकात ज्ञानेश्वरांनी गीतेवर ज्ञानेश्वरी हे भाष्य लिहून त्याचा प्रारंभ केला. वास्तवात भक्ती चळवळ सामाजिक व धार्मिक सुधारणा घडवून आणण्यासाठी चालविली गेलेली चळवळ होती. त्याचा मार्ग ईश्वर भक्ती असला तरी वास्तवात समाजसुधारणा घडवून आणणे हा त्यामगचा उद्देश होता. म्हणूनच वारकरी संप्रदायाने जात, वर्ण, वर्ग, धर्म, लिंग असा कुठलाही भेदभाव न मानता या कार्यात सर्वांना स्थान दिले. समाजामध्ये जातीयवस्था, कर्मकांड, रुढी, परंपरा, प्रथा इत्यादींच्या विरोधात जागृती घडवून आणली. संपूर्ण भारताच्या इतिहासाचा आढावा घेतल्यास वर्तमानकाळात जो आधुनिक समाज निर्माण झालेला आहे, तो एकाएकी निर्माण झालेला नाही. त्यामध्ये आधुनिक काळातील समाजसुधारकांप्रमाणेच संतांचे सुद्धा योगदान महत्त्वपूर्ण आहे. जो ज्यांनी समाजामध्ये अस्तित्वात असलेली वाईट व्यवस्था बदलविण्यासाठी मध्ययुगात प्रथम प्रयत्न संतांनी केला. त्यांचे पूर्ण फळ आधुनिक काळात मिळाले.

संदर्भ:

१. महाजन व्ही.डी., मध्यकाळातील भारत, एस. चन्द्र एण्ड कंपनी लि., नई दिल्ली, नववी आवृत्ती, १९९०, पृ. २३८.

२. कठारे अनिल व इतर, मध्ययुगीन भारत, अखन प्रकाशन, सोलापूर, प्रथमवृत्ती २०११, पृ. ३५१
३. सतीश चंद्र, मध्यकालीन भारत— दिल्लीची मुल्तानशाही, पृ. २८६
४. कित्ता, पृ. २८६
५. सतीश चंद्र, अनिल काळे, मध्यकालीन भारत—दिल्लीची मुल्तानशाही, के सागर पब्लिकेशन, खंड पहिला, २००६ पृ. २९६
६. माळुंखे आ. ह., विदोही तुकाराम, लोकायत, सातारा, २००३ पृ. १०३
७. सतीश चंद्र, उपरोक्त, पृ. २१२
८. कित्ता, पृ. २१२
९. महाजन व्ही. डी., उपरोक्त, पृ. २३८
१०. कठारे अनिल, उपरोक्त, पृ. ३४९



SUSTAINABLE DEVELOPMENT IN RURAL INDIA: ISSUES AND POLICY INITIATIVES



EDITORS

Dr. Mansingh S. Dabade Dr. Deepak V. Suryawanshi

NAAC RE-ACCREDITATION
'B' GRADE (CGPA:2.79)

**Sahakarbhushan S.K.Patil College, Kurundwad Tal: Shirol,
Dist: Kolhapur 416106 (MS) INDIA
(AFFILIATED TO SHIVAJI UNIVERSITY KOLHAPUR)**

INDEX

Sr. No.	Title	Page No.
1	Cadastrial Information System (CIS) - GIS Based Application A Case Study for Salu Village (Tara Tekad, Kolhapur District) Dr. Vishal S. Mason, Dr. Jyotish D. Chitambar	1
2	Overview Of Rural Development Programmes In India Mr. Abhijit Kumbhar	4
3	Importance Of Sports In Our Life Prof. Prasad Limbaji Kashinori	7
4	Role Of Sugar Co-Operatives In Rural India: A Case Study Of Shri Datta Karkhana Shirdi Dr. Mansingh S. Dabade	8
5	Need Of The Inclusion Of Differently Aabled Persons In Sustainable Developmental Process Prof. Akshata Anurkumar Gowade	12
6	A Study Of Social Maturity Among College Students Shri Anil Babasaheb Bagale	14
7	Agricultural And Rural Tourism In India Ms. Pranali Aji Nandagore	15
8	Green Marketing In Rural India Ms. Ankita Sanjay Satvadi	19
9	Rural Economy Towards Cashless: A Case Study Of Nagpur Ms. Srusmita Shaminath Chougale	21
10	Irrigation And Agricultural Development Dr. Dattatray Sataran Bagade	22
11	Social Reforms In Marathi Region: Special Reference To Tribal Rural Child Education Dr. Harji Sadaf, Mr. Gaudhile V. A.	26
12	Agro Tourism For Rural Development Ms. Ashwini Babasaheb Patil	28
13	Role Of Green Marketing In Rural Development Ms. Shah Shivani Shiral	29
14	Agro-Tourism In Rural India Ms. Ashvini Sonil Mali	31
15	Digital India Ms. Rasika Tanaji Maskar	32
16	Green Marketing & Rural India Ms. Varsha Gajanan Patil	33
17	Make In India & Rural India Ms. Snehal Dadasa Aade	34
18	Role Of Co-Operative In India Ms. Arpita Adinath Bahwan	36
19	Role Of Women Entrepreneurs In Sustainable Development Of Rural Economy And Sustainable Development For Rural Women Empowerment Ms. Patil Shweta Rangunda	38
20	Rural Development And Food Problem In India Dr. Pandit S. Waghmare	39
21	Cashless Society Ms. Borgave Sunita Ganpati	40
22	Rural Road Infrastructure In India: A Need Ms. Sabina Rizwan Matwal	41
23	Role Of Maharashtra State Road Transport Corporation In India Ms. Reshma Babasaheb Ekanbe	43
24	Digital India: With Reference To Digital Empowerment Of Citizens Ms. Kagale Pallavi Laxman	44

124	प्रथम भारतीय संविधान समीक्षा-एन एन	डॉ. सीतल चक्रवर्ती	244
125	सामाजिक अर्थशास्त्र - एन.ए. कर्कर	अनन्त कर्कर	245
126	प्रथम भारतीय संविधान - संविधान के अन्तर्गत	डॉ. सीतल चक्रवर्ती	248
127	प्रथम भारतीय संविधान के अन्तर्गत भारतीय संविधान का विकास एक विचारधारा अन्तर्गत	डॉ. रामचन्द्र शर्मा	250
128	प्रथम भारतीय संविधान के अन्तर्गत भारतीय संविधान के अन्तर्गत	विश्व कर्कर	251
129	प्रथम भारतीय संविधान के अन्तर्गत	डॉ. सीतल चक्रवर्ती	253
130	प्रथम भारतीय संविधान के अन्तर्गत भारतीय संविधान	डॉ. रामचन्द्र शर्मा	255
131	प्रथम भारतीय संविधान के अन्तर्गत भारतीय संविधान के अन्तर्गत	डॉ. रामचन्द्र शर्मा	258
132	14 वां विधान संशोधन के अन्तर्गत भारतीय संविधान	डॉ. सीतल चक्रवर्ती	260
133	प्रथम भारतीय संविधान के अन्तर्गत भारतीय संविधान	डॉ. रामचन्द्र शर्मा	261
134	प्रथम भारतीय संविधान के अन्तर्गत	डॉ. रामचन्द्र शर्मा	263
135	भारतीय संविधान के अन्तर्गत भारतीय संविधान के अन्तर्गत	डॉ. सी. श्रीराम शर्मा	264
136	भारतीय संविधान के अन्तर्गत भारतीय संविधान के अन्तर्गत	डॉ. सी. श्रीराम शर्मा	266
137	भारतीय संविधान के अन्तर्गत भारतीय संविधान के अन्तर्गत	डॉ. सी. श्रीराम शर्मा	267
138	भारतीय संविधान के अन्तर्गत भारतीय संविधान के अन्तर्गत	डॉ. सी. श्रीराम शर्मा	269
139	भारतीय संविधान के अन्तर्गत भारतीय संविधान के अन्तर्गत	डॉ. सी. श्रीराम शर्मा	273
140	भारतीय संविधान के अन्तर्गत भारतीय संविधान के अन्तर्गत	डॉ. सी. श्रीराम शर्मा	274
141	भारतीय संविधान के अन्तर्गत भारतीय संविधान के अन्तर्गत	डॉ. सी. श्रीराम शर्मा	276
142	भारतीय संविधान के अन्तर्गत भारतीय संविधान के अन्तर्गत	डॉ. सी. श्रीराम शर्मा	278
143	भारतीय संविधान के अन्तर्गत भारतीय संविधान के अन्तर्गत	डॉ. सी. श्रीराम शर्मा	280
144	भारतीय संविधान के अन्तर्गत भारतीय संविधान के अन्तर्गत	डॉ. सी. श्रीराम शर्मा	281

A Review on Superhydrophobic Surfaces: Fundamentals, Fabrications and Applications

Mehejbin R. Mujawar¹, Rajesh B. Sawant¹, Govind D. Salunke¹, Rajaram S. Sutar², Sanjay S. Latthe³, Ankush M. Sargar^{4*}, Raghunath K. Mane⁵, Krishna K. Rangar¹, Shivaji R. Kulal^{1*}

¹Department of Chemistry, Raje Ramrao Mahavidyalaya, Jath, Dist. - Sangli (MS) India

²Self-cleaning Research Laboratory, Department of Physics, Raje Ramrao Mahavidyalaya, Jath, Dist. - Sangli (MS) India.

³Self-cleaning Research Laboratory, Department of Physics, Vivekanand College (Autonomous), Kolhapur, Dist. - Kolhapur (MS) India.

⁴Department of Chemistry, Bharati Vidyapeeth's Dr. Patangrao Kadam Mahavidyalaya, Sangli, Dist. - Sangli (MS) India

⁵Department of Chemistry, Smt. Kusumtai Rajarambhapu Patil Kanya Mahavidyalaya, Islampur, Dist. - Sangli (MS) India

**Corresponding author's E-mail: stkulal@gmail.com, amsargar2012@gmail.com*

Abstract

Superhydrophobic surfaces are highly hydrophobic i.e., it extremely difficult to wet. Superhydrophobic surfaces are the tendency to repel water drops and absorb oil drops. The water contact angle of superhydrophobic surfaces is greater than 150° , the oil contact angle is less than 5° , and the sliding angle is less than 5° . It is showing the lotus effect. Superhydrophobicity is observed in the lotus leaves, insects, and some other plants in which their leaves would not get wet. This phenomenon is due to the unique surface structure of the lotus leaf and also the presence of a low surface energy material on the surface of the leaf. For the formation of a superhydrophobic surface, the surface must show hierarchical micro- and nano-roughness and low surface energy. Efforts have been taken to form superhydrophobic surfaces for a variety of applications. There are many applications of superhydrophobic surfaces such as self-cleaning surfaces, oil-water separation surfaces, anti-icing surfaces, anti-corrosion surfaces, anti-fogging surfaces, and water-resistant surfaces. In this article, the fundamental principles of superhydrophobic surfaces, some recent trends in the fabrication of superhydrophobic surfaces, and their applications are reviewed and discussed.

Keyword: Superhydrophobicity, Superoleophobicity, Lotus effect, Self-cleaning, Oil-water separation, Water-repelling, Oil Contact Angle, Water Contact angle, Anti-icing, Anti-corrosion.

“Dissemination of Education for Knowledge, Science and Culture”
-Shikshanmaharshi Dr. Bapuji Salunkhe



KOLHAPUR
NAAC Accredited "A"
in 3rd cycle
With CGPA - 3.24
58th Rank in NIRF -2017

Vivekanand College, Kolhapur

Dept. of History & Political Science



PROCEEDINGS

One day International Multidisciplinary Seminar

"Emerging Movements & Trends
in Humanities and Sciences"

22nd September, 2017

A Special issue of

Aayushi International Interdisciplinary Research Journal

Special Issue- XV ISSN -2349-638x

Impact Factor 3.025

Dr. S. R. Kattimani
Editor

Dr.M.S. Ghorpade
Co-Editor

Mr.D. A. Pawar
Co-Editor

Dr. S. Y. Hongekar
Principal,
Vivekanand College, Kolhapur

Sr.No.	Author Name	Research Paper / Article Name	Page No.
101.	पल्लवी रोहिदास मिरजकर	सोलापूरमधील महिला विडी-कामगार चळवळ	428 To 431
102.	पी.जे. चौधरी	भारताच्या स्वातंत्र्य चळवळीत वृत्तपत्रांचे योगदान	432 To 437
103.	शिवप्रसाद सुनिल शेवाळे	महाराणी जिजाबाई कालीन वेदोक्त चळवळ : एक अभ्यास	438 To 439
104.	गोविंद नागनाथराव ढोबळे	कामगार चळवळ	440 To 444
105.	डॉ.शिवाजी दत्तात्रय जाधव	सामाजिक बदल आणि भारतातील सामाजिक चळवळी	445 To 448
106.	डॉ.कल्पणा पाटोळे	स्त्री-जागरण में हिंदी उपन्यासों की भूमिका (नासिरा शर्मा के उपन्यासों के संदर्भ में)	449 To 451
107.	डॉ.ज्योती व्हटकर -खरात	डॉ.बाबासाहेब आंबेडकरांचे धर्मांतर : सामाजिक सुधारणा चळवळीतील एक ऐतिहासिक निर्णय	452 To 455
108.	डॉ.संजय सागरु सपकाळ	भारतातील सामाजिक व राजकीय चळवळीत महिला विकासाची वाटचाल	456 To 459
109.	डॉ.वसंत भूपाल शिंदे	भारतंबंध परराष्ट्र धोरण - सातत्य आणि स्थित्यंतर अलिप्ततवादी चळवळ : विकास आणि प्रस्तुतता	460 To 468
110.	डॉ.राहुल दत्ता मांडणीकर	दलित चळवळीची स्थित्यंतरे	469 To 474
111.	काशिलिंग रघुनाथ गावडे	छोडो भारत, प्रतिसरकार आणि शिराळा पेठा	475 To 479
112.	सागरकुमार राहुल जाधव यशवंत नागुर्डेकर	महाराष्ट्रातील पर्यावरण चळवळी	480 To 484
113.	अनिल गाडेकर डॉ.उल्का देशमुख	धनगर समाजाच्या आरक्षण चळवळीचा समाजशास्त्रीय अभ्यास	485 To 487
114.	डॉ.प्रा.संपदा टिपकुर्ले	दारुबंदी चळवळ - आर्थिक आणि सामाजिक परिणाम	488 To 491
115.	अनिल प्रभाकर कांबळे	नारी मुक्ति आंदोलन : उद्भव और विकास	492 To 493
116.	पद्माकर बळीराम तटाळे	भारतातील सहकारी चळवळ	494 To 496
117.	डॉ.मधुकर धुतुरे	माहितीचा अधिकार एक सामाजिक चळवळ	497 To 501
118.	डॉ.सौ. सुनिता एस.राठोड	नोटबंदी : यश अपयश	502 To 505
119.	डॉ.एम. आर.खोत	स्वातंत्र्यसैनिक अरुणा असफ अली यांचे जीवन व कार्य	506 To 508

भारताच्या स्वातंत्र्य चळवळीत वृत्तपत्रांचे योगदान

वौधरी पी.जे.

राजे रामराव महाविद्यालय, जत.

प्रास्ताविक :

भारतीय स्वातंत्र्य चळवळीच्या इतिहासामध्ये वृत्तपत्रांना महत्वपूर्ण स्थान आहे. वृत्तपत्रांचे प्रमुख कार्य सरकारची ध्येय-धोरणे जनतेपर्यंत पोहचणे, जनतेच्या समस्या सरकारच्या लक्षात आणून देणे आणि सरकारच्या धोरणाविषयी असलेल्या जनतेच्या प्रतिक्रिया सरकारच्या लक्षात आणून देणे असते. त्याचबरोबर देश-विदेशातील घडणा-या घडामोडींची माहिती लोकांपर्यंत पोचवणे असते. या सार्वजनिक गरजामधून वृत्तपत्रांचा विकास झाला. वृत्तपत्रांनी भारतीय स्वातंत्र्य चळवळीत जागृती भारतीय जनतेत निर्माण करण्याचे कार्य केले. १८५७ पासून तर १९४७ पर्यंतच्या काळात ब्रिटीश सत्तेचे वर्चस्व संपूर्णतः आनण्यासाठी भारतीयांनी अनेक चळवळी केल्या त्या संपूर्ण स्वतंत्र्य चळवळीत वृत्तपत्रांनी प्रचार प्रसार केला. भारतीय लोकांना एकत्रीत अनण्याचे कार्य केले. ब्रिटीश सरकारची शोषण कारी धोरणे जनतेसमोर मांडून जनतेत ब्रिटीश विरोधी जागृती निर्माण केली. इ.स. १८८५ मध्ये राष्ट्रीय सत्तेची स्थापना झाल्यावर राष्ट्रीय सभेच्या नेतृत्वात ब्रिटीश सत्तेच्या पासून भारताला स्वातंत्र्य प्राप्त करण्यासाठी १८५७ चा उठाव, स्वदेशी चळवळ, होमरूल चळवळ, असहकार चळवळ, संविनय कायदेभंग चळवळ आणि 'चले जाव चळवळ' इत्यादी प्रमुख चळवळी झाल्या. या चळवळी यशस्वी करण्यासाठी वृत्तपत्रांनी केलेले कार्य हे चळवळीत सहभागी असलेल्या नेत्यांनी केलेल्या प्रचार सभेपेक्षा कमी नव्हते. वृत्तपत्रांनी या चळवळीमध्ये भारतीय जनतेला जास्तीत-जास्त संख्येने सहभागी होण्यास प्रेरित केले. वृत्तपत्रे ही शहरी भागापूरते सीमित नव्हती तर खेड्या-पाड्यापर्यंत पोहचत होते.

त्यामुळे ब्रिटीशांच्या सर्व ध्येय धोरणांची माहिती त्या ध्येय धोरणांच्या विरोधी भारतीय नेत्यांनी केलेल्या प्रतिक्रियांची माहिती भारतीय स्वातंत्र्याच्या चळवळीत ग्रामीण भागातील भारतीय लोकांना सुध्दा होत होती. त्यामुळे अनेक शेतकरी कामगार स्त्रीयांनी भाग घेतला व या चळवळीला व्यापक स्वरूप प्राप्त करून दिले सर्व देशवासीयांना एकत्रीत आणून भारतीय स्वातंत्र्य चळवळीला बळ निर्माण करून देण्याचे कार्य वृत्तपत्रांनी केले. त्या अनुषंगाने या स्वातंत्र्य चळवळीच्या संदर्भात वृत्तपत्रांच्या कार्याचा आढावा घेणे गरजेचे आहे.

भारतात वृत्तपत्रांचा उगम :

युरोपीय वसाहती आल्यानंतरच भारतात वृत्तपत्रांचा प्रारंभ झाला. ब्रिटीशांची सत्ता भारतावर प्रस्थापीत होण्याअगोदरच भारतात बातमीदार व बातमीपत्रे अस्तीत्वात होती परंतु वृत्तपत्रांचा प्रारंभ करण्याचे श्रेय वास्तवात ब्रिटीश सरकारलाच द्यावे लागते. भारतात पहिले वृत्तपत्र काढण्याचा प्रयत्न ब्रिटीशांच्या असंतुष्ट अधिन्यांनी केला. त्या मागचा उद्देश ब्रिटीश अधिकाऱ्यांमधील भ्रष्टाचार उघडकीस आणणे हा होता. १७७६ मॅ विलीयम बोल्ट्स की कोर्ट ऑफ डायरेक्टर्स ने निजी व्यापार के लिये निंदा की और उससे त्यागपत्र देकर यह इच्छा प्रकट की की वह समाचार पत्र निकलेगा और फीर यह कहा की उसके पास हस्तलिखित रुप मे बहुत सें तथ्य हैं जो सभी व्यक्तियोंसे गहरा संबंध रखते हैं , इस्ट इंडीया कंपनीच्या अधिकाऱ्यात लवकरच त्याची प्रतिक्रिया तयार झाली. आणि विलीयम बोल्ट्सची वृत्तपत्र स्थापन करण्याची योजना धुळीस मिळाली. त्यामुळे भारतात प्रथम वृत्तपत्र स्थापन करण्याचे श्रेय जेम्स ऑगस्टस हिक्की यांना प्राप्त झाले. त्याने १७८० मध्ये दि बंगाल गॅझेट या नावाने वृत्तपत्र प्रकाशित झाले. आणि भारतात वृत्तपत्रांचा प्रारंभ झाला. त्यानंतर कलकत्ता गॅझेट १७८४ बंगाल जर्नल १७८५ कलकत्ता क्रोनिकल १७८८, मद्रस कुरिअर इत्यादी इंग्रजी वृत्तपत्रे एकामागून एक प्रकाशित झाली. या वृत्तपत्रांचा उद्देश युरोपियन आणि अँग्लो इंडियन लोकांचे मनोरंजन करणे हा होता. कारण यांना ब्रिटीश अधिकाऱ्यांचा रोष ओढावून घ्यावयचा नव्हता तरीही या वृत्तपत्रांतून ब्रिटीश अधिकाऱ्यांच्या भ्रष्टाचाराच्या बातम्या प्रकाशित होत होत्या. त्या बातम्या इंग्लंडच्या पार्लमेंटकडे जाऊ नये याची खबरदारी घेतली जात होती. ही वृत्तपत्रे सरकारी अधिकाऱ्यांच्या दयेवर टिकून होती. या वृत्तपत्रांचे महत्व हळुहळु भारतीय नवशीक्षित मध्यमवर्गाच्या लक्षात येवू लागले. आणि भारतीयांनीही वृत्तपत्रे प्रकाशित करायला प्रारंभ केला. समाचार दर्पन,

संवाद कौमुदी, अमृतबझार पत्रीका, दर्पन, केशरी, मराठा, बंगाली, रास्तगोप्तार, यंग इंडीया आशी अनेक वृत्तपत्रे भारतीयानी प्रकाशीत केली. या वृत्तपत्रांनी स्वातंत्र्य चळवळीच्या काळात ब्रिटीशविरोधी भारतीय जनमत तयार करण्यात महत्वाची भुमीका बजावली.

विषय विवेचन :

भारतीय स्वातंत्र्य चळवळीत वृत्तपत्रांचे कार्य पाहतांना १८५७ च्या उठावापासून तर १९४७ पर्यंत झालेल्या प्रमुख चळवळीचा उल्लेख करावा लागतो. त्यानुसार १८८५ पुर्विचे वृत्तपत्रांचे कार्य मवाळ कालखंड, जहाल काजखंड आणि गांधी युग इत्यादी कालखंडाचा ब्रिटीश सरकारच्या विरोधात झालेल्या छोट्या*मोठ्या चळवळीत ब्रिटीश सरकारने आखलेल्या ध्येय धोरणांविषयी वृत्तपत्रातून झालेल्या प्रतिक्रियांचा वृत्तपत्रातून मांडलेल्या भारतीय जनतेच्या समस्या आदींचा विचार करावा लागतो.

१८८५ पुर्विचे वृत्तपत्रांचे कार्य :

१८५७ च्या उठावाने भारतीयानी मोठ्या प्रमाणावर ब्रिटीश सत्तेला प्रथम विरोध करून भारतातून ब्रिटीशांची सत्ता संपुष्टात आणण्याचा पहीला प्रयत्न केला तेव्हापासून खऱ्या अर्थाने भारतीय स्वातंत्र्य चळवळीचा प्रारंभ झाला. १८५७ च्या उठावाचा प्रचार -प्रसार करण्यात वृत्तपत्रांनी महत्वाचे योगदान दिले त्या काळात बंगालमध्ये आघाडीवर असलेले वृत्तपत्र म्हणजे 'हिंदु पेटीयर'. १८५७ च्या उठावाचे खरे स्वरूप जनतेपुढे स्पष्ट मांडणे ब्रिटीशांच्या जुलमी नीतीवर प्रखर टीका करणे, त्या मजुरांच्या हालअपेष्टांना वाचा फोडून त्यांच्या जुलमी मालकाविरुद्ध प्रतिकाराला त्यांना उद्युक्त करणे अशा स्वरूपाचे कार्य त्या वृत्तपत्राने चालविले होते. त्यानंतर कीशोरीचंद्र मित्र यांचे बंगाल नवगोपाल मित्र यांचे 'द नॅशनल पेपर' आदि वृत्तपत्रांनी बंगालमध्ये राष्ट्रीय भावना जागृत करण्यात अतिशय महत्वाची कामगिरी केली. १८५७ च्या उठावाने भारतीय लोकांमध्ये राष्ट्रीय जागृती निर्माण झाली. १८५७ च्या उठावानंतर सुशिक्षित मध्यम वर्गाचा उदय झाला. या वर्गाने चळवळीचे नेतृत्व करण्यात पुढाकार घेतला. ब्रिटीशांच्या शोषणकारी नीतीच्या विरोधात आपल्या विचारांचा प्रचार करण्यासाठी या मध्यम वर्गाला वृत्तपत्रांची आवश्यकता भासू लागली. प्रत्येक गावो-गावी जावून आपल्या विचारांचा प्रसार करणे शक्य नव्हते त्यासाठी वृत्तपत्रे ही त्यासाठी उपयोगी माध्यम होते. म्हणून या सूशिक्षित भारतीय नेत्यांनी अनेक वृत्तपत्रे काढून ब्रिटीशकालीन व्यवस्थेची माहिती प्रकाशित केली. १८७५ साली खानदेश वैभव या पत्राने "दबून राहणाऱ्यांना सरकार अधिकच दडपून टाकत होते हा नित्याचा अनुभव आहे. म्हणून बळाचे उत्तर बळानेच द्यायला पाहिजे." असा धाडसी संदेश भारतीय जनतेला दिला. तर भारतातील एकाही राज्यकर्त्याने केले नाही इतके भारताचे नुकसान ब्रिटीश शासनाने केले आहे." असे 'महाराष्ट्र मित्र' या पत्रकाने ठामपणे प्रतिपादन केले. त्याच साली ब्रिटीश राजपुत्राच्या भारतभेटीच्यावेळी त्याच्या स्वागतात लोकांनी सहभागी होऊ नये. आपल्या तक्रारी शिवाय इतर काहीही त्याच्या कानी पडू देवू नये असा संदेश मुंबईतून प्रकाशित होणा*या 'शिवाजी' या वृत्तपत्राने आपल्या वाचकांना दिला. बडोदे? याचे राजे मल्हारराव गायकवाड यांना ब्रिटीश सरकारने पदच्युत करून बंदिस्त केल्याचे पडसाद संपूर्ण भारतभर उमटले आणि महाराष्ट्रपासून तर बंगालपर्यंतच्या वृत्तपत्रांतून ब्रिटीश सरकारवर टीका झाली की, ब्रिटीश सरकार त्या मल्हारराव गायकवाड यांना पदच्युत करण्याचा अधिकार कसा पोहचला असा प्रश्न वृत्तपत्रामधून प्रकाशित करून ब्रिटीश सरकारला विचारणा केली. अमृतबझार पत्रिकेने तर एक पाउल पुढे टाकून एका राष्ट्राचे रक्तशोषण करून त्याला रक्तहीन बनविणे हा एका सामान्य ब्रिटीश अधिका*यावर विषप्रयोग करण्यापेक्षा कितीतरी गंभीर गुन्हा आहे अशी टीका ब्रिटीश सरकारवर केली. १८७८ साली या वृत्तपत्राने ब्रिटीशांनी लादलेली गुलामगिरी फार काळ टिकणार नाही. स्वातंत्र्य हाच यशाचा व सुखाचा बालेकिल्ला आहे असे मत मांडून भारतीयानी स्वतंत्रता या वृत्तपत्राने स्वातंत्र्याचा मंत्र दिला. राष्ट्रीय सभेची स्थापना होण्याअगोदरच वृत्तपत्रांनी भारतीय जनतेमध्ये राजकिय जागृती निर्माण करण्याचे कार्य केले होते. अनेक वृत्तपत्रांनी ब्रिटीशांच्या शोषणकारी नीतीवर टीका केली. भारतीय जनतेच्या समस्या वृत्तपत्रातील बातम्यामधून ब्रिटीश सरकारला दाखवून दिल्या. १८५७ च्या उठावापूर्वीच्या वृत्तपत्रापेक्षा या उठावानंतर वृत्तपत्रांची संख्या ही वेगाने वाढू लागली. १८५७ च्या उठावापासून तर १८७५ पर्यंतच्या काळात ही संख्या वेगाने वाढत जावून भारताच्या भिन्न भागात आणि त्या-त्या भागातील भाषांमध्ये प्रकाशित होणा-या वृत्तपत्रांची संख्या ३७४ झाली तर १९४७ वृत्तपत्रे इंग्रजी भाषेत प्रकाशित होवू लागली. या काळातील वृत्तपत्रे ही भारतीय समाजाची मुखपत्रेच होती, की ज्या मुखपत्रांनी ब्रिटीशांना

भारतीय समाजाची गा-हानी समजावून दिली. ब्रिटिशांचा अन्यायी बुरखा फाडून लोकांना दाखविले आणि जनतेच्या असंतोषाला वाचा फोडण्याचे कार्य या वृत्तपत्रांनी केले.

मवाळ कालखंडातील वृत्तपत्रांचे कार्य:

१८५७ च्या उठावानंतर भारतीय जनतेत राष्ट्रीय भावना जागृत होवू लागली. ब्रिटिशांची सत्ता भारतातून समाप्त करायची असेल किंवा भारतीयांच्या मागण्या ब्रिटिशांकडून मान्य करून घ्यावयाचे असतील तर वेगवेगळ्या भागात ब्रिटिश विरोधी चळवळी चालविणा-या संघटनांनी एकत्रित येवून राष्ट्रीय संघटना निर्माण करावी. आणि या संघटनेच्या नेतृत्वात देशव्यापी चळवळ चालवावी अशी अपेक्षा विविध भागातील नेतृत्वातून व्यक्त होऊ लागली. त्याचे अंतिम परिणाम म्हणजे १८८५ ला झालेली राष्ट्रीय सभेची स्थापना राष्ट्रीय सभेची स्थापना होताच त्याचे पडसाद वृत्तपत्रांवरही उमटले १८८५ ते १९०५ या कार्यकाळात राष्ट्रीय सभेवर मवाळ विचारसरणीच्या नेत्यांचे प्रभुत्व होते. यामध्ये दादाभाई नौरोजी, सुरेंद्रनाथ बॅनर्जी, व्यमेशचंद्र बॅनर्जी, दिनशा वाचा, गोपाळकृष्ण गोखले आदि नेत्यांचा समावेश होता. या नेत्यांनी ब्रिटिश सरकारविषयी मवाळ भुमिका स्विकारून अर्ज विनंत्याच्या माध्यमाने भारताच्या समस्या सोडविणे, ब्रिटिश जनतेचा कौल आपल्या बाजूने तयार करणे, ब्रिटिश सरकारची मर्जी संपादन करणे इत्यादी तत्वांचा अवलंब केला. यांची भुमिका शांततामय असली तरी राष्ट्रीय सभेच्या प्रत्येक अधिवेशनामध्ये भारतीयांच्या समस्या सोडविण्याचे ठराव पारित करण्यात येत होते. त्या ठरावांची माहिती वृत्तपत्रातून प्रकाशित करून जनतेपर्यंत पोहचविण्याचे कार्य केले जात होते. त्यातून जनतेत जनजागृती निर्माण होण्यास मदत झाली. बिटीशंअ या शालिग्राम प्रतिमेचा खटला कलकत्ता उच्च न्यायालयात चालू असताना ही प्रतिमा शंभर वर्षांपेक्षा पुरानी नाही असा निर्णय न्यायाधीश नॉरीश ने दिलेला होता. त्या निर्णयाचा विरोध म्हणून सुरेंद्रनाथ बॅनर्जींनी २ एप्रिल १८८३ को अपेन अखबार बंगालीमें लिखा था की, नॉरीसने सबूत दे दिया है की वह इस उच्च और जिम्मेदार पद के लायक नहीं है। इस युवा और नौसिखिया न्यायाधिष की सनदपर लगाम लगाने के लिए कुछ ना कुछ किया ही जाना चाहिए। यासाठी त्यांना दोन महिन्याची सजा झाली होती. या विरोधात कलकत्ता आणि बंगालच्या विविध भागात आंदोलने झालीत. त्याचे पडसाद लाहोर, अमृतसर, आगरा, फैजाबाद, पुना इत्यादि ठिकाणी ही पडून त्या निर्णयाचा विरोध करण्यात आला. गो. ग. आगरकर आणि लोकमान्य टिळक यांनी १८८१ मध्ये मराठी भाषेत केसरी आणि इंग्रजी भाषेत मराठा वृत्तपत्रे प्रकाशित केली. या वृत्तपत्रांच्या माध्यमाने लोकमान्य टिळकांनी लोकांना ब्रिटिशांच्या विरोधात जागृत करण्याचे कार्य केले. त्याबरोबरच राष्ट्रीय आंदोलनात सहभागी होण्यासाठी जनतेला प्रेरित केले. १८९६-९७ मध्ये पुणे परिसरात दुष्काळ पडलेला होता. त्यावेळी या परिसरातील जनतेला शेतक-यांनी सरकारचा महसूल भरू नये असा प्रसार केसरी आणि मराठा ही वृत्तपत्रे आणि आपल्या प्रचार सभांच्या माध्यमाने लोकमान्य टिळकांनी केली. १८९७ मध्ये दुष्काळानंतर प्लेगची साथ पुण्याच्या परिसरात आली होती. प्लेगच्या साथीचे निवारण करण्यासाठी ब्रिटिश सरकारने रॅड आणि आयस्ट ह्या दोन अधिका-यांच्या नियंत्रणाखाली प्लेग निवारण यंत्रणा राबविली होती. परंतु प्लेग निवारणाच्या नावाखाली या ब्रिटिश अधिका-यांनी पुण्यातील लोकांवर अत्याचार करणे प्रारंभ केले. प्लेग ग्रस्तांची घरे जाळली अनेक स्त्रीयांचे शोषण केले या ब्रिटिशांच्या अमानविय कृत्यांच्या विरोधात टिळक ने अपने समाचार पत्र मराठा में इसपर टिप्पणी करते हुए लिखा था, आजकल नगर में राज कर रही प्लेग अपने मानवीय रुपांतरोसे अधिक दयालू है।, असा टोला वृत्तपत्रात हाणून या काळातील ब्रिटिशांची जुलूमशाही प्लेगपेक्षाही वाईट आहे हे स्पष्ट केले. त्याचे पडसाद पुण्यातील क्रांतीकारकांवर पडले. चाफेकर बंधूंनी या दोन्हा अधिका-यांची गोळ्या घालून हत्या केली. त्यात लोकमान्य टिळकांनाही ब्रिटिश सरकारने दोषी मानून त्यांच्यावर देशद्रोहाचा आरोप लावून अठरा महिन्याची शिक्षा दिली. लोकमान्य टिळकांनी ब्रिटिश सरकारच्या कैदेच्या शिक्षेला न जुमानता भारताला स्वातंत्र्य मिळवून देण्यासाठी या वृत्तपत्रांच्या माध्यमाने जनजागृती करित राहिले.

जहाल कालखंडातील वृत्तपत्रांचे कार्य :

राष्ट्रीय सभेच्या स्वातंत्र्य चळवळीची विभागणी केल्याप्रमाणे १८८५ ते १९०५ या काळात मवाळचा प्रभाव असला तरी लोकमान्य टिळकांच्या जहालवादी विचारांची सुरुवात जहाल कालखंडात झाली होती. या काळातच आपले जहालवादी विचार वृत्तपत्रातून मांडून ब्रिटिश सरकारचा विरोध केला होता. १९०५ ते १९२० या काळातील ब्रिटिश विरोधी चळवळीवर जहाल विचारसरणीचा प्रभाव पडला. भारतीय जनता या विचारांना प्रेरित झाली. त्याचा परिणाम वृत्तपत्रावर

होवून ब्रिटिश अधिका-या विषयी परखड विचार मांडून या काळात झालेल्या चळवळीचा प्रचार-प्रसार करण्यात 'बंगाली', 'केसरी', 'मराठा', 'न्यु इंडिया' इत्यादी वृत्तपत्रांनी महत्वाचे कार्य केले. या काळातील वृत्तपत्राच्या कार्याची सुरुवात १९०५ च्या वंग भंग चळवळीच्या प्रसार-प्रचारापासून झाली. बंगाल फाळणीच्या विरोधामध्ये बंगाल मध्ये राष्ट्रीय काँग्रेसने वंग भंग आंदोलन सुरु केले. सुरेंद्रनाथ बॅनर्जी, कृष्णकुमार मित्र, पृथ्वीसचंद्र राव व अन्य नेताओं ने विभाजन प्रस्ताव के खिलाफ बंगाली हीतवादी संजीवनी जैसे अखबारो और पत्रिकाओं के माध्यम से आंदोलन छेडा। आणि वंगभंग आंदोलनाची सुरुवात झाली. १६ ऑक्टोबर १९०५ हा दिवस 'दूखवटा दिवस' म्हणून साजरा करून या आधारे फाळणीचा विरोध केला. वंग भंग आंदोलनाविषयी जागृती निर्माण करण्याचे कार्य वृत्तपत्रांनी केले. त्यानुसार लॉर्ड कर्झनने केलेल्या कार्यावर वृत्तापत्रातून मोठ्या प्रमाणावर टिका झाली. 'अमृत बाजार पत्रिका' या वृत्तपत्राने लॉर्ड कर्झनचे १९०५ मध्ये झालेले कलकत्ता विद्यापीठातील भाषण दूस-याच दिवशी छापले. त्याबरोबरच लॉर्ड कर्झनची पुस्तक पद प्रॉब्लेम्स ऑफ ईस्टची माहिती बॉक्स बनवून प्रकाशित केली. त्यामध्ये लॉर्ड कर्झनने महाराणी व्हिक्टोरियाच्या असलेल्या आपल्या संबंधाचा उल्लेख केला होता. त्यामुळे लॉर्ड कर्झनचा खोटेपणा जनतेसमोर आला. त्याची बदनामी झाली. त्याबरोबरच ब्रिटनच्या 'विकली टाईम्स' ने यह खबर छाप दी की, श्लगता है की सत्य का सम्मान करना लॉर्ड कर्झनने अपने विवाह के बाद पत्नी के मार्गदर्शन में ही सिखा है यह अमेरिकीओं का खास गुण है। १९०६-०७ मध्ये हिंदू-मुस्लिमांमध्ये ब्रिटिश अधिका-यांनी दिलेल्या चिथावणीमुळे दंगली झाल्या असा स्पष्ट अभिप्राय 'लंडन डेली न्युज' या वृत्तपत्राने दिलेला आठवतो. वंग भंग चळवळीच्या काळात ब्रिटिशांनी बंगाल प्रांतातील जनतेवर जे अत्याचार केले त्याचा वृत्तात लंडन डेली न्युज या वृत्तपत्राने प्रकाशित केला आणि रशियन जुलुमशाहीला लाजविणारे अत्याचार बंगालमध्ये घडत असल्याचे त्याने ब्रिटिश जनतेच्या निर्दशनास आणून दिले. कर्झनच्या भारत विरोधी व प्रतीगामी धोरणाची माहिती 'बंगाल', 'संध्या', 'युगांतर' या वृत्तपत्रांच्या माध्यमानेही भारतीय जनतेला होत होती. १९०५ साली लोकमान्य टिळकांनी केसरी वृत्तपत्रातील लेखात 'कर्झनची तुलना औरंगजेबाशी' केली होती. लोकमान्य टिळकांनी एका लेखात सरकारी अधिकारी कोणतेही कारण नसताना लोकामध्ये दहशत निर्माण करतात अशी लोकांना वेगवेगळ्या प्रकारची भीती दाखवून त्यांच्यात नैराश्य निर्माण करतात तेंव्हा स्फोटक बॉम्बचा आवाज या अधिका-यांना आणि सरकारला चेतावणी देते की, लोक शांत आणि निष्क्रीय बसने आणि दडपशाही शोषणाला सहन करण्याच्या सीमा पलिकडे गेलेले आहेत आणि आता काहीतर करण्याच्या मार्गावर आहेत हे वृत्त ब्रिटिश सरकारला सहन झाले नाही आणि त्यांना राजद्रोहाच्या खटल्याखाली २४ जून १९०८ मध्ये सहा वर्षांची काळ्यापाण्याची शिक्षा दिली. या काळापासून १९१४ पर्यंत निष्क्रीय झालेली राष्ट्रीय काँग्रेस लोकमान्य टिळकांच्या सुटकेनंतर पुन्हा जागृत झाली. लोकमान्य टिळक आणि अॅनी बेझंट यांनी जहाल आणि मवाळ त्याचबरोबर मुस्लिम लीग यांच्यात १९१६ च्या लखनौ अधिवेशनात एकता घडवून ब्रिटिश विरोधी चळवळ पुन्हा प्रारंभ झाली. या काळातील महत्त्वपूर्ण चळवळ म्हणजे होमरूल चळवळ होय. होमरूल याचा अर्थ स्वशासन असा होतो. अॅनी बेझंट ने आयर्लंड प्रमाणे भारतालाही स्वशासन मिळावे म्हणून होमरूल चळवळ प्रारंभ केली. १९१५ च्या सुरुवातीलाच अॅनी बेझंटने 'न्यु इंडिया' आणि 'कॉमनवेल' या वृत्तपत्रांच्या माध्यमाने होमरूल चळवळीची घोषणा केली. राष्ट्रीय काँग्रेसच्या नेत्यांना या चळवळीला पाठिंबा मागितला. त्यात लोकमान्य टिळकांनी पुढाकार घेवून देशातील प्रमुख दोन केंद्रातून ही चळवळ चालविली. लोकमान्य टिळकांचे केंद्र बेळगांव तर अॅनी बेझंटचे केंद्र अड्यार मद्रासजवळ होते. दोघांनीही आपआपले भाग वाटून घेवून होमरूल चळवळ चालविली होती. लोकमान्य टिळकांच्या नेतृत्वातील चळवळ जोमात चालू असताना २३ जुलै १९१६ रोजी भारतात असंतोष निर्माण करण्याच्या आरोपाखाली त्यांना अटक करून त्यांना प्रथम मॅजीस्ट्रेटच्या न्यायालयात खटला चालवण्यात येवून दोषी करार देण्यात आला. परंतु लोकमान्य टिळकांनी उच्च न्यायालयात अपील केली तेंव्हा उच्च न्यायालयाने निर्दोष करार दिला होता. 'इस जीत के लिए गांधीने 'यंग इंडिया' अखबार में लिखा यह अभिव्यक्ती की आजादी की, बहुत बड़ी जीत है। होमरूल आंदोलन के लिए एक बहुत बड़ी सफलता है। अॅनी बेझंटच्या होमरूल चळवळीत सहभागी असलेल्या लोकांना व्यक्तीगतरित्या निर्देश देण्यात येत होते. किंवा 'न्यु इंडिया' या वृत्तपत्रात अरुंडेलने प्रकाशित केलेली बातमी वाचून पुढे चळवळीत काय करायचे आहे हे सदस्यांना कळत होते. आणि त्यानुसार अॅनी बेझंटची होमरूल चळवळ व्यवस्थित चालत होती. होमरूल चळवळीचा प्रसार करण्यात या वृत्तपत्राने चळवळीतील सहभागी नेत्यांप्रमाणेच सहकार्य दिले.

गांधीयुगातील वृत्तपत्रांचे कार्य :

१९२० पासूनच्या चळवळीवर महात्मा गांधींच्या विचारांचा प्रभाव होता म्हणून १९२० ते १९४७ या स्वातंत्र्य चळवळीच्या काळाला गांधी युग म्हणून ओळखले जाते. गांधीजींनी सत्य, अहिंसा आणि सत्याग्रह या तत्वांच्या आधारे या काळातील चळवळी चालविल्या. भारताला स्वातंत्र्य अहिंसा आणि असहकार या तत्वांनी प्राप्त करता येईल असे त्याचे ठाम मत होते. उन्होने यंग इंडिया नामक पत्रिकांमै लिखा था, 'जिन ऋषियों ने हिंसा के बिच अहिंसा के सिध्दांत को खोज निकाला वे 'न्युटन' से अधिक प्रखर बुध्दीवाले लोग थे, वे स्वयं वैलिंगटन से अधिक विर योध्दा थे। स्वयं हथियारों का प्रयोग जानते हूए भी उन्होने इसकी व्यवस्था को अनुभव किया और उन्होंने युध्द से दुःखी संसार को बतलाया की इसकी मुक्ती हिंसाद्वारा नहीं अपितु अहिंसाद्वारा ही है।',^{१०} हिंसेने हिंसाच निर्माण होत असते. त्यामुळे अहिंसेच्या मार्गाने सत्याग्रह केल्यास स्वातंत्र्याबरोबर शांतताही मिळेल अशी आशा आपल्या विचारातून व्यक्त केली. त्यांनी ब्रिटिश सरकारला सहाय्य न करणे ब्रिटिशांनी निर्माण केलेले अन्यायी कायदे सत्याग्रह करून तोडण्याचा प्रयोग त्यांनी आपल्या चळवळीमध्ये केला. गांधीजींच्या नेतृत्वातील चळवळीचे एक महत्वपूर्ण वैशिष्ट्य की त्यांनी कामगार, शेतकरी, स्त्री यांचा सहभाग चळवळीत करून घेतला त्यामुळे या काळातील चळवळीची व्यापकता देशव्यापी होती. खेड्या-पाड्यापासून लोक स्वातंत्र्याच्या चळवळीमध्ये सहभागी झाले होते. या कालखंडात १९२० ला असहकार चळवळ व्यापक स्वरूपात झाली. त्यात सरकारला सहकार्य न करण्यावर भर देण्यात आला होता. पदव्यांचा त्याग करणे, वकिली व्यवसाय सोडणे, सरकारी शाळांचा त्याग करणे, परदेशी मालाचा बहिष्कार करणे इत्यादी असहकारात्मक बाबींवर भर देण्यात आला होता. या चळवळीचा प्रसार करण्यामध्ये सभा, भाषणे या बरोबर वृत्तपत्रांनीसुध्दा मोलाचे सहकार्य केले. 'नवजीवन', 'यंग इंडिया', 'हिंदुस्तान टाइम्स', 'इनडिपेंडंट' इत्यादी वृत्तपत्रांनी असहकार चळवळीचा प्रचार-प्रसार खेड्यापाड्यापर्यंत केला. १९२० ते १९२२ पर्यंत असहकार चळवळ जोमात चालू असताना ५ फेब्रुवारी १९२२ रोजी असहकार चळवळीतील सत्याग्रही आणि ब्रिटिश सैनिक यांच्यात हिंसा घडून आली. त्यानंतर महात्मा गांधींनी असहकार चळवळ मागे घेण्याचा निर्णय घेतला. ब्रिटिश सरकारने असहकार चळवळीस महात्मा गांधींना कारणीभूत ठरविले आणि त्यांच्या अटकेची बातमी येवू लागली. तेंव्हा ९ मार्च १९२२ च्या यंग इंडिया या अंकात गांधीजींनी 'मी जर पकडलो गेलो तर' ह्या मथळ्याचा लेख लिहला व राष्ट्रीय सभेच्या कार्यकर्त्यांना खादी, राष्ट्रीय शिक्षण, हिंदु-मुस्लिमांचे ऐक्य, अस्पृश्यता निवारण वैगरे विधायक कार्यक्रम करित रहा व अनत्याचाराचे व्रत पाळा असा उपदेश केला. सायमन कमिशनमध्ये एकही सदस्य भारतीय नसल्यामुळे राष्ट्रीय काँग्रेसने त्यांचा विरोध केला आणि ब्रिटिश सरकारचा बहिष्कार करण्याचा निर्णय घेतला, त्यानंतर १९२९ मध्ये पूर्ण स्वराज्याचा ठराव पारित करण्यात आला. तेंव्हा महात्मा गांधींनी १२ जून १९२८ के 'यंग इंडिया' में करा था। कहा जाता है की स्वतंत्रता का प्रस्ताव ही उचीत जवाब है..... आयोग की नियुक्ती (सायमन आयोग) को उचित उत्तर मिलना चाहिए, भाषण चाहे कितने भी बहादुरी से भरे हो, घोषणाएँ चाहे जितनी भी साहसपूर्ण हों, उसको इसकी आवश्यकता नहीं है, इसके लिए उचित कार्रवाई की जानी चाहिए।^{१२} हा गांधीजींचा विचार भारतीयांना स्वातंत्र्याच्या चळवळीसाठी प्रेरित करित होता. पुढील चळवळीला भारतीय लोकांना तयार करण्याचे कार्य करित होता. ब्रिटिश सरकारने काँग्रेसची पुर्ण स्वराज्याची मागणी मान्य केली नाही भारताच्या संदर्भात विचार-विनिमय करण्यासाठी १९३० ते १९३२ च्या दरम्यान गोलमेज परिषदाचे आयोजन ब्रिटिश सरकारने केले होते. त्या गोलमेज परिषदांना राष्ट्रीय सभेचे नेते गांधीजींना इंग्लंडला जाणे अपेक्षित होते परंतु एक वर्षानंतर 'सविनय कायदेभंग' चळवळ चालविण्याचे गांधीजींनी ठरविले होते म्हणून इंग्लंडला जाण्याची योजना रद्द केली आणि जनवरी १९२९ के 'यंग इंडिया' में लिखा: मुझे ऐसा लगता है की, यदि मैं यूरोप चला गया तो लोगों के साथ धोखा करने का अपराधी होऊंगा। मेरी अंतरात्मा मुझसे कहती है की वह सिर्फ जो मेरे सामने आता है उसका मुकाबला करने के लिए मुझे तयार रहना चाहिए बल्कि मुझे सोच विचार कर कोई कार्यक्रम सुझाना चाहिए। इन सबसे उपर मुझे अगले वर्ष के संघर्ष के लिए तयार रहना चाहिए, इसकी शकल चाहे जो भी हो।^{१३} १९३० मध्ये महात्मा गांधींनी सविनय कायदेभंगाची चळवळ प्रारंभ करण्यासाठी मिठाचा कायदा मोडण्याचा निर्णय घेतला. १२ मार्च १९३० रोजी साबरमती आश्रमातून ७९ अनुयायासह समुद्र किना-यावरील दांडी ची यात्रा प्रारंभ करून ५ एप्रिल १९३० रोजी मीठ हातात घेवून मीठाचा कायदा तोडला आणि सविनय कायदेभंगाच्या चळवळीला सुरुवात झाली. ज्या भागात समुद्र किनारा होता तेथे मीठ तयार करून कायदा तोडण्यात आला. काही भागात जंगल सत्याग्रह झाले

त्यात जंगला संबंधीचे कायदे तोडण्यात आले. या चळवळीमध्येही वृत्तपत्रे विविध भागात घडणा-या घटना प्रकाशित करित होते. ज्यामुळे देशभरातील लोक या चळवळीत सहभागी होवून अनेक ब्रिटिशांचे अन्यायी कायदे लोकांनी या काळात तोडले. १९३३ मध्ये महात्मा गांधींनी 'हरिजन' वृत्तपत्र काढले त्यानंतर चलेजाव चळवळ प्रारंभ होण्याच्या अगोदरच ब्रिटिशांनी हा देश सोडून जावे या उपदेशातून महात्मा गांधी १० मे १९४२ च्या हरिजन वृत्तपत्रात म्हणाले की, Undertereted non-cooperation: "so his suggestion was that Britain should be colled Upon to quit India and "Leave the country in the hand of god" 15 याचवृत्तपत्रातून १९४२ च्या चलेजाव चळवळीत २३ ऑगस्ट १९४२ ला श्री किशोरलाल मूंझुवाला यांनी अहिंसक क्रांतीत यापैकी कोणत्या गोष्टी बसू शकतील व कोणत्या बसू शकणार नाहीत या संबंधी आपले मत महात्मा गांधींनी पुढील प्रमाणे जाहिर केले ते म्हणतात, सरकारी कचे-या, बँका, धान्य-कोठारे इत्यादींची लुट अथवा मारपीट या गोष्टी करू देता कामा नयेत. दळणवळणाची साधने जीविताला धोका न होईल अशा प्रकारे अनत्याचारी मार्गाने तोडणे शक्य आहे. संघ करणे हा सर्वात श्रेष्ठ मार्ग आहे, तो जर करता येईल तर ते पुरेसा प्रभावी होईल त्यात अनत्याचाराच्या दृष्टीने मुळीच दोष राहणार नाही. आजच्या सारख्या लढ्यात तारा तोडणे रुल उखडणे, लहान-लहान पुल पाडून टाकणे या गोष्टी करताना जीविताला धोका येणार नाही याबद्दल जर पूर्ण सावधगिरी घेण्यात आली तर त्या करण्यास हरकत नाही. १४ अशी मते चलेजाव चळवळीतील अहिंसात्मक मार्गाने चालविण्याच्या संदर्भात मांडले होते. या चळवळीच्या काळात जेव्हा ८ ऑगस्टला काँग्रेसच्या नेत्यांना अटक करण्यात आली आणि ९ ऑगस्ट १९४२ रोजी लोकांनीच चळवळ प्रारंभ केल्यावर या चळवळीत लोकांची लोकप्रियता तयार करण्यात आणि जागृती निर्माण करण्यास महत्वाचे सहकार्य केले.

अशा त-हेने जवळ-जवळ १८५७ च्या उठावापासून प्रारंभ झालेल्या आणि १९४२ च्या चलेजाव चळवळीपर्यंतच्या काळातील झालेल्या अनेक चळवळीमध्ये भारतीय वृत्तपत्रांनी मोलाची कामगिरी केली. जनतेला सर्वच स्तरातील बातम्या पुरविण्याचे कार्य केले. चळवळीमध्ये चालविलेल्या हालचालींची माहिती भारताच्या एका भागातून दुस-या भागातील जनतेला पोहचविण्याचे कार्य या वृत्तपत्रांनी केले. परकियांचे भारतीय जनतेवर होणारे अन्याय, जुलुम, शोषणाच्या व्यथा उघड्यावर आणल्या. ब्रिटिश विरोधी भारतीय जनतेत जागृती घडवून आणली. स्वातंत्र्यासाठी चाललेल्या चळवळीमध्ये जनतेला सहभागी होण्यास प्रेरित करण्याचे कार्य वृत्तपत्रांनी केले. एकंदरीत स्वातंत्र्य चळवळीतील वृत्तपत्रांनी बजावलेली भूमिका आपल्याला नाकारता येत नाही. त्यात वृत्तपत्राचा बहूमोल वाटा आहे.

संदर्भग्रंथ सूची:





1. ग्रोवर बी. एल., आधुनिक भारत का इतिहास, एस. चंन्द एण्ड कम्पनी प्रा. लि., नई दिल्ली, ३४ वॉ. संस्करण-२०१४, पृ.क्रं. २६४
2. डॉ.वैदय सुमन, डॉ. शांता कोठेकर, आधुनिक भारताचा इतिहास, श्री साईनाथ प्रकाशन, नागपूर, तृतीयावृत्ती-२००० पृ.क्रं. ३८५
3. कित्ता पृ.क्रं. २१८
4. बिपिन चंद्र एंव अन्य, भारत का स्वतंत्रता संघर्ष, हिंदी माध्यम कार्यान्वय निर्देशालय दिल्ली विश्वविद्यालय, २८ वॉ पुर्नमुद्रण-२००८, पृ.क्रं. ६९
5. ग्रोवर बी. एल. एंव अन्य, आधुनिक भारत का इतिहास, पृ. क्रं. ३१०
6. बिपिन चंद्र एंव अन्य, भारत का स्वतंत्रता संघर्ष, पृ. क्रं. ८६
7. कित्ता पृ.क्रं. ६९
8. डॉ. वैदय सुमन, आधुनिक भारताचा इतिहास पृ. क्रं. २६३
9. बिपिन चंद्र एंव अन्य, भारत का स्वतंत्रता संघर्ष, पृ. क्रं. ११८
10. ग्रोवर बी. एल. एंव अन्य, आधुनिक भारत का इतिहास, पृ. क्रं. ३३३
11. डॉ. जावडेकर शं. द. आधुनिक भारत, सुलभ राष्ट्रीय ग्रंथमाला, पुणे तृतीयावृत्ती पृ. क्रं. ३८२
12. बिपिन चंद्र एंव अन्य, भारत का स्वतंत्रता संघर्ष, पृ. क्रं. २०१
13. कित्ता पृ.क्रं. २०४
14. डॉ. जावडेकर शं. द. आधुनिक भारत, पृ. क्रं. ४७६



Colloids and Surfaces A: Physicochemical and Engineering Aspects

Volume 657, Part B, 20 January 2023, 130561

Facile approach to fabricate a high-performance superhydrophobic PS/OTS modified SS mesh for oil-water separation

Rajaram S. Sutar^a, **Sanjay S. Latthe**^b  , Nilam B. Gharge^a, Pradip P. Gaikwad^a, Akshay R. Jundle^a, Sagar S. Ingole^a, Rutuja A. Ekunde^a, Saravanan Nagappan^c, Kang Hyun Park^c, Appasaheb K. Bhosale^a, Shanhu Liu^d  

Show more 

 Share  Cite

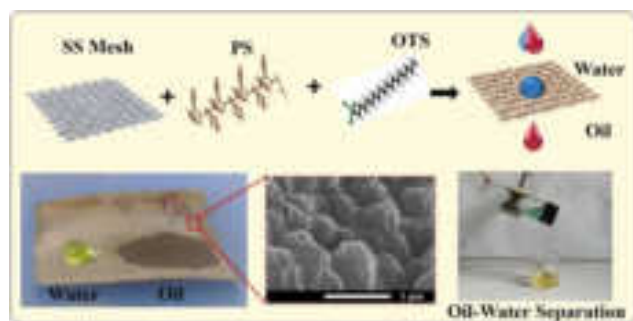
<https://doi.org/10.1016/j.colsurfa.2022.130561> 

[Get rights and content](#) 

Abstract

Special wetting materials have been used for the oil and water separation due to their different interfacial attraction of oil and water. Herein, we successfully fabricated superhydrophobic coatings on stainless steel (SS) mesh by depositing successive layers of polystyrene (PS) and octadecyltrichlorosilane (OTS) through the dip-coating method. The as-prepared coating showed a water contact angle (WCA) of $157.5 \pm 2^\circ$, a rolling angle of $6 \pm 2^\circ$ and an oil contact angle (OCA) of around 0° . The surface microstructure analysis of the coating revealed a regular pattern of microscale bumps with nanoscale folds on it, both of which improve the overall superhydrophobicity of the surface. The capacity of coatings to separate oil and water was examined by employing a variety of mixtures of oil and water, including petrol, diesel, kerosene, vegetable oil, and coconut oil. In case of low viscosity oil, the coated mesh demonstrated separation effectiveness of more than 97% and on the other hand, high viscosity oil demonstrated just 89% efficiency. Low viscosity oils showed a greater permeation flux through the mesh than extremely viscous oil. The mechanical strength of the coating was examined using bending, twisting, adhesive tape testing, sandpaper abrasion tests, and the findings indicated that coated mesh had exceptional mechanical resilience. In addition, the developed superhydrophobic mesh demonstrated excellent thermal stability and self-cleaning properties. Therefore, this superhydrophobic/superoleophilic mesh has a significant deal of application potential in practical.

Graphical Abstract



[Download : Download high-res image \(229KB\)](#)

[Download : Download full-size image](#)

Introduction

Oil spills and industrial effluents inflict significant harm to the ecosystems of the seas, human health, and the surrounding environment [1], [2]. The safe and responsible disposal of wastewater containing oil has been shown to be a challenging problem on a global scale. Many approaches have been used for the treatment of oil-water pollution, including oil skimmers, filtration, oil-absorbing materials, magnetic separations, centrifugal machine, flotation technologies, and combustion [3], [4], [5]. Traditional methods have various drawbacks, including limited separation efficiency, time consumption, cost-effectiveness, and the generation of secondary pollutants [6], [7], [8]. Therefore, cutting-edge technologies are an absolute necessity for the disposal of oily wastewater and the protection of the environment. Many efforts have been reported in the fabrication of separation membranes with controlled surface wetting property [9], [10]. The utilization of bio-inspired superhydrophobic materials in oil-water separation processes is a popular area of study due to its high water repellency and ability to allow oil to enter in it [4], [11], [12]. Therefore, superhydrophobic materials have been added to commercially available cotton textiles, 3D porous materials, different polymer membranes, filter papers, and metal meshes for considerable oil-water separation [13], [14]. Chemical etching [15], [16], spray deposition [17], [18], dip coating [19], hydrothermal method [20], sol-gel processing [21], [22], chemical vapor deposition [23], electrospinning [24], [25], and layer by layer [26] methods have been used for modification of porous surfaces. Among these, dip-coating is a quick and effective method of producing bulky, intricately formed products [27]. Metal meshes have sparked a lot of attention since they are long-lasting, reusable, and may be used in industry [2], [23]. Porous materials can absorb or filter liquids, and when their surface structure is adjusted with a specific wettability material, they can help separate oil or water from oil-water mixtures [28], [29]. Numerous types of porous metal meshes, including those constructed of nickel, copper, and stainless steel (SS), among other materials were used for oil-water separation [30], [31], [32], [33]. Among them, SS meshes have found widespread use for oil-water separation owing to their high electrical and electrothermal capabilities as well as their superior resistance to thermal shock [33].

OTS has been used to tune the surface wettability of porous substrates so that oil and water can be effectively separated. The OTS has low surface energy, hence it improves the hydrophobicity of the rough surface and also shows high oil absorption capacity [35], [36]. Li et al. [34] recently made superhydrophobic SS mesh by spraying it with a mixture of OTS-modified SiO₂ nanoparticles and waterborne PU. This superhydrophobic mesh was able to separate a mixture of kerosene and water at a rate of 98.3%. Latthe et al. [27] created a superhydrophobic surface by varying the concentration of OTS in PS solution and the number of dipping cycles. At first, they prepared a homogenous solution containing PS and OTS using tetrahydrofuran (THF) as a solvent. The pre-cleaned glass substrate was dip-coated (4 times) on the homogenous solution and air-dried to get a superhydrophobic surface with a contact angle of $154 \pm 2^\circ$. Ke et al. [37] have built a superhydrophobic and superoleophilic sponge by immersing it in OTS solution. This kind of sponge has shown an absorption capacity of 42–68 times more than the mass of the sponge for toluene, light oil, and

methyl silicone oil. Even after being put through 50 separation cycles, this adsorption capacity remained the same. Liang et al. [38] modified a polyurethane sponge by immersing in an OTS solution for oil-water separation. Cheng et al. [24] used coaxial electrospinning with PVDF solution as a lumen solution and reactive silicon-containing monomers as the outer solution to generate superhydrophobic nanofiber membranes with hierarchical micro nano-scale morphology. The outstanding separation efficiency of 99.6% is achieved with the as-prepared asymmetric composite membrane, which has an extremely rapid permeation flux. They show a water-in-n-octane permeation flux of 17331 L/(m²h) and retain 88% of their original permeance after 20 cycles of operation [24]. Rasouli et al. [13] briefly reviewed the various aspects of fabrication of superhydrophobic/superoleophilic membranes having mesh, films, and porous substrates for efficient oil-water separation applications. In order to modify the surface energy of superhydrophobic/superoleophilic membranes, it is usual practice to use low surface energy chemicals such as fatty acids, thiols, silanes, polymers based on polyethylene, and carbon nanotubes [13]. These membranes have >99% oil separation efficiency in oil-water combinations.

In this research work, a layer of PS was first applied on SS mesh using a dip coating process, followed by an OTS dip layer to achieve superhydrophobicity. The dip coating cycles were consequently carried out by dip and dry in both PS in THF and OTS in hexane. The surface structure of a red rose petal was obtained on SS mesh. SEM and EDS were used to describe the surface morphology and chemical composition, respectively. The gravity-driven oil-water separation technique was used to determine the oil-water separation efficiency and permeation flux using a custom-made setup. The mechanical durability of superhydrophobic mesh was evaluated using adhesive tape tests, sandpaper abrasion tests, bending, twisting, and folding tests. We have achieved the contact angles of 157.5±2° for OPS-2 as well as 154±2° for OPS-3 in superhydrophobic range and a comparable contact angle of 148.5±2° for OPS-1. The stable and robust self-cleaning coating was produced by this method as compared with the reported methods.

Section snippets

Materials

Polystyrene (PS) having average molecular weight ~ 280,000 and octadecyltrichlorosilane (OTS) were obtained from Sigma Aldrich, St. Louis, MO, USA. Tetrahydrofuran (THF) and hexane were purchased from Spectrochem, Mumbai, India. Stainless steel (SS) mesh with pore sizes of about 50µm was obtained from Shanghai Titan Technology Co. Ltd. China. The petrol, diesel, kerosene (from Bharat Petroleum Corporation Limited, India), vegetable oil (from Garud, India), and coconut oil (from Parachute...

Surface morphology and chemical composition

Fig. 2(a-f) depicts the surface morphology of meshes after being treated with varying doses of OTS. At low OTS concentrations, ten successive coating layers of PS and OTS create a rougher surface with nanoscale folds, as seen in Fig. 2(a). The enlarged view shows that there is a regular micro and nanoscale rough texture, which is essential for improving hydrophobicity and can be observed in Fig. 2(d). Surprisingly, regular shaped bumps emerged after raising the OTS concentration by twofold, as...

Conclusions

In conclusion, we have successfully fabricated superhydrophobic and superoleophilic SS mesh by depositing consecutive layers of polystyrene (PS) and octadecyltrichlorosilane (OTS) using an easy and inexpensive dip coating method. This allowed us to create a superhydrophobic and superoleophilic surface on the SS mesh. The WCA of 157.5 ±

2°, the OCA of about 0°, and the rolling angle of $6 \pm 2^\circ$ were all attained by adjusting the concentration of OTS in successive layered deposition. The...

CRedit authorship contribution statement

Rajaram S. Sutar: Conceptualization, Methodology, Investigation, Writing – original draft, Writing – review & editing, **Sanjay S. Latthe:** Supervision, Writing – review & editing, Visualization, **Nilam B. Gharge:** Methodology, **Pradip P. Gaikwad:** Methodology, Investigation, **Akshay R. Jundle:** Methodology, Investigation, **Sagar S. Ingole:** Methodology, Investigation, **Rutuja A. Ekunde:** Methodology, **Saravanan Nagappan:** Formal analysis, Writing – review & editing, **Kang Hyun Park:** Validation, Investigation, ...

Declaration of Competing Interest

The authors declare that they have no known competing financial interests or personal relationships that could have appeared to influence the work reported in this paper....

Acknowledgement

This work is financially supported by DST – INSPIRE Faculty Scheme, Department of Science and Technology (DST), Govt. of India. [DST/INSPIRE/04/2015/000281]....

[Recommended articles](#)

References (54)

Y. Liu *et al.*

[Bioinspired structured superhydrophobic and superoleophilic stainless steel mesh for efficient oil-water separation](#)

Colloids Surf. A: Physicochem. Eng. Asp. (2016)

M. Bennett *et al.*

[Monitoring the operation of an oil/water separator using impedance tomography](#)

Miner. Eng. (2004)

Y. Deng *et al.*

[Recent development of super-wettable materials and their applications in oil-water separation](#)

J. Clean. Prod. (2020)

S.S. Latthe *et al.*

[Superhydrophobic surfaces for oil-water separation, in](#)

[Superhydrophobic Polymer Coatings](#)(2019)

S. Rasouli *et al.*

[Superhydrophobic and superoleophilic membranes for oil-water separation application: a comprehensive review](#)

Mater. Des. (2021)

Y. Liu *et al.*

[On-demand oil/water separation of 3D Fe foam by controllable wettability](#)

Chem. Eng. J. (2018)

R. Liao *et al.*

[Fabrication of superhydrophobic surface on aluminum by continuous chemical etching and its anti-icing property](#)

Appl. Surf. Sci. (2014)

W. Ma *et al.*

[Lightweight, elastic and superhydrophobic multifunctional nanofibrous aerogel for self-cleaning, oil/water separation and pressure sensing](#)

Chem. Eng. J. (2022)

Y. Wan *et al.*

[The research on preparation of superhydrophobic surfaces of pure copper by hydrothermal method and its corrosion resistance](#)

Electrochim. Acta (2018)

Y. Xiu *et al.*

[UV and thermally stable superhydrophobic coatings from sol-gel processing](#)

J. Colloid Interface Sci. (2008)



[View more references](#)

Cited by (19)

[Oil/water separation copper membranes modified by laser induced ZnO nanowires growth with enhanced catalytic function](#)

2024, Colloids and Surfaces A: Physicochemical and Engineering Aspects

[Show abstract](#)

[Magnetic superhydrophobic sponge with 3D interpenetrating network structure coating for multimodal driven oil/water separation](#)

2024, Progress in Organic Coatings

[Show abstract](#)

[Multifunctional carbonized Zn-MOF coatings for cotton fabric: Unveiling synergistic effects of superhydrophobic, oil-water separation, self-cleaning, and UV protection features](#)

2023, Surface and Coatings Technology

[Show abstract](#)

[Ecofriendly superhydrophobic fabrics for ultra-fast oil/water separation by self-assembly](#)

2023, Surface and Coatings Technology

[Show abstract](#)

Efficient separation of oil-water emulsions: Competent design of superwetting materials for practical applications

2023, Journal of Environmental Chemical Engineering

[Show abstract](#) 

Sustainable approach to oil recovery from oil spills through superhydrophobic jute fabric

2023, Marine Pollution Bulletin

[Show abstract](#) 

[> View all citing articles on Scopus](#) 

[View full text](#)

© 2022 Elsevier B.V. All rights reserved.



All content on this site: Copyright © 2024 Elsevier B.V., its licensors, and contributors. All rights are reserved, including those for text and data mining, AI training, and similar technologies. For all open access content, the Creative Commons licensing terms apply.





**International Symposium
on**

Sustainable Environment and Smart Technology



Jointly Organized by

Pune District Education Association's

**Prof. Ramkrishna More Arts,
Commerce and Science College**

Akurdi, Pune - 411044

and

**Department of Technology
Savitribai Phule Pune University, Pune 411007**

10-11 March, 2023

Editor

Prin. Dr. M. G. Chaskar



**Self Study
Publication**

ABSTRACT BOOK

[ISBN-978-81-948795-2-7]

15	“On-Water” Reaction of (Thio)isocyanate: A Sustainable Process for the Synthesis of Unsymmetrical (Thio)ureas	Karche Amit Dattatray	12
16	Studies on Gut Fungal Diversity from Organic Waste Feeding Beetle.	Ganesh E Gore, Dhiraj Dhotre, Deepak Shelke, Hiralal Sonawane	13
17	Fe ₂ O ₃ – Polyaniline thin films: A Smart Material for the Ammonia gas Sensing	Somnath Dattinge, Dipali Dubal, Shamal Ballal, Sunil Kandalkar, Dnyaneshwar Shinde	13
18	Antioxidant Activities of Mycogenically Synthesized Nanoparticles from Combination of Medicinally Important Mushroom <i>Inonotus</i> Sp. and Chitosan	Pallavi Champaneria, H B Sonawane, B N zaware	14
19	Account of Wood Rotting Fungi from Madhe Ghat and Connecting Area of Velha Tehsil.	Bhagat S. P., Sonawane H. B., Borde M. Y.	14
20	A Green Protocol for One-Pot Synthesis of 3,4-Dihydropyrano[C]Chromenes and Biscoumarins by Employing WEB as an Internal Base.	Kumbhar Vikrant Vasudev	14
21	Investigations on CuO: ZnO Composites for Photocatalytic Performance.	Akanksha S Chougale, Snehal S Wagh, Harshad D Shelake, Habib M. Pathan and Dnyaneshwar R Shinde	11
22	Magnetic Hyperthermia with Fe ₃ O ₄ Nanoparticles	Pandhare Amol Babaso	11
23	Studies on Induced Mutation in Barnyard Millet (<i>Echinochloa esculanta</i>) L.	Jagtap Bhavana D. and Danai-Tambhale S. D.	11
24	Determination of Physicochemical Parameters and Adulteration Of Multifloral Honey by FTIR-ATR spectroscopy	Rekha J. Shinde, Indira M. Patil and Rashmi A. Morey	14
25	Ni-Ferrite an Efficient Catalyst for Synthesis of 3-Aryl Substituted Isoxazole-5-Carboxylic Acids Via One-Pot Multicomponent Reaction	Ganesh Totre, Dnyaneshwar Shinde, Prakash Patil and Pramod Kulkarni	14
26	Degradation of Textile Reactive Azodyes by <i>Hapalosiphon arboreus</i>	Rutuja Pund and K. M. Nitnaware	15
27	Fabrication of Durable Candle Soot-Wax Composite Coated Superhydrophobic Sponges for Oil-Water Separation	Mehejbin R. Mujawar , Rajesh B. Sawant, Amol B. Pandhare, Rajaram S. Sutar, Sanjay S. Latthe, Ankush M. Sargar, Raghunath K. Mane, Shivaji R. Kulal	15
28	NiFe ₂ O ₄ : An Efficient and Magnetically Recoverable Catalyst for Synthesis of 2-amino-3-cyanopyridines Derivatives	Sandip Rathod	18
29	Phytochemical and Anti-Microbial Studies of Underutilized, Neglected, Endemic and Threatened Wild Crop Relative <i>Vigna khandalensis</i> (Santapau) Raghavan et Wadhwa	Sarika A. Bhumkar, Sandip S. Thorve, Sadashiv N. Bolbhat, Vinayak H. Lokhande	18
30	Decolourization of Spent Wash Colour under Sun Light using Mesoporous Cu-TiO ₂ Nanoparticles Synthesized By Sol-Gel Assisted Hydrothermal (SGAH) Method	Shrikant. P.Takle, Aarti S. Tarlekar, Amol Bhosale, Netaji Mali, Shaila Dhotre, Digambar B. Bankar, Namdeo N. Bhujbal	19
31	Synthesis of Organic Nano Semiconductor for Photocatalytic and Antimicrobial study Performance	Vivekanand Jawale, Gulab Gugale, Vikram Pandit	19
32	Endophytes Isolated from <i>Ophiorrhiza rugosa</i> Plant Producing a Good Source of Camptothecin.	Vaishnavi Chavan, Hiralal Sonawane and Mahesh Borde	20

Abstract-26**Degradation of textile reactive azodyes by *Hapalosiphon arboreus*****Miss Rutuja Pund and Dr. K. M. Nitnaware***

Department of Botany, Hutatma Rajguru Mahavidyalaya, Rajgurunagar

Corresponding Email: kmnbotany@gmail.com

Abstract: Azodyes widely used in textile industries are toxic to life. Dye degradation using microorganism gained more attention due to cost effectiveness and eco-friendly. There is need to investigate more indigenous species. In the present study the filamentous cyanobacteria *Hapalosiphon vulgaris* was examined for its degrading ability of azodyes Methyl Orange, Tartrazine Yellow, Scarlet Red, Reactive Black 5 and Sudan III. The axenic culture of *Hapalosiphon* was inoculated with various concentrations of dyes (5, 10 and 20 ppm) and incubated for 3, 5 and 7 days. Dye degradation was based on initial dye concentration. The maximum decolorization was observed in Scarlet red and Sudan III 92.5% and 82.02% respectively after 7 days of incubation. Azoreductase enzyme in algae responsible for degradation of azodyes into aromatic amines. Maximum azoreductase activity 6.02 Umg-1 protein was observed for scarlet red. Influence of azo dyes on Chlorophyll a and b content and Phycobilin Proteins was also examined. The degradation product after decolourization was confirmed and identified by spectroscopic analysis and Fourier transformed infrared spectroscopic analysis.

Keywords: Azoreductase enzyme, Methyl Orange, Scarlet Red, FTIR

Abstract-27**Fabrication of Durable Candle Soot-Wax Composite Coated Superhydrophobic Sponges for Oil-Water Separation****Mehejbin R. Mujawar¹, Rajesh B. Sawant¹, Amol B. Pandhare², Rajaram S. Sutar³, Sanjay S. Latthe⁴, Ankush M. Sargar^{5*}, Raghunath K. Mane⁶, Shivaji R. Kulal***¹ Department of Chemistry, Raje Ramrao Mahavidyalaya, Jath, (Affiliated to Shivaji University, Kolhapur)² Department of Chemistry, Shivaji University, Kolhapur, (MS) India³ Self-cleaning Research Laboratory, Department of Physics, Raje Ramrao Mahavidyalaya, Jath,⁴ Self-cleaning Research Laboratory, Department of Physics, Vivekanand College, Kolhapur,⁵ Department of Chemistry, Bharati Vidyapeeth's Dr. Patangrao Kadam Mahavidyalaya, Sangli,⁶ Department of Chemistry, Smt. Kusumtai Rajarambhapu Patil Kanya Mahavidyalaya, Islampur,*Corresponding authors E-mail: srkulal@gmail.com, amsargar2012@gmail.com

Abstract: A novel superhydrophobic candle soot-wax composite coated surfaces for oil-water separation was fabricated via a facile two-step strategy. The decomposition of candle soot on the surface and then it was fixed via deposition of wax on CS-coated surfaces. The candle soot was synthesized by paraffin candle combustion flame. The CS-coated surface was prepared by via the dip-coating method without further surface modification and pre-treatments. Candle soot was firmly immobilized on the wax skeleton constructing a nanoscale rough surface with superhydrophobicity. The coated surfaces exhibit superhydrophobicity with a water contact angle of $> 150^\circ$ and a sliding angle of nearly 0° . The thermal stability, pH tolerance, compression tolerance, chemical durability, reusability, emulsion oil-water separation, and muddy water-oil separation was tested by using these superhydrophobic surfaces. The superhydrophobic surfaces have a sustainable, anti-wetting property under cross-sectional cutting, pressing, paper peel test, abrasion resistance test, and different pH environments. The superhydrophobic surface is suitable for practical application on a large scale. The simple CS-wax coating method can be applied to various surfaces, such as stainless steel and polyurethane sponges. These research results show evidence that the CS-wax-coated surface is promising in environmental remediation for large-scale, low-cost, removal of oil spills from water.

Keywords: Candle soot nanoparticles, oil-water separation, sliding angle, superhydrophobic surfaces, water contact angle, waxes.

१८५७ च्या उठावात आदिवासी क्रांतीकारकांचे योगदान

चौधरी पी. जे.

सहा. प्राध्यापक (इतिहास)

राजे रामराव महाविद्यालय, जत.

pichoudhary72@gmail.com

Mo.No. 7057491078

प्रस्तावना :-

भारतीय स्वातंत्र्याच्या चळवळीतील १८५७ चा उठाव एक महत्त्वपूर्ण घटना होय. या उठावाने भारतीयांनी ब्रिटीशांचे वर्चस्व संपुष्टात आणण्याचा पहिला प्रयत्न केला. १८५७ च्या उठावापासून आदिवासी समुदायही अलिप्त नव्हता. आदिवासींनी आपल्या क्षेत्रामध्ये ब्रिटीशांच्या विरोधात उठाव घडवून आणला होता. वास्तवात १८५७ च्या उठावापूर्वी पासूनच ब्रिटीश सत्तेच्या विरोधात भारतातील अनेक क्षेत्रात छोट्या- मोठ्या प्रांतीय स्वरूपाचे उठाव घडून आले होते. त्या उठावात आदिवासी उठावांचा समावेश होतो. आदिवासींच्या हक्कांना धोका पोहचविणाऱ्या ब्रिटीश सत्तेचा विरोध अनेक आदिवासी जमातींनी केला होता. त्यामध्ये चौरा उठाव (१७६८) भील उठाव (१८१८) हो आंदोलन (१८२०), कोळी उठाव (१८२४) कोल उठाव (१८३१) सिंगपो उठाव (१८३०) संधाल उठाव (१८५५) आदिंचा समावेश होतो. ब्रिटीशांनी आधुनिक शस्त्रांच्या बळावर भारतीयांची कोणतीही तमा न बळगता हे क्षेत्रीय व प्रांतीय स्वरूपाचे उठाव दडपून टाकले होते. भारतीयांमध्ये संघटन निर्माण होवू नये म्हणून त्यांच्यात छोटे-मोठे गट निर्माण करण्यास प्रारंभ करून फुटीरवत्ती वाढविण्याच्या प्रयत्न केला. ब्रिटीशांच्या साम्राज्यावादी धोरणाचा आणि त्यांच्या शोषणकरी नीतीचा परिणाम संस्थानिक, सैनीक, कामगार, शेतकरी आणि आदिवासी इत्यादी या सर्वांवरच झाला होता. त्यासाठी राजकीय, प्रशासकीय, आर्थिक, धार्मिक, सामाजिक, लष्करी इत्यादी अनेक कारणे भारतीयांनी केलेल्या ब्रिटीशांच्या विरोधासाठी तेवढीच जबाबदार होती. आदिवासींच्या हक्कांना ब्रिटीशांनी बाधा निर्माण करून आदिवासींच्या क्षेत्रातील त्यांचे जल, जंगल आणि जमीनी वरील हक्क ब्रिटीशांनी हिरावण्याचे कार्य केले होते ते हक्क अबाधित ठेवण्यासाठी आदिवासींनी १८५७ च्या उठावापूर्वीच क्षेत्रीय व प्रांतीय स्वरूपाचे उठाव केले होते. परंतु आदिवासींना त्यात यश आलेले नव्हते. त्यामुळे आदिवासींचे ब्रिटीशांनी हिरावलेले हक्क आणि ब्रिटीशांची सत्ता भारतातून संपुष्टात आणण्यासाठी १८५७ च्या उठावात भाग घेवून ब्रिटीशांच्या विरोधात भारताला स्वातंत्र्य मिळवून देण्यासाठी चाललेल्या १८५७ च्या स्वातंत्र्यसमरात आदिवासी क्रांतीकारांनी मोलाचे योगदान दिले.

१८५७ चा उठाव :-

१८५७ चा उठाव अचानक घडून येणारी घटना नव्हती. तर अनेक वर्षांपासून भारतीयांमध्ये असलेला ब्रिटीश विरोधी असंतोष होता. चरबीयुक्त काडतुसाच्या तत्कालीक प्रकरणामुळे १८५७ च्या उठावाने ब्रिटीशांच्या विरोधात भारतीयांनी या असंतोषाचा स्फोट घडवून आणला. १८५६ मध्ये कंपनीने ब्राउन बेस बंदुकीच्या जागी एनफील्ड नावाच्या रायफली आणल्या. या बंदुकीला लागणाऱ्या काडतुसांना गाई व डुकरांची चरबी लावली जात होती. गाय हिंदूना पवित्र तर डुक्कर मुस्लीमांना अपवित्र होते. त्या प्रकरणाने हिंदू- मुस्लीमांच्या धार्मिक भावना दुखावल्या त्याची माहिती भारतीय सैनिकांना लागताच ती वाऱ्यासारखी पसरत गेली. बराकपूर छावणीमध्ये ३४ व्या रेजीमेंटच्या मंगल पांडे या भारतीय सैनिकाने काडतुसे वापरण्यास विरोध करून २९ मार्च १८५७ रोजी ब्रिटीश अधिकारी सार्जंट मेजर हयुसन हडसन यांची गोळी घालून हत्या केली आणि १८५७ च्या उठावाला सुरुवात झाली.

१८५७ चा उठाव आणि आदिवासी क्रांतीकारक :-

१० मे १८५७ मध्ये मीरत छावणीतील भारतीय सैनिकांनी उठाव करून तुरुंगावर हल्ला केला. तेथील कैद्यांची मुक्तता केली आणि खजिना शस्त्रास्त्रे लुटून क्रांतीकारक ११ मे १८५७ रोजी दिल्लीला पोहचले. १२ मे १८५७ रोजी बहादुरशहाला 'बादशहा' घोषित केले. बहादुरशहाला आपला नेता म्हणून घोषित केल्यानंतर दिल्ली स्वतंत्र झाल्याची घोषणा केली. कानपूर मध्ये नानासाहेब पेशव, झाशी मध्ये राणी लक्ष्मीबाई, लखनौ मध्ये बेगम हजरत महल, बिहारमध्ये कुंवरसिंह यांनी उठावाचे नेतृत्व केले. १८५७ च्या उठावापासून आदिवासी क्रांतीकारकही अलीप्त नव्हते. आदिवासी क्रांतीकारकांनी आप-आपल्या प्रदेशामध्ये उठावाचे नेतृत्व केले होते. महाराष्ट्रातील सातपूडा परिसरात (धुळे, नंदूरबार) तत्कालीन मध्य प्रांतामध्ये आदिवासी शासकांनी, छत्तीसगड मध्ये इत्यादी भागात आदिवासी क्रांतीकारांनी उठावाचे नेतृत्व केले होते. वास्तवात आदिवासींनी १८५७ च्या उठावाच्या पूर्वीपासूनच ब्रिटिश सत्तेचा विरोध केलेला होता. त्यामुळे आदिवासी क्रांतीकारक अशा व्यापक स्वरूपात झालेल्या उठावापासून अलिप्त असणे शक्य नव्हते. आदिवासींनी आपल्या परंपरागत शस्त्रास्त्रांच्या माध्यमाने ब्रिटिश सैन्याबरोबर सशस्त्र क्रांती या उठावामध्ये घडवून आणली आणि अनेक आदिवासी क्रांतीकारकांनी १८५७च्या उठावात आपल्या प्राणाचे बलीदान दिले तत्कालीन गोंडवाना, छत्तीसगड (रायपूर), चांदागड, खानदेश (सातपूडा भाग) इत्यादी आदिवासी राहत असलेल्या भागात आदिवासी क्रांतीकारकांनी उठावाचे नेतृत्व करून ब्रिटिशामध्ये दहशत निर्माण केली. १८५७ ते १८५८ या दरम्यान झालेल्या या स्वातंत्र्यसमराच्या काळात ब्रिटिशांना राज्य करणे कठीण करून ठेवले त्या आदिवासी क्रांतीकारकांच्या कार्याचा आढावा या ठिकाणी घेण्यात आलेला आहे.

शंकरशहा आणि रधूनाथशहा :-

ब्रिटिश भारतातील मध्य प्रांतात गढा— मडंला येथे आदिवासींचे राज्य होते. १८५७ च्या उठावाच्या वेळी शंकरशहा मडावी गढा—मडंल्याचा शासक होता. शंकरशहा मडावी हे राजे संग्रामशहा च्या घराण्यातील असून मध्ययुगीन काळातील इतिहास प्रसिध्द गढा—मडंल्याची राणी दुर्गावती चे दीर चंद्रशहा यांचे नातू आहेत. १८५७ च्या उठावापूर्वीपासूनच शंकरशहा यांनी ब्रिटिशांचा विरोध करून छोटे—मोठे उठाव ब्रिटीश धोरणाच्या विरोधात मध्य प्रांतात केले होते. परंतु १८५७ च्या उठावातील त्यांचे कार्य महत्त्वपूर्ण आहे जवळ— जवळ संपूर्ण देशभर १८५७ चा उठाव घडून आल्याबरोबर शंकरशहा आणि रधूनाथशहा या पिता—पुत्राने उठावात भाग घेतला आणि ब्रिटिशांची सत्ता भारतातून संपविण्यासाठी तत्कालीन मध्य प्रांतात उठाव घडवून आणला. १८५७ च्या उठावाच्या वेळी जबलपूर परिसरात ब्रिटिशांची ५२ वी रेजिमेंट तेथील उठावाचा बंदोबस्त करण्यासाठी ठेवण्यात आली होती. या रेजिमेंटचा कमांडर क्लार्क अतिशय क्रूर होता. त्या परिसरातील छोटे—मोठे राजे, जमिनदार आणि जनतेला त्रास देण्याचे कार्य क्लार्क या ब्रिटिश अधिकाऱ्याने चालविले होते. तेथील जनतेकडून अतिरिक्त महसूल वसूल करणे, लोकांना जंगलात जाण्यास बंदी घालणे, ब्रिटीश सत्तेच्या विरोध करणाऱ्यांना मारहान करणे आदि. दडपशाहीचे धोरण या ब्रिटिश कमांडरने जबलपूर परिसरात चालविले होते. गोंडवाणाचा राजा शंकरशहा याने क्लार्कच्या या अन्यायकारी धोरणाचा विरोध करण्याचे ठरविले, आणि १८५७ च्या उठावाची सुरुवात गोंडवाणा परिसरात झाली या उठावामध्ये शंकरशहा बरोबर त्याचा मुलगा रधूनाथशहा यानेही भाग घेतला. आणि दोघाही पिता —पुत्रांनी गोंडवाना परिसरात १८५७ च्या उठावाचे नेतृत्व केले दोघेही पिता—पुत्र चांगले कवी होते. त्यांनी आपल्या कवितांच्या माध्यमाने १८५७ च्या उठावाचा प्रसार संपूर्ण गोंडवाना परिसरात केला आणि तेथील जनतेला ब्रिटिश विरोधी उठावामध्ये सहभागी होण्यास प्रेरित केले. शंकरशहाने आपल्या दरबारातील कर्मचारी गिरधारीलाल दास याला गोंडवाना

राज्यातून बाहेर काढले कारण गिरधारीलाल दास १८५७ च्या उठावामध्ये ब्रिटिश सरकारला मदत करित होता. शंकरशहा आणि रधूनाथशहा हे दोघेही पिता—पुत्र ज्या कवितांच्या माध्यमाने गोंडवाना परिसरातील जनतेला १८५७ च्या उठावात सहभागी होण्यास प्रेरित करित होते. त्या कवितांचा अर्थ गिरधारीलाल दास ब्रिटिशांना सांगत होता. त्यामुळे ते दोघेही पिता पुत्र काय काय करतात याची माहिती ब्रिटिशांना मिळत होती. त्यामुळे गोंडवानाच्या जन सामान्याचा राजा शंकरशहा ब्रिटिश विरोधी योजनेवर काम करित आहे हे क्लार्कच्या लक्षात येत होते. ब्रिटिशांनी गोंडवाना परिसरात आपले गुप्तचर पेरून शंकरशहा आणि रधूनाथशहा यांच्या १८५७ च्या उठावातील सहभागाची माहिती काढली. क्लार्कच्या गुप्तचरांनी राजाच्या राजमहलात जावून शंकरशहाच्या हालचालीची माहिती काढली. गुप्तचरांच्या माध्यमाने शंकरशहा आणि रधूनाथशहा दोन दिवसानंतर ब्रिटिशांच्या छावणीवर हमला करणार ही बातमी मिळाली. ब्रिटिश अधिकारी क्लार्कला छावणीवरील हल्ल्याची बातमी गुप्तचरांच्या माध्यमातून अगोदरच मिळाल्यामुळे त्याने १४ सप्टेंबर १८५७ रोजी आपल्या ब्रिटिश सैन्यांच्या तुकडीने घेरले आणि शंकरशहा आणि रधूनाथशहा या दोघांही पिता —पुत्रांना ब्रिटिशांनी बंदी बनविले. १८५७ च्या उठावात सहभागी होवून ब्रिटिशांच्या छावणीवर हल्ला करण्याची योजना बनविल्यामुळे शंकरशहा आणि रधूनाथशहा या दोघांही पिता—पुत्राला १८ सप्टेंबर १८५७ रोजी वेगवेगळ्या दोन तोंफांच्या तोंडी ब्रिटिशांनी बांधले. दोघांही पिता—पुत्राचा मरण समोर असतानांही ब्रिटिशांनविरुद्ध आपल्या विचारांची आणि कृतीची प्रतिक्रिया त्यांनी त्यावेळी कवितेच्या माध्यमांनी व्यक्त केली. त्यात कवितेचा पहिला कडवा राजाने आणि दुसरा कडवा त्यांच्या मुलाने म्हटले :

मलेच्छों का मर्दन करो, कालिका माई ।

मुंद मुख डंडिन को, चुगली को चबाई खाई,

खुंद डार दुष्टन को, शत्रु संहारिका ॥

दुसरा कडवा राजांचा मुलगा म्हणाला :

कालिका भवानी माय अरज हमारी सुन

डार मुण्डमाल गरे खडग कर धर ले। ३

शंकरशहा आणि रधूनाथशहा या दोघांही पिता —पुत्रांचे कवितेतील कडवे पूर्ण होता बरोबर गोंडवानाची जनता ब्रिटिशांच्या विरुद्ध आक्रमक होवून राजा आणि राजकुमारांचा मोठया प्रमाणावर जय जय कार करू लागली. त्यामुळे ब्रिटिश छावणीवर जनतेचा हल्ला होईल अशी परिस्थिती निर्माण झाली. क्लार्कच्या मनात भिती निर्माण झाली आणि दोंन्ही तोफांना आग लावण्यात येवून दोघांही पिता —पुत्राला तोफेच्या तोंडी उडवून देण्यात आले. शंकरशहा आणि रधूनाथशहा या दोघांही पिता —पुत्राने भारताच्या स्वातंत्र्यासाठी १८५७ च्या उठावात प्राणाची आहुती दिली.

वीर नारायनसिंह :-

१८५७ च्या उठावात छत्तीसगड च्या भागात उठाव घडवून आणण्यात वीरनारायनसिंह चे महत्वपूर्ण योगदान आहे . वीर नारायनसिंह छत्तीसगड मधील सोनाखान जमीनदारीचा जमीनदार होता. १८९५ मध्ये वीरनारायनसिंह यांचा जन्म झाला. त्यांच्या वडीलांचे नाव रामराय होते. लहानपणापासूनच आपल्या जमीनदारीतील लोकांच्या समस्या विषयी त्याला तळमळ होती. त्यामुळे जमीनदार झाल्यावर तेथील लोकांच्या कल्याणासाठीच जगणार असा सोनाखान जमीनदारीतील जनतेचा

विश्वास होता. वीर नारायनसिंहचा लोकांच्या समस्या विषयी असलेल्या तळमळीचे दर्शन १८५६ मध्ये छत्तीसगड परिसरात पडलेल्या दुष्काळाच्या वेळी त्यांनी लोकांसाठी केलेल्या कार्यातून होते. त्यावेळी छत्तीसगड परिसरात भयंकर दुष्काळ पडला होता. लोकांसमोर अन्न —पाण्याची मोठी समस्या निर्माण झाली होती. अशा प्रसंगाच्या वेळी वीर नारायनसिंहसारख्या लोक कल्याणाची तळमळ असलेल्या जमीनदाराने शांत बसणे शक्य नव्हते. छत्तीसगड मधील जनता अन्न —पाण्याविना दुष्काळाची सामना करित होती आणि व्यापारांनी मात्र अन्न धान्य गोदामांमध्ये साठवून ठेवले होते. अशा दुष्काळी परिस्थितीत ब्रिटिश सरकारला सांगून व्यापारांच्या गोदामातील धान्य लुटून लोकांमध्ये वाटून दिले. त्यामुळे व्यापाऱ्यांनी ब्रिटिश सरकारकडे वीरनारायनसिंहाची तक्रार केली. ब्रिटिशांना सुध्दा बहानाच पाहिजे होता. ब्रिटिश सरकारने कोणताही विचार न करता वीरनारायनसिंहाला २४ ऑक्टोबर १८५६ रोजी संबलपुरात अटक केली. चोरी आणि लुटमार करण्याचा आरोप त्यांच्यावर लावून रायपूरच्या तुरुंगात कैद करण्यात आले. ब्रिटिश सरकारने दुष्काळ ग्रस्त शेतकऱ्यांची मदत करणाऱ्या वीर नारायनसिंहला तुरुंगात डांबून जनेतेचे शोषण करणाऱ्या व्यापाऱ्यांना मात्र संरक्षण दिले. १८५७ मध्ये उठावाची सुरवात झाली. भारतीय सैनिकांनी ब्रिटिश सरकारच्या विरोधात उठाव घडवून आणला त्याचे पडसाद छत्तीसगड परिसरामध्येही पडले त्यावेळी वीर नारायनसिंह रायपूरच्या तुरुंगामध्ये सजा भोगत होते. रायपूर मधील सैनिक ब्रिटिश विरोधी भारतीयांच्या असंतोषाची वाट पाहत होते ती १८५७ च्या उठावाने त्यांच्या समोर चालून आली. रायपूर मधील भारतीय सैनिकांनी उठाव घडवून आणला आणि वीर नारायनसिंह ला आपला नेता नियुक्त केले २८ ऑगस्ट १८५७ मध्ये भारतीय सैनिक आणि जनतेच्या मदतीने रायपूरच्या तुरुंगातून वीरनारायनसिंह बाहेर पडले आणि सोनाखानला पोहचले त्याला पाहून तेथील जनता आनंदीत झाली. अगोदर पासूनच ब्रिटिशांच्या विरोधामध्ये उठाव करण्यासाठी लोक तत्पर होते. त्यांना फक्त कुशल संघटक आणि चांगल्या नेतृत्वाची आवश्यकता होती ते नेतृत्व सोनाखानच्या जनतेला वीर नारायनसिंहच्या रूपात प्राप्त झाले. त्यांने ५०० निवडक सैनिकांची एक तुकडी तयार केली आणि ब्रिटिशांची सत्ता संपविण्यासाठी उठाव करण्याचा निर्णय घेतला भारताला इंग्रजांच्या गुलामगिरीतून मुक्त करण्यासाठी लपून छपून ब्रिटिशांच्या अनेक छावण्यावर हल्ले करायला प्रारंभ केला त्याची माहिती रायपूर चा डेप्टी कमिश्नर स्मिथला मिळताच तो अचंबित झाला त्याने वीर नारायनसिंह ने केलेला उठाव दडपून काढण्याचा निर्णय घेतला. २० नोव्हेंबर १८५७ मध्ये ब्रिटिशांची सेना खरोद पोलीस स्टेशनला पोहचली. परंतु वीर नारायनसिंह च्या ब्रिटिश विरोधी आक्रमण कार्यवाहीमुळे डेप्टी कमीश्नर स्मित घाबरून गेला. त्यामुळे आपल्या मदतीसाठी कंटगी, भटगांव, भिलाईगड आणि देवरी च्या जमीनदारांना बोलावून घेतले. २९ नोव्हेंबर १८५७ रोजी स्मित ने सोनाखान ला ब्रिटिश सैन्ये हलविले यावेळी वीर नारायनसिंहच्या भितीमुळे रायपूर आणि बिलासपूर वरून स्मिथने जे घोडस्वार बोलावले ते सर्व ब्रिटिश होते. सोनाखानला ब्रिटिश सैनिक पहोचले तेंव्हा सोनाखान मध्ये एकही लोक नव्हते तेथील सर्व जनतने अरण्यांत आश्रय घेतला होता. वीर नारायनसिंह च्या नेतृत्वात ब्रिटिश विरोधी उठावात तेथील जनता सहभागी होती. ब्रिटिशांनी सोनाखान गावाला आग लावून जाळून टाकले. गावाला लावलेल्या आगीमुळे सोनाखान गाव संपूर्ण जळून खाक झाला होता. गावाला आग लावून परत जाणाऱ्या ब्रिटिशांवर वीर नारायनसिंह ने आपल्या सहकार्यानिशी सोनाखानच्या पहाडीवरून गोळीबार केला अगोदर पासूनच ब्रिटिशांसोबत लढण्याची पूर्व तयारी वीर नारायनसिंह ने केली होती. युध्दाला सुरुवात झाली. २ डिसेंबर १८५७ रोजी कंटगी वरून ब्रिटिशांची एक अतिरिक्त सैनिक तुकडी स्मितच्या मदतीसाठी आली आणि या पाहाडीला ब्रिटिशांनी चारही बाजूने घेरले होते. वीर नारायनसिंह आणि स्मितच्या सैन्यामध्ये लढाई चालू झाली. परंतु वीर नारायनसिंह आणि त्यांच्या सहकार्यांकडील शस्त्रसाठा समाप्त झाला. त्यामुळे ब्रिटिशांनी वीर नारायनसिंह ला पकडले आणि रायपूरच्या तुरुंगात ठेवण्यात आले. त्यांच्यावर

राजद्रोहाचा खटला चालविण्यात आला आणि १० डिसेंबर १८५७ रोजी रायपूर मधील जय स्तंभ चौकात फाशी देण्यात आली. वीरनारायनसिंह आदिवासी वीर भारतीयांना ब्रिटिशांच्या गुलामगिरीतून मुक्त करण्यासाठी हसत हसत फासावर गेला.

बाबूराव शेडमाके :-

महाराष्ट्रातील चांदागड (चंद्रपूर) परिसरात १८५७ च्या उठावाचे नेतृत्व बाबूराव पुल्लेसुर शेडमाके यांनी केले होते. तो मोल्लमपली जमीनदारीचा जमीनदार होता. विवाहानंतर या जमीनदारीची जिम्मेदारी त्यांच्यावर आली आणि १८ डिसेंबर १८५४ मध्ये जमीनदारीचे अधिकार त्यांने ताब्यात घेतले होते या काळापर्यंत ब्रिटिशांची सत्ता संपूर्ण देशात प्रस्थापित होवून बळकट झाली होती. चांदागडचा परिसर ही ब्रिटिशांनी आपल्या ताब्यात घेतला होता. ब्रिटिशांनी आपल्या फायद्यासाठी योग्य – अयोग्यतेचा कसलाही विचार न करता भारतीयांचे जास्तीत जास्त शोषण करण्याचे धोरण चालविले होते. या ब्रिटिशांच्या शोषणकारी धोरणाचे परिणाम चांदागड परिसरातील जनतावरही झाले होते. ब्रिटिशांचे या परिसरातील जनतेवरील अन्याय, अत्याचार आणि जुलूम वाढत चालले होते. त्यांचा विरोध करण्याचा निर्णय बाबूराव शेडमाकेने घेतला सुरुवातीला त्यांनी चालविलेली चळवळ राजकीय आणि सामाजिक स्वरूपाची होती. अहिंसेच्या मार्गाने जनतेच्या समस्या सोडविण्याचा प्रयत्न बाबूराव शेडमाकेनी केला. परंतु ब्रिटिश सरकार त्याला न्याय देत नव्हती चांदागड परिसरातील जनतेमध्ये ब्रिटिशविरोधी प्रबोधने करून जनजागृती करण्याचे कार्य केले ब्रिटिशांनी काढलेल्या अन्यायी कायद्याचा तो विरोध करित होता. त्यामुळे त्या परिसरातील लोकांमध्येही त्याच्या विषयी आपुलकी निर्माण झाला होती. आपला नेता आपल्याला ब्रिटिशांच्या गुलामगिरीतून मुक्त करेल असा ठाव विश्वास जनतेत निर्माण झाला होता. ब्रिटिश सरकार शांततेने मांडलेल्या मागण्यांना प्रतिसाद न देता तेथील जनतेवर अन्याय करून दडपशाहीचे धोरण अवलंबिले. त्यामुळे बाबूराव शेडमाके या आदिवासी क्रांतीकारकाने अहिंसेच्या मार्गाने आपल्या जनतेला न्याय मिळत नाही म्हणून सशस्त्र क्रांतीचा मार्ग अवलंबिला १८५७ मध्ये ब्रिटिशांच्या विरोधात भारतीयांनी उठाव केला. तेव्हा चांदागड परिसरात उठावाचे नेतृत्व बाबूराव शेडमाके यांनी केले. त्यांनी २४ सप्टेंबर १८५७ रोजी 'जंगोम सेनेची' स्थापना केली.

shedmake consolidated 500 tribal youth from the region and prepared an army and with this army he was able to capture Rajghad area. चांदागड परिसरातून ब्रिटिशांची सत्ता संपविण्यासाठी उठाव केला. बाबूराव शेडमाके यांनी केलेल्या उठावाची माहिती चंद्रपूरचा उपजिल्हाधिकारी क्विकटोनला लागताच उठाव दडपून टाकण्यासाठी ब्रिटिशांनी त्याच्या विरोधात हालचाली केल्या. नांगगाव घोसारी येथे झालेल्या युद्धात ब्रिटिशांचा पराभव झाला. त्यानंतर क्विकटोनने ब्रिटिश सेनेची दुसरी तुकडी उठाव दडपून टाकण्यासाठी पाठविली. संगनपूर व बामनपेठ च्या युद्धात बाबूराव शेडमाकेचा विजय झाला. या दोन्ही विषयातून त्याला प्रोत्साहन प्राप्त झाले की आपण ब्रिटिशांनी सत्ता या देशातून संपुष्टात आणून आपल्या देशवासियांना गुलामगिरीतून मुक्त करू शकतो. २९ एप्रिल १८५८ मध्ये चींचगुडी येथील टेलीफोन ऑफीसवर हल्ला केला. या हल्ल्यामध्ये ब्रिटिश अधिकारी हाल आणि गार्टलॅंड यांना ठार केले परंतु ब्रिटिश अधिकारी पेटर या हल्ल्याची बातमी चंद्रपूरचा जिल्हाधिकारी क्विकटोनला पोहचविण्यात यशस्वी झाला. मोल्लमपलीच्या अंरण्याच्या आणि डोंगराळ भागात वीर बाबूराव शेडमाके या आदिवासी क्रांतीकारकांचा पराभव करणे शक्य नाही म्हणून चतूर उपाय योजून त्याला बंदी बनविण्याचा निर्णय घेतला. १८ सप्टेंबर १८५८ ला राणी लक्ष्मीबाईंच्या अहेरी येथील राजघराण्यात बाबूराव शेडमाके जेवण करित असतांना ब्रिटिशांनी त्याला पकडले आणि २१ ऑक्टोबर १८५८ रोजी चांदागड येथील गोंड राजाच्या किल्ल्यात त्याच्या चेहरावर कोणताही बुरखा न घालता महालांच्या

पटांगणात पिंपळाच्या झाडाला फाशी देण्यात आली. १८५७ च्या उठावात ब्रिटिशांच्या गुलामगिरीतुन भारतीय जनतेला मुक्त करण्यासाठी ब्रिटिशांच्या अन्यायी शोषणकारी धोरणाचा विरोध करण्यासाठी चांदागड परिसरात उठाव घडून आणला आणि देशाच्या स्वातंत्र्यासाठी आपल्या प्राणाचे बलिदान दिले.

क्रांतीवीर खाज्या नाईक :-

खानदेशातील सातपुडा भागात (धुळे, नंदुरबार) आदिवासी भिल्लांनी १८५७ च्या उठावात भाग घेवून ब्रिटिशांच्या विरोधात उठाव घडवून आणला त्या उठावाचे नेतृत्व क्रांतीवीर खाज्या नाईक यांनी केले होते. १८३१ ते १८५१ च्या दरम्यान क्रांतीवीर खाज्या नाईक ब्रिटिशांचा नोकरदार होता. संधवा घाटातून चालणाऱ्या व्यापाराचे संरक्षण करण्याचे कार्य करित होता. परंतु त्यांच्या हातून एक लुटारु मारल्या गेल्यामुळे ब्रिटिश सरकारने त्यांच्यावर खटला चालवून १० वर्षांची शिक्षा दिली. १८५५ मध्ये सजा पूर्ण करून परत आल्यावर आपल्या पूर्वीच्या नोकरीवर घ्यावे अशी विनंती ब्रिटिशांना क्रांतीवीर खाज्या नाईक यांनी केली परंतु ब्रिटिशांनी ती मान्य केली नाही. १८५७ मध्ये इतिहास प्रसिध्द अशा स्वातंत्र संग्रामाला सुरवात झाली भारतातील विविध भागात अनेक क्रांतीकारकांच्या नेतृत्वात ब्रिटिश विरोधी उठाव झाला. त्यामुळे ब्रिटिशांना सातपुडा परिसराच्या संरक्षणासाठी खाज्या नाईकची गरज भासू लागली परंतु यावेळी तो दिल्लीच्या बादशहाच्या संपर्कात आला होता त्याला १८५७ च्या उठावाची सुचना मिळताच सातपुडा परिसरात क्रांतीवीर खाज्या नाईक ने उठाव घडवून आणला भिमा नाईक , मेवाश्या नाईक यांना सोबतला घेवून ७०० भिल्लांचे संघटन निर्माण केले आणि ब्रिटिशांच्या विरोधात उठाव केला. गावच्या गावे लुटून ब्रिटिशासमोर मोठे आव्हान निर्माण केले क्रांतीवीर खाज्या नाईकने उठावाचे आव्हान करताच हनुमंतराय नाईक आपल्या भिल्ल सहकाऱ्यांसह येवून त्यांना मिळाला.

संधवा घाटावर ताबा व लुट :-

सातपुडा परिसरातील भागात ब्रिटिशामध्ये दहशत निर्माण करून संधवा घाटावर ताबा मिळविण्यात यश संपादन केले. त्या घाटातून चालणाऱ्या व्यापारातून ब्रिटिश सरकारला कर मिळत होता. हा कर क्रांतीवीर खाज्या नाईक ने स्वतः गोळा करायला सुरवात केली. आणि त्या करातून मिळालेला पैसा गोर गरीबांना मदत करण्यासाठी खर्च केला. त्या बरोबरच ब्रिटिशांचा खजिना लुटण्याची मोहिम क्रांतीवीर खाज्या नाईक यांनी चालविली. १७ नोव्हेंबर १८५७ पर्यंत खाज्या नाईक आणि भिमा नाईक यांनी ५०० भिल्लांची सेना तयार केली. त्यावेळच्या खानदेशच्या हददीतून ३० मैलावर उत्तरेस होळकरांच्या हददीतून जामली चोकी जवळ इंदोर वरून मंबईकडे होळकरांच्या राज्यातून वसूल केलेली सात लाखाची खंडणी ब्रिटिश ३०० सैनिकांच्या सुरक्षेत घेवून चालले होते. तो खजिना क्रांतीवीर खाज्या नाईक याने आपल्या सैनिकांच्या सहाय्याने लुटला. ब्रिटिश सरकार मात्र त्याला धक्काही लावू शकली नव्हती. खाज्या नाईकाच्या उठावातील क्रांतीकारकांची संख्या दिवसेंदिवस वाढत होती महादेव नाईक , दौलत नाईक यांच्या बरोबरच अक्काणी महाल भागात ब्रिटिशांच्या विरोधात उठाव घडवून आणणारे काळूबाबा नाईकही आता खाज्या नाईकाला येवून मिळाले होते. होळकरांच्या भोर संस्थानातील रोहिले, मकरानी आणि अरब सैनिक येवून मिळाल्यामुळे खाज्या नाईकच्या भिल्ल सेनेत मोठया प्रमाणावर वाढ झाली होती. सातपुडा भागात ब्रिटिशांच्या विरोधात उठाव करण्यासाठी भिल्ल आदिवासी सैनिकांचा मोठा जमाव निर्माण झाला होता सुलतानपुरच्या भिल्ल सेनेने सारंगखेडा गावावर कल्ला करून त्या ठिकाणाहून ब्रिटिशांना पळवून लावले होते.

अंबापाणीचे युध्द :- (११ एप्रिल १८५८)

सातपुडा परिसरात ब्रिटीश विरोधी उठावाची व्याप्ती वाढली होती. टेलीफोनच्या तारा तोडणे, पोस्ट ऑफिस फोडणे, खजिना लुटणे इत्यादी ब्रिटीश विरोधी कार्ये भिल्लांनी चालवून ब्रिटीशांना त्या भागातून पळवून लावण्याचा प्रयत्न केला होता त्यामुळे ब्रिटीशांनी खाज्या नाईकाच्या नेतृत्वात झालेला उठाव दडपून टाकण्यासाठी सैन्यांच्या तुकड्या वाढविल्या मेजर इव्हासन्स, कॅप्टन बर्च, ले. वेसवी, ले. स्टुअर्ट, कॅप्टन मॉन्टेगोमेरी इत्यादी आधिकाऱ्यांच्या नियुक्त्याही ब्रिटीशांनी उठावाचा बंदोबस्त करण्यासाठी केल्या होत्या. सातपुडा भागातील भिल्लांशी लढण्यासाठी भिल्लांचेच बांधव असलेले महादेव कोळी जमातीची सैनिक तुकडी ब्रिटीशांनी निर्माण केली होती. भिल्लांसोबत ब्रिटीश सैन्यांच्या जागोजागी चकमकी होत होत्या. अशा परिस्थितीत खानदेशातील शिरपूर पासून २४ किमी. अंतरावर असलेल्या अंबापाणीच्या जंगलात खाज्या नाईक आणि त्यांची भिल्ल सेना आश्रयाला असल्याची माहिती ब्रिटीशांना लागली. ११ एप्रिल १८५८ रोजी खाज्या नाईक, दौलतसिंग नाईक, काळूबाबा नाईक, यांच्यासह १५०० भिल्ल सैनिकांना ब्रिटीश अधिकारी मेजर ईव्हासन्सने अंबापाणीच्या जंगलात घेराव घालून हल्ला केला. ब्रिटीशाकडे आधुनिक शस्त्रास्त्रे होती व भिल्ल सेना परंपरागत शस्त्रास्त्रांच्या सहाय्याने लढत होते. त्यामध्ये भिल्ल सेनेचा टिकाव लागणे शक्य नव्हते. या युद्धात ६५ भिल्ल क्रांतीवीर शहीद झाले. १७० जखमी झाले कॅप्टन बर्च, ले. वेसवी हे ब्रिटीश अधिकारी जखमी होवून एक ब्रिटीश अधिकारी युद्धात मारला गेला. खाज्या नाईक सह ६२ लोकांवर डम टायल खटला चालविण्यात येवून डमच्या आवाजावर ५७ आरोपींना गोळ्या घालण्यात आल्या आणि खाज्या नाईकाचा शिर कापून सेंधवाच्या किल्ल्याबाहेर लटकविण्यात आले होते. ते या दृष्टीकोनातून की पुन्हा त्या भागातील कोणीही ब्रिटीशांच्या विरोधामध्ये उठाव करू नये अन्यथा अशी शिक्षा दिली जाईल याची चेतावणी भिल्लांसाठी होती. ही लढाई १८५७ च्या उठावातील अंबापाणीची लढाई म्हणून ओळखली जाते. खाज्या नाईकाने या लढाईमध्ये भिल्ल सेनेचे नेतृत्व केले.

अशाप्रकारे आदिवासी क्रांतीकारकांनी १८५७ च्या उठावात आपल्या क्षेत्रात उठावाचे नेतृत्व केले. आणि ब्रिटीशांची गुलामगिरी संपविण्यासाठी झालेल्या या लढयात बाहदूरशहा, नानासाहेब पेशवे, राणी लक्ष्मीबाई, बेगम हजरत महल, कुवरसिंह आदि. प्रमाणे आपल्या प्राणांचे बलिदान दिले. स्वातंत्र्य सैनिकांनी प्रारंभ केलेल्या १८५७ च्या स्वातंत्र्यसमरात शंकरशहा, रधूनाथशहा(गोंडवाना), नारायणसिंह (छत्तीसगढ), बाबूराम शेडमाके(चांदागड), खाज्या नाईक (खानदेश) इत्यादी आदिवासी क्रांतीकारांनी उठावाचे नेतृत्व केले. ब्रिटीशांच्या विरोधात आदिवासी समुदाय यांच्या नेतृत्वात एकत्रित झाला आणि ब्रिटीशांच्या शोषणकारी व्यवस्थेचा विरोध आदिवासींच्या माध्यमाने १८५७ च्या उठावात करण्यात आला. हे नाकारता येत नाही.

संदर्भ:





- १) मडावी शेषराव एन., गोंडवानाचा सांस्कृतिक इतिहास, सुधीर प्रकाशन, वर्धा, प्रथमावृत्ती, २०११ पृ. क्र. २८१
- २) www.shankarshaha.in
- ३) कित्ता
- ४) www.virnarayansinh.in
- ५) मडावी शेषराव एन., गोंडवानाचा सांस्कृतिक इतिहास पृ. क्र. २८२
- ६) www.virbaburaoshedmake.in
- ७) मडावी शेषराव एन., गोंडवानाचा सांस्कृतिक इतिहास पृ. क्र. २८६
- ८) डॉ. आर.एस.पवार, स्वातंत्र्य युद्धात खानदेशातील आदिवासींचे योगदान, आदिवासी समाज, तिसरी आ. २०१५ पृ. क्र. ५०
- ९) www.khajyanaik.in



Colloids and Surfaces A: Physicochemical and Engineering Aspects

Volume 657, Part B, 20 January 2023, 130561

Facile approach to fabricate a high-performance superhydrophobic PS/OTS modified SS mesh for oil-water separation

Rajaram S. Sutar^a, Sanjay S. Latthe^b  , Nilam B. Gharge^a, Pradip P. Gaikwad^a, Akshay R. Jundale^a, Sagar S. Ingole^a, Rutuja A. Ekunde^a, Saravanan Nagappan^c, Kang Hyun Park^c, Appasaheb K. Bhosale^a, Shanhu Liu^d  

Show more 

 Share  Cite

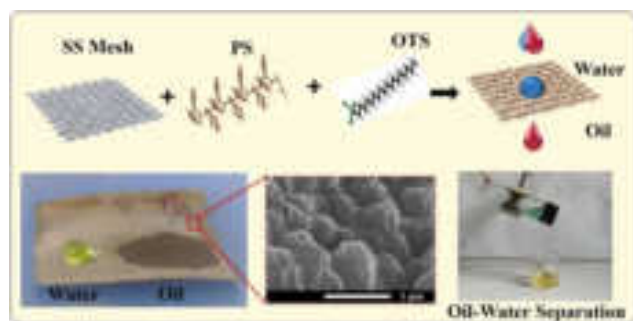
<https://doi.org/10.1016/j.colsurfa.2022.130561> 

[Get rights and content](#) 

Abstract

Special wetting materials have been used for the oil and water separation due to their different interfacial attraction of oil and water. Herein, we successfully fabricated superhydrophobic coatings on stainless steel (SS) mesh by depositing successive layers of polystyrene (PS) and octadecyltrichlorosilane (OTS) through the dip-coating method. The as-prepared coating showed a water contact angle (WCA) of $157.5 \pm 2^\circ$, a rolling angle of $6 \pm 2^\circ$ and an oil contact angle (OCA) of around 0° . The surface microstructure analysis of the coating revealed a regular pattern of microscale bumps with nanoscale folds on it, both of which improve the overall superhydrophobicity of the surface. The capacity of coatings to separate oil and water was examined by employing a variety of mixtures of oil and water, including petrol, diesel, kerosene, vegetable oil, and coconut oil. In case of low viscosity oil, the coated mesh demonstrated separation effectiveness of more than 97% and on the other hand, high viscosity oil demonstrated just 89% efficiency. Low viscosity oils showed a greater permeation flux through the mesh than extremely viscous oil. The mechanical strength of the coating was examined using bending, twisting, adhesive tape testing, sandpaper abrasion tests, and the findings indicated that coated mesh had exceptional mechanical resilience. In addition, the developed superhydrophobic mesh demonstrated excellent thermal stability and self-cleaning properties. Therefore, this superhydrophobic/superoleophilic mesh has a significant deal of application potential in practical.

Graphical Abstract



[Download : Download high-res image \(229KB\)](#)

[Download : Download full-size image](#)

Introduction

Oil spills and industrial effluents inflict significant harm to the ecosystems of the seas, human health, and the surrounding environment [1], [2]. The safe and responsible disposal of wastewater containing oil has been shown to be a challenging problem on a global scale. Many approaches have been used for the treatment of oil-water pollution, including oil skimmers, filtration, oil-absorbing materials, magnetic separations, centrifugal machine, flotation technologies, and combustion [3], [4], [5]. Traditional methods have various drawbacks, including limited separation efficiency, time consumption, cost-effectiveness, and the generation of secondary pollutants [6], [7], [8]. Therefore, cutting-edge technologies are an absolute necessity for the disposal of oily wastewater and the protection of the environment. Many efforts have been reported in the fabrication of separation membranes with controlled surface wetting property [9], [10]. The utilization of bio-inspired superhydrophobic materials in oil-water separation processes is a popular area of study due to its high water repellency and ability to allow oil to enter in it [4], [11], [12]. Therefore, superhydrophobic materials have been added to commercially available cotton textiles, 3D porous materials, different polymer membranes, filter papers, and metal meshes for considerable oil-water separation [13], [14]. Chemical etching [15], [16], spray deposition [17], [18], dip coating [19], hydrothermal method [20], sol-gel processing [21], [22], chemical vapor deposition [23], electrospinning [24], [25], and layer by layer [26] methods have been used for modification of porous surfaces. Among these, dip-coating is a quick and effective method of producing bulky, intricately formed products [27]. Metal meshes have sparked a lot of attention since they are long-lasting, reusable, and may be used in industry [2], [23]. Porous materials can absorb or filter liquids, and when their surface structure is adjusted with a specific wettability material, they can help separate oil or water from oil-water mixtures [28], [29]. Numerous types of porous metal meshes, including those constructed of nickel, copper, and stainless steel (SS), among other materials were used for oil-water separation [30], [31], [32], [33]. Among them, SS meshes have found widespread use for oil-water separation owing to their high electrical and electrothermal capabilities as well as their superior resistance to thermal shock [33].

OTS has been used to tune the surface wettability of porous substrates so that oil and water can be effectively separated. The OTS has low surface energy, hence it improves the hydrophobicity of the rough surface and also shows high oil absorption capacity [35], [36]. Li et al. [34] recently made superhydrophobic SS mesh by spraying it with a mixture of OTS-modified SiO₂ nanoparticles and waterborne PU. This superhydrophobic mesh was able to separate a mixture of kerosene and water at a rate of 98.3%. Latthe et al. [27] created a superhydrophobic surface by varying the concentration of OTS in PS solution and the number of dipping cycles. At first, they prepared a homogenous solution containing PS and OTS using tetrahydrofuran (THF) as a solvent. The pre-cleaned glass substrate was dip-coated (4 times) on the homogenous solution and air-dried to get a superhydrophobic surface with a contact angle of $154 \pm 2^\circ$. Ke et al. [37] have built a superhydrophobic and superoleophilic sponge by immersing it in OTS solution. This kind of sponge has shown an absorption capacity of 42–68 times more than the mass of the sponge for toluene, light oil, and

methyl silicone oil. Even after being put through 50 separation cycles, this adsorption capacity remained the same. Liang et al. [38] modified a polyurethane sponge by immersing in an OTS solution for oil-water separation. Cheng et al. [24] used coaxial electrospinning with PVDF solution as a lumen solution and reactive silicon-containing monomers as the outer solution to generate superhydrophobic nanofiber membranes with hierarchical micro nano-scale morphology. The outstanding separation efficiency of 99.6% is achieved with the as-prepared asymmetric composite membrane, which has an extremely rapid permeation flux. They show a water-in-n-octane permeation flux of 17331 L/(m²h) and retain 88% of their original permeance after 20 cycles of operation [24]. Rasouli et al. [13] briefly reviewed the various aspects of fabrication of superhydrophobic/superoleophilic membranes having mesh, films, and porous substrates for efficient oil-water separation applications. In order to modify the surface energy of superhydrophobic/superoleophilic membranes, it is usual practice to use low surface energy chemicals such as fatty acids, thiols, silanes, polymers based on polyethylene, and carbon nanotubes [13]. These membranes have >99% oil separation efficiency in oil-water combinations.

In this research work, a layer of PS was first applied on SS mesh using a dip coating process, followed by an OTS dip layer to achieve superhydrophobicity. The dip coating cycles were consequently carried out by dip and dry in both PS in THF and OTS in hexane. The surface structure of a red rose petal was obtained on SS mesh. SEM and EDS were used to describe the surface morphology and chemical composition, respectively. The gravity-driven oil-water separation technique was used to determine the oil-water separation efficiency and permeation flux using a custom-made setup. The mechanical durability of superhydrophobic mesh was evaluated using adhesive tape tests, sandpaper abrasion tests, bending, twisting, and folding tests. We have achieved the contact angles of 157.5±2° for OPS-2 as well as 154±2° for OPS-3 in superhydrophobic range and a comparable contact angle of 148.5±2° for OPS-1. The stable and robust self-cleaning coating was produced by this method as compared with the reported methods.

Section snippets

Materials

Polystyrene (PS) having average molecular weight ~ 280,000 and octadecyltrichlorosilane (OTS) were obtained from Sigma Aldrich, St. Louis, MO, USA. Tetrahydrofuran (THF) and hexane were purchased from Spectrochem, Mumbai, India. Stainless steel (SS) mesh with pore sizes of about 50µm was obtained from Shanghai Titan Technology Co. Ltd. China. The petrol, diesel, kerosene (from Bharat Petroleum Corporation Limited, India), vegetable oil (from Garud, India), and coconut oil (from Parachute...

Surface morphology and chemical composition

Fig. 2(a-f) depicts the surface morphology of meshes after being treated with varying doses of OTS. At low OTS concentrations, ten successive coating layers of PS and OTS create a rougher surface with nanoscale folds, as seen in Fig. 2(a). The enlarged view shows that there is a regular micro and nanoscale rough texture, which is essential for improving hydrophobicity and can be observed in Fig. 2(d). Surprisingly, regular shaped bumps emerged after raising the OTS concentration by twofold, as...

Conclusions

In conclusion, we have successfully fabricated superhydrophobic and superoleophilic SS mesh by depositing consecutive layers of polystyrene (PS) and octadecyltrichlorosilane (OTS) using an easy and inexpensive dip coating method. This allowed us to create a superhydrophobic and superoleophilic surface on the SS mesh. The WCA of 157.5 ±

2°, the OCA of about 0°, and the rolling angle of $6 \pm 2^\circ$ were all attained by adjusting the concentration of OTS in successive layered deposition. The...

CRedit authorship contribution statement

Rajaram S. Sutar: Conceptualization, Methodology, Investigation, Writing – original draft, Writing – review & editing, **Sanjay S. Latthe:** Supervision, Writing – review & editing, Visualization, **Nilam B. Gharge:** Methodology, **Pradip P. Gaikwad:** Methodology, Investigation, **Akshay R. Jundle:** Methodology, Investigation, **Sagar S. Ingole:** Methodology, Investigation, **Rutuja A. Ekunde:** Methodology, **Saravanan Nagappan:** Formal analysis, Writing – review & editing, **Kang Hyun Park:** Validation, Investigation, ...

Declaration of Competing Interest

The authors declare that they have no known competing financial interests or personal relationships that could have appeared to influence the work reported in this paper....

Acknowledgement

This work is financially supported by DST – INSPIRE Faculty Scheme, Department of Science and Technology (DST), Govt. of India. [DST/INSPIRE/04/2015/000281]....

[Recommended articles](#)

References (54)

Y. Liu *et al.*

[Bioinspired structured superhydrophobic and superoleophilic stainless steel mesh for efficient oil-water separation](#)

Colloids Surf. A: Physicochem. Eng. Asp. (2016)

M. Bennett *et al.*

[Monitoring the operation of an oil/water separator using impedance tomography](#)

Miner. Eng. (2004)

Y. Deng *et al.*

[Recent development of super-wettable materials and their applications in oil-water separation](#)

J. Clean. Prod. (2020)

S.S. Latthe *et al.*

[Superhydrophobic surfaces for oil-water separation, in](#)

[Superhydrophobic Polymer Coatings](#)(2019)

S. Rasouli *et al.*

[Superhydrophobic and superoleophilic membranes for oil-water separation application: a comprehensive review](#)

Mater. Des. (2021)

Y. Liu *et al.*

[On-demand oil/water separation of 3D Fe foam by controllable wettability](#)

Chem. Eng. J. (2018)

R. Liao *et al.*

[Fabrication of superhydrophobic surface on aluminum by continuous chemical etching and its anti-icing property](#)

Appl. Surf. Sci. (2014)

W. Ma *et al.*

[Lightweight, elastic and superhydrophobic multifunctional nanofibrous aerogel for self-cleaning, oil/water separation and pressure sensing](#)

Chem. Eng. J. (2022)

Y. Wan *et al.*

[The research on preparation of superhydrophobic surfaces of pure copper by hydrothermal method and its corrosion resistance](#)

Electrochim. Acta (2018)

Y. Xiu *et al.*

[UV and thermally stable superhydrophobic coatings from sol-gel processing](#)

J. Colloid Interface Sci. (2008)



[View more references](#)

Cited by (19)

[Oil/water separation copper membranes modified by laser induced ZnO nanowires growth with enhanced catalytic function](#)

2024, Colloids and Surfaces A: Physicochemical and Engineering Aspects

[Show abstract](#)

[Magnetic superhydrophobic sponge with 3D interpenetrating network structure coating for multimodal driven oil/water separation](#)

2024, Progress in Organic Coatings

[Show abstract](#)

[Multifunctional carbonized Zn-MOF coatings for cotton fabric: Unveiling synergistic effects of superhydrophobic, oil-water separation, self-cleaning, and UV protection features](#)

2023, Surface and Coatings Technology

[Show abstract](#)

[Ecofriendly superhydrophobic fabrics for ultra-fast oil/water separation by self-assembly](#)

2023, Surface and Coatings Technology

[Show abstract](#)

Efficient separation of oil-water emulsions: Competent design of superwetting materials for practical applications

2023, Journal of Environmental Chemical Engineering

[Show abstract](#) 

Sustainable approach to oil recovery from oil spills through superhydrophobic jute fabric

2023, Marine Pollution Bulletin

[Show abstract](#) 

[> View all citing articles on Scopus](#) 

[View full text](#)

© 2022 Elsevier B.V. All rights reserved.



All content on this site: Copyright © 2024 Elsevier B.V., its licensors, and contributors. All rights are reserved, including those for text and data mining, AI training, and similar technologies. For all open access content, the Creative Commons licensing terms apply.



A Review on Superhydrophobic Surfaces: Fundamentals, Fabrications and Applications

Mehejbin R. Mujawar¹, Rajesh B. Sawant¹, Govind D. Salunke¹, Rajaram S. Sutar², Sanjay S. Lathe³, Ankush M. Sargar⁴, Raghunath K. Mane⁵, Krishna K. Rangar¹, Shivaji R. Kulal^{1*}

¹ Department of Chemistry, Raje Ramrao Mahavidyalaya, Jath, Dist. - Sangli (MS) India

² Self-cleaning Research Laboratory, Department of Physics, Raje Ramrao Mahavidyalaya, Jath, Dist. - Sangli (MS) India.

³ Self-cleaning Research Laboratory, Department of Physics, Vivekanand College (Autonomous), Kolhapur, Dist. - Kolhapur (MS) India.

⁴ Department of Chemistry, Bharati Vidyapeeth's Dr. Patangrao Kadam Mahavidyalaya, Sangli, Dist. - Sangli (MS) India

⁵ Department of Chemistry, Smt. Kusumtai Rajarambhapu Patil Kanya Mahavidyalaya, Islampur, Dist. - Sangli (MS) India

*Corresponding author's E-mail: srkulal@gmail.com, amsargar2012@gmail.com

Abstract

Superhydrophobic surfaces are highly hydrophobic i.e., it extremely difficult to wet. Superhydrophobic surfaces are the tendency to repel water drops and absorb oil drops. The water contact angle of superhydrophobic surfaces is greater than 150° , the oil contact angle is less than 5° , and the sliding angle is less than 5° . It is showing the lotus effect. Superhydrophobicity is observed in the lotus leaves, insects, and some other plants in which their leaves would not get wet. This phenomenon is due to the unique surface structure of the lotus leaf and also the presence of a low surface energy material on the surface of the leaf. For the formation of a superhydrophobic surface, the surface must show hierarchical micro- and nano-roughness and low surface energy. Efforts have been taken to form superhydrophobic surfaces for a variety of applications. There are many applications of superhydrophobic surfaces such as self-cleaning surfaces, oil-water separation surfaces, anti-icing surfaces, anti-corrosion surfaces, anti-fogging surfaces, and water-resistant surfaces. In this article, the fundamental principles of superhydrophobic surfaces, some recent trends in the fabrication of superhydrophobic surfaces, and their applications are reviewed and discussed.

Keyword: Superhydrophobicity, Superoleophobicity, Lotus effect, Self-cleaning, Oil-water separation, Water-repelling, Oil Contact Angle, Water Contact angle, Anti-icing, Anti-corrosion.



REVIEW OF RESEARCH

ISSN: 2249-894X

IMPACT FACTOR : 5. 7631 (UIF)

भारतीय पर्यटनात आदिवासी लोककलांचे योगदान

चौधरी पी. जे.^१, डॉ. स्वाती काळभोर^२

^१राजे रामराव महाविद्यालय, जत

^२श्रीमती सी. के. गोयल महाविद्यालय, दापोडी, पुणे.

प्रस्तावना :-

आदिवासी लोककलांना भारतीय पर्यटनात महत्त्वाचे स्थान आहे. पर्यटक ज्ञान आणि आनंद या दोन्ही गोष्टी साध्य करण्यासाठी पर्यटन करतात. आदिवासी लोककलांमध्ये या दोन्ही गोष्टी समाविष्ट आहेत. आदिवासींच्या लोक चित्रकला, लोकगीते, लोकनृत्य इत्यादी लोककलांना ऐतिहासिक वारसा आहे. आदिवासींच्या प्रथा, परंपरा, भावना, त्यांचा निसर्गवादी दृष्टीकोन इत्यादी गोष्टींची माहिती आपल्याला त्यांच्या लोककलांमधून मिळते. त्याचबरोबर लोककला सादर करण्याची कला आकर्षक आहे. ज्यातून पाहणाऱ्यांना आनंद मिळतो. त्यामुळे पर्यटक आदिवासींची लोकसंस्कृती पाहण्यासाठी भारतातील आदिवासी क्षेत्रामध्ये येतात. त्यांच्या लोककला पाहून आनंदीत होतात आणि आदिवासींच्या संस्कृतीचे ज्ञानही मिळवतात. या लोककलांनी भारतीय पर्यटनाला गती मिळवून देण्यात महत्त्वाची भूमिका बजावलेली आहे. आदिवासींच्या लोककलांना ग्रामीण संस्कृतीच्या उदयापासूनची परंपरा लाभलेली आहे. त्यामुळेच ह्या लोककला वैशिष्ट्यपूर्ण आहेत. काळाच्या ओघात मानव जसा आधुनिक बनत गेला तशा या प्राचीन प्रथा, परंपरा लोप पावल्या परंतु आदिवासींनी त्या आजही लोककलांच्या माध्यमातून टिकवून ठेवलेल्या आहे. त्यामुळेच आदिवासींच्या लोककला दुर्मिळ आणि वैशिष्ट्यपूर्ण वाटतात. वाली लोकचित्रकला आदिवासी लोकगीते, गोंडी लोकनृत्य, नागा नृत्य इत्यादी लोककलाची परंपरा प्रागैतिहासिक काळापासूनच असल्याचे निदर्शनास आलेली आहे. ज्यांनी देश - विदेशी पर्यटकांना भारतामध्ये आदिवासींची लोकसंस्कृती पाहण्यासाठी येण्यास भाग पाडले आहे. भारतातील पर्यटकाबरोबर विदेशी पर्यटक ही मुंबई जवळील वाली जमातीचा प्रदेश, सातपुड्यातील भिल्ल जमातीचा प्रदेश, गडचिरोली जिल्ह्यातील गोंड जमातीचा प्रदेश, झारखंड मधील मुंडा जमातीचा प्रदेश, नागालँड - आसाम भागातील नागा जमातीचा प्रदेश, हिमाचल प्रदेशातील आदिवासी लोकसंस्कृती पाहण्यासाठी पर्यटन करतात. ज्या मुळे पर्यटन व्यवसायाचा विकास घडून येतो. आदिवासींच्या लोककलांचा अभ्यास करणे आवश्यक आहे. त्याबरोबर पर्यटनात या लोककलांच्या योगदानाची माहिती घेणेही गरजेचे आहे.



लोककलांचा अर्थ :-

लोककला ग्रामीण आणि आदिवासी भागातून निर्माण झालेल्या आहेत. त्यामुळे भारतातील लोककलांचे निर्माते ग्रामीण आणि आदिवासींच आहेत हे स्पष्ट होते. लोकांनी लोकांच्या भाषेत (बोलीभाषा) लोकांसाठी निर्माण केलेली कला म्हणजे लोककला होय. लोककलांचा निर्माता कोणीही एक व्यक्ती नाही तर व्यक्तीच्या समुहाकडून चालत आलेल्या कला आहेत. या ठिकाणी एक व्यक्ती नाही तर व्यक्तींचा समुह असतो त्यामुळे या कलांना लोककला असे म्हणतात. लोकचित्रकला, लोकगीते, लोकनृत्य या आदिवासी लोककलांचा निर्माता अज्ञात असतो. त्यामुळे त्यांच्या लोककलांच्या निर्मातीचे श्रेय आदिवासी समुहाला जाते. त्याबरोबरच या लोककलाचे सादरीकरण समुहाने होत असल्यामुळे लोककलांचे स्वरूप सामुहिक असते. हेच या कलांमधील प्राथमिक वैशिष्ट्य म्हणता येईल ज्यामुळे पर्यटकांसाठी ह्या लोककला पर्यटनीय ठरतात.

आदिवासी लोककलांचा उगम :-

भारतामध्ये ग्रामीण संस्कृतीची सुरुवात झाल्यापासूनच लोककलांचा उगम झाला असावा परंतु ऐतिहासिक साधना अभावी वर्तमान काळात लोककलांच्या उगमाचा निश्चित कालक्रम ठरविणे शक्य नाही. प्रागैतिहासिक काळातील गुफा चित्रकारी, सिंधु संस्कृतीच्या काळातील लोककलांशी संबंधीत अवशेष इत्यादी वरून लोककलांचा इतिहास ग्रामीण जीवनाच्या उगमा एवढाच जुना असावा. भाषा आणि लिपी मानवाला अवगत होण्यापूर्वीच आपल्या भावना व्यक्त करण्यासाठी चित्रकलेसारख्या लोककलांचा वापर मानवाने केलेले असल्याचे पुरावे भिमबेटका सारख्या गुफेतील चित्रकलेतून मिळतात. सिंधु संस्कृतीच्या काळातील भावचित्र लिपी, मातीच्या भांड्यावरील चित्रे इत्यादी लोककलांच्या उगमाची उदाहरणे आहेत. आदिवासी संस्कृती भारतातील मुळ संस्कृती आहे त्यामुळे ह्या लोककला आदिवासींनीच निर्माण केलेल्या असल्यात कारण प्रगैतिहासिक काळातील भिमबेटका सारख्या गुफेतील चित्रकलांचे नमुने आदिवासी चित्रकलेत पाहावयास मिळतात. त्याबरोबरच प्रगैतिहासिक काळातील पाषाण हत्यारे आज थोड्याफार फरकाने आपणास मागासलेल्या आदिवासी लोकांच्या वापरात असल्याचे बघावयास मिळतात. ३ गोंदिया जिल्ह्यातील कचारगड गुफेत ५०००० वर्षापूर्वी मानवाचा समुह निवासास असावा असा पुरावा उत्खननातून आढळला आहे. ४ ही गुफा आदिवासी गोंड जमीतीचे आराध्य स्थळ आहे. या आराध्य स्थळाच्या कथेवरून गोंडी नृत्याचा उगम या आराध्य स्थळातून झाला असावा अशी माहिती मिळते. ५ यावरून आदिवासी लोककलांचा उगम ग्रामीण संस्कृतीच्या उदयाबरोबर झाला असावा हे स्पष्ट होते.

आदिवासी लोककला :-

लोकचित्रकला, लोकगीते, लोकनृत्य इत्यादी आदिवासींच्या लोककला आहेत. प्राचीन काळापासून तर वर्तमान काळापर्यंत भारतीय संस्कृतीत अनेकवेळा संक्रमण झालेले आहे. त्यामुळे आदिवासींच्या सर्वच लोकलांना वेगळे करता येणार नाही. परंतु काही लोककला आदिवासींमध्येच प्रसिद्ध आहेत किंवा त्या लोककला आदिवासींमध्येच सादर केल्या जातात. त्यांचाच उल्लेख यामध्ये करण्यात येईल. आदिवासींच्या लोककला सामाजिक, धार्मिक आणि त्यांच्या नैसर्गिक जीवनाच्या दृष्यांशी संबंधीत आहेत.

आदिवासी लोकचित्रकला :-

आदिवासींमध्ये प्राचीन काळापासून अंगनात, घराच्या भिंतीवर, लग्नांच्या मुंडयांवर निसर्गाशी संबंधीत विविध देवी - देवतांची चित्रे काढण्यात येतात. "ये चित्र प्रागैतिहासिक गुफा चित्रांची तरहेर दिखते हे। ६ ज्यामध्ये वन्य प्राण्याची शिकार करताना किंवा शिकार केलेला प्राणी घेवून जाताना, नृत्य करताना, शेतात पेरणी, शेतीची कापणी करतानाची चित्रे आदिवासी काढतात. जी पर्यटकासाठी आकर्षनीय आहेत. या लोक चित्रकलांचे नमुने आज विक्रीचे वस्तु बनल्या आहेत. त्यांचे वास्तव चित्र पाहण्यासाठी वाली जमाती राहात असलेल्या प्रदेशामध्ये पर्यटक मोठ्या प्रमाणात येतात. वाली आदिवासी जमातीची लोकचित्रकला भारतामध्ये प्रसिद्ध आहे ही जमात मुंबई महानगराच्या बाजूच्या प्रदेशात वसलेली आहे. भारतातील एवढ्या मोठ्या महानगराजवळ ही जमात राहात असूनही वाली जमातीने प्राचीन काळापासूनची आपली परंपरा जपून ठेवलेली आहे. पूर्वी ही चित्रकारी स्त्रीयाच करायच्या परंतु आज पुरुषही ही चित्रकारी काढतात. वाली जमातीचे लोक या चित्रकलेचा उपयोग आपल्या घराच्या भिंती सुंदर दिसण्यासाठी भिंतीवर चित्रे काढतात. ही चित्रकला आज कागद, कापड इत्याद्यावर काढण्यात येते आणि त्याचे नमुने बाजारपेठामध्ये विकले जातात. त्याचे प्रदर्शन केले जाते. कापडाच्या अनेक डिझाईन बनविण्यासाठी या चित्रकलेचा वापर करण्यात येतो. या चित्रकले मध्ये भारतातील प्रारंभीच्या ग्रामीण संस्कृतीचे ज्ञान साठवलेले आहे. त्यामुळेच देश - परदेशातील पर्यटक ही चित्रकला पाहण्यासाठी भारतामध्ये येतात. व या चित्रकलांचे नमुने विकत घेतात. त्यामुळे भारतीय पर्यटन व्यवसाय वृद्धीगत होण्यास मदत झाली. वास्तवात वाली लोकचित्रकला साधारण चित्रकला आहे. ज्यामध्ये तांदळाच्या चुर्णापासून बनविण्यात येणाऱ्या पांढऱ्या रंगाचा वापर केला जातो. सामान्यपणे वर्तुळाकार चित्रकला काढण्यात येते ज्यामध्ये मध्ये - मध्ये लाल व पिवळ्या रंगाचे बिंदु बनविण्यात येतात. वाली चित्रकलेमध्ये वाली जमातीच्या दैनंदिन जीवनाचे व त्यांच्या सामाजिक जीवनाचे चित्रण केलेले आहे. या चित्रकलेला प्राचीन परंपरा आहे. परंतु पुराव्या अभावी या चित्रकलेचा प्रारंभ केव्हा झाला हे निश्चित सांगता येणार नाही दसवी सदी ई. पु.के. आरंभीक काल में इसके होने के संकेत मिलते हे। तेंव्हापासून ही लोकचित्रकला वाली जमातीमध्ये परंपरेनुसार चालत आलेली असावी. ७ १९७० च्या पूर्वी वाली जमाती बाहेरच्या जगाला या लोकचित्रकलेची माहिती झाल्यानंतर या लोककलेला जगभर प्रसिद्धी मिळाली. त्यानंतर ही चित्रकला पर्यटन व्यवसायाचे महत्त्वाचे साधन बनले. वाली जमाती प्रमाणेच इतर आदिवासी जमातीमध्येही चित्रकला काढण्यात येतात. घराच्या मातीच्या भिंती सुंदर बनविण्यासाठी मातीची भांडी, वादय इत्यादीवर सुबक चित्रकारी करण्यात येत असते. बांबुपासून बनविण्यात येणाऱ्या कलाकुसरीच्या वस्तुवर सुबक चित्रकला काढतात. चित्रकले सारखाच गोदवन प्रकारही आदिवासीमध्ये पहावयास मिळतो. आदिवासी स्त्रीया हात, पाय, नाक, कपाळ, गाल इत्यादी शरीराच्या अंगावर पशु, पक्षी, देवी - देवता, फुले - फळे, सूर्य, चंद्र, तारे इत्यादींचे चित्रे नैसर्गिक रंगाच्या सहाय्याने काढतात. जो आदिवासींच्या उत्तम चित्रकारीचा एक भाग आहे. की आदिवासी स्त्रीया आपल्या शरीराला सुंदर - सुबक बनविण्यासाठी आपल्या अंगावर नैसर्गिक रंगाने चित्रे काढतात. गोदवनातील चित्रेही त्यांच्या संस्कृतीची माहिती देतात.

आदिवासी लोकगीते :-

भारतामध्ये आदिवासींच्या अनेक जमाती आहेत. प्रत्येक जमातीची भाषा वेगवेगळी आहे. त्यांच्या भाषेमध्ये त्यांची लोकगीते आहेत. त्यांच्या दैनंदिन जीवनामध्ये लोकगीतांना अनन्य साधारण महत्त्व आहे. शेतातील कामे, विवाह, नविन अपत्याचा जन्म, मृत्यू, सण - उत्सव इत्यादी वेळी आदिवासी लोकगीते म्हणत असतात. लोककला आदिवासी भागातुन निर्माण झाल्यामुळे लोकगीतांचे निर्माण आदिवासी आहेत, असे म्हटल्यास अतिशयोक्ती होणार नाही. ८) आदिवासींची लोकगीते अलिखित स्वरूपात आहेत. परंपरेनुसार मौखिक पध्दतीने चालत आलेली आहेत. प्राचीन काळापासून चालत आलेले आदिवासींचे शिक्षा केंद्र "गोटुल" चा गाणे आणि नाचणे प्राणच होता. या गोटुल मध्ये संध्याकाळी आदिवासी मुले - मुली लोकगीते म्हणत व नृत्य करित असत. यातुनच आदिवासींच्या सामुहिक जीवनामध्ये लोकगीतांनी आपले स्थान मिळवाचे आदिवासींच्या लोकगीतांची भाषा आणि शब्द कला आदिवासींच्या रोजच्या व्यवहारी जगण्या वागण्यातुन रिती रिवाजातुन उदयास आल्या असल्याचे दिसते. त्यामुळे या लोकगीतांना मोठी परंपरा प्राप्त झाली आहे. ९) आदिवासींच्या लोक गीतामधील भावना पर्यटकांना लुभावणाऱ्या असतात. आदिवासी भागातुन पर्यटक प्रवास करित असतांना शेतात काम करणाऱ्या स्त्रीयाची गाणी ऐकुन ते स्थळ पर्यटकांसाठी समनिय झालेले असते. वर्षभर शहरी भागात राहुन नेहमी मोटार गाड्यांचा आवाज ऐकनारे पर्यटक अरण्यात आदिवासींच्या गीतातील मधुर आवाज आणि त्या मधुर आवाजातील अर्थांमुळे आनंदीत होतात. पर्यटक उन्हाळ्यात आदिवासींच्या विवाह प्रसंगी गायल्या जाणाऱ्या गीतांचा आस्वाद घेतात. नंदुरबार, कोकण, गडचिरोली इत्यादी भागामध्ये पर्यटक मोठ्या संस्थेने येतात. त्यांचा उद्देश त्या भागातील निसर्ग सौंदर्याबरोबर त्या भागातील आदिवासी संस्कृती पाहणे हा असतो. आदिवासी आपल्या लोकगीतामधुन आपल्या सुख - दुःखाच्या भावना व्यक्त करतात. त्यांच्या देवी - देवता, निसर्ग प्रेम इत्यादी संबंधी गीते पर्यटकास आकर्षनीय असतात. आदिवासींमध्ये पुरुष लोकगीतापेक्षा स्त्री लोकगीतांची संख्या जास्त असताना दिसुन येते. स्त्री जीवनाशी संबंधीत भाव - भावनांचे चित्रण लोकगीतात जास्त प्रमाणात रेखाटले गेल्याचे दिसुन येते. आदिवासीं शेतातील कामे सोपे करण्यासाठी, विवाह समारंभ मनोरंजक करण्यासाठी लोकगीताचा वापर करतात. या लोकगीतांनी पर्यटकांना आदिवासी भागामध्ये येण्यास भाग पाडल्यामुळे पर्यटन व्यवसायात वाढ होवून तोरणमाळ, चिखलदरा, गडचिरोली इत्यादी भागामध्ये पर्यटन आदिवासींच्या रोजगाराचे साधन बनला आहे. ज्यातुन त्या भागातील स्थानिक लोकांना पैसा मिळतो त्याबरोबरच भारत सरकारलाही देश - विदेशी चलन मिळत असते.

आदिवासी लोकनृत्य :-

आदिवासी उत्तम प्रकारे लोकनृत्य सादर करतात. भारतातील आदिवासी लोकनृत्यांना जागतीक प्रसिध्दी मिळालेली आहे. भारतीय लोकसंस्कृतीला सादर करण्याच्या कार्यात आदिवासींच्या या लोकनृत्यांना महत्त्वाचे स्थान आहे. भिल्ल नृत्य, गोंडी नृत्य, मुंडारी नृत्य, नागा नृत्य इत्यादी आदिवासी नृत्य भारतामध्ये प्रसिध्द आहेत. या लोकनृत्यांना पाहण्यासाठी देश - विदेशातुन पर्यटक आदिवासी भागामध्ये स्थलांतरित होतात. सण - उत्सवाच्या वेळेला आदिवासी लोकनृत्यांमध्ये सहभागी होवून मनोरंजन करतात. आदिवासी लोकनृत्यामुळे पर्यटकांना त्यांच्या प्रथा, परंपरा, चालीरितीची माहिती होते. ज्यामुळे भारतांच्या संस्कृतीची ओळख आंतरराष्ट्रीय स्तरावर या लोकनृत्यामुळे होते. आदिवासींच्या लोकनृत्याची परंपरा फार प्राचीन आहे. यांचा संदर्भ कचारगड गुफेच्या संबंधीत कथेवरुन मिळतो की, काली कंकालीची मुले नदीवर स्नान करण्यासाठी गेलेले असताना वाटेत सुगंधित फुलावरती भौरे गोल - गोल फिरत असताना दिसले हे दृष्य बघुन ती मुले आनंदीत झाले आणि त्या भौऱ्याप्रमाणे गोल - गोल कडे करुन नाचायला लागले त्यातुनच आदिवासी गोंड समाजामध्ये गोंडी नृत्य करण्याची परंपरा निर्माण झाली. १०) आजही आदिवासी हातात हात घालुन गोल कडे करुन समुहाने नृत्य करतात. आदिवासींच्या लोकनृत्यांना प्राचीन इतिहास आहे. त्यामुळे अभ्यासक, संशोधक व ज्ञानी पर्यटकांना अशा पर्यटकांच्या ठिकाणी जाणे आवडते. असे पर्यटक आदिवासी भागामध्ये आदिवासींच्या संस्कृतीची माहिती घेण्यासाठी स्थलांतरित होतात. आदिवासींची क्षेत्रे लोकसंस्कृतीने समृध्द आहेत. त्याचबरोबर निसर्ग सौंदर्यानेही नटलेली आहेत. करण आदिवासी दऱ्या - खोऱ्यानी युक्त अशा जंगलात वास्तव्याला असतात. त्यांची लोकनृत्य निसर्ग सौंदर्यानी युक्त अशा वातावरणात सादर करण्यात येतात. त्यांच्या लोकनृत्यात अरण्यातील झाडाच्या फांद्या, पाणे अंगाला बांधतात. डोक्याला मोरपीसे, नकली चेहरे, मुखवटे विशिष्ट अंगविक्षेप आणि त्याला साजेसे संगीत की ज्या संगीतामधुन नृत्य करण्याची आवड निर्माण होईल इत्यादी तयारी करुन नृत्य सादर करतात. आदिवासींच्या लोकनृत्यामध्ये इच्छुक असणाऱ्या पर्यटकांनाही सहभागी होता येते. त्यामुळे त्यांच्या लोकनृत्यांचा प्रत्यक्ष आनंद घेता येतो. नृत्यामध्ये पशु- पक्ष्यांच्या नकला करतात. कोलाम आणि हलबा /हलबी जमातीमध्ये डंडार नृत्य प्रसिध्द आहे. या नृत्यामध्ये बांबू आणि कागदाच्या लगदयापासून शेना मातीचे मिश्रनाचे लेप लावून आणि त्यावर रंग रंगोटी करुन मुखवटे तयार करतात. हे मुखवटे घालुन डंडार नृत्य करतात. गोंड जमातीमध्ये कर्मा, रेला, डेमसा नृत्य प्रसिध्द आहेत. ज्यामध्ये नगारा, ढोलकी, बासरी, टिपऱ्या इत्यादी वाद्य वाजविण्यात येतात. आदिवासींचे जीवन जंगलाशी संबंधीत असते. शेती, पशुपालन, जंगलाशी संबंधीत रोजगार, वन्य प्राण्याची शिकार इत्यादीवर त्यांचा उदरनिर्वाह चालतो. त्यामुळे निसर्ग देवतांना आपल्या नृत्याच्या माध्यमातुन कृतज्ञता व्यक्त करतात. आदिवासी लोकनृत्यामध्ये सामाजिक दृष्टिकोन असतो. हा ज्ञान पर्यटकांना त्यांच्या लोकनृत्यामधुन मिळतो. त्याच बरोबर पर्यटकांचे मनोरंजनही होत असते. ज्ञान आणि आनंद मिळवणे हा जो पर्यटकांचा उद्देश असतो तो उद्देश खऱ्या अर्थाने आदिवासींच्या लोकनृत्यातुन साध्य होतो. त्यामुळेच आदिवासींची लोकनृत्य पाहण्यासाठी देश - विदेशातुन पर्यटक आदिवासी भागामध्ये येतात.

आदिवासी लोककला आणि पर्यटन :-

आदिवासींच्या लोककला त्यांच्या संस्कृतीचाच एक भाग आहेत. त्यामुळे पर्यटनाच्या विविध प्रकारांपैकी सांस्कृतिक पर्यटनामध्ये या लोककलांचा समावेश होईल. या लोककलांमधून आदिवासींच्या संस्कृतीची माहिती मिळते. चित्रकला, लोकगीते, लोकनृत्य या लोककलांमधून आदिवासींचे राहणीमान, त्यांच्या सवई, त्यांचा इतिहास, प्रथा, परंपरा, धार्मिक कृत्य आणि त्यांच्या जीवन पध्दतीची माहिती मिळते. सांस्कृतिक पर्यटन के माध्यम से पर्यटकों को सम्बन्धित देश की संस्कृती के बारे में पता चलता है। संस्कृती ही वह माध्यम है, जिससे किसी देश या स्थान की महानता का पता चलता है। ११ म्हणुन जिज्ञासु पर्यटक अशा संस्कृतीची निवड करतात जी संस्कृती प्रचलित संस्कृतीपेक्षा भिन्न आहे, आणि त्या संस्कृतीला ऐतिहासिक परंपरा आहे. भारतातील आदिवासींच्या लोकसंस्कृतीला किंवा लोककलांना हा समृद्ध ऐतिहासिक वारसा लाभलेला आहे. त्याचबरोबर इतर संस्कृत्यापेक्षा आदिवासी संस्कृती भिन्न आहे. त्यामुळे पर्यटक भारताच्या आदिवासी भागातील ही लोकसंस्कृती पाहण्यासाठी येतात. त्यामुळे भारतीय पर्यटनाचा विकास घडून येतो. आज पर्यटनाचे स्वरूप व्यावसायिक बनलेले आहे. त्यामध्ये ऐतिहासिक स्थळे, भौगोलिक स्थळे, धार्मिक स्थळे इत्यादीबरोबर लोककलांच्या स्वरूपातील आदिवासींच्या लोकसंस्कृतीचेही योगदान आहे. पर्यटनामुळे अनेक व्यवसाय विकसीत होतात ट्रॅव्हलिंग, हॉटेल, अनेक कलाकुशरीच्या वस्तु, खादय वस्तु, इत्यादीच्या विक्रीला वेग आला. पर्यटन मार्गदर्शकांना रोजगार मिळाला. पर्यटनासाठी निर्माण करण्यात आलेल्या पर्यटन विभागाचा विकास होवून त्याच्या अनेक शाखा भारतात आणि परदेशामध्ये निर्माण झाल्या. भारत सरकारला पर्यटनातून पैसा मिळू लागला. विदेशी पर्यटक भारतामध्ये पर्यटन करण्यासाठी येवू लागल्यामुळे विदेशी चलन भारत सरकारला मिळू लागले. ज्यामुळे कोणतीही गुंतवणुक न करता विदेशी चलनाची गरज पर्यटनामुळे पुर्ण होऊ लागली आहे. या सर्व गोष्टी भारताला मिळविण्यात आदिवासी लोककलांचाही महत्त्वाचा वाटा आहे. लोकसंस्कृती पाहण्याची आवड अभ्यासक व ज्ञानी व्यक्तीनांच असली तरी आदिवासींचे क्षेत्र नैसर्गिक रित्या समृद्ध आहेत. पर्यटकांना स्वाथ्यांच्या दृष्टीकोनातून पर्यावरणही महत्त्वाचा असतो, आणि आदिवासींच्या लोककलांमधून त्यांना ज्ञान आणि आनंदही मिळत असतो. त्यामुळे आदिवासी भागामध्ये प्रवास करणे पर्यटकांना आवडत असते. त्या भागातील लोककला वनराई, वन्यजीव, त्या भागातील आदिवासींचे जीवन इत्यादींचे अटुत नाते निर्माण झालेले असते हेच पर्यटकांना लुभावनारे असते.

भारत सरकार आदिवासी लोकसंस्कृती टिकवून ठेवण्यासाठी प्रयत्न करते. त्यासाठी त्यांच्या भागामध्ये कमीत - कमी हस्तक्षेप होईल असे कायदे करताना दिसून येते. कारण आदिवासी क्षेत्र निसर्ग रम्य क्षेत्र आहे. त्यातच अशा वातावरणात असणारी आदिवासींची संस्कृती त्या ठिकाणी जाणाऱ्यांना चक्रीत करून ठेवते. प्राचीन काळापासून चालत आलेली आदिवासीमधील लोककलांची परंपरा टिकून रहावी हा भारत सरकारचा दृष्टीकोन आहे. त्यासाठी ग्रामीण स्थरापासून तर राष्ट्रीय स्तरापर्यंत सांस्कृतिक कार्यक्रमांचे आयोजन करून आदिवासींच्या लोकसंस्कृतीचे प्रदर्शन करण्यात येते. त्यामुळे देश - विदेशातील पर्यटकांना या लोककलांची माहिती मिळते. त्यातून भारतातील आदिवासींच्या या लोककला प्रत्यक्ष पाहण्याची आवड पर्यटकांमध्ये निर्माण होते आणि पर्यटक आदिवासी भागामध्ये येतात. भारतातील पर्यटन विकासाला स्वातंत्र्यापूर्वीच सुरुवात झालेली होती. विकसनशिल देशांना पर्यटनाच्या विकासावर जोर द्यावा लागतो. कारण त्यांना विकसीत होण्यासाठी परकीय चलन प्राप्त करणे गरजेचे असते. त्या बरोबर आपल्या देशातील तरुणांना रोजगार उपलब्ध करून देणे हे उद्दिष्ट असते. त्यासाठी पर्यटन विकास हा त्यावरचा उत्तम उपाय असतो स्वातंत्र्यानंतर भारत सरकारने विकासाला गती देण्यासाठी इ. स. १९६७ मध्ये भारतीय पर्यटन व नागरी हवाई वाहतुक मंत्रालय स्थापन करण्यात आले. भारतीय पर्यटन विकास महामंडळाचे अनेक केंद्र भारताच्या विविध राज्यात निर्माण करण्यात आले. त्या बरोबरच इंग्लंड, फ्रान्स, जर्मनी, अमेरिका इत्यादी देशामध्ये भारतीय पर्यटन विकास महामंडळाने आपले केंद्र स्थापन केले. आदिवासींच्या या लोककलांचे पर्यटन विकासात महत्त्व लक्षात घेवून परदेशातील स्थापन करण्यात आलेल्या पर्यटन केंद्रातून परदेशात या लोककलांचा प्रसार करण्यात येतो. महाराष्ट्र पर्यटन विकास महामंडळाची स्थापना १९७५ साली झाली. या मंडळाने महाराष्ट्रातील पर्यटन विकासाला चालना देण्यासाठी महाराष्ट्रातील पर्यटनीय क्षेत्राच्या जाहीराती करित असते. त्यामध्ये महाराष्ट्राच्या आदिवासी भागातील कोणत्या लोककला प्रसिद्ध आहेत. त्यांची माहिती पर्यटकांना पुरविण्यात महत्त्वाचे योगदान देते. महाराष्ट्राच्या पर्यटन विकासात कोकण, नंदुरबार, मेळघाट, गडचिरोली इत्यादी आदिवासी क्षेत्रातील लोककलांनी महत्त्वाचे कार्य केले आहे. परंतु आधुनिक काळात आदिवासींमध्ये होत असलेल्या शिक्षणाच्या प्रसारामुळे आदिवासींमधील तरुण वर्ग या लोककलांकडे मागासलेपणाचे लक्षण आहेत. ह्या दृष्टीने पाहत असतो. त्यामुळे या लोककला लोप पावण्यांच्या स्थितीमध्ये आहेत. दिवसेंदिवस लोककलांना सादरीकरणाचे प्रमाण आदिवासी भागामध्ये कमी होत चालले आहे. आज लोककला आदिवासींच्या रोजच्या जीवनाचा भाग राहिलेल्या नाहीत. आदिवासी सामुहीक मेळावे, यात्रा, सामुहिक विवाह सोहळे, आराध्य स्थळांशी संबंधीत धार्मिक उत्सव इत्यादी वेळेला आदिवासी या लोककला सादर करतात. त्यामुळे पुढील काळात पर्यटनामध्ये या लोककलांचे महत्त्व लक्षात घेवून त्यांच्या सुरक्षितेसाठी अधिक प्रयत्न करणे आवश्यक आहे. ज्यामुळे या लोककलांची भारतीय पर्यटन विकासाला गती देण्यात मदत होईल.

मुल्यमापन :-

आधुनिक काळात ज्ञान, मनोरंजन, रोजगार, परकीय चलन, आंतरराष्ट्रीय संबंध, राष्ट्रीय एक्य इत्यादी दृष्टीकोनातून पर्यटनाला महत्त्वपूर्ण स्थान आहे. त्यासाठी पर्यटनाचा विकास करणे आवश्यक आहे. आणि पर्यटनाच्या विकासासाठी पर्यटकांना आकर्षित करणाऱ्या भारतातील प्रत्येक बाबींना महत्त्व देणे आवश्यक आहे. आदिवासी चित्रकला, लोकगीते, लोकनृत्य इत्यादी लोककला पर्यटनाच्या विकासासाठी

आवश्यक आहेत. कारण या लोककलामधील ऐतिहासिक परंपरा, आदिवासींच्या लोकसंस्कृतीचे दर्शन ह्या गोष्टी पर्यटकांना आदिवासी भागामध्ये स्थलांतरित होवून वास्तव्याला येण्यास भाग पाडतात. पर्यटकांच्या भेटीमुळे आणि त्यांच्या वास्तव्यामुळे त्यांना भारतातील आदिवासींच्या संस्कृतीची माहिती होते. त्यांचा इतिहास समजण्यास मदत होते. त्यामुळे परकीय देशामध्ये भारताच्या संदर्भामध्ये जो गैरसमज असतो तो दुर होतो. त्यातून आंतरराष्ट्रीय संबंध निर्माण होण्यास मदत होते. आणि देश - विदेशातील पर्यटक कोणतीही भीती न बाळगता भारतातील आदिवासी क्षेत्रामध्ये पर्यटन करण्यासाठी येतात. त्यामुळे पर्यटनाचा विकास होण्यास मदत होते. आदिवासी लोककलांनी भारताच्या संस्कृती संवर्धनाबरोबर पर्यटन व्यवसायातून ज्ञान, मनोरंजन, रोजगार, परकीय चलन, राष्ट्रीय ऐक्य, आंतरराष्ट्रीय संबंध निर्माण करण्यात महत्त्वाचे योगदान दिलेले आहे.

संदर्भग्रंथ सूची

- १) डॉ. कठारे आणि इतर, पुरातत्त्व विदय वस्तुसंग्रहालय शास्त्र आणि पर्यटन, विदया बुक पब्लिशर्स, औरंगाबाद, २०११ पृ. क्र. २१०
- २) मडावी एस. एन. गोंडवानाचा सांस्कृतिक इतिहास, सुधीर प्रकाशन, वर्धा, प्रथमावृत्ती मे. २०११ पृ. क्र. ११०
- ३) डॉ. बोरकर र. रा. चंद्रपूर - गडचिरोली जिल्ह्याचे पुरातत्त्व, सुयश प्रकाशन, नागपुर, प्रथमावृत्ती २००९ पृ. क्र. ३४
- ४) डॉ. टेंभेकर नलिनी खे., पूर्व विदर्भातील ऐतिहासिक व प्रेक्षणीय स्थळे, पिंपळापूरे बुक डिस्ट्रीब्युटर्स, नागपूर पृ. क्र. २४१
- ५) मडावी एस. एन. गोंडवानाचा सांस्कृतिक इतिहास पृ. क्र. १००
- ६) lok kala in hindi
- ७) lok kala in hindi
- ८) मडावी एस. एन. गोंडवानाचा सांस्कृतिक इतिहास पृ. क्र. ११०
- ९) भुसारे एम. एल. आदिवासी लोकगीतांतील स्त्री दर्शन, आदिवासी समाज, राष्ट्रीय चर्चासत्र, पंकज महाविद्यालय, चोपडा, २०१५ पृ. क्र. ३५
- १०) मडावी एस. एन. गोंडवानाचा सांस्कृतिक इतिहास पृ. क्र. १००
- ११) जोशी अतुल व इतर, भारत मे. आधुनिक पर्यटन, रावत पब्लिकेशन, जयपूर पृ. क्र. १७.

A Review on Superhydrophobic Surfaces: Fundamentals, Fabrications and Applications

Mehejbin R. Mujawar¹, Rajesh B. Sawant¹, Govind D. Salunke¹, Rajaram S. Sutar², Sanjay S. Lathe³, Ankush M. Sargar⁴, Raghunath K. Mane⁵, Krishna K. Rangar¹, Shivaji R. Kulal^{1*}

¹ Department of Chemistry, Raje Ramrao Mahavidyalaya, Jath, Dist. - Sangli (MS) India

² Self-cleaning Research Laboratory, Department of Physics, Raje Ramrao Mahavidyalaya, Jath, Dist. - Sangli (MS) India.

³ Self-cleaning Research Laboratory, Department of Physics, Vivekanand College (Autonomous), Kolhapur, Dist. - Kolhapur (MS) India.

⁴ Department of Chemistry, Bharati Vidyapeeth's Dr. Patangrao Kadam Mahavidyalaya, Sangli, Dist. - Sangli (MS) India

⁵ Department of Chemistry, Smt. Kusumtai Rajarambhapu Patil Kanya Mahavidyalaya, Islampur, Dist. - Sangli (MS) India

*Corresponding author's E-mail: srkulal@gmail.com, amsargar2012@gmail.com

Abstract

Superhydrophobic surfaces are highly hydrophobic i.e., it extremely difficult to wet. Superhydrophobic surfaces are the tendency to repel water drops and absorb oil drops. The water contact angle of superhydrophobic surfaces is greater than 150° , the oil contact angle is less than 5° , and the sliding angle is less than 5° . It is showing the lotus effect. Superhydrophobicity is observed in the lotus leaves, insects, and some other plants in which their leaves would not get wet. This phenomenon is due to the unique surface structure of the lotus leaf and also the presence of a low surface energy material on the surface of the leaf. For the formation of a superhydrophobic surface, the surface must show hierarchical micro- and nano-roughness and low surface energy. Efforts have been taken to form superhydrophobic surfaces for a variety of applications. There are many applications of superhydrophobic surfaces such as self-cleaning surfaces, oil-water separation surfaces, anti-icing surfaces, anti-corrosion surfaces, anti-fogging surfaces, and water-resistant surfaces. In this article, the fundamental principles of superhydrophobic surfaces, some recent trends in the fabrication of superhydrophobic surfaces, and their applications are reviewed and discussed.

Keyword: Superhydrophobicity, Superoleophobicity, Lotus effect, Self-cleaning, Oil-water separation, Water-repelling, Oil Contact Angle, Water Contact angle, Anti-icing, Anti-corrosion.



SHIVAJI UNIVERSITY, KOLHAPUR

Volume-49 Issue-1 (January, 2023)

ISSN-Science-0250-5347

Estd. 1962
"A++" Accredited by NAAC (2021)
with CGPA 3.52



JOURNAL OF SHIVAJI UNIVERSITY : SCIENCE AND TECHNOLOGY

(Peer Reviewed Journal)

Journal of Shivaji University: Science and Technology
Volume-49, Issue-1 (January,2023)
INDEX

Sr. No.	Title of Research Article with Name of Author/s	Page No.
1.	Synthesis and Characterization of g-C₃N₄ Decorated ZnONanorods and their Binder Free Deposited Photoanodes for Photoelectrochemical Water Splitting Studies Pramod A. Koyale, Prakash S. Pawar, Swapnajit V. Mulik, Vijay S. Ghodake, Amol B. Pandhare, Ankita K. Dhukate, Sagar D. Delekar	1
2.	Thiamine Hydrochloride (VB₁) Catalyzed Synthesis of 5-aryl-4-phenyl-1,2,4-triazolidine-3-thiones in Aqueous Medium Pradeep P. Patil, Prasad M. Swami, Shankar P. Hangirgekar, Sandeep A. Sankpal	10
3.	Evaluation of Acute Toxic Effect of Gallic Acid Loaded Eudragit's 100 Nanoparticles on <i>Artemia Salina</i> Brine Shrimp Bioassay Poornima S. Sankpal, Sachinkumar V. Patil, Sayali S. Patil	20
4.	Surface Modifications of Binder Free ZnONanorod Thin Films through Cds Quantum Dots for Dye Sensitized Solar Cells Krantiveer V. More, Anant G. Dhodamani, Sajid B. Mullani, Tukaram D. Dongale, Prakash S. Pawar, Satish M. Patil, Sunil J. Kadam, Sagar D. Delekar	36
5.	Review on Candle Soot based Superhydrophobic Surfaces for Oil-Water Separation Mehejbin R. Mujawar, Rajesh B. Sawant, Amol B. Pandhare, Prashant D. Sanadi, Sanjay S. Latthe, Ankush M. Sargar, Raghunath K. Mane, Shivaji R. Kulal	50
6.	A Review on Current Advancements in Magnetic Nanomaterials for Magnetic Hyperthermia Applications Amol B. Pandhare, Prakash S. Pawar, Vijay S. Ghodake, Swapnajit V. Mulik, Pramod A. Koyale, Ankita K. Dhukate, Deepak B. Mohite, Karishma V. Shikhare, Rajendra P. Patil, Sagar D. Delekar	62
7.	One-Step Synthesis of Biomass-Derived Carbon Dots: Study of Optical Properties Akanksha G. Kolekar, Omkar S. Nille, Shubham J. Kumbhar, Priyanka S. Mahadar, Sayali B. Lohar, Govind B. Kolekar, Gavisiddappa S. Gokavi, Vishalkumar R. More	87
8.	Synthesis and Characterization of Plant-Mediated CuO Nanoparticles Omkar S. Nille, Harshad A. Mirgane, Sneha V. Koparde, Akanksha G. Kolekar, Ashlesha R. Pawar, Pallavi J. Pawar, Abhishek A. Waghmode, Tanaji R. Dhage, Vijay S. Ghodake, Prasad M. Swami, Sarita D. Shinde, Govind B. Kolekar	95

Review on Candle Soot based Superhydrophobic Surfaces for Oil-Water Separation

Mehejbin R. Mujawar^{a,*}, Rajesh B. Sawant^a, Amol B. Pandhare^{b,f},
Prashant D. Sanadi^g, Sanjay S. Latthe^c, Ankush M. Sargar^d,
Raghunath K. Mane^e, Shivaji R. Kulal^{a,*}

^aDepartment of Chemistry, Raje Ramrao Mahavidyalaya, Jath, Sangli 416 404 (MS) India.

^bDepartment of Chemistry, Shivaji University, Kolhapur 416 004 (MS) India.

^cDepartment of Physics, Vivekanand College, Kolhapur 416 003 (MS) India.

^dDepartment of Chemistry, Bharati Vidyapeeth's Dr. Patangrao Kadam Mahavidyalaya, Sangli 416 416 (MS) India.

^eDepartment of Chemistry, Smt. Kusumtai Rajarambhapu Patil Kanya Mahavidyalaya, Islampur, Sangli 416 409 (MS) India.

^fDepartment of Chemistry, M.H. Shinde Mahavidyalaya, Tisangi, Gaganbavda, Kolhapur 416 206 (MS) India.

^gDepartment of Engginring, Chemistry, Institute of Technology's College of Engineering (Autonomous), Kolhapur 416 234 (MS) India.

*Corresponding authors: srkulal@gmail.com and mehejabeenmujawar@gmail.com

ABSTRACT

Over the many years, the oceanic oil spill accidents and most industries worldwide discharging immense levels of oil in the surroundings is a serious problem for the environment. There is a need to develop technology for oil-water separation because the spilled oil affects the ecological and environmental system. Candle soot nanoparticles are hydrophobic (water repellent) in nature and has the advantages of cost-effectiveness and production scalability over other carbons like graphene, Carbon Nanotubes (CNTs), Carbon Nanodots (CNDs), etc. in their synthesis. Candle soot based superhydrophobic materials have outstanding water repulsion and oil absorption capacity, highly selectivity, chemical inertness and excellent recyclability. In this paper, we discuss applications of candle soot based superhydrophobic materials applied on sponge and mesh substrates for oil-water separation.

KEYWORDS

Carbon Nanotubes, Carbon Nanodots.

.....

1. INTRODUCTION

The oil spilling and discharge of industrial organic solvents causes several damages to water resources and aquatic ecosystems [1-3], which became a global problem and need to solve it urgently to save the ecosystems. A new technology in material science has been developed for oil-water separation using superhydrophobic nanomaterial. As like the lotus leaf, superhydrophobic surface having water contact angle greater than 150° and oil contact angle near 0°[4]. Different chemical methods

are used for the fabrication of the superhydrophobic mesh/sponge for efficient oil-water separation. As the carbon nanoparticles are hydrophobic in nature, it shows strong affinity toward oil. At the same time, huge amount of candle soot waste is produced. Undoubtedly, it is of great benefit to turn candle soot waste into high value oil absorbent materials [5]. The superhydrophobic mesh/sponge exhibited high selectivity toward different oil and organic pollutants, fast and efficient oil-water separation capability, good repeatability, good reusability, mechanically stable, chemically stable and thermally stable [6]. Candle soot-based absorbents demonstrate superior efficiency in the removal of oils. However, the high production costs of carbon nanotube[7], graphene[8], activated carbon [9], expanded graphite [10], etc. So, these absorbents limit their wide adoption at large scale. Candle soot (CS) generated from incomplete combustion of paraffin wax has demonstrated the advantages of cost effectiveness and production scalability over CNTs, graphene and activated carbons in their synthesis [11]. However, candle soot coated superhydrophobic materials are the best solution from these. The superhydrophobic surfaces on which water achieves water contact angle higher than 150° and sliding angle less than 5° are attracting minds of researchers due to their efficient oil-water separation abilities [12-14]. J. Song et al. [15] fabricated CS-coated mesh by using dip-coating method. The cleaned stainless-steel mesh (SSM) was dipped in the glue solution for 10 min and then dried at 80°C to obtain the CS-glue coated mesh. The CS coating is close packed because of using superglue as a binder. The CS-glue coated mesh revealed the separation efficiency higher than 99.95%. Even after 20 cycle separation tests, it was shown superior reusability and durability. Li et al. [16] prepared the hydrophobic CS by incomplete combustion of hydrocarbons from the middle of candle flame. The PU sponge dipped in the solution of CS, SiO_2 and PU resin to achieve stable superhydrophobicity. The CS- SiO_2 -PU sponge showed excellent oil-water separation efficiency. The CS- SiO_2 -PU sponge was also shown superior separation efficiency from hot water, acidic solutions, alkaline solutions and salt solutions. Zulfiqar et al. [17] deposited cheaply available sawdust on polychloroprene adhesive-coated stainless-steel mesh with deposition of silicone polymer by using dip-coating method. Then, a thin layer of CS particle was applied on the prepared stainless-steel mesh by simply holding it above a candle flame. The CS particles get uniformly deposited on silicone covered sawdust which exhibited highly rough and porous morphology required for superhydrophobicity. It showed excellent oil-water separation efficiency greater than 95% which showed its recyclability, reusability and mechanical stability. In this article, we will mostly discuss on the simple, low-cost, rapid and innovative methods for the fabrication of superhydrophobic/superoleophilic CS coated sponges/meshes for efficient oil-water separation application.

2. SUPERHYDROPHOBIC-SUPEROLEOPHILIC SURFACES FOR OIL-WATER SEPARATION

2.1 Oil-water separation using Superhydrophobic-superoleophilic sponges

2.1.1 Highly efficient carbon soot sponge

The CS particles obtained from ethylene-oxygen combustion flame with flow rate of 5:3. These CS particles were dispersed in 1, 2-dichloroethane followed by sonication. The sponge was dipped in CS dispersion solution to attain superhydrophobic sponge. The superhydrophobic sponge achieved by a uniform coating of as-grown CS particles onto the porous skeleton through simple immersion in CS dispersion. The CS-modified sponge exhibited excellent oil-water separation efficiency without further chemical modification. The fast and easy recovery of engine oil floating on the water surface by CS-modified sponge confirms its high oil-water separation efficiency. The CS-sponge was shown an absorption capacity in the range of 25-80 times its original weight. The absorption capacity of the CS-sponge does not show severe degradation after 10 cycles which indicating a highly stable absorption performance of CS-sponge. After 10 cycles which indicating a highly stable absorption capacity is kept for CS-modified sponge, which much higher than that of the CS-sponge [18].

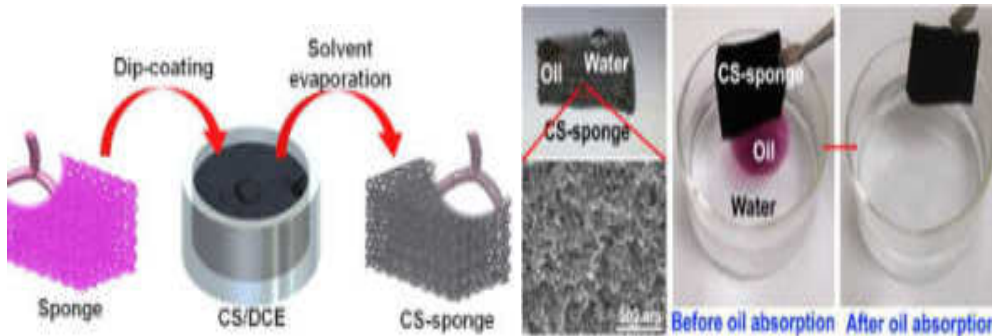


Figure-1. Schematic showing the carbon soot-sponge preparation by dip-coating and carbon soot sponge before & after oil absorption. Images reprinted from [18], with permission from American Chemical Society, Copyright 2014.

2.1.2 Recyclable superhydrophobic straw soot sponge

The straw soot on the glass slide was collected by shaving soot from the glass using a spatula. The colloidal suspension of CS was prepared by simply mixing the soot in ethanolic medium. The sponge was dipped into straw soot solution by using dip-coating method to form superhydrophobic sponge. The modified sponge was shown the water contact angle up to 154° . This superhydrophobic sample had good hydrophobic stability even in acidic condition and it can show the efficient oil-water separation. The amount of the absorbed oil was about 30 times of sponges own

weight which can be shown that the evaluation of the mass based on absorption capacity. The absorption capacity based on density, viscosity and surface tension of the absorbed liquids. This superhydrophobic sponge shows highly recyclability. The experiments demonstrate that the sponge can absorb the oil more than 30 cyclic applications without any significant change in the absorption. This method shows the benefits of easy preparation using natural soot source, better performance, oil absorption in a very short time in comparison with previous works [19].

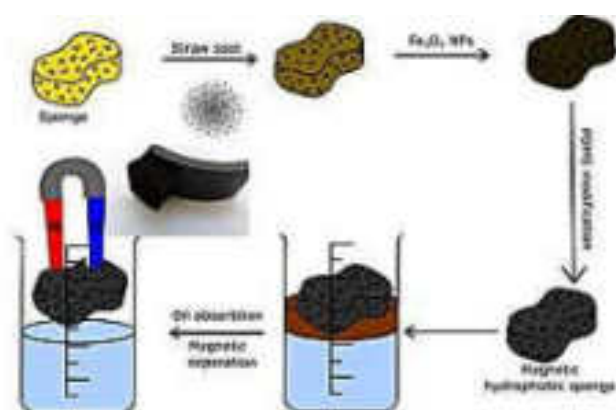


Figure-2. Schematic illustration of preparation of modified polyurethane sponge and oil separation process. Images reprinted from [19], with permission from Elsevier, Copyright 2017.

2.1.3 Durable PVDF/CS sponge

The superhydrophobic surface was fabricated by using PVDF and candle soot via sugar template method. It was shown the water contact angle of 158.3° and roll on angle of 6.7° . The oil quickly absorbed by superhydrophobic sponge which can be shows the superoleophilic property of superhydrophobic sponge. The solar value of candle soot is up to 99.4% which shows excellent light absorbing property. The sponge shows excellent oil-water separation property even after 25 cycles without destroying the sponge. The strong elasticity & high stretch resistance confirms that the modified superhydrophobic surface is highly mechanical durable. The modified sponge maintains the 89% of recovery rate even after 10 cycles. The absorption capability recovered up to 96% without obvious change of morphology of the sponge surface. This method was used to prepare a photothermal & porous PVDF/CS sponge with structural, chemical and mechanical property. It was shown high photothermal property.

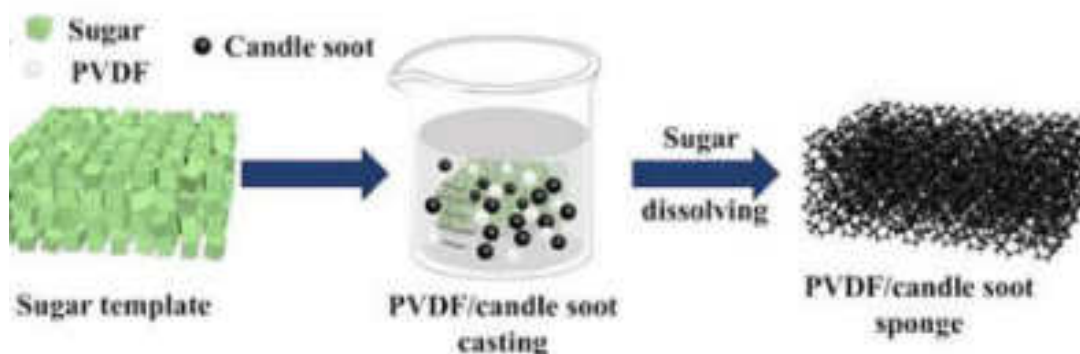


Figure-3. Schematic illustration of the fabrication of porous PVDF/candle soot sponge using sugar template. Images reprinted from [20], with permission from Elsevier, Copyright 2021.

2.2 Oil-water separation using superhydrophobic-superoleophilic meshes

2.2.1 Superhydrophobic SiO_2 /Carbon mesh

The candle soot was collected on the surface of stainless-steel mesh by placing the mesh above the wick of candle. Then by using chemical vapour deposition method the SiO_2 /carbon layer deposited on stainless steel mesh. Modify this mesh by using PFOTS and PDPA-PFO respectively to form the superhydrophobic and superoleophilic mesh membrane. This modified superhydrophobic stainless steel mesh exhibits excellent repellence for all the tested strong acids, strong bases and saturated salts, indicating a good stability of modified mesh under a series of hard environment. The separation efficiencies obtained repeatedly even after 15 cycles without any noticeable deterioration. Both superhydrophobic and superoleophilic modified stainless steel mesh membranes shows stability, durability and reusability. The SiO_2 /Carbon modified stainless steel mesh indicates good material for treating real oil-polluted water in different practical applications as well as in oil spill clean-up. This method shows higher performance, oil-water separation in a short time and repeatedly in comparison with earlier works [20].

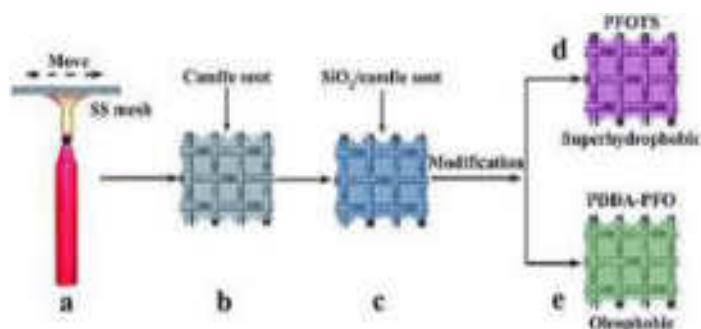


Figure-4. Process of superhydrophobic and oleophobic mesh membranes preparation: (a) coating stainless steel mesh with carbon nanoparticle (candle

soot), (b) carbon nanoparticle coated stainless steel mesh, (c) SiO₂/carbon stainless steel mesh, (d) PFOTS modified SiO₂/carbon stainless steel mesh, (e) PDDA–PFO modified SiO₂/carbon stainless steel mesh. Images reprinted from [21], with permission from Royal Society of Chemistry, Copyright 2017.

2.2.2 Durable PDMS-CS based superhydrophobic mesh

The candle soot was deposited on stainless steel mesh by simply placed above the candle flame for 15 sec. Then this CS coated stainless steel mesh was dipped in solution of PDMS & Xylene for 10 min by using immersion method. After that same process will be carried out for deposition of candle soot on this modified stainless-steel mesh was prepared. It shows 156° water contact angle & nearly 0° oil contact angle. Also, it shows 3° sliding angles. It shows higher water contact angle even after 10 times tests of oil-water separation. The oil-water separation efficiency was nearly 91% by using this modified superhydrophobic stainless steel mesh. It exhibits high thermal stability, good corrosion resistance and reusability. It was modified though combine mesh & polymer foam the composite adsorbent material successfully separate the oil from water via magnet drive method. This modified method was very useful than other research work. So, it was very useful than any other works [21].

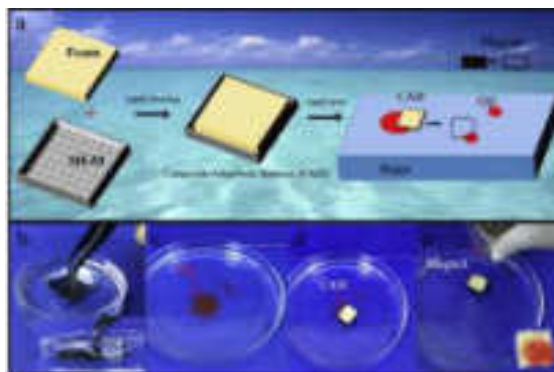


Figure-5. a) Schematic for the preparation process of composite adsorbent material (CAM) from the SH-M square boat and polymer foam, as well as its application of magnet drive for oil/water separation; b) SH-M square boat immersion in water by force; c–e) picture of the magnet drive CAM oil adsorption process. Images reprinted from [22], with permission from Progress in Organic Coatings, Copyright 2019.

2.2.3 CS templated superhydrophobic silica coating on SS mesh

The superhydrophobic coating was prepared through placing the cleaned substrate over candle flame until a few microns thick layer of candle soot deposited on

stainless steel mesh. The candle soot coated substrate together with SiCl_4 was placed in a drier for chemical vapour deposition. Then, though calcination at $600\text{ }^\circ\text{C}$ for half in air, CS composed NPs thermally degraded and diffused through the silica shell gradually. It shows highly oil-water separation efficiency even after 30 times cycle separation superhydrophobic surface remained. The superhydrophobic coating revealed excellent separation efficiency even after 6 times reuses of same superhydrophobic material. It could be potentially used in optical and visual application scenarios where in harsh & oily environments, like goggles, building façade, visual oil-water separation device & touch screen, etc. Among the all-other research work it shows tremendous oil-water separation properties [22].

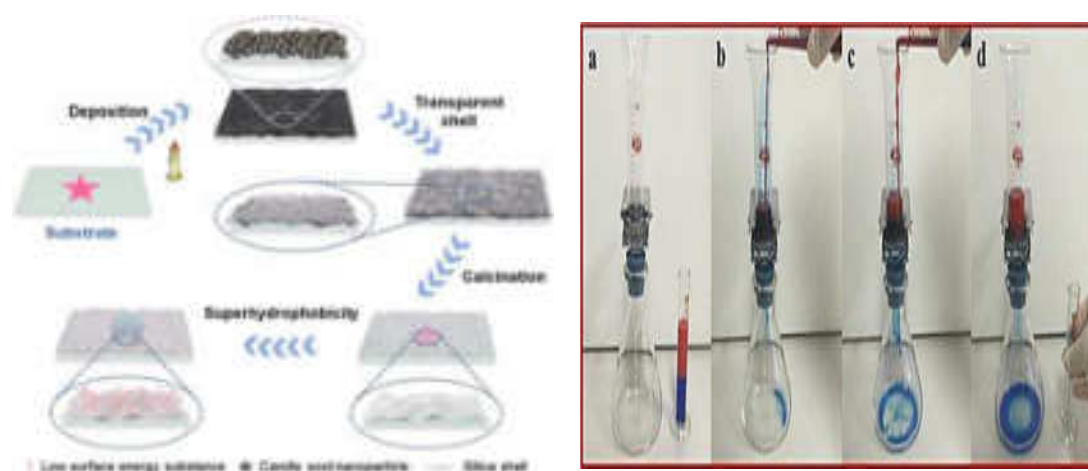


Figure-6. Schematic of preparation and properties of the transparent and robust superhydrophobic coating and oil–water separation. Images reprinted from [23], with permission from Nature, Copyright 2022.

3.CONCLUSION

As this review highlights, candle soot nanoparticles are unique in that, their fabrication requires little control of external parameters. It is very economical beneficial, facile and straightforward to synthesize. Candle soot coated sponge/mesh for use in oil-water separation has been developed by using CS-nanoparticles and different polymers. The candle soot synthesis, candle soot coated sponge/mesh preparation, procedures are simple, cost-effective and scalable. The absorption/separation investigation demonstrates that, the candle soot sponge/mesh is highly efficient and stable in absorbing a wide range of oil and organic solvents. It can be believed that, the candle soot coated superhydrophobic materials are very useful for oil-water separation. It shows various tremendous results with candle soot-

polymer composite in various mechanical conditions. A candle soot nanoparticle shows significant surface area to volume ratio, high electronic and ionic conductivity. Candle soot is produced by simply burning of candles and hence, it is ecofriendly, economical and useful. Candle soot coated sponge/mesh can show stability, durability, reusability and reproducibility.

ACKNOWLEDGEMENT

This work was supported by Department of Chemistry and Department of Physics, RajeRamrao Mahavidyalaya, Jath. We also acknowledge Prof. (Dr.) Suresh S. Patil, Principal, RajeRamrao Mahavidyalaya, Jath.

REFERENCES

1. Yao, T.,Zhang, Y.,Xiao, Y.,Zhao, P.,Li, G.,Yang, H., Li, F.(2016) *Journal of Molecular Liquids*, 218, 611–614.
2. Bi, H., Xie, X., Yin, K., Zhou, Y., Wan, S., He, L., Xu, F., Banhart, F., Sun, L., Ruoff, R.S. (2012) *Advanced Functional Materials*, 22, 4421-4425.
3. Cong, H.P., Ren, X.C., Wang, P., Yu, S.H. (2012) *American Chemical SocietyNano*, 6, 2693-2703.
4. Li, L., Li, B., Dong, J., Zhang, J. (2016) *Journal of Materials Chemistry A*, 4, 13677-13725.
5. Gao, J., Huang, X., Xue, H., Tang, L., Li, R.K. (2017) *Chemical Engineering Journal*, 326, 443-453.
6. Bayat A., Aghamiri, S. F., Moheb, A.,Vakili-Nezhaad, G. R.(2005) *Chemical Engineering & Technology*, 12, 28-40.
7. Li, J., Zhu, L.,Luo, Z.(2016) *Chemical Engineering Journal*, 287, 474-481.
8. Wu, Z., Li, C., Liang, H., Zhang, Y.,Wang, X., Chen, J.,Yu, S. (2014) *Scientific Reports*, 4, 4079.
9. Bi, H., Xie, X., Yin, K., Zhou, Y., Wan, S., He, L., Xu, F., Banhart, F.,Sun, L.,Ruof, R. S.(2012), *Advanced Functional Materials*, 22, 4421-4425.
10. Sam, E. K., Sam, D. K., Lv, X., Liu, B., Xiao, X., Gong, S., Yu, W., Chen, J., Liu, J.(2019) *Chemical Engineering Journal*, 19, 3012-3018.
11. Zulfiqar, U., Hussain, S. Z., Subhani, T., Hussain, I., Rehman, H.(2018), *Colloids and Surfaces A: Physicochemical and Engineering Aspects*, 539, 391–398.
12. Gao, Y., Zhou, Y. S., Xiong, W., Wang, M., Fan, L., Golgir, H., Jiang, L., Hou, W., Huang, X., Jiang, L., Silvain, J.,Lu, Y. F. (2014) *ACS Applied Materials & Interfaces*, 6, 5924–5929.
13. Ren, G., Song, Y., Li, X., Zhou, Y.,Zhang, Z., Zhu, X.(2018) *Applied Surface Science*, 428, 520-525.





14. Choi, S., Kwon, T., Im, H., Moon, D., Baek, D., Seol, M., Duarte, J., Choi, Y.(2011) *ACS Applied Materials & Interfaces*, 3, 4552–4556.
15. Song, J., Na, L., Li, J., Cao, Y., Cao, H.(2022) *Nanomaterials*, 12, 761-775.
16. Li, J., Zhao, Z., Kang, R., Zhang, Y., Lv, W., Li, M., Jia, R., Luo, L.(2017)*Journal of Sol-Gel Science and Technology*, 3, 817–826.
17. Zulfiqar, U., Hussain, S., Subhani, T., Hussain, I., Rehman, H.(2018) *Colloids and Surfaces A: Physicochemical and Engineering Aspects*, 539, 391–398.
18. Gao, Y., Zhou, Y., Xiong, W., Wang, M., Fan, L., Rabiee-Golgir, H., Jiang, L., Hou, W., Xi, H., Jiang, L., Silvain, J., Lu, F.(2014) *ACS Applied Materials & Interfaces*, 6, 5924–5929.
19. Beshkar, F., Khojasteh, H., Niasari, M.(2017) *Journal of Colloid and Interface Science*, 497, 57–65.
20. Liu, D., Yu, Y., Chen, X., Zheng, Y.(2017) *RSC Advances*, 7, 12908–12915.
21. Zhang, R., Zhou, Z., Ge, W., Lu, Y., Liu, T., Yang, W., Dai, J. (2020) *Chinese Journal of Chemical Engineering*, 5, 30292-30294.
22. Chen, B., Zhang, R., Fu, H., Xu, J., Jing, Y., Xu, G., Wang, B., Xu, H.(2022)*Scientific Reports*, 8, 1-9.



Colloids and Surfaces A: Physicochemical and Engineering Aspects

Volume 657, Part B, 20 January 2023, 130561

Facile approach to fabricate a high-performance superhydrophobic PS/OTS modified SS mesh for oil-water separation

Rajaram S. Sutar^a, Sanjay S. Latthe^b  , Nilam B. Gharge^a, Pradip P. Gaikwad^a, Akshay R. Jundle^a, Sagar S. Ingole^a, Rituja A. Ekunde^a, Saravanan Nagappan^c, Kang Hyun Park^c, Appasaheb K. Bhosale^a, Shanhu Liu^d  

Show more 

 Share  Cite

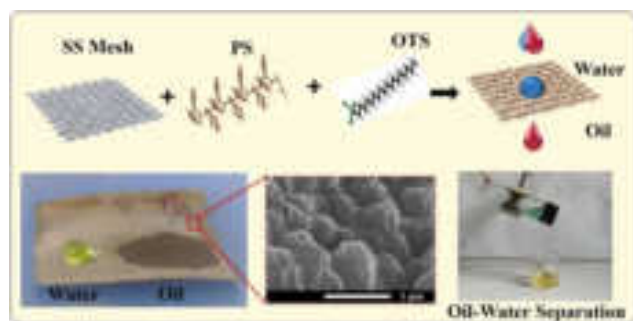
<https://doi.org/10.1016/j.colsurfa.2022.130561> 

[Get rights and content](#) 

Abstract

Special wetting materials have been used for the oil and water separation due to their different interfacial attraction of oil and water. Herein, we successfully fabricated superhydrophobic coatings on stainless steel (SS) mesh by depositing successive layers of polystyrene (PS) and octadecyltrichlorosilane (OTS) through the dip-coating method. The as-prepared coating showed a water contact angle (WCA) of $157.5 \pm 2^\circ$, a rolling angle of $6 \pm 2^\circ$ and an oil contact angle (OCA) of around 0° . The surface microstructure analysis of the coating revealed a regular pattern of microscale bumps with nanoscale folds on it, both of which improve the overall superhydrophobicity of the surface. The capacity of coatings to separate oil and water was examined by employing a variety of mixtures of oil and water, including petrol, diesel, kerosene, vegetable oil, and coconut oil. In case of low viscosity oil, the coated mesh demonstrated separation effectiveness of more than 97% and on the other hand, high viscosity oil demonstrated just 89% efficiency. Low viscosity oils showed a greater permeation flux through the mesh than extremely viscous oil. The mechanical strength of the coating was examined using bending, twisting, adhesive tape testing, sandpaper abrasion tests, and the findings indicated that coated mesh had exceptional mechanical resilience. In addition, the developed superhydrophobic mesh demonstrated excellent thermal stability and self-cleaning properties. Therefore, this superhydrophobic/superoleophilic mesh has a significant deal of application potential in practical.

Graphical Abstract



[Download : Download high-res image \(229KB\)](#)

[Download : Download full-size image](#)

Introduction

Oil spills and industrial effluents inflict significant harm to the ecosystems of the seas, human health, and the surrounding environment [1], [2]. The safe and responsible disposal of wastewater containing oil has been shown to be a challenging problem on a global scale. Many approaches have been used for the treatment of oil-water pollution, including oil skimmers, filtration, oil-absorbing materials, magnetic separations, centrifugal machine, flotation technologies, and combustion [3], [4], [5]. Traditional methods have various drawbacks, including limited separation efficiency, time consumption, cost-effectiveness, and the generation of secondary pollutants [6], [7], [8]. Therefore, cutting-edge technologies are an absolute necessity for the disposal of oily wastewater and the protection of the environment. Many efforts have been reported in the fabrication of separation membranes with controlled surface wetting property [9], [10]. The utilization of bio-inspired superhydrophobic materials in oil-water separation processes is a popular area of study due to its high water repellency and ability to allow oil to enter in it [4], [11], [12]. Therefore, superhydrophobic materials have been added to commercially available cotton textiles, 3D porous materials, different polymer membranes, filter papers, and metal meshes for considerable oil-water separation [13], [14]. Chemical etching [15], [16], spray deposition [17], [18], dip coating [19], hydrothermal method [20], sol-gel processing [21], [22], chemical vapor deposition [23], electrospinning [24], [25], and layer by layer [26] methods have been used for modification of porous surfaces. Among these, dip-coating is a quick and effective method of producing bulky, intricately formed products [27]. Metal meshes have sparked a lot of attention since they are long-lasting, reusable, and may be used in industry [2], [23]. Porous materials can absorb or filter liquids, and when their surface structure is adjusted with a specific wettability material, they can help separate oil or water from oil-water mixtures [28], [29]. Numerous types of porous metal meshes, including those constructed of nickel, copper, and stainless steel (SS), among other materials were used for oil-water separation [30], [31], [32], [33]. Among them, SS meshes have found widespread use for oil-water separation owing to their high electrical and electrothermal capabilities as well as their superior resistance to thermal shock [33].

OTS has been used to tune the surface wettability of porous substrates so that oil and water can be effectively separated. The OTS has low surface energy, hence it improves the hydrophobicity of the rough surface and also shows high oil absorption capacity [35], [36]. Li et al. [34] recently made superhydrophobic SS mesh by spraying it with a mixture of OTS-modified SiO₂ nanoparticles and waterborne PU. This superhydrophobic mesh was able to separate a mixture of kerosene and water at a rate of 98.3%. Latthe et al. [27] created a superhydrophobic surface by varying the concentration of OTS in PS solution and the number of dipping cycles. At first, they prepared a homogenous solution containing PS and OTS using tetrahydrofuran (THF) as a solvent. The pre-cleaned glass substrate was dip-coated (4 times) on the homogenous solution and air-dried to get a superhydrophobic surface with a contact angle of $154 \pm 2^\circ$. Ke et al. [37] have built a superhydrophobic and superoleophilic sponge by immersing it in OTS solution. This kind of sponge has shown an absorption capacity of 42–68 times more than the mass of the sponge for toluene, light oil, and

methyl silicone oil. Even after being put through 50 separation cycles, this adsorption capacity remained the same. Liang et al. [38] modified a polyurethane sponge by immersing in an OTS solution for oil-water separation. Cheng et al. [24] used coaxial electrospinning with PVDF solution as a lumen solution and reactive silicon-containing monomers as the outer solution to generate superhydrophobic nanofiber membranes with hierarchical micro nano-scale morphology. The outstanding separation efficiency of 99.6% is achieved with the as-prepared asymmetric composite membrane, which has an extremely rapid permeation flux. They show a water-in-n-octane permeation flux of 17331 L/(m²h) and retain 88% of their original permeance after 20 cycles of operation [24]. Rasouli et al. [13] briefly reviewed the various aspects of fabrication of superhydrophobic/superoleophilic membranes having mesh, films, and porous substrates for efficient oil-water separation applications. In order to modify the surface energy of superhydrophobic/superoleophilic membranes, it is usual practice to use low surface energy chemicals such as fatty acids, thiols, silanes, polymers based on polyethylene, and carbon nanotubes [13]. These membranes have >99% oil separation efficiency in oil-water combinations.

In this research work, a layer of PS was first applied on SS mesh using a dip coating process, followed by an OTS dip layer to achieve superhydrophobicity. The dip coating cycles were consequently carried out by dip and dry in both PS in THF and OTS in hexane. The surface structure of a red rose petal was obtained on SS mesh. SEM and EDS were used to describe the surface morphology and chemical composition, respectively. The gravity-driven oil-water separation technique was used to determine the oil-water separation efficiency and permeation flux using a custom-made setup. The mechanical durability of superhydrophobic mesh was evaluated using adhesive tape tests, sandpaper abrasion tests, bending, twisting, and folding tests. We have achieved the contact angles of 157.5±2° for OPS-2 as well as 154±2° for OPS-3 in superhydrophobic range and a comparable contact angle of 148.5±2° for OPS-1. The stable and robust self-cleaning coating was produced by this method as compared with the reported methods.

Section snippets

Materials

Polystyrene (PS) having average molecular weight ~ 280,000 and octadecyltrichlorosilane (OTS) were obtained from Sigma Aldrich, St. Louis, MO, USA. Tetrahydrofuran (THF) and hexane were purchased from Spectrochem, Mumbai, India. Stainless steel (SS) mesh with pore sizes of about 50µm was obtained from Shanghai Titan Technology Co. Ltd. China. The petrol, diesel, kerosene (from Bharat Petroleum Corporation Limited, India), vegetable oil (from Garud, India), and coconut oil (from Parachute...

Surface morphology and chemical composition

Fig. 2(a-f) depicts the surface morphology of meshes after being treated with varying doses of OTS. At low OTS concentrations, ten successive coating layers of PS and OTS create a rougher surface with nanoscale folds, as seen in Fig. 2(a). The enlarged view shows that there is a regular micro and nanoscale rough texture, which is essential for improving hydrophobicity and can be observed in Fig. 2(d). Surprisingly, regular shaped bumps emerged after raising the OTS concentration by twofold, as...

Conclusions

In conclusion, we have successfully fabricated superhydrophobic and superoleophilic SS mesh by depositing consecutive layers of polystyrene (PS) and octadecyltrichlorosilane (OTS) using an easy and inexpensive dip coating method. This allowed us to create a superhydrophobic and superoleophilic surface on the SS mesh. The WCA of 157.5 ±

2°, the OCA of about 0°, and the rolling angle of $6 \pm 2^\circ$ were all attained by adjusting the concentration of OTS in successive layered deposition. The...

CRedit authorship contribution statement

Rajaram S. Sutar: Conceptualization, Methodology, Investigation, Writing – original draft, Writing – review & editing, **Sanjay S. Latthe:** Supervision, Writing – review & editing, Visualization, **Nilam B. Gharge:** Methodology, **Pradip P. Gaikwad:** Methodology, Investigation, **Akshay R. Jundle:** Methodology, Investigation, **Sagar S. Ingole:** Methodology, Investigation, **Rutuja A. Ekunde:** Methodology, **Saravanan Nagappan:** Formal analysis, Writing – review & editing, **Kang Hyun Park:** Validation, Investigation, ...

Declaration of Competing Interest

The authors declare that they have no known competing financial interests or personal relationships that could have appeared to influence the work reported in this paper....

Acknowledgement

This work is financially supported by DST – INSPIRE Faculty Scheme, Department of Science and Technology (DST), Govt. of India. [DST/INSPIRE/04/2015/000281]....

[Recommended articles](#)

References (54)

Y. Liu *et al.*

[Bioinspired structured superhydrophobic and superoleophilic stainless steel mesh for efficient oil-water separation](#)

Colloids Surf. A: Physicochem. Eng. Asp. (2016)

M. Bennett *et al.*

[Monitoring the operation of an oil/water separator using impedance tomography](#)

Miner. Eng. (2004)

Y. Deng *et al.*

[Recent development of super-wettable materials and their applications in oil-water separation](#)

J. Clean. Prod. (2020)

S.S. Latthe *et al.*

[Superhydrophobic surfaces for oil-water separation, in](#)

[Superhydrophobic Polymer Coatings](#)(2019)

S. Rasouli *et al.*

[Superhydrophobic and superoleophilic membranes for oil-water separation application: a comprehensive review](#)

Mater. Des. (2021)

Y. Liu *et al.*

[On-demand oil/water separation of 3D Fe foam by controllable wettability](#)

Chem. Eng. J. (2018)

R. Liao *et al.*

[Fabrication of superhydrophobic surface on aluminum by continuous chemical etching and its anti-icing property](#)

Appl. Surf. Sci. (2014)

W. Ma *et al.*

[Lightweight, elastic and superhydrophobic multifunctional nanofibrous aerogel for self-cleaning, oil/water separation and pressure sensing](#)

Chem. Eng. J. (2022)

Y. Wan *et al.*

[The research on preparation of superhydrophobic surfaces of pure copper by hydrothermal method and its corrosion resistance](#)

Electrochim. Acta (2018)

Y. Xiu *et al.*

[UV and thermally stable superhydrophobic coatings from sol-gel processing](#)

J. Colloid Interface Sci. (2008)



[View more references](#)

Cited by (19)

[Oil/water separation copper membranes modified by laser induced ZnO nanowires growth with enhanced catalytic function](#)

2024, Colloids and Surfaces A: Physicochemical and Engineering Aspects

[Show abstract](#)

[Magnetic superhydrophobic sponge with 3D interpenetrating network structure coating for multimodal driven oil/water separation](#)

2024, Progress in Organic Coatings

[Show abstract](#)

[Multifunctional carbonized Zn-MOF coatings for cotton fabric: Unveiling synergistic effects of superhydrophobic, oil-water separation, self-cleaning, and UV protection features](#)

2023, Surface and Coatings Technology

[Show abstract](#)

[Ecofriendly superhydrophobic fabrics for ultra-fast oil/water separation by self-assembly](#)

2023, Surface and Coatings Technology

[Show abstract](#)

Efficient separation of oil-water emulsions: Competent design of superwetting materials for practical applications

2023, Journal of Environmental Chemical Engineering

[Show abstract](#) 

Sustainable approach to oil recovery from oil spills through superhydrophobic jute fabric

2023, Marine Pollution Bulletin

[Show abstract](#) 

[>](#) [View all citing articles on Scopus](#) 

[View full text](#)

© 2022 Elsevier B.V. All rights reserved.



All content on this site: Copyright © 2024 Elsevier B.V., its licensors, and contributors. All rights are reserved, including those for text and data mining, AI training, and similar technologies. For all open access content, the Creative Commons licensing terms apply.





**International Symposium
on**

Sustainable Environment and Smart Technology



Jointly Organized by

Pune District Education Association's

**Prof. Ramkrishna More Arts,
Commerce and Science College**

Akurdi, Pune - 411044

and

**Department of Technology
Savitribai Phule Pune University, Pune 411007**

10-11 March, 2023

Editor

Prin. Dr. M. G. Chaskar



**Self Study
Publication**

ABSTRACT BOOK

[ISBN-978-81-948795-2-7]

15	“On-Water” Reaction of (Thio)isocyanate: A Sustainable Process for the Synthesis of Unsymmetrical (Thio)ureas	Karche Amit Dattatray	12
16	Studies on Gut Fungal Diversity from Organic Waste Feeding Beetle.	Ganesh E Gore, Dhiraj Dhotre, Deepak Shelke, Hiralal Sonawane	13
17	Fe ₂ O ₃ – Polyaniline thin films: A Smart Material for the Ammonia gas Sensing	Somnath Dattinge, Dipali Dubal, Shamal Ballal, Sunil Kandalkar, Dnyaneshwar Shinde	13
18	Antioxidant Activities of Mycogenically Synthesized Nanoparticles from Combination of Medicinally Important Mushroom <i>Inonotus</i> Sp. and Chitosan	Pallavi Champaneria, H B Sonawane, B N zaware	14
19	Account of Wood Rotting Fungi from Madhe Ghat and Connecting Area of Velha Tehsil.	Bhagat S. P., Sonawane H. B., Borde M. Y.	14
20	A Green Protocol for One-Pot Synthesis of 3,4-Dihydropyrano[C]Chromenes and Biscoumarins by Employing WEB as an Internal Base.	Kumbhar Vikrant Vasudev	14
21	Investigations on CuO: ZnO Composites for Photocatalytic Performance.	Akanksha S Chougale, Snehal S Wagh, Harshad D Shelake, Habib M. Pathan and Dnyaneshwar R Shinde	11
22	Magnetic Hyperthermia with Fe ₃ O ₄ Nanoparticles	Pandhare Amol Babaso	11
23	Studies on Induced Mutation in Barnyard Millet (<i>Echinochloa esculanta</i>) L.	Jagtap Bhavana D. and Danai-Tambhale S. D.	11
24	Determination of Physicochemical Parameters and Adulteration Of Multifloral Honey by FTIR-ATR spectroscopy	Rekha J. Shinde, Indira M. Patil and Rashmi A. Morey	14
25	Ni-Ferrite an Efficient Catalyst for Synthesis of 3-Aryl Substituted Isoxazole-5-Carboxylic Acids Via One-Pot Multicomponent Reaction	Ganesh Totre, Dnyaneshwar Shinde, Prakash Patil and Pramod Kulkarni	14
26	Degradation of Textile Reactive Azodyes by <i>Hapalosiphon arboreus</i>	Rutuja Pund and K. M. Nitnaware	15
27	Fabrication of Durable Candle Soot-Wax Composite Coated Superhydrophobic Sponges for Oil-Water Separation	Mehejbin R. Mujawar, Rajesh B. Sawant, Amol B. Pandhare, Rajaram S. Sutar , Sanjay S. Latthe, Ankush M. Sargar, Raghunath K. Mane, Shivaji R. Kulal	15
28	NiFe ₂ O ₄ : An Efficient and Magnetically Recoverable Catalyst for Synthesis of 2-amino-3-cyanopyridines Derivatives	Sandip Rathod	18
29	Phytochemical and Anti-Microbial Studies of Underutilized, Neglected, Endemic and Threatened Wild Crop Relative <i>Vigna khandalensis</i> (Santapau) Raghavan et Wadhwa	Sarika A. Bhumkar, Sandip S. Thorve, Sadashiv N. Bolbhat, Vinayak H. Lokhande	18
30	Decolourization of Spent Wash Colour under Sun Light using Mesoporous Cu-TiO ₂ Nanoparticles Synthesized By Sol-Gel Assisted Hydrothermal (SGAH) Method	Shrikant. P.Takle, Aarti S. Tarlekar, Amol Bhosale, Netaji Mali, Shaila Dhotre, Digambar B. Bankar, Namdeo N. Bhujbal	19
31	Synthesis of Organic Nano Semiconductor for Photocatalytic and Antimicrobial study Performance	Vivekanand Jawale, Gulab Gugale, Vikram Pandit	19
32	Endophytes Isolated from <i>Ophiorrhiza rugosa</i> Plant Producing a Good Source of Camptothecin.	Vaishnavi Chavan, Hiralal Sonawane and Mahesh Borde	20

Abstract-26**Degradation of textile reactive azodyes by *Hapalosiphon arboreus*****Miss Rutuja Pund and Dr. K. M. Nitnaware***

Department of Botany, Hutatma Rajguru Mahavidyalaya, Rajgurunagar

Corresponding Email: kmnbotany@gmail.com

Abstract: Azodyes widely used in textile industries are toxic to life. Dye degradation using microorganism gained more attention due to cost effectiveness and eco-friendly. There is need to investigate more indigenous species. In the present study the filamentous cyanobacteria *Hapalosiphon vulgaris* was examined for its degrading ability of azodyes Methyl Orange, Tartrazine Yellow, Scarlet Red, Reactive Black 5 and Sudan III. The axenic culture of *Hapalosiphon* was inoculated with various concentrations of dyes (5, 10 and 20 ppm) and incubated for 3, 5 and 7 days. Dye degradation was based on initial dye concentration. The maximum decolorization was observed in Scarlet red and Sudan III 92.5% and 82.02% respectively after 7 days of incubation. Azoreductase enzyme in algae responsible for degradation of azodyes into aromatic amines. Maximum azoreductase activity 6.02 Umg-1 protein was observed for scarlet red. Influence of azo dyes on Chlorophyll a and b content and Phycobilin Proteins was also examined. The degradation product after decolourization was confirmed and identified by spectroscopic analysis and Fourier transformed infrared spectroscopic analysis.

Keywords: Azoreductase enzyme, Methyl Orange, Scarlet Red, FTIR

Abstract-27**Fabrication of Durable Candle Soot-Wax Composite Coated Superhydrophobic Sponges for Oil-Water Separation****Mehejbin R. Mujawar¹, Rajesh B. Sawant¹, Amol B. Pandhare², Rajaram S. Sutar³, Sanjay S. Latthe⁴, Ankush M. Sargar^{5*}, Raghunath K. Mane⁶, Shivaji R. Kulal^{*}**¹ Department of Chemistry, Raje Ramrao Mahavidyalaya, Jath, (Affiliated to Shivaji University, Kolhapur)² Department of Chemistry, Shivaji University, Kolhapur, (MS) India³ Self-cleaning Research Laboratory, Department of Physics, Raje Ramrao Mahavidyalaya, Jath,⁴ Self-cleaning Research Laboratory, Department of Physics, Vivekanand College, Kolhapur,⁵ Department of Chemistry, Bharati Vidyapeeth's Dr. Patangrao Kadam Mahavidyalaya, Sangli,⁶ Department of Chemistry, Smt. Kusumtai Rajarambhapu Patil Kanya Mahavidyalaya, Islampur,*Corresponding authors E-mail: srkulal@gmail.com, amsargar2012@gmail.com

Abstract: A novel superhydrophobic candle soot-wax composite coated surfaces for oil-water separation was fabricated via a facile two-step strategy. The decomposition of candle soot on the surface and then it was fixed via deposition of wax on CS-coated surfaces. The candle soot was synthesized by paraffin candle combustion flame. The CS-coated surface was prepared by via the dip-coating method without further surface modification and pre-treatments. Candle soot was firmly immobilized on the wax skeleton constructing a nanoscale rough surface with superhydrophobicity. The coated surfaces exhibit superhydrophobicity with a water contact angle of $> 150^\circ$ and a sliding angle of nearly 0° . The thermal stability, pH tolerance, compression tolerance, chemical durability, reusability, emulsion oil-water separation, and muddy water-oil separation was tested by using these superhydrophobic surfaces. The superhydrophobic surfaces have a sustainable, anti-wetting property under cross-sectional cutting, pressing, paper peel test, abrasion resistance test, and different pH environments. The superhydrophobic surface is suitable for practical application on a large scale. The simple CS-wax coating method can be applied to various surfaces, such as stainless steel and polyurethane sponges. These research results show evidence that the CS-wax-coated surface is promising in environmental remediation for large-scale, low-cost, removal of oil spills from water.

Keywords: Candle soot nanoparticles, oil-water separation, sliding angle, superhydrophobic surfaces, water contact angle, waxes.



**International Symposium
on**

Sustainable Environment and Smart Technology



Jointly Organized by

Pune District Education Association's

**Prof. Ramkrishna More Arts,
Commerce and Science College**

Akurdi, Pune - 411044

and

Department of Technology

Savitribai Phule Pune University, Pune 411007

10-11 March, 2023

Editor

Prin. Dr. M. G. Chaskar



**Self Study
Publication**

ABSTRACT BOOK

[ISBN-978-81-948795-2-7]

15	“On-Water” Reaction of (Thio)isocyanate: A Sustainable Process for the Synthesis of Unsymmetrical (Thio)ureas	Karche Amit Dattatray	12
16	Studies on Gut Fungal Diversity from Organic Waste Feeding Beetle.	Ganesh E Gore, Dhiraj Dhotre, Deepak Shelke, Hiralal Sonawane	13
17	Fe ₂ O ₃ – Polyaniline thin films: A Smart Material for the Ammonia gas Sensing	Somnath Dattinge, Dipali Dubal, Shamal Ballal, Sunil Kandalkar, Dnyaneshwar Shinde	13
18	Antioxidant Activities of Mycogenically Synthesized Nanoparticles from Combination of Medicinally Important Mushroom <i>Inonotus</i> Sp. and Chitosan	Pallavi Champaneria, H B Sonawane, B N zaware	14
19	Account of Wood Rotting Fungi from Madhe Ghat and Connecting Area of Velha Tehsil.	Bhagat S. P., Sonawane H. B., Borde M. Y.	14
20	A Green Protocol for One-Pot Synthesis of 3,4-Dihydropyrano[C]Chromenes and Biscoumarins by Employing WEB as an Internal Base.	Kumbhar Vikrant Vasudev	14
21	Investigations on CuO: ZnO Composites for Photocatalytic Performance.	Akanksha S Chougale, Snehal S Wagh, Harshad D Shelake, Habib M. Pathan and Dnyaneshwar R Shinde	11
22	Magnetic Hyperthermia with Fe ₃ O ₄ Nanoparticles	Pandhare Amol Babaso	11
23	Studies on Induced Mutation in Barnyard Millet (<i>Echinochloa esculanta</i>) L.	Jagtap Bhavana D. and Danai-Tambhale S. D.	11
24	Determination of Physicochemical Parameters and Adulteration Of Multifloral Honey by FTIR-ATR spectroscopy	Rekha J. Shinde, Indira M. Patil and Rashmi A. Morey	14
25	Ni-Ferrite an Efficient Catalyst for Synthesis of 3-Aryl Substituted Isoxazole-5-Carboxylic Acids Via One-Pot Multicomponent Reaction	Ganesh Totre, Dnyaneshwar Shinde, Prakash Patil and Pramod Kulkarni	14
26	Degradation of Textile Reactive Azodyes by <i>Hapalosiphon arboreus</i>	Rutuja Pund and K. M. Nitnaware	15
27	Fabrication of Durable Candle Soot-Wax Composite Coated Superhydrophobic Sponges for Oil-Water Separation	Mehejbin R. Mujawar, Rajesh B. Sawant , Amol B. Pandhare, Rajaram S. Sutar, Sanjay S. Latthe, Ankush M. Sargar, Raghunath K. Mane, Shivaji R. Kulal	15
28	NiFe ₂ O ₄ : An Efficient and Magnetically Recoverable Catalyst for Synthesis of 2-amino-3-cyanopyridines Derivatives	Sandip Rathod	18
29	Phytochemical and Anti-Microbial Studies of Underutilized, Neglected, Endemic and Threatened Wild Crop Relative <i>Vigna khandalensis</i> (Santapau) Raghavan et Wadhwa	Sarika A. Bhumkar, Sandip S. Thorve, Sadashiv N. Bolbhat, Vinayak H. Lokhande	18
30	Decolourization of Spent Wash Colour under Sun Light using Mesoporous Cu-TiO ₂ Nanoparticles Synthesized By Sol-Gel Assisted Hydrothermal (SGAH) Method	Shrikant. P.Takle, Aarti S. Tarlekar, Amol Bhosale, Netaji Mali, Shaila Dhotre, Digambar B. Bankar, Namdeo N. Bhujbal	19
31	Synthesis of Organic Nano Semiconductor for Photocatalytic and Antimicrobial study Performance	Vivekanand Jawale, Gulab Gugale, Vikram Pandit	19
32	Endophytes Isolated from <i>Ophiorrhiza rugosa</i> Plant Producing a Good Source of Camptothecin.	Vaishnavi Chavan, Hiralal Sonawane and Mahesh Borde	20

Abstract-26**Degradation of textile reactive azodyes by *Hapalosiphon arboreus*****Miss Rutuja Pund and Dr. K. M. Nitnaware***

Department of Botany, Hutatma Rajguru Mahavidyalaya, Rajgurunagar

Corresponding Email: kmnbotany@gmail.com

Abstract: Azodyes widely used in textile industries are toxic to life. Dye degradation using microorganism gained more attention due to cost effectiveness and eco-friendly. There is need to investigate more indigenous species. In the present study the filamentous cyanobacteria *Hapalosiphon vulgaris* was examined for its degrading ability of azodyes Methyl Orange, Tartrazine Yellow, Scarlet Red, Reactive Black 5 and Sudan III. The axenic culture of *Hapalosiphon* was inoculated with various concentrations of dyes (5, 10 and 20 ppm) and incubated for 3, 5 and 7 days. Dye degradation was based on initial dye concentration. The maximum decolorization was observed in Scarlet red and Sudan III 92.5% and 82.02% respectively after 7 days of incubation. Azoreductase enzyme in algae responsible for degradation of azodyes into aromatic amines. Maximum azoreductase activity 6.02 Umg-1 protein was observed for scarlet red. Influence of azo dyes on Chlorophyll a and b content and Phycobilin Proteins was also examined. The degradation product after decolourization was confirmed and identified by spectroscopic analysis and Fourier transformed infrared spectroscopic analysis.

Keywords: Azoreductase enzyme, Methyl Orange, Scarlet Red, FTIR

Abstract-27**Fabrication of Durable Candle Soot-Wax Composite Coated Superhydrophobic Sponges for Oil-Water Separation****Mehejbin R. Mujawar¹, Rajesh B. Sawant¹, Amol B. Pandhare², Rajaram S. Sutar³, Sanjay S. Latthe⁴, Ankush M. Sargar^{5*}, Raghunath K. Mane⁶, Shivaji R. Kulal***¹ Department of Chemistry, Raje Ramrao Mahavidyalaya, Jath, (Affiliated to Shivaji University, Kolhapur)² Department of Chemistry, Shivaji University, Kolhapur, (MS) India³ Self-cleaning Research Laboratory, Department of Physics, Raje Ramrao Mahavidyalaya, Jath,⁴ Self-cleaning Research Laboratory, Department of Physics, Vivekanand College, Kolhapur,⁵ Department of Chemistry, Bharati Vidyapeeth's Dr. Patangrao Kadam Mahavidyalaya, Sangli,⁶ Department of Chemistry, Smt. Kusumtai Rajarambhapu Patil Kanya Mahavidyalaya, Islampur,*Corresponding authors E-mail: srkulal@gmail.com, amsargar2012@gmail.com

Abstract: A novel superhydrophobic candle soot-wax composite coated surfaces for oil-water separation was fabricated via a facile two-step strategy. The decomposition of candle soot on the surface and then it was fixed via deposition of wax on CS-coated surfaces. The candle soot was synthesized by paraffin candle combustion flame. The CS-coated surface was prepared by via the dip-coating method without further surface modification and pre-treatments. Candle soot was firmly immobilized on the wax skeleton constructing a nanoscale rough surface with superhydrophobicity. The coated surfaces exhibit superhydrophobicity with a water contact angle of $> 150^\circ$ and a sliding angle of nearly 0° . The thermal stability, pH tolerance, compression tolerance, chemical durability, reusability, emulsion oil-water separation, and muddy water-oil separation was tested by using these superhydrophobic surfaces. The superhydrophobic surfaces have a sustainable, anti-wetting property under cross-sectional cutting, pressing, paper peel test, abrasion resistance test, and different pH environments. The superhydrophobic surface is suitable for practical application on a large scale. The simple CS-wax coating method can be applied to various surfaces, such as stainless steel and polyurethane sponges. These research results show evidence that the CS-wax-coated surface is promising in environmental remediation for large-scale, low-cost, removal of oil spills from water.

Keywords: Candle soot nanoparticles, oil-water separation, sliding angle, superhydrophobic surfaces, water contact angle, waxes.

A Review on Superhydrophobic Surfaces: Fundamentals, Fabrications and Applications

Mehejbin R. Mujawar¹, Rajesh B. Sawant¹, Govind D. Salunke¹, Rajaram S. Sutar², Sanjay S. Lathe³, Ankush M. Sargar⁴, Raghunath K. Mane⁵, Krishna K. Rangar¹, Shivaji R. Kulal^{1*}

¹ Department of Chemistry, Raje Ramrao Mahavidyalaya, Jath, Dist. - Sangli (MS) India

² Self-cleaning Research Laboratory, Department of Physics, Raje Ramrao Mahavidyalaya, Jath, Dist. - Sangli (MS) India.

³ Self-cleaning Research Laboratory, Department of Physics, Vivekanand College (Autonomous), Kolhapur, Dist. - Kolhapur (MS) India.

⁴ Department of Chemistry, Bharati Vidyapeeth's Dr. Patangrao Kadam Mahavidyalaya, Sangli, Dist. - Sangli (MS) India

⁵ Department of Chemistry, Smt. Kusumtai Rajarambhapu Patil Kanya Mahavidyalaya, Islampur, Dist. - Sangli (MS) India

*Corresponding author's E-mail: srkulal@gmail.com, amsargar2012@gmail.com

Abstract

Superhydrophobic surfaces are highly hydrophobic i.e., it extremely difficult to wet. Superhydrophobic surfaces are the tendency to repel water drops and absorb oil drops. The water contact angle of superhydrophobic surfaces is greater than 150° , the oil contact angle is less than 5° , and the sliding angle is less than 5° . It is showing the lotus effect. Superhydrophobicity is observed in the lotus leaves, insects, and some other plants in which their leaves would not get wet. This phenomenon is due to the unique surface structure of the lotus leaf and also the presence of a low surface energy material on the surface of the leaf. For the formation of a superhydrophobic surface, the surface must show hierarchical micro- and nano-roughness and low surface energy. Efforts have been taken to form superhydrophobic surfaces for a variety of applications. There are many applications of superhydrophobic surfaces such as self-cleaning surfaces, oil-water separation surfaces, anti-icing surfaces, anti-corrosion surfaces, anti-fogging surfaces, and water-resistant surfaces. In this article, the fundamental principles of superhydrophobic surfaces, some recent trends in the fabrication of superhydrophobic surfaces, and their applications are reviewed and discussed.

Keyword: Superhydrophobicity, Superoleophobicity, Lotus effect, Self-cleaning, Oil-water separation, Water-repelling, Oil Contact Angle, Water Contact angle, Anti-icing, Anti-corrosion.



**International Symposium
on**

Sustainable Environment and Smart Technology



Jointly Organized by

Pune District Education Association's

**Prof. Ramkrishna More Arts,
Commerce and Science College**

Akurdi, Pune - 411044

and

**Department of Technology
Savitribai Phule Pune University, Pune 411007**

10-11 March, 2023

Editor

Prin. Dr. M. G. Chaskar



**Self Study
Publication**

ABSTRACT BOOK

[ISBN-978-81-948795-2-7]

15	“On-Water” Reaction of (Thio)isocyanate: A Sustainable Process for the Synthesis of Unsymmetrical (Thio)ureas	Karche Amit Dattatray	12
16	Studies on Gut Fungal Diversity from Organic Waste Feeding Beetle.	Ganesh E Gore, Dhiraj Dhotre, Deepak Shelke, Hiralal Sonawane	13
17	Fe ₂ O ₃ – Polyaniline thin films: A Smart Material for the Ammonia gas Sensing	Somnath Dattinge, Dipali Dubal, Shamal Ballal, Sunil Kandalkar, Dnyaneshwar Shinde	13
18	Antioxidant Activities of Mycogenically Synthesized Nanoparticles from Combination of Medicinally Important Mushroom <i>Inonotus</i> Sp. and Chitosan	Pallavi Champaneria, H B Sonawane, B N zaware	14
19	Account of Wood Rotting Fungi from Madhe Ghat and Connecting Area of Velha Tehsil.	Bhagat S. P., Sonawane H. B., Borde M. Y.	14
20	A Green Protocol for One-Pot Synthesis of 3,4-Dihydropyrano[C]Chromenes and Biscoumarins by Employing WEB as an Internal Base.	Kumbhar Vikrant Vasudev	14
21	Investigations on CuO: ZnO Composites for Photocatalytic Performance.	Akanksha S Chougale, Snehal S Wagh, Harshad D Shelake, Habib M. Pathan and Dnyaneshwar R Shinde	11
22	Magnetic Hyperthermia with Fe ₃ O ₄ Nanoparticles	Pandhare Amol Babaso	11
23	Studies on Induced Mutation in Barnyard Millet (<i>Echinochloa esculanta</i>) L.	Jagtap Bhavana D. and Danai-Tambhale S. D.	11
24	Determination of Physicochemical Parameters and Adulteration Of Multifloral Honey by FTIR-ATR spectroscopy	Rekha J. Shinde, Indira M. Patil and Rashmi A. Morey	14
25	Ni-Ferrite an Efficient Catalyst for Synthesis of 3-Aryl Substituted Isoxazole-5-Carboxylic Acids Via One-Pot Multicomponent Reaction	Ganesh Totre, Dnyaneshwar Shinde, Prakash Patil and Pramod Kulkarni	14
26	Degradation of Textile Reactive Azodyes by <i>Hapalosiphon arboreus</i>	Rutuja Pund and K. M. Nitnaware	15
27	Fabrication of Durable Candle Soot-Wax Composite Coated Superhydrophobic Sponges for Oil-Water Separation	Mehejbin R. Mujawar, Rajesh B. Sawant, Amol B. Pandhare, Rajaram S. Sutar, Sanjay S. Latthe , Ankush M. Sargar, Raghunath K. Mane, Shivaji R. Kulal	15
28	NiFe ₂ O ₄ : An Efficient and Magnetically Recoverable Catalyst for Synthesis of 2-amino-3-cyanopyridines Derivatives	Sandip Rathod	18
29	Phytochemical and Anti-Microbial Studies of Underutilized, Neglected, Endemic and Threatened Wild Crop Relative <i>Vigna khandalensis</i> (Santapau) Raghavan et Wadhwa	Sarika A. Bhumkar, Sandip S. Thorve, Sadashiv N. Bolbhat, Vinayak H. Lokhande	18
30	Decolourization of Spent Wash Colour under Sun Light using Mesoporous Cu-TiO ₂ Nanoparticles Synthesized By Sol-Gel Assisted Hydrothermal (SGAH) Method	Shrikant. P.Takle, Aarti S. Tarlekar, Amol Bhosale, Netaji Mali, Shaila Dhotre, Digambar B. Bankar, Namdeo N. Bhujbal	19
31	Synthesis of Organic Nano Semiconductor for Photocatalytic and Antimicrobial study Performance	Vivekanand Jawale, Gulab Gugale, Vikram Pandit	19
32	Endophytes Isolated from <i>Ophiorrhiza rugosa</i> Plant Producing a Good Source of Camptothecin.	Vaishnavi Chavan, Hiralal Sonawane and Mahesh Borde	20

Abstract-26**Degradation of textile reactive azodyes by *Hapalosiphon arboreus*****Miss Rutuja Pund and Dr. K. M. Nitnaware***

Department of Botany, Hutatma Rajguru Mahavidyalaya, Rajgurunagar

Corresponding Email: kmnbotany@gmail.com

Abstract: Azodyes widely used in textile industries are toxic to life. Dye degradation using microorganism gained more attention due to cost effectiveness and eco-friendly. There is need to investigate more indigenous species. In the present study the filamentous cyanobacteria *Hapalosiphon vulgaris* was examined for its degrading ability of azodyes Methyl Orange, Tartrazine Yellow, Scarlet Red, Reactive Black 5 and Sudan III. The axenic culture of *Hapalosiphon* was inoculated with various concentrations of dyes (5, 10 and 20 ppm) and incubated for 3, 5 and 7 days. Dye degradation was based on initial dye concentration. The maximum decolorization was observed in Scarlet red and Sudan III 92.5% and 82.02% respectively after 7 days of incubation. Azoreductase enzyme in algae responsible for degradation of azodyes into aromatic amines. Maximum azoreductase activity 6.02 Umg-1 protein was observed for scarlet red. Influence of azo dyes on Chlorophyll a and b content and Phycobilin Proteins was also examined. The degradation product after decolourization was confirmed and identified by spectroscopic analysis and Fourier transformed infrared spectroscopic analysis.

Keywords: Azoreductase enzyme, Methyl Orange, Scarlet Red, FTIR

Abstract-27**Fabrication of Durable Candle Soot-Wax Composite Coated Superhydrophobic Sponges for Oil-Water Separation****Mehejbin R. Mujawar¹, Rajesh B. Sawant¹, Amol B. Pandhare², Rajaram S. Sutar³, Sanjay S. Latthe⁴, Ankush M. Sargar^{5*}, Raghunath K. Mane⁶, Shivaji R. Kulal^{*}**¹ Department of Chemistry, Raje Ramrao Mahavidyalaya, Jath, (Affiliated to Shivaji University, Kolhapur)² Department of Chemistry, Shivaji University, Kolhapur, (MS) India³ Self-cleaning Research Laboratory, Department of Physics, Raje Ramrao Mahavidyalaya, Jath,⁴ Self-cleaning Research Laboratory, Department of Physics, Vivekanand College, Kolhapur,⁵ Department of Chemistry, Bharati Vidyapeeth's Dr. Patangrao Kadam Mahavidyalaya, Sangli,⁶ Department of Chemistry, Smt. Kusumtai Rajarambhapu Patil Kanya Mahavidyalaya, Islampur,*Corresponding authors E-mail: srkulal@gmail.com, amsargar2012@gmail.com

Abstract: A novel superhydrophobic candle soot-wax composite coated surfaces for oil-water separation was fabricated via a facile two-step strategy. The decomposition of candle soot on the surface and then it was fixed via deposition of wax on CS-coated surfaces. The candle soot was synthesized by paraffin candle combustion flame. The CS-coated surface was prepared by via the dip-coating method without further surface modification and pre-treatments. Candle soot was firmly immobilized on the wax skeleton constructing a nanoscale rough surface with superhydrophobicity. The coated surfaces exhibit superhydrophobicity with a water contact angle of $> 150^\circ$ and a sliding angle of nearly 0° . The thermal stability, pH tolerance, compression tolerance, chemical durability, reusability, emulsion oil-water separation, and muddy water-oil separation was tested by using these superhydrophobic surfaces. The superhydrophobic surfaces have a sustainable, anti-wetting property under cross-sectional cutting, pressing, paper peel test, abrasion resistance test, and different pH environments. The superhydrophobic surface is suitable for practical application on a large scale. The simple CS-wax coating method can be applied to various surfaces, such as stainless steel and polyurethane sponges. These research results show evidence that the CS-wax-coated surface is promising in environmental remediation for large-scale, low-cost, removal of oil spills from water.

Keywords: Candle soot nanoparticles, oil-water separation, sliding angle, superhydrophobic surfaces, water contact angle, waxes.

A Review on Superhydrophobic Surfaces: Fundamentals, Fabrications and Applications

Mehejbin R. Mujawar¹, Rajesh B. Sawant¹, Govind D. Salunke¹, Rajaram S. Sutar², Sanjay S. Lathe³, Ankush M. Sargar⁴, Raghunath K. Mane⁵, Krishna K. Rangar¹, Shivaji R. Kulal^{1*}

¹ Department of Chemistry, Raje Ramrao Mahavidyalaya, Jath, Dist. - Sangli (MS) India

² Self-cleaning Research Laboratory, Department of Physics, Raje Ramrao Mahavidyalaya, Jath, Dist. - Sangli (MS) India.

³ Self-cleaning Research Laboratory, Department of Physics, Vivekanand College (Autonomous), Kolhapur, Dist. - Kolhapur (MS) India.

⁴ Department of Chemistry, Bharati Vidyapeeth's Dr. Patangrao Kadam Mahavidyalaya, Sangli, Dist. - Sangli (MS) India

⁵ Department of Chemistry, Smt. Kusumtai Rajarambhapu Patil Kanya Mahavidyalaya, Islampur, Dist. - Sangli (MS) India

*Corresponding author's E-mail: srkulal@gmail.com, amsargar2012@gmail.com

Abstract

Superhydrophobic surfaces are highly hydrophobic i.e., it extremely difficult to wet. Superhydrophobic surfaces are the tendency to repel water drops and absorb oil drops. The water contact angle of superhydrophobic surfaces is greater than 150° , the oil contact angle is less than 5° , and the sliding angle is less than 5° . It is showing the lotus effect. Superhydrophobicity is observed in the lotus leaves, insects, and some other plants in which their leaves would not get wet. This phenomenon is due to the unique surface structure of the lotus leaf and also the presence of a low surface energy material on the surface of the leaf. For the formation of a superhydrophobic surface, the surface must show hierarchical micro- and nano-roughness and low surface energy. Efforts have been taken to form superhydrophobic surfaces for a variety of applications. There are many applications of superhydrophobic surfaces such as self-cleaning surfaces, oil-water separation surfaces, anti-icing surfaces, anti-corrosion surfaces, anti-fogging surfaces, and water-resistant surfaces. In this article, the fundamental principles of superhydrophobic surfaces, some recent trends in the fabrication of superhydrophobic surfaces, and their applications are reviewed and discussed.

Keyword: Superhydrophobicity, Superoleophobicity, Lotus effect, Self-cleaning, Oil-water separation, Water-repelling, Oil Contact Angle, Water Contact angle, Anti-icing, Anti-corrosion.



SHIVAJI UNIVERSITY, KOLHAPUR

Volume-49 Issue-1 (January, 2023)

ISSN-Science-0250-5347

Estd. 1962
"A++" Accredited by NAAC (2021)
with CGPA 3.52



JOURNAL OF SHIVAJI UNIVERSITY : SCIENCE AND TECHNOLOGY

(Peer Reviewed Journal)

Journal of Shivaji University: Science and Technology
Volume-49, Issue-1 (January,2023)
INDEX

Sr. No.	Title of Research Article with Name of Author/s	Page No.
1.	Synthesis and Characterization of g-C₃N₄ Decorated ZnONanorods and their Binder Free Deposited Photoanodes for Photoelectrochemical Water Splitting Studies Pramod A. Koyale, Prakash S. Pawar, Swapnajit V. Mulik, Vijay S. Ghodake, Amol B. Pandhare, Ankita K. Dhukate, Sagar D. Delekar	1
2.	Thiamine Hydrochloride (VB₁) Catalyzed Synthesis of 5-aryl-4-phenyl-1,2,4-triazolidine-3-thiones in Aqueous Medium Pradeep P. Patil, Prasad M. Swami, Shankar P. Hangirgekar, Sandeep A. Sankpal	10
3.	Evaluation of Acute Toxic Effect of Gallic Acid Loaded Eudragit's 100 Nanoparticles on <i>Artemia Salina</i> Brine Shrimp Bioassay Poornima S. Sankpal, Sachinkumar V. Patil, Sayali S. Patil	20
4.	Surface Modifications of Binder Free ZnONanorod Thin Films through Cds Quantum Dots for Dye Sensitized Solar Cells Krantiveer V. More, Anant G. Dhodamani, Sajid B. Mullani, Tukaram D. Dongale, Prakash S. Pawar, Satish M. Patil, Sunil J. Kadam, Sagar D. Delekar	36
5.	Review on Candle Soot based Superhydrophobic Surfaces for Oil-Water Separation Mehejbin R. Mujawar, Rajesh B. Sawant, Amol B. Pandhare, Prashant D. Sanadi, Sanjay S. Latthe, Ankush M. Sargar, Raghunath K. Mane, Shivaji R. Kulal	50
6.	A Review on Current Advancements in Magnetic Nanomaterials for Magnetic Hyperthermia Applications Amol B. Pandhare, Prakash S. Pawar, Vijay S. Ghodake, Swapnajit V. Mulik, Pramod A. Koyale, Ankita K. Dhukate, Deepak B. Mohite, Karishma V. Shikhare, Rajendra P. Patil, Sagar D. Delekar	62
7.	One-Step Synthesis of Biomass-Derived Carbon Dots: Study of Optical Properties Akanksha G. Kolekar, Omkar S. Nille, Shubham J. Kumbhar, Priyanka S. Mahadar, Sayali B. Lohar, Govind B. Kolekar, Gavisiddappa S. Gokavi, Vishalkumar R. More	87
8.	Synthesis and Characterization of Plant-Mediated CuO Nanoparticles Omkar S. Nille, Harshad A. Mirgane, Sneha V. Koparde, Akanksha G. Kolekar, Ashlesha R. Pawar, Pallavi J. Pawar, Abhishek A. Waghmode, Tanaji R. Dhage, Vijay S. Ghodake, Prasad M. Swami, Sarita D. Shinde, Govind B. Kolekar	95

Review on Candle Soot based Superhydrophobic Surfaces for Oil-Water Separation

Mehejbin R. Mujawar^{a,*}, Rajesh B. Sawant^a, Amol B. Pandhare^{b,f},
Prashant D. Sanadi^g, Sanjay S. Latthe^c, Ankush M. Sargar^d,
Raghunath K. Mane^e, Shivaji R. Kulal^{a,*}

^aDepartment of Chemistry, Raje Ramrao Mahavidyalaya, Jath, Sangli 416 404 (MS) India.

^bDepartment of Chemistry, Shivaji University, Kolhapur 416 004 (MS) India.

^cDepartment of Physics, Vivekanand College, Kolhapur 416 003 (MS) India.

^dDepartment of Chemistry, Bharati Vidyapeeth's Dr. Patangrao Kadam Mahavidyalaya, Sangli 416 416 (MS) India.

^eDepartment of Chemistry, Smt. Kusumtai Rajarambhapu Patil Kanya Mahavidyalaya, Islampur, Sangli 416 409 (MS) India.

^fDepartment of Chemistry, M.H. Shinde Mahavidyalaya, Tisangi, Gaganbavda, Kolhapur 416 206 (MS) India.

^gDepartment of Engginring, Chemistry, Institute of Technology's College of Engineering (Autonomous), Kolhapur 416 234 (MS) India.

*Corresponding authors: srkulal@gmail.com and mehejabeenmujawar@gmail.com

ABSTRACT

Over the many years, the oceanic oil spill accidents and most industries worldwide discharging immense levels of oil in the surroundings is a serious problem for the environment. There is a need to develop technology for oil-water separation because the spilled oil affects the ecological and environmental system. Candle soot nanoparticles are hydrophobic (water repellent) in nature and has the advantages of cost-effectiveness and production scalability over other carbons like graphene, Carbon Nanotubes (CNTs), Carbon Nanodots (CNDs), etc. in their synthesis. Candle soot based superhydrophobic materials have outstanding water repulsion and oil absorption capacity, highly selectivity, chemical inertness and excellent recyclability. In this paper, we discuss applications of candle soot based superhydrophobic materials applied on sponge and mesh substrates for oil-water separation.

KEYWORDS

Carbon Nanotubes, Carbon Nanodots.

.....

1. INTRODUCTION

The oil spilling and discharge of industrial organic solvents causes several damages to water resources and aquatic ecosystems [1-3], which became a global problem and need to solve it urgently to save the ecosystems. A new technology in material science has been developed for oil-water separation using superhydrophobic nanomaterial. As like the lotus leaf, superhydrophobic surface having water contact angle greater than 150° and oil contact angle near 0°[4]. Different chemical methods

are used for the fabrication of the superhydrophobic mesh/sponge for efficient oil-water separation. As the carbon nanoparticles are hydrophobic in nature, it shows strong affinity toward oil. At the same time, huge amount of candle soot waste is produced. Undoubtedly, it is of great benefit to turn candle soot waste into high value oil absorbent materials [5]. The superhydrophobic mesh/sponge exhibited high selectivity toward different oil and organic pollutants, fast and efficient oil-water separation capability, good repeatability, good reusability, mechanically stable, chemically stable and thermally stable [6]. Candle soot-based absorbents demonstrate superior efficiency in the removal of oils. However, the high production costs of carbon nanotube[7], graphene[8], activated carbon [9], expanded graphite [10], etc. So, these absorbents limit their wide adoption at large scale. Candle soot (CS) generated from incomplete combustion of paraffin wax has demonstrated the advantages of cost effectiveness and production scalability over CNTs, graphene and activated carbons in their synthesis [11]. However, candle soot coated superhydrophobic materials are the best solution from these. The superhydrophobic surfaces on which water achieves water contact angle higher than 150° and sliding angle less than 5° are attracting minds of researchers due to their efficient oil-water separation abilities [12-14]. J. Song et al. [15] fabricated CS-coated mesh by using dip-coating method. The cleaned stainless-steel mesh (SSM) was dipped in the glue solution for 10 min and then dried at 80°C to obtain the CS-glue coated mesh. The CS coating is close packed because of using superglue as a binder. The CS-glue coated mesh revealed the separation efficiency higher than 99.95%. Even after 20 cycle separation tests, it was shown superior reusability and durability. Li et al. [16] prepared the hydrophobic CS by incomplete combustion of hydrocarbons from the middle of candle flame. The PU sponge dipped in the solution of CS, SiO_2 and PU resin to achieve stable superhydrophobicity. The CS- SiO_2 -PU sponge showed excellent oil-water separation efficiency. The CS- SiO_2 -PU sponge was also shown superior separation efficiency from hot water, acidic solutions, alkaline solutions and salt solutions. Zulfiqar et al. [17] deposited cheaply available sawdust on polychloroprene adhesive-coated stainless-steel mesh with deposition of silicone polymer by using dip-coating method. Then, a thin layer of CS particle was applied on the prepared stainless-steel mesh by simply holding it above a candle flame. The CS particles get uniformly deposited on silicone covered sawdust which exhibited highly rough and porous morphology required for superhydrophobicity. It showed excellent oil-water separation efficiency greater than 95% which showed its recyclability, reusability and mechanical stability. In this article, we will mostly discuss on the simple, low-cost, rapid and innovative methods for the fabrication of superhydrophobic/superoleophilic CS coated sponges/meshes for efficient oil-water separation application.

2. SUPERHYDROPHOBIC-SUPEROLEOPHILIC SURFACES FOR OIL-WATER SEPARATION

2.1 Oil-water separation using Superhydrophobic-superoleophilic sponges

2.1.1 Highly efficient carbon soot sponge

The CS particles obtained from ethylene-oxygen combustion flame with flow rate of 5:3. These CS particles were dispersed in 1, 2-dichloroethane followed by sonication. The sponge was dipped in CS dispersion solution to attain superhydrophobic sponge. The superhydrophobic sponge achieved by a uniform coating of as-grown CS particles onto the porous skeleton through simple immersion in CS dispersion. The CS-modified sponge exhibited excellent oil-water separation efficiency without further chemical modification. The fast and easy recovery of engine oil floating on the water surface by CS-modified sponge confirms its high oil-water separation efficiency. The CS-sponge was shown an absorption capacity in the range of 25-80 times its original weight. The absorption capacity of the CS-sponge does not show severe degradation after 10 cycles which indicating a highly stable absorption performance of CS-sponge. After 10 cycles which indicating a highly stable absorption capacity is kept for CS-modified sponge, which much higher than that of the CS-sponge [18].

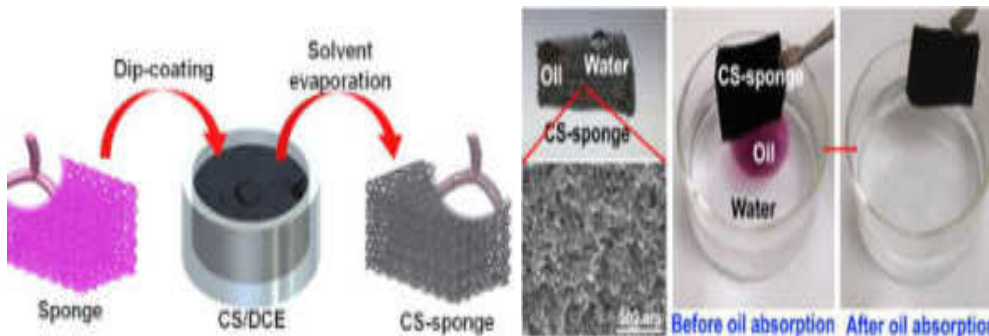


Figure-1. Schematic showing the carbon soot-sponge preparation by dip-coating and carbon soot sponge before & after oil absorption. Images reprinted from [18], with permission from American Chemical Society, Copyright 2014.

2.1.2 Recyclable superhydrophobic straw soot sponge

The straw soot on the glass slide was collected by shaving soot from the glass using a spatula. The colloidal suspension of CS was prepared by simply mixing the soot in ethanolic medium. The sponge was dipped into straw soot solution by using dip-coating method to form superhydrophobic sponge. The modified sponge was shown the water contact angle up to 154° . This superhydrophobic sample had good hydrophobic stability even in acidic condition and it can show the efficient oil-water separation. The amount of the absorbed oil was about 30 times of sponges own

weight which can be shown that the evaluation of the mass based on absorption capacity. The absorption capacity based on density, viscosity and surface tension of the absorbed liquids. This superhydrophobic sponge shows highly recyclability. The experiments demonstrate that the sponge can absorb the oil more than 30 cyclic applications without any significant change in the absorption. This method shows the benefits of easy preparation using natural soot source, better performance, oil absorption in a very short time in comparison with previous works [19].

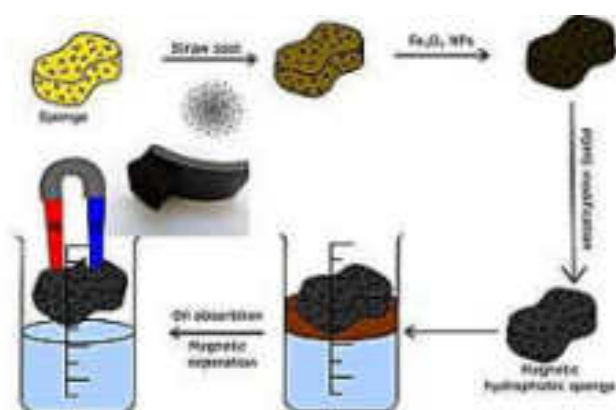


Figure-2. Schematic illustration of preparation of modified polyurethane sponge and oil separation process. Images reprinted from [19], with permission from Elsevier, Copyright 2017.

2.1.3 Durable PVDF/CS sponge

The superhydrophobic surface was fabricated by using PVDF and candle soot via sugar template method. It was shown the water contact angle of 158.3° and roll on angle of 6.7° . The oil quickly absorbed by superhydrophobic sponge which can be shows the superoleophilic property of superhydrophobic sponge. The solar value of candle soot is up to 99.4% which shows excellent light absorbing property. The sponge shows excellent oil-water separation property even after 25 cycles without destroying the sponge. The strong elasticity & high stretch resistance confirms that the modified superhydrophobic surface is highly mechanical durable. The modified sponge maintains the 89% of recovery rate even after 10 cycles. The absorption capability recovered up to 96% without obvious change of morphology of the sponge surface. This method was used to prepare a photothermal & porous PVDF/CS sponge with structural, chemical and mechanical property. It was shown high photothermal property.

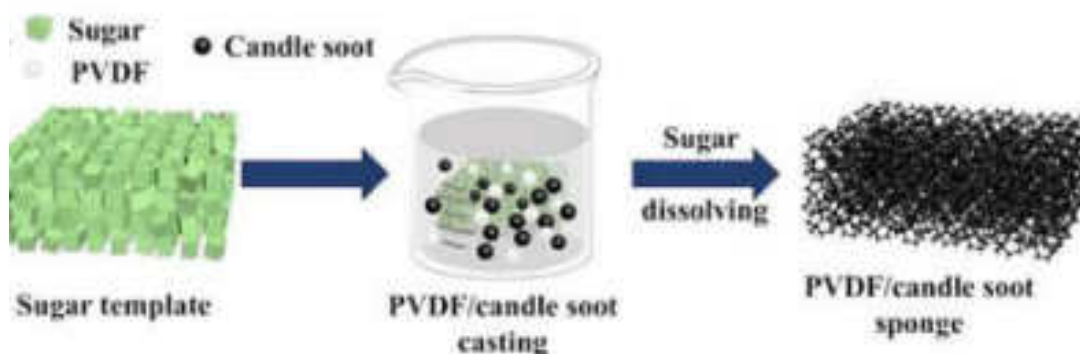


Figure-3. Schematic illustration of the fabrication of porous PVDF/candle soot sponge using sugar template. Images reprinted from [20], with permission from Elsevier, Copyright 2021.

2.2 Oil-water separation using superhydrophobic-superoleophilic meshes

2.2.1 Superhydrophobic SiO_2 /Carbon mesh

The candle soot was collected on the surface of stainless-steel mesh by placing the mesh above the wick of candle. Then by using chemical vapour deposition method the SiO_2 /carbon layer deposited on stainless steel mesh. Modify this mesh by using PFOTS and PDPA-PFO respectively to form the superhydrophobic and superoleophilic mesh membrane. This modified superhydrophobic stainless steel mesh exhibits excellent repellence for all the tested strong acids, strong bases and saturated salts, indicating a good stability of modified mesh under a series of hard environment. The separation efficiencies obtained repeatedly even after 15 cycles without any noticeable deterioration. Both superhydrophobic and superoleophilic modified stainless steel mesh membranes shows stability, durability and reusability. The SiO_2 /Carbon modified stainless steel mesh indicates good material for treating real oil-polluted water in different practical applications as well as in oil spill clean-up. This method shows higher performance, oil-water separation in a short time and repeatedly in comparison with earlier works [20].

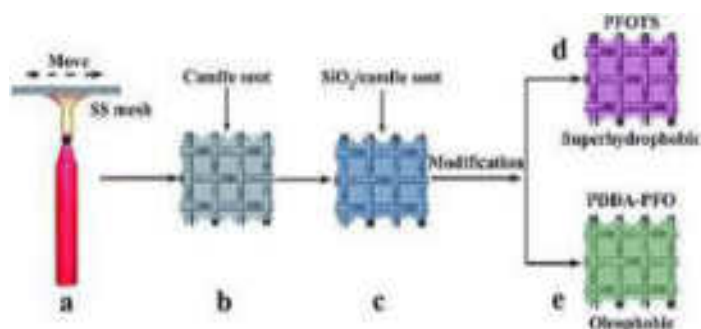


Figure-4. Process of superhydrophobic and oleophobic mesh membranes preparation: (a) coating stainless steel mesh with carbon nanoparticle (candle

soot), (b) carbon nanoparticle coated stainless steel mesh, (c) SiO₂/carbon stainless steel mesh, (d) PFOTS modified SiO₂/carbon stainless steel mesh, (e) PDDA–PFO modified SiO₂/carbon stainless steel mesh. Images reprinted from [21], with permission from Royal Society of Chemistry, Copyright 2017.

2.2.2 Durable PDMS-CS based superhydrophobic mesh

The candle soot was deposited on stainless steel mesh by simply placed above the candle flame for 15 sec. Then this CS coated stainless steel mesh was dipped in solution of PDMS & Xylene for 10 min by using immersion method. After that same process will be carried out for deposition of candle soot on this modified stainless-steel mesh was prepared. It shows 156° water contact angle & nearly 0° oil contact angle. Also, it shows 3° sliding angles. It shows higher water contact angle even after 10 times tests of oil-water separation. The oil-water separation efficiency was nearly 91% by using this modified superhydrophobic stainless steel mesh. It exhibits high thermal stability, good corrosion resistance and reusability. It was modified though combine mesh & polymer foam the composite adsorbent material successfully separate the oil from water via magnet drive method. This modified method was very useful than other research work. So, it was very useful than any other works [21].

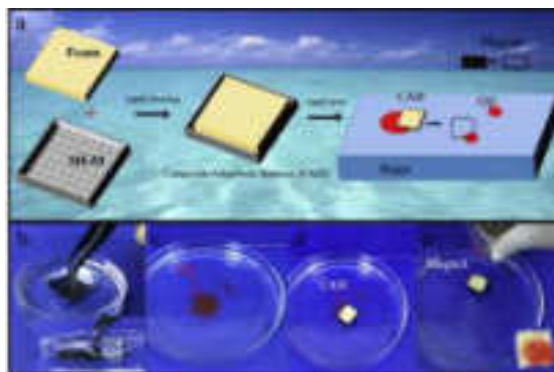


Figure-5. a) Schematic for the preparation process of composite adsorbent material (CAM) from the SH-M square boat and polymer foam, as well as its application of magnet drive for oil/water separation; b) SH-M square boat immersion in water by force; c–e) picture of the magnet drive CAM oil adsorption process. Images reprinted from [22], with permission from Progress in Organic Coatings, Copyright 2019.

2.2.3 CS templated superhydrophobic silica coating on SS mesh

The superhydrophobic coating was prepared through placing the cleaned substrate over candle flame until a few microns thick layer of candle soot deposited on

stainless steel mesh. The candle soot coated substrate together with SiCl_4 was placed in a drier for chemical vapour deposition. Then, though calcination at $600\text{ }^\circ\text{C}$ for half in air, CS composed NPs thermally degraded and diffused through the silica shell gradually. It shows highly oil-water separation efficiency even after 30 times cycle separation superhydrophobic surface remained. The superhydrophobic coating revealed excellent separation efficiency even after 6 times reuses of same superhydrophobic material. It could be potentially used in optical and visual application scenarios where in harsh & oily environments, like goggles, building façade, visual oil-water separation device & touch screen, etc. Among the all-other research work it shows tremendous oil-water separation properties [22].

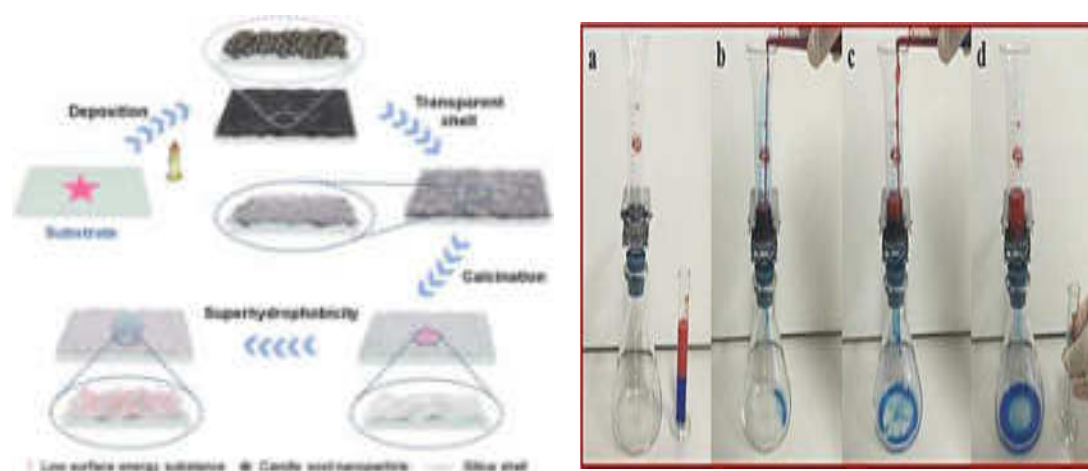


Figure-6. Schematic of preparation and properties of the transparent and robust superhydrophobic coating and oil–water separation. Images reprinted from [23], with permission from Nature, Copyright 2022.

3.CONCLUSION

As this review highlights, candle soot nanoparticles are unique in that, their fabrication requires little control of external parameters. It is very economical beneficial, facile and straightforward to synthesize. Candle soot coated sponge/mesh for use in oil-water separation has been developed by using CS-nanoparticles and different polymers. The candle soot synthesis, candle soot coated sponge/mesh preparation, procedures are simple, cost-effective and scalable. The absorption/separation investigation demonstrates that, the candle soot sponge/mesh is highly efficient and stable in absorbing a wide range of oil and organic solvents. It can be believed that, the candle soot coated superhydrophobic materials are very useful for oil-water separation. It shows various tremendous results with candle soot-

polymer composite in various mechanical conditions. A candle soot nanoparticle shows significant surface area to volume ratio, high electronic and ionic conductivity. Candle soot is produced by simply burning of candles and hence, it is ecofriendly, economical and useful. Candle soot coated sponge/mesh can show stability, durability, reusability and reproducibility.

ACKNOWLEDGEMENT

This work was supported by Department of Chemistry and Department of Physics, RajeRamrao Mahavidyalaya, Jath. We also acknowledge Prof. (Dr.) Suresh S. Patil, Principal, RajeRamrao Mahavidyalaya, Jath.

REFERENCES

1. Yao, T.,Zhang, Y.,Xiao, Y.,Zhao, P.,Li, G.,Yang, H., Li, F.(2016) Journal of Molecular Liquids, 218, 611–614.
2. Bi, H., Xie, X., Yin, K., Zhou, Y., Wan, S., He, L., Xu, F., Banhart, F., Sun, L., Ruoff, R.S. (2012) Advanced Functional Materials, 22, 4421-4425.
3. Cong, H.P., Ren, X.C., Wang, P., Yu, S.H. (2012) American Chemical SocietyNano, 6, 2693-2703.
4. Li, L., Li, B., Dong, J., Zhang, J. (2016) Journal of Materials Chemistry A, 4, 13677-13725.
5. Gao, J., Huang, X., Xue, H., Tang, L., Li, R.K. (2017) Chemical Engineering Journal, 326, 443-453.
6. Bayat A., Aghamiri, S. F., Moheb, A.,Vakili-Nezhaad, G. R.(2005) Chemical Engineering & Technology, 12, 28-40.
7. Li, J., Zhu, L.,Luo, Z.(2016) Chemical Engineering Journal, 287, 474-481.
8. Wu, Z., Li, C., Liang, H., Zhang, Y.,Wang, X., Chen, J.,Yu, S. (2014) Scientific Reports, 4, 4079.
9. Bi, H., Xie, X., Yin, K., Zhou, Y., Wan, S., He, L., Xu, F., Banhart, F.,Sun, L.,Ruof, R. S.(2012), Advanced Functional Materials, 22, 4421-4425.
10. Sam, E. K., Sam, D. K., Lv, X., Liu, B., Xiao, X., Gong, S., Yu, W., Chen, J., Liu, J.(2019) Chemical Engineering Journal, 19, 3012-3018.
11. Zulfiqar, U., Hussain, S. Z., Subhani, T., Hussain, I., Rehman, H.(2018), Colloids and Surfaces A: Physicochemical and Engineering Aspects, 539, 391–398.
12. Gao, Y., Zhou, Y. S., Xiong, W., Wang, M., Fan, L., Golgir, H., Jiang, L., Hou, W., Huang, X., Jiang, L., Silvain, J.,Lu, Y. F. (2014) ACS Applied Materials & Interfaces, 6, 5924–5929.
13. Ren, G., Song, Y., Li, X., Zhou, Y.,Zhang, Z., Zhu, X.(2018) Applied Surface Science, 428, 520-525.

14. Choi, S., Kwon, T., Im, H., Moon, D., Baek, D., Seol, M., Duarte, J., Choi, Y.(2011) *ACS Applied Materials & Interfaces*, 3, 4552–4556.
15. Song, J., Na, L., Li, J., Cao, Y., Cao, H.(2022) *Nanomaterials*, 12, 761-775.
16. Li, J., Zhao, Z., Kang, R., Zhang, Y., Lv, W., Li, M., Jia, R., Luo, L.(2017)*Journal of Sol-Gel Science and Technology*, 3, 817–826.
17. Zulfiqar, U., Hussain, S., Subhani, T., Hussain, I., Rehman, H.(2018) *Colloids and Surfaces A: Physicochemical and Engineering Aspects*, 539, 391–398.
18. Gao, Y., Zhou, Y., Xiong, W., Wang, M., Fan, L., Rabiee-Golgir, H., Jiang, L., Hou, W., Xi, H., Jiang, L., Silvain, J., Lu, F.(2014) *ACS Applied Materials & Interfaces*, 6, 5924–5929.
19. Beshkar, F., Khojasteh, H., Niasari, M.(2017) *Journal of Colloid and Interface Science*, 497, 57–65.
20. Liu, D., Yu, Y., Chen, X., Zheng, Y.(2017) *RSC Advances*, 7, 12908–12915.
21. Zhang, R., Zhou, Z., Ge, W., Lu, Y., Liu, T., Yang, W., Dai, J. (2020) *Chinese Journal of Chemical Engineering*, 5, 30292-30294.
22. Chen, B., Zhang, R., Fu, H., Xu, J., Jing, Y., Xu, G., Wang, B., Xu, H.(2022)*Scientific Reports*, 8, 1-9.

A Review on Superhydrophobic Surfaces: Fundamentals, Fabrications and Applications

Mehejbin R. Mujawar¹, Rajesh B. Sawant¹, Govind D. Salunke¹, Rajaram S. Sutar², Sanjay S. Lathe³, Ankush M. Sargar⁴, Raghunath K. Mane⁵, Krishna K. Rangar¹, Shivaji R. Kulal^{1*}

¹ Department of Chemistry, Raje Ramrao Mahavidyalaya, Jath, Dist. - Sangli (MS) India

² Self-cleaning Research Laboratory, Department of Physics, Raje Ramrao Mahavidyalaya, Jath, Dist. - Sangli (MS) India.

³ Self-cleaning Research Laboratory, Department of Physics, Vivekanand College (Autonomous), Kolhapur, Dist. - Kolhapur (MS) India.

⁴ Department of Chemistry, Bharati Vidyapeeth's Dr. Patangrao Kadam Mahavidyalaya, Sangli, Dist. - Sangli (MS) India

⁵ Department of Chemistry, Smt. Kusumtai Rajarambhapu Patil Kanya Mahavidyalaya, Islampur, Dist. - Sangli (MS) India

*Corresponding author's E-mail: srkulal@gmail.com, amsargar2012@gmail.com

Abstract

Superhydrophobic surfaces are highly hydrophobic i.e., it extremely difficult to wet. Superhydrophobic surfaces are the tendency to repel water drops and absorb oil drops. The water contact angle of superhydrophobic surfaces is greater than 150° , the oil contact angle is less than 5° , and the sliding angle is less than 5° . It is showing the lotus effect. Superhydrophobicity is observed in the lotus leaves, insects, and some other plants in which their leaves would not get wet. This phenomenon is due to the unique surface structure of the lotus leaf and also the presence of a low surface energy material on the surface of the leaf. For the formation of a superhydrophobic surface, the surface must show hierarchical micro- and nano-roughness and low surface energy. Efforts have been taken to form superhydrophobic surfaces for a variety of applications. There are many applications of superhydrophobic surfaces such as self-cleaning surfaces, oil-water separation surfaces, anti-icing surfaces, anti-corrosion surfaces, anti-fogging surfaces, and water-resistant surfaces. In this article, the fundamental principles of superhydrophobic surfaces, some recent trends in the fabrication of superhydrophobic surfaces, and their applications are reviewed and discussed.

Keyword: Superhydrophobicity, Superoleophobicity, Lotus effect, Self-cleaning, Oil-water separation, Water-repelling, Oil Contact Angle, Water Contact angle, Anti-icing, Anti-corrosion.

अक्षर वाङ्मय

वर्ष तेरावे, पुरवणी अंक ४, खंड. २

फेब्रुवारी २०२३



मुख्य संपादक
डॉ. नानासाहेब सुर्यवंशी



अक्षर वाङ्मय

वर्ष तेरावे, पुरवणी अंक ४, खंड. २

फेब्रुवारी २०२३

संपादक
डॉ. नानासाहेब सूर्यवंशी

कार्यकारी संपादक
डॉ. शिवाजीराव देशमुख

प्रकाशक : सौ. रेखाताई नानासाहेब सूर्यवंशी, प्रतीक प्रकाशन
'प्रणव' रुक्मिणी नगर, थोडगा रोड, अहमदपूर ४१३५१५
मुद्रक: श्री. जे प्रिंटिंग प्रा लिमिटेड १४१६ सदाशिव पेठ पुणे- ४११०३०
साहित्य व वर्गणी पाठवण्याचा पत्ता: डॉ. नानासाहेब सूर्यवंशी
'प्रणव' रुक्मिणी नगर, थोडगा रोड, अहमदपूर,
जि. लातूर, ४१३५१५
E-mail : suryawanshinanasahab67@gmail.com

वार्षिक वर्गणी: रु ५००/-

पंचवार्षिक वर्गणी : रु २०००/-

द्विवार्षिक वर्गणी : रु ९००/-

अंक मूल्य : रु १२५/-

-
- महाराष्ट्र राज्य साहित्य व सांस्कृतिक मंडळ या नियतकालकाच्या प्रकाशनात अनुदान दिले असले तरी या नियतकालिकेतील लेख लेखांच्या विचाराशी मंडळ व शासन सहमत असेलच असे नाही.
 - या अंकातील लेखातून व्यक्त झालेले लेखकांच्या मतांशी संपादक, संपादक मंडळ, प्रकाशक व मुद्रक सहमत असतीलच असं नाही.



24	Search for Inner Self in Techno savvy era: Kim Scott's <i>True Country</i> Shital Anandran Mohite, Dr. Rajashri Barvekar	74-76
25	Impact of Technology on Education Miss. Sawant Ashwini Arjun	77-79
26	Teaching and Studying Literature in The Digital Age Dr. Sarangpani Ramchandra Shinde	80-84
27	A Study on Significant Role of Technology in Financial Sector Prof. Ms. Manju shri Kadam, Dr. Shabana A. Memon	85-89
28	The Era Of E-Literature Ms Sweta Shalish Thakkar, Dr. Mahavir Sankala	90-92
29	Death Trap of Technology - A Dystopia Vision of 20 th Century Sci Fi Mr. Ananda Pandhare, Dr. Mahavir Sankala	93-96
30	Impact of Technology on Book Publication and Library Services A Comparative Study: Digital and Library Niche Ms Swati Shree	97-99
31	A study of Technological advancement: A pathway to Utopia Mr. Marewad Atul Balaji, Dr. Sankla Mahavir R	100-102
32	The Depiction of Uneven Dissemination of the Technological Advancement in <i>Generosity</i> by Richard Powers Abhijeet S. Dalavi, Prof. (Dr) Satish R. Ghatge	103-105
33	Use of Digital Tools and E-resources in Teaching Literature Mr. Shaikh Firoj Husen,	106-108
34	The analysis of Technological Advancements in the Entertainment Sector with respect to shift in Language and Audience Base. Snehal S. Warekar	109-111
35	Technological Prospects in Avatar 2: Merely Imagination or Realism Mr. Prashant P. Ingole, Ms. Shraddha M. Sankla	112-115
36	भूमंडलीकरण, मीडिया और हिंदी साहित्य डॉ. गणेश हुंदा गभाले	116-119
37	भूमंडलीकरण के परिप्रेक्ष्य में हिंदी सिनेमा डॉ. सुबराज राजाराम मुळगे	120-123
38	भूमंडलीकरण के दौर में नारी डॉ. सुसंधा हिंदुराव परपणकर	124-126
39	भूमंडलीकरण और हिंदी साहित्य (कहानी विधा के विशेष संदर्भ में) डॉ. नितीन हिंदुराव कुंभार	127-129
40	भूमंडलीकरण के परिप्रेक्ष्य में हिंदी कविता: विशेष संदर्भ 'नवी कविताएँ' प्रा. हिरामन टोंगारे, डॉ. सतीशकुमार पडोळकर	130-133
41	वेदग्रन्थ उपन्यास में चित्रित किसान आन्दोलन विद्या आनंदराव जाधव	134-136
42	भूमंडलीकरण और उपन्यास साहित्य (युवावर्ग के संदर्भ में) सु. श्री. अर्चना चसंत ठराल	137-138
43	भारतवर्षीय विज्ञानम् । डॉ. सविन चंद्रशेखर कंदले	139-143
44	संस्कृत साहित्यापीय संमीनजायीय अध्यायनामधे संयजानापी भूमिका डु. मधुरा प्रमोद किरयेकर	144-146
45	Technology and Sanskrit literature Aayush	147-149
46	संस्कृतसाहित्ये नन्वज्ञानम् Guneendra Arya	150-152

भूमंडलीकरण के परिप्रेक्ष्य में हिंदी कविता: विशेष संदर्भ ' लंबी कविताएँ'

प्रा.श्रीरामचण टोंगारे, डॉ.रातीशभुगार पडोळकर,

अध्यक्ष, हिंदी विभाग, राजे रामराय महाविद्यालय, जत जिला- गांगली
महा. प्राध्यापक, राजे रामराय महाविद्यालय, जत जिला- गांगली

अभेद्य :-

कविता अथवा काव्य बहुत प्राचीन साहित्य विधा है। भूमंडलीकरण के दौर में काव्य विधा काफ़ी हद तक परिवर्तित हुई। इसका प्रमुख कारण भूमंडलीकरण के समय में मानवी जीवन में आया हुआ परिवर्तन। इसी कारण कविता की संरचना में भी परिवर्तन हुआ। परिणामतः लंबी कविता का उद्भव हुआ। लंबी कविता में कथन की अपेक्षा संवेदना, बोध, कल्पनात्मकता अथवा किसी चिंतन की अभिव्यक्ति अथवा सांकेतिक अभिव्यक्ति की जाती है। किंतु लंबी कविता नई का निर्धारण, चिंतन की सृष्टि, शैली-विधान आदि पर अधिक बल दिया गया है। पुरानी प्रबन्धात्मक कविताओं में कथा की यह निर्बाध सघनता बहुत कम दिखाई देती है, जैसी की आज की लंबी कविताओं में हुआ करता है। भूमंडलीकरण के दौर में रचित आधुनिक कविताएँ या प्रवीत कविता में लंबी कविता का अंतर बहुत साफ-साफ दृष्टिगोचर होता है। नये कविताएँ अनुभूति और अभिव्यक्ति दोनों में मंचित हुआ करती हैं। उनका कथा जल्दी ही खूब जाता है किंतु लंबा आकार देखकर भी किसी कविता को लंबी कविता कहना उचित नहीं है। आज लंबी कविता का शिल्प काफी विकसित हो चुका है। इस वैशिष्ट्य को ठीक ढंग में न पकड़ पानेवाले लोक लंबी कविता को किसी नेता का भाषण मात्र समझते हैं। ऐसा भी नहीं है कि दम-भंडह पंक्तियों से अधिक विकसित हो जाने पर किसी कविता को लंबी कविता कह दिया जाए। संवेदना की निर्बाध अभिव्यक्ति, चेतना प्रवाह, वयार्थ का स्पष्ट बोध और उनके बीच से मूल्यों का निर्धारण लंबी कविता का मुख्य वैशिष्ट्य है। इनमें आज के जीवन का बदलता हुआ वयार्थ, विवशता, तनाव, त्रास आदि सब कुछ लंबी कविता में व्यक्त हो जाता है। डॉ. शम्भुनाथसिंह जैसे गीतकार कविता की संरचना एवं विशेषताएँ जाने मर उमे केवल नेता का भाषण मान लेते हैं- "लंबी कविता नेता के भाषण के समान होती हैं जिसमें कुछ भी लिख सकते हैं।" अपनी इस अवधारणा के आधारपर वे यह निष्कर्ष निकालते हैं कि भावानुभूति को जहाँ प्रकट करना है वहाँ छोटी कविता ही लिखी जाएगी, लंबी कविता नहीं। (नई कविता की लंबी कविताएँ- डॉ. रामसुधार सिंह, पृ. 1)

कविता के विकास के साथ लंबी कविताओं की अधिक से अधिक रचनाएँ हुई हैं। किंतु इसके स्वतंत्र अस्तित्व के संबंध में विद्वानों में मतभिन्नता है। कुछ विद्वान इसे स्वतंत्र विधा के रूप में स्वीकार करते हैं, लेकिन कुछ विद्वान इससे सहमत नहीं हैं। 'दुमरा समक' के प्रमुख कवि नरेश मेहता के विचार में भूमंडलीकरण के दौर की लंबी कविता यह एक स्वतंत्र विधा है, क्योंकि किसी विचार को विस्तृत करके ही लंबी कविता लिखी जा सकती है। अपनी इस विशेषता के कारण लंबी कविता का महाकाव्य का छण्डकाव्य से अलग अस्तित्व होता है। महाकाव्य और छण्डकाव्य के लिए सीमित परिवेश और सीमित काल आवश्यक है। लेकिन लंबी कविता इससे पूर्णतः अलग है। (वहीं, पृ.2) नरेश मेहता की तरह डॉ. शुक्देवसिंह भी लंबी कविता को एक अलग विधा मानते हुए कहते हैं- प्रत्येक काल की छंद, लय आदि से संबंधित कोई न कोई विशेषता रही है और नई कविता की शैली में हम लंबी कविता को ही रख सकते हैं। (वहीं, पृ.2) लेकिन बहुत मारे विद्वान इस मत से सहमत नहीं होते हैं। इन विद्वानों में डॉ. जगदीश गुप्त, श्री लक्ष्मीकांत वर्मा, श्रीराम वर्मा और श्री नीलाभ प्रमुख हैं। श्री जगदीश गुप्त की अवधारणा है कि पर्याप्त रचना होने पर ही कोई काव्यधारा अलग विधा बन सकती है। श्रीराम वर्मा भी इस मत से सहमत हैं। उनके अनुसार 'लंबी कविता कोई विधा नहीं है।' (वहीं, पृ.2) इन विद्वानों के नये विचार अपनी परंपरावादी विचारक के परिचायक हैं।

भूमंडलीकरण और लंबी कविता स्वरूप:

'लंबी कविता' को कविता की एक स्वतंत्र विधा स्वीकार करने पर सबसे पहला यह प्रश्न सामने आता है कि अगर यह एक स्वतंत्र विधा है तो उसका स्वरूप क्या होगा? उसकी संरचना कैसी होगी? इस संदर्भ में दो-तीन बातें महत्वपूर्ण हैं। कविता के स्वरूप निर्धारण में देश और काल का महत्वपूर्ण योगदान रहता है। जिस देश और काल में लंबी कविता लिखी गयी है वही उसके स्वरूप का निर्धारण करता है। इसमें कवि का व्यक्तिगत महत्व भी होता है और प्रत्येक कवि की शूनित पर भी इसका स्वरूप निर्भर करता है। कवि की तीव्रता ही उसे स्वरूप प्रदान करती है। इन्हीं दृष्टियों से लंबी कविता के स्वरूप पर विचार करना समीचीन

होया। औद्योगीकरण और और महानगरीकरण के परिणाम स्वरूप आज की जिंदगी दुहर-नी गयी है। भारत के स्वधीनताप का में नई पीढ़ी के सारे मपने टूट-बिखर गनये हैं और उन्हें वेकारी, भूख, कुण्ठा, घुटन, उपहार स्वरूप प्राप्त हुए है। इन कारण युवा पीढ़ी समकालीन व्यवस्था के खिलाफ हो गयी। जीवन समस्त स्तरों पर निराशा एवं अनास्था मिलने के कारण युवा पीढ़ी का एक शिकायती और बिद्रोही हो जाना स्वाभाविक ही था। लंबी कविता इसी शिकायत का एकाग्रण है। धूमिल ने एक उदाहरण के लिए 'बौबलाए' हुए आदमी का एकाग्रण। आज का युग विशिष्ट समस्याका युग है और इसी व्यापकता को व्यक्त करने के लिए छोटे-मोटे अपर्याप्त घोषित किनये गनये और फलस्वरूप लंबी कविता का मृजन संभव हो सका। कविता के लंबेपन में कवि का व्यक्तित्व का सहायक होता है। व्यक्ति के अनुसार अनुभूति में अंतर हो जाता है। कविता के निजी बोध अथवा गहराण में उपती गविना के फलस्वरूप उस कविता का आकार बन जाता है। इसी संदर्भ में कुछ कविताएँ लंबी और कुछ छोटी बन जाती है। लंबी कविता के बोध और संवेदना का फलक विस्तृत होता है। 'तार रातक के द्वितीय संस्करण में कवि एक नई कविता 'एक आत्ममंतव' की रचना जो कुल मिलाकर छः पृष्ठों की कविता है और उसके विषय में कवि का कथन है कि, 'यहाँ जो नई कविता दी जा रही है, और यह 1963 की ही रचना है, अपेक्षाकृत छोटी है। इससे छोटी रचनाएँ शायद मे अब नहीं लिख सकता।' (वहीं, पृ.3) इन प्रकार स्पष्ट है कि कविता का लंबा होना कवि की वैज्ञानिकता पर निर्भर है।

लंबी कविता में कथा को अभिव्यक्त करने का अपना एक अलग ढंग है। कथन की भंगिमा मुख्यतः तीन बातों पर निर्भर करती है- कौन कह रहा है, नया कह रहा है और किससे कह रहा है। (वहीं पृ.4) छायावादोत्तर कवियों का अपना कौशल था कि वे हल्की-सी बात को उपस्थित कर गुरु गंभीरता को शटके से तोड़ना- "सुनता रहा मधुर नुपुर ध्वनि, यदिप बजती थी चप्पल" (वहीं, पृ.4) आदि पर आज कवि लंबी कविताओं में 'टीम' को बड़ाजक ढंग से कहना चाहता है। धूमिल की 'भोबीराम' इसका उदाहरण है। 'लंबी कविता में सिवा इसके कि वे लंबी होती हैं और उनका फलक बड़ा होता है' में कोई और अलग बड़ी सूची को मानता। उनमें एक विचार या मनःस्थिति विस्तार से और सालंकार यानी खूब दिखाई दे मके ऐसे ढंग में कही जा सकती है- "अनुपात तो उनमें भी होता है। छोटी कविता में बात को सात-सात, आठ-आठ पहलुओं से नहीं देखा जा सकता है। 'अनाम तुम उसे हो'का अनाम पूरी कविता में व्याप्त कविता में व्याप्त है। कभी सूरज की किरन की भाँति, कभी धारा की तरह, कभी गति की उप वह कवि को प्रभावित करता है और कवि के होठों को प्वाले की भाँति छू लेता है। 'अनाम' को कवि कई पहलुओं में रचका देता है। 'अनाम' का नाम जानने के लिए कवि की उत्सुकता देखने लायक है।" (वहीं, पृ.4)

छोटी कविता में इतने विस्तार के लिए अवकाश नहीं रहता है। छोटी कविताओं में कवि एक निश्चित अंग ही प्रस्तुत कर पाता है। भवानीप्रसाद मिश्र की ही एक छोटी कविता से इसे स्पष्ट समझा जा जा सकता है। पूरी कविता इसप्रकार है-

मैंने पूछा
तुम क्यों आ गई
वह हँसी
और बोली
तुम्हें कुरुप से
बचाने के लिए
कुरुप है
जरुरत से ज्यादा
धूप
मे छाया है
जरुरत से ज्यादा धूप
कुरुप है। (वहीं, पृ.4-5)

कविता में धूप और छाया की एक हल्की-मी झलक भर दिखायी पड़ती है। लेकिन लंबी कविताओं का फलक बड़ा हो है और कवि बाह्य एवं अन्तः दोनों स्थितियों का विस्तार पूर्वक उद्घाटन करता है। कविता के अनेक दृश्यपटन उपस्थित किनये जाते हैं जो कहीं पाठक को सुख और संतोष के प्रीतिकर विस्तार में देखेजाते चले जाते हैं, कहीं भयानक उत्पात और संसट के रूप संवेदना को क्षुब्ध करते रहते हैं। प्रबंध कविता में एक केंद्रीय कथा के अनेक परिप्रेक्ष्य होते हैं और प्रबंधकार उन्हें अनेक नदनों में बाँटकर अलग-अलग सगों या अध्यायों में विभाजित कर देता है। आखिर किमी सर्ग में रूप-चित्रण प्रधान हो जाता है, वहीं कवि

का विकास दिखायी पड़ता है, कहीं मूल्यों का निर्धारण होता है और कहीं वैयक्तिक अनुभूतियों की विवृति दिखाई पड़ती है। इन प्रकार विभिन्न परिप्रेक्ष्यों के आधारपर कई मंदर्भ उपस्थित किये जा सकते हैं, लेकिन लंबी कविता का समग्र विकास किसी एक केंद्रीय चेतना से जुड़ा होता है। उन्नी केंद्रीय दम्बुचेतना अथवा संवेदना को कवि अनेक मंदर्भों में विकसित करता हुआ आगे बढ़ता है। इस तरह से लंबी कविता से रूप का चित्रण, संवेदना की विवृति, मूल्यों का निर्धारण और उनका अंकन जुड़ जाता है।

कमला की विभिन्न मनःस्थितियों का पूरी कविता में भिन्न-भिन्न रूपों में चित्रण किया गया है। कहीं रूप- कविता नारी के रूप में, कहीं गुलरदेश की रानी के रूप में, कहीं वीरांगना के रूप में, कहीं अपमानित नारी के रूप में, कहीं दीन-हीन करुणा की स्फूर्ति के रूप में कमला उपस्थित होती है। अंत में बहलोभा, लालसा एवं महत्त्वकांक्षा की प्रतिस्फूर्ति बनकर हमारे समझ आती है, जब समस्त शाही परिवार की हत्या कर दी जाती है।

'राम की शक्ति पूजा' के केंद्र में संघर्षमय राम के जीवन में व्याप्त निराशान्धकार है। 'रावण महिमा श्यामा विमावरी अंधकार' ही राम को घेरे हुए हैं। रावण का भव और रात्रि का अंधकार दोनों एक हैं। कवि का लक्ष्य यहाँ राम-रावण के युद्ध का वर्णन नहीं है इसीलिए कविता का आरंभ होता है- 'रवि हुआ अस्त, ज्योति के पत्र पर लिखा अमरा रह गया राम रावण का अपराजित समरा आज का....। (निराला और मुक्तिबोध की चार लंबी कविताएँ पृ. ४४)' राक्षस, लंका आदि सभी एक व्यापक सांकेतिक अर्थ के लिए एकत्र किये गये हैं। वास्तविक संघर्ष का स्थल तो राम का अंतस्वभाव है। शूनित-माधना की सिद्धि में यह संघर्ष समाप्त हो जाता है। इसी बीच जो भी राम की मानसिक स्थिति बनी है उन्नी का मूल्य चित्रांकन करना कवि का उद्देश्य है। राम बानर सेना के साथ शिविर में लौट आते हैं। राम की जय खुलकर चारों ओर पीठ झाड़ों पर टूटती हुई है। वे पूरी तरह जीवन युद्ध से निराश हो गये हैं, हिंखर भी आशा की एक झलक राम की आँखों में दिखाई पड़ती है। कवि उपमानों के सहारे उनका चित्र खींच देता है-

"उतरा ज्यों दुर्गम पर्वत पर नेशांधकार,

चमकती दूर तराएँ ज्यों कहीं पारा।' (नई कविता की लंबी कविताएँ, पृ. 6)

तदुपरांत राम जहाँ अपने सेनानियों के साथ बैठते हैं वहाँ की स्थिति का वर्णन कवि इसप्रकार करता है-

'हे अमा-निशा, उगलता गगनपग अंधकार,

खो रहा गिा का ज्ञानख सत्वध है पवन-पारा

अप्रतिहत बरज रहा पीछे, अम्बुधि विशाल,

भूधर ज्यों ध्यान मग, केवल जलनी मशाला" (वहीं, पृ. 6)

हिंदी साहित्य में फैंटेसी आधुनिक युग की देन है। आधुनिक युग में जीवन की विचंगति, मानसिक निर्वलता आदि को कवि फैंटेसी के सहारे प्रस्तुत करने लगा है। हिंदी साहित्य में इसकी उपज विदेशी प्रभाव के कारण मानी जा सकती है जो नाटकों में होती हुई काव्य में आयी है। यह फैंटेसी कहीं कवि की मनोवैज्ञानिक दृष्टि प्रगट करती है और कहीं कविता में प्रभावोत्पादकता लाती है। 'राम की शक्ति पूजा' शीर सीता का अपहरण होने का दृश्य फैंटेसी के सहारे चित्रित किया गया है। सण भर के लिए पाठक जनक-वाटिका में पहुँच जाता है और राम सीता के 'नयनों का नयनों गोपन-प्रिय संभाषण' के दर्शन करता है। यहाँ एक ओर राम के मन की दुर्वलता लक्षित होती है वहीं दूसरी ओर कविता में एक चमत्कार भी पैदा किया गया है। इसी समय रावण का अद्भुतहान मुनाई देना भी फैंटेसी के अंतर्गत है। कविता का यह स्थल फैंटेसी सर्वना के कारण इतना महत्वपूर्ण हो गया है कि पूरी कविता का केंद्र-बिंदु बन गया है। लेकिन फैंटेसी की सफल अभिव्यक्ति मुक्तिबोध ने ही प्रारंभ होती है। श्री. सुरेश ऋतुपूर्व के अनुसार- 'मुक्तिबोध ने अपनी कविताओं में भयानक फैंटेसी की रचना करके, छायावादियों के देशकी मनमन से महीन बाचवीय वातावरण को जिनमें रजनीगंधा की महल में डूबे हुए कुंज हैं, लाज भरा सौंदर्य है- शिप्र-भिन्न कर दिया।' (वहीं, पृ. 8) 'अंधेरे में' के अंतर्गत अनेक सफल फैंटेसी की सर्वना हुई है। विचारों की धुन कवि के मिर में घूमती है और वह इसकी खोज में चेतन में अवचेतन एवं स्वप्न से जागृति अवस्थाओं में संचरण करती हुई बंधार्थ को उछालती चमती है। पूरी कविता का संसार संसार और अंधेरे का संसार है। मुक्तिबोध के अतिरिक्त विजयदेव नारायण साही, धूमिल, राजकमल चौधरी और सीमित्र इकोहन की कविताओं में भी सफल फैंटेसी की रचना की गई है। विजयदेव नारायण साही की लंबी कविताओं में भी मुक्तिबोध के समान फैंटेसी की सर्वना हुई है।

परमानन्द श्रीवास्तव के अनुसार "फैटेसी की दुनिया की यह तलाश, उस जटिल की तलाश है- जहाँ अरिष्ट कठोर मूल्यों और मानव-अस्तित्व की बुनियादी जिज्ञासाओं या चिन्ताओं का एक साथ सामना किया जा सकता है।" (वहीं, पृ.9)

धूमिल की 'पटकथा' एक चित्रकथा है। जिसमें सामाजिक और राजनैतिक यथार्थ के अनेक दृश्य फैटेसी के माहुरि पदों पर उपस्थित किये गये हैं। पूरी कविता एक सपाट बगानी है जिसमें गहनत भाषा का अभाव महसूस होता है। इस कारण ही अशोक वाजपेयी इस कविता को एक दिनचर्या असफलता मानते हैं जिसे पढ़ने में ऊब और कभी-कभी शिष्ट पैदा होती है।" (वहीं, पृ.9)

अशोक वाजपेयी का यह कथन एकांकी दृष्टि का परिचायक है। इसे जड़ों-का-तड़ों स्वीकार नहीं किया जा सकता है। कविता में फैटेसी के सच्चे कवि ने हिंदुस्थान का दृश्य उपस्थित किया गया है जो पूरी कविता को एक गहरे दृष्टिकोण पर आधारित बना कर देता है। फैटेसी की सफल अभिव्यक्ति निम्नलिखित पंक्तियों में देखी जा सकती है। धून और आंगूओं से तर चेहरे में हिंदुस्तान की गथाय धूमिल की फैटेसी की देन है-

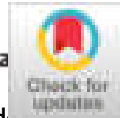
उसका हाथ ऊपर उठा था
धून और आंगू से तर चेहरा
'दुखी मत हो। यही मेरी नियति है।
मे हिंदुस्तान है।

हत्बारा। हत्बारा। हत्बारा।' (वहीं, पृ.9)

कुल मिलाकर भूमंडलीकरण के दौर में लिखी लंबी कविता की फैटेसी एक महत्वपूर्ण विशेषता है जिसकी प्रत्येक लंबी कविताओं में सफल सृष्टि की गयी है। इसके प्रयोग से लंबी कविताओं में जहाँ एक ओर चमत्कार उत्पन्न किया गया है वहीं एक नवीन शैली के प्रयोग द्वारा प्रभाव भी पैदा करने की कोशिश की गई है। भूमंडलीकरण के दौर में घटित जटिल मनोव्यापारों को अभिव्यक्त करने के लिए लंबी कविताओं ने फैटेसी का भरपूर उपयोग किया हुआ है। भूमंडलीकरण के समय की लंबी कविता की संरचना में फैटेसी का भी महत्वपूर्ण स्थान होता है। फैटेसी द्वारा जहाँ एक ओर कविता लंबी होती है वहीं दूसरी ओर उगम गद्यात्मकता प्रधान होती है। डॉ. आत्म-संघर्ष और सामाजिक संघर्ष, आत्म और अनात्म के संघर्ष के फलस्वरूप आज की कविता का कथय पूर्णतः जटिल हो गया है। इस जटिल कथा की अभिव्यक्ति के लिए कवि स्वप्न और फैटेसी की शैली अपनाता है। यह लंबी कविता की अपनी निजी विशेषता है। कवि के भीतर का संश्राम पूरे समाज में फैला हुआ है जिसके भीतर अनेक जाती-पड़वासी आकृतियाँ उभरती दिखायी देती हैं। कविता के प्रारंभ में ही उस अंधेरे का वर्णन शुरू होता है जो जिंदगी के कमरों में लगातार चक्कर लगाता है। इसी अंधेरे के बीच कविता के अंत तक कवि हूर सड़क हूर गली में प्रत्येक चेहरे की ओर झांककर पठार, पहाड़ और समुद्र तक अपनी खोई हुई अभिव्यक्ति को छुड़ता है। सफल फैटेसी की रचना के लिए भाषा का संघटन आवश्यक है जिसमें प्राचीन वाच्यता को नष्ट किया जा सके। मुक्तिबोध में भाषा का यह संहारक रूप सबसे अधिक उभरकर आया है। इसी कारण मुक्तिबोध फैटेसी की रचना में अधिक सफल हुई है।

संदर्भ:

- 1) नई कविता की लंबी कविताएँ डॉ. रामसुधारसिंह; राधा पब्लिकेशन, नई दिल्ली-110002; प्रथम संस्करण 1993
- 2) लंबी कविताएँ वैचारिक सरोकार; डॉ. बलदेव बंशी; वाणी प्रकाशन नई दिल्ली; प्रथम संस्करण 2009
- 3) पाब्लो नेरुदा: एक कैदी की खुली दुनिया; अरुण माहेश्वरी; वाणी प्रकाशन नई दिल्ली.
- 4) कविता से लंबी कविता: दिनोदकुमार शुक्ल; वाणी प्रकाशन नई दिल्ली.
- 5) मापेक्ष संपादक-महावीर अग्रवाल
- 6) लंबी कविताएँ और नरेंद्र मोहन; संपा. डॉ. रमेश सोनी



Superhydrophobic PVC/SiO₂ Coating for Self-Cleaning Application

Rajaram S. Sutar, Prashant J. Kalel, Sanjay S. Latthe, Deepak A. Kumbhar, Smita S. Mahajan, Prashant P. Chikode, Swati S. Patil, Sunita S. Kadam, V. H. Gaikwad, Appasaheb K. Bhosale, Kishor Kumar Sadasivuni, Shanhu Liu,* and Ruimin Xing*

A lotus leaf like self-cleaning superhydrophobic coating has high demand in industrial applications. Such coatings are prepared by alternative dip and spray deposition techniques. A layer of polyvinyl chloride is applied on glass substrate by dip coating and then spray coated a suspension of hydrophobic silica nanoparticles at substrate temperature of 50 °C. This coating procedure is repeated for three times to achieve rough surface morphology which exhibits a water contact angle of $169 \pm 2^\circ$ and sliding angle of 6° . The superhydrophobic state of the coating is still preserved when water volume of 1.2 L is used to impact the water drops on coating surface. The stability of the wetting state of the coating is analyzed against the water jet, adhesive tape and sandpaper abrasion tests. The prepared superhydrophobic coating strongly repelled the muddy water suggesting its importance in self-cleaning applications.

which inspired to create artificial superhydrophobic surface by increasing surface roughness along with decreasing surface energy. Such superhydrophobic surfaces have numerous applications including self-cleaning, anti-corrosion, drag-reduction, oil-water separation, and etc.^[3–8] So far, SiO₂, TiO₂, ZnO, Al₂O₃, candle soot and various polymers have been used to fabricate self-cleaning superhydrophobic coatings.^[9–14] Among them, polymer/SiO₂ nanocomposite is a promising in preparation of self-cleaning superhydrophobic coatings.^[15,16]

The self-cleaning property of superhydrophobic coatings has attracted significant interest in industrial applications. Recently, Latthe et al. have applied suspension of hydrophobic SiO₂ nanoparticles

(NPs) on different types of substrates including body of motorcycle, building wall, mini boat, solar cell panel, window glass, cotton shirt, fabric shoes, cellulose paper, metal, wood, sponges, plastic, and marble which revealed high water repellency and excellent self-cleaning property.^[17] Many reports are available on the preparation of superhydrophobic polyvinyl chloride (PVC) thin films using ethanol.^[18–20] Seyfi et al. have drop casted a mixture of PVC, Ag₃PO₄, and ethanol on thermoplastic

1. Introduction

Lotus leaf is a perfect model of self-cleaning superhydrophobic surface with specific combination of surface chemistry (surface energy) and surface topography (surface roughness).^[1,2] A low surface energy hierarchical surface structure of lotus leaf surface revealed unusual wettability (water contact angle (WCA) greater than 150° and sliding angle less than 10°)

R. S. Sutar, P. J. Kalel, S. S. Latthe, S. Liu, R. Xing
Self-cleaning Research Laboratory
Department of Physics
Raje Ramrao College
Jath
Affiliated to Shivaji University
Kolhapur, Maharashtra 416404, India
E-mail: liushanhu@vip.henu.edu.cn; rmxing@henu.edu.cn

S. S. Latthe, A. K. Bhosale
Henan Key Laboratory of Polyoxometalate Chemistry
Henan Joint International Research Laboratory of Environmental
Pollution Control Materials
College of Chemistry and Chemical Engineering
Henan University
Kaifeng 475004 P. R. China

D. A. Kumbhar
Department of Chemistry
Raje Ramrao College
Jath Maharashtra 416404, India

DOI: 10.1002/masy.202000034

S. S. Mahajan, P. P. Chikode
Department of Physics
Jaysingpur College
Jaysingpur Maharashtra 416404, India

S. S. Patil
Department of Physics
ACS College
Palus Maharashtra 416404, India

S. S. Kadam
Department of Physics
KNP College
Walwa Maharashtra 416404, India

V. H. Gaikwad
School of Chemistry
MIT World Peace University, Kothrud
Pune Maharashtra 416404, India

K. K. Sadasivuni
Center for Advanced Materials
Qatar University
Doha 2713 Qatar

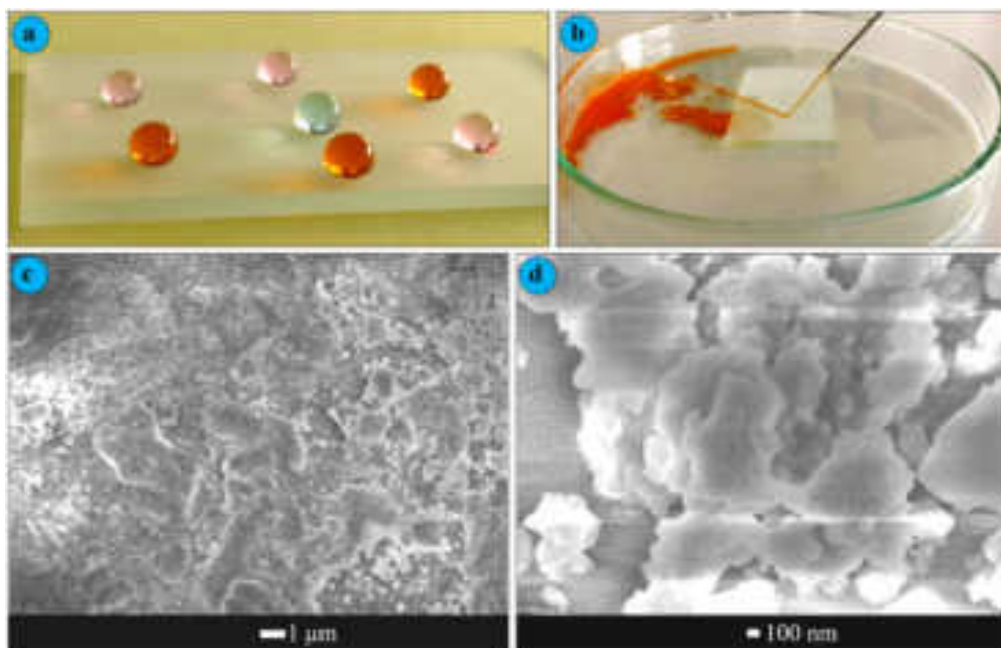


Figure 1. a) Optical photograph of color water drop on superhydrophobic coating, b) the image of water jet impacting on coating, c and d) different magnification SEM images of superhydrophobic coating.

polyurethane (TPU) substrate and achieved antibacterial superhydrophobic surface.^[21] The as prepared superhydrophobic TPU surface showed WCA $\approx 156^\circ$ and SA $\approx 2^\circ$ with self-cleaning performance. Also, Guo et al.^[15] have reported that water drops rolled off immediately on the coating prepared by casting of polymer (PVC, PMMA, and PE) and SiO₂ NPs composite on various substrates like copper, aluminum, stainless steel, silicon, glass and filter paper. Rivero et al.^[22] have prepared superhydrophobic surface by depositing ZnO NPs incorporated polystyrene (PS) and PVC polymeric solution on aluminum alloy substrate using the electrospinning technique. Yuan et al.^[23] have obtained lotus-leaf-like superhydrophobic PVC film by casting PVC solution on negative template of PDMS. Other than this, Zhang et al.^[24] have obtained superhydrophobic coating by pouring PVC/SiO₂ mixture on negative template of PDMS and reported that superhydrophobicity depends on weight percentage of SiO₂ particles in PVC. Chen et al.^[25] have prepared water-repellent SiO₂/polymer (PS and PVC) composite coating without any surface chemical modification by spin coating. The amount of hydrophobic SiO₂ NPs in PVC or PS affects the surface roughness and hence the wettability of the coating.

Herein, we have prepared superhydrophobic surface on glass by dip coating followed by spray coating method. The hydrophobic SiO₂ NPs were prepared by sol-gel technique. A thin layer of PVC was applied on glass substrate by dip coating and dried at room temperature. After that, a suspension of SiO₂ NPs in hexane was sprayed on PVC coated glass substrate at substrate temperature of 50 °C. The superhydrophobic coating was obtained by applying multiple alternative layers of PVC and SiO₂ NPs on glass substrate.

2. Result and Discussion

2.1. Surface Microstructure and Wettability

The multiple layers of PVC/SiO₂ were applied on glass substrate to obtain desired surface roughness which is the main requirement of extreme water repellency. **Figure 1c** represents the surface microstructure of three bilayer of PVC/SiO₂ coating, where the aggregated SiO₂ NPs were distributed on the PVC layer. The PVC layer can help SiO₂ NPs to adhere firmly on the coating surface. The aggregation of SiO₂ NPs is not uniform and the grain sizes from 5 μm to 100 nm were observed (**Figure 1d**). These different size scale grains provide hierarchical surface morphology. Nearly similar surface morphology was reported for the PVC/SiO₂ nanocomposite coating prepared by spin coat technique.^[25] This hierarchical surface morphology tends to trap small air pockets in the rough voids and hence a water drop can sit on the air-solid composite structure with minimum contact to the solid fraction of the surface. A water drop can only touch a small solid fraction of the coating, as the trapped air pushes away the water drops and not allowing the water drops to wet the inner portion of a rough surface. As shown in the **Figure 1a**, the water drops hardly stay on the three bilayer of PVC/SiO₂ superhydrophobic coating. Every water drop takes spherical shape at different positions on the coating surface confirming the uniform deposition of PVC/SiO₂ on the substrate. The superhydrophobic coating was appeared opaque due to the presence of micrometer scaled grains which allows scattering of the visible light. Also the water jet was impacted on the superhydrophobic coating which rebounds off the surface quickly after impacting (**Figure 1b**). The trapped air in the rough surface resists the water jet to invade the

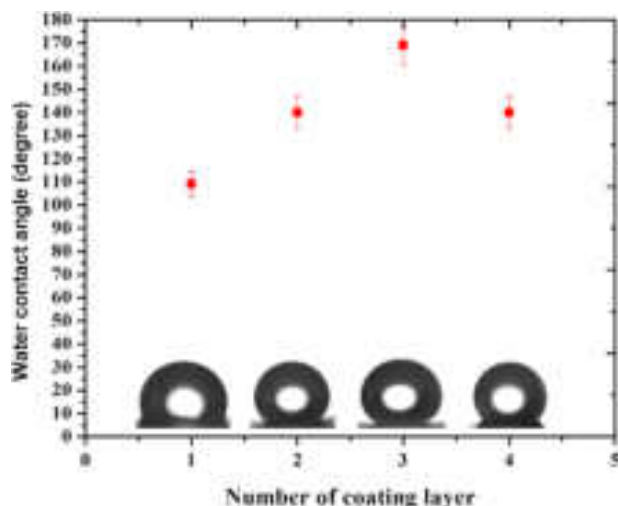


Figure 2. The variation of water contact angle with layer of polyvinyl chloride and SiO_2 particles.

rough structure. Also water jet rebounding confirms the robustness of the coating.

A systematic study was performed on the dependence of numbers of bilayers on the wettability of the coating (**Figure 2**). A first bilayer coating exhibited a WCA of $110 \pm 5^\circ$ confirming hydrophobic nature of the coating. The surface roughness of the coating is quite low to trap the air pockets and hence the wettability falls in the Wenzel's state^[26] where the solid fraction of the coating was partially wetted by the water drops. Though the WCA increased to $140 \pm 6^\circ$ with considerable decrease in solid-liquid contact area in case of two bilayer coating, the wettability was still in the Wenzel's wetting state. The WCA of $169 \pm 7^\circ$ and SA of 6° was observed for three bilayer coating confirming superhydrophobicity in Cassie-Baxter's wetting state.^[27] A water drop floats on the layer of air having minimum contact with solid fraction of the coating surface and hence readily roll off the surface. For next bilayer coatings, the WCA tends to decrease as a result of increase in thickness which creates visible cracks in the coatings during evaporation of solvent.

2.2. Durability Tests

The mechanical durability of superhydrophobic coating can be evaluated by water jet and water drop impact, sand paper abrasion and adhesive tape peeling test.^[28] Here, the water jet was developed by 15 mL syringe. The water jet was immediately spread on uncoated glass slide due to smooth surface structure with hydrophilic nature. On the other hand, the water jet bounced off the superhydrophobic coating as shown in **Figure 1b**. The air trapped hierarchical structure strongly avoids pinning of water jet on the surface.^[5,29] The wettability of the coating was checked after water jet impact study and the coating showed no change in its superhydrophobic property confirming its robustness. Water drop impact test was carried out by adjusting the distance between superhydrophobic coating and tip of tap about 10 cm as shown in schematic (**Figure 3a**). Nearly 2 L of water was dropped on the superhydrophobic coating inclined at 30° with drop falling rate

of 90 drops min^{-1} . The effect of water drop impact on the wetting properties of the superhydrophobic coating was estimated. The superhydrophobic state of the coating was intact for the impact of 1.2 L of the water as a result of stable air pockets in the rough microstructure of the coating which avoids water drop penetration inside the coating structure. However, the trapped air starts to evacuate from the rough structure and also the rough structure might have partly ruined due to continuous impact of water drops and as a result, WCA decreased to less than 140° for impacting 2.0 L of water (**Figure 3b**).

The adhesive tape peeling test was carried by using Cellotape No.405 having adhesiveness of 3.93 N/10 mm. A tape was applied firmly on the superhydrophobic coating with the help of 200 g weighted disk rolling back and forth on it (**Figure 4a**).^[28] After slowly peeling off the tape, some amount of the coating material was observed stacked on the adhesive tape; however, the coating showed the WCA of 165° (**Figure 4b**). The superhydrophobicity of the coating was found intact for two cycles of adhesive tape test, and then the WCA decreased to 80° for five cycles of adhesive tape test confirming the exhaustive loss of PVC/ SiO_2 from the coating (**Figure 4c**).

In large scale applications, superhydrophobic coatings can be damaged by scratch, rubbing and finger contact. To sustain the hierarchical micro/nanostructure and low surface energy of superhydrophobic coating under mechanical abrasion is one of the important issue. Here, the mechanical abrasion test was performed using sandpaper grit no. 400. The schematic of sandpaper abrasion process is illustrated in **Figure 5a**. A weight (100 g) was placed on superhydrophobic coating and dragged for 10 cm length on sandpaper at the average speed of 0.5 cm sec^{-1} . The effect of abrasion distance on the wettability of the superhydrophobic coating was studied (**Figure 5b**). The wettability of the coating was found in the superhydrophobic state for dragging the coating for nearly 30 cm on the sandpaper which confirms no significant loss in the surface roughness of the coating. However, the WCA decreased to 93° for dragging the coating for 60 cm on sandpaper confirming substantial damage to the coating.

2.3. Self-Cleaning Property

High water repellent property of the surface with low water sliding angle helps to keep the surface clean like a lotus leaf. In open air, many solid surfaces are contaminated by various types of dust particles. On superhydrophobic surface, spherical shaped water drop roll away easily by collecting dust particles, performing self-clean ability. The self-cleaning ability of the prepared superhydrophobic coating was tested by muddy water. The muddy water was prepared by dispersing fine particles of soil in water. This muddy water was poured on the superhydrophobic coating. In the process of pouring muddy water, it eventually get repelled off the superhydrophobic coating (**Figure 6a–c**). After pouring 50 mL of muddy water, surface becomes clean similar to lotus leaf (**Figure 6c**). This indicates prepared superhydrophobic coating was highly water repellent with excellent self-cleaning property.

3. Conclusions

We have used a conventional dip and spray coating techniques to prepare superhydrophobic coating by applying consecutive layers

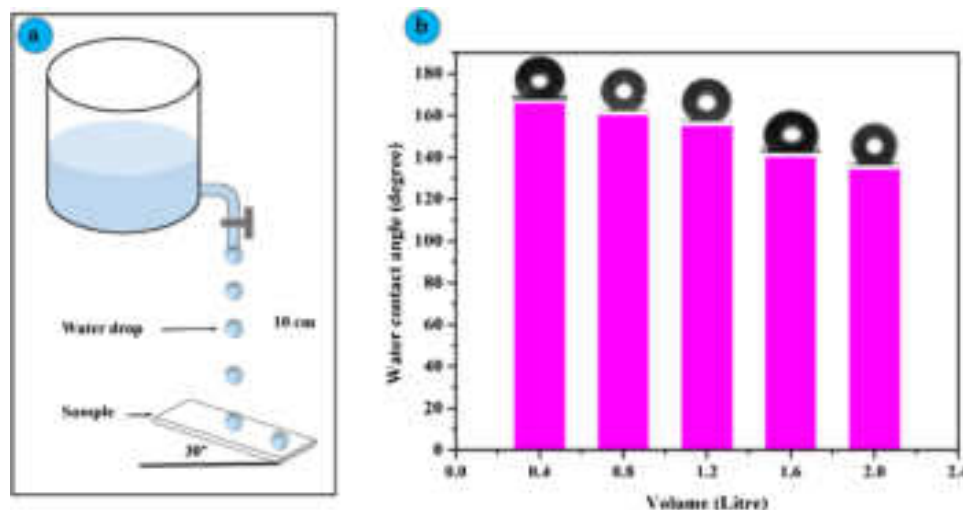


Figure 3. a) A schematic of water drop impact test, b) the effect of water drop impact on wettability of the superhydrophobic coating.

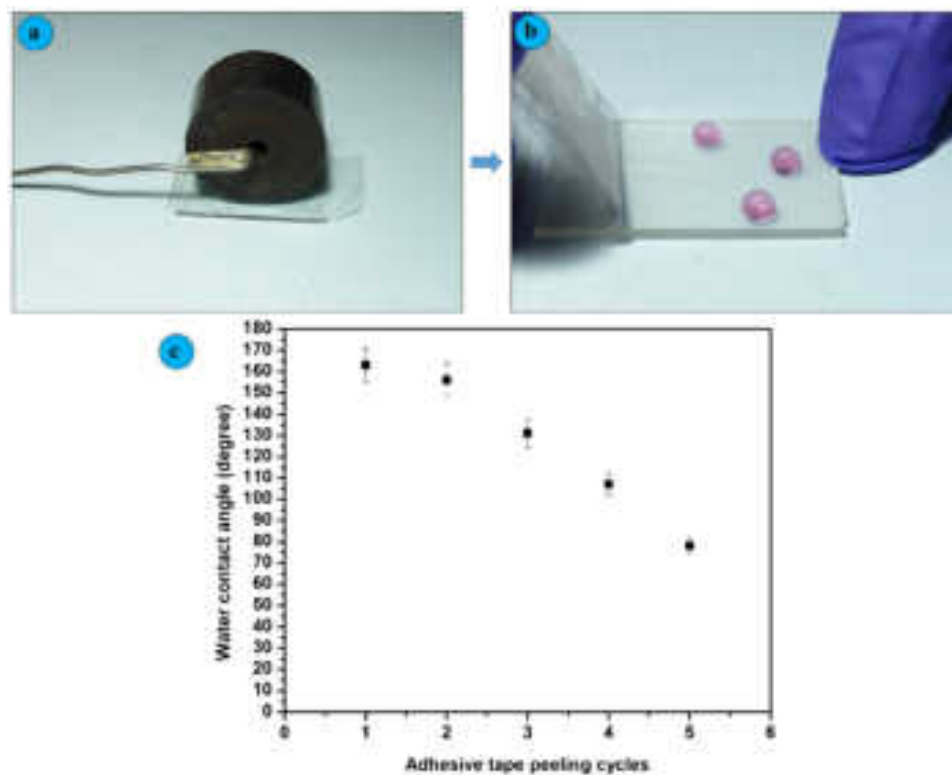


Figure 4. a) Rolling of 200 g weighted disc on adhesive tape placed on coating, b) adhesive tape peeling off and c) effect of adhesive tape peeling cycles on the wettability of the superhydrophobic coating.

of PVC and hydrophobic SiO₂ NPs on glass substrate. The hierarchical rough microstructure with different scaled grains of SiO₂ NPs was observed. The self-cleaning superhydrophobic coating with WCA of 169 ± 2° and sliding angle of 6° was achieved by applying three bilayers of alternate PVC followed by hydrophobic SiO₂ NPs. The water jet bouncing off the surface indicates the air pockets trapped in dual scale rough structure. After dripping the

water of volume 1.2 L, the water drop impacted coating showed invariable wettability. The superhydrophobic coatings were moderately stable against adhesive tape and sandpaper abrasion tests. Future practical applications of these coating can be found in windshields of vehicles, solar cell panels and windows of buildings, if their transparency and mechanical stability could be further enhanced.

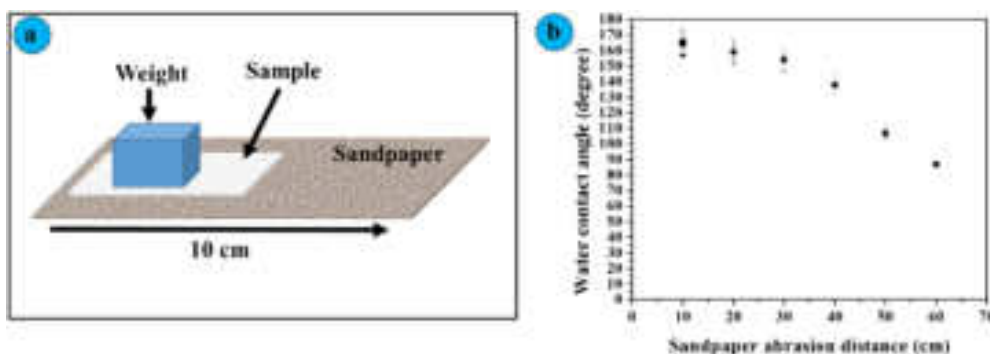


Figure 5. a) Schematic of sandpaper abrasion test and b) the variation of water contact angle with sandpaper abrasion distance.



Figure 6. a-c) Self-cleaning behavior of superhydrophobic coating.

4. Experimental Section

Materials: Methyltrimethoxysilane (MTMS) and PVC were purchased from Sigma-Aldrich, USA. Ethanol, methanol, ammonia solution, tetrahydrofuron (THF) and hexane were bought from Spectrochem PVT. LTD., India. Micro-Glass slides ($75 \times 25 \times 1.35$ mm) were obtained from Blue star, Polar Industrial Corporation, India.

Synthesis of Hydrophobic SiO_2 NPs: The hydrophobic SiO_2 NPs were synthesized using sol-gel method reported in literature.^[30] The mixture of 2 mL MTMS, 20 mL methanol and 4 mL distilled water was stirred for 20 min. After that ammonia solution was added dropwise and kept for stirring for 30 min. The prepared gel was aged for overnight and dried at 80°C for 5 h. The dried gel was grinded well using mortar and pestle to obtain fine powder of silica particles.

Preparation of Superhydrophobic Coating: At first, the glass substrates were ultrasonically cleaned with distilled water and ethanol for 30 min and dried at room temperature. The cleaned glass substrate was dipped in the PVC solution for 30 s. The solution was prepared by dissolving 100 mg PVC powder in 10 mL THF using magnetic stirrer (200 rpm for 30 min). A thin layer of PVC deposited glass substrate was dried at room temperature. A suspension of SiO_2 NPs (100 mg) was prepared by dispersing in 10 mL hexane and sprayed on PVC deposited glass substrate at substrate temperature of 50°C . Finally PVC/ SiO_2 deposited glass substrate was annealed at 100°C for 1 h. In this way, one bilayer of PVC/ SiO_2 was applied on glass substrate. This procedure was repeated to deposit two, three and four bilayers of PVC/ SiO_2 on glass substrate.

Characterizations: The wettability of prepared coatings was evaluated by measuring WCA and sliding angle (SA) using contact angle meter (HO-IAD-CAM-01, Holmarc Opto-Mechatronics Pvt. Ltd. India). The surface morphology of coating was characterized by field emission scanning electron microscopy (FESEM, JEOL, JSM-7610F, Japan). The water jet impact test was carried out by using 15 mL syringe. For water drop impact test, the coated glass substrate was kept at 30° inclination and water drops were dropped from the height of 10 cm. The mechanical stability of the coating was checked by adhesive tape peeling and sandpaper abrasion test. The self-cleaning behavior was observed by pouring muddy water on the coating.

Acknowledgements

This work was financially supported by DST-INSPIRE Faculty Scheme, Department of Science and Technology (DST), Govt. of India. [DST/INSPIRE/04/2015/000281]. SSL acknowledges financial assistance from the Henan University, Kaifeng, P. R. China. The authors greatly appreciate the support of the National Natural Science Foundation of China (21950410531).

Conflict of Interest

The authors declare no conflict of interest.

Keywords

PVC, roughness, superhydrophobic and self-cleaning, wetting

- [1] L. Feng, S. Li, Y. Li, H. Li, L. Zhang, J. Zhai, Y. Song, B. Liu, L. Jiang, D. Zhu, *Adv. Mater.* **2002**, *14*, 1857.
- [2] C. Neinhuis, W. Barthlott, *Annal. Botany* **1997**, *79*, 667.
- [3] S. P. Dalawai, M. A. S. Aly, S. S. Latthe, R. Xing, R. S. Sutar, S. Nagappan, C.-S. Ha, K. K. Sadasivuni, S. Liu, *Prog. Org. Coat.* **2020**, *138*, 105381.
- [4] S. S. Latthe, V. S. Kodag, R. S. Sutar, A. K. Bhosale, S. Nagappan, C.-S. Ha, K. K. Sadasivuni, S. R. Kural, S. Liu, R. Xing, *Mater. Chem. Phys.* **2020**, *243*, 122634.
- [5] S. S. Latthe, P. Sudhagar, A. Devadoss, A. M. Kumar, S. Liu, C. Terashima, K. Nakataa, A. Fujishima, *J. Mater. Chem. A* **2015**, *3*, 14263.
- [6] S. S. Latthe, et al. *Superhydrophobic Polymer Coatings*, **2019**, Elsevier. pp. 339–356.
- [7] S. S. Latthe, R. S. Sutar, A. K. Bhosale, S. Nagappan, C.-S. Ha, K. K. Sadasivuni, S. Liu, R. Xing, *Prog. Org. Coat.* **2019**, *137*, 105373.

- [8] S. S. Latthe, R. S. Sutar, T. B. Shinde, S. B. Pawar, T. M. Khot, A. K. Bhosale, K. K. Sadasivuni, R. Xing, L. Mao, S. Liu, *ACS Appl. Nano Mater.* **2019**, 2, 799.
- [9] A. B. Gurav, S. S. Latthe, R. S. Vhatkar, J. G. Lee, D. Y. Kim, J. J. Park, S. S. Yoon, *Ceram. Int.* **2014**, 40, 7151.
- [10] A. M. Kokare, et al. *AIP Conference Proceedings*, AIP Publishing. **2018**.
- [11] S. S. Latthe, et al. *Green Chemistry for Surface Coatings, Inks and Adhesives*. **2019**. pp. 92–119.
- [12] R. S. Sutar, et al. *Macromolecular Symposia*, **2019**. Wiley Online Library.
- [13] S. Bilgin, M. Isik, E. Yilgor, *Polymer* **2012**, 53, 1180.
- [14] H. Yoon, H. Kim, S. S. Latthe, M.-W. Kim, S. Al-Deyabd, S. S. Yoon, *J. Mater. Chem. A* **2015**, 3, 11403.
- [15] Y. Guo, Q. Wang, *Appl. Surf. Sci.* **2010**, 257, 33.
- [16] P. G. Pawar, R. Xing, R. C. Kambale, A. M. Kumar, S. Liu, S. S. Latthe, *Prog. Org. Coat.* **2017**, 105, 235.
- [17] S. S. Latthe, R. S. Sutar, V. S. Kodag, A. K. Bhosale, A. M. Kumar, K. K. Sadasivuni, R. Xing, S. Liu, *Prog. Org. Coat.* **2019**, 128, 52.
- [18] H. Chen, Z. Yuan, J. Zhang, Y. Liu, K. Li, D. Zhao, S. Li, P. Shi, J. Tang, *J. Porous Mater.* **2009**, 16, 447.
- [19] Z. Khoryani, J. Seyfi, M. Nekoei, *Appl. Surf. Sci.* **2018**, 428, 933.
- [20] X. Li, G. Chen, Y. Ma, L. Feng, H. Zhao, L. Jiang, F. Wang, *Polymer* **2006**, 47, 506.
- [21] J. Seyfi, M. Panahi-Sarmad, A. OraeiGhodousi, V. Goodarzi, H. A. Khonakdar, A. Asefnejad, S. Shojaei, *Colloids Surf., B* **2019**, 183, 110438.
- [22] P. J. Rivero, A. Iribarren, S. Larumbe, J. F. Palacio, R. Rodríguez, *Coatings* **2019**, 9, 367.
- [23] Z. Yuan, H. Chen, J. Zhang, *Appl. Surf. Sci.* **2008**, 254, 1593.
- [24] X. Zhang, B. Ding, R. Cheng, S. C. Dixon, Y. Lu, *Adv. Sci.* **2018**, 5, 1700520.
- [25] H. Chen, X. Zhang, P. Zhang, Z. Zhang, *Appl. Surf. Sci.* **2012**, 261, 628.
- [26] R. N. Wenzel, *Ind. Eng. Chem.* **1936**, 28, 988.
- [27] A. Cassie, S. Baxter, *Trans. Faraday Soc.* **1944**, 40, 546.
- [28] N. Wang, D. Xiong, S. Pan, K. Wang, Y. Shi, Y. Deng, *New J. Chem.* **2017**, 41, 1846.
- [29] A. Kibar, H. Karabay, K. Yigit, I. Ucar, H. Erbil, *Exp. Fluids* **2010**, 49, 1135.
- [30] S. S. Latthe, A. V. Rao, *Surf. Coat. Technol.* **2012**, 207, 489.



**International Symposium
on**

Sustainable Environment and Smart Technology



Jointly Organized by

Pune District Education Association's

**Prof. Ramkrishna More Arts,
Commerce and Science College**

Akurdi, Pune - 411044

and

Department of Technology

Savitribai Phule Pune University, Pune 411007

10-11 March, 2023

Editor

Prin. Dr. M. G. Chaskar



**Self Study
Publication**

ABSTRACT BOOK

[ISBN-978-81-948795-2-7]

15	“On-Water” Reaction of (Thio)isocyanate: A Sustainable Process for the Synthesis of Unsymmetrical (Thio)ureas	Karche Amit Dattatray	12
16	Studies on Gut Fungal Diversity from Organic Waste Feeding Beetle.	Ganesh E Gore, Dhiraj Dhotre, Deepak Shelke, Hiralal Sonawane	13
17	Fe ₂ O ₃ – Polyaniline thin films: A Smart Material for the Ammonia gas Sensing	Somnath Dattinge, Dipali Dubal, Shamal Ballal, Sunil Kandalkar, Dnyaneshwar Shinde	13
18	Antioxidant Activities of Mycogenically Synthesized Nanoparticles from Combination of Medicinally Important Mushroom <i>Inonotus</i> Sp. and Chitosan	Pallavi Champaneria, H B Sonawane, B N zaware	14
19	Account of Wood Rotting Fungi from Madhe Ghat and Connecting Area of Velha Tehsil.	Bhagat S. P., Sonawane H. B., Borde M. Y.	14
20	A Green Protocol for One-Pot Synthesis of 3,4-Dihydropyrano[C]Chromenes and Biscoumarins by Employing WEB as an Internal Base.	Kumbhar Vikrant Vasudev	14
21	Investigations on CuO: ZnO Composites for Photocatalytic Performance.	Akanksha S Chougale, Snehal S Wagh, Harshad D Shelake, Habib M. Pathan and Dnyaneshwar R Shinde	11
22	Magnetic Hyperthermia with Fe ₃ O ₄ Nanoparticles	Pandhare Amol Babaso	11
23	Studies on Induced Mutation in Barnyard Millet (<i>Echinochloa esculanta</i>) L.	Jagtap Bhavana D. and Danai-Tambhale S. D.	11
24	Determination of Physicochemical Parameters and Adulteration Of Multifloral Honey by FTIR-ATR spectroscopy	Rekha J. Shinde, Indira M. Patil and Rashmi A. Morey	14
25	Ni-Ferrite an Efficient Catalyst for Synthesis of 3-Aryl Substituted Isoxazole-5-Carboxylic Acids Via One-Pot Multicomponent Reaction	Ganesh Totre, Dnyaneshwar Shinde, Prakash Patil and Pramod Kulkarni	14
26	Degradation of Textile Reactive Azodyes by <i>Hapalosiphon arboreus</i>	Rutuja Pund and K. M. Nitnaware	15
27	Fabrication of Durable Candle Soot-Wax Composite Coated Superhydrophobic Sponges for Oil-Water Separation	Mehejbin R. Mujawar, Rajesh B. Sawant, Amol B. Pandhare, Rajaram S. Sutar, Sanjay S. Latthe, Ankush M. Sargar, Raghunath K. Mane, Shivaji R. Kulal	15
28	NiFe ₂ O ₄ : An Efficient and Magnetically Recoverable Catalyst for Synthesis of 2-amino-3-cyanopyridines Derivatives	Sandip Rathod	18
29	Phytochemical and Anti-Microbial Studies of Underutilized, Neglected, Endemic and Threatened Wild Crop Relative <i>Vigna khandalensis</i> (Santapau) Raghavan et Wadhwa	Sarika A. Bhumkar, Sandip S. Thorve, Sadashiv N. Bolbhat, Vinayak H. Lokhande	18
30	Decolourization of Spent Wash Colour under Sun Light using Mesoporous Cu-TiO ₂ Nanoparticles Synthesized By Sol-Gel Assisted Hydrothermal (SGAH) Method	Shrikant. P.Takle, Aarti S. Tarlekar, Amol Bhosale, Netaji Mali, Shaila Dhotre, Digambar B. Bankar, Namdeo N. Bhujbal	19
31	Synthesis of Organic Nano Semiconductor for Photocatalytic and Antimicrobial study Performance	Vivekanand Jawale, Gulab Gugale, Vikram Pandit	19
32	Endophytes Isolated from <i>Ophiorrhiza rugosa</i> Plant Producing a Good Source of Camptothecin.	Vaishnavi Chavan, Hiralal Sonawane and Mahesh Borde	20

Abstract-26**Degradation of textile reactive azodyes by Hapalosiphon arboreus****Miss Rutuja Pund and Dr. K. M. Nitnaware***

Department of Botany, Hutatma Rajguru Mahavidyalaya, Rajgurunagar

Corresponding Email: kmnbotany@gmail.com

Abstract: Azodyes widely used in textile industries are toxic to life. Dye degradation using microorganism gained more attention due to cost effectiveness and eco-friendly. There is need to investigate more indigenous species. In the present study the filamentous cyanobacteria Hapalosiphon vulgaris was examined for its degrading ability of azodyes Methyl Orange, Tartrazine Yellow, Scarlet Red, Reactive Black 5 and Sudan III. The axenic culture of Hapalosiphon was inoculated with various concentrations of dyes (5, 10 and 20 ppm) and incubated for 3, 5 and 7 days. Dye degradation was based on initial dye concentration. The maximum decolorization was observed in Scarlet red and Sudan III 92.5% and 82.02% respectively after 7 days of incubation. Azoreductase enzyme in algae responsible for degradation of azodyes into aromatic amines. Maximum azoreductase activity 6.02 Umg-1 protein was observed for scarlet red. Influence of azo dyes on Chlorophyll a and b content and Phycobilin Proteins was also examined. The degradation product after decolourization was confirmed and identified by spectroscopic analysis and Fourier transformed infrared spectroscopic analysis.

Keywords: Azoreductase enzyme, Methyl Orange, Scarlet Red, FTIR

Abstract-27**Fabrication of Durable Candle Soot-Wax Composite Coated Superhydrophobic Sponges for Oil-Water Separation****Mehejbin R. Mujawar¹, Rajesh B. Sawant¹, Amol B. Pandhare², Rajaram S. Sutar³, Sanjay S. Latthe⁴, Ankush M. Sargar^{5*}, Raghunath K. Mane⁶, Shivaji R. Kulal^{1*}**¹ Department of Chemistry, Raje Ramrao Mahavidyalaya, Jath, (Affiliated to Shivaji University, Kolhapur)² Department of Chemistry, Shivaji University, Kolhapur, (MS) India³ Self-cleaning Research Laboratory, Department of Physics, Raje Ramrao Mahavidyalaya, Jath,⁴ Self-cleaning Research Laboratory, Department of Physics, Vivekanand College, Kolhapur,⁵ Department of Chemistry, Bharati Vidyapeeth's Dr. Patangrao Kadam Mahavidyalaya, Sangli,⁶ Department of Chemistry, Smt. Kusumtai Rajarambhapu Patil Kanya Mahavidyalaya, Islampur,*Corresponding authors E-mail: srkulal@gmail.com, amsargar2012@gmail.com

Abstract: A novel superhydrophobic candle soot-wax composite coated surfaces for oil-water separation was fabricated via a facile two-step strategy. The decomposition of candle soot on the surface and then it was fixed via deposition of wax on CS-coated surfaces. The candle soot was synthesized by paraffin candle combustion flame. The CS-coated surface was prepared by via the dip-coating method without further surface modification and pre-treatments. Candle soot was firmly immobilized on the wax skeleton constructing a nanoscale rough surface with superhydrophobicity. The coated surfaces exhibit superhydrophobicity with a water contact angle of $> 150^\circ$ and a sliding angle of nearly 0° . The thermal stability, pH tolerance, compression tolerance, chemical durability, reusability, emulsion oil-water separation, and muddy water-oil separation was tested by using these superhydrophobic surfaces. The superhydrophobic surfaces have a sustainable, anti-wetting property under cross-sectional cutting, pressing, paper peel test, abrasion resistance test, and different pH environments. The superhydrophobic surface is suitable for practical application on a large scale. The simple CS-wax coating method can be applied to various surfaces, such as stainless steel and polyurethane sponges. These research results show evidence that the CS-wax-coated surface is promising in environmental remediation for large-scale, low-cost, removal of oil spills from water.

Keywords: Candle soot nanoparticles, oil-water separation, sliding angle, superhydrophobic surfaces, water contact angle, waxes.

A Review on Superhydrophobic Surfaces: Fundamentals, Fabrications and Applications

Mehejbin R. Mujawar¹, Rajesh B. Sawant¹, Govind D. Salunke¹, Rajaram S. Sutar², Sanjay S. Lathe³, Ankush M. Sargar⁴, Raghunath K. Mane⁵, Krishna K. Rangar¹, Shivaji R. Kulal^{1*}

¹ Department of Chemistry, Raje Ramrao Mahavidyalaya, Jath, Dist. - Sangli (MS) India

² Self-cleaning Research Laboratory, Department of Physics, Raje Ramrao Mahavidyalaya, Jath, Dist. - Sangli (MS) India.

³ Self-cleaning Research Laboratory, Department of Physics, Vivekanand College (Autonomous), Kolhapur, Dist. - Kolhapur (MS) India.

⁴ Department of Chemistry, Bharati Vidyapeeth's Dr. Patangrao Kadam Mahavidyalaya, Sangli, Dist. - Sangli (MS) India

⁵ Department of Chemistry, Smt. Kusumtai Rajarambhapu Patil Kanya Mahavidyalaya, Islampur, Dist. - Sangli (MS) India

*Corresponding author's E-mail: srkulal@gmail.com, amsargar2012@gmail.com

Abstract

Superhydrophobic surfaces are highly hydrophobic i.e., it extremely difficult to wet. Superhydrophobic surfaces are the tendency to repel water drops and absorb oil drops. The water contact angle of superhydrophobic surfaces is greater than 150° , the oil contact angle is less than 5° , and the sliding angle is less than 5° . It is showing the lotus effect. Superhydrophobicity is observed in the lotus leaves, insects, and some other plants in which their leaves would not get wet. This phenomenon is due to the unique surface structure of the lotus leaf and also the presence of a low surface energy material on the surface of the leaf. For the formation of a superhydrophobic surface, the surface must show hierarchical micro- and nano-roughness and low surface energy. Efforts have been taken to form superhydrophobic surfaces for a variety of applications. There are many applications of superhydrophobic surfaces such as self-cleaning surfaces, oil-water separation surfaces, anti-icing surfaces, anti-corrosion surfaces, anti-fogging surfaces, and water-resistant surfaces. In this article, the fundamental principles of superhydrophobic surfaces, some recent trends in the fabrication of superhydrophobic surfaces, and their applications are reviewed and discussed.

Keyword: Superhydrophobicity, Superoleophobicity, Lotus effect, Self-cleaning, Oil-water separation, Water-repelling, Oil Contact Angle, Water Contact angle, Anti-icing, Anti-corrosion.



SHIVAJI UNIVERSITY, KOLHAPUR

Volume-49 Issue-1 (January, 2023)

ISSN-Science-0250-5347

Estd. 1962
"A++" Accredited by NAAC (2021)
with CGPA 3.52



JOURNAL OF SHIVAJI UNIVERSITY : SCIENCE AND TECHNOLOGY

(Peer Reviewed Journal)

Journal of Shivaji University: Science and Technology
Volume-49, Issue-1 (January,2023)

INDEX

Sr. No.	Title of Research Article with Name of Author/s	Page No.
1.	Synthesis and Characterization of g-C₃N₄ Decorated ZnONanorods and their Binder Free Deposited Photoanodes for Photoelectrochemical Water Splitting Studies Pramod A. Koyale, Prakash S. Pawar, Swapnajit V. Mulik, Vijay S. Ghodake, Amol B. Pandhare, Ankita K. Dhukate, Sagar D. Delekar	1
2.	Thiamine Hydrochloride (VB₁) Catalyzed Synthesis of 5-aryl-4-phenyl-1,2,4-triazolidine-3-thiones in Aqueous Medium Pradeep P. Patil, Prasad M. Swami, Shankar P. Hangirgekar, Sandeep A. Sankpal	10
3.	Evaluation of Acute Toxic Effect of Gallic Acid Loaded Eudragit's 100 Nanoparticles on <i>Artemia Salina</i> Brine Shrimp Bioassay PoornimaS. Sankpal, Sachinkumar V.Patil,SayaliS. Patil	20
4.	Surface Modifications of Binder Free ZnONanorod Thin Films through Cds Quantum Dots for Dye Sensitized Solar Cells Krantiveer V. More, Anant G. Dhodamani, Sajid B. Mullani, Tukaram D. Dongale,Prakash S. Pawar,Satish M. Patil, Sunil J. Kadam, Sagar D. Delekar	36
5.	Review on Candle Soot based Superhydrophobic Surfaces for Oil-Water Separation Mehejbin R. Mujawar, Rajesh B. Sawant, Amol B. Pandhare, Prashant D. Sanadi, Sanjay S. Latthe, Ankush M. Sargar, Raghunath K. Mane, Shivaji R. Kulal	50
6.	A Review on Current Advancements in Magnetic Nanomaterials for Magnetic Hyperthermia Applications Amol B. Pandhare, Prakash S. Pawar, Vijay S. Ghodake, Swapnajit V. Mulik, Pramod A. Koyale, Ankita K. Dhukate, Deepak B. Mohite, Karishma V. Shikhare, Rajendra P. Patil, Sagar D. Delekar	62
7.	One-Step Synthesis of Biomass-Derived Carbon Dots: Study of Optical Properties Akanksha G. Kolekar, Omkar S. Nille,Shubham J. Kumbhar, Priyanka S. Mahadar, Sayali B. Lohar, Govind B. Kolekar, Gavisiddappa S. Gokavi, Vishalkumar R. More	87
8.	Synthesis and Characterization of Plant-Mediated CuO Nanoparticles Omkar S. Nille, Harshad A. Mirgane, Sneha V. Koparde, Akanksha G. Kolekar, Ashlesha R. Pawar, Pallavi J. Pawar, Abhishek A. Waghmode, Tanaji R. Dhage, Vijay S. Ghodake, Prasad M. Swami, Sarita D. Shinde,Govind B. Kolekar	95

Review on Candle Soot based Superhydrophobic Surfaces for Oil-Water Separation

Mehejbin R. Mujawar^{a,*}, Rajesh B. Sawant^a, Amol B. Pandhare^{b,f},
Prashant D. Sanadi^g, Sanjay S. Latthe^c, Ankush M. Sargar^d,
Raghunath K. Mane^e, Shivaji R. Kulal^{a,*}

^aDepartment of Chemistry, Raje Ramrao Mahavidyalaya, Jath, Sangli 416 404 (MS) India.

^bDepartment of Chemistry, Shivaji University, Kolhapur 416 004 (MS) India.

^cDepartment of Physics, Vivekanand College, Kolhapur 416 003 (MS) India.

^dDepartment of Chemistry, Bharati Vidyapeeth's Dr. Patangrao Kadam Mahavidyalaya, Sangli 416 416 (MS) India.

^eDepartment of Chemistry, Smt. Kusumtai Rajarambhapu Patil Kanya Mahavidyalaya, Islampur, Sangli 416 409 (MS) India.

^fDepartment of Chemistry, M.H. Shinde Mahavidyalaya, Tisangi, Gaganbavda, Kolhapur 416 206 (MS) India.

^gDepartment of Engginring, Chemistry, Institute of Technology's College of Engineering (Autonomous), Kolhapur 416 234 (MS) India.

*Corresponding authors: srkulal@gmail.com and mehejabeenmujawar@gmail.com

ABSTRACT

Over the many years, the oceanic oil spill accidents and most industries worldwide discharging immense levels of oil in the surroundings is a serious problem for the environment. There is a need to develop technology for oil-water separation because the spilled oil affects the ecological and environmental system. Candle soot nanoparticles are hydrophobic (water repellent) in nature and has the advantages of cost-effectiveness and production scalability over other carbons like graphene, Carbon Nanotubes (CNTs), Carbon Nanodots (CNDs), etc. in their synthesis. Candle soot based superhydrophobic materials have outstanding water repulsion and oil absorption capacity, highly selectivity, chemical inertness and excellent recyclability. In this paper, we discuss applications of candle soot based superhydrophobic materials applied on sponge and mesh substrates for oil-water separation.

KEYWORDS

Carbon Nanotubes, Carbon Nanodots.

.....

1. INTRODUCTION

The oil spilling and discharge of industrial organic solvents causes several damages to water resources and aquatic ecosystems [1-3], which became a global problem and need to solve it urgently to save the ecosystems. A new technology in material science has been developed for oil-water separation using superhydrophobic nanomaterial. As like the lotus leaf, superhydrophobic surface having water contact angle greater than 150° and oil contact angle near 0°[4]. Different chemical methods

are used for the fabrication of the superhydrophobic mesh/sponge for efficient oil-water separation. As the carbon nanoparticles are hydrophobic in nature, it shows strong affinity toward oil. At the same time, huge amount of candle soot waste is produced. Undoubtedly, it is of great benefit to turn candle soot waste into high value oil absorbent materials [5]. The superhydrophobic mesh/sponge exhibited high selectivity toward different oil and organic pollutants, fast and efficient oil-water separation capability, good repeatability, good reusability, mechanically stable, chemically stable and thermally stable [6]. Candle soot-based absorbents demonstrate superior efficiency in the removal of oils. However, the high production costs of carbon nanotube[7], graphene[8], activated carbon [9], expanded graphite [10], etc. So, these absorbents limit their wide adoption at large scale. Candle soot (CS) generated from incomplete combustion of paraffin wax has demonstrated the advantages of cost effectiveness and production scalability over CNTs, graphene and activated carbons in their synthesis [11]. However, candle soot coated superhydrophobic materials are the best solution from these. The superhydrophobic surfaces on which water achieves water contact angle higher than 150° and sliding angle less than 5° are attracting minds of researchers due to their efficient oil-water separation abilities [12-14]. J. Song et al. [15] fabricated CS-coated mesh by using dip-coating method. The cleaned stainless-steel mesh (SSM) was dipped in the glue solution for 10 min and then dried at 80°C to obtain the CS-glue coated mesh. The CS coating is close packed because of using superglue as a binder. The CS-glue coated mesh revealed the separation efficiency higher than 99.95%. Even after 20 cycle separation tests, it was shown superior reusability and durability. Li et al. [16] prepared the hydrophobic CS by incomplete combustion of hydrocarbons from the middle of candle flame. The PU sponge dipped in the solution of CS, SiO_2 and PU resin to achieve stable superhydrophobicity. The CS- SiO_2 -PU sponge showed excellent oil-water separation efficiency. The CS- SiO_2 -PU sponge was also shown superior separation efficiency from hot water, acidic solutions, alkaline solutions and salt solutions. Zulfiqar et al. [17] deposited cheaply available sawdust on polychloroprene adhesive-coated stainless-steel mesh with deposition of silicone polymer by using dip-coating method. Then, a thin layer of CS particle was applied on the prepared stainless-steel mesh by simply holding it above a candle flame. The CS particles get uniformly deposited on silicone covered sawdust which exhibited highly rough and porous morphology required for superhydrophobicity. It showed excellent oil-water separation efficiency greater than 95% which showed its recyclability, reusability and mechanical stability. In this article, we will mostly discuss on the simple, low-cost, rapid and innovative methods for the fabrication of superhydrophobic/superoleophilic CS coated sponges/meshes for efficient oil-water separation application.

2. SUPERHYDROPHOBIC-SUPEROLEOPHILIC SURFACES FOR OIL-WATER SEPARATION

2.1 Oil-water separation using Superhydrophobic-superoleophilic sponges

2.1.1 Highly efficient carbon soot sponge

The CS particles obtained from ethylene-oxygen combustion flame with flow rate of 5:3. These CS particles were dispersed in 1, 2-dichloroethane followed by sonication. The sponge was dipped in CS dispersion solution to attain superhydrophobic sponge. The superhydrophobic sponge achieved by a uniform coating of as-grown CS particles onto the porous skeleton through simple immersion in CS dispersion. The CS-modified sponge exhibited excellent oil-water separation efficiency without further chemical modification. The fast and easy recovery of engine oil floating on the water surface by CS-modified sponge confirms its high oil-water separation efficiency. The CS-sponge was shown an absorption capacity in the range of 25-80 times its original weight. The absorption capacity of the CS-sponge does not show severe degradation after 10 cycles which indicating a highly stable absorption performance of CS-sponge. After 10 cycles which indicating a highly stable absorption capacity is kept for CS-modified sponge, which much higher than that of the CS-sponge [18].

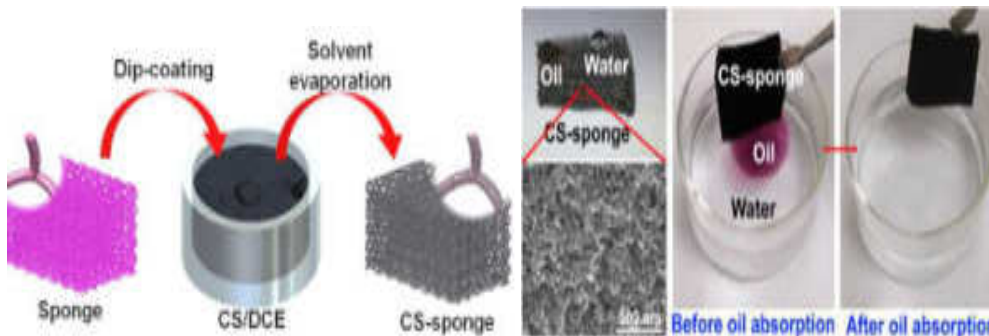


Figure-1. Schematic showing the carbon soot-sponge preparation by dip-coating and carbon soot sponge before & after oil absorption. Images reprinted from [18], with permission from American Chemical Society, Copyright 2014.

2.1.2 Recyclable superhydrophobic straw soot sponge

The straw soot on the glass slide was collected by shaving soot from the glass using a spatula. The colloidal suspension of CS was prepared by simply mixing the soot in ethanolic medium. The sponge was dipped into straw soot solution by using dip-coating method to form superhydrophobic sponge. The modified sponge was shown the water contact angle up to 154° . This superhydrophobic sample had good hydrophobic stability even in acidic condition and it can show the efficient oil-water separation. The amount of the absorbed oil was about 30 times of sponges own

weight which can be shown that the evaluation of the mass based on absorption capacity. The absorption capacity based on density, viscosity and surface tension of the absorbed liquids. This superhydrophobic sponge shows highly recyclability. The experiments demonstrate that the sponge can absorb the oil more than 30 cyclic applications without any significant change in the absorption. This method shows the benefits of easy preparation using natural soot source, better performance, oil absorption in a very short time in comparison with previous works [19].

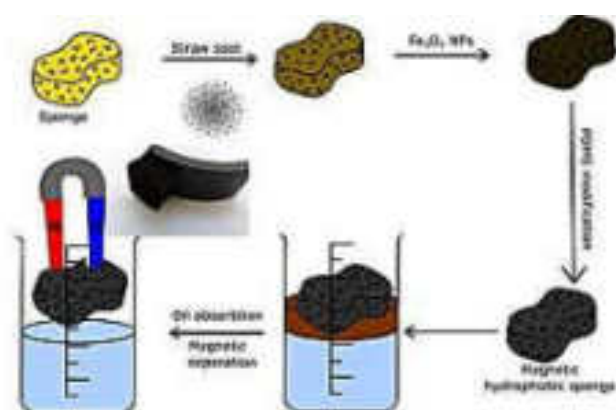


Figure-2. Schematic illustration of preparation of modified polyurethane sponge and oil separation process. Images reprinted from [19], with permission from Elsevier, Copyright 2017.

2.1.3 Durable PVDF/CS sponge

The superhydrophobic surface was fabricated by using PVDF and candle soot via sugar template method. It was shown the water contact angle of 158.3° and roll on angle of 6.7° . The oil quickly absorbed by superhydrophobic sponge which can be shows the superoleophilic property of superhydrophobic sponge. The solar value of candle soot is up to 99.4% which shows excellent light absorbing property. The sponge shows excellent oil-water separation property even after 25 cycles without destroying the sponge. The strong elasticity & high stretch resistance confirms that the modified superhydrophobic surface is highly mechanical durable. The modified sponge maintains the 89% of recovery rate even after 10 cycles. The absorption capability recovered up to 96% without obvious change of morphology of the sponge surface. This method was used to prepare a photothermal & porous PVDF/CS sponge with structural, chemical and mechanical property. It was shown high photothermal property.

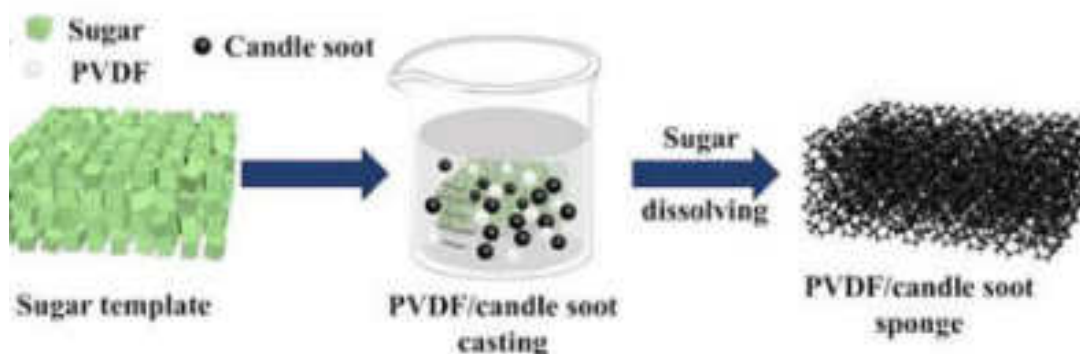


Figure-3. Schematic illustration of the fabrication of porous PVDF/candle soot sponge using sugar template. Images reprinted from [20], with permission from Elsevier, Copyright 2021.

2.2 Oil-water separation using superhydrophobic-superoleophilic meshes

2.2.1 Superhydrophobic SiO_2 /Carbon mesh

The candle soot was collected on the surface of stainless-steel mesh by placing the mesh above the wick of candle. Then by using chemical vapour deposition method the SiO_2 /carbon layer deposited on stainless steel mesh. Modify this mesh by using PFOTS and PDPA-PFO respectively to form the superhydrophobic and superoleophilic mesh membrane. This modified superhydrophobic stainless steel mesh exhibits excellent repellence for all the tested strong acids, strong bases and saturated salts, indicating a good stability of modified mesh under a series of hard environment. The separation efficiencies obtained repeatedly even after 15 cycles without any noticeable deterioration. Both superhydrophobic and superoleophilic modified stainless steel mesh membranes shows stability, durability and reusability. The SiO_2 /Carbon modified stainless steel mesh indicates good material for treating real oil-polluted water in different practical applications as well as in oil spill clean-up. This method shows higher performance, oil-water separation in a short time and repeatedly in comparison with earlier works [20].

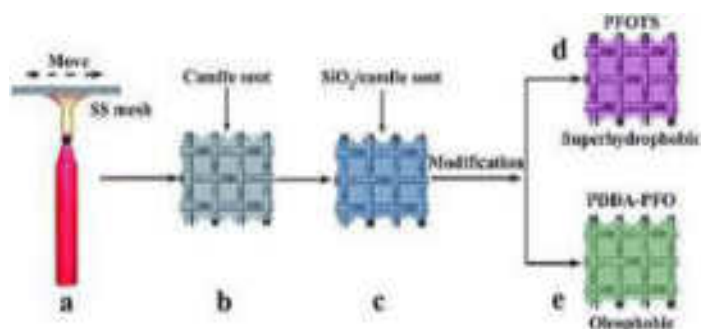


Figure-4. Process of superhydrophobic and oleophobic mesh membranes preparation: (a) coating stainless steel mesh with carbon nanoparticle (candle

soot), (b) carbon nanoparticle coated stainless steel mesh, (c) SiO₂/carbon stainless steel mesh, (d) PFOTS modified SiO₂/carbon stainless steel mesh, (e) PDDA–PFO modified SiO₂/carbon stainless steel mesh. Images reprinted from [21], with permission from Royal Society of Chemistry, Copyright 2017.

2.2.2 Durable PDMS-CS based superhydrophobic mesh

The candle soot was deposited on stainless steel mesh by simply placed above the candle flame for 15 sec. Then this CS coated stainless steel mesh was dipped in solution of PDMS & Xylene for 10 min by using immersion method. After that same process will be carried out for deposition of candle soot on this modified stainless-steel mesh was prepared. It shows 156° water contact angle & nearly 0° oil contact angle. Also, it shows 3° sliding angles. It shows higher water contact angle even after 10 times tests of oil-water separation. The oil-water separation efficiency was nearly 91% by using this modified superhydrophobic stainless steel mesh. It exhibits high thermal stability, good corrosion resistance and reusability. It was modified though combine mesh & polymer foam the composite adsorbent material successfully separate the oil from water via magnet drive method. This modified method was very useful than other research work. So, it was very useful than any other works [21].

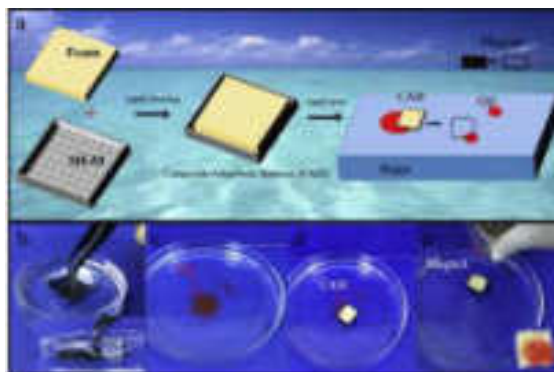


Figure-5. a) Schematic for the preparation process of composite adsorbent material (CAM) from the SH-M square boat and polymer foam, as well as its application of magnet drive for oil/water separation; b) SH-M square boat immersion in water by force; c–e) picture of the magnet drive CAM oil adsorption process. Images reprinted from [22], with permission from Progress in Organic Coatings, Copyright 2019.

2.2.3 CS templated superhydrophobic silica coating on SS mesh

The superhydrophobic coating was prepared through placing the cleaned substrate over candle flame until a few microns thick layer of candle soot deposited on

stainless steel mesh. The candle soot coated substrate together with SiCl_4 was placed in a drier for chemical vapour deposition. Then, though calcination at $600\text{ }^\circ\text{C}$ for half in air, CS composed NPs thermally degraded and diffused through the silica shell gradually. It shows highly oil-water separation efficiency even after 30 times cycle separation superhydrophobic surface remained. The superhydrophobic coating revealed excellent separation efficiency even after 6 times reuses of same superhydrophobic material. It could be potentially used in optical and visual application scenarios where in harsh & oily environments, like goggles, building façade, visual oil-water separation device & touch screen, etc. Among the all-other research work it shows tremendous oil-water separation properties [22].

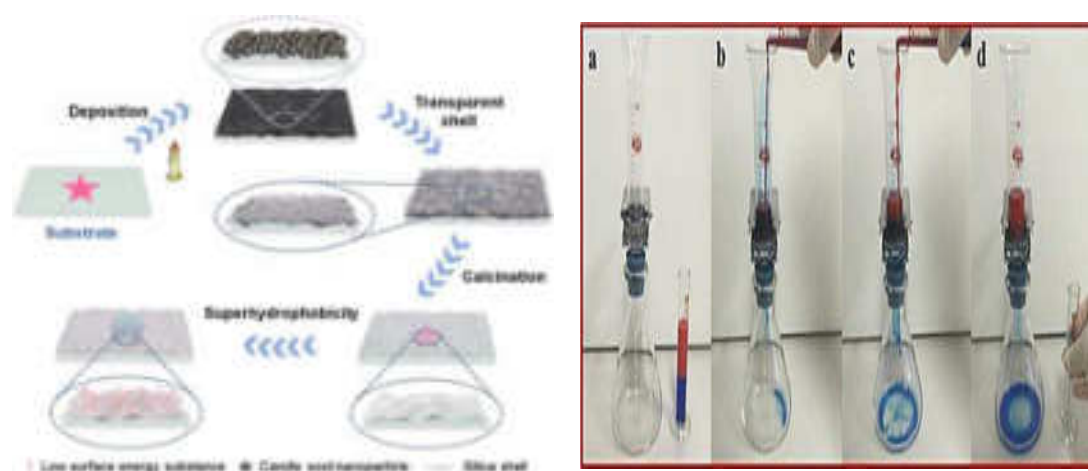


Figure-6. Schematic of preparation and properties of the transparent and robust superhydrophobic coating and oil–water separation. Images reprinted from [23], with permission from Nature, Copyright 2022.

3.CONCLUSION

As this review highlights, candle soot nanoparticles are unique in that, their fabrication requires little control of external parameters. It is very economical beneficial, facile and straightforward to synthesize. Candle soot coated sponge/mesh for use in oil-water separation has been developed by using CS-nanoparticles and different polymers. The candle soot synthesis, candle soot coated sponge/mesh preparation, procedures are simple, cost-effective and scalable. The absorption/separation investigation demonstrates that, the candle soot sponge/mesh is highly efficient and stable in absorbing a wide range of oil and organic solvents. It can be believed that, the candle soot coated superhydrophobic materials are very useful for oil-water separation. It shows various tremendous results with candle soot-

polymer composite in various mechanical conditions. A candle soot nanoparticle shows significant surface area to volume ratio, high electronic and ionic conductivity. Candle soot is produced by simply burning of candles and hence, it is ecofriendly, economical and useful. Candle soot coated sponge/mesh can show stability, durability, reusability and reproducibility.

ACKNOWLEDGEMENT

This work was supported by Department of Chemistry and Department of Physics, RajeRamrao Mahavidyalaya, Jath. We also acknowledge Prof. (Dr.) Suresh S. Patil, Principal, RajeRamrao Mahavidyalaya, Jath.

REFERENCES

1. Yao, T.,Zhang, Y.,Xiao, Y.,Zhao, P.,Li, G.,Yang, H., Li, F.(2016) *Journal of Molecular Liquids*, 218, 611–614.
2. Bi, H., Xie, X., Yin, K., Zhou, Y., Wan, S., He, L., Xu, F., Banhart, F., Sun, L., Ruoff, R.S. (2012) *Advanced Functional Materials*, 22, 4421-4425.
3. Cong, H.P., Ren, X.C., Wang, P., Yu, S.H. (2012) *American Chemical SocietyNano*, 6, 2693-2703.
4. Li, L., Li, B., Dong, J., Zhang, J. (2016) *Journal of Materials Chemistry A*, 4, 13677-13725.
5. Gao, J., Huang, X., Xue, H., Tang, L., Li, R.K. (2017) *Chemical Engineering Journal*, 326, 443-453.
6. Bayat A., Aghamiri, S. F., Moheb, A.,Vakili-Nezhaad, G. R.(2005) *Chemical Engineering & Technology*, 12, 28-40.
7. Li, J., Zhu, L.,Luo, Z.(2016) *Chemical Engineering Journal*, 287, 474-481.
8. Wu, Z., Li, C., Liang, H., Zhang, Y.,Wang, X., Chen, J.,Yu, S. (2014) *Scientific Reports*, 4, 4079.
9. Bi, H., Xie, X., Yin, K., Zhou, Y., Wan, S., He, L., Xu, F., Banhart, F.,Sun, L.,Ruof, R. S.(2012), *Advanced Functional Materials*, 22, 4421-4425.
10. Sam, E. K., Sam, D. K., Lv, X., Liu, B., Xiao, X., Gong, S., Yu, W., Chen, J., Liu, J.(2019) *Chemical Engineering Journal*, 19, 3012-3018.
11. Zulfiqar, U., Hussain, S. Z., Subhani, T., Hussain, I., Rehman, H.(2018), *Colloids and Surfaces A: Physicochemical and Engineering Aspects*, 539, 391–398.
12. Gao, Y., Zhou, Y. S., Xiong, W., Wang, M., Fan, L., Golgir, H., Jiang, L., Hou, W., Huang, X., Jiang, L., Silvain, J.,Lu, Y. F. (2014) *ACS Applied Materials & Interfaces*, 6, 5924–5929.
13. Ren, G., Song, Y., Li, X., Zhou, Y.,Zhang, Z., Zhu, X.(2018) *Applied Surface Science*, 428, 520-525.

14. Choi, S., Kwon, T., Im, H., Moon, D., Baek, D., Seol, M., Duarte, J., Choi, Y. (2011) *ACS Applied Materials & Interfaces*, 3, 4552–4556.
15. Song, J., Na, L., Li, J., Cao, Y., Cao, H. (2022) *Nanomaterials*, 12, 761–775.
16. Li, J., Zhao, Z., Kang, R., Zhang, Y., Lv, W., Li, M., Jia, R., Luo, L. (2017) *Journal of Sol-Gel Science and Technology*, 3, 817–826.
17. Zulfiqar, U., Hussain, S., Subhani, T., Hussain, I., Rehman, H. (2018) *Colloids and Surfaces A: Physicochemical and Engineering Aspects*, 539, 391–398.
18. Gao, Y., Zhou, Y., Xiong, W., Wang, M., Fan, L., Rabiee-Golgir, H., Jiang, L., Hou, W., Xi, H., Jiang, L., Silvain, J., Lu, F. (2014) *ACS Applied Materials & Interfaces*, 6, 5924–5929.
19. Beshkar, F., Khojasteh, H., Niasari, M. (2017) *Journal of Colloid and Interface Science*, 497, 57–65.
20. Liu, D., Yu, Y., Chen, X., Zheng, Y. (2017) *RSC Advances*, 7, 12908–12915.
21. Zhang, R., Zhou, Z., Ge, W., Lu, Y., Liu, T., Yang, W., Dai, J. (2020) *Chinese Journal of Chemical Engineering*, 5, 30292–30294.
22. Chen, B., Zhang, R., Fu, H., Xu, J., Jing, Y., Xu, G., Wang, B., Xu, H. (2022) *Scientific Reports*, 8, 1–9.



SHIVAJI UNIVERSITY, KOLHAPUR

Volume-49 Issue-1 (January, 2023)

ISSN-Science-0250-5347

Estd. 1962
"A++" Accredited by NAAC (2021)
with CGPA 3.52



JOURNAL OF SHIVAJI UNIVERSITY : SCIENCE AND TECHNOLOGY

(Peer Reviewed Journal)

Journal of Shivaji University: Science and Technology
Volume-49, Issue-1 (January,2023)
INDEX

Sr. No.	Title of Research Article with Name of Author/s	Page No.
1.	Synthesis and Characterization of g-C₃N₄ Decorated ZnONanorods and their Binder Free Deposited Photoanodes for Photoelectrochemical Water Splitting Studies Pramod A. Koyale, Prakash S. Pawar, Swapnajit V. Mulik, Vijay S. Ghodake, Amol B. Pandhare, Ankita K. Dhukate, Sagar D. Delekar	1
2.	Thiamine Hydrochloride (VB₁) Catalyzed Synthesis of 5-aryl-4-phenyl-1,2,4-triazolidine-3-thiones in Aqueous Medium Pradeep P. Patil, Prasad M. Swami, Shankar P. Hangirgekar, Sandeep A. Sankpal	10
3.	Evaluation of Acute Toxic Effect of Gallic Acid Loaded Eudragit's 100 Nanoparticles on <i>Artemia Salina</i> Brine Shrimp Bioassay PoournimaS. Sankpal, Sachinkumar V.Patil,SayaliS. Patil	20
4.	Surface Modifications of Binder Free ZnONanorod Thin Films through Cds Quantum Dots for Dye Sensitized Solar Cells Krantiveer V. More, Anant G. Dhodamani, Sajid B. Mullani, Tukaram D. Dongale,Prakash S. Pawar,Satish M. Patil, Sunil J. Kadam, Sagar D. Delekar	36
5.	Review on Candle Soot based Superhydrophobic Surfaces for Oil-Water Separation Mehejbin R. Mujawar, Rajesh B. Sawant, Amol B. Pandhare, Prashant D. Sanadi, Sanjay S. Latthe, Ankush M. Sargar, Raghunath K. Mane, Shivaji R. Kulal	50
6.	A Review on Current Advancements in Magnetic Nanomaterials for Magnetic Hyperthermia Applications Amol B. Pandhare, Prakash S. Pawar, Vijay S. Ghodake, Swapnajit V. Mulik, Pramod A. Koyale, Ankita K. Dhukate, Deepak B. Mohite, Karishma V. Shikhare, Rajendra P. Patil, Sagar D. Delekar	62
7.	One-Step Synthesis of Biomass-Derived Carbon Dots: Study of Optical Properties Akanksha G. Kolekar, Omkar S. Nille,Shubham J. Kumbhar, Priyanka S. Mahadar, Sayali B. Lohar, Govind B. Kolekar, Gavisiddappa S. Gokavi, Vishalkumar R. More	87
8.	Synthesis and Characterization of Plant-Mediated CuO Nanoparticles Omkar S. Nille, Harshad A. Mirgane, Sneha V. Koparde, Akanksha G. Kolekar, Ashlesha R. Pawar, Pallavi J. Pawar, Abhishek A. Waghmode, Tanaji R. Dhage, Vijay S. Ghodake, Prasad M. Swami, Sarita D. Shinde,Govind B. Kolekar	95

Review on Candle Soot based Superhydrophobic Surfaces for Oil-Water Separation

Mehejbin R. Mujawar^{a,*}, Rajesh B. Sawant^a, Amol B. Pandhare^{b,f},
Prashant D. Sanadi^g, Sanjay S. Latthe^c, Ankush M. Sargar^d,
Raghunath K. Mane^e, Shivaji R. Kulal^{a,*}

^aDepartment of Chemistry, Raje Ramrao Mahavidyalaya, Jath, Sangli 416 404 (MS) India.

^bDepartment of Chemistry, Shivaji University, Kolhapur 416 004 (MS) India.

^cDepartment of Physics, Vivekanand College, Kolhapur 416 003 (MS) India.

^dDepartment of Chemistry, Bharati Vidyapeeth's Dr. Patangrao Kadam Mahavidyalaya, Sangli 416 416 (MS) India.

^eDepartment of Chemistry, Smt. Kusumtai Rajarambhapu Patil Kanya Mahavidyalaya, Islampur, Sangli 416 409 (MS) India.

^fDepartment of Chemistry, M.H. Shinde Mahavidyalaya, Tisangi, Gaganbavda, Kolhapur 416 206 (MS) India.

^gDepartment of Engginring, Chemistry, Institute of Technology's College of Engineering (Autonomous), Kolhapur 416 234 (MS) India.

*Corresponding authors: srkulal@gmail.com and mehejabeenmujawar@gmail.com

ABSTRACT

Over the many years, the oceanic oil spill accidents and most industries worldwide discharging immense levels of oil in the surroundings is a serious problem for the environment. There is a need to develop technology for oil-water separation because the spilled oil affects the ecological and environmental system. Candle soot nanoparticles are hydrophobic (water repellent) in nature and has the advantages of cost-effectiveness and production scalability over other carbons like graphene, Carbon Nanotubes (CNTs), Carbon Nanodots (CNDs), etc. in their synthesis. Candle soot based superhydrophobic materials have outstanding water repulsion and oil absorption capacity, highly selectivity, chemical inertness and excellent recyclability. In this paper, we discuss applications of candle soot based superhydrophobic materials applied on sponge and mesh substrates for oil-water separation.

KEYWORDS

Carbon Nanotubes, Carbon Nanodots.

.....

1. INTRODUCTION

The oil spilling and discharge of industrial organic solvents causes several damages to water resources and aquatic ecosystems [1-3], which became a global problem and need to solve it urgently to save the ecosystems. A new technology in material science has been developed for oil-water separation using superhydrophobic nanomaterial. As like the lotus leaf, superhydrophobic surface having water contact angle greater than 150° and oil contact angle near 0°[4]. Different chemical methods

are used for the fabrication of the superhydrophobic mesh/sponge for efficient oil-water separation. As the carbon nanoparticles are hydrophobic in nature, it shows strong affinity toward oil. At the same time, huge amount of candle soot waste is produced. Undoubtedly, it is of great benefit to turn candle soot waste into high value oil absorbent materials [5]. The superhydrophobic mesh/sponge exhibited high selectivity toward different oil and organic pollutants, fast and efficient oil-water separation capability, good repeatability, good reusability, mechanically stable, chemically stable and thermally stable [6]. Candle soot-based absorbents demonstrate superior efficiency in the removal of oils. However, the high production costs of carbon nanotube[7], graphene[8], activated carbon [9], expanded graphite [10], etc. So, these absorbents limit their wide adoption at large scale. Candle soot (CS) generated from incomplete combustion of paraffin wax has demonstrated the advantages of cost effectiveness and production scalability over CNTs, graphene and activated carbons in their synthesis [11]. However, candle soot coated superhydrophobic materials are the best solution from these. The superhydrophobic surfaces on which water achieves water contact angle higher than 150° and sliding angle less than 5° are attracting minds of researchers due to their efficient oil-water separation abilities [12-14]. J. Song et al. [15] fabricated CS-coated mesh by using dip-coating method. The cleaned stainless-steel mesh (SSM) was dipped in the glue solution for 10 min and then dried at 80°C to obtain the CS-glue coated mesh. The CS coating is close packed because of using superglue as a binder. The CS-glue coated mesh revealed the separation efficiency higher than 99.95%. Even after 20 cycle separation tests, it was shown superior reusability and durability. Li et al. [16] prepared the hydrophobic CS by incomplete combustion of hydrocarbons from the middle of candle flame. The PU sponge dipped in the solution of CS, SiO_2 and PU resin to achieve stable superhydrophobicity. The CS- SiO_2 -PU sponge showed excellent oil-water separation efficiency. The CS- SiO_2 -PU sponge was also shown superior separation efficiency from hot water, acidic solutions, alkaline solutions and salt solutions. Zulfiqar et al. [17] deposited cheaply available sawdust on polychloroprene adhesive-coated stainless-steel mesh with deposition of silicone polymer by using dip-coating method. Then, a thin layer of CS particle was applied on the prepared stainless-steel mesh by simply holding it above a candle flame. The CS particles get uniformly deposited on silicone covered sawdust which exhibited highly rough and porous morphology required for superhydrophobicity. It showed excellent oil-water separation efficiency greater than 95% which showed its recyclability, reusability and mechanical stability. In this article, we will mostly discuss on the simple, low-cost, rapid and innovative methods for the fabrication of superhydrophobic/superoleophilic CS coated sponges/meshes for efficient oil-water separation application.

2. SUPERHYDROPHOBIC-SUPEROLEOPHILIC SURFACES FOR OIL-WATER SEPARATION

2.1 Oil-water separation using Superhydrophobic-superoleophilic sponges

2.1.1 Highly efficient carbon soot sponge

The CS particles obtained from ethylene-oxygen combustion flame with flow rate of 5:3. These CS particles were dispersed in 1, 2-dichloroethane followed by sonication. The sponge was dipped in CS dispersion solution to attain superhydrophobic sponge. The superhydrophobic sponge achieved by a uniform coating of as-grown CS particles onto the porous skeleton through simple immersion in CS dispersion. The CS-modified sponge exhibited excellent oil-water separation efficiency without further chemical modification. The fast and easy recovery of engine oil floating on the water surface by CS-modified sponge confirms its high oil-water separation efficiency. The CS-sponge was shown an absorption capacity in the range of 25-80 times its original weight. The absorption capacity of the CS-sponge does not show severe degradation after 10 cycles which indicating a highly stable absorption performance of CS-sponge. After 10 cycles which indicating a highly stable absorption capacity is kept for CS-modified sponge, which much higher than that of the CS-sponge [18].

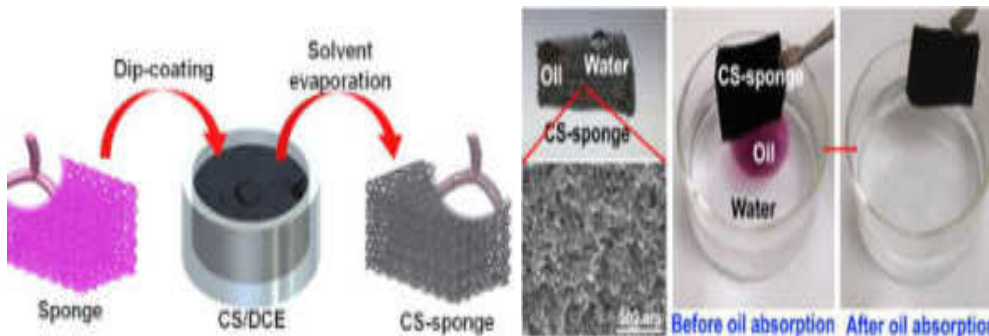


Figure-1. Schematic showing the carbon soot-sponge preparation by dip-coating and carbon soot sponge before & after oil absorption. Images reprinted from [18], with permission from American Chemical Society, Copyright 2014.

2.1.2 Recyclable superhydrophobic straw soot sponge

The straw soot on the glass slide was collected by shaving soot from the glass using a spatula. The colloidal suspension of CS was prepared by simply mixing the soot in ethanolic medium. The sponge was dipped into straw soot solution by using dip-coating method to form superhydrophobic sponge. The modified sponge was shown the water contact angle up to 154° . This superhydrophobic sample had good hydrophobic stability even in acidic condition and it can show the efficient oil-water separation. The amount of the absorbed oil was about 30 times of sponges own

weight which can be shown that the evaluation of the mass based on absorption capacity. The absorption capacity based on density, viscosity and surface tension of the absorbed liquids. This superhydrophobic sponge shows highly recyclability. The experiments demonstrate that the sponge can absorb the oil more than 30 cyclic applications without any significant change in the absorption. This method shows the benefits of easy preparation using natural soot source, better performance, oil absorption in a very short time in comparison with previous works [19].

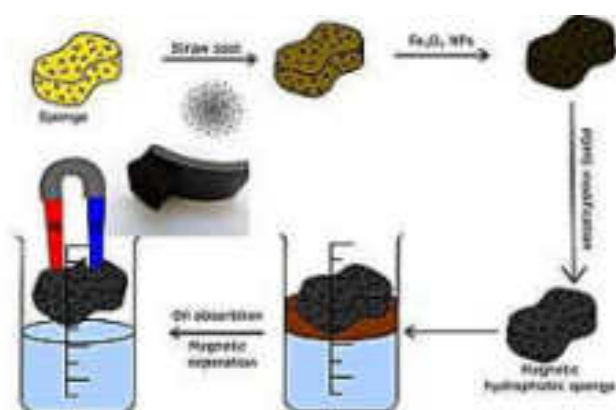


Figure-2. Schematic illustration of preparation of modified polyurethane sponge and oil separation process. Images reprinted from [19], with permission from Elsevier, Copyright 2017.

2.1.3 Durable PVDF/CS sponge

The superhydrophobic surface was fabricated by using PVDF and candle soot via sugar template method. It was shown the water contact angle of 158.3° and roll on angle of 6.7° . The oil quickly absorbed by superhydrophobic sponge which can be shows the superoleophilic property of superhydrophobic sponge. The solar value of candle soot is up to 99.4% which shows excellent light absorbing property. The sponge shows excellent oil-water separation property even after 25 cycles without destroying the sponge. The strong elasticity & high stretch resistance confirms that the modified superhydrophobic surface is highly mechanical durable. The modified sponge maintains the 89% of recovery rate even after 10 cycles. The absorption capability recovered up to 96% without obvious change of morphology of the sponge surface. This method was used to prepare a photothermal & porous PVDF/CS sponge with structural, chemical and mechanical property. It was shown high photothermal property.

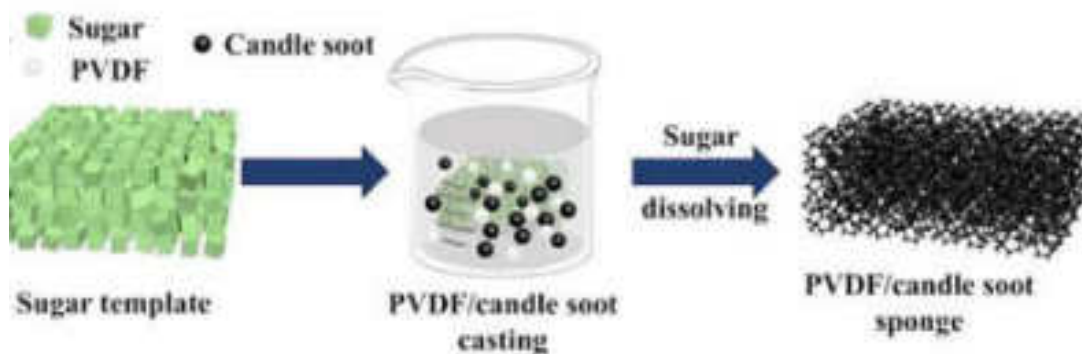


Figure-3. Schematic illustration of the fabrication of porous PVDF/candle soot sponge using sugar template. Images reprinted from [20], with permission from Elsevier, Copyright 2021.

2.2 Oil-water separation using superhydrophobic-superoleophilic meshes

2.2.1 Superhydrophobic SiO_2 /Carbon mesh

The candle soot was collected on the surface of stainless-steel mesh by placing the mesh above the wick of candle. Then by using chemical vapour deposition method the SiO_2 /carbon layer deposited on stainless steel mesh. Modify this mesh by using PFOTS and PDPA-PFO respectively to form the superhydrophobic and superoleophilic mesh membrane. This modified superhydrophobic stainless steel mesh exhibits excellent repellence for all the tested strong acids, strong bases and saturated salts, indicating a good stability of modified mesh under a series of hard environment. The separation efficiencies obtained repeatedly even after 15 cycles without any noticeable deterioration. Both superhydrophobic and superoleophilic modified stainless steel mesh membranes shows stability, durability and reusability. The SiO_2 /Carbon modified stainless steel mesh indicates good material for treating real oil-polluted water in different practical applications as well as in oil spill clean-up. This method shows higher performance, oil-water separation in a short time and repeatedly in comparison with earlier works [20].

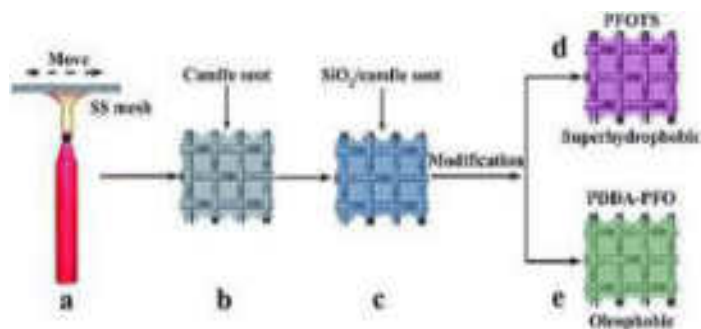


Figure-4. Process of superhydrophobic and oleophobic mesh membranes preparation: (a) coating stainless steel mesh with carbon nanoparticle (candle

soot), (b) carbon nanoparticle coated stainless steel mesh, (c) SiO₂/carbon stainless steel mesh, (d) PFOTS modified SiO₂/carbon stainless steel mesh, (e) PDDA–PFO modified SiO₂/carbon stainless steel mesh. Images reprinted from [21], with permission from Royal Society of Chemistry, Copyright 2017.

2.2.2 Durable PDMS-CS based superhydrophobic mesh

The candle soot was deposited on stainless steel mesh by simply placed above the candle flame for 15 sec. Then this CS coated stainless steel mesh was dipped in solution of PDMS & Xylene for 10 min by using immersion method. After that same process will be carried out for deposition of candle soot on this modified stainless-steel mesh was prepared. It shows 156° water contact angle & nearly 0° oil contact angle. Also, it shows 3° sliding angles. It shows higher water contact angle even after 10 times tests of oil-water separation. The oil-water separation efficiency was nearly 91% by using this modified superhydrophobic stainless steel mesh. It exhibits high thermal stability, good corrosion resistance and reusability. It was modified though combine mesh & polymer foam the composite adsorbent material successfully separate the oil from water via magnet drive method. This modified method was very useful than other research work. So, it was very useful than any other works [21].

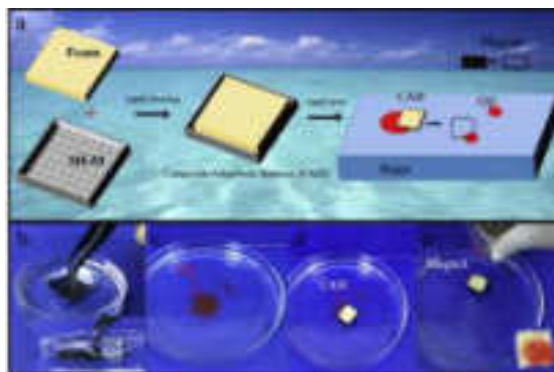


Figure-5. a) Schematic for the preparation process of composite adsorbent material (CAM) from the SH-M square boat and polymer foam, as well as its application of magnet drive for oil/water separation; b) SH-M square boat immersion in water by force; c–e) picture of the magnet drive CAM oil adsorption process. Images reprinted from [22], with permission from Progress in Organic Coatings, Copyright 2019.

2.2.3 CS templated superhydrophobic silica coating on SS mesh

The superhydrophobic coating was prepared through placing the cleaned substrate over candle flame until a few microns thick layer of candle soot deposited on

stainless steel mesh. The candle soot coated substrate together with SiCl_4 was placed in a drier for chemical vapour deposition. Then, though calcination at $600\text{ }^\circ\text{C}$ for half in air, CS composed NPs thermally degraded and diffused through the silica shell gradually. It shows highly oil-water separation efficiency even after 30 times cycle separation superhydrophobic surface remained. The superhydrophobic coating revealed excellent separation efficiency even after 6 times reuses of same superhydrophobic material. It could be potentially used in optical and visual application scenarios where in harsh & oily environments, like goggles, building façade, visual oil-water separation device & touch screen, etc. Among the all-other research work it shows tremendous oil-water separation properties [22].

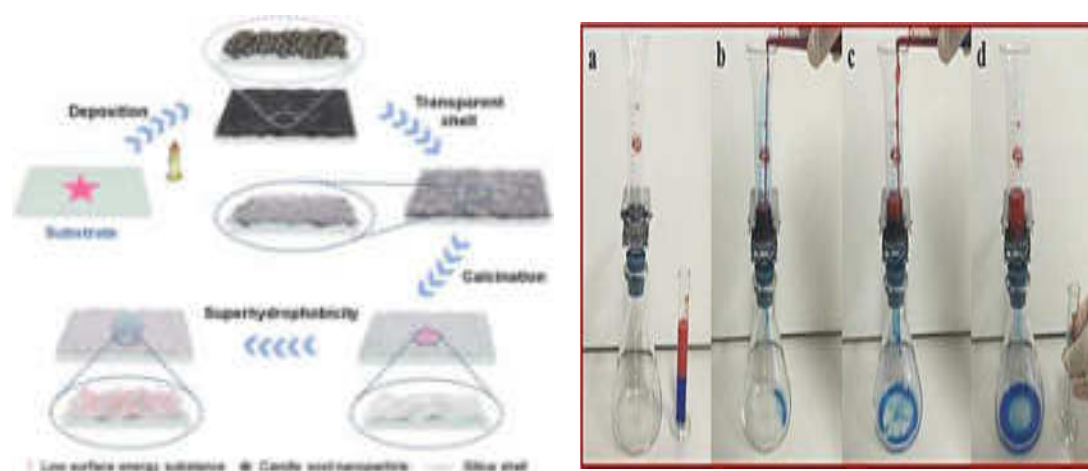


Figure-6. Schematic of preparation and properties of the transparent and robust superhydrophobic coating and oil–water separation. Images reprinted from [23], with permission from Nature, Copyright 2022.

3.CONCLUSION

As this review highlights, candle soot nanoparticles are unique in that, their fabrication requires little control of external parameters. It is very economical beneficial, facile and straightforward to synthesize. Candle soot coated sponge/mesh for use in oil-water separation has been developed by using CS-nanoparticles and different polymers. The candle soot synthesis, candle soot coated sponge/mesh preparation, procedures are simple, cost-effective and scalable. The absorption/separation investigation demonstrates that, the candle soot sponge/mesh is highly efficient and stable in absorbing a wide range of oil and organic solvents. It can be believed that, the candle soot coated superhydrophobic materials are very useful for oil-water separation. It shows various tremendous results with candle soot-

polymer composite in various mechanical conditions. A candle soot nanoparticle shows significant surface area to volume ratio, high electronic and ionic conductivity. Candle soot is produced by simply burning of candles and hence, it is ecofriendly, economical and useful. Candle soot coated sponge/mesh can show stability, durability, reusability and reproducibility.

ACKNOWLEDGEMENT

This work was supported by Department of Chemistry and Department of Physics, RajeRamrao Mahavidyalaya, Jath. We also acknowledge Prof. (Dr.) Suresh S. Patil, Principal, RajeRamrao Mahavidyalaya, Jath.

REFERENCES

1. Yao, T.,Zhang, Y.,Xiao, Y.,Zhao, P.,Li, G.,Yang, H., Li, F.(2016) *Journal of Molecular Liquids*, 218, 611–614.
2. Bi, H., Xie, X., Yin, K., Zhou, Y., Wan, S., He, L., Xu, F., Banhart, F., Sun, L., Ruoff, R.S. (2012) *Advanced Functional Materials*, 22, 4421-4425.
3. Cong, H.P., Ren, X.C., Wang, P., Yu, S.H. (2012) *American Chemical SocietyNano*, 6, 2693-2703.
4. Li, L., Li, B., Dong, J., Zhang, J. (2016) *Journal of Materials Chemistry A*, 4, 13677-13725.
5. Gao, J., Huang, X., Xue, H., Tang, L., Li, R.K. (2017) *Chemical Engineering Journal*, 326, 443-453.
6. Bayat A., Aghamiri, S. F., Moheb, A.,Vakili-Nezhaad, G. R.(2005) *Chemical Engineering & Technology*, 12, 28-40.
7. Li, J., Zhu, L.,Luo, Z.(2016) *Chemical Engineering Journal*, 287, 474-481.
8. Wu, Z., Li, C., Liang, H., Zhang, Y.,Wang, X., Chen, J.,Yu, S. (2014) *Scientific Reports*, 4, 4079.
9. Bi, H., Xie, X., Yin, K., Zhou, Y., Wan, S., He, L., Xu, F., Banhart, F.,Sun, L.,Ruof, R. S.(2012), *Advanced Functional Materials*, 22, 4421-4425.
10. Sam, E. K., Sam, D. K., Lv, X., Liu, B., Xiao, X., Gong, S., Yu, W., Chen, J., Liu, J.(2019) *Chemical Engineering Journal*, 19, 3012-3018.
11. Zulfiqar, U., Hussain, S. Z., Subhani, T., Hussain, I., Rehman, H.(2018), *Colloids and Surfaces A: Physicochemical and Engineering Aspects*, 539, 391–398.
12. Gao, Y., Zhou, Y. S., Xiong, W., Wang, M., Fan, L., Golgir, H., Jiang, L., Hou, W., Huang, X., Jiang, L., Silvain, J.,Lu, Y. F. (2014) *ACS Applied Materials & Interfaces*, 6, 5924–5929.
13. Ren, G., Song, Y., Li, X., Zhou, Y.,Zhang, Z., Zhu, X.(2018) *Applied Surface Science*, 428, 520-525.

14. Choi, S., Kwon, T., Im, H., Moon, D., Baek, D., Seol, M., Duarte, J., Choi, Y. (2011) *ACS Applied Materials & Interfaces*, 3, 4552–4556.
15. Song, J., Na, L., Li, J., Cao, Y., Cao, H. (2022) *Nanomaterials*, 12, 761–775.
16. Li, J., Zhao, Z., Kang, R., Zhang, Y., Lv, W., Li, M., Jia, R., Luo, L. (2017) *Journal of Sol-Gel Science and Technology*, 3, 817–826.
17. Zulfiqar, U., Hussain, S., Subhani, T., Hussain, I., Rehman, H. (2018) *Colloids and Surfaces A: Physicochemical and Engineering Aspects*, 539, 391–398.
18. Gao, Y., Zhou, Y., Xiong, W., Wang, M., Fan, L., Rabiee-Golgir, H., Jiang, L., Hou, W., Xi, H., Jiang, L., Silvain, J., Lu, F. (2014) *ACS Applied Materials & Interfaces*, 6, 5924–5929.
19. Beshkar, F., Khojasteh, H., Niasari, M. (2017) *Journal of Colloid and Interface Science*, 497, 57–65.
20. Liu, D., Yu, Y., Chen, X., Zheng, Y. (2017) *RSC Advances*, 7, 12908–12915.
21. Zhang, R., Zhou, Z., Ge, W., Lu, Y., Liu, T., Yang, W., Dai, J. (2020) *Chinese Journal of Chemical Engineering*, 5, 30292–30294.
22. Chen, B., Zhang, R., Fu, H., Xu, J., Jing, Y., Xu, G., Wang, B., Xu, H. (2022) *Scientific Reports*, 8, 1–9.

ISBN : 978-93-83797-52-1



‘ज्ञान, विज्ञान आणि सुसंस्कार यांसाठी शिक्षण प्रसार’
-शिक्षणमहर्षी डॉ. बापूजी साळुंखे



Shri Swami Vivekanand Shikshan Sanstha, Kolhapur's
Raje Ramrao Mahavidyalaya, Jath

(Dist: Sangli 416404)

(Affiliated to Shivaji University, Kolhapur)

Re-accredited 'B' by NAAC (CGPA 2.50)

Website: www.rrcollege.org

Proceeding of ICSSR Sponsored National Seminar on
**CHANGING PARADIGMS OF SOCIAL
MOVEMENTS**

17th and 18th February, 2017

Dr. S. Y. Hongekar
Editor in Chief

Miss. Samiksha Farakate
Co-Editor

Dr. B. M. Dahalake
Editor

Publisher:



Swachhand Publication
Kolhapur 416 008
Mob.: 98231 18300

Editor in Chief: **Dr. S.Y. Hongekar**
Principal
Shri Swami Vivekanand Shikshan Sanstha, Kolhapur's
Raje Ramrao Mahavidyalaya, Jath
Dist: Sangli 416404

ISBN: 978-93-83797-52-1

No part of this publication may be reproduced or transmitted in any form by any means, electronic or mechanical, including photocopy, recording or any information storage and retrieval systems without permission in writing from the copy right.

Disclaimer:

The publisher or editors do not take any responsibility for the same in any manner. Errors, if any, are purely unintentional and readers are requested to communicate such errors to the editors or publishers to avoid discrepancies in future

Publication : 2017

Co-Editor

Miss. Samiksha Farakate
Assistant Professor
Raje Ramrao Mahavidyalaya,
Jath, Dist: Sangli 416404

Editor

Dr. B. M. Dahalake
Assistant Professor
Raje Ramrao Mahavidyalaya,
Jath, Dist: Sangli 416404

Printed by:

Shrikant Printer
Opp. Khare Mangal Karyalaya,
Shivaji University Road Kolhapur
Mob. 9890499466, 8483829154

Price: 250/-

CONTENT

Sr. No.	Title	Author	Page No.
1	SOCIAL MOVEMENTS IN INDIA: MEANING, NATURE, CAUSES AND PRESENT STATUS	Shekhar B. Ashtikar Dr. Sunil V. Shinde	1
2	SOCIO-POLITICAL DIMENSIONS OF LABOUR MOVEMENT IN INDIA	Prof. D.A. Pawar Prof. R. B. Patil	5
3	CHANGING DYNAMICS OF SOCIAL AND LITERARY DALIT MOVEMENTS IN INDIA	Mr. Sannake Tukaram Umesh, Prof. R. D. Karande	8
4	"FEMINISTIC PARADIGMS OF SUBVERSION OF HIERARCHY AND INDEPENDENT POSITION OF WOMEN	Mr. Bansode Ramdas Shamrao	14
5	THE ROLE OF NON-GOVERNMENTAL ORGANIZATIONS (NGOs) IN CONSERVATION OF NATURAL RESOURCES: SOME ISSUES	Sanjay S. Sathe, Suresh P. Dharigouda, Appasaheb K. Bhosale, Rajendra A. Lavate & Vidya C. Mali	19
6	CHANGING INTERACTION AND BEHAVIOUR BETWEEN HUMAN AND BIRDS WITH THE HELP OF NGO'S AND VARIOUS ORGANISATIONS.	Miss. Deshmukh .S.B., Miss.Saptal.L.P	26
7	ROLE OF DR. B.R. AMBEDKAR'S SOCIAL MOVEMENTS TO EMERGE HIM AS AN EMANCIPATOR OF UNTOUCHABLES	Lavate Rajendra A., Sathe Sanjay S., Sajjan, Mallappa B., Kumbhar Dipak A., Salunke Govind D. & Borate Santosh D.	29
8	INFORMATION AND COMMUNICATION TECHNOLOGIES FOR DEVELOPMENT: AN INCLUSIVE FRAMEWORK FOR E-GOVERNANCE	Prof. A.R.Herwade	38
9	ENVIRONMENT MOVEMENT IN INDIA	Dr.Hanumant Kurkute	48

Raje Ramrao Mahavidyalaya, Jath

10	SUPERSTITION: A LAW, MOVEMENT AND AN EXPERIENCE	Shrikant Kokare Sanjay Latthe	54
11	'दलित आंदोलन और हिंदी साहित्य'	प्रा. हिरामन देवराम टोंगारे	58
12	"स्त्रीवादी और भारतीय समाज"	प्रा. डॉ. सविता भाऊलाल नागरे	63
13	शिक्षणमहर्षी बापुजी साळुंखे यांचे सामाजिक चळवळीतील योगदान	प्रा. डॉ. भिमार्शंकर मधुसुदन डहाळके	68
14	स्वातंत्र्योत्तर काळातील सामाजिक चळवळीचे मूल्यमापन	श्री. ज्ञानेश्वर शामराव आवाळे, श्री.दिपक सर्जेराव पाटील	73
15	बदलत्या सामाजिक चळवळीच्या परिपेक्षातून भारतीय पर्यावरणीय चळवळीचा अभ्यास.	श्री. आबासाहेब बद्रुवान गायकवाड	77
16	डॉ. बाबासाहेब आंबेडकरांच्या राजकीय चळवळींचा इतिहास	प्रा. डॉ. सोमनाथ डॉ. कदम	83
17	राजर्षी शाहू महाराजांचा सत्यशोधक चळवळ	डॉ. संतोष कोल्हे प्रा. संदीप पाटील	89
18	भारताच्या राजकीय, सामाजिक चळवळींचे बदलते स्वरूप व मर्यादा	प्रा. चालीकवार राजेश सुभाष	94
19	महाराष्ट्रातील सामाजिक चळवळी : एक मूल्यमापन	प्रा. दत्तात्रय दादासो जाधव प्रा. अनिल टी. शिंदे	97
20	नक्षलवादी चळवळ संदर्भात सलवा जुद्धम मोहीमेबाबत कृती कार्यक्रम	प्रा. रावसाहेब स. कांबळे	101
21	कल्याणकारी कृतीकार्यक्रम आणि राजकीय कृतीप्रवणता	श्री. श्याम रोकडे	106
22	स्वातंत्र्योत्तर दलित पॅथर चळवळ	प्रा. कु.शिलेदार चंद्रकला बसाप्पा	110
23	सामाजिक चळवळींचे बदलते आयाम व चळवळी समोरील अडथळे	प्रा. डॉ. शामराव महादेव लेंडवे	116
24	महात्मा फुले आणि सत्यशोधक समाज	चौधरी पुंडलिक जयपाल	121
25	पर्यावरणवादी एक नव-सामाजिक चळवळ	प्रा. निलेश गोकुळ शेंरे.	129

महात्मा फुले आणि सत्यशोधक समाज

चौधरी पुंडलिक जयपाल

सहा.प्राध्यापक, इतिहास

राजे रामराव महाविद्यालय, जत, जि.सांगली

email-pjchoudhary72@gmail.com

१९ व्या शतकात संपुर्ण भारतात समाजसुधारणेच्या चळवळी चालू होत्या. त्यामध्ये महात्मा फुले यांनी अपृश्य बहुजन समाजाला ब्राम्हणांच्या मानसिक गुलामगिरीतून मुक्त करून सामाजिक विषमता दूर करण्यासाठी २४ सप्टेंबर १८७३ मध्ये सत्यशोधक समाजाची स्थापना केली. अपृश्य बहुजन समाजाला जागृत करून कनिष्ठ वर्गातील आन्यायाला वाचा फोडण्यासाठी प्रथम १८७३ मध्ये 'गुलामगिरी' ह्या ग्रंथाची निर्मिती केली. ब्राम्हणी व्यवस्थेने लादविलेल्या गुलामगिरीची जाणीव अपृश्य वर्गाला करून देवून त्यातून मुक्त होण्याची प्रेरणा निर्माण केली. महात्मा फुले कृतीवादी समाजसुधारक होते त्यामुळे समाजात सुधारणा घडवून आणण्यासाठी नुसते प्रबोधने नाही तर प्रत्यक्ष कार्य केले पाहिजे हा दृष्टीकोन त्यांच्यामध्ये होता. त्यासाठी त्यांना समाजाला जागृत करण्यासाठी पोषक तत्वज्ञान आणि संघटीत व्यासपीठाची आवश्यकता निर्माण होत होती. सत्यशोधक समाज स्थापन करण्याच्या कितीतरी आधिपासून महात्मा फुले आपले विचार सभा, पत्रके, पुस्तिका इत्यादींच्या माध्यमाने समाजात मांडत होते. देवा धर्माच्या नावाखाली भटभिक्षुणी प्राचीन ग्रंथाचा आधार घेवून अपृश्य बहुजन समाजाला मानसिक गुलामगिरीत ठेवले होते. त्यांच्यावर प्रथा, परंपरा, चालीरिती लादविण्यात आल्या होत्या त्या विषयी जागृत करण्यासाठी अपृश्य बहुजनांच्या शिक्षणाची कास धरली होती ते आपल्या भाषणाच्या माध्यमाने अपृश्य समाजाला शिक्षण घेण्यास प्रेरित करित होते व जातीभेद संपुष्टात आणून समानता निर्माण करण्याचे प्रयत्न केले. जोतीरावांनी आपली भाषणे व ग्रंथ यांच्या व्दारा शेतकरी आणि कामगार यांच्या गा-हाण्याकडे सरकारचे लक्ष वेधावे यासाठी प्रयत्न केला. सरकारी खात्यात भ्रष्टाचार कसा होतो. त्यात शेतक-याची पिळवणूक कशी होते व त्याकडे सरकारी अधिकारी कसे दुर्लक्ष करतात हे उघडकीस आणण्याचे कार्य त्यांनी केले. शेतकरी व कामगारांची व्यथा सरकारला दाखवून दिला. परंतु झगडा केल्याशिवाय समुळ समाप्त झालेले अधिकार अपृश्यांना परत मिळणार नाही याची जाणीव महात्मा फुल्यांना झाली व त्यासाठी संस्थेची आवश्यकता भासू लागली. म्हणून आपल्या विचारांचा प्रचार आणि प्रसार करण्यासाठी संघटीत व्यासपीठ निर्माण करण्याचा बेत केला. त्यांनी २४ सप्टेंबर १८७३ मध्ये पुणे येथे आपल्या कार्यकर्त्यांची सभा आयोजित केली

या सभेत केंद्रीय संस्थेचे महत्व महात्मा फुले यांनी पटवून दिले. आणि सर्वांच्या विचाराने २४ सप्टेंबर १९७३ रोजी सत्यशोधक समाजाची स्थापना झाली.

सत्यशोधक समाजाचे तत्व आणि प्रतिज्ञा:

सत्यशोधक समाजाचे पहिले अध्यक्ष व कोषाध्यक्ष या पदावर महात्मा फुले यांचीच निवड करण्यात आली. नारायणराव गोविंदराव कडलक यांची सत्यशोधक समाजाचे कार्यवाह म्हणून निवड करण्यात आली. सामाजिक विषमता व अपृश्यांचे दुःख नाहीसे करणे, अपृश्यांची ब्राम्हण पुरोहिताकडून होणारी पिळवणूक बंद करणे, त्यांना त्यांच्या मानवी हक्क व अधिकारांची जाणीव करून देणे, पुरोहितांच्या मानसिक आणि धार्मिक गुलामगिरीतून अपृश्यांची मुक्तता करणे इत्यादी उद्देश सत्यशोधक समाज स्थापने मागे होते. महात्मा फुले यांच्या मृत्युनंतर १९११ साली सत्यशोधक समाजाचे ठराव प्रसिध्द झाले. त्यात सत्यशोधक समाजप्रणीत तीन तत्त्वे गोवली होतील ती अशी अज सर्व मनुष्य एकाच देवाची लेकरे आहेत व तोच त्यांचा सर्वे सर्वा आहे बज देवाची प्रार्थना करण्यात कोणत्या मध्यस्त किंवा दलालाची आवश्यकता नाही कज वरिल तत्त्व कबुल असल्यास कोणासही सत्यशोधक समाजाचा सभासद होता येते. छत्र्येक सभासदाला पुढीलप्रमाणे प्रतिष्ठा घ्यावी लागेल सर्व मानवप्राणी एकाच देवाची लेकरे आहेत, सबब ती माझी भावंडे आहेत, अशा बुध्दीने मी त्यांच्याशी वागेन. परमेश्वराची पुजा, भक्ती अगर ध्यानधारणा करतेवेळी अगर धार्मिक विधिचे वेळी मी मध्यस्थांची गरज ठेवणार नाही. मी माझ्या मुला मुलींना सुशिक्षित करीन. मी नेहमी राज निष्ठेने वागेन परमेश्वरास साक्ष ठेवून मी ही प्रतिज्ञा करीत आहे ह्या प्रतिज्ञेप्रमाणे वागण्यास मला सामर्थ्य येईल व आयुष्य जाण्यास योग्य प्रकारे इश्वर मला मदत करे. सत्यशोधक समाजाचे सदस्यत्व सर्वांना खुले होते. ब्राम्हण, महार, मांग, ज्यु आणि मुसलमान हे चळवळीच्या सुरुवातीला सभासद होते असे दिसते. अनेक ठिकाणी सत्यशोधक समाजाच्या शाखा स्थापन करण्यात आलेल्या होत्या प्रत्येक आठवड्याला सभा होत असे. षणुण्यातील सोमवार पेठेतील डॉ. गावडे यांच्या घरी दर आठवड्याला सभा भरत असेल या सभेमध्ये दारुबंदी, सक्तीचे शिक्षण, स्वदेशी मालाचा पुरस्कार, अल्पखर्चात लग्न लावणे, धार्मिक क्षेत्रातील ब्राम्हणांची पुरोहीतशाही संपविणे, जातीभेद, मुर्तीपूजा यांचा विरोध करणे इत्यादी गोष्टींवर चर्चा घडवून आणली जात असे. व ती सोडविण्यासाठी विचार विमर्स केला जात होता. ब्राम्हणांनी सत्यशोधक समाजाच्या विरुध्द प्रचार चालविला होता. ब्राम्हनांनी ज्या गरिबांना घाबरवून सोडले ते महात्मा फुले यांच्याकडे येत आणि मराठीत प्रार्थना चालते काय? असा प्रश्न त्यांना विचारीत असत. तेव्हा महात्मा फुले म्हणत की संस्कृत व्यतिरीक्त भारतीय भाषेत प्रार्थना केली तर देवाला चालत नाही असे म्हणने चुकीचे आहे. देव मानसाचे मन ओळखतो. मानवाने व्यक्त केलेल्या इच्छा त्याला समजतात लॅटीन, इंग्रजी, फ्रेंच इत्यादी भाषातील केलेल्या प्रार्थना देवाला

समजल्या नाही काय? तुकाराम, नामदेव, चोखामेळा यांनी केलेल्या प्रार्थना देवाला कळल्या नाहीत काय? असे विविध प्रश्न विचारून गरीबांना समजवून देण्याचे कार्य करीत असत. सत्यशोधक समाजाचे कोणीही सभासद होवू नये यासाठी ब्राम्हणांनी खेडयापाडयात विरोधी प्रचार केला. नोकरीत असणा—या अपृश्यावर अन्याय केला. सत्यशोधक समाजाच्या सभासदांना नोक—या मिळू नयेत यासाठी प्रयत्न केले. ब्राम्हणां व्यतिरीक्त कोणाच्याही माध्यमाने होम—हवन, पूजा विधी केला तर निःसंतान राहशील अशी भिती दाखवित होते.

सत्यशोधक समाजाचे तत्त्वज्ञान:

महात्मा फुले यांनी सत्य आणि वास्तव यांचा आधार घेवून कार्य करण्यास प्रारंभ केला. एखादी गोष्ट बुध्दीला पटल्यानंतरच तिचा स्विकार केला पाहिजे याकडे त्याचा बेत होता. मिशनरी शाळेतून शिक्षण घेतल्यानंतर महात्मा फुले यांनी थॉमस पेन यांचा 'राईट्स ऑफ मॅन' हा ग्रंथ वाचला. या ग्रंथातील मानवी मुल्यांचा प्रभाव त्यांच्यावर पडला आणि त्यांनी समाजातील दृष्ट प्रवृत्ती व परंपरेवर कोरडे ओढण्यास सुरुवात केली. महात्मा फुले यांच्या सत्यशोधक समाजाचा जातीव्यवस्थेवर अजिबात विश्वास नव्हता. त्याबरोबर परमेश्वराने वर्णव्यवस्था निर्माण केली यावरही विश्वास नव्हता म्हणून त्यांनी धार्मिक कार्यातील आवश्यक तेवढ्याच विधी ठेवल्या त्याच बरोबर यातून मध्यस्थ किंवा दलालांची उचल बांगडी करण्याचे कार्य केले. मुर्तीपूजेचाही विरोध केला. तत्कालीन समाजात प्रार्थना करण्याचे अधिकार ब्राम्हण व्यतिरीक्त लोकांना नाकारण्यात आलेले होते. सत्यशोधक समाजाने मिळवून दिले. सर्वांना प्रार्थना करण्याचा अधिकार दिला. वेद, पुराण हे इश्वराने निर्माण केलेले नसून मानसानेच निर्माण केलेले आहे. बायबल किंवा कुराण या सारखे धार्मिक ग्रंथ इश्वराने लिहिलेले आहेत हे त्यांना कधीच वाटले नाही. म्हणून समाजातील जाती व्यवस्था, वर्णव्यवस्था, परंपरा, चालिरीती इत्यादींना प्राचीन धार्मिक ग्रंथाचा आधार घेवून ब्राम्हणीव्यवस्थेने समाजव्यवस्थेवर लादविल्या व समाजात अपृश्यता निर्माण केली त्याच्या विरोधात बंड करण्याचे कार्य सत्यशोधक समाजाने केले. छत्रपती शिवाजी महाराज आणि जॉर्ज वॉशिंग्टन यांच्या चरित्रामुळे महात्मा फुले यांचे विचार समतामुलक बनले. त्यांच्या विचारापासून प्रेरित होवून समतावादी समाज निर्माण करणे हे आपल्या जीवनाचे ध्येय ठरविले होते. त्यासाठी अगोदर कनिष्ठ वर्गाचा उध्दार करण्याचा निर्णय घेतला. सत्यशोधक समाजात फार बुध्दीमान लोक होते अशातला भाग नाही तर त्यांचा तत्त्वज्ञानी साधा शेतकरी होता. कौ ज्याला अपृश्य, बहुजन वर्गाचा उध्दार करण्याची उर्मी निर्माण झाली होती त्यातून त्याला आंतरिक प्रेरणा व बुध्दिप्रामाण्याची देणगी निसर्गातून लाभलेली होती. सत्यशोधक समाजाच्या कार्याचे प्रेरणास्थान शेतकरी, कामगार यांचे दुःख दुर करण्याची तळमळ होती. सत्यशोधक समाजाचे अनुयायी शेतात जावून सभा, बैठक भरवून सामान्यांच्या भाषेत आपले

विचार मांडत असत. घोगडी, पागोडे, धोतर आणि हातात टप घेवून आपल्या आपल्या भाषणात शेतकर-यांच्या कर्जाचा उल्लेख करीत असत त्यांच्या समस्या जाणून घेत व त्यासाठी कोण जबाबदार आहे हे समजावून सांगत असत. धर्मविधी, पूजापाठ या नावाखाली धुर्त ब्राम्हण किंवा मध्यस्थ शेतक-याची लुबाडणूक करतात हे समजावून देत होते. या दुःखातून बाहेर पडायचे असेल तर शिक्षण कसे उपयुक्त आहे हे सांगून समाजाला नवी दिशा दाखविण्याचे कार्य सत्यशोधक समाज करीत होता.

सत्यशोधक समाजाचे कार्य:

समाजाची एकात्मता हिच राष्ट्रीय एकात्मता या मजबूत पायावर सत्यशोधक समाजाचे अधिष्ठान होते.^५ ही सामाजिक समता निर्माण करण्यासाठी अपृश्य, शेतकरी, कामगार यांच्या समस्या सोडविणे, वर्गविरहीत समाज निर्माण करणे यासाठी सत्यशोधक समाजाने ध्येय आणि उद्दीष्टे प्रत्यक्ष कृतीत आणण्याचा निर्णय घेतला. विद्यार्थ्यांकडून शिष्यवृत्तीसाठी अर्ज मागवून घेतले व दहा विद्यार्थ्यांना शिष्यवृत्ती दिली.^६ या कार्याविषयी ब्राम्हणेत्तर समाजाने त्यांना धन्यवाद दिले व त्यांच्या कार्यात सहभाग नोंदविला त्यामुळे सत्यशोधक समाजाची सदस्य संख्या वाढली. कनिष्ठ वर्गाने लगेचच सत्यशोधक समाजाची धार्मिक शिकवण कृतीत उतरविण्यात सुरुवात केली. महात्मा फुले यांचा दुरचा नातलग त्यांच्या दुकानात कामाला होता. तो अशिक्षित होता. त्याला केंव्हा केंव्हा लिहायला वाचायला महात्मा फुले शिकवित होते. त्याचे लग्न सत्यशोधक समाजाच्या नियमानुसार करण्याचे ठरविले मुलाने ही होकार दिला. त्याची बातमी पुण्यातील ब्राम्हणाना लागताच त्यांनी मुलीच्या वडीलांना त्या लग्नाविरुद्ध चेतविले परंतु मुलीची आई सावित्रीबाईची मैत्रीण असल्यामुळे ह्या विवाहाला ब्राम्हण विरोध टळला आणि कमी खर्चात २५ डिसेंबर १८७३ रोजी सत्यशोधक समाजाच्या वतीने पहिला विवाह झाला.

ब्राम्हण पुरोहिता शिवाय हिंदू विवाह होणे ही त्या काळात घडलेली आश्चर्यकारक घटना होय. सत्यशोधक समाजाच्या वतीने हे उचललेले पहिलेच पाऊल असल्यामुळे भट ब्राम्हणांचा फारसा विरोध झाला नाही. परंतु सत्य शोधक समाजाच्या वतीने ब्राम्हणाशिवाय दुसरा विवाह करण्याचे जेव्हा महात्मा फुल्यांनी ठरविले तेव्हा मात्र ब्राम्हणांनी त्रिव विरोध केला. ग्यानोबा ससाणे यांचे लग्न ब्राम्हणाशिवाय करण्याचा निर्णय घेतला तेव्हा भट ब्राम्हण पुरोहितशिवाय लग्न लावणे धर्मबाह्य आहे हे सांगण्यासाठी ससाणे रहात असलेल्या खेड्यात गुंड पाठवून हा निर्णय मागे घेण्यास भाग पाडण्याचा प्रयत्न केला. त्याला सामाजिक बहिष्काराची धमकी सुध्दा दाखविण्यात आली. तेव्हा महात्मा फुले यांनी तुझे संरक्षण ब्रिटिश करतील त्याचबरोबर नोकर-यात सुधारक ब्राम्हण तुला मदत करतील असे सांगितले ग्यानोबा ससाणेला आपल्या नातलगाकडूनही विरोध होवू

लागला. त्याला मारण्याच्या धमक्याही देण्यात आल्या. परंतु महात्मा फुले यांनी महात्मा फुले यांच्या घरी ७ मे १८७४ मध्ये व्यवस्थित पार पडला. विवाहाला सत्यशोधक समाजाचे अनुयायी मोठ्या संख्येने उपस्थित होते. या विवाहाची खळबळजनक बातमी अनेक वृत्तपत्रातून प्रसिध्द झाली. ब्राम्हण पुरोहितांशिवाय हिंदू विवाह असा त्यांनी मधळा दिला होता. सत्यशोधक समाजाने ब्राम्हण पुरोहितांशिवाय केलेल्या दोन विवाहामुळे ब्राम्हण, धर्मांध समाजाने तिघ्न विरोध केला. अपृश्य, बहूजन समाजाला मात्र त्याचा अभिमान वाटला.

सामाजिक चळवळीतील बरेच नेते भाषणे, सभा यांच्या माध्यमाने वाईट रुढी, परंपरा, चालीरिती इत्यादींचा विरोध करित परंतु कृती मात्र काहीही करित नव्हते अशा स्वतःला समाजसुधारक म्हणविणा-या नेतृत्वाची झडती घेत असत. एकदा माधवराव रानडे यांनी आपल्या विधवा बहिणीची कथा महात्मा फुल्यांना सांगितली तेव्हा त्यांनी जे तुम्ही लोकांना करावयास उपदेश करता तेच स्वतः करून दाखविण्याची देवाने तुम्हांस नामी संधी दिली आहे. आपल्या बहिणीचा पुर्नविवाह करून आपले बोल खरे करा. लढल्याशिवाय कोणतीही गोष्ट मिळत नाही. समाजसुधारणा आपोआप होत नसते. ते आपण घडवायचे असते हे लोकांना घेयाने पटवून द्या त्यावर रानडे म्हणाले जर बहिणीचा पुर्नविवाह केला तर माझ्या बडीलांना अपार दुःख होईल आणि पुण्यातील ब्राम्हण माझ्यावर बहिष्कार टाकतील. त्यावर ज्योतीरावांनी रानड्यांना खरमरीत उत्तर दिले रावसाहेब, मग सुधारकांचे डोंग करू नका." अशा शब्दात कानउघाडणी केली. पुन्हा एकदा माधवराव रानड्यांनी त्यांच्या पत्नीचे निधन झाल्यावर बत्तीस वर्षांचे असताना अकरा वर्षांच्या मुलीशी पुर्नविवाह केला. त्याविषयी महात्मा फुल्यांनी समाज सुधारणेचा विश्वास घात केल्याबद्दल विरोध केला व भारतातील विचारवंत लोक एवढे अवनतीला व अधोगतीला गेलेले आहेत की आम्हाला सांगावयास दुःख वाटते. स्वतःला समाजसेवक म्हणवून घेताना सामाजिक व्यवस्थेतील दोषांचा विरोध करण्याचे सामर्थ्य आमच्यात नाही याची शोकांतिका निर्माण होते. लोकहितवादी गोपालराव देशमुख यांनी आपला मुलगा शिक्षणासाठी इंग्लंडला पाठवून आपण धर्मबाह्य वर्तन केले अशी त्यांनी कबुली दिली." कारण त्याकाळी समुद्र पर्यटन करणे धर्मबाह्य समजण्यात येत होते. त्यामुळे धर्म, जात, कुळ यांना काळीमा लागते अशी ब्राम्हणी व्यवस्थेची समजूत होती. परंतु एका समाजसुधारकाकडून याचा विरोध न होणे हे समाजसुधारणेच्या विचाराला पटण्यासारखे नव्हते. नेटिव्ह ओपिनियन ने सांगितलेल्या कसोटीनुसार बोटावर मोजण्याइतके समाजसुधारक शिल्लक राहतील ज्यामध्ये आपले तत्वज्ञान आणि त्यानुसार कृती केलेल्यांचा समावेश असेल अशा समाजसुधारकामध्ये महात्मा फुले यांचा समावेश होतो. की ज्यांनी आपल्या तत्वज्ञानाला कृतीची जोड दिली व अपृश्य मागासलेल्या

समाजासाठी कार्य केले. समाजसेवेचे ढोंग करणा-या नेतृत्वांना जसा चोप दिला तसेच बोले तैसा चाले या कृतीनुसार कार्य करणा-या सामाजिक सुधारकांची प्रशंसाही केली. त्यासाठी विष्णूशास्त्री चिपळूनकरांचे उदाहरण देता येईल त्यांची पत्नी मरण पावल्यानंतर त्यांनी १८७४ मध्ये विधवेशी आपला पुर्नविवाह केला त्यामुळे महात्मा फुल्यांनी त्यांची प्रशंसा केली भारतातील इतर समाजसुधारकांच्या कार्याविषयी त्यांना आपुलकी होती. जे समाजसुधारक सोशीत पिडीत जनतेच्या कल्याणासाठी झडत असत त्यांना त्यांच्या कार्यात मदत करत स्वामी दयानंद सरस्वती यांनी १८७५ मध्ये मुंबईत आर्य समाजाची स्थापना केली. त्यांचा उद्देश सामान्य जनतेच्या उध्दारासाठी कार्य करणे हा होता. आपल्या मताचा प्रचार करण्यासाठी जुलै १८७५ मध्ये पुण्यात आले होते. तेव्हा ब्राम्हणवाद्यांनी त्यांना मिरवणूक काढण्यास विरोध केला होता. तेव्हा महात्मा फुल्यांनी आपण स्वतः व आपले अनुयायी मिरवणूकीत आणून स्वामी दयानंद सरस्वतींची मिरवणूक यशस्वी केली होती. महात्मा फुले हे खरे संघटक होते. आपल्यानंतरही हे कार्य चालू ठेवण्यासाठी नेतृत्व निर्माण करून ठेवण्याची गरज त्यांना वाटत होती. त्यामुळे काहीवेळा महत्वाची कामे आणि कार्याचे नेतृत्व आपल्या अनुयायांवर सोपवित होते. याचे उदाहरण म्हणजे १८७५ मध्ये सत्यशोधक समाजाचा दुसरा वार्षिक समारंभ झाला तेव्हा सत्यशोधक समाजाच्या अध्यक्ष पदाची धुरा महात्मा फुले यांनी प्रभावी व तरुण नेते डॉ. विश्राम रामजी घोले यांच्यावर सोपविली. कोषाध्यक्ष पद रामशेट उरवणे यांना दिले.^{१३} कार्यकर्तृत्वाचा हेवा त्यांनी कधीच केला नाही तर समाजकार्यासाठी कार्यकर्ते तयार करण्याचे कार्य केले प्रत्येक रविवारी सत्यशोधक समाजाच्या कार्यकर्त्यांची सभा आयोजित केली जात असे. व त्या ठिकाणी व्याख्याने होत असत. त्यात वकृत्वकलेची शिकवण देण्यात येत होती. सत्यशोधक समाजाने महात्मा फुल्यांनी देणगी म्हणून दिलेल्या श्गुलामगिरीश आणि श्ब्राम्हणांचे कसबश या ग्रंथाच्या प्रती समाजातील प्रतिष्ठीत नामवंत लोकांमध्ये विनामुल्य वाटल्या. सत्यशोधक समाजाचे उद्देश शोषित, पिडीत, अपृश्य, शेतकरी, कामगार इत्यादींच्या सुधाराचे असल्यामुळे आपले विचार समाजापर्यंत पोहचविण्यासाठी अधिक परिश्रम केले. ष्भालेकर यांनी दिनबंधु नावाचे नियतकालीक काढले इ.स. १८७७ ते १८८० असे ३ वर्षे सत्यशोधक समाजाच्या नियमांवर हे वृत्तपत्र चालले.^{१३} दिनबंधु नियतकालीकामागे सत्यशोधक समाजाची प्रेरणा होती त्यामुळे त्यामधून एखादी बातमी छापून येणे म्हणजे एक प्रकारचा झंझावात होता या वृत्तपत्राने सत्यशोधक समाजाचे बहूजन अपृश्य समाजाला जागृत करण्याचे कार्य केले. निबंध स्पर्धा, वकृत्व स्पर्धा आयोजित केल्या जात होत्या.त्याच्या माध्यमाने शेतक-यांच्या विकासासाठी शेतीपध्दती कशी असावी किंवा मुर्तीपूजा उपयुक्त आहे किंवा नाही अशा विषयावर भर देवून सामान्य वर्गाला जागृत करण्याचे कार्य केले. स्वतः महात्मा फुले आपल्या भाषणात शिक्षकांनी विद्यार्थ्यांना

आदर्श पाठ द्यावा, वास्तव्य परिस्थिती शिकवावी, समाजात जावून सामान्य लोकांना जागृत करावे असे उपदेश देत असत. महात्मा फुले आणि त्यांचा सत्यशोधक समाज यांनी व्याख्यानावरोबर प्रत्यक्ष कृती करून समाज जागृतीचे कार्य केले. त्यामुळे अपूश्य, शोषित, पिडीत वर्गाला विकास करण्यासाठी प्रेरणा प्राप्त झाली. व त्यांच्या कार्यकर्त्यांत वाढ होत गेली. सत्यशोधक समाजाच्या सभासदांची संख्या २३१ वरून ३१६ पर्यंत पोहचली आणि सत्यशोधक समाज अपूश्य, कनिष्ठ वर्गाला गुलामगिरी झुगारून देण्याचा संघटक मंच प्राप्त झाला.

निष्कर्ष:

सत्यशोधक समाजाने अपूश्य, बहुजन समाजाला ब्राम्हण्यव्यवस्थेपासून जागृत करण्याचे कार्य केले. प्राचीन साहित्याची वेद, पुराणे निर्मिती देवाने केलेली नसून माणसानेच केलेली आहे. भट, ब्राम्हणांनी आपल्या फायद्यासाठी रुढी, परंपरा निर्माण केल्या. देव आणि मानव यामधील स्वतःला मध्यस्थ दाखविले व अपूश्य समाजावर गुलामगिरी लादविली हे स्पष्ट करून दिले. जातीव्यवस्था, वर्णव्यवस्था इश्वराने निर्माण केलेली नसून ब्राम्हणी व्यवस्थेने केलेली आहे. ती दुर सारण्यासाठी शिक्षणाचा पुरस्कार केला व समाजामध्ये समता निर्माण करण्यासाठी कार्य केले. समाजाला जागृत करण्यासाठी नुसते भाषणे किंवा सभा घेतल्या नाहीत तर प्रत्यक्ष कृती करून दाखविली. शोषित, पिडीतांना मदत करण्याचे कार्य केले. स्त्री शिक्षणावर भर देवून १८४८ मध्ये मुलींची पहिली शाळा काढली. १८६३ मध्ये बालहत्या प्रतिबंधक गृहाची स्थापना केली, अपूश्यासाठी शाळा काढल्या त्याचबरोबर समाजसेवेचे सोंग करणा-यांना खडसाविण्याचेही कार्य केले. समाजसेवा करू इच्छिणा-यांना सहकार्यही केले. शेतकरी, कामगार यांच्या गुलामगिरीची खंत त्यांना असल्यामुळे त्यांनी आत्मियतेने कार्य केले. ज्या ठिकाणी जमेल त्या ठिकाणी जाऊन सभा आयोजित करून समाजाला जागृत करण्याचे कार्य केले. समाजातील प्रतिष्ठीत व्यक्तींनी या कार्यात सहकार्य करावे यासाठी प्रयत्न केले. अपूश्य, शेतकरी, कामगार यांच्या समस्या चवाट्यावर आणून त्यांच्या समस्या सोडविण्यावर भर दिला. वर्णभेद संपुष्टात आल्याशिवाय समस्या मिटणार नाही हे महात्मा फुले यांना माहित होते. त्यामुळे जातीव्यवस्था, वर्णव्यवस्था, धर्मातील मध्यस्थ किंवा पुरोहीतशाही, अनिष्ट रुढी, परंपरा यांना विरोध केला. व अपूश्य, बहुजन समाजाला जगण्याचा मार्ग दाखविला. गुलामगिरी समुळ नष्ट करण्याची अपूश्य, कनिष्ठ वर्गात प्रेरणा निर्माण केली.

संदर्भ ग्रंथ सुची

१. कौर धनंजय, महात्मा जोतीराव फुले, पॉप्युलर प्रकाशन, मुंबई, पाचवी आवृत्ती, २०१२ पृष्ठ क्र. १५८
२. कित्ता, पृष्ठ क्र. १५९
३. कित्ता, पृष्ठ क्र. १५९

४. कित्ता, पृष्ठ कं. १६०
५. डॉ. रामटेके बी. एम. अपृश्यता निवारणात सत्यशोधक समाजाचे योगदान, लोकशाही वार्ता, वृत्तपत्र लेख, दिनांक ०९ ऑक्टोबर २०१६, पृष्ठ कं. ८
६. कित्ता, पृष्ठ कं. ८
७. डॉ. जगताप वामनराव, फुलेच्या सत्यशोधक समाजाची केलेली वाताहत, लोकमत वृत्तपत्र लेख, दि. २३ सप्टेंबर २०१६ पृष्ठ कं. ४
८. कीर धनंजय, महात्मा जोतीराव फुले, पृष्ठ कं. १६४
९. कित्ता, पृष्ठ कं. १६६
१०. कित्ता, पृष्ठ कं. १७१
११. कित्ता, पृष्ठ कं. १७६
१२. कित्ता पृष्ठ कं. १७६
१३. डॉ. रामटेके बी. एम., अपृश्यता निवारणात सत्यशोधक समाजाचे योगदान, वृत्तपत्रलेख पृष्ठ कं. ८



Superhydrophobic PVC/SiO₂ Coating for Self-Cleaning Application

Rajaram S. Sutar, Prashant J. Kalel, Sanjay S. Latthe, Deepak A. Kumbhar, Smita S. Mahajan, Prashant P. Chikode, Swati S. Patil, Sunita S. Kadam, V. H. Gaikwad, Appasaheb K. Bhosale, Kishor Kumar Sadasivuni, Shanhu Liu,* and Ruimin Xing*

A lotus leaf like self-cleaning superhydrophobic coating has high demand in industrial applications. Such coatings are prepared by alternative dip and spray deposition techniques. A layer of polyvinyl chloride is applied on glass substrate by dip coating and then spray coated a suspension of hydrophobic silica nanoparticles at substrate temperature of 50 °C. This coating procedure is repeated for three times to achieve rough surface morphology which exhibits a water contact angle of $169 \pm 2^\circ$ and sliding angle of 6° . The superhydrophobic state of the coating is still preserved when water volume of 1.2 L is used to impact the water drops on coating surface. The stability of the wetting state of the coating is analyzed against the water jet, adhesive tape and sandpaper abrasion tests. The prepared superhydrophobic coating strongly repelled the muddy water suggesting its importance in self-cleaning applications.

which inspired to create artificial superhydrophobic surface by increasing surface roughness along with decreasing surface energy. Such superhydrophobic surfaces have numerous applications including self-cleaning, anti-corrosion, drag-reduction, oil-water separation, and etc.^[3–8] So far, SiO₂, TiO₂, ZnO, Al₂O₃, candle soot and various polymers have been used to fabricate self-cleaning superhydrophobic coatings.^[9–14] Among them, polymer/SiO₂ nanocomposite is a promising in preparation of self-cleaning superhydrophobic coatings.^[15,16]

The self-cleaning property of superhydrophobic coatings has attracted significant interest in industrial applications. Recently, Latthe et al. have applied suspension of hydrophobic SiO₂ nanoparticles

(NPs) on different types of substrates including body of motorcycle, building wall, mini boat, solar cell panel, window glass, cotton shirt, fabric shoes, cellulose paper, metal, wood, sponges, plastic, and marble which revealed high water repellency and excellent self-cleaning property.^[17] Many reports are available on the preparation of superhydrophobic polyvinyl chloride (PVC) thin films using ethanol.^[18–20] Seyfi et al. have drop casted a mixture of PVC, Ag₃PO₄, and ethanol on thermoplastic

1. Introduction

Lotus leaf is a perfect model of self-cleaning superhydrophobic surface with specific combination of surface chemistry (surface energy) and surface topography (surface roughness).^[1,2] A low surface energy hierarchical surface structure of lotus leaf surface revealed unusual wettability (water contact angle (WCA) greater than 150° and sliding angle less than 10°)

R. S. Sutar, P. J. Kalel, S. S. Latthe, S. Liu, R. Xing
Self-cleaning Research Laboratory
Department of Physics
Raje Ramrao College
Jath
Affiliated to Shivaji University
Kolhapur, Maharashtra 416404, India
E-mail: liushanhu@vip.henu.edu.cn; rmxing@henu.edu.cn

S. S. Latthe, A. K. Bhosale
Henan Key Laboratory of Polyoxometalate Chemistry
Henan Joint International Research Laboratory of Environmental
Pollution Control Materials
College of Chemistry and Chemical Engineering
Henan University
Kaifeng 475004 P. R. China

D. A. Kumbhar
Department of Chemistry
Raje Ramrao College
Jath Maharashtra 416404, India

DOI: 10.1002/masy.202000034

S. S. Mahajan, P. P. Chikode
Department of Physics
Jaysingpur College
Jaysingpur Maharashtra 416404, India

S. S. Patil
Department of Physics
ACS College
Palus Maharashtra 416404, India

S. S. Kadam
Department of Physics
KNP College
Walwa Maharashtra 416404, India

V. H. Gaikwad
School of Chemistry
MIT World Peace University, Kothrud
Pune Maharashtra 416404, India

K. K. Sadasivuni
Center for Advanced Materials
Qatar University
Doha 2713 Qatar

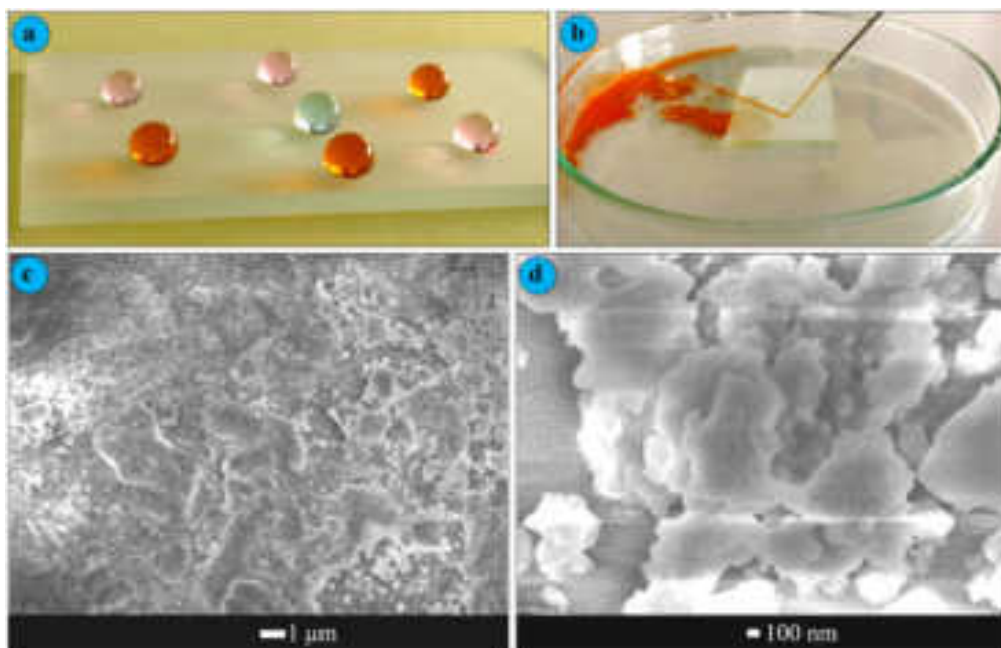


Figure 1. a) Optical photograph of color water drop on superhydrophobic coating, b) the image of water jet impacting on coating, c and d) different magnification SEM images of superhydrophobic coating.

polyurethane (TPU) substrate and achieved antibacterial superhydrophobic surface.^[21] The as prepared superhydrophobic TPU surface showed WCA $\approx 156^\circ$ and SA $\approx 2^\circ$ with self-cleaning performance. Also, Guo et al.^[15] have reported that water drops rolled off immediately on the coating prepared by casting of polymer (PVC, PMMA, and PE) and SiO₂ NPs composite on various substrates like copper, aluminum, stainless steel, silicon, glass and filter paper. Rivero et al.^[22] have prepared superhydrophobic surface by depositing ZnO NPs incorporated polystyrene (PS) and PVC polymeric solution on aluminum alloy substrate using the electrospinning technique. Yuan et al.^[23] have obtained lotus-leaf-like superhydrophobic PVC film by casting PVC solution on negative template of PDMS. Other than this, Zhang et al.^[24] have obtained superhydrophobic coating by pouring PVC/SiO₂ mixture on negative template of PDMS and reported that superhydrophobicity depends on weight percentage of SiO₂ particles in PVC. Chen et al.^[25] have prepared water-repellent SiO₂/polymer (PS and PVC) composite coating without any surface chemical modification by spin coating. The amount of hydrophobic SiO₂ NPs in PVC or PS affects the surface roughness and hence the wettability of the coating.

Herein, we have prepared superhydrophobic surface on glass by dip coating followed by spray coating method. The hydrophobic SiO₂ NPs were prepared by sol-gel technique. A thin layer of PVC was applied on glass substrate by dip coating and dried at room temperature. After that, a suspension of SiO₂ NPs in hexane was sprayed on PVC coated glass substrate at substrate temperature of 50 °C. The superhydrophobic coating was obtained by applying multiple alternative layers of PVC and SiO₂ NPs on glass substrate.

2. Result and Discussion

2.1. Surface Microstructure and Wettability

The multiple layers of PVC/SiO₂ were applied on glass substrate to obtain desired surface roughness which is the main requirement of extreme water repellency. **Figure 1c** represents the surface microstructure of three bilayer of PVC/SiO₂ coating, where the aggregated SiO₂ NPs were distributed on the PVC layer. The PVC layer can help SiO₂ NPs to adhere firmly on the coating surface. The aggregation of SiO₂ NPs is not uniform and the grain sizes from 5 μm to 100 nm were observed (**Figure 1d**). These different size scale grains provide hierarchical surface morphology. Nearly similar surface morphology was reported for the PVC/SiO₂ nanocomposite coating prepared by spin coat technique.^[25] This hierarchical surface morphology tends to trap small air pockets in the rough voids and hence a water drop can sit on the air-solid composite structure with minimum contact to the solid fraction of the surface. A water drop can only touch a small solid fraction of the coating, as the trapped air pushes away the water drops and not allowing the water drops to wet the inner portion of a rough surface. As shown in the **Figure 1a**, the water drops hardly stay on the three bilayer of PVC/SiO₂ superhydrophobic coating. Every water drop takes spherical shape at different positions on the coating surface confirming the uniform deposition of PVC/SiO₂ on the substrate. The superhydrophobic coating was appeared opaque due to the presence of micrometer scaled grains which allows scattering of the visible light. Also the water jet was impacted on the superhydrophobic coating which rebounds off the surface quickly after impacting (**Figure 1b**). The trapped air in the rough surface resists the water jet to invade the

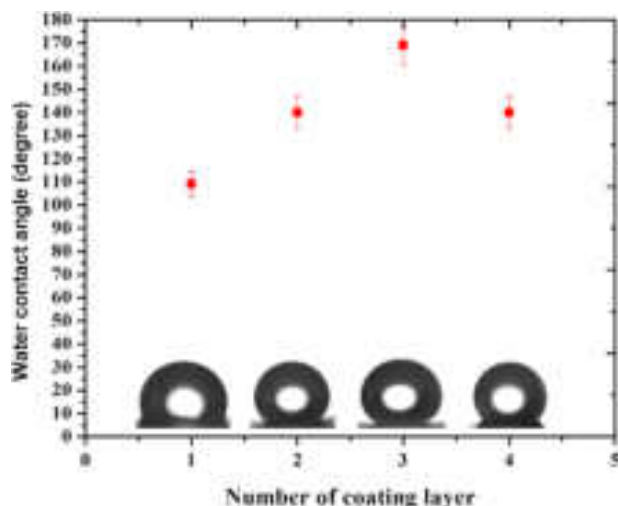


Figure 2. The variation of water contact angle with layer of polyvinyl chloride and SiO_2 particles.

rough structure. Also water jet rebounding confirms the robustness of the coating.

A systematic study was performed on the dependence of numbers of bilayers on the wettability of the coating (**Figure 2**). A first bilayer coating exhibited a WCA of $110 \pm 5^\circ$ confirming hydrophobic nature of the coating. The surface roughness of the coating is quite low to trap the air pockets and hence the wettability falls in the Wenzel's state^[26] where the solid fraction of the coating was partially wetted by the water drops. Though the WCA increased to $140 \pm 6^\circ$ with considerable decrease in solid-liquid contact area in case of two bilayer coating, the wettability was still in the Wenzel's wetting state. The WCA of $169 \pm 7^\circ$ and SA of 6° was observed for three bilayer coating confirming superhydrophobicity in Cassie-Baxter's wetting state.^[27] A water drop floats on the layer of air having minimum contact with solid fraction of the coating surface and hence readily roll off the surface. For next bilayer coatings, the WCA tends to decrease as a result of increase in thickness which creates visible cracks in the coatings during evaporation of solvent.

2.2. Durability Tests

The mechanical durability of superhydrophobic coating can be evaluated by water jet and water drop impact, sand paper abrasion and adhesive tape peeling test.^[28] Here, the water jet was developed by 15 mL syringe. The water jet was immediately spread on uncoated glass slide due to smooth surface structure with hydrophilic nature. On the other hand, the water jet bounced off the superhydrophobic coating as shown in **Figure 1b**. The air trapped hierarchical structure strongly avoids pinning of water jet on the surface.^[5,29] The wettability of the coating was checked after water jet impact study and the coating showed no change in its superhydrophobic property confirming its robustness. Water drop impact test was carried out by adjusting the distance between superhydrophobic coating and tip of tap about 10 cm as shown in schematic (**Figure 3a**). Nearly 2 L of water was dropped on the superhydrophobic coating inclined at 30° with drop falling rate

of 90 drops min^{-1} . The effect of water drop impact on the wetting properties of the superhydrophobic coating was estimated. The superhydrophobic state of the coating was intact for the impact of 1.2 L of the water as a result of stable air pockets in the rough microstructure of the coating which avoids water drop penetration inside the coating structure. However, the trapped air starts to evacuate from the rough structure and also the rough structure might have partly ruined due to continuous impact of water drops and as a result, WCA decreased to less than 140° for impacting 2.0 L of water (**Figure 3b**).

The adhesive tape peeling test was carried by using Cellotape No.405 having adhesiveness of 3.93 N/10 mm. A tape was applied firmly on the superhydrophobic coating with the help of 200 g weighted disk rolling back and forth on it (**Figure 4a**).^[28] After slowly peeling off the tape, some amount of the coating material was observed stacked on the adhesive tape; however, the coating showed the WCA of 165° (**Figure 4b**). The superhydrophobicity of the coating was found intact for two cycles of adhesive tape test, and then the WCA decreased to 80° for five cycles of adhesive tape test confirming the exhaustive loss of PVC/ SiO_2 from the coating (**Figure 4c**).

In large scale applications, superhydrophobic coatings can be damaged by scratch, rubbing and finger contact. To sustain the hierarchical micro/nanostructure and low surface energy of superhydrophobic coating under mechanical abrasion is one of the important issue. Here, the mechanical abrasion test was performed using sandpaper grit no. 400. The schematic of sandpaper abrasion process is illustrated in **Figure 5a**. A weight (100 g) was placed on superhydrophobic coating and dragged for 10 cm length on sandpaper at the average speed of 0.5 cm sec^{-1} . The effect of abrasion distance on the wettability of the superhydrophobic coating was studied (**Figure 5b**). The wettability of the coating was found in the superhydrophobic state for dragging the coating for nearly 30 cm on the sandpaper which confirms no significant loss in the surface roughness of the coating. However, the WCA decreased to 93° for dragging the coating for 60 cm on sandpaper confirming substantial damage to the coating.

2.3. Self-Cleaning Property

High water repellent property of the surface with low water sliding angle helps to keep the surface clean like a lotus leaf. In open air, many solid surfaces are contaminated by various types of dust particles. On superhydrophobic surface, spherical shaped water drop roll away easily by collecting dust particles, performing self-cleaning ability. The self-cleaning ability of the prepared superhydrophobic coating was tested by muddy water. The muddy water was prepared by dispersing fine particles of soil in water. This muddy water was poured on the superhydrophobic coating. In the process of pouring muddy water, it eventually get repelled off the superhydrophobic coating (**Figure 6a–c**). After pouring 50 mL of muddy water, surface becomes clean similar to lotus leaf (**Figure 6c**). This indicates prepared superhydrophobic coating was highly water repellent with excellent self-cleaning property.

3. Conclusions

We have used a conventional dip and spray coating techniques to prepare superhydrophobic coating by applying consecutive layers

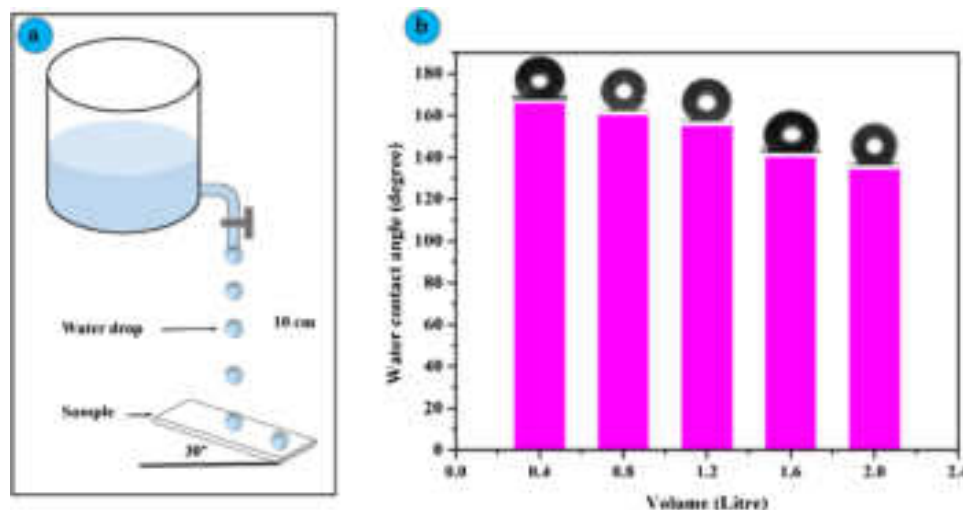


Figure 3. a) A schematic of water drop impact test, b) the effect of water drop impact on wettability of the superhydrophobic coating.

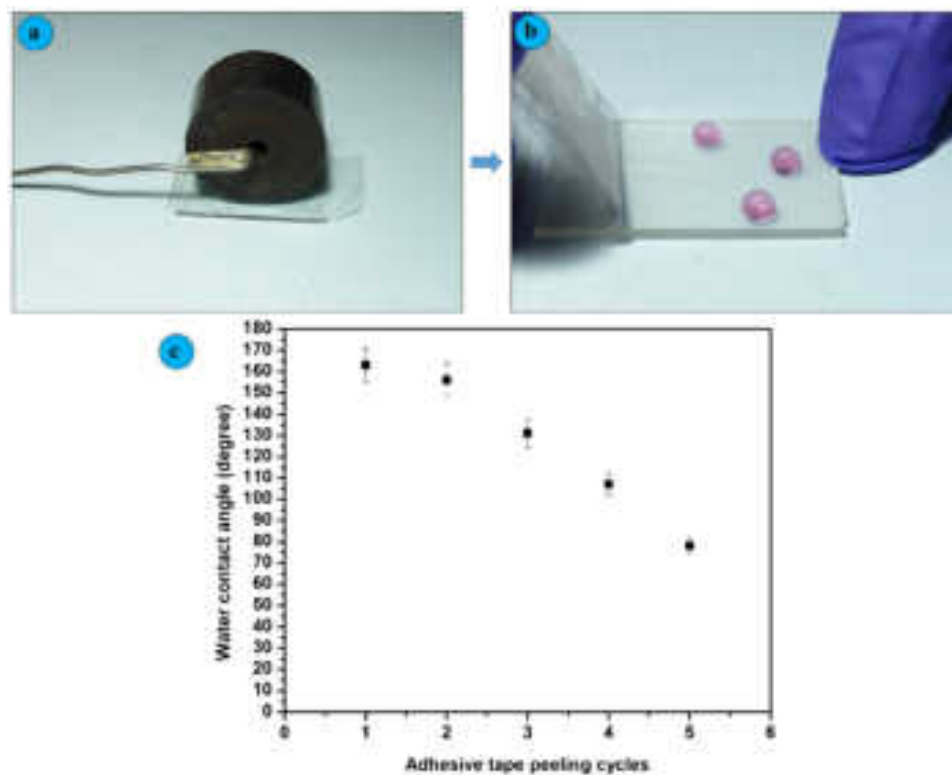


Figure 4. a) Rolling of 200 g weighted disc on adhesive tape placed on coating, b) adhesive tape peeling off and c) effect of adhesive tape peeling cycles on the wettability of the superhydrophobic coating.

of PVC and hydrophobic SiO₂ NPs on glass substrate. The hierarchical rough microstructure with different scaled grains of SiO₂ NPs was observed. The self-cleaning superhydrophobic coating with WCA of 169 ± 2° and sliding angle of 6° was achieved by applying three bilayers of alternate PVC followed by hydrophobic SiO₂ NPs. The water jet bouncing off the surface indicates the air pockets trapped in dual scale rough structure. After dripping the

water of volume 1.2 L, the water drop impacted coating showed invariable wettability. The superhydrophobic coatings were moderately stable against adhesive tape and sandpaper abrasion tests. Future practical applications of these coating can be found in windshields of vehicles, solar cell panels and windows of buildings, if their transparency and mechanical stability could be further enhanced.

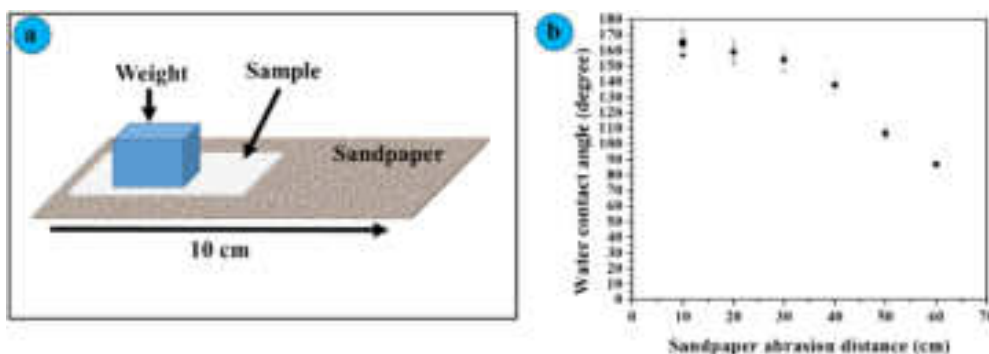


Figure 5. a) Schematic of sandpaper abrasion test and b) the variation of water contact angle with sandpaper abrasion distance.



Figure 6. a-c) Self-cleaning behavior of superhydrophobic coating.

4. Experimental Section

Materials: Methyltrimethoxysilane (MTMS) and PVC were purchased from Sigma-Aldrich, USA. Ethanol, methanol, ammonia solution, tetrahydrofuron (THF) and hexane were bought from Spectrochem PVT. LTD., India. Micro-Glass slides ($75 \times 25 \times 1.35$ mm) were obtained from Blue star, Polar Industrial Corporation, India.

Synthesis of Hydrophobic SiO_2 NPs: The hydrophobic SiO_2 NPs were synthesized using sol-gel method reported in literature.^[30] The mixture of 2 mL MTMS, 20 mL methanol and 4 mL distilled water was stirred for 20 min. After that ammonia solution was added dropwise and kept for stirring for 30 min. The prepared gel was aged for overnight and dried at 80°C for 5 h. The dried gel was grinded well using mortar and pestle to obtain fine powder of silica particles.

Preparation of Superhydrophobic Coating: At first, the glass substrates were ultrasonically cleaned with distilled water and ethanol for 30 min and dried at room temperature. The cleaned glass substrate was dipped in the PVC solution for 30 s. The solution was prepared by dissolving 100 mg PVC powder in 10 mL THF using magnetic stirrer (200 rpm for 30 min). A thin layer of PVC deposited glass substrate was dried at room temperature. A suspension of SiO_2 NPs (100 mg) was prepared by dispersing in 10 mL hexane and sprayed on PVC deposited glass substrate at substrate temperature of 50°C . Finally PVC/ SiO_2 deposited glass substrate was annealed at 100°C for 1 h. In this way, one bilayer of PVC/ SiO_2 was applied on glass substrate. This procedure was repeated to deposit two, three and four bilayers of PVC/ SiO_2 on glass substrate.

Characterizations: The wettability of prepared coatings was evaluated by measuring WCA and sliding angle (SA) using contact angle meter (HO-IAD-CAM-01, Holmarc Opto-Mechatronics Pvt. Ltd. India). The surface morphology of coating was characterized by field emission scanning electron microscopy (FESEM, JEOL, JSM-7610F, Japan). The water jet impact test was carried out by using 15 mL syringe. For water drop impact test, the coated glass substrate was kept at 30° inclination and water drops were dropped from the height of 10 cm. The mechanical stability of the coating was checked by adhesive tape peeling and sandpaper abrasion test. The self-cleaning behavior was observed by pouring muddy water on the coating.

Acknowledgements

This work was financially supported by DST-INSPIRE Faculty Scheme, Department of Science and Technology (DST), Govt. of India. [DST/INSPIRE/04/2015/000281]. SSL acknowledges financial assistance from the Henan University, Kaifeng, P. R. China. The authors greatly appreciate the support of the National Natural Science Foundation of China (21950410531).

Conflict of Interest

The authors declare no conflict of interest.

Keywords

PVC, roughness, superhydrophobic and self-cleaning, wetting

- [1] L. Feng, S. Li, Y. Li, H. Li, L. Zhang, J. Zhai, Y. Song, B. Liu, L. Jiang, D. Zhu, *Adv. Mater.* **2002**, *14*, 1857.
- [2] C. Neinhuis, W. Barthlott, *Annal. Botany* **1997**, *79*, 667.
- [3] S. P. Dalawai, M. A. S. Aly, S. S. Latthe, R. Xing, R. S. Sutar, S. Nagappan, C.-S. Ha, K. K. Sadasivuni, S. Liu, *Prog. Org. Coat.* **2020**, *138*, 105381.
- [4] S. S. Latthe, V. S. Kodag, R. S. Sutar, A. K. Bhosale, S. Nagappan, C.-S. Ha, K. K. Sadasivuni, S. R. Kural, S. Liu, R. Xing, *Mater. Chem. Phys.* **2020**, *243*, 122634.
- [5] S. S. Latthe, P. Sudhagar, A. Devadoss, A. M. Kumar, S. Liu, C. Terashima, K. Nakataa, A. Fujishima, *J. Mater. Chem. A* **2015**, *3*, 14263.
- [6] S. S. Latthe, et al. *Superhydrophobic Polymer Coatings*, **2019**, Elsevier. pp. 339–356.
- [7] S. S. Latthe, R. S. Sutar, A. K. Bhosale, S. Nagappan, C.-S. Ha, K. K. Sadasivuni, S. Liu, R. Xing, *Prog. Org. Coat.* **2019**, *137*, 105373.

- [8] S. S. Latthe, R. S. Sutar, T. B. Shinde, S. B. Pawar, T. M. Khot, A. K. Bhosale, K. K. Sadasivuni, R. Xing, L. Mao, S. Liu, *ACS Appl. Nano Mater.* **2019**, 2, 799.
- [9] A. B. Gurav, S. S. Latthe, R. S. Vhatkar, J. G. Lee, D. Y. Kim, J. J. Park, S. S. Yoon, *Ceram. Int.* **2014**, 40, 7151.
- [10] A. M. Kokare, et al. *AIP Conference Proceedings*, AIP Publishing. **2018**.
- [11] S. S. Latthe, et al. *Green Chemistry for Surface Coatings, Inks and Adhesives*. **2019**. pp. 92–119.
- [12] R. S. Sutar, et al. *Macromolecular Symposia*, **2019**. Wiley Online Library.
- [13] S. Bilgin, M. Isik, E. Yilgor, *Polymer* **2012**, 53, 1180.
- [14] H. Yoon, H. Kim, S. S. Latthe, M.-W. Kim, S. Al-Deyabd, S. S. Yoon, *J. Mater. Chem. A* **2015**, 3, 11403.
- [15] Y. Guo, Q. Wang, *Appl. Surf. Sci.* **2010**, 257, 33.
- [16] P. G. Pawar, R. Xing, R. C. Kambale, A. M. Kumar, S. Liu, S. S. Latthe, *Prog. Org. Coat.* **2017**, 105, 235.
- [17] S. S. Latthe, R. S. Sutar, V. S. Kodag, A. K. Bhosale, A. M. Kumar, K. K. Sadasivuni, R. Xing, S. Liu, *Prog. Org. Coat.* **2019**, 128, 52.
- [18] H. Chen, Z. Yuan, J. Zhang, Y. Liu, K. Li, D. Zhao, S. Li, P. Shi, J. Tang, *J. Porous Mater.* **2009**, 16, 447.
- [19] Z. Khoryani, J. Seyfi, M. Nekoei, *Appl. Surf. Sci.* **2018**, 428, 933.
- [20] X. Li, G. Chen, Y. Ma, L. Feng, H. Zhao, L. Jiang, F. Wang, *Polymer* **2006**, 47, 506.
- [21] J. Seyfi, M. Panahi-Sarmad, A. OraeiGhodousi, V. Goodarzi, H. A. Khonakdar, A. Asefnejad, S. Shojaei, *Colloids Surf., B* **2019**, 183, 110438.
- [22] P. J. Rivero, A. Iribarren, S. Larumbe, J. F. Palacio, R. Rodríguez, *Coatings* **2019**, 9, 367.
- [23] Z. Yuan, H. Chen, J. Zhang, *Appl. Surf. Sci.* **2008**, 254, 1593.
- [24] X. Zhang, B. Ding, R. Cheng, S. C. Dixon, Y. Lu, *Adv. Sci.* **2018**, 5, 1700520.
- [25] H. Chen, X. Zhang, P. Zhang, Z. Zhang, *Appl. Surf. Sci.* **2012**, 261, 628.
- [26] R. N. Wenzel, *Ind. Eng. Chem.* **1936**, 28, 988.
- [27] A. Cassie, S. Baxter, *Trans. Faraday Soc.* **1944**, 40, 546.
- [28] N. Wang, D. Xiong, S. Pan, K. Wang, Y. Shi, Y. Deng, *New J. Chem.* **2017**, 41, 1846.
- [29] A. Kibar, H. Karabay, K. Yigit, I. Ucar, H. Erbil, *Exp. Fluids* **2010**, 49, 1135.
- [30] S. S. Latthe, A. V. Rao, *Surf. Coat. Technol.* **2012**, 207, 489.



SHIVAJI UNIVERSITY, KOLHAPUR

Volume-49 Issue-2 (July, 2023)

ISSN-Science-0250-5347

Estd. 1962
"A++" Accredited by NAAC (2021)
with CGPA 3.52



Journal of Shivaji University SCIENCE & TECHNOLOGY

(Peer Reviewed Journal)

Journal of Shivaji University: Science and Technology
Volume-49, Issue-2 (July, 2023)

INDEX

Sr. No.	Title of Research Article with Name of Author/s	Page No.
1.	Silica Coated Superhydrophobic Materials for Oil-Water Separation Application-A Short Review Rajesh B. Sawant, Mehejbin R. Mujawar, Amol B. Pandhare, Sanjay S. Latthe, Ankush M. Sargar, Raghunath K. Mane, Shivaji R. Kulal	1
2.	Green Synthesis of NiO Nanoparticles from <i>Partheniumhysterophorus</i> Plant Sneha V. Koparde, Akanksha G. Kolekar, Shital S. Shendage, Aniket H. Sawat, Snehal D. Patil, Snehal S. Patil, Reshma B. Darekar, Amol B. Pandhare, Vijay S. Ghodake, Samadhan P. Pawar, Govind B. Kolekar	12
3.	Microwave-Assisted Synthesis of Pyrazole and Its Hybrid Scaffolds as Potent Biological and Pharmacological Agents: A Short Review Pravin. R. Kharade, Uttam. B. Chougale, Satish. S. Kadam, Kiran. N. Patil, Prakash S. Pawar, Savita. S. Desai	19
4.	Biosynthesis and Catalytic Transformation of Ruthenium Nanoparticles in Biomimetic Applications Komal M. Dhumal, Anita R. Mali	36
5.	Third Generation Solar Cells: Importance and Measurements Techniques for knowing Photovoltaic Device Performance Prakash S. Pawar, Pramod A. Koyale, Amol B. Pandhare, Vijay S. Ghodake, Swapnijit V. Mulik, Ankita K. Dhukate, Waleed Dabdoub, Sagar D. Delekar	48
6.	Aggregation-Induced Emission, Mechanochromism, and Applications of Tetraphenylethene/Triphenylamine-based Molecules Kishor. S. Jagadhane, Govind. B. Kolekar, Prasad. M. Swami, Prashant. V. Anbhule	68
7.	Greener and Environmentally Benign Methodologies for the Synthesis of Bis(indolyl)methane and Trisindolines Aboli C. Sapkal, Suraj R. Attar, Santosh B. Kamble	75

Silica Coated Superhydrophobic Materials for Oil-Water Separation Application-A Short Review

Rajesh B. Sawant^{a,*}, Mehejbin R. Mujawar^a, Amol B. Pandhare^{b,f},
Sanjay S. Latthe^c, Ankush M. Sargar^d,
Raghunath K. Mane^e, Shivaji R. Kulal^{a*}

^aDepartment of Chemistry, Raje Ramrao Mahavidyalaya, Jath, Sangli 416 404 (MS) India.

^bDepartment of Chemistry, Shivaji University, Kolhapur 416 004 (MS) India.

^cDepartment of Physics, Vivekanand College, Kolhapur 416 003 (MS) India.

^dDepartment of Chemistry, Bharati Vidyapeeth's Dr. Patangrao Kadam Mahavidyalaya, Sangli 416 416 (MS) India.

^e Department of Chemistry, Smt. Kusumtai Rajarambhapu Patil Kanya Mahavidyalaya, Islampur, Sangli 416 409 (MS) India.

^fDepartment of Chemistry, M.H. Shinde Mahavidyalaya, Tisangi, Gaganbavda, Kolhapur 416 206 (MS) India.

*Corresponding authors: srkulal@gmail.com and rbsawant2@gmail.com

ABSTRACT

Contamination like oil and organic pollutants in water has a severe problem for aquatic life and human being; it is a need to preserve their life. These contaminants are added due to frequent oil spill accidents, and industrial as well as domestic waste. There is a need to develop methods and materials that show excellent ability to separate the oil and organic contaminants from water. Recently, superhydrophobic coated sponges, metals mesh, membranes and porous materials plays crucial role to separate oil and water from oil-water mixture. The micro and nonporous of substrate facilitate to enter liquid into it and superhydrophobic/superoleophilic property of substrate surface resist water and allows oil to enter into porous substrate. The various surface modified organic metal oxide nanoparticles are used to develop superhydrophobic surface on porous substrate. Among them SiO₂ nanoparticles is promising material to preparation of superhydrophobic surface because of their cost-effectiveness and easy synthesis techniques. This review focused on silica modified porous sponge, metal meshes, membrane and porous substrate for scalable oil-water separation application.

KEYWORDS

Superhydrophobic, Oil-water separation, porous sponge, Metal mesh and membrane.

.....

1. INTRODUCTION

Frequent oil spill accidents and industrial chemical spills occurred in the sea and the ecosystem damage; such incidents have spread to impact the offspring. Therefore, considerable surviving organisms for several years after the impact [1-2] efforts have been done to remove oil and organic solvents from water. Due to this extensive current research is focussed on the development of superhydrophobic materials for effective oil-water separation. To achieve superhydrophobic sponges, surface roughness and low surface energy materials play a crucial role. The various methods such as dip coating, immersion, spray coating; hydrothermal methods, chemical vapor deposition, surface etching, solvothermal methods, layer-by-layer assembly and electrochemical treatment describe a modification of sponges for oil and water separation [3-4]. At present, traditional technologies, including in situ burning [5], bioremediation [6], chemical dispersant methods [7], skimming [8], and the use of sorbents [9] are used to clean up spilled oils or organic pollutants. However, many of these strategies involve energy intensive and slow processes, have low clean-up capacities or create secondary pollution during the clean-up process, restricting their widespread practical applications [10-11]. To realize the hierarchical structures on different material surfaces, a series of strategies, such as sol-gel coating [12], chemical vapor deposition [13], plasma etching [14], template processing [15], lithographic patterning [16], etc. have been adopted [17]. The superhydrophobic surfaces on which water achieves water contact angle higher than 150° and sliding angle less than 5° are attracting minds of researchers due to their efficient oil-water separation efficiency [18].

Recently, Wu et al. [19] have prepared a highly flexible superhydrophobic PDMS@F-SiO₂ coating for self-cleaning and drag-reduction applications via a two-step spraying of PDMS and F-SiO₂ nanoparticles. However, it is common that inorganic particles normally tend to agglomerate due to the interparticle forces stemming from the Vander Waals, capillary and electrostatic forces [20], which leads to phase separation during the fabrication process and tends to diminish the quality of the coating through cracks or weak adhesive to the substrates. Gao et al. [21] prepared PVDF/SiO₂ coated superhydrophobic porous membranes using a spraying technique. These membranes could be used to separate the oil-water mixtures but are not applicable to surfactant stabilized water-in-oil emulsions because of their large pore sizes. Li et al. [22] prepared the hydrophobic CS by incomplete combustion of hydrocarbons from the middle of a candle flame. The PU sponge was immersed in the solution of CS, SiO₂ and PU resin to achieve stable superhydrophobicity. The CS-SiO₂-PU sponge was shown excellent oil-water separation efficiency. The CS-SiO₂-PU sponge showed excellent oil-water separation efficiency from hot water, acidic solutions, alkaline solutions and salt solutions.

In this review, the sophisticated, facile and low-cost methods for fabrication of superhydrophobic porous material for oil-water separation application are discussed.

The 3D sponges, metal meshes, membrane and cotton fabrics are used as substrate for scalable oil-water separation application.

2. SUPERHYDROPHOBIC SURFACES FOR OIL-WATER SEPARATION

2.1 Superhydrophobic SiO₂ Modified Sponges for Oil-Water Separation

Zhang et al. [23] have fabricated the superhydrophobic surface by using VTMS and SiO₂ via immersion method. The schematic of preparation of superhydrophobic sponge is shown in **Figure-1**. It was shown a water contact angle of 153.2° and roll-on angle of 4.8°. The oil is quickly absorbed by superhydrophobic sponge which can be shown the superoleophilic property of a modified sponge. The IR peak at 1078 cm⁻¹ shows the presence of the O-Si-O bond present in the material. It was showing the high separation efficiency of about 99.5%. It exhibited good saturated adsorption properties exceeding 70 g/g for all oils. It shows outstanding characteristics of superhydrophobic sponge such as high porosity, small pore size and ultra-light mass. After 20 cycles, it was found that the adsorption ability of the modified melamine sponge for different oils decreased slightly. It shows outstanding stability and reusable performance. The modified sponge maintains an 89% of recovery rate even after 20 cycles. This method was used to prepare porosity and provides storage space for the adsorption of oil pollution. This superhydrophobic composite melamine sponge provided the possibility for practical application of oil-water separation.

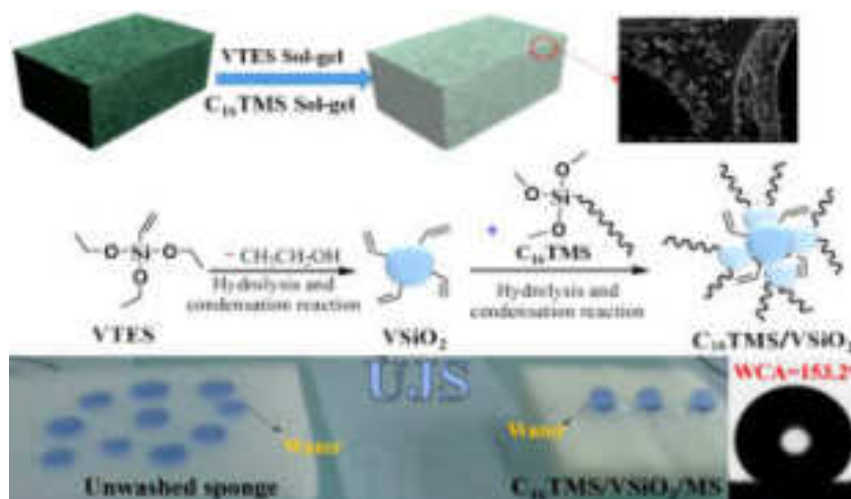


Figure-1. Schematic illustration of the preparation of superhydrophobic sponge. Images reprinted from [23], with permission from Elsevier, Journal of Chemical Engineering, Copyright 2020.

Liu et al. [24]. have fabricated a superhydrophobic sponge and polyester coated with SiO₂-DTMS through an entrapment method. The **Figure-2** reveals the fabrication process of superhydrophobic sponge and polyester. The SiO₂ particles were introduced by growth on the substrate through the polymerization process, followed by the addition of DTMS as an adhesive, leading to a homogeneous and dense superhydrophobic membrane. The modified sponge was shown the water contact angle up to 172° indicating the water repellence was superior. This superhydrophobic sample had good hydrophobic stability even in acidic condition and it can show efficient oil-water separation. The amount of the absorbed oil was about 43-65 times of sponge own weight can be shown that the evaluation of the mass based on absorbed surface tension, density, viscosity of absorbed liquids. It exhibits stable oil storage under harsh environmental conditions in oil-water separation. The performance remained constant after 100 recycling sequences, even in a harsh water environment.

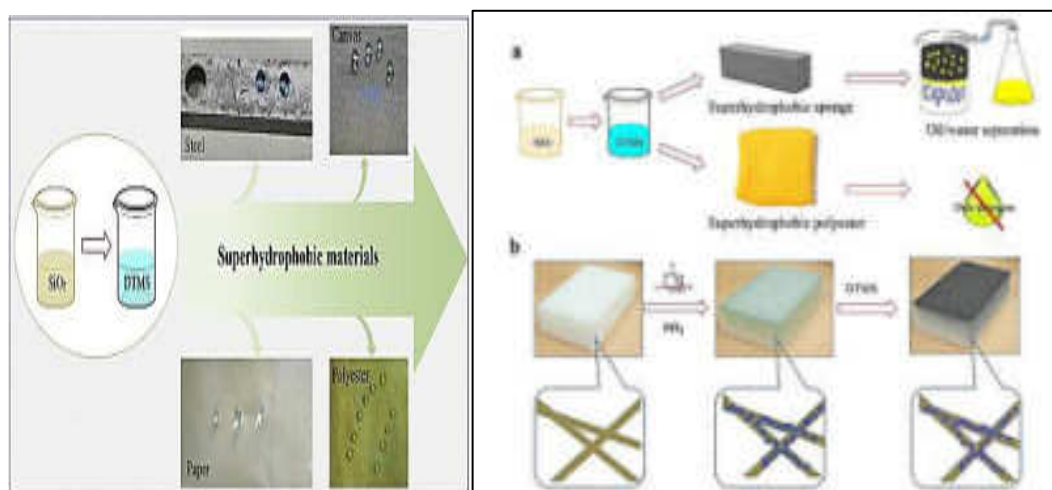


Figure-2. Schematic illustration of the fabrication of a modified sponge and polyester. Images reprinted from [24], with permission from Elsevier, Copyright 2019.

2.2 Superhydrophobic SiO₂ Modified Metal Meshes for Oil-Water Separation

Zhao et al. [25] have prepared superhydrophobic SiO₂ nanoparticles by improved Stober method and then coated on a chemically etched stainless steel mesh by one step dipping method to fabricate superhydrophobic SiO₂ coated stainless steel mesh. The preparation process was simple, efficient and environmentally friendly. The experimental procedure is shown in **Figure-3**. It shows excellent oil-water separation properties, which can be widely used in oil-water separation. It was showing 153.3° water contact angle and 0° oil contact angle. The oil-water separation efficiency was nearly 96% by using this modified stainless-steel mesh.

The separation efficiencies were obtained repeatedly even after 40 cycles without noticeable deterioration. The superhydrophobic modified stainless steel mesh shows stability, durability and reusability. The SiO₂ modified stainless steel mesh indicates good material for treating real oil-polluted water in different practical applications. This method shows high performance, oil-water separation in a short time and repeatedly in comparison with earlier works.

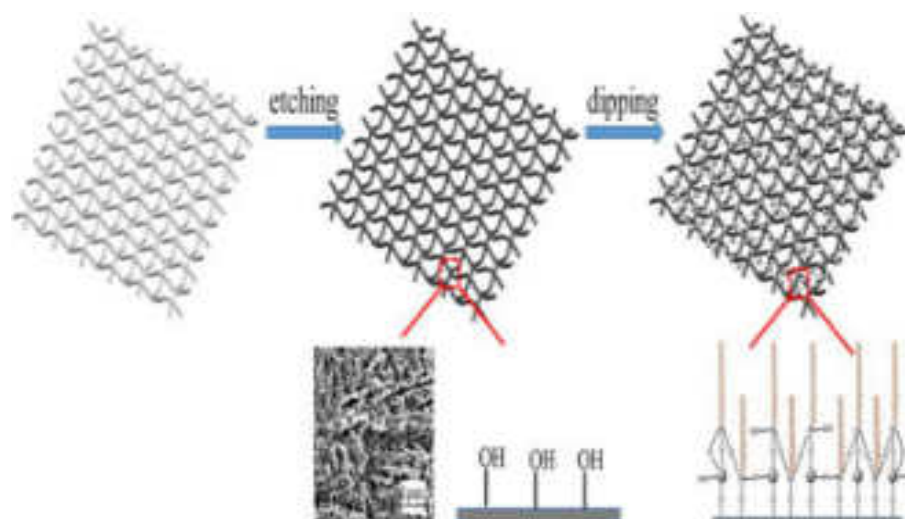


Figure-3. Schematic illustration of the preparation of FSSM. Images reprinted from [25], with permission from Elsevier, Copyright 2019.

Xiong et al. [26] have prepared SiO₂ nanoparticles by an improved modified method by using TEOS and then coated on a stainless-steel mesh by spraying method to fabricate SiO₂ coated stainless steel mesh. The **Figure-4** illustrates schematic of preparation of the superhydrophobic stainless-steel mesh. The preparation process was efficient, simple and environmentally friendly. It shows good mechanical properties and oil/water separation performance. It was showing 156.4° oil contact angle and less than 10° water contact angles. The oil-water separation efficiency was nearly 98.69% by using this modified stainless-steel mesh. The separation efficiencies obtained repeatedly even after 20 cycles without noticeable deterioration. The superhydrophobic modified stainless steel mesh shows stability, durability and reusability. The SiO₂ modified stainless steel mesh indicates excellent material for treating oil-polluted water in different practical applications. This method shows an easily scaled-up preparation process, stable mechanical and thermal properties, offering new prospects for efficient oil/water separation in comparison with earlier works.

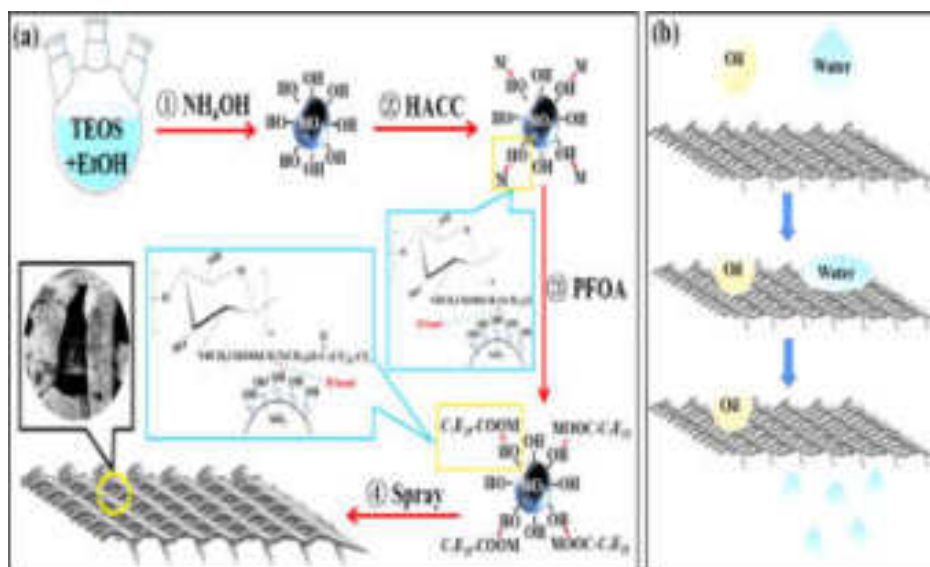


Figure-4 (a) Schematic diagram illustrating the fabrication of air superhydrophilic-superoleophobic membrane. (b) Scheme of the oil/water separation. Images reprinted from [26], with permission from Elsevier, Journal of Colloid and Interface Science, Copyright 2021.

2.3 Superhydrophobic SiO₂ Modified Porous Substrates for Oil-Water Separation

Gu et al. [27] have prepared a membrane (SiO₂/Polyurethane membrane) with porous structure rough surface and hydrophobic epidermis by surface modification to construct a rough surface and low-energy epidermis on electrospun polyurethane membrane. The schematic of experimental procedure is shown in **Figure-5**. The superhydrophobic SiO₂/PU porous membrane prepared by chemical modification on the membrane shows a water contact angle 152.1° and low sliding angle 6°. This membrane was used for different aqueous solutions like water, saline solution, alkaline solution acidic solution. The porous membrane shows low air permeability and high-water vapor transmission rate. It shown good oil absorption capacity. It was shows high oil-water separation efficiency above 98.5%. The absorption capacity of the modified membrane does not show severe degradation even after 30 separation cycles which indicating a highly stable absorption performance of modified membrane. It provided the potential for eater repellent, breathable applications and oil-water separation in long term use.

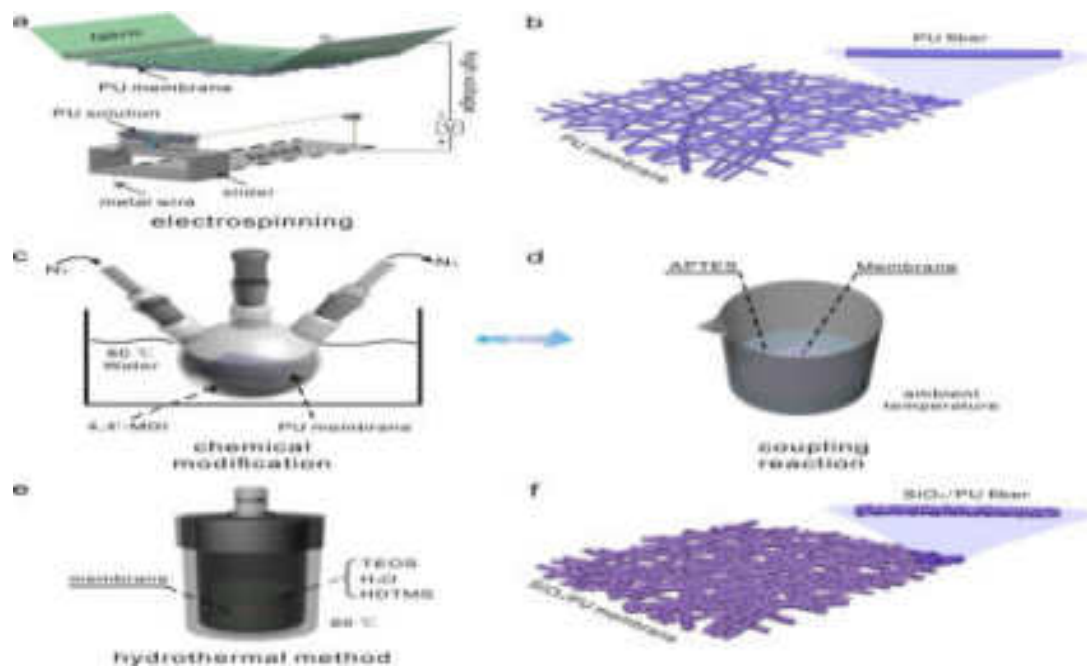


Figure-5. The preparation scheme of superhydrophobic SiO₂/PU membrane. Images reprinted from [27], with permission from Elsevier, App. Sur. Sci. Copyright 2019.

Wei and their co-researchers [28] have obtained the SiO₂ nanoparticles from ethanol and ammonium hydroxide with TEOS. The SiO₂ nanoparticles were isolated by repeated centrifugation in ethanol followed by drying in a vacuum oven. A facile strategy was presented to prepare silica particles grafting. The sprayable solution be easily applied to different porous substrates to achieve durable superhydrophobic coating (schematically shown in **Figure-6**). The surface shows a separation efficiency of 98.8% dealing with oil-water mixture. The oil absorption capacity of immersion coated polyurethane sponge was demonstrated higher than pristine polyurethane sponge an 39 g/g which would benefit from the presence of lipophilic PSAN and higher porosity contributed by abundant nanoparticles. After 10 cycles of abrasion test the remained separation efficiency of above 96% and water contact angle of 151° confirmed the mechanical durability. This sponge shows facile, environmentally friendly, mechanical and chemical stability.

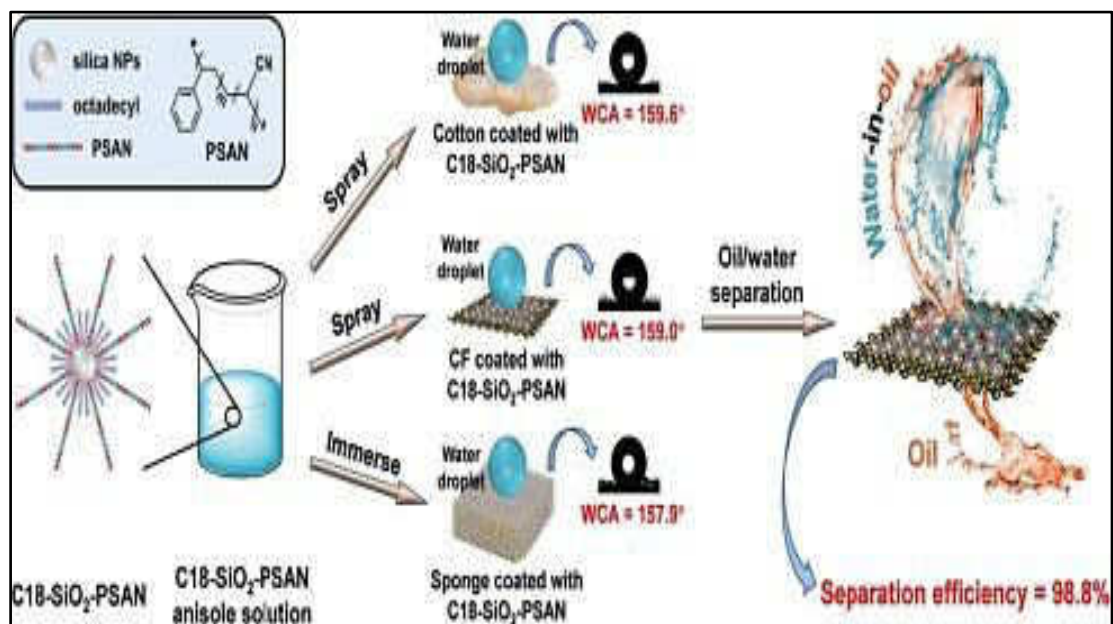


Figure-6. Schematic illustration of preparation of modified superhydrophobic surface for oil-water separation. Images reprinted from [28], with permission from Elsevier, Copyright 2021.

2.4 Superhydrophobic SiO₂- Polymer Composite Based Membrane for Oil-Water Separation

Li and their co-workers [29] have fabricated the superhydrophobic surface by using PVDF and SiO₂ via sugar template method. The schematic of preparation method is shown **Figure-7**. It was shown in a water contact angle of 155.68° and roll-on angle of nearly 6°. The prepared superhydrophobic PVDF oil/water separation membrane had low water adhesion performance and ultrahigh separation efficiency of nearly 99.98% in terms of the oil purity in the filtrate. The recycling performance over 20 cycles. This membrane has excellent potential for use in various large-scale practical applications, water purification treatment and the separation of commercially relevant emulsions. The possibility of large-scale production and low manufacturing costs of this sponge is very promising advantages for oil-water separation application.

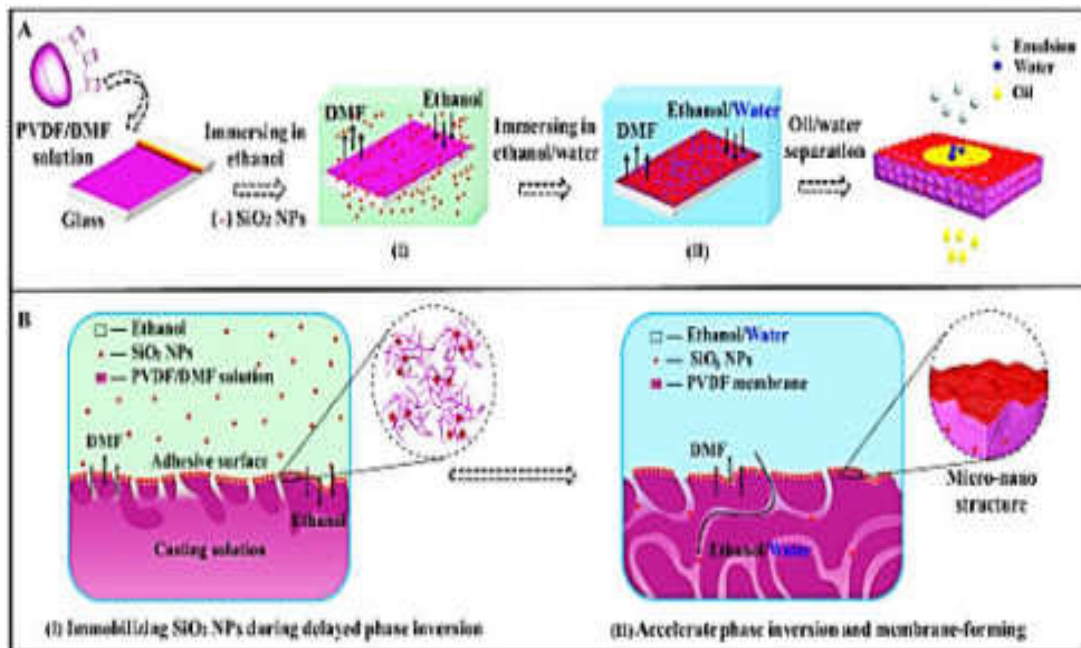


Figure-7. Schematic illustration (A) and structural evolution (B) for the formation of adhesive-free superhydrophobic SiO₂ nanoparticles decorated PVDF oil-water separation membranes [29]. Images reprinted from [29], with permission from Elsevier, Copyright 2018.

Bai et al. [30] have coated cotton fabric by sol-gel processed SiO₂. The as-prepared fabric was immersed in the solution of FeCl₃, thiophene and CH₂Cl₂ solution. Then, the modified fabric was washed with ethanol and dry it. **Figure-8** reveals the experimental procedure of preparation of superhydrophobic fabric. The modified fabric shows water contact angles above 160°. The strongest peak at 1050 cm⁻¹ belongs to the Si-O bond indicating that SiO₂ particles have been coated on the cotton fabric. The modified cotton fabric shows outstanding resistance to ultraviolet irradiation, high temperature, low temperature, organic solvent, immersion and excellent durability even after 8 months. The as-prepared fabric was showing the capability in various chemical exposures. It was showing good anti-dirt and anti-frost properties. The modified superhydrophobic cotton fabric was used as filter membrane for the gravity driven oil-water separation with high separation efficiency and excellent reusability. By using, this modified cotton fabric, both immiscible and emulsified oil-water mixtures could be separated. The efficient oil-water separation was also achieved under harsh conditions. The superhydrophobic fabric shows potential for the fast, coat-effective treatment of oil spill accidents and industrial oily sewage.

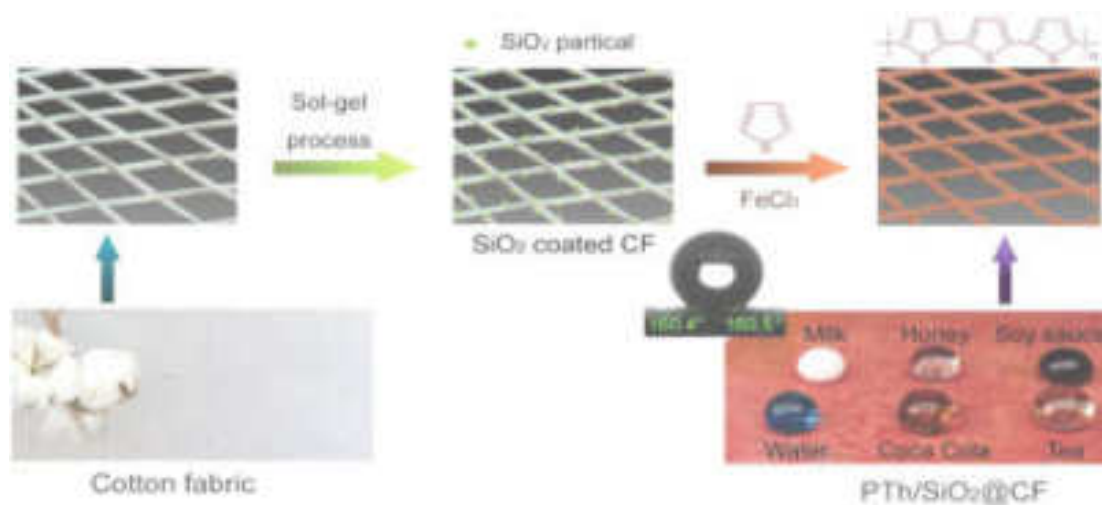


Figure-8. Schematic Illustration of the fabrication process of the PTh/SiO₂@CF [30]. Images reprinted from [30], with permission from Elsevier, Adv. Mater. Interfaces, Copyright 2021.

3. CONCLUSION

This review highlights, SiO₂ nanoparticles are unique, their fabrication requires little control of external parameters such as surface modification. It is very beneficial economically, facile and straightforward to synthesize. The SiO₂ nanoparticles coated sponge/mesh has been developed by using SiO₂ nanoparticles and different polymers. The absorption/separation investigation demonstrates that, the SiO₂ surface is highly efficient and stable in absorbing a wide range of oil and organic solvents. It can be believed that, the SiO₂ coated superhydrophobic materials are very useful for oil-water separation. It shows various tremendous results with SiO₂-polymer composite in various mechanical conditions. Hence this review is helpful to upcoming researchers to develop highly scalable superhydrophobic surfaces for efficient oil-water separation applications.

ACKNOWLEDGEMENT

This work was supported by Department of Chemistry and Department of Physics, Raje Ramrao Mahavidyalaya, Jath. We also acknowledge Prof. (Dr.) Suresh S. Patil, Principal, Raje Ramrao Mahavidyalaya, Jath.

REFERENCES

1. Alsbaiee A., Smith B. J., Xiao L., Ling Y., Helbling D. E. & Dichtel W. R. (2016) *Nature*, 529, 190-194.
2. Li Y., Zhang Z., Ge B., Men X., and Xue Q. (2016) *Green Chemistry*, 18, 5266-5272.
3. Ma Q., Cheng H., Fane A. G., Wang R., and Zhang H. (2016) *Small*, 12, 2186-2202.
4. Li L., Li B., Dong J., and Zhang J. (2016) *Journal of Materials Chemistry A*, 4, 13677–13725.
5. Yuan J., Liu X., Akbulut O., Hu J., Sui S. L., Kong J., Stellacci F. (2008) *Nature*, 3, 332-337.
6. Broje V., Keller A. A. (2006) *Environmental Science & Technology*, 40, 7914-7918.
7. Wu Z. Y., Li C., Liang H. W., Zhang Y. N., Wang X., Chen J. F. & Yu S. H. (2014) *Science Reports*, 4, 4079-4091.
8. Keshavarz A., Zilouei H., Abdol maleki A. (2015) *Journal of Environmental Management*, 157, 279-286.
9. Wang Z., Xu Y., Liu Y., Shao L. (2015) *Journal of Materials Chemistry A*, 3, 266-273.
10. Li J., Zhao Z., Kang R., Zhang Y., Lv W., Li M., Jia R., Luo L. (2017) *Journal of Sol-Gel Science and Technology*, 3, 817–826.
11. Keshavarz A., Zilouei H., Abdolmaleki A., Asadinezhad A. (2015) *Journal of Environmental Management*, 157, 279-286.
12. Sam E. K., Sam D. K., Lv X., Liu B., Xiao X., Gong S., Yu W., Chen J., Liu J. (2019) *Chemical Engineering Journal*, 19, 1103-1109.
13. Jin M., Feng X., Xi J., Zhai J., Cho K., Feng L., Jiang L. (2005) *Macromolecular Rapid Communications*, 26, 1805-1818.
14. Yao T., Zhang Y., Xiao Y., Zhao P., Guo L., Yang H., Li F. (2016) *Journal of Molecular Liquids*, 218, 611–614.
15. Gao Y., Zhou Y. S., Xiong W., Wang M., Fan L., Golgir H. R., Jiang L., Hou W., Huang X., Jiang L., Silvain J. F., Lu Y. F. (2014) *ACS Applied Materials & Interfaces*, 6, 5924–5929.
16. Erbil H. Y., Demirel A. L., Avcı Y., Mert O. (2003) *Science*, 299, 1377-1391.

17. Fard A. K., Mckay G., Manawi Y., Malaibari Z., Hussien M. A. (2016) *Chemsphere*, 164, 142-155.
18. Ren G., Song Y., Li X., Zhou Y., Zhang Z., Zhu X. (2018) *Applied Surface Science*, 428, 520-525.
19. Gu J., Xiao P., Chen J., Liu F., Huang Y., Li G., Zhang J., Chen T. (2014) *Journal of Materials Chemistry A*, 2, 15268–15272.
20. Li J., Kang R., Tang X., She H., Yang Y., Zha F. (2016) *Nanoscale*, 8, 7638–7645.
21. Gao Y., Zhou Y. S., Xiong W., Wang M., Fan L., Golgir H. R., Jiang L., Hou W., Huang X., Jiang L., Silvain J. F., Lu Y. F. (2014) *ACS Applied Materials & Interfaces*, 6, 5924–5929.
22. Li J., Zhao Z., Kang R., Zhang Y., Li M. (2017) *Journal of Sol-Gel Science and Technology*, 83, 817-826.
23. Zhang R., Zhou Z., Ge W., Lu Y., Liu T., Yang W., Dai J. (2020) *Chinese Journal of Chemical Engineering*, 5, 30292-30310.
24. Liu D., Yu Y., Chen X., Zheng Y. (2017) *RSC Advances*, 7, 12908–12915.
25. Zhao L., Du Z., Tai X., Ma Y. (2021) *Colloids and Surfaces A: Physicochemical and Engineering Aspects*, 623, 126404-126415.
26. Xiong W., Li L., Qiao F., Chen J., Chen Z., Zhou X., Hu K., Zhao X., Xie Y. (2021) *Journal of Colloid and Interface Science*, 6, 118–126.
27. Gu J., Xiao P., Chen J., Liu F., Huang Y., Li G., Zhang J., Chen T. (2014) *Journal of Materials Chemistry A*, 2, 15268–15272.
28. Wei C., Deu F., Lin L., An Z., He Y., Chen X., Chen L., Zhao Y. (2018) *Journal of Membrane Science*, 555, 220-228.
29. Li X., Wang X., Yuan Y., Wu M., Wu Q., Liu J., Yang J., Zhang J. (2021) *European Polymer Journal*, 159, 110729-110742.
30. Bai W., Lin H., Chen K., Zeng R., Lin Y., Xu Y. (2021) *Advanced Materials Interfaces*, 254, 725-740.

PAPER



Cite this: *New J. Chem.*, 2023, 47, 20171

Pd(OAc)₂/[C₁₈-DABCO-C₁₈]2Br: a nano palladium catalytic approach for Mizoroki–Heck and Suzuki–Miyaura coupling reactions in water†

Archana Rajmane,^a Chunilal Pawara,^{bc} Sumit Kamble,^{bc} Utkarsh More,^d **Suresh Patil^e** and Arjun Kumbhar^{✉*}^a

In this study, we have successfully used a new catalytic system comprised of Pd(OAc)₂ and [C₁₈-DABCO-C₁₈]2Br (at a ratio of 1:10 mol%) for various types of C–C coupling reactions, including Mizoroki–Heck and Suzuki–Miyaura, in a water-based medium. The catalyst system was analyzed using TEM, which revealed the presence of stable Pd nanoparticles (PdNPs) that were less than 5 nm in size and were protected by a “Gemini” type [C₁₈-DABCO-C₁₈]2Br surfactant. X-ray photoelectron spectroscopy (XPS) was used to determine the oxidation states of Pd. Our optimization study revealed that this catalytic system was highly effective in coupling a range of aryl iodides and bromides with different olefins and aryl boronic acids. The reactions were performed at 80–100 °C with K₂CO₃ as a base, and high yields ranging from 80–93% were obtained. The selectivity of all reactions was excellent, ranging from 92–100%, with a turnover number (TON) of 79.72–92.77 and a turnover frequency (TOF) of 0.997–2.059 min⁻¹. Similarly, the catalytic system was highly efficient in Suzuki–Miyaura coupling of various aryl iodides and bromides with different aryl boronic acids, yielding good to excellent product yields (87–95%) with TON of 86.86–94.84 and TOF of 1.996–3.161 min⁻¹. One of the advantages of this catalyst is that it can be recycled at least three times for Mizoroki–Heck coupling reactions with only a marginal loss in product yields.

Received 28th August 2023,
Accepted 12th October 2023

DOI: 10.1039/d3nj04035f

rsc.li/njc

Introduction

Palladium-catalyzed coupling reactions have become an important tool in organic synthesis, using various aryl and vinyl halides and nucleophiles.¹ Two prominent examples of these reactions are the Mizoroki–Heck olefination² and Suzuki–Miyaura coupling, which enable the construction of carbon–carbon bonds and the synthesis of new biomolecules, compounds of theoretical interest, and organic polymers.³ Traditionally, these reactions have relied on the use of various phosphines,⁴ amines,⁵ carbenes,⁶ and mixed ligands,⁷ but

recent research has focused on alternative ligand systems, especially those that address issues of toxicity and sensitivity to air and moisture. These new methods rely on environmentally friendly protocols, particularly those involving water as a solvent.⁸ Water is widely used in biological as well as many chemical processes,⁹ but water-mediated cross-coupling reactions usually require the use of toxic and air-sensitive phosphine ligands.^{10,11} As a result, there is a need for phosphine-free catalysts, which can require low reaction temperatures.¹²

Therefore, the development of a new catalytic system for use in organic reactions that is economically and environmentally viable, works at low temperatures, and is free of phosphine and ligands in aqueous media has garnered a lot of attention. Although organic reactions in water have several advantages,¹³ the limited aqueous solubility of most neutral organic substrates and functional group reactivity are the main obstacles to water as a solvent in organic reactions. By adding common additives such as tetrabutylammonium bromide, various polymers, and ionic liquids, along with different Pd sources,¹⁴ remarkable rate enhancements have been achieved in these cross-coupling reactions of aryl iodides in various solvents. The formation of colloid PdNPs under the so-called ‘Jeffery conditions’¹⁵ takes place in these catalytic systems. Despite all these

^a Department of Chemistry, Vivekanad College, Kolhapur (Empowered Autonomous), (Affiliated to Shivaji University, Kolhapur), Maharashtra, 416312, India.

E-mail: arjun22win@rediffmail.com

^b Department of Salt and Marine Chemicals, CSIR-Central Salt and Marine Chemicals Research Institute, Bhavnagar, Gujarat 364002, India

^c Academy of Scientific and Innovative Research (AcSIR), Ghaziabad 201002, Uttar Pradesh, India

^d Department of Chemistry, Shivaji University, Kolhapur, Maharashtra, India

^e Department of Chemistry, P. D. V. P. College, Tasgaon, Maharashtra, 416312, India

† Electronic supplementary information (ESI) available. See DOI: <https://doi.org/10.1039/d3nj04035f>

developments, many of the catalytic systems still require polar aprotic solvents. Recently, Pd catalysts in the form of Pd dispersions containing PdNPs have gained increasing scientific interest for many cross-coupling reactions.¹⁶ It is generally observed that the activity and selectivity of PdNPs depend on the size and morphology of PdNPs, as they show superior catalytic properties and do not require ligands. Various strategies have been reported regarding the development of nano-catalysts in water for Mizoroki–Heck and Suzuki–Miyaura coupling reactions under environmentally sustainable conditions.¹⁷

In our previous research, we studied the development of Pd-catalyzed coupling reactions using various Pd catalysts in different reaction media, including biosurfactants and hydrotropes.¹⁸ In this study, we present a new catalytic system comprising Pd(OAc)₂ and [C₁₈-DABCO-C₁₈]2Br (1:10 mol%) that demonstrates outstanding efficiency and reusability in Mizoroki–Heck and Suzuki–Miyaura coupling reactions conducted in an aqueous medium. The Gemini-type surfactant [C₁₈-DABCO-C₁₈]2Br¹⁹ serves as a great stabilizing agent, allowing Pd(OAc)₂ to act as a source of Pd nanoparticles (PdNPs). This catalytic system facilitates the coupling of various aryl iodides and bromides with different nucleophiles, using K₂CO₃ as a base and operating at 80 °C. The reactions provide the desired products in good to excellent yields, exhibiting exceptional selectivity and short reaction times. We evaluated the stereoselectivity of the catalytic system by calculating *E/Z* ratios, confirming its favorable tendency towards the formation of the *E*-isomer (92–100%) in Mizoroki–Heck coupling reactions.

Results and discussion

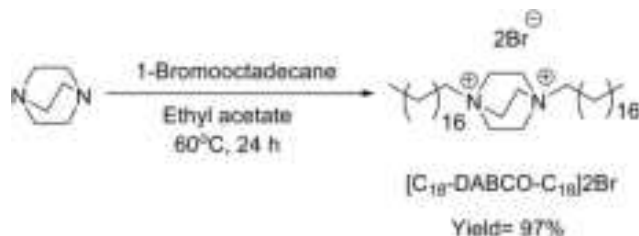
1. Synthesis of [C₁₈-DABCO-C₁₈]2Br

The diquaternization of the DABCO with 1-bromooctadecane in ethyl acetate at 60 °C provided about 97% yield of the [C₁₈-DABCO-C₁₈]2Br as reported in the literature procedure (Scheme 1).²⁰

The obtained DABCO salt could be easily soluble in water and various organic solvents like MeOH, CHCl₃, acetone, DMF, and DMSO, that further characterized and confirmed using ¹H NMR, ¹³C NMR, and HR-MS (Fig. 1).

2. Study of micellization behavior of prepared [C₁₈-DABCO-C₁₈]2Br in aqueous solution

The micellization behavior of the pure [C₁₈-DABCO-C₁₈]2Br in an aqueous solution was studied using conductivity and UV-absorption measurements.



Scheme 1 Synthesis of [C₁₈-DABCO-C₁₈]2Br.

(a) Conductivity measurements. The conductivity method provides reliable information regarding the micellization behavior of the surfactants before and after the formation of micelles. The concentration above which the surfactant changes its behavior in physical and spectral properties is known as critical micelle concentration (CMC).^{21a} In the current study, we measured the CMC of pure dimeric [C₁₈-DABCO-C₁₈]2Br in an aqueous solution. The graph for conductance measurements concerning the concentration of aqueous pure [C₁₈-DABCO-C₁₈]2Br at 298.15 K is shown in Fig. 2.

Conductance measurements based on the Onsager theory of electrolyte conductivity revealed a change in slope between the pre- and post-micellar regions, indicating the formation of micelles. The intersection point of the two straight lines representing the critical micelle concentration (CMC) of the surfactants was also observed.^{21b} The slope after reaching the CMC decreased, suggesting the presence of micelles. The determined CMC of pure [C₁₈-DABCO-C₁₈]2Br at 298.15 K was found to be 0.027 mM, which is in good agreement with the CMC of the dimeric surfactant [C₁₆-C₃-C₁₆] (0.025 mM). Notably, the CMC of the pure dimeric [C₁₈-DABCO-C₁₈]2Br was much lower than that of the single-chain [C₁₈-DABCO]Br surfactant (1.15 mM).^{22a} This significant difference in CMC values may be attributed to the increased surface activity and enhanced hydrophobic–hydrophobic interactions observed in dimeric surfactants.^{22b}

(b) UV-Vis absorption study. The dye-solubilization method is used for this study which works on the principle of the solution polarity. To study the micellar behavior of [C₁₈-DABCO-C₁₈]2Br in an aqueous solution we used methyl orange as an anionic dye (MO) for the UV-visible measurements due to the cationic nature of the surfactant.

The absorption spectra, obtained by plotting the absorbance *versus* wavelength, were recorded for aqueous solutions of MO dye with varying concentrations of [C₁₈-DABCO-C₁₈]2Br surfactant, as shown in Fig. 3. The absorption peak for pure MO dye (without the addition of surfactant) was observed at a wavelength of λ_{max} 465 nm. Upon increasing the concentration of the surfactant, a noticeable shift in the absorption peak towards shorter wavelengths (hypsochromic shift or higher frequency) was observed. This shift can be attributed to the association of dye molecules with surfactant monomers, leading to a decrease in the local polarity around the dye molecules. In the micellar pseudo-phase, the dye molecules become solubilized, resulting in a decrease in absorbance. In the presence of the surfactant, the λ_{max} for the methyl orange dye shifted from 465 nm to 370 nm. This shift suggests that the dye molecules are either solubilized or incorporated into the core of the surfactant molecules. Additionally, the intensity of the absorption peak decreases as the concentration of the surfactant is increased. This intensity reduction may be attributed to interactions between the surfactant and dye molecules, specifically hydrophobic–hydrophobic interactions occurring between the dye and surfactant molecules.

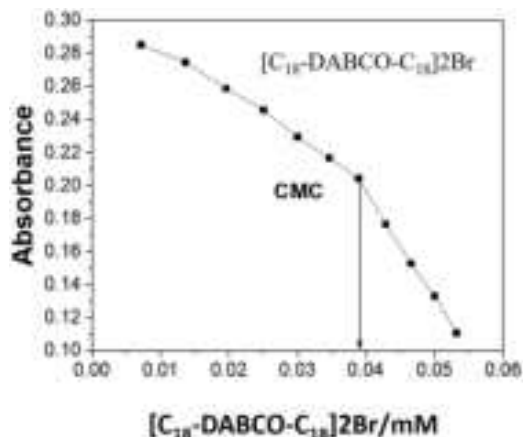


Fig. 4 Absorbance versus concentration of pure $[C_{18}\text{-DABCO-}C_{18}]2\text{Br}$ surfactants in aqueous solution at 298.15 K.

protected from the water, while the hydrophilic headgroups face the solvent, which makes the arrangement of surfactant molecules in the water a stable one. Micelles can effectively dissolve hydrophobic compounds, such as dye molecules, which results in a decrease in absorbance intensity. The micellization process is facilitated by the interactions between dye-surfactant and hydrophobic-hydrophobic compounds, which play significant roles in the formation and stability of micelles.

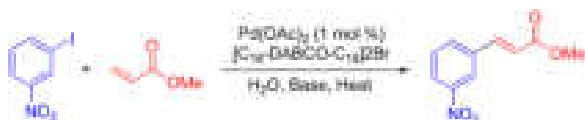
The CMC value by using the conductivity method is 0.025 mM and by UV-visible measurements is 0.039 mM. This may be due to that in UV-visible measurements we use methyl orange dye for CMC determination and due to the dye-surfactant interaction the CMC values are different by UV-visible measurements.

3. Applications of $\text{Pd}(\text{OAc})_2/[C_{18}\text{-DABCO-}C_{18}]2\text{Br}$

(a) Mizoroki-Heck coupling reactions. The Mizoroki-Heck reaction, which was discovered in the early 1970s,²⁴ is a highly effective catalytic tool for developing carbon-carbon bonds. It has remarkable versatility in accommodating various functional groups.²⁵

To optimize the reaction conditions, a model reaction was conducted using 3-nitroiodobenzene and methyl acrylate in the presence of a $\text{Pd}(\text{OAc})_2/[C_{18}\text{-DABCO-}C_{18}]2\text{Br}$ catalytic system in water. (Scheme 2).

We used a simple *in situ* method to prepare colloidal PdNPs. First, we suspended $\text{Pd}(\text{OAc})_2$ and $[C_{18}\text{-DABCO-}C_{18}]2\text{Br}$ in water and then reacted them with 3-nitroiodobenzene and methyl acrylate in the presence of K_2CO_3 as a base. Adding $\text{Pd}(\text{OAc})_2$ directly to water caused the formation of



Scheme 2 $\text{Pd}(\text{OAc})_2/[C_{18}\text{-DABCO-}C_{18}]2\text{Br}$ for the ligand-free Mizoroki-Heck coupling reaction.

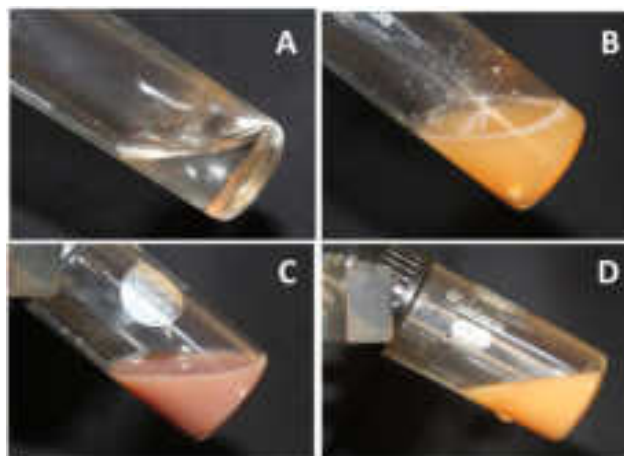


Fig. 5 Observations of reaction mixture: (A) $\text{Pd}(\text{OAc})_2$ in neat water (heterogeneous appearance); (B) $\text{Pd}(\text{OAc})_2/[C_{18}\text{-DABCO-}C_{18}]2\text{Br}$ in water; (C) reaction mixture at $t = 2$ min; and (D) aqueous phase containing catalyst after extraction of the product at $t = 45$ min.

heterogeneous phases, making it insoluble. However, combining 1 mol% $\text{Pd}(\text{OAc})_2$ with 10 mol% $[C_{18}\text{-DABCO-}C_{18}]2\text{Br}$ in water resulted in a stable dispersion with a yellow color (Fig. 5A and B). Stirring the reaction mixture at 100°C turned the solution into a wine-red color. This color change is likely due to the formation of colloidal PdNPs, stabilized by an excess of ammonium ions present in $[C_{18}\text{-DABCO-}C_{18}]2\text{Br}$, as shown in Fig. 5C.²⁶

The colloidal wine-red colored reaction mixture²⁷ was analyzed using TEM at various time intervals: (a) 2 minutes (Fig. 6A), (b) 30 minutes (Fig. 6B), and (c) 45 minutes (Fig. 6C) after the product was extracted. The TEM analysis clearly showed the uniform distribution of PdNPs, which had a particle size smaller than 5 nm.

The EDS spectrum of the PdNPs present in the reaction mixture after 2 min (Fig. 7) showed signals for Pd, which indicates the presence of substantial amounts of Pd in reaction mixture.

To study the change in oxidation states of Pd present in the reaction mixture the high-resolution XPS spectra (Fig. 8) of the Pd 3d were recorded after (a) 2 min, (b) 30 min, and (c) after extraction of the product (45 min) respectively. The XPS spectrum displayed two peaks with binding energies at 336.2 eV and 341.5 eV, corresponding to Pd 3d_{5/2} and Pd 3d_{3/2}. The spin-orbit coupling results in a binding energy (B.E) difference of 5.2 eV between the Pd 3d_{5/2} and 3d_{3/2} orbitals attributed to the spin-orbit interaction. The observed binding energy (B.E) values for Pd (336.2 eV) do not precisely correspond to the B.E value for Pd⁰ (335.1 eV), suggesting that the oxidation state of Pd falls within the range of 0 to +2 in all three samples.^{28,29}

The impact of the quantity of $[C_{18}\text{-DABCO-}C_{18}]2\text{Br}$ was examined in controlled experiments. No conversion was observed when the reaction was initiated without the use of $[C_{18}\text{-DABCO-}C_{18}]2\text{Br}$, even after extending the reaction time for 120 minutes (Table 1, entry 1). However, the addition of $[C_{18}\text{-DABCO-}C_{18}]2\text{Br}$ (1 to 10 mol%) resulted in a consistent

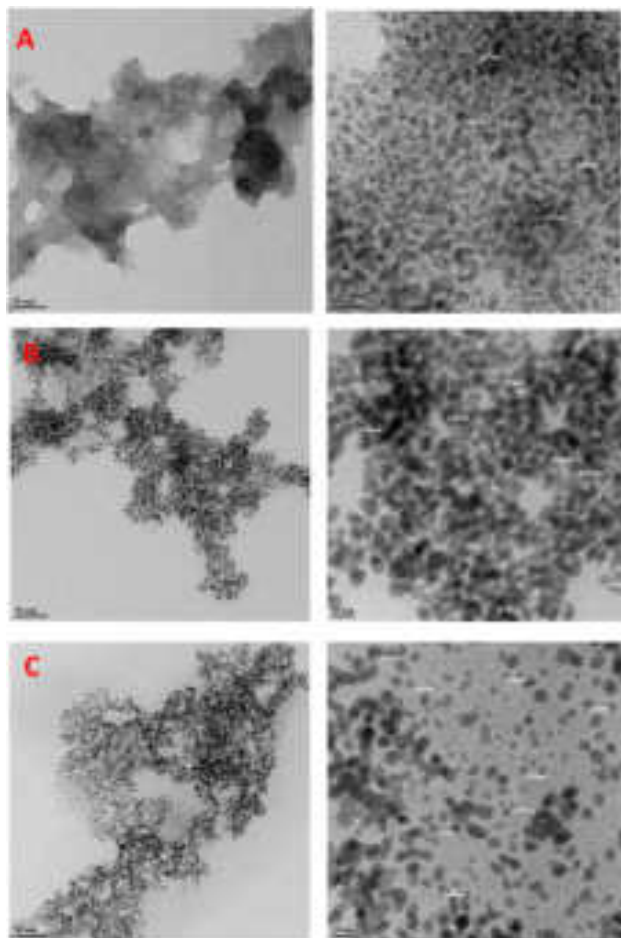


Fig. 6 TEM images of reaction mixture; (A) after 2 min, (B) after 30 min, and (C) after 45 min.

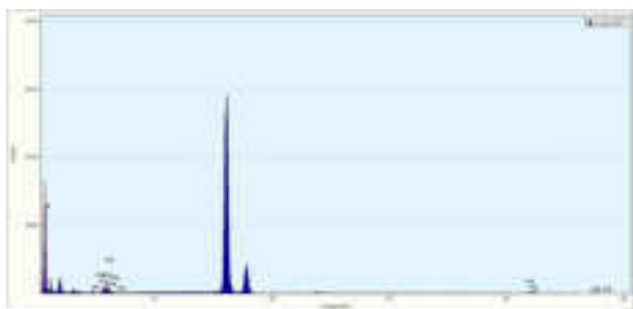


Fig. 7 EDX spectrum of reaction mixture after 2 min.

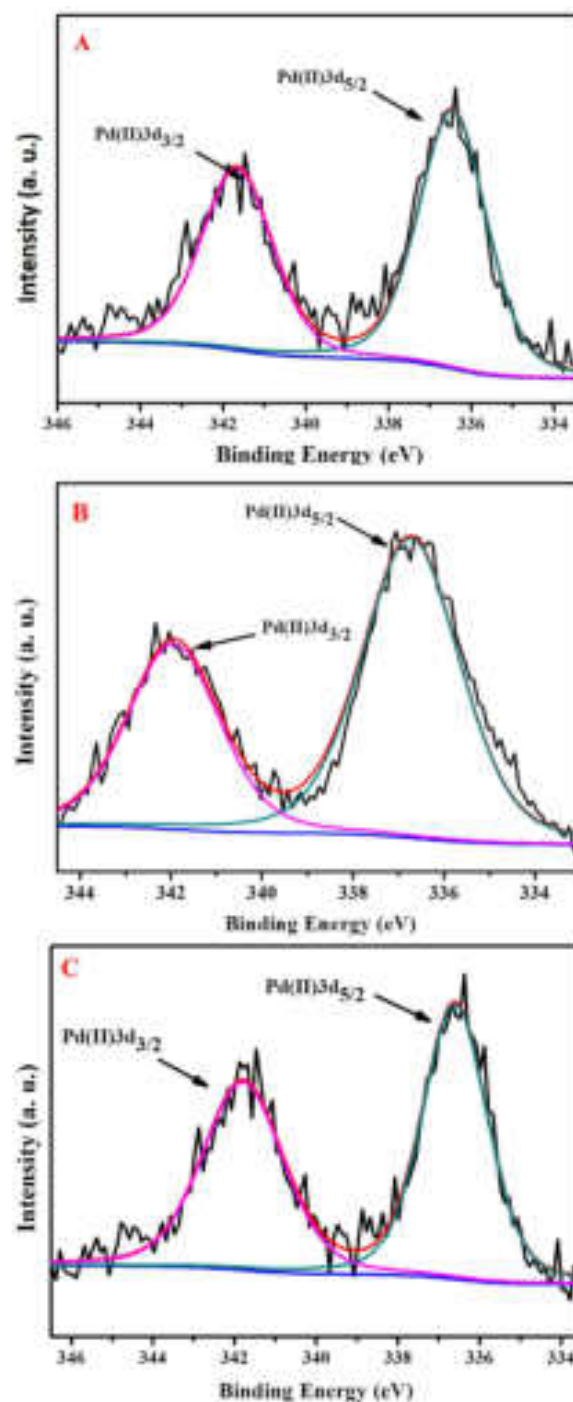


Fig. 8 XPS analysis of reaction mixture; (a) after 2 min, (b) after 30 min, and (c) after 45 min (extraction of product).

increase in the yield, up to 94% after 45 min (Table 1, entries 2–4). In general, using 10 mol% of $[\text{C}_{18}\text{-DABCO-C}_{18}]_2\text{Br}$ in pure water was adequate to achieve satisfactory conversions, while increasing the concentration to 15 mol% did not significantly improve the yield under otherwise identical conditions (Table 1, entry 5). Interestingly, the *trans* selectivity increased from 92% to 96% as the quantity of $[\text{C}_{18}\text{-DABCO-C}_{18}]_2\text{Br}$ increased from 1 mol% to 5 mol% (Table 1, entry 2 and 3),

but later increases in the quantity only marginally affected the selectivity (Table 1, entry 4 and 5).

Different bases and amounts of K_2CO_3 were tested in a model reaction. No product was observed when no base was used (Table 1, entry 6). The use of 1 mmol of K_2CO_3 gave the highest yield (Table 1, entry 4). Increasing the amount of K_2CO_3 did not improve the yield or reaction time (Table 1, entry 8). Among the tested bases, K_2CO_3 was the most effective in

Table 1 The effect of [C₁₈-DABCO-C₁₈]2Br and base in Mizoroki-Heck coupling reaction^a

Entry	[C ₁₈ -DABCO-C ₁₈]2Br (mol%)	Base (mmol)	Time (min)	Yield ^b (%)	TON	TOF (min ⁻¹)	Selectivity ^c (%)	
							<i>E</i>	<i>Z</i>
1	—	K ₂ CO ₃ (1.0)	45	Trace	—	—	—	—
2	1	K ₂ CO ₃ (1.0)	45	81	80.67	1.792	92	8
3	5	K ₂ CO ₃ (1.0)	45	81	80.67	1.792	96	4
4	10	K ₂ CO ₃ (1.0)	45	94	93.71	2.082	96	4
5	15	K ₂ CO ₃ (1.0)	45	94	93.71	2.082	97	3
6	10	Base-free	120	—	—	—	—	—
7	10	K ₂ CO ₃ (0.5)	120	45	44.92	0.374	94	6
8	10	K ₂ CO ₃ (1.5)	45	94	93.71	2.082	97	3
9	10	NaOAc (1.0)	120	56	55.55	0.462	96	4
10	10	KOH (1.0)	120	70	69.56	0.579	99	1

^a All the reactions were carried out using 3-nitro-iodobenzene (1.0 mmol), methyl acrylate (1.10 mmol), base (1–1.5 mmol), Pd(OAc)₂ (1 mol%), [C₁₈-DABCO-C₁₈]2Br (1–10 mol%) in water (5.0 mL) at 100 °C under air. ^b By HPLC. ^c By HPLC.

activating the reactant. However, NaOAc was highly inactive, resulting in only 46% conversion even after 120 minutes of reaction time (Table 1, entry 9). Although KOH showed a lower yield (70%) and longer reaction time (120 min), it exhibited the highest selectivity (99% *E*-isomer) (Table 1, entry 10). K₃PO₄ showed good yield (85%) but the lowest selectivity (89% *E*-isomer) among the tested bases (Table 1, entry 11).

In a study on Mizoroki-Heck coupling reactions,³⁰ the impact of temperature was investigated by maintaining the ratio of Pd(OAc)₂/[C₁₈-DABCO-C₁₈]2Br (1 : 10 mol%) constant with K₂CO₃ as a base in water at four different temperatures. The results showed that temperature played a crucial role in catalyst activation, as no reaction was observed at 60 and 80 °C (Table 2, entries 1 and 2). However, at 100 °C, an excellent conversion was achieved within 45 minutes (Table 2, entry 3). Further increasing the temperature to 120 °C did not result in significant improvements in yield or selectivity (Table 2, entry 4).

The impact of the amount of Pd(OAc)₂ was examined by maintaining the amount of [C₁₈-DABCO-C₁₈]2Br at 10 mol% and reaction temperature at 100 °C. The results showed that 1.0 mol% of Pd(OAc)₂ was highly efficient, providing almost complete conversion with consistent selectivity. Though the maximum Turnover Number (TON) 115.94 was obtained for 0.5 mol% Pd(OAc)₂ (Table 2, entries 5), 1 mol% Pd(OAc)₂ was found to be best in terms of product yield (Table 2, entries 3).

Thus, 1 mol% Pd(OAc)₂, 1 mmol K₂CO₃, and 10 mol% [C₁₈-DABCO-C₁₈]2Br in water at 100 °C is considered as optimum reaction condition for exploration of next study.

To showcase the versatility and wide applicability of the developed protocol, different aryl halides were subjected to coupling reactions with various acrylates under optimized reaction conditions. The reaction conditions were as follows: aryl halides (1.0 mmol), acrylates (1.1 mmol), K₂CO₃ (1.0 mmol), Pd(OAc)₂ (1 mol%), [C₁₈-DABCO-C₁₈]2Br (10 mol%), water (5.0 mL) at 100 °C. The desired products were obtained with good to excellent yields and showed high selectivity. Substrates that contained electron-donating groups exhibited slightly lower yields, which could be improved by extending the reaction time.³¹ Additionally, it was observed that aryl iodides displayed higher reactivity compared to aryl bromides. Notably, the para-substituted compounds consistently yielded almost 100% of the *E*-isomer (Table 3).

(b) Suzuki-Miyaura coupling reactions. The successful outcomes achieved through Mizoroki-Heck coupling reactions motivated us to extend the applicability of the developed catalytic system to Suzuki-Miyaura coupling reactions. Suzuki-Miyaura coupling reaction is widely known for its efficiency in carbon-carbon bond formation and compatibility with different functional groups.^{32,33} In this study, we explored the potential of our protocol for the Suzuki-Miyaura coupling reaction using various aryl iodides and bromides with aryl boronic acids in an aqueous environment with K₂CO₃ as the

Table 2 The influence of temperature and amount of catalyst in the Mizoroki-Heck reaction^a

Entry	Pd(OAc) ₂ (mol%)	Temperature (°C)	Time (min)	Yield ^b (%)	TON	TOF	Selectivity ^c (%)	
							<i>E</i>	<i>Z</i>
1	1.0	60	120	—	—	—	—	—
2	1.0	80	120	—	—	—	—	—
3	1.0	100	45	94	93.71	2.082	89	97
4	1.0	120	45	94	93.71	2.082	90	96
5	0.5	100	60	58	115.94	1.932	58	98
6	1.0	100	45	89	88.88	1.975	89	96
7	2.0	100	45	95	47.34	1.052	91	95

^a All the reactions were carried out using 3-nitro-iodobenzene (1.0 mmol), methyl acrylate (1.1 mmol), K₂CO₃ (1.0 mmol), Pd(OAc)₂ (1 mol%), [C₁₈-DABCO-C₁₈]2Br (10 mol%) in water (5.0 mL) at 60–120 °C under air. ^b By HPLC. ^c By HPLC.

Table 3 A substrate scope for Mizoroki–Heck reaction using Pd(OAc)₂/[C₁₈-DABCO-C₁₈]2Br^a

X = Br and I

Entry	Aryl halides	Products	Time (min)	Yield ^b (%)	TON	TOF (min ⁻¹)	E/Z ^c
1			50	92	91.85	1.837	100/0
2			45	93	92.67	2.059	100/0
3			65	80	79.72	1.226	100/0
4			65	82	81.63	1.255	100/0
5			50	91	90.82	1.816	100/0
6			60	83	82.63	1.377	100/0
7			50	90	89.83	1.796	100/0
8			65	85	85.00	1.307	100/0
9			60	89	88.96	1.482	100/0
10			50	93	92.77	1.855	88/12
11			90	90	89.74	0.997	88/12
12			80	88	87.61	1.095	100/0
13			80	87	86.66	1.083	100/0

^a All the reactions were carried out using aryl halides (1.0 mmol), acrylates (1.1 mmol), K₂CO₃ (1.0 mmol), Pd(OAc)₂ (1 mol%), [C₁₈-DABCO-C₁₈]2Br (10 mol%) in water (5.0 mL) at 100 °C under air. ^b Isolated yield. ^c By HPLC.

base, in Pd(OAc)₂/[C₁₈-DABCO-C₁₈]2Br catalyst at 80 °C. The results, presented in Table 4, demonstrate that all tested substrates could be easily converted into the expected products with yields ranging from 80% to 95%, achieved within a reaction time of 30 to 60 minutes.

Recycling study

The lifetime and reusability of a catalyst are essential for its practical applications. To evaluate the recyclability of the Pd(OAc)₂/[C₁₈-DABCO-C₁₈]2Br system, consecutive Mizoroki–Heck coupling reactions were carried out using 3-nitro-

Table 4 Scope of Pd(OAc)₂/[C₁₈-DABCO-C₁₈]2Br catalytic system for Suzuki–Miyaura coupling reaction^a

X = Br and I

Entry	Aryl halides	Arylboronic acids	Products	Time (min)	Yield ^b (%)	TON	TOF (min ⁻¹)
1				30	95	94.84	3.161
2				45	90	89.89	1.997
3				45	91	90.64	2.014
4				40	88	87.91	2.197
5				35	87	86.86	2.481
6				35	90	89.88	2.568
7				40	92	91.54	2.288
8				30	93	92.91	3.097
9				45	90	89.82	1.996
10				40	91	90.88	2.272

^a All the reactions were carried out using aryl halides (1.0 mmol), aryl boronic acids (1.1 mmol), K₂CO₃ (2.0 mmol), Pd(OAc)₂ (1 mol%), [C₁₈-DABCO-C₁₈]2Br (10 mol%) in water (5.0 mL) at 80 °C under air. ^b Isolated yield.

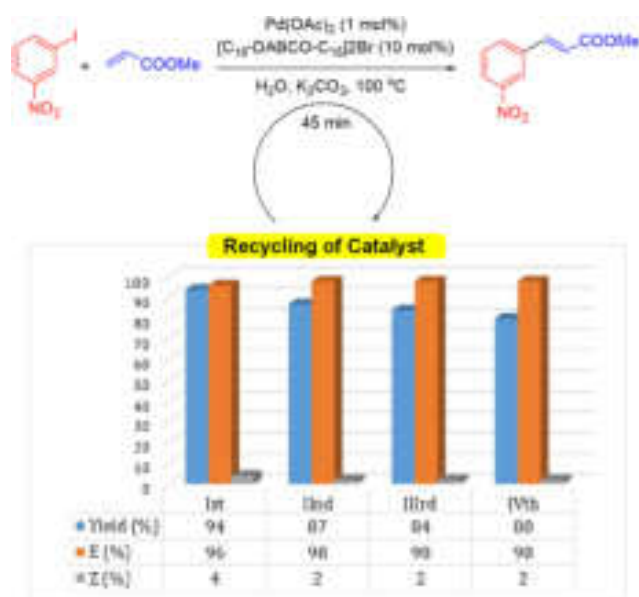


Fig. 9 Recycling of catalytic system for Mizoroki–Heck coupling reaction.

iodobenzene and methyl acrylate. After the fresh reaction product was separated from the reaction mixture with ethyl acetate extraction, the aqueous phase containing the catalyst was used for the subsequent reaction cycle without any additional treatment. The catalytic system could be effectively recovered and reused for at least three cycles, with a decrease in product yields from 94–80%, which could be attributed to the handling loss of the catalysts. However, the *E/Z* selectivity was not significantly impacted (Fig. 9).

Conclusion

Conclusively, our study successfully demonstrated the synthesis and characterization of a novel Gemini-type diquaternalized DABCO surfactant which further stabilized PdNPs as depicted in TEM and XPS studies and designated as Pd(OAc)₂/[C₁₈-DABCO-C₁₈]₂Br. The catalytic system provides a straightforward and efficient approach for synthesizing diversely functionalized acrylates through ligand-free Mizoroki–Heck cross-coupling reactions in an aqueous medium at 100 °C. Additionally, we also demonstrated the effectiveness of this method for ligand-free Suzuki–Miyaura cross-coupling reactions under similar reaction conditions. The Mizoroki–Heck reactions exhibited remarkable Turnover Numbers (TON) ranging from 79.72 to 92.77, and Turnover Frequencies (TOF) ranging from 0.997 to 2.059 min⁻¹. Similarly, the Suzuki–Miyaura reactions displayed TON values of 86.86 to 94.84 and TOF values of 1.996 to 3.161 min⁻¹. This methodology offers notable environmental advantages, including shorter reaction times, mild reaction conditions, high product yields, excellent selectivity, and operational simplicity. Furthermore, the catalytic system showcased reusability for at least four runs, although with slightly decreased product yields while maintaining selectivity. This research contributes to the development of efficient

and sustainable catalytic systems and provides promising avenues for future applications.

Data availability statement

The data that support the findings of this study are available in the supporting information of this article.

Author contributions

Archana Rajmane: study conception and design, data collection, experimental work and designing of manuscript; Chunilal Pawara: data characterization and analysis; Sumit Kamble: data characterization and analysis; Utkarsh More: physical study; Suresh Patil: project co-supervisor; Arjun Kumbhar: project supervisor.

Conflicts of interest

There are no conflicts to declare.

Acknowledgements

Archana Rajmane is a BARTI-Fellow and grateful to the Government of Maharashtra (India) for the financial support under Dr Babasaheb Ambedkar National Research Fellowship (BANRF-2020) [BANRF-2020/21-22/850 dated 16/02/2022]. Arjun Kumbhar is grateful to the Science and Engineering Research Board-Department of Science and Technology (SERB-DST), Government of India, New Delhi, for supporting this work under the scheme of Start-Up research grants for Young Scientists (SB/FT/CS-153/2013). Sumit Kamble is thankful to SERB-EEQ (EEQ/2020/000249) for financial support and AcSIR Gaziaabad for academic support.

References

- (a) S. Bräse and A. D. Meijere, *Metal-Catalyzed Cross-Coupling Reactions*, Wiley-VCH, Verlag GmbH, 2008, 217; (b) I. P. Beletskaya and A. V. Cheprakov, *Chem. Rev.*, 2000, **100**, 3009–3066; (c) R. F. Heck and J. P. Nolley, *J. Org. Chem.*, 1972, **37**, 2320–2322; (d) T. Mizoroki, K. Mori and A. Ozaki, *Bull. Chem. Soc. Jpn.*, 1971, **44**, 581; (e) C. C. Carin, J. Seechurn, M. O. Kitching, T. J. Colacot and V. Snieckus, *Angew. Chem., Int. Ed.*, 2012, **51**, 5062–5085.
- (a) G. B. Smith, G. C. Dezeny, D. L. Hughes, A. O. King and T. R. Verhoeven, *J. Org. Chem.*, 1994, **59**, 8151–8156; (b) S. J. Danishefsky, J. J. Masters, W. B. Young, J. T. Link, L. B. Snyder, T. V. Magee, D. K. Jung, R. C. A. Isaacs, W. G. Bornmann, C. A. Alaimo, C. A. Coburn and M. J. Di Grandi, *J. Am. Chem. Soc.*, 1996, **118**, 2843–2859; (c) A. B. Dounay and L. E. Overman, *Chem. Rev.*, 2003, **103**, 2945–2964; (d) M. Prashad, *Top. Organomet. Chem.*, 2004, **6**, 181; (e) K. C. Nicolaou, P. G. Bulger and D. Sarlah, *Angew. Chem., Int. Ed.*, 2005, **44**, 4413.

- 3 (a) C. Torborg and M. Beller, *Adv. Synth. Catal.*, 2009, **18**(351), 3027–3043; (b) N. Hussain and A. Hussain, *RSC Adv.*, 2021, **11**, 34369–34391; (c) M. Farhang, A. R. Akbarzadeh, M. Rabbani and A. M. Ghadiri, *Polyhedron*, 2022, **227**, 116–124.
- 4 (a) C. A. Fleckenstein and H. Plenio, *Chem. Soc. Rev.*, 2010, **39**, 694–711; (b) K. B. Gan, R.-L. Zhong, Z.-W. Zhang and F. Y. Kwong, *J. Am. Chem. Soc.*, 2022, **144**, 14864–14873.
- 5 A. Kumbhar, *J. Orgmet. Chem.*, 2017, **848**, 22e88.
- 6 A. Kumbhar, *J. Orgmet. Chem.*, 2019, **881**, 79e129.
- 7 (a) A. Rajmane, S. Jadhav and A. Kumbhar, *J. Orgmet. Chem.*, 2022, **957**, 122147; (b) A. Rajmane and A. Kumbhar, *Mol. Catal.*, 2022, **532**, 112699.
- 8 (a) F. Alonso, I. P. Beletskaya and M. Yus, *Tetrahedron*, 2005, **61**, 11771–11835; (b) S. N. Jadhav, A. S. Kumbhar, C. V. Rode and R. S. Salunkhe, *Green Chem.*, 2016, **18**, 1898–1911.
- 9 (a) A. Chanda and V. V. Fokin, *Chem. Rev.*, 2009, **109**, 725–748; (b) C. J. Li and L. Chen, *Chem. Soc. Rev.*, 2006, **35**, 68; (c) *Organic Reactions in Water: Principles, Strategies and Applications* ed. U. Marcus Lindström, Blackwell Pub. Ltd, 2007; (d) C. J. Li, *Green Chemical Syntheses and Processes ACS Symposium Series*, 2000, ch. 6, vol. 767, pp. 66–73; (e) T. Kitanosono, K. Masuda, P. Xu and S. Kobayashi, *Chem. Rev.*, 2018, **118**, 679–746.
- 10 W. A. Herrmann, V. P. W. Böhm and C. P. Reisinger, *J. Organomet. Chem.*, 1999, **576**, 23–41.
- 11 A. N. Marziale, D. Jantke, S. H. Faul, T. Reiner, E. Herdtweck and J. Eppinger, *Green Chem.*, 2011, **13**, 169–177.
- 12 (a) A. H. M. de Vries, J. M. C. A. Mulders, J. H. M. Mommers, H. J. W. Henderickx and J. G. de Vries, *Org. Lett.*, 2003, **5**, 3285–3288; (b) Q. Yao, E. P. Kinney and Z. Yang, *J. Org. Chem.*, 2003, **68**, 7528–7531; (c) J. G. de Vries, *Dalton Trans.*, 2006, 421.
- 13 (a) E. Alacid and C. Najera, *Synlett*, 2006, **18**, 2959–2964; (b) D. Schonfelder, O. Nuyken and R. J. Weberskirch, *Organomet. Chem.*, 2005, **690**, 4648–4655; (c) D. Schonfelder, K. Fischer, M. Schmidt, O. Nuyken and R. Weberskirch, *Macromolecules*, 2005, **38**, 254–262; (d) J. P. Genet and M. Savignac, *J. Organomet. Chem.*, 1999, **576**, 305–317.
- 14 (a) Y. Cui and L. Zhang, *J. Mol. Catal. A: Chem.*, 2005, **237**, 120–125; (b) F. Bellina and C. Chiappe, *Molecules*, 2010, **15**, 2211–2245.
- 15 (a) T. Jeffery, *J. Chem. Soc., Chem. Commun.*, 1984, 1287–1289; (b) T. Jeffery, *Advances in Metal–Organic Chemistry*, ed. L. S. Liebeskind, Jai Press Inc., London, 5 1996, pp. 153.
- 16 (a) X. Yang, Z. Fei, D. Zhao, W. H. Ang, Y. Li and P. Dyson, *J. Inorg. Chem.*, 2008, **47**, 3292–3297; (b) P. Migowski and J. Dupont, *Chem. – Eur. J.*, 2007, **13**, 32–39; (c) C. Chiappe, D. Pieraccini, D. Zhao, Z. Fei and P. J. Dyson, *Adv. Synth. Catal.*, 2006, **348**, 68–74; (d) D. Zhao, Z. Fei, T. J. Geldbach, R. Scopelliti and P. J. Dyson, *J. Am. Chem. Soc.*, 2004, **126**, 15876–15882; (e) Z. Fei, D. Zhao, D. Pieraccini, W. H. Ang, T. J. Geldbach, R. Scopelliti, C. Chiappe and P. Dyson, *J. Organometall.*, 2007, **26**, 1588–1598; (f) A. Biffis, M. Zecca and M. Basato, *J. Mol. Catal. A: Chem.*, 2001, **173**, 249–274; (g) A. Balanta, C. Godard and C. Claver, *Chem. Soc. Rev.*, 2011, **40**, 4973–4985.
- 17 (a) M. T. Reetz and E. Westermann, *Angew. Chem., Int. Ed.*, 2000, **39**, 165–168; (b) J. Evans, L. O'Neill, V. L. Kambhampati, G. Rayner, S. Turin, A. Genge, A. J. Dent and T. Neisius, *J. Chem. Soc., Dalton Trans.*, 2002, 2207–2212; (c) J. G. de Vries, *J. Chem. Soc., Dalton Trans.*, 2006, 421–429; (d) A. H. M. de Vries, F. J. Parlevliet, L. Schmieder-van de Vondervoort, J. H. M. Mommers, H. J. W. Henderickx, M. A. M. Walet and J. G. de Vries, *Adv. Synth. Catal.*, 2002, **344**, 996–1002; (e) R. S. Varmam, *Green Chem.*, 2014, **16**, 2027–2041; (f) H. Pang, Y. Hu, J. Yu, F. Gallou and B. H. Lipshutz, *J. Am. Chem. Soc.*, 2021, **143**, 3373–3382; (g) S. Handa, Y. Wang, F. Gallou and B. H. Lipshutz, *Science*, 2015, **349**, 1087–1091.
- 18 (a) S. N. Jadhav, A. S. Kumbhar, S. S. Mali, C. K. Hong and R. S. Salunkhe, *New J. Chem.*, 2015, **39**, 2333–2341; (b) A. Kumbhar, S. Jadhav, S. Kamble, G. Rashinkar and R. Salunkhe, *Tetrahedron Lett.*, 2013, **54**, 1331–1337; (c) A. Kumbhar, S. Kamble, S. Jadhav, G. Rashinkar and R. Salunkhe, *Catal. Lett.*, 2012, **142**, 1388–1396; (d) A. Kumbhar and R. Salunkhe, *Curr. Org. Chem.*, 2015, **19**, 2075–2121; (e) A. Kumbhar, *Top. Curr. Chem.*, 2017, **375**, 2; (f) S. N. Jadhav and C. V. Rode, *Green Chem.*, 2017, **19**, 5958–5970.
- 19 (a) K. S. Kim, A. F. Gossmann and N. Winograd, *J. Oleo Sci.*, 2006, **55**, 381; (b) S. K. Hait and S. P. Moulik, *Curr. Sci.*, 2002, **82**, 1101–1111; (c) P. Quagliotto, G. Viscardi, C. Barolo, E. Barni, S. Bellinvia, E. Fiscaro and C. Compari, *J. Org. Chem.*, 2003, **68**, 7651–7660; (d) R. Oda, S. J. Candau and I. Huc, *J. Chem. Commun.*, 1997, 2105–2106; (e) J. H. Mathias, M. J. Rosen and L. Davenport, *Langmuir*, 2001, **17**, 6148–6154; (f) F. M. Menger and J. S. Keiper, *Angew. Chem., Int. Ed.*, 2000, **39**, 1906–1920.
- 20 T. Lohar, A. Kumbhar, M. Barge and R. Salunkhe, *J. Mol. Liq.*, 2016, **224**, 1102–1108.
- 21 (a) U. More, P. Kumari, Z. Vaid, K. Behera and N. Malek, *J. Surfactant Detergent.*, 2016, **19**, 75–89; (b) M. J. Jones and D. Chapman, *Micelles, Monolayers, and Biomembranes*, Wiley-LISS, New York, 1995.
- 22 (a) A. Rajmane, R. Bandal, S. Shirke, U. More, S. Patil and A. Kumbhar, *J. Mol. Liq.*, 2023, 123247, DOI: [10.1016/j.molliq.2023.123247](https://doi.org/10.1016/j.molliq.2023.123247); (b) U. More, Z. Vaid, S. Rajput, N. Malek and O. A. Eleoud, *J. Colloid Polym. Sci.*, 2017, **295**, 2351–2361.
- 23 U. More, Z. Vaid, S. Rajput, Y. Kadam and N. Malek, *J. Dispersion Sci., Technol.*, 2017, **38**, 393–402.
- 24 (a) R. F. Heck, *J. Am. Chem. Soc.*, 1968, **90**, 5518–5526; (b) T. Mizoroki, K. Miori and A. Ozaki, *Bull. Chem. Soc. Jap.*, 1971, **44**, 581; (c) K. F. Heck and J. P. Nolley, *J. Org. Chem.*, 1972, **37**, 2320.
- 25 A. B. Dounay and L. E. Overman, *Chem. Rev.*, 2003, **103**, 2945–2964.
- 26 (a) S. Klingelhofer, W. Heitz, A. Greiner, S. Oestreich, S. Förster and M. Antonietti, *J. Am. Chem. Soc.*, 1997, **119**, 10116–10120; (b) M. Belier, H. Fischer, K. Kuhlein, C.-P. Reisinger and W. A. Herrmarm, *J. Organomet. Chem.*, 1996, **520**, 257–259; (c) M. T. Reetz, R. Breinbauer and K. Wanninger, *Tetrahedron Lett.*, 1996, **37**, 4499–4502.

- 27 (a) A. H. M. de Vries, J. M. C. A. Mulders, J. H. M. Mommers, H. J. W. Henderickx and J. G. de Vries, *Org. Lett.*, 2003, **5**, 3285–3288; (b) M. T. Reetz, G. Lohmer and R. Schwickardi, *Angew. Chem., Int. Ed.*, 1998, **37**, 481–483.
- 28 (a) L. Chen, A. Yelon and E. Sacher, *J. Phys. Chem. C*, 2011, **115**, 7896–7905; (b) N. Semagina, A. Renken, D. Laub and L. Kiwi-Minsker, *J. Catal.*, 2007, **246**, 308–314; (c) S. Yang, J. Dong, Z. Yao, C. Shen, X. Shi, Y. Tian, S. Lin and X. Zhang, *Sci. Rep.*, 2014, **4**, 4501; (d) R. Venkatesan, M. H. G. Precht, J. D. Scholten, R. P. Pezzi, G. Machado and J. Dupont, *J. Mater. Chem.*, 2011, **21**, 3030.
- 29 (a) S. A. Tressaud and Z. Khairou, *Anorg. Allg. Chem.*, 1986, **540/541**, 291; (b) S. Kukunuri, P. M. Austeria and S. Sampath, *Chem. Commun.*, 2016, **52**, 206–209.
- 30 V. K. Aggarwal, A. C. Staubitz and M. Owen, *Org. Process Res. Dev.*, 2006, **10**, 64–69.
- 31 Q. Yang, N. Sane, D. Klosowski, M. Lee, T. Rosenthal, N. X. Wang and E. Wiensch, *Org. Process Res. Dev.*, 2019, **23**, 2148–2156.
- 32 (a) N. Miyaura, K. Yamada and A. Suzuki, *Tetrahedron Lett.*, 1979, **20**, 3437–3440; (b) T. E. Barder, S. D. Walker, J. R. Martinelli and S. L. Buchwald, *J. Am. Chem. Soc.*, 2005, **127**(13), 4685–4696; (c) A. Fihri, M. Bouhrara, B. Nekoueshahraki, J. M. Basset and V. Polshettiwar, *Chem. Soc. Rev.*, 2011, **40**, 5181–5203.
- 33 (a) S. E. Hooshmand, B. Heidari, R. Sedghi and R. S. Varma, *Green Chem.*, 2019, **21**, 381–405; (b) M. Farhang, A. R. Akbarzadeh, M. Rabbani and A. M. Ghadiri, *Polyhedron*, 2022, **227**, 116124.

KI-Oxone catalyzed ultrasound-promoted synthesis of imidazo[1,2-a]pyridine-3-carboxylates (IPCs) and evaluation of their antitubercular activity

Vikram Desai^{1,3}, Sandip Patil³, Sandip Nipane¹, Vijay Sawant¹, Rajanikant Kurane⁴, Madhukar Deshmukh² and Suresh Patil^{5*}

¹*Smt. Kasturbai Walchand College, Sangli, Maharashtra (India)*

²*Department of Chemistry, Shivaji University, Kolhapur, Maharashtra (India)*

³*PG Department of Chemistry, P.D.V.P. College, Tasgaon-Sangli, Maharashtra (India)*

⁴*Rajarambapu Institute of Technology, Rajaramnagar, Maharashtra (India)*

⁵*Department of Chemistry, Raje Ramrao Mahavidyalaya, Jath-Sangli, Maharashtra (India)*

*Corresponding author: Email: pgchemistrysangli@gmail.com

Abstract

The present work involved ultrasound promoted KI-Oxone mediated oxidative C-N bond formation from reaction of β -keto ester and 2-aminopyridines leading to novel functional imidazo[1,2-a]pyridine-3-carboxylates (IPCs). The α -halogenation of β -keto ester have been easily carried out by *in situ* formed $I^+ OH^-$ species from KI-Oxone system. All derivatives were characterized by IR, NMR and mass spectra. The structure of the synthesized IPCs was confirmed by X-ray crystallographic analysis. Transition metal free protocol, one pot synthesis, non-toxic reagents, benign reaction conditions, high yield, short reaction time and synthesis of highly functional IPCs are the remarkable features of the present method. The synthesised IPCs shows remarkable antitubercular activity.

Keywords

Oxone, Ultrasound irradiation, β -ketoester, 2-aminopyridine, KI, IPCs

Introduction

Heterocyclic scaffolds especially fused N-heterocyclic structures are promising building blocks in various bioactive, natural and synthetic products. [1] Construction of substituted N-heterocycles therefore considered as immortal platform and thus, continuous effort have been made for their advancement. [2] The main objective in advancement was to develop hybrid molecules where two or more new potent small bioactive heterocyclic scaffolds are assembled in a single molecule which possessing multiple or combined biological activities. [3-5]

Imidazo[1,2-a]pyridines are very important heterocycles which have been found to be the core scaffold of many natural products and drugs [Fig. 1]. They have received considerable

interest from the pharmaceutical industry because of their important biological activities and interesting therapeutic properties [6] including antibacterial [7], antifungal [8], antiviral [9], antiulcer [10], and anti-inflammatory behaviour [11].

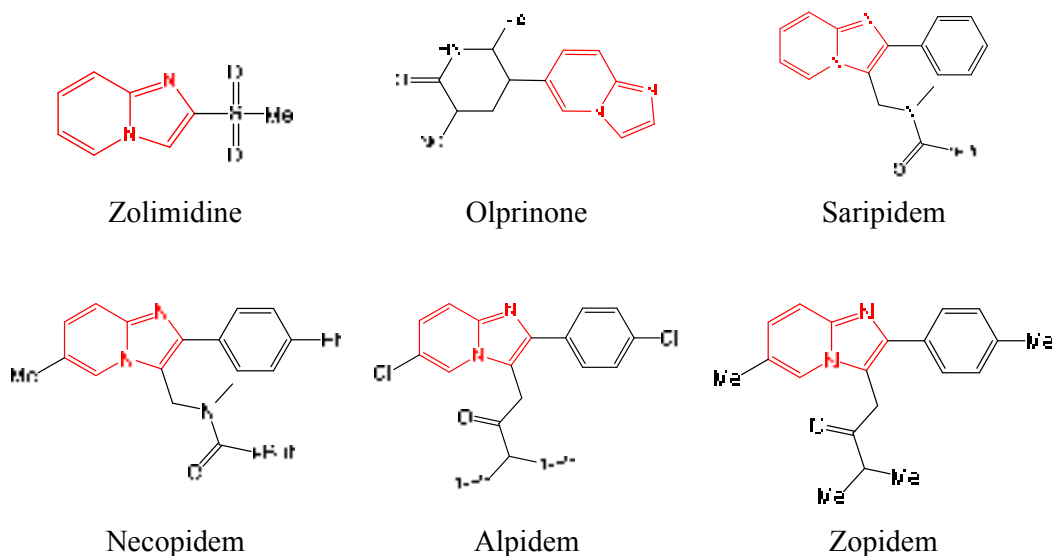


Fig. 1: The drugs containing imidazo[1,2-a]pyridine skeleton

Several synthetic methodologies have been developed to access functionalized imidazo[1,2]pyridine derivatives using condensation, tandem reaction, multicomponent strategy, intramolecular C–H amination, oxidative coupling. Among them, the common approaches were cyclocondensations of 2-aminopyridines with α -halocarbonyl compounds [12], 1,3-dicarbonyl compounds [13], nitroolefins or alkynes [14], tandem imine formation-oxidative cyclization of 2-aminopyridine with ketone [15] /alkyne [16] /diketone[17] /chalcone [18] multicomponent coupling of 2-aminopyridine, aldehyde, and ketone [19]/alkyne [20] /isonitrile [21] /nitroalkane [22]. In most of the strategies imidazo[1,2-a]pyridines were achieved through transition metal catalysed coupling reactions and generated highly functional derivatives. However, transition metal free approaches are commonly preferred in view of benign and green synthetic methodology.

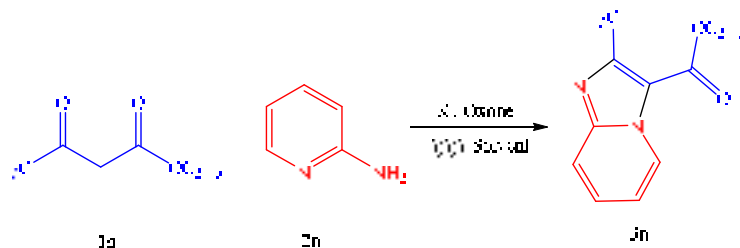
The development of an efficient catalytic oxidizing systems where only a catalytic amount of hypervalent iodine (III) reagent is required are focused as they provide environmental and economic advantages. These reagents can be generated *in situ* used with another cheap and nontoxic oxidant. [23] The hypervalent iodine(III) reagents such as (diacetoxyiodo)benzene (DIB), phenyliodine diacetate (PIDA), iodosobenzene diacetate (IBD or IBDA), [bis(trifluoroacetoxy)iodo]benzene and phenyliodine bis(trifluoroacetate) (PIFA) are very useful oxidants in organic synthesis. [24] The most highlighted application of hypervalent iodine (III) reagents is the α -functionalization of carbonyl groups. These strategies

involved the α -acetoxylation and α -tosylation of ketones using PIDA and HTIB as the oxidant, respectively. [25] The reagent for synthesis of α -tosyloxy ketones is the combination of iodosylbenzene and 4-toluenesulfonic acid. [26] The α -halogenated functional carbonyl groups were reacts with 2-aminopyridines to afford substituted imidazo[1,2-a]pyridines. The synthesis of imidazo[1,2-a]pyridine-3-carboxylate from hypervalent iodine (III) catalysed α -halogenated β -ketoester with 2-amino pyridine is practically convenient method however, there are many drawbacks of such hypervalent iodine catalysts viz. low solubility and stability, explosive nature, expensive and light weight. [27-28] We explored herewith ultrasound promoted utility of KI-Oxone as catalyst for an efficient synthesis of imidazo[1,2-a]pyridine-3-carboxylates from the reaction of 2-amino pyridine with β -ketoester.

Result and discussion

The study was instigated by investigation of reaction conditions performing reaction of ethyl acetoacetate (1a), 2-aminopyridine (2a) in presence of KI-Oxone under ultrasonication as model reaction. Initially, the reaction was performed without solvent to check the effect of solvent, which revealed that suitable solvent must be required [Table 1, entry 1] In acetonitrile 45 % yield of desired product was obtained. [Table 1, entry 2] The use of acetone, THF, DMF and 1,4-dioxane as solvents at 50 °C led to not formation of products. (Table 1, entries 3-6) Protic solvents viz. H₂O, EtOH and MeOH were found to be less suitable to form desired product. (Table 1, entries 7-9) In DCM low yield was obtained. [Table 1, entry 10] Considering the yield in ethanol and water, we tested EtOH:H₂O (1:1) mixed solvent system to model reaction. Surprisingly, 80 % yield was obtained within 30 min only. [Table 1, entry 11] The reaction was also performed at room temperature to check the effect of temperature which resulted excellent yield of desired product in 22 min only. [Table 1, entry 12] The reaction was subjected at high amount of KI-Oxone equivalent such as 1.5, 2.0 and 3.0 however, no appreciable change in yield was obtained. (Table 1, entries 13-15) Further the reaction was also performed at 80 °C which gave 89 % yield. [Table 1, entry 16] In absence of KI-Oxone the reaction preceded with no formation of product. [Table 1, entry 17] Thus it was concluded that KI-Oxone (1.0 equiv) at room temperature in EtOH:H₂O (1:1) under ultrasonication were the optimal reaction conditions.

Table 1: Optimization of reaction conditions for synthesis of imidazo[1,2-a]-pyridine-3-carboxylates



Entry	KI-Oxone (equiv.)	Solvent	Temp (°C)	Time (min)	Yield ^b (%)
1	1.0	-	50	60	16
2	1.0	MeCN	50	45	45
3	1.0	Acetone	50	60	NR
4	1.0	1,4-dioxane	50	45	NR
5	1.0	THF	50	60	NR
6	1.0	DMF	50	60	NR
7	1.0	H ₂ O	50	45	68
8	1.0	EtOH	50	45	66
9	10	MeOH	50	45	46
10	1.0	DCM	50	60	44
11	1.0	EtOH:H ₂ O (1:1)	50	30	80
12	1.0	EtOH:H₂O (1:1)	rt	22	94
13	1.5	EtOH:H ₂ O (1:1)	rt	30	92
14	2.0	EtOH:H ₂ O (1:1)	rt	30	91
15	3.0	EtOH:H ₂ O (1:1)	rt	60	64
16	1.0	EtOH:H ₂ O (1:1)	80	30	86
17	00	EtOH:H ₂ O (1:1)	rt	60	NR

The bold values represent the best reaction conditions

^aReaction conditions: a reaction mixture of β -ketoester (**1a**) (1 mmol, 1 equiv) and 2-aminopyridines (**2b**) (1 mmol, 1 equiv) with KI-Oxone (1equiv), solvent (3ml), ultrasonication.

^bIsolated yields

^{NR}No reaction

The generality of the present methodology was extended employing optimized reaction conditions. For synthesis of highly functional imidazo[1,2-a]-pyridine-3-carboxylates diverse alkyl or aryl substituents at the keto moiety of β -ketoester were treated with simple and substituted 2-amino pyridines (Scheme 1). The reaction of ethyl acetoacetate with 2-aminopyridine and 3-methyl-2-aminopyridine furnished excellent yield in short reaction time. (Table 2, entries 1-2] Methyl benzoylacetate, an aromatic functional β -ketoester on reaction with 2-aminopyridine and 3-methyl-2-aminopyridine resulted 92 and 91 % yields, respectively. (Table 2, entries 3-4) Further the generality was extended for synthesis of novel derivatives of imidazo[1,2-a]-pyridine-3-carboxylates using bulky substitution on keto moiety. High yields

were obtained for the reaction of tert-butyl substituted β -ketoester with 2-amino pyridine and 3-methyl-2-aminopyridine. (Table 2, entries 5-6) A heterocycle substituted β -ketoester furnished 90 to 92 % yields of desired products. (Table 2, entry 7-8). Cyclopropyl functionalized β -ketoester also gave remarkable yields with 2-aminopyridine derivatives. (Table 2, entries 9-10) Overall, alkyl, aryl, tert-butyl, thiophenyl and cyclo-propyl substituted β -ketoester furnished high yield of imidazo[1,2-a]-pyridine-3-carboxylates by reaction with simple and alkyl substituted 2-aminopyridine.

Scheme 1: Synthesis of imidazo[1,2-a]-pyridine-3-carboxylates

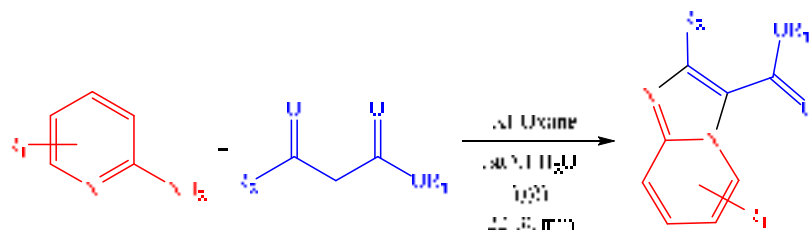
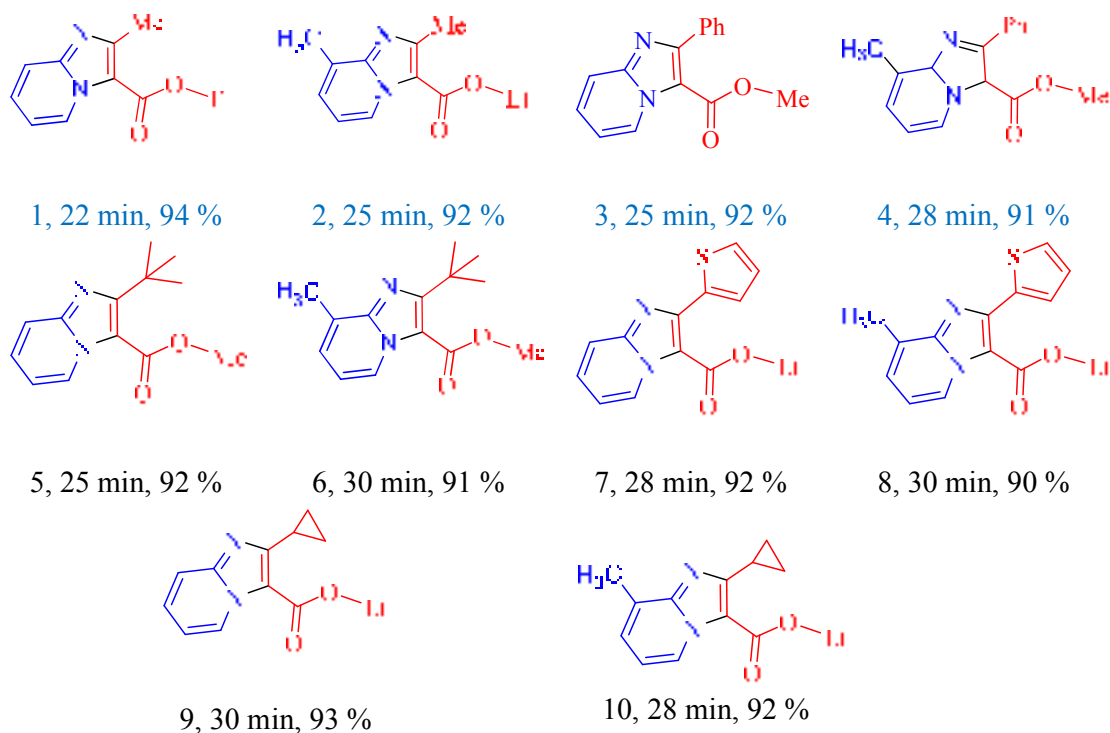


Table 2: Library of synthesized imidazo[1,2-a]-pyridine-3-carboxylates



X-Ray Crystallography

The data were collected at 100 K and the thermal ellipsoid drawn at 50% probability level. For this the purified compound 3e is dissolved in a mixed solvent of dichloromethane and hexanes to slowly evaporate which resulted the formation of colourless crystals. ORTEP

diagram of the molecule (Fig. 2) in a crystal of 3e displacement ellipsoids are drawn at 50 % probability level and H atoms are shown as small spheres of arbitrary radii (CCDC no. 1982684). The crystallography data confirms the formation the structure of synthesized product (3e) and literature reveals the absence of the crystallographic data of the present molecule (3e).

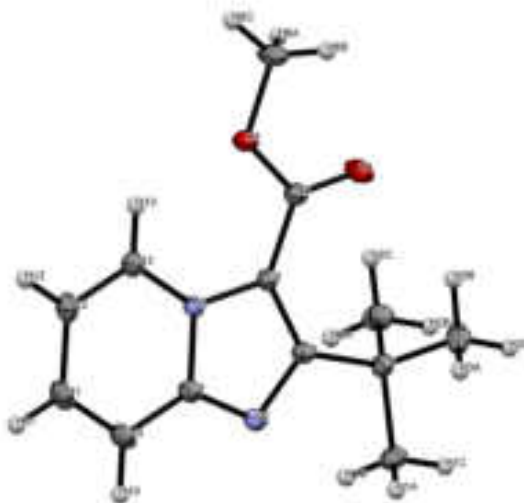


Fig. 2: Crystallographic structure of 3e

The plausible mechanism for synthesis of imidazo[1,2-a]-pyridine-3-carboxylates is depicted in figure 2. Under ultrasonic irradiation, the halide (I^-) is released initially from iodide source and can be reoxidized by oxone resulted *in situ* generation of halogenated species. (I^+OH^-). The α -iodination of tautomeric enol form of β -ketoester stabilized by intramolecular hydrogen bonding furnish 3-iodo β -ketoester (3). The nucleophilic addition of 2-aminopyridine (2) under tandem oxidative annulation strategy with intermediate 3 affords intermediate 4 by releasing halide (I^-) which can be reoxidized by oxone to generate the electrophile (I^+). Subsequent intramolecular nucleophilic addition of 4 provided intermediate 5. Finally, the proton transfer followed by subsequent dehydration and dehydrogenation produced final product Imidazo[1,2-a]pyridine (6).

3h	S	S	S	S	S	S	R	R
3i	S	S	S	S	S	S	S	R
3j	S	S	S	S	S	S	S	R
S- Sensitive, R- Resistance Standard Strain used: Mycobacteria tuberculosis (Vaccine strain, H37 RV strain): ATCC No- 27294. Standard values for the Anti-Tb test which was performed. Pyrazinamide-3.125µg/ml, Ciprofloxacin-3.125µg/ml, Streptomycin- 6.25µg/ml								

Experimental

General

All aminopyridines, Ketoesters, oxone, KI and other chemicals were commercially obtained and used without further purification. IR spectra were recorded with IRAffinity-1 SHIMADZU instrument. The NMR spectra were recorded on AV 400 Bruker (400 MHz for ^1H NMR and 100 MHz for ^{13}C NMR) spectrometer using TMS as an internal standard in CDCl_3 as solvent. The chemical shift (δ values) are expressed in parts per million (ppm) and coupling constants (J) are expressed in hertz (Hz). Mass spectra were recorded on a Perkin Elmer Clarus 600 mass spectrometer using EI ionization. Microwave Irradiations were carried out in a Microwave Synthesizer System (850 W power; *Cata R* System).

General procedure for synthesis of imidazo[1,2-a]-pyridine-3-carboxylic acid esters:

KI-Oxone (1.0 equiv) was slowly added to a well stirred solution β -ketoester (1 mmol) and 2-aminopyridines (1 mmol) in ethanol: H_2O (3ml) and the reaction mixture was allowed to stir under ultrasonic irradiation at room temperature for the 22-30 min. On completion of reaction, as indicated by TLC (ethyl acetate: ether, 25:75), the solvent was evaporated under reduced pressure. Then obtained solid was dissolved in sodium hydrogen carbonate saturated solution and extracted three times with chloroform. The combined organic extracts were washed with water, dried over anhydrous Na_2SO_4 , concentrated under vacuum to afford the products. The crude products were purified by silica gel (60-120 mesh; 5.5 g) column chromatography using hexane /ethyl acetate (9:1 v/v) as eluent.

Conclusion

In summary we have synthesized imidazo[1,2-a]-pyridine-3-carboxylates from 2-aminopyridine and β -ketoester employing highly efficient KI-Oxone catalytic system. The reaction preceded through tandem oxidative annulation strategy. Highly functional imidazo[1,2-a]-pyridine-3-carboxylates have been synthesized under ultrasound irradiation with high yield in short reaction time. The crystallography data confirms the formation the imidazo[1,2-a]-pyridine-3-carboxylate (3e) and literature reveals the absence of the

crystallographic data of the synthesized derivative. The remarkable features of present protocol are metal free, non-toxic, benign reaction conditions. The synthesized imidazo[1,2-a]-pyridine-3-carboxylates screened for antitubercular and antioxidant evaluation. Most of the derivatives show admirable biological activity.

Acknowledgement

We gratefully acknowledge the financial support from Shivaji University, Kolhapur, Maharashtra (India) under Research Initiation Scheme [SU/C&U.D.Section/Prop. No.:4/1335].

Conflict of interest

The authors declare that there is no conflict of interests regarding the publication of this article.

References

1. T. S. Harrison, G. M. Keating, *CNS Drugs* 19, 65 (2005).
2. (a) P. G. Baraldi, M. A. Tabrizi, S. Gessi, P. A. Borea, *Chem. Rev.* 108, 238 (2008); (b) J. E. Coughlin, Z. B. Henson, G. C. Welch, G. C. Bazan, *Acc. Chem. Res.* 47, 257, (2014); (c) D. Chen, S. J. Su, Y. Cao, *J. Mater. Chem.*, 2, 9565 (2014).
3. (a) F. W. Muregi, A. Ishih, *Drug Dev. Res.* 71, 20 (2010); (b) T. G. M. Treptow, F. Figueirô, E. H. F. Jandrey, A. M. O. Battastini, C. G. Salbego, J. B. Hoppe, P. S. Taborda, S. B. Rosa, L. A. Piovesan, C. R. M. D'Oca, D. Russowsky, M. G. M. D'Oca, *Eur. J. Med. Chem.* 95, 552 (2015).
4. R. Echemend, A. F. de La Torre, J. L. Monteiro, M. Pila, A. G. Corrêa, B. Westermann, D. G. Rivera, M. W. Paixio, *Angew. Chem. Int. Ed.* 54, 7621 (2015).
5. (a) K. Nepali, S. Sharma, M. Sharma, P. M. S. Bedi, K. L. Dhar, *Eur. J. Med. Chem.* 77, 422 (2014); (b) C. Hubschwerlen, J. L. Specklin, C. Sigwalt, S. Schoeder, H. H. Locher, *Bioorg. Med. Chem.* 11, 2313, (2003); (c) A. A. Bekhit, A. M. Hassan, H. A. Abd El Razik, M. M. ElMiligy, E. J. El-Agroudy, D. Bekhit Ael, *Eur. J. Med. Chem.* 94, 30 (2015); (d) K. M. Amin, A. A. Eissa, S. M. AbouSeri, F. M. Awadallah, G. S. Hassan, *Eur. J. Med. Chem.* 60, 187 (2013); (e) R. Pingaew, A. Saekee, P. Mandi, C. Nantasenamat, S. Prachayasittikul, S. Ruchirawat, V. Prachayasittikul, *Eur. J. Med. Chem.* 22, 112 (2014).
6. A. R. Katritzky, Y.-J. Xu, H. Tu, *J. Org. Chem.* 68(12), 4935 (2003),.
7. Y. Rival, G. Grassy, G. Michel, *Chem. Pharm. Bull.* 40, 1170 (1992).
8. M.H. Fisher, A. Lusi, *J. Med. Chem.* 15, 982 (1972).
9. M. Lhassani, O. Chavignon, J.M. Chezal, *Eur. J. Med. Chem.* 34, 271 (1999).

10. J. J. Kaminsky, A. M. Doweiko, *J. Med. Chem.* 40, 427 (1999).
11. K. C. Rupert, J. R. Henry, J. H. Dodd, *Bioorg. Med. Chem. Lett.* 13, 347 (2003).
12. (a) S. Ulloora, A.V. Adhikari, R. Shabaraya, *Chin. Chem. Lett.* 24, 853 (2013); (b) A. Herath, R. Dahl, N. D. P. Cosford, *Org. Lett.* 12, 412 (2010).
13. (a) X. Wang, L. Ma, W. Yu, *Synthesis*, 2445 (2011); (b) L. J. Ma, X. P. Wang, W. Yu, B. Han, *Chem. Commun.* 47, 11333 (2011).
14. (a) R. L. Yan, H. Han, C. Ma, *J. Org. Chem.* 77, 2024 (2012); (b) J. Zeng, Y. J. Tan, M. L. Leow, X. W. Liu, *Org. Lett.* 14, 4386 (2012); (c) C. L. Zong, R. S. Zeng, J. P. Zou, *Chem. J. Chin. Univ.* 30, 632 (2014).
15. (a) A. K. Bagdi, M. Rahman, S. Santra, A. Majee, A. Hajra, *Adv. Synth. Catal.* 355, 1741 (2013); (b) Cai, Z.; Wang, S.; Ji, S. *Adv. Synth. Catal.* 355, 2686 (2013); (c) Z. Fei, Y. -P.Zhu, M. -C. Liu, F. -C Jia, A. -X. Wu, *Tetrahedron Lett.* 54, 1222 (2013).
16. (a) C. He, J. Hao, H. Xu, Y. Mo, H. Liu, J. Han, A. Lei, *Chem. Commun.* 11073 (2012); (b) Y. Gao, M. Yin, W. Wu, H. Huang, H. Jiang, *Adv. Synth. Catal.* 355, 2263 (2013).
17. L. Ma, X. Wang, W. Yu, B. Han, *Chem. Commun.* 11333 (2011).
18. (a) K. Monir, B. A. Kumar, S. Mishra, A. Majee, A. Hajra, *Adv. Synth. Catal.* 356, 1105 (2014); (b) P. Kaswan,; P. K. Rajnikant, A. Kumar, *Tetrahedron* 70, 8539 (2014).
19. P. Kaswan, K. Pericherla, H. K. Saini, A. Kumar, *RSC Adv.* 5, 3670 (2015).
20. N. Chernyak, V. Gevorgyan, *Angew. Chem., Int. Ed.* 49, 2743 (2010).
21. (a) E. F. DiMauro, J. M. Kennedy, *J. Org. Chem.* 72, 1013 (2007); (b) G. Xi, Z. Liu, *Tetrahedron* 71, 9602 (2015).
22. Yan, H.; Wang, Y.; Pan, C.; Zhang, H.; Yang, S.; Ren, X.; Li, J.; Huang, G. *Eur. J. Org. Chem.* 2754 (2014).
23. (a) R. D. Richardson, T. Wirth, *Angew. Chem., Int. Ed.* 45, 4402 (2006); (b) M. Ochiai, K. Miyamoto, *Eur. J. Org. Chem.* 4229 (2008); (c) T. Dohi, Y. Kita, *Chem. Commun.*, 2009, 2073; (d) T. Dohi, *Chem. Pharm. Bull.* 58, 135 (2010).
24. (a) V. V. Zhdankin,; Stang, P. J. *Chem. Rev.* 102, 2523 (2002). (b) Zhdankin, V. V.; Stang, P. J. *Chem. Rev.* 108, 5299 (2008).
25. (a) R. M. Moriarty, O. Prakash, *Org. React.* 54, 273 (1999); (b) G. Koser, *Aldrichimica Acta* 34, 89 (2001).
26. M. Ueno, T. Nabana, H. Togo, *J. Org. Chem.* 68, 6424 (2003).
27. C. Huo, J. Tang, H. Xie, Y. Wang, J. Dong, *Org. Lett.*, 2016, 18, 5, 1016.
28. X. Wang, L. Ma, W. Yu, *Synthesis* 2011, 15, 2445.
29. R. S. Kumar, T. Sivakumar, R. S. Sundaram, P. Sivakumar, R. Nethaji, M. Gupta, U. K. Mazumdar, *Iran. J. Pharmacol. Ther.*, 2006, 5, 35.



Alginate acid in water at room temperature: a natural combination for the environmental benign synthesis of 2,3-dihydroquinazolin-4(1H)-ones

Archana Rajmane¹ · Dipti Jadhav¹ · Kiran Bagade¹ · Suresh Patil² · Arjun Kumbhar¹

Received: 23 June 2023 / Accepted: 18 September 2023
© The Author(s), under exclusive licence to Springer Nature B.V. 2023

Abstract

We have successfully synthesized 2,3-dihydroquinazolin-4(1H)-ones (DHQs) using naturally sourced alginate acid as a solid acid catalyst. Our synthetic method was performed in pure water at room temperature and yielded good to excellent results. We achieved this by directly cyclo-condensing anthranilamide with various aldehydes or ketones in the presence of alginate acid in water at room temperature. Furthermore, the alginate acid can be easily separated from the reaction mixture and reused up to five times with consistent yields and reaction time. This method is energy efficient and can be applied on a large scale, with excellent green credentials. Our evaluation of green metrics highlights the sustainable features of the alginate acid-catalyzed DHQ synthesis process.

Graphical abstract



Keywords Alginate acid · Green synthesis · 2,3-Dihydroquinazolin-4(1H)-ones · Aqueous medium · Biopolymers

Extended author information available on the last page of the article

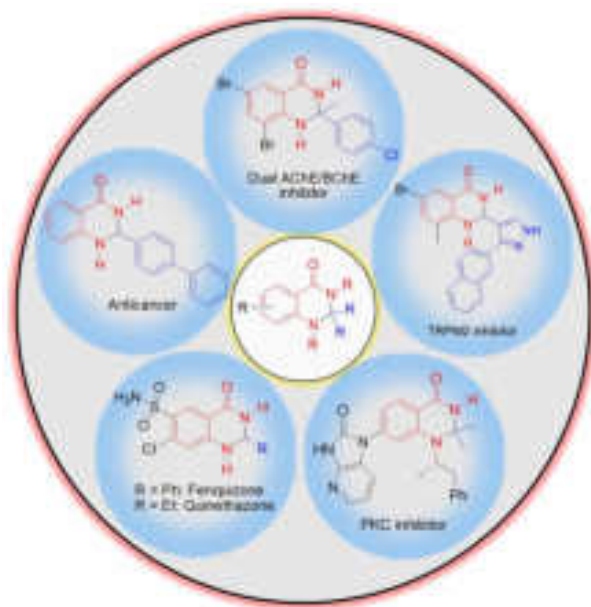


Fig. 1 Crucial pharmaceutical active compounds containing DHQ framework

Introduction

Quinazolinone scaffolds are a type of fused heterocycles that have potential pharmacological and biological activities [1, 2]. They are essential units found in natural products, agrochemicals, pharmaceuticals, and synthetic drugs (Fig. 1) [3]. One particular type of heterocyclic framework, 2,3-dihydroquinazolin-4(1H)-ones (DHQs), plays a crucial role in various medications due to its potent pharmacological and biological effects, such as anticancer, anticonvulsant, analgesic, diuretic, antihistamine, and antihypertensive activities [4–13].

DHQs are essential in many fields, and various methods have been reported for their synthesis, such as two and three-component reactions under different reaction conditions [14] (Fig. 2). The simplest and most direct method is the two-component condensation of anthranilamide with aldehydes or ketones. On the other hand, the three-component condensation of isatoic anhydride and different amines with aldehydes is another method. However, a two-component reaction is more environmentally friendly than a three-component reaction, according to green chemistry matrices. Many of the reported protocols use costly reagents, require extended reaction times and high temperatures, and involve tedious work-up procedures. The atom economy (AE) indicates that a two-component reaction is better than a three-component reaction.

In recent years, various catalysts have been used to catalyze these reactions such as cyanuric chloride [15], morpholinoethanesulfonic acid [16], *p*-TSA [11], 5,5'-indogodisulfonic acid [17], lactic acid [18], oxalic acid [19], citric acid [20], amino acid

[21], $\text{Sc}(\text{OTf})_3$ [22], $\text{Y}(\text{OTf})_3$ [23], $\text{Ga}(\text{OTf})_3$ [24], $\text{SrCl}_2 \cdot 6\text{H}_2\text{O}$ [25], $\text{H}_3\text{PW}_{12}\text{O}_{40}$ [26], NH_4Cl [27], $\text{H}[\text{Gly}_2\text{B}]$ [28], $[\text{Bmim}]\text{BF}_4$ [22], choline-sulfuric acid ionic liquid [9], basic ionic liquid [29], magnetic supported catalysts like Fe_3O_4 -Schiff base of $\text{Cu}(\text{II})$ [30], $\text{Fe}_3\text{O}_4 @ \text{SiO}_2\text{-SO}_3\text{H}$ [31], $\text{IL} @ \text{MNP}$ [32], $\text{Fe}_3\text{O}_4 @ \text{PEG-Ni}$ [33], $\text{Fe}_3\text{O}_4 @ \text{L-proline-SO}_3\text{H}$ [34] silica-supported catalysts such as MCM-41-dtz-Ni [35], $\text{SBA-16/GPTMS-TSC-CuI}$ [36], $\text{CoFe}_2\text{O}_4 @ \text{SiO}_2\text{-CPTES-Guanidine-Cu}(\text{II})$ [37] Hb zeolite [38], zinc oxide micelles [39], mono-ammonium phosphate fertilizer modified by cadmium [40], cerium(IV) ammonium nitrate [41], trifluoroethanol [42], $[\text{PEG-TEA}]\text{OH}$ [43], polyethylene glycol [44], and biocomposites such as β -cyclodextrin- SO_3H [45], $\text{Fe}_3\text{O}_4 @ \text{nano-cellulose-OPO}_3\text{H}$ [46], β -cyclodextrin [47], Ag-CNTs [48] has been also used for the synthesis of DHQs.

Over the past 20 years, there has been a growing need for more sustainable organic transformations that reduce waste [49–51]. DHQs are important, so it is highly appreciated when organic synthesis are environmentally friendly, high-yielding, and clean. Biopolymers, including solid support and catalysts, are commonly used in various organic transformations [52, 53]. Alginic acid is a binary, block polysaccharide consisting of (1–4) connected β -D-mannuronic acid (M) and α -L-guluronic acid (G) residues of varying compositions and sequences. It is a structural

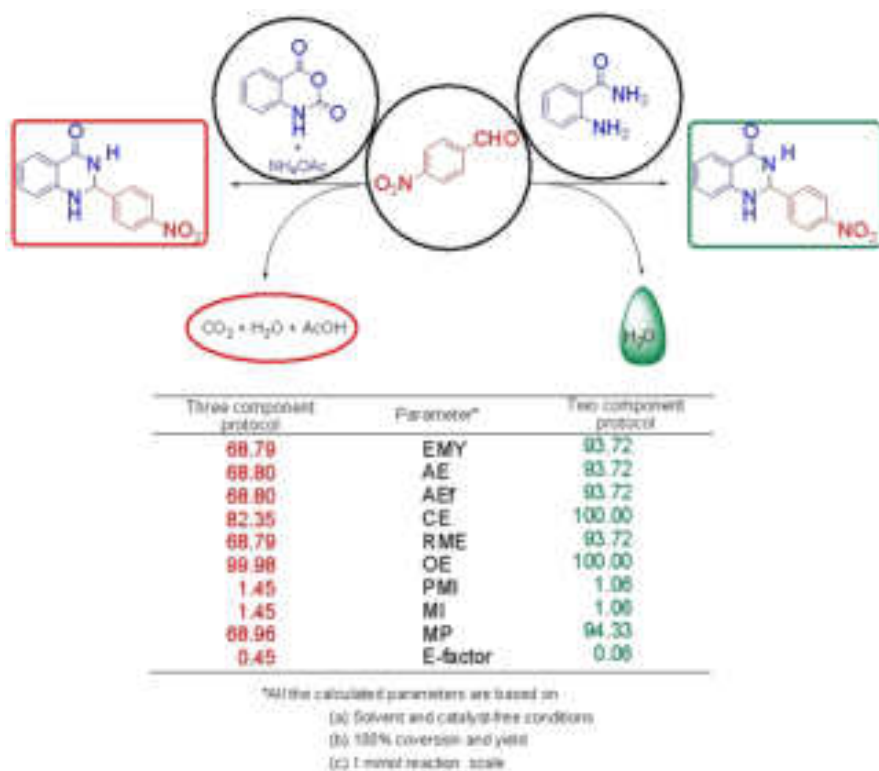
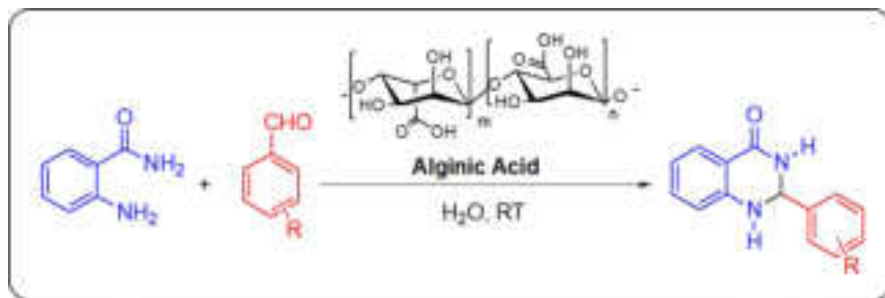


Fig. 2 Two protocols and green chemistry matrices for the synthesis of DHQs



Scheme 1. Alginic acid-catalyzed synthesis of DHQ in water at room temperature

component found in marine brown algae and many bacteria [54]. It can be extracted as water-soluble sodium alginate by adding an excess of alkali [55]. The carboxyl and hydroxyl groups of adjacent chains help to stabilize reactants during the reaction [56]. Alginic acids are biodegradable, biocompatible, and easily accessible, making them a popular choice as environmentally friendly catalysts for traditional inorganic and organic solid acids [57–59].

Water is a crucial solvent in many biological processes and is widely recognized for its advantages in organic reactions, such as being safe, cost-effective, and environmentally compatible. Recently, new methodologies including multicomponent reactions have been developed that are highly efficient and compatible [60] with green chemistry principles for the synthesis of various heterocyclic scaffolds and cross-coupling reactions [61–64].

We have recently made an effort to introduce new, more efficient methodologies that adhere to green chemistry principles for synthesizing various heterocyclic scaffolds [65, 66] and cross-coupling reactions [67–69]. Alginic acid, due to its unique properties and ability to act as an excellent Brønsted organic acid catalyst, was used as a solid acid catalyst. This involved the cyclo-condensation of anthranilamides and various aldehydes/ketones in water at room temperature (Scheme 1). The resulting products were obtained in good to excellent yields, and the alginic acid can be easily separated from the reaction mixture and recycled at least five times with consistent yield and reaction time.

Materials and methods

General remarks

All reactions were carried out in a round-bottom flask at RT. Chemical reagents and anhydrous solvents were purchased from commercial suppliers (TCI and Sigma-Aldrich chemical companies) and used as purchased. Thin layer chromatography (TLC) was performed using silica gel pre-coated aluminum plates, which were visualized with UV light at 254 nm or under iodine. ^1H NMR and ^{13}C NMR were recorded with Bruker (600 Mz) spectrometers using CDCl_3 and DMSO solvents

Chemical shifts for ^1H NMR are referred to as internal TMS (0 ppm), and chemical shifts for ^{13}C NMR are referenced to the carbon resonance of the solvent (CDCl_3 : δ 77.0 ppm). Data are reported as follows: chemical shift (δ ppm), multiplicity (s=singlet, d=doublet, t=triplet, q=quartet, m=multiplet), coupling constant (Hz), and integration.

General procedure for the synthesis of 2,3-dihydroquinazolin-4(1H)-ones

A mixture of anthranilamide (1 mmol), aldehyde/ketone (1 mmol), and alginate acid (5 mg) in water (5 mL) was stirred at room temperature. Reaction progress was monitored by TLC (ethyl acetate: *n*-hexane, 1:9). After completion of the reaction, 0.1 N NaOH (5 mL) was added to the reaction mixture to separate alginate acid as sodium alginate. The resultant solid product was collected by simple filtration and washed with water (5 mL). This crude product was recrystallized by using ethanol.

Result and discussion

The alginate acid was characterized by FTIR spectroscopy [70]. The broadband IR absorption at 3434 cm^{-1} is for the COOH group which was confirmed by the sharp band at 1744 cm^{-1} (Fig. 3). The weak signal at 2924 and 2854 cm^{-1} is due to C–H stretching vibrations. The asymmetric stretching of carboxylate vibration (O–C–O) is shown at 1628 cm^{-1} . The band at 1402 cm^{-1} may be due to C–OH deformation vibration with the contribution of O–C–O symmetric stretching vibration of the carboxylate group. The band at 1029 cm^{-1} may be assigned to C–O stretching, and C–O and C–C stretching vibrations of pyranose rings.

The porous nature of the alginate acid was evident in scanning electron microscopy (SEM) images. An image shows a relatively fibrous smooth surface about $50\text{ }\mu\text{m}$ thick (Fig. 4a and b) while elemental mapping is highlighted in the EDS micrograph (Fig. 4c).

In order to find the best reaction conditions for synthesizing DHQ, we first reacted anthranilamide with 4-nitrobenzaldehyde under various conditions. Initially,

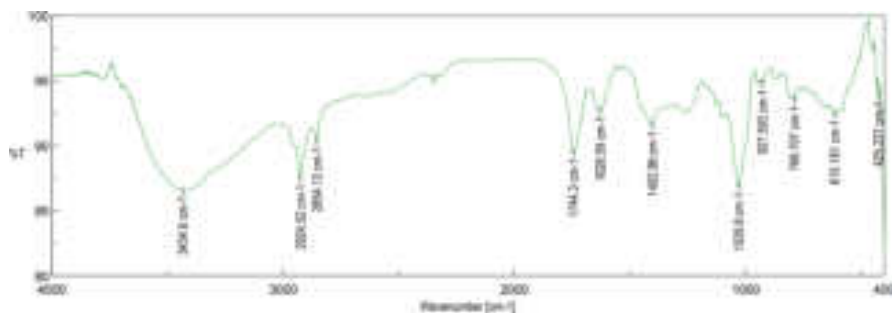


Fig. 3 The FTIR spectrum of alginate acid

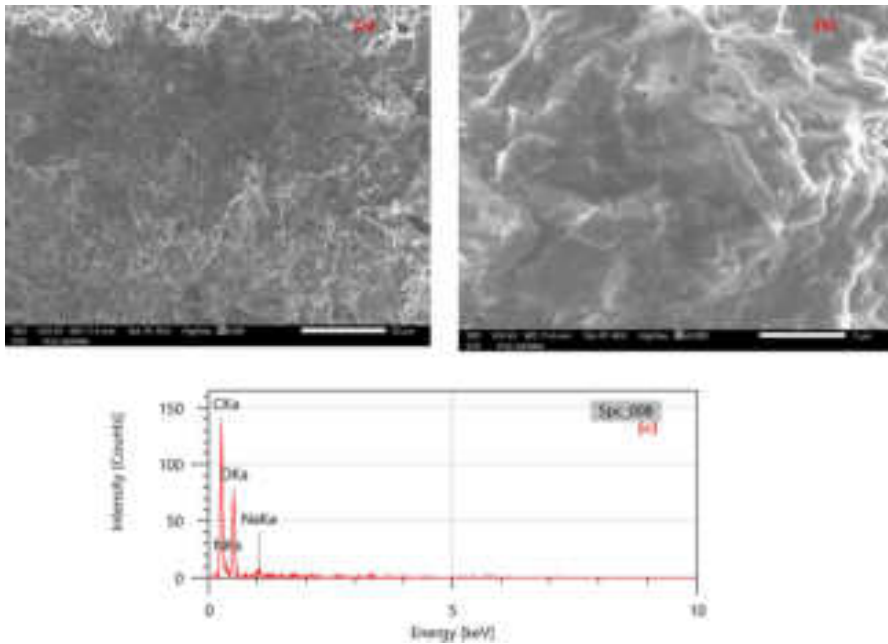
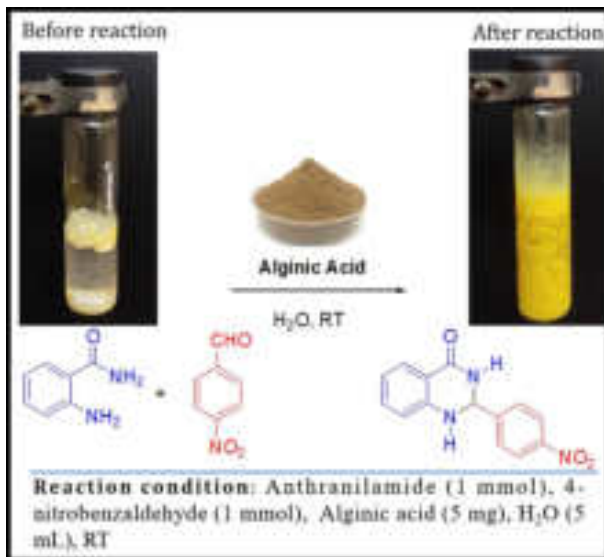


Fig. 4 SEM images (a and b) and EDS micrograph c of alginate acid



Scheme 2. Alginic acid-catalyzed synthesis of DHQ in water at room temperature

Table 1 Influence of quantity of alginic acid on the yield and reaction time of DHQ in water at room temperature^{a,b}

Entry	Amount of alginic acid (mg)	Time (min)	Yield ^b (%)
1	0	60	Trace
2	2	60	72
3	5	30	94
4	10	30	95
5	20	30	96
6	30	25	95
7	40	25	96
8	50	25	96

^aReaction conditions: Anthranilamide (1 mmol), 4-nitrobenzaldehyde (1 mmol), alginic acid (2–50 mg), H₂O (5 mL), RT

^bIsolated yields

Table 2 Effect of temperature and screening of various solvents for the synthesis of DHQ^{a,b}

Entry	Solvent	T (°C)	Time (min)	Yield ^b (%)
1	H ₂ O	RT	30	94
2	H ₂ O	40	20	96
3	H ₂ O	60	20	95
4	H ₂ O	80	15	95
5	EtOH	RT	25	96
6	50% Aq. EtOH	RT	30	95
7	DMF	RT	40	95
8	DCM	RT	55	54
9	Toluene	RT	40	76
10	Acetonitrile	RT	45	81

^aReaction conditions: anthranilamide (1 mmol), 4-nitrobenzaldehyde (1 mmol), alginic acid (5 mg, 2.84 mol%), solvent (5 mL), RT–80 °C

^bIsolated yields

we tested all reactions using water as a safe and environmentally friendly solvent [70] at room temperature (27–30 °C) (Scheme 2).

To determine the proper amount of catalyst, we conducted the model reaction using different concentrations of alginic acid (Table 1). Our findings showed that product formation ranged from 72 to 96% for all concentrations tested. Although the yield was similar across all concentrations, the reaction time for 5 mg of catalyst was 30 min compared to only 25–30 min for the other amounts. This suggests that 5 mg of alginic acid is sufficient for a smooth reaction.

To assess how solvents impact the model reaction, we tested a variety of solvents, including EtOH, methanol, toluene, DMF, acetonitrile, and aqueous ethanol (50%), using 5 mg of alginic acid at room temperature (Table 2). Aqueous ethanol proved to be the most effective in terms of product yield and reaction time, while organic

solvents like DCM, toluene, and acetonitrile were less effective. Water is considered the preferred solvent for reactions from a green chemistry perspective, and solvent selection guides often prioritize SH&E criteria (Table S6).

In an effort to reduce the reaction time, we tested the model reaction at various temperatures (Table 2). Increasing the temperature resulted in a decrease in reaction time from 30 to 15 min, but the higher temperature was ultimately more effective. For economic reasons, we carried out further reactions at ambient temperature.

We tested the effectiveness of our optimized conditions by synthesizing different DHQ derivatives (Table 3). This process is important as it shows how well the method can tolerate various functional groups and handle diverse substrates with different properties. We found that a wide range of aromatic aldehydes worked well in this reaction, indicating that our method is highly versatile. All reactions were performed on a 1 mmol scale in water with 5 mg of alginic acid at room temperature, unless otherwise noted. The yields were excellent, ranging from 84–94%. Even aromatic heterocyclic aldehydes were successfully reacted, yielding the desired product with a 84–94% yield.

As we were successful in using different aromatic aldehydes as electrophiles we then used ketones as another electrophiles for the synthesis of different DHQs. By reacting different ketones with anthranilamide, we obtained the desired products with good to excellent yields (86–94%) as shown in Table 4. The reaction also worked well with cyclic ketones such as cyclopentanone, cyclohexanone, and isatin.

We then expanded the scope of our work by creating bis-quinazolinone through the reaction of anthranilamide with terephthalaldehyde under optimized conditions (Scheme 3). The reaction was able to produce the desired products with a yield of 92% in just 35 min.

Based on our results, we have a possible mechanism for the formation of DHQ (3a) shown in Scheme 4. In the first step, alginic acid acts as a powerful Brønsted acid and activates aldehyde (2a) through protonation of the carbonyl group to form an intermediate I. The activated aldehyde I then undergoes a nucleophilic attack by anthranilamide (2) to form imine adduct II. In the presence of alginic acid, imine II is then converted into an iminium intermediate III through a protonation-cyclization process. Finally, DHQ (3a) is generated from III via deprotonation and the catalyst is released for the next cycle.

The efficient recycling of catalysts with consistent activity after a catalytic reaction is very important for green and sustainable development. In addition, recycling the catalyst is an important requirement for the industry's practical application of a catalyst.

After completion of reaction, the alginic acid was extracted using 0.1 N NaOH. The resulting product was separated through simple filtration. The aqueous extract containing sodium alginate was re-precipitated by 0.1N HCl. The solid alginic acid obtained was separated through centrifugation, dried in a vacuum, and reused for the next reaction cycle. The catalyst was observed to be recyclable at least five times, with a slight loss in activity with increased reaction time from 30–55 min. The catalyst also showed good TON and TOF values (Fig. 5).

To test the effectiveness of this protocol, a gram-scale (10 mmol scale) experiment was conducted for the reaction of anthranilamide with 4-nitrobenzaldehyde

Table 3 Exploration of the substrate scope of the developed synthetic method^{a,b}

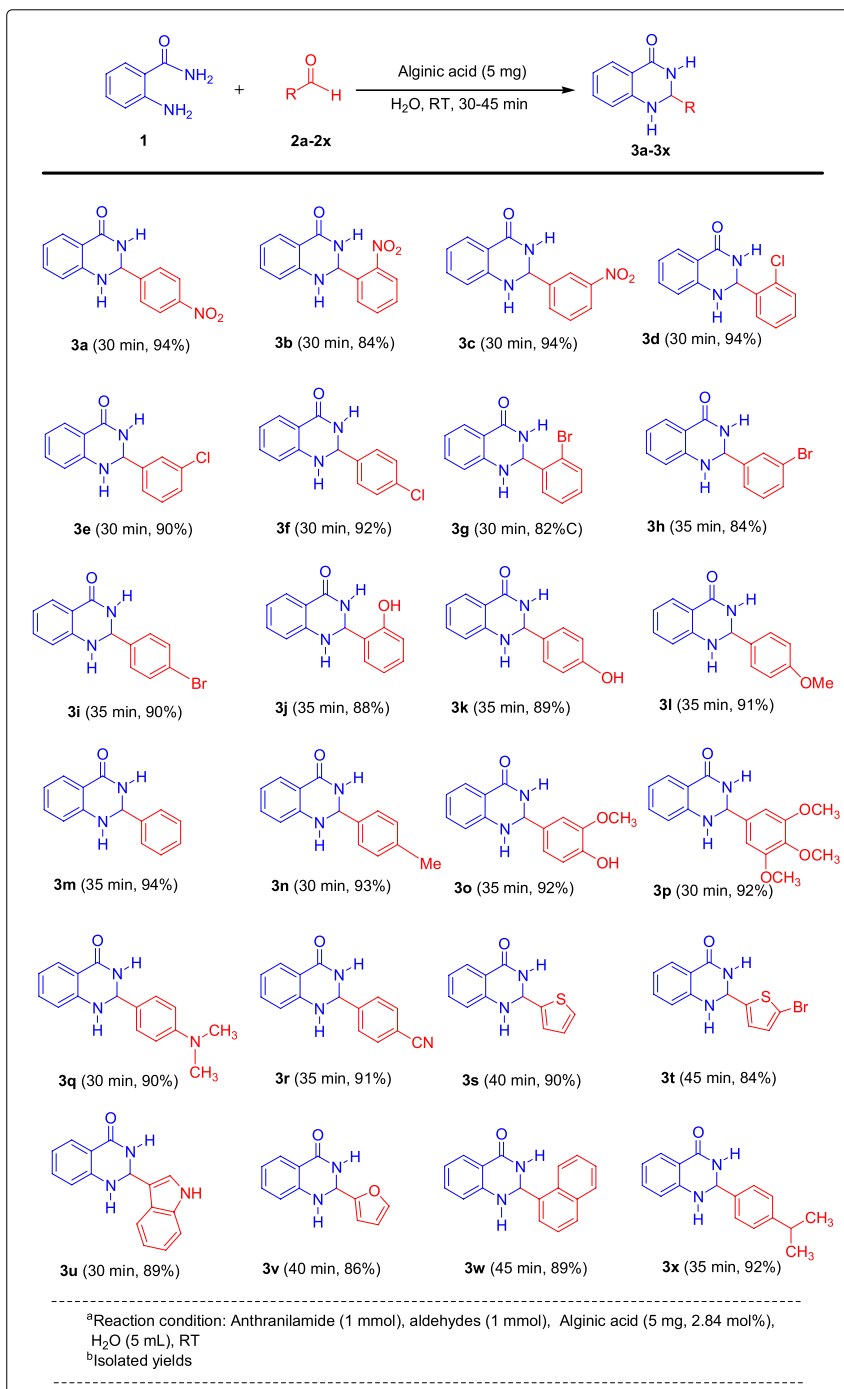
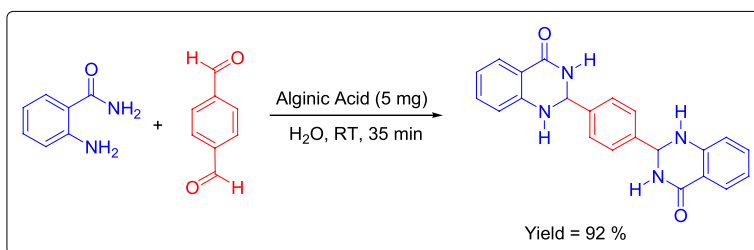
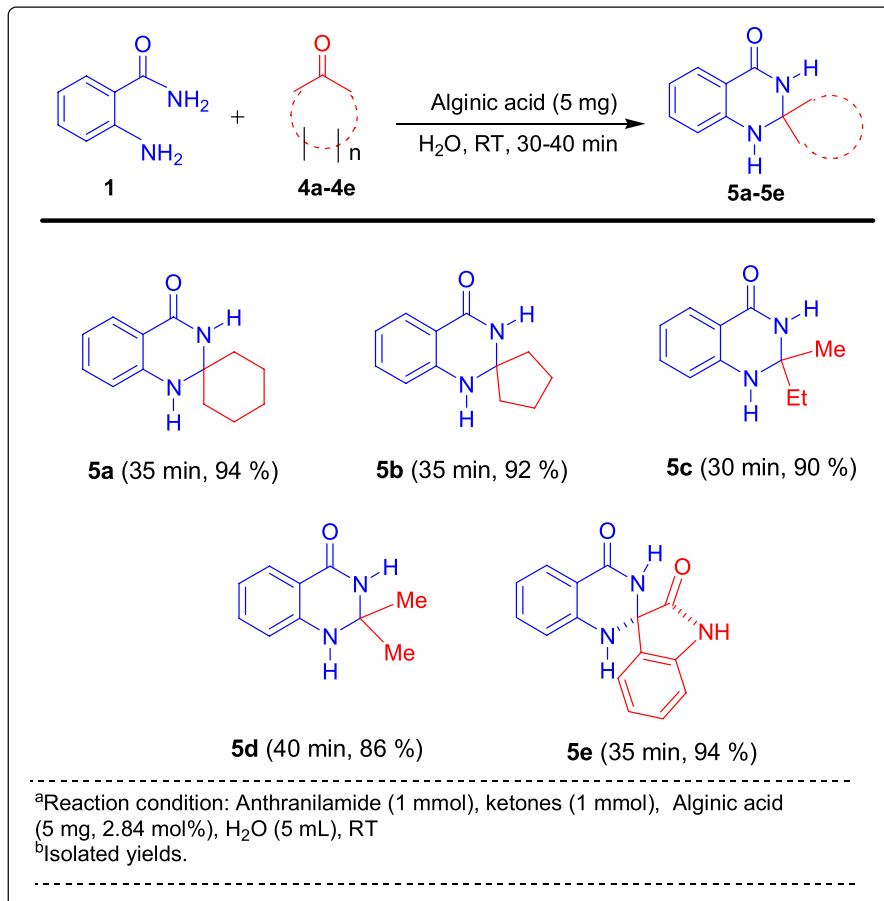
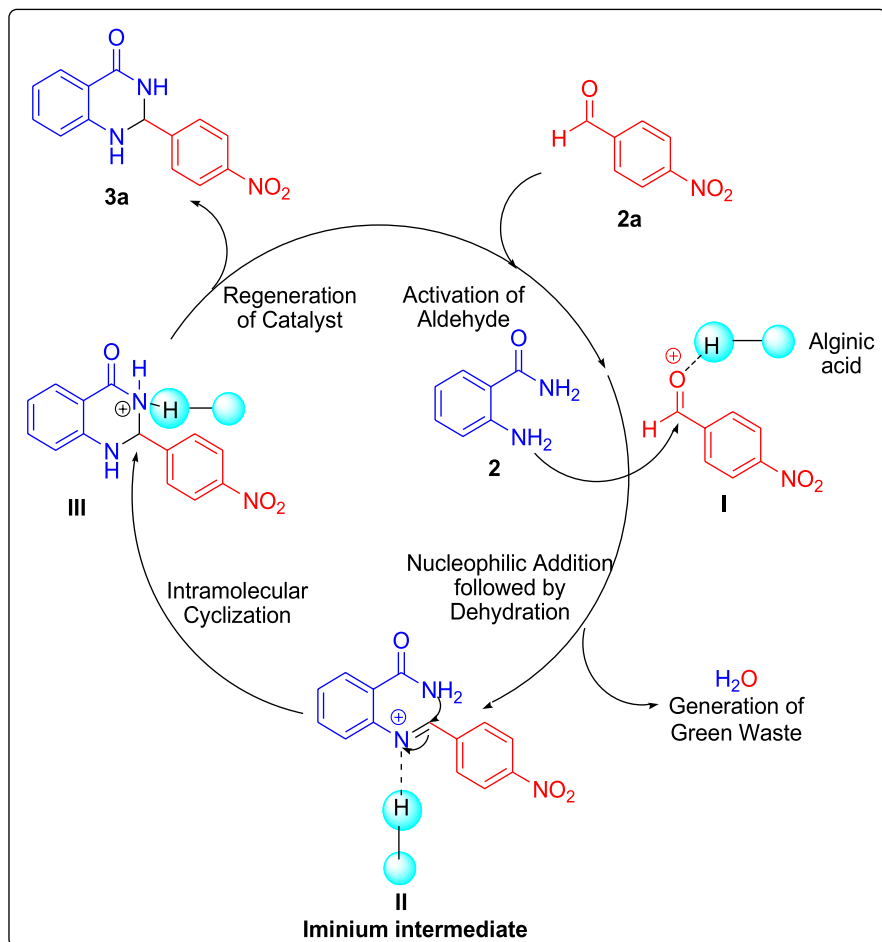


Table 4 Exploration of the substrate scope of the developed synthetic method by using various ketones^{a,b}**Scheme 3.** Synthesis of bis-quinazolinone

or cyclohexanone under optimized reaction conditions (Scheme 5). The large-scale process delivered the target products (**3a**), with 92% and (**5a**) 91% yields within 65 and 70 min, respectively. It was observed that the gram-scale synthesis



Scheme 4. A plausible mechanism for the synthesis of DHQ catalyzed by alginate acid

is almost similar to mmol scale entry in terms of yield but requires more time to complete. The TON and TOF were also high for the gram scale.

To avoid the consumption of solvents during the isolation process, different methods (Method I and Method II) were attempted and their green metric values were calculated with a catalyst (Fig. 6). Method I involved the extraction of products with CHCl_3 (2×5 mL), while Method II involved the treatment of the reaction mixture with NaOH (5 mL, 0.1 N NaOH), followed by filtration. The use of aqueous NaOH treatment dramatically reduced the green metrics.

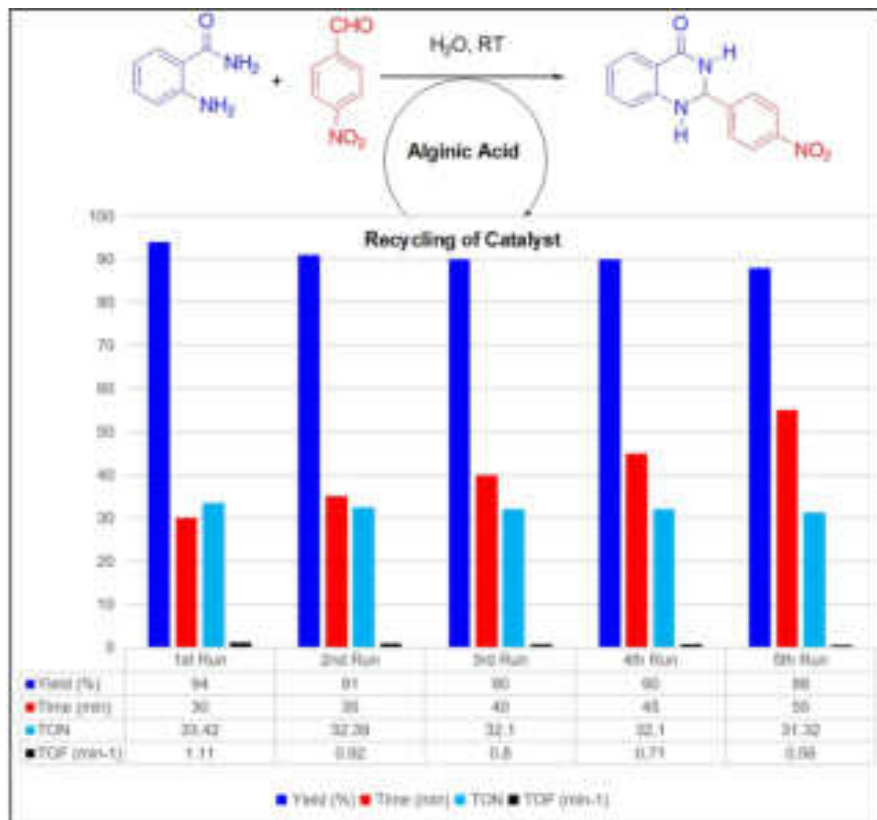
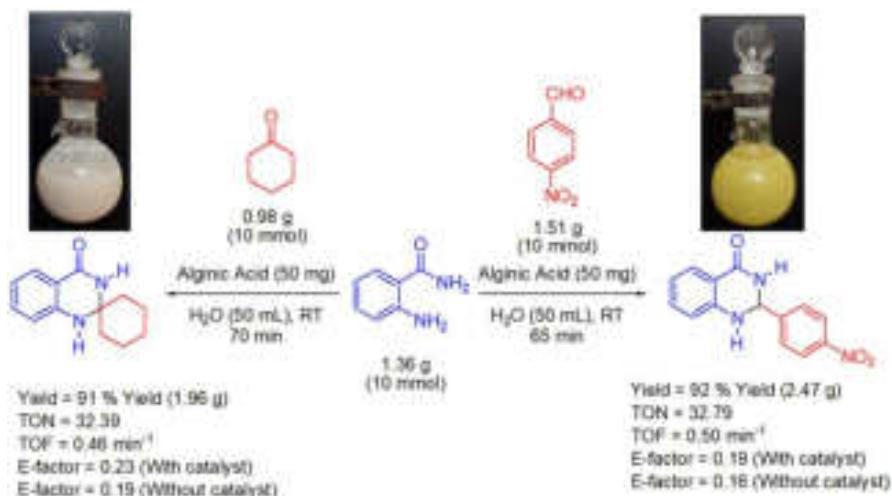


Fig. 5 Recyclability of the alginic acids for the synthesis of DHQ

General reflections on the evaluation of green metrics (estimation of greenness of present method)

Various sets of metrics were analyzed to estimate the "greenness" of syntheses [71, 72]. Green metrics measure the efficiency and environmental concert of chemical processes and can be better measured by environmental factor (E factor), turnover number (TON), turnover frequency (TOF), atom economy (AE), atom efficiency (AEf), carbon efficiency (CE), optimum efficiency (OE), effective mass yield (EMY), reaction mass efficiency (RME), mass productivity (MP), mass intensity (MI), and process mass intensity (PMI), as well as solvent and water intensity (SI and WI). These green chemistry metrics were measured for all reactions and depicted in Table S5.

The representative results of the model reaction under optimized reaction conditions are depicted in Fig. 7. The matrices were calculated by considering both the with and without catalyst. The results demonstrated that the values of green chemistry metrics are nearly close to their ideal values.



Scheme 5. Gram scale synthesis of products 3a and 5a

Extarion of product in 2 x 5 mL CHCl ₃		Reaction Mixture	Extarion of catalyst in 5 mL 0.1 N NaOH	
Product				Product
	Method-I	Parameter*		Method-II
	47.62	PMI		60.69
	27.78	MI (Excluding water)		1.15
	3.59	MP		86.95
	26.62	SI (Excluding water)		00
	19.84	WI		59.52

*All the parameters are calculated for model reaction with catalyst (Scheme 2)

Fig. 6 The green metrics analysis for the isolation of DHQ

- The green credentials such as safety, health, and environmental scores, and the overall ranking of solvents assessed in the present protocol by using the CHEM21 solvent selection guide [73] and COSMO-RS [74]. Thus, we used water as a solvent for the reaction, which is a highly recommended solvent for chemical processes (Table S6). Though we used EtOH for the recrystallization of crude products, its use is recommended. This was also supported by solvent intensity (SI=0) and water intensity (WI) parameters of the present protocol, which are found to be 52.08 – 81.52 g/g.

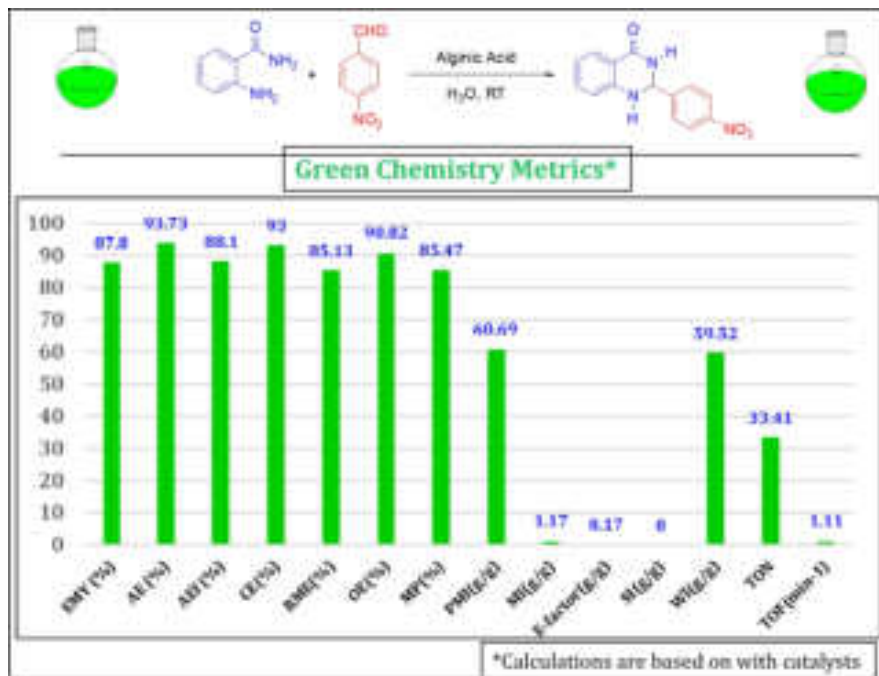


Fig. 7 The green metrics analysis for the synthesis of DHQ

- In current years the efficiency of the catalytic process has been evaluated by turnover number (TON) and turnover frequency (TOF) values [75]. The present catalyst attained TON = 29.17–33.46 and TOF = 0.66–1.11 min⁻¹.
- Effective mass yield (EMY) measures the environmental acceptability of a process. This metric defines yield in terms of the product made from non-toxic materials [76]. In the present method, EMY is 76.94–87.80% indicating the considerable greenness of the method.
- The DHQ can be synthesized straightforwardly in high yields. There is only the elimination of water as green waste. As all the products are obtained with good to excellent yields, the atom efficiency (AEf) for the present method is also excellent at 92.19–94.57% atom economy (AE) and 77.10–88.10% AEf.
- Carbon Efficiency (CE) and Mass productivity (MP) are used to elucidate reaction process consumption. The CE and MP for the present work are 81–100% and 75.18–85.47%, much better than the reported catalysts.
- Reaction mass efficiency (RME) is a realistic metric for describing the greenness of a process [77]. It accounts for yield, stoichiometry, and atom economy. In the present protocol, up to 85.13% RME is attained for 4-nitrobenzaldehyde, while 74.84% for 2-bromobenzaldehyde.
- Process mass intensity (PMI) is the total mass of materials used to produce a specified product. This is the key, high-level matrix for evaluating and benchmarking progress toward more sustainable manufacturing [71]. PMI evaluation (53.26–82.83 g/g) supports the above fact.

- Mass intensity (MI) accounts for the yield, stoichiometry, solvent, and reagent used in the reaction. The present method has MI ranges from 1.17 to 1.33 (g/g), which is near the ideal value of MI (MI = 1 g/g).
- Environmental Factor (E-factor) is a simple and fast metric for the evaluation of the environmental impact of industrial processes. It accounts for chemical yield and includes reagents; solvent loss and all process aids. The lower the E-factor, the lesser the waste generated in the process. The E-factor of the present method is between 0.17 and 0.33 (g/g) indicating the considerable greenness of the present protocol (the ideal E-factor is 0).
- In chemical reactions, a large amount of solvent used can be accounted for and assessed for the green matrix in terms of solvent intensity (SI) because of the significant environmental impact of solvents [78, 79]. Because SI excludes water from the calculations [71], the water intensity (WI) of a process should be calculated separately [80].

Conclusion

To summarize, a natural and eco-friendly process for creating 2,3-dihydroquinazolin-4(1H)-one analog has been developed using alginic acid as a catalyst. This method is advantageous because it has a low environmental impact and operates under mild conditions. The reaction occurs at room temperature through a simple stirring process, resulting in high yields. Additionally, this approach has a wide range of applications, can be easily scaled up, and allows for hassle-free product recovery. Its sustainability credentials have also been verified through green metrics evaluation. Overall, this alginic acid-catalyzed DHQ synthesis represents a promising greener alternative.

Supplementary Information The online version contains supplementary material available at <https://doi.org/10.1007/s11164-023-05147-8>.

Acknowledgements A. R. is a BARTI-Fellow and grateful to the Government of Maharashtra (India) for the financial support under Dr. Babasaheb Ambedkar National Research Fellowship (BANRF-2020) [BANRF-2020/21-22/850 dated 16/02/2022]. A. K. is grateful to the University Grants Commission, Government of India, New Delhi, for partially supporting this work under the scheme Major Research Project [F. No. 41-182/2014 (SR)].

Author's contributions The author confirms sole responsibility for the following: Principal author collected the data, carried out experimental work, drafted the manuscript preparation, and designed the schemes and figures. Second author: All second authors partly helped to characterize and calculate green matrices. Corresponding author designed the manuscript, formatted figures and schemes, and contributed to analysis and interpretation of data.

Funding There is no funding available for publication.

Availability of data and materials The data will be available upon reasonable request.

Declarations

Conflict of interest The authors declare that they have no known competing financial interests or personal relationships that could have appeared to influence the work reported in this paper.

Ethical approval There are no human subjects in this research article, and informed consent is not applicable.

References

1. M. Asif, *Int. J. Med. Chem.* **2014**, 395637 (2014)
2. S.B. Mhaske, N.P. Argade, *Tetrahedron* **62**, 9787 (2006)
3. R.S.M. Ismail, N.S.M. Ismail, S. Abuserii et al., *Fut. J. Pharmaceutical Sci.* **2**, 9 (2016)
4. H. Zhang, H. Liu, X. Luo et al., *Eur. J. Med. Chem.* **25**, 235 (2018)
5. S. Seyedmousavi, H. Rafati, M. Ilkit et al., *Methods Protocols.* **1508**, 107 (2016)
6. D.A. Horton, G.T. Bourne, M.L. Smythe, *Chem. Rev.* **103**, 893 (2003)
7. R. Williams, C.M. Niswender, Q. Luo et al., *Bioorg. Med. Chem. Lett.* **19**, 962 (2009)
8. A.V.Dhanunjaya Rao, B. P. Vykuteswararao, T. Bhaskarkumar et al., *Tetrahedron Lett.* **56**, 4714 (2015)
9. N. Azizi, F. Shirde, *Res. Chem. Intermed.* **43**, 3873 (2017)
10. K.S. Gajulaa, N. Mamedaa, S.K.D. Chevella et al., *Synth. Commun.* **48**, 2866 (2018)
11. G. Yashwantrao, V.P. Jejurkar, R. Kshatriya et al., *ACS Sustain. Chem. Eng.* **7**, 13551 (2019)
12. K.H. Narasimhamurthy, Y.R. Girishb, N. Thimmarajuc et al., *Chem. Data Collec.* **21**, 100230 (2019)
13. F. Olivito, N. Amodio, M.L. Di Gioia et al., *Med. Chem. Commun.* **10**, 116 (2019)
14. M. Badolato, F. Aiello, N. Neamat, *RSC Adv.* **8**, 20894 (2018)
15. M. Sharma, S. Pandey, K.Chauhan et al. *J. Org. Chem.* **77**, 929 (2012)
16. V.B. Labade, P.V. Shinde, M.S. Shingare, *Tetrahedron Lett.* **54**, 5778 (2013)
17. C. Liu, Q. Wang, Z. Xu et al., *Synth. Commun.* **52**, 1537 (2022)
18. S. Zhaleh, N. Hazeri, M. Maghsoodlou, *Res. Chem. Intermed.* **42**, 6381 (2016)
19. S. Karhale, D. Survase, R. Bhat et al., *Res. Chem. Intermed.* **43**, 3915 (2017)
20. Q. Ding, J. Zhang, J. Chen et al., *J. Heterocycl. Chem.* **49**, 375 (2012)
21. K.M. Mustaque, A. Subramani, T.K. Shabeer et al., *Lett. in Org. Chem.* **15**, 246 (2018)
22. J. Chen, W. Su, H. Wu et al., *Green Chem.* **9**, 972 (2007)
23. Y.H. Shang, L.Y. Fan, X.X. Li et al., *Chin. Chem. Lett.* **26**, 1355 (2015)
24. D. Shi, L. Rong, J. Wang et al., *Tetrahedron Lett.* **44**, 3199 (2003)
25. Z.H. Zhang, H.Y. Lu, S.H. Yang et al., *J. Comb. Chem.* **12**, 643 (2010)
26. Y.X. Zong, Y. Zhao, W.C. Luo et al., *Chin. Chem. Lett.* **21**, 778 (2010)
27. A. Shaabani, A. Maleki, H. Mofakham et al., *Synth. Commun.* **38**, 3751 (2008)
28. P.V.N.S. Murthy, D. Rambabu, G.R. Krishna et al., *Tetrahedron Lett.* **53**, 863 (2012)
29. O. Obaiah, N.N. Kebbahalli, R.M. Goravanahalli et al., *Eur. J. Chem.* **5**, 671 (2014)
30. A. Ghorbani-Choghamarani, Z. Darvishnejad, M. Norouzi *Appl. Organomet. Chem.* **29**, 707 (2015)
31. M. Beyki, M. Fallah-Mehrjardi *Lett. in Org.Chem.* **15**, 1 (2018)
32. H. N. Dadhania, D. K. Raval, A. N. Dadhania *Res. Chem. Intermed.* **44**, 117 (2017)
33. N.N. Pesyan, A.D. Asl, S. Namdar. *Appl. Organomet. Chem.* **34**, e5710 (2020)
34. G. K. Kharmawlong, R. Nongrum, B. Chhetri et al., *Synth. Commun.* **1** (2019)
35. F. Havasi, A. Ghorbani-Choghamarani, F. Nikpour. *Microporous Mesoporous Mater.* **224**, 26 (2016)
36. M.A. Erfan, B. Akhlaghinia, S. S. E. Ghodsinia *Chem. Select* **5**, 2306 (2020)
37. L. Heidari, L. Shiri. *Appl. Organomet. Chem.* **33**, e4636 (2019)
38. K.S. Gajulaa, N. Mamedaa, S. Kodumuria et al., *Synth. Commun.* **48**, 2866 (2018)
39. J. Mou, N. Chen, Y. Zhao et al., **8**, 239 (2020) www.frontiersin.org
40. S. Chehab, Y. Merroun, T. Ghailane et al., *Polycycl. Aromat. Compd.* **42**, (2022)
41. M. Wang, J.J. Gao, Z.G. Song et al., *Chem. Heterocycl. Compd.* **47**, 851 (2011)
42. R.Z. Qiao, B.L. Xu, Y. H. Wang. *Chin. Chem. Lett.* **18**, 656 (2007)
43. H.R. Safaei, M. Shekouhy, S. Ghorbanzadeh *Chem. Select.* **3**, 4750 (2018)
44. P.Yerram, R. Chowrasia, S. Seeka et al., *Eur. J. Chem.* **4**, 462 (2013)
45. J. Wu, X. Du, J. Ma et al., *Green Chem.* **16**, 3210 (2014)
46. B.B.F. Mirjalili, Z. Zagbaghi, A. Monfared. *J. Chin. Chem. Soc.* **67**, 197 (2020)
47. K. Ramesh, K. Karnakar, G. Satish et al., *Tetrahedron Lett.* **53**, 6936 (2012)
48. J. Safari, S. Gandomi-Ravandi, *RSC Adv.* **00**, 1 (2013)
49. G. Hedouin, D. Ogulu, G. Kaur et al., *Chem. Commun.* **59**, 2842 (2023)

50. L.L. Mao, L.X. Quan, Y. Liu et al., *Curr. Opin. Green Sustain. Chem.* **40**, 100756 (2023)
51. S. Kamat, Y. Indi, A. Kumbhar et al., *Res. Chem. Intermed.* **48**, 3223 (2022)
52. A. Kumbhar, R. Salunkhe, *Curr. Org. Chem.* **19**, 2075 (2015)
53. Á. Molnár, A. Papp, *Catal. Sci. Technol.* **4**, 295 (2014)
54. A. Haug, B. Larsen, O. Smidsrød, *Carbohydr. Res.* **32**, 217 (1974)
55. S. Saji, A. Hebden, P. Goswami et al., *Sustainability* **14**, 5181 (2022)
56. L. Li, Y. Fang, R. Vreeker et al., *Biomacromol* **8**, 464 (2007)
57. X. Guo, Y. Wang, Y. Qin et al., *Int. J. Biol. Macromol.* **162**, 618 (2020)
58. A. Srivastava, A. Yadav, S. Samanta, *Tetrahedron Lett.* **56**, 6003 (2015)
59. A. Maleki, Z. Varzi, F. Hassanzadeh-Afrouzi, *Polyhedron* **171**, 193 (2019)
60. T. Kitanosono, K. Masuda, P. Xu et al., *Chem. Rev.* **118**, 679 (2018)
61. Y.S. Zhu, L. Shi, L. Fu et al., *Chin. Chem. Lett.* **33**, 1497 (2022)
62. Y. Guo, Y. Liu, J. Wan, *Chin. Chem. Lett.* **19**, 23 (2021)
63. J. Lu, E. Ma, Y. Liu et al., *RSC Adv.* **5**, 59167 (2015)
64. L. Shen, Z. Chen, Q. Zheng et al., *ACS Catal.* **11**, 12833 (2021)
65. A. Kumbhar, S. Kamble, M. Barge et al., *Tetrahedron Lett.* **53**, 2756 (2012)
66. A. Kumbhar, S. Jadhav, R. Shejwal et al., *RSC Adv.* **6**, 19612 (2016)
67. A. Kumbhar, S. Jadhav, S. Kamble et al., *Tetrahedron Lett.* **54**, 1331 (2013)
68. S. Jadhav, A. Kumbhar, R. Salunkhe, *Appl. Organomet. Chem.* **29**, 339 (2015)
69. S. Jadhav, A. Jagdale, S. Kamble et al., *R. Salunkhe. RSC Adv.* **6**, 3406 (2016)
70. M.G. Dekamin, Z. Karimi, Z. Latifidoost et al., *Int. J. Biol. Macromol.* **108**, 1273 (2018)
71. C. Jimenez-Gonzalez, C.S. Ponder, Q.B. Broxterman et al., *Org. Process Res. Dev.* **15**, 912 (2011)
72. G. Brahmachari, M. Mandal, I. Karmakar et al., *ACS Sustainable Chem. Eng.* **7**, 6369 (2019)
73. D. Prat, A. Wells, J. Hayler et al., *Green Chem.* **18**, 288 (2015)
74. J. Esteban, A.J. Vorholt, W. Leitner, *Green Chem.* **22**, 2097 (2020)
75. S. Kozuch, Jan M. L. Martin, *ACS Catal.* **12**, 2787 (2012)
76. T. Hudlicky, D. A. Frey, L. Koroniak et al., *Green Chem.* **57** (1999)
77. D.J.C. Constable, A.D. Curzons, V.L. Cunningham, *Green Chem.* **4**, 521 (2002)
78. A.D. Curzons, D.C. Constable, V.L. Cunningham, *Clean Prod. Process.* **1**, 82 (1999)
79. K. Alfonsi, J. Colberg, P.J. Dunn et al., *Green Chem.* **10**, 31 (2008)
80. C. Jiménez-González, A.D. Curzons, D.J.C. Constable et al., *Clean Prod. Process.* **7**, 42 (2004)

Publisher's Note Springer Nature remains neutral with regard to jurisdictional claims in published maps and institutional affiliations.

Springer Nature or its licensor (e.g. a society or other partner) holds exclusive rights to this article under a publishing agreement with the author(s) or other rightsholder(s); author self-archiving of the accepted manuscript version of this article is solely governed by the terms of such publishing agreement and applicable law.

Authors and Affiliations

Archana Rajmane¹ · Dipti Jadhav¹ · Kiran Bagade¹ · Suresh Patil² · Arjun Kumbhar¹

✉ Arjun Kumbhar
arjun22win@rediffmail.com

¹ Department of Chemistry, Vivekanand College (Empowered Autonomous), Kolhapur, Maharashtra 416003, India

² P. D. V. P. College (Affiliated to Shivaji University, Kolhapur), Tasgaon, Maharashtra 416312, India

MAH/MUL/ 03051/2012

ISSN :2319 9318



One Day National Interdisciplinary Conference 28 April 2023
Organized by Rayat Shikshan Sanstha's Prof. Dr. N.D. Patil Mahavidyalaya, Malkapur
(Perid)



Rayat Shikshan Sanstha's
Prof. Dr. N. D. Patil Mahavidyalaya, Malkapur (Perid)
One Day National Interdisciplinary Conference
On

Literary Trends and Issues in 21st Century

Friday, 28 April 2023

Organized by

Departments of Marathi, Hindi, English, and IQAC

Chief Editor: - Dr. Gholap Babu Ganpat

❖ विद्यावार्ता या आंतरविद्याशाखीय बहुभाषिक त्रैमासिकात व्यक्त झालेल्या मतांशी मालक, प्रकाशक, मुद्रक, संपादक सहमत असतीलच असे नाही. न्यायक्षेत्र:बीड

"Printed by: Harshwardhan Publication Pvt.Ltd. Published by Ghodke Archana Rajendra & Printed & published at Harshwardhan Publication Pvt.Ltd.,At.Post. Limbaganesh Dist,Beed -431122 (Maharashtra) and Editor Dr. Gholap Babu Ganpat.

Reg.No.U74120 MH2013 PTC 251205

Harshwardhan Publication Pvt.Ltd.

At.Post.Limbaganesh,Tq.Dist.Beed

Pin-431126 (Maharashtra) Cell:07588057695,09850203295

harshwardhanpubli@gmail.com, vidyawarta@gmail.com

All Types Educational & Reference Book Publisher & Distributors / www.vidyawarta.com

- 25) एकविसाव्या शतकातील मराठी कादंबरी
मंगेश सुभाष दुर्तोडे, जिल्हा अहमदनगर ||116
- 26) एकविसाव्या शतकातील आदिवासी कविता
प्रा.डॉ.बी.टी.दाभाडे, जि.रत्नागिरी ||118
- 27) मुस्लीम समाजाचे वास्तव चित्रण करणारा कवी अजीम नवाज राही
डॉ.संभाजी बाबाराव सावंत, जि.जळगाव ||121
- 28) एकवीसाव्या शतकातील शेतकरी आणि 'अवकाळी पावसाच्या दरम्यानची गोष्ट'
प्रा. प्रमोद नेताजी पाटील, कोल्हापूर ||124
- 29) मराठी साहित्यातील जीवनमूल्यांचा वेध व 'वडार वेदना' कादंबरीचे आकलन
प्रा. स्वाती प्रभाकर मगदूम, रामानंदनगर (बुर्ली) ||127
- 30) 'निंभार': आत्मनिष्ठ जाणिवेचा आविष्कार
प्रा. संजय शंकर सुतार, डॉ. ज्ञानेश्वर रामचंद्र कांबळे, इचलकरंजी ||131
- 31) मराठीतील ललित स्तंभलेखन : संकल्पना, स्वरूप आणि व्याप्ती
डॉ.नावडकर विद्या विजय, सातारा (स्वायत्त) ||135
- 32) दिनेश काळे यांच्या कादंबरीतील प्रतिनायिका व प्रतिनायक
प्रा.डॉ. प्रियदर्शनी वसंतराव देशमुख, जि.अमरावती ||141
- 33) ठाकर आदिवासींचे संचित: पिंगुळीच्या अंगणात
प्रा. वसंत पानसरे, माटुंगा ||144
- 34) मेंढपाळ कुटुंबामधील तरुणाच्या संघर्षमय जीवनाची गाथा : फेसाटी
प्रा.कोटरंगे दत्ता नामदेव, जि.धाराशिव ||148
- 35) परिघावरील लैंगिकता आणि मराठी साहित्य
डॉ. शीतल पावसकर भोसले, उल्हासनगर ||151
- 36) एकविसाव्या शतकातील 'साठेचं काय करायचं?' जागतिकीकरणाच्या परिप्रेक्ष्यातून..
वैशाली योगेश जोशी, मुंबई ||159

२) मध्ययुगीन कालखंडातील साहित्याने मूल्यांचा पाया घातला परंतु स्वातंत्र्योत्तर काळातील साहित्यातून मूल्यांचा विकास अधिक होणे आवश्यक होते तसे चित्र दिसत नाही.

३) मानवी जीवन विकसित व यशस्वी करण्याची क्षमता मूल्यांमध्ये आहे. शाश्वत मूल्यांची परखण नवोदित साहित्यातून होणे गरजेचे आहे.

४) साहित्यातून मानवी जीवनमूल्य जपली जात नसतील तर ते साहित्य समृद्ध आहे असे म्हणणे निरर्थक ठरते.

५) मानवी जीवनात मूल्यांना फार महत्त्व आहे ते साहित्यिकांनी आपल्या साहित्यातून जोपासणे तितकेच महत्त्वाचे आहे.

संदर्भग्रंथ

१.कोत्तापल्ले, डॉ. नागनाथ, 'आधुनिक मराठी कविता एक दृष्टिक्षेप' प्रतिभास प्रकाशन, परभणी, २००७.

२. राऊत, डॉ. अनंत, 'मूल्यनिष्ठ समाजघडणीत साहित्याची भूमिका', कैलास पब्लिकेशन्स, औरंगाबाद, प्रथमावृत्ती २६ जानेवारी २००८.

३. गोसावी, र. रा. 'पाच भक्तीसंप्रदाय', प्रतिमा प्रकाशन, पुणे तृतीयावृत्ती, १५ ऑगस्ट २००८

४. खैरनार, डॉ. दिलीप, 'भारतीय समाजातील नैतिक मूल्ये', डायमंड पब्लिकेशन्स, पुणे, प्रथमावृत्ती २००६.

५. गायकवाड, लक्ष्मण . वडार वेदना, प्रथमावृत्ती २०००

ॐॐॐ

30

'निंभार': आत्मनिष्ठ जाणिवेचा आविष्कार

प्रा. संजय शंकर सुतार

मराठी, विभागप्रमुख,

दत्ताजीराव कदम आर्ट्स, सायन्स अण्ड कॉमर्स
कॉलेज, इचलकरंजी

डॉ. ज्ञानेश्वर रामचंद्र कांबळे

सहायक प्राध्यापक,

दत्ताजीराव कदम आर्ट्स, सायन्स अण्ड कॉमर्स
कॉलेज, इचलकरंजी

प्रत्येक व्यक्तीच्या अंतर्मनात एखादा लेखक दडलेला असतो. एखाद्या पाषाणातून पाझर फुटावा व त्या उमाळ्यातून ओलावा निर्माण होऊन त्यातून अंकुर फुटावेत अशा अंतःप्रेरणेतून लेखक आपलं जगण साहित्याच्या परिघात मांडत असतो. अशा अनुभवसंपन्न आशय विचारामधून साहित्यकृती जन्म घेते. अशी साहित्यकृती त्या वाङ्मयप्रवाहातील मैलाचा दगड म्हणून ठसठशीतपणे उभी राहते. तिचे अस्तित्व त्या साहित्य प्रकारातील नवे संदर्भमूल्य म्हणून अधोरेखित होते. या अनुषंगाने साहित्य जगतात 'दीर्घ कथनात्मक गद्याचा आविष्कार म्हणून कादंबरीकडे पाहिले गेले आहे'. कादंबरी हा मुद्रणोत्तर जगतातील आधुनिक साहित्यप्रकार म्हणून ओळखला गेला आहे. या साहित्य प्रकारातून व्यक्ती आणि समाज यांच्यामधील नातेसंबंधांची वीण प्रामुख्याने गुंतलेली असते. त्या नात्यासंबंधाच्या भोवतालच्या परिघात घडलेल्या स्थित्यंतराचे वैश्विक रूप कादंबरीतून प्रकटत जाते. पाश्चात्य जगात आधुनिकतेमधून निर्माण झालेल्या नवमध्यमवर्गातून आकारास आलेल्या या वाङ्मय प्रकारात जागतिकीकरणानंतर मानवी जीवनावर झालेल्या अनुकूल-प्रतिकूल बदलांकडे समग्र दृष्टीने लक्ष

वेधले आहे. तदनंतर झालेल्या वैश्विक बदलांकडे विविध साहित्य प्रवाहांप्रमाणे कादंबरीच्या माध्यमातूनही मानवी भावभावना, माणूस व समाजामधील नातेसंबंधांची गुंतागुंत, त्यासह भोवतालच्या वास्तवाच्या विविध परि आणि सीमा अधोरेखित करित भाषिक प्रयोगाच्या आणि अर्थाच्या शक्यता कादंबरीमधून पडताळले गेलेले दिसून येतात.

काळाच्या प्रत्येक टप्प्यांवर बदलत्या स्थित्यंतरानुसार 'वर्तमानाचे नवे रचित साकारणारी कादंबरी नवी भाषा, नवे रचनाबंध, नवी मूल्ये रुजवण्याचे आणि वाचकांची अभिरुची घडवण्याचे काम करत आहे.' विशेषतः एकविसाव्या शतकातील बहुतांश कादंबऱ्यांमधून सिमित अवकाशाच्या पलीकडे नवी परिमाणे शोधत आधुनिक जगातील बदलत्या मूल्यदृष्टीचा वेध घेत एक नवी जीवनदृष्टी साहित्यातून प्रकट झालेली दिसते. त्यामध्ये प्रामुख्याने 'बारोमास', 'भूमी', 'गाथा सप्तपती', 'संभुती', 'वारूळ', 'चाळेगत', 'इळनमाळ', 'शाळा', 'आगळ', 'अवकाळी पावसाच्या दरम्यानची गोष्ट', 'जोहार', 'नवं कटवन', 'पोटमारा', 'सायड', 'अवघाचि संसार', 'आटपाट देशातल्या गोष्टी', 'स्वतःला फालतू समजण्याची गोष्ट', 'उद्या', 'रौदाळा', 'पडझड', 'धुळपावल', 'बगळा', 'निशाणी डावा अंगठा', 'लॅडमाफिया', 'रिबोट', 'रहबर', 'जुगाड', 'उजव्या सोंडेच्या बाहुल्या', 'झडझिंबड', 'गाज', 'ईश्वर डॉट कॉम', इत्यादी प्राथमिक कादंबऱ्यांमधून भोवतालच्या काळाचे संदर्भ शोधत मानवी जीवनाच्या अवस्थांतरांचे प्रतिबिंब शोधण्याचा जाणीवपूर्वक प्रयत्न केल्याचे दिसून येते. या स्थित्यंतराच्या कालौघात सामान्य माणूस त्याच्या उध्वस्तपणाचे, रितेपणाचे, गारठलेल्या संवेदनाचे, शेतीच्या अधोगतीतून चक्रव्यूहात सापडलेल्या कृषिसंस्कृतीचे विदारक सत्य मांडताना माणसाचे एकाकीपण संस्कृतीचा पोकळ बडिवार, सामाजिक संबंधातील बदलते संदर्भ, मानवी जीवनातील अतर्क्य, असंगततेला स्पर्श करणारी परिस्थिती यांचे वेगळेपण अधोरेखित करणाऱ्या वरील कादंबऱ्यांच्या वर्तुळविश्वात 'निंभार' ही आशय आकाराचे अभिनत्व मांडणारी एक प्रयोगशील कादंबरी म्हणून तीचे महत्त्व अधोरेखित होते. वास्तवाच्या अंतरंगात जाऊन जे जाणवले त्याचा आत्मसाक्षात्कार करताना

दिसून येते. 'निंभार' म्हणजे मध्यान्हीचे तळपतं ऊन. प्रत्येक व्यक्तीच्या आयुष्यात ऊन सावल्यांचा खेळ चालत असतो. धगधगत्या उन्हात होणारी तगमग ही अस्वस्थता निर्माण करते. ही अस्वस्थता लेखक संतोष तेंडुलकर यांच्या लेखन सामग्रीचे आत्मबळ म्हणून पुढे येते आणि त्यातून 'निंभार' सारख्या प्रयोगशील कादंबरीची रचनानिर्मितीची प्रक्रिया घडते.

जीवनानुभवाचे 'समृद्ध स्तर मांडणारी प्रस्तुत कादंबरी समाजजीवनाच्या अनेकस्तरीय वाटा धुंडाळताना दिसते.' या कादंबरीचा निवेदक हा ताऊन सुलाखून निघालेल्या परिस्थितीवर मात करित शिक्षणाची उमेद जागवण्याचे आत्मभान जपतो. कोकणातल्या कोंडये गावाच्या केंद्रावर्ती घटनांचा पसारा मांडताना कोकणातील नैसर्गिक स्थित्यंतरे कौटुंबिक, सामाजिक अस्थिरता यामधून शिक्षणासाठीची झालेली धावाधाव या सर्वांच्या रेखतून निवेदक आपली इच्छाशक्तीची उमेद जपून ठेवतो. माध्यमिक शिक्षण घेत असताना घडत गेलेल्या घटनाक्रमामधून मॅकेनिकल डिप्लोमा झालेला निवेदक सौदी अरेबिया येथील तैवान मधील मिळालेल्या संधीमधून स्वतःला सिद्ध करण्याचा प्रयत्न करतो. येणार्या प्रत्येक संकटांशी सामना करित स्वतःला घडवत जातो. तेथे वास्तव्यास असताना आंतरराष्ट्रीय देशातील सांस्कृतिक संदर्भ तेथील व्यक्तिस्वातंत्र्य, संस्कृति-सभ्यता, परंपरा, स्त्री-पुरुष विचारधारा या सर्वांमध्ये भारत देश कसा उजवा आहे. याची प्रचिती या निमित्ताने निवेदकाने कादंबरीच्या माध्यमातून स्वानुभवातून विस्तृतपणे रेखाटली आहे. तैवान मधील भाषा, लोकविचार, भाव भावना, आचार-विचार यातील प्रस्तुत कादंबरीच्या रचना सौंदर्या बरोबर भाषा-सौंदर्यात वेगळेपणाची अनुभूती देते. व्यावसायिक जीवनदृष्टिकोनासह लेखकाने गावखेड्यांच्या वैशिष्ट्यांचा माणसांचा, तेथील ग्रामीण जीवनाचे दिलेले संदर्भ कादंबरीत विशेषत्वाने नजरेत भरते.

कोकणातल्या गतस्मृतींना उजाळा देणारा निवेदक कादंबरीच्या माध्यमातून त्यामध्ये विरघळून जातो. कोकणातल्या भोवतालात आपले बालपण शोधताना तिथल्या नैसर्गिक वातावरणातील संस्कृतिविशेषामधील झालेले बदल अत्यंत मार्मिक

पद्धतीने टिपले आहेत. कोकण म्हणजे निसर्ग, समुद्र आणि फणसासारखी माणसे त्यांच्या व्यथा वेदनांचे मनोरे लेखकाने कादंबरीत उभारलेले आहेत. कोकणी माणसांमधला चिकित्सकपणा त्याच्यामधील काटकपणा या स्वाभाविक वैशिष्ट्यंमधून अनेक पात्रांमधून वेगळेपण दृष्टीक्षेपात येते. विविध प्रसंगामधून अनेक वृत्ती-प्रवृत्तीच्या माणसांमुळे 'निवेदकाचे' जीवन बदलण्यास ही माणसं कारणीभूत झालेली दिसतात. निवेदकाच्या वडिलांनी आयुष्यभर भली-बुरी माणसं जपली व वाढवली पण नंतरच्या काळात त्यांनी सोडलेली साथ ही विचार करण्यास प्रवृत्त करते.

वरील मानवी वैशिष्ट्यंखेरीज कोकणातील पावसाळ्यापूर्वी व नंतरचे जीवन, निसर्गाच्या प्रतिकूलतेनुसार कोकणी माणसाची वाटचाल खाचे विशेष कादंबरीतून पुढे येते. यामध्ये मसाल्याचे काम करणारी सखू सोनारीन, उबदार गोधड्य शिवणारी जनाबाई. पाडाला आलेले रायवळ आंबे उतरून आडी लावणारा आबा शिवगण, भातलागणीच्या वेळी चिखलावर काटेरी गुफा (दाता) फिरवणारा वासु व त्यावर उभा राहणारा नाता परब, अनैतिकतेच्या चक्रव्यूहात सापडलेला गोपाळ तसेच निवेदकाच्या घरी गोठ्यातील जनावरांची काळजी घेणारा पांडू या शिवाय लेखकाचं जीवन बदलण्यास कारणीभूत ठरलेली आई, वडील, भाऊ व बना मावशी, सर्व भावंड ही पात्रे निवेदकाच्या जगण्यावर खोलवर परिणाम करताना दिसून येतात.

प्रस्तुत कादंबरीतील ही जीवाभावाची माणसं हीच निवेदकाच्या जगण्याला अर्थ प्राप्त करून देणारे घटक आहेत. इथल्या सामान्य माणसांमध्ये देवपण शोधणारा नायक कोकणातल्या रिती, परंपरा संस्कृतिसंघर्ष, उत्सवातील वेगळेपण या कादंबरीच्या रूपाने मांडत जातो. प्रत्येक सण उत्सवातील कोकणी माणसांनी जपलेलं वैभव भातशेतीच्या दरवळाप्रमाणे खर्गाअर्थाने कादंबरीतून पाझरताना दिसते. 'कादंबरीकार अशा घटनांची निवड आणि मांडणी करीत असतो. ज्यांच्या द्वारा भोवतीच्या विश्वातील माणसे, त्यांचे परस्पर संबंध व सामाजिक संस्था व त्यांची तत्वे यावर प्रकाश पडावा तसेच त्या विशिष्ट काळातील सामाजिक व नैतिक मूल्ये आणि तो वर्णन करीत असलेल्या कल्पित

विश्वातील सामाजिक वा नैतिक मूल्ये यांच्याशी वाचक कुठेतरी नाते जोडू शकेल' या भूमिकेतून लेखक संतोष तेंडुलकरांनी निवेदकाच्या जीवनव्यवहाराशी आपली नाळ कायम ठेवत वाचकाला प्रेरित केले आहे. कोकणातून स्थलांतर होणारे चाकरमानी त्यांचे प्रश्न याशिवाय मुंबईत राहणाऱ्या सामान्य माणूस हा केवळ ग्राहक' याच केंद्रस्थानी राहिल्याने त्यामुळे निर्माण झालेल्या परिस्थितीचे आत्मचिंतन कादंबरीच्या वर्तुळ परीघातून घडताना जाणवते. साहजिकच आधुनिकतेच्या जगतात नवमूल्यांची होणारी हेळसांड या कादंबरीच्या रूपाने समोर येते. प्रस्तुत कादंबरीच्या निवेदकाच्या वाटचला आयुष्यभर संघर्ष आला. त्यामधून स्वतःला शोधताना आपल्या आशा-आकांशा याचं निर्माल्य करावं लागलं. तरीही उद्याच्या नव्या दिवसाचा शोध घेणारा निवेदक प्रेरणास्रोत म्हणूनच पुढे येताना जाणवतो. जीवनाच्या या कोलाहलात स्वत्व जपताना आई-वडील हीच उर्जा निवेदकाच्या प्रत्येक प्रतिकूल परिस्थितीशी संघर्ष करण्यासाठी बळ देते. कुटुंब जपणारी आई ही कर्त्या पुरुषाची जागा घेताना दिसते. तर आजारपणात वडिलांची काळजी घेणारी कुटुंबवत्सल आई मध्ये लेखक श्यामच्या आईचे रूप शोधताना दिसतो. आयुष्यभर कष्टणारी आई बरोबरच ज्यांनी गावाला 'दिशा' दिली व गाव जपला त्या वडिलांनी समाजाला आधुनिक विचार देण्याचा प्रयत्न केला. सतत नव्या उद्योग व्यवसायातून वेगळेपण शोधण्याचा ध्यास घेतला. पण लोकांनी त्यांच्या पडत्या काळात पाठ फिरविली ही अस्वीकार्य गोष्ट लेखकाच्या अंतर्मनाला छेदून टाकते. समाज व्यवस्थेतील वेगाने होणारे बदल लेखकाने सूक्ष्म तपशिलांसह मांडत हरवत चाललेल्या मानवी मूल्यांकडे लक्ष वेधले आहे. आयुष्यभर कष्टमय जीवन जगलेल्या निवेदकाच्या वडिलांच्या वाटचाला नियतीने लिह्वर कॅन्सरचे व्याधीग्रस्त जगणे बहाल करून निवेदकाला पुन्हा चक्रव्यूहात टाकले. आजारपणात त्यांची शुश्रूषा घेणाऱ्या व जीवापाड प्रेम करणाऱ्या नायकाच्या वाटचला शेवटी अत्यंतदर्शन घ्यावे लागले अन् त्याच वेळी काही अंतराने गेलेल्या आईच्या निधनाने दुहेरी संकटात नायकाच्या भोवती आभाळ कोसळते.

सारं उसवतं आयुष्य आम्ही टाके हे घालतो
इथं वैशाख वणवा आम्ही पाऊस शोधतो

अशा संघर्षमयी जीवनाच्या विविधांगी
कोनांमधून लेखक आपल्या अस्तित्वाचा खुणा
शोधताना दिसून येतात.

प्रस्तुत कादंबरीत मराठी, हिंदी मिश्रित व
कोकणी भाषेची रूपे आविष्कृत झालेली दिसतात
याशिवाय कोकणात नाव घेऊन बोलावण्याची पद्धती
त्यामधील गोडवा, प्रादेशिक म्हणीमधून कादंबरीच्या
भाषा सौंदर्यात भर पडलेली दिसून येते. संतोष तेंडुलकर
व लिखित या आत्मनिवेदनपर कादंबरीत
व्यवधानांमधून समाज, गावखेडे, शोषणव्यवस्था,
शहरीकरणाच्या समस्या, मुंबईतील स्थित्यंतरे, जागतिक
संदर्भातील भारत या सर्वांचे परि आणि सीमा यांना
अधोरेखित करण्याचा यशस्वी प्रयत्न केला आहे. ज्या
पद्धतीने भालचंद्र नेमाडे यांच्या 'बिठार', 'जरीला',
'झूल' तसेच विलास सारंग यांच्या 'एन्कीच्या राज्यात',
भाऊ पाध्ये यांची 'बॅरिस्टर अनिरुद्ध धोपेश्वर', किरण
नगरकर यांची 'सात सक्कं त्रेचाळीस', दीनानाथ मनोहर
यांच्या 'मन्वंतर' प्रमाणे 'निंभार' मधून माणसांच्या दैनंदिन
जीवन व्यवहारांमधील अनाकलनीयता, असंगतता,
एकाकीपणाची आत्मजाणीव व त्यातील अस्वस्थता
यामधील आत्मनिष्ठ जाणिवेतून स्व-शोधार्थ निघालेल्या
लेखकाने भोवतालचा जगाचे दर्शन घडविले आहे.
अशा काल व अवकाशाचा विस्तृत पटात अस्तित्वाचा
शोध घेणारी ही कादंबरी संकल्पनात्मक बदलांकडे
लक्ष वेधून घेते. तसेच मानवतेच्या संचिताचे भाष्य
करणारी कादंबरी म्हणून 'निंभार' तळपत्या मध्यानहीच्या
उन्हाप्रमाणे विचारांचे 'काहूर निर्माण करण्यात यशस्वी
होईल अशी आशा वाटते.

संदर्भ ग्रंथसूची :

- १) तेंडुलकर, संतोष 'निंभार', तेजश्री प्रकाशन,
कबनूर, २०२३.
- २) थोरात, हरिश्चंद्र 'कादंबरी विषयी' पद्मगंधा
प्रकाशन, पुणे, २००६.
- ३) इनामदार-साने, रेखा' अस्तित्त्ववाद आणि मराठी
कादंबरी', राजहंस प्रकाशन, पुणे, २००४.
- ४) जाधव, रा.ग (संपा.) 'मराठी वाङ्मयाचा इतिहास'

खंड- सातवा, भाग तिसरा, महाराष्ट्र साहित्य परिषद, पुणे,
२०१०.

५) सानप, किशोर 'मराठी कादंबरी नव्या दिशा'
निर्मल प्रकाशन, नांदेड, २००५.

६) घोंगडे, बाळासाहेब' अक्षर पेरणी - कादंबरी
निर्मिती प्रक्रिया' विशेषांक' ऑक्टोबर - नोव्हेंबर-डिसेंबर,
२०१६.

७) थोरात, हरिश्चंद्र 'कादंबरी: एक साहित्यप्रकार'
, शब्द पब्लिकेशन, मुंबई, २०१०.

८) काळे, मंगेश नारायणराव '१९६० नंतरचे बदलते
संदर्भ आणि मराठी कादंबरी', 'खेळ' नव्वदोत्तर कादंबरी
विशेषांक, जून २०१४.

९) गणोरकर, प्रभा आणि इतर (संपा.) वाङ्मयीन
संज्ञा संकल्पना कोश, ग.रा. भटकळ फाउण्डेशन, मुंबई,
२००१.

१०) राज्याध्यक्ष, विजया 'मराठी वाङ्मयकोश',
समीक्षा - संज्ञा, खंड - चौथा, महाराष्ट्र राज्य साहित्य
आणि संस्कृती मंडळ, मुंबई, २०११.

ॐॐॐ



SHIVAJI UNIVERSITY, KOLHAPUR

Volume-49 Issue-2 (July, 2023)

ISSN-Science-0250-5347

Estd. 1962
"A++" Accredited by NAAC (2021)
with CGPA 3.52



Journal of Shivaji University SCIENCE & TECHNOLOGY

(Peer Reviewed Journal)

Journal of Shivaji University: Science and Technology
Volume-49, Issue-2 (July, 2023)

INDEX

Sr. No.	Title of Research Article with Name of Author/s	Page No.
1.	Silica Coated Superhydrophobic Materials for Oil-Water Separation Application-A Short Review Rajesh B. Sawant, Mehejbin R. Mujawar, Amol B. Pandhare, Sanjay S. Latthe, Ankush M. Sargar, Raghunath K. Mane, Shivaji R. Kulal	1
2.	Green Synthesis of NiO Nanoparticles from <i>Partheniumhysterophorus</i> Plant Sneha V. Koparde, Akanksha G. Kolekar, Shital S. Shendage, Aniket H. Sawat, Snehal D. Patil, Snehal S. Patil, Reshma B. Darekar, Amol B. Pandhare, Vijay S. Ghodake, Samadhan P. Pawar, Govind B. Kolekar	12
3.	Microwave-Assisted Synthesis of Pyrazole and Its Hybrid Scaffolds as Potent Biological and Pharmacological Agents: A Short Review Pravin. R. Kharade, Uttam. B. Chougale, Satish. S. Kadam, Kiran. N. Patil, Prakash S. Pawar, Savita. S. Desai	19
4.	Biosynthesis and Catalytic Transformation of Ruthenium Nanoparticles in Biomimetic Applications Komal M. Dhumal, Anita R. Mali	36
5.	Third Generation Solar Cells: Importance and Measurements Techniques for knowing Photovoltaic Device Performance Prakash S. Pawar, Pramod A. Koyale, Amol B. Pandhare, Vijay S. Ghodake, Swapnijit V. Mulik, Ankita K. Dhukate, Waleed Dabdoub, Sagar D. Delekar	48
6.	Aggregation-Induced Emission, Mechanochromism, and Applications of Tetraphenylethene/Triphenylamine-based Molecules Kishor. S. Jagadhane, Govind. B. Kolekar, Prasad. M. Swami, Prashant. V. Anbhule	68
7.	Greener and Environmentally Benign Methodologies for the Synthesis of Bis(indolyl)methane and Trisindolines Aboli C. Sapkal, Suraj R. Attar, Santosh B. Kamble	75

Silica Coated Superhydrophobic Materials for Oil-Water Separation Application-A Short Review

Rajesh B. Sawant^{a,*}, Mehejbin R. Mujawar^a, Amol B. Pandhare^{b,f},
Sanjay S. Latthe^c, Ankush M. Sargar^d,
Raghunath K. Mane^e, Shivaji R. Kulal^{a,*}

^aDepartment of Chemistry, Raje Ramrao Mahavidyalaya, Jath, Sangli 416 404 (MS) India.

^bDepartment of Chemistry, Shivaji University, Kolhapur 416 004 (MS) India.

^cDepartment of Physics, Vivekanand College, Kolhapur 416 003 (MS) India.

^dDepartment of Chemistry, Bharati Vidyapeeth's Dr. Patangrao Kadam Mahavidyalaya, Sangli 416 416 (MS) India.

^e Department of Chemistry, Smt. Kusumtai Rajarambhapu Patil Kanya Mahavidyalaya, Islampur, Sangli 416 409 (MS) India.

^fDepartment of Chemistry, M.H. Shinde Mahavidyalaya, Tisangi, Gaganbavda, Kolhapur 416 206 (MS) India.

*Corresponding authors: srkulal@gmail.com and rbsawant2@gmail.com

ABSTRACT

Contamination like oil and organic pollutants in water has a severe problem for aquatic life and human being; it is a need to preserve their life. These contaminants are added due to frequent oil spill accidents, and industrial as well as domestic waste. There is a need to develop methods and materials that show excellent ability to separate the oil and organic contaminants from water. Recently, superhydrophobic coated sponges, metals mesh, membranes and porous materials plays crucial role to separate oil and water from oil-water mixture. The micro and nonporous of substrate facilitate to enter liquid into it and superhydrophobic/superoleophilic property of substrate surface resist water and allows oil to enter into porous substrate. The various surface modified organic metal oxide nanoparticles are used to develop superhydrophobic surface on porous substrate. Among them SiO₂ nanoparticles is promising material to preparation of superhydrophobic surface because of their cost-effectiveness and easy synthesis techniques. This review focused on silica modified porous sponge, metal meshes, membrane and porous substrate for scalable oil-water separation application.

KEYWORDS

Superhydrophobic, Oil-water separation, porous sponge, Metal mesh and membrane.

.....

1. INTRODUCTION

Frequent oil spill accidents and industrial chemical spills occurred in the sea and the ecosystem damage; such incidents have spread to impact the offspring. Therefore, considerable surviving organisms for several years after the impact [1-2] efforts have been done to remove oil and organic solvents from water. Due to this extensive current research is focussed on the development of superhydrophobic materials for effective oil-water separation. To achieve superhydrophobic sponges, surface roughness and low surface energy materials play a crucial role. The various methods such as dip coating, immersion, spray coating; hydrothermal methods, chemical vapor deposition, surface etching, solvothermal methods, layer-by-layer assembly and electrochemical treatment describe a modification of sponges for oil and water separation [3-4]. At present, traditional technologies, including in situ burning [5], bioremediation [6], chemical dispersant methods [7], skimming [8], and the use of sorbents [9] are used to clean up spilled oils or organic pollutants. However, many of these strategies involve energy intensive and slow processes, have low clean-up capacities or create secondary pollution during the clean-up process, restricting their widespread practical applications [10-11]. To realize the hierarchical structures on different material surfaces, a series of strategies, such as sol-gel coating [12], chemical vapor deposition [13], plasma etching [14], template processing [15], lithographic patterning [16], etc. have been adopted [17]. The superhydrophobic surfaces on which water achieves water contact angle higher than 150° and sliding angle less than 5° are attracting minds of researchers due to their efficient oil-water separation efficiency [18].

Recently, Wu et al. [19] have prepared a highly flexible superhydrophobic PDMS@F-SiO₂ coating for self-cleaning and drag-reduction applications via a two-step spraying of PDMS and F-SiO₂ nanoparticles. However, it is common that inorganic particles normally tend to agglomerate due to the interparticle forces stemming from the Vander Waals, capillary and electrostatic forces [20], which leads to phase separation during the fabrication process and tends to diminish the quality of the coating through cracks or weak adhesive to the substrates. Gao et al. [21] prepared PVDF/SiO₂ coated superhydrophobic porous membranes using a spraying technique. These membranes could be used to separate the oil-water mixtures but are not applicable to surfactant stabilized water-in-oil emulsions because of their large pore sizes. Li et al. [22] prepared the hydrophobic CS by incomplete combustion of hydrocarbons from the middle of a candle flame. The PU sponge was immersed in the solution of CS, SiO₂ and PU resin to achieve stable superhydrophobicity. The CS-SiO₂-PU sponge was shown excellent oil-water separation efficiency. The CS-SiO₂-PU sponge showed excellent oil-water separation efficiency from hot water, acidic solutions, alkaline solutions and salt solutions.

In this review, the sophisticated, facile and low-cost methods for fabrication of superhydrophobic porous material for oil-water separation application are discussed.

The 3D sponges, metal meshes, membrane and cotton fabrics are used as substrate for scalable oil-water separation application.

2. SUPERHYDROPHOBIC SURFACES FOR OIL-WATER SEPARATION

2.1 Superhydrophobic SiO₂ Modified Sponges for Oil-Water Separation

Zhang et al. [23] have fabricated the superhydrophobic surface by using VTMS and SiO₂ via immersion method. The schematic of preparation of superhydrophobic sponge is shown in **Figure-1**. It was shown a water contact angle of 153.2° and roll-on angle of 4.8°. The oil is quickly absorbed by superhydrophobic sponge which can be shown the superoleophilic property of a modified sponge. The IR peak at 1078 cm⁻¹ shows the presence of the O-Si-O bond present in the material. It was showing the high separation efficiency of about 99.5%. It exhibited good saturated adsorption properties exceeding 70 g/g for all oils. It shows outstanding characteristics of superhydrophobic sponge such as high porosity, small pore size and ultra-light mass. After 20 cycles, it was found that the adsorption ability of the modified melamine sponge for different oils decreased slightly. It shows outstanding stability and reusable performance. The modified sponge maintains an 89% of recovery rate even after 20 cycles. This method was used to prepare porosity and provides storage space for the adsorption of oil pollution. This superhydrophobic composite melamine sponge provided the possibility for practical application of oil-water separation.

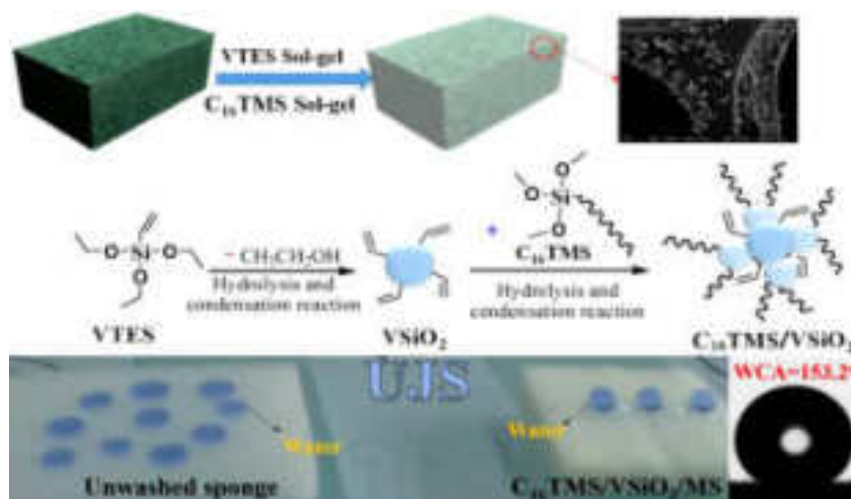


Figure-1. Schematic illustration of the preparation of superhydrophobic sponge. Images reprinted from [23], with permission from Elsevier, Journal of Chemical Engineering, Copyright 2020.

Liu et al. [24]. have fabricated a superhydrophobic sponge and polyester coated with SiO₂-DTMS through an entrapment method. The **Figure-2** reveals the fabrication process of superhydrophobic sponge and polyester. The SiO₂ particles were introduced by growth on the substrate through the polymerization process, followed by the addition of DTMS as an adhesive, leading to a homogeneous and dense superhydrophobic membrane. The modified sponge was shown the water contact angle up to 172° indicating the water repellence was superior. This superhydrophobic sample had good hydrophobic stability even in acidic condition and it can show efficient oil-water separation. The amount of the absorbed oil was about 43-65 times of sponge own weight can be shown that the evaluation of the mass based on absorbed surface tension, density, viscosity of absorbed liquids. It exhibits stable oil storage under harsh environmental conditions in oil-water separation. The performance remained constant after 100 recycling sequences, even in a harsh water environment.

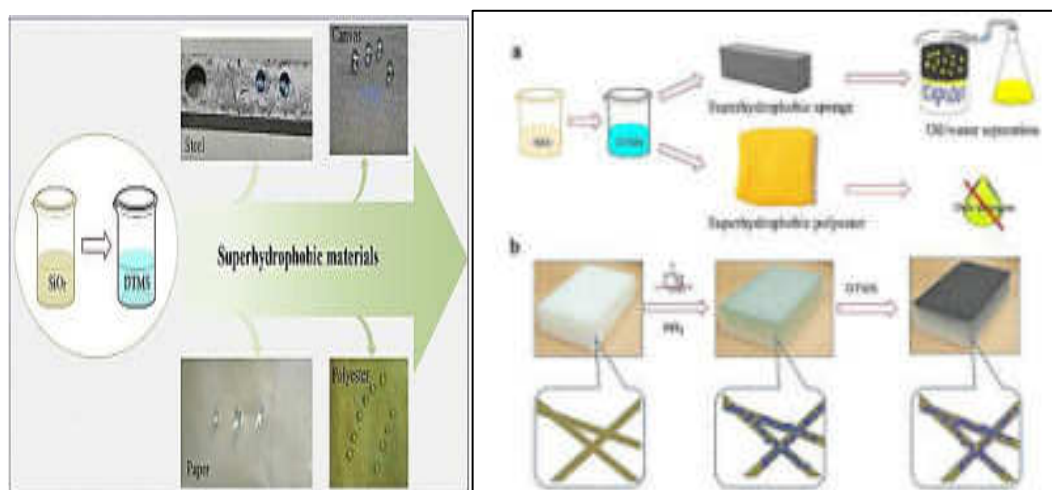


Figure-2. Schematic illustration of the fabrication of a modified sponge and polyester. Images reprinted from [24], with permission from Elsevier, Copyright 2019.

2.2 Superhydrophobic SiO₂ Modified Metal Meshes for Oil-Water Separation

Zhao et al. [25] have prepared superhydrophobic SiO₂ nanoparticles by improved Stober method and then coated on a chemically etched stainless steel mesh by one step dipping method to fabricate superhydrophobic SiO₂ coated stainless steel mesh. The preparation process was simple, efficient and environmentally friendly. The experimental procedure is shown in **Figure-3**. It shows excellent oil-water separation properties, which can be widely used in oil-water separation. It was showing 153.3° water contact angle and 0° oil contact angle. The oil-water separation efficiency was nearly 96% by using this modified stainless-steel mesh.

The separation efficiencies were obtained repeatedly even after 40 cycles without noticeable deterioration. The superhydrophobic modified stainless steel mesh shows stability, durability and reusability. The SiO₂ modified stainless steel mesh indicates good material for treating real oil-polluted water in different practical applications. This method shows high performance, oil-water separation in a short time and repeatedly in comparison with earlier works.

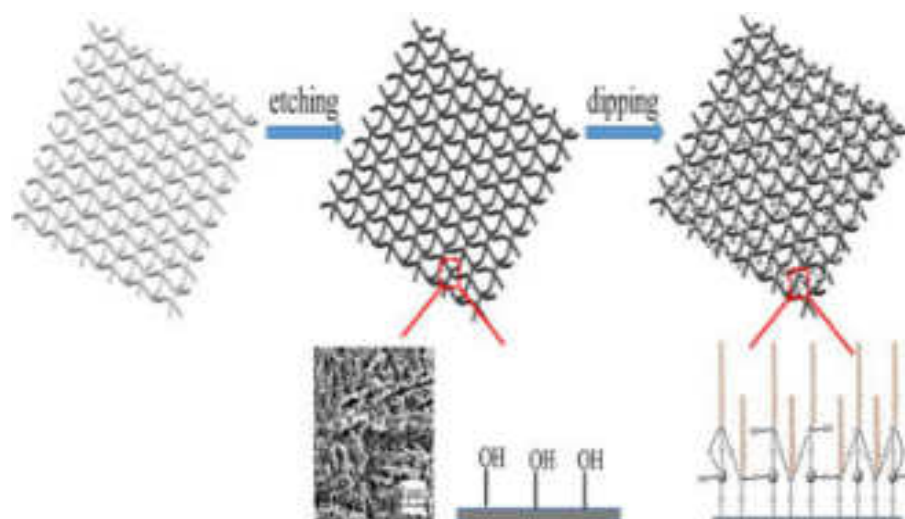


Figure-3. Schematic illustration of the preparation of FSSM. Images reprinted from [25], with permission from Elsevier, Copyright 2019.

Xiong et al. [26] have prepared SiO₂ nanoparticles by an improved modified method by using TEOS and then coated on a stainless-steel mesh by spraying method to fabricate SiO₂ coated stainless steel mesh. The **Figure-4** illustrates schematic of preparation of the superhydrophobic stainless-steel mesh. The preparation process was efficient, simple and environmentally friendly. It shows good mechanical properties and oil/water separation performance. It was showing 156.4° oil contact angle and less than 10° water contact angles. The oil-water separation efficiency was nearly 98.69% by using this modified stainless-steel mesh. The separation efficiencies obtained repeatedly even after 20 cycles without noticeable deterioration. The superhydrophobic modified stainless steel mesh shows stability, durability and reusability. The SiO₂ modified stainless steel mesh indicates excellent material for treating oil-polluted water in different practical applications. This method shows an easily scaled-up preparation process, stable mechanical and thermal properties, offering new prospects for efficient oil/water separation in comparison with earlier works.

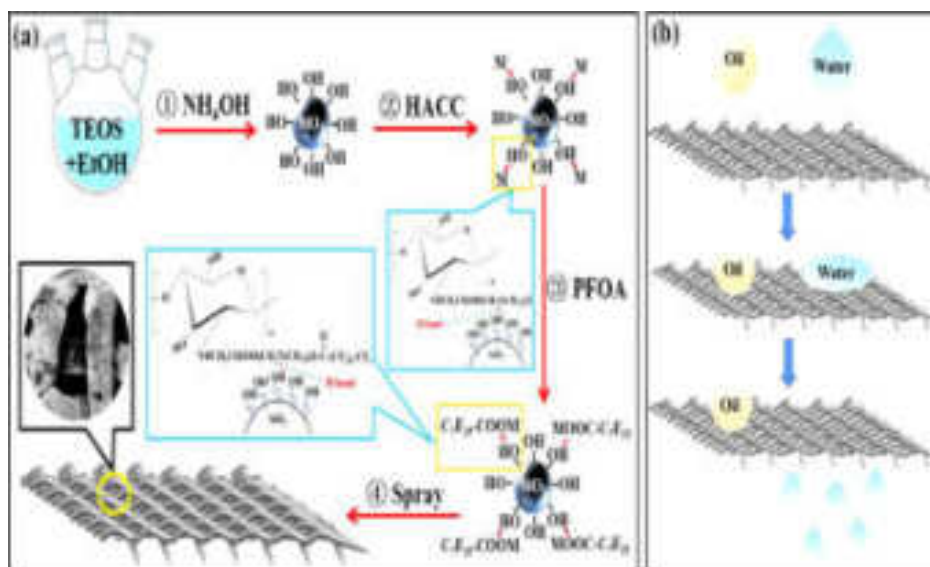


Figure-4 (a) Schematic diagram illustrating the fabrication of air superhydrophilic-superoleophobic membrane. (b) Scheme of the oil/water separation. Images reprinted from [26], with permission from Elsevier, Journal of Colloid and Interface Science, Copyright 2021.

2.3 Superhydrophobic SiO₂ Modified Porous Substrates for Oil-Water Separation

Gu et al. [27] have prepared a membrane (SiO₂/Polyurethane membrane) with porous structure rough surface and hydrophobic epidermis by surface modification to construct a rough surface and low-energy epidermis on electrospun polyurethane membrane. The schematic of experimental procedure is shown in **Figure-5**. The superhydrophobic SiO₂/PU porous membrane prepared by chemical modification on the membrane shows a water contact angle 152.1° and low sliding angle 6°. This membrane was used for different aqueous solutions like water, saline solution, alkaline solution acidic solution. The porous membrane shows low air permeability and high-water vapor transmission rate. It shown good oil absorption capacity. It was shows high oil-water separation efficiency above 98.5%. The absorption capacity of the modified membrane does not show severe degradation even after 30 separation cycles which indicating a highly stable absorption performance of modified membrane. It provided the potential for eater repellent, breathable applications and oil-water separation in long term use.

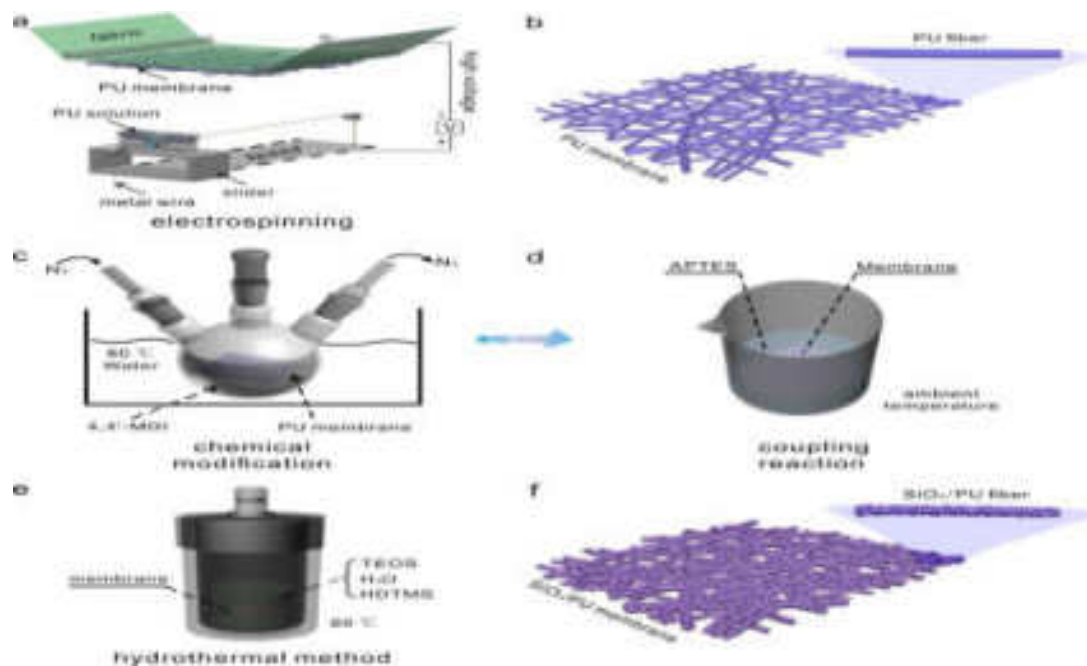


Figure-5. The preparation scheme of superhydrophobic SiO₂/PU membrane. Images reprinted from [27], with permission from Elsevier, App. Sur. Sci. Copyright 2019.

Wei and their co-researchers [28] have obtained the SiO₂ nanoparticles from ethanol and ammonium hydroxide with TEOS. The SiO₂ nanoparticles were isolated by repeated centrifugation in ethanol followed by drying in a vacuum oven. A facile strategy was presented to prepare silica particles grafting. The sprayable solution be easily applied to different porous substrates to achieve durable superhydrophobic coating (schematically shown in **Figure-6**). The surface shows a separation efficiency of 98.8% dealing with oil-water mixture. The oil absorption capacity of immersion coated polyurethane sponge was demonstrated higher than pristine polyurethane sponge an 39 g/g which would benefit from the presence of lipophilic PSAN and higher porosity contributed by abundant nanoparticles. After 10 cycles of abrasion test the remained separation efficiency of above 96% and water contact angle of 151° confirmed the mechanical durability. This sponge shows facile, environmentally friendly, mechanical and chemical stability.

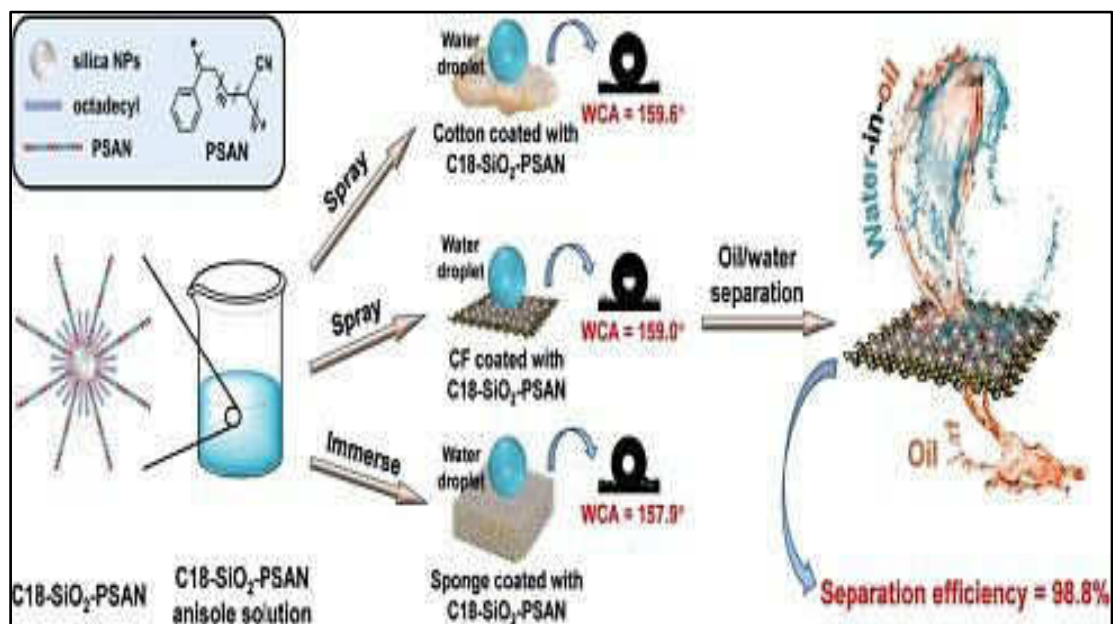


Figure-6. Schematic illustration of preparation of modified superhydrophobic surface for oil-water separation. Images reprinted from [28], with permission from Elsevier, Copyright 2021.

2.4 Superhydrophobic SiO₂- Polymer Composite Based Membrane for Oil-Water Separation

Li and their co-workers [29] have fabricated the superhydrophobic surface by using PVDF and SiO₂ via sugar template method. The schematic of preparation method is shown **Figure-7**. It was shown in a water contact angle of 155.68° and roll-on angle of nearly 6°. The prepared superhydrophobic PVDF oil/water separation membrane had low water adhesion performance and ultrahigh separation efficiency of nearly 99.98% in terms of the oil purity in the filtrate. The recycling performance over 20 cycles. This membrane has excellent potential for use in various large-scale practical applications, water purification treatment and the separation of commercially relevant emulsions. The possibility of large-scale production and low manufacturing costs of this sponge is very promising advantages for oil-water separation application.

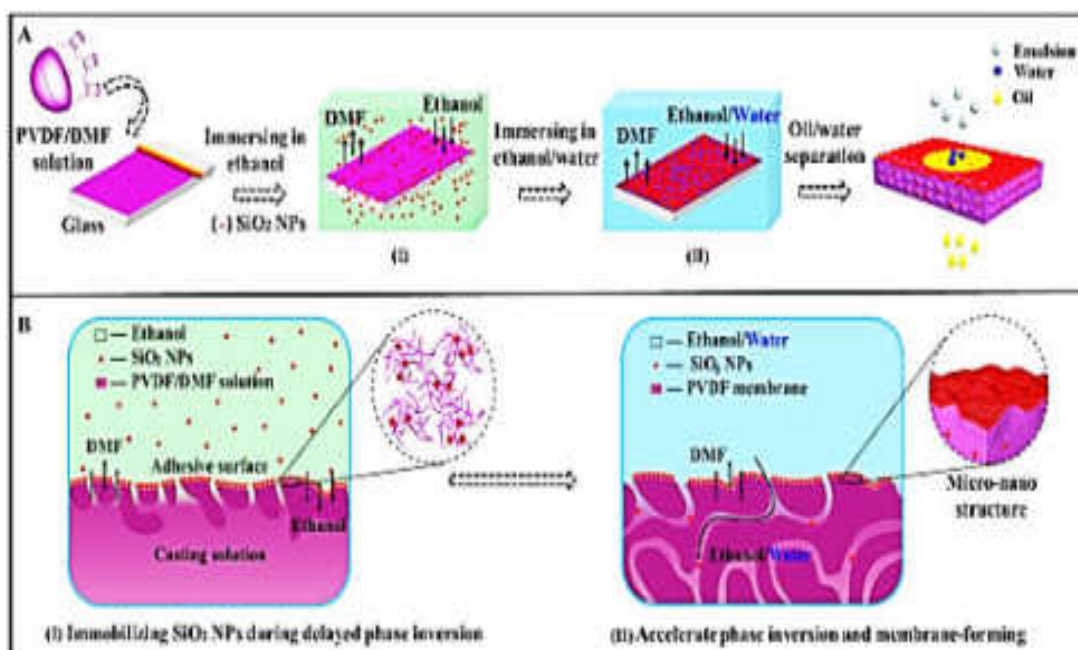


Figure-7. Schematic illustration (A) and structural evolution (B) for the formation of adhesive-free superhydrophobic SiO₂ nanoparticles decorated PVDF oil-water separation membranes [29]. Images reprinted from [29], with permission from Elsevier, Copyright 2018.

Bai et al. [30] have coated cotton fabric by sol-gel processed SiO₂. The as-prepared fabric was immersed in the solution of FeCl₃, thiophene and CH₂Cl₂ solution. Then, the modified fabric was washed with ethanol and dry it. **Figure-8** reveals the experimental procedure of preparation of superhydrophobic fabric. The modified fabric shows water contact angles above 160°. The strongest peak at 1050 cm⁻¹ belongs to the Si-O bond indicating that SiO₂ particles have been coated on the cotton fabric. The modified cotton fabric shows outstanding resistance to ultraviolet irradiation, high temperature, low temperature, organic solvent, immersion and excellent durability even after 8 months. The as-prepared fabric was showing the capability in various chemical exposures. It was showing good anti-dirt and anti-frost properties. The modified superhydrophobic cotton fabric was used as filter membrane for the gravity driven oil-water separation with high separation efficiency and excellent reusability. By using, this modified cotton fabric, both immiscible and emulsified oil-water mixtures could be separated. The efficient oil-water separation was also achieved under harsh conditions. The superhydrophobic fabric shows potential for the fast, coat-effective treatment of oil spill accidents and industrial oily sewage.

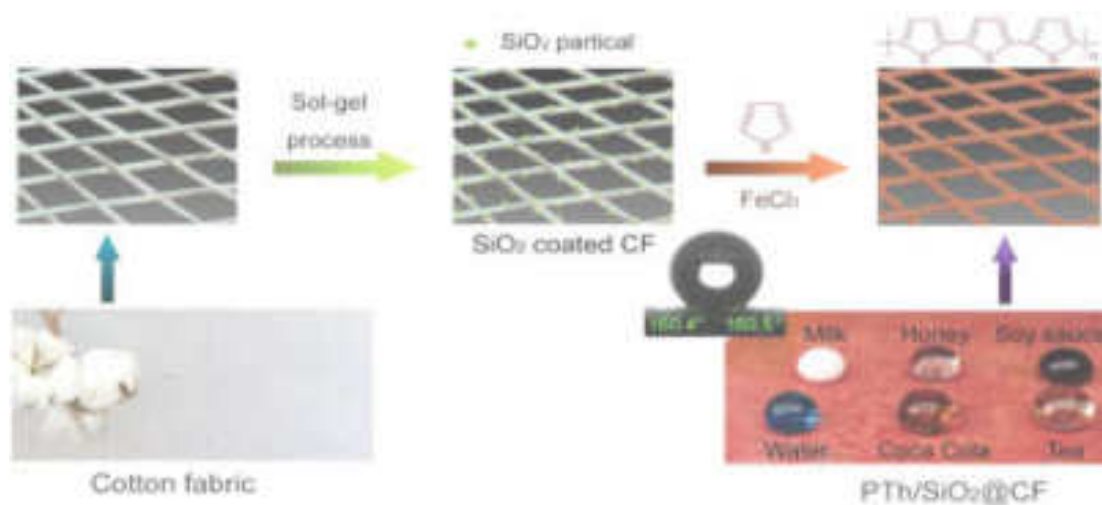


Figure-8. Schematic Illustration of the fabrication process of the PTh/SiO₂@CF [30]. Images reprinted from [30], with permission from Elsevier, Adv. Mater. Interfaces, Copyright 2021.

3. CONCLUSION

This review highlights, SiO₂ nanoparticles are unique, their fabrication requires little control of external parameters such as surface modification. It is very beneficial economically, facile and straightforward to synthesize. The SiO₂ nanoparticles coated sponge/mesh has been developed by using SiO₂ nanoparticles and different polymers. The absorption/separation investigation demonstrates that, the SiO₂ surface is highly efficient and stable in absorbing a wide range of oil and organic solvents. It can be believed that, the SiO₂ coated superhydrophobic materials are very useful for oil-water separation. It shows various tremendous results with SiO₂-polymer composite in various mechanical conditions. Hence this review is helpful to upcoming researchers to develop highly scalable superhydrophobic surfaces for efficient oil-water separation applications.

ACKNOWLEDGEMENT

This work was supported by Department of Chemistry and Department of Physics, Raje Ramrao Mahavidyalaya, Jath. We also acknowledge Prof. (Dr.) Suresh S. Patil, Principal, Raje Ramrao Mahavidyalaya, Jath.

REFERENCES

1. Alsbaiee A., Smith B. J., Xiao L., Ling Y., Helbling D. E. & Dichtel W. R. (2016) *Nature*, 529, 190-194.
2. Li Y., Zhang Z., Ge B., Men X., and Xue Q. (2016) *Green Chemistry*, 18, 5266-5272.
3. Ma Q., Cheng H., Fane A. G., Wang R., and Zhang H. (2016) *Small*, 12, 2186-2202.
4. Li L., Li B., Dong J., and Zhang J. (2016) *Journal of Materials Chemistry A*, 4, 13677–13725.
5. Yuan J., Liu X., Akbulut O., Hu J., Sui S. L., Kong J., Stellacci F. (2008) *Nature*, 3, 332-337.
6. Broje V., Keller A. A. (2006) *Environmental Science & Technology*, 40, 7914-7918.
7. Wu Z. Y., Li C., Liang H. W., Zhang Y. N., Wang X., Chen J. F. & Yu S. H. (2014) *Science Reports*, 4, 4079-4091.
8. Keshavarz A., Zilouei H., Abdol maleki A. (2015) *Journal of Environmental Management*, 157, 279-286.
9. Wang Z., Xu Y., Liu Y., Shao L. (2015) *Journal of Materials Chemistry A*, 3, 266-273.
10. Li J., Zhao Z., Kang R., Zhang Y., Lv W., Li M., Jia R., Luo L. (2017) *Journal of Sol-Gel Science and Technology*, 3, 817–826.
11. Keshavarz A., Zilouei H., Abdolmaleki A., Asadinezhad A. (2015) *Journal of Environmental Management*, 157, 279-286.
12. Sam E. K., Sam D. K., Lv X., Liu B., Xiao X., Gong S., Yu W., Chen J., Liu J. (2019) *Chemical Engineering Journal*, 19, 1103-1109.
13. Jin M., Feng X., Xi J., Zhai J., Cho K., Feng L., Jiang L. (2005) *Macromolecular Rapid Communications*, 26, 1805-1818.
14. Yao T., Zhang Y., Xiao Y., Zhao P., Guo L., Yang H., Li F. (2016) *Journal of Molecular Liquids*, 218, 611–614.
15. Gao Y., Zhou Y. S., Xiong W., Wang M., Fan L., Golgir H. R., Jiang L., Hou W., Huang X., Jiang L., Silvain J. F., Lu Y. F. (2014) *ACS Applied Materials & Interfaces*, 6, 5924–5929.
16. Erbil H. Y., Demirel A. L., Avcı Y., Mert O. (2003) *Science*, 299, 1377-1391.

17. Fard A. K., Mckay G., Manawi Y., Malaibari Z., Hussien M. A. (2016) *Chemsphere*, 164, 142-155.
18. Ren G., Song Y., Li X., Zhou Y., Zhang Z., Zhu X. (2018) *Applied Surface Science*, 428, 520-525.
19. Gu J., Xiao P., Chen J., Liu F., Huang Y., Li G., Zhang J., Chen T. (2014) *Journal of Materials Chemistry A*, 2, 15268–15272.
20. Li J., Kang R., Tang X., She H., Yang Y., Zha F. (2016) *Nanoscale*, 8, 7638–7645.
21. Gao Y., Zhou Y. S., Xiong W., Wang M., Fan L., Golgir H. R., Jiang L., Hou W., Huang X., Jiang L., Silvain J. F., Lu Y. F. (2014) *ACS Applied Materials & Interfaces*, 6, 5924–5929.
22. Li J., Zhao Z., Kang R., Zhang Y., Li M. (2017) *Journal of Sol-Gel Science and Technology*, 83, 817-826.
23. Zhang R., Zhou Z., Ge W., Lu Y., Liu T., Yang W., Dai J. (2020) *Chinese Journal of Chemical Engineering*, 5, 30292-30310.
24. Liu D., Yu Y., Chen X., Zheng Y. (2017) *RSC Advances*, 7, 12908–12915.
25. Zhao L., Du Z., Tai X., Ma Y. (2021) *Colloids and Surfaces A: Physicochemical and Engineering Aspects*, 623, 126404-126415.
26. Xiong W., Li L., Qiao F., Chen J., Chen Z., Zhou X., Hu K., Zhao X., Xie Y. (2021) *Journal of Colloid and Interface Science*, 6, 118–126.
27. Gu J., Xiao P., Chen J., Liu F., Huang Y., Li G., Zhang J., Chen T. (2014) *Journal of Materials Chemistry A*, 2, 15268–15272.
28. Wei C., Deu F., Lin L., An Z., He Y., Chen X., Chen L., Zhao Y. (2018) *Journal of Membrane Science*, 555, 220-228.
29. Li X., Wang X., Yuan Y., Wu M., Wu Q., Liu J., Yang J., Zhang J. (2021) *European Polymer Journal*, 159, 110729-110742.
30. Bai W., Lin H., Chen K., Zeng R., Lin Y., Xu Y. (2021) *Advanced Materials Interfaces*, 254, 725-740.

अक्षर वाङ्मय

वर्ष तेरावे, पुरवणी अंक ४, खंड. २

फेब्रुवारी २०२३



मुख्य संपादक
डॉ. नानासाहेब सुर्यवंशी



अक्षर वाङ्मय

वर्ष तेरावे, पुरवणी अंक ४, खंड. २

फेब्रुवारी २०२३

संपादक
डॉ. नानासाहेब सूर्यवंशी

कार्यकारी संपादक
डॉ. शिवाजीराव देशमुख

प्रकाशक : सौ. रेखाताई नानासाहेब सूर्यवंशी, प्रतीक प्रकाशन
'प्रणव' रुक्मिणी नगर, थोडगा रोड, अहमदपूर ४१३५१५
मुद्रक: श्री. जे प्रिंटिंग प्रा लिमिटेड १४१६ सदाशिव पेठ पुणे- ४११०३०
साहित्य व वर्गणी पाठवण्याचा पत्ता: डॉ. नानासाहेब सूर्यवंशी
'प्रणव' रुक्मिणी नगर, थोडगा रोड, अहमदपूर,
जि. लातूर, ४१३५१५
E-mail : suryawanshinanasahab67@gmail.com

वार्षिक वर्गणी: रु ५००/-

पंचवार्षिक वर्गणी : रु २०००/-

द्विवार्षिक वर्गणी : रु ९००/-

अंक मूल्य : रु १२५/-

-
- महाराष्ट्र राज्य साहित्य व सांस्कृतिक मंडळ या नियतकालकाच्या प्रकाशनात अनुदान दिले असले तरी या नियतकालिकेतील लेख लेखांच्या विचाराशी मंडळ व शासन सहमत असेलच असे नाही.
 - या अंकातील लेखातून व्यक्त झालेले लेखकांच्या मतांशी संपादक, संपादक मंडळ, प्रकाशक व मुद्रक सहमत असतीलच असं नाही.



24	Search for Inner Self in Techno savvy era: Kim Scott's <i>True Country</i> Shital Anandran Mohite, Dr. Rajashri Barvekar	74-76
25	Impact of Technology on Education Miss. Sawant Ashwini Arjun	77-79
26	Teaching and Studying Literature in The Digital Age Dr. Sarangpani Ramchandra Shinde	80-84
27	A Study on Significant Role of Technology in Financial Sector Prof. Ms. Manju shri Kadam, Dr. Shabana A. Memon	85-89
28	The Era Of E-Literature Ms Sweta Shalish Thakkar, Dr. Mahavir Sankala	90-92
29	Death Trap of Technology - A Dystopia Vision of 20 th Century Sci Fi Mr. Ananda Pandhare, Dr. Mahavir Sankala	93-96
30	Impact of Technology on Book Publication and Library Services A Comparative Study: Digital and Library Niche Ms Swati Shree	97-99
31	A study of Technological advancement: A pathway to Utopia Mr. Marewad Atul Balaji, Dr. Sankla Mahavir R	100-102
32	The Depiction of Uneven Dissemination of the Technological Advancement in <i>Generosity</i> by Richard Powers Abhijeet S. Dalavi, Prof. (Dr) Satish R. Ghatge	103-105
33	Use of Digital Tools and E-resources in Teaching Literature Mr. Shaikh Firoj Husen,	106-108
34	The analysis of Technological Advancements in the Entertainment Sector with respect to shift in Language and Audience Base. Snehal S. Warekar	109-111
35	Technological Prospects in Avatar 2: Merely Imagination or Realism Mr. Prashant P. Ingole, Ms. Shraddha M. Sankla	112-115
36	भूमंडलीकरण, मीडिया और हिंदी साहित्य डॉ. गणेश हुंदा गभाले	116-119
37	भूमंडलीकरण के परिप्रेक्ष्य में हिंदी सिनेमा डॉ. सुबराज राजाराम मुळगे	120-123
38	भूमंडलीकरण के दौर में नारी डॉ. सुसंधा हिंदुराव परपणकर	124-126
39	भूमंडलीकरण और हिंदी साहित्य (कहानी विधा के विशेष संदर्भ में) डॉ. नितीन हिंदुराव कुंभार	127-129
40	भूमंडलीकरण के परिप्रेक्ष्य में हिंदी कविता: विशेष संदर्भ 'नवी कविताएँ' प्रा. हिरामन टोंगारे, डॉ. सतीशकुमार पडोळकर	130-133
41	वेदग्रन्थ उपन्यास में चित्रित किसान आन्दोलन विद्या आनंदराव जाधव	134-136
42	भूमंडलीकरण और उपन्यास साहित्य (युवावर्ग के संदर्भ में) सु. धी. अर्चना चसंत ठराल	137-138
43	भारतवर्षी विज्ञानम् । डॉ. सविन चंद्रशेखर कंदले	139-143
44	संस्कृत साहित्यापीठ संमीलनाधीन अध्यापनामध्ये संयोजनापी भूमिका डु. मधुरा प्रमोद किरयेकर	144-146
45	Technology and Sanskrit literature Aayush	147-149
46	संस्कृतसाहित्ये नवज्ञानम् Guneendra Arya	150-152

भूमंडलीकरण के परिप्रेक्ष्य में हिंदी कविता: विशेष संदर्भ ' लंबी कविताएँ'

प्रा.श्रीरामचण्डेकर, डॉ.रातीशकुमार पटोकरकर,

अध्यक्ष, हिंदी विभाग, राजे रामराय महाविद्यालय, जत जिला- सांगली
महा. प्राध्यापक, राजे रामराय महाविद्यालय, जत जिला- सांगली

अभिलेख :-

कविता अथवा काव्य बहुत प्राचीन साहित्य विधा है। भूमंडलीकरण के दौर में काव्य विधा काफ़ी हद तक परिवर्तित हुई। इसका प्रमुख कारण भूमंडलीकरण के समय में मानवी जीवन में आया हुआ परिवर्तन। इसी कारण कविता की संरचना में भी परिवर्तन हुआ। परिणामतः लंबी कविता का उद्भव हुआ। लंबी कविता में कथन की अपेक्षा संवेदना, बोध, कल्पनात्मकता अथवा किसी चिंतन की अभिव्यक्ति अथवा सांकेतिक अभिव्यक्ति की जाती है। किंतु लंबी कविता नई का निर्धारण, चिंतन की सृष्टि, शैली-विधान आदि पर अधिक बल दिया गया है। पुरानी प्रचन्धात्मक कविताओं में कथा की यह निर्बाध सघनता बहुत कम दिखाई देती है, जैसी की आज की लंबी कविताओं में हुआ करता है। भूमंडलीकरण के दौर में रचित आधुनिक कविताएँ या प्रवीत कविता ये तो लंबी कविता का अंतर बहुत साफ-साफ दृष्टिगोचर होता है। नये कविताएँ अनुभूति और अभिव्यक्ति दोनों में मंचित हुआ करती हैं। उनका कथा जल्दी ही खूब जाता है किंतु लंबा आकार देखकर भी किसी कविता को लंबी कविता कहना उचित नहीं है। आज लंबी कविता का शिल्प काफ़ी विकसित हो चुका है। इस वैशिष्ट्य को ठीक ढंग में न पकड़ पानेवाले लोक लंबी कविता को किसी नेता का भाषण मात्र समझते हैं। ऐसा भी नहीं है कि दम-भंडह पंक्तियों से अधिक विकसित हो जाने पर किसी कविता को लंबी कविता कह दिया जाए। संवेदना की निर्बाध अभिव्यक्ति, चेतना प्रवाह, वयार्थ का स्पष्ट बोध और उनके बीच से मूल्यों का निर्धारण लंबी कविता का मुख्य वैशिष्ट्य है। इनमें आज के जीवन का बदलता हुआ वयार्थ, विवशता, तनाव, त्रास आदि सब कुछ लंबी कविता में व्यक्त हो जाता है। डॉ. शम्भुनाथसिंह जैसे गीतकार कविता की संरचना एवं विशेषताएँ जाने मर उमे केवल नेता का भाषण मान लेते हैं- "लंबी कविता नेता के भाषण के समान होती हैं जिसमें कुछ भी लिख सकते हैं।" अपनी इस अवधारणा के आधारपर वे यह निष्कर्ष निकालते हैं कि भावानुभूति को जहाँ प्रकट करना है वहाँ छोटी कविता ही लिखी जाएगी, लंबी कविता नहीं। (नई कविता की लंबी कविताएँ- डॉ. रामसुधार सिंह, पृ. 1)

कविता के विकास के साथ लंबी कविताओं की अधिक से अधिक रचनाएँ हुई हैं। किंतु इसके स्वतंत्र अस्तित्व के संबंध में विद्वानों में मतभिन्नता है। कुछ विद्वान इसे स्वतंत्र विधा के रूप में स्वीकार करते हैं, लेकिन कुछ विद्वान इससे सहमत नहीं हैं। 'दुमरा समक' के प्रमुख कवि नरेश मेहता के विचार में भूमंडलीकरण के दौर की लंबी कविता यह एक स्वतंत्र विधा है, क्योंकि किसी विचार को विस्तृत करके ही लंबी कविता लिखी जा सकती है। अपनी इस विशेषता के कारण लंबी कविता का महाकाव्य का छण्डकाव्य से अलग अस्तित्व होता है। महाकाव्य और छण्डकाव्य के लिए सीमित परिवेश और सीमित काल आवश्यक है। लेकिन लंबी कविता इससे पूर्णतः अलग है। (वहीं, पृ.2) नरेश मेहता की तरह डॉ. शुक्देवसिंह भी लंबी कविता को एक अलग विधा मानते हुए कहते हैं- प्रत्येक काल की छंद, लय आदि से संबंधित कोई न कोई विशेषता रही है और नई कविता की शैली में हम लंबी कविता को ही रख सकते हैं। (वहीं, पृ.2) लेकिन बहुत मारे विद्वान इस मत से सहमत नहीं होते हैं। इन विद्वानों में डॉ. जगदीश गुप्त, श्री लक्ष्मीकांत वर्मा, श्रीराम वर्मा और श्री नीलाभ प्रमुख हैं। श्री जगदीश गुप्त की अवधारणा है कि पर्याप्त रचना होने पर ही कोई काव्यधारा अलग विधा बन सकती है। श्रीराम वर्मा भी इस मत से सहमत हैं। उनके अनुसार 'लंबी कविता कोई विधा नहीं है।' (वहीं, पृ.2) इन विद्वानों के नये विचार अपनी परंपरावादी विचारक के परिचायक हैं।

भूमंडलीकरण और लंबी कविता स्वरूप:

'लंबी कविता' को कविता की एक स्वतंत्र विधा स्वीकार करने पर सबसे पहला यह प्रश्न सामने आता है कि अगर यह एक स्वतंत्र विधा है तो उसका स्वरूप क्या होगा? उसकी संरचना कैसी होगी? इस संदर्भ में दो-तीन बातें महत्वपूर्ण हैं। कविता के स्वरूप निर्धारण में देश और काल का महत्वपूर्ण योगदान रहता है। जिस देश और काल में लंबी कविता लिखी गयी है वही उसके स्वरूप का निर्धारण करता है। इसमें कवि का व्यक्तिगत महत्व भी होता है और प्रत्येक कवि की शूनित पर भी इसका स्वरूप निर्भर करता है। कवि की तीव्रता ही उसे स्वरूप प्रदान करती है। इन्हीं दृष्टियों से लंबी कविता के स्वरूप पर विचार करना समीचीन

होगा। औद्योगीकरण और और महानगरीकरण के परिणाम स्वरूप आज की जिंदगी दुहर-नी गयी है। भारत के स्वधीनतापन का
में नई पीढ़ी के सारे मपने टूट-बिखर गनये हैं और उन्हें वेकारी, भूख, कुण्ठा, घुटन, उपहार स्वरूप प्राप्त हुए है। इन कारण युवा
पीढ़ी समकालीन व्यवस्था के खिलाफ हो गयी। जीवन समस्त स्तरों पर निराशा एवं अनास्था मिलने के कारण युवा पीढ़ी का एक
शिकायती और बिद्रोही हो जाना स्वाभाविक ही था। लंबी कविता इसी शिकायत का एकाग्रताप है। धूमिल ने एक उदाहरण देते हुए
'बौबलाए' हुए आदमी का एकालाप। आज का युग विशिष्ट समस्याका युग है और इसी व्यापकता को व्यन करने के लिए छोटे-मोटे
अपर्याप्त घोषित किनये गनये और फलस्वरूप लंबी कविता का मृजन संभव हो सका। कविता के लंबेपन में कवि का व्यनित्य का
सहायक होता है। व्यक्ति के अनुसार अनुभूति में अंतर हो जाता है। कविता के निजी बोध अथवा गहराण में उपती गविना के
फलस्वरूप उस कविता का आकार बन जाता है। इसी संदर्भ में कुछ कविताएँ लंबी और कुछ छोटी बन जाती है। लंबी कविता के
बोध और संवेदना का फलक विस्तृत होता है। 'तार रातक के द्वितीय संस्करण में कवि एक नई कविता 'एक आत्ममंतन' की रचना
जो कुल मिलाकर छः पृष्ठों की कविता है और उसके विषय में कवि का कथन है कि, 'यहाँ जो नई कविता दी जा रही है, और यह
1963 की ही रचना है, अपेक्षाकृत छोटी है। इससे छोटी रचनाएँ शायद मे अब नहीं लिख सकता।' (वहीं, पृ.3) इन प्रकार स्पष्ट है
कि कविता का लंबा होना कवि की वैज्ञानिकता पर निर्भर है।

लंबी कविता में कथा को अभिव्यक्त करने का अपना एक अलग ढंग है। कथन की भंगिमा मुख्यतः तीन बातों पर निर्भर
करती है- कौन कह रहा है, नया कह रहा है और किससे कह रहा है। (वहीं पृ.4) छायावादोत्तर कवियों का अपना कौशल था कि
हल्की-सी बात को उपस्थित कर गुरु गंभीरता को शटके से तोड़ना-" सुनता रहा मधुर नुपुर ध्वनि, यदिप बजती थी चप्पल" (वहीं
पृ.4) आदि पर आज कवि लंबी कविताओं में 'टीम' को बड़ाजक ढंग से कहना चाहता है। धूमिल की 'भोनीराम' इसका उत्कृष्ट
उदाहरण है। 'लंबी कविता में सिवा इसके कि वे लंबी होती हैं और उनका फलक बड़ा होता है' में कोई और अलग बड़ी सूची को
मानता। उनमें एक विचार या मनःस्थिति विस्तार से और सालंकार यानी खूब दिखाई दे मके ऐसे ढंग में कही जा सकती है-
"अनुपात तो उनमें भी होता है। छोटी कविता में बात को सात-सात, आठ-आठ पहलुओं से नहीं देखा जा सकता है। 'अनाम तुम उले
हो'का अनाम पूरी कविता में व्याप्त कविता में व्याप्त है। कभी सूरज की किरन की भाँति, कभी धारा की तरह, कभी गति की उप
वह कवि को प्रभावित करता है और कवि के होठों को प्वाले की भाँति छू लेता है। 'अनाम' को कवि कई पहलुओं में रचका देता
है। 'अनाम' का नाम जानने के लिए कवि की उत्सुकता देखने लायक है।" (वहीं, पृ.4)

छोटी कविता में इतने विस्तार के लिए अवकाश नहीं रहता है। छोटी कविताओं में कवि एक निश्चित अंग ही प्रस्तुत क
पाता है। भवानीप्रसाद मिश्र की ही एक छोटी कविता से इसे स्पष्ट समझा जा जा सकता है। पूरी कविता इसप्रकार है-

मैंने पूछा
तुम क्यों आ गई
वह हँसी
और बोली
तुम्हें कुरूप से
बचाने के लिए
कुरूप है
जरुरत से ज्यादा
धूप
मैं छाया हूँ
जरुरत से ज्यादा धूप
कुरूप हूँ। (वहीं, पृ.4-5)

कविता में धूप और छाया की एक हल्की-सी झलक भर दिखायी पड़ती है। लेकिन लंबी कविताओं का फलक बड़ा होता
है और कवि बाह्य एवं अन्तः दोनों स्थितियों का विस्तार पूर्वक उद्घाटन करता है। कविता के अनेक दृश्यपटन उपस्थित किनये जाते
हैं जो कहीं पाठक को सुख और संतोष के प्रीतिकर विस्तार में देखेलाते चले जाते हैं, कहीं भयानक उत्पात और संसट के इन
संवेदना को क्षुब्ध करते रहते हैं। प्रबंध कविता में एक केंद्रीय कथा के अनेक परिप्रेक्ष्य होते हैं और प्रबंधकार उन्हें अनेक नदनों में
बाँटकर अलग-अलग सगों या अध्यायों में विभाजित कर देता है। आखिर किमी सर्ग में रूप-चित्रण प्रधान हो जाता है, वहीं कहीं

का विकास दिखायी पड़ता है, कहीं मूल्यों का निर्धारण होता है और कहीं वैयक्तिक अनुभूतियों की विवृति दिखाई पड़ती है। इन प्रकार विभिन्न परिप्रेक्ष्यों के आधार पर कई संदर्भ उपस्थित किये जा सकते हैं, लेकिन लंबी कविता का समग्र विकास किसी एक केंद्रीय चेतना से जुड़ा होता है। उन्नी केंद्रीय दम्बुचेतना अथवा संवेदना को कवि अनेक संदर्भों में विकसित करता हुआ आगे बढ़ता है। इस तरह से लंबी कविता से रूप का चित्रण, संवेदना की विवृति, मूल्यों का निर्धारण और उनका अंकन जुड़ जाता है।

कमला की विभिन्न मनःस्थितियों का पूरी कविता में भिन्न-भिन्न रूपों में चित्रण किया गया है। कहीं रूप- कविता नारी के रूप में, कहीं गुलरदेश की रानी के रूप में, कहीं वीरांगना के रूप में, कहीं अपमानित नारी के रूप में, कहीं दीन-हीन करुणा की स्फूर्ति के रूप में कमला उपस्थित होती है। अंत में बहलोभा, लालसा एवं महत्त्वकांक्षा की प्रतिस्फूर्ति बनकर हमारे समझ आती है, जब समस्त शाही परिवार की हत्या कर दी जाती है।

'राम की शक्ति पूजा' के केंद्र में संघर्षमय राम के जीवन में व्याप्त निराशान्धकार है। 'रावण महिमा श्यामा विनाशरी अंधकार' ही राम को घेरे हुए हैं। रावण का भव और रात्रि का अंधकार दोनों एक हैं। कवि का लक्ष्य यहाँ राम-रावण के युद्ध का वर्णन नहीं है इसीलिए कविता का आरंभ होता है- 'रवि हुआ अस्त, ज्योति के पत्र पर लिखा अमरा रह गया राम रावण का अपराजित समरा आज का....। (निराला और मुक्तिबोध की चार लंबी कविताएँ पृ. ४४)' राक्षस, लंका आदि सभी एक व्यापक सांकेतिक अर्थ के लिए एकत्र किये गये हैं। वास्तविक संघर्ष का स्थल तो राम का अंतस्वभाव है। शूनित-माधना की सिद्धि में यह संघर्ष समाप्त हो जाता है। इसी बीच जो भी राम की मानसिक स्थिति बनी है उन्नी का मूल्य चित्रांकन करना कवि का उद्देश्य है। राम बानर सेना के साथ शिविर में लौट आते हैं। राम की जय गुलकर चारों ओर पीठ झाड़ों पर टूटती हुई है। वे पूरी तरह जीवन युद्ध से निराश हो गये हैं, हिंखर भी आशा की एक झलक राम की आँखों में दिखाई पड़ती है। कवि उपमानों के सहारे उनका चित्र खींच देता है-

"उतरा ज्यों दुर्गम पर्वत पर नेशांधकार,

चमकती दूर तराएँ ज्यों कहीं पारा।' (नई कविता की लंबी कविताएँ, पृ. 6)

तदुपरांत राम जहाँ अपने सेनानियों के साथ बैठते हैं वहाँ की स्थिति का वर्णन कवि इसप्रकार करता है-

'हे अमा-निशा, उगलता गगनपग अंधकार,

खो रहा गिा का ज्ञानख सत्वध है पवन-पारा

अप्रतिहत बरज रहा पीछे, अम्बुधि विशाल,

भूधर ज्यों ध्यान मग, केवल जलनी मशाला" (वहीं, पृ. 6)

हिंदी साहित्य में फैंटेसी आधुनिक युग की देन है। आधुनिक युग में जीवन की विचंगति, मानसिक निर्वलता आदि को कवि फैंटेसी के सहारे प्रस्तुत करने लगा है। हिंदी साहित्य में इसकी उपज विदेशी प्रभाव के कारण मानी जा सकती है जो नाटकों में होती हुई काव्य में आयी है। यह फैंटेसी कहीं कवि की मनोवैज्ञानिक दृष्टि प्रगट करती है और कहीं कविता में प्रभावोत्पादकता लाती है। 'राम की शक्ति पूजा' शीर सीता का अपहरण होने का दृश्य फैंटेसी के सहारे चित्रित किया गया है। सप्त भर के लिए पाठक जनक-वाटिका में पहुँच जाता है और राम सीता के 'नयनों का नयनों गोपन-प्रिय संभाषण' के दर्शन करता है। यहाँ एक ओर राम के मन की दुर्वलता लक्षित होती है वहीं दूसरी ओर कविता में एक चमत्कार भी पैदा किया गया है। इसी समय रावण का अद्भुतानुसार्द देना भी फैंटेसी के अंतर्गत है। कविता का यह स्थल फैंटेसी सर्वना के कारण इतना महत्वपूर्ण हो गया है कि पूरी कविता का केंद्र-बिंदु बन गया है। लेकिन फैंटेसी की सफल अभिव्यक्ति मुक्तिबोध ने ही प्रारंभ होती है। श्री. सुरेश ऋतुपूर्व के अनुसार- 'मुक्तिबोध ने अपनी कविताओं में भयानक फैंटेसी की रचना करके, छायावादियों के देशकी मनमन से महीन बाचवीय वातावरण को जिनमें रजनीगंधा की महल में डूबे हुए कुंज हैं, लाज भरा सौंदर्य है- शिप्र-भिन्न कर दिया।' (वहीं, पृ. 8) 'अंधेरे में' के अंतर्गत अनेक सफल फैंटेसी की सर्वना हुई है। विचारों की धुन कवि के मिर में घूमती है और वह इसकी खोज में चेतन में अवचेतन एवं स्वप्न से जागृति अवस्थाओं में संचरण करती हुई बंधार्थ को उछालती चमती है। पूरी कविता का संसार संसार और अंधेरे का संसार है। मुक्तिबोध के अतिरिक्त विजयदेव नारायण साही, धूमिल, राजकमल चौधरी और सीमित्र इकोहन की कविताओं में भी सफल फैंटेसी की रचना की गई है। विजयदेव नारायण साही की लंबी कविताओं में भी मुक्तिबोध के समान फैंटेसी की सर्वना हुई है।

परमानन्द श्रीवास्तव के अनुसार "फैटेसी की दुनिया की यह तलाश, उस जटिल की तलाश है- जहाँ अरिष्ट कठोर मूल्यों और मानव-अस्तित्व की बुनियादी जिज्ञासाओं या चिंताओं का एक साथ सामना किया जा सकता है।" (वहीं, पृ.9)

धूमिल की 'पटकथा' एक चित्रकथा है। जिसमें सामाजिक और राजनैतिक यथार्थ के अनेक दृश्य फैटेसी के माहौल पर उपस्थित किये गये हैं। पूरी कविता एक सपाट बगानी है जिसमें गहनत भाषा का अभाव महसूस होता है। इस कारण ही अशोक वाजपेयी इस कविता को एक दिनचर्या असफलता मानते हैं जिसे पढ़ने में ऊब और कभी-कभी थिड़ पैदा होती है।" (वहीं, पृ.9) अशोक वाजपेयी का यह कथन एकांकी दृष्टि का परिचायक है। इसे ज्यों-का-त्यों स्वीकार नहीं किया जा सकता है। कविता में फैटेसी के सहारे कवि ने हिंदुस्थान का दृश्य उपस्थित किया गया है जो पूरी कविता को एक गहरे दृष्टिकोण पर आधारित बना कर देता है। फैटेसी की सफल अभिव्यक्ति निम्नलिखित पंक्तियों में देखी जा सकती है। धून और आंगूओं से तर चेहरे में हिंदुस्तान की गथाय धूमिल की फैटेसी की देन है-

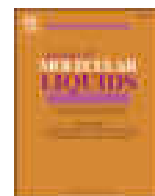
उसका हाथ ऊपर उठा था
धून और आंगू से तर चेहरा
'दुखी मत हो। यही मेरी नियति है।
मे हिंदुस्तान है।

हत्बारा। हत्बारा। हत्बारा।' (वहीं, पृ.9)

कुल मिलाकर भूमंडलीकरण के दौर में लिखी लंबी कविता की फैटेसी एक महत्वपूर्ण विशेषता है जिसकी प्रत्येक लंबी कविताओं में सफल सृष्टि की गयी है। इसके प्रयोग से लंबी कविताओं में जहाँ एक ओर चमत्कार उत्पन्न किया गया है वहीं एक नवीन शैली के प्रयोग द्वारा प्रभाव भी पैदा करने की कोशिश की गई है। भूमंडलीकरण के दौर में घटित जटिल मनोव्यापारों को अभिव्यक्त करने के लिए लंबी कविताओं ने फैटेसी का भरपूर उपयोग किया हुआ है। भूमंडलीकरण के समय की लंबी कविता की संरचना में फैटेसी का भी महत्वपूर्ण स्थान होता है। फैटेसी द्वारा जहाँ एक ओर कविता लंबी होती है वहीं दूसरी ओर उगम गद्यात्मकता प्रधान होती है। डॉ. आत्म-संघर्ष और सामाजिक संघर्ष, आत्म और अनात्म के संघर्ष के फलस्वरूप आज की कविता का कथय पूर्णतः जटिल हो गया है। इस जटिल कथा की अभिव्यक्ति के लिए कवि स्वप्न और फैटेसी की शैली अपनाता है। यह लंबी कविता की अपनी निजी विशेषता है। कवि के भीतर का संघर्ष पूरे समाज में फैला हुआ है जिसके भीतर अनेक जातीय-पड़पानी आकृतियाँ उभरती दिखायी देती हैं। कविता के प्रारंभ में ही उस अंधेरे का वर्णन शुरू होता है जो जिंदगी के कमरों में लगातार चक्कर लगाता है। इसी अंधेरे के बीच कविता के अंत तक कवि हूर सड़क हूर गली में प्रत्येक चेहरे की ओर झाँककर पठार, पहाड़ और समुद्र तक अपनी खोई हुई अभिव्यक्ति को ढूँढता है। सफल फैटेसी की रचना के लिए भाषा का संघटन आवश्यक है जिसमें प्राचीन वाच्यता को नष्ट किया जा सके। मुक्तिबोध में भाषा का यह संहारक रूप सबसे अधिक उभरकर आया है। इसी कारण मुक्तिबोध फैटेसी की रचना में अधिक सफल हुई है।

संदर्भ:

- 1) नई कविता की लंबी कविताएँ डॉ. रामसुधारसिंह; राधा पब्लिकेशन, नई दिल्ली-110002; प्रथम संस्करण 1993
- 2) लंबी कविताएँ वैचारिक सरोकार; डॉ. बलदेव बंशी; वाणी प्रकाशन नई दिल्ली; प्रथम संस्करण 2009
- 3) पाब्लो नेरुदा: एक कैदी की खुली दुनिया; अरुण माहेश्वरी; वाणी प्रकाशन नई दिल्ली.
- 4) कविता से लंबी कविता: दिनोदकुमार शुक्ल; वाणी प्रकाशन नई दिल्ली.
- 5) मापेक्ष संपादक-महावीर अग्रवाल
- 6) लंबी कविताएँ और नरेंद्र मोहन; संपा. डॉ. रमेश सोनी



[DABCO-C₁₈]Br: A novel basic surfactant for the synthesis of dihydropyrano[3,2-c]chromenes and 2-aminobenzochromenes under ambient conditions

Archana Rajmane^a, Rupesh Bandal^a, Sunita Shirke^a, Utkarsh More^b, Suresh Patil^c, Arjun Kumbhar^{a,*}

^a Department of Chemistry, Vivekanad College, Kolhapur (Empowered Autonomous), Maharashtra 416003, India

^b Department of Chemistry, Shivaji University, Kolhapur 416004, India

^c Department of Chemistry, P. D. V. P. College, Tasgaon, Maharashtra 416312, India

ARTICLE INFO

Keywords:

Multi-component reactions
Chromenes
[DABCO-C₁₈]Br
Surfactants
CMC
Recyclability

ABSTRACT

We successfully produced a new surfactant called [DABCO-C₁₈]Br, which is a monoquaternized octadecyl-1,4-diazabicyclo[2.2.2]octane bromide. The yield was good. The surfactant that was created was analyzed using techniques such as ¹H NMR, ¹³CNMR, and Mass characterization. We analyzed the synthesized [DABCO-C₁₈]Br salt and found that it has great surfactant properties. Its critical micelle concentration (CMC) is 1.15 mM as determined by the conductivity method and 1.0 mM by UV-Vis absorption measurement at 298.15 K. The values align well with the critical micelle concentration (CMC) of the commonly used surfactant [C16TAB]. We have studied the catalytic efficiency of [DABCO-C₁₈]Br, a tertiary base surfactant, for the synthesis of dihydropyrano [3,2-c]chromenes. This synthesis is achieved through one-pot three-component reactions involving aromatic aldehydes, malononitrile, and 4-hydroxycoumarin in water at room temperature. The method was also extended for the synthesis of 2-aminobenzochromenes via one-pot three-component reactions of aromatic aldehydes, malononitrile, and lawsone in water at 80 °C. The products were achieved in yields ranging from good to excellent within a timeframe of 30–60 min. In addition, the aqueous solution with [DABCO-C₁₈]Br was reused up to four times with a minor reduction in product output. This protocol is fast, energy-efficient, and can be used on a large scale for synthetic purposes. Additionally, it boasts impressive environmentally-friendly credentials.

1. Introduction

One of the most valuable methods for creating chemically and biologically significant structures is through the use of multicomponent reactions (MCRs) [1–3]. The approach includes combining multiple substrates in a single reaction, resulting in domino methods [4–7]. Another option is to add one or more reactants sequentially without isolating intermediates. MCR provides exceptional rewards thanks to its simplicity, easy automation, and waste reduction resulting from reduced work-up and purification stages. In green chemistry, a significant focus is on developing active and eco-friendly procedures for synthesizing biologically important compounds [8,9]. Using green solvents, like water, in various initiatives to replace volatile organic solvents [10,11] is crucial. This work aims to create and implement innovative methods for synthesizing materials using water as a sustainable and eco-friendly

reaction medium [12–14]. Sometimes, organic compounds may have limited solubility in water. However, this issue can be resolved by incorporating surface-active compounds like surfactants [15–17].

Dihydropyrano[3,2-c]chromenes, which are a type of chromene derivative [9], are an intriguing group of fused heterocyclic scaffolds. They have been found to have various beneficial properties, including anti-HIV, antimicrobial, antibacterial, anticancer, spasmolytic, and anticoagulant activities [18–20]. Additionally, these derivatives have shown potential as a treatment for various neurodegenerative diseases, such as Alzheimer's disease, Parkinson's disease, Down's syndrome, AIDS-associated dementia, Huntington's disease, schizophrenia, and myoclonus [21,22] (Fig. 1).

In connection with this, many substantial efforts have been made for the synthesis of dihydropyrano[3,2-c]chromenes in the presence of piperidine [23] cetyltrimethylammonium chloride (CTAC) [24]

* Corresponding author.

E-mail address: arjun22win@rediffmail.com (A. Kumbhar).

<https://doi.org/10.1016/j.molliq.2023.123247>

Received 17 August 2023; Received in revised form 29 September 2023; Accepted 3 October 2023

Available online 5 October 2023

0167-7322/© 2023 Elsevier B.V. All rights reserved.

cetyltrimethylammonium bromide (CTAB) coupled with ultrasound [25], alumina [26], K_2CO_3 under microwave irradiation [27], MgO nanoparticles [28], heteropolyacid [29], hexadecyltrimethylammonium bromide (HTMAB) [30], triethylbenzylammonium chloride (TEBA) [31], $TiCl_4$ [32], $(NH_4)_2HPO_4$ -(S)-proline [33], sodium carbonate [34], NaOAc/KF [35], NaBr coupled with electrochemical technique [36], indium with NaI [37], sodium dodecyl sulfate (SDS) [38], tetrabutylammonium chloride [39], 3-hydroxypropanaminium acetate (HPAA) [40] ZIF@ZnTiO₃ Nanocomposite [41], DTP/SiO₂ [42], MnONPs [43] WEB [44], IRA 400-Cl resin [18], [Ch][TAPSO] [45], $NH(CH_2)_7NH_3BiCl_5$ [46], DES [47], NiO-NPs using mucilage of Cordia myxa fruit [48] and many more. While most of these methodologies have become established, some of them have presented more or fewer drawbacks. For instance, many of these pose environmental hazards, longer reaction times, modest yields, and higher amounts of catalysts.

We have recently introduced new and efficient methods for synthesizing different heterocyclic frameworks [49,50] and for Pd-catalysed coupling reactions [51], which are in line with green chemistry principles and involve the use of various additives. In this communication, we would like to share our findings on a surfactant called [DABCO-C₁₈]Br, which acts as an effective and reusable 'Gemini type surfactant' with basic properties [52]. This surfactant has been used for synthesizing dihydropyrano[3,2-c]chromene and 2-aminobenzochromene derivatives in a water-based medium.

2. Experimental

2.1. General remarks

All reactions were carried out in a round-bottom flask at RT or heating. Chemical reagents and anhydrous solvents were purchased

from commercial suppliers (TCI and Sigma-Aldrich chemical companies) and used as purchased. Thin layer chromatography (TLC) was performed using silica gel pre-coated aluminum plates, which were visualized with UV light at 254 nm or under iodine. ¹H NMR and ¹³C NMR were recorded with Bruker (600 MHz) spectrometers using CDCl₃ and DMSO solvents. Chemical shifts for ¹H NMR are referred to as internal TMS (0 ppm). Data are reported as follows: chemical shift (δ ppm), multiplicity (s = singlet, d = doublet, t = triplet, q = quartet, m = multiplet), coupling constant (Hz), and integration.

2.2. General procedure for the synthesis of [DABCO-C₁₈]Br surfactant

In a round-bottom flask, containing DABCO (1,4-diazabicyclo[2.2.2]octane) (2.13 g, 19.01 mmol) and 1-Bromooctadecane (5.0 g, 5.15 mL, 15.01 mmol) was stirred in ethyl acetate (20 mL) at 60 °C for 24 h. The obtained white solid was filtered, and washed with ethyl acetate (3 × 15 mL) and dried in oven. The yield of product was 89 %.

2.3. General procedure for the synthesis of dihydropyrano[3,2-c]chromenes

In a round-bottom flask containing 4-nitrobenzaldehyde (0.151 g, 1 mmol), malononitrile (0.066 g, 1 mmol) and 4-hydroxycoumarin (0.162 g, 1 mmol) was stirred in water (5 mL) in the presence of [DABCO-C₁₈]Br (20 mg, 0.044 mmol) at room temperature. The progress of the reaction was monitored by TLC in ethyl acetate:n-hexane (4:6). For TLC analysis the reaction mixture was extracted in ethyl acetate. After completion of reaction, the solid product was filtered, washed with water (5 mL) and dried in oven. The crude product was recrystallized by hot ethanol.

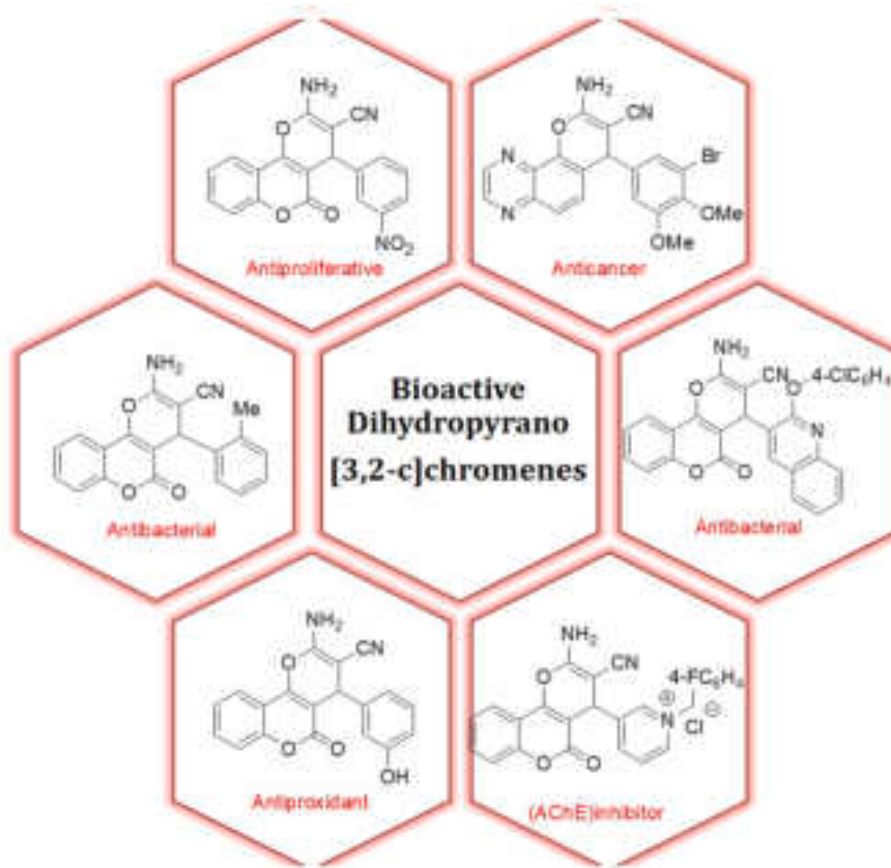


Fig. 1. Critical pharmaceutical active compounds containing chromene framework.

2.4. General procedure for the 2-aminobenzochromene

In a round-bottom flask containing 4-nitrobenzaldehyde (1 mmol, 0.151 g), malononitrile (1 mmol, 0.066 g) and Lawsone (1 mmol, 0.174 g) was stirred in water (5 mL) in the presence of [DABCO-C₁₈]Br (20 mg, 0.044 mmol) at 80 °C temperature. The progress of the reaction was monitored by TLC in ethyl acetate:*n*-hexane (2:8). For TLC analysis the reaction mixture was extracted in ethyl acetate. After completion of reaction, the solid product was filtered, washed with water (5 mL) and dried in oven. The crude product was recrystallized by hot ethanol.

3. Results and discussion

3.1. Synthesis of [DABCO-C₁₈]Br

The [DABCO-C₁₈]Br salt was synthesized with ease by mono-quaternizing DABCO (1,4-diazabicyclo[2.2.2]octane) with 1-bromooctadecane in ethyl acetate at 60 °C. The yield of the final product was 89 % (Scheme 1) [53].

3.2. Micellization behavior of [DABCO-C₁₈]Br in aqueous solution

The conductivity and UV measurements were used to determine the micellization behavior (CMC) of pure [DABCO-C₁₈]Br in an aqueous solution.

3.2.1. Conductivity measurements

The critical micelle concentration (CMC) refers to the point at which the behavior of the surfactant alters in physical and spectral properties [54]. The method of conductivity is a reliable way to gather information about the behavior of surfactants, both before and after they form micelles [55]. As part of our current investigation, we have assessed the CMC of pure [DABCO-C₁₈]Br in an aqueous solution. To take conductivity measurements, we added incremental amounts of aqueous surfactant solution from the stock solution (which was 5 times higher than CMC), to the conductivity cell. We also added an appropriate volume of distilled water. After the solutions were mixed, we recorded stable conductivity values. For each concentration, we made five measurements and only the mean values were used. The standard uncertainty of the measurements was less than 0.3 % [56]. Fig. 2 displays the plots for the conductivity technique utilized in this study to determine the concentration of the pure aqueous [DABCO-C₁₈]Br at a temperature of 298.15 K. In this method, we noticed a distinct shift in the property's slope in the CMC area as 'c' (surfactant) increased. Based on the Onsager theory of electrolyte conductivity, we saw a change in slope between the pre- and post-micellar regions in conductance measurements. The intersection points of the two straight lines representing the CMC of surfactants were also observed. The CMC of the pure [DABCO-C₁₈]Br at 298.15 K was obtained as 1.15 mM, which is in agreement with the CMC of the common surfactant [C₁₆TAB], which is 0.98 mM [57].

The degree of counter ion binding (β) was determined through $\beta = 1 - \alpha$ (where, $\alpha = S_2/S_1$, S_2/S_1 is the ratio of the post-micellar slopes to pre-micellar slopes), in the conductivity versus concentration plots [58,59]. The values for the degree of counter ion binding (β) using conductivity measurements for pure [DABCO-C₁₈]Br is 0.828.

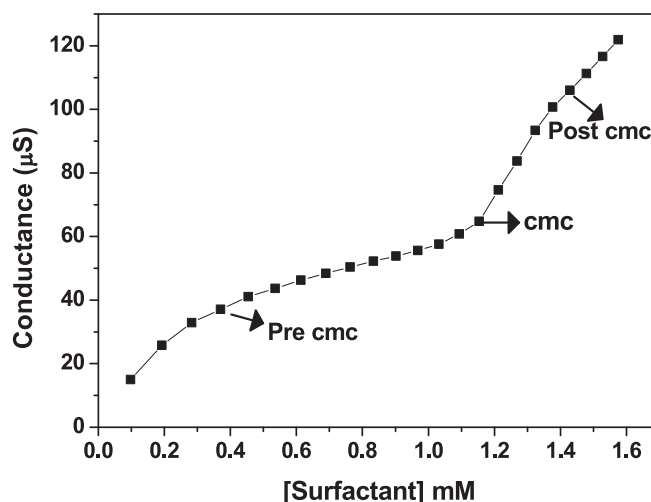


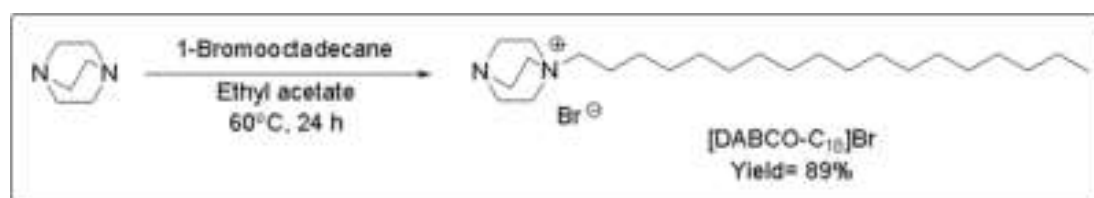
Fig. 2. Conductometric profile of pure [DABCO-C₁₈]Br in aqueous solution at 298.15 K.

3.2.2. UV-Vis absorption measurements

For the measurements of UV-Visible spectra, we used UV-Vis spectrophotometer (Varian Carry 50, Switzerland) equipped with a thermostated cell compartment for the temperature control. We determined the micellization behavior of [DABCO-C₁₈]Br in an aqueous solution by measuring dye solubilization based on UV-Vis absorption. Specifically, we used an anionic dye, methyl orange, since [DABCO-C₁₈]Br is a cationic surfactant. The dye solubilization method operates on the principle of solution polarity [60]. In Fig. 3, we can see the plot of absorbance versus wavelength for various concentrations of [DABCO-C₁₈]Br, a surfactant in an aqueous solution using methyl orange dye. The plot shows that the peak for pure dye (without the addition of surfactant) is obtained at λ_{max} 465 nm. However, as the concentration of surfactant increases, the absorption peak shifts towards a shorter wavelength (known as a hypsochromic shift or higher frequency). This occurs because the dye molecules start associating with surfactant monomers, which decreases the microscopic polarity near the dye molecules. At the micellar pseudo-phase, the dye molecules become solubilized and a decrease in absorbance is observed. Additionally, in the presence of a surfactant, the λ_{max} for the methyl orange dye shifts from 465 to 435 nm, which may be due to the dye being solubilized or incorporated into the core of the surfactant molecule.

Fig. 4 displays the absorption spectra of methyl orange dye at varying concentrations of pure [DABCO-C₁₈]Br in an aqueous solution at 298.15 K. The CMC was determined by where two lines intersected. The CMC of [DABCO-C₁₈]Br is 1.0 mM. The concentration range for CMC by UV-Visible measurements is from 0.98 mM to 1.2 mM, which aligns well with the conductance measurements and literature value of [C₁₆TAB] (i. e. 0.98 mM) [57].

Fig. 5 illustrates the graphical mechanism of micellization for [DABCO-C₁₈]Br surfactant, as determined by the experiments described above.



Scheme 1. Synthesis of [DABCO-C₁₈]Br surfactant.

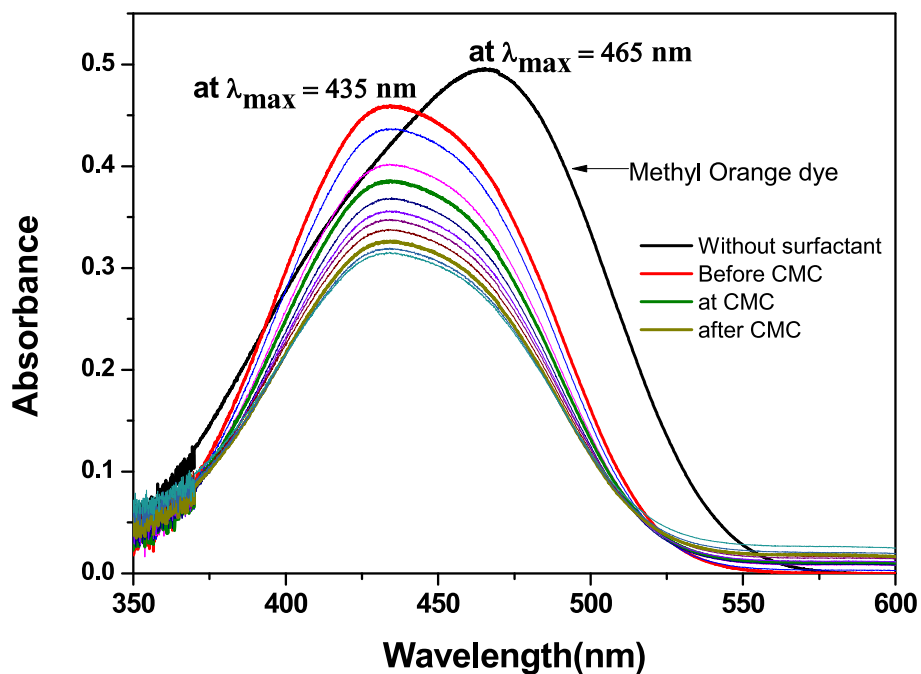


Fig. 3. The absorption spectra of methyl orange dye in aqueous solution of pure [DABCO-C₁₈]Br at 298.15 K ($c(\text{MO})$ is 1.15×10^{-4} M). (For interpretation of the references to colour in this figure legend, the reader is referred to the web version of this article.)

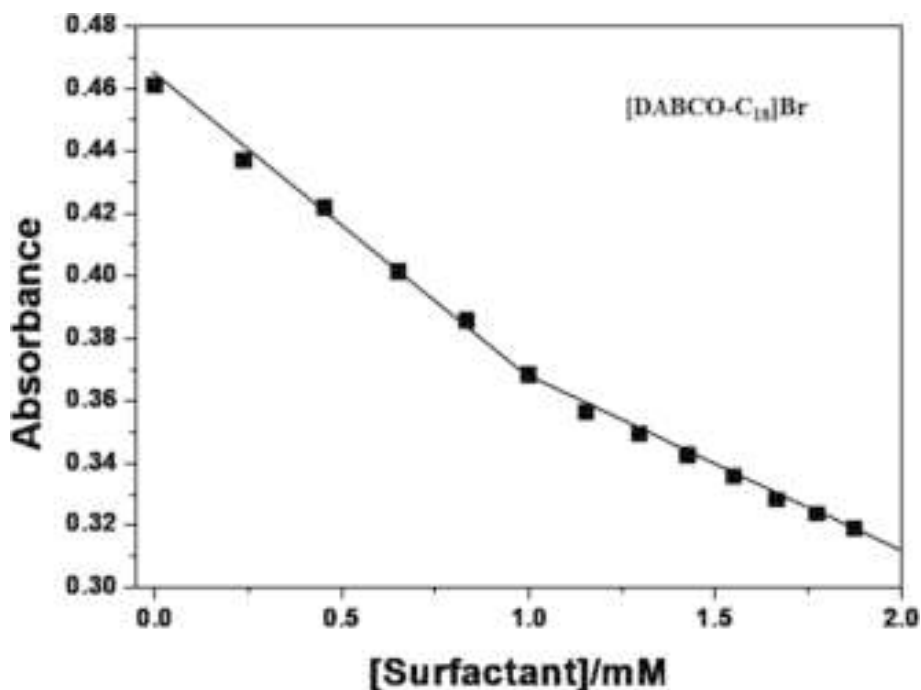


Fig. 4. Absorbance versus concentration of pure [DABCO-C₁₈]Br surfactants in aqueous solution at 298.15 K.

3.3. Applications of [DABCO-C₁₈]Br in the synthesis of dihydropyrano [3,2-c]chromenes

Based on the favorable surfactant characteristics of [DABCO-C₁₈]Br, as well as the alkaline properties provided by DABCO, we intended to investigate its catalytic abilities in producing dihydropyrano[3,2-c]chromenes using eco-friendly conditions.

At first, to improve different reaction conditions, we selected 4-nitrobenzaldehyde (0.151 g, 1 mmol), malononitrile (0.066 g, 1 mmol), and 4-hydroxycoumarin (0.162 g, 1 mmol) as the model reaction partners in

an aqueous solution of [DABCO-C₁₈]Br (Scheme 2).

We conducted the model reaction with different conditions to determine the appropriate amount of surfactant, reaction temperature, and type of solvent (Table 1). It's worth noting that the reaction didn't take place under conditions without a catalyst (Table 1, entry 1). Table 1 shows that with the addition of 5 mg surfactant, the product yield increased to 84 % (Table 1, entry 2). When the amount of surfactant was increased from 5 to 50 mg, the yield improved from 84 to 96 % and the reaction time reduced from 30 to 25 min. at room temperature. (Table 1, entries 2–7). Raising the temperature of the reaction

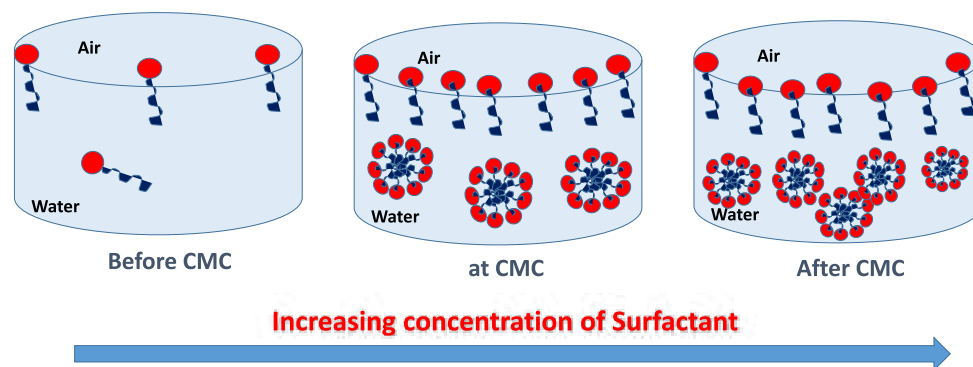
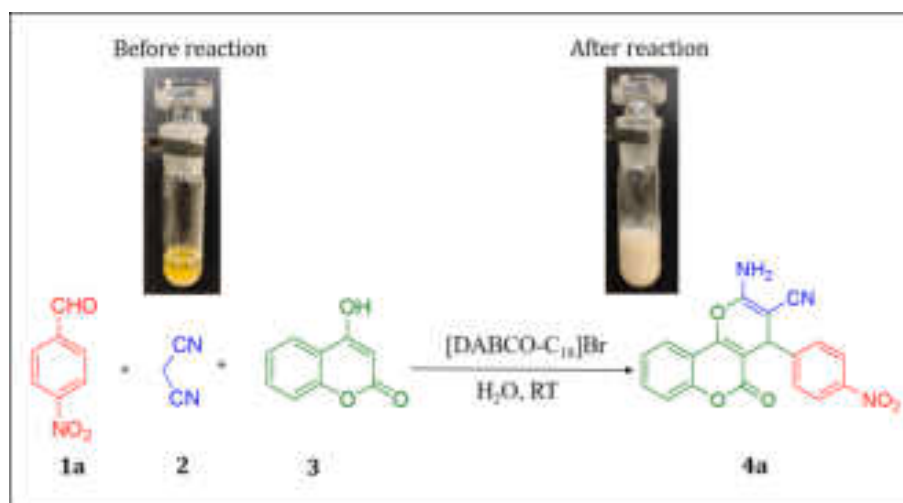


Fig. 5. Graphical representation of micellization of [DABCO- C_{18}]Br in water.



Scheme 2. Synthesis of dihydropyrano[3,2-c]chromene using [DABCO- C_{18}]Br surfactant in aqueous solution.

Table 1

Influence of quantity of surfactant, nature of solvent, and temperature on the yield and reaction time of dihydropyrano[3,2-c]chromene.^a

Entry	Amount of [DABCO- C_{18}]Br (mg)	Solvent	Temperature (°C)	Time (min)	Yield ^b (%)
1	0	H ₂ O	RT	60	Trace
2	5	H ₂ O	RT	30	84
3	10	H ₂ O	RT	30	90
4	20	H ₂ O	RT	30	96
5	30	H ₂ O	RT	25	95
6	40	H ₂ O	RT	25	96
7	50	H ₂ O	RT	25	96
8	20	H ₂ O	40	30	95
9	20	H ₂ O	80	20	94
11	20	EtOH	RT	30	94
12	20	EtOH:H ₂ O (1:1)	RT	30	89
13	20	DMF	RT	35	88
14	20	DCM	RT	45	85
15	20	CH ₃ CN	RT	50	78
16	20	Toluene	RT	60	70

^a Reaction conditions: 4-Nitrobenzaldehyde (1 mmol), malononitrile (1 mmol), 4-hydroxycoumarin (1 mmol), [DABCO- C_{18}]Br (5–50 mg), solvent (5 mL), RT to 80 °C.

^b Isolated yields.

mixture from room temperature to 80 °C significantly affects the reaction time. (Table 1, entries 8–9). We tested the catalytic activity of surfactant in various organic solvents. While it did work in these

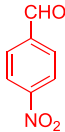
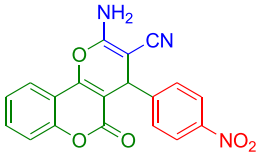
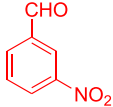
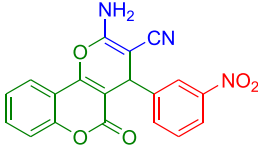
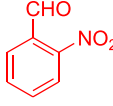
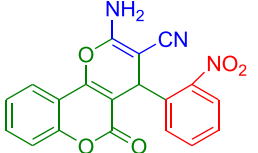
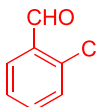
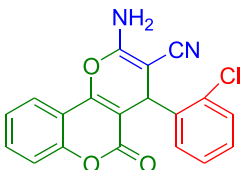
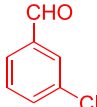
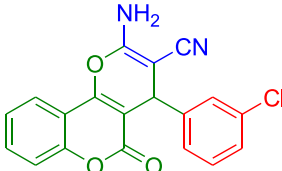
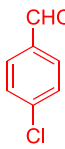
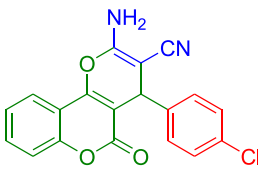
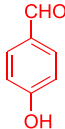
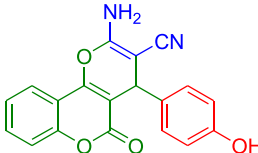
solvents, its activity was lower than in water (Table 1, entries 10–15). Therefore, we determined that the best reaction condition is using 20 mg of surfactant in water at room temperature (Table 1, entry 4).

Using the optimized conditions, we explored the current procedure for synthesizing different derivatives of dihydropyrano[3,2-c]chromenes (Table 2). The reaction was feasible with a wide range of aromatic aldehydes. All reactions were conducted at room temperature, on a 1 mmol scale, with the presence of 20 mg surfactant in water, unless otherwise stated. The reactants were converted efficiently into the desired products, with yields ranging from 87 to 96 %. Additionally, aromatic heterocyclic aldehydes were able to react successfully, producing the product with 87–93 % yield.

3.4. Applications of [DABCO- C_{18}]Br in the synthesis of 2-aminobenzochromene

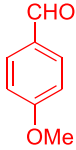
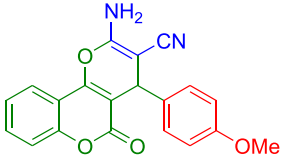
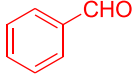
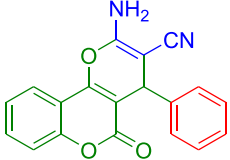
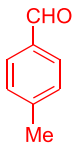
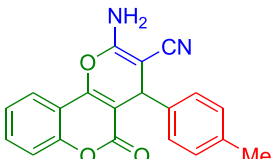
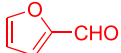
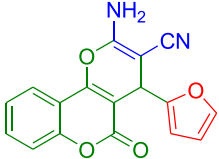
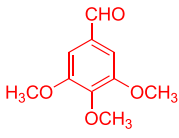
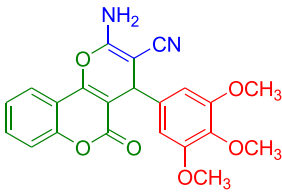
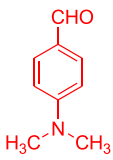
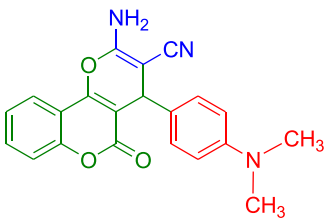
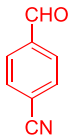
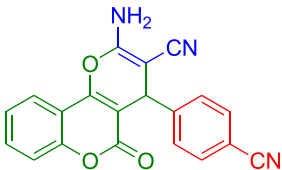
There are a variety of biological activities associated with benzo[g]chromenes, such as anti-cancer, anti-inflammatory, and anti-malaria effects [61]. In addition, the benzo[g]chromenes occurring naturally are also used as drugs for the treatment of tumor [62,63]. In this connection, many 2-aminobenzochromenes were synthesized by different synthetic methods from aromatic aldehyde, lawsone, and malononitrile in the presence of different catalysts such as TEBA [64], Potassium phthalimide-N-oxyl [65], propylpiperazine-N-sulfamic acid (SBPPSA) [66], Zn(L-proline)₂ [67], Et₃N [68], urea [69], [bmim]OH [70], L-proline [71], [Et₃NH][HSO₄] [72], Fe₂O₃@SiO₂ NPs [73], ammonium acetate [74], Fe₃O₄@SiO₂@NH₂-TCT-Mesalamine – Cu(II) MNPs [75], and IRA 400-Cl resin [18]. However, there is a need to

Table 2Exploration of the substrate scope for the synthesis of dihydropyrano[3,2-c]chromenes in aqueous [DABCO-C₁₈]Br solution at room temperature.^a

Entry	Aldehydes	Products	Time (min)	Yield ^b (%)	M.P (°C)
1			30	96	258–260
2			35	93	262–264
3			30	92	250–252
4			30	92	264–266
5			35	91	244–246
6			30	94	260–262
7			45	90	258–260

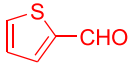
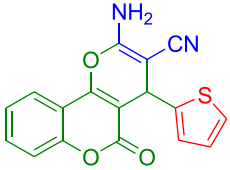
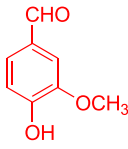
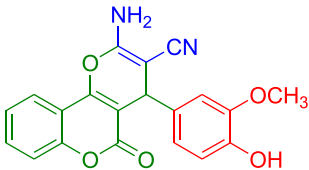
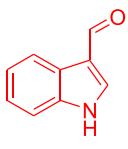
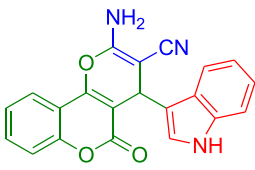
(continued on next page)

Table 2 (continued)

Entry	Aldehydes	Products	Time (min)	Yield ^b (%)	M.P (°C)
8			40	90	240–242
9			40	89	256–258
10			35	88	250–252
11			45	88	250–252
12			35	93	238–240
13			30	92	222–224
14			30	91	286–288

(continued on next page)

Table 2 (continued)

Entry	Aldehydes	Products	Time (min)	Yield ^b (%)	M.P (°C)
15			45	87	226–228
16			30	92	250–252
17			35	93	200–202

^a Reaction conditions: Aromatic aldehydes (1 mmol), malononitrile (1 mmol), 4-hydroxycoumarin (1 mmol), [DABCO-C₁₈]Br (20 mg), Water (5 mL), RT.

^b Isolated yields.

develop a new better, and more efficient method that can lead to enhanced yields under green conditions.

We experimented with using lawsone to synthesize 2-aminobenzochromene after successfully utilizing 4-hydroxycoumarin as a nucleophile. The procedure entails combining aryl aldehydes (1 mmol), malononitrile (0.066 g, 1 mmol), lawsone (0.174 g, 1 mmol) under varying reaction conditions (Scheme 3).

To determine the appropriate amount of surfactant, reaction temperature, and solvent type, the model reaction was tested under different conditions (Table 3). It was found that no reaction took place when there was no catalyst present (Table 3, entry 1). After conducting different experiments, it was determined that the ideal reaction conditions involve use of 20 mg surfactant in water at a temperature of 80 °C (Table 3, entry 9).

After obtaining the optimized conditions, we investigated the reaction scope for the synthesis of different 2-aminobenzochromene derivatives (Table 4). Our findings showed that numerous aromatic

Table 3

Influence of quantity of surfactant, nature of solvent, and temperature on the yield and reaction time of 2-aminobenzochromene.^a

Entry	Amount of [DABCO-C ₁₈]Br (mg)	Solvent	Temperature (°C)	Time (min)	Yield ^b (%)
1	0	H ₂ O	RT	60	NR
2	5	H ₂ O	RT	180	94
3	10	H ₂ O	RT	160	95
4	20	H ₂ O	RT	140	96
5	30	H ₂ O	RT	100	95
6	40	H ₂ O	RT	90	96
7	50	H ₂ O	RT	90	96
8	5	H ₂ O	40	90	90
9	20	H ₂ O	80	60	96
11	20	EtOH	80	90	80
12	20	EtOH:H ₂ O (1:1)	80	90	89
13	20	DMF	80	70	86
14	20	DCM	80	120	85
15	20	CH ₃ CN	80	150	78
16	20	Toluene	80	160	70

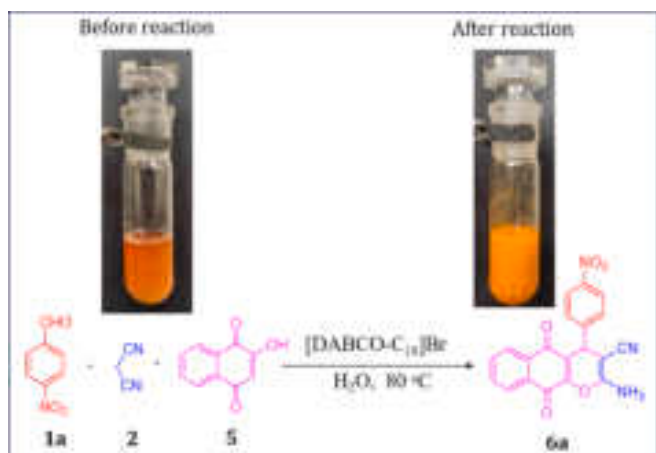
^a Reaction conditions: 4-Nitrobenzaldehyde (1 mmol), malononitrile (1 mmol), lawsone (1 mmol), [DABCO-C₁₈]Br (5–50 mg), solvent (5 mL), RT to 80 °C.

^b Isolated yields.

aldehydes can be effortlessly converted into the intended products with yields ranging from good to excellent.

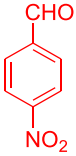
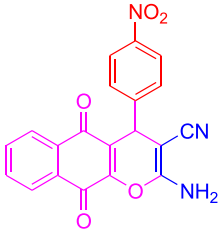
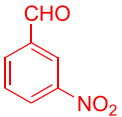
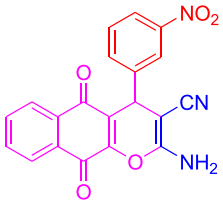
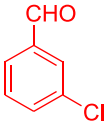
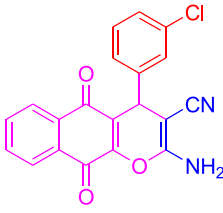
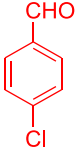
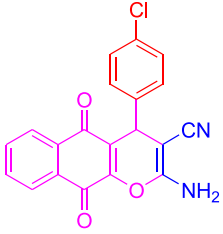
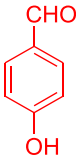
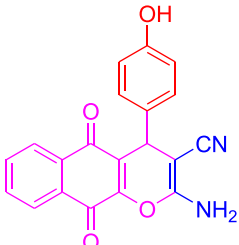
3.5. Gram-scale synthesis of dihydropyrano[3,2-c]chromene and 2-aminobenzochromene

We examined the effectiveness of the current approach for creating dihydropyrano[3,2-c]chromene and 2-aminobenzochromene on a gram scale (10 mmol scale). This was achieved by reacting 4-nitrobenzaldehyde (1.51 g, 10 mmol), malononitrile (0.66 g, 10 mmol), and 4-hydroxycoumarin (1.62 g, 10 mmol) under standard conditions. Within 90 min, the process yielded 94 % of the target product **4a**. Similarly, **6a** was



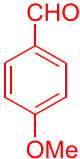
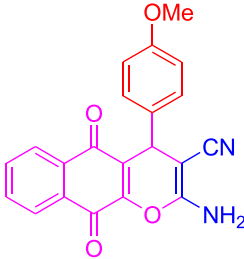
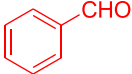
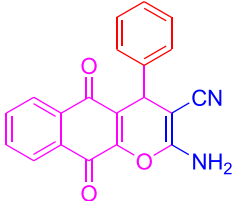
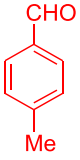
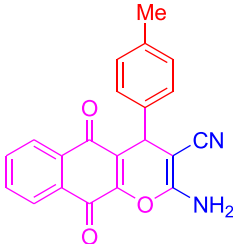
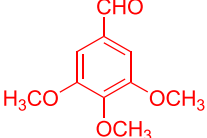
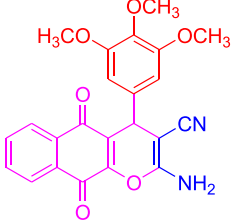
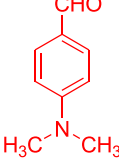
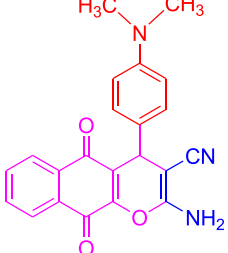
Scheme 3. Synthesis of 2-aminobenzochromene using [DABCO-C₁₈]Br surfactant in aqueous solution.

Table 4
Exploration of the substrate scope for the synthesis of 2-aminobenzochromenes.^a

Entry	Aldehydes	Products	Time (min)	Yield ^b (%)	M.P (°C)
1			60	96	228–230
2			65	94	246–248
3			60	88	242–244
4			70	96	278–280
5			60	93	250–252

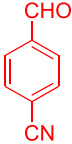
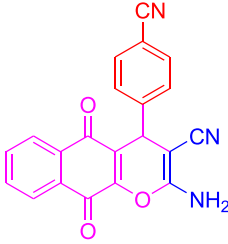
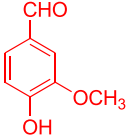
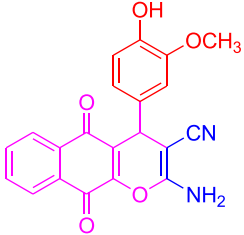
(continued on next page)

Table 4 (continued)

Entry	Aldehydes	Products	Time (min)	Yield ^b (%)	M.P (°C)
6			75	90	248–250
7			70	91	258–260
8			70	90	240–242
9			60	95	228–230
10			60	95	246–248

(continued on next page)

Table 4 (continued)

Entry	Aldehydes	Products	Time (min)	Yield ^b (%)	M.P (°C)
11			60	94	238–240
12			65	96	248–250

^a Reaction conditions: Aromatic aldehydes (1 mmol), malononitrile (1 mmol), Lawsone (1 mmol), [DABCO-C₁₈]Br (20 mg), Water (5 mL), 80 °C.

^b Isolated yields.

produced with a 92 % yield by reacting 4-nitrobenzaldehyde (1.51 g, 10 mmol), malononitrile (0.66 g, 10 mmol), and lawsone (1.74 g, 10 mmol) at 80 °C (Scheme 4).

3.6. Mechanism of synthesis of dihydropyrano[3,2-c]chromenes and 2-aminobenzochromenes

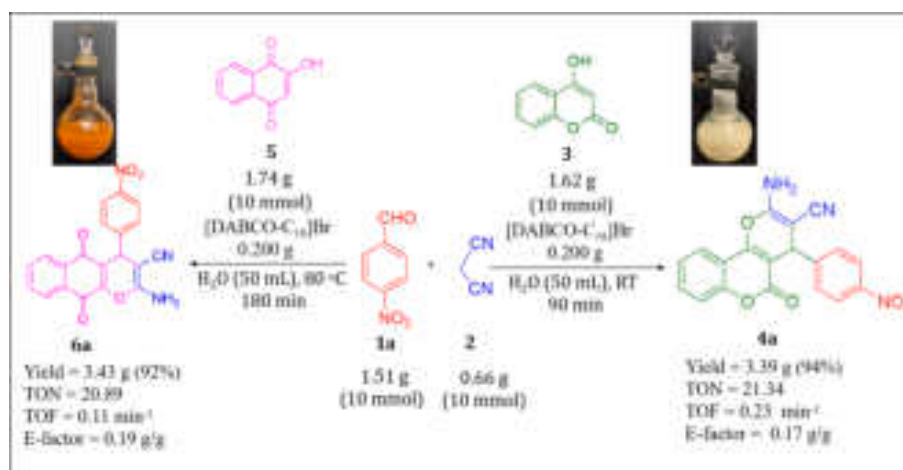
According to the results shown above, Scheme 5 provides a plausible mechanism for the creation of chromenes (4) and (6). Initially, [DABCO-C₁₈]Br acts as a base, abstracting the acidic proton of malononitrile (2) producing anionic intermediate I. The resulting intermediate I attacks the carbonyl group of aldehyde (1) to form a Knoevenagel adduct II. In the second step, the 4-hydroxycoumarin (3) or lawsone (5) reacts with adduct II to create Michael adduct III and III' respectively. These adducts undergo intramolecular cyclization via intermediate IV and IV' followed by tautomerization and delivered the desired products 4a and 6a respectively.

3.7. Recyclability

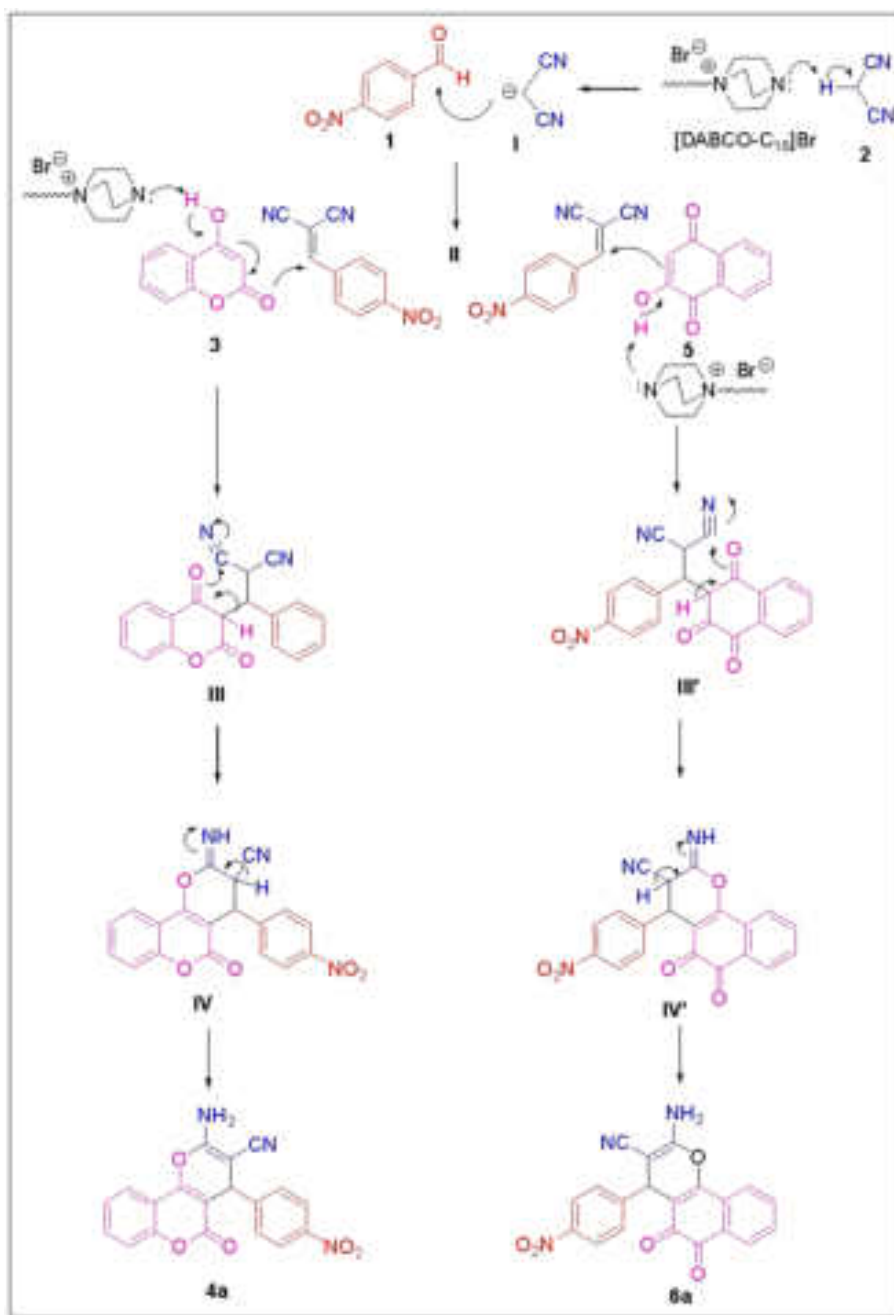
Efficient recycling of catalytic systems with consistent activity is crucial for sustainable organic transformations. To study the recyclability of the catalytic system for dihydropyrano[3,2-c]chromene synthesis, a model reaction was used. The [DABCO-C₁₈]Br containing aqueous solution can be easily separated from the reaction mixture through filtration. The aqueous layer was then washed with ethyl acetate, and the aqueous layer containing [DABCO-C₁₈]Br was recycled at least four times with a slight decrease in activity (Fig. 6).

3.8. Estimation of greenness of the present protocol

Later on, several metrics were analyzed to determine the level of environmental friendliness of the current protocol [76,77]. Green metrics quantify the efficiency and environmental impact of chemical processes. These can be better measured by various factors such as environmental factor (E factor), turnover number (TON), turnover frequency (TOF), atom economy (AE), atom efficiency (Aef), carbon



Scheme 4. Gram scale synthesis of products 4a and 6a using [DABCO-C₁₈]Br.



Scheme 5. A plausible mechanism for the synthesis of dihydropyrano[3,2-c]chromenes and 2-aminobenzochromenes using [DABCO-C₁₈]Br.

efficiency (CE), optimum efficiency (OE), effective mass yield (EMY), reaction mass efficiency (RME), mass productivity (MP), mass intensity (MI) and process mass intensity (PMI), as well as solvent and water intensity (SI and WI). Table 5 displays the green chemistry metrics that were measured for all the reactions (See Supporting Information, Tables S3–S6).

The representative results of the model reaction under optimized reaction conditions are depicted in Fig. 7. The metrics were calculated by considering both the with and without catalyst. The results demonstrated that the values of green chemistry metrics are nearly close to their ideal values.

- We evaluated the efficiency of the catalytic system by measuring the TON and TOF values [78]. Our system achieved TON values ranging from 19.54 to 21.59 and 19.77 to 21.59, with corresponding TOF values of 0.43–0.71 min⁻¹ and 0.26–0.35 min⁻¹.

- To assess the environmental impact, we used EMY [79]. Our method showed an EMY between 82.35 and 91.29 % for compounds 4a–q and 83.68–95.14 % for compounds 6a–l which, demonstrates its significant environmental friendliness.
- In the current protocol, the CE is 100 %, while MP is in between 78.12 % and 86.95 % for compounds 4a–q and 80.00–90.90 % for compounds 6a–l.
- Additionally, the AEf for this method is excellent, ranging from 94.44–95.26 % and 94.79–95.87 % for compounds 4a–4q and 6a–6l respectively.
- As all products being obtained with good to excellent yields, the AE is also high, ranging from 82.38–91.44 % and 95.19–83.84 % for compounds 4a–4q and 6a–6l respectively.
- RME is a faithful metrics for relating the greenness of a process [80], and it accounts for yield, stoichiometry, and atom economy. The present protocol has achieved RME of up to 86.71 % for compound

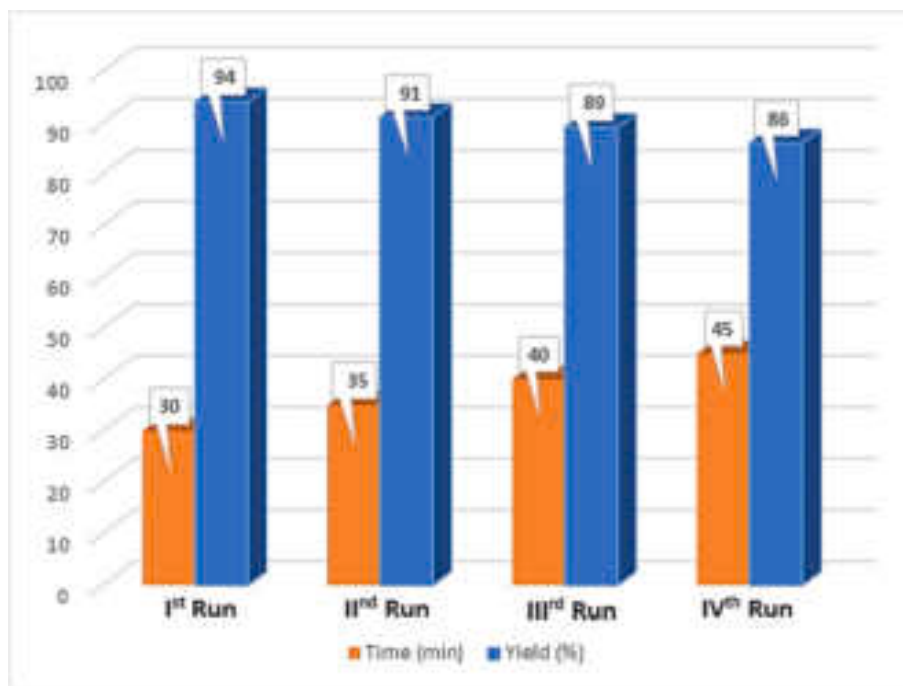


Fig. 6. Recyclability of the [DABCO-C₁₈]Br for the synthesis of dihydropyrano[3,2-c]chromenes.

Table 5

A range of green chemistry metrics for all the products.

Sr. No.	Green Metrics	Dihydropyrano[3,2-c]chromenes	2-Aminobenzo chromenes
1	EMY (%)	82.35–91.29	83.68–95.14
2	AE (%)	94.44–95.26	94.79–95.87
3	AEf (%)	82.38–91.44	83.84–95.19
4	CE (%)	100	100
5	RME (%)	77.77–86.71	79.50–90.28
6	OE (%)	82.12–91.03	83.43–91.34
7	MP (%)	78.12–86.95	80.00–90.90
8	PMI (g/g)	14.14–19.86	13.74–18.00
9	MI (g/g)	1.15–1.28	1.10–1.25
10	E-factor (g/g)	0.14–0.28	0.10–0.25
11	SI (g/g)	0	0
12	WI (g/g)	26.52–37.17	25.18–33.55
13	TON	19.54–21.59	19.77–21.59
14	TOF min ⁻¹	0.43–0.71	0.26–0.35

4a and 77.77 % for compound 4o. Similarly, RME 90.28 % for compound 6k and 79.50 % for compound 6c.

- PMI is a decisive metrics for evaluating and benchmarking progress toward sustainable manufacturing processes. It measures the total mass of materials used to produce a product. The PMI values of this protocol range from 14.44–19.86 g/g for compounds 4a–q and 13.74–18.00 g/g for compounds 6a–l.
- MI takes into account the yield, stoichiometry, solvent, and reagent used in the reaction. The MI for compounds 4a–q are 1.15–1.28 g/g and 1.10–1.25 g/g for compounds 6a–l, which is close to the ideal value of MI (MI = 1 g/g).
- The E-factor is an easy way to measure the environmental impact of chemical methods. It takes into account the chemical yield and consider reagents, solvent loss, and all process aids. The lower the E-factor, the less waste is produced during the process. The E-factor for current protocol is 0.14–0.28 g/g for compounds 4a–q and 0.10–0.25 g/g for compounds 6a–l indicating its significant environmental friendliness (the optimal E-factor is 0).

- In chemical reactions, the amount of solvent used is typically substantial, and its impact on sustainability is measured through SI [81,82]. The SI value of a process is zero in the present protocol since water is excluded from the calculations and organic solvents are not used, except for EtOH in recrystallization.

4. Conclusion

In summary, a new surfactant called octadecyl diazabicyclooctadecane bromide [DABCO-C₁₈]Br has impressive surfactant properties. Two different methods were used to determine the critical micelle concentration (CMC), conductivity analysis yielded a value of 1.15 mM, while UV–Vis absorption measurement gave a value of 1.0 mM. The degree of counter ion binding (β) for pure [DABCO-C₁₈]Br was found to be 0.828 as determined by conductivity measurements. As [DABCO-C₁₈]Br is a strong tertiary base and an excellent surfactant, it proved to be a highly efficient catalyst for the synthesis of dihydropyrano[3,2-c]chromenes in water at room temperature. Additionally, it demonstrated good to excellent activity in creating 2-aminobenzo chromenes in water at 80 °C. The aqueous solution containing [DABCO-C₁₈]Br could be recycled up to four times with a slight decrease in product yield from 94 % (1st run) to 86 % (4th run). This protocol is quick, energy-efficient, and applicable for large-scale synthesis, with excellent green credentials. From a sustainability point of view, green chemistry parameters like E-factor, atom economy, and carbon efficiency are in good agreement with the ideal values. All of the green metrics are found to be highly satisfactory, thereby supporting substantial green credentials of the process.

Author contributions

Archana Rajmane: Study conception and design, data collection, experimental work and designing of manuscript; **Sunita Shirke:** Formal analysis; **Rupesh Bandal:** Formal analysis; **Utkarsh More:** Physical study; **Suresh Patil:** Project co-supervisor; **Arjun Kumbhar:** Project supervisor.

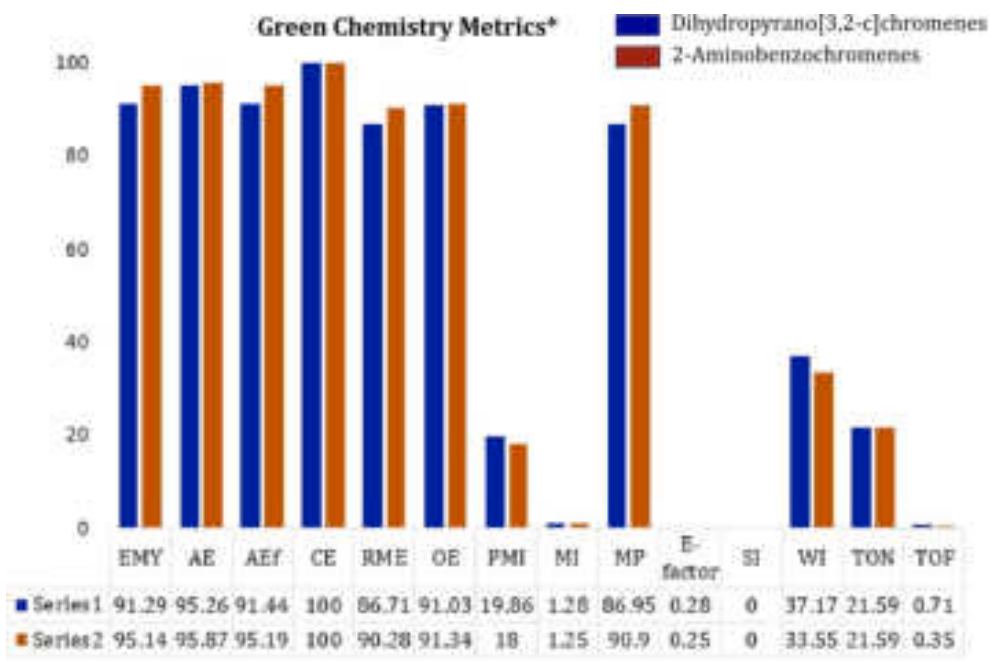


Fig. 7. The green metrics analysis for the synthesis of dihydropyrano[3,2-c]chromenes and 2-aminobenzochromenes (* For compounds 4a and 6a). (For interpretation of the references to colour in this figure legend, the reader is referred to the web version of this article.)

Declaration of Competing Interest

The authors declare that they have no known competing financial interests or personal relationships that could have appeared to influence the work reported in this paper.

Data availability

Data will be made available on request.

Acknowledgments

Archana Rajmane is grateful to the Government of Maharashtra (India) for the financial support under Dr. Babasaheb Ambedkar National Research Fellowship (BANRF-2020) [BANRF-2020/21-22/850 dated 16/02/2022]. We also like to show our appreciation to the University Grants Commission, Government of India, New Delhi, for enduring this work under the scheme of Major Research Project [F.No. 41-182/2014(SR)].

Appendix A. Supplementary material

Supplementary data to this article can be found online at <https://doi.org/10.1016/j.molliq.2023.123247>.

References

- [1] S.E. John, S. Gulatia, N. Shankaraiah, Recent advances in multi-component reactions and their mechanistic insights: a triennium review, *Org. Chem. Front.* 8 (2021) 4237–4287, <https://doi.org/10.1039/D0QO01480J>.
- [2] A. Dömling, W. Wang, K. Wang, Chemistry and biology of multicomponent reactions, *Chem. Rev.* 112 (2012) 3083–3135, <https://doi.org/10.1021/cr100233r>.
- [3] C.S. Graebin, F.V. Ribeiro, K.R. Rogério, A.E. Kümmerle, Multicomponent reactions for the synthesis of bioactive compounds: a review, *Curr. Org. Synth.* 16 (2019) 855–899, <https://doi.org/10.2174/1570179416666190718153703>.
- [4] L.F. Tietze, Domino reactions in organic synthesis, *Chem. Rev.* 96 (1996) 115–136, <https://doi.org/10.1021/cr950027e>.
- [5] H. Pellissier, Stereocontrolled domino reactions, *Chem. Rev.* 113 (2013) 442–524, <https://doi.org/10.1021/cr300271k>.
- [6] S. Pandey, R.K. Shukla, C.M.R. Volla, Access to polysubstituted furan derivatives via cascade oxy-palladation and hydrocarbofunctionalization of unactivated alkenes, *Org. Lett.* 25 (2023) 4694–4699, <https://doi.org/10.1021/acs.orglett.3c01571>.
- [7] M. Braun, Stereoselective domino Heck-Suzuki reactions, *Eur. J. Org. Chem.* 26 (2023), e202201282, <https://doi.org/10.1002/ejoc.202201282>.
- [8] C. Michelin, N. Hoffmann, Photocatalysis applied to organic synthesis – a green chemistry approach, *Curr. Opin. Green Sustain. Chem.* 10 (2018) 40–45, <https://doi.org/10.1016/j.cogsc.2018.02.009>.
- [9] W. Zhang, Green chemistry aspects of fluoros techniques—opportunities and challenges for small-scale organic synthesis, *Green Chem.* 11 (2009) 911–920, <https://doi.org/10.1039/B820740B>.
- [10] F. Gao, H. Chang, J. Li, R. Wang, Y. Gu, Replacing polar aprotic solvents with water in organic synthesis, *Curr. Opin. Green Sustain. Chem.* 40 (2023), 100774, <https://doi.org/10.1016/j.cogsc.2023.100774>.
- [11] M.B. Gawande, V.D.B. Bonifácio, R. Luque, P.S. Branco, R.S. Varma, Benign by design: catalyst-free in-water, on-water green chemical methodologies in organic synthesis, *Chem. Soc. Rev.* 42 (2013) 5522–5551, <https://doi.org/10.1039/C3CS60025D>.
- [12] T. Kitanosono, S. Kobayashi, Synthetic organic “Aquachemistry” that relies on neither cosolvents nor surfactants, *ACS Cent. Sci.* 7 (2021) 739–747, <https://doi.org/10.1021/acscentsci.1c00045>.
- [13] T. Kitanosono, K. Masuda, P. Xu, S. Kobayashi, Catalytic organic reactions in water toward sustainable society, *Chem. Rev.* 118 (2018) 679–746, <https://doi.org/10.1021/acs.chemrev.7b00417>.
- [14] A. Chanda, V.V. Fokin, Organic synthesis “On Water”, *Chem. Rev.* 109 (2009) 725–748, <https://doi.org/10.1021/cr800448g>.
- [15] F. Fabris, M. Illner, J.U. Repke, A. Scarso, M. Schwarze, Is micellar catalysis green chemistry? *Molecules* 28 (2023), 4809 <https://doi.org/10.3390/molecules28124809>.
- [16] H. Kumar, G. Kaur, Scrutinizing self-assembly, surface activity and aggregation behavior of mixtures of imidazolium based ionic liquids and surfactants: a comprehensive review, *Front. Chem.* 9 (2021), <https://doi.org/10.3389/fchem.2021.667941>.
- [17] S. Kamat, Y. Indi, A. Kumbhar, S. Kamble, An aqueous hydrotropic solution as environmentally benign reaction medium for organic transformations: a short review, *Res. Chem. Intermed.* 48 (2022) 3223–3245, <https://doi.org/10.1007/s11164-022-04761-2>.
- [18] S.C. Palapetta, H. Gurusamy, S. Ganapasam, Synthesis, characterization, computational studies, molecular docking, and in vitro anticancer activity of dihydropyrano[3,2-c]chromene and 2-aminobenzochromene derivatives, *ACS Omega* 8 (2023) 7415–7429, <https://doi.org/10.1021/acsomega.2c06049>.
- [19] T.H. Afifi, S.M. Riyadh, A.A. Deawaly, A. Naqvi, Novel chromenes and benzochromenes bearing arylazo moiety: molecular docking, in-silico admet, in-vitro antimicrobial and anticancer screening, *Med. Chem. Res.* 28 (2019) 1471–1487, <https://doi.org/10.1007/s00044-019-02387-5>.
- [20] K.A. Ali, N.A.A. Abdelhazef, E.A. Ragab, A.A. Ibrahim, A.E. Amr, Design and synthesis of novel fused heterocycles using 4-chromanone as synthon, *Russ. J. Gen. Chem.* 85 (2015) 2853–2860, <https://doi.org/10.1134/S107036321512035X>.
- [21] K.S. Lee, L.Y. Khil, S.H. Chae, D. Kim, B.H. Lee, G.S. Hwang, C.H. Moon, T. S. Chang, C.K. Moon, Effects of DK-002, a synthesized (6a*s*, *cis*)-9,10-Dimethoxy-

- 7,11b-dihydro-indeno[2,1-c]chromene-3,6a-diol, on platelet activity, *Life Sci.* 78 (2006) 1091–1097, <https://doi.org/10.1016/j.lfs.2005.06.017>.
- [22] K.V. Sashidhara, M. Kumar, R.K. Modukuri, A. Srivastava, A. Puri, Discovery and synthesis of novel substituted benzocoumarins as orally active lipid modulating agents, *Bioorg. Med. Chem. Lett.* 21 (2011) 6709–6713, <https://doi.org/10.1016/j.bmcl.2011.09.053>.
- [23] J. Bloxham, C.P. Dell, C.W. Smith, Preparation of some new benzylidenemalononitriles by an SNAr reaction: application to naphtho[1,2-b]pyran synthesis, *Heterocycles* 38 (1994) 399–408, <https://doi.org/10.3987/COM-93-6594>.
- [24] R. Ballini, G. Bosica, M.L. Conforti, R. Maggi, A. Mazzacanni, P. Righi, G. Sartori, Three-component process for the synthesis of 2-amino-2-chromenes in aqueous media, *Tetrahedron* 57 (2001) 1395–1398, [https://doi.org/10.1016/S0040-4020\(00\)01121-2](https://doi.org/10.1016/S0040-4020(00)01121-2).
- [25] T.S. Jin, J.C. Xiao, S.J. Wang, T.S. Li, Ultrasound-assisted synthesis of 2-amino-2-chromenes with cetyltrimethylammonium bromide in aqueous media, *Ultrason. Sonochem.* 11 (2004) 393–397, <https://doi.org/10.1016/j.ulsonch.2003.10.002>.
- [26] R. Maggi, R. Ballini, G. Sartori, R. Sartorio, Basic alumina catalyzed synthesis of substituted 2-amino-2-chromenes via three-component reaction, *Tetrahedron Lett.* 45 (2004) 2297–2299, <https://doi.org/10.1016/j.tetlet.2004.01.115>.
- [27] M. Kidwai, S. Saxena, M.K. Rahman Khan, S.S. Thukral, Aqua mediated synthesis of substituted 2-amino-4H-chromenes and in vitro study as antibacterial agents, *Bioorg. Med. Chem. Lett.* 15 (2005) 4295–4298, <https://doi.org/10.1016/j.bmcl.2005.06.041>.
- [28] D. Kumar, V.B. Reddy, G.B. Mishra, R.K. Rana, M.N. Nadagouda, R.S. Varma, Nanosized magnesium oxide as catalyst for the rapid and green synthesis of substituted 2-amino-2-chromenes, *Tetrahedron* 63 (2007) 3093–3097, <https://doi.org/10.1016/j.tet.2007.02.019>.
- [29] M.M. Heravi, K. Bakhtiari, V. Zadsirjan, F.F. Bamoharram, O.M. Heravi, Aqua mediated synthesis of substituted 2-amino-4H-chromenes catalyzed by green and reusable Preyssler heteropolyacid, *Bioorg. Med. Chem. Lett.* 17 (2007) 4262–4265, <https://doi.org/10.1016/j.bmcl.2007.05.023>.
- [30] T.S. Jin, J.S. Zhang, L.B. Liu, A.Q. Wang, T.S. Li, Clean, one-pot synthesis of naphthopyran derivatives in aqueous media, *Synth. Commun.* 36 (2006) 2009–2015, <https://doi.org/10.1080/00397910600632096>.
- [31] D.Q. Shi, S. Zhang, Q.Y. Zhuang, X.S. Wang, H. Hu, Clean synthesis of benzo[h]chromene derivatives in water, *Chin. J. Org. Chem.* 23 (2003) 1419–1421.
- [32] B.S. Kumar, N. Srinivasulu, R.H. Udipi, B. Rajitha, Y.T. Reddy, P.N. Reddy, P. S. Kumar, An efficient approach towards three component coupling of one pot reaction for synthesis of functionalized benzopyrans, *J. Heterocycl. Chem.* 43 (2006) 1691–1693, <https://doi.org/10.1002/jhet.5570430641>.
- [33] S. Abdolmohammadi, S. Balalaie, Novel and efficient catalysts for the one-pot synthesis of 3,4-dihydropyrano[c]chromene derivatives in aqueous media, *Tetrahedron Lett.* 48 (2007) 3299–3303, <https://doi.org/10.1016/j.tetlet.2007.02.135>.
- [34] M.R. Naimi-Jamal, S. Mashkouri, A. Sharifi, An efficient, multicomponent approach for solvent-free synthesis of 2-amino-4H-chromene scaffold, *Mol. Divers.* 14 (2010) 473–477, <https://doi.org/10.1007/s11030-010-9246-5>.
- [35] M.N. Elinson, A.I. Ilovaisky, V.M. Merkulova, P.A. Belyakov, A.O. Chizhov, G. I. Nikishin, Solvent-free cascade reaction: direct multicomponent assembling of 2-amino-4H-chromene scaffold from salicylaldehyde, malononitrile or cyanoacetate and nitroalkanes, *Tetrahedron* 66 (2010) 4043–4048, <https://doi.org/10.1016/j.tet.2010.04.024>.
- [36] S. Makarem, A.A. Mohammadi, A.R. Fakhari, A multi-component electro-organic synthesis of 2-amino-4H-chromenes, *Tetrahedron Lett.* 49 (2008) 7194–7196, <https://doi.org/10.1016/j.tetlet.2008.10.006>.
- [37] G. Shanthi, P.T. Perumal, Indium-Mediated One-Pot Synthesis of New 4-Allyl-2-amino-4H-chromenes in Water, *Synlett.* (2008) 2791–2794, doi: 10.1055/s-0028-1087297.
- [38] H. Mehrabi, H. Abusaidi, Synthesis of biscoumarin and 3,4-dihydropyrano[c]chromene derivatives catalyzed by sodium dodecyl sulfate (SDS) in neat water, *J. Iran. Chem. Soc.* 7 (2010) 890–894, <https://doi.org/10.1007/BF03246084>.
- [39] H. Mehrabi, N. Kamali, Efficient and eco-friendly synthesis of 2-amino-4H-chromene derivatives using catalytic amount of tetrabutylammonium chloride (TBAC) in water and solvent-free conditions, *J. Iran. Chem. Soc.* 9 (2012) 599–605, <https://doi.org/10.1007/s13738-012-0073-8>.
- [40] H.R. Shaterian, A.R. Oveisi, A simple Green approach to the synthesis of 2-amino-5-oxo-4,5-dihydropyrano[3,2-c]chromene-3-carbonitrile derivatives catalyzed by 3-hydroxypropanaminium acetate (HPAA) as a new ionic liquid, *J. Iran. Chem. Soc.* 8 (2011) 545–552, <https://doi.org/10.1007/BF03249089>.
- [41] T. Farahmand, S. Hashemian, A. Shihani, ZIF@ZnTiO₃ nanocomposite as a reusable organocatalyst for the synthesis of 3, 4-dihydropyrano[c]chromene derivatives, *Curr. Organocatal.* 6 (2019) 248–256, <https://doi.org/10.2174/2213337206666190610094227>.
- [42] R.D. Kamble, M.V. Gaikwad, M.R. Tapare, S.V. Hese, S.N. Kadam, A.N. Ambhore, B.S. Dawane, Dtp/SiO₂: an efficient and reusable heterogeneous catalyst for synthesis of dihydropyrano [3, 2-c] chromene-3-carbonitrile derivatives, *J. Appl. Organomet. Chem.* 1 (2021) 22–28.
- [43] S. Shaikh, I. Yellapurkar, M.M.V. Raman, Mn₂O₃ NPs: a versatile catalyst for the syntheses of pyrano[3,2-c]chromenes, pyrano[3,2-b]pyrans and spirooxindoles, *Chem. Africa* 4 (2021) 821–834, <https://doi.org/10.1007/s42250-021-00270-8>.
- [44] V. Kumbhar, S. Gaiki, R. Raskar, A. Kumbhar, B. Khairnar, A green protocol for one-pot synthesis of 3,4-dihydropyrano[c]chromenes and biscoumarins by employing WEB as an internal base, *Results Chem.* 4 (2022), 100589, <https://doi.org/10.1016/j.rechem.2022.100589>.
- [45] U.K. Verma, A. Manhas, K.K. Kapoor, [Ch][TAPSO] as an efficient ionic liquid catalyst for one-pot synthesis of tetrahydro-4H-chromenes and 3,4-dihydropyrano [c]chromenes, 8 (2023) e202204961, doi: 10.1002/slct.202204961.
- [46] Z. Benzekri, S. Sibous, H. Anahmadi, F.E. hajri, D.E. Mekkaoui, R. Hissou, A. Ouasri, A. Souizi, A. Rhandour, S. Boukhris, Novel hybrid perovskite crystal NH₃(CH₂)₇NH₃BiCl₅ as a potential catalytic performance and eco-friendly for the synthesis of 3,4-dihydropyrano [3,2-c] chromenes derivatives, *J. Mol. Struct.* 1281 (2023) 135064, doi: 10.1016/j.molstruc.2023.135064.
- [47] Z. Valipour, R. Hosseinzadeh, Y. Sarrafi, B. Maleki, Natural Deep Eutectic Solvent as a Green Catalyst for the One-pot Synthesis of Chromene and 4H-Pyran Derivatives, *Orag. Preparation Procedure Int.* (2023), doi: 10.1080/00304948.2023.2232917.
- [48] F. Mirsalari, E. Tahanpesar, H. Sanaeishoar, Biosynthesis of NiO-NPs using mucilage of Cordia myxa fruit and their potential application as an efficient catalyst for the synthesis of chromenes, *Res. Chem. Intermed.* 49 (2023) 4127–4148, <https://doi.org/10.1007/s11164-023-05067-7>.
- [49] A. Kumbhar, S. Kamble, M. Barge, G. Rashinkar, R. Salunkhe, Brønsted acid hydrotrope combined catalyst for environmentally benign synthesis of quinoxalines and pyrido[2,3-b]pyrazines in aqueous medium, *Tetrahedron Lett.* 53 (2012) 2756–2760, <https://doi.org/10.1016/j.tetlet.2012.03.097>.
- [50] A. Kumbhar, S. Jadhav, R. Shejwal, G. Rashinkar, R. Salunkhe, Application of novel multi-cationic ionic liquids in microwave assisted 2-amino-4H-chromene synthesis, *RSC Adv.* 6 (2016) 19612–19619, <https://doi.org/10.1039/C6RA01062H>.
- [51] A. Kumbhar, S. Jadhav, S. Kamble, G. Rashinkar, R. Salunkhe, Palladium supported hybrid cellulose–aluminum oxide composite for Suzuki-Miyaura cross coupling reaction, *Tetrahedron Lett.* 54 (2013) 1331–1337, <https://doi.org/10.1016/j.tetlet.2012.11.140>.
- [52] C.S. Buettner, A. Cognigni, C. Schröder, K.B. Schröder, Surface-active ionic liquids: a review, *J. Mol. Liq.* 347 (2022), 118160, <https://doi.org/10.1016/j.molliq.2021.118160>.
- [53] T. Lohar, A. Kumbhar, M. Barge, R. Salunkhe, DABCO functionalized dicationic ionic liquid (DDL): a novel green benchmark in multicomponent synthesis of heterocyclic scaffolds under sustainable reaction conditions, *J. Mol. Liquids* 224 (2016) 1102–1108, <https://doi.org/10.1016/j.molliq.2016.10.039>.
- [54] M.M. Mabrouk, N.A. Hamed, F.R. Mansour, Spectroscopic methods for determination of critical micelle concentrations of surfactants; a comprehensive review, *App. Spectro. Rev.* 58 (2023) 206–234, <https://doi.org/10.1080/05704928.2021.1955702>.
- [55] U. More, P. Kumari, Z. Vaid, K. Behera, N.I. Malek, Interaction between ionic liquids and Gemini surfactant: a detailed investigation into the role of ionic liquids in modifying properties of aqueous Gemini surfactant, *J. Surfactant Detergent* 19 (2016) 75–89, <https://doi.org/10.1007/s11743-015-1747-x>.
- [56] U.U. More, Z.S. Vaid, S.M. Rajput, N.I. Malek, O.A. El Seoud, Effects of 1-alkyl-3-methylimidazolium bromide ionic liquids on the micellar properties of [butanediy-1,4-bis(dimethyldodecylammonium bromide)] gemini surfactant in aqueous solution, *J. Coll. Polym. Sci.* 295 (2017) 2351–2361, <https://doi.org/10.1007/s00396-017-4210-x>.
- [57] U. More, Z.S. Vaid, S. Rajput, Y. Kadam, N. Malek, Effect of imidazolium-based ionic liquids on the aggregation behavior of twin-tailed cationic Gemini surfactant in aqueous solution, *J. Disper. Sci. Technol.* 38 (2017) 393–402, <https://doi.org/10.1080/01932691.2016.1170610>.
- [58] M.R. Amin, S. Mahbub, S. Hidayathulla, M.M. Alam, M.A. Hoque, M.A. Rub, An estimation of the effect of mono/poly-hydroxy organic compounds on the interaction of tetradecyltrimethylammonium bromide with levofloxacin hemihydrate antibiotic drug, *J. Mol. Liq.* 269 (2018) 417–425, <https://doi.org/10.1016/j.molliq.2018.08.0431>.
- [59] S. Aktar, M. Saha, S. Mahbub, M.A. Halim, M.A. Rub, M.A. Hoque, D.M.S. Islam, D. Kumar, Y.G. Alghamdi, A.M. Asiri, Influence of polyethylene glycol on the aggregation/clouding phenomena of cationic and non-ionic surfactants in attendance of electrolytes (NaCl & Na₂SO₄): an experimental and theoretical analysis, *J. Mol. Liq.* 306 (2020), 112880, <https://doi.org/10.1016/j.molliq.2020.112880>.
- [60] U. More, Z. Vaid, P. Bhamoria, A. Kumar, N.I. Malek, Effect of [C n mim][Br] based ionic liquids on the aggregation behavior of tetradecyltrimethylammonium bromide in aqueous medium, *J. Sol. Chem.* 44 (2015) 850–874, <https://doi.org/10.1007/s10953-015-0318-0>.
- [61] C.J. Li, Y.L. Li, U.S. Patent Appl. Publ. US 2005222246 A1 20051006.
- [62] P.E. da S. Júnior, N.M. de Araujo, F. da S. Emery, Claisen rearrangement of hydroxynaphthoquinones: selectivity toward naphthofuran or α -iloidone using copper salts and iodine, *J. Heterocyclic Chem.* 52 (2015) 518–521, doi: 10.1002/jhet.2087.
- [63] A. Shaabani, R. Ghadari, S. Ghasemi, M. Pedarpour, A.H. Rezayan, A. Sarvary, S. W. Ng, Novel one-pot three- and pseudo-five-component reactions: synthesis of functionalized benzo[g]- and dihydropyrano[2,3-g]chromene derivatives, *J. Comb. Chem.* 11 (2009) 956–959, <https://doi.org/10.1021/cc900101w>.
- [64] C. Yao, C. Yu, T. Li, S. Tu, An efficient synthesis of 4H-benzo[g]chromene-5,10-dione derivatives through triethylbenzylammonium chloride catalyzed multicomponent reaction under solvent-free conditions, *Chin. J. Chem.* 27 (2009) 1989–1994, <https://doi.org/10.1002/cjoc.200990334>.
- [65] M.G. Dekamin, M. Eslami, A. Maleki, Potassium phthalimide-N-oxyl: a novel, efficient, and simple organocatalyst for the one-pot three-component synthesis of various 2-amino-4H-chromene derivatives in water, *Tetrahedron* 69 (2013) 1074–1085, <https://doi.org/10.1016/j.tet.2012.11.068>.
- [66] F. Khorami, H.R. Shaterian, Silica-bonded propylpiperazine-N-sulfamic acid as recyclable solid acid catalyst for preparation of 2-amino-3-cyano-4-aryl-5,10-dioxo-5,10-dihydro-4H-benzo[g]chromenes and hydroxy-substituted naphthalene-

- 1,4-dione derivatives, *Chin. J. Catal.* 35 (2014) 242–246, [https://doi.org/10.1016/S1872-2067\(12\)60761-X](https://doi.org/10.1016/S1872-2067(12)60761-X).
- [67] B. Maleki, S. Babae, R. Tayebee, Zn(L-proline)₂ as a powerful and reusable organometallic catalyst for the very fast synthesis of 2-amino-4H-benzo[g]chromene derivatives under solvent-free conditions, *Appl. Organometal. Chem.* 29 (2015) 408–411, <https://doi.org/10.1002/aoc.3306>.
- [68] B. Maleki, M. Baghayeri, S. Sheikh, S. Babae, S. Farhadi, One-pot synthesis of some 2-amino-4H-chromene derivatives using triethanolamine as a novel reusable organocatalyst under solvent-free conditions and its application in electrosynthesis of silver nanoparticles, *Russ. J. Gen. Chem.* 87 (2017) 1064–1072, <https://doi.org/10.1134/S1070363217050280>.
- [69] G. Brahmachari, B. Banerjee, Facile and one-pot access to diverse and densely functionalized 2-amino-3-cyano-4H-pyrans and pyran-annulated heterocyclic scaffolds via an eco-friendly multicomponent reaction at room temperature using urea as a novel organo-catalyst, *ACS Sustain. Chem. Eng.* 2 (2014) 411–422, <https://doi.org/10.1021/sc400312n>.
- [70] K. Gong, H.L. Wang, J. Luo, Z.L. Liu, One-pot synthesis of polyfunctionalized pyrans catalyzed by basic ionic liquid in aqueous media, *J. Het. Chem.* 46 (2009) 1145–1150, <https://doi.org/10.1002/jhet.193>.
- [71] F.K. Behbahani, M. Ghorbani, M. Sadeghpour, M. Mirzaei, L-proline as reusable and organo catalyst for the one-pot synthesis of substituted 2-amino-4H-chromenes, *Lett. Org. Chem.* 10 (2013) 191–194.
- [72] F. Khorami, H.R. Shaterian, Preparation of 2-amino-3-cyano-4-aryl-5,10-dioxo-5,10-dihydro-4H-benzo[g]chromene and hydroxyl naphthalene-1,4-dione derivatives, *Res. Chem. Intermed.* 41 (2015) 3171–3191, <https://doi.org/10.1007/s11164-013-1423-6>.
- [73] R. Nongrum, G.S. Nongthombam, M. Kharkongor, J.W.S. Rani, N. Rahman, C. Kathing, B. Myrboh, R. Nongkhaw, A nano-organo catalyzed route towards the efficient synthesis of benzo[b]pyran derivatives under ultrasonic irradiation, *RSC Adv.* 6 (2016) 108384–108392, <https://doi.org/10.1039/C6RA24108E>.
- [74] S.N. Gracious, N. Kerru, S. Maddila, W.E.V. Zyl, S.B. Jonnalagadda, Facile one-pot green synthesis of 2-amino-4H-benzo[g]chromenes in aqueous ethanol under ultrasound irradiation, *Synth. Commun.* 50 (2020) 1960–1971, <https://doi.org/10.1080/00397911.2020.1761393>.
- [75] H. Taherkhani, A. Ramazani, S. Sajjadifar, H. Aghahosseini, A. Rezaei, Design and preparation of copper(II)-mesalamine complex functionalized on silica-coated magnetite nanoparticles and study of its catalytic properties for green and multicomponent synthesis of highly substituted 4H-chromenes and pyridines, *ACS Omega* 7 (2022) 14972–14984, <https://doi.org/10.1021/acsomega.2c00731>.
- [76] C.J. Gonzalez, C.S. Ponder, Q.B. Broxterman, J.B. Manley, Using the right green yardstick: why process mass intensity is used in the pharmaceutical industry to drive more sustainable processes, *Org. Process Res. Dev.* 15 (2011) 912–917, <https://doi.org/10.1021/op200097d>.
- [77] G. Brahmachari, M. Mandal, I. Karmakar, K. Nurjamal, B. Mandal, Ultrasound-promoted expedient and green synthesis of diversely functionalized 6-amino-5-((4-hydroxy-2-oxo-2H-chromen-3-yl)(aryl)methyl)pyrimidine-2,4(1H,3H)-diones via one-pot multicomponent reaction under sulfamic acid catalysis at ambient conditions, *ACS Sustain. Chem. Eng.* 7 (2019) 6369–6380, <https://doi.org/10.1021/acssuschemeng.9b00133>.
- [78] S. Kozuch, J.M.L. Martin, “Turning Over” definitions in catalytic cycles, *ACS Catal.* 12 (2012) 2787–2794, <https://doi.org/10.1021/cs3005264>.
- [79] T. Hudlicky, D.A. Frey, L. Koroniak, C.D. Claeboe, L.E. Brammer, Toward a ‘reagent-free’ synthesis, *Green Chem.* 1 (1999) 57–59, <https://doi.org/10.1039/A901397K>.
- [80] D.J.C. Constable, A.D. Curzons, V.L. Cunningham, Metrics to ‘green’ chemistry—which are the best? *Green Chem.* 4 (2002) 521–527, <https://doi.org/10.1039/B206169B>.
- [81] A.D. Curzons, D.C. Constable, V.L. Cunningham, Solvent selection guide: a guide to the integration of environmental, health and safety criteria into the selection of solvents, *Clean Prod. Process.* 1 (1999) 82–90, <https://doi.org/10.1007/s100980050014>.
- [82] K. Alfonsi, J. Colberg, P.J. Dunn, T. Fevig, S. Jennings, T.A. Johnson, H.P. Kleine, C. Knight, M.A. Nagy, D.A. Perry, M. Stefaniak, Green chemistry tools to influence a medicinal chemistry and research chemistry based organisation, *Green Chem.* 10 (2008) 31–36, <https://doi.org/10.1039/B711717E>.



SHIVAJI UNIVERSITY, KOLHAPUR

Volume-49 Issue-2 (July, 2023)

ISSN-Science-0250-5347

Estd. 1962
"A++" Accredited by NAAC (2021)
with CGPA 3.52



Journal of Shivaji University SCIENCE & TECHNOLOGY

(Peer Reviewed Journal)

INDEX

Sr. No.	Title of Research Article with Name of Author/s	Page No.
1.	Silica Coated Superhydrophobic Materials for Oil-Water Separation Application-A Short Review Rajesh B. Sawant, Mehejbin R. Mujawar, Amol B. Pandhare, Sanjay S. Latthe, Ankush M. Sargar, Raghunath K. Mane, Shivaji R. Kulal	1
2.	Green Synthesis of NiO Nanoparticles from <i>Partheniumhysterophorus</i> Plant Sneha V. Koparde, Akanksha G. Kolekar, Shital S. Shendage, Aniket H. Sawat, Snehal D. Patil, Snehal S. Patil, Reshma B. Darekar, Amol B. Pandhare, Vijay S. Ghodake, Samadhan P. Pawar, Govind B. Kolekar	12
3.	Microwave-Assisted Synthesis of Pyrazole and Its Hybrid Scaffolds as Potent Biological and Pharmacological Agents: A Short Review Pravin. R. Kharade, Uttam. B. Chougale, Satish. S. Kadam, Kiran. N. Patil, Prakash S. Pawar, Savita. S. Desai	19
4.	Biosynthesis and Catalytic Transformation of Ruthenium Nanoparticles in Biomimetic Applications Komal M. Dhumal, Anita R. Mali	36
5.	Third Generation Solar Cells: Importance and Measurements Techniques for knowing Photovoltaic Device Performance Prakash S. Pawar, Pramod A. Koyale, Amol B. Pandhare, Vijay S. Ghodake, Swapnijit V. Mulik, Ankita K. Dhukate, Waleed Dabdoub, Sagar D. Delekar	48
6.	Aggregation-Induced Emission, Mechanochromism, and Applications of Tetraphenylethene/Triphenylamine-based Molecules Kishor. S. Jagadhane, Govind. B. Kolekar, Prasad. M. Swami, Prashant. V. Anbhule	68
7.	Greener and Environmentally Benign Methodologies for the Synthesis of Bis(indolyl)methane and Trisindolines Aboli C. Sapkal, Suraj R. Attar, Santosh B. Kamble	75

Silica Coated Superhydrophobic Materials for Oil-Water Separation Application-A Short Review

Rajesh B. Sawant^{a,*}, Mehejbin R. Mujawar^a, Amol B. Pandhare^{b,f},
Sanjay S. Latthe^c, Ankush M. Sargar^d,
Raghunath K. Mane^e, Shivaji R. Kulal^{a*}

^aDepartment of Chemistry, Raje Ramrao Mahavidyalaya, Jath, Sangli 416 404 (MS) India.

^bDepartment of Chemistry, Shivaji University, Kolhapur 416 004 (MS) India.

^cDepartment of Physics, Vivekanand College, Kolhapur 416 003 (MS) India.

^dDepartment of Chemistry, Bharati Vidyapeeth's Dr. Patangrao Kadam Mahavidyalaya, Sangli 416 416 (MS) India.

^e Department of Chemistry, Smt. Kusumtai Rajarambhapu Patil Kanya Mahavidyalaya, Islampur, Sangli 416 409 (MS) India.

^fDepartment of Chemistry, M.H. Shinde Mahavidyalaya, Tisangi, Gaganbavda, Kolhapur 416 206 (MS) India.

*Corresponding authors: srkulal@gmail.com and rbsawant2@gmail.com

ABSTRACT

Contamination like oil and organic pollutants in water has a severe problem for aquatic life and human being; it is a need to preserve their life. These contaminants are added due to frequent oil spill accidents, and industrial as well as domestic waste. There is a need to develop methods and materials that show excellent ability to separate the oil and organic contaminants from water. Recently, superhydrophobic coated sponges, metals mesh, membranes and porous materials plays crucial role to separate oil and water from oil-water mixture. The micro and nonporous of substrate facilitate to enter liquid into it and superhydrophobic/superoleophilic property of substrate surface resist water and allows oil to enter into porous substrate. The various surface modified organic metal oxide nanoparticles are used to develop superhydrophobic surface on porous substrate. Among them SiO₂ nanoparticles is promising material to preparation of superhydrophobic surface because of their cost-effectiveness and easy synthesis techniques. This review focused on silica modified porous sponge, metal meshes, membrane and porous substrate for scalable oil-water separation application.

KEYWORDS

Superhydrophobic, Oil-water separation, porous sponge, Metal mesh and membrane.

.....

1. INTRODUCTION

Frequent oil spill accidents and industrial chemical spills occurred in the sea and the ecosystem damage; such incidents have spread to impact the offspring. Therefore, considerable surviving organisms for several years after the impact [1-2] efforts have been done to remove oil and organic solvents from water. Due to this extensive current research is focussed on the development of superhydrophobic materials for effective oil-water separation. To achieve superhydrophobic sponges, surface roughness and low surface energy materials play a crucial role. The various methods such as dip coating, immersion, spray coating; hydrothermal methods, chemical vapor deposition, surface etching, solvothermal methods, layer-by-layer assembly and electrochemical treatment describe a modification of sponges for oil and water separation [3-4]. At present, traditional technologies, including in situ burning [5], bioremediation [6], chemical dispersant methods [7], skimming [8], and the use of sorbents [9] are used to clean up spilled oils or organic pollutants. However, many of these strategies involve energy intensive and slow processes, have low clean-up capacities or create secondary pollution during the clean-up process, restricting their widespread practical applications [10-11]. To realize the hierarchical structures on different material surfaces, a series of strategies, such as sol-gel coating [12], chemical vapor deposition [13], plasma etching [14], template processing [15], lithographic patterning [16], etc. have been adopted [17]. The superhydrophobic surfaces on which water achieves water contact angle higher than 150° and sliding angle less than 5° are attracting minds of researchers due to their efficient oil-water separation efficiency [18].

Recently, Wu et al. [19] have prepared a highly flexible superhydrophobic PDMS@F-SiO₂ coating for self-cleaning and drag-reduction applications via a two-step spraying of PDMS and F-SiO₂ nanoparticles. However, it is common that inorganic particles normally tend to agglomerate due to the interparticle forces stemming from the Vander Waals, capillary and electrostatic forces [20], which leads to phase separation during the fabrication process and tends to diminish the quality of the coating through cracks or weak adhesive to the substrates. Gao et al. [21] prepared PVDF/SiO₂ coated superhydrophobic porous membranes using a spraying technique. These membranes could be used to separate the oil-water mixtures but are not applicable to surfactant stabilized water-in-oil emulsions because of their large pore sizes. Li et al. [22] prepared the hydrophobic CS by incomplete combustion of hydrocarbons from the middle of a candle flame. The PU sponge was immersed in the solution of CS, SiO₂ and PU resin to achieve stable superhydrophobicity. The CS-SiO₂-PU sponge was shown excellent oil-water separation efficiency. The CS-SiO₂-PU sponge showed excellent oil-water separation efficiency from hot water, acidic solutions, alkaline solutions and salt solutions.

In this review, the sophisticated, facile and low-cost methods for fabrication of superhydrophobic porous material for oil-water separation application are discussed.

The 3D sponges, metal meshes, membrane and cotton fabrics are used as substrate for scalable oil-water separation application.

2. SUPERHYDROPHOBIC SURFACES FOR OIL-WATER SEPARATION

2.1 Superhydrophobic SiO₂ Modified Sponges for Oil-Water Separation

Zhang et al. [23] have fabricated the superhydrophobic surface by using VTMS and SiO₂ via immersion method. The schematic of preparation of superhydrophobic sponge is shown in **Figure-1**. It was shown a water contact angle of 153.2° and roll-on angle of 4.8°. The oil is quickly absorbed by superhydrophobic sponge which can be shown the superoleophilic property of a modified sponge. The IR peak at 1078 cm⁻¹ shows the presence of the O-Si-O bond present in the material. It was showing the high separation efficiency of about 99.5%. It exhibited good saturated adsorption properties exceeding 70 g/g for all oils. It shows outstanding characteristics of superhydrophobic sponge such as high porosity, small pore size and ultra-light mass. After 20 cycles, it was found that the adsorption ability of the modified melamine sponge for different oils decreased slightly. It shows outstanding stability and reusable performance. The modified sponge maintains an 89% of recovery rate even after 20 cycles. This method was used to prepare porosity and provides storage space for the adsorption of oil pollution. This superhydrophobic composite melamine sponge provided the possibility for practical application of oil-water separation.

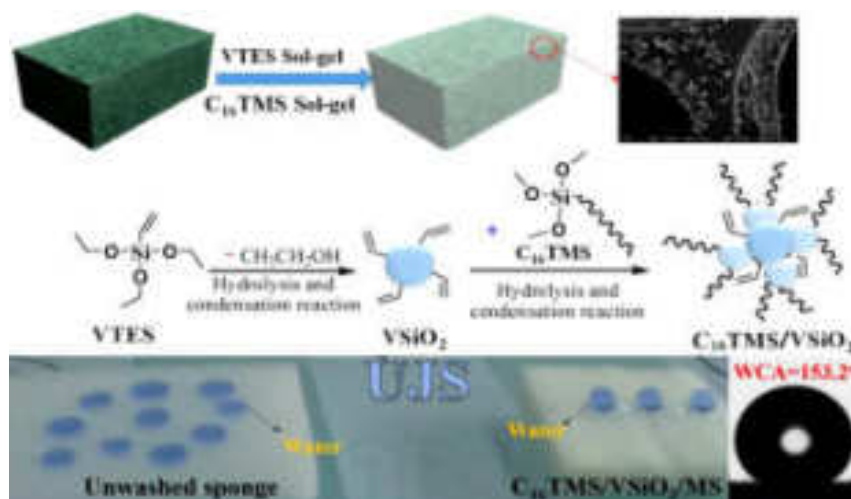


Figure-1. Schematic illustration of the preparation of superhydrophobic sponge. Images reprinted from [23], with permission from Elsevier, Journal of Chemical Engineering, Copyright 2020.

Liu et al. [24]. have fabricated a superhydrophobic sponge and polyester coated with SiO₂-DTMS through an entrapment method. The **Figure-2** reveals the fabrication process of superhydrophobic sponge and polyester. The SiO₂ particles were introduced by growth on the substrate through the polymerization process, followed by the addition of DTMS as an adhesive, leading to a homogeneous and dense superhydrophobic membrane. The modified sponge was shown the water contact angle up to 172° indicating the water repellence was superior. This superhydrophobic sample had good hydrophobic stability even in acidic condition and it can show efficient oil-water separation. The amount of the absorbed oil was about 43-65 times of sponge own weight can be shown that the evaluation of the mass based on absorbed surface tension, density, viscosity of absorbed liquids. It exhibits stable oil storage under harsh environmental conditions in oil-water separation. The performance remained constant after 100 recycling sequences, even in a harsh water environment.

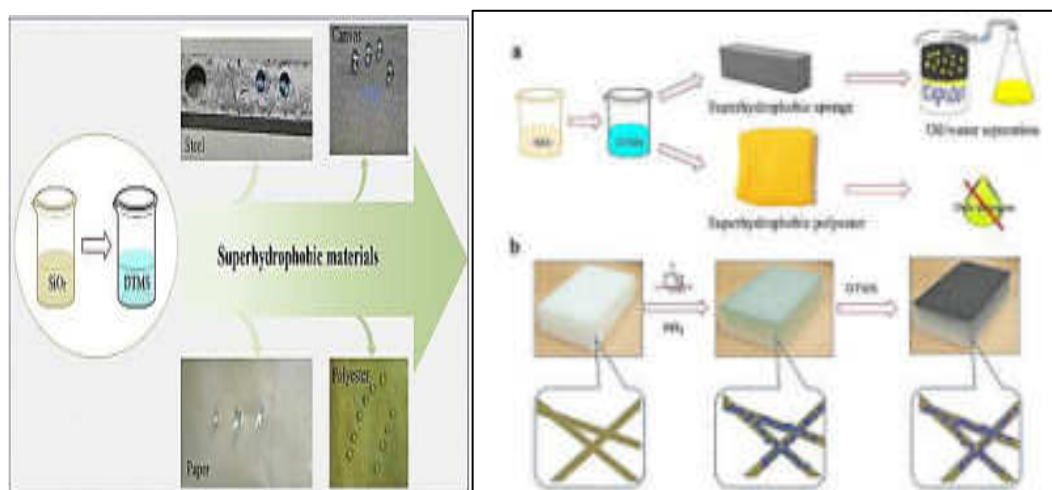


Figure-2. Schematic illustration of the fabrication of a modified sponge and polyester. Images reprinted from [24], with permission from Elsevier, Copyright 2019.

2.2 Superhydrophobic SiO₂ Modified Metal Meshes for Oil-Water Separation

Zhao et al. [25] have prepared superhydrophobic SiO₂ nanoparticles by improved Stober method and then coated on a chemically etched stainless steel mesh by one step dipping method to fabricate superhydrophobic SiO₂ coated stainless steel mesh. The preparation process was simple, efficient and environmentally friendly. The experimental procedure is shown in **Figure-3**. It shows excellent oil-water separation properties, which can be widely used in oil-water separation. It was showing 153.3° water contact angle and 0° oil contact angle. The oil-water separation efficiency was nearly 96% by using this modified stainless-steel mesh.

The separation efficiencies were obtained repeatedly even after 40 cycles without noticeable deterioration. The superhydrophobic modified stainless steel mesh shows stability, durability and reusability. The SiO₂ modified stainless steel mesh indicates good material for treating real oil-polluted water in different practical applications. This method shows high performance, oil-water separation in a short time and repeatedly in comparison with earlier works.

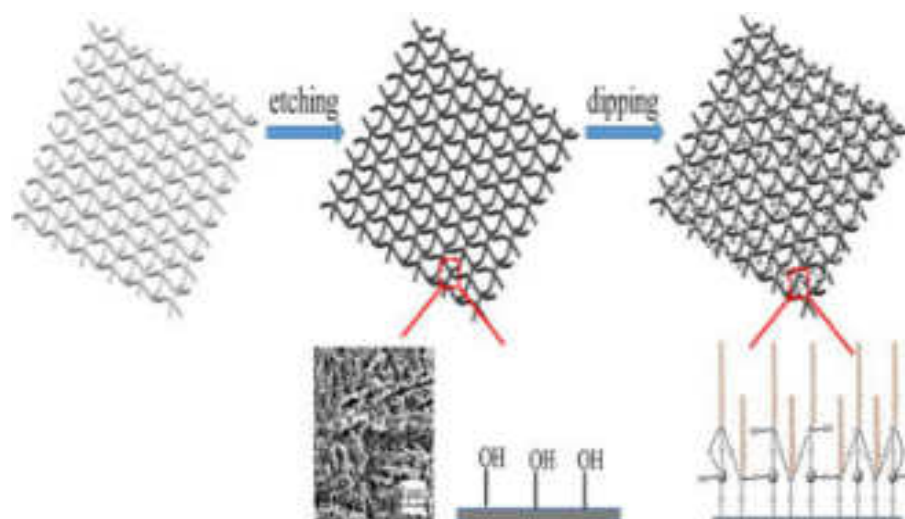


Figure-3. Schematic illustration of the preparation of FSSM. Images reprinted from [25], with permission from Elsevier, Copyright 2019.

Xiong et al. [26] have prepared SiO₂ nanoparticles by an improved modified method by using TEOS and then coated on a stainless-steel mesh by spraying method to fabricate SiO₂ coated stainless steel mesh. The **Figure-4** illustrates schematic of preparation of the superhydrophobic stainless-steel mesh. The preparation process was efficient, simple and environmentally friendly. It shows good mechanical properties and oil/water separation performance. It was showing 156.4° oil contact angle and less than 10° water contact angles. The oil-water separation efficiency was nearly 98.69% by using this modified stainless-steel mesh. The separation efficiencies obtained repeatedly even after 20 cycles without noticeable deterioration. The superhydrophobic modified stainless steel mesh shows stability, durability and reusability. The SiO₂ modified stainless steel mesh indicates excellent material for treating oil-polluted water in different practical applications. This method shows an easily scaled-up preparation process, stable mechanical and thermal properties, offering new prospects for efficient oil/water separation in comparison with earlier works.

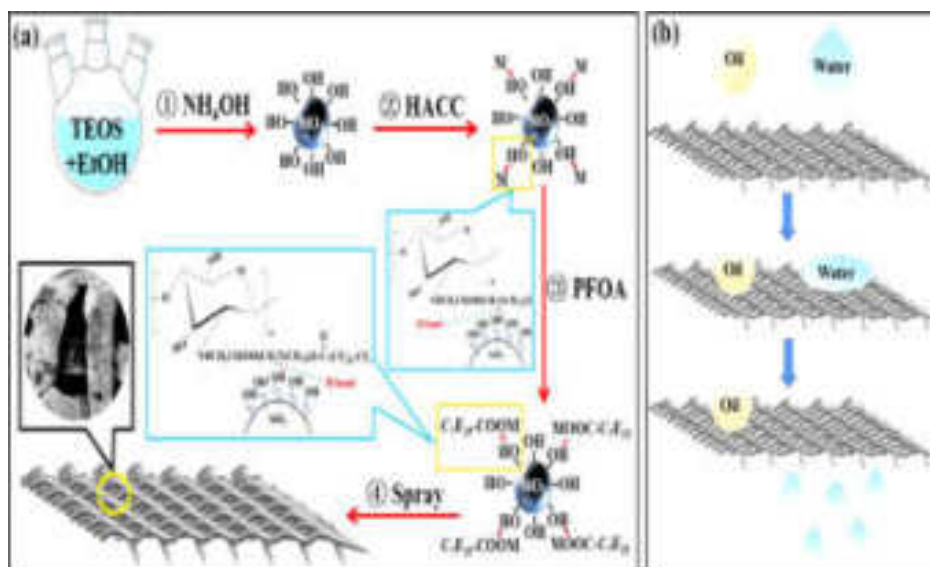


Figure-4 (a) Schematic diagram illustrating the fabrication of air superhydrophilic-superoleophobic membrane. (b) Scheme of the oil/water separation. Images reprinted from [26], with permission from Elsevier, Journal of Colloid and Interface Science, Copyright 2021.

2.3 Superhydrophobic SiO₂ Modified Porous Substrates for Oil-Water Separation

Gu et al. [27] have prepared a membrane (SiO₂/Polyurethane membrane) with porous structure rough surface and hydrophobic epidermis by surface modification to construct a rough surface and low-energy epidermis on electrospun polyurethane membrane. The schematic of experimental procedure is shown in **Figure-5**. The superhydrophobic SiO₂/PU porous membrane prepared by chemical modification on the membrane shows a water contact angle 152.1° and low sliding angle 6°. This membrane was used for different aqueous solutions like water, saline solution, alkaline solution acidic solution. The porous membrane shows low air permeability and high-water vapor transmission rate. It shown good oil absorption capacity. It was shows high oil-water separation efficiency above 98.5%. The absorption capacity of the modified membrane does not show severe degradation even after 30 separation cycles which indicating a highly stable absorption performance of modified membrane. It provided the potential for eater repellent, breathable applications and oil-water separation in long term use.

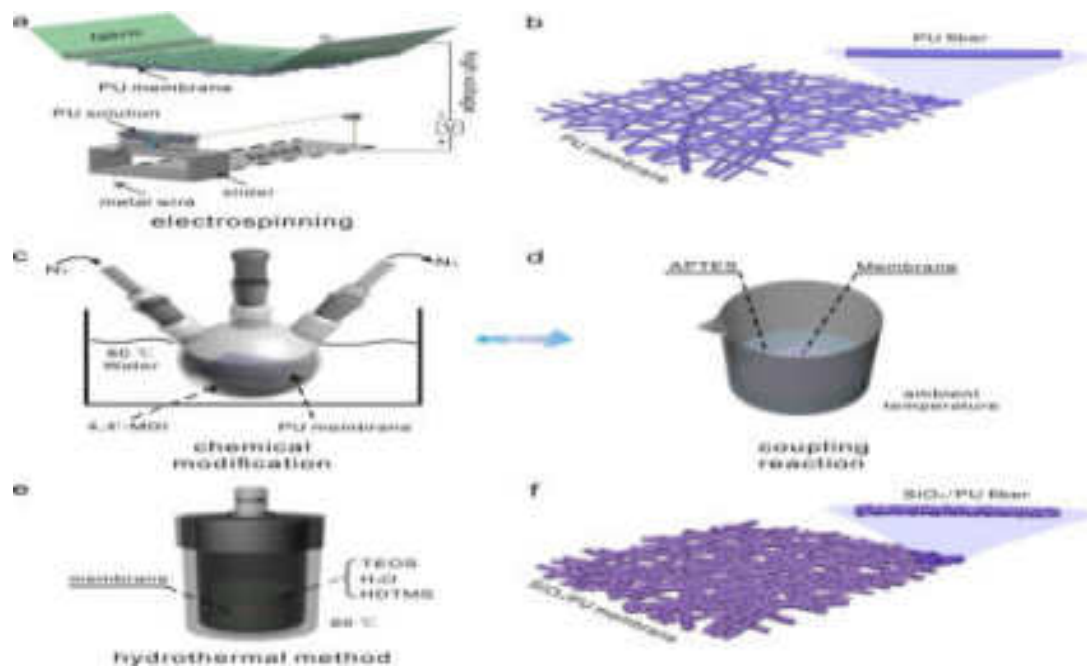


Figure-5. The preparation scheme of superhydrophobic SiO₂/PU membrane. Images reprinted from [27], with permission from Elsevier, App. Sur. Sci. Copyright 2019.

Wei and their co-researchers [28] have obtained the SiO₂ nanoparticles from ethanol and ammonium hydroxide with TEOS. The SiO₂ nanoparticles were isolated by repeated centrifugation in ethanol followed by drying in a vacuum oven. A facile strategy was presented to prepare silica particles grafting. The sprayable solution be easily applied to different porous substrates to achieve durable superhydrophobic coating (schematically shown in **Figure-6**). The surface shows a separation efficiency of 98.8% dealing with oil-water mixture. The oil absorption capacity of immersion coated polyurethane sponge was demonstrated higher than pristine polyurethane sponge an 39 g/g which would benefit from the presence of lipophilic PSAN and higher porosity contributed by abundant nanoparticles. After 10 cycles of abrasion test the remained separation efficiency of above 96% and water contact angle of 151° confirmed the mechanical durability. This sponge shows facile, environmentally friendly, mechanical and chemical stability.

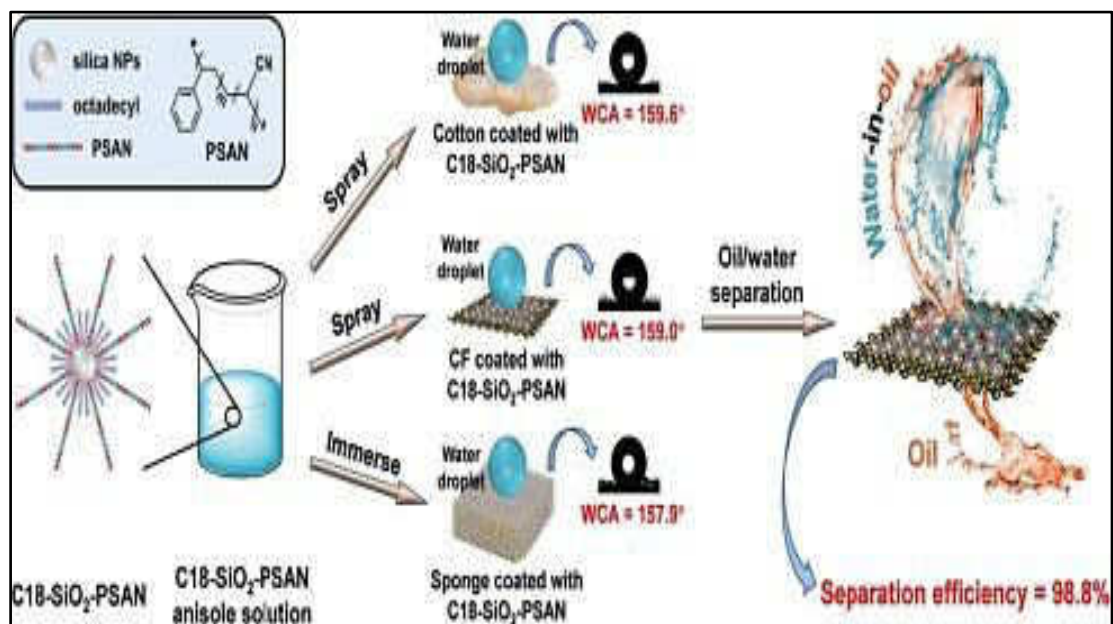


Figure-6. Schematic illustration of preparation of modified superhydrophobic surface for oil-water separation. Images reprinted from [28], with permission from Elsevier, Copyright 2021.

2.4 Superhydrophobic SiO₂- Polymer Composite Based Membrane for Oil-Water Separation

Li and their co-workers [29] have fabricated the superhydrophobic surface by using PVDF and SiO₂ via sugar template method. The schematic of preparation method is shown **Figure-7**. It was shown in a water contact angle of 155.68° and roll-on angle of nearly 6°. The prepared superhydrophobic PVDF oil/water separation membrane had low water adhesion performance and ultrahigh separation efficiency of nearly 99.98% in terms of the oil purity in the filtrate. The recycling performance over 20 cycles. This membrane has excellent potential for use in various large-scale practical applications, water purification treatment and the separation of commercially relevant emulsions. The possibility of large-scale production and low manufacturing costs of this sponge is very promising advantages for oil-water separation application.

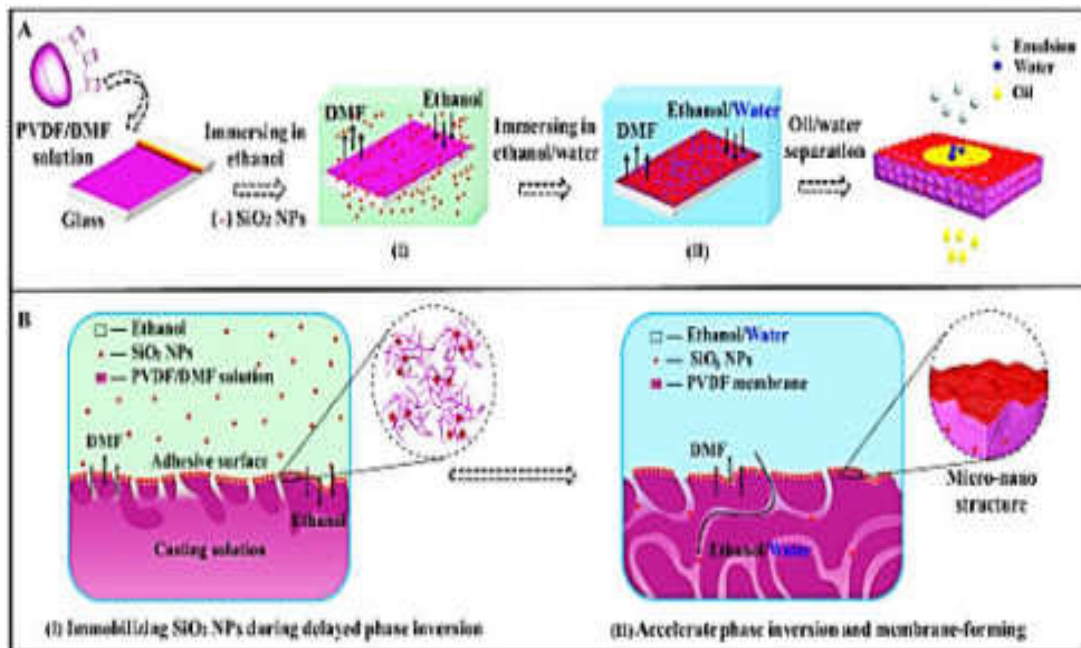


Figure-7. Schematic illustration (A) and structural evolution (B) for the formation of adhesive-free superhydrophobic SiO₂ nanoparticles decorated PVDF oil-water separation membranes [29]. Images reprinted from [29], with permission from Elsevier, Copyright 2018.

Bai et al. [30] have coated cotton fabric by sol-gel processed SiO₂. The as-prepared fabric was immersed in the solution of FeCl₃, thiophene and CH₂Cl₂ solution. Then, the modified fabric was washed with ethanol and dry it. **Figure-8** reveals the experimental procedure of preparation of superhydrophobic fabric. The modified fabric shows water contact angles above 160°. The strongest peak at 1050 cm⁻¹ belongs to the Si-O bond indicating that SiO₂ particles have been coated on the cotton fabric. The modified cotton fabric shows outstanding resistance to ultraviolet irradiation, high temperature, low temperature, organic solvent, immersion and excellent durability even after 8 months. The as-prepared fabric was showing the capability in various chemical exposures. It was showing good anti-dirt and anti-frost properties. The modified superhydrophobic cotton fabric was used as filter membrane for the gravity driven oil-water separation with high separation efficiency and excellent reusability. By using, this modified cotton fabric, both immiscible and emulsified oil-water mixtures could be separated. The efficient oil-water separation was also achieved under harsh conditions. The superhydrophobic fabric shows potential for the fast, coat-effective treatment of oil spill accidents and industrial oily sewage.

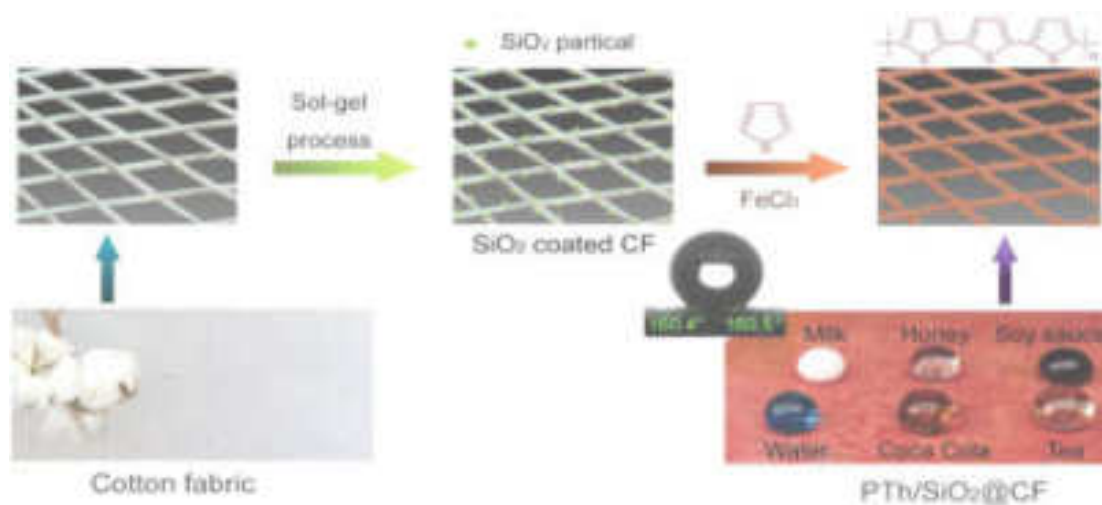


Figure-8. Schematic Illustration of the fabrication process of the PTh/SiO₂@CF [30]. Images reprinted from [30], with permission from Elsevier, Adv. Mater. Interfaces, Copyright 2021.

3. CONCLUSION

This review highlights, SiO₂ nanoparticles are unique, their fabrication requires little control of external parameters such as surface modification. It is very beneficial economically, facile and straightforward to synthesize. The SiO₂ nanoparticles coated sponge/mesh has been developed by using SiO₂ nanoparticles and different polymers. The absorption/separation investigation demonstrates that, the SiO₂ surface is highly efficient and stable in absorbing a wide range of oil and organic solvents. It can be believed that, the SiO₂ coated superhydrophobic materials are very useful for oil-water separation. It shows various tremendous results with SiO₂-polymer composite in various mechanical conditions. Hence this review is helpful to upcoming researchers to develop highly scalable superhydrophobic surfaces for efficient oil-water separation applications.

ACKNOWLEDGEMENT

This work was supported by Department of Chemistry and Department of Physics, Raje Ramrao Mahavidyalaya, Jath. We also acknowledge Prof. (Dr.) Suresh S. Patil, Principal, Raje Ramrao Mahavidyalaya, Jath.

REFERENCES

1. Alsbaiee A., Smith B. J., Xiao L., Ling Y., Helbling D. E. & Dichtel W. R. (2016) *Nature*, 529, 190-194.
2. Li Y., Zhang Z., Ge B., Men X., and Xue Q. (2016) *Green Chemistry*, 18, 5266-5272.
3. Ma Q., Cheng H., Fane A. G., Wang R., and Zhang H. (2016) *Small*, 12, 2186-2202.
4. Li L., Li B., Dong J., and Zhang J. (2016) *Journal of Materials Chemistry A*, 4, 13677–13725.
5. Yuan J., Liu X., Akbulut O., Hu J., Sui S. L., Kong J., Stellacci F. (2008) *Nature*, 3, 332-337.
6. Broje V., Keller A. A. (2006) *Environmental Science & Technology*, 40, 7914-7918.
7. Wu Z. Y., Li C., Liang H. W., Zhang Y. N., Wang X., Chen J. F. & Yu S. H. (2014) *Science Reports*, 4, 4079-4091.
8. Keshavarz A., Zilouei H., Abdol maleki A. (2015) *Journal of Environmental Management*, 157, 279-286.
9. Wang Z., Xu Y., Liu Y., Shao L. (2015) *Journal of Materials Chemistry A*, 3, 266-273.
10. Li J., Zhao Z., Kang R., Zhang Y., Lv W., Li M., Jia R., Luo L. (2017) *Journal of Sol-Gel Science and Technology*, 3, 817–826.
11. Keshavarz A., Zilouei H., Abdolmaleki A., Asadinezhad A. (2015) *Journal of Environmental Management*, 157, 279-286.
12. Sam E. K., Sam D. K., Lv X., Liu B., Xiao X., Gong S., Yu W., Chen J., Liu J. (2019) *Chemical Engineering Journal*, 19, 1103-1109.
13. Jin M., Feng X., Xi J., Zhai J., Cho K., Feng L., Jiang L. (2005) *Macromolecular Rapid Communications*, 26, 1805-1818.
14. Yao T., Zhang Y., Xiao Y., Zhao P., Guo L., Yang H., Li F. (2016) *Journal of Molecular Liquids*, 218, 611–614.
15. Gao Y., Zhou Y. S., Xiong W., Wang M., Fan L., Golgir H. R., Jiang L., Hou W., Huang X., Jiang L., Silvain J. F., Lu Y. F. (2014) *ACS Applied Materials & Interfaces*, 6, 5924–5929.
16. Erbil H. Y., Demirel A. L., Avcı Y., Mert O. (2003) *Science*, 299, 1377-1391.

17. Fard A. K., Mckay G., Manawi Y., Malaibari Z., Hussien M. A. (2016) *Chemsphere*, 164, 142-155.
18. Ren G., Song Y., Li X., Zhou Y., Zhang Z., Zhu X. (2018) *Applied Surface Science*, 428, 520-525.
19. Gu J., Xiao P., Chen J., Liu F., Huang Y., Li G., Zhang J., Chen T. (2014) *Journal of Materials Chemistry A*, 2, 15268–15272.
20. Li J., Kang R., Tang X., She H., Yang Y., Zha F. (2016) *Nanoscale*, 8, 7638–7645.
21. Gao Y., Zhou Y. S., Xiong W., Wang M., Fan L., Golgir H. R., Jiang L., Hou W., Huang X., Jiang L., Silvain J. F., Lu Y. F. (2014) *ACS Applied Materials & Interfaces*, 6, 5924–5929.
22. Li J., Zhao Z., Kang R., Zhang Y., Li M. (2017) *Journal of Sol-Gel Science and Technology*, 83, 817-826.
23. Zhang R., Zhou Z., Ge W., Lu Y., Liu T., Yang W., Dai J. (2020) *Chinese Journal of Chemical Engineering*, 5, 30292-30310.
24. Liu D., Yu Y., Chen X., Zheng Y. (2017) *RSC Advances*, 7, 12908–12915.
25. Zhao L., Du Z., Tai X., Ma Y. (2021) *Colloids and Surfaces A: Physicochemical and Engineering Aspects*, 623, 126404-126415.
26. Xiong W., Li L., Qiao F., Chen J., Chen Z., Zhou X., Hu K., Zhao X., Xie Y. (2021) *Journal of Colloid and Interface Science*, 6, 118–126.
27. Gu J., Xiao P., Chen J., Liu F., Huang Y., Li G., Zhang J., Chen T. (2014) *Journal of Materials Chemistry A*, 2, 15268–15272.
28. Wei C., Deu F., Lin L., An Z., He Y., Chen X., Chen L., Zhao Y. (2018) *Journal of Membrane Science*, 555, 220-228.
29. Li X., Wang X., Yuan Y., Wu M., Wu Q., Liu J., Yang J., Zhang J. (2021) *European Polymer Journal*, 159, 110729-110742.
30. Bai W., Lin H., Chen K., Zeng R., Lin Y., Xu Y. (2021) *Advanced Materials Interfaces*, 254, 725-740.



Photocatalytic and Superhydrophilic TiO₂ Coatings on Marble for Self-Cleaning Applications

Journal:	<i>Macromolecular Symposia</i>
Manuscript ID	Draft
Wiley - Manuscript type:	Research Article
Date Submitted by the Author:	n/a
Complete List of Authors:	Sutar, Rajaram; Raje Ramrao college jath, Department of Physics Patil, Pratiksha; Self-Cleaning Research Laboratory, Department of Physics, Raje Ramrao Mahavidyalaya, Jath, Physics Bhosale, Appasaheb; Raje Ramrao mahavidyalaya, Jath, Physics Department Sadasivuni , Kishor Kumar ; Center for Advanced Materials, Qatar University, Qatar.
Keywords:	Photocatalytic, superhydrophilic, Self-cleaning, TiO ₂ coating

SCHOLARONE™
Manuscripts

Photocatalytic and Superhydrophilic TiO₂ Coatings on Marble for Self-Cleaning Applications

Rajaram S. Sutar¹, Pratiksha B. Patil¹, Appasaheb K. Bhosale¹, Shital R. Shinde², P. G. Pawar³, C. E. Patil⁴, Sunita S. Kadam⁵, P.M. Kadam⁶, C. R. Bobade⁷, Kishor Kumar Sadasivuni⁸ and Sanjay S. Latthe^{1*}

¹Self-Cleaning Research Laboratory, Department of Physics, Raje Ramrao Mahavidyalaya, Jath, Dist: Sangli – 416404, (Affiliated to Shivaji University, Kolhapur) Maharashtra, India.

²Vidnyan Mahavidyalaya, Sangola, 413307, Maharashtra, India.

³Shivaji Polytechnic College, Sangola - 413307, Maharashtra, India.

⁴Department of Physics, Bharti Vidyapeeth's Dr. Patangrao Kadam Mahavidyalaya, Sangli, Maharashtra, India.

⁵Krantisinh Nana Patil College, Walwa, Sangli, Maharashtra.

⁶KWC Sangli, Maharashtra, India

⁷Balwant College, Vita. Dist: Sangli (M.S.) India

⁸Center for Advanced Materials, Qatar University, P. O. Box 2713, Doha, Qatar.

Corresponding Author: latthes@gmail.com

Abstract

The application of photocatalytic and self-cleaning titanium dioxide (TiO₂) nanomaterials coating on the stone of architectural heritage (particularly on marble) can be to preserve their aesthetic qualities. The present work describes the effect of dipping time in TiO₂ - SiO₂ coating and effect of UV irradiation on coating in term of hydrophilicity. The SiO₂ solution prepared by tetraethylorthosilicate (TEOS) through sol-gel process and 30-50 nm sized TiO₂ particles added to prepare coating solution. The water contact angle decreases with increasing dipping time of piece of marble in TiO₂ - SiO₂ solution. Also the hydrophilicity of coating increases with increasing UV illumination time. The 2-D and 3-D laser microscope analysis revealed surface structure and stable surface roughness of 1.0 μm. Such type of superhydrophilic TiO₂ - SiO₂ coating on marble may be used to apply architectural heritage and buildings.

Keywords: Photocatalytic, superhydrophilic, Self-cleaning and TiO₂ coating.

1. Introduction

From last decade, scientific research has been paid attention to developing novel surface for protection of aesthetic qualities of stone surfaces of historic buildings. Marbles have been extensively used in cultural heritages and historical architectures like statues and monuments. Increasing concentration of pollutants (soil particles, organisms, bird droppings, fire damage, etc.), may cause the deterioration of surfaces architectures. Photocatalytic and superhydrophilic TiO_2 coating is one of the best solution to avoid this problem. TiO_2 can generate oxidative ($\bullet\text{OH}$) and reductive ($\bullet\text{O}_2$) species under UV light irradiation, which are helps to degrade different organic and inorganic compounds ^[1, 2]. Moreover, the hydrophilicity enhanced by $-\text{OH}$, which easily remove the fouling substances on TiO_2 coated surfaces by flow water film; this is called self-cleaning ability. Munafo et al. ^[3] have sprayed colloidal suspensions of TiO_2 on travertine stone to deposit photocatalytic self-cleaning coating. After long-term aging under UV-A irradiation, the microstructure of coating was unaltered but reduced photoactivity and self-cleaning properties. Bergamonti et al. ^[4] have applied TiO_2 -sol on the stone samples by brush, repeating the procedure for three times to obtain self-cleaning coating. Lettieri et al. ^[5] have applied nanostructured TiO_2 as a photoactive coating onto a compact limestone and a highly porous calcarenite. The both types of stone has showed self-cleaning ability by photodegradation test of rhodamine B. Luna et al. ^[6] have applied sol-gel processed $\text{Au-TiO}_2/\text{SiO}_2$ photocatalysts coating on building stone by spray coating . Integrated TiO_2 in a silica matrix can enhanced its adherence to the substrate and the subsequent coating durability. Au nanoparticles enhance the TiO_2 photoactivity and the self-cleaning and depolluting performance of the coated building stone. Aminian et al. ^[7] have deposited nanolayer of TiO_2 on glass substrate by dip coating method and reported that addition of SiO_2 nanolayer under the TiO_2 layer increase the hydrophilicity due to the increase in the roughness and surface area of the nano-grains.

In the present work, we have deposited TiO_2 - SiO_2 coating on white marble by dip coating technique. The sol-gel processed silica sol were prepared by using TEOS and TiO_2 added in silica sol to prepare coating solution. The study of photodegradation of methylene blue revealed prepared coating has excellent self-cleaning ability.

2. Experimental

2.1. Materials

Tetraethylorthosilicate (TEOS, $\geq 99.0\%$) and TiO_2 nanoparticles (< 25 nm particle size, 99.7%) were purchased from Sigma-Aldrich, USA. Ethanol and nitric acid (Extra Pure AR) were bought spectrochem pvt. Mumbai, India. Methylene blue dye was obtained from Poona Laboratory, Poona, India. A small pieces of white marble (L x W x H, 5 cm x 2 cm x 1 cm) collected from local market

2.2. Preparation of TiO_2 coating on Marble

The silica sol was prepared by sol-gel processing of TEOS using nitric acid as catalyst. 11.2 ml distilled water and 0.6 ml nitric acid mixed well by magnetic stirrer. 7.5 ml of TEOS was added drop-by-drop in above mixture and kept at constant stirring (500 RPM). After 5 hr. stirring 10 ml ethanol was added slowly and stirring further continued for overnight to get silica (SiO_2) sol. Thereafter, 60 mg TiO_2 nanoparticles were dispersed in prepared silica sol and stirred for 2 hr. to get uniform coating solution. The marble pieces were washed by laboratory detergent and later by distilled water and dried well by dryer with hot air. The cleaned piece of marble dipped in coating solution with various dipping time. Deposited marble pieces were dried at 110°C for 6 hr to rid of solvents. The schematic process of deposition of superhydrophilic $\text{TiO}_2 - \text{SiO}_2$ coating on marble as shown in **Fig.1**. The dip-withdraw speed and dipping time were controlled by Dip-coater machine. The dipping time varied from 1 minute to 7 minutes at constant dip-withdraw speed of 50 mm/sec

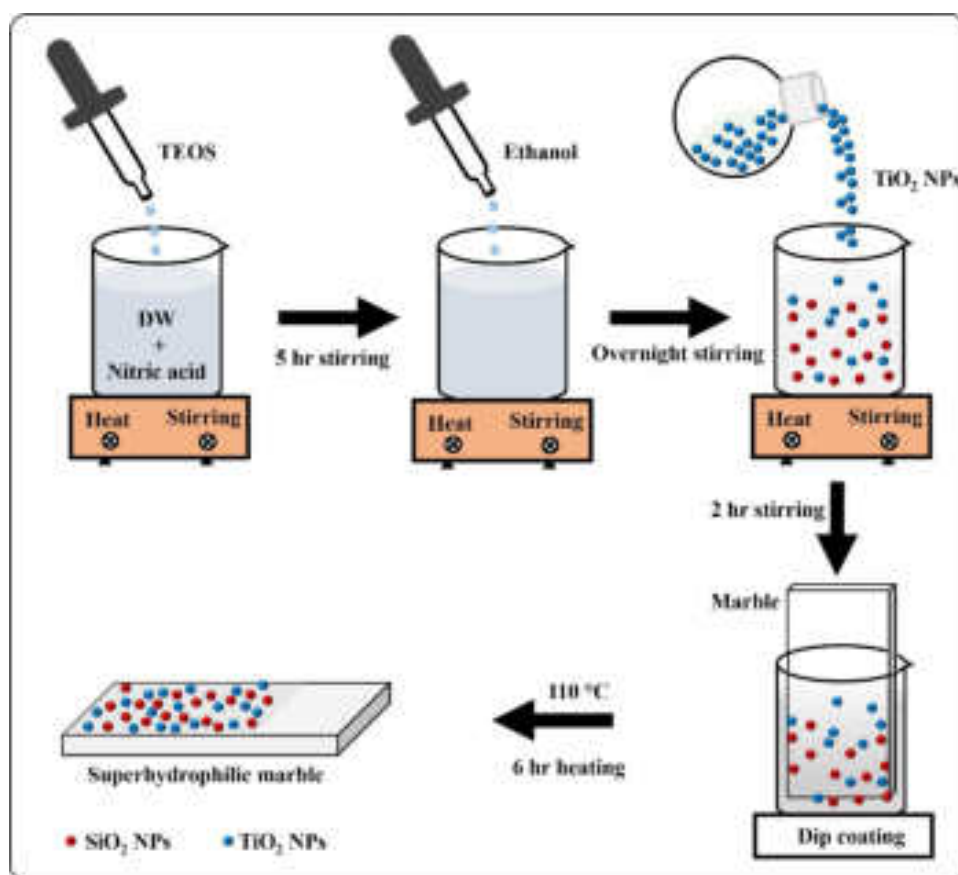


Fig. 1: Preparation of TiO₂ coating on marble.

2.3. Characterizations

A laser microscope (KEYENCE, VK-X200 series) was used to characterize the 2D and 3D surface topography of coated marble. A closed metal box with one open side covered by black napkin was fabricated and UV lamps (Intensity=1 mW/cm²) was fitted onto the ceiling of the box. The photocatalytic property of the coating was confirmed by the decrease in water contact angle (WCA) with UV illumination time. The wetting properties of the coating surface before and after UV irradiation was confirmed by WCA measurements. A contact angle meter (Kyowa, Drop Master; Saitama, Japan) was used to measure the WCAs. A small water drop was gently placed on the surface by using syringe. The self-cleaning ability of the TiO₂ coating under exposure to UV irradiation were checked using methylene blue (MB) as a stain.

3. Result and Discussion

3.1. Surface Topography and Roughness of the Prepared Coating on Marble

The surface topography plays an important role on the wettability of the thin films (**Fig. 2**). The TiO_2 - SiO_2 coating prepared by 01 minute dipping showed relatively smooth surface with RMS roughness of nearly $0.74 \mu\text{m}$. The increase in dipping time significantly affects on thickness as well as roughness of the film. The TiO_2 - SiO_2 thin films prepared by 07 minute dipping showed remarkably rough surface structure with RMS roughness of $\sim 01.00 \mu\text{m}$. Such surface structure along with highly roughness is helps to achieve the superhydrophilic. The deposition time was further increased to 10 minutes, however the visible cracks were observed on the thin film, which can be easily removed by the gentle fingertip touching.

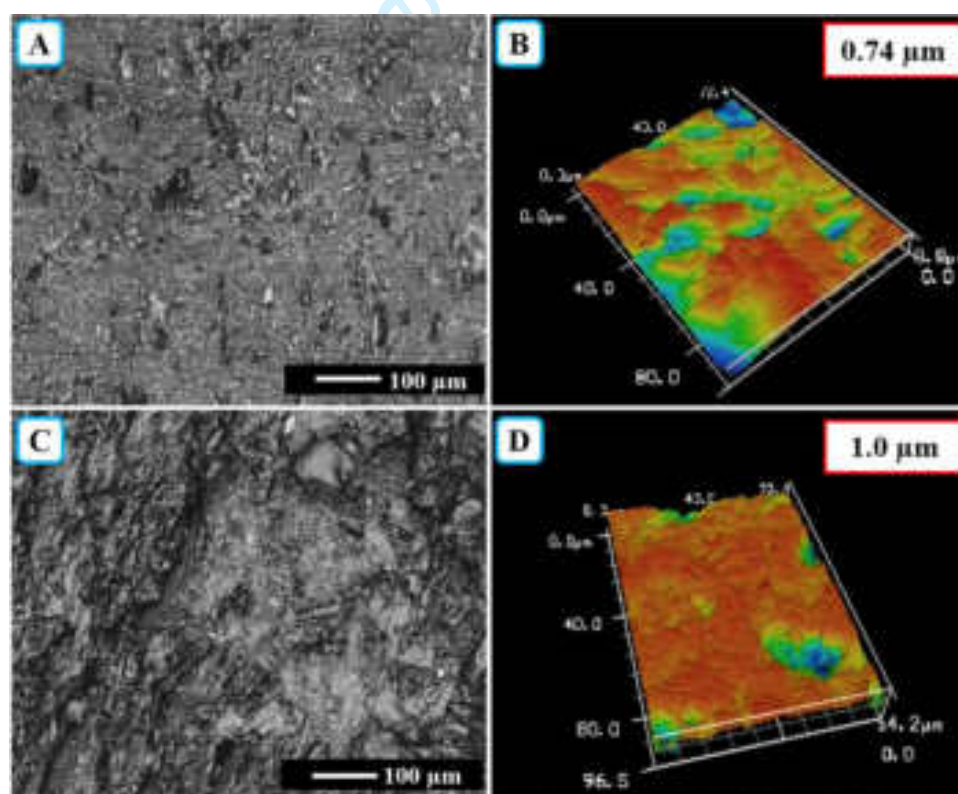


Fig. 2: The 2-D and 3-D Laser Microscope images of the SiO_2 - TiO_2 thin films prepared from (A, B) 01 minute and (C, D) 07 minute deposition time, respectively.

3.2. Surface Wettability, Photocatalytic Activity and Self-cleaning property

The coating of TiO_2 - SiO_2 thin film were applied on pre-cleaned marble by dipping at different time in coating solution. The dipping time were varied from 01 to 07 minute. As usual, 01 minute deposited coating showed WCA of 27° due to smoothness of the thin film. However, the WCA gradually decreased to 14° for 07 minute deposited TiO_2 - SiO_2 thin films. The wetting property changes with dipping time of marble in coating solution. The variation of WCA with dipping time as shown in the **Fig. 3**. This is due to the increased in roughness of the coating which eventually helps to decrease the wettability of the thin film [8].

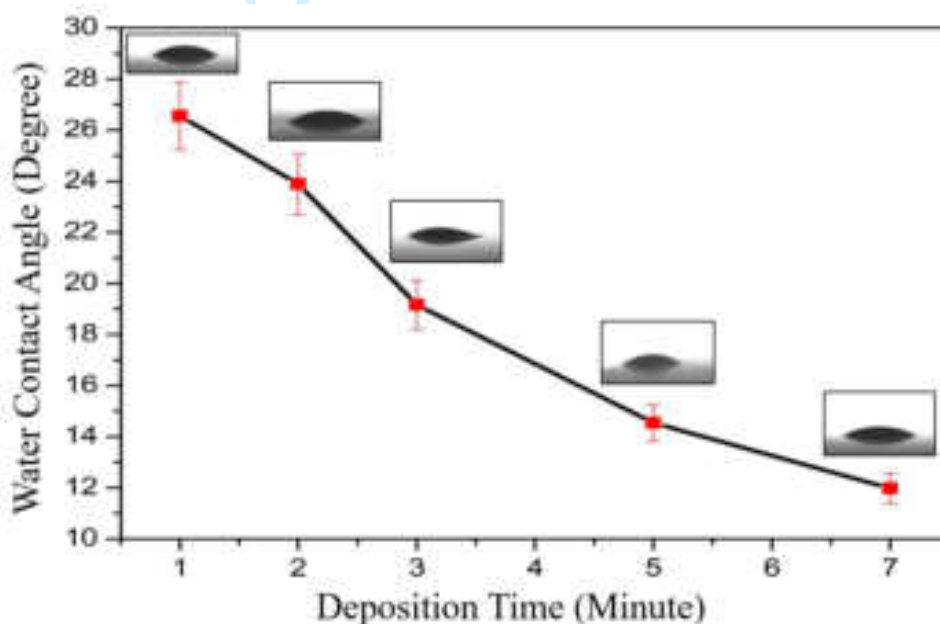


Fig. 3: An effect of dipping times on wettability of the coating.

When water drop deposited on uncoated marble, water drop stacked with WCA $> 40^\circ$. Other hand, water drop spread on coated marble. The colour dyed water on coated and uncoated marble as shown in **Fig.4**.

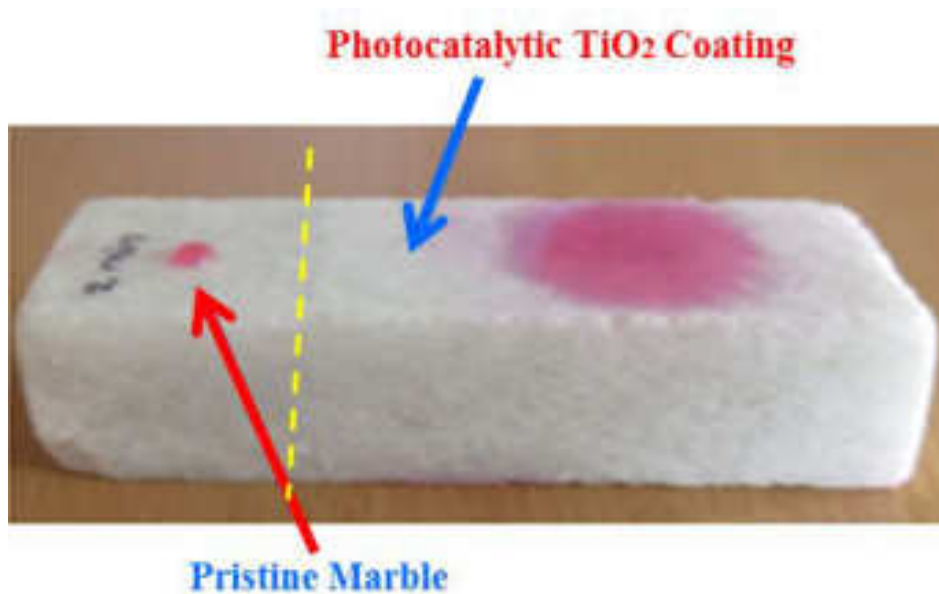


Fig. 4: Optical photograph of behaviour of water drop on coated and uncoated part of the marble.

The effect of UV irradiation on dip-coated marble (07 minute dipping marble) were observed. The hydrophilicity of coating increases with duration of UV irradiation ^[9, 10]. The variation of WCA with duration of UV irradiation as shown in **Fig. 5**. After 8 minute UV irradiation duration, the WCA of coating reached to $< 5^\circ$, which confirms hydrophilic coating become superhydrophilic. This contradict to some reports where superhydrophilicity was only achieved after long period of time of UV irradiation. UV irradiation causes to form stable hydroxyl groups on TiO₂ - SiO₂ surface and consequently surface becomes more hydrophilic ^[7]. Mostly, fast reducing WCA of hydrophilic coating under UVA radiation, which resulting that superhydrophilic self-cleaning TiO₂ - SiO₂ coating.

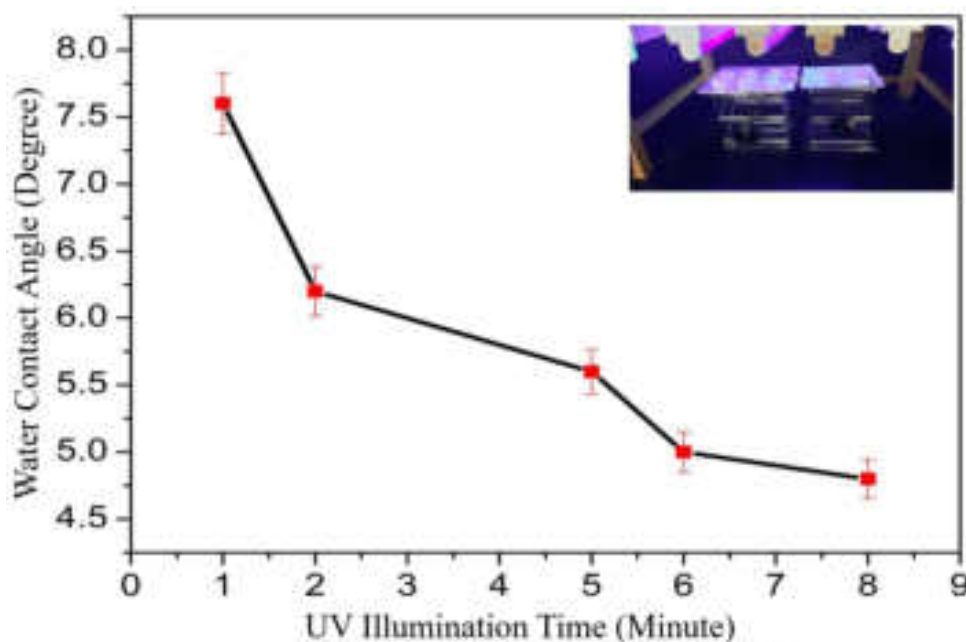


Fig. 5: An effect on UV illumination time on the wettability of the TiO_2 - SiO_2 coated marble.

Mostly white marbles are prone to damage by air and water pollution. The continuous degradation of monuments due to organic pollutants may soon become irreversible. The degradation of MB has extensively used to evaluate self-cleaning ability of coated marble [4, 11]. The systematically evaluated self-cleaning activity by adopting standard procedure. 0.5 ml of MB was poured on coated marble as shown in Fig.6 (A). Later, this marble placed at 10 cm from UV source in degradation chamber for degradation of MB. 30 hrs exposure to UV irradiation caused more than 90% degradation of MB (Fig.6 (B)). This confirms the prepared TiO_2 - SiO_2 coated marble exhibited excellent self-cleaning ability under exposure to UV illumination.



Fig. 6: Photograph of self-cleaning photodegradation test by MB, (A) before UV exposure and (B) after 30 hrs exposure to UV irradiation.

4. Conclusion

Superhydrophilic TiO₂ - SiO₂ thin films were successfully applied on marble for photocatalytic and self-cleaning application. A coating with 07 minutes of deposition time revealed hydrophilic property with contact angle nearly 14°. After exposure to UV irradiation for 8 minutes the contact angled reduced < 5°. The surface roughness of coating was found increased with deposition time. A transformation of surface wettability of TiO₂ film into superhydrophilic state and subsequent decomposition of organic pollutants by UV exposure leads to self-cleaning phenomena.

References:

1. Hoffmann, M.R., et al., *Environmental applications of semiconductor photocatalysis*. Chemical reviews, 1995. **95**(1): p. 69-96.
2. Miyauchi, M., et al., *Reversible wettability control of TiO₂ surface by light irradiation*. Surface Science, 2002. **511**(1-3): p. 401-407.
3. Munafò, P., et al., *Durability of nano-engineered TiO₂ self-cleaning treatments on limestone*. Construction and Building Materials, 2014. **65**: p. 218-231.
4. Bergamonti, L., et al., *Photocatalytic self-cleaning TiO₂ coatings on carbonatic stones*. Applied Physics A, 2016. **122**(2): p. 124.
5. Lettieri, M., et al., *Nanostructured TiO₂ for stone coating: Assessing compatibility with basic stone's properties and photocatalytic effectiveness*. Bulletin of Engineering Geology and the Environment, 2017. **76**(1): p. 101-114.
6. Luna, M., et al., *Au-TiO₂/SiO₂ photocatalysts for building materials: Self-cleaning and depolluting performance*. Building and Environment, 2019. **164**: p. 106347.
7. Khajeh Aminian, M., et al., *Hydrophilic and Photocatalytic Properties of TiO₂/SiO₂ Nano-layers in Dry Weather*. Progress in Color, Colorants and Coatings, 2021. **14**(3): p. 221-232.
8. Syafiq, A., et al., *Superhydrophilic smart coating for self-cleaning application on glass substrate*. Journal of Nanomaterials, 2018. **2018**.
9. Fateh, R., R. Dillert, and D. Bahnemann, *Preparation and characterization of transparent hydrophilic photocatalytic TiO₂/SiO₂ thin films on polycarbonate*. Langmuir, 2013. **29**(11): p. 3730-3739.
10. Shayan, M., et al., *Improved osteoblast response to UV-irradiated PMMA/TiO₂ nanocomposites with controllable wettability*. Journal of Materials Science: Materials in Medicine, 2014. **25**(12): p. 2721-2730.
11. Luna, M., et al., *TiO₂-SiO₂ coatings with a low content of AuNPs for producing self-cleaning building materials*. Nanomaterials, 2018. **8**(3): p. 177.



Superhydrophobic PVC/SiO₂ Coating for Self-Cleaning Application

Rajaram S. Sutar, Prashant J. Kalel, Sanjay S. Latthe, **Deepak A. Kumbhar**, Smita S. Mahajan, Prashant P. Chikode, Swati S. Patil, Sunita S. Kadam, V. H. Gaikwad, Appasaheb K. Bhosale, Kishor Kumar Sadasivuni, Shanhu Liu,* and Ruimin Xing*

A lotus leaf like self-cleaning superhydrophobic coating has high demand in industrial applications. Such coatings are prepared by alternative dip and spray deposition techniques. A layer of polyvinyl chloride is applied on glass substrate by dip coating and then spray coated a suspension of hydrophobic silica nanoparticles at substrate temperature of 50 °C. This coating procedure is repeated for three times to achieve rough surface morphology which exhibits a water contact angle of $169 \pm 2^\circ$ and sliding angle of 6° . The superhydrophobic state of the coating is still preserved when water volume of 1.2 L is used to impact the water drops on coating surface. The stability of the wetting state of the coating is analyzed against the water jet, adhesive tape and sandpaper abrasion tests. The prepared superhydrophobic coating strongly repelled the muddy water suggesting its importance in self-cleaning applications.

which inspired to create artificial superhydrophobic surface by increasing surface roughness along with decreasing surface energy. Such superhydrophobic surfaces have numerous applications including self-cleaning, anti-corrosion, drag-reduction, oil-water separation, and etc.^[3–8] So far, SiO₂, TiO₂, ZnO, Al₂O₃, candle soot and various polymers have been used to fabricate self-cleaning superhydrophobic coatings.^[9–14] Among them, polymer/SiO₂ nanocomposite is a promising in preparation of self-cleaning superhydrophobic coatings.^[15,16]

The self-cleaning property of superhydrophobic coatings has attracted significant interest in industrial applications. Recently, Latthe et al. have applied suspension of hydrophobic SiO₂ nanoparticles

(NPs) on different types of substrates including body of motorcycle, building wall, mini boat, solar cell panel, window glass, cotton shirt, fabric shoes, cellulose paper, metal, wood, sponges, plastic, and marble which revealed high water repellency and excellent self-cleaning property.^[17] Many reports are available on the preparation of superhydrophobic polyvinyl chloride (PVC) thin films using ethanol.^[18–20] Seyfi et al. have drop casted a mixture of PVC, Ag₃PO₄, and ethanol on thermoplastic

1. Introduction

Lotus leaf is a perfect model of self-cleaning superhydrophobic surface with specific combination of surface chemistry (surface energy) and surface topography (surface roughness).^[1,2] A low surface energy hierarchical surface structure of lotus leaf surface revealed unusual wettability (water contact angle (WCA) greater than 150° and sliding angle less than 10°)

R. S. Sutar, P. J. Kalel, S. S. Latthe, S. Liu, R. Xing
Self-cleaning Research Laboratory
Department of Physics
Raje Ramrao College
Jath
Affiliated to Shivaji University
Kolhapur, Maharashtra 416404, India
E-mail: liushanhu@vip.henu.edu.cn; rmxing@henu.edu.cn

S. S. Latthe, A. K. Bhosale
Henan Key Laboratory of Polyoxometalate Chemistry
Henan Joint International Research Laboratory of Environmental
Pollution Control Materials
College of Chemistry and Chemical Engineering
Henan University
Kaifeng 475004 P. R. China

D. A. Kumbhar
Department of Chemistry
Raje Ramrao College
Jath Maharashtra 416404, India

DOI: 10.1002/masy.202000034

S. S. Mahajan, P. P. Chikode
Department of Physics
Jaysingpur College
Jaysingpur Maharashtra 416404, India

S. S. Patil
Department of Physics
ACS College
Palus Maharashtra 416404, India

S. S. Kadam
Department of Physics
KNP College
Walwa Maharashtra 416404, India

V. H. Gaikwad
School of Chemistry
MIT World Peace University, Kothrud
Pune Maharashtra 416404, India

K. K. Sadasivuni
Center for Advanced Materials
Qatar University
Doha 2713 Qatar

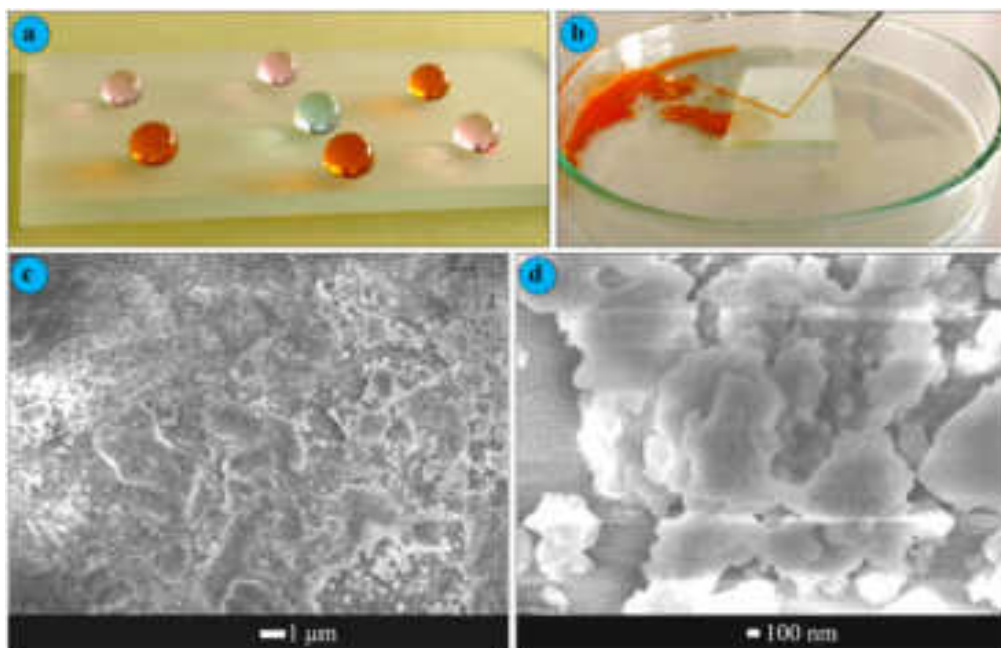


Figure 1. a) Optical photograph of color water drop on superhydrophobic coating, b) the image of water jet impacting on coating, c and d) different magnification SEM images of superhydrophobic coating.

polyurethane (TPU) substrate and achieved antibacterial superhydrophobic surface.^[21] The as prepared superhydrophobic TPU surface showed WCA $\approx 156^\circ$ and SA $\approx 2^\circ$ with self-cleaning performance. Also, Guo et al.^[15] have reported that water drops rolled off immediately on the coating prepared by casting of polymer (PVC, PMMA, and PE) and SiO₂ NPs composite on various substrates like copper, aluminum, stainless steel, silicon, glass and filter paper. Rivero et al.^[22] have prepared superhydrophobic surface by depositing ZnO NPs incorporated polystyrene (PS) and PVC polymeric solution on aluminum alloy substrate using the electrospinning technique. Yuan et al.^[23] have obtained lotus-leaf-like superhydrophobic PVC film by casting PVC solution on negative template of PDMS. Other than this, Zhang et al.^[24] have obtained superhydrophobic coating by pouring PVC/SiO₂ mixture on negative template of PDMS and reported that superhydrophobicity depends on weight percentage of SiO₂ particles in PVC. Chen et al.^[25] have prepared water-repellent SiO₂/polymer (PS and PVC) composite coating without any surface chemical modification by spin coating. The amount of hydrophobic SiO₂ NPs in PVC or PS affects the surface roughness and hence the wettability of the coating.

Herein, we have prepared superhydrophobic surface on glass by dip coating followed by spray coating method. The hydrophobic SiO₂ NPs were prepared by sol-gel technique. A thin layer of PVC was applied on glass substrate by dip coating and dried at room temperature. After that, a suspension of SiO₂ NPs in hexane was sprayed on PVC coated glass substrate at substrate temperature of 50 °C. The superhydrophobic coating was obtained by applying multiple alternative layers of PVC and SiO₂ NPs on glass substrate.

2. Result and Discussion

2.1. Surface Microstructure and Wettability

The multiple layers of PVC/SiO₂ were applied on glass substrate to obtain desired surface roughness which is the main requirement of extreme water repellency. **Figure 1c** represents the surface microstructure of three bilayer of PVC/SiO₂ coating, where the aggregated SiO₂ NPs were distributed on the PVC layer. The PVC layer can help SiO₂ NPs to adhere firmly on the coating surface. The aggregation of SiO₂ NPs is not uniform and the grain sizes from 5 μm to 100 nm were observed (**Figure 1d**). These different size scale grains provide hierarchical surface morphology. Nearly similar surface morphology was reported for the PVC/SiO₂ nanocomposite coating prepared by spin coat technique.^[25] This hierarchical surface morphology tends to trap small air pockets in the rough voids and hence a water drop can sit on the air-solid composite structure with minimum contact to the solid fraction of the surface. A water drop can only touch a small solid fraction of the coating, as the trapped air pushes away the water drops and not allowing the water drops to wet the inner portion of a rough surface. As shown in the **Figure 1a**, the water drops hardly stay on the three bilayer of PVC/SiO₂ superhydrophobic coating. Every water drop takes spherical shape at different positions on the coating surface confirming the uniform deposition of PVC/SiO₂ on the substrate. The superhydrophobic coating was appeared opaque due to the presence of micrometer scaled grains which allows scattering of the visible light. Also the water jet was impacted on the superhydrophobic coating which rebounds off the surface quickly after impacting (**Figure 1b**). The trapped air in the rough surface resists the water jet to invade the

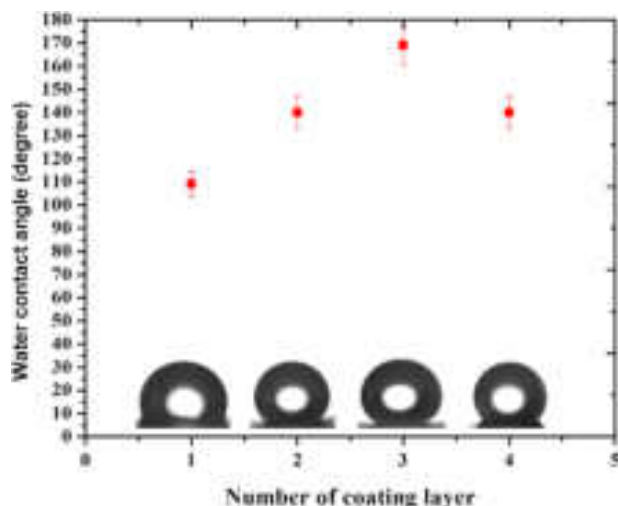


Figure 2. The variation of water contact angle with layer of polyvinyl chloride and SiO_2 particles.

rough structure. Also water jet rebounding confirms the robustness of the coating.

A systematic study was performed on the dependence of numbers of bilayers on the wettability of the coating (Figure 2). A first bilayer coating exhibited a WCA of $110 \pm 5^\circ$ confirming hydrophobic nature of the coating. The surface roughness of the coating is quite low to trap the air pockets and hence the wettability falls in the Wenzel's state^[26] where the solid fraction of the coating was partially wetted by the water drops. Though the WCA increased to $140 \pm 6^\circ$ with considerable decrease in solid-liquid contact area in case of two bilayer coating, the wettability was still in the Wenzel's wetting state. The WCA of $169 \pm 7^\circ$ and SA of 6° was observed for three bilayer coating confirming superhydrophobicity in Cassie-Baxter's wetting state.^[27] A water drop floats on the layer of air having minimum contact with solid fraction of the coating surface and hence readily roll off the surface. For next bilayer coatings, the WCA tends to decrease as a result of increase in thickness which creates visible cracks in the coatings during evaporation of solvent.

2.2. Durability Tests

The mechanical durability of superhydrophobic coating can be evaluated by water jet and water drop impact, sand paper abrasion and adhesive tape peeling test.^[28] Here, the water jet was developed by 15 mL syringe. The water jet was immediately spread on uncoated glass slide due to smooth surface structure with hydrophilic nature. On the other hand, the water jet bounced off the superhydrophobic coating as shown in Figure 1b. The air trapped hierarchical structure strongly avoids pinning of water jet on the surface.^[5,29] The wettability of the coating was checked after water jet impact study and the coating showed no change in its superhydrophobic property confirming its robustness. Water drop impact test was carried out by adjusting the distance between superhydrophobic coating and tip of tap about 10 cm as shown in schematic (Figure 3a). Nearly 2 L of water was dropped on the superhydrophobic coating inclined at 30° with drop falling rate

of 90 drops min^{-1} . The effect of water drop impact on the wetting properties of the superhydrophobic coating was estimated. The superhydrophobic state of the coating was intact for the impact of 1.2 L of the water as a result of stable air pockets in the rough microstructure of the coating which avoids water drop penetration inside the coating structure. However, the trapped air starts to evacuate from the rough structure and also the rough structure might have partly ruined due to continuous impact of water drops and as a result, WCA decreased to less than 140° for impacting 2.0 L of water (Figure 3b).

The adhesive tape peeling test was carried by using Cellotape No.405 having adhesiveness of 3.93 N/10 mm. A tape was applied firmly on the superhydrophobic coating with the help of 200 g weighted disk rolling back and forth on it (Figure 4a).^[28] After slowly peeling off the tape, some amount of the coating material was observed stacked on the adhesive tape; however, the coating showed the WCA of 165° (Figure 4b). The superhydrophobicity of the coating was found intact for two cycles of adhesive tape test, and then the WCA decreased to 80° for five cycles of adhesive tape test confirming the exhaustive loss of PVC/ SiO_2 from the coating (Figure 4c).

In large scale applications, superhydrophobic coatings can be damaged by scratch, rubbing and finger contact. To sustain the hierarchical micro/nanostructure and low surface energy of superhydrophobic coating under mechanical abrasion is one of the important issue. Here, the mechanical abrasion test was performed using sandpaper grit no. 400. The schematic of sandpaper abrasion process is illustrated in Figure 5a. A weight (100 g) was placed on superhydrophobic coating and dragged for 10 cm length on sandpaper at the average speed of 0.5 cm sec^{-1} . The effect of abrasion distance on the wettability of the superhydrophobic coating was studied (Figure 5b). The wettability of the coating was found in the superhydrophobic state for dragging the coating for nearly 30 cm on the sandpaper which confirms no significant loss in the surface roughness of the coating. However, the WCA decreased to 93° for dragging the coating for 60 cm on sandpaper confirming substantial damage to the coating.

2.3. Self-Cleaning Property

High water repellent property of the surface with low water sliding angle helps to keep the surface clean like a lotus leaf. In open air, many solid surfaces are contaminated by various types of dust particles. On superhydrophobic surface, spherical shaped water drop roll away easily by collecting dust particles, performing self-cleaning ability. The self-cleaning ability of the prepared superhydrophobic coating was tested by muddy water. The muddy water was prepared by dispersing fine particles of soil in water. This muddy water was poured on the superhydrophobic coating. In the process of pouring muddy water, it eventually get repelled off the superhydrophobic coating (Figure 6a–c). After pouring 50 mL of muddy water, surface becomes clean similar to lotus leaf (Figure 6c). This indicates prepared superhydrophobic coating was highly water repellent with excellent self-cleaning property.

3. Conclusions

We have used a conventional dip and spray coating techniques to prepare superhydrophobic coating by applying consecutive layers

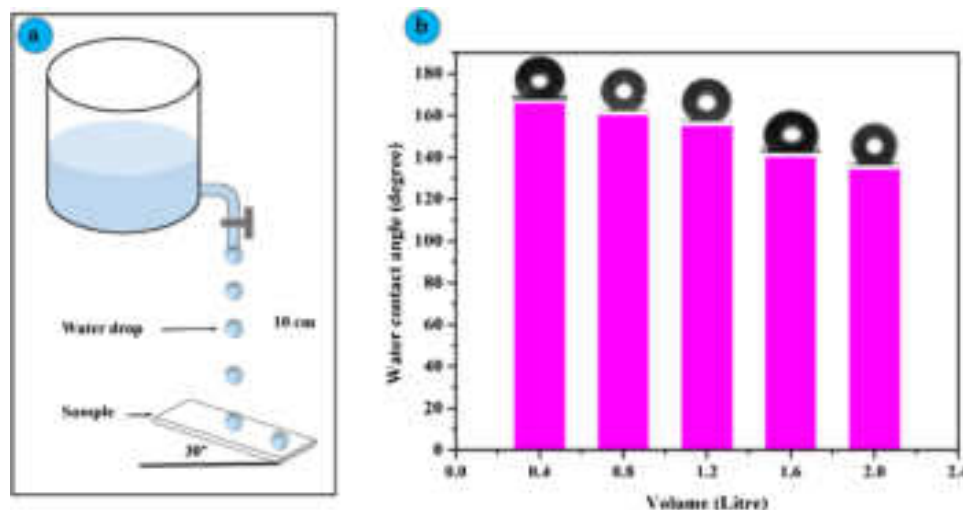


Figure 3. a) A schematic of water drop impact test, b) the effect of water drop impact on wettability of the superhydrophobic coating.

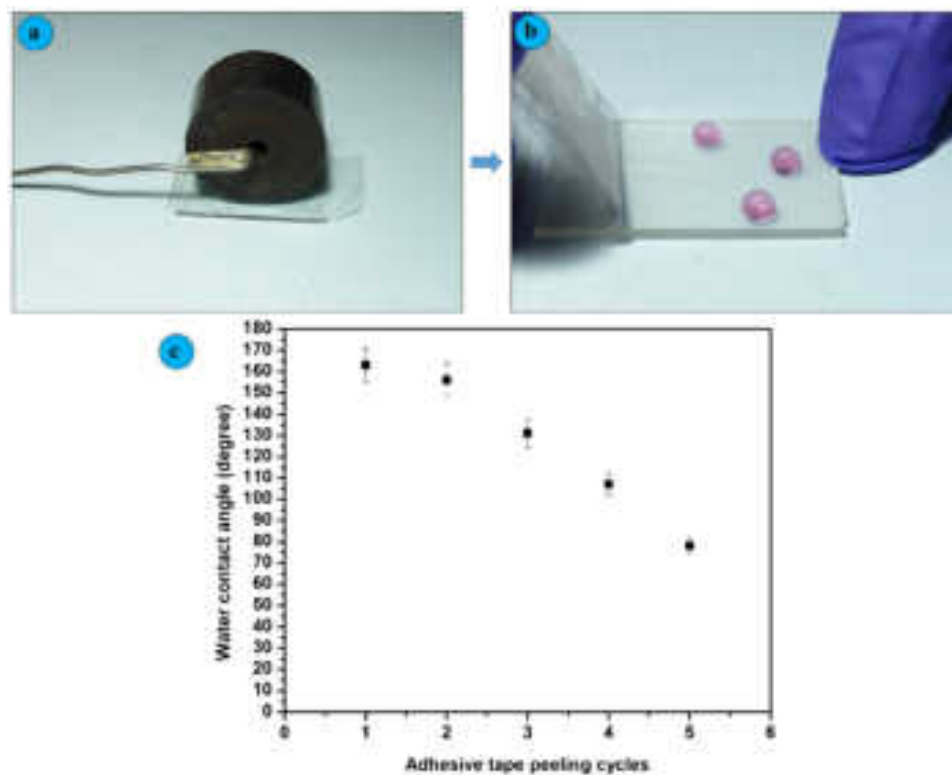


Figure 4. a) Rolling of 200 g weighted disc on adhesive tape placed on coating, b) adhesive tape peeling off and c) effect of adhesive tape peeling cycles on the wettability of the superhydrophobic coating.

of PVC and hydrophobic SiO₂ NPs on glass substrate. The hierarchical rough microstructure with different scaled grains of SiO₂ NPs was observed. The self-cleaning superhydrophobic coating with WCA of 169 ± 2° and sliding angle of 6° was achieved by applying three bilayers of alternate PVC followed by hydrophobic SiO₂ NPs. The water jet bouncing off the surface indicates the air pockets trapped in dual scale rough structure. After dripping the

water of volume 1.2 L, the water drop impacted coating showed invariable wettability. The superhydrophobic coatings were moderately stable against adhesive tape and sandpaper abrasion tests. Future practical applications of these coating can be found in windshields of vehicles, solar cell panels and windows of buildings, if their transparency and mechanical stability could be further enhanced.

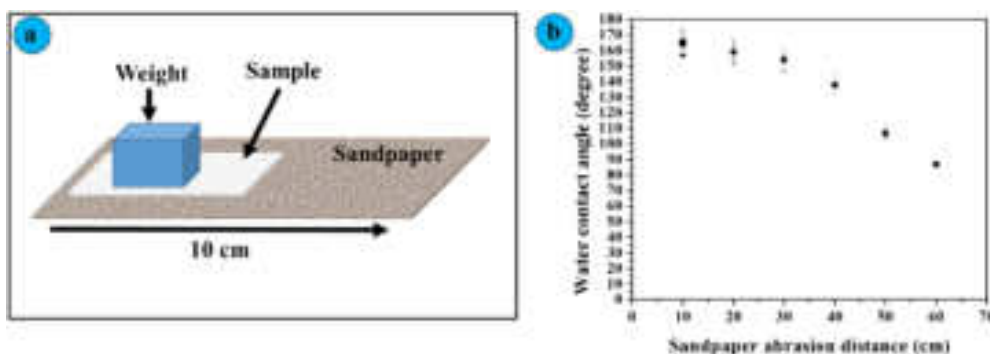


Figure 5. a) Schematic of sandpaper abrasion test and b) the variation of water contact angle with sandpaper abrasion distance.



Figure 6. a-c) Self-cleaning behavior of superhydrophobic coating.

4. Experimental Section

Materials: Methyltrimethoxysilane (MTMS) and PVC were purchased from Sigma-Aldrich, USA. Ethanol, methanol, ammonia solution, tetrahydrofuron (THF) and hexane were bought from Spectrochem PVT. LTD., India. Micro-Glass slides ($75 \times 25 \times 1.35$ mm) were obtained from Blue star, Polar Industrial Corporation, India.

Synthesis of Hydrophobic SiO_2 NPs: The hydrophobic SiO_2 NPs were synthesized using sol-gel method reported in literature.^[30] The mixture of 2 mL MTMS, 20 mL methanol and 4 mL distilled water was stirred for 20 min. After that ammonia solution was added dropwise and kept for stirring for 30 min. The prepared gel was aged for overnight and dried at 80°C for 5 h. The dried gel was grinded well using mortar and pestle to obtain fine powder of silica particles.

Preparation of Superhydrophobic Coating: At first, the glass substrates were ultrasonically cleaned with distilled water and ethanol for 30 min and dried at room temperature. The cleaned glass substrate was dipped in the PVC solution for 30 s. The solution was prepared by dissolving 100 mg PVC powder in 10 mL THF using magnetic stirrer (200 rpm for 30 min). A thin layer of PVC deposited glass substrate was dried at room temperature. A suspension of SiO_2 NPs (100 mg) was prepared by dispersing in 10 mL hexane and sprayed on PVC deposited glass substrate at substrate temperature of 50°C . Finally PVC/ SiO_2 deposited glass substrate was annealed at 100°C for 1 h. In this way, one bilayer of PVC/ SiO_2 was applied on glass substrate. This procedure was repeated to deposit two, three and four bilayers of PVC/ SiO_2 on glass substrate.

Characterizations: The wettability of prepared coatings was evaluated by measuring WCA and sliding angle (SA) using contact angle meter (HO-IAD-CAM-01, Holmarc Opto-Mechatronics Pvt. Ltd. India). The surface morphology of coating was characterized by field emission scanning electron microscopy (FESEM, JEOL, JSM-7610F, Japan). The water jet impact test was carried out by using 15 mL syringe. For water drop impact test, the coated glass substrate was kept at 30° inclination and water drops were dropped from the height of 10 cm. The mechanical stability of the coating was checked by adhesive tape peeling and sandpaper abrasion test. The self-cleaning behavior was observed by pouring muddy water on the coating.

Acknowledgements

This work was financially supported by DST-INSPIRE Faculty Scheme, Department of Science and Technology (DST), Govt. of India. [DST/INSPIRE/04/2015/000281]. SSL acknowledges financial assistance from the Henan University, Kaifeng, P. R. China. The authors greatly appreciate the support of the National Natural Science Foundation of China (21950410531).

Conflict of Interest

The authors declare no conflict of interest.

Keywords

PVC, roughness, superhydrophobic and self-cleaning, wetting

- [1] L. Feng, S. Li, Y. Li, H. Li, L. Zhang, J. Zhai, Y. Song, B. Liu, L. Jiang, D. Zhu, *Adv. Mater.* **2002**, *14*, 1857.
- [2] C. Neinhuis, W. Barthlott, *Annal. Botany* **1997**, *79*, 667.
- [3] S. P. Dalawai, M. A. S. Aly, S. S. Latthe, R. Xing, R. S. Sutar, S. Nagappan, C.-S. Ha, K. K. Sadasivuni, S. Liu, *Prog. Org. Coat.* **2020**, *138*, 105381.
- [4] S. S. Latthe, V. S. Kodag, R. S. Sutar, A. K. Bhosale, S. Nagappan, C.-S. Ha, K. K. Sadasivuni, S. R. Kural, S. Liu, R. Xing, *Mater. Chem. Phys.* **2020**, *243*, 122634.
- [5] S. S. Latthe, P. Sudhagar, A. Devadoss, A. M. Kumar, S. Liu, C. Terashima, K. Nakataa, A. Fujishima, *J. Mater. Chem. A* **2015**, *3*, 14263.
- [6] S. S. Latthe, et al. *Superhydrophobic Polymer Coatings*, **2019**, Elsevier. pp. 339–356.
- [7] S. S. Latthe, R. S. Sutar, A. K. Bhosale, S. Nagappan, C.-S. Ha, K. K. Sadasivuni, S. Liu, R. Xing, *Prog. Org. Coat.* **2019**, *137*, 105373.

- [8] S. S. Latthe, R. S. Sutar, T. B. Shinde, S. B. Pawar, T. M. Khot, A. K. Bhosale, K. K. Sadasivuni, R. Xing, L. Mao, S. Liu, *ACS Appl. Nano Mater.* **2019**, 2, 799.
- [9] A. B. Gurav, S. S. Latthe, R. S. Vhatkar, J. G. Lee, D. Y. Kim, J. J. Park, S. S. Yoon, *Ceram. Int.* **2014**, 40, 7151.
- [10] A. M. Kokare, et al. *AIP Conference Proceedings*, AIP Publishing. **2018**.
- [11] S. S. Latthe, et al. *Green Chemistry for Surface Coatings, Inks and Adhesives*. **2019**. pp. 92–119.
- [12] R. S. Sutar, et al. *Macromolecular Symposia*, **2019**. Wiley Online Library.
- [13] S. Bilgin, M. Isik, E. Yilgor, *Polymer* **2012**, 53, 1180.
- [14] H. Yoon, H. Kim, S. S. Latthe, M.-W. Kim, S. Al-Deyabd, S. S. Yoon, *J. Mater. Chem. A* **2015**, 3, 11403.
- [15] Y. Guo, Q. Wang, *Appl. Surf. Sci.* **2010**, 257, 33.
- [16] P. G. Pawar, R. Xing, R. C. Kambale, A. M. Kumar, S. Liu, S. S. Latthe, *Prog. Org. Coat.* **2017**, 105, 235.
- [17] S. S. Latthe, R. S. Sutar, V. S. Kodag, A. K. Bhosale, A. M. Kumar, K. K. Sadasivuni, R. Xing, S. Liu, *Prog. Org. Coat.* **2019**, 128, 52.
- [18] H. Chen, Z. Yuan, J. Zhang, Y. Liu, K. Li, D. Zhao, S. Li, P. Shi, J. Tang, *J. Porous Mater.* **2009**, 16, 447.
- [19] Z. Khoryani, J. Seyfi, M. Nekoei, *Appl. Surf. Sci.* **2018**, 428, 933.
- [20] X. Li, G. Chen, Y. Ma, L. Feng, H. Zhao, L. Jiang, F. Wang, *Polymer* **2006**, 47, 506.
- [21] J. Seyfi, M. Panahi-Sarmad, A. OraeiGhodousi, V. Goodarzi, H. A. Khonakdar, A. Asefnejad, S. Shojaei, *Colloids Surf., B* **2019**, 183, 110438.
- [22] P. J. Rivero, A. Iribarren, S. Larumbe, J. F. Palacio, R. Rodríguez, *Coatings* **2019**, 9, 367.
- [23] Z. Yuan, H. Chen, J. Zhang, *Appl. Surf. Sci.* **2008**, 254, 1593.
- [24] X. Zhang, B. Ding, R. Cheng, S. C. Dixon, Y. Lu, *Adv. Sci.* **2018**, 5, 1700520.
- [25] H. Chen, X. Zhang, P. Zhang, Z. Zhang, *Appl. Surf. Sci.* **2012**, 261, 628.
- [26] R. N. Wenzel, *Ind. Eng. Chem.* **1936**, 28, 988.
- [27] A. Cassie, S. Baxter, *Trans. Faraday Soc.* **1944**, 40, 546.
- [28] N. Wang, D. Xiong, S. Pan, K. Wang, Y. Shi, Y. Deng, *New J. Chem.* **2017**, 41, 1846.
- [29] A. Kibar, H. Karabay, K. Yigit, I. Ucar, H. Erbil, *Exp. Fluids* **2010**, 49, 1135.
- [30] S. S. Latthe, A. V. Rao, *Surf. Coat. Technol.* **2012**, 207, 489.



SHIVAJI UNIVERSITY, KOLHAPUR

Volume-49 Issue-2 (July, 2023)

ISSN-Science-0250-5347

Estd. 1962
"A++" Accredited by NAAC (2021)
with CGPA 3.52



Journal of Shivaji University SCIENCE & TECHNOLOGY

(Peer Reviewed Journal)

Journal of Shivaji University: Science and Technology
Volume-49, Issue-2 (July, 2023)

INDEX

Sr. No.	Title of Research Article with Name of Author/s	Page No.
1.	Silica Coated Superhydrophobic Materials for Oil-Water Separation Application-A Short Review Rajesh B. Sawant, Mehejbin R. Mujawar, Amol B. Pandhare, Sanjay S. Latthe, Ankush M. Sargar, Raghunath K. Mane, Shivaji R. Kulal	1
2.	Green Synthesis of NiO Nanoparticles from <i>Partheniumhysterophorus</i> Plant Sneha V. Koparde, Akanksha G. Kolekar, Shital S. Shendage, Aniket H. Sawat, Snehal D. Patil, Snehal S. Patil, Reshma B. Darekar, Amol B. Pandhare, Vijay S. Ghodake, Samadhan P. Pawar, Govind B. Kolekar	12
3.	Microwave-Assisted Synthesis of Pyrazole and Its Hybrid Scaffolds as Potent Biological and Pharmacological Agents: A Short Review Pravin. R. Kharade, Uttam. B. Chougale, Satish. S. Kadam, Kiran. N. Patil, Prakash S. Pawar, Savita. S. Desai	19
4.	Biosynthesis and Catalytic Transformation of Ruthenium Nanoparticles in Biomimetic Applications Komal M. Dhumal, Anita R. Mali	36
5.	Third Generation Solar Cells: Importance and Measurements Techniques for knowing Photovoltaic Device Performance Prakash S. Pawar, Pramod A. Koyale, Amol B. Pandhare, Vijay S. Ghodake, Swapnijit V. Mulik, Ankita K. Dhukate, Waleed Dabdoub, Sagar D. Delekar	48
6.	Aggregation-Induced Emission, Mechanochromism, and Applications of Tetraphenylethene/Triphenylamine-based Molecules Kishor. S. Jagadhane, Govind. B. Kolekar, Prasad. M. Swami, Prashant. V. Anbhule	68
7.	Greener and Environmentally Benign Methodologies for the Synthesis of Bis(indolyl)methane and Trisindolines Aboli C. Sapkal, Suraj R. Attar, Santosh B. Kamble	75

Silica Coated Superhydrophobic Materials for Oil-Water Separation Application-A Short Review

Rajesh B. Sawant^{a,*}, Mehejbin R. Mujawar^a, Amol B. Pandhare^{b,f},
Sanjay S. Latthe^c, Ankush M. Sargar^d,
Raghunath K. Mane^e, Shivaji R. Kulal^{a*}

^aDepartment of Chemistry, Raje Ramrao Mahavidyalaya, Jath, Sangli 416 404 (MS) India.

^bDepartment of Chemistry, Shivaji University, Kolhapur 416 004 (MS) India.

^cDepartment of Physics, Vivekanand College, Kolhapur 416 003 (MS) India.

^dDepartment of Chemistry, Bharati Vidyapeeth's Dr. Patangrao Kadam Mahavidyalaya, Sangli 416 416 (MS) India.

^e Department of Chemistry, Smt. Kusumtai Rajarambhapu Patil Kanya Mahavidyalaya, Islampur, Sangli 416 409 (MS) India.

^fDepartment of Chemistry, M.H. Shinde Mahavidyalaya, Tisangi, Gaganbavda, Kolhapur 416 206 (MS) India.

*Corresponding authors: srkulal@gmail.com and rbsawant2@gmail.com

ABSTRACT

Contamination like oil and organic pollutants in water has a severe problem for aquatic life and human being; it is a need to preserve their life. These contaminants are added due to frequent oil spill accidents, and industrial as well as domestic waste. There is a need to develop methods and materials that show excellent ability to separate the oil and organic contaminants from water. Recently, superhydrophobic coated sponges, metals mesh, membranes and porous materials plays crucial role to separate oil and water from oil-water mixture. The micro and nonporous of substrate facilitate to enter liquid into it and superhydrophobic/superoleophilic property of substrate surface resist water and allows oil to enter into porous substrate. The various surface modified organic metal oxide nanoparticles are used to develop superhydrophobic surface on porous substrate. Among them SiO₂ nanoparticles is promising material to preparation of superhydrophobic surface because of their cost-effectiveness and easy synthesis techniques. This review focused on silica modified porous sponge, metal meshes, membrane and porous substrate for scalable oil-water separation application.

KEYWORDS

Superhydrophobic, Oil-water separation, porous sponge, Metal mesh and membrane.

.....

1. INTRODUCTION

Frequent oil spill accidents and industrial chemical spills occurred in the sea and the ecosystem damage; such incidents have spread to impact the offspring. Therefore, considerable surviving organisms for several years after the impact [1-2] efforts have been done to remove oil and organic solvents from water. Due to this extensive current research is focussed on the development of superhydrophobic materials for effective oil-water separation. To achieve superhydrophobic sponges, surface roughness and low surface energy materials play a crucial role. The various methods such as dip coating, immersion, spray coating; hydrothermal methods, chemical vapor deposition, surface etching, solvothermal methods, layer-by-layer assembly and electrochemical treatment describe a modification of sponges for oil and water separation [3-4]. At present, traditional technologies, including in situ burning [5], bioremediation [6], chemical dispersant methods [7], skimming [8], and the use of sorbents [9] are used to clean up spilled oils or organic pollutants. However, many of these strategies involve energy intensive and slow processes, have low clean-up capacities or create secondary pollution during the clean-up process, restricting their widespread practical applications [10-11]. To realize the hierarchical structures on different material surfaces, a series of strategies, such as sol-gel coating [12], chemical vapor deposition [13], plasma etching [14], template processing [15], lithographic patterning [16], etc. have been adopted [17]. The superhydrophobic surfaces on which water achieves water contact angle higher than 150° and sliding angle less than 5° are attracting minds of researchers due to their efficient oil-water separation efficiency [18].

Recently, Wu et al. [19] have prepared a highly flexible superhydrophobic PDMS@F-SiO₂ coating for self-cleaning and drag-reduction applications via a two-step spraying of PDMS and F-SiO₂ nanoparticles. However, it is common that inorganic particles normally tend to agglomerate due to the interparticle forces stemming from the Vander Waals, capillary and electrostatic forces [20], which leads to phase separation during the fabrication process and tends to diminish the quality of the coating through cracks or weak adhesive to the substrates. Gao et al. [21] prepared PVDF/SiO₂ coated superhydrophobic porous membranes using a spraying technique. These membranes could be used to separate the oil-water mixtures but are not applicable to surfactant stabilized water-in-oil emulsions because of their large pore sizes. Li et al. [22] prepared the hydrophobic CS by incomplete combustion of hydrocarbons from the middle of a candle flame. The PU sponge was immersed in the solution of CS, SiO₂ and PU resin to achieve stable superhydrophobicity. The CS-SiO₂-PU sponge was shown excellent oil-water separation efficiency. The CS-SiO₂-PU sponge showed excellent oil-water separation efficiency from hot water, acidic solutions, alkaline solutions and salt solutions.

In this review, the sophisticated, facile and low-cost methods for fabrication of superhydrophobic porous material for oil-water separation application are discussed.

The 3D sponges, metal meshes, membrane and cotton fabrics are used as substrate for scalable oil-water separation application.

2. SUPERHYDROPHOBIC SURFACES FOR OIL-WATER SEPARATION

2.1 Superhydrophobic SiO₂ Modified Sponges for Oil-Water Separation

Zhang et al. [23] have fabricated the superhydrophobic surface by using VTMS and SiO₂ via immersion method. The schematic of preparation of superhydrophobic sponge is shown in **Figure-1**. It was shown a water contact angle of 153.2° and roll-on angle of 4.8°. The oil is quickly absorbed by superhydrophobic sponge which can be shown the superoleophilic property of a modified sponge. The IR peak at 1078 cm⁻¹ shows the presence of the O-Si-O bond present in the material. It was showing the high separation efficiency of about 99.5%. It exhibited good saturated adsorption properties exceeding 70 g/g for all oils. It shows outstanding characteristics of superhydrophobic sponge such as high porosity, small pore size and ultra-light mass. After 20 cycles, it was found that the adsorption ability of the modified melamine sponge for different oils decreased slightly. It shows outstanding stability and reusable performance. The modified sponge maintains an 89% of recovery rate even after 20 cycles. This method was used to prepare porosity and provides storage space for the adsorption of oil pollution. This superhydrophobic composite melamine sponge provided the possibility for practical application of oil-water separation.

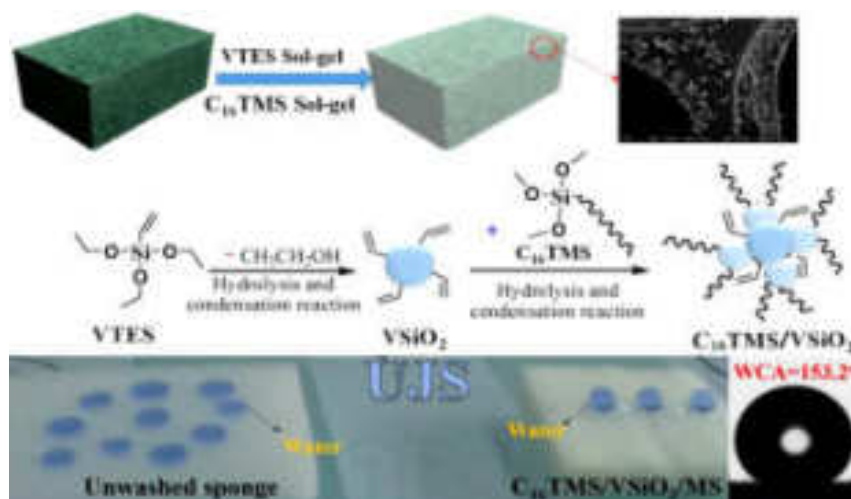


Figure-1. Schematic illustration of the preparation of superhydrophobic sponge. Images reprinted from [23], with permission from Elsevier, Journal of Chemical Engineering, Copyright 2020.

Liu et al. [24]. have fabricated a superhydrophobic sponge and polyester coated with SiO₂-DTMS through an entrapment method. The **Figure-2** reveals the fabrication process of superhydrophobic sponge and polyester. The SiO₂ particles were introduced by growth on the substrate through the polymerization process, followed by the addition of DTMS as an adhesive, leading to a homogeneous and dense superhydrophobic membrane. The modified sponge was shown the water contact angle up to 172° indicating the water repellence was superior. This superhydrophobic sample had good hydrophobic stability even in acidic condition and it can show efficient oil-water separation. The amount of the absorbed oil was about 43-65 times of sponge own weight can be shown that the evaluation of the mass based on absorbed surface tension, density, viscosity of absorbed liquids. It exhibits stable oil storage under harsh environmental conditions in oil-water separation. The performance remained constant after 100 recycling sequences, even in a harsh water environment.

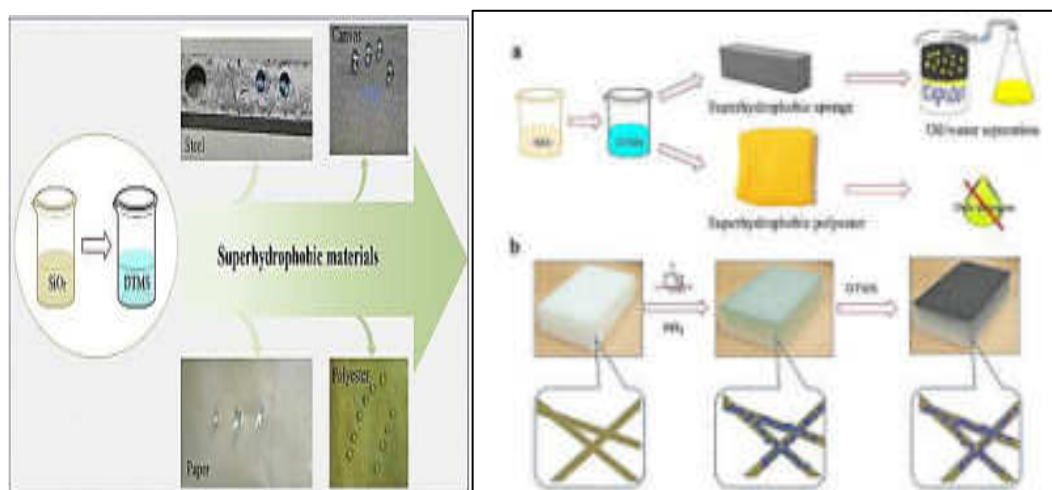


Figure-2. Schematic illustration of the fabrication of a modified sponge and polyester. Images reprinted from [24], with permission from Elsevier, Copyright 2019.

2.2 Superhydrophobic SiO₂ Modified Metal Meshes for Oil-Water Separation

Zhao et al. [25] have prepared superhydrophobic SiO₂ nanoparticles by improved Stober method and then coated on a chemically etched stainless steel mesh by one step dipping method to fabricate superhydrophobic SiO₂ coated stainless steel mesh. The preparation process was simple, efficient and environmentally friendly. The experimental procedure is shown in **Figure-3**. It shows excellent oil-water separation properties, which can be widely used in oil-water separation. It was showing 153.3° water contact angle and 0° oil contact angle. The oil-water separation efficiency was nearly 96% by using this modified stainless-steel mesh.

The separation efficiencies were obtained repeatedly even after 40 cycles without noticeable deterioration. The superhydrophobic modified stainless steel mesh shows stability, durability and reusability. The SiO₂ modified stainless steel mesh indicates good material for treating real oil-polluted water in different practical applications. This method shows high performance, oil-water separation in a short time and repeatedly in comparison with earlier works.

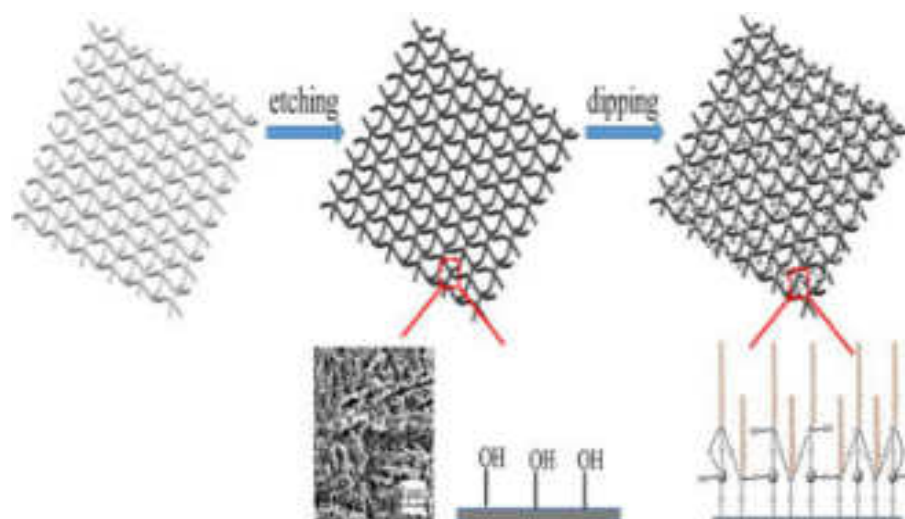


Figure-3. Schematic illustration of the preparation of FSSM. Images reprinted from [25], with permission from Elsevier, Copyright 2019.

Xiong et al. [26] have prepared SiO₂ nanoparticles by an improved modified method by using TEOS and then coated on a stainless-steel mesh by spraying method to fabricate SiO₂ coated stainless steel mesh. The **Figure-4** illustrates schematic of preparation of the superhydrophobic stainless-steel mesh. The preparation process was efficient, simple and environmentally friendly. It shows good mechanical properties and oil/water separation performance. It was showing 156.4° oil contact angle and less than 10° water contact angles. The oil-water separation efficiency was nearly 98.69% by using this modified stainless-steel mesh. The separation efficiencies obtained repeatedly even after 20 cycles without noticeable deterioration. The superhydrophobic modified stainless steel mesh shows stability, durability and reusability. The SiO₂ modified stainless steel mesh indicates excellent material for treating oil-polluted water in different practical applications. This method shows an easily scaled-up preparation process, stable mechanical and thermal properties, offering new prospects for efficient oil/water separation in comparison with earlier works.

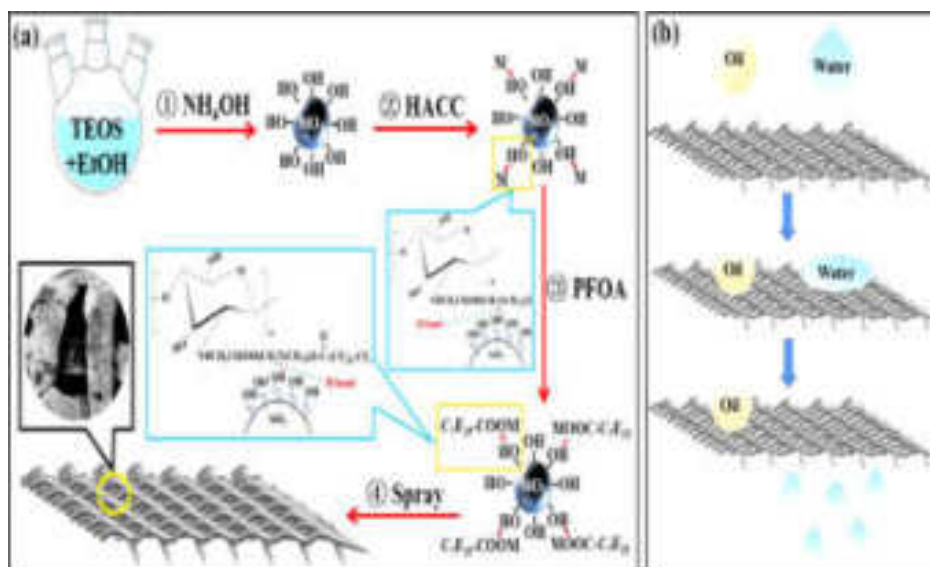


Figure-4 (a) Schematic diagram illustrating the fabrication of air superhydrophilic-superoleophobic membrane. (b) Scheme of the oil/water separation. Images reprinted from [26], with permission from Elsevier, Journal of Colloid and Interface Science, Copyright 2021.

2.3 Superhydrophobic SiO₂ Modified Porous Substrates for Oil-Water Separation

Gu et al. [27] have prepared a membrane (SiO₂/Polyurethane membrane) with porous structure rough surface and hydrophobic epidermis by surface modification to construct a rough surface and low-energy epidermis on electrospun polyurethane membrane. The schematic of experimental procedure is shown in **Figure-5**. The superhydrophobic SiO₂/PU porous membrane prepared by chemical modification on the membrane shows a water contact angle 152.1° and low sliding angle 6°. This membrane was used for different aqueous solutions like water, saline solution, alkaline solution acidic solution. The porous membrane shows low air permeability and high-water vapor transmission rate. It shown good oil absorption capacity. It was shows high oil-water separation efficiency above 98.5%. The absorption capacity of the modified membrane does not show severe degradation even after 30 separation cycles which indicating a highly stable absorption performance of modified membrane. It provided the potential for eater repellent, breathable applications and oil-water separation in long term use.

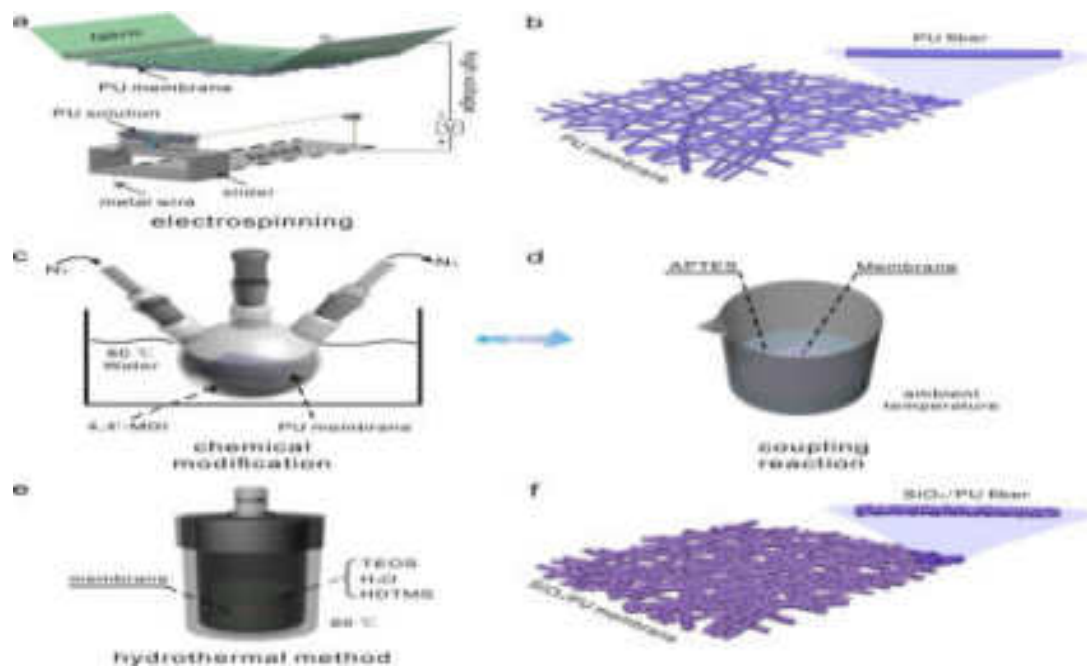


Figure-5. The preparation scheme of superhydrophobic SiO₂/PU membrane. Images reprinted from [27], with permission from Elsevier, App. Sur. Sci. Copyright 2019.

Wei and their co-researchers [28] have obtained the SiO₂ nanoparticles from ethanol and ammonium hydroxide with TEOS. The SiO₂ nanoparticles were isolated by repeated centrifugation in ethanol followed by drying in a vacuum oven. A facile strategy was presented to prepare silica particles grafting. The sprayable solution be easily applied to different porous substrates to achieve durable superhydrophobic coating (schematically shown in **Figure-6**). The surface shows a separation efficiency of 98.8% dealing with oil-water mixture. The oil absorption capacity of immersion coated polyurethane sponge was demonstrated higher than pristine polyurethane sponge an 39 g/g which would benefit from the presence of lipophilic PSAN and higher porosity contributed by abundant nanoparticles. After 10 cycles of abrasion test the remained separation efficiency of above 96% and water contact angle of 151° confirmed the mechanical durability. This sponge shows facile, environmentally friendly, mechanical and chemical stability.

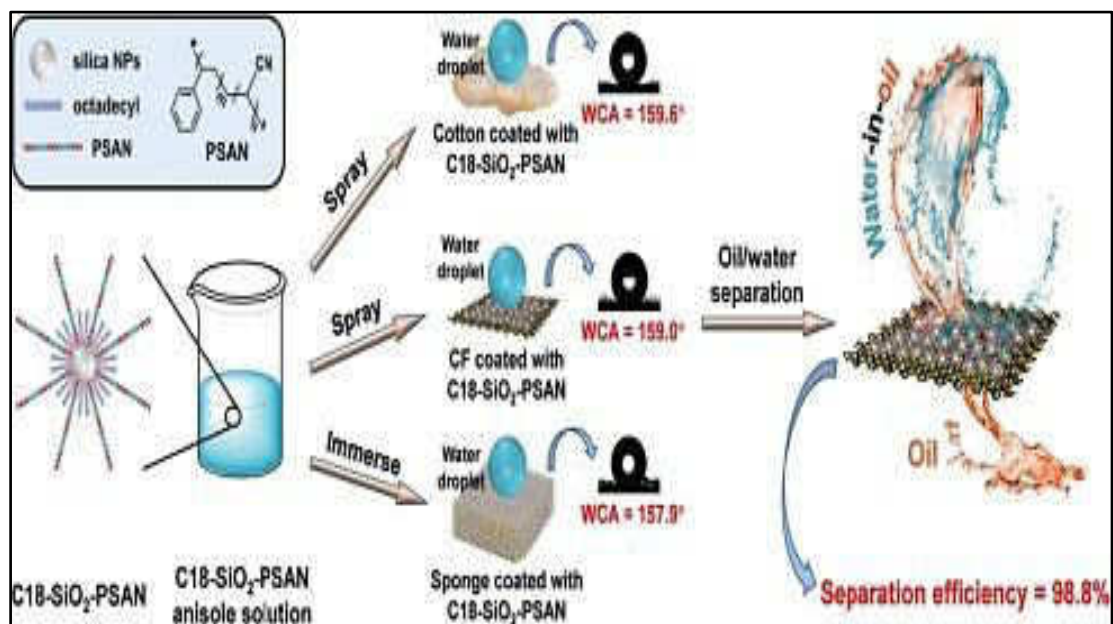


Figure-6. Schematic illustration of preparation of modified superhydrophobic surface for oil-water separation. Images reprinted from [28], with permission from Elsevier, Copyright 2021.

2.4 Superhydrophobic SiO₂- Polymer Composite Based Membrane for Oil-Water Separation

Li and their co-workers [29] have fabricated the superhydrophobic surface by using PVDF and SiO₂ via sugar template method. The schematic of preparation method is shown **Figure-7**. It was shown in a water contact angle of 155.68° and roll-on angle of nearly 6°. The prepared superhydrophobic PVDF oil/water separation membrane had low water adhesion performance and ultrahigh separation efficiency of nearly 99.98% in terms of the oil purity in the filtrate. The recycling performance over 20 cycles. This membrane has excellent potential for use in various large-scale practical applications, water purification treatment and the separation of commercially relevant emulsions. The possibility of large-scale production and low manufacturing costs of this sponge is very promising advantages for oil-water separation application.

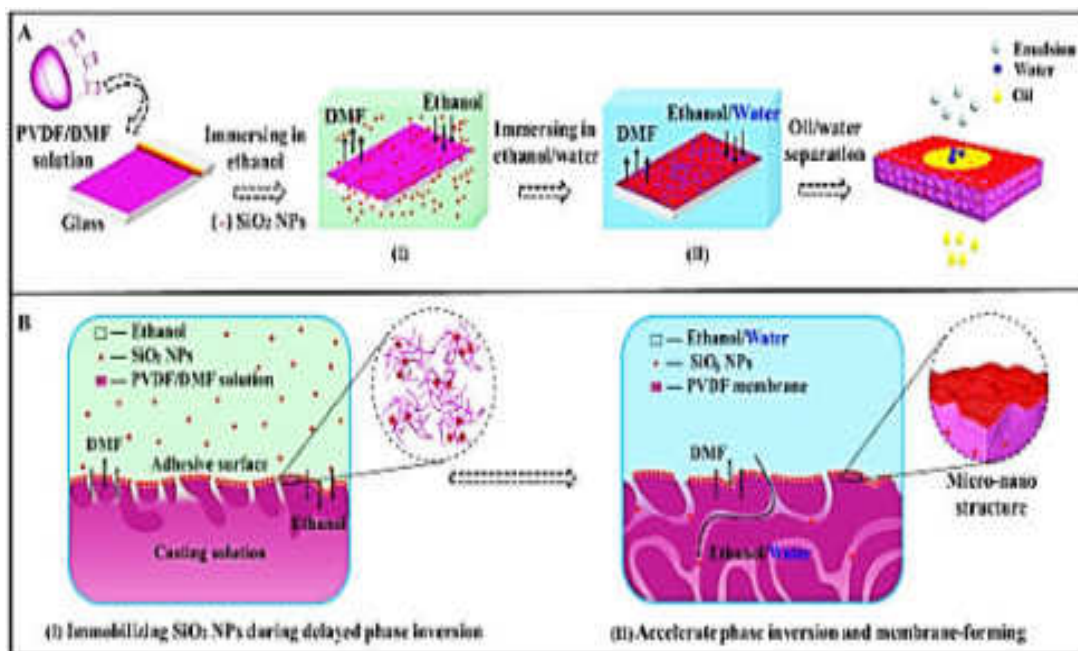


Figure-7. Schematic illustration (A) and structural evolution (B) for the formation of adhesive-free superhydrophobic SiO₂ nanoparticles decorated PVDF oil-water separation membranes [29]. Images reprinted from [29], with permission from Elsevier, Copyright 2018.

Bai et al. [30] have coated cotton fabric by sol-gel processed SiO₂. The as-prepared fabric was immersed in the solution of FeCl₃, thiophene and CH₂Cl₂ solution. Then, the modified fabric was washed with ethanol and dry it. **Figure-8** reveals the experimental procedure of preparation of superhydrophobic fabric. The modified fabric shows water contact angles above 160°. The strongest peak at 1050 cm⁻¹ belongs to the Si-O bond indicating that SiO₂ particles have been coated on the cotton fabric. The modified cotton fabric shows outstanding resistance to ultraviolet irradiation, high temperature, low temperature, organic solvent, immersion and excellent durability even after 8 months. The as-prepared fabric was showing the capability in various chemical exposures. It was showing good anti-dirt and anti-frost properties. The modified superhydrophobic cotton fabric was used as filter membrane for the gravity driven oil-water separation with high separation efficiency and excellent reusability. By using, this modified cotton fabric, both immiscible and emulsified oil-water mixtures could be separated. The efficient oil-water separation was also achieved under harsh conditions. The superhydrophobic fabric shows potential for the fast, coat-effective treatment of oil spill accidents and industrial oily sewage.

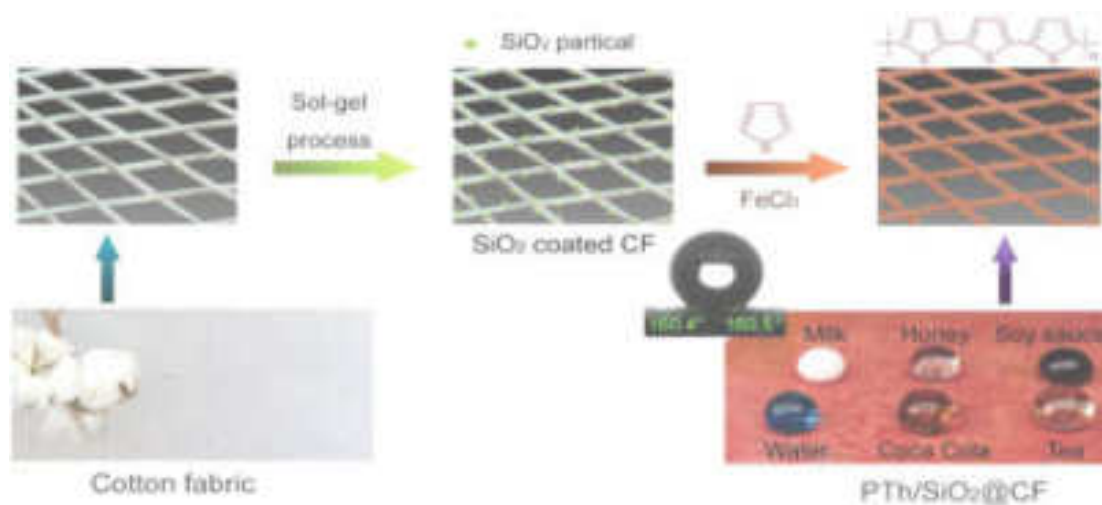


Figure-8. Schematic Illustration of the fabrication process of the PTh/SiO₂@CF [30]. Images reprinted from [30], with permission from Elsevier, Adv. Mater. Interfaces, Copyright 2021.

3. CONCLUSION

This review highlights, SiO₂ nanoparticles are unique, their fabrication requires little control of external parameters such as surface modification. It is very beneficial economically, facile and straightforward to synthesize. The SiO₂nanoparticles coated sponge/mesh has been developed by using SiO₂nanoparticles and different polymers. The absorption/separation investigation demonstrates that, the SiO₂surface is highly efficient and stable in absorbing a wide range of oil and organic solvents. It can be believed that, the SiO₂coated superhydrophobic materials are very useful for oil-water separation. It shows various tremendous results with SiO₂-polymer composite in various mechanical conditions. Hence this review is helpful to upcoming researchers to develop highly scalable superhydrophobic surfaces for efficient oil-water separation applications.

ACKNOWLEDGEMENT

This work was supported by Department of Chemistry and Department of Physics, Raje Ramrao Mahavidyalaya, Jath. We also acknowledge Prof. (Dr.) Suresh S. Patil, Principal, Raje Ramrao Mahavidyalaya, Jath.

REFERENCES

1. Alsbaiee A., Smith B. J., Xiao L., Ling Y., Helbling D. E. & Dichtel W. R. (2016) *Nature*, 529, 190-194.
2. Li Y., Zhang Z., Ge B., Men X., and Xue Q. (2016) *Green Chemistry*, 18, 5266-5272.
3. Ma Q., Cheng H., Fane A. G., Wang R., and Zhang H. (2016) *Small*, 12, 2186-2202.
4. Li L., Li B., Dong J., and Zhang J. (2016) *Journal of Materials Chemistry A*, 4, 13677–13725.
5. Yuan J., Liu X., Akbulut O., Hu J., Sui S. L., Kong J., Stellacci F. (2008) *Nature*, 3, 332-337.
6. Broje V., Keller A. A. (2006) *Environmental Science & Technology*, 40, 7914-7918.
7. Wu Z. Y., Li C., Liang H. W., Zhang Y. N., Wang X., Chen J. F. & Yu S. H. (2014) *Science Reports*, 4, 4079-4091.
8. Keshavarz A., Zilouei H., Abdol maleki A. (2015) *Journal of Environmental Management*, 157, 279-286.
9. Wang Z., Xu Y., Liu Y., Shao L. (2015) *Journal of Materials Chemistry A*, 3, 266-273.
10. Li J., Zhao Z., Kang R., Zhang Y., Lv W., Li M., Jia R., Luo L. (2017) *Journal of Sol-Gel Science and Technology*, 3, 817–826.
11. Keshavarz A., Zilouei H., Abdolmaleki A., Asadinezhad A. (2015) *Journal of Environmental Management*, 157, 279-286.
12. Sam E. K., Sam D. K., Lv X., Liu B., Xiao X., Gong S., Yu W., Chen J., Liu J. (2019) *Chemical Engineering Journal*, 19, 1103-1109.
13. Jin M., Feng X., Xi J., Zhai J., Cho K., Feng L., Jiang L. (2005) *Macromolecular Rapid Communications*, 26, 1805-1818.
14. Yao T., Zhang Y., Xiao Y., Zhao P., Guo L., Yang H., Li F. (2016) *Journal of Molecular Liquids*, 218, 611–614.
15. Gao Y., Zhou Y. S., Xiong W., Wang M., Fan L., Golgir H. R., Jiang L., Hou W., Huang X., Jiang L., Silvain J. F., Lu Y. F. (2014) *ACS Applied Materials & Interfaces*, 6, 5924–5929.
16. Erbil H. Y., Demirel A. L., Avcı Y., Mert O. (2003) *Science*, 299, 1377-1391.

17. Fard A. K., Mckay G., Manawi Y., Malaibari Z., Hussien M. A. (2016) *Chemsphere*, 164, 142-155.
18. Ren G., Song Y., Li X., Zhou Y., Zhang Z., Zhu X. (2018) *Applied Surface Science*, 428, 520-525.
19. Gu J., Xiao P., Chen J., Liu F., Huang Y., Li G., Zhang J., Chen T. (2014) *Journal of Materials Chemistry A*, 2, 15268–15272.
20. Li J., Kang R., Tang X., She H., Yang Y., Zha F. (2016) *Nanoscale*, 8, 7638–7645.
21. Gao Y., Zhou Y. S., Xiong W., Wang M., Fan L., Golgir H. R., Jiang L., Hou W., Huang X., Jiang L., Silvain J. F., Lu Y. F. (2014) *ACS Applied Materials & Interfaces*, 6, 5924–5929.
22. Li J., Zhao Z., Kang R., Zhang Y., Li M. (2017) *Journal of Sol-Gel Science and Technology*, 83, 817-826.
23. Zhang R., Zhou Z., Ge W., Lu Y., Liu T., Yang W., Dai J. (2020) *Chinese Journal of Chemical Engineering*, 5, 30292-30310.
24. Liu D., Yu Y., Chen X., Zheng Y. (2017) *RSC Advances*, 7, 12908–12915.
25. Zhao L., Du Z., Tai X., Ma Y. (2021) *Colloids and Surfaces A: Physicochemical and Engineering Aspects*, 623, 126404-126415.
26. Xiong W., Li L., Qiao F., Chen J., Chen Z., Zhou X., Hu K., Zhao X., Xie Y. (2021) *Journal of Colloid and Interface Science*, 6, 118–126.
27. Gu J., Xiao P., Chen J., Liu F., Huang Y., Li G., Zhang J., Chen T. (2014) *Journal of Materials Chemistry A*, 2, 15268–15272.
28. Wei C., Deu F., Lin L., An Z., He Y., Chen X., Chen L., Zhao Y. (2018) *Journal of Membrane Science*, 555, 220-228.
29. Li X., Wang X., Yuan Y., Wu M., Wu Q., Liu J., Yang J., Zhang J. (2021) *European Polymer Journal*, 159, 110729-110742.
30. Bai W., Lin H., Chen K., Zeng R., Lin Y., Xu Y. (2021) *Advanced Materials Interfaces*, 254, 725-740.

A REVIEW ON SUPERHYDROPHOBIC SURFACES: FUNDAMENTALS, FABRICATIONS AND APPLICATIONS

Mehejbin R. Mujawar¹, Rajesh B. Sawant¹, Deepak A. Kumbhar², Ankush M. Sargar³,
Shivaji R. Kulal¹

ABSTRACT

Superhydrophobic surfaces are highly hydrophobic i.e., it extremely difficult to wet. Superhydrophobic surfaces are the tendency to repel water drops and absorb oil drops. The water contact angle of superhydrophobic surfaces is greater than 150° , the oil contact angle is less than 5° , and the sliding angle is less than 5° . It is showing the lotus effect. Super hydrophobicity is observed in the lotus leaves, insects, and some other plants in which their leaves would not get wet. This phenomenon is due to the unique surface structure of the lotus leaf and also the presence of a low surface energy material on the surface of the leaf. For the formation of a superhydrophobic surface, the surface must show hierarchical micro- and nano-roughness and low surface energy. Efforts have been taken to form superhydrophobic surfaces for a variety of applications. There are many applications of superhydrophobic surfaces such as self-cleaning surfaces, oil-water separation surfaces, anti-icing surfaces, anti-corrosion surfaces, anti-fogging surfaces, and water-resistant surfaces. In this article, the fundamental principles of superhydrophobic surfaces, some recent trends in the fabrication of superhydrophobic surfaces, and their applications are reviewed and discussed.

Keywords: Super hydrophobicity, Superoleophobicity, Lotus effect, Self-cleaning, Anti-icing.

1 Department of Chemistry, Raje Ramrao Mahavidyalaya, Jath, Dist. - Sangli (MS) India

2 Department of Chemistry, Dattajirao Kadam Arts, Science and Commerce College, Ichalkaranji, Dist. - Kolhapur (MS) India.

3 Department of Chemistry, Bharati Vidyapeeth's Dr. Patangrao Kadam Mahavidyalaya, Sangli, Dist. - Sangli (MS) India

INTRODUCTION:

Many plants and insects are water-repellent due to their hydrophobic surface with microscopic roughness. These surfaces show self-adhesive properties against particulate contamination. This mechanism is like the Lotus effect which is the most important function of many microstructures and biological surfaces. Barthlott et. al. discovers the Lotus effect; two things caused the leaf surface to be superhydrophobic: one a waxy material and the second numerous microscopic bumps. The hydrophobic nature of the waxy surface shows high contact angle. The microscopic bumps show the hydrophobic surface to behave superhydrophobic surface. The air trapped between the spaces of microscopic bumps increases the water contact angle to greater than 160°. Due to the greater water contact angle, the drop of water becomes nearly spherical and rolls across the leaf [1-6]. Lotus leaf plant is not only single plants that exhibit superhydrophobic surface but also different insects and plants that show superhydrophobic surfaces [7-9]. Some of them are shown in figure 1 and the water contact angle of some plants and insects are shown in Table 1.

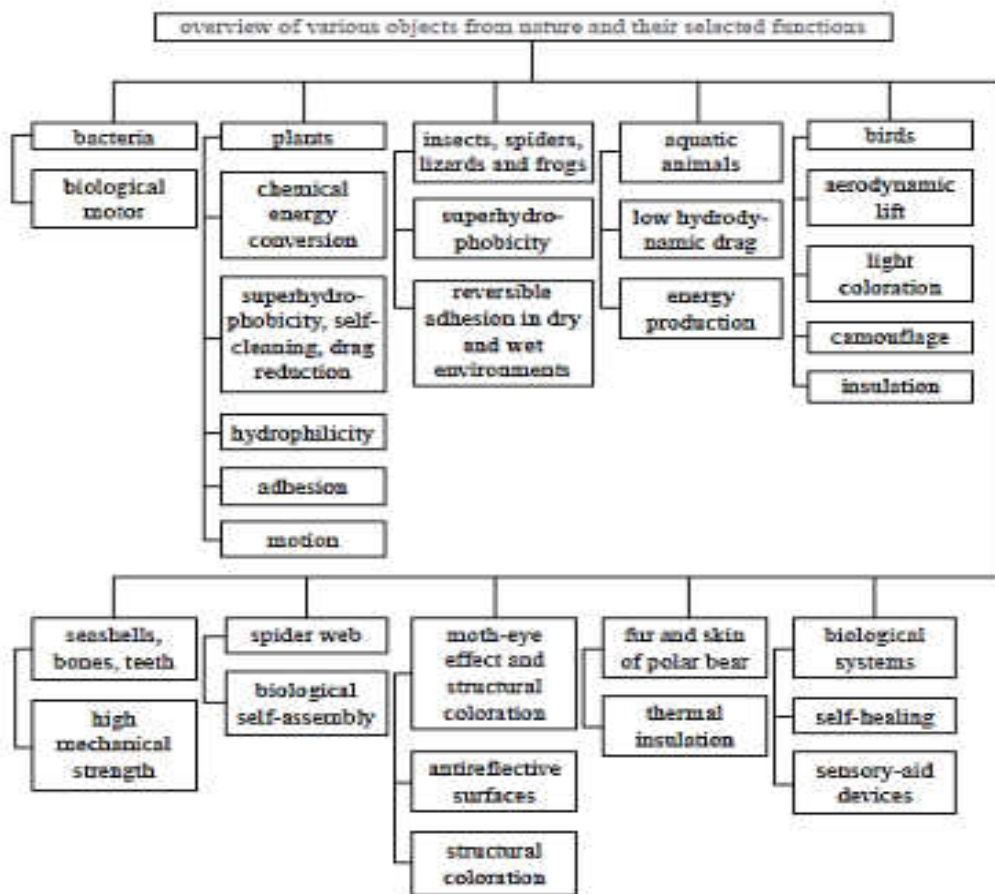


Figure 1. Schematic illustration of an overview of various objects from nature and their selected functions. Images reprinted from [10], with permission from Phil. Trans. R. Soc. A, Copyright 2009.

Table 1: Water contact angles of some plants and insects

Plant Name	Contact angle (°)
Purple setcreasea	167
Ramee leaf	164
Taro plant leaf	164
Perfoliate knotweed	162
Leymus arenarius leaf	161
Chinese watermelon	159
Rice leaf	157
Indian Cress	140
Insect Name	Contact angle (°)
Water striders	167.6
Homoptera	165
Diptera Tabanus Chrysurus	156

Efforts have been taken in the form of artificial superhydrophobic surfaces. The artificial superhydrophobic surfaces for a variety of applications, such as anti-fogging mirrors and displays, water-resistant fabrics, anti-icing, self-cleaning windows and panels, Superdry surfaces, corrosion-resistant surfaces, drag reduction, anti-reflection, water-resistant concrete, and walls, etc [11-15]. Based on contact angle and wetting behavior, the solid surfaces are classified into four different types: (i) superhydrophobic, if the water contact angle is less than 10° , (ii) hydrophilic if the water contact angle is between 10° and 90° , (iii) hydrophobic if the water contact angle is between 90° and 150° , and (iv) superhydrophilic if the water contact angle is above 150° as shown in figure 2 [16-17].

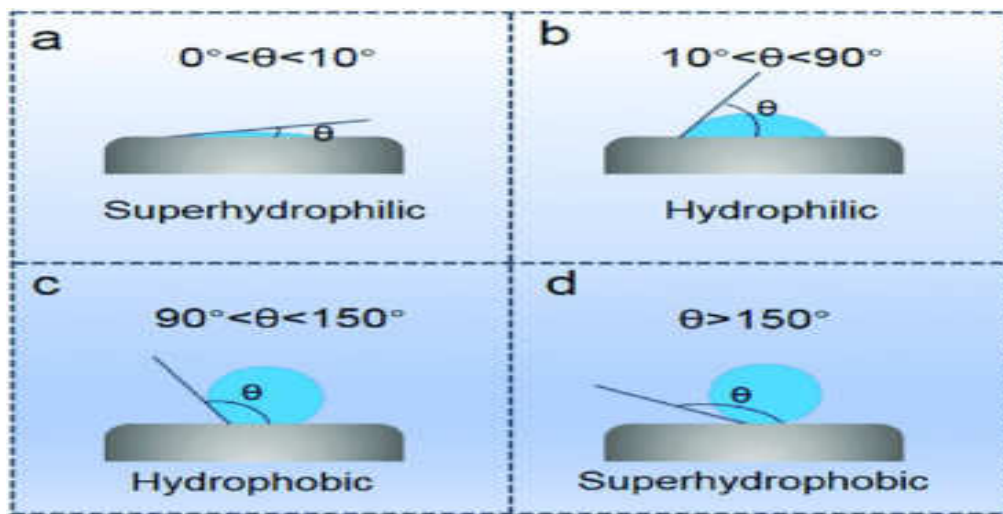


Figure 2. Schematic illustration of (a) superhydrophilic, (b) hydrophilic, (c) hydrophobic, and (d) superhydrophobic surfaces with different wetting/non-wetting states. Images reprinted from [17], with permission from New J. Chem, Copyright 2021.

2. Fundamentals of superhydrophobic surfaces

Thomas Young formulated the basic law from which the shape of a water drop on a solid surface can be determined. From Young's Model, small drop sizes, it is clear that the contact angle is sufficient for determining the shape of the water drop and wettability [18-19]. The required condition for a drop to spread is the energy to create a solid-vapor interface should be greater than that of a liquid-vapor interface. If this condition is not satisfied, the drop does not spread and a contact angle exists. The contact angle should be less than 90° for the wetting property and the contact angle should be greater than 90° for repelling property. If the contact angle is less than 90° , the surface becomes hydrophilic while if the contact angle is greater than 90° , the surface becomes hydrophobic. If the contact angle is reduced to a value less than 90° , the hydrophilicity increases, and the surface wets readily. If the contact angle increases i.e., greater than 90° then the hydrophobicity also increases and the surface is water-repellent. The contact angle for a completely hydrophobic spherical drop is 180° and for a completely hydrophilic wet surface is 0° . Since Young's Model applies to smooth surfaces not to rough surfaces as shown in figure 3 [20-21].

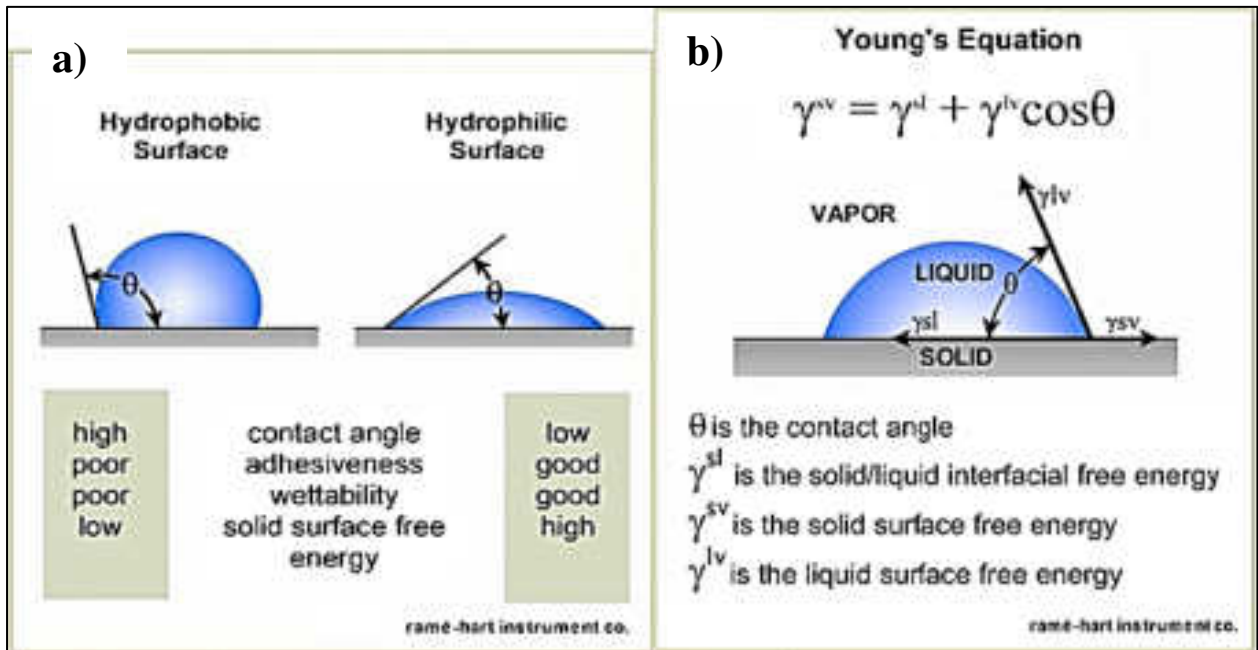


Figure 3. a) Contact angle of hydrophobic and hydrophilic surfaces b) Young's equation correlating contact angle to surface energies (Reprinted with permission from Rame-hart Instrument Co.)

In reality, the solid surfaces are rough. The relation between roughness and contact angle was explained by Wenzel Model. Wenzel modified young's model by introducing the term, roughness factor. It is important to note that the contact angle is applicable only for smooth surfaces whereas the apparent contact angle is applied for rough surfaces. According to the Wenzel model, solid-liquid and solid-vapor interfacial surface tensions are slightly increased due to increased rough surface area, and liquid-air interfacial surface tensions as shown in figure 4.

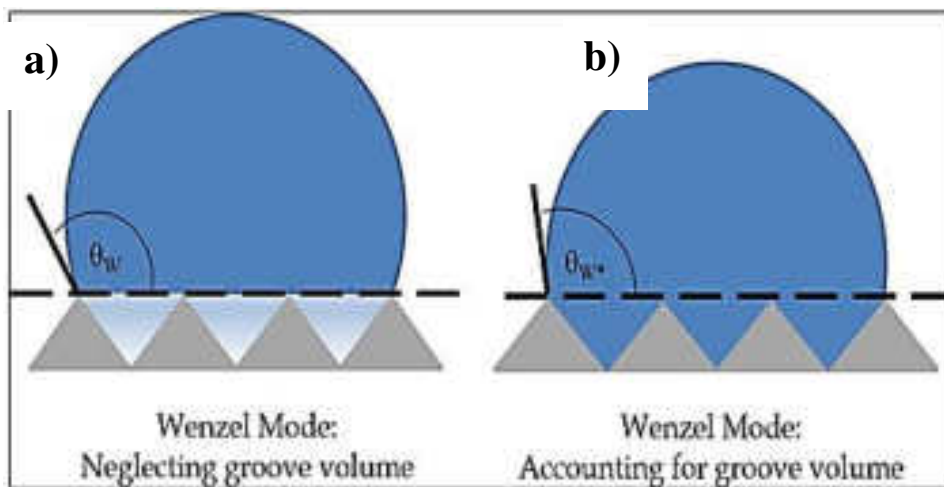


Figure 4. Schematic illustration of (a) Wenzel Mode: Neglecting groove volume (b) Wenzel Mode: Accounting for groove volume. Images reprinted from [23], with permission from ACS Omega, Copyright 2020.

The work of the Wenzel model was extended by Cassie and Baxter for porous surfaces. When the surface roughness is higher, the liquid doesn't need to fill the complete solid surface. The liquid contacts only the peaks of the surface and does not enter into the valleys as shown in figure 5. A mass fraction of liquid contacts with the peaks of the solid surface making a solid-liquid interface. An important observation is shown between the Wenzel model and the Cassie-Baxter model. In the Wenzel model, the drop of liquid contacts the completely rough solid surface without the presence of air. Since the contact is greater the movement of the drop is difficult across the solid surface. Cassie-Baxter model, the drop of liquid does not make complete contact with the surface due to the presence of air. If the Cassie-Baxter state the drop of liquid can easily roll across the solid surface. The Cassie-Baxter model is highly preferred over the Wenzel model to obtain superhydrophobic surfaces [24-25].

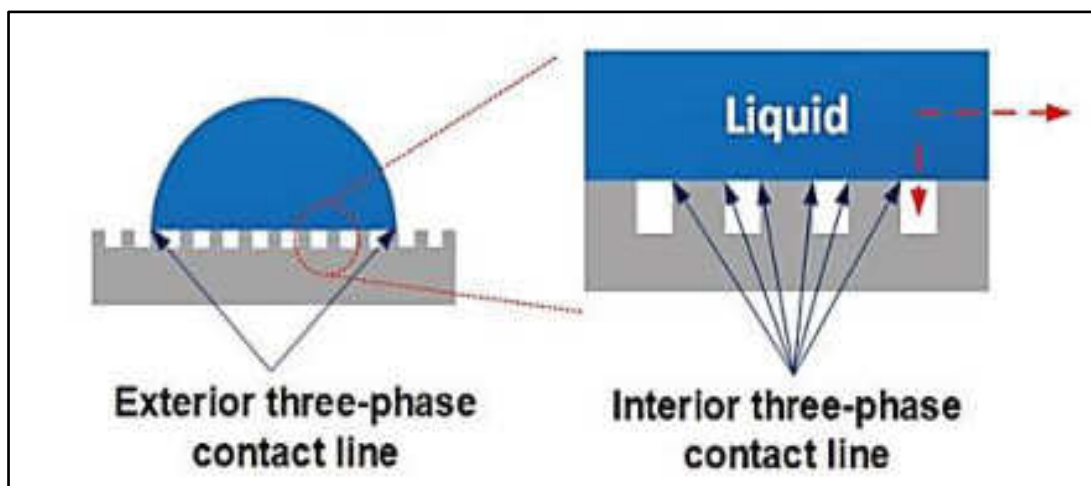


Figure 5. Schematic illustration of the existence of exterior and interior three-phase contact lines for Cassie-Baxter wetting configurations. The red dotted arrow represents the possible direction of droplet movement in response to the supply of external energy. Images reprinted from [24], with permission from Adv. Mater. Interface, Copyright 2019.

3. Fabrication of superhydrophobic surfaces

3.1. Natural Superhydrophobic Surfaces

Number of superhydrophobic surfaces examples are found in nature. One of the most well-known examples is lotus leaf, it shows high resolution scanning electron microscopy (SEM). The lotus leaf shows that the surface contains randomly distributed bumps at a scale of 5-10 μm and hairy nanostructures with a typical diameter of 100-200 nm as shown in figure 6 [26]. This complex surface consisting of micro- and nano-scale hierarchical structures amplify the hydrophobicity of the wax film at the leaf surface to attain a water contact angle of 150° –

160° and a sliding angle lower than ~2°. The leaf surface can always be kept clean to maximize the uptake of sun light. Other plants with superhydrophobic leaves include eucalyptus, tulipa, asphodelus, drosera, iris, euphorbia and gingko biloba [27].

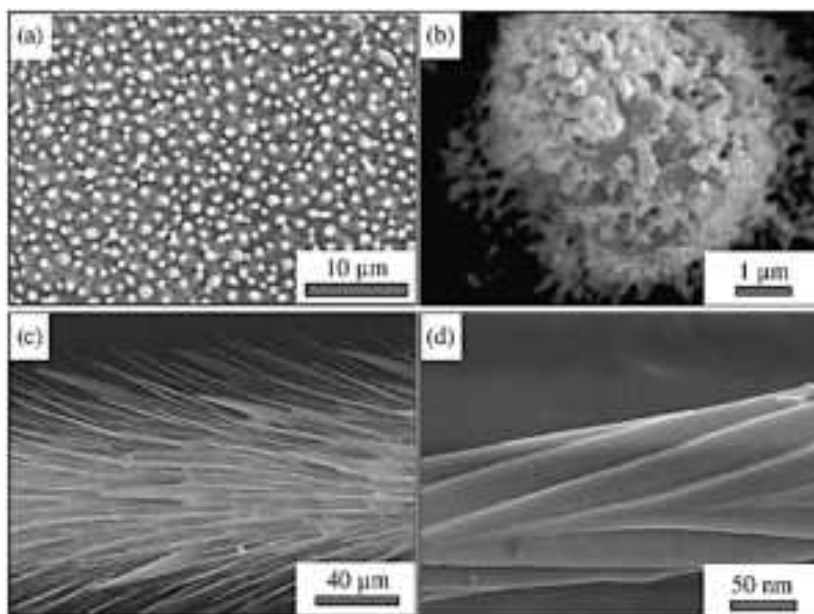


Figure 6. SEM images of naturally superhydrophobic surfaces: (a, b) lotus leaf and (c, d) water strider leg. Images reprinted with permission from Wiley Inter Science, Copyright 2002 [26].

3.2 Synthetic Superhydrophobic Surfaces

The key theme of all the examples found in nature is that hydrophobicity is amplified to superhydrophobicity surface. These surfaces consist of micro- and nano-scale hierarchical structures (Fig. 6) [26, 27]. This roughness is necessary for both high water contact angle and low sliding angle [28]. Depends on these principles, various synthetic approaches have been developed for preparation of superhydrophobic surfaces as shown in figure 7 [29]. The superhydrophobic fabrics formed by dipping textiles in a toluene solution of 4 wt.% methyl silicone followed by drying at 100°C. The fabrics processed water contact angles higher than 150°.

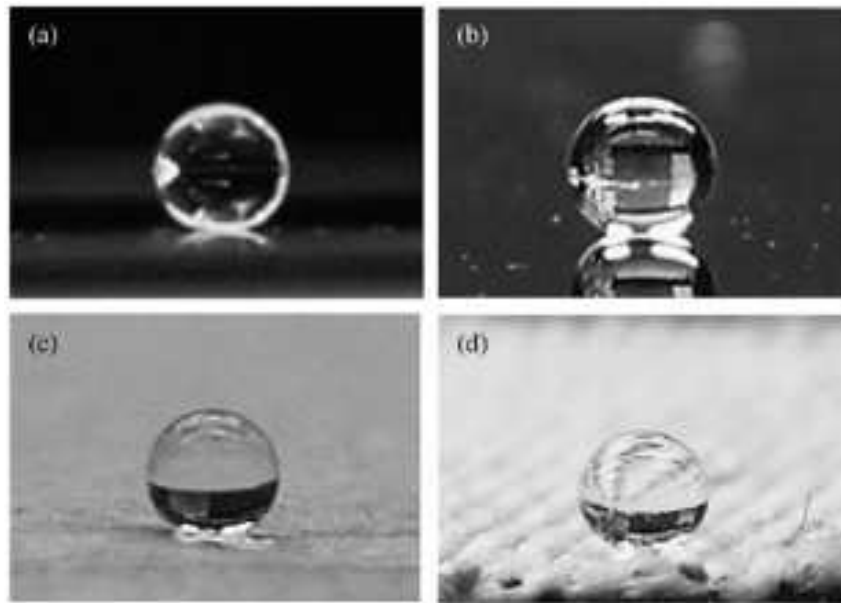


Figure 7. Optical images of water droplets on a superhydrophobic coating deposited on (a) gold film, (b) Si wafer, (c) Kimwipe tissue and (d) cotton. Images reprinted with permission from American Chemical Society, Copyright 2005 [29].

4. Applications of Superhydrophobic Surfaces:

The application of the superhydrophobic surfaces can be classified as shown in Figure 8. There are different materials used for formation of superhydrophobic surfaces, such as glass, polymers, metals, composites and micro- and nanoparticles, are fabricated by using various techniques to generate superhydrophobic surfaces. The superhydrophobic surfaces is formed by the functional requirements related to some of the fields, such as aerospace, automotive, medical devices, nuclear reactors, textiles, marine applications, clinical diagnostics and sensing, as shown in Figure 8.

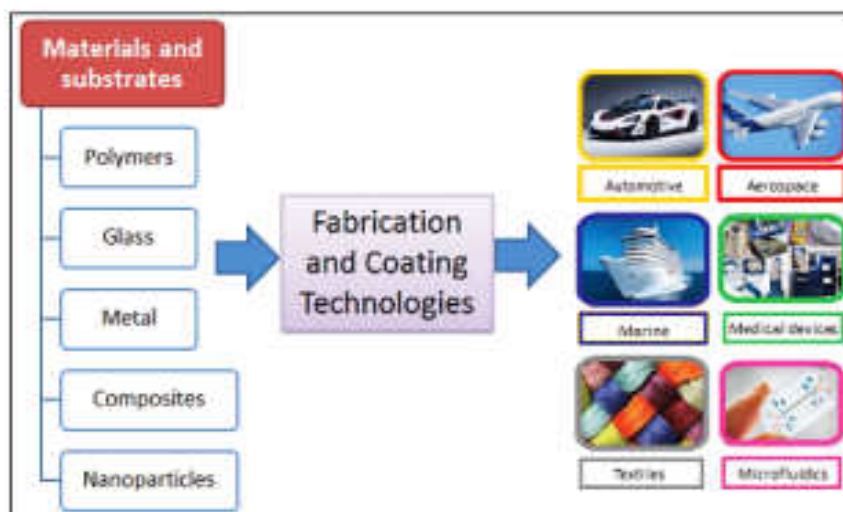


Figure 8. Application landscape of superhydrophobic surfaces. Images reprinted with permission from Journal of Micromanufacturing, Copyright 2019 [30].

4.1 Anti-icing:

Icephobicity is one of the examples of superhydrophobicity, e.g., ice adhesive may modify the effective shape of the aircrafts. So, icing affects the reliability of aircrafts. Superhydrophobic coating prevent the formation of ice as shown in figure 9. From figure 9, it is seen that, the uncoated aluminium plate gets iced, while the composite coated plate remained ice free. The anti-icing essential for aircraft applications, ships, wind turbines, refrigerators, air-conditioners, etc.

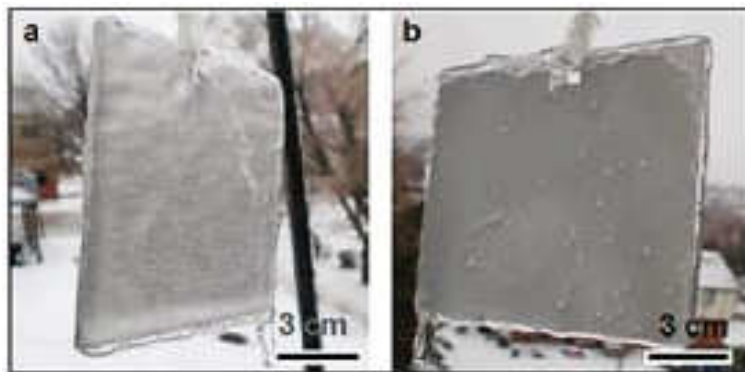


Figure 9. Testing of the anti-icing properties of a superhydrophobic surface in the ‘freezing rain’: (a) untreated side of an aluminium plate and (b) the aluminium plate coated with the superhydrophobic composites, after the rain. Images reprinted with permission from Langmuir, Copyright 2009 [31].

4.2 Self-cleaning superhydrophobic surfaces:

The self-cleaning superhydrophobic surfaces are combination of superhydrophobicity and photocatalytic behaviour to break down the dirt and wash it away from the surface. There are many superhydrophobic surfaces which are synthesized with different methods and used in industries. The self-cleaning superhydrophobic surfaces are extremely dry and repel water drops. These surfaces are not clean themselves but when the water drops roll on it they wash the dirt from the surface as shown in the figure 10.

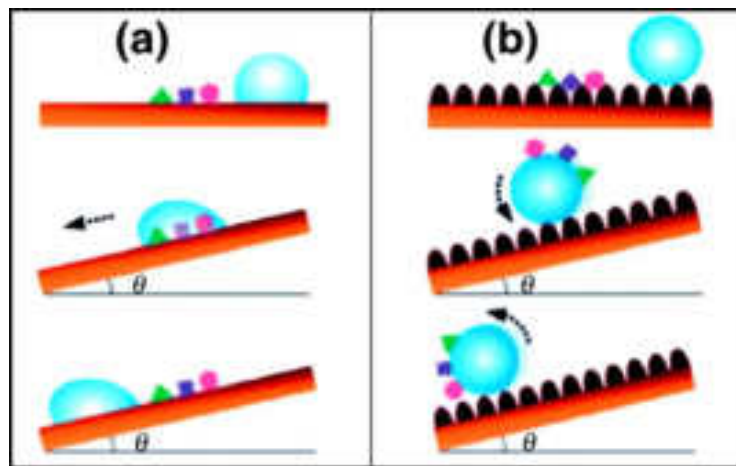


Figure 10. Schematic representation of (a) a smooth surface without self-cleaning properties and (b) a superhydrophobic surfaces with self-cleaning properties. Images reprinted with permission from Journal of Materials Chemistry A, Copyright 2013 [32].

4.3 Oil-water separation:

Superhydrophobic surfaces are also used for the separation of various oils from the water. In the oil-water separation filtration method is used, the oil-water mixture is pouring on the superhydrophobic surfaces the oil separated out easily from the oil-water mixture. The superhydrophobic surfaces are water repellent and oil absorbent. For the absorption process, the superhydrophobic surface is dipped in the oil-water mixture. Due to superhydrophobic nature of surface, it will repel water while absorbing the dispersed oil from oil-water mixture, so it is helpful to separate oil and water from oil-water mixture effectively as shown in figure 11 [33].

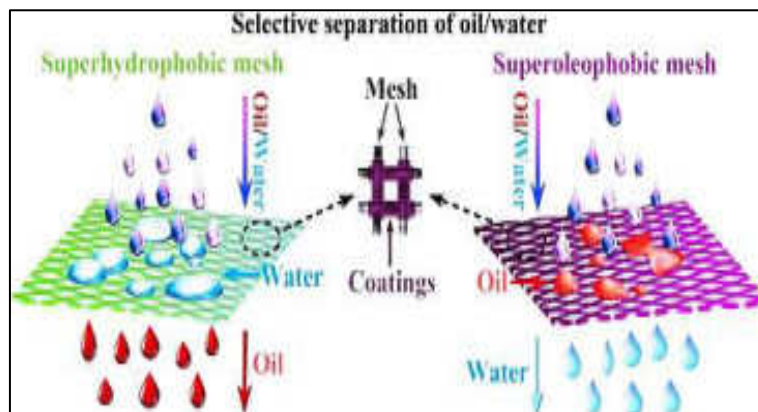


Figure 11. Separation of oil and water from oil-water mixture with superhydrophobic mesh. Images reprinted with permission from Advances in Colloid and Interface Science, Copyright 2016 [33].

5. CONCLUSION

In this article, the fundamentals of superhydrophobic surfaces, fabrication of superhydrophobic surfaces and the applications of superhydrophobic surfaces were reviewed and discussed. The natural and synthetic superhydrophobic surfaces are shows strong water repellent surfaces that shows the excellent superhydrophobicity capacity. There are number of fabrication methods used for producing a superhydrophobic surface with robustness surface, mechanically durable and stable. Self-cleaning property is one the most important function of superhydrophobic surfaces, it shows optical transparency, superoleophobicity, anti-biofouling, anti-icing and low cost coating. Superhydrophobic surfaces have vast use in industry.

REFERENCES:

1. W. Barthlott, C. Neinhuis, "Purity of the sacred lotus, or escape from contamination in biological surfaces" *Self-cleaning of biological surfaces*, 202 (1997) 1-8.
2. Chee Huei Lee, Nick Johnson, Jaroslaw Drelich, Yoke Khin Yap, "The performance of superhydrophobic and superoleophilic carbon nanotube meshes in water–oil filtration" *CARBON*, 49 (2011) 669 – 676.
3. Michael J. Kreder, Jack Alvarenga, Philseok Kim and Joanna Aizenberg, "Design of anti-icing surfaces: smooth, textured or slippery?" *NATURE REVIEWS*, 1 (2016) 1-15.
4. Juliana Lasprilla-Botero, Sergio Torres-Giner, Maria Pardo-Figuerez, Mónica Álvarez-Láinez and Jose M. Lagaron, "Superhydrophobic Bilayer Coating Based on Annealed Electrospun Ultrathin Poly (ϵ -caprolactone) Fibers and Electrospayed Nanostructured Silica Microparticles for Easy Emptying Packaging Applications" *Coatings* 8 (2018) 1-15.
5. John T Simpson, Scott R Hunter and Tolga Aytug, "Superhydrophobic materials and coatings: a review" *Rep. Prog. Phys.* 78 (2015) 1-15.
6. Xuelin Tian, Tuukka Verho, Robin H. A. Ras, "Moving superhydrophobic surfaces toward real-world applications" *SCIENCE*, 352 (2016) 142-144.
7. Thierry Darmanin, Elisabeth Taffi n de Givenchy, Sonia Amigoni, and Frederic Guittard, "Superhydrophobic Surfaces by Electrochemical Processes" *Adv. Mater.*, 25 (2013) 1378–1394.

8. H.B. Eral, D.J.C.M.'t Mannetje and J.M. Oh, "Contact angle hysteresis: A review of fundamentals and applications" *Colloid Polym. Sci.*, 291 (2013) 247–260.
9. Shuhui Li, Jianying Huang, Zhong Chen, Guoqiang Chen and Yuekun Lai, "Review on special wettability textiles: theoretical models, fabrication technologies and multifunctional applications" *Journal of Materials Chemistry A*, 13 (2013) 1-21.
10. Bharat Bhushan, "Biomimetics: lessons from nature-an overview" *Phil. Trans. R. Soc. A*, 367 (2009) 1445–1486.
11. L. B. Boinovich, "Superhydrophobic Coatings as a New Class of Polyfunctional Materials" *Herald of The Russian Academy of Sciences*, 83 (2013) 1-11.
12. Yang-Tse Cheng, "Is the lotus leaf superhydrophobic?" *Applied Physics Letters*, 86 (2005) 144101-4.
13. Shunsuke Nishimoto and Bharat Bhushan, "Bioinspired self-cleaning surfaces with superhydrophobicity, superoleophobicity, and superhydrophilicity" *The Royal Society of Chemistry*, (2012) 1-13.
14. Kerstin Koch and Wilhelm Barthlott, "Superhydrophobic and superhydrophilic plant surfaces: an inspiration for biomimetic materials" *Phil. Trans. R. Soc. A* 367 (2009) 1487–1509.
15. Kesong Liu and Lei Jiang, "Bio-Inspired Self-Cleaning Surfaces" *Annu. Rev. Mater. Res.* 42 (2012) 231–63.
16. V. Anand Ganesh, Hemant Kumar Raut, A. Sreekumaran Nair and Seeram Ramakrishna, "A review on self-cleaning coatings" *J. Mater. Chem.*, 21 (2011) 16304–16322.
17. Binbin Zhang and Weichen Xu, "Superhydrophobic, superamphiphobic and SLIPS materials as anti-corrosion and antibiofouling barriers" *New J. Chem.*, 45 (2021) 15170–15179.
18. Colin R. Crick and Ivan P. Parkin, "Preparation and Characterisation of Superhydrophobic Surfaces" *Chem. Eur. J.* 16 (2010) 3568 – 3588.
19. Xiao-Song Wang, Shu-Wen Cuie, Long Zhou, Sheng-Hua Xu, Zhi-Wei Sun & Ru-Zeng Zhu, "A generalized Young's equation for contact angles of droplets on homogeneous and rough substrates" *Journal of Adhesion Science and Technology*, 28 (2014)161–170.

20. Tania Dey and Daragh Naughton, “Cleaning and anti-reflective (AR) hydrophobic coating of glass surface: a review from materials science perspective” *J Sol-Gel Sci Technol*, (2015) 1-27.
21. Peng Wang, Mingji Chen, Huilong Han, Xiaoliang Fan, Qing Liu, and Jinfeng Wang, “Transparent and abrasion-resistant superhydrophobic coating with robust self-cleaning function in either air or oil” *J. Name.*, (2013) 1-3.
22. Junlong Song and Orlando J. Rojas, “Approaching super-hydrophobicity from cellulosic materials: A Review” *Nordic Pulp & Paper Research Journal*, 28 (2013) 216-238.
23. Michael S. Bell and Ali Borhan, “A Volume-Corrected Wenzel Model” *ACS Omega* 5 (2020) 8875–8884.
24. Chun Haow Kung, Pradeep Kumar Sow, Beniamin Zahiri, and Walter Mérida, “Assessment and Interpretation of Surface Wettability Based on Sessile Droplet Contact Angle Measurement: Challenges and Opportunities” *Adv. Mater. Interfaces* 1900839 (2019) 1-27.
25. Bharat Bhushan and Yong Chae Jung, “Natural and biomimetic artificial surfaces for superhydrophobicity, self-cleaning, low adhesion, and drag reduction” *Progress in Materials Science* 56 (2011) 1–108.
26. Lin Feng, Shuhong Li, Yingshan Li, Huanjun Li, Lingjaun Zhang, Jin Zhai, Yanlin Song, “Super-hydrophobic Surfaces: From Natural to Artificial” *Adv. Mater.* 14 (2002) 1857-1860.
27. Woo Lee, Mi-Kyoung Jin, Won-Cheol Yoo, and Jin-Kyu Lee, “Nanostructuring of a Polymeric Substrate with Well-Defined Nanometer-Scale Topography and Tailored Surface Wettability” *Langmuir* 20 (2004) 7665-7669.
28. Lichao Gao and Thomas J. McCarthy, “Contact Angle Hysteresis Explained” *Langmuir* 22 (2006) 6234-6237.
29. Seong H. Kim, Jeong-Hoon Kim, Bang-Kwon Kang, and Han S. Uhm, “Superhydrophobic CF_x Coating via In-Line Atmospheric RF Plasma of He-CF₄-H₂” *Langmuir* 21 (2005) 12213-12217.
30. Kapil Manoharan and Shantanu Bhattacharya, “Superhydrophobic surfaces review: Functional application, fabrication techniques and limitations” *Journal of Micromanufacturing*, 2 (2019) 59–78.

31. Liangliang Cao, Andrew K. Jones, Vinod K. Sikka, Jianzhong Wu, and Di Gao, “Anti-Icing Superhydrophobic Coatings” *Langmuir* 25 (2009) 12444–12448.
32. Mehdi Khodaei, “Introductory Chapter: Superhydrophobic Surfaces- Introduction and Applications” *Superhydrophobic Surfaces - Fabrications to Practical Applications* (2019) 1-11.
33. Yuanlie Yu, Hua Chen, Yun Liu, Vincent S.J. Craig, Zhiping Lai, “Selective separation of oil and water with mesh membranes by capillarity” *Advances in Colloid and Interface Science* (2016) 1-10.



Superhydrophobic PVC/SiO₂ Coating for Self-Cleaning Application

Rajaram S. Sutar, Prashant J. Kalel, **Sanjay S. Latthe**, Deepak A. Kumbhar, Smita S. Mahajan, Prashant P. Chikode, Swati S. Patil, Sunita S. Kadam, V. H. Gaikwad, Appasaheb K. Bhosale, Kishor Kumar Sadasivuni, Shanhu Liu,* and Ruimin Xing*

A lotus leaf like self-cleaning superhydrophobic coating has high demand in industrial applications. Such coatings are prepared by alternative dip and spray deposition techniques. A layer of polyvinyl chloride is applied on glass substrate by dip coating and then spray coated a suspension of hydrophobic silica nanoparticles at substrate temperature of 50 °C. This coating procedure is repeated for three times to achieve rough surface morphology which exhibits a water contact angle of $169 \pm 2^\circ$ and sliding angle of 6° . The superhydrophobic state of the coating is still preserved when water volume of 1.2 L is used to impact the water drops on coating surface. The stability of the wetting state of the coating is analyzed against the water jet, adhesive tape and sandpaper abrasion tests. The prepared superhydrophobic coating strongly repelled the muddy water suggesting its importance in self-cleaning applications.

which inspired to create artificial superhydrophobic surface by increasing surface roughness along with decreasing surface energy. Such superhydrophobic surfaces have numerous applications including self-cleaning, anti-corrosion, drag-reduction, oil-water separation, and etc.^[3–8] So far, SiO₂, TiO₂, ZnO, Al₂O₃, candle soot and various polymers have been used to fabricate self-cleaning superhydrophobic coatings.^[9–14] Among them, polymer/SiO₂ nanocomposite is a promising in preparation of self-cleaning superhydrophobic coatings.^[15,16]

The self-cleaning property of superhydrophobic coatings has attracted significant interest in industrial applications. Recently, Latthe et al. have applied suspension of hydrophobic SiO₂ nanoparticles

(NPs) on different types of substrates including body of motorcycle, building wall, mini boat, solar cell panel, window glass, cotton shirt, fabric shoes, cellulose paper, metal, wood, sponges, plastic, and marble which revealed high water repellency and excellent self-cleaning property.^[17] Many reports are available on the preparation of superhydrophobic polyvinyl chloride (PVC) thin films using ethanol.^[18–20] Seyfi et al. have drop casted a mixture of PVC, Ag₃PO₄, and ethanol on thermoplastic

1. Introduction

Lotus leaf is a perfect model of self-cleaning superhydrophobic surface with specific combination of surface chemistry (surface energy) and surface topography (surface roughness).^[1,2] A low surface energy hierarchical surface structure of lotus leaf surface revealed unusual wettability (water contact angle (WCA) greater than 150° and sliding angle less than 10°)

R. S. Sutar, P. J. Kalel, S. S. Latthe, S. Liu, R. Xing
Self-cleaning Research Laboratory
Department of Physics
Raje Ramrao College
Jath
Affiliated to Shivaji University
Kolhapur, Maharashtra 416404, India
E-mail: liushanhu@vip.henu.edu.cn; rmxing@henu.edu.cn

S. S. Latthe, A. K. Bhosale
Henan Key Laboratory of Polyoxometalate Chemistry
Henan Joint International Research Laboratory of Environmental
Pollution Control Materials
College of Chemistry and Chemical Engineering
Henan University
Kaifeng 475004 P. R. China

D. A. Kumbhar
Department of Chemistry
Raje Ramrao College
Jath Maharashtra 416404, India

DOI: 10.1002/masy.202000034

S. S. Mahajan, P. P. Chikode
Department of Physics
Jaysingpur College
Jaysingpur Maharashtra 416404, India

S. S. Patil
Department of Physics
ACS College
Palus Maharashtra 416404, India

S. S. Kadam
Department of Physics
KNP College
Walwa Maharashtra 416404, India

V. H. Gaikwad
School of Chemistry
MIT World Peace University, Kothrud
Pune Maharashtra 416404, India

K. K. Sadasivuni
Center for Advanced Materials
Qatar University
Doha 2713 Qatar

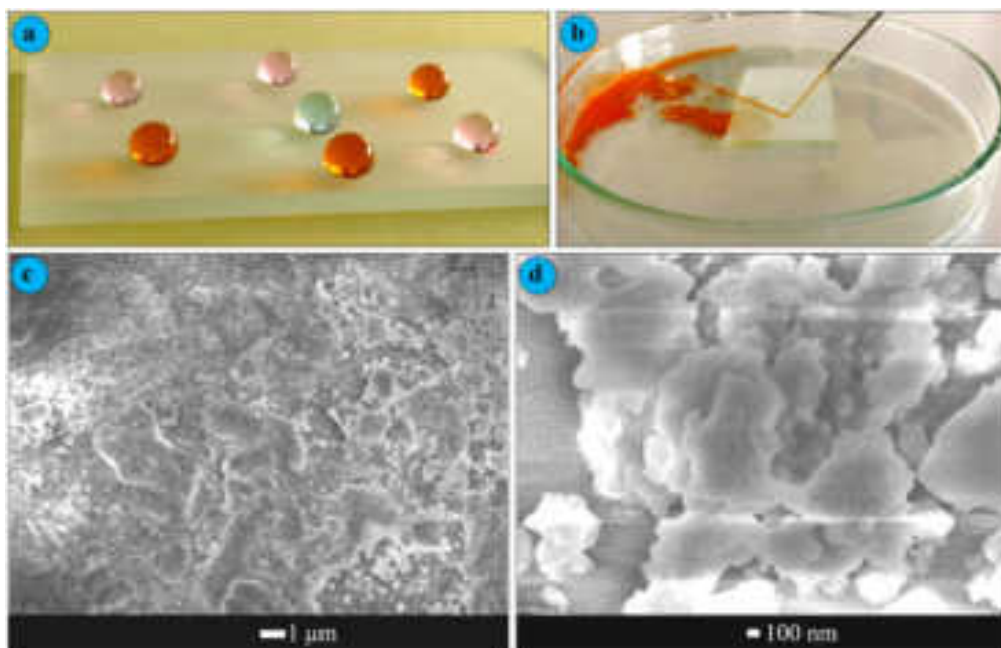


Figure 1. a) Optical photograph of color water drop on superhydrophobic coating, b) the image of water jet impacting on coating, c and d) different magnification SEM images of superhydrophobic coating.

polyurethane (TPU) substrate and achieved antibacterial superhydrophobic surface.^[21] The as prepared superhydrophobic TPU surface showed WCA $\approx 156^\circ$ and SA $\approx 2^\circ$ with self-cleaning performance. Also, Guo et al.^[15] have reported that water drops rolled off immediately on the coating prepared by casting of polymer (PVC, PMMA, and PE) and SiO₂ NPs composite on various substrates like copper, aluminum, stainless steel, silicon, glass and filter paper. Rivero et al.^[22] have prepared superhydrophobic surface by depositing ZnO NPs incorporated polystyrene (PS) and PVC polymeric solution on aluminum alloy substrate using the electrospinning technique. Yuan et al.^[23] have obtained lotus-leaf-like superhydrophobic PVC film by casting PVC solution on negative template of PDMS. Other than this, Zhang et al.^[24] have obtained superhydrophobic coating by pouring PVC/SiO₂ mixture on negative template of PDMS and reported that superhydrophobicity depends on weight percentage of SiO₂ particles in PVC. Chen et al.^[25] have prepared water-repellent SiO₂/polymer (PS and PVC) composite coating without any surface chemical modification by spin coating. The amount of hydrophobic SiO₂ NPs in PVC or PS affects the surface roughness and hence the wettability of the coating.

Herein, we have prepared superhydrophobic surface on glass by dip coating followed by spray coating method. The hydrophobic SiO₂ NPs were prepared by sol-gel technique. A thin layer of PVC was applied on glass substrate by dip coating and dried at room temperature. After that, a suspension of SiO₂ NPs in hexane was sprayed on PVC coated glass substrate at substrate temperature of 50 °C. The superhydrophobic coating was obtained by applying multiple alternative layers of PVC and SiO₂ NPs on glass substrate.

2. Result and Discussion

2.1. Surface Microstructure and Wettability

The multiple layers of PVC/SiO₂ were applied on glass substrate to obtain desired surface roughness which is the main requirement of extreme water repellency. **Figure 1c** represents the surface microstructure of three bilayer of PVC/SiO₂ coating, where the aggregated SiO₂ NPs were distributed on the PVC layer. The PVC layer can help SiO₂ NPs to adhere firmly on the coating surface. The aggregation of SiO₂ NPs is not uniform and the grain sizes from 5 μm to 100 nm were observed (**Figure 1d**). These different size scale grains provide hierarchical surface morphology. Nearly similar surface morphology was reported for the PVC/SiO₂ nanocomposite coating prepared by spin coat technique.^[25] This hierarchical surface morphology tends to trap small air pockets in the rough voids and hence a water drop can sit on the air-solid composite structure with minimum contact to the solid fraction of the surface. A water drop can only touch a small solid fraction of the coating, as the trapped air pushes away the water drops and not allowing the water drops to wet the inner portion of a rough surface. As shown in the **Figure 1a**, the water drops hardly stay on the three bilayer of PVC/SiO₂ superhydrophobic coating. Every water drop takes spherical shape at different positions on the coating surface confirming the uniform deposition of PVC/SiO₂ on the substrate. The superhydrophobic coating was appeared opaque due to the presence of micrometer scaled grains which allows scattering of the visible light. Also the water jet was impacted on the superhydrophobic coating which rebounds off the surface quickly after impacting (**Figure 1b**). The trapped air in the rough surface resists the water jet to invade the

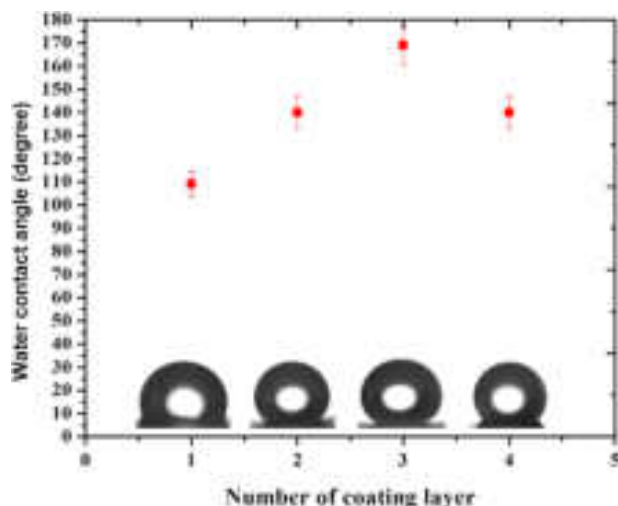


Figure 2. The variation of water contact angle with layer of polyvinyl chloride and SiO_2 particles.

rough structure. Also water jet rebounding confirms the robustness of the coating.

A systematic study was performed on the dependence of numbers of bilayers on the wettability of the coating (Figure 2). A first bilayer coating exhibited a WCA of $110 \pm 5^\circ$ confirming hydrophobic nature of the coating. The surface roughness of the coating is quite low to trap the air pockets and hence the wettability falls in the Wenzel's state^[26] where the solid fraction of the coating was partially wetted by the water drops. Though the WCA increased to $140 \pm 6^\circ$ with considerable decrease in solid-liquid contact area in case of two bilayer coating, the wettability was still in the Wenzel's wetting state. The WCA of $169 \pm 7^\circ$ and SA of 6° was observed for three bilayer coating confirming superhydrophobicity in Cassie-Baxter's wetting state.^[27] A water drop floats on the layer of air having minimum contact with solid fraction of the coating surface and hence readily roll off the surface. For next bilayer coatings, the WCA tends to decrease as a result of increase in thickness which creates visible cracks in the coatings during evaporation of solvent.

2.2. Durability Tests

The mechanical durability of superhydrophobic coating can be evaluated by water jet and water drop impact, sand paper abrasion and adhesive tape peeling test.^[28] Here, the water jet was developed by 15 mL syringe. The water jet was immediately spread on uncoated glass slide due to smooth surface structure with hydrophilic nature. On the other hand, the water jet bounced off the superhydrophobic coating as shown in Figure 1b. The air trapped hierarchical structure strongly avoids pinning of water jet on the surface.^[5,29] The wettability of the coating was checked after water jet impact study and the coating showed no change in its superhydrophobic property confirming its robustness. Water drop impact test was carried out by adjusting the distance between superhydrophobic coating and tip of tap about 10 cm as shown in schematic (Figure 3a). Nearly 2 L of water was dropped on the superhydrophobic coating inclined at 30° with drop falling rate

of 90 drops min^{-1} . The effect of water drop impact on the wetting properties of the superhydrophobic coating was estimated. The superhydrophobic state of the coating was intact for the impact of 1.2 L of the water as a result of stable air pockets in the rough microstructure of the coating which avoids water drop penetration inside the coating structure. However, the trapped air starts to evacuate from the rough structure and also the rough structure might have partly ruined due to continuous impact of water drops and as a result, WCA decreased to less than 140° for impacting 2.0 L of water (Figure 3b).

The adhesive tape peeling test was carried by using Cellotape No.405 having adhesiveness of 3.93 N/10 mm. A tape was applied firmly on the superhydrophobic coating with the help of 200 g weighted disk rolling back and forth on it (Figure 4a).^[28] After slowly peeling off the tape, some amount of the coating material was observed stacked on the adhesive tape; however, the coating showed the WCA of 165° (Figure 4b). The superhydrophobicity of the coating was found intact for two cycles of adhesive tape test, and then the WCA decreased to 80° for five cycles of adhesive tape test confirming the exhaustive loss of PVC/ SiO_2 from the coating (Figure 4c).

In large scale applications, superhydrophobic coatings can be damaged by scratch, rubbing and finger contact. To sustain the hierarchical micro/nanostructure and low surface energy of superhydrophobic coating under mechanical abrasion is one of the important issue. Here, the mechanical abrasion test was performed using sandpaper grit no. 400. The schematic of sandpaper abrasion process is illustrated in Figure 5a. A weight (100 g) was placed on superhydrophobic coating and dragged for 10 cm length on sandpaper at the average speed of 0.5 cm sec^{-1} . The effect of abrasion distance on the wettability of the superhydrophobic coating was studied (Figure 5b). The wettability of the coating was found in the superhydrophobic state for dragging the coating for nearly 30 cm on the sandpaper which confirms no significant loss in the surface roughness of the coating. However, the WCA decreased to 93° for dragging the coating for 60 cm on sandpaper confirming substantial damage to the coating.

2.3. Self-Cleaning Property

High water repellent property of the surface with low water sliding angle helps to keep the surface clean like a lotus leaf. In open air, many solid surfaces are contaminated by various types of dust particles. On superhydrophobic surface, spherical shaped water drop roll away easily by collecting dust particles, performing self-cleaning ability. The self-cleaning ability of the prepared superhydrophobic coating was tested by muddy water. The muddy water was prepared by dispersing fine particles of soil in water. This muddy water was poured on the superhydrophobic coating. In the process of pouring muddy water, it eventually get repelled off the superhydrophobic coating (Figure 6a–c). After pouring 50 mL of muddy water, surface becomes clean similar to lotus leaf (Figure 6c). This indicates prepared superhydrophobic coating was highly water repellent with excellent self-cleaning property.

3. Conclusions

We have used a conventional dip and spray coating techniques to prepare superhydrophobic coating by applying consecutive layers

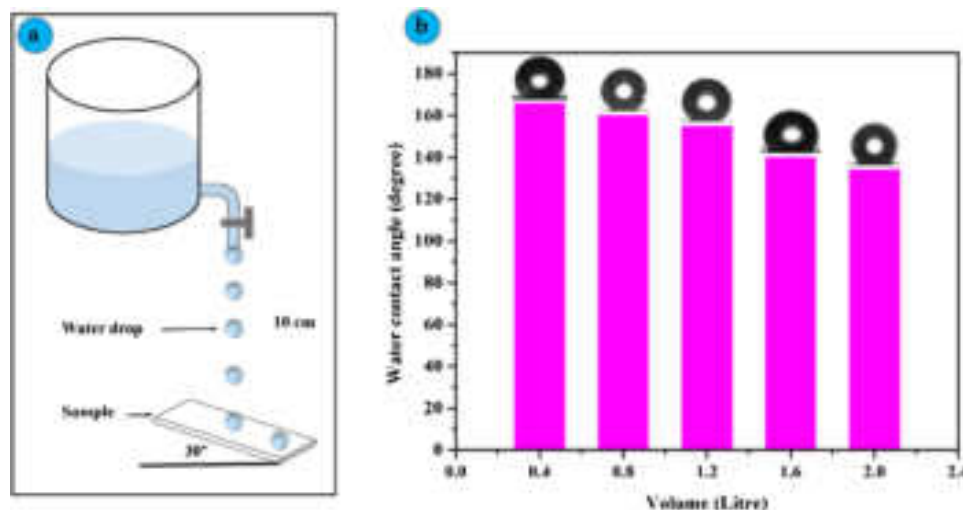


Figure 3. a) A schematic of water drop impact test, b) the effect of water drop impact on wettability of the superhydrophobic coating.

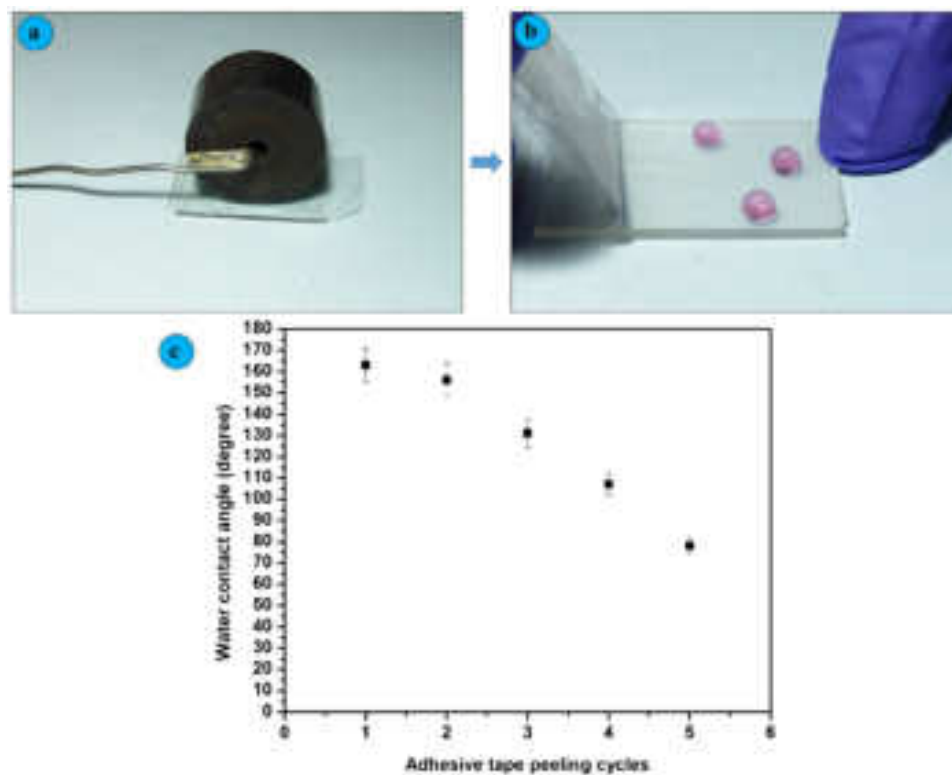


Figure 4. a) Rolling of 200 g weighted disc on adhesive tape placed on coating, b) adhesive tape peeling off and c) effect of adhesive tape peeling cycles on the wettability of the superhydrophobic coating.

of PVC and hydrophobic SiO₂ NPs on glass substrate. The hierarchical rough microstructure with different scaled grains of SiO₂ NPs was observed. The self-cleaning superhydrophobic coating with WCA of 169 ± 2° and sliding angle of 6° was achieved by applying three bilayers of alternate PVC followed by hydrophobic SiO₂ NPs. The water jet bouncing off the surface indicates the air pockets trapped in dual scale rough structure. After dripping the

water of volume 1.2 L, the water drop impacted coating showed invariable wettability. The superhydrophobic coatings were moderately stable against adhesive tape and sandpaper abrasion tests. Future practical applications of these coating can be found in windshields of vehicles, solar cell panels and windows of buildings, if their transparency and mechanical stability could be further enhanced.

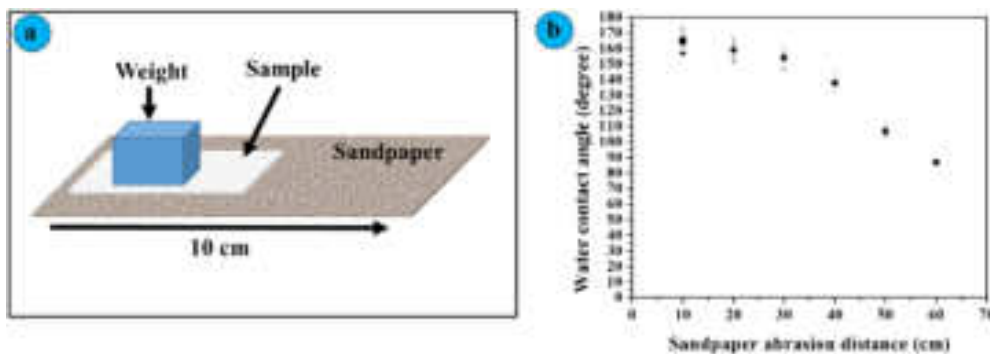


Figure 5. a) Schematic of sandpaper abrasion test and b) the variation of water contact angle with sandpaper abrasion distance.



Figure 6. a-c) Self-cleaning behavior of superhydrophobic coating.

4. Experimental Section

Materials: Methyltrimethoxysilane (MTMS) and PVC were purchased from Sigma-Aldrich, USA. Ethanol, methanol, ammonia solution, tetrahydrofuran (THF) and hexane were bought from Spectrochem PVT. LTD., India. Micro-Glass slides (75 × 25 × 1.35 mm) were obtained from Blue star, Polar Industrial Corporation, India.

Synthesis of Hydrophobic SiO₂ NPs: The hydrophobic SiO₂ NPs were synthesized using sol-gel method reported in literature.^[30] The mixture of 2 mL MTMS, 20 mL methanol and 4 mL distilled water was stirred for 20 min. After that ammonia solution was added dropwise and kept for stirring for 30 min. The prepared gel was aged for overnight and dried at 80°C for 5 h. The dried gel was grinded well using mortar and pestle to obtain fine powder of silica particles.

Preparation of Superhydrophobic Coating: At first, the glass substrates were ultrasonically cleaned with distilled water and ethanol for 30 min and dried at room temperature. The cleaned glass substrate was dipped in the PVC solution for 30 s. The solution was prepared by dissolving 100 mg PVC powder in 10 mL THF using magnetic stirrer (200 rpm for 30 min). A thin layer of PVC deposited glass substrate was dried at room temperature. A suspension of SiO₂ NPs (100 mg) was prepared by dispersing in 10 mL hexane and sprayed on PVC deposited glass substrate at substrate temperature of 50 °C. Finally PVC/SiO₂ deposited glass substrate was annealed at 100 °C for 1 h. In this way, one bilayer of PVC/SiO₂ was applied on glass substrate. This procedure was repeated to deposit two, three and four bilayers of PVC/SiO₂ on glass substrate.

Characterizations: The wettability of prepared coatings was evaluated by measuring WCA and sliding angle (SA) using contact angle meter (HO-IAD-CAM-01, Holmarc Opto-Mechatronics Pvt. Ltd. India). The surface morphology of coating was characterized by field emission scanning electron microscopy (FESEM, JEOL, JSM-7610F, Japan). The water jet impact test was carried out by using 15 mL syringe. For water drop impact test, the coated glass substrate was kept at 30° inclination and water drops were dropped from the height of 10 cm. The mechanical stability of the coating was checked by adhesive tape peeling and sandpaper abrasion test. The self-cleaning behavior was observed by pouring muddy water on the coating.

Acknowledgements

This work was financially supported by DST-INSPIRE Faculty Scheme, Department of Science and Technology (DST), Govt. of India. [DST/INSPIRE/04/2015/000281]. SSL acknowledges financial assistance from the Henan University, Kaifeng, P. R. China. The authors greatly appreciate the support of the National Natural Science Foundation of China (21950410531).

Conflict of Interest

The authors declare no conflict of interest.

Keywords

PVC, roughness, superhydrophobic and self-cleaning, wetting

- [1] L. Feng, S. Li, Y. Li, H. Li, L. Zhang, J. Zhai, Y. Song, B. Liu, L. Jiang, D. Zhu, *Adv. Mater.* **2002**, *14*, 1857.
- [2] C. Neinhuis, W. Barthlott, *Annal. Botany* **1997**, *79*, 667.
- [3] S. P. Dalawai, M. A. S. Aly, S. S. Latthe, R. Xing, R. S. Sutar, S. Nagappan, C.-S. Ha, K. K. Sadasivuni, S. Liu, *Prog. Org. Coat.* **2020**, *138*, 105381.
- [4] S. S. Latthe, V. S. Kodag, R. S. Sutar, A. K. Bhosale, S. Nagappan, C.-S. Ha, K. K. Sadasivuni, S. R. Kural, S. Liu, R. Xing, *Mater. Chem. Phys.* **2020**, *243*, 122634.
- [5] S. S. Latthe, P. Sudhagar, A. Devadoss, A. M. Kumar, S. Liu, C. Terashima, K. Nakataa, A. Fujishima, *J. Mater. Chem. A* **2015**, *3*, 14263.
- [6] S. S. Latthe, et al. *Superhydrophobic Polymer Coatings*, **2019**, Elsevier. pp. 339–356.
- [7] S. S. Latthe, R. S. Sutar, A. K. Bhosale, S. Nagappan, C.-S. Ha, K. K. Sadasivuni, S. Liu, R. Xing, *Prog. Org. Coat.* **2019**, *137*, 105373.

- [8] S. S. Latthe, R. S. Sutar, T. B. Shinde, S. B. Pawar, T. M. Khot, A. K. Bhosale, K. K. Sadasivuni, R. Xing, L. Mao, S. Liu, *ACS Appl. Nano Mater.* **2019**, 2, 799.
- [9] A. B. Gurav, S. S. Latthe, R. S. Vhatkar, J. G. Lee, D. Y. Kim, J. J. Park, S. S. Yoon, *Ceram. Int.* **2014**, 40, 7151.
- [10] A. M. Kokare, et al. *AIP Conference Proceedings*, AIP Publishing. **2018**.
- [11] S. S. Latthe, et al. *Green Chemistry for Surface Coatings, Inks and Adhesives*. **2019**. pp. 92–119.
- [12] R. S. Sutar, et al. *Macromolecular Symposia*, **2019**. Wiley Online Library.
- [13] S. Bilgin, M. Isik, E. Yilgor, *Polymer* **2012**, 53, 1180.
- [14] H. Yoon, H. Kim, S. S. Latthe, M.-W. Kim, S. Al-Deyabd, S. S. Yoon, *J. Mater. Chem. A* **2015**, 3, 11403.
- [15] Y. Guo, Q. Wang, *Appl. Surf. Sci.* **2010**, 257, 33.
- [16] P. G. Pawar, R. Xing, R. C. Kambale, A. M. Kumar, S. Liu, S. S. Latthe, *Prog. Org. Coat.* **2017**, 105, 235.
- [17] S. S. Latthe, R. S. Sutar, V. S. Kodag, A. K. Bhosale, A. M. Kumar, K. K. Sadasivuni, R. Xing, S. Liu, *Prog. Org. Coat.* **2019**, 128, 52.
- [18] H. Chen, Z. Yuan, J. Zhang, Y. Liu, K. Li, D. Zhao, S. Li, P. Shi, J. Tang, *J. Porous Mater.* **2009**, 16, 447.
- [19] Z. Khoryani, J. Seyfi, M. Nekoei, *Appl. Surf. Sci.* **2018**, 428, 933.
- [20] X. Li, G. Chen, Y. Ma, L. Feng, H. Zhao, L. Jiang, F. Wang, *Polymer* **2006**, 47, 506.
- [21] J. Seyfi, M. Panahi-Sarmad, A. OraeiGhodousi, V. Goodarzi, H. A. Khonakdar, A. Asefnejad, S. Shojaei, *Colloids Surf., B* **2019**, 183, 110438.
- [22] P. J. Rivero, A. Iribarren, S. Larumbe, J. F. Palacio, R. Rodríguez, *Coatings* **2019**, 9, 367.
- [23] Z. Yuan, H. Chen, J. Zhang, *Appl. Surf. Sci.* **2008**, 254, 1593.
- [24] X. Zhang, B. Ding, R. Cheng, S. C. Dixon, Y. Lu, *Adv. Sci.* **2018**, 5, 1700520.
- [25] H. Chen, X. Zhang, P. Zhang, Z. Zhang, *Appl. Surf. Sci.* **2012**, 261, 628.
- [26] R. N. Wenzel, *Ind. Eng. Chem.* **1936**, 28, 988.
- [27] A. Cassie, S. Baxter, *Trans. Faraday Soc.* **1944**, 40, 546.
- [28] N. Wang, D. Xiong, S. Pan, K. Wang, Y. Shi, Y. Deng, *New J. Chem.* **2017**, 41, 1846.
- [29] A. Kibar, H. Karabay, K. Yigit, I. Ucar, H. Erbil, *Exp. Fluids* **2010**, 49, 1135.
- [30] S. S. Latthe, A. V. Rao, *Surf. Coat. Technol.* **2012**, 207, 489.



Photocatalytic and Superhydrophilic TiO₂ Coatings on Marble for Self-Cleaning Applications

Journal:	<i>Macromolecular Symposia</i>
Manuscript ID	Draft
Wiley - Manuscript type:	Research Article
Date Submitted by the Author:	n/a
Complete List of Authors:	Sutar, Rajaram; Raje Ramrao college jath, Department of Physics Patil, Pratiksha; Self-Cleaning Research Laboratory, Department of Physics, Raje Ramrao Mahavidyalaya, Jath, Physics Bhosale, Appasaheb; Raje Ramrao mahavidyalaya, Jath, Physics Department Sadasivuni, Kishor Kumar; Center for Advanced Materials, Qatar University, Qatar.
Keywords:	Photocatalytic, superhydrophilic, Self-cleaning, TiO ₂ coating

SCHOLARONE™
Manuscripts

Photocatalytic and Superhydrophilic TiO₂ Coatings on Marble for Self-Cleaning Applications

Rajaram S. Sutar¹, Pratiksha B. Patil¹, Appasaheb K. Bhosale¹, Shital R. Shinde², P. G. Pawar³, C. E. Patil⁴, Sunita S. Kadam⁵, P.M. Kadam⁶, C. R. Bobade⁷, Kishor Kumar Sadasivuni⁸ and Sanjay S. Latthe^{1*}

¹Self-Cleaning Research Laboratory, Department of Physics, Raje Ramrao Mahavidyalaya, Jath, Dist: Sangli – 416404, (Affiliated to Shivaji University, Kolhapur) Maharashtra, India.

²Vidnyan Mahavidyalaya, Sangola, 413307, Maharashtra, India.

³Shivaji Polytechnic College, Sangola - 413307, Maharashtra, India.

⁴Department of Physics, Bharti Vidyapeeth's Dr. Patangrao Kadam Mahavidyalaya, Sangli, Maharashtra, India.

⁵Krantisinh Nana Patil College, Walwa, Sangli, Maharashtra.

⁶KWC Sangli, Maharashtra, India

⁷Balwant College, Vita. Dist: Sangli (M.S.) India

⁸Center for Advanced Materials, Qatar University, P. O. Box 2713, Doha, Qatar.

Corresponding Author: latthes@gmail.com

Abstract

The application of photocatalytic and self-cleaning titanium dioxide (TiO₂) nanomaterials coating on the stone of architectural heritage (particularly on marble) can be to preserve their aesthetic qualities. The present work describes the effect of dipping time in TiO₂ - SiO₂ coating and effect of UV irradiation on coating in term of hydrophilicity. The SiO₂ solution prepared by tetraethylorthosilicate (TEOS) through sol-gel process and 30-50 nm sized TiO₂ particles added to prepare coating solution. The water contact angle decreases with increasing dipping time of piece of marble in TiO₂ - SiO₂ solution. Also the hydrophilicity of coating increases with increasing UV illumination time. The 2-D and 3-D laser microscope analysis revealed surface structure and stable surface roughness of 1.0 μm. Such type of superhydrophilic TiO₂ - SiO₂ coating on marble may be used to apply architectural heritage and buildings.

Keywords: Photocatalytic, superhydrophilic, Self-cleaning and TiO₂ coating.

1. Introduction

From last decade, scientific research has been paid attention to developing novel surface for protection of aesthetic qualities of stone surfaces of historic buildings. Marbles have been extensively used in cultural heritages and historical architectures like statues and monuments. Increasing concentration of pollutants (soil particles, organisms, bird droppings, fire damage, etc.), may cause the deterioration of surfaces architectures. Photocatalytic and superhydrophilic TiO_2 coating is one of the best solution to avoid this problem. TiO_2 can generate oxidative ($\bullet\text{OH}$) and reductive ($\bullet\text{O}_2$) species under UV light irradiation, which are helps to degrade different organic and inorganic compounds ^[1, 2]. Moreover, the hydrophilicity enhanced by $-\text{OH}$, which easily remove the fouling substances on TiO_2 coated surfaces by flow water film; this is called self-cleaning ability. Munafo et al. ^[3] have sprayed colloidal suspensions of TiO_2 on travertine stone to deposit photocatalytic self-cleaning coating. After long-term aging under UV-A irradiation, the microstructure of coating was unaltered but reduced photoactivity and self-cleaning properties. Bergamonti et al. ^[4] have applied TiO_2 -sol on the stone samples by brush, repeating the procedure for three times to obtain self-cleaning coating. Lettieri et al. ^[5] have applied nanostructured TiO_2 as a photoactive coating onto a compact limestone and a highly porous calcarenite. The both types of stone has showed self-cleaning ability by photodegradation test of rhodamine B. Luna et al. ^[6] have applied sol-gel processed $\text{Au-TiO}_2/\text{SiO}_2$ photocatalysts coating on building stone by spray coating . Integrated TiO_2 in a silica matrix can enhanced its adherence to the substrate and the subsequent coating durability. Au nanoparticles enhance the TiO_2 photoactivity and the self-cleaning and depolluting performance of the coated building stone. Aminian et al. ^[7] have deposited nanolayer of TiO_2 on glass substrate by dip coating method and reported that addition of SiO_2 nanolayer under the TiO_2 layer increase the hydrophilicity due to the increase in the roughness and surface area of the nano-grains.

In the present work, we have deposited TiO_2 - SiO_2 coating on white marble by dip coating technique. The sol-gel processed silica sol were prepared by using TEOS and TiO_2 added in silica sol to prepare coating solution. The study of photodegradation of methylene blue revealed prepared coating has excellent self-cleaning ability.

2. Experimental

2.1. Materials

Tetraethylorthosilicate (TEOS, $\geq 99.0\%$) and TiO_2 nanoparticles (< 25 nm particle size, 99.7%) were purchased from Sigma-Aldrich, USA. Ethanol and nitric acid (Extra Pure AR) were bought spectrochem pvt. Mumbai, India. Methylene blue dye was obtained from Poona Laboratory, Poona, India. A small pieces of white marble (L x W x H, 5 cm x 2 cm x 1 cm) collected from local market

2.2. Preparation of TiO_2 coating on Marble

The silica sol was prepared by sol-gel processing of TEOS using nitric acid as catalyst. 11.2 ml distilled water and 0.6 ml nitric acid mixed well by magnetic stirrer. 7.5 ml of TEOS was added drop-by-drop in above mixture and kept at constant stirring (500 RPM). After 5 hr. stirring 10 ml ethanol was added slowly and stirring further continued for overnight to get silica (SiO_2) sol. Thereafter, 60 mg TiO_2 nanoparticles were dispersed in prepared silica sol and stirred for 2 hr. to get uniform coating solution. The marble pieces were washed by laboratory detergent and later by distilled water and dried well by dryer with hot air. The cleaned piece of marble dipped in coating solution with various dipping time. Deposited marble pieces were dried at 110°C for 6 hr to rid of solvents. The schematic process of deposition of superhydrophilic $\text{TiO}_2 - \text{SiO}_2$ coating on marble as shown in **Fig.1**. The dip-withdraw speed and dipping time were controlled by Dip-coater machine. The dipping time varied from 1 minute to 7 minutes at constant dip-withdraw speed of 50 mm/sec

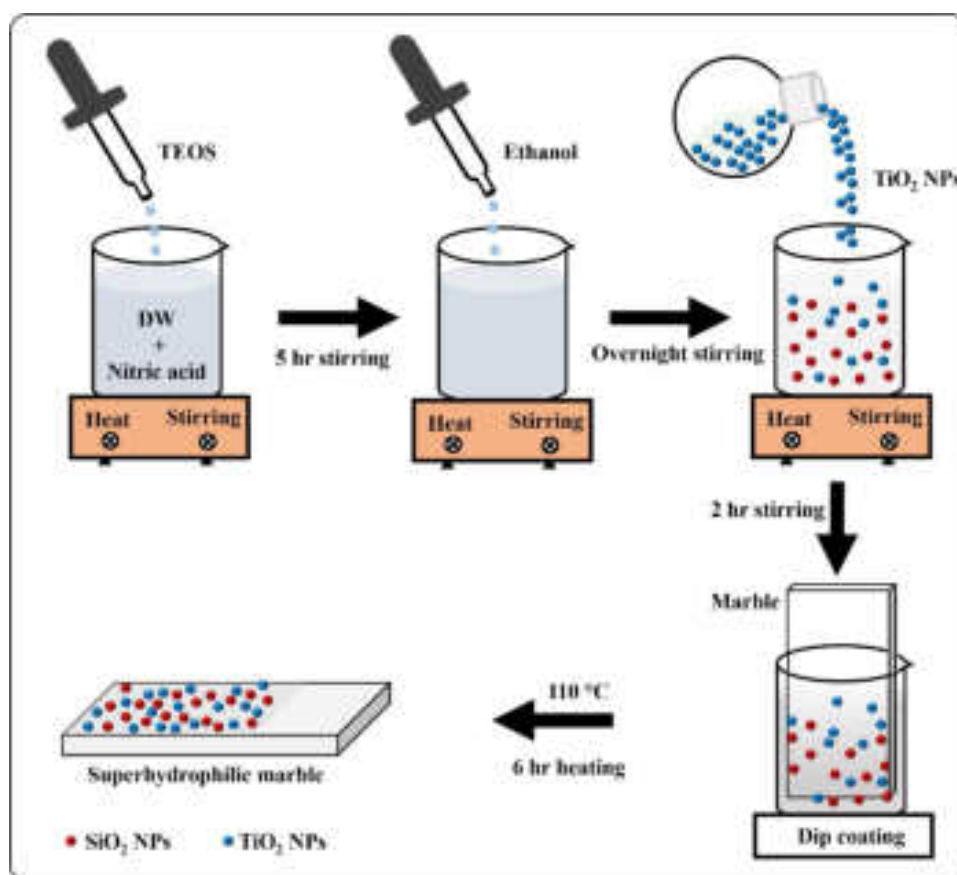


Fig. 1: Preparation of TiO₂ coating on marble.

2.3. Characterizations

A laser microscope (KEYENCE, VK-X200 series) was used to characterize the 2D and 3D surface topography of coated marble. A closed metal box with one open side covered by black napkin was fabricated and UV lamps (Intensity=1 mW/cm²) was fitted onto the ceiling of the box. The photocatalytic property of the coating was confirmed by the decrease in water contact angle (WCA) with UV illumination time. The wetting properties of the coating surface before and after UV irradiation was confirmed by WCA measurements. A contact angle meter (Kyowa, Drop Master; Saitama, Japan) was used to measure the WCAs. A small water drop was gently placed on the surface by using syringe. The self-cleaning ability of the TiO₂ coating under exposure to UV irradiation were checked using methylene blue (MB) as a stain.

3. Result and Discussion

3.1. Surface Topography and Roughness of the Prepared Coating on Marble

The surface topography plays an important role on the wettability of the thin films (**Fig. 2**). The TiO_2 - SiO_2 coating prepared by 01 minute dipping showed relatively smooth surface with RMS roughness of nearly $0.74 \mu\text{m}$. The increase in dipping time significantly affects on thickness as well as roughness of the film. The TiO_2 - SiO_2 thin films prepared by 07 minute dipping showed remarkably rough surface structure with RMS roughness of $\sim 01.00 \mu\text{m}$. Such surface structure along with highly roughness is helps to achieve the superhydrophilic. The deposition time was further increased to 10 minutes, however the visible cracks were observed on the thin film, which can be easily removed by the gentle fingertip touching.

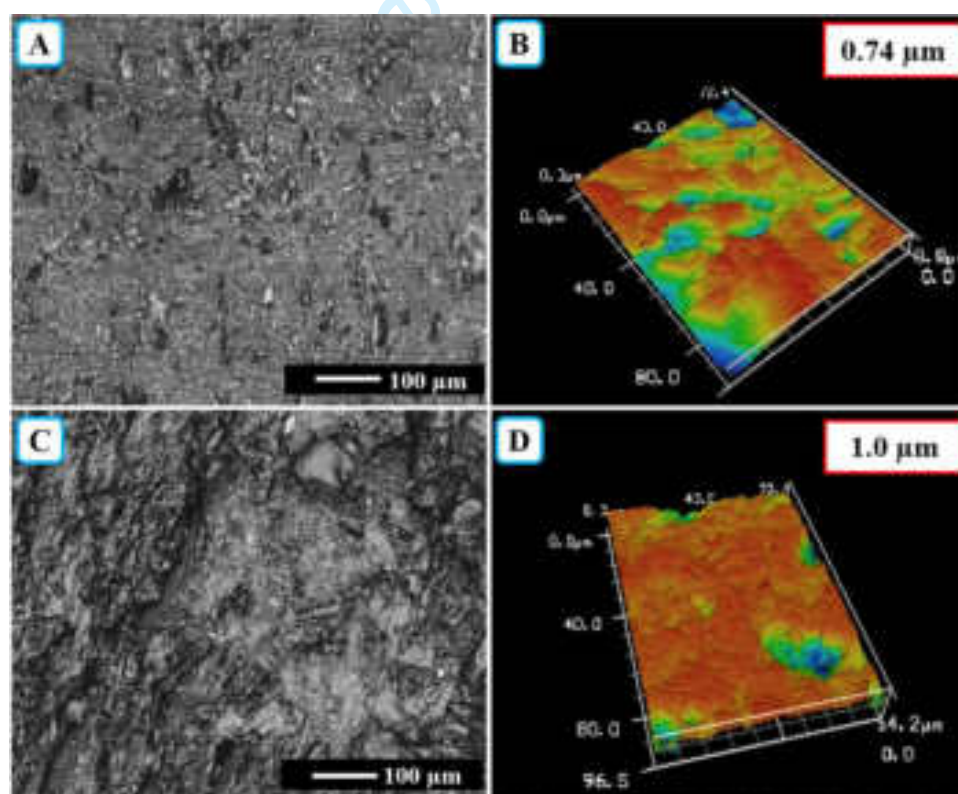


Fig. 2: The 2-D and 3-D Laser Microscope images of the SiO_2 - TiO_2 thin films prepared from (A, B) 01 minute and (C, D) 07 minute deposition time, respectively.

3.2. Surface Wettability, Photocatalytic Activity and Self-cleaning property

The coating of TiO_2 - SiO_2 thin film were applied on pre-cleaned marble by dipping at different time in coating solution. The dipping time were varied from 01 to 07 minute. As usual, 01 minute deposited coating showed WCA of 27° due to smoothness of the thin film. However, the WCA gradually decreased to 14° for 07 minute deposited TiO_2 - SiO_2 thin films. The wetting property changes with dipping time of marble in coating solution. The variation of WCA with dipping time as shown in the **Fig. 3**. This is due to the increased in roughness of the coating which eventually helps to decrease the wettability of the thin film [8].

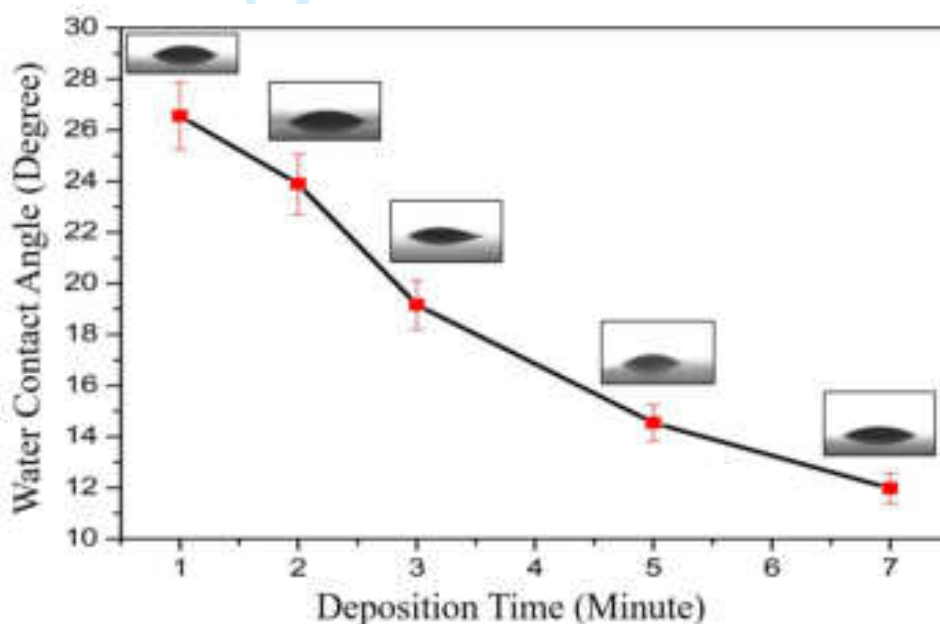


Fig. 3: An effect of dipping times on wettability of the coating.

When water drop deposited on uncoated marble, water drop stacked with WCA $> 40^\circ$. Other hand, water drop spread on coated marble. The colour dyed water on coated and uncoated marble as shown in **Fig.4**.

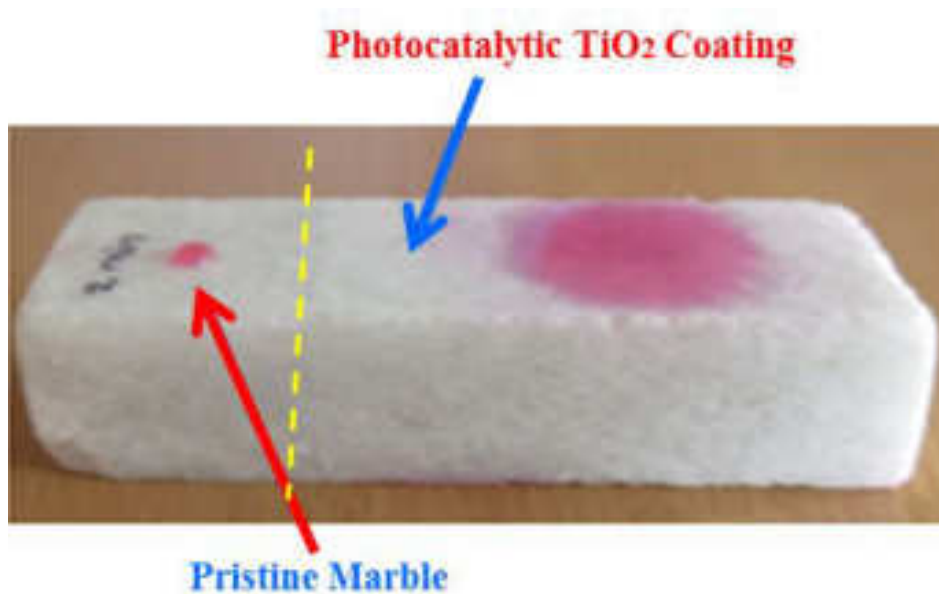


Fig. 4: Optical photograph of behaviour of water drop on coated and uncoated part of the marble.

The effect of UV irradiation on dip-coated marble (07 minute dipping marble) were observed. The hydrophilicity of coating increases with duration of UV irradiation ^[9, 10]. The variation of WCA with duration of UV irradiation as shown in **Fig. 5**. After 8 minute UV irradiation duration, the WCA of coating reached to $< 5^\circ$, which confirms hydrophilic coating become superhydrophilic. This contradict to some reports where superhydrophilicity was only achieved after long period of time of UV irradiation. UV irradiation causes to form stable hydroxyl groups on TiO₂ - SiO₂ surface and consequently surface becomes more hydrophilic ^[7]. Mostly, fast reducing WCA of hydrophilic coating under UVA radiation, which resulting that superhydrophilic self-cleaning TiO₂ - SiO₂ coating.

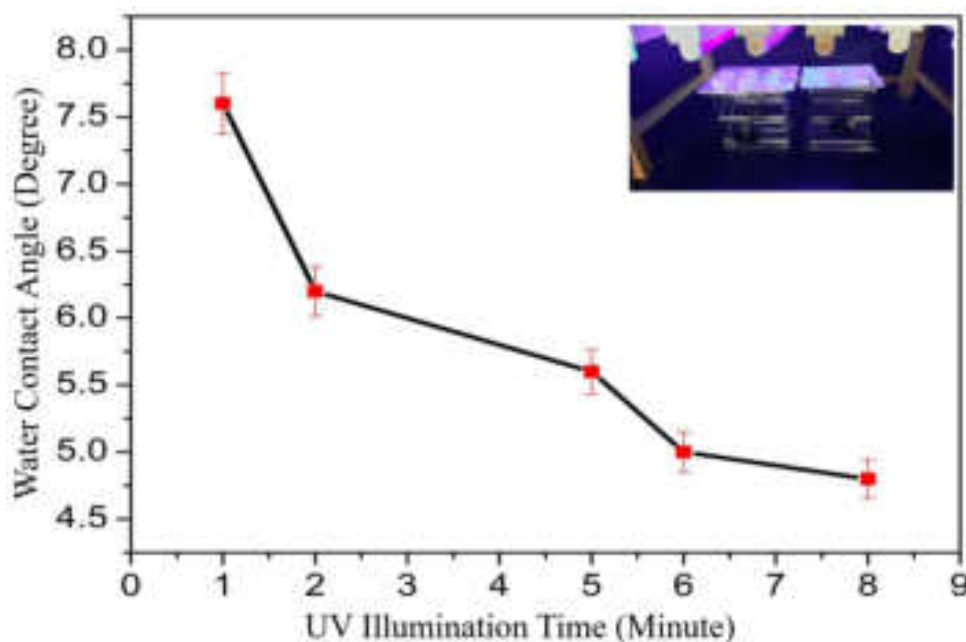


Fig. 5: An effect on UV illumination time on the wettability of the TiO_2 - SiO_2 coated marble.

Mostly white marbles are prone to damage by air and water pollution. The continuous degradation of monuments due to organic pollutants may soon become irreversible. The degradation of MB has extensively used to evaluate self-cleaning ability of coated marble [4, 11]. The systematically evaluated self-cleaning activity by adopting standard procedure. 0.5 ml of MB was poured on coated marble as shown in Fig.6 (A). Later, this marble placed at 10 cm from UV source in degradation chamber for degradation of MB. 30 hrs exposure to UV irradiation caused more than 90% degradation of MB (Fig.6 (B)). This confirms the prepared TiO_2 - SiO_2 coated marble exhibited excellent self-cleaning ability under exposure to UV illumination.



Fig. 6: Photograph of self-cleaning photodegradation test by MB, (A) before UV exposure and (B) after 30 hrs exposure to UV irradiation.

4. Conclusion

Superhydrophilic TiO₂ - SiO₂ thin films were successfully applied on marble for photocatalytic and self-cleaning application. A coating with 07 minutes of deposition time revealed hydrophilic property with contact angle nearly 14°. After exposure to UV irradiation for 8 minutes the contact angled reduced < 5°. The surface roughness of coating was found increased with deposition time. A transformation of surface wettability of TiO₂ film into superhydrophilic state and subsequent decomposition of organic pollutants by UV exposure leads to self-cleaning phenomena.

References:

1. Hoffmann, M.R., et al., *Environmental applications of semiconductor photocatalysis*. Chemical reviews, 1995. **95**(1): p. 69-96.
2. Miyauchi, M., et al., *Reversible wettability control of TiO₂ surface by light irradiation*. Surface Science, 2002. **511**(1-3): p. 401-407.
3. Munafò, P., et al., *Durability of nano-engineered TiO₂ self-cleaning treatments on limestone*. Construction and Building Materials, 2014. **65**: p. 218-231.
4. Bergamonti, L., et al., *Photocatalytic self-cleaning TiO₂ coatings on carbonatic stones*. Applied Physics A, 2016. **122**(2): p. 124.
5. Lettieri, M., et al., *Nanostructured TiO₂ for stone coating: Assessing compatibility with basic stone's properties and photocatalytic effectiveness*. Bulletin of Engineering Geology and the Environment, 2017. **76**(1): p. 101-114.
6. Luna, M., et al., *Au-TiO₂/SiO₂ photocatalysts for building materials: Self-cleaning and depolluting performance*. Building and Environment, 2019. **164**: p. 106347.
7. Khajeh Aminian, M., et al., *Hydrophilic and Photocatalytic Properties of TiO₂/SiO₂ Nano-layers in Dry Weather*. Progress in Color, Colorants and Coatings, 2021. **14**(3): p. 221-232.
8. Syafiq, A., et al., *Superhydrophilic smart coating for self-cleaning application on glass substrate*. Journal of Nanomaterials, 2018. **2018**.
9. Fateh, R., R. Dillert, and D. Bahnemann, *Preparation and characterization of transparent hydrophilic photocatalytic TiO₂/SiO₂ thin films on polycarbonate*. Langmuir, 2013. **29**(11): p. 3730-3739.
10. Shayan, M., et al., *Improved osteoblast response to UV-irradiated PMMA/TiO₂ nanocomposites with controllable wettability*. Journal of Materials Science: Materials in Medicine, 2014. **25**(12): p. 2721-2730.
11. Luna, M., et al., *TiO₂-SiO₂ coatings with a low content of AuNPs for producing self-cleaning building materials*. Nanomaterials, 2018. **8**(3): p. 177.



Photocatalytic and Superhydrophilic TiO₂ Coatings on Marble for Self-Cleaning Applications

Journal:	<i>Macromolecular Symposia</i>
Manuscript ID	Draft
Wiley - Manuscript type:	Research Article
Date Submitted by the Author:	n/a
Complete List of Authors:	Sutar, Rajaram; Raje Ramrao college jath, Department of Physics Patil, Pratiksha; Self-Cleaning Research Laboratory, Department of Physics, Raje Ramrao Mahavidyalaya, Jath, Physics Bhosale, Appasaheb; Raje Ramrao mahavidyalaya, Jath, Physics Department Sadasivuni , Kishor Kumar ; Center for Advanced Materials, Qatar University, Qatar.
Keywords:	Photocatalytic, superhydrophilic, Self-cleaning, TiO ₂ coating

SCHOLARONE™
Manuscripts

Photocatalytic and Superhydrophilic TiO₂ Coatings on Marble for Self-Cleaning Applications

Rajaram S. Sutar¹, Pratiksha B. Patil¹, Appasaheb K. Bhosale¹, Shital R. Shinde², P. G. Pawar³, C. E. Patil⁴, Sunita S. Kadam⁵, P.M. Kadam⁶, C. R. Bobade⁷, Kishor Kumar Sadasivuni⁸ and Sanjay S. Latthe^{1*}

¹Self-Cleaning Research Laboratory, Department of Physics, Raje Ramrao Mahavidyalaya, Jath, Dist: Sangli – 416404, (Affiliated to Shivaji University, Kolhapur) Maharashtra, India.

²Vidnyan Mahavidyalaya, Sangola, 413307, Maharashtra, India.

³Shivaji Polytechnic College, Sangola - 413307, Maharashtra, India.

⁴Department of Physics, Bharti Vidyapeeth's Dr. Patangrao Kadam Mahavidyalaya, Sangli, Maharashtra, India.

⁵Krantisinh Nana Patil College, Walwa, Sangli, Maharashtra.

⁶KWC Sangli, Maharashtra, India

⁷Balwant College, Vita. Dist: Sangli (M.S.) India

⁸Center for Advanced Materials, Qatar University, P. O. Box 2713, Doha, Qatar.

Corresponding Author: latthes@gmail.com

Abstract

The application of photocatalytic and self-cleaning titanium dioxide (TiO₂) nanomaterials coating on the stone of architectural heritage (particularly on marble) can be to preserve their aesthetic qualities. The present work describes the effect of dipping time in TiO₂ - SiO₂ coating and effect of UV irradiation on coating in term of hydrophilicity. The SiO₂ solution prepared by tetraethylorthosilicate (TEOS) through sol-gel process and 30-50 nm sized TiO₂ particles added to prepare coating solution. The water contact angle decreases with increasing dipping time of piece of marble in TiO₂ - SiO₂ solution. Also the hydrophilicity of coating increases with increasing UV illumination time. The 2-D and 3-D laser microscope analysis revealed surface structure and stable surface roughness of 1.0 μm. Such type of superhydrophilic TiO₂ - SiO₂ coating on marble may be used to apply architectural heritage and buildings.

Keywords: Photocatalytic, superhydrophilic, Self-cleaning and TiO₂ coating.

1. Introduction

From last decade, scientific research has been paid attention to developing novel surface for protection of aesthetic qualities of stone surfaces of historic buildings. Marbles have been extensively used in cultural heritages and historical architectures like statues and monuments. Increasing concentration of pollutants (soil particles, organisms, bird droppings, fire damage, etc.), may cause the deterioration of surfaces architectures. Photocatalytic and superhydrophilic TiO_2 coating is one of the best solution to avoid this problem. TiO_2 can generate oxidative ($\bullet\text{OH}$) and reductive ($\bullet\text{O}_2$) species under UV light irradiation, which are helps to degrade different organic and inorganic compounds [1, 2]. Moreover, the hydrophilicity enhanced by $-\text{OH}$, which easily remove the fouling substances on TiO_2 coated surfaces by flow water film; this is called self-cleaning ability. Munafo et al. [3] have sprayed colloidal suspensions of TiO_2 on travertine stone to deposit photocatalytic self-cleaning coating. After long-term aging under UV-A irradiation, the microstructure of coating was unaltered but reduced photoactivity and self-cleaning properties. Bergamonti et al. [4] have applied TiO_2 -sol on the stone samples by brush, repeating the procedure for three times to obtain self-cleaning coating. Lettieri et al. [5] have applied nanostructured TiO_2 as a photoactive coating onto a compact limestone and a highly porous calcarenite. The both types of stone has showed self-cleaning ability by photodegradation test of rhodamine B. Luna et al. [6] have applied sol-gel processed $\text{Au-TiO}_2/\text{SiO}_2$ photocatalysts coating on building stone by spray coating . Integrated TiO_2 in a silica matrix can enhanced its adherence to the substrate and the subsequent coating durability. Au nanoparticles enhance the TiO_2 photoactivity and the self-cleaning and depolluting performance of the coated building stone. Aminian et al. [7] have deposited nanolayer of TiO_2 on glass substrate by dip coating method and reported that addition of SiO_2 nanolayer under the TiO_2 layer increase the hydrophilicity due to the increase in the roughness and surface area of the nano-grains.

In the present work, we have deposited TiO_2 - SiO_2 coating on white marble by dip coating technique. The sol-gel processed silica sol were prepared by using TEOS and TiO_2 added in silica sol to prepare coating solution. The study of photodegradation of methylene blue revealed prepared coating has excellent self-cleaning ability.

2. Experimental

2.1. Materials

Tetraethylorthosilicate (TEOS, $\geq 99.0\%$) and TiO_2 nanoparticles (< 25 nm particle size, 99.7%) were purchased from Sigma-Aldrich, USA. Ethanol and nitric acid (Extra Pure AR) were bought spectrochem pvt. Mumbai, India. Methylene blue dye was obtained from Poona Laboratory, Poona, India. A small pieces of white marble (L x W x H, 5 cm x 2 cm x 1 cm) collected from local market

2.2. Preparation of TiO_2 coating on Marble

The silica sol was prepared by sol-gel processing of TEOS using nitric acid as catalyst. 11.2 ml distilled water and 0.6 ml nitric acid mixed well by magnetic stirrer. 7.5 ml of TEOS was added drop-by-drop in above mixture and kept at constant stirring (500 RPM). After 5 hr. stirring 10 ml ethanol was added slowly and stirring further continued for overnight to get silica (SiO_2) sol. Thereafter, 60 mg TiO_2 nanoparticles were dispersed in prepared silica sol and stirred for 2 hr. to get uniform coating solution. The marble pieces were washed by laboratory detergent and later by distilled water and dried well by dryer with hot air. The cleaned piece of marble dipped in coating solution with various dipping time. Deposited marble pieces were dried at 110°C for 6 hr to rid of solvents. The schematic process of deposition of superhydrophilic $\text{TiO}_2 - \text{SiO}_2$ coating on marble as shown in **Fig.1**. The dip-withdraw speed and dipping time were controlled by Dip-coater machine. The dipping time varied from 1 minute to 7 minutes at constant dip-withdraw speed of 50 mm/sec

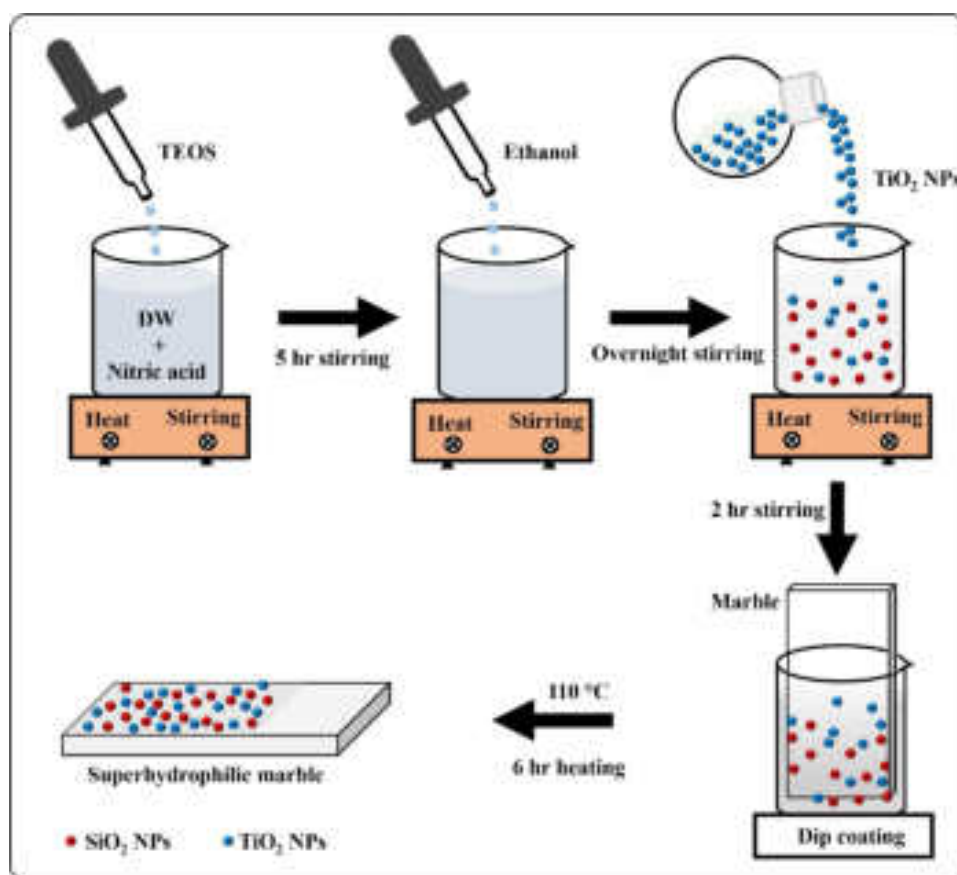


Fig. 1: Preparation of TiO₂ coating on marble.

2.3. Characterizations

A laser microscope (KEYENCE, VK-X200 series) was used to characterize the 2D and 3D surface topography of coated marble. A closed metal box with one open side covered by black napkin was fabricated and UV lamps (Intensity=1 mW/cm²) was fitted onto the ceiling of the box. The photocatalytic property of the coating was confirmed by the decrease in water contact angle (WCA) with UV illumination time. The wetting properties of the coating surface before and after UV irradiation was confirmed by WCA measurements. A contact angle meter (Kyowa, Drop Master; Saitama, Japan) was used to measure the WCAs. A small water drop was gently placed on the surface by using syringe. The self-cleaning ability of the TiO₂ coating under exposure to UV irradiation were checked using methylene blue (MB) as a stain.

3. Result and Discussion

3.1. Surface Topography and Roughness of the Prepared Coating on Marble

The surface topography plays an important role on the wettability of the thin films (**Fig. 2**). The TiO_2 - SiO_2 coating prepared by 01 minute dipping showed relatively smooth surface with RMS roughness of nearly $0.74 \mu\text{m}$. The increase in dipping time significantly affects on thickness as well as roughness of the film. The TiO_2 - SiO_2 thin films prepared by 07 minute dipping showed remarkably rough surface structure with RMS roughness of $\sim 01.00 \mu\text{m}$. Such surface structure along with highly roughness is helps to achieve the superhydrophilic. The deposition time was further increased to 10 minutes, however the visible cracks were observed on the thin film, which can be easily removed by the gentle fingertip touching.

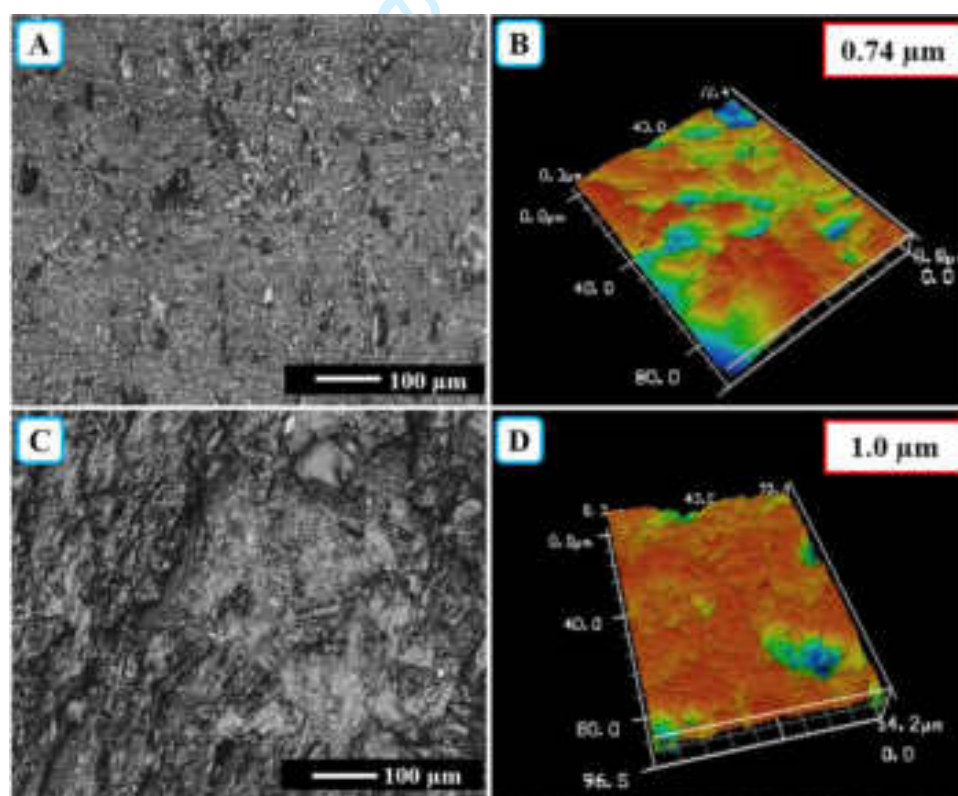


Fig. 2: The 2-D and 3-D Laser Microscope images of the SiO_2 - TiO_2 thin films prepared from (A, B) 01 minute and (C, D) 07 minute deposition time, respectively.

3.2. Surface Wettability, Photocatalytic Activity and Self-cleaning property

The coating of TiO_2 - SiO_2 thin film were applied on pre-cleaned marble by dipping at different time in coating solution. The dipping time were varied from 01 to 07 minute. As usual, 01 minute deposited coating showed WCA of 27° due to smoothness of the thin film. However, the WCA gradually decreased to 14° for 07 minute deposited TiO_2 - SiO_2 thin films. The wetting property changes with dipping time of marble in coating solution. The variation of WCA with dipping time as shown in the **Fig. 3**. This is due to the increased in roughness of the coating which eventually helps to decrease the wettability of the thin film [8].

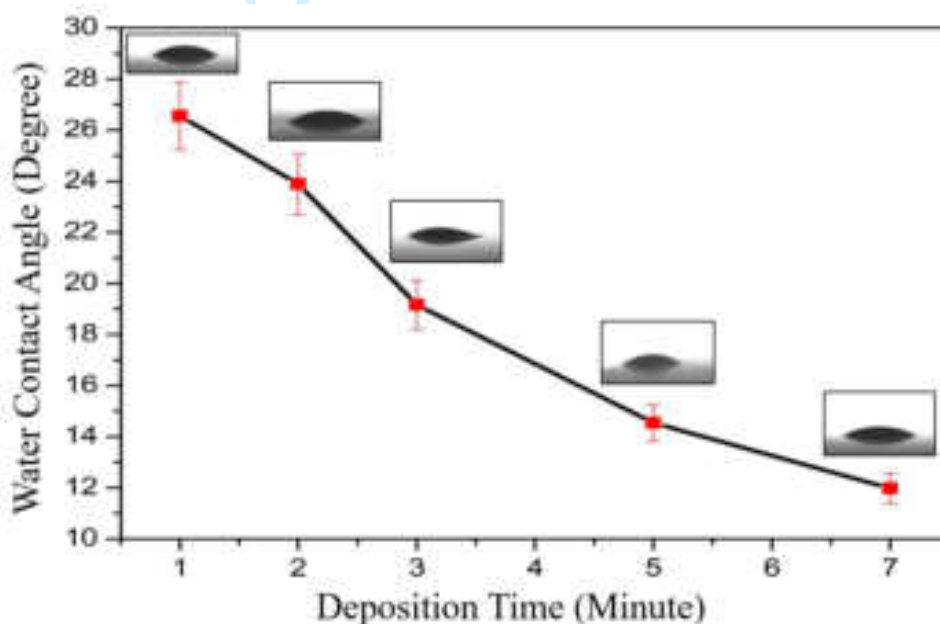


Fig. 3: An effect of dipping times on wettability of the coating.

When water drop deposited on uncoated marble, water drop stacked with WCA $> 40^\circ$. Other hand, water drop spread on coated marble. The colour dyed water on coated and uncoated marble as shown in **Fig.4**.

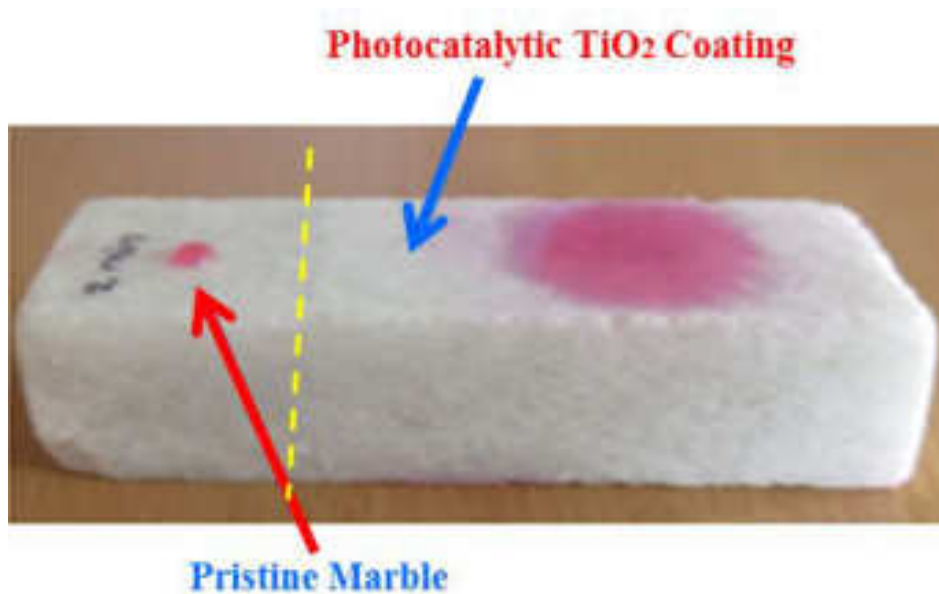


Fig. 4: Optical photograph of behaviour of water drop on coated and uncoated part of the marble.

The effect of UV irradiation on dip-coated marble (07 minute dipping marble) were observed. The hydrophilicity of coating increases with duration of UV irradiation ^[9, 10]. The variation of WCA with duration of UV irradiation as shown in **Fig. 5**. After 8 minute UV irradiation duration, the WCA of coating reached to $< 5^\circ$, which confirms hydrophilic coating become superhydrophilic. This contradict to some reports where superhydrophilicity was only achieved after long period of time of UV irradiation. UV irradiation causes to form stable hydroxyl groups on TiO_2 - SiO_2 surface and consequently surface becomes more hydrophilic ^[7]. Mostly, fast reducing WCA of hydrophilic coating under UVA radiation, which resulting that superhydrophilic self-cleaning TiO_2 - SiO_2 coating.

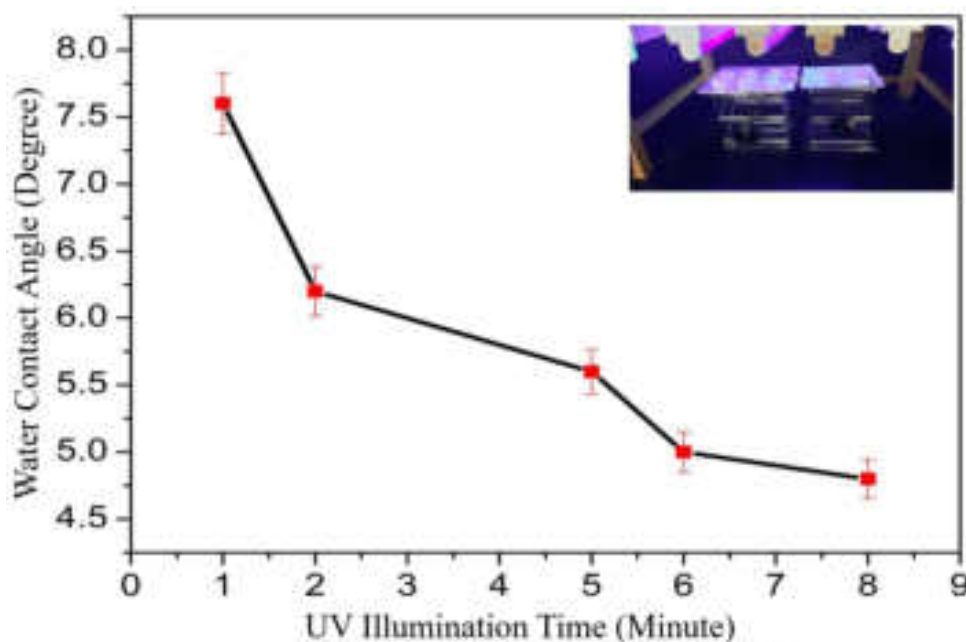


Fig. 5: An effect on UV illumination time on the wettability of the TiO_2 - SiO_2 coated marble.

Mostly white marbles are prone to damage by air and water pollution. The continuous degradation of monuments due to organic pollutants may soon become irreversible. The degradation of MB has extensively used to evaluate self-cleaning ability of coated marble [4, 11]. The systematically evaluated self-cleaning activity by adopting standard procedure. 0.5 ml of MB was poured on coated marble as shown in Fig.6 (A). Later, this marble placed at 10 cm from UV source in degradation chamber for degradation of MB. 30 hrs exposure to UV irradiation caused more than 90% degradation of MB (Fig.6 (B)). This confirms the prepared TiO_2 - SiO_2 coated marble exhibited excellent self-cleaning ability under exposure to UV illumination.



Fig. 6: Photograph of self-cleaning photodegradation test by MB, (A) before UV exposure and (B) after 30 hrs exposure to UV irradiation.

4. Conclusion

Superhydrophilic TiO₂ - SiO₂ thin films were successfully applied on marble for photocatalytic and self-cleaning application. A coating with 07 minutes of deposition time revealed hydrophilic property with contact angle nearly 14°. After exposure to UV irradiation for 8 minutes the contact angled reduced < 5°. The surface roughness of coating was found increased with deposition time. A transformation of surface wettability of TiO₂ film into superhydrophilic state and subsequent decomposition of organic pollutants by UV exposure leads to self-cleaning phenomena.

References:

1. Hoffmann, M.R., et al., *Environmental applications of semiconductor photocatalysis*. Chemical reviews, 1995. **95**(1): p. 69-96.
2. Miyauchi, M., et al., *Reversible wettability control of TiO₂ surface by light irradiation*. Surface Science, 2002. **511**(1-3): p. 401-407.
3. Munafò, P., et al., *Durability of nano-engineered TiO₂ self-cleaning treatments on limestone*. Construction and Building Materials, 2014. **65**: p. 218-231.
4. Bergamonti, L., et al., *Photocatalytic self-cleaning TiO₂ coatings on carbonatic stones*. Applied Physics A, 2016. **122**(2): p. 124.
5. Lettieri, M., et al., *Nanostructured TiO₂ for stone coating: Assessing compatibility with basic stone's properties and photocatalytic effectiveness*. Bulletin of Engineering Geology and the Environment, 2017. **76**(1): p. 101-114.
6. Luna, M., et al., *Au-TiO₂/SiO₂ photocatalysts for building materials: Self-cleaning and depolluting performance*. Building and Environment, 2019. **164**: p. 106347.
7. Khajeh Aminian, M., et al., *Hydrophilic and Photocatalytic Properties of TiO₂/SiO₂ Nano-layers in Dry Weather*. Progress in Color, Colorants and Coatings, 2021. **14**(3): p. 221-232.
8. Syafiq, A., et al., *Superhydrophilic smart coating for self-cleaning application on glass substrate*. Journal of Nanomaterials, 2018. **2018**.
9. Fateh, R., R. Dillert, and D. Bahnemann, *Preparation and characterization of transparent hydrophilic photocatalytic TiO₂/SiO₂ thin films on polycarbonate*. Langmuir, 2013. **29**(11): p. 3730-3739.
10. Shayan, M., et al., *Improved osteoblast response to UV-irradiated PMMA/TiO₂ nanocomposites with controllable wettability*. Journal of Materials Science: Materials in Medicine, 2014. **25**(12): p. 2721-2730.
11. Luna, M., et al., *TiO₂-SiO₂ coatings with a low content of AuNPs for producing self-cleaning building materials*. Nanomaterials, 2018. **8**(3): p. 177.

Chief Guest



Dr. Achyut Godbole
MD, Softexcel Consultancy



Hon. Abhaykumar Salunkhe
Executive President



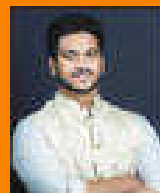
Prof. D. T. Shirke
Vice Chancellor, SUK



Prof. P. S. Patil
Pro-Vice Chancellor, SUK



Hon. Shubhangi Gavade
Secretary



Hon. Kaustabh Gavade
Chief Executive Officer



Prin. Dr. R. V. Shejwal
Joint Secretary
(Administration)



Prin. S. M. Gavali
Joint Secretary (Finance)



Dr. Milind S. Hujare
Principal

Dr. Milind S. Hujare

Principal, PDVP Mahavidyalaya, Tasgaon. Dist. Sangli

Prin. (Dr.) R. R. Kumbhar

Vivekanand College, Kolhapur

I/C Prin. Prof. (Dr.) S. R. Ghatage

S.M.D.B.S. Mahavidyalaya, Miraj

I/C Prin. Prof. (Dr.) S. S. Patil

R. R. College, Jath

Prin. (Dr.) A. N. Patil

D. K. A. S. C. College, Ichalkaranji

Prin. (Dr.) J. S. Deshmukh

R. P. College, Osmanabad

I/C Prin. (Dr.) S. S. Desai

Smt. M. M. College, Panchgani

Conveners

Prof. S. K. Khade

Dr. A. N. Ambhore

Treasurers

Mr. P. V. Patil

Dr. P. B. Teli

Dr. S. K. Shinde

Co-conveners

Dr. J. S. Ghodake

Dr. S. D. Jadhav

Organizing Secretaries

Dr. A. P. Inamdar

Dr. M. U. Patil

Dr. R. A. Kalel

Coordinators

Prof. N. A. Kulkarni

Prof. S. A. Khabade

Technocrats

Mr. B. S. Harale

Prof. R. M. Ganeshwade

Dr. P. S. Bhandare

Local Organizing Committee

Mr. J. A. Yadav	Mr. V. J. Jadhav	Prof. T. K. Badame	Mr. P. R. Khade	Mr. R. B. Mankar	Dr. A. S. Wagh
Dr. S. J. Patil	Mr. A. R. Patil	Dr. V. D. Kumbhar	Mrs. P. R. Mirajkar	Mr. S. S. Gavil	Dr. A. G. Sonawale
Mr. A. K. Patil	Mr. D. Y. Sakhare	Mr. A. A. Jagdale	Ms. V. D. Jagdale	Ms. V. V. Patil	Mr. R. S. Mote
Mr. S. R. Ghogare	Dr. K. N. Patil	Dr. B. J. Kadam	Dr. A. M. Mali	Mr. A. S. Bagal	Mr. V. T. Kumbhar
Mr. D. S. Shinde	Ms. S. R. Mali	Dr. G. R. Patil	Dr. R. J. Gore	Mr. G. S. Pawar	Mr. J. H. Lavand
Mr. D. J. Nalawade	Mr. D. D. Patil	Mr. S. A. Patil	Dr. A. S. Magdum	Mr. V. R. Patil	Mr. V. M. Jadhav
Mr. R. S. Kumbhar	Dr. S. L. Andhelwar	Ms. S. D. Ghatage	Ms. P. A. Kashid	Ms. P. R. Zambre	Ms. P. S. Jadhav
Mr. A. H. Tarange	Ms. A. S. Yadav	Mr. S. M. Patil	Ms. N. V. More	Ms. S. G. Patil	Ms. D. M. Gosavi
Dr. M. M. Patil	Mr. S. A. Karande	Ms. S. S. Panari	Ms. S. M. Kolekar	Mrs. N. V. Kumbhar	Ms. S. P. Patil
Ms. S. S. Patil	Ms. S. S. Patil	Ms. P. V. Shinde	Mr. S. V. Mane	Ms. S. S. Patil	Ms. S. T. Wagh
Mr. A. A. Wagh					Ms. S. K. Patil
Mr. M. B. Kadam					Mr. S. P. Salunkhe
Mr. M. K. Patil					Mr. A. R. Lavand

All Teaching and non Teaching Staff PDVP Mahavidyalaya, Tasgaon.

Multidisciplinary Approach in Basic and Applied Sciences (MABAS - 2023)



“Dissemination of Education for Knowledge, Science & Culture”

- Shikshanmaharshi Dr. Babuji Salunkhe

Shri Swami Vivekanand Shikshan Sanstha Kolhapur's

Padmabhushan Dr. Vasantodada Patil Mahavidyalaya, Tasgaon

Dist.: Sangli (MS) India Pin : 416 312

Knowledge Partner

Department of Biotechnology, Shivaji University, Kolhapur

Third International Conference

On

“Multidisciplinary Approach in Basic and Applied Sciences (MABAS - 2023)”

(23rd & 24th February - 2023)

Souvenir

ISBN: 978-93-95369-30-5



TABLE OF CONTENTS

Sr. No.	Title	Page no.
1	Diversity of millipedes (myriapoda: diplopoda) in selected lateritic soil habitats in satara tehsil, western ghat, Maharashtra - <i>Shaikh N. A., Abdar M. R., Kengar S. B.</i>	01
2	“Peanut shell extract mediated Biogenic synthesis of palladium nanoparticles (PdNPs) and its application as a homogeneous catalyst for the Suzuki-Miyaura coupling”- <i>Pranoti P. Patil, Utkarsha B. Patil, Utkarsha U. Patil, Shashikant R. Sawant, Rahul A. Kalel</i>	02
3	A study on causes and impact of laterite mining on environment and on the life of Dhangarwada people in Kudchire village of Goa state.- <i>Mr. Vinay Takale</i>	03
4	Morphological Investigation of Rhyzopertha dominica Using Light Microscopy and Scanning Electron Microscopy - <i>Mahure Y.R. and S.K. Zilpe</i>	04
5	Synthesis of Carbon Dot from Couropita Guianensis (Cannon Ball) Flower and applied for the Sensing of an anti-Diabetic drug Metformin.- <i>P. R. Khandagale, Dr. S. V. Nipane, Dr. S. R. Sabale, Dr. R. S. Dhabe.</i>	05
6	Morphological And Histological Cyclic Changes In Theovary Of Freshwater Fish : <i>Channa gachua, Dr. Ashwini G. Ghanbahadur, Prof. Y. K. Khillare</i>	06
7	Cordyceps militaris – An Important Medicinal Mushroom- <i>Trupti D. Kadam, Dr. Ashok V. Kharde.</i>	07
8	Morphometric Analysis Of Hiranyakeshi River, Sindhudurg District Using GIS Technology- <i>Aishwarya Pramod Hingmire, Shrikant Ghadage, Mayur Goud.</i>	08
9	Isolation of urease producing bacteria to produce biocement via MICP process.- <i>P. S. Rayate, B. A. Bhanjale, S. S Yeulkar</i>	09
10	Studies On Web Structure Of Two Spiders From Family Araneidae In Akola District <i>Satyavijay S. Dhande</i>	10
11	Attempts To Improve The Eye Dropper Deigne For Better Patient Compliance <i>Ms. Arte Aakanksha Sachin</i>	11
12	Aegle marmelos ash: A heterogeneous catalyst for Henry reaction <i>Rupesh C. Patil and Suresh S. Patil</i>	12
13	BMIM]-Glycine: A Sustainable Benchmark For Multicomponent Chromene Synthesis <i>Mr. Ashutosh A. Jagdale, Prin. (Dr.) Bhaskar V. Tamhankar and Prof. (Dr.) Suresh S. Patil</i>	13

110	Studies on Livestock Predation and Human Leopard (<i>Panthera pardus</i>) Conflicts in Shirala Tehasil of Sangli District Maharashtra, India. - Jadhav V.M	112
111	Epidermal Growth Factor accelerated wound contraction in wound licking permitted and prevented groups in sialoadenectomised mice.- Sirinbanu R. Matwal, Nitin D. Potphode, Vasant M. Patole and Madhuri V. Walvekar	113
112	A green and highly efficient synthesis of pyrazolopyranopyrimidines- Chandrakant M. Mang, Satyajit S. Jadhav, Vishal Y. Khule, Soham B. Khot, Sachinkumar K. Shinde, Megha U. Patil, Suresh S. Patil	114
113	Liquid – Liquid Extraction and Separation of Zirconium (IV) from Succinate Media and Its Separation from Other Toxic Metals- A. M. Nalawade, M. R. Nalawade, R. A. Nalawade, R.V. Shejawal, C. P. Mane	115
114	Synthesis, and Characterization of Zn Substituted Li–Ni Nano Ferrites- Dr.R.G.Kharabe, Miss A. Y. Sanadi and Mr.S.B.Vairat	116
115	Investigation of antiglycation and antioxidant potential of <i>Morus alba</i> and <i>Garcinia indica</i> plant leaves.- Satish G. Parte & A.U.Sutar	117
116	Nesting Site And Nesting Material Of House Crow (<i>Corvus splendens</i>) In Rajee Ramrao College Campus, Jath, Dist. Sangli (M.S.), India.-Dr. L.P. Saptal, Dr. S. B. Deshmukh, Dr. M. B. Sajjan, Mr. M. H. Karenavar	118
117	Green Synthesis, Characterization, Catalytic and Antibacterial Applications of ZnO Nanoparticles- N. P. Patila, Dr. D. S. Gaikwada, Dr. K. A. Undalea	119
118	Evaluation of E. Coli Contamination in Drinking Water in Chiplun City - Samruddhi Ghumare	120
119	Impact of anthropogenic activities on water quality and plankton communities in the Warana River- Priyanka Pharane	121
120	Brief review on <i>Gliricidia sepium</i> - Santosh Jagatap, Dr. B.S. Wali	122
121	"Synthesis And Spectroscopic Characterization Of Some Novel 2-Amino- 1,3,4-Thiadiazole"- More A. L., Dr. Chougule A. M.	123
122	"2-Amino- 1,3,4-Thiadiazole As An Antimicrobial Scaffold"- More A. L., Dr. Chougule A. M., J. V. Kuwar	124
123	Antifungal activity and Preliminary Phytochemical Analysis of Leaf Extracts of <i>Anodendron paniculatum</i> and <i>Ellertonia rheedii</i> Wight- Bommegowdha A Mauna, Manasa C. K., Dr. Parameshwar Naik T.	125
124	Inland water quality monitoring using sentinel-2 and Landsat-8: A Comparative Study on Different Lakes in Uttarakhand, India- Shalini, Rakesh Singh, Virendra Bahadur Singh	126
125	Impact Of Farmponds On Agricultural Development Of Nashik District - Handge Satish Balasaheb & Dr. Nikam Subhash Namdeo	127
126	Anticancer and Antioxidant β -D-Glucopyranose (1 \rightarrow 2) α -D-	128

Nesting Site and Nesting Material of House Crow (*Corvus splendens*) In Raje Ramrao College Campus, Jath, Dist. Sangli (M.S.), India.

Dr. L.P. Saptal^{1*}, Dr. S. B. Deshmukh², Dr. M. B. Sajjan³, Mr. M. H. Karenavar⁴

Asst. Prof. Department of Zoology, Raje Ramrao Mahavidyalaya, Jath.

*Corresponding author: saptallalita@gmail.com

Abstract

The present study was carried out the nesting site and nesting material of house crow in Raje Ramrao College campus, Jath. The total area of campus is 28.33 acres. Total 33 nests were reported to identify the nest materials. Out of these 6 nests on Neem tree, 16 on Nilgiri, 1 on Peepal, 8 on Ashoka tree and 2 on Coconut tree. The majority of nests which were observed on Nilgiri trees in between 2 to 3 branches. The observed nest materials are twigs, dried large sticks, dried grass, paper piece, pieces of wire, plastic threads, fibers of coconut tree. Plant leaf and unidentified material are also present inside of the nest. The majority of material which is used for constructing the nests are dried sticks and grasses. To identify the nest materials unused nest was observed.

The present work is focused on nesting sites and nesting material of *Carvus splendens* at because there is no detail study available in this campus area.

Keywords: Nesting site, nesting material, College campus, Maharashtra.

Chief Guest



Dr. Achyut Godbole
MD, Softexcel Consultancy



Hon. Abhaykumar Salunkhe
Executive President



Prof. D. T. Shirke
Vice Chancellor, SUK



Prof. P. S. Patil
Pro-Vice Chancellor, SUK



Hon. Shubhangi Gavade
Secretary



Hon. Kaustabh Gavade
Chief Executive Officer



Prin. Dr. R. V. Shejwal
Joint Secretary
(Administration)



Prin. S. M. Gavali
Joint Secretary (Finance)



Dr. Milind S. Hujare
Principal

Dr. Milind S. Hujare

Principal, PDVP Mahavidyalaya, Tasgaon. Dist. Sangli

Prin. (Dr.) R. R. Kumbhar

Vivekanand College, Kolhapur

I/C Prin. Prof. (Dr.) S. R. Ghatage

S.M.D.B.S. Mahavidyalaya, Miraj

I/C Prin. Prof. (Dr.) S. S. Patil

R. R. College, Jath

Prin. (Dr.) A. N. Patil

D. K. A. S. C. College, Ichalkaranji

Prin. (Dr.) J. S. Deshmukh

R. P. College, Osmanabad

I/C Prin. (Dr.) S. S. Desai

Smt. M. M. College, Panchgani

Conveners

Prof. S. K. Khade

Dr. A. N. Ambhore

Treasurers

Mr. P. V. Patil

Dr. P. B. Teli

Dr. S. K. Shinde

Co-conveners

Dr. J. S. Ghodake

Dr. S. D. Jadhav

Organizing Secretaries

Dr. A. P. Inamdar

Dr. M. U. Patil

Dr. R. A. Kalel

Coordinators

Prof. N. A. Kulkarni

Prof. S. A. Khabade

Technocrats

Mr. B. S. Harale

Prof. R. M. Ganeshwade

Dr. P. S. Bhandare

Local Organizing Committee

Mr. J. A. Yadav	Mr. V. J. Jadhav	Prof. T. K. Badame	Mr. P. R. Khade	Mr. R. B. Mankar	Dr. A. S. Wagh
Dr. S. J. Patil	Mr. A. R. Patil	Dr. V. D. Kumbhar	Mrs. P. R. Mirajkar	Mr. S. S. Gavil	Dr. A. G. Sonawale
Mr. A. K. Patil	Mr. D. Y. Sakhare	Mr. A. A. Jagdale	Ms. V. D. Jagdale	Ms. V. V. Patil	Mr. R. S. Mote
Mr. S. R. Ghogare	Dr. K. N. Patil	Dr. B. J. Kadam	Dr. A. M. Mali	Mr. A. S. Bagal	Mr. V. T. Kumbhar
Mr. D. S. Shinde	Ms. S. R. Mali	Dr. G. R. Patil	Dr. R. J. Gore	Mr. G. S. Pawar	Mr. J. H. Lavand
Mr. D. J. Nalawade	Mr. D. D. Patil	Mr. S. A. Patil	Dr. A. S. Magdum	Mr. V. R. Patil	Mr. V. M. Jadhav
Mr. R. S. Kumbhar	Dr. S. L. Andhelwar	Ms. S. D. Ghatage	Ms. P. A. Kashid	Ms. P. R. Zambre	Ms. P. S. Jadhav
Mr. A. H. Tarange	Ms. A. S. Yadav	Mr. S. M. Patil	Ms. N. V. More	Ms. S. G. Patil	Ms. D. M. Gosavi
Dr. M. M. Patil	Mr. S. A. Karande	Ms. S. S. Panari	Ms. S. M. Kolekar	Mrs. N. V. Kumbhar	Ms. S. P. Patil
Ms. S. S. Patil	Ms. S. S. Patil	Ms. P. V. Shinde	Mr. S. V. Mane	Ms. S. S. Patil	Ms. S. T. Wagh
Mr. A. A. Wagh					Ms. S. K. Patil
Mr. M. B. Kadam					Mr. S. P. Salunkhe
Mr. M. K. Patil					Mr. A. R. Lavand

All Teaching and non Teaching Staff PDVP Mahavidyalaya, Tasgaon.

Multidisciplinary Approach in Basic and Applied Sciences (MABAS - 2023)



“Dissemination of Education for Knowledge, Science & Culture”

- Shikshanmaharshi Dr. Bapuji Salunkhe

Shri Swami Vivekanand Shikshan Sanstha Kolhapur's

Padmabhushan Dr. Vasantodada Patil Mahavidyalaya, Tasgaon

Dist.: Sangli (MS) India Pin : 416 312

Knowledge Partner

Department of Biotechnology, Shivaji University, Kolhapur

Third International Conference

On

“Multidisciplinary Approach in Basic and Applied Sciences (MABAS - 2023)”

(23rd & 24th February - 2023)

Souvenir

ISBN: 978-93-95369-30-5



TABLE OF CONTENTS

Sr. No.	Title	Page no.
1	Diversity of millipedes (myriapoda: diplopoda) in selected lateritic soil habitats in satara tehsil, western ghat, Maharashtra - <i>Shaikh N. A., Abdar M. R., Kengar S. B.</i>	01
2	“Peanut shell extract mediated Biogenic synthesis of palladium nanoparticles (PdNPs) and its application as a homogeneous catalyst for the Suzuki-Miyaura coupling”- <i>Pranoti P. Patil, Utkarsha B. Patil, Utkarsha U. Patil, Shashikant R. Sawant, Rahul A. Kalel</i>	02
3	A study on causes and impact of laterite mining on environment and on the life of Dhangarwada people in Kudchire village of Goa state.- <i>Mr. Vinay Takale</i>	03
4	Morphological Investigation of Rhyzopertha dominica Using Light Microscopy and Scanning Electron Microscopy - <i>Mahure Y.R. and S.K. Zilpe</i>	04
5	Synthesis of Carbon Dot from Couropita Guianensis (Cannon Ball) Flower and applied for the Sensing of an anti-Diabetic drug Metformin.- <i>P. R. Khandagale, Dr. S. V. Nipane, Dr. S. R. Sabale, Dr. R. S. Dhabe.</i>	05
6	Morphological And Histological Cyclic Changes In Theovary Of Freshwater Fish : <i>Channa gachua, Dr. Ashwini G. Ghanbahadur, Prof. Y. K. Khillare</i>	06
7	Cordyceps militaris – An Important Medicinal Mushroom- <i>Trupti D. Kadam, Dr. Ashok V. Kharde.</i>	07
8	Morphometric Analysis Of Hiranyakeshi River, Sindhudurg District Using GIS Technology- <i>Aishwarya Pramod Hingmire, Shrikant Ghadage, Mayur Goud.</i>	08
9	Isolation of urease producing bacteria to produce biocement via MICP process.- <i>P. S. Rayate, B. A. Bhanjale, S. S Yeulkar</i>	09
10	Studies On Web Structure Of Two Spiders From Family Araneidae In Akola District <i>Satyavijay S. Dhande</i>	10
11	Attempts To Improve The Eye Dropper Deigne For Better Patient Compliance <i>Ms. Arte Aakanksha Sachin</i>	11
12	Aegle marmelos ash: A heterogeneous catalyst for Henry reaction <i>Rupesh C. Patil and Suresh S. Patil</i>	12
13	BMIM]-Glycine: A Sustainable Benchmark For Multicomponent Chromene Synthesis <i>Mr. Ashutosh A. Jagdale, Prin. (Dr.) Bhaskar V. Tamhankar and Prof. (Dr.) Suresh S. Patil</i>	13

110	Studies on Livestock Predation and Human Leopard (<i>Panthera pardus</i>) Conflicts in Shirala Tehasil of Sangli District Maharashtra, India. - Jadhav V.M	112
111	Epidermal Growth Factor accelerated wound contraction in wound licking permitted and prevented groups in sialoadenectomised mice.- Sirinbanu R. Matwal, Nitin D. Potphode, Vasant M. Patole and Madhuri V. Walvekar	113
112	A green and highly efficient synthesis of pyrazolopyranopyrimidines- Chandrakant M. Mang, Satyajit S. Jadhav, Vishal Y. Khule, Soham B. Khot, Sachinkumar K. Shinde, Megha U. Patil, Suresh S. Patil	114
113	Liquid – Liquid Extraction and Separation of Zirconium (IV) from Succinate Media and Its Separation from Other Toxic Metals- A. M. Nalawade, M. R. Nalawade, R. A. Nalawade, R.V. Shejawal, C. P. Mane	115
114	Synthesis, and Characterization of Zn Substituted Li–Ni Nano Ferrites- Dr.R.G.Kharabe, Miss A. Y. Sanadi and Mr.S.B.Vairat	116
115	Investigation of antiglycation and antioxidant potential of <i>Morus alba</i> and <i>Garcinia indica</i> plant leaves.- Satish G. Parte & A.U.Sutar	117
116	Nesting Site And Nesting Material Of House Crow (<i>Corvus splendens</i>) In Rajee Ramrao College Campus, Jath, Dist. Sangli (M.S.), India.-Dr. L.P. Saptal, Dr. S. B. Deshmukh, Dr. M. B. Sajjan, Mr. M. H. Karenavar	118
117	Green Synthesis, Characterization, Catalytic and Antibacterial Applications of ZnO Nanoparticles- N. P. Patila, Dr. D. S. Gaikwada, Dr. K. A. Undalea	119
118	Evaluation of E. Coli Contamination in Drinking Water in Chiplun City - Samruddhi Ghumare	120
119	Impact of anthropogenic activities on water quality and plankton communities in the Warana River- Priyanka Pharane	121
120	Brief review on <i>Gliricidia sepium</i> - Santosh Jagatap, Dr. B.S. Wali	122
121	"Synthesis And Spectroscopic Characterization Of Some Novel 2-Amino- 1,3,4-Thiadiazole"- More A. L., Dr. Chougule A. M.	123
122	"2-Amino- 1,3,4-Thiadiazole As An Antimicrobial Scaffold"- More A. L., Dr. Chougule A. M., J. V. Kuwar	124
123	Antifungal activity and Preliminary Phytochemical Analysis of Leaf Extracts of <i>Anodendron paniculatum</i> and <i>Ellertonia rheedii</i> Wight- Bommegowdha A Mauna, Manasa C. K., Dr. Parameshwar Naik T.	125
124	Inland water quality monitoring using sentinel-2 and Landsat-8: A Comparative Study on Different Lakes in Uttarakhand, India- Shalini, Rakesh Singh, Virendra Bahadur Singh	126
125	Impact Of Farmponds On Agricultural Development Of Nashik District - Handge Satish Balasaheb & Dr. Nikam Subhash Namdeo	127
126	Anticancer and Antioxidant β -D-Glucopyranose (1 \rightarrow 2) α -D-	128

Nesting Site and Nesting Material of House Crow (*Corvus splendens*) In Raje Ramrao College Campus, Jath, Dist. Sangli (M.S.), India.

Dr. L.P. Saptal^{1*}, Dr. S. B. Deshmukh², Dr. M. B. Sajjan³, Mr. M. H. Karenavar⁴

Asst. Prof. Department of Zoology, Raje Ramrao Mahavidyalaya, Jath.

*Corresponding author: saptallalita@gmail.com

Abstract

The present study was carried out the nesting site and nesting material of house crow in Raje Ramrao College campus, Jath. The total area of campus is 28.33 acres. Total 33 nests were reported to identify the nest materials. Out of these 6 nests on Neem tree, 16 on Nilgiri, 1 on Peepal, 8 on Ashoka tree and 2 on Coconut tree. The majority of nests which were observed on Nilgiri trees in between 2 to 3 branches. The observed nest materials are twigs, dried large sticks, dried grass, paper piece, pieces of wire, plastic threads, fibers of coconut tree. Plant leaf and unidentified material are also present inside of the nest. The majority of material which is used for constructing the nests are dried sticks and grasses. To identify the nest materials unused nest was observed.

The present work is focused on nesting sites and nesting material of *Carvus splendens* at because there is no detail study available in this campus area.

Keywords: Nesting site, nesting material, College campus, Maharashtra.

Chief Guest



Dr. Achyut Godbole
MD, Softexcel Consultancy



Hon. Abhaykumar Salunkhe
Executive President



Prof. D. T. Shirke
Vice Chancellor, SUK



Prof. P. S. Patil
Pro-Vice Chancellor, SUK



Hon. Shubhangi Gavade
Secretary



Hon. Kaustabh Gavade
Chief Executive Officer



Prin. Dr. R. V. Shejwal
Joint Secretary
(Administration)



Prin. S. M. Gavali
Joint Secretary (Finance)



Dr. Milind S. Hujare
Principal

Dr. Milind S. Hujare

Principal, PDVP Mahavidyalaya, Tasgaon. Dist. Sangli

Prin. (Dr.) R. R. Kumbhar

Vivekanand College, Kolhapur

I/C Prin. Prof. (Dr.) S. R. Ghatage

S.M.D.B.S. Mahavidyalaya, Miraj

I/C Prin. Prof. (Dr.) S. S. Patil

R. R. College, Jath

Prin. (Dr.) A. N. Patil

D. K. A. S. C. College, Ichalkaranji

Prin. (Dr.) J. S. Deshmukh

R. P. College, Osmanabad

I/C Prin. (Dr.) S. S. Desai

Smt. M. M. College, Panchgani

Conveners

Prof. S. K. Khade

Dr. A. N. Ambhore

Treasurers

Mr. P. V. Patil

Dr. P. B. Teli

Dr. S. K. Shinde

Co-conveners

Dr. J. S. Ghodake

Dr. S. D. Jadhav

Organizing Secretaries

Dr. A. P. Inamdar

Dr. M. U. Patil

Dr. R. A. Kalel

Coordinators

Prof. N. A. Kulkarni

Prof. S. A. Khabade

Technocrats

Mr. B. S. Harale

Prof. R. M. Ganeshwade

Dr. P. S. Bhandare

Local Organizing Committee

Mr. J. A. Yadav	Mr. V. J. Jadhav	Prof. T. K. Badame	Mr. P. R. Khade	Mr. R. B. Mankar	Dr. A. S. Wagh
Dr. S. J. Patil	Mr. A. R. Patil	Dr. V. D. Kumbhar	Mrs. P. R. Mirajkar	Mr. S. S. Gavil	Dr. A. G. Sonawale
Mr. A. K. Patil	Mr. D. Y. Sakhare	Mr. A. A. Jagdale	Ms. V. D. Jagdale	Ms. V. V. Patil	Mr. R. S. Mote
Mr. S. R. Ghogare	Dr. K. N. Patil	Dr. B. J. Kadam	Dr. A. M. Mali	Mr. A. S. Bagal	Mr. V. T. Kumbhar
Mr. D. S. Shinde	Ms. S. R. Mali	Dr. G. R. Patil	Dr. R. J. Gore	Mr. G. S. Pawar	Mr. J. H. Lavand
Mr. D. J. Nalawade	Mr. D. D. Patil	Mr. S. A. Patil	Dr. A. S. Magdum	Mr. V. R. Patil	Mr. V. M. Jadhav
Mr. R. S. Kumbhar	Dr. S. L. Andhelwar	Ms. S. D. Ghatage	Ms. P. A. Kashid	Ms. P. R. Zambre	Ms. P. S. Jadhav
Mr. A. H. Tarange	Ms. A. S. Yadav	Mr. S. M. Patil	Ms. N. V. More	Ms. S. G. Patil	Ms. D. M. Gosavi
Dr. M. M. Patil	Mr. S. A. Karande	Ms. S. S. Panari	Ms. S. M. Kolekar	Mrs. N. V. Kumbhar	Ms. S. P. Patil
Ms. S. S. Patil	Ms. S. S. Patil	Ms. P. V. Shinde	Mr. S. V. Mane	Ms. S. S. Patil	Ms. S. T. Wagh
Mr. A. A. Wagh					Ms. S. K. Patil
Mr. M. B. Kadam					Mr. S. P. Salunkhe
Mr. M. K. Patil					Mr. A. R. Lavand

All Teaching and non Teaching Staff PDVP Mahavidyalaya, Tasgaon.

Multidisciplinary Approach in Basic and Applied Sciences (MABAS - 2023)



“Dissemination of Education for Knowledge, Science & Culture”

- Shikshanmaharshi Dr. Babuji Salunkhe

Shri Swami Vivekanand Shikshan Sanstha Kolhapur's

Padmabhushan Dr. Vasantodada Patil Mahavidyalaya, Tasgaon

Dist.: Sangli (MS) India Pin : 416 312

Knowledge Partner

Department of Biotechnology, Shivaji University, Kolhapur

Third International Conference

On

“Multidisciplinary Approach in Basic and Applied Sciences (MABAS - 2023)”

(23rd & 24th February - 2023)

Souvenir

ISBN: 978-93-95369-30-5



TABLE OF CONTENTS

Sr. No.	Title	Page no.
1	Diversity of millipedes (myriapoda: diplopoda) in selected lateritic soil habitats in satara tehsil, western ghat, Maharashtra - <i>Shaikh N. A., Abdar M. R., Kengar S. B.</i>	01
2	“Peanut shell extract mediated Biogenic synthesis of palladium nanoparticles (PdNPs) and its application as a homogeneous catalyst for the Suzuki-Miyaura coupling”- <i>Pranoti P. Patil, Utkarsha B. Patil, Utkarsha U. Patil, Shashikant R. Sawant, Rahul A. Kalel</i>	02
3	A study on causes and impact of laterite mining on environment and on the life of Dhangarwada people in Kudchire village of Goa state.- <i>Mr. Vinay Takale</i>	03
4	Morphological Investigation of Rhyzopertha dominica Using Light Microscopy and Scanning Electron Microscopy - <i>Mahure Y.R. and S.K. Zilpe</i>	04
5	Synthesis of Carbon Dot from Couropita Guianensis (Cannon Ball) Flower and applied for the Sensing of an anti-Diabetic drug Metformin.- <i>P. R. Khandagale, Dr. S. V. Nipane, Dr. S. R. Sabale, Dr. R. S. Dhabe.</i>	05
6	Morphological And Histological Cyclic Changes In Theovary Of Freshwater Fish : <i>Channa gachua, Dr. Ashwini G. Ghanbahadur, Prof. Y. K. Khillare</i>	06
7	Cordyceps militaris – An Important Medicinal Mushroom- <i>Trupti D. Kadam, Dr. Ashok V. Kharde.</i>	07
8	Morphometric Analysis Of Hiranyakeshi River, Sindhudurg District Using GIS Technology- <i>Aishwarya Pramod Hingmire, Shrikant Ghadage, Mayur Goud.</i>	08
9	Isolation of urease producing bacteria to produce biocement via MICP process.- <i>P. S. Rayate, B. A. Bhanjale, S. S Yeulkar</i>	09
10	Studies On Web Structure Of Two Spiders From Family Araneidae In Akola District <i>Satyavijay S. Dhande</i>	10
11	Attempts To Improve The Eye Dropper Deigne For Better Patient Compliance <i>Ms. Arte Aakanksha Sachin</i>	11
12	Aegle marmelos ash: A heterogeneous catalyst for Henry reaction <i>Rupesh C. Patil and Suresh S. Patil</i>	12
13	BMIM]-Glycine: A Sustainable Benchmark For Multicomponent Chromene Synthesis <i>Mr. Ashutosh A. Jagdale, Prin. (Dr.) Bhaskar V. Tamhankar and Prof. (Dr.) Suresh S. Patil</i>	13

110	Studies on Livestock Predation and Human Leopard (<i>Panthera pardus</i>) Conflicts in Shirala Tehasil of Sangli District Maharashtra, India. - Jadhav V.M	112
111	Epidermal Growth Factor accelerated wound contraction in wound licking permitted and prevented groups in sialoadenectomised mice.- Sirinbanu R. Matwal, Nitin D. Potphode, Vasant M. Patole and Madhuri V. Walvekar	113
112	A green and highly efficient synthesis of pyrazolopyranopyrimidines- Chandrakant M. Mang, Satyajit S. Jadhav, Vishal Y. Khule, Soham B. Khot, Sachinkumar K. Shinde, Megha U. Patil, Suresh S. Patil	114
113	Liquid – Liquid Extraction and Separation of Zirconium (IV) from Succinate Media and Its Separation from Other Toxic Metals- A. M. Nalawade, M. R. Nalawade, R. A. Nalawade, R.V. Shejawal, C. P. Mane	115
114	Synthesis, and Characterization of Zn Substituted Li–Ni Nano Ferrites- Dr.R.G.Kharabe, Miss A. Y. Sanadi and Mr.S.B.Vairat	116
115	Investigation of antiglycation and antioxidant potential of <i>Morus alba</i> and <i>Garcinia indica</i> plant leaves.- Satish G. Parte & A.U.Sutar	117
116	Nesting Site And Nesting Material Of House Crow (<i>Corvus splendens</i>) In Rajee Ramrao College Campus, Jath, Dist. Sangli (M.S.), India.-Dr. L.P. Saptal, Dr. S. B. Deshmukh, Dr. M. B. Sajjan, Mr. M. H. Karenavar	118
117	Green Synthesis, Characterization, Catalytic and Antibacterial Applications of ZnO Nanoparticles- N. P. Patila, Dr. D. S. Gaikwada, Dr. K. A. Undalea	119
118	Evaluation of E. Coli Contamination in Drinking Water in Chiplun City - Samruddhi Ghumare	120
119	Impact of anthropogenic activities on water quality and plankton communities in the Warana River- Priyanka Pharane	121
120	Brief review on <i>Gliricidia sepium</i> - Santosh Jagatap, Dr. B.S. Wali	122
121	"Synthesis And Spectroscopic Characterization Of Some Novel 2-Amino- 1,3,4-Thiadiazole"- More A. L., Dr. Chougule A. M.	123
122	"2-Amino- 1,3,4-Thiadiazole As An Antimicrobial Scaffold"- More A. L., Dr. Chougule A. M., J. V. Kuwar	124
123	Antifungal activity and Preliminary Phytochemical Analysis of Leaf Extracts of <i>Anodendron paniculatum</i> and <i>Ellertonia rheedii</i> Wight- Bommegowdha A Mauna, Manasa C. K., Dr. Parameshwar Naik T.	125
124	Inland water quality monitoring using sentinel-2 and Landsat-8: A Comparative Study on Different Lakes in Uttarakhand, India- Shalini, Rakesh Singh, Virendra Bahadur Singh	126
125	Impact Of Farmponds On Agricultural Development Of Nashik District - Handge Satish Balasaheb & Dr. Nikam Subhash Namdeo	127
126	Anticancer and Antioxidant β -D-Glucopyranose (1 \rightarrow 2) α -D-	128

Nesting Site and Nesting Material of House Crow (*Corvus splendens*) In Raje Ramrao College Campus, Jath, Dist. Sangli (M.S.), India.

Dr. L.P. Saptal^{1*}, Dr. S. B. Deshmukh², Dr. M. B. Sajjan³, Mr. M. H. Karenavar⁴

Asst. Prof. Department of Zoology, Raje Ramrao Mahavidyalaya, Jath.

*Corresponding author: saptallalita@gmail.com

Abstract

The present study was carried out the nesting site and nesting material of house crow in Raje Ramrao College campus, Jath. The total area of campus is 28.33 acres. Total 33 nests were reported to identify the nest materials. Out of these 6 nests on Neem tree, 16 on Nilgiri, 1 on Peepal, 8 on Ashoka tree and 2 on Coconut tree. The majority of nests which were observed on Nilgiri trees in between 2 to 3 branches. The observed nest materials are twigs, dried large sticks, dried grass, paper piece, pieces of wire, plastic threads, fibers of coconut tree. Plant leaf and unidentified material are also present inside of the nest. The majority of material which is used for constructing the nests are dried sticks and grasses. To identify the nest materials unused nest was observed.

The present work is focused on nesting sites and nesting material of *Carvus splendens* at because there is no detail study available in this campus area.

Keywords: Nesting site, nesting material, College campus, Maharashtra.

Chief Guest



Dr. Achyut Godbole
MD, Softexcel Consultancy



Hon. Abhaykumar Salunkhe
Executive President



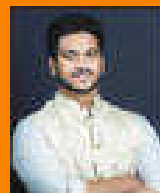
Prof. D. T. Shirke
Vice Chancellor, SUK



Prof. P. S. Patil
Pro-Vice Chancellor, SUK



Hon. Shubhangi Gavade
Secretary



Hon. Kaustabh Gavade
Chief Executive Officer



Prin. Dr. R. V. Shejwal
Joint Secretary
(Administration)



Prin. S. M. Gavali
Joint Secretary (Finance)



Dr. Milind S. Hujare
Principal

Dr. Milind S. Hujare

Principal, PDVP Mahavidyalaya, Tasgaon. Dist. Sangli

Prin. (Dr.) R. R. Kumbhar

Vivekanand College, Kolhapur

I/C Prin. Prof. (Dr.) S. R. Ghatage

S.M.D.B.S. Mahavidyalaya, Miraj

I/C Prin. Prof. (Dr.) S. S. Patil

R. R. College, Jath

Prin. (Dr.) A. N. Patil

D. K. A. S. C. College, Ichalkaranji

Prin. (Dr.) J. S. Deshmukh

R. P. College, Osmanabad

I/C Prin. (Dr.) S. S. Desai

Smt. M. M. College, Panchgani

Conveners

Prof. S. K. Khade

Dr. A. N. Ambhore

Treasurers

Mr. P. V. Patil

Dr. P. B. Teli

Dr. S. K. Shinde

Co-conveners

Dr. J. S. Ghodake

Dr. S. D. Jadhav

Organizing Secretaries

Dr. A. P. Inamdar

Dr. M. U. Patil

Dr. R. A. Kalel

Coordinators

Prof. N. A. Kulkarni

Prof. S. A. Khabade

Technocrats

Mr. B. S. Harale

Prof. R. M. Ganeshwade

Dr. P. S. Bhandare

Local Organizing Committee

Mr. J. A. Yadav	Mr. V. J. Jadhav	Prof. T. K. Badame	Mr. P. R. Khade	Mr. R. B. Mankar	Dr. A. S. Wagh
Dr. S. J. Patil	Mr. A. R. Patil	Dr. V. D. Kumbhar	Mrs. P. R. Mirajkar	Mr. S. S. Gavil	Dr. A. G. Sonawale
Mr. A. K. Patil	Mr. D. Y. Sakhare	Mr. A. A. Jagdale	Ms. V. D. Jagdale	Ms. V. V. Patil	Mr. R. S. Mote
Mr. S. R. Ghogare	Dr. K. N. Patil	Dr. B. J. Kadam	Dr. A. M. Mali	Mr. A. S. Bagal	Mr. V. T. Kumbhar
Mr. D. S. Shinde	Ms. S. R. Mali	Dr. G. R. Patil	Dr. R. J. Gore	Mr. G. S. Pawar	Mr. J. H. Lavand
Mr. D. J. Nalawade	Mr. D. D. Patil	Mr. S. A. Patil	Dr. A. S. Magdum	Mr. V. R. Patil	Mr. V. M. Jadhav
Mr. R. S. Kumbhar	Dr. S. L. Andhelwar	Ms. S. D. Ghatage	Ms. P. A. Kashid	Ms. P. R. Zambre	Ms. P. S. Jadhav
Mr. A. H. Tarange	Ms. A. S. Yadav	Mr. S. M. Patil	Ms. N. V. More	Ms. S. G. Patil	Ms. D. M. Gosavi
Dr. M. M. Patil	Mr. S. A. Karande	Ms. S. S. Panari	Ms. S. M. Kolekar	Mrs. N. V. Kumbhar	Ms. S. P. Patil
Ms. S. S. Patil	Ms. S. S. Patil	Ms. P. V. Shinde	Mr. S. V. Mane	Ms. S. S. Patil	Ms. S. T. Wagh
Mr. A. A. Wagh					Ms. S. K. Patil
Mr. M. B. Kadam					Mr. S. P. Salunkhe
Mr. M. K. Patil					Mr. A. R. Lavand

All Teaching and non Teaching Staff PDVP Mahavidyalaya, Tasgaon.



“Dissemination of Education for Knowledge, Science & Culture”

- Shikshanmaharshi Dr. Bapuji Salunkhe

Shri Swami Vivekanand Shikshan Sanstha Kolhapur's

Padmabhushan Dr. Vasantodada Patil Mahavidyalaya, Tasgaon

Dist.: Sangli (MS) India Pin : 416 312

Knowledge Partner

Department of Biotechnology, Shivaji University, Kolhapur

Third International Conference

On

“Multidisciplinary Approach in Basic and Applied Sciences (MABAS - 2023)”

(23rd & 24th February - 2023)

Souvenir

ISBN: 978-93-95369-30-5

Multidisciplinary Approach in Basic and Applied Sciences (MABAS - 2023)



TABLE OF CONTENTS

Sr. No.	Title	Page no.
1	Diversity of millipedes (myriapoda: diplopoda) in selected lateritic soil habitats in satara tehsil, western ghat, Maharashtra - <i>Shaikh N. A., Abdar M. R., Kengar S. B.</i>	01
2	“Peanut shell extract mediated Biogenic synthesis of palladium nanoparticles (PdNPs) and its application as a homogeneous catalyst for the Suzuki-Miyaura coupling”- <i>Pranoti P. Patil, Utkarsha B. Patil, Utkarsha U. Patil, Shashikant R. Sawant, Rahul A. Kalel</i>	02
3	A study on causes and impact of laterite mining on environment and on the life of Dhangarwada people in Kudchire village of Goa state.- <i>Mr. Vinay Takale</i>	03
4	Morphological Investigation of Rhyzopertha dominica Using Light Microscopy and Scanning Electron Microscopy - <i>Mahure Y.R. and S.K. Zilpe</i>	04
5	Synthesis of Carbon Dot from Couropita Guianensis (Cannon Ball) Flower and applied for the Sensing of an anti-Diabetic drug Metformin.- <i>P. R. Khandagale, Dr. S. V. Nipane, Dr. S. R. Sabale, Dr. R. S. Dhabe.</i>	05
6	Morphological And Histological Cyclic Changes In Theovary Of Freshwater Fish : <i>Channa gachua, Dr. Ashwini G. Ghanbahadur, Prof. Y. K. Khillare</i>	06
7	Cordyceps militaris – An Important Medicinal Mushroom- <i>Trupti D. Kadam, Dr. Ashok V. Kharde.</i>	07
8	Morphometric Analysis Of Hiranyakeshi River, Sindhudurg District Using GIS Technology- <i>Aishwarya Pramod Hingmire, Shrikant Ghadage, Mayur Goud.</i>	08
9	Isolation of urease producing bacteria to produce biocement via MICP process.- <i>P. S. Rayate, B. A. Bhanjale, S. S Yeulkar</i>	09
10	Studies On Web Structure Of Two Spiders From Family Araneidae In Akola District <i>Satyavijay S. Dhande</i>	10
11	Attempts To Improve The Eye Dropper Deigne For Better Patient Compliance <i>Ms. Arte Aakanksha Sachin</i>	11
12	Aegle marmelos ash: A heterogeneous catalyst for Henry reaction <i>Rupesh C. Patil and Suresh S. Patil</i>	12
13	BMIM]-Glycine: A Sustainable Benchmark For Multicomponent Chromene Synthesis <i>Mr. Ashutosh A. Jagdale, Prin. (Dr.) Bhaskar V. Tamhankar and Prof. (Dr.) Suresh S. Patil</i>	13

110	Studies on Livestock Predation and Human Leopard (<i>Panthera pardus</i>) Conflicts in Shirala Tehasil of Sangli District Maharashtra, India. - Jadhav V.M	112
111	Epidermal Growth Factor accelerated wound contraction in wound licking permitted and prevented groups in sialoadenectomised mice.- Sirinbanu R. Matwal, Nitin D. Potphode, Vasant M. Patole and Madhuri V. Walvekar	113
112	A green and highly efficient synthesis of pyrazolopyranopyrimidines- Chandrakant M. Mang, Satyajit S. Jadhav, Vishal Y. Khule, Soham B. Khot, Sachinkumar K. Shinde, Megha U. Patil, Suresh S. Patil	114
113	Liquid – Liquid Extraction and Separation of Zirconium (IV) from Succinate Media and Its Separation from Other Toxic Metals- A. M. Nalawade, M. R. Nalawade, R. A. Nalawade, R.V. Shejawal, C. P. Mane	115
114	Synthesis, and Characterization of Zn Substituted Li–Ni Nano Ferrites- Dr.R.G.Kharabe, Miss A. Y. Sanadi and Mr.S.B.Vairat	116
115	Investigation of antiglycation and antioxidant potential of <i>Morus alba</i> and <i>Garcinia indica</i> plant leaves.- Satish G. Parte & A.U.Sutar	117
116	Nesting Site And Nesting Material Of House Crow (<i>Corvus splendens</i>) In Rajee Ramrao College Campus, Jath, Dist. Sangli (M.S.), India.-Dr. L.P. Saptal, Dr. S. B. Deshmukh, Dr. M. B. Sajjan, Mr. M. H. Karenavar	118
117	Green Synthesis, Characterization, Catalytic and Antibacterial Applications of ZnO Nanoparticles- N. P. Patila, Dr. D. S. Gaikwada, Dr. K. A. Undalea	119
118	Evaluation of E. Coli Contamination in Drinking Water in Chiplun City - Samruddhi Ghumare	120
119	Impact of anthropogenic activities on water quality and plankton communities in the Warana River- Priyanka Pharane	121
120	Brief review on <i>Gliricidia sepium</i> - Santosh Jagatap, Dr. B.S. Wali	122
121	"Synthesis And Spectroscopic Characterization Of Some Novel 2-Amino- 1,3,4-Thiadiazole"- More A. L., Dr. Chougule A. M.	123
122	"2-Amino- 1,3,4-Thiadiazole As An Antimicrobial Scaffold"- More A. L., Dr. Chougule A. M., J. V. Kuwar	124
123	Antifungal activity and Preliminary Phytochemical Analysis of Leaf Extracts of <i>Anodendron paniculatum</i> and <i>Ellertonia rheedii</i> Wight- Bommegowdha A Mauna, Manasa C. K., Dr. Parameshwar Naik T.	125
124	Inland water quality monitoring using sentinel-2 and Landsat-8: A Comparative Study on Different Lakes in Uttarakhand, India- Shalini, Rakesh Singh, Virendra Bahadur Singh	126
125	Impact Of Farmponds On Agricultural Development Of Nashik District - Handge Satish Balasaheb & Dr. Nikam Subhash Namdeo	127
126	Anticancer and Antioxidant β -D-Glucopyranose (1 \rightarrow 2) α -D-	128

Nesting Site and Nesting Material of House Crow (*Corvus splendens*) In Raje Ramrao College Campus, Jath, Dist. Sangli (M.S.), India.

Dr. L.P. Saptal^{1*}, Dr. S. B. Deshmukh², Dr. M. B. Sajjan³, Mr. M. H. Karenavar⁴

Asst. Prof. Department of Zoology, Raje Ramrao Mahavidyalaya, Jath.

*Corresponding author: saptallalita@gmail.com

Abstract

The present study was carried out the nesting site and nesting material of house crow in Raje Ramrao College campus, Jath. The total area of campus is 28.33 acres. Total 33 nests were reported to identify the nest materials. Out of these 6 nests on Neem tree, 16 on Nilgiri, 1 on Peepal, 8 on Ashoka tree and 2 on Coconut tree. The majority of nests which were observed on Nilgiri trees in between 2 to 3 branches. The observed nest materials are twigs, dried large sticks, dried grass, paper piece, pieces of wire, plastic threads, fibers of coconut tree. Plant leaf and unidentified material are also present inside of the nest. The majority of material which is used for constructing the nests are dried sticks and grasses. To identify the nest materials unused nest was observed.

The present work is focused on nesting sites and nesting material of *Carvus splendens* at because there is no detail study available in this campus area.

Keywords: Nesting site, nesting material, College campus, Maharashtra.

Chief Guest



Dr. Achyut Godbole
MD, Softexcel Consultancy



Hon. Abhaykumar Salunkhe
Executive President



Prof. D. T. Shirke
Vice Chancellor, SUK



Prof. P. S. Patil
Pro-Vice Chancellor, SUK



Hon. Shubhangi Gavade
Secretary



Hon. Kaustabh Gavade
Chief Executive Officer



Prin. Dr. R. V. Shejwal
Joint Secretary
(Administration)



Prin. S. M. Gavali
Joint Secretary (Finance)



Dr. Milind S. Hujare
Principal

Dr. Milind S. Hujare

Principal, PDVP Mahavidyalaya, Tasgaon. Dist. Sangli

Prin. (Dr.) R. R. Kumbhar

Vivekanand College, Kolhapur

I/C Prin. Prof. (Dr.) S. R. Ghatage

S.M.D.B.S. Mahavidyalaya, Miraj

I/C Prin. Prof. (Dr.) S. S. Patil

R. R. College, Jath

Prin. (Dr.) A. N. Patil

D. K. A. S. C. College, Ichalkaranji

Prin. (Dr.) J. S. Deshmukh

R. P. College, Osmanabad

I/C Prin. (Dr.) S. S. Desai

Smt. M. M. College, Panchgani

Conveners

Prof. S. K. Khade

Dr. A. N. Ambhore

Treasurers

Mr. P. V. Patil

Dr. P. B. Teli

Dr. S. K. Shinde

Co-conveners

Dr. J. S. Ghodake

Dr. S. D. Jadhav

Organizing Secretaries

Dr. A. P. Inamdar

Dr. M. U. Patil

Dr. R. A. Kalel

Coordinators

Prof. N. A. Kulkarni

Prof. S. A. Khabade

Technocrats

Mr. B. S. Harale

Prof. R. M. Ganeshwade

Dr. P. S. Bhandare

Local Organizing Committee

Mr. J. A. Yadav	Mr. V. J. Jadhav	Prof. T. K. Badame	Mr. P. R. Khade	Mr. R. B. Mankar	Dr. A. S. Wagh
Dr. S. J. Patil	Mr. A. R. Patil	Dr. V. D. Kumbhar	Mrs. P. R. Mirajkar	Mr. S. S. Gavil	Dr. A. G. Sonawale
Mr. A. K. Patil	Mr. D. Y. Sakhare	Mr. A. A. Jagdale	Ms. V. D. Jagdale	Ms. V. V. Patil	Mr. R. S. Mote
Mr. S. R. Ghogare	Dr. K. N. Patil	Dr. B. J. Kadam	Dr. A. M. Mali	Mr. A. S. Bagal	Mr. V. T. Kumbhar
Mr. D. S. Shinde	Ms. S. R. Mali	Dr. G. R. Patil	Dr. R. J. Gore	Mr. G. S. Pawar	Mr. J. H. Lavand
Mr. D. J. Nalawade	Mr. D. D. Patil	Mr. S. A. Patil	Dr. A. S. Magdum	Mr. V. R. Patil	Mr. V. M. Jadhav
Mr. R. S. Kumbhar	Dr. S. L. Andhelwar	Ms. S. D. Ghatage	Ms. P. A. Kashid	Ms. P. R. Zambre	Ms. P. S. Jadhav
Mr. A. H. Tarange	Ms. A. S. Yadav	Mr. S. M. Patil	Ms. N. V. More	Ms. S. G. Patil	Ms. D. M. Gosavi
Dr. M. M. Patil	Mr. S. A. Karande	Ms. S. S. Panari	Ms. S. M. Kolekar	Mrs. N. V. Kumbhar	Ms. S. P. Patil
Ms. S. S. Patil	Ms. S. S. Patil	Ms. P. V. Shinde	Mr. S. V. Mane	Ms. S. S. Patil	Ms. S. T. Wagh
Mr. A. A. Wagh					Ms. S. K. Patil
Mr. M. B. Kadam					Mr. S. P. Salunkhe
Mr. M. K. Patil					Mr. A. R. Lavand

All Teaching and non Teaching Staff PDVP Mahavidyalaya, Tasgaon.

Multidisciplinary Approach in Basic and Applied Sciences (MABAS - 2023)



“Dissemination of Education for Knowledge, Science & Culture”

- Shikshanmaharshi Dr. Bapuji Salunkhe

Shri Swami Vivekanand Shikshan Sanstha Kolhapur's

Padmabhushan Dr. Vasantodada Patil Mahavidyalaya, Tasgaon

Dist.: Sangli (MS) India Pin : 416 312

Knowledge Partner

Department of Biotechnology, Shivaji University, Kolhapur

Third International Conference

On

“Multidisciplinary Approach in Basic and Applied Sciences (MABAS - 2023)”

(23rd & 24th February - 2023)

Souvenir

ISBN: 978-93-95369-30-5



TABLE OF CONTENTS

Sr. No.	Title	Page no.
1	Diversity of millipedes (myriapoda: diplopoda) in selected lateritic soil habitats in satara tehsil, western ghat, Maharashtra - <i>Shaikh N. A., Abdar M. R., Kengar S. B.</i>	01
2	“Peanut shell extract mediated Biogenic synthesis of palladium nanoparticles (PdNPs) and its application as a homogeneous catalyst for the Suzuki-Miyaura coupling”- <i>Pranoti P. Patil, Utkarsha B. Patil, Utkarsha U. Patil, Shashikant R. Sawant, Rahul A. Kalel</i>	02
3	A study on causes and impact of laterite mining on environment and on the life of Dhangarwada people in Kudchire village of Goa state.- <i>Mr. Vinay Takale</i>	03
4	Morphological Investigation of Rhyzopertha dominica Using Light Microscopy and Scanning Electron Microscopy - <i>Mahure Y.R. and S.K. Zilpe</i>	04
5	Synthesis of Carbon Dot from Couropita Guianensis (Cannon Ball) Flower and applied for the Sensing of an anti-Diabetic drug Metformin.- <i>P. R. Khandagale, Dr. S. V. Nipane, Dr. S. R. Sabale, Dr. R. S. Dhabe.</i>	05
6	Morphological And Histological Cyclic Changes In Theovary Of Freshwater Fish : <i>Channa gachua, Dr. Ashwini G. Ghanbahadur, Prof. Y. K. Khillare</i>	06
7	Cordyceps militaris – An Important Medicinal Mushroom- <i>Trupti D. Kadam, Dr. Ashok V. Kharde.</i>	07
8	Morphometric Analysis Of Hiranyakeshi River, Sindhudurg District Using GIS Technology- <i>Aishwarya Pramod Hingmire, Shrikant Ghadage, Mayur Goud.</i>	08
9	Isolation of urease producing bacteria to produce biocement via MICP process.- <i>P. S. Rayate, B. A. Bhanjale, S. S Yeulkar</i>	09
10	Studies On Web Structure Of Two Spiders From Family Araneidae In Akola District <i>Satyavijay S. Dhande</i>	10
11	Attempts To Improve The Eye Dropper Deigne For Better Patient Compliance <i>Ms. Arte Aakanksha Sachin</i>	11
12	Aegle marmelos ash: A heterogeneous catalyst for Henry reaction <i>Rupesh C. Patil and Suresh S. Patil</i>	12
13	BMIM]-Glycine: A Sustainable Benchmark For Multicomponent Chromene Synthesis <i>Mr. Ashutosh A. Jagdale, Prin. (Dr.) Bhaskar V. Tamhankar and Prof. (Dr.) Suresh S. Patil</i>	13

183	General Assessment Of Solid Waste Management In India- Dr. Arjun Shivaji Wagh, Mrs. Dipali Pol	185
184	The application of solar technologies for sustainable development of agricultural sector in India- Dr. Arjun Shivaji Wagh, Mrs. Dipali Pol	186
185	Human Development Index (HDI): A Study of Satara District of Maharashtra (India)- Dr. Arjun Shivaji Wagh, Mr. Sushil Yadav	187
186	Synthesis, Characterization and catalytic application of Al-MCM-41 for the preparation of 2H-indazolo[2,1-b]phthalazine-trione derivatives Jayshri V. Mendhea and Santosh L. Khillare	188
187	Effect of Carbon and Nitrogen on The Growth of <i>Sclerotium rolfsii</i> Sacc., Causing Fruit Rot of Ridge Gourd- S. L. Soudagar, N. K. Khandare, M. B. Waghmare	189
188	Protective Effect Of <i>Petroselinum Crispum</i> Extract On Histology Of Sublingual Gland Of- Galactose Induced Aged Male Mice- S. N. Khandare	190
189	Seasonal Variations in Physico-Chemical Parameters of Bhagyanagar Lake in Khanapur Tehsil, District Sangli (M.S), India.- P. P. Patil, S. A. Khabade and G. K. Sontakke	191
190	A Study on Butterflies (Rhopalocera) Diversity in Raje Ramrao Mahavidyalaya Campus, Jath, Sangli District, Maharashtra State, India.- M. B. Sajjan, R. A. Lavate, M. H. Karenavar and P. B. Teli	192
191	Seasonal Variations in Physico-Chemical Parameters of Bhagyanagar lake in Khanapur Tehsil, District Sangli (M.S), India.- Patil Punam, Khabade, S. A and Sontakke G. K	193
192	Study of Diversity of Birds in Chandgad City and Near Area of Chandgad, Dist- Kolhapur (Maharashtra)- Kedari N. Nikam	194
193	Vegetative Morphology Study For species Identification- Ranjan B. Kalbande	195
194	Ionic Liquid Catalyzed Green and Efficient One Pot Four Component Synthesis of Pyranopyrazoles - S. S. Kadama, P. R. Kharade, D. S. Gaikwada, S. S. Desai	196
195	Use of natural colors in pharmaceutical preparations- Tejaswini Padale	197
196	In vitro Screening and Molecular Docking of Some Euphorbiaceae L. Plants as Anti-HIV- Shravani Majgaonkar, Dhanshree Rajput, Aaditya Chayani, Dr. Sandeep Patil Shankar Joshi.	198
197	Control of Insect Pest with the help of Spiders in the Orange Fields of Jalgaon jamod Tahsil, District Buldhana, Maharashtra State- Dr. AMIT BABANRAO VAIRALE	199
198	[P-DABCO]Cl/PEG-400: An efficient recyclable catalytic system for the synthesis of quinoline derivatives- Bhosale D. Y., Londhe B. S.	200
199	<i>In vitro</i> Screening and Molecular Docking of Some Euphorbiaceae L. Plants as Anti-HIV- Shravani Majgaonkar, Dhanshree Rajput, Aaditya Chayani, Dr. Sandeep Patil, Shankar Joshi.	201

A Study on Butterflies (Rhopalocera) Diversity in Raje Ramrao Mahavidyalaya Campus, Jath, Sangli District, Maharashtra State, India.

^{1*}**M. B. Sajjan**, ²R. A. Lavate, ¹M. H. Karenavar and ³P. B. Teli

^{1*,1}Department of Zoology, Raje Ramrao Mahavidyalaya, Jath, Dist-Sangli, (MS)

²Department of Botany, Raje Ramrao Mahavidyalaya, Jath, Dist-Sangli, (MS)

³Department of Zoology, P. D. V. P. Mahavidyalaya, Tasgaon, Dist-Sangli, (MS)

**Corresponding author E-mail: sajjan_mb73@yahoo.com*

Abstract

A study on butterfly diversity was carried out in Raje Ramrao College Campus, Jath Tehsil of Sangli district, Maharashtra state, India. Field studies were made to record the diversity of butterflies at college campus in Jath during 2020 to 2022, a total of 35 species of butterflies were recorded from 30 genera belong to 4 families. Butterflies are wonderfully diverse in shape, size and their colours. They also perform some important ecological significance. The most important function they involved in pollination. They also act as an ecological indicator.

The study area (College campus) is rich in butterfly diversity and further research could be conducted to obtain more details and documentation on butterfly diversity for the conservation and development of butterfly garden.

Keywords: Diversity, Butterfly, Conservation, Campus

Chief Guest



Dr. Achyut Godbole
MD, Softexcel Consultancy



Hon. Abhaykumar Salunkhe
Executive President



Prof. D. T. Shirke
Vice Chancellor, SUK



Prof. P. S. Patil
Pro-Vice Chancellor, SUK



Hon. Shubhangi Gavade
Secretary



Hon. Kaustabh Gavade
Chief Executive Officer



Prin. Dr. R. V. Shejwal
Joint Secretary
(Administration)



Prin. S. M. Gavali
Joint Secretary (Finance)



Dr. Milind S. Hujare
Principal

Dr. Milind S. Hujare

Principal, PDVP Mahavidyalaya, Tasgaon. Dist. Sangli

Prin. (Dr.) R. R. Kumbhar

Vivekanand College, Kolhapur

I/C Prin. Prof. (Dr.) S. R. Ghatage

S.M.D.B.S. Mahavidyalaya, Miraj

I/C Prin. Prof. (Dr.) S. S. Patil

R. R. College, Jath

Prin. (Dr.) A. N. Patil

D. K. A. S. C. College, Ichalkaranji

Prin. (Dr.) J. S. Deshmukh

R. P. College, Osmanabad

I/C Prin. (Dr.) S. S. Desai

Smt. M. M. College, Panchgani

Conveners

Prof. S. K. Khade

Dr. A. N. Ambhore

Treasurers

Mr. P. V. Patil

Dr. P. B. Teli

Dr. S. K. Shinde

Co-conveners

Dr. J. S. Ghodake

Dr. S. D. Jadhav

Organizing Secretaries

Dr. A. P. Inamdar

Dr. M. U. Patil

Dr. R. A. Kalel

Coordinators

Prof. N. A. Kulkarni

Prof. S. A. Khabade

Technocrats

Mr. B. S. Harale

Prof. R. M. Ganeshwade

Dr. P. S. Bhandare

Local Organizing Committee

Mr. J. A. Yadav	Mr. V. J. Jadhav	Prof. T. K. Badame	Mr. P. R. Khade	Mr. R. B. Mankar	Dr. A. S. Wagh
Dr. S. J. Patil	Mr. A. R. Patil	Dr. V. D. Kumbhar	Mrs. P. R. Mirajkar	Mr. S. S. Gavil	Dr. A. G. Sonawale
Mr. A. K. Patil	Mr. D. Y. Sakhare	Mr. A. A. Jagdale	Ms. V. D. Jagdale	Ms. V. V. Patil	Mr. R. S. Mote
Mr. S. R. Ghogare	Dr. K. N. Patil	Dr. B. J. Kadam	Dr. A. M. Mali	Mr. A. S. Bagal	Mr. V. T. Kumbhar
Mr. D. S. Shinde	Ms. S. R. Mali	Dr. G. R. Patil	Dr. R. J. Gore	Mr. G. S. Pawar	Mr. J. H. Lavand
Mr. D. J. Nalawade	Mr. D. D. Patil	Mr. S. A. Patil	Dr. A. S. Magdum	Mr. V. R. Patil	Mr. V. M. Jadhav
Mr. R. S. Kumbhar	Dr. S. L. Andhelwar	Ms. S. D. Ghatage	Ms. P. A. Kashid	Ms. P. R. Zambre	Ms. P. S. Jadhav
Mr. A. H. Tarange	Ms. A. S. Yadav	Mr. S. M. Patil	Ms. N. V. More	Ms. S. G. Patil	Ms. D. M. Gosavi
Dr. M. M. Patil	Mr. S. A. Karande	Ms. S. S. Panari	Ms. S. M. Kolekar	Mrs. N. V. Kumbhar	Ms. S. P. Patil
Ms. S. S. Patil	Ms. S. S. Patil	Ms. P. V. Shinde	Mr. S. V. Mane	Ms. S. S. Patil	Ms. S. T. Wagh
Mr. A. A. Wagh					Ms. S. K. Patil
Mr. M. B. Kadam					Mr. S. P. Salunkhe
Mr. M. K. Patil					Mr. A. R. Lavand

All Teaching and non Teaching Staff PDVP Mahavidyalaya, Tasgaon.

Multidisciplinary Approach in Basic and Applied Sciences (MABAS - 2023)



“Dissemination of Education for Knowledge, Science & Culture”

- Shikshanmaharshi Dr. Babuji Salunkhe

Shri Swami Vivekanand Shikshan Sanstha Kolhapur's

Padmabhushan Dr. Vasantodada Patil Mahavidyalaya, Tasgaon

Dist.: Sangli (MS) India Pin : 416 312

Knowledge Partner

Department of Biotechnology, Shivaji University, Kolhapur

Third International Conference

On

“Multidisciplinary Approach in Basic and Applied Sciences (MABAS - 2023)”

(23rd & 24th February - 2023)

Souvenir

ISBN: 978-93-95369-30-5



TABLE OF CONTENTS

Sr. No.	Title	Page no.
1	Diversity of millipedes (myriapoda: diplopoda) in selected lateritic soil habitats in satara tehsil, western ghat, Maharashtra - <i>Shaikh N. A., Abdar M. R., Kengar S. B.</i>	01
2	“Peanut shell extract mediated Biogenic synthesis of palladium nanoparticles (PdNPs) and its application as a homogeneous catalyst for the Suzuki-Miyaura coupling”- <i>Pranoti P. Patil, Utkarsha B. Patil, Utkarsha U. Patil, Shashikant R. Sawant, Rahul A. Kalel</i>	02
3	A study on causes and impact of laterite mining on environment and on the life of Dhangarwada people in Kudchire village of Goa state.- <i>Mr. Vinay Takale</i>	03
4	Morphological Investigation of Rhyzopertha dominica Using Light Microscopy and Scanning Electron Microscopy - <i>Mahure Y.R. and S.K. Zilpe</i>	04
5	Synthesis of Carbon Dot from Couropita Guianensis (Cannon Ball) Flower and applied for the Sensing of an anti-Diabetic drug Metformin.- <i>P. R. Khandagale, Dr. S. V. Nipane, Dr. S. R. Sabale, Dr. R. S. Dhabe.</i>	05
6	Morphological And Histological Cyclic Changes In Theovary Of Freshwater Fish : <i>Channa gachua, Dr. Ashwini G. Ghanbahadur, Prof. Y. K. Khillare</i>	06
7	Cordyceps militaris – An Important Medicinal Mushroom- <i>Trupti D. Kadam, Dr. Ashok V. Kharde.</i>	07
8	Morphometric Analysis Of Hiranyakeshi River, Sindhudurg District Using GIS Technology- <i>Aishwarya Pramod Hingmire, Shrikant Ghadage, Mayur Goud.</i>	08
9	Isolation of urease producing bacteria to produce biocement via MICP process.- <i>P. S. Rayate, B. A. Bhanjale, S. S Yeulkar</i>	09
10	Studies On Web Structure Of Two Spiders From Family Araneidae In Akola District <i>Satyavijay S. Dhande</i>	10
11	Attempts To Improve The Eye Dropper Deigne For Better Patient Compliance <i>Ms. Arte Aakanksha Sachin</i>	11
12	Aegle marmelos ash: A heterogeneous catalyst for Henry reaction <i>Rupesh C. Patil and Suresh S. Patil</i>	12
13	BMIM]-Glycine: A Sustainable Benchmark For Multicomponent Chromene Synthesis <i>Mr. Ashutosh A. Jagdale, Prin. (Dr.) Bhaskar V. Tamhankar and Prof. (Dr.) Suresh S. Patil</i>	13

183	General Assessment Of Solid Waste Management In India- Dr. Arjun Shivaji Wagh, Mrs. Dipali Pol	185
184	The application of solar technologies for sustainable development of agricultural sector in India- Dr. Arjun Shivaji Wagh, Mrs. Dipali Pol	186
185	Human Development Index (HDI): A Study of Satara District of Maharashtra (India)- Dr. Arjun Shivaji Wagh, Mr. Sushil Yadav	187
186	Synthesis, Characterization and catalytic application of Al-MCM-41 for the preparation of 2H-indazolo[2,1-b]phthalazine-trione derivatives Jayshri V. Mendhea and Santosh L. Khillare	188
187	Effect of Carbon and Nitrogen on The Growth of Sclerotium rolfsii Sacc., Causing Fruit Rot of Ridge Gourd- S. L. Soudagar, N. K. Khandare, M. B. Waghmare	189
188	Protective Effect Of Petroselinum Crispum Extract On Histology Of Sublingual Gland Of- Galactose Induced Aged Male Mice- S. N. Khandare	190
189	Seasonal Variations in Physico-Chemical Parameters of Bhagyanagar Lake in Khanapur Tehsil, District Sangli (M.S), India.- P. P. Patil, S. A. Khabade and G. K. Sontakke	191
190	A Study on Butterflies (Rhopalocera) Diversity in Raje Ramrao Mahavidyalaya Campus, Jath, Sangli District, Maharashtra State, India.- M. B. Sajjan, R. A. Lavate, M. H. Karenavar and P. B. Teli	192
191	Seasonal Variations in Physico-Chemical Parameters of Bhagyanagar lake in Khanapur Tehsil, District Sangli (M.S), India.- Patil Punam, Khabade, S. A and Sontakke G. K	193
192	Study of Diversity of Birds in Chandgad City and Near Area of Chandgad, Dist- Kolhapur (Maharashtra)- Kedari N. Nikam	194
193	Vegetative Morphology Study Forspecies Identification- Ranjan B. Kalbande	195
194	Ionic Liquid Catalyzed Green and Efficient One Pot Four Component Synthesis of Pyranopyrazoles - S. S. Kadama, P. R. Kharade, D. S. Gaikwada, S. S. Desai	196
195	Use of natural colors in pharmaceutical preparations- Tejaswini Padale	197
196	In vitro Screening and Molecular Docking of Some Euphorbiaceae L. Plants as Anti-HIV- Shravani Majgaonkar, Dhanshree Rajput, Aaditya Chayani, Dr. Sandeep Patil Shankar Joshi.	198
197	Control of Insect Pest with the help of Spiders in the Orange Fields of Jalgaon jamod Tahsil, District Buldhana, Maharashtra State- Dr. AMIT BABANRAO VAIRALE	199
198	[P-DABCO]Cl/PEG-400: An efficient recyclable catalytic system for the synthesis of quinoline derivatives- Bhosale D. Y., Londhe B. S.	200
199	<i>In vitro</i> Screening and Molecular Docking of Some Euphorbiaceae L. Plants as Anti-HIV- Shravani Majgaonkar, Dhanshree Rajput, Aaditya Chayani, Dr. Sandeep Patil, Shankar Joshi.	201

A Study on Butterflies (Rhopalocera) Diversity in Raje Ramrao Mahavidyalaya Campus, Jath, Sangli District, Maharashtra State, India.

^{1*}M. B. Sajjan, ²R. A. Lavate, ¹M. H. Karenavar and ³P. B. Teli

^{1*,1}Department of Zoology, Raje Ramrao Mahavidyalaya, Jath, Dist-Sangli, (MS)

²Department of Botany, Raje Ramrao Mahavidyalaya, Jath, Dist-Sangli, (MS)

³Department of Zoology, P. D. V. P. Mahavidyalaya, Tasgaon, Dist-Sangli, (MS)

**Corresponding author E-mail: sajjan_mb73@yahoo.com*

Abstract

A study on butterfly diversity was carried out in Raje Ramrao College Campus, Jath Tehsil of Sangli district, Maharashtra state, India. Field studies were made to record the diversity of butterflies at college campus in Jath during 2020 to 2022, a total of 35 species of butterflies were recorded from 30 genera belong to 4 families. Butterflies are wonderfully diverse in shape, size and their colours. They also perform some important ecological significance. The most important function they involved in pollination. They also act as an ecological indicator.

The study area (College campus) is rich in butterfly diversity and further research could be conducted to obtain more details and documentation on butterfly diversity for the conservation and development of butterfly garden.

Keywords: Diversity, Butterfly, Conservation, Campus

Chief Guest



Dr. Achyut Godbole
MD, Softexcel Consultancy



Hon. Abhaykumar Salunkhe
Executive President



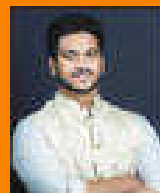
Prof. D. T. Shirke
Vice Chancellor, SUK



Prof. P. S. Patil
Pro-Vice Chancellor, SUK



Hon. Shubhangi Gavade
Secretary



Hon. Kaustabh Gavade
Chief Executive Officer



Prin. Dr. R. V. Shejwal
Joint Secretary
(Administration)



Prin. S. M. Gavali
Joint Secretary (Finance)



Dr. Milind S. Hujare
Principal

Dr. Milind S. Hujare

Principal, PDVP Mahavidyalaya, Tasgaon. Dist. Sangli

Prin. (Dr.) R. R. Kumbhar

Vivekanand College, Kolhapur

I/C Prin. Prof. (Dr.) S. R. Ghatage

S.M.D.B.S. Mahavidyalaya, Miraj

I/C Prin. Prof. (Dr.) S. S. Patil

R. R. College, Jath

Prin. (Dr.) A. N. Patil

D. K. A. S. C. College, Ichalkaranji

Prin. (Dr.) J. S. Deshmukh

R. P. College, Osmanabad

I/C Prin. (Dr.) S. S. Desai

Smt. M. M. College, Panchgani

Conveners

Prof. S. K. Khade

Dr. A. N. Ambhore

Treasurers

Mr. P. V. Patil

Dr. P. B. Teli

Dr. S. K. Shinde

Co-conveners

Dr. J. S. Ghodake

Dr. S. D. Jadhav

Organizing Secretaries

Dr. A. P. Inamdar

Dr. M. U. Patil

Dr. R. A. Kalel

Coordinators

Prof. N. A. Kulkarni

Prof. S. A. Khabade

Technocrats

Mr. B. S. Harale

Prof. R. M. Ganeshwade

Dr. P. S. Bhandare

Local Organizing Committee

Mr. J. A. Yadav	Mr. V. J. Jadhav	Prof. T. K. Badame	Mr. P. R. Khade	Mr. R. B. Mankar	Dr. A. S. Wagh
Dr. S. J. Patil	Mr. A. R. Patil	Dr. V. D. Kumbhar	Mrs. P. R. Mirajkar	Mr. S. S. Gavil	Dr. A. G. Sonawale
Mr. A. K. Patil	Mr. D. Y. Sakhare	Mr. A. A. Jagdale	Ms. V. D. Jagdale	Ms. V. V. Patil	Mr. R. S. Mote
Mr. S. R. Ghogare	Dr. K. N. Patil	Dr. B. J. Kadam	Dr. A. M. Mali	Mr. A. S. Bagal	Mr. V. T. Kumbhar
Mr. D. S. Shinde	Ms. S. R. Mali	Dr. G. R. Patil	Dr. R. J. Gore	Mr. G. S. Pawar	Mr. J. H. Lavand
Mr. D. J. Nalawade	Mr. D. D. Patil	Mr. S. A. Patil	Dr. A. S. Magdum	Mr. V. R. Patil	Mr. V. M. Jadhav
Mr. R. S. Kumbhar	Dr. S. L. Andhelwar	Ms. S. D. Ghatage	Ms. P. A. Kashid	Ms. P. R. Zambre	Ms. P. S. Jadhav
Mr. A. H. Tarange	Ms. A. S. Yadav	Mr. S. M. Patil	Ms. N. V. More	Ms. S. G. Patil	Ms. D. M. Gosavi
Dr. M. M. Patil	Mr. S. A. Karande	Ms. S. S. Panari	Ms. S. M. Kolekar	Mrs. N. V. Kumbhar	Ms. S. P. Patil
Ms. S. S. Patil	Ms. S. S. Patil	Ms. P. V. Shinde	Mr. S. V. Mane	Ms. S. S. Patil	Ms. S. T. Wagh
Mr. A. A. Wagh					Ms. S. K. Patil
Mr. M. B. Kadam					Mr. S. P. Salunkhe
Mr. M. K. Patil					Mr. A. R. Lavand

All Teaching and non Teaching Staff PDVP Mahavidyalaya, Tasgaon.

Multidisciplinary Approach in Basic and Applied Sciences (MABAS - 2023)



“Dissemination of Education for Knowledge, Science & Culture”

- Shikshanmaharshi Dr. Bapuji Salunkhe

Shri Swami Vivekanand Shikshan Sanstha Kolhapur's

Padmabhushan Dr. Vasantodada Patil Mahavidyalaya, Tasgaon

Dist.: Sangli (MS) India Pin : 416 312

Knowledge Partner

Department of Biotechnology, Shivaji University, Kolhapur

Third International Conference

On

“Multidisciplinary Approach in Basic and Applied Sciences (MABAS - 2023)”

(23rd & 24th February - 2023)

Souvenir

ISBN: 978-93-95369-30-5



TABLE OF CONTENTS

Sr. No.	Title	Page no.
1	Diversity of millipedes (myriapoda: diplopoda) in selected lateritic soil habitats in satara tehsil, western ghat, Maharashtra - <i>Shaikh N. A., Abdar M. R., Kengar S. B.</i>	01
2	“Peanut shell extract mediated Biogenic synthesis of palladium nanoparticles (PdNPs) and its application as a homogeneous catalyst for the Suzuki-Miyaura coupling”- <i>Pranoti P. Patil, Utkarsha B. Patil, Utkarsha U. Patil, Shashikant R. Sawant, Rahul A. Kalel</i>	02
3	A study on causes and impact of laterite mining on environment and on the life of Dhangarwada people in Kudchire village of Goa state.- <i>Mr. Vinay Takale</i>	03
4	Morphological Investigation of Rhyzopertha dominica Using Light Microscopy and Scanning Electron Microscopy - <i>Mahure Y.R. and S.K. Zilpe</i>	04
5	Synthesis of Carbon Dot from Couropita Guianensis (Cannon Ball) Flower and applied for the Sensing of an anti-Diabetic drug Metformin.- <i>P. R. Khandagale, Dr. S. V. Nipane, Dr. S. R. Sabale, Dr. R. S. Dhabe.</i>	05
6	Morphological And Histological Cyclic Changes In Theovary Of Freshwater Fish : <i>Channa gachua, Dr. Ashwini G. Ghanbahadur, Prof. Y. K. Khillare</i>	06
7	Cordyceps militaris – An Important Medicinal Mushroom- <i>Trupti D. Kadam, Dr. Ashok V. Kharde.</i>	07
8	Morphometric Analysis Of Hiranyakeshi River, Sindhudurg District Using GIS Technology- <i>Aishwarya Pramod Hingmire, Shrikant Ghadage, Mayur Goud.</i>	08
9	Isolation of urease producing bacteria to produce biocement via MICP process.- <i>P. S. Rayate, B. A. Bhanjale, S. S Yeulkar</i>	09
10	Studies On Web Structure Of Two Spiders From Family Araneidae In Akola District <i>Satyavijay S. Dhande</i>	10
11	Attempts To Improve The Eye Dropper Deigne For Better Patient Compliance <i>Ms. Arte Aakanksha Sachin</i>	11
12	Aegle marmelos ash: A heterogeneous catalyst for Henry reaction <i>Rupesh C. Patil and Suresh S. Patil</i>	12
13	BMIM]-Glycine: A Sustainable Benchmark For Multicomponent Chromene Synthesis <i>Mr. Ashutosh A. Jagdale, Prin. (Dr.) Bhaskar V. Tamhankar and Prof. (Dr.) Suresh S. Patil</i>	13

183	General Assessment Of Solid Waste Management In India- <i>Dr. Arjun Shivaji Wagh, Mrs. Dipali Pol</i>	185
184	The application of solar technologies for sustainable development of agricultural sector in India- <i>Dr. Arjun Shivaji Wagh, Mrs. Dipali Pol</i>	186
185	Human Development Index (HDI): A Study of Satara District of Maharashtra (India)- <i>Dr. Arjun Shivaji Wagh, Mr. Sushil Yadav</i>	187
186	Synthesis, Characterization and catalytic application of Al-MCM-41 for the preparation of 2H-indazolo[2,1-b]phthalazine-trione derivatives <i>Jayshri V. Mendhea and Santosh L. Khillare</i>	188
187	Effect of Carbon and Nitrogen on The Growth of <i>Sclerotium rolfsii</i> Sacc., Causing Fruit Rot of Ridge Gourd- <i>S. L. Soudagar, N. K. Khandare, M. B. Waghmare</i>	189
188	Protective Effect Of <i>Petroselinum Crispum</i> Extract On Histology Of Sublingual Gland Of- <i>Galactose Induced Aged Male Mice- S. N. Khandare</i>	190
189	Seasonal Variations in Physico-Chemical Parameters of Bhagyanagar Lake in Khanapur Tehsil, District Sangli (M.S), India.- <i>P. P. Patil, S. A. Khabade and G. K. Sontakke</i>	191
190	A Study on Butterflies (Rhopalocera) Diversity in Raje Ramrao Mahavidyalaya Campus, Jath, Sangli District, Maharashtra State, India.- M. B. Sajjan, R. A. Lavate, M. H. Karenavar and P. B. Teli	192
191	Seasonal Variations in Physico-Chemical Parameters of Bhagyanagar lake in Khanapur Tehsil, District Sangli (M.S), India.- <i>Patil Punam, Khabade, S. A and Sontakke G. K</i>	193
192	Study of Diversity of Birds in Chandgad City and Near Area of Chandgad, Dist- Kolhapur (Maharashtra)- <i>Kedari N. Nikam</i>	194
193	Vegetative Morphology Study For species Identification- <i>Ranjan B. Kalbande</i>	195
194	Ionic Liquid Catalyzed Green and Efficient One Pot Four Component Synthesis of Pyranopyrazoles - <i>S. S. Kadama, P. R. Kharade, D. S. Gaikwada, S. S. Desai</i>	196
195	Use of natural colors in pharmaceutical preparations- <i>Tejaswini Padale</i>	197
196	In vitro Screening and Molecular Docking of Some Euphorbiaceae L. Plants as Anti-HIV- <i>Shravani Majgaonkar, Dhanshree Rajput, Aaditya Chayani, Dr. Sandeep Patil Shankar Joshi.</i>	198
197	Control of Insect Pest with the help of Spiders in the Orange Fields of Jalgaon jamod Tahsil, District Buldhana, Maharashtra State- <i>Dr. AMIT BABANRAO VAIRALE</i>	199
198	[P-DABCO]Cl/PEG-400: An efficient recyclable catalytic system for the synthesis of quinoline derivatives- <i>Bhosale D. Y., Londhe B. S.</i>	200
199	<i>In vitro</i> Screening and Molecular Docking of Some Euphorbiaceae L. Plants as Anti-HIV- <i>Shravani Majgaonkar, Dhanshree Rajput, Aaditya Chayani, Dr. Sandeep Patil, Shankar Joshi.</i>	201

A Study on Butterflies (Rhopalocera) Diversity in Raje Ramrao Mahavidyalaya Campus, Jath, Sangli District, Maharashtra State, India.

^{1*}M. B. Sajjan, ²R. A. Lavate, ¹M. H. Karennavar and ³P. B. Teli

^{1*,1}Department of Zoology, Raje Ramrao Mahavidyalaya, Jath, Dist-Sangli, (MS)

²Department of Botany, Raje Ramrao Mahavidyalaya, Jath, Dist-Sangli, (MS)

³Department of Zoology, P. D. V. P. Mahavidyalaya, Tasgaon, Dist-Sangli, (MS)

**Corresponding author E-mail: sajjan_mb73@yahoo.com*

Abstract

A study on butterfly diversity was carried out in Raje Ramrao College Campus, Jath Tehsil of Sangli district, Maharashtra state, India. Field studies were made to record the diversity of butterflies at college campus in Jath during 2020 to 2022, a total of 35 species of butterflies were recorded from 30 genera belong to 4 families. Butterflies are wonderfully diverse in shape, size and their colours. They also perform some important ecological significance. The most important function they involved in pollination. They also act as an ecological indicator.

The study area (College campus) is rich in butterfly diversity and further research could be conducted to obtain more details and documentation on butterfly diversity for the conservation and development of butterfly garden.

Keywords: Diversity, Butterfly, Conservation, Campus

Chief Guest



Dr. Achyut Godbole
MD, Softexcel Consultancy



Hon. Abhaykumar Salunkhe
Executive President



Prof. D. T. Shirke
Vice Chancellor, SUK



Prof. P. S. Patil
Pro-Vice Chancellor, SUK



Hon. Shubhangi Gavade
Secretary



Hon. Kaustabh Gavade
Chief Executive Officer



Prin. Dr. R. V. Shejwal
Joint Secretary
(Administration)



Prin. S. M. Gavali
Joint Secretary (Finance)



Dr. Milind S. Hujare
Principal

Dr. Milind S. Hujare

Principal, PDVP Mahavidyalaya, Tasgaon. Dist. Sangli

Prin. (Dr.) R. R. Kumbhar

Vivekanand College, Kolhapur

I/C Prin. Prof. (Dr.) S. R. Ghatage

S.M.D.B.S. Mahavidyalaya, Miraj

I/C Prin. Prof. (Dr.) S. S. Patil

R. R. College, Jath

Prin. (Dr.) A. N. Patil

D. K. A. S. C. College, Ichalkaranji

Prin. (Dr.) J. S. Deshmukh

R. P. College, Osmanabad

I/C Prin. (Dr.) S. S. Desai

Smt. M. M. College, Panchgani

Conveners

Prof. S. K. Khade

Dr. A. N. Ambhore

Treasurers

Mr. P. V. Patil

Dr. P. B. Teli

Dr. S. K. Shinde

Co-conveners

Dr. J. S. Ghodake

Dr. S. D. Jadhav

Organizing Secretaries

Dr. A. P. Inamdar

Dr. M. U. Patil

Dr. R. A. Kalel

Coordinators

Prof. N. A. Kulkarni

Prof. S. A. Khabade

Technocrats

Mr. B. S. Harale

Prof. R. M. Ganeshwade

Dr. P. S. Bhandare

Local Organizing Committee

Mr. J. A. Yadav	Mr. V. J. Jadhav	Prof. T. K. Badame	Mr. P. R. Khade	Mr. R. B. Mankar	Dr. A. S. Wagh
Dr. S. J. Patil	Mr. A. R. Patil	Dr. V. D. Kumbhar	Mrs. P. R. Mirajkar	Mr. S. S. Gavil	Dr. A. G. Sonawale
Mr. A. K. Patil	Mr. D. Y. Sakhare	Mr. A. A. Jagdale	Ms. V. D. Jagdale	Ms. V. V. Patil	Mr. R. S. Mote
Mr. S. R. Ghogare	Dr. K. N. Patil	Dr. B. J. Kadam	Dr. A. M. Mali	Mr. A. S. Bagal	Mr. V. T. Kumbhar
Mr. D. S. Shinde	Ms. S. R. Mali	Dr. G. R. Patil	Dr. R. J. Gore	Mr. G. S. Pawar	Mr. J. H. Lavand
Mr. D. J. Nalawade	Mr. D. D. Patil	Mr. S. A. Patil	Dr. A. S. Magdum	Mr. V. R. Patil	Mr. V. M. Jadhav
Mr. R. S. Kumbhar	Dr. S. L. Andhelwar	Ms. S. D. Ghatage	Ms. P. A. Kashid	Ms. P. R. Zambre	Ms. P. S. Jadhav
Mr. A. H. Tarange	Ms. A. S. Yadav	Mr. S. M. Patil	Ms. N. V. More	Ms. S. G. Patil	Ms. D. M. Gosavi
Dr. M. M. Patil	Mr. S. A. Karande	Ms. S. S. Panari	Ms. S. M. Kolekar	Mrs. N. V. Kumbhar	Ms. S. P. Patil
Ms. S. S. Patil	Ms. S. S. Patil	Ms. P. V. Shinde	Mr. S. V. Mane	Ms. S. S. Patil	Ms. S. T. Wagh
Mr. A. A. Wagh					Ms. S. K. Patil
Mr. M. B. Kadam					Mr. S. P. Salunkhe
Mr. M. K. Patil					Mr. A. R. Lavand

All Teaching and non Teaching Staff PDVP Mahavidyalaya, Tasgaon.

Multidisciplinary Approach in Basic and Applied Sciences (MABAS - 2023)



“Dissemination of Education for Knowledge, Science & Culture”

- Shikshanmaharshi Dr. Bapuji Salunkhe

Shri Swami Vivekanand Shikshan Sanstha Kolhapur's

Padmabhushan Dr. Vasantodada Patil Mahavidyalaya, Tasgaon

Dist.: Sangli (MS) India Pin : 416 312

Knowledge Partner

Department of Biotechnology, Shivaji University, Kolhapur

Third International Conference

On

“Multidisciplinary Approach in Basic and Applied Sciences (MABAS - 2023)”

(23rd & 24th February - 2023)

Souvenir

ISBN: 978-93-95369-30-5



TABLE OF CONTENTS

Sr. No.	Title	Page no.
1	Diversity of millipedes (myriapoda: diplopoda) in selected lateritic soil habitats in satara tehsil, western ghat, Maharashtra - <i>Shaikh N. A., Abdar M. R., Kengar S. B.</i>	01
2	“Peanut shell extract mediated Biogenic synthesis of palladium nanoparticles (PdNPs) and its application as a homogeneous catalyst for the Suzuki-Miyaura coupling”- <i>Pranoti P. Patil, Utkarsha B. Patil, Utkarsha U. Patil, Shashikant R. Sawant, Rahul A. Kalel</i>	02
3	A study on causes and impact of laterite mining on environment and on the life of Dhangarwada people in Kudchire village of Goa state.- <i>Mr. Vinay Takale</i>	03
4	Morphological Investigation of Rhyzopertha dominica Using Light Microscopy and Scanning Electron Microscopy - <i>Mahure Y.R. and S.K. Zilpe</i>	04
5	Synthesis of Carbon Dot from Couropita Guianensis (Cannon Ball) Flower and applied for the Sensing of an anti-Diabetic drug Metformin.- <i>P. R. Khandagale, Dr. S. V. Nipane, Dr. S. R. Sabale, Dr. R. S. Dhabe.</i>	05
6	Morphological And Histological Cyclic Changes In Theovary Of Freshwater Fish : <i>Channa gachua, Dr. Ashwini G. Ghanbahadur, Prof. Y. K. Khillare</i>	06
7	Cordyceps militaris – An Important Medicinal Mushroom- <i>Trupti D. Kadam, Dr. Ashok V. Kharde.</i>	07
8	Morphometric Analysis Of Hiranyakeshi River, Sindhudurg District Using GIS Technology- <i>Aishwarya Pramod Hingmire, Shrikant Ghadage, Mayur Goud.</i>	08
9	Isolation of urease producing bacteria to produce biocement via MICP process.- <i>P. S. Rayate, B. A. Bhanjale, S. S Yeulkar</i>	09
10	Studies On Web Structure Of Two Spiders From Family Araneidae In Akola District <i>Satyavijay S. Dhande</i>	10
11	Attempts To Improve The Eye Dropper Deigne For Better Patient Compliance <i>Ms. Arte Aakanksha Sachin</i>	11
12	Aegle marmelos ash: A heterogeneous catalyst for Henry reaction <i>Rupesh C. Patil and Suresh S. Patil</i>	12
13	BMIM]-Glycine: A Sustainable Benchmark For Multicomponent Chromene Synthesis <i>Mr. Ashutosh A. Jagdale, Prin. (Dr.) Bhaskar V. Tamhankar and Prof. (Dr.) Suresh S. Patil</i>	13

183	General Assessment Of Solid Waste Management In India- Dr. Arjun Shivaji Wagh, Mrs. Dipali Pol	185
184	The application of solar technologies for sustainable development of agricultural sector in India- Dr. Arjun Shivaji Wagh, Mrs. Dipali Pol	186
185	Human Development Index (HDI): A Study of Satara District of Maharashtra (India)- Dr. Arjun Shivaji Wagh, Mr. Sushil Yadav	187
186	Synthesis, Characterization and catalytic application of Al-MCM-41 for the preparation of 2H-indazolo[2,1-b]phthalazine-trione derivatives Jayshri V. Mendhea and Santosh L. Khillare	188
187	Effect of Carbon and Nitrogen on The Growth of <i>Sclerotium rolfsii</i> Sacc., Causing Fruit Rot of Ridge Gourd- S. L. Soudagar, N. K. Khandare, M. B. Waghmare	189
188	Protective Effect Of <i>Petroselinum Crispum</i> Extract On Histology Of Sublingual Gland Of- Galactose Induced Aged Male Mice- S. N. Khandare	190
189	Seasonal Variations in Physico-Chemical Parameters of Bhagyanagar Lake in Khanapur Tehsil, District Sangli (M.S), India.- P. P. Patil, S. A. Khabade and G. K. Sontakke	191
190	A Study on Butterflies (Rhopalocera) Diversity in Raje Ramrao Mahavidyalaya Campus, Jath, Sangli District, Maharashtra State, India.- M. B. Sajjan, R. A. Lavate, M. H. Karenavar and P. B. Teli	192
191	Seasonal Variations in Physico-Chemical Parameters of Bhagyanagar lake in Khanapur Tehsil, District Sangli (M.S), India.- Patil Punam, Khabade, S. A and Sontakke G. K	193
192	Study of Diversity of Birds in Chandgad City and Near Area of Chandgad, Dist- Kolhapur (Maharashtra)- Kedari N. Nikam	194
193	Vegetative Morphology Study For species Identification- Ranjan B. Kalbande	195
194	Ionic Liquid Catalyzed Green and Efficient One Pot Four Component Synthesis of Pyranopyrazoles - S. S. Kadama, P. R. Kharade, D. S. Gaikwada, S. S. Desai	196
195	Use of natural colors in pharmaceutical preparations- Tejaswini Padale	197
196	In vitro Screening and Molecular Docking of Some Euphorbiaceae L. Plants as Anti-HIV- Shravani Majgaonkar, Dhanshree Rajput, Aaditya Chayani, Dr. Sandeep Patil Shankar Joshi.	198
197	Control of Insect Pest with the help of Spiders in the Orange Fields of Jalgaon jamod Tahsil, District Buldhana, Maharashtra State- Dr. AMIT BABANRAO VAIRALE	199
198	[P-DABCO]Cl/PEG-400: An efficient recyclable catalytic system for the synthesis of quinoline derivatives- Bhosale D. Y., Londhe B. S.	200
199	<i>In vitro</i> Screening and Molecular Docking of Some Euphorbiaceae L. Plants as Anti-HIV- Shravani Majgaonkar, Dhanshree Rajput, Aaditya Chayani, Dr. Sandeep Patil, Shankar Joshi.	201

A Study on Butterflies (Rhopalocera) Diversity in Raje Ramrao Mahavidyalaya Campus, Jath, Sangli District, Maharashtra State, India.

^{1*}M. B. Sajjan, ²R. A. Lavate, ¹M. H. Karenavar and ³P. B. Teli

^{1*,1}Department of Zoology, Raje Ramrao Mahavidyalaya, Jath, Dist-Sangli, (MS)

²Department of Botany, Raje Ramrao Mahavidyalaya, Jath, Dist-Sangli, (MS)

³Department of Zoology, P. D. V. P. Mahavidyalaya, Tasgaon, Dist-Sangli, (MS)

**Corresponding author E-mail: sajjan_mb73@yahoo.com*

Abstract

A study on butterfly diversity was carried out in Raje Ramrao College Campus, Jath Tehsil of Sangli district, Maharashtra state, India. Field studies were made to record the diversity of butterflies at college campus in Jath during 2020 to 2022, a total of 35 species of butterflies were recorded from 30 genera belong to 4 families. Butterflies are wonderfully diverse in shape, size and their colours. They also perform some important ecological significance. The most important function they involved in pollination. They also act as an ecological indicator.

The study area (College campus) is rich in butterfly diversity and further research could be conducted to obtain more details and documentation on butterfly diversity for the conservation and development of butterfly garden.

Keywords: Diversity, Butterfly, Conservation, Campus

Chief Guest



Dr. Achyut Godbole
MD, Softexcel Consultancy



Hon. Abhaykumar Salunkhe
Executive President



Prof. D. T. Shirke
Vice Chancellor, SUK



Prof. P. S. Patil
Pro-Vice Chancellor, SUK



Hon. Shubhangi Gavade
Secretary



Hon. Kaustabh Gavade
Chief Executive Officer



Prin. Dr. R. V. Shejwal
Joint Secretary
(Administration)



Prin. S. M. Gavali
Joint Secretary (Finance)



Dr. Milind S. Hujare
Principal

Dr. Milind S. Hujare

Principal, PDVP Mahavidyalaya, Tasgaon. Dist. Sangli

Prin. (Dr.) R. R. Kumbhar

Vivekanand College, Kolhapur

I/C Prin. Prof. (Dr.) S. R. Ghatage

S.M.D.B.S. Mahavidyalaya, Miraj

I/C Prin. Prof. (Dr.) S. S. Patil

R. R. College, Jath

Prin. (Dr.) A. N. Patil

D. K. A. S. C. College, Ichalkaranji

Prin. (Dr.) J. S. Deshmukh

R. P. College, Osmanabad

I/C Prin. (Dr.) S. S. Desai

Smt. M. M. College, Panchgani

Conveners

Prof. S. K. Khade

Dr. A. N. Ambhore

Treasurers

Mr. P. V. Patil

Dr. P. B. Teli

Dr. S. K. Shinde

Co-conveners

Dr. J. S. Ghodake

Dr. S. D. Jadhav

Organizing Secretaries

Dr. A. P. Inamdar

Dr. M. U. Patil

Dr. R. A. Kalel

Coordinators

Prof. N. A. Kulkarni

Prof. S. A. Khabade

Technocrats

Mr. B. S. Harale

Prof. R. M. Ganeshwade

Dr. P. S. Bhandare

Local Organizing Committee

Mr. J. A. Yadav	Mr. V. J. Jadhav	Prof. T. K. Badame	Mr. P. R. Khade	Mr. R. B. Mankar	Dr. A. S. Wagh
Dr. S. J. Patil	Mr. A. R. Patil	Dr. V. D. Kumbhar	Mrs. P. R. Mirajkar	Mr. S. S. Gavil	Dr. A. G. Sonawale
Mr. A. K. Patil	Mr. D. Y. Sakhare	Mr. A. A. Jagdale	Ms. V. D. Jagdale	Ms. V. V. Patil	Mr. R. S. Mote
Mr. S. R. Ghogare	Dr. K. N. Patil	Dr. B. J. Kadam	Dr. A. M. Mali	Mr. A. S. Bagal	Mr. V. T. Kumbhar
Mr. D. S. Shinde	Ms. S. R. Mali	Dr. G. R. Patil	Dr. R. J. Gore	Mr. G. S. Pawar	Mr. J. H. Lavand
Mr. D. J. Nalawade	Mr. D. D. Patil	Mr. S. A. Patil	Dr. A. S. Magdum	Mr. V. R. Patil	Mr. V. M. Jadhav
Mr. R. S. Kumbhar	Dr. S. L. Andhelwar	Ms. S. D. Ghatage	Ms. P. A. Kashid	Ms. P. R. Zambre	Ms. P. S. Jadhav
Mr. A. H. Tarange	Ms. A. S. Yadav	Mr. S. M. Patil	Ms. N. V. More	Ms. S. G. Patil	Ms. D. M. Gosavi
Dr. M. M. Patil	Mr. S. A. Karande	Ms. S. S. Panari	Ms. S. M. Kolekar	Mrs. N. V. Kumbhar	Ms. S. P. Patil
Ms. S. S. Patil	Ms. S. S. Patil	Ms. P. V. Shinde	Mr. S. V. Mane	Ms. S. S. Patil	Ms. S. T. Wagh
Mr. A. A. Wagh					Ms. S. K. Patil
Mr. M. B. Kadam					Mr. S. P. Salunkhe
Mr. M. K. Patil					Mr. A. R. Lavand

All Teaching and non Teaching Staff PDVP Mahavidyalaya, Tasgaon.

Multidisciplinary Approach in Basic and Applied Sciences (MABAS - 2023)



“Dissemination of Education for Knowledge, Science & Culture”

- Shikshanmaharshi Dr. Bapuji Salunkhe

Shri Swami Vivekanand Shikshan Sanstha Kolhapur's

Padmabhushan Dr. Vasantodada Patil Mahavidyalaya, Tasgaon

Dist.: Sangli (MS) India Pin : 416 312

Knowledge Partner

Department of Biotechnology, Shivaji University, Kolhapur

Third International Conference

On

“Multidisciplinary Approach in Basic and Applied Sciences (MABAS - 2023)”

(23rd & 24th February - 2023)

Souvenir

ISBN: 978-93-95369-30-5



TABLE OF CONTENTS

Sr. No.	Title	Page no.
1	Diversity of millipedes (myriapoda: diplopoda) in selected lateritic soil habitats in satara tehsil, western ghat, Maharashtra - <i>Shaikh N. A., Abdar M. R., Kengar S. B.</i>	01
2	“Peanut shell extract mediated Biogenic synthesis of palladium nanoparticles (PdNPs) and its application as a homogeneous catalyst for the Suzuki-Miyaura coupling”- <i>Pranoti P. Patil, Utkarsha B. Patil, Utkarsha U. Patil, Shashikant R. Sawant, Rahul A. Kalel</i>	02
3	A study on causes and impact of laterite mining on environment and on the life of Dhangarwada people in Kudchire village of Goa state.- <i>Mr. Vinay Takale</i>	03
4	Morphological Investigation of Rhyzopertha dominica Using Light Microscopy and Scanning Electron Microscopy - <i>Mahure Y.R. and S.K. Zilpe</i>	04
5	Synthesis of Carbon Dot from Couropita Guianensis (Cannon Ball) Flower and applied for the Sensing of an anti-Diabetic drug Metformin.- <i>P. R. Khandagale, Dr. S. V. Nipane, Dr. S. R. Sabale, Dr. R. S. Dhabe.</i>	05
6	Morphological And Histological Cyclic Changes In Theovary Of Freshwater Fish : <i>Channa gachua, Dr. Ashwini G. Ghanbahadur, Prof. Y. K. Khillare</i>	06
7	Cordyceps militaris – An Important Medicinal Mushroom- <i>Trupti D. Kadam, Dr. Ashok V. Kharde.</i>	07
8	Morphometric Analysis Of Hiranyakeshi River, Sindhudurg District Using GIS Technology- <i>Aishwarya Pramod Hingmire, Shrikant Ghadage, Mayur Goud.</i>	08
9	Isolation of urease producing bacteria to produce biocement via MICP process.- <i>P. S. Rayate, B. A. Bhanjale, S. S Yeulkar</i>	09
10	Studies On Web Structure Of Two Spiders From Family Araneidae In Akola District <i>Satyavijay S. Dhande</i>	10
11	Attempts To Improve The Eye Dropper Deigne For Better Patient Compliance <i>Ms. Arte Aakanksha Sachin</i>	11
12	Aegle marmelos ash: A heterogeneous catalyst for Henry reaction <i>Rupesh C. Patil and Suresh S. Patil</i>	12
13	BMIM]-Glycine: A Sustainable Benchmark For Multicomponent Chromene Synthesis <i>Mr. Ashutosh A. Jagdale, Prin. (Dr.) Bhaskar V. Tamhankar and Prof. (Dr.) Suresh S. Patil</i>	13

	performance- Komal P. Patil & Vishwas Y. Deshpande	
30	Health Fitness and Wellness- Miss. Komal Prakash Jadhav	31
31	Abhrak Bhasma and SiO ₂ Mediated Protection of Phospholipid Turnover in Carbon Tetrachloride Induced Acute Hepato-Steatosis and Allied Nephrotoxicity Showing Male Albino Rat”- Parashuram B. Teli and Aruna A. Kanase	32
32	Synthesis of chromium-D-phenylalanine complexa nd exploring its effects on reproduction and development in Drosophila melanogaster- Mallinath S. Kalshetti and Shivsharan B. Dhadde	33
33	Effect Of Am Fungi On Protein, Chlorophyll And Enzyme Activity In Finger Millet Under Salt Stress- S. V. HAJARE, DR. A. A. KULKARNI	34
34	Synthesis and Screening of Multifunctional Potential of C-3 Substituted Coumarin Derivatives- Anees Pangal and Khursheed Ahmed	35
35	Aquatic Biodiversity of Nimbavade Reservoir of Sangli District, Maharashtra, India- Alka P. Inamdr	36
36	Biodiversity of aerobiocomponents with reference to groundnut crop at Patan - M. R. Shinde	37
37	Cobalt Oxide (Co ₃ O ₄) Thin Films for Supercapacitor Application- Avdhut Sutar, Jayshree Patil and Sachin Pawar	38
38	Exploring Anti-Inflammatory Properties Of Indian Herbs For Treating Rheumatoid Arthritis- Aayushi Bhakta, Ph.D Biotechnology, Shri Guru Ram Rai University, Dehradun	39
39	Review of Charging systems for Electric Vehicle- Nayan J. Kotmire, Dr. A.B. Kakade	40
40	Click reaction for 1, 4-disubstituted 1, 2, 3 triazoles- Arvind Pawar A. T. Birajdar Gajanan Rashinkar Suresh Patil	41
41	Cyber Security - Zahra Jabeen’ Prof. Dr. B.K. Mishra	42
42	Diversity of Wetland Avifauna from Kadegaon Tahsil, Sangli District, Maharashtra. Jyoti S. Sathe and Vijay S. Jadhav	43
43	DNA barcoding and phylogenetics of freshwater fish fauna of Upper Krishna River, Maharashtra- Sachin K. Shelake, Suraj A. Sudney, Abhijeet R. Pathare, Pratik P. Badade, Rahul R. Tayade, Vishwas Y. Deshpande	44
44	Studies On The Electrical And Magnetic Properties Of Magnesium Ferrite With Samarium And Dysprosium Substitutes- R. N. Kumbhar, T. J. Shinde, V. L. Mathe, P.P. Chikode, J. S. Ghodake	45
45	Evaluation of E. Coli Contamination in Drinking Water in Chiplun City - Samruddhi Ghumare	46
46	Morphological And Anatomical Studiesoniphigenia Stellatablatt. Dr. A. P. Patil, Manish Kumar Karnani and M.S. Sawant	47

Click reaction for 1, 4-disubstituted 1, 2, 3 triazoles

Arvind Pawar^a A. T. Birajdar^a Gajanan Rashinkar^b Suresh*Patil

^aDepartment of Chemistry, S. M. Dr. Bapuji Salunkhe, Miraj ,
Dist. Sangli., 416312, M. S., India

^bDepartment of Chemistry, Shivaji University, Kolhapur, 416004, M. S., India
E-mail: gsr_chem@unishivaji.ac.in

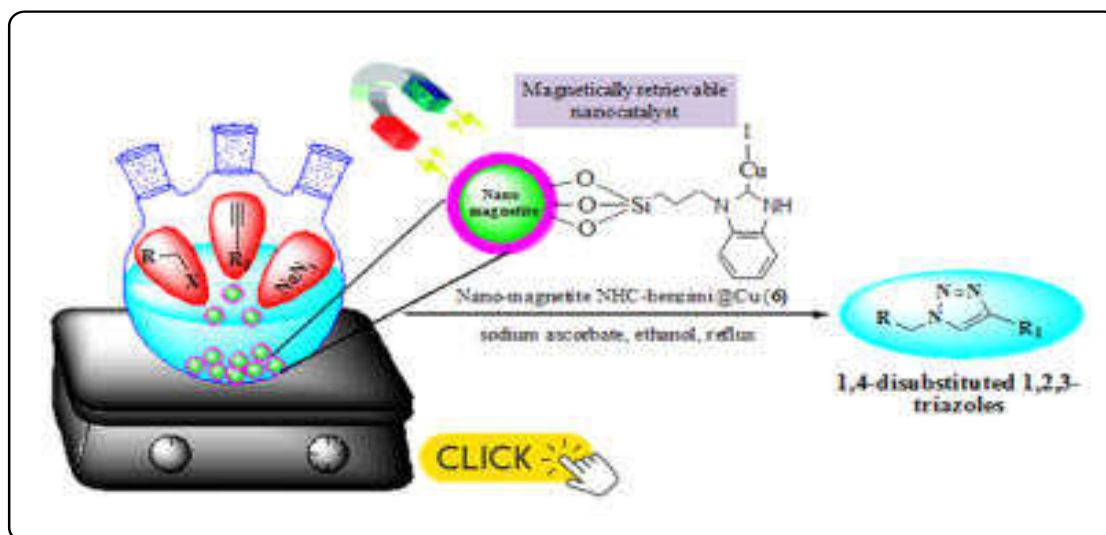
^cDepartment of Chemistry, Raje Ramrao College. Jath, Dist. Sangli, 416410, M. S. India

*Corresponding author E-mail: sanyujapatil@yahoo.com

Abstract

In this paper, we report a novel magnetically separable silica coated copper nano-magnetite NHC-benzimidazole@Cu complex as heterogeneous catalyst for the multicomponent click reaction via Huisgen 1,3-dipolar cycloaddition reaction of alkyl or aryl halide, sodium azide and terminal alkyne, which affords various 1,4-disubstituted 1,2,3-triazoles. The multistep repaired nano catalyst has been characterized by various spectroscopic methods such as FT-IR, TGA, EDX, XRD, TEM and VSM. The heterogeneous nano catalyst structures coated on the copper surface are responsible for the excellent catalyst performances in the reaction. The reusability of the catalyst makes the present protocol more fascinating from an environmental and economic point of view.

Graphic ABSTRACT



Keywords: Magnetically retrievable nanocatalyst · Click reaction · Copper iodide · 1,2,3-triazoles · Reusability

Chief Guest



Dr. Achyut Godbole
MD, Softexcel Consultancy



Hon. Abhaykumar Salunkhe
Executive President



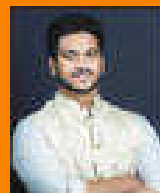
Prof. D. T. Shirke
Vice Chancellor, SUK



Prof. P. S. Patil
Pro-Vice Chancellor, SUK



Hon. Shubhangi Gavade
Secretary



Hon. Kaustabh Gavade
Chief Executive Officer



Prin. Dr. R. V. Shejwal
Joint Secretary
(Administration)



Prin. S. M. Gavali
Joint Secretary (Finance)



Dr. Milind S. Hujare
Principal

Dr. Milind S. Hujare

Principal, PDVP Mahavidyalaya, Tasgaon. Dist. Sangli

Prin. (Dr.) R. R. Kumbhar

Vivekanand College, Kolhapur

I/C Prin. Prof. (Dr.) S. R. Ghatage

S.M.D.B.S. Mahavidyalaya, Miraj

I/C Prin. Prof. (Dr.) S. S. Patil

R. R. College, Jath

Prin. (Dr.) A. N. Patil

D. K. A. S. C. College, Ichalkaranji

Prin. (Dr.) J. S. Deshmukh

R. P. College, Osmanabad

I/C Prin. (Dr.) S. S. Desai

Smt. M. M. College, Panchgani

Conveners

Prof. S. K. Khade

Dr. A. N. Ambhore

Treasurers

Mr. P. V. Patil

Dr. P. B. Teli

Dr. S. K. Shinde

Co-conveners

Dr. J. S. Ghodake

Dr. S. D. Jadhav

Organizing Secretaries

Dr. A. P. Inamdar

Dr. M. U. Patil

Dr. R. A. Kalel

Coordinators

Prof. N. A. Kulkarni

Prof. S. A. Khabade

Technocrats

Mr. B. S. Harale

Prof. R. M. Ganeshwade

Dr. P. S. Bhandare

Local Organizing Committee

Mr. J. A. Yadav	Mr. V. J. Jadhav	Prof. T. K. Badame	Mr. P. R. Khade	Mr. R. B. Mankar	Dr. A. S. Wagh
Dr. S. J. Patil	Mr. A. R. Patil	Dr. V. D. Kumbhar	Mrs. P. R. Mirajkar	Mr. S. S. Gavil	Dr. A. G. Sonawale
Mr. A. K. Patil	Mr. D. Y. Sakhare	Mr. A. A. Jagdale	Ms. V. D. Jagdale	Ms. V. V. Patil	Mr. R. S. Mote
Mr. S. R. Ghogare	Dr. K. N. Patil	Dr. B. J. Kadam	Dr. A. M. Mali	Mr. A. S. Bagal	Mr. V. T. Kumbhar
Mr. D. S. Shinde	Ms. S. R. Mali	Dr. G. R. Patil	Dr. R. J. Gore	Mr. G. S. Pawar	Mr. J. H. Lavand
Mr. D. J. Nalawade	Mr. D. D. Patil	Mr. S. A. Patil	Dr. A. S. Magdum	Mr. V. R. Patil	Mr. V. M. Jadhav
Mr. R. S. Kumbhar	Dr. S. L. Andhelwar	Ms. S. D. Ghatage	Ms. P. A. Kashid	Ms. P. R. Zambre	Ms. P. S. Jadhav
Mr. A. H. Tarange	Ms. A. S. Yadav	Mr. S. M. Patil	Ms. N. V. More	Ms. S. G. Patil	Ms. D. M. Gosavi
Dr. M. M. Patil	Mr. S. A. Karande	Ms. S. S. Panari	Ms. S. M. Kolekar	Mrs. N. V. Kumbhar	Ms. S. P. Patil
Ms. S. S. Patil	Ms. S. S. Patil	Ms. P. V. Shinde	Mr. S. V. Mane	Ms. S. S. Patil	Ms. S. T. Wagh
Mr. A. A. Wagh					Ms. S. K. Patil
Mr. M. B. Kadam					Mr. S. P. Salunkhe
Mr. M. K. Patil					Mr. A. R. Lavand

All Teaching and non Teaching Staff PDVP Mahavidyalaya, Tasgaon.

Multidisciplinary Approach in Basic and Applied Sciences (MABAS - 2023)



“Dissemination of Education for Knowledge, Science & Culture”

- Shikshanmaharshi Dr. Babuji Salunkhe

Shri Swami Vivekanand Shikshan Sanstha Kolhapur's

Padmabhushan Dr. Vasantodada Patil Mahavidyalaya, Tasgaon

Dist.: Sangli (MS) India Pin : 416 312

Knowledge Partner

Department of Biotechnology, Shivaji University, Kolhapur

Third International Conference

On

“Multidisciplinary Approach in Basic and Applied Sciences (MABAS - 2023)”

(23rd & 24th February - 2023)

Souvenir

ISBN: 978-93-95369-30-5



TABLE OF CONTENTS

Sr. No.	Title	Page no.
1	Diversity of millipedes (myriapoda: diplopoda) in selected lateritic soil habitats in satara tehsil, western ghat, Maharashtra - <i>Shaikh N. A., Abdar M. R., Kengar S. B.</i>	01
2	“Peanut shell extract mediated Biogenic synthesis of palladium nanoparticles (PdNPs) and its application as a homogeneous catalyst for the Suzuki-Miyaura coupling”- <i>Pranoti P. Patil, Utkarsha B. Patil, Utkarsha U. Patil, Shashikant R. Sawant, Rahul A. Kalel</i>	02
3	A study on causes and impact of laterite mining on environment and on the life of Dhangarwada people in Kudchire village of Goa state.- <i>Mr. Vinay Takale</i>	03
4	Morphological Investigation of Rhyzopertha dominica Using Light Microscopy and Scanning Electron Microscopy - <i>Mahure Y.R. and S.K. Zilpe</i>	04
5	Synthesis of Carbon Dot from Couropita Guianensis (Cannon Ball) Flower and applied for the Sensing of an anti-Diabetic drug Metformin.- <i>P. R. Khandagale, Dr. S. V. Nipane, Dr. S. R. Sabale, Dr. R. S. Dhabe.</i>	05
6	Morphological And Histological Cyclic Changes In Theovary Of Freshwater Fish : <i>Channa gachua, Dr. Ashwini G. Ghanbahadur, Prof. Y. K. Khillare</i>	06
7	Cordyceps militaris – An Important Medicinal Mushroom- <i>Trupti D. Kadam, Dr. Ashok V. Kharde.</i>	07
8	Morphometric Analysis Of Hiranyakeshi River, Sindhudurg District Using GIS Technology- <i>Aishwarya Pramod Hingmire, Shrikant Ghadage, Mayur Goud.</i>	08
9	Isolation of urease producing bacteria to produce biocement via MICP process.- <i>P. S. Rayate, B. A. Bhanjale, S. S Yeulkar</i>	09
10	Studies On Web Structure Of Two Spiders From Family Araneidae In Akola District <i>Satyavijay S. Dhande</i>	10
11	Attempts To Improve The Eye Dropper Deigne For Better Patient Compliance <i>Ms. Arte Aakanksha Sachin</i>	11
12	Aegle marmelos ash: A heterogeneous catalyst for Henry reaction <i>Rupesh C. Patil and Suresh S. Patil</i>	12
13	BMIM]-Glycine: A Sustainable Benchmark For Multicomponent Chromene Synthesis <i>Mr. Ashutosh A. Jagdale, Prin. (Dr.) Bhaskar V. Tamhankar and Prof. (Dr.) Suresh S. Patil</i>	13

	<i>Bommegowdna A Mauna, Manasa C. K., Dr. Parameshwar Naik T.</i>	
97	Role of pH in the Synthesis of Metal Sulphide Nanomaterials Thin Film: Review <i>N. B. Pawar, K. V. Khot, V. V. Kondalkar, R. K. Mane, P. N. Bhosale</i>	98
98	Laboratory Scale Magnetostriction Setup and Measurement of Coefficient of Magnetostriction on $\text{Co}_{0.9}\text{Ni}_{0.1}\text{Fe}_{2-x}\text{Mn}_x\text{O}_4$ Ferrite- <i>M. M. Sutar, R. T. Pandhare, D. Y. Bhosale, H. P. Gaikwad, N. M. Kumbhare, S. V. Malgaonkar, V. B. Bansode, A. T. Birajdar, J. S. Ghodake, A. N. Pati</i>	100
99	Synthesis and characterization of NiCoLDH for supercapacitors application <i>V. L. Shinde, A. P. Torane</i>	101
100	Structural and Optical Properties of PVA Thin film doped with CuSO_4 <i>R. Risodkar</i>	102
101	Kinetics and mechanism of oxidation of metformin hydrochloride by enneamolybdomanganate (IV) in hydrochloric acid medium <i>S. I. Mujawar, R. S. Yalgudre, D. J. Sutar, G. S. Gokavi</i>	103
102	New records of Meliolaceous Black Mildew Microfungi from Maharashtra State - <i>Pratik D. Natekar, Anjali P. Patil, Chandrahas R. Patil</i>	104
103	Effect Of Am Fungi On Protein, Chlorophyll And Enzyme Activity In Finger Millet Under Salt Stress- <i>S. V. Hajare, Dr. A.A. Kulkarni</i>	105
104	Sustainable and Green chemistry: Need of Current Scenario- <i>Dr. Prashant R. Mahalle</i>	106
105	Biology of Pseudoscorpion from Sangli District of Western Maharashtra.(India)-Gavali <i>C.S., Nikalje S. B. and Khabade S. A.</i>	107
106	Green synthesis of iron oxide nanoparticle from Ficus Carcia: Characterization and application towards heterocyclization- <i>Komal Mali, Nikita Sabale, Pranita Mali, Snehal Mainkar, Ajay Ambhore</i>	108
107	Iron Nanoparticle-Bentonite Hybrid Using Leaves of Syzygium Cumini Plant from India: Design and Assessment in Heterocyclization- <i>Arya S. Patil, Kirti S. Patil, Ujjwala B. Patil, Kalyani S. Shinde, Pushpa A. Kashid, Ajay N. Ambhore</i>	109
108	One-pot multi-component green synthesis of some new benzylidene-imino-thiazolyl-pyrazol-3-ol derivatives and evaluation of their anticancer, DNA binding and antioxidant activities <i>Ajay N. Ambhore, Shuddhodan N. Kadam, Amit S. Waghmare, Dilip A. Sonwane</i>	110
109	Bael Fruit Ash Water Extract (BFAWE): A greener benchmark for the synthesis of 4H-benzochromenes <i>Megha U. Patil, Sachin K. Shinde, Suresh S. Patil, Omkar Mali, Akshay Jadhav, Vaibhav Patil, Pravin Bhosale</i>	111

Bael Fruit Ash Water Extract (BFAWE): A greener benchmark for the synthesis of 4*H*-benzochromenes

Megha U. Patil, * [a] Sachin K. Shinde, [a] Suresh S. Patil, [b] Omkar Mali, AkshayJadhav, [a]
Vaibhav Patil, [a] Pravin Bhosale [a]

[a] Synthetic Research Laboratory, PG Department of Chemistry, PDVP College, Tasgaon,
Sangli-416 312 (MS), India. Affiliated to Shivaji University, Kolhapur.

[b] Raje Ramrao College, Jat

*Corresponding Author: E-mail: mupatil30@gmail.com; Fax. (0233) 223 2181.

Abstract

A simple and environmental-friendly synthetic protocol has been developed for the synthesis of tetrahydrochromeno[4,3-*b*]chromene-6,8-dione derivatives by condensation of 4-hydroxycoumarin with aromatic aldehydes and dimedone in the presence of bael fruit ash water extract (BFAWE) in aqueous medium. This green protocol was further extended for structurally diverse benzylpyrazolylcoumarins by condensation of equimolar quantity of ethylaceto acetate, hydrazine hydrates, 4-hydroxycoumarin and aromatic aldehydes in good to excellent yields. The advantage of this method includes a mild, an efficient and highly economical protocol under aerobic conditions at very short reaction time, under ligand/external catalyst/external promoter-free conditions. This protocol is better and more practical alternative to the existing protocols for green processes.

Chief Guest



Dr. Achyut Godbole
MD, Softexcel Consultancy



Hon. Abhaykumar Salunkhe
Executive President



Prof. D. T. Shirke
Vice Chancellor, SUK



Prof. P. S. Patil
Pro-Vice Chancellor, SUK



Hon. Shubhangi Gavade
Secretary



Hon. Kaustabh Gavade
Chief Executive Officer



Prin. Dr. R. V. Shejawal
Joint Secretary
(Administration)



Prin. S. M. Gavali
Joint Secretary (Finance)



Dr. Milind S. Hujare
Principal

Dr. Milind S. Hujare

Principal, PDVP Mahavidyalaya, Tasgaon. Dist. Sangli

Prin. (Dr.) R. R. Kumbhar

Vivekanand College, Kolhapur

I/C Prin. Prof. (Dr.) S. R. Ghatage

S.M.D.B.S. Mahavidyalaya, Miraj

I/C Prin. Prof. (Dr.) S. S. Patil

R. R. College, Jath

Prin. (Dr.) A. N. Patil

D. K. A. S. C. College, Ichalkaranji

Prin. (Dr.) J. S. Deshmukh

R. P. College, Osmanabad

I/C Prin. (Dr.) S. S. Desai

Smt. M. M. College, Panchgani

Conveners

Prof. S. K. Khade

Dr. A. N. Ambhore

Treasurers

Mr. P. V. Patil

Dr. P. B. Teli

Dr. S. K. Shinde

Co-conveners

Dr. J. S. Ghodake

Dr. S. D. Jadhav

Organizing Secretaries

Dr. A. P. Inamdar

Dr. M. U. Patil

Dr. R. A. Kalel

Coordinators

Prof. N. A. Kulkarni

Prof. S. A. Khabade

Technocrats

Mr. B. S. Harale

Prof. R. M. Ganeshwade

Dr. P. S. Bhandare

Local Organizing Committee

Mr. J. A. Yadav	Mr. V. J. Jadhav	Prof. T. K. Badame	Mr. P. R. Khade	Mr. R. B. Mankar	Dr. A. S. Wagh
Dr. S. J. Patil	Mr. A. R. Patil	Dr. V. D. Kumbhar	Mrs. P. R. Mirajkar	Mr. S. S. Gavil	Dr. A. G. Sonawale
Mr. A. K. Patil	Mr. D. Y. Sakhare	Mr. A. A. Jagdale	Ms. V. D. Jagdale	Ms. V. V. Patil	Mr. R. S. Mote
Mr. S. R. Ghogare	Dr. K. N. Patil	Dr. B. J. Kadam	Dr. A. M. Mali	Mr. A. S. Bagal	Mr. V. T. Kumbhar
Mr. D. S. Shinde	Ms. S. R. Mali	Dr. G. R. Patil	Dr. R. J. Gore	Mr. G. S. Pawar	Mr. J. H. Lavand
Mr. D. J. Nalawade	Mr. D. D. Patil	Mr. S. A. Patil	Dr. A. S. Magdum	Mr. V. R. Patil	Mr. V. M. Jadhav
Mr. R. S. Kumbhar	Dr. S. L. Andhelwar	Ms. S. D. Ghatage	Ms. P. A. Kashid	Ms. P. R. Zambre	Ms. P. S. Jadhav
Mr. A. H. Tarange	Ms. A. S. Yadav	Mr. S. M. Patil	Ms. N. V. More	Ms. S. G. Patil	Ms. D. M. Gosavi
Dr. M. M. Patil	Mr. S. A. Karande	Ms. S. S. Panari	Ms. S. M. Kolekar	Mrs. N. V. Kumbhar	Ms. S. P. Patil
Ms. S. S. Patil	Ms. S. S. Patil	Ms. P. V. Shinde	Mr. S. V. Mane	Ms. S. S. Patil	Ms. S. T. Wagh
Mr. A. A. Wagh					Ms. S. K. Patil
Mr. M. B. Kadam					Mr. S. P. Salunkhe
Mr. M. K. Patil					Mr. A. R. Lavand

All Teaching and non Teaching Staff PDVP Mahavidyalaya, Tasgaon.

Multidisciplinary Approach in Basic and Applied Sciences (MABAS - 2023)



“Dissemination of Education for Knowledge, Science & Culture”

- Shikshanmaharshi Dr. Bapuji Salunkhe

Shri Swami Vivekanand Shikshan Sanstha Kolhapur's

Padmabhushan Dr. Vasantodada Patil Mahavidyalaya, Tasgaon

Dist.: Sangli (MS) India Pin : 416 312

Knowledge Partner

Department of Biotechnology, Shivaji University, Kolhapur

Third International Conference

On

“Multidisciplinary Approach in Basic and Applied Sciences (MABAS - 2023)”

(23rd & 24th February - 2023)

Souvenir

ISBN: 978-93-95369-30-5



TABLE OF CONTENTS

Sr. No.	Title	Page no.
1	Diversity of millipedes (myriapoda: diplopoda) in selected lateritic soil habitats in satara tehsil, western ghat, Maharashtra - <i>Shaikh N. A., Abdar M. R., Kengar S. B.</i>	01
2	“Peanut shell extract mediated Biogenic synthesis of palladium nanoparticles (PdNPs) and its application as a homogeneous catalyst for the Suzuki-Miyaura coupling”- <i>Pranoti P. Patil, Utkarsha B. Patil, Utkarsha U. Patil, Shashikant R. Sawant, Rahul A. Kalel</i>	02
3	A study on causes and impact of laterite mining on environment and on the life of Dhangarwada people in Kudchire village of Goa state.- <i>Mr. Vinay Takale</i>	03
4	Morphological Investigation of Rhyzopertha dominica Using Light Microscopy and Scanning Electron Microscopy - <i>Mahure Y.R. and S.K. Zilpe</i>	04
5	Synthesis of Carbon Dot from Couropita Guianensis (Cannon Ball) Flower and applied for the Sensing of an anti-Diabetic drug Metformin.- <i>P. R. Khandagale, Dr. S. V. Nipane, Dr. S. R. Sabale, Dr. R. S. Dhabe.</i>	05
6	Morphological And Histological Cyclic Changes In Theovary Of Freshwater Fish : <i>Channa gachua, Dr. Ashwini G. Ghanbahadur, Prof. Y. K. Khillare</i>	06
7	Cordyceps militaris – An Important Medicinal Mushroom- <i>Trupti D. Kadam, Dr. Ashok V. Kharde.</i>	07
8	Morphometric Analysis Of Hiranyakeshi River, Sindhudurg District Using GIS Technology- <i>Aishwarya Pramod Hingmire, Shrikant Ghadage, Mayur Goud.</i>	08
9	Isolation of urease producing bacteria to produce biocement via MICP process.- <i>P. S. Rayate, B. A. Bhanjale, S. S Yeulkar</i>	09
10	Studies On Web Structure Of Two Spiders From Family Araneidae In Akola District <i>Satyavijay S. Dhande</i>	10
11	Attempts To Improve The Eye Dropper Deigne For Better Patient Compliance <i>Ms. Arte Aakanksha Sachin</i>	11
12	Aegle marmelos ash: A heterogeneous catalyst for Henry reaction <i>Rupesh C. Patil and Suresh S. Patil</i>	12
13	BMIM]-Glycine: A Sustainable Benchmark For Multicomponent Chromene Synthesis <i>Mr. Ashutosh A. Jagdale, Prin. (Dr.) Bhaskar V. Tamhankar and Prof. (Dr.) Suresh S. Patil</i>	13

	<i>Jayashree P. Gadade, Ajit B. Telave and Swaroopa A. Patil</i>	
141	Cost effective fodder from sugarcane waste –bagasse by fungal lignin degradation- <i>Pawar N.A., Sabale R.M., Chavan V.V., More K.S., Jagtap S.A., Dr. Jayant Rathod</i>	143
142	Degradation of vegetable waste into organic compost along with mitigation of greenhouse gases- <i>Dhanashree Nevase and Dr. Jayant Rathod</i>	144
143	Evaluating The Potential For Growth Of Artificial Intelligence <i>A. R. Swami, V. S. Kumbhar, K. G. Kharade</i>	145
144	“Green synthesis of nanoparticles in advance various methods” <i>Swati D. Ghatage, Supriya P. Patil, Sanyuja S. Patil, Ankita S. Yadav</i>	146
145	Study the variability in UV irradiance over Kolhapur using Microtops-II <i>Dada P. Nade, Rani P. Pawar, Akshay S. Patil and Sambhaji M. Pawar</i>	147
146	Development of a Sustainable Superhydrophobic Coating by Polymer Layer Deposition on Candle Soot Surface via Dip Coating Technique <i>Rutuja A. Ekunde, Akshay R. Jundle, Sagar S. Ingole, Pradip P. Gaikwad, Rajaram S. Sutar, A. K. Bhosale and Sanjay S. Latthe</i>	148
147	Nutritional Evaluation of plant leaf powder of Brassica nigra as feedstuff in formulated diet for growth of Indian major carp, Cirrhinus mrigala.- <i>Dr. Sheetal Londhe</i>	149
148	Bacillus siamensis as Biocontrol agent against rhizome rot causing plant pathogens.- <i>Saddamhusen Pinjari, Shirishkumar Supanekar, Jyoti Jadhav.</i>	150
149	Review On The Development Of Xrd In Samarium - Dysprosium Substituted Magnesium Ferrite- <i>R. N. Kumbhar1, T. J. Shinde, V. L. Mathe, P.P. Chikode, A. S. Yadav, J. S. Ghodake</i>	151
150	BMI a simple and easy method to assess probable health issues in Students.- <i>Komal Prithviraj Patil 1 & Vishwas Y. Deshpande 2</i>	152
151	Investigation of luminescence properties of Ce ³⁺ doped Li ₂ Al ₄ O ₇ phosphor- <i>Mahendra R. Thomare1, Siddharth D. Nimbalkar 2, Arun B. Chavan3, Dinesh S. Bobade4</i>	153
152	Some Results of Differential Subordination And Superordination by Using Generalized Differential Operator- <i>Miss. Sarika Nilapgol</i>	154
153	Bioefficacy Of Phenylmethane Sulfonyl Fluoride On Larval Triacylglycerol Acylhydrolase Activity Of Hellula Undalis (Fabricius)- <i>R. J. Sawant And R. M. Gejage</i>	155
154	Polystyrene and Octadecyltrichlorosilane Dip Coated Superhydrophobic SS Mesh for Oil-Water Separation- <i>Akshay R. Jundle, Sagar S. Ingole, Pradip P. Gaikwad, Rutuja A. Ekunde, Rajaram S.</i>	156

Development of a Sustainable Superhydrophobic Coating by Polymer Layer Deposition on Candle Soot Surface via Dip Coating Technique

Rutuja A. Ekunde¹, Akshay R. Jundle¹, Sagar S. Ingole¹, Pradip P. Gaikwad¹, Rajaram S. Sutar¹, A. K. Bhosale¹ and Sanjay S. Latthe^{2*}

¹Self-Cleaning Research Laboratory, Department of Physics, Raje Ramrao College, Jath, Dist: Sangli – 416404, (Affiliated to Shivaji University, Kolhapur) Maharashtra, India.

² Self-cleaning Research Laboratory, Department of Physics, Vivekanand College, Kolhapur (Autonomous), Kolhapur–416003, (Affiliated to Shivaji University, Kolhapur) Maharashtra, India

*Corresponding authors E-mail: latthes@gmail.com, akbhosale1@gmail.com

Abstract

A robust superhydrophobic coating has been developed by depositing the polymer layer on the candle soot (CS) surface via dip coating technique. The weak physical interaction of the CS particles with the substrate, results in weaker stability and robustness. In order to improve the mechanical properties of CS surface, we applied a thin layer of polystyrene (PS), polyethylene (PE), polypropylene (PP), and polyvinylidene fluoride (PVDF) on CS surface. The PS, PE, PP and PVDF layer deposited on CS surface revealed water contact angles around 170°, 174°, 175°, and 171° with sliding angles of 2°, 1°, 1°, and 3° respectively. All polymer layer deposited CS surfaces not only exhibited excellent superhydrophobic but also self-cleaning surface property. Among them PP coated CS surface showed better stability against water jet impact as well as water drop impact tests. Even after 50 cycles of sandpaper abrasion and 20 cycles of adhesive tape peeling tests, the PP polymer deposited CS surface maintained superhydrophobic properties. The PP is a better polymer to improve the long-term durability of CS surface confirmed by the mechanical durability tests. Therefore this approach can be used for potential industrial application.

Keywords: Candle Soot, Lotus leaf, polymer coating, Self-Cleaning, and Superhydrophobic.

Chief Guest



Dr. Achyut Godbole
MD, Softexcel Consultancy



Hon. Abhaykumar Salunkhe
Executive President



Prof. D. T. Shirke
Vice Chancellor, SUK



Prof. P. S. Patil
Pro-Vice Chancellor, SUK



Hon. Shubhangi Gavade
Secretary



Hon. Kaustabh Gavade
Chief Executive Officer



Prin. Dr. R. V. Shejwal
Joint Secretary
(Administration)



Prin. S. M. Gavali
Joint Secretary (Finance)



Dr. Milind S. Hujare
Principal

Dr. Milind S. Hujare

Principal, PDVP Mahavidyalaya, Tasgaon. Dist. Sangli

Prin. (Dr.) R. R. Kumbhar

Vivekanand College, Kolhapur

I/C Prin. Prof. (Dr.) S. R. Ghatage

S.M.D.B.S. Mahavidyalaya, Miraj

I/C Prin. Prof. (Dr.) S. S. Patil

R. R. College, Jath

Prin. (Dr.) A. N. Patil

D. K. A. S. C. College, Ichalkaranji

Prin. (Dr.) J. S. Deshmukh

R. P. College, Osmanabad

I/C Prin. (Dr.) S. S. Desai

Smt. M. M. College, Panchgani

Conveners

Prof. S. K. Khade

Dr. A. N. Ambhore

Treasurers

Mr. P. V. Patil

Dr. P. B. Teli

Dr. S. K. Shinde

Co-conveners

Dr. J. S. Ghodake

Dr. S. D. Jadhav

Organizing Secretaries

Dr. A. P. Inamdar

Dr. M. U. Patil

Dr. R. A. Kalel

Coordinators

Prof. N. A. Kulkarni

Prof. S. A. Khabade

Technocrats

Mr. B. S. Harale

Prof. R. M. Ganeshwade

Dr. P. S. Bhandare

Local Organizing Committee

Mr. J. A. Yadav	Mr. V. J. Jadhav	Prof. T. K. Badame	Mr. P. R. Khade	Mr. R. B. Mankar	Dr. A. S. Wagh
Dr. S. J. Patil	Mr. A. R. Patil	Dr. V. D. Kumbhar	Mrs. P. R. Mirajkar	Mr. S. S. Gavil	Dr. A. G. Sonawale
Mr. A. K. Patil	Mr. D. Y. Sakhare	Mr. A. A. Jagdale	Ms. V. D. Jagdale	Ms. V. V. Patil	Mr. R. S. Mote
Mr. S. R. Ghogare	Dr. K. N. Patil	Dr. B. J. Kadam	Dr. A. M. Mali	Mr. A. S. Bagal	Mr. V. T. Kumbhar
Mr. D. S. Shinde	Ms. S. R. Mali	Dr. G. R. Patil	Dr. R. J. Gore	Mr. G. S. Pawar	Mr. J. H. Lavand
Mr. D. J. Nalawade	Mr. D. D. Patil	Mr. S. A. Patil	Dr. A. S. Magdum	Mr. V. R. Patil	Mr. V. M. Jadhav
Mr. R. S. Kumbhar	Dr. S. L. Andhelwar	Ms. S. D. Ghatage	Ms. P. A. Kashid	Ms. P. R. Zambre	Ms. P. S. Jadhav
Mr. A. H. Tarange	Ms. A. S. Yadav	Mr. S. M. Patil	Ms. N. V. More	Ms. S. G. Patil	Ms. D. M. Gosavi
Dr. M. M. Patil	Mr. S. A. Karande	Ms. S. S. Panari	Ms. S. M. Kolekar	Mrs. N. V. Kumbhar	Ms. S. P. Patil
Ms. S. S. Patil	Ms. S. S. Patil	Ms. P. V. Shinde	Mr. S. V. Mane	Ms. S. S. Patil	Ms. S. T. Wagh
Mr. A. A. Wagh					Ms. S. K. Patil
Mr. M. B. Kadam					Mr. S. P. Salunkhe
Mr. M. K. Patil					Mr. A. R. Lavand

All Teaching and non Teaching Staff PDVP Mahavidyalaya, Tasgaon.

Multidisciplinary Approach in Basic and Applied Sciences (MABAS - 2023)



“Dissemination of Education for Knowledge, Science & Culture”

- Shikshanmaharshi Dr. Babuji Salunkhe

Shri Swami Vivekanand Shikshan Sanstha Kolhapur's

Padmabhushan Dr. Vasantodada Patil Mahavidyalaya, Tasgaon

Dist.: Sangli (MS) India Pin : 416 312

Knowledge Partner

Department of Biotechnology, Shivaji University, Kolhapur

Third International Conference

On

“Multidisciplinary Approach in Basic and Applied Sciences (MABAS - 2023)”

(23rd & 24th February - 2023)

Souvenir

ISBN: 978-93-95369-30-5



TABLE OF CONTENTS

Sr. No.	Title	Page no.
1	Diversity of millipedes (myriapoda: diplopoda) in selected lateritic soil habitats in satara tehsil, western ghat, Maharashtra - <i>Shaikh N. A., Abdar M. R., Kengar S. B.</i>	01
2	“Peanut shell extract mediated Biogenic synthesis of palladium nanoparticles (PdNPs) and its application as a homogeneous catalyst for the Suzuki-Miyaura coupling”- <i>Pranoti P. Patil, Utkarsha B. Patil, Utkarsha U. Patil, Shashikant R. Sawant, Rahul A. Kalel</i>	02
3	A study on causes and impact of laterite mining on environment and on the life of Dhangarwada people in Kudchire village of Goa state.- <i>Mr. Vinay Takale</i>	03
4	Morphological Investigation of Rhyzopertha dominica Using Light Microscopy and Scanning Electron Microscopy - <i>Mahure Y.R. and S.K. Zilpe</i>	04
5	Synthesis of Carbon Dot from Couropita Guianensis (Cannon Ball) Flower and applied for the Sensing of an anti-Diabetic drug Metformin.- <i>P. R. Khandagale, Dr. S. V. Nipane, Dr. S. R. Sabale, Dr. R. S. Dhabe.</i>	05
6	Morphological And Histological Cyclic Changes In Theovary Of Freshwater Fish : <i>Channa gachua, Dr. Ashwini G. Ghanbahadur, Prof. Y. K. Khillare</i>	06
7	Cordyceps militaris – An Important Medicinal Mushroom- <i>Trupti D. Kadam, Dr. Ashok V. Kharde.</i>	07
8	Morphometric Analysis Of Hiranyakeshi River, Sindhudurg District Using GIS Technology- <i>Aishwarya Pramod Hingmire, Shrikant Ghadage, Mayur Goud.</i>	08
9	Isolation of urease producing bacteria to produce biocement via MICP process.- <i>P. S. Rayate, B. A. Bhanjale, S. S Yeulkar</i>	09
10	Studies On Web Structure Of Two Spiders From Family Araneidae In Akola District <i>Satyavijay S. Dhande</i>	10
11	Attempts To Improve The Eye Dropper Deigne For Better Patient Compliance <i>Ms. Arte Aakanksha Sachin</i>	11
12	Aegle marmelos ash: A heterogeneous catalyst for Henry reaction <i>Rupesh C. Patil and Suresh S. Patil</i>	12
13	BMIM]-Glycine: A Sustainable Benchmark For Multicomponent Chromene Synthesis <i>Mr. Ashutosh A. Jagdale, Prin. (Dr.) Bhaskar V. Tamhankar and Prof. (Dr.) Suresh S. Patil</i>	13

	<i>Jayashree P. Gadade, Ajit B. Telave and Swaroopa A. Patil</i>	
141	Cost effective fodder from sugarcane waste –bagasse by fungal lignin degradation- <i>Pawar N.A., Sabale R.M., Chavan V.V., More K.S., Jagtap S.A., Dr. Jayant Rathod</i>	143
142	Degradation of vegetable waste into organic compost along with mitigation of greenhouse gases- <i>Dhanashree Nevase and Dr. Jayant Rathod</i>	144
143	Evaluating The Potential For Growth Of Artificial Intelligence <i>A. R. Swami, V. S. Kumbhar, K. G. Kharade</i>	145
144	“Green synthesis of nanoparticles in advance various methods” <i>Swati D. Ghatage, Supriya P. Patil, Sanyuja S. Patil, Ankita S. Yadav</i>	146
145	Study the variability in UV irradiance over Kolhapur using Microtops-II <i>Dada P. Nade, Rani P. Pawar, Akshay S. Patil and Sambhaji M. Pawar</i>	147
146	Development of a Sustainable Superhydrophobic Coating by Polymer Layer Deposition on Candle Soot Surface via Dip Coating Technique <i>Rutuja A. Ekunde, Akshay R. Jundle, Sagar S. Ingole, Pradip P. Gaikwad, Rajaram S. Sutar, A. K. Bhosale and Sanjay S. Lathe</i>	148
147	Nutritional Evaluation of plant leaf powder of Brassica nigra as feedstuff in formulated diet for growth of Indian major carp, Cirrhinus mrigala.- <i>Dr. Sheetal Londhe</i>	149
148	Bacillus siamensis as Biocontrol agent against rhizome rot causing plant pathogens.- <i>Saddamhusen Pinjari, Shirishkumar Supanekar, Jyoti Jadhav.</i>	150
149	Review On The Development Of Xrd In Samarium - Dysprosium Substituted Magnesium Ferrite- <i>R. N. Kumbhar1, T. J. Shinde, V. L. Mathe, P.P. Chikode, A. S. Yadav, J. S. Ghodake</i>	151
150	BMI a simple and easy method to assess probable health issues in Students.- <i>Komal Prithviraj Patil 1 & Vishwas Y. Deshpande 2</i>	152
151	Investigation of luminescence properties of Ce ³⁺ doped Li ₂ Al ₄ O ₇ phosphor- <i>Mahendra R. Thomare1, Siddharth D. Nimbalkar 2, Arun B. Chavan3, Dinesh S. Bobade4</i>	153
152	Some Results of Differential Subordination And Superordination by Using Generalized Differential Operator- <i>Miss. Sarika Nilapgol</i>	154
153	Bioefficacy Of Phenylmethane Sulfonyl Fluoride On Larval Triacylglycerol Acylhydrolase Activity Of Hellula Undalis (Fabricius)- <i>R. J. Sawant And R. M. Gejage</i>	155
154	Polystyrene and Octadecyltrichlorosilane Dip Coated Superhydrophobic SS Mesh for Oil-Water Separation- <i>Akshay R. Jundle, Sagar S. Ingole, Pradip P. Gaikwad, Rutuja A. Ekunde, Rajaram S.</i>	156

Development of a Sustainable Superhydrophobic Coating by Polymer Layer Deposition on Candle Soot Surface via Dip Coating Technique

Rutuja A. Ekunde¹, Akshay R. Jundle¹, Sagar S. Ingole¹, Pradip P. Gaikwad¹, Rajaram S. Sutar¹, A. K. Bhosale¹ and Sanjay S. Latthe^{2*}

¹Self-Cleaning Research Laboratory, Department of Physics, Raje Ramrao College, Jath, Dist: Sangli – 416404, (Affiliated to Shivaji University, Kolhapur) Maharashtra, India.

² Self-cleaning Research Laboratory, Department of Physics, Vivekanand College, Kolhapur (Autonomous), Kolhapur–416003, (Affiliated to Shivaji University, Kolhapur) Maharashtra, India

*Corresponding authors E-mail: latthes@gmail.com, akbhosale1@gmail.com

Abstract

A robust superhydrophobic coating has been developed by depositing the polymer layer on the candle soot (CS) surface via dip coating technique. The weak physical interaction of the CS particles with the substrate, results in weaker stability and robustness. In order to improve the mechanical properties of CS surface, we applied a thin layer of polystyrene (PS), polyethylene (PE), polypropylene (PP), and polyvinylidene fluoride (PVDF) on CS surface. The PS, PE, PP and PVDF layer deposited on CS surface revealed water contact angles around 170°, 174°, 175°, and 171° with sliding angles of 2°, 1°, 1°, and 3° respectively. All polymer layer deposited on CS surface not only exhibited excellent superhydrophobic but also self-cleaning surface property. Among them PP coated CS surface showed better stability against water jet impact as well as water drop impact tests. Even after 50 cycles of sandpaper abrasion and 20 cycles of adhesive tape peeling tests, the PP polymer deposited on CS surface maintained superhydrophobic properties. The PP is a better polymer to improve the long-term durability of CS surface confirmed by the mechanical durability tests. Therefore this approach can be used for potential industrial application.

Keywords: Candle Soot, Lotus leaf, polymer coating, Self-Cleaning, and Superhydrophobic.

Chief Guest



Dr. Achyut Godbole
MD, Softexcel Consultancy



Hon. Abhaykumar Salunkhe
Executive President



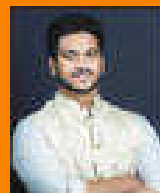
Prof. D. T. Shirke
Vice Chancellor, SUK



Prof. P. S. Patil
Pro-Vice Chancellor, SUK



Hon. Shubhangi Gavade
Secretary



Hon. Kaustabh Gavade
Chief Executive Officer



Prin. Dr. R. V. Shejwal
Joint Secretary
(Administration)



Prin. S. M. Gavali
Joint Secretary (Finance)



Dr. Milind S. Hujare
Principal

Dr. Milind S. Hujare

Principal, PDVP Mahavidyalaya, Tasgaon. Dist. Sangli

Prin. (Dr.) R. R. Kumbhar

Vivekanand College, Kolhapur

I/C Prin. Prof. (Dr.) S. R. Ghatage

S.M.D.B.S. Mahavidyalaya, Miraj

I/C Prin. Prof. (Dr.) S. S. Patil

R. R. College, Jath

Prin. (Dr.) A. N. Patil

D. K. A. S. C. College, Ichalkaranji

Prin. (Dr.) J. S. Deshmukh

R. P. College, Osmanabad

I/C Prin. (Dr.) S. S. Desai

Smt. M. M. College, Panchgani

Conveners

Prof. S. K. Khade

Dr. A. N. Ambhore

Treasurers

Mr. P. V. Patil

Dr. P. B. Teli

Dr. S. K. Shinde

Co-conveners

Dr. J. S. Ghodake

Dr. S. D. Jadhav

Organizing Secretaries

Dr. A. P. Inamdar

Dr. M. U. Patil

Dr. R. A. Kalel

Coordinators

Prof. N. A. Kulkarni

Prof. S. A. Khabade

Technocrats

Mr. B. S. Harale

Prof. R. M. Ganeshwade

Dr. P. S. Bhandare

Local Organizing Committee

Mr. J. A. Yadav	Mr. V. J. Jadhav	Prof. T. K. Badame	Mr. P. R. Khade	Mr. R. B. Mankar	Dr. A. S. Wagh
Dr. S. J. Patil	Mr. A. R. Patil	Dr. V. D. Kumbhar	Mrs. P. R. Mirajkar	Mr. S. S. Gavil	Dr. A. G. Sonawale
Mr. A. K. Patil	Mr. D. Y. Sakhare	Mr. A. A. Jagdale	Ms. V. D. Jagdale	Ms. V. V. Patil	Mr. R. S. Mote
Mr. S. R. Ghogare	Dr. K. N. Patil	Dr. B. J. Kadam	Dr. A. M. Mali	Mr. A. S. Bagal	Mr. V. T. Kumbhar
Mr. D. S. Shinde	Ms. S. R. Mali	Dr. G. R. Patil	Dr. R. J. Gore	Mr. G. S. Pawar	Mr. J. H. Lavand
Mr. D. J. Nalawade	Mr. D. D. Patil	Mr. S. A. Patil	Dr. A. S. Magdum	Mr. V. R. Patil	Mr. V. M. Jadhav
Mr. R. S. Kumbhar	Dr. S. L. Andhelwar	Ms. S. D. Ghatage	Ms. P. A. Kashid	Ms. P. R. Zambre	Ms. P. S. Jadhav
Mr. A. H. Tarange	Ms. A. S. Yadav	Mr. S. M. Patil	Ms. N. V. More	Ms. S. G. Patil	Ms. D. M. Gosavi
Dr. M. M. Patil	Mr. S. A. Karande	Ms. S. S. Panari	Ms. S. M. Kolekar	Mrs. N. V. Kumbhar	Ms. S. P. Patil
Ms. S. S. Patil	Ms. S. S. Patil	Ms. P. V. Shinde	Mr. S. V. Mane	Ms. S. S. Patil	Ms. S. T. Wagh
Mr. A. A. Wagh					Ms. S. K. Patil
Mr. M. B. Kadam					Mr. S. P. Salunkhe
Mr. M. K. Patil					Mr. A. R. Lavand

All Teaching and non Teaching Staff PDVP Mahavidyalaya, Tasgaon.

Multidisciplinary Approach in Basic and Applied Sciences (MABAS - 2023)



“Dissemination of Education for Knowledge, Science & Culture”

- Shikshanmaharshi Dr. Babuji Salunkhe

Shri Swami Vivekanand Shikshan Sanstha Kolhapur's

Padmabhushan Dr. Vasantodada Patil Mahavidyalaya, Tasgaon

Dist.: Sangli (MS) India Pin : 416 312

Knowledge Partner

Department of Biotechnology, Shivaji University, Kolhapur

Third International Conference

On

“Multidisciplinary Approach in Basic and Applied Sciences (MABAS - 2023)”

(23rd & 24th February - 2023)

Souvenir

ISBN: 978-93-95369-30-5



TABLE OF CONTENTS

Sr. No.	Title	Page no.
1	Diversity of millipedes (myriapoda: diplopoda) in selected lateritic soil habitats in satara tehsil, western ghat, Maharashtra - <i>Shaikh N. A., Abdar M. R., Kengar S. B.</i>	01
2	“Peanut shell extract mediated Biogenic synthesis of palladium nanoparticles (PdNPs) and its application as a homogeneous catalyst for the Suzuki-Miyaura coupling”- <i>Pranoti P. Patil, Utkarsha B. Patil, Utkarsha U. Patil, Shashikant R. Sawant, Rahul A. Kalel</i>	02
3	A study on causes and impact of laterite mining on environment and on the life of Dhangarwada people in Kudchire village of Goa state.- <i>Mr. Vinay Takale</i>	03
4	Morphological Investigation of Rhyzopertha dominica Using Light Microscopy and Scanning Electron Microscopy - <i>Mahure Y.R. and S.K. Zilpe</i>	04
5	Synthesis of Carbon Dot from Couropita Guianensis (Cannon Ball) Flower and applied for the Sensing of an anti-Diabetic drug Metformin.- <i>P. R. Khandagale, Dr. S. V. Nipane, Dr. S. R. Sabale, Dr. R. S. Dhabe.</i>	05
6	Morphological And Histological Cyclic Changes In Theovary Of Freshwater Fish : <i>Channa gachua, Dr. Ashwini G. Ghanbahadur, Prof. Y. K. Khillare</i>	06
7	Cordyceps militaris – An Important Medicinal Mushroom- <i>Trupti D. Kadam, Dr. Ashok V. Kharde.</i>	07
8	Morphometric Analysis Of Hiranyakeshi River, Sindhudurg District Using GIS Technology- <i>Aishwarya Pramod Hingmire, Shrikant Ghadage, Mayur Goud.</i>	08
9	Isolation of urease producing bacteria to produce biocement via MICP process.- <i>P. S. Rayate, B. A. Bhanjale, S. S Yeulkar</i>	09
10	Studies On Web Structure Of Two Spiders From Family Araneidae In Akola District <i>Satyavijay S. Dhande</i>	10
11	Attempts To Improve The Eye Dropper Deigne For Better Patient Compliance <i>Ms. Arte Aakanksha Sachin</i>	11
12	Aegle marmelos ash: A heterogeneous catalyst for Henry reaction <i>Rupesh C. Patil and Suresh S. Patil</i>	12
13	BMIM]-Glycine: A Sustainable Benchmark For Multicomponent Chromene Synthesis <i>Mr. Ashutosh A. Jagdale, Prin. (Dr.) Bhaskar V. Tamhankar and Prof. (Dr.) Suresh S. Patil</i>	13

	<i>Jayashree P. Gadade, Ajit B. Telave and Swaroopa A. Patil</i>	
141	Cost effective fodder from sugarcane waste –bagasse by fungal lignin degradation- <i>Pawar N.A., Sabale R.M., Chavan V.V., More K.S., Jagtap S.A., Dr. Jayant Rathod</i>	143
142	Degradation of vegetable waste into organic compost along with mitigation of greenhouse gases- <i>Dhanashree Nevase and Dr. Jayant Rathod</i>	144
143	Evaluating The Potential For Growth Of Artificial Intelligence <i>A. R. Swami, V. S. Kumbhar, K. G. Kharade</i>	145
144	“Green synthesis of nanoparticles in advance various methods” <i>Swati D. Ghatage, Supriya P. Patil, Sanyuja S. Patil, Ankita S. Yadav</i>	146
145	Study the variability in UV irradiance over Kolhapur using Microtops-II <i>Dada P. Nade, Rani P. Pawar, Akshay S. Patil and Sambhaji M. Pawar</i>	147
146	Development of a Sustainable Superhydrophobic Coating by Polymer Layer Deposition on Candle Soot Surface via Dip Coating Technique <i>Rutuja A. Ekunde, Akshay R. Jundle, Sagar S. Ingole, Pradip P. Gaikwad, Rajaram S. Sutar, A. K. Bhosale and Sanjay S. Lathe</i>	148
147	Nutritional Evaluation of plant leaf powder of Brassica nigra as feedstuff in formulated diet for growth of Indian major carp, Cirrhinus mrigala.- <i>Dr. Sheetal Londhe</i>	149
148	Bacillus siamensis as Biocontrol agent against rhizome rot causing plant pathogens.- <i>Saddamhusen Pinjari, Shirishkumar Supanekar, Jyoti Jadhav.</i>	150
149	Review On The Development Of Xrd In Samarium - Dysprosium Substituted Magnesium Ferrite- <i>R. N. Kumbhar1, T. J. Shinde, V. L. Mathe, P.P. Chikode, A. S. Yadav, J. S. Ghodake</i>	151
150	BMI a simple and easy method to assess probable health issues in Students.- <i>Komal Prithviraj Patil 1 & Vishwas Y. Deshpande 2</i>	152
151	Investigation of luminescence properties of Ce ³⁺ doped Li ₂ Al ₄ O ₇ phosphor- <i>Mahendra R. Thomare1, Siddharth D. Nimbalkar 2, Arun B. Chavan3, Dinesh S. Bobade4</i>	153
152	Some Results of Differential Subordination And Superordination by Using Generalized Differential Operator- <i>Miss. Sarika Nilapgol</i>	154
153	Bioefficacy Of Phenylmethane Sulfonyl Fluoride On Larval Triacylglycerol Acylhydrolase Activity Of Hellula Undalis (Fabricius)- <i>R. J. Sawant And R. M. Gejage</i>	155
154	Polystyrene and Octadecyltrichlorosilane Dip Coated Superhydrophobic SS Mesh for Oil-Water Separation- <i>Akshay R. Jundle, Sagar S. Ingole, Pradip P. Gaikwad, Rutuja A. Ekunde, Rajaram S.</i>	156

Development of a Sustainable Superhydrophobic Coating by Polymer Layer Deposition on Candle Soot Surface via Dip Coating Technique

Rutuja A. Ekunde¹, Akshay R. Jundle¹, Sagar S. Ingole¹, Pradip P. Gaikwad¹, Rajaram S. Sutar¹, A. K. Bhosale¹ and Sanjay S. Latthe^{2*}

¹Self-Cleaning Research Laboratory, Department of Physics, Raje Ramrao College, Jath, Dist: Sangli – 416404, (Affiliated to Shivaji University, Kolhapur) Maharashtra, India.

² Self-cleaning Research Laboratory, Department of Physics, Vivekanand College, Kolhapur (Autonomous), Kolhapur–416003, (Affiliated to Shivaji University, Kolhapur) Maharashtra, India

*Corresponding authors E-mail: latthes@gmail.com, akbhosale1@gmail.com

Abstract

A robust superhydrophobic coating has been developed by depositing the polymer layer on the candle soot (CS) surface via dip coating technique. The weak physical interaction of the CS particles with the substrate, results in weaker stability and robustness. In order to improve the mechanical properties of CS surface, we applied a thin layer of polystyrene (PS), polyethylene (PE), polypropylene (PP), and polyvinylidene fluoride (PVDF) on CS surface. The PS, PE, PP and PVDF layer deposited on CS surface revealed water contact angles around 170°, 174°, 175°, and 171° with sliding angles of 2°, 1°, 1°, and 3° respectively. All polymer layer deposited on CS surface not only exhibited excellent superhydrophobic but also self-cleaning surface property. Among them PP coated CS surface showed better stability against water jet impact as well as water drop impact tests. Even after 50 cycles of sandpaper abrasion and 20 cycles of adhesive tape peeling tests, the PP polymer deposited on CS surface maintained superhydrophobic properties. The PP is a better polymer to improve the long-term durability of CS surface confirmed by the mechanical durability tests. Therefore this approach can be used for potential industrial application.

Keywords: Candle Soot, Lotus leaf, polymer coating, Self-Cleaning, and Superhydrophobic.

Chief Guest



Dr. Achyut Godbole
MD, Softexcel Consultancy



Hon. Abhaykumar Salunkhe
Executive President



Prof. D. T. Shirke
Vice Chancellor, SUK



Prof. P. S. Patil
Pro-Vice Chancellor, SUK



Hon. Shubhangi Gavade
Secretary



Hon. Kaustabh Gavade
Chief Executive Officer



Prin. Dr. R. V. Shejwal
Joint Secretary
(Administration)



Prin. S. M. Gavali
Joint Secretary (Finance)



Dr. Milind S. Hujare
Principal

Dr. Milind S. Hujare

Principal, PDVP Mahavidyalaya, Tasgaon. Dist. Sangli

Prin. (Dr.) R. R. Kumbhar

Vivekanand College, Kolhapur

I/C Prin. Prof. (Dr.) S. R. Ghatage

S.M.D.B.S. Mahavidyalaya, Miraj

I/C Prin. Prof. (Dr.) S. S. Patil

R. R. College, Jath

Prin. (Dr.) A. N. Patil

D. K. A. S. C. College, Ichalkaranji

Prin. (Dr.) J. S. Deshmukh

R. P. College, Osmanabad

I/C Prin. (Dr.) S. S. Desai

Smt. M. M. College, Panchgani

Conveners

Prof. S. K. Khade

Dr. A. N. Ambhore

Treasurers

Mr. P. V. Patil

Dr. P. B. Teli

Dr. S. K. Shinde

Co-conveners

Dr. J. S. Ghodake

Dr. S. D. Jadhav

Organizing Secretaries

Dr. A. P. Inamdar

Dr. M. U. Patil

Dr. R. A. Kalel

Coordinators

Prof. N. A. Kulkarni

Prof. S. A. Khabade

Technocrats

Mr. B. S. Harale

Prof. R. M. Ganeshwade

Dr. P. S. Bhandare

Local Organizing Committee

Mr. J. A. Yadav	Mr. V. J. Jadhav	Prof. T. K. Badame	Mr. P. R. Khade	Mr. R. B. Mankar	Dr. A. S. Wagh
Dr. S. J. Patil	Mr. A. R. Patil	Dr. V. D. Kumbhar	Mrs. P. R. Mirajkar	Mr. S. S. Gavil	Dr. A. G. Sonawale
Mr. A. K. Patil	Mr. D. Y. Sakhare	Mr. A. A. Jagdale	Ms. V. D. Jagdale	Ms. V. V. Patil	Mr. R. S. Mote
Mr. S. R. Ghogare	Dr. K. N. Patil	Dr. B. J. Kadam	Dr. A. M. Mali	Mr. A. S. Bagal	Mr. V. T. Kumbhar
Mr. D. S. Shinde	Ms. S. R. Mali	Dr. G. R. Patil	Dr. R. J. Gore	Mr. G. S. Pawar	Mr. J. H. Lavand
Mr. D. J. Nalawade	Mr. D. D. Patil	Mr. S. A. Patil	Dr. A. S. Magdum	Mr. V. R. Patil	Mr. V. M. Jadhav
Mr. R. S. Kumbhar	Dr. S. L. Andhelwar	Ms. S. D. Ghatage	Ms. P. A. Kashid	Ms. P. R. Zambre	Ms. P. S. Jadhav
Mr. A. H. Tarange	Ms. A. S. Yadav	Mr. S. M. Patil	Ms. N. V. More	Ms. S. G. Patil	Ms. D. M. Gosavi
Dr. M. M. Patil	Mr. S. A. Karande	Ms. S. S. Panari	Ms. S. M. Kolekar	Mrs. N. V. Kumbhar	Ms. S. P. Patil
Ms. S. S. Patil	Ms. S. S. Patil	Ms. P. V. Shinde	Mr. S. V. Mane	Ms. S. S. Patil	Ms. S. T. Wagh
Mr. A. A. Wagh					Ms. S. K. Patil
Mr. M. B. Kadam					Mr. S. P. Salunkhe
Mr. M. K. Patil					Mr. A. R. Lavand

All Teaching and non Teaching Staff PDVP Mahavidyalaya, Tasgaon.

Multidisciplinary Approach in Basic and Applied Sciences (MABAS - 2023)



“Dissemination of Education for Knowledge, Science & Culture”

- Shikshanmaharshi Dr. Babuji Salunkhe

Shri Swami Vivekanand Shikshan Sanstha Kolhapur's

Padmabhushan Dr. Vasantodada Patil Mahavidyalaya, Tasgaon

Dist.: Sangli (MS) India Pin : 416 312

Knowledge Partner

Department of Biotechnology, Shivaji University, Kolhapur

Third International Conference

On

“Multidisciplinary Approach in Basic and Applied Sciences (MABAS - 2023)”

(23rd & 24th February - 2023)

Souvenir

ISBN: 978-93-95369-30-5



TABLE OF CONTENTS

Sr. No.	Title	Page no.
1	Diversity of millipedes (myriapoda: diplopoda) in selected lateritic soil habitats in satara tehsil, western ghat, Maharashtra - <i>Shaikh N. A., Abdar M. R., Kengar S. B.</i>	01
2	“Peanut shell extract mediated Biogenic synthesis of palladium nanoparticles (PdNPs) and its application as a homogeneous catalyst for the Suzuki-Miyaura coupling”- <i>Pranoti P. Patil, Utkarsha B. Patil, Utkarsha U. Patil, Shashikant R. Sawant, Rahul A. Kalel</i>	02
3	A study on causes and impact of laterite mining on environment and on the life of Dhangarwada people in Kudchire village of Goa state.- <i>Mr. Vinay Takale</i>	03
4	Morphological Investigation of Rhyzopertha dominica Using Light Microscopy and Scanning Electron Microscopy - <i>Mahure Y.R. and S.K. Zilpe</i>	04
5	Synthesis of Carbon Dot from Couropita Guianensis (Cannon Ball) Flower and applied for the Sensing of an anti-Diabetic drug Metformin.- <i>P. R. Khandagale, Dr. S. V. Nipane, Dr. S. R. Sabale, Dr. R. S. Dhabe.</i>	05
6	Morphological And Histological Cyclic Changes In Theovary Of Freshwater Fish : <i>Channa gachua, Dr. Ashwini G. Ghanbahadur, Prof. Y. K. Khillare</i>	06
7	Cordyceps militaris – An Important Medicinal Mushroom- <i>Trupti D. Kadam, Dr. Ashok V. Kharde.</i>	07
8	Morphometric Analysis Of Hiranyakeshi River, Sindhudurg District Using GIS Technology- <i>Aishwarya Pramod Hingmire, Shrikant Ghadage, Mayur Goud.</i>	08
9	Isolation of urease producing bacteria to produce biocement via MICP process.- <i>P. S. Rayate, B. A. Bhanjale, S. S Yeulkar</i>	09
10	Studies On Web Structure Of Two Spiders From Family Araneidae In Akola District <i>Satyavijay S. Dhande</i>	10
11	Attempts To Improve The Eye Dropper Deigne For Better Patient Compliance <i>Ms. Arte Aakanksha Sachin</i>	11
12	Aegle marmelos ash: A heterogeneous catalyst for Henry reaction <i>Rupesh C. Patil and Suresh S. Patil</i>	12
13	BMIM]-Glycine: A Sustainable Benchmark For Multicomponent Chromene Synthesis <i>Mr. Ashutosh A. Jagdale, Prin. (Dr.) Bhaskar V. Tamhankar and Prof. (Dr.) Suresh S. Patil</i>	13

	<i>Jayashree P. Gadade, Ajit B. Telave and Swaroopa A. Patil</i>	
141	Cost effective fodder from sugarcane waste –bagasse by fungal lignin degradation- <i>Pawar N.A., Sabale R.M., Chavan V.V., More K.S., Jagtap S.A., Dr. Jayant Rathod</i>	143
142	Degradation of vegetable waste into organic compost along with mitigation of greenhouse gases- <i>Dhanashree Nevase and Dr. Jayant Rathod</i>	144
143	Evaluating The Potential For Growth Of Artificial Intelligence <i>A. R. Swami, V. S. Kumbhar, K. G. Kharade</i>	145
144	“Green synthesis of nanoparticles in advance various methods” <i>Swati D. Ghatage, Supriya P. Patil, Sanyuja S. Patil, Ankita S. Yadav</i>	146
145	Study the variability in UV irradiance over Kolhapur using Microtops-II <i>Dada P. Nade, Rani P. Pawar, Akshay S. Patil and Sambhaji M. Pawar</i>	147
146	Development of a Sustainable Superhydrophobic Coating by Polymer Layer Deposition on Candle Soot Surface via Dip Coating Technique <i>Rutuja A. Ekunde, Akshay R. Jundle, Sagar S. Ingole, Pradip P. Gaikwad, Rajaram S. Sutar, A. K. Bhosale and Sanjay S. Latthe</i>	148
147	Nutritional Evaluation of plant leaf powder of Brassica nigra as feedstuff in formulated diet for growth of Indian major carp, Cirrhinus mrigala.- <i>Dr. Sheetal Londhe</i>	149
148	Bacillus siamensis as Biocontrol agent against rhizome rot causing plant pathogens.- <i>Saddamhusen Pinjari, Shirishkumar Supanekar, Jyoti Jadhav.</i>	150
149	Review On The Development Of Xrd In Samarium - Dysprosium Substituted Magnesium Ferrite- <i>R. N. Kumbhar¹, T. J. Shinde, V. L. Mathe, P.P. Chikode, A. S. Yadav, J. S. Ghodake</i>	151
150	BMI a simple and easy method to assess probable health issues in Students.- <i>Komal Prithviraj Patil¹ & Vishwas Y. Deshpande²</i>	152
151	Investigation of luminescence properties of Ce ³⁺ doped Li ₂ Al ₄ O ₇ phosphor- <i>Mahendra R. Thomare¹, Siddharth D. Nimbalkar², Arun B. Chavan³, Dinesh S. Bobade⁴</i>	153
152	Some Results of Differential Subordination And Superordination by Using Generalized Differential Operator- <i>Miss. Sarika Nilapgol</i>	154
153	Bioefficacy Of Phenylmethane Sulfonyl Fluoride On Larval Triacylglycerol Acylhydrolase Activity Of Hellula Undalis (Fabricius)- <i>R. J. Sawant And R. M. Gejage</i>	155
154	Polystyrene and Octadecyltrichlorosilane Dip Coated Superhydrophobic SS Mesh for Oil-Water Separation- <i>Akshay R. Jundle, Sagar S. Ingole, Pradip P. Gaikwad, Rutuja A. Ekunde, Rajaram S.</i>	156

Development of a Sustainable Superhydrophobic Coating by Polymer Layer Deposition on Candle Soot Surface via Dip Coating Technique

Rutuja A. Ekunde¹, Akshay R. Jundle¹, Sagar S. Ingole¹, Pradip P. Gaikwad¹, Rajaram S. Sutar¹, A. K. Bhosale¹ and Sanjay S. Latthe^{2*}

¹Self-Cleaning Research Laboratory, Department of Physics, Raje Ramrao College, Jath, Dist: Sangli – 416404, (Affiliated to Shivaji University, Kolhapur) Maharashtra, India.

² Self-cleaning Research Laboratory, Department of Physics, Vivekanand College, Kolhapur (Autonomous), Kolhapur–416003, (Affiliated to Shivaji University, Kolhapur) Maharashtra, India

*Corresponding authors E-mail: latthes@gmail.com, akbhosale1@gmail.com

Abstract

A robust superhydrophobic coating has been developed by depositing the polymer layer on the candle soot (CS) surface via dip coating technique. The weak physical interaction of the CS particles on the substrate, results in weaker stability and robustness. In order to improve the mechanical properties of CS surface, we applied a thin layer of polystyrene (PS), polyethylene (PE), polypropylene (PP), and polyvinylidene fluoride (PVDF) on CS surface. The PS, PE, PP and PVDF layer deposited on CS surface revealed water contact angles around 170°, 174°, 175°, and 171° with sliding angles of 2°, 1°, 1°, and 3° respectively. All polymer layer deposited on CS surface not only exhibited excellent superhydrophobic but also self-cleaning surface property. Among them PP coated CS surface showed better stability against water jet impact as well as water drop impact tests. Even after 50 cycles of sandpaper abrasion and 20 cycles of adhesive tape peeling tests, the PP polymer deposited on CS surface maintained superhydrophobic properties. The PP is a better polymer to improve the long-term durability of CS surface confirmed by the mechanical durability tests. Therefore this approach can be used for potential industrial application.

Keywords: Candle Soot, Lotus leaf, polymer coating, Self-Cleaning, and Superhydrophobic.

Chief Guest



Dr. Achyut Godbole
MD, Softexcel Consultancy



Hon. Abhaykumar Salunkhe
Executive President



Prof. D. T. Shirke
Vice Chancellor, SUK



Prof. P. S. Patil
Pro-Vice Chancellor, SUK



Hon. Shubhangi Gavade
Secretary



Hon. Kaustabh Gavade
Chief Executive Officer



Prin. Dr. R. V. Shejwal
Joint Secretary
(Administration)



Prin. S. M. Gavali
Joint Secretary (Finance)



Dr. Milind S. Hujare
Principal

Dr. Milind S. Hujare

Principal, PDVP Mahavidyalaya, Tasgaon. Dist. Sangli

Prin. (Dr.) R. R. Kumbhar

Vivekanand College, Kolhapur

I/C Prin. Prof. (Dr.) S. R. Ghatage

S.M.D.B.S. Mahavidyalaya, Miraj

I/C Prin. Prof. (Dr.) S. S. Patil

R. R. College, Jath

Prin. (Dr.) A. N. Patil

D. K. A. S. C. College, Ichalkaranji

Prin. (Dr.) J. S. Deshmukh

R. P. College, Osmanabad

I/C Prin. (Dr.) S. S. Desai

Smt. M. M. College, Panchgani

Conveners

Prof. S. K. Khade

Dr. A. N. Ambhore

Treasurers

Mr. P. V. Patil

Dr. P. B. Teli

Dr. S. K. Shinde

Co-conveners

Dr. J. S. Ghodake

Dr. S. D. Jadhav

Organizing Secretaries

Dr. A. P. Inamdar

Dr. M. U. Patil

Dr. R. A. Kalel

Coordinators

Prof. N. A. Kulkarni

Prof. S. A. Khabade

Technocrats

Mr. B. S. Harale

Prof. R. M. Ganeshwade

Dr. P. S. Bhandare

Local Organizing Committee

Mr. J. A. Yadav	Mr. V. J. Jadhav	Prof. T. K. Badame	Mr. P. R. Khade	Mr. R. B. Mankar	Dr. A. S. Wagh
Dr. S. J. Patil	Mr. A. R. Patil	Dr. V. D. Kumbhar	Mrs. P. R. Mirajkar	Mr. S. S. Gavil	Dr. A. G. Sonawale
Mr. A. K. Patil	Mr. D. Y. Sakhare	Mr. A. A. Jagdale	Ms. V. D. Jagdale	Ms. V. V. Patil	Mr. R. S. Mote
Mr. S. R. Ghogare	Dr. K. N. Patil	Dr. B. J. Kadam	Dr. A. M. Mali	Mr. A. S. Bagal	Mr. V. T. Kumbhar
Mr. D. S. Shinde	Ms. S. R. Mali	Dr. G. R. Patil	Dr. R. J. Gore	Mr. G. S. Pawar	Mr. J. H. Lavand
Mr. D. J. Nalawade	Mr. D. D. Patil	Mr. S. A. Patil	Dr. A. S. Magdum	Mr. V. R. Patil	Mr. V. M. Jadhav
Mr. R. S. Kumbhar	Dr. S. L. Andhelwar	Ms. S. D. Ghatage	Ms. P. A. Kashid	Ms. P. R. Zambre	Ms. P. S. Jadhav
Mr. A. H. Tarange	Ms. A. S. Yadav	Mr. S. M. Patil	Ms. N. V. More	Ms. S. G. Patil	Ms. D. M. Gosavi
Dr. M. M. Patil	Mr. S. A. Karande	Ms. S. S. Panari	Ms. S. M. Kolekar	Mrs. N. V. Kumbhar	Ms. S. P. Patil
Ms. S. S. Patil	Ms. S. S. Patil	Ms. P. V. Shinde	Mr. S. V. Mane	Ms. S. S. Patil	Ms. S. T. Wagh
Mr. A. A. Wagh					Ms. S. K. Patil
Mr. M. B. Kadam					Mr. S. P. Salunkhe
Mr. M. K. Patil					Mr. A. R. Lavand

All Teaching and non Teaching Staff PDVP Mahavidyalaya, Tasgaon.

Multidisciplinary Approach in Basic and Applied Sciences (MABAS - 2023)



“Dissemination of Education for Knowledge, Science & Culture”

- Shikshanmaharshi Dr. Bapuji Salunkhe

Shri Swami Vivekanand Shikshan Sanstha Kolhapur's

Padmabhushan Dr. Vasantodada Patil Mahavidyalaya, Tasgaon

Dist.: Sangli (MS) India Pin : 416 312

Knowledge Partner

Department of Biotechnology, Shivaji University, Kolhapur

Third International Conference

On

“Multidisciplinary Approach in Basic and Applied Sciences (MABAS - 2023)”

(23rd & 24th February - 2023)

Souvenir

ISBN: 978-93-95369-30-5



TABLE OF CONTENTS

Sr. No.	Title	Page no.
1	Diversity of millipedes (myriapoda: diplopoda) in selected lateritic soil habitats in satara tehsil, western ghat, Maharashtra - <i>Shaikh N. A., Abdar M. R., Kengar S. B.</i>	01
2	“Peanut shell extract mediated Biogenic synthesis of palladium nanoparticles (PdNPs) and its application as a homogeneous catalyst for the Suzuki-Miyaura coupling”- <i>Pranoti P. Patil, Utkarsha B. Patil, Utkarsha U. Patil, Shashikant R. Sawant, Rahul A. Kalel</i>	02
3	A study on causes and impact of laterite mining on environment and on the life of Dhangarwada people in Kudchire village of Goa state.- <i>Mr. Vinay Takale</i>	03
4	Morphological Investigation of Rhyzopertha dominica Using Light Microscopy and Scanning Electron Microscopy - <i>Mahure Y.R. and S.K. Zilpe</i>	04
5	Synthesis of Carbon Dot from Couropita Guianensis (Cannon Ball) Flower and applied for the Sensing of an anti-Diabetic drug Metformin.- <i>P. R. Khandagale, Dr. S. V. Nipane, Dr. S. R. Sabale, Dr. R. S. Dhabe.</i>	05
6	Morphological And Histological Cyclic Changes In Theovary Of Freshwater Fish : <i>Channa gachua, Dr. Ashwini G. Ghanbahadur, Prof. Y. K. Khillare</i>	06
7	Cordyceps militaris – An Important Medicinal Mushroom- <i>Trupti D. Kadam, Dr. Ashok V. Kharde.</i>	07
8	Morphometric Analysis Of Hiranyakeshi River, Sindhudurg District Using GIS Technology- <i>Aishwarya Pramod Hingmire, Shrikant Ghadage, Mayur Goud.</i>	08
9	Isolation of urease producing bacteria to produce biocement via MICP process.- <i>P. S. Rayate, B. A. Bhanjale, S. S Yeulkar</i>	09
10	Studies On Web Structure Of Two Spiders From Family Araneidae In Akola District <i>Satyavijay S. Dhande</i>	10
11	Attempts To Improve The Eye Dropper Deigne For Better Patient Compliance <i>Ms. Arte Aakanksha Sachin</i>	11
12	Aegle marmelos ash: A heterogeneous catalyst for Henry reaction <i>Rupesh C. Patil and Suresh S. Patil</i>	12
13	BMIM]-Glycine: A Sustainable Benchmark For Multicomponent Chromene Synthesis <i>Mr. Ashutosh A. Jagdale, Prin. (Dr.) Bhaskar V. Tamhankar and Prof. (Dr.) Suresh S. Patil</i>	13

	<i>Jayashree P. Gadade, Ajit B. Telave and Swaroopa A. Patil</i>	
141	Cost effective fodder from sugarcane waste –bagasse by fungal lignin degradation- <i>Pawar N.A., Sabale R.M., Chavan V.V., More K.S., Jagtap S.A., Dr. Jayant Rathod</i>	143
142	Degradation of vegetable waste into organic compost along with mitigation of greenhouse gases- <i>Dhanashree Nevase and Dr. Jayant Rathod</i>	144
143	Evaluating The Potential For Growth Of Artificial Intelligence <i>A. R. Swami, V. S. Kumbhar, K. G. Kharade</i>	145
144	“Green synthesis of nanoparticles in advance various methods” <i>Swati D. Ghatage, Supriya P. Patil, Sanyuja S. Patil, Ankita S. Yadav</i>	146
145	Study the variability in UV irradiance over Kolhapur using Microtops-II <i>Dada P. Nade, Rani P. Pawar, Akshay S. Patil and Sambhaji M. Pawar</i>	147
146	Development of a Sustainable Superhydrophobic Coating by Polymer Layer Deposition on Candle Soot Surface via Dip Coating Technique <i>Rutuja A. Ekunde, Akshay R. Jundle, Sagar S. Ingole, Pradip P. Gaikwad, Rajaram S. Sutar, A. K. Bhosale and Sanjay S. Latthe</i>	148
147	Nutritional Evaluation of plant leaf powder of Brassica nigra as feedstuff in formulated diet for growth of Indian major carp, Cirrhinus mrigala.- <i>Dr. Sheetal Londhe</i>	149
148	Bacillus siamensis as Biocontrol agent against rhizome rot causing plant pathogens.- <i>Saddamhusen Pinjari, Shirishkumar Supanekar, Jyoti Jadhav.</i>	150
149	Review On The Development Of Xrd In Samarium - Dysprosium Substituted Magnesium Ferrite- <i>R. N. Kumbhar¹, T. J. Shinde, V. L. Mathe, P.P. Chikode, A. S. Yadav, J. S. Ghodake</i>	151
150	BMI a simple and easy method to assess probable health issues in Students.- <i>Komal Prithviraj Patil¹ & Vishwas Y. Deshpande²</i>	152
151	Investigation of luminescence properties of Ce ³⁺ doped Li ₂ Al ₄ O ₇ phosphor- <i>Mahendra R. Thomare¹, Siddharth D. Nimbalkar², Arun B. Chavan³, Dinesh S. Bobade⁴</i>	153
152	Some Results of Differential Subordination And Superordination by Using Generalized Differential Operator- <i>Miss. Sarika Nilapgol</i>	154
153	Bioefficacy Of Phenylmethane Sulfonyl Fluoride On Larval Triacylglycerol Acylhydrolase Activity Of Hellula Undalis (Fabricius)- <i>R. J. Sawant And R. M. Gejage</i>	155
154	Polystyrene and Octadecyltrichlorosilane Dip Coated Superhydrophobic SS Mesh for Oil-Water Separation- <i>Akshay R. Jundle, Sagar S. Ingole, Pradip P. Gaikwad, Rutuja A. Ekunde, Rajaram S.</i>	156

Polystyrene and Octadecyltrichlorosilane Dip Coated Superhydrophobic SS Mesh for Oil-Water Separation

Akshay R. Jundle¹, Sagar S. Ingole¹, Pradip P. Gaikwad¹, Rutuja A. Ekunde¹, Rajaram S. Sutar¹, A. K. Bhosale¹ and Sanjay S. Latthe^{2*}

¹Self-Cleaning Research Laboratory, Department of Physics, Raje Ramrao College, Jath, Dist: Sangli – 416404, (Affiliated to Shivaji University, Kolhapur) Maharashtra, India.

² Self-cleaning Research Laboratory, Department of Physics, Vivekanand College, Kolhapur (Autonomous), Kolhapur–416003, (Affiliated to Shivaji University, Kolhapur) Maharashtra, India

*Corresponding authors E-mail: latthes@gmail.com

Abstract

A superhydrophobic coating was produced on stainless steel (SS) mesh using the dip coating technique. On stainless steel mesh (SS), a layer of polystyrene (PS) and followed by a layer of octadecyltrichlorosilane (OTS) was deposited back-to-back eight times. The water contact angle (WCA), rolling angle, and oil contact angle (OCA) of the prepared coatings were $155\pm 2^\circ$, $7\pm 2^\circ$ and 0° , respectively. The nano-level folds on micro-level bumps were observed on the stainless-steel mesh (SS) surface during the surface microstructure study, which contributed to the surface's superhydrophobicity. The oil and water separation ability of coatings was tested using various oil and water mixtures, including petrol, diesel, kerosene, vegetable oil, and coconut oil. The superhydrophobic mesh has shown a separation effectiveness of more than 97% for low viscous fluids and less than 85% for high viscous oils. Low-viscous oils penetrated into the mesh at a higher rate than high-viscous oils. Bending, twisting, adhesive tape peeling, and sandpaper abrasion testing were used to assess the mechanical strength of the coating; the results demonstrated that coated mesh exhibited outstanding mechanical rigidity. Furthermore, the superhydrophobic mesh has revealed exceptional heat stability and self-cleaning ability.

Keywords: *Oil-water separation, stainless steel mesh, superhydrophobic, and superoleophilic.*

Chief Guest



Dr. Achyut Godbole
MD, Softexcel Consultancy



Hon. Abhaykumar Salunkhe
Executive President



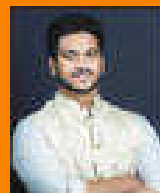
Prof. D. T. Shirke
Vice Chancellor, SUK



Prof. P. S. Patil
Pro-Vice Chancellor, SUK



Hon. Shubhangi Gavade
Secretary



Hon. Kaustabh Gavade
Chief Executive Officer



Prin. Dr. R. V. Shejwal
Joint Secretary
(Administration)



Prin. S. M. Gavali
Joint Secretary (Finance)



Dr. Milind S. Hujare
Principal

Dr. Milind S. Hujare

Principal, PDVP Mahavidyalaya, Tasgaon. Dist. Sangli

Prin. (Dr.) R. R. Kumbhar

Vivekanand College, Kolhapur

I/C Prin. Prof. (Dr.) S. R. Ghatage

S.M.D.B.S. Mahavidyalaya, Miraj

I/C Prin. Prof. (Dr.) S. S. Patil

R. R. College, Jath

Prin. (Dr.) A. N. Patil

D. K. A. S. C. College, Ichalkaranji

Prin. (Dr.) J. S. Deshmukh

R. P. College, Osmanabad

I/C Prin. (Dr.) S. S. Desai

Smt. M. M. College, Panchgani

Conveners

Prof. S. K. Khade

Dr. A. N. Ambhore

Treasurers

Mr. P. V. Patil

Dr. P. B. Teli

Dr. S. K. Shinde

Co-conveners

Dr. J. S. Ghodake

Dr. S. D. Jadhav

Organizing Secretaries

Dr. A. P. Inamdar

Dr. M. U. Patil

Dr. R. A. Kalel

Coordinators

Prof. N. A. Kulkarni

Prof. S. A. Khabade

Technocrats

Mr. B. S. Harale

Prof. R. M. Ganeshwade

Dr. P. S. Bhandare

Local Organizing Committee

Mr. J. A. Yadav	Mr. V. J. Jadhav	Prof. T. K. Badame	Mr. P. R. Khade	Mr. R. B. Mankar	Dr. A. S. Wagh
Dr. S. J. Patil	Mr. A. R. Patil	Dr. V. D. Kumbhar	Mrs. P. R. Mirajkar	Mr. S. S. Gavil	Dr. A. G. Sonawale
Mr. A. K. Patil	Mr. D. Y. Sakhare	Mr. A. A. Jagdale	Ms. V. D. Jagdale	Ms. V. V. Patil	Mr. R. S. Mote
Mr. S. R. Ghogare	Dr. K. N. Patil	Dr. B. J. Kadam	Dr. A. M. Mali	Mr. A. S. Bagal	Mr. V. T. Kumbhar
Mr. D. S. Shinde	Ms. S. R. Mali	Dr. G. R. Patil	Dr. R. J. Gore	Mr. G. S. Pawar	Mr. J. H. Lavand
Mr. D. J. Nalawade	Mr. D. D. Patil	Mr. S. A. Patil	Dr. A. S. Magdum	Mr. V. R. Patil	Mr. V. M. Jadhav
Mr. R. S. Kumbhar	Dr. S. L. Andhelwar	Ms. S. D. Ghatage	Ms. P. A. Kashid	Ms. P. R. Zambre	Ms. P. S. Jadhav
Mr. A. H. Tarange	Ms. A. S. Yadav	Mr. S. M. Patil	Ms. N. V. More	Ms. S. G. Patil	Ms. D. M. Gosavi
Dr. M. M. Patil	Mr. S. A. Karande	Ms. S. S. Panari	Ms. S. M. Kolekar	Mrs. N. V. Kumbhar	Ms. S. P. Patil
Ms. S. S. Patil	Ms. S. S. Patil	Ms. P. V. Shinde	Mr. S. V. Mane	Ms. S. S. Patil	Ms. S. T. Wagh
Mr. A. A. Wagh					Ms. S. K. Patil
Mr. M. B. Kadam					Mr. S. P. Salunkhe
Mr. M. K. Patil					Mr. A. R. Lavand

All Teaching and non Teaching Staff PDVP Mahavidyalaya, Tasgaon.

Multidisciplinary Approach in Basic and Applied Sciences (MABAS - 2023)



“Dissemination of Education for Knowledge, Science & Culture”

- Shikshanmaharshi Dr. Bapuji Salunkhe

Shri Swami Vivekanand Shikshan Sanstha Kolhapur's

Padmabhushan Dr. Vasantodada Patil Mahavidyalaya, Tasgaon

Dist.: Sangli (MS) India Pin : 416 312

Knowledge Partner

Department of Biotechnology, Shivaji University, Kolhapur

Third International Conference

On

“Multidisciplinary Approach in Basic and Applied Sciences (MABAS - 2023)”

(23rd & 24th February - 2023)

Souvenir

ISBN: 978-93-95369-30-5



TABLE OF CONTENTS

Sr. No.	Title	Page no.
1	Diversity of millipedes (myriapoda: diplopoda) in selected lateritic soil habitats in satara tehsil, western ghat, Maharashtra - <i>Shaikh N. A., Abdar M. R., Kengar S. B.</i>	01
2	“Peanut shell extract mediated Biogenic synthesis of palladium nanoparticles (PdNPs) and its application as a homogeneous catalyst for the Suzuki-Miyaura coupling”- <i>Pranoti P. Patil, Utkarsha B. Patil, Utkarsha U. Patil, Shashikant R. Sawant, Rahul A. Kalel</i>	02
3	A study on causes and impact of laterite mining on environment and on the life of Dhangarwada people in Kudchire village of Goa state.- <i>Mr. Vinay Takale</i>	03
4	Morphological Investigation of Rhyzopertha dominica Using Light Microscopy and Scanning Electron Microscopy - <i>Mahure Y.R. and S.K. Zilpe</i>	04
5	Synthesis of Carbon Dot from Couropita Guianensis (Cannon Ball) Flower and applied for the Sensing of an anti-Diabetic drug Metformin.- <i>P. R. Khandagale, Dr. S. V. Nipane, Dr. S. R. Sabale, Dr. R. S. Dhabe.</i>	05
6	Morphological And Histological Cyclic Changes In Theovary Of Freshwater Fish : <i>Channa gachua, Dr. Ashwini G. Ghanbahadur, Prof. Y. K. Khillare</i>	06
7	Cordyceps militaris – An Important Medicinal Mushroom- <i>Trupti D. Kadam, Dr. Ashok V. Kharde.</i>	07
8	Morphometric Analysis Of Hiranyakeshi River, Sindhudurg District Using GIS Technology- <i>Aishwarya Pramod Hingmire, Shrikant Ghadage, Mayur Goud.</i>	08
9	Isolation of urease producing bacteria to produce biocement via MICP process.- <i>P. S. Rayate, B. A. Bhanjale, S. S Yeulkar</i>	09
10	Studies On Web Structure Of Two Spiders From Family Araneidae In Akola District <i>Satyavijay S. Dhande</i>	10
11	Attempts To Improve The Eye Dropper Deigne For Better Patient Compliance <i>Ms. Arte Aakanksha Sachin</i>	11
12	Aegle marmelos ash: A heterogeneous catalyst for Henry reaction <i>Rupesh C. Patil and Suresh S. Patil</i>	12
13	BMIM]-Glycine: A Sustainable Benchmark For Multicomponent Chromene Synthesis <i>Mr. Ashutosh A. Jagdale, Prin. (Dr.) Bhaskar V. Tamhankar and Prof. (Dr.) Suresh S. Patil</i>	13

	<i>Jayashree P. Gadade, Ajit B. Telave and Swaroopa A. Patil</i>	
141	Cost effective fodder from sugarcane waste –bagasse by fungal lignin degradation- <i>Pawar N.A., Sabale R.M., Chavan V.V., More K.S., Jagtap S.A., Dr. Jayant Rathod</i>	143
142	Degradation of vegetable waste into organic compost along with mitigation of greenhouse gases- <i>Dhanashree Nevase and Dr. Jayant Rathod</i>	144
143	Evaluating The Potential For Growth Of Artificial Intelligence <i>A. R. Swami, V. S. Kumbhar, K. G. Kharade</i>	145
144	“Green synthesis of nanoparticles in advance various methods” <i>Swati D. Ghatage, Supriya P. Patil, Sanyuja S. Patil, Ankita S. Yadav</i>	146
145	Study the variability in UV irradiance over Kolhapur using Microtops-II <i>Dada P. Nade, Rani P. Pawar, Akshay S. Patil and Sambhaji M. Pawar</i>	147
146	Development of a Sustainable Superhydrophobic Coating by Polymer Layer Deposition on Candle Soot Surface via Dip Coating Technique <i>Rutuja A. Ekunde, Akshay R. Jundle, Sagar S. Ingole, Pradip P. Gaikwad, Rajaram S. Sutar, A. K. Bhosale and Sanjay S. Latthe</i>	148
147	Nutritional Evaluation of plant leaf powder of Brassica nigra as feedstuff in formulated diet for growth of Indian major carp, Cirrhinus mrigala.- <i>Dr. Sheetal Londhe</i>	149
148	Bacillus siamensis as Biocontrol agent against rhizome rot causing plant pathogens.- <i>Saddamhusen Pinjari, Shirishkumar Supanekar, Jyoti Jadhav.</i>	150
149	Review On The Development Of Xrd In Samarium - Dysprosium Substituted Magnesium Ferrite- <i>R. N. Kumbhar1, T. J. Shinde, V. L. Mathe, P.P. Chikode, A. S. Yadav, J. S. Ghodake</i>	151
150	BMI a simple and easy method to assess probable health issues in Students.- <i>Komal Prithviraj Patil 1 & Vishwas Y. Deshpande 2</i>	152
151	Investigation of luminescence properties of Ce ³⁺ doped Li ₂ Al ₄ O ₇ phosphor- <i>Mahendra R. Thomare1, Siddharth D. Nimbalkar 2, Arun B. Chavan3, Dinesh S. Bobade4</i>	153
152	Some Results of Differential Subordination And Superordination by Using Generalized Differential Operator- <i>Miss. Sarika Nilapgol</i>	154
153	Bioefficacy Of Phenylmethane Sulfonyl Fluoride On Larval Triacylglycerol Acylhydrolase Activity Of Hellula Undalis (Fabricius)- <i>R. J. Sawant And R. M. Gejage</i>	155
154	Polystyrene and Octadecyltrichlorosilane Dip Coated Superhydrophobic SS Mesh for Oil-Water Separation- <i>Akshay R. Jundle, Sagar S. Ingole, Pradip P. Gaikwad, Rutuja A. Ekunde, Rajaram S.</i>	156

Polystyrene and Octadecyltrichlorosilane Dip Coated Superhydrophobic SS Mesh for Oil-Water Separation

Akshay R. Jundle¹, Sagar S. Ingole¹, Pradip P. Gaikwad¹, Rutuja A. Ekunde¹, Rajaram S. Sutar¹, A. K. Bhosale¹ and Sanjay S. Latthe^{2*}

¹Self-Cleaning Research Laboratory, Department of Physics, Raje Ramrao College, Jath, Dist: Sangli – 416404, (Affiliated to Shivaji University, Kolhapur) Maharashtra, India.

² Self-cleaning Research Laboratory, Department of Physics, Vivekanand College, Kolhapur (Autonomous), Kolhapur–416003, (Affiliated to Shivaji University, Kolhapur) Maharashtra, India

*Corresponding authors E-mail: latthes@gmail.com

Abstract

A superhydrophobic coating was produced on stainless steel (SS) mesh using the dip coating technique. On stainless steel mesh (SS), a layer of polystyrene (PS) and followed by a layer of octadecyltrichlorosilane (OTS) was deposited back-to-back eight times. The water contact angle (WCA), rolling angle, and oil contact angle (OCA) of the prepared coatings were $155\pm 2^\circ$, $7\pm 2^\circ$ and 0° , respectively. The nano-level folds on micro-level bumps were observed on the stainless-steel mesh (SS) surface during the surface microstructure study, which contributed to the surface's superhydrophobicity. The oil and water separation ability of coatings was tested using various oil and water mixtures, including petrol, diesel, kerosene, vegetable oil, and coconut oil. The superhydrophobic mesh has shown a separation effectiveness of more than 97% for low viscous fluids and less than 85% for high viscous oils. Low-viscous oils penetrated into the mesh at a higher rate than high-viscous oils. Bending, twisting, adhesive tape peeling, and sandpaper abrasion testing were used to assess the mechanical strength of the coating; the results demonstrated that coated mesh exhibited outstanding mechanical rigidity. Furthermore, the superhydrophobic mesh has revealed exceptional heat stability and self-cleaning ability.

Keywords: *Oil-water separation, stainless steel mesh, superhydrophobic, and superoleophilic.*

Chief Guest



Dr. Achyut Godbole
MD, Softexcel Consultancy



Hon. Abhaykumar Salunkhe
Executive President



Prof. D. T. Shirke
Vice Chancellor, SUK



Prof. P. S. Patil
Pro-Vice Chancellor, SUK



Hon. Shubhangi Gavade
Secretary



Hon. Kaustabh Gavade
Chief Executive Officer



Prin. Dr. R. V. Shejwal
Joint Secretary
(Administration)



Prin. S. M. Gavali
Joint Secretary (Finance)



Dr. Milind S. Hujare
Principal

Dr. Milind S. Hujare

Principal, PDVP Mahavidyalaya, Tasgaon. Dist. Sangli

Prin. (Dr.) R. R. Kumbhar

Vivekanand College, Kolhapur

I/C Prin. Prof. (Dr.) S. R. Ghatage

S.M.D.B.S. Mahavidyalaya, Miraj

I/C Prin. Prof. (Dr.) S. S. Patil

R. R. College, Jath

Prin. (Dr.) A. N. Patil

D. K. A. S. C. College, Ichalkaranji

Prin. (Dr.) J. S. Deshmukh

R. P. College, Osmanabad

I/C Prin. (Dr.) S. S. Desai

Smt. M. M. College, Panchgani

Conveners

Prof. S. K. Khade

Dr. A. N. Ambhore

Treasurers

Mr. P. V. Patil

Dr. P. B. Teli

Dr. S. K. Shinde

Co-conveners

Dr. J. S. Ghodake

Dr. S. D. Jadhav

Organizing Secretaries

Dr. A. P. Inamdar

Dr. M. U. Patil

Dr. R. A. Kalel

Coordinators

Prof. N. A. Kulkarni

Prof. S. A. Khabade

Technocrats

Mr. B. S. Harale

Prof. R. M. Ganeshwade

Dr. P. S. Bhandare

Local Organizing Committee

Mr. J. A. Yadav	Mr. V. J. Jadhav	Prof. T. K. Badame	Mr. P. R. Khade	Mr. R. B. Mankar	Dr. A. S. Wagh
Dr. S. J. Patil	Mr. A. R. Patil	Dr. V. D. Kumbhar	Mrs. P. R. Mirajkar	Mr. S. S. Gavil	Dr. A. G. Sonawale
Mr. A. K. Patil	Mr. D. Y. Sakhare	Mr. A. A. Jagdale	Ms. V. D. Jagdale	Ms. V. V. Patil	Mr. R. S. Mote
Mr. S. R. Ghogare	Dr. K. N. Patil	Dr. B. J. Kadam	Dr. A. M. Mali	Mr. A. S. Bagal	Mr. V. T. Kumbhar
Mr. D. S. Shinde	Ms. S. R. Mali	Dr. G. R. Patil	Dr. R. J. Gore	Mr. G. S. Pawar	Mr. J. H. Lavand
Mr. D. J. Nalawade	Mr. D. D. Patil	Mr. S. A. Patil	Dr. A. S. Magdum	Mr. V. R. Patil	Mr. V. M. Jadhav
Mr. R. S. Kumbhar	Dr. S. L. Andhelwar	Ms. S. D. Ghatage	Ms. P. A. Kashid	Ms. P. R. Zambre	Ms. P. S. Jadhav
Mr. A. H. Tarange	Ms. A. S. Yadav	Mr. S. M. Patil	Ms. N. V. More	Ms. S. G. Patil	Ms. D. M. Gosavi
Dr. M. M. Patil	Mr. S. A. Karande	Ms. S. S. Panari	Ms. S. M. Kolekar	Mrs. N. V. Kumbhar	Ms. S. P. Patil
Ms. S. S. Patil	Ms. S. S. Patil	Ms. P. V. Shinde	Mr. S. V. Mane	Ms. S. S. Patil	Ms. S. T. Wagh
Mr. A. A. Wagh					Ms. S. K. Patil
Mr. M. B. Kadam					Mr. S. P. Salunkhe
Mr. M. K. Patil					Mr. A. R. Lavand

All Teaching and non Teaching Staff PDVP Mahavidyalaya, Tasgaon.

Multidisciplinary Approach in Basic and Applied Sciences (MABAS - 2023)



“Dissemination of Education for Knowledge, Science & Culture”

- Shikshanmaharshi Dr. Bapuji Salunkhe

Shri Swami Vivekanand Shikshan Sanstha Kolhapur's

Padmabhushan Dr. Vasantodada Patil Mahavidyalaya, Tasgaon

Dist.: Sangli (MS) India Pin : 416 312

Knowledge Partner

Department of Biotechnology, Shivaji University, Kolhapur

Third International Conference

On

“Multidisciplinary Approach in Basic and Applied Sciences (MABAS - 2023)”

(23rd & 24th February - 2023)

Souvenir

ISBN: 978-93-95369-30-5



TABLE OF CONTENTS

Sr. No.	Title	Page no.
1	Diversity of millipedes (myriapoda: diplopoda) in selected lateritic soil habitats in satara tehsil, western ghat, Maharashtra - <i>Shaikh N. A., Abdar M. R., Kengar S. B.</i>	01
2	“Peanut shell extract mediated Biogenic synthesis of palladium nanoparticles (PdNPs) and its application as a homogeneous catalyst for the Suzuki-Miyaura coupling”- <i>Pranoti P. Patil, Utkarsha B. Patil, Utkarsha U. Patil, Shashikant R. Sawant, Rahul A. Kalel</i>	02
3	A study on causes and impact of laterite mining on environment and on the life of Dhangarwada people in Kudchire village of Goa state.- <i>Mr. Vinay Takale</i>	03
4	Morphological Investigation of Rhyzopertha dominica Using Light Microscopy and Scanning Electron Microscopy - <i>Mahure Y.R. and S.K. Zilpe</i>	04
5	Synthesis of Carbon Dot from Couropita Guianensis (Cannon Ball) Flower and applied for the Sensing of an anti-Diabetic drug Metformin.- <i>P. R. Khandagale, Dr. S. V. Nipane, Dr. S. R. Sabale, Dr. R. S. Dhabe.</i>	05
6	Morphological And Histological Cyclic Changes In Theovary Of Freshwater Fish : <i>Channa gachua, Dr. Ashwini G. Ghanbahadur, Prof. Y. K. Khillare</i>	06
7	Cordyceps militaris – An Important Medicinal Mushroom- <i>Trupti D. Kadam, Dr. Ashok V. Kharde.</i>	07
8	Morphometric Analysis Of Hiranyakeshi River, Sindhudurg District Using GIS Technology- <i>Aishwarya Pramod Hingmire, Shrikant Ghadage, Mayur Goud.</i>	08
9	Isolation of urease producing bacteria to produce biocement via MICP process.- <i>P. S. Rayate, B. A. Bhanjale, S. S Yeulkar</i>	09
10	Studies On Web Structure Of Two Spiders From Family Araneidae In Akola District <i>Satyavijay S. Dhande</i>	10
11	Attempts To Improve The Eye Dropper Deigne For Better Patient Compliance <i>Ms. Arte Aakanksha Sachin</i>	11
12	Aegle marmelos ash: A heterogeneous catalyst for Henry reaction <i>Rupesh C. Patil and Suresh S. Patil</i>	12
13	BMIM]-Glycine: A Sustainable Benchmark For Multicomponent Chromene Synthesis <i>Mr. Ashutosh A. Jagdale, Prin. (Dr.) Bhaskar V. Tamhankar and Prof. (Dr.) Suresh S. Patil</i>	13

	<i>Jayashree P. Gadade, Ajit B. Telave and Swaroopa A. Patil</i>	
141	Cost effective fodder from sugarcane waste –bagasse by fungal lignin degradation- <i>Pawar N.A., Sabale R.M., Chavan V.V., More K.S., Jagtap S.A., Dr. Jayant Rathod</i>	143
142	Degradation of vegetable waste into organic compost along with mitigation of greenhouse gases- <i>Dhanashree Nevase and Dr. Jayant Rathod</i>	144
143	Evaluating The Potential For Growth Of Artificial Intelligence <i>A. R. Swami, V. S. Kumbhar, K. G. Kharade</i>	145
144	“Green synthesis of nanoparticles in advance various methods” <i>Swati D. Ghatage, Supriya P. Patil, Sanyuja S. Patil, Ankita S. Yadav</i>	146
145	Study the variability in UV irradiance over Kolhapur using Microtops-II <i>Dada P. Nade, Rani P. Pawar, Akshay S. Patil and Sambhaji M. Pawar</i>	147
146	Development of a Sustainable Superhydrophobic Coating by Polymer Layer Deposition on Candle Soot Surface via Dip Coating Technique <i>Rutuja A. Ekunde, Akshay R. Jundle, Sagar S. Ingole, Pradip P. Gaikwad, Rajaram S. Sutar, A. K. Bhosale and Sanjay S. Latthe</i>	148
147	Nutritional Evaluation of plant leaf powder of Brassica nigra as feedstuff in formulated diet for growth of Indian major carp, Cirrhinus mrigala.- <i>Dr. Sheetal Londhe</i>	149
148	Bacillus siamensis as Biocontrol agent against rhizome rot causing plant pathogens.- <i>Saddamhusen Pinjari, Shirishkumar Supanekar, Jyoti Jadhav.</i>	150
149	Review On The Development Of Xrd In Samarium - Dysprosium Substituted Magnesium Ferrite- <i>R. N. Kumbhar¹, T. J. Shinde, V. L. Mathe, P.P. Chikode, A. S. Yadav, J. S. Ghodake</i>	151
150	BMI a simple and easy method to assess probable health issues in Students.- <i>Komal Prithviraj Patil¹ & Vishwas Y. Deshpande²</i>	152
151	Investigation of luminescence properties of Ce ³⁺ doped Li ₂ Al ₄ O ₇ phosphor- <i>Mahendra R. Thomare¹, Siddharth D. Nimbalkar², Arun B. Chavan³, Dinesh S. Bobade⁴</i>	153
152	Some Results of Differential Subordination And Superordination by Using Generalized Differential Operator- <i>Miss. Sarika Nilapgol</i>	154
153	Bioefficacy Of Phenylmethane Sulfonyl Fluoride On Larval Triacylglycerol Acylhydrolase Activity Of Hellula Undalis (Fabricius)- <i>R. J. Sawant And R. M. Gejage</i>	155
154	Polystyrene and Octadecyltrichlorosilane Dip Coated Superhydrophobic SS Mesh for Oil-Water Separation- <i>Akshay R. Jundle, Sagar S. Ingole, Pradip P. Gaikwad, Rutuja A. Ekunde, Rajaram S.</i>	156

Polystyrene and Octadecyltrichlorosilane Dip Coated Superhydrophobic SS Mesh for Oil-Water Separation

Akshay R. Jundle¹, Sagar S. Ingole¹, Pradip P. Gaikwad¹, Rutuja A. Ekunde¹, Rajaram S. Sutar¹, A. K. Bhosale¹ and Sanjay S. Latthe^{2*}

¹Self-Cleaning Research Laboratory, Department of Physics, Raje Ramrao College, Jath, Dist: Sangli – 416404, (Affiliated to Shivaji University, Kolhapur) Maharashtra, India.

² Self-cleaning Research Laboratory, Department of Physics, Vivekanand College, Kolhapur (Autonomous), Kolhapur–416003, (Affiliated to Shivaji University, Kolhapur) Maharashtra, India

*Corresponding authors E-mail: latthes@gmail.com

Abstract

A superhydrophobic coating was produced on stainless steel (SS) mesh using the dip coating technique. On stainless steel mesh (SS), a layer of polystyrene (PS) and followed by a layer of octadecyltrichlorosilane (OTS) was deposited back-to-back eight times. The water contact angle (WCA), rolling angle, and oil contact angle (OCA) of the prepared coatings were $155\pm 2^\circ$, $7\pm 2^\circ$ and 0° , respectively. The nano-level folds on micro-level bumps were observed on the stainless-steel mesh (SS) surface during the surface microstructure study, which contributed to the surface's superhydrophobicity. The oil and water separation ability of coatings was tested using various oil and water mixtures, including petrol, diesel, kerosene, vegetable oil, and coconut oil. The superhydrophobic mesh has shown a separation effectiveness of more than 97% for low viscous fluids and less than 85% for high viscous oils. Low-viscous oils penetrated into the mesh at a higher rate than high-viscous oils. Bending, twisting, adhesive tape peeling, and sandpaper abrasion testing were used to assess the mechanical strength of the coating; the results demonstrated that coated mesh exhibited outstanding mechanical rigidity. Furthermore, the superhydrophobic mesh has revealed exceptional heat stability and self-cleaning ability.

Keywords: *Oil-water separation, stainless steel mesh, superhydrophobic, and superoleophilic.*

Chief Guest



Dr. Achyut Godbole
MD, Softexcel Consultancy



Hon. Abhaykumar Salunkhe
Executive President



Prof. D. T. Shirke
Vice Chancellor, SUK



Prof. P. S. Patil
Pro-Vice Chancellor, SUK



Hon. Shubhangi Gavade
Secretary



Hon. Kaustabh Gavade
Chief Executive Officer



Prin. Dr. R. V. Shejwal
Joint Secretary
(Administration)



Prin. S. M. Gavali
Joint Secretary (Finance)



Dr. Milind S. Hujare
Principal

Dr. Milind S. Hujare

Principal, PDVP Mahavidyalaya, Tasgaon. Dist. Sangli

Prin. (Dr.) R. R. Kumbhar

Vivekanand College, Kolhapur

I/C Prin. Prof. (Dr.) S. R. Ghatage

S.M.D.B.S. Mahavidyalaya, Miraj

I/C Prin. Prof. (Dr.) S. S. Patil

R. R. College, Jath

Prin. (Dr.) A. N. Patil

D. K. A. S. C. College, Ichalkaranji

Prin. (Dr.) J. S. Deshmukh

R. P. College, Osmanabad

I/C Prin. (Dr.) S. S. Desai

Smt. M. M. College, Panchgani

Conveners

Prof. S. K. Khade

Dr. A. N. Ambhore

Treasurers

Mr. P. V. Patil

Dr. P. B. Teli

Dr. S. K. Shinde

Co-conveners

Dr. J. S. Ghodake

Dr. S. D. Jadhav

Organizing Secretaries

Dr. A. P. Inamdar

Dr. M. U. Patil

Dr. R. A. Kalel

Coordinators

Prof. N. A. Kulkarni

Prof. S. A. Khabade

Technocrats

Mr. B. S. Harale

Prof. R. M. Ganeshwade

Dr. P. S. Bhandare

Local Organizing Committee

Mr. J. A. Yadav	Mr. V. J. Jadhav	Prof. T. K. Badame	Mr. P. R. Khade	Mr. R. B. Mankar	Dr. A. S. Wagh
Dr. S. J. Patil	Mr. A. R. Patil	Dr. V. D. Kumbhar	Mrs. P. R. Mirajkar	Mr. S. S. Gavil	Dr. A. G. Sonawale
Mr. A. K. Patil	Mr. D. Y. Sakhare	Mr. A. A. Jagdale	Ms. V. D. Jagdale	Ms. V. V. Patil	Mr. R. S. Mote
Mr. S. R. Ghogare	Dr. K. N. Patil	Dr. B. J. Kadam	Dr. A. M. Mali	Mr. A. S. Bagal	Mr. V. T. Kumbhar
Mr. D. S. Shinde	Ms. S. R. Mali	Dr. G. R. Patil	Dr. R. J. Gore	Mr. G. S. Pawar	Mr. J. H. Lavand
Mr. D. J. Nalawade	Mr. D. D. Patil	Mr. S. A. Patil	Dr. A. S. Magdum	Mr. V. R. Patil	Mr. V. M. Jadhav
Mr. R. S. Kumbhar	Dr. S. L. Andhelwar	Ms. S. D. Ghatage	Ms. P. A. Kashid	Ms. P. R. Zambre	Ms. P. S. Jadhav
Mr. A. H. Tarange	Ms. A. S. Yadav	Mr. S. M. Patil	Ms. N. V. More	Ms. S. G. Patil	Ms. D. M. Gosavi
Dr. M. M. Patil	Mr. S. A. Karande	Ms. S. S. Panari	Ms. S. M. Kolekar	Mrs. N. V. Kumbhar	Ms. S. P. Patil
Ms. S. S. Patil	Ms. S. S. Patil	Ms. P. V. Shinde	Mr. S. V. Mane	Ms. S. S. Patil	Ms. S. T. Wagh
Mr. A. A. Wagh					Ms. S. K. Patil
Mr. M. B. Kadam					Mr. S. P. Salunkhe
Mr. M. K. Patil					Mr. A. R. Lavand

All Teaching and non Teaching Staff PDVP Mahavidyalaya, Tasgaon.

Multidisciplinary Approach in Basic and Applied Sciences (MABAS - 2023)



“Dissemination of Education for Knowledge, Science & Culture”

- Shikshanmaharshi Dr. Babuji Salunkhe

Shri Swami Vivekanand Shikshan Sanstha Kolhapur's

Padmabhushan Dr. Vasantodada Patil Mahavidyalaya, Tasgaon

Dist.: Sangli (MS) India Pin : 416 312

Knowledge Partner

Department of Biotechnology, Shivaji University, Kolhapur

Third International Conference

On

“Multidisciplinary Approach in Basic and Applied Sciences (MABAS - 2023)”

(23rd & 24th February - 2023)

Souvenir

ISBN: 978-93-95369-30-5



TABLE OF CONTENTS

Sr. No.	Title	Page no.
1	Diversity of millipedes (myriapoda: diplopoda) in selected lateritic soil habitats in satara tehsil, western ghat, Maharashtra - <i>Shaikh N. A., Abdar M. R., Kengar S. B.</i>	01
2	“Peanut shell extract mediated Biogenic synthesis of palladium nanoparticles (PdNPs) and its application as a homogeneous catalyst for the Suzuki-Miyaura coupling”- <i>Pranoti P. Patil, Utkarsha B. Patil, Utkarsha U. Patil, Shashikant R. Sawant, Rahul A. Kalel</i>	02
3	A study on causes and impact of laterite mining on environment and on the life of Dhangarwada people in Kudchire village of Goa state.- <i>Mr. Vinay Takale</i>	03
4	Morphological Investigation of Rhyzopertha dominica Using Light Microscopy and Scanning Electron Microscopy - <i>Mahure Y.R. and S.K. Zilpe</i>	04
5	Synthesis of Carbon Dot from Couropita Guianensis (Cannon Ball) Flower and applied for the Sensing of an anti-Diabetic drug Metformin.- <i>P. R. Khandagale, Dr. S. V. Nipane, Dr. S. R. Sabale, Dr. R. S. Dhabe.</i>	05
6	Morphological And Histological Cyclic Changes In Theovary Of Freshwater Fish : <i>Channa gachua, Dr. Ashwini G. Ghanbahadur, Prof. Y. K. Khillare</i>	06
7	Cordyceps militaris – An Important Medicinal Mushroom- <i>Trupti D. Kadam, Dr. Ashok V. Kharde.</i>	07
8	Morphometric Analysis Of Hiranyakeshi River, Sindhudurg District Using GIS Technology- <i>Aishwarya Pramod Hingmire, Shrikant Ghadage, Mayur Goud.</i>	08
9	Isolation of urease producing bacteria to produce biocement via MICP process.- <i>P. S. Rayate, B. A. Bhanjale, S. S Yeulkar</i>	09
10	Studies On Web Structure Of Two Spiders From Family Araneidae In Akola District <i>Satyavijay S. Dhande</i>	10
11	Attempts To Improve The Eye Dropper Deigne For Better Patient Compliance <i>Ms. Arte Aakanksha Sachin</i>	11
12	Aegle marmelos ash: A heterogeneous catalyst for Henry reaction <i>Rupesh C. Patil and Suresh S. Patil</i>	12
13	BMIM]-Glycine: A Sustainable Benchmark For Multicomponent Chromene Synthesis <i>Mr. Ashutosh A. Jagdale, Prin. (Dr.) Bhaskar V. Tamhankar and Prof. (Dr.) Suresh S. Patil</i>	13

	<i>Jayashree P. Gadade, Ajit B. Telave and Swaroopa A. Patil</i>	
141	Cost effective fodder from sugarcane waste –bagasse by fungal lignin degradation- <i>Pawar N.A., Sabale R.M., Chavan V.V., More K.S., Jagtap S.A., Dr. Jayant Rathod</i>	143
142	Degradation of vegetable waste into organic compost along with mitigation of greenhouse gases- <i>Dhanashree Nevase and Dr. Jayant Rathod</i>	144
143	Evaluating The Potential For Growth Of Artificial Intelligence <i>A. R. Swami, V. S. Kumbhar, K. G. Kharade</i>	145
144	“Green synthesis of nanoparticles in advance various methods” <i>Swati D. Ghatage, Supriya P. Patil, Sanyuja S. Patil, Ankita S. Yadav</i>	146
145	Study the variability in UV irradiance over Kolhapur using Microtops-II <i>Dada P. Nade, Rani P. Pawar, Akshay S. Patil and Sambhaji M. Pawar</i>	147
146	Development of a Sustainable Superhydrophobic Coating by Polymer Layer Deposition on Candle Soot Surface via Dip Coating Technique <i>Rutuja A. Ekunde, Akshay R. Jundle, Sagar S. Ingole, Pradip P. Gaikwad, Rajaram S. Sutar, A. K. Bhosale and Sanjay S. Latthe</i>	148
147	Nutritional Evaluation of plant leaf powder of Brassica nigra as feedstuff in formulated diet for growth of Indian major carp, Cirrhinus mrigala.- <i>Dr. Sheetal Londhe</i>	149
148	Bacillus siamensis as Biocontrol agent against rhizome rot causing plant pathogens.- <i>Saddamhusen Pinjari, Shirishkumar Supanekar, Jyoti Jadhav.</i>	150
149	Review On The Development Of Xrd In Samarium - Dysprosium Substituted Magnesium Ferrite- <i>R. N. Kumbhar¹, T. J. Shinde, V. L. Mathe, P.P. Chikode, A. S. Yadav, J. S. Ghodake</i>	151
150	BMI a simple and easy method to assess probable health issues in Students.- <i>Komal Prithviraj Patil 1 & Vishwas Y. Deshpande 2</i>	152
151	Investigation of luminescence properties of Ce ³⁺ doped Li ₂ Al ₄ O ₇ phosphor- <i>Mahendra R. Thomare¹, Siddharth D. Nimbalkar², Arun B. Chavan³, Dinesh S. Bobade⁴</i>	153
152	Some Results of Differential Subordination And Superordination by Using Generalized Differential Operator- <i>Miss. Sarika Nilapgol</i>	154
153	Bioefficacy Of Phenylmethane Sulfonyl Fluoride On Larval Triacylglycerol Acylhydrolase Activity Of Hellula Undalis (Fabricius)- <i>R. J. Sawant And R. M. Gejage</i>	155
154	Polystyrene and Octadecyltrichlorosilane Dip Coated Superhydrophobic SS Mesh for Oil-Water Separation- <i>Akshay R. Jundle, Sagar S. Ingole, Pradip P. Gaikwad, Rutuja A. Ekunde, Rajaram S.</i>	156

Polystyrene and Octadecyltrichlorosilane Dip Coated Superhydrophobic SS Mesh for Oil-Water Separation

Akshay R. Jundle¹, Sagar S. Ingole¹, Pradip P. Gaikwad¹, Rutuja A. Ekunde¹, Rajaram S. Sutar¹, A. K. Bhosale¹ and Sanjay S. Latthe^{2*}

¹Self-Cleaning Research Laboratory, Department of Physics, Raje Ramrao College, Jath, Dist: Sangli – 416404, (Affiliated to Shivaji University, Kolhapur) Maharashtra, India.

² Self-cleaning Research Laboratory, Department of Physics, Vivekanand College, Kolhapur (Autonomous), Kolhapur–416003, (Affiliated to Shivaji University, Kolhapur) Maharashtra, India

*Corresponding authors E-mail: latthes@gmail.com

Abstract

A superhydrophobic coating was produced on stainless steel (SS) mesh using the dip coating technique. On stainless steel mesh (SS), a layer of polystyrene (PS) and followed by a layer of octadecyltrichlorosilane (OTS) was deposited back-to-back eight times. The water contact angle (WCA), rolling angle, and oil contact angle (OCA) of the prepared coatings were $155\pm 2^\circ$, $7\pm 2^\circ$ and 0° , respectively. The nano-level folds on micro-level bumps were observed on the stainless-steel mesh (SS) surface during the surface microstructure study, which contributed to the surface's superhydrophobicity. The oil and water separation ability of coatings was tested using various oil and water mixtures, including petrol, diesel, kerosene, vegetable oil, and coconut oil. The superhydrophobic mesh has shown a separation effectiveness of more than 97% for low viscous fluids and less than 85% for high viscous oils. Low-viscous oils penetrated into the mesh at a higher rate than high-viscous oils. Bending, twisting, adhesive tape peeling, and sandpaper abrasion testing were used to assess the mechanical strength of the coating; the results demonstrated that coated mesh exhibited outstanding mechanical rigidity. Furthermore, the superhydrophobic mesh has revealed exceptional heat stability and self-cleaning ability.

Keywords: *Oil-water separation, stainless steel mesh, superhydrophobic, and superoleophilic.*

Chief Guest



Dr. Achyut Godbole
MD, Softexcel Consultancy



Hon. Abhaykumar Salunkhe
Executive President



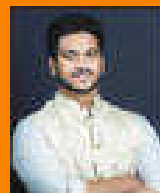
Prof. D. T. Shirke
Vice Chancellor, SUK



Prof. P. S. Patil
Pro-Vice Chancellor, SUK



Hon. Shubhangi Gavade
Secretary



Hon. Kaustabh Gavade
Chief Executive Officer



Prin. Dr. R. V. Shejwal
Joint Secretary
(Administration)



Prin. S. M. Gavali
Joint Secretary (Finance)



Dr. Milind S. Hujare
Principal

Dr. Milind S. Hujare

Principal, PDVP Mahavidyalaya, Tasgaon. Dist. Sangli

Prin. (Dr.) R. R. Kumbhar

Vivekanand College, Kolhapur

I/C Prin. Prof. (Dr.) S. R. Ghatage

S.M.D.B.S. Mahavidyalaya, Miraj

I/C Prin. Prof. (Dr.) S. S. Patil

R. R. College, Jath

Prin. (Dr.) A. N. Patil

D. K. A. S. C. College, Ichalkaranji

Prin. (Dr.) J. S. Deshmukh

R. P. College, Osmanabad

I/C Prin. (Dr.) S. S. Desai

Smt. M. M. College, Panchgani

Conveners

Prof. S. K. Khade

Dr. A. N. Ambhore

Treasurers

Mr. P. V. Patil

Dr. P. B. Teli

Dr. S. K. Shinde

Co-conveners

Dr. J. S. Ghodake

Dr. S. D. Jadhav

Organizing Secretaries

Dr. A. P. Inamdar

Dr. M. U. Patil

Dr. R. A. Kalel

Coordinators

Prof. N. A. Kulkarni

Prof. S. A. Khabade

Technocrats

Mr. B. S. Harale

Prof. R. M. Ganeshwade

Dr. P. S. Bhandare

Local Organizing Committee

Mr. J. A. Yadav	Mr. V. J. Jadhav	Prof. T. K. Badame	Mr. P. R. Khade	Mr. R. B. Mankar	Dr. A. S. Wagh
Dr. S. J. Patil	Mr. A. R. Patil	Dr. V. D. Kumbhar	Mrs. P. R. Mirajkar	Mr. S. S. Gavil	Dr. A. G. Sonawale
Mr. A. K. Patil	Mr. D. Y. Sakhare	Mr. A. A. Jagdale	Ms. V. D. Jagdale	Ms. V. V. Patil	Mr. R. S. Mote
Mr. S. R. Ghogare	Dr. K. N. Patil	Dr. B. J. Kadam	Dr. A. M. Mali	Mr. A. S. Bagal	Mr. V. T. Kumbhar
Mr. D. S. Shinde	Ms. S. R. Mali	Dr. G. R. Patil	Dr. R. J. Gore	Mr. G. S. Pawar	Mr. J. H. Lavand
Mr. D. J. Nalawade	Mr. D. D. Patil	Mr. S. A. Patil	Dr. A. S. Magdum	Mr. V. R. Patil	Mr. V. M. Jadhav
Mr. R. S. Kumbhar	Dr. S. L. Andhelwar	Ms. S. D. Ghatage	Ms. P. A. Kashid	Ms. P. R. Zambre	Ms. P. S. Jadhav
Mr. A. H. Tarange	Ms. A. S. Yadav	Mr. S. M. Patil	Ms. N. V. More	Ms. S. G. Patil	Ms. D. M. Gosavi
Dr. M. M. Patil	Mr. S. A. Karande	Ms. S. S. Panari	Ms. S. M. Kolekar	Mrs. N. V. Kumbhar	Ms. S. P. Patil
Ms. S. S. Patil	Ms. S. S. Patil	Ms. P. V. Shinde	Mr. S. V. Mane	Ms. S. S. Patil	Ms. S. T. Wagh
Mr. A. A. Wagh					Ms. S. K. Patil
Mr. M. B. Kadam					Mr. S. P. Salunkhe
Mr. M. K. Patil					Mr. A. R. Lavand

All Teaching and non Teaching Staff PDVP Mahavidyalaya, Tasgaon.

Multidisciplinary Approach in Basic and Applied Sciences (MABAS - 2023)



“Dissemination of Education for Knowledge, Science & Culture”

- Shikshanmaharshi Dr. Babuji Salunkhe

Shri Swami Vivekanand Shikshan Sanstha Kolhapur's

Padmabhushan Dr. Vasantodada Patil Mahavidyalaya, Tasgaon

Dist.: Sangli (MS) India Pin : 416 312

Knowledge Partner

Department of Biotechnology, Shivaji University, Kolhapur

Third International Conference

On

“Multidisciplinary Approach in Basic and Applied Sciences (MABAS - 2023)”

(23rd & 24th February - 2023)

Souvenir

ISBN: 978-93-95369-30-5



TABLE OF CONTENTS

Sr. No.	Title	Page no.
1	Diversity of millipedes (myriapoda: diplopoda) in selected lateritic soil habitats in satara tehsil, western ghat, Maharashtra - <i>Shaikh N. A., Abdar M. R., Kengar S. B.</i>	01
2	“Peanut shell extract mediated Biogenic synthesis of palladium nanoparticles (PdNPs) and its application as a homogeneous catalyst for the Suzuki-Miyaura coupling”- <i>Pranoti P. Patil, Utkarsha B. Patil, Utkarsha U. Patil, Shashikant R. Sawant, Rahul A. Kalel</i>	02
3	A study on causes and impact of laterite mining on environment and on the life of Dhangarwada people in Kudchire village of Goa state.- <i>Mr. Vinay Takale</i>	03
4	Morphological Investigation of Rhyzopertha dominica Using Light Microscopy and Scanning Electron Microscopy - <i>Mahure Y.R. and S.K. Zilpe</i>	04
5	Synthesis of Carbon Dot from Couropita Guianensis (Cannon Ball) Flower and applied for the Sensing of an anti-Diabetic drug Metformin.- <i>P. R. Khandagale, Dr. S. V. Nipane, Dr. S. R. Sabale, Dr. R. S. Dhabe.</i>	05
6	Morphological And Histological Cyclic Changes In Theovary Of Freshwater Fish : <i>Channa gachua, Dr. Ashwini G. Ghanbahadur, Prof. Y. K. Khillare</i>	06
7	Cordyceps militaris – An Important Medicinal Mushroom- <i>Trupti D. Kadam, Dr. Ashok V. Kharde.</i>	07
8	Morphometric Analysis Of Hiranyakeshi River, Sindhudurg District Using GIS Technology- <i>Aishwarya Pramod Hingmire, Shrikant Ghadage, Mayur Goud.</i>	08
9	Isolation of urease producing bacteria to produce biocement via MICP process.- <i>P. S. Rayate, B. A. Bhanjale, S. S Yeulkar</i>	09
10	Studies On Web Structure Of Two Spiders From Family Araneidae In Akola District <i>Satyavijay S. Dhande</i>	10
11	Attempts To Improve The Eye Dropper Deigne For Better Patient Compliance <i>Ms. Arte Aakanksha Sachin</i>	11
12	Aegle marmelos ash: A heterogeneous catalyst for Henry reaction <i>Rupesh C. Patil and Suresh S. Patil</i>	12
13	BMIM]-Glycine: A Sustainable Benchmark For Multicomponent Chromene Synthesis <i>Mr. Ashutosh A. Jagdale, Prin. (Dr.) Bhaskar V. Tamhankar and Prof. (Dr.) Suresh S. Patil</i>	13

155	The SiO₂-PS Composite Coated Superhydrophobic Tectona Grandis Leaf Mesh for Oil-water Separation – <i>Sagar S. Ingole, Akshay R. Jundle, Pradip P. Gaikwad, Rutuja A. Ekunde, Rajaram S. Sutar, A. K. Bhosale and, Sanjay S. Latthe</i>	157
156	A New Validated UHPLC-PDA Method for Simultaneous Quantification of Abiraterone Acetate, its Six Specified Process Impurities, and Four Degradation Products and Confirmation of all analytes based on Molecular Weight - <i>Deepak Mhaske, Archana Rajmane, Arjun Kumbhar</i>	158
157	Title - Isolation of ponceau 4R degrading bacteria from textile effluent <i>Rashmi Rokade, Jyoti Jadhav</i>	159
158	“Synthesis and Characterizations of Nickel Oxide thin film for Supercapacitor Application”- <i>Akash N. Pasale and Gaurav B. Gaikwad</i>	160
159	Today's Impact of Environmental Changes on Biodiversity Conservation – <i>Dr. Nilima M. Kankale</i>	161
160	“A study of the mechanisms underlying the anti-inflammatory effect of Mucuna atropurpurea in carrageenan-induced paw edema in rats” <i>Pratibha Malia, Manali Raneb Jyoti Jadhava</i>	162
161	The development of Self-cleaning Superhydrophobic Coating using PDMS and Candle Soot Nanoparticles Composite by Spray Technique <i>Pradip P. Gaikwad, Sagar S. Ingole, Akshay R. Jundle, Rutuja A. Ekunde, Rajaram S. Sutar, A. K. Bhosale, and Sanjay S. Latthe</i>	163
162	Development And Evaluation Of Herbal Nanoemulgel Formulation For Psoriasis Managem Ent- <i>Mr. Ravindra G. Gaikwad, Dr. Sachin S. Mali, Dr. Anilkumar J. Shinde</i>	164
163	Comparative study on incidence of seasonal diseases in commercial silkworm crossbreeds MV1 × S8 and PM × FC2 (Bombyx mori L.) in Kolhapur, Maharashtra.- <i>Rohitkumar. S. Kadam, Surat. A. Manjare, Venkata S. Manne and Manish D. Mahindrakar</i>	165
164	Studies on the plants used in Kolhapur district for the treatment of skin diseases and burns- <i>S. A. Apate and A. A. Kengar</i>	166
165	Metal Oxide Composite for Biomedical field- G.B. Takle, P.A. Kamble, P. D. Gaikwad	167
166	Development of Alkynyl Functionalized Mixed Ligand Ni(II) and Zn(II) Complexes- <i>Sharad Kamble, S. S. Chavan</i>	168
167	Analysing and Minimizing Complexity of the Triangular-Rectangular Number algorithm using Pells Equation using Python 3.- <i>Mr. Aniket S. Jadhav Mr. Mehul A. Jadhav, Mr. Thorat Sanjay Pandurang, Mr. S. S. Khopade</i>	169
168	Oneness Of Natural Number: Special Series And Their Mappings- <i>Mr. Mehul A. Jadhav, Mr. Kapil P. Gidde, Mr. Thorat Sanjay</i>	170

The SiO₂-PS Composite Coated Superhydrophobic *Tectona Grandis* Leaf Mesh for Oil-Water Separation

Sagar S. Ingole¹, Akshay R. Jundle¹, Pradip P. Gaikwad¹, Rutuja A. Ekunde¹, Rajaram S. Sutar¹, A.
K. Bhosale¹ and, Sanjay S. Latthe^{2*}

¹Self-Cleaning Research Laboratory, Department of Physics, Raje Ramrao College, Jath, Dist: Sangli –
416404, (Affiliated to Shivaji University, Kolhapur) Maharashtra, India.

² Self-cleaning Research Laboratory, Department of Physics, Vivekanand College, Kolhapur
(Autonomous), Kolhapur–416003, (Affiliated to Shivaji University, Kolhapur) Maharashtra, India

*Corresponding authors E-mail: latthes@gmail.com

Abstract

In the present study, the nanocomposite of SiO₂ nanoparticles and polystyrene (SiO₂-PS) was deposited on the naturally dried *Tectona grandis leaf* mesh through the dip coating method. The leaf mesh demonstrated a water contact angle of $157 \pm 2^\circ$ and $8 \pm 1^\circ$ of water roll-off angle after being coated with 40 mg/ml of hydrophobic SiO₂ nanoparticles in a 15 mg/ml of PS solution. The crater-like structure of the superhydrophobic leaf mesh effectively separates oils with an absolute viscosity of less than 55 cP from oil-water mixtures such as petrol, kerosene, diesel, and coconut oil using gravity-driven oil-water separation. The coated mesh also maintains its separation efficiency of 95% for up to 18 separation cycles. This low-cost and eco-friendly approach is a promising method for reducing oil-water pollution in future.

Keywords: Tectona Grandis Leaf Mesh; Wettability; Superhydrophobic; Superoleophilic; Oil-Water Separation.

Chief Guest



Dr. Achyut Godbole
MD, Softexcel Consultancy



Hon. Abhaykumar Salunkhe
Executive President



Prof. D. T. Shirke
Vice Chancellor, SUK



Prof. P. S. Patil
Pro-Vice Chancellor, SUK



Hon. Shubhangi Gavade
Secretary



Hon. Kaustabh Gavade
Chief Executive Officer



Prin. Dr. R. V. Shejawal
Joint Secretary
(Administration)



Prin. S. M. Gavali
Joint Secretary (Finance)



Dr. Milind S. Hujare
Principal

Dr. Milind S. Hujare

Principal, PDVP Mahavidyalaya, Tasgaon. Dist. Sangli

Prin. (Dr.) R. R. Kumbhar

Vivekanand College, Kolhapur

I/C Prin. Prof. (Dr.) S. R. Ghatage

S.M.D.B.S. Mahavidyalaya, Miraj

I/C Prin. Prof. (Dr.) S. S. Patil

R. R. College, Jath

Prin. (Dr.) A. N. Patil

D. K. A. S. C. College, Ichalkaranji

Prin. (Dr.) J. S. Deshmukh

R. P. College, Osmanabad

I/C Prin. (Dr.) S. S. Desai

Smt. M. M. College, Panchgani

Conveners

Prof. S. K. Khade

Dr. A. N. Ambhore

Treasurers

Mr. P. V. Patil

Dr. P. B. Teli

Dr. S. K. Shinde

Co-conveners

Dr. J. S. Ghodake

Dr. S. D. Jadhav

Organizing Secretaries

Dr. A. P. Inamdar

Dr. M. U. Patil

Dr. R. A. Kalel

Coordinators

Prof. N. A. Kulkarni

Prof. S. A. Khabade

Technocrats

Mr. B. S. Harale

Prof. R. M. Ganeshwade

Dr. P. S. Bhandare

Local Organizing Committee

Mr. J. A. Yadav	Mr. V. J. Jadhav	Prof. T. K. Badame	Mr. P. R. Khade	Mr. R. B. Mankar	Dr. A. S. Wagh
Dr. S. J. Patil	Mr. A. R. Patil	Dr. V. D. Kumbhar	Mrs. P. R. Mirajkar	Mr. S. S. Gavil	Dr. A. G. Sonawale
Mr. A. K. Patil	Mr. D. Y. Sakhare	Mr. A. A. Jagdale	Ms. V. D. Jagdale	Ms. V. V. Patil	Mr. R. S. Mote
Mr. S. R. Ghogare	Dr. K. N. Patil	Dr. B. J. Kadam	Dr. A. M. Mali	Mr. A. S. Bagal	Mr. V. T. Kumbhar
Mr. D. S. Shinde	Ms. S. R. Mali	Dr. G. R. Patil	Dr. R. J. Gore	Mr. G. S. Pawar	Mr. J. H. Lavand
Mr. D. J. Nalawade	Mr. D. D. Patil	Mr. S. A. Patil	Dr. A. S. Magdum	Mr. V. R. Patil	Mr. V. M. Jadhav
Mr. R. S. Kumbhar	Dr. S. L. Andhelwar	Ms. S. D. Ghatage	Ms. P. A. Kashid	Ms. P. R. Zambre	Ms. P. S. Jadhav
Mr. A. H. Tarange	Ms. A. S. Yadav	Mr. S. M. Patil	Ms. N. V. More	Ms. S. G. Patil	Ms. D. M. Gosavi
Dr. M. M. Patil	Mr. S. A. Karande	Ms. S. S. Panari	Ms. S. M. Kolekar	Mrs. N. V. Kumbhar	Ms. S. P. Patil
Ms. S. S. Patil	Ms. S. S. Patil	Ms. P. V. Shinde	Mr. S. V. Mane	Ms. S. S. Patil	Ms. S. T. Wagh
Mr. A. A. Wagh					Ms. S. K. Patil
Mr. M. B. Kadam					Mr. S. P. Salunkhe
Mr. M. K. Patil					Mr. A. R. Lavand

All Teaching and non Teaching Staff PDVP Mahavidyalaya, Tasgaon.

Multidisciplinary Approach in Basic and Applied Sciences (MABAS - 2023)



“Dissemination of Education for Knowledge, Science & Culture”

- Shikshanmaharshi Dr. Babuji Salunkhe

Shri Swami Vivekanand Shikshan Sanstha Kolhapur's

Padmabhushan Dr. Vasantodada Patil Mahavidyalaya, Tasgaon

Dist.: Sangli (MS) India Pin : 416 312

Knowledge Partner

Department of Biotechnology, Shivaji University, Kolhapur

Third International Conference

On

“Multidisciplinary Approach in Basic and Applied Sciences (MABAS - 2023)”

(23rd & 24th February - 2023)

Souvenir

ISBN: 978-93-95369-30-5



TABLE OF CONTENTS

Sr. No.	Title	Page no.
1	Diversity of millipedes (myriapoda: diplopoda) in selected lateritic soil habitats in satara tehsil, western ghat, Maharashtra - <i>Shaikh N. A., Abdar M. R., Kengar S. B.</i>	01
2	“Peanut shell extract mediated Biogenic synthesis of palladium nanoparticles (PdNPs) and its application as a homogeneous catalyst for the Suzuki-Miyaura coupling”- <i>Pranoti P. Patil, Utkarsha B. Patil, Utkarsha U. Patil, Shashikant R. Sawant, Rahul A. Kalel</i>	02
3	A study on causes and impact of laterite mining on environment and on the life of Dhangarwada people in Kudchire village of Goa state.- <i>Mr. Vinay Takale</i>	03
4	Morphological Investigation of Rhyzopertha dominica Using Light Microscopy and Scanning Electron Microscopy - <i>Mahure Y.R. and S.K. Zilpe</i>	04
5	Synthesis of Carbon Dot from Couropita Guianensis (Cannon Ball) Flower and applied for the Sensing of an anti-Diabetic drug Metformin.- <i>P. R. Khandagale, Dr. S. V. Nipane, Dr. S. R. Sabale, Dr. R. S. Dhabe.</i>	05
6	Morphological And Histological Cyclic Changes In Theovary Of Freshwater Fish : <i>Channa gachua, Dr. Ashwini G. Ghanbahadur, Prof. Y. K. Khillare</i>	06
7	Cordyceps militaris – An Important Medicinal Mushroom- <i>Trupti D. Kadam, Dr. Ashok V. Kharde.</i>	07
8	Morphometric Analysis Of Hiranyakeshi River, Sindhudurg District Using GIS Technology- <i>Aishwarya Pramod Hingmire, Shrikant Ghadage, Mayur Goud.</i>	08
9	Isolation of urease producing bacteria to produce biocement via MICP process.- <i>P. S. Rayate, B. A. Bhanjale, S. S Yeulkar</i>	09
10	Studies On Web Structure Of Two Spiders From Family Araneidae In Akola District <i>Satyavijay S. Dhande</i>	10
11	Attempts To Improve The Eye Dropper Deigne For Better Patient Compliance <i>Ms. Arte Aakanksha Sachin</i>	11
12	Aegle marmelos ash: A heterogeneous catalyst for Henry reaction <i>Rupesh C. Patil and Suresh S. Patil</i>	12
13	BMIM]-Glycine: A Sustainable Benchmark For Multicomponent Chromene Synthesis <i>Mr. Ashutosh A. Jagdale, Prin. (Dr.) Bhaskar V. Tamhankar and Prof. (Dr.) Suresh S. Patil</i>	13

155	The SiO₂-PS Composite Coated Superhydrophobic Tectona Grandis Leaf Mesh for Oil-water Separation – <i>Sagar S. Ingole, Akshay R. Jundle, Pradip P. Gaikwad, Rutuja A. Ekunde, Rajaram S. Sutar, A. K. Bhosale and, Sanjay S. Lathe</i>	157
156	A New Validated UHPLC-PDA Method for Simultaneous Quantification of Abiraterone Acetate, its Six Specified Process Impurities, and Four Degradation Products and Confirmation of all analytes based on Molecular Weight - <i>Deepak Mhaske, Archana Rajmane, Arjun Kumbhar</i>	158
157	Title - Isolation of ponceau 4R degrading bacteria from textile effluent <i>Rashmi Rokade, Jyoti Jadhav</i>	159
158	“Synthesis and Characterizations of Nickel Oxide thin film for Supercapacitor Application”- <i>Akash N. Pasale and Gaurav B. Gaikwad</i>	160
159	Today's Impact of Environmental Changes on Biodiversity Conservation – <i>Dr. Nilima M. Kankale</i>	161
160	“A study of the mechanisms underlying the anti-inflammatory effect of Mucuna atropurpurea in carrageenan-induced paw edema in rats” <i>Pratibha Malia, Manali Raneb Jyoti Jadhava</i>	162
161	The development of Self-cleaning Superhydrophobic Coating using PDMS and Candle Soot Nanoparticles Composite by Spray Technique <i>Pradip P. Gaikwad, Sagar S. Ingole, Akshay R. Jundle, Rutuja A. Ekunde, Rajaram S. Sutar, A. K. Bhosale, and Sanjay S. Lathe</i>	163
162	Development And Evaluation Of Herbal Nanoemulgel Formulation For Psoriasis Managem Ent- <i>Mr. Ravindra G. Gaikwad, Dr. Sachin S. Mali, Dr. Anilkumar J. Shinde</i>	164
163	Comparative study on incidence of seasonal diseases in commercial silkworm crossbreeds MV1 × S8 and PM × FC2 (Bombyx mori L.) in Kolhapur, Maharashtra.- <i>Rohitkumar. S. Kadam, Surat. A. Manjare, Venkata S. Manne and Manish D. Mahindrakar</i>	165
164	Studies on the plants used in Kolhapur district for the treatment of skin diseases and burns- <i>S. A. Apate and A. A. Kengar</i>	166
165	Metal Oxide Composite for Biomedical field- G.B. Takle, P.A. Kamble, P. D. Gaikwad	167
166	Development of Alkynyl Functionalized Mixed Ligand Ni(II) and Zn(II) Complexes- <i>Sharad Kamble, S. S. Chavan</i>	168
167	Analysing and Minimizing Complexity of the Triangular-Rectangular Number algorithm using Pells Equation using Python 3.- <i>Mr. Aniket S. Jadhav Mr. Mehul A. Jadhav, Mr. Thorat Sanjay Pandurang, Mr. S. S. Khopade</i>	169
168	Oneness Of Natural Number: Special Series And Their Mappings- <i>Mr. Mehul A. Jadhav, Mr. Kapil P. Gidde, Mr. Thorat Sanjay</i>	170

The SiO₂-PS Composite Coated Superhydrophobic *Tectona Grandis* Leaf Mesh for Oil-Water Separation

Sagar S. Ingole¹, Akshay R. Jundle¹, Pradip P. Gaikwad¹, Rutuja A. Ekunde¹, **Rajaram S. Sutar¹**, A.
K. Bhosale¹ and, Sanjay S. Latthe^{2*}

¹Self-Cleaning Research Laboratory, Department of Physics, Raje Ramrao College, Jath, Dist: Sangli –
416404, (Affiliated to Shivaji University, Kolhapur) Maharashtra, India.

² Self-cleaning Research Laboratory, Department of Physics, Vivekanand College, Kolhapur
(Autonomous), Kolhapur–416003, (Affiliated to Shivaji University, Kolhapur) Maharashtra, India

*Corresponding authors E-mail: latthes@gmail.com

Abstract

In the present study, the nanocomposite of SiO₂ nanoparticles and polystyrene (SiO₂-PS) was deposited on the naturally dried *Tectona grandis leaf* mesh through the dip coating method. The leaf mesh demonstrated a water contact angle of $157 \pm 2^\circ$ and $8 \pm 1^\circ$ of water roll-off angle after being coated with 40 mg/ml of hydrophobic SiO₂ nanoparticles in a 15 mg/ml of PS solution. The crater-like structure of the superhydrophobic leaf mesh effectively separates oils with an absolute viscosity of less than 55 cP from oil-water mixtures such as petrol, kerosene, diesel, and coconut oil using gravity-driven oil-water separation. The coated mesh also maintains its separation efficiency of 95% for up to 18 separation cycles. This low-cost and eco-friendly approach is a promising method for reducing oil-water pollution in future.

Keywords: Tectona Grandis Leaf Mesh; Wettability; Superhydrophobic; Superoleophilic; Oil-Water Separation.

Chief Guest



Dr. Achyut Godbole
MD, Softexcel Consultancy



Hon. Abhaykumar Salunkhe
Executive President



Prof. D. T. Shirke
Vice Chancellor, SUK



Prof. P. S. Patil
Pro-Vice Chancellor, SUK



Hon. Shubhangi Gavade
Secretary



Hon. Kaustabh Gavade
Chief Executive Officer



Prin. Dr. R. V. Shejawal
Joint Secretary
(Administration)



Prin. S. M. Gavali
Joint Secretary (Finance)



Dr. Milind S. Hujare
Principal

Dr. Milind S. Hujare

Principal, PDVP Mahavidyalaya, Tasgaon. Dist. Sangli

Prin. (Dr.) R. R. Kumbhar

Vivekanand College, Kolhapur

I/C Prin. Prof. (Dr.) S. R. Ghatage

S.M.D.B.S. Mahavidyalaya, Miraj

I/C Prin. Prof. (Dr.) S. S. Patil

R. R. College, Jath

Prin. (Dr.) A. N. Patil

D. K. A. S. C. College, Ichalkaranji

Prin. (Dr.) J. S. Deshmukh

R. P. College, Osmanabad

I/C Prin. (Dr.) S. S. Desai

Smt. M. M. College, Panchgani

Conveners

Prof. S. K. Khade

Dr. A. N. Ambhore

Treasurers

Mr. P. V. Patil

Dr. P. B. Teli

Dr. S. K. Shinde

Co-conveners

Dr. J. S. Ghodake

Dr. S. D. Jadhav

Organizing Secretaries

Dr. A. P. Inamdar

Dr. M. U. Patil

Dr. R. A. Kalel

Coordinators

Prof. N. A. Kulkarni

Prof. S. A. Khabade

Technocrats

Mr. B. S. Harale

Prof. R. M. Ganeshwade

Dr. P. S. Bhandare

Local Organizing Committee

Mr. J. A. Yadav	Mr. V. J. Jadhav	Prof. T. K. Badame	Mr. P. R. Khade	Mr. R. B. Mankar	Dr. A. S. Wagh
Dr. S. J. Patil	Mr. A. R. Patil	Dr. V. D. Kumbhar	Mrs. P. R. Mirajkar	Mr. S. S. Gavil	Dr. A. G. Sonawale
Mr. A. K. Patil	Mr. D. Y. Sakhare	Mr. A. A. Jagdale	Ms. V. D. Jagdale	Ms. V. V. Patil	Mr. R. S. Mote
Mr. S. R. Ghogare	Dr. K. N. Patil	Dr. B. J. Kadam	Dr. A. M. Mali	Mr. A. S. Bagal	Mr. V. T. Kumbhar
Mr. D. S. Shinde	Ms. S. R. Mali	Dr. G. R. Patil	Dr. R. J. Gore	Mr. G. S. Pawar	Mr. J. H. Lavand
Mr. D. J. Nalawade	Mr. D. D. Patil	Mr. S. A. Patil	Dr. A. S. Magdum	Mr. V. R. Patil	Mr. V. M. Jadhav
Mr. R. S. Kumbhar	Dr. S. L. Andhelwar	Ms. S. D. Ghatage	Ms. P. A. Kashid	Ms. P. R. Zambre	Ms. P. S. Jadhav
Mr. A. H. Tarange	Ms. A. S. Yadav	Mr. S. M. Patil	Ms. N. V. More	Ms. S. G. Patil	Ms. D. M. Gosavi
Dr. M. M. Patil	Mr. S. A. Karande	Ms. S. S. Panari	Ms. S. M. Kolekar	Mrs. N. V. Kumbhar	Ms. S. P. Patil
Ms. S. S. Patil	Ms. S. S. Patil	Ms. P. V. Shinde	Mr. S. V. Mane	Ms. S. S. Patil	Ms. S. T. Wagh
Mr. A. A. Wagh					Ms. S. K. Patil
Mr. M. B. Kadam					Mr. S. P. Salunkhe
Mr. M. K. Patil					Mr. A. R. Lavand

All Teaching and non Teaching Staff PDVP Mahavidyalaya, Tasgaon.

Multidisciplinary Approach in Basic and Applied Sciences (MABAS - 2023)



“Dissemination of Education for Knowledge, Science & Culture”

- Shikshanmaharshi Dr. Bapuji Salunkhe

Shri Swami Vivekanand Shikshan Sanstha Kolhapur's

Padmabhushan Dr. Vasantodada Patil Mahavidyalaya, Tasgaon

Dist.: Sangli (MS) India Pin : 416 312

Knowledge Partner

Department of Biotechnology, Shivaji University, Kolhapur

Third International Conference

On

“Multidisciplinary Approach in Basic and Applied Sciences (MABAS - 2023)”

(23rd & 24th February - 2023)

Souvenir

ISBN: 978-93-95369-30-5



TABLE OF CONTENTS

Sr. No.	Title	Page no.
1	Diversity of millipedes (myriapoda: diplopoda) in selected lateritic soil habitats in satara tehsil, western ghat, Maharashtra - <i>Shaikh N. A., Abdar M. R., Kengar S. B.</i>	01
2	“Peanut shell extract mediated Biogenic synthesis of palladium nanoparticles (PdNPs) and its application as a homogeneous catalyst for the Suzuki-Miyaura coupling”- <i>Pranoti P. Patil, Utkarsha B. Patil, Utkarsha U. Patil, Shashikant R. Sawant, Rahul A. Kalel</i>	02
3	A study on causes and impact of laterite mining on environment and on the life of Dhangarwada people in Kudchire village of Goa state.- <i>Mr. Vinay Takale</i>	03
4	Morphological Investigation of Rhyzopertha dominica Using Light Microscopy and Scanning Electron Microscopy - <i>Mahure Y.R. and S.K. Zilpe</i>	04
5	Synthesis of Carbon Dot from Couropita Guianensis (Cannon Ball) Flower and applied for the Sensing of an anti-Diabetic drug Metformin.- <i>P. R. Khandagale, Dr. S. V. Nipane, Dr. S. R. Sabale, Dr. R. S. Dhabe.</i>	05
6	Morphological And Histological Cyclic Changes In Theovary Of Freshwater Fish : <i>Channa gachua, Dr. Ashwini G. Ghanbahadur, Prof. Y. K. Khillare</i>	06
7	Cordyceps militaris – An Important Medicinal Mushroom- <i>Trupti D. Kadam, Dr. Ashok V. Kharde.</i>	07
8	Morphometric Analysis Of Hiranyakeshi River, Sindhudurg District Using GIS Technology- <i>Aishwarya Pramod Hingmire, Shrikant Ghadage, Mayur Goud.</i>	08
9	Isolation of urease producing bacteria to produce biocement via MICP process.- <i>P. S. Rayate, B. A. Bhanjale, S. S Yeulkar</i>	09
10	Studies On Web Structure Of Two Spiders From Family Araneidae In Akola District <i>Satyavijay S. Dhande</i>	10
11	Attempts To Improve The Eye Dropper Deigne For Better Patient Compliance <i>Ms. Arte Aakanksha Sachin</i>	11
12	Aegle marmelos ash: A heterogeneous catalyst for Henry reaction <i>Rupesh C. Patil and Suresh S. Patil</i>	12
13	BMIM]-Glycine: A Sustainable Benchmark For Multicomponent Chromene Synthesis <i>Mr. Ashutosh A. Jagdale, Prin. (Dr.) Bhaskar V. Tamhankar and Prof. (Dr.) Suresh S. Patil</i>	13

155	The SiO₂-PS Composite Coated Superhydrophobic Tectona Grandis Leaf Mesh for Oil-water Separation – Sagar S. Ingole, Akshay R. Jundle, Pradip P. Gaikwad, Rutuja A. Ekunde, Rajaram S. Sutar, A. K. Bhosale and, Sanjay S. Lathe	157
156	A New Validated UHPLC-PDA Method for Simultaneous Quantification of Abiraterone Acetate, its Six Specified Process Impurities, and Four Degradation Products and Confirmation of all analytes based on Molecular Weight - Deepak Mhaske, Archana Rajmane, Arjun Kumbhar	158
157	Title - Isolation of ponceau 4R degrading bacteria from textile effluent Rashmi Rokade, Jyoti Jadhav	159
158	“Synthesis and Characterizations of Nickel Oxide thin film for Supercapacitor Application”- Akash N. Pasale and Gaurav B. Gaikwad	160
159	Today's Impact of Environmental Changes on Biodiversity Conservation – Dr. Nilima M. Kankale	161
160	“A study of the mechanisms underlying the anti-inflammatory effect of Mucuna atropurpurea in carrageenan-induced paw edema in rats” Pratibha Malia, Manali Raneb Jyoti Jadhava	162
161	The development of Self-cleaning Superhydrophobic Coating using PDMS and Candle Soot Nanoparticles Composite by Spray Technique Pradip P. Gaikwad, Sagar S. Ingole, Akshay R. Jundle, Rutuja A. Ekunde, Rajaram S. Sutar, A. K. Bhosale, and Sanjay S. Lathe	163
162	Development And Evaluation Of Herbal Nanoemulgel Formulation For Psoriasis Managem Ent- Mr. Ravindra G. Gaikwad, Dr. Sachin S. Mali, Dr. Anilkumar J. Shinde	164
163	Comparative study on incidence of seasonal diseases in commercial silkworm crossbreeds MV1 × S8 and PM × FC2 (Bombyx mori L.) in Kolhapur, Maharashtra.- Rohitkumar. S. Kadam, Surat. A. Manjare, Venkata S. Manne and Manish D. Mahindrakar	165
164	Studies on the plants used in Kolhapur district for the treatment of skin diseases and burns- S. A. Apate and A. A. Kengar	166
165	Metal Oxide Composite for Biomedical field- G.B. Takle, P.A. Kamble, P. D. Gaikwad	167
166	Development of Alkynyl Functionalized Mixed Ligand Ni(II) and Zn(II) Complexes- Sharad Kamble, S. S. Chavan	168
167	Analysing and Minimizing Complexity of the Triangular-Rectangular Number algorithm using Pells Equation using Python 3.- Mr. Aniket S. Jadhav Mr. Mehul A. Jadhav, Mr. Thorat Sanjay Pandurang, Mr. S. S. Khopade	169
168	Oneness Of Natural Number: Special Series And Their Mappings- Mr. Mehul A. Jadhav, Mr. Kapil P. Gidde, Mr. Thorat Sanjay	170

The SiO₂-PS Composite Coated Superhydrophobic *Tectona Grandis* Leaf Mesh for Oil-Water Separation

Sagar S. Ingole¹, Akshay R. Jundle¹, Pradip P. Gaikwad¹, Rutuja A. Ekunde¹, Rajaram S. Sutar¹, A.
K. Bhosale¹ and, Sanjay S. Latthe^{2*}

¹Self-Cleaning Research Laboratory, Department of Physics, Raje Ramrao College, Jath, Dist: Sangli –
416404, (Affiliated to Shivaji University, Kolhapur) Maharashtra, India.

² Self-cleaning Research Laboratory, Department of Physics, Vivekanand College, Kolhapur
(Autonomous), Kolhapur–416003, (Affiliated to Shivaji University, Kolhapur) Maharashtra, India

*Corresponding authors E-mail: latthes@gmail.com

Abstract

In the present study, the nanocomposite of SiO₂ nanoparticles and polystyrene (SiO₂-PS) was deposited on the naturally dried *Tectona grandis leaf* mesh through the dip coating method. The leaf mesh demonstrated a water contact angle of $157 \pm 2^\circ$ and $8 \pm 1^\circ$ of water roll-off angle after being coated with 40 mg/ml of hydrophobic SiO₂ nanoparticles in a 15 mg/ml of PS solution. The crater-like structure of the superhydrophobic leaf mesh effectively separates oils with an absolute viscosity of less than 55 cP from oil-water mixtures such as petrol, kerosene, diesel, and coconut oil using gravity-driven oil-water separation. The coated mesh also maintains its separation efficiency of 95% for up to 18 separation cycles. This low-cost and eco-friendly approach is a promising method for reducing oil-water pollution in future.

Keywords: Tectona Grandis Leaf Mesh; Wettability; Superhydrophobic; Superoleophilic; Oil-Water Separation.

Chief Guest



Dr. Achyut Godbole
MD, Softexcel Consultancy



Hon. Abhaykumar Salunkhe
Executive President



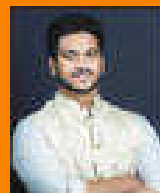
Prof. D. T. Shirke
Vice Chancellor, SUK



Prof. P. S. Patil
Pro-Vice Chancellor, SUK



Hon. Shubhangi Gavade
Secretary



Hon. Kaustabh Gavade
Chief Executive Officer



Prin. Dr. R. V. Shejwal
Joint Secretary
(Administration)



Prin. S. M. Gavali
Joint Secretary (Finance)



Dr. Milind S. Hujare
Principal

Dr. Milind S. Hujare

Principal, PDVP Mahavidyalaya, Tasgaon. Dist. Sangli

Prin. (Dr.) R. R. Kumbhar

Vivekanand College, Kolhapur

I/C Prin. Prof. (Dr.) S. R. Ghatage

S.M.D.B.S. Mahavidyalaya, Miraj

I/C Prin. Prof. (Dr.) S. S. Patil

R. R. College, Jath

Prin. (Dr.) A. N. Patil

D. K. A. S. C. College, Ichalkaranji

Prin. (Dr.) J. S. Deshmukh

R. P. College, Osmanabad

I/C Prin. (Dr.) S. S. Desai

Smt. M. M. College, Panchgani

Conveners

Prof. S. K. Khade

Dr. A. N. Ambhore

Treasurers

Mr. P. V. Patil

Dr. P. B. Teli

Dr. S. K. Shinde

Co-conveners

Dr. J. S. Ghodake

Dr. S. D. Jadhav

Organizing Secretaries

Dr. A. P. Inamdar

Dr. M. U. Patil

Dr. R. A. Kalel

Coordinators

Prof. N. A. Kulkarni

Prof. S. A. Khabade

Technocrats

Mr. B. S. Harale

Prof. R. M. Ganeshwade

Dr. P. S. Bhandare

Local Organizing Committee

Mr. J. A. Yadav	Mr. V. J. Jadhav	Prof. T. K. Badame	Mr. P. R. Khade	Mr. R. B. Mankar	Dr. A. S. Wagh
Dr. S. J. Patil	Mr. A. R. Patil	Dr. V. D. Kumbhar	Mrs. P. R. Mirajkar	Mr. S. S. Gavil	Dr. A. G. Sonawale
Mr. A. K. Patil	Mr. D. Y. Sakhare	Mr. A. A. Jagdale	Ms. V. D. Jagdale	Ms. V. V. Patil	Mr. R. S. Mote
Mr. S. R. Ghogare	Dr. K. N. Patil	Dr. B. J. Kadam	Dr. A. M. Mali	Mr. A. S. Bagal	Mr. V. T. Kumbhar
Mr. D. S. Shinde	Ms. S. R. Mali	Dr. G. R. Patil	Dr. R. J. Gore	Mr. G. S. Pawar	Mr. J. H. Lavand
Mr. D. J. Nalawade	Mr. D. D. Patil	Mr. S. A. Patil	Dr. A. S. Magdum	Mr. V. R. Patil	Mr. V. M. Jadhav
Mr. R. S. Kumbhar	Dr. S. L. Andhelwar	Ms. S. D. Ghatage	Ms. P. A. Kashid	Ms. P. R. Zambre	Ms. P. S. Jadhav
Mr. A. H. Tarange	Ms. A. S. Yadav	Mr. S. M. Patil	Ms. N. V. More	Ms. S. G. Patil	Ms. D. M. Gosavi
Dr. M. M. Patil	Mr. S. A. Karande	Ms. S. S. Panari	Ms. S. M. Kolekar	Mrs. N. V. Kumbhar	Ms. S. P. Patil
Ms. S. S. Patil	Ms. S. S. Patil	Ms. P. V. Shinde	Mr. S. V. Mane	Ms. S. S. Patil	Ms. S. T. Wagh
Mr. A. A. Wagh					Ms. S. K. Patil
Mr. M. B. Kadam					Mr. S. P. Salunkhe
Mr. M. K. Patil					Mr. A. R. Lavand

All Teaching and non Teaching Staff PDVP Mahavidyalaya, Tasgaon.

Multidisciplinary Approach in Basic and Applied Sciences (MABAS - 2023)



“Dissemination of Education for Knowledge, Science & Culture”

- Shikshanmaharshi Dr. Bapuji Salunkhe

Shri Swami Vivekanand Shikshan Sanstha Kolhapur's

Padmabhushan Dr. Vasantodada Patil Mahavidyalaya, Tasgaon

Dist.: Sangli (MS) India Pin : 416 312

Knowledge Partner

Department of Biotechnology, Shivaji University, Kolhapur

Third International Conference

On

“Multidisciplinary Approach in Basic and Applied Sciences (MABAS - 2023)”

(23rd & 24th February - 2023)

Souvenir

ISBN: 978-93-95369-30-5



TABLE OF CONTENTS

Sr. No.	Title	Page no.
1	Diversity of millipedes (myriapoda: diplopoda) in selected lateritic soil habitats in satara tehsil, western ghat, Maharashtra - <i>Shaikh N. A., Abdar M. R., Kengar S. B.</i>	01
2	“Peanut shell extract mediated Biogenic synthesis of palladium nanoparticles (PdNPs) and its application as a homogeneous catalyst for the Suzuki-Miyaura coupling”- <i>Pranoti P. Patil, Utkarsha B. Patil, Utkarsha U. Patil, Shashikant R. Sawant, Rahul A. Kalel</i>	02
3	A study on causes and impact of laterite mining on environment and on the life of Dhangarwada people in Kudchire village of Goa state.- <i>Mr. Vinay Takale</i>	03
4	Morphological Investigation of Rhyzopertha dominica Using Light Microscopy and Scanning Electron Microscopy - <i>Mahure Y.R. and S.K. Zilpe</i>	04
5	Synthesis of Carbon Dot from Couropita Guianensis (Cannon Ball) Flower and applied for the Sensing of an anti-Diabetic drug Metformin.- <i>P. R. Khandagale, Dr. S. V. Nipane, Dr. S. R. Sabale, Dr. R. S. Dhabe.</i>	05
6	Morphological And Histological Cyclic Changes In Theovary Of Freshwater Fish : <i>Channa gachua, Dr. Ashwini G. Ghanbahadur, Prof. Y. K. Khillare</i>	06
7	Cordyceps militaris – An Important Medicinal Mushroom- <i>Trupti D. Kadam, Dr. Ashok V. Kharde.</i>	07
8	Morphometric Analysis Of Hiranyakeshi River, Sindhudurg District Using GIS Technology- <i>Aishwarya Pramod Hingmire, Shrikant Ghadage, Mayur Goud.</i>	08
9	Isolation of urease producing bacteria to produce biocement via MICP process.- <i>P. S. Rayate, B. A. Bhanjale, S. S Yeulkar</i>	09
10	Studies On Web Structure Of Two Spiders From Family Araneidae In Akola District <i>Satyavijay S. Dhande</i>	10
11	Attempts To Improve The Eye Dropper Deigne For Better Patient Compliance <i>Ms. Arte Aakanksha Sachin</i>	11
12	Aegle marmelos ash: A heterogeneous catalyst for Henry reaction <i>Rupesh C. Patil and Suresh S. Patil</i>	12
13	BMIM]-Glycine: A Sustainable Benchmark For Multicomponent Chromene Synthesis <i>Mr. Ashutosh A. Jagdale, Prin. (Dr.) Bhaskar V. Tamhankar and Prof. (Dr.) Suresh S. Patil</i>	13

155	The SiO₂-PS Composite Coated Superhydrophobic Tectona Grandis Leaf Mesh for Oil-water Separation – <i>Sagar S. Ingole, Akshay R. Jundle, Pradip P. Gaikwad, Rutuja A. Ekunde, Rajaram S. Sutar, A. K. Bhosale and, Sanjay S. Latthe</i>	157
156	A New Validated UHPLC-PDA Method for Simultaneous Quantification of Abiraterone Acetate, its Six Specified Process Impurities, and Four Degradation Products and Confirmation of all analytes based on Molecular Weight - <i>Deepak Mhaske, Archana Rajmane, Arjun Kumbhar</i>	158
157	Title - Isolation of ponceau 4R degrading bacteria from textile effluent <i>Rashmi Rokade, Jyoti Jadhav</i>	159
158	“Synthesis and Characterizations of Nickel Oxide thin film for Supercapacitor Application”- <i>Akash N. Pasale and Gaurav B. Gaikwad</i>	160
159	Today's Impact of Environmental Changes on Biodiversity Conservation – <i>Dr. Nilima M. Kankale</i>	161
160	“A study of the mechanisms underlying the anti-inflammatory effect of Mucuna atropurpurea in carrageenan-induced paw edema in rats” <i>Pratibha Malia, Manali Raneb Jyoti Jadhava</i>	162
161	The development of Self-cleaning Superhydrophobic Coating using PDMS and Candle Soot Nanoparticles Composite by Spray Technique <i>Pradip P. Gaikwad, Sagar S. Ingole, Akshay R. Jundle, Rutuja A. Ekunde, Rajaram S. Sutar, A. K. Bhosale, and Sanjay S. Latthe</i>	163
162	Development And Evaluation Of Herbal Nanoemulgel Formulation For Psoriasis Managem Ent- <i>Mr. Ravindra G. Gaikwad, Dr. Sachin S. Mali, Dr. Anilkumar J. Shinde</i>	164
163	Comparative study on incidence of seasonal diseases in commercial silkworm crossbreeds MV1 × S8 and PM × FC2 (Bombyx mori L.) in Kolhapur, Maharashtra.- <i>Rohitkumar. S. Kadam, Surat. A. Manjare, Venkata S. Manne and Manish D. Mahindrakar</i>	165
164	Studies on the plants used in Kolhapur district for the treatment of skin diseases and burns- <i>S. A. Apate and A. A. Kengar</i>	166
165	Metal Oxide Composite for Biomedical field- G.B. Takle, P.A. Kamble, P. D. Gaikwad	167
166	Development of Alkynyl Functionalized Mixed Ligand Ni(II) and Zn(II) Complexes- <i>Sharad Kamble, S. S. Chavan</i>	168
167	Analysing and Minimizing Complexity of the Triangular-Rectangular Number algorithm using Pells Equation using Python 3.- <i>Mr. Aniket S. Jadhav Mr. Mehul A. Jadhav, Mr. Thorat Sanjay Pandurang, Mr. S. S. Khopade</i>	169
168	Oneness Of Natural Number: Special Series And Their Mappings- <i>Mr. Mehul A. Jadhav, Mr. Kapil P. Gidde, Mr. Thorat Sanjay</i>	170

The SiO₂-PS Composite Coated Superhydrophobic *Tectona Grandis* Leaf Mesh for Oil-Water Separation

Sagar S. Ingole¹, Akshay R. Jundle¹, Pradip P. Gaikwad¹, Rutuja A. Ekunde¹, Rajaram S. Sutar¹, A.
K. Bhosale¹ and, Sanjay S. Latthe^{2*}

¹Self-Cleaning Research Laboratory, Department of Physics, Raje Ramrao College, Jath, Dist: Sangli –
416404, (Affiliated to Shivaji University, Kolhapur) Maharashtra, India.

² Self-cleaning Research Laboratory, Department of Physics, Vivekanand College, Kolhapur
(Autonomous), Kolhapur–416003, (Affiliated to Shivaji University, Kolhapur) Maharashtra, India

*Corresponding authors E-mail: latthes@gmail.com

Abstract

In the present study, the nanocomposite of SiO₂ nanoparticles and polystyrene (SiO₂-PS) was deposited on the naturally dried *Tectona grandis leaf* mesh through the dip coating method. The leaf mesh demonstrated a water contact angle of $157 \pm 2^\circ$ and $8 \pm 1^\circ$ of water roll-off angle after being coated with 40 mg/ml of hydrophobic SiO₂ nanoparticles in a 15 mg/ml of PS solution. The crater-like structure of the superhydrophobic leaf mesh effectively separates oils with an absolute viscosity of less than 55 cP from oil-water mixtures such as petrol, kerosene, diesel, and coconut oil using gravity-driven oil-water separation. The coated mesh also maintains its separation efficiency of 95% for up to 18 separation cycles. This low-cost and eco-friendly approach is a promising method for reducing oil-water pollution in future.

Keywords: Tectona Grandis Leaf Mesh; Wettability; Superhydrophobic; Superoleophilic; Oil-Water Separation.

Chief Guest



Dr. Achyut Godbole
MD, Softexcel Consultancy



Hon. Abhaykumar Salunkhe
Executive President



Prof. D. T. Shirke
Vice Chancellor, SUK



Prof. P. S. Patil
Pro-Vice Chancellor, SUK



Hon. Shubhangi Gavade
Secretary



Hon. Kaustabh Gavade
Chief Executive Officer



Prin. Dr. R. V. Shejwal
Joint Secretary
(Administration)



Prin. S. M. Gavali
Joint Secretary (Finance)



Dr. Milind S. Hujare
Principal

Dr. Milind S. Hujare

Principal, PDVP Mahavidyalaya, Tasgaon. Dist. Sangli

Prin. (Dr.) R. R. Kumbhar

Vivekanand College, Kolhapur

I/C Prin. Prof. (Dr.) S. R. Ghatage

S.M.D.B.S. Mahavidyalaya, Miraj

I/C Prin. Prof. (Dr.) S. S. Patil

R. R. College, Jath

Prin. (Dr.) A. N. Patil

D. K. A. S. C. College, Ichalkaranji

Prin. (Dr.) J. S. Deshmukh

R. P. College, Osmanabad

I/C Prin. (Dr.) S. S. Desai

Smt. M. M. College, Panchgani

Conveners

Prof. S. K. Khade

Dr. A. N. Ambhore

Treasurers

Mr. P. V. Patil

Dr. P. B. Teli

Dr. S. K. Shinde

Co-conveners

Dr. J. S. Ghodake

Dr. S. D. Jadhav

Organizing Secretaries

Dr. A. P. Inamdar

Dr. M. U. Patil

Dr. R. A. Kalel

Coordinators

Prof. N. A. Kulkarni

Prof. S. A. Khabade

Technocrats

Mr. B. S. Harale

Prof. R. M. Ganeshwade

Dr. P. S. Bhandare

Local Organizing Committee

Mr. J. A. Yadav	Mr. V. J. Jadhav	Prof. T. K. Badame	Mr. P. R. Khade	Mr. R. B. Mankar	Dr. A. S. Wagh
Dr. S. J. Patil	Mr. A. R. Patil	Dr. V. D. Kumbhar	Mrs. P. R. Mirajkar	Mr. S. S. Gavil	Dr. A. G. Sonawale
Mr. A. K. Patil	Mr. D. Y. Sakhare	Mr. A. A. Jagdale	Ms. V. D. Jagdale	Ms. V. V. Patil	Mr. R. S. Mote
Mr. S. R. Ghogare	Dr. K. N. Patil	Dr. B. J. Kadam	Dr. A. M. Mali	Mr. A. S. Bagal	Mr. V. T. Kumbhar
Mr. D. S. Shinde	Ms. S. R. Mali	Dr. G. R. Patil	Dr. R. J. Gore	Mr. G. S. Pawar	Mr. J. H. Lavand
Mr. D. J. Nalawade	Mr. D. D. Patil	Mr. S. A. Patil	Dr. A. S. Magdum	Mr. V. R. Patil	Mr. V. M. Jadhav
Mr. R. S. Kumbhar	Dr. S. L. Andhelwar	Ms. S. D. Ghatage	Ms. P. A. Kashid	Ms. P. R. Zambre	Ms. P. S. Jadhav
Mr. A. H. Tarange	Ms. A. S. Yadav	Mr. S. M. Patil	Ms. N. V. More	Ms. S. G. Patil	Ms. D. M. Gosavi
Dr. M. M. Patil	Mr. S. A. Karande	Ms. S. S. Panari	Ms. S. M. Kolekar	Mrs. N. V. Kumbhar	Ms. S. P. Patil
Ms. S. S. Patil	Ms. S. S. Patil	Ms. P. V. Shinde	Mr. S. V. Mane	Ms. S. S. Patil	Ms. S. T. Wagh
Mr. A. A. Wagh					Ms. S. K. Patil
Mr. M. B. Kadam					Mr. S. P. Salunkhe
Mr. M. K. Patil					Mr. A. R. Lavand

All Teaching and non Teaching Staff PDVP Mahavidyalaya, Tasgaon.

Multidisciplinary Approach in Basic and Applied Sciences (MABAS - 2023)



“Dissemination of Education for Knowledge, Science & Culture”

- Shikshanmaharshi Dr. Babuji Salunkhe

Shri Swami Vivekanand Shikshan Sanstha Kolhapur's

Padmabhushan Dr. Vasantraodada Patil Mahavidyalaya, Tasgaon

Dist.: Sangli (MS) India Pin : 416 312

Knowledge Partner

Department of Biotechnology, Shivaji University, Kolhapur

Third International Conference

On

“Multidisciplinary Approach in Basic and Applied Sciences (MABAS - 2023)”

(23rd & 24th February - 2023)

Souvenir

ISBN: 978-93-95369-30-5



TABLE OF CONTENTS

Sr. No.	Title	Page no.
1	Diversity of millipedes (myriapoda: diplopoda) in selected lateritic soil habitats in satara tehsil, western ghat, Maharashtra - <i>Shaikh N. A., Abdar M. R., Kengar S. B.</i>	01
2	“Peanut shell extract mediated Biogenic synthesis of palladium nanoparticles (PdNPs) and its application as a homogeneous catalyst for the Suzuki-Miyaura coupling”- <i>Pranoti P. Patil, Utkarsha B. Patil, Utkarsha U. Patil, Shashikant R. Sawant, Rahul A. Kalel</i>	02
3	A study on causes and impact of laterite mining on environment and on the life of Dhangarwada people in Kudchire village of Goa state.- <i>Mr. Vinay Takale</i>	03
4	Morphological Investigation of Rhyzopertha dominica Using Light Microscopy and Scanning Electron Microscopy - <i>Mahure Y.R. and S.K. Zilpe</i>	04
5	Synthesis of Carbon Dot from Couropita Guianensis (Cannon Ball) Flower and applied for the Sensing of an anti-Diabetic drug Metformin.- <i>P. R. Khandagale, Dr. S. V. Nipane, Dr. S. R. Sabale, Dr. R. S. Dhabe.</i>	05
6	Morphological And Histological Cyclic Changes In Theovary Of Freshwater Fish : <i>Channa gachua, Dr. Ashwini G. Ghanbahadur, Prof. Y. K. Khillare</i>	06
7	Cordyceps militaris – An Important Medicinal Mushroom- <i>Trupti D. Kadam, Dr. Ashok V. Kharde.</i>	07
8	Morphometric Analysis Of Hiranyakeshi River, Sindhudurg District Using GIS Technology- <i>Aishwarya Pramod Hingmire, Shrikant Ghadage, Mayur Goud.</i>	08
9	Isolation of urease producing bacteria to produce biocement via MICP process.- <i>P. S. Rayate, B. A. Bhanjale, S. S Yeulkar</i>	09
10	Studies On Web Structure Of Two Spiders From Family Araneidae In Akola District <i>Satyavijay S. Dhande</i>	10
11	Attempts To Improve The Eye Dropper Deigne For Better Patient Compliance <i>Ms. Arte Aakanksha Sachin</i>	11
12	Aegle marmelos ash: A heterogeneous catalyst for Henry reaction <i>Rupesh C. Patil and Suresh S. Patil</i>	12
13	BMIM]-Glycine: A Sustainable Benchmark For Multicomponent Chromene Synthesis <i>Mr. Ashutosh A. Jagdale, Prin. (Dr.) Bhaskar V. Tamhankar and Prof. (Dr.) Suresh S. Patil</i>	13

155	The SiO ₂ -PS Composite Coated Superhydrophobic Tectona Grandis Leaf Mesh for Oil-water Separation – Sagar S. Ingole, Akshay R. Jundle, Pradip P. Gaikwad, Rutuja A. Ekunde, Rajaram S. Sutar, A. K. Bhosale and, Sanjay S. Latthe	157
156	A New Validated UHPLC-PDA Method for Simultaneous Quantification of Abiraterone Acetate, its Six Specified Process Impurities, and Four Degradation Products and Confirmation of all analytes based on Molecular Weight - Deepak Mhaske, Archana Rajmane, Arjun Kumbhar	158
157	Title - Isolation of ponceau 4R degrading bacteria from textile effluent Rashmi Rokade, Jyoti Jadhav	159
158	“Synthesis and Characterizations of Nickel Oxide thin film for Supercapacitor Application”- Akash N. Pasale and Gaurav B. Gaikwad	160
159	Today's Impact of Environmental Changes on Biodiversity Conservation – Dr. Nilima M. Kankale	161
160	“A study of the mechanisms underlying the anti-inflammatory effect of Mucuna atropurpurea in carrageenan-induced paw edema in rats” Pratibha Malia, Manali Raneb Jyoti Jadhava	162
161	The development of Self-cleaning Superhydrophobic Coating using PDMS and Candle Soot Nanoparticles Composite by Spray Technique Pradip P. Gaikwad, Sagar S. Ingole, Akshay R. Jundle, Rutuja A. Ekunde, Rajaram S. Sutar, A. K. Bhosale, and Sanjay S. Latthe	163
162	Development And Evaluation Of Herbal Nanoemulgel Formulation For Psoriasis Managem Ent- Mr. Ravindra G. Gaikwad, Dr. Sachin S. Mali, Dr. Anilkumar J. Shinde	164
163	Comparative study on incidence of seasonal diseases in commercial silkworm crossbreeds MV1 × S8 and PM × FC2 (Bombyx mori L.) in Kolhapur, Maharashtra.- Rohitkumar. S. Kadam, Surat. A. Manjare, Venkata S. Manne and Manish D. Mahindrakar	165
164	Studies on the plants used in Kolhapur district for the treatment of skin diseases and burns- S. A. Apate and A. A. Kengar	166
165	Metal Oxide Composite for Biomedical field- G.B. Takle, P.A. Kamble, P. D. Gaikwad	167
166	Development of Alkynyl Functionalized Mixed Ligand Ni(II) and Zn(II) Complexes- Sharad Kamble, S. S. Chavan	168
167	Analysing and Minimizing Complexity of the Triangular-Rectangular Number algorithm using Pells Equation using Python 3.- Mr. Aniket S. Jadhav Mr. Mehul A. Jadhav, Mr. Thorat Sanjay Pandurang, Mr. S. S. Khopade	169
168	Oneness Of Natural Number: Special Series And Their Mappings- Mr. Mehul A. Jadhav, Mr. Kapil P. Gidde, Mr. Thorat Sanjay	170

“Synthesis and Characterizations of Nickel Oxide Thin Film for Supercapacitor Application”

Akash N. Pasale^{1*} and **Gaurav B. Gaikwad²**

¹Department of Physics, Raje Ramrao College, Jath.

²Department of Physics, Sadguru Ghadage Maharaj College, Karad.

Corresponding author* – akashpasale1995@gmail.com

Abstract

Nickel Oxide (NiO) thin films were successfully deposited by simple Electrodeposition Technique by using Nickel Chloride onto copper substrate at room temperature. Influence of substrate temperature on structural, surface morphological, optical and, electrical properties were studied using X- ray Diffraction, Scanning Electron Microscope and, Contact angle meter. XRD results reveal that, films are average grain size is 40.83 nm. XRD results reveal that films are polycrystalline with single phase cubic structure and crystallinity of the film increases as the temperature increases. Scanning electron microscopy studies indicate that, a strong dependence of the surface texture and grain size on the various experimental conditions. It shows that particles shown is micaceous an of lakes with dispersed sandwich and cauliflower in shape. This may be occurred due to urea used in the synthesis process as hydrolysis controlling agent. The porosity of the films increases after annealing which was observed from the SEM study. Contact angle of nearly 0° correspond to complete wetting. This clearly indicates the films having superhydrophilic nature.

Keywords: Electrodeposition method, XRD, SEM, Nickel oxide etc.

Original Research Article

महात्मा गांधीजींची ग्रामविकास संकल्पना व कार्य

सी. डे. चौधरी

इतिहास विभाग, राधे राजराज बहुविद्यालय, ७४ वि. कावली ४१८४०४ महाराष्ट्र, भारत

Corresponding author E-mail: gschoudhary71@gmail.com

इस्ताविक

भारतातील ग्रामीण भागाच्या विकासात महात्मा गांधीजींच्या विचारांना व कार्यांना महत्त्वाचे स्थान आहे. गांधीजींनी भारताच्या सर्वांगीण विकासासाठी ग्रामीण भागाच्या विकासाची आवश्यकता लक्षात घेऊन ग्रामीण भागाच्या विकासाची संकल्पना आपली बुलपणे व ग्रंथांमध्ये मांडलेली आहे. त्याचबरोबर ग्रामीण भागाच्या विकासासाठी प्रत्यक्ष कृत्रियुक्त कार्यक्रम राबविले. भारताच्या सर्वांगीण विकासासाठी खेड्यांना स्वयंपूर्ण बनविणे आवश्यक आहे असे गांधीजींचे मत होते. भारतातील लोकसाह्यीच्या बळकटीकरणामाठी शहर व खेड्यातील लोकांचे जीवन समान पातळीवर विकसीत होणे आवश्यक आहे. याची जाणीव घेऊन ग्रामीण भागात रोजगार निर्मिती करण्यावर भर देता ज्यामुळे खेड्यातील लोकांच्या गरजा खेड्यांमध्ये पूर्ण होतील. ग्रामीण भागातील लोकांना मानवी मूल्य व रोजगार निर्मिती करून देणारी शैक्षणिक व्यवस्था खेड्यांमध्ये राबविता जावी. यावर गांधीजींचा भर होता. गांधीजींच्या ग्राम विकासाच्या संकल्पनेत खेड्यांच्या आर्थिक विकासाबरोबर शिक्षण, रस्ते, स्वच्छता, रोजगार, संस्कृतीचे जतन व संवर्धन यादींचा समावेश होता. गांधीजींची ग्राम विकासाची संकल्पना आदर्श गाव निर्माण करणारी आहे. त्यामुळे गांधीजींच्या ग्रामविकास संकल्पनेचा व त्यांच्या कृत्रिकार्यक्रमांचा आढावा घेणे आवश्यक आहे.

विषय विवेचन

महात्मा गांधीजींनी भारताच्या विकासासाठी ग्रामीण भागाच्या विकासाकडे आपले लक्ष केंद्रित केले. त्यासाठी शहर, बुलपणीय लेखन व ग्रंथांमधून आपले विचार मांडले. त्याचबरोबर ग्रामीण भागाच्या विकासासाठी विविध योजना पारिष्कारून भर दिला. त्यामध्ये तालमी संघ, ग्राम उद्योग संघ व गो रक्षा संघ यांचा समावेश आहे.

ग्रामीण विकास संकल्पना

गांधीजींनी आपल्या ग्राम विकास संकल्पनेत आर्थिक विकेंद्रीकरण, खेड्यांची रचना व सत्तेच्या विकेंद्रीकारणावर भर दिला आहे.

आर्थिक विकेंद्रीकरण

गांधीजींनी भारतातील ग्रामीण भागाच्या विकासासाठी आर्थिक विकेंद्रीकरणाची आवश्यकता असण्याचे मत मांडले. त्यांनी ९ जानेवारी १९३० च्या हरिजन वृत्तपत्रातील लेखात आदर्श खेड्यांची संकल्पना मांडलेली आहे. गांधीजींच्या आदर्श खेड्यांच्या संकल्पनेत भारतातील खेड्यांना सर्वांगीण विकास अंतर्भूत आहे. गांधीजींच्या आदर्श खेड्यांच्या संकल्पनेत गांधीजींना ग्रामांचा स्वायत्त विकास अपेक्षित आहे. गावातील लोकांच्या गरजा गावांमध्येच पूर्ण व्हाव्यात. छोटा-मोठ्या गरजेच्या वस्तू गावांमध्येच निर्माण व्हाव्यात. पाहिलेच, भाजीपाला, फळे इत्यादींचे उत्पादन गावात झाले पाहिजे.

खेड्यांची रचना

गांधीजींच्या ग्राम विकास संकल्पनेत ग्रामांच्या रचनेला महत्त्व आहे. गावातील घरांची रचना अशी असावी की, घरांमध्ये पुरेसा प्रकाश व हवा वेईल. घरांच्या मागे-पुढे अंगण असावे. गावात पिण्याच्या पाण्याच्या विहिरी असल्यात. गावातील रस्ते व सल्या स्वच्छ असल्यात. रस्त्यांच्या दोन्ही कडेला सांडपाण्याच्या नाल्या असल्यात. गावात स्वच्छता असावी. खेड्यातील लोकांना प्राचना करण्यासाठी मंदिर किंवा प्रायनागृह असावे. गावात प्राथमिक व माध्यमिक शाळा असावी. गावातील तटे गावातच सोडविले जावेत. ग्रामासाठी ग्रामपंचायत असावी. गांधीजींच्या संरक्षणासाठी गौशाला असावी. असे मत मांडले आहे.

मतेचे विकेंद्रीकरण

गांधीजींनी ग्रामांच्या सर्वांगीण विकासासाठी मतेच्या विकेंद्रीकरणाची आवश्यकता असल्याचे मत व्यक्त केले आहे. ग्रामपंचायतींना गावाच्या निर्णयाचे सर्व अधिकार दिले जावेत. असे गांधीजींना वाटत होते. त्यासाठी गांधीजींनी स्वातंत्र्यपूर्व काळातच आपल्या 'यंग इंडिया' या वृत्तपत्रातील लेखात पंचायतीविषयी मार्गदर्शनासाठी काही नियम प्रस्तुत केले आहेत. त्यामध्ये ग्रामस्वच्छता, शिक्षण, आरोग्य विषयक सुविधा, पिण्याच्या पाण्याची व्यवस्था, शोषीत-पीडितांची उन्नती, गावातील तटे पंचायतीच्या माध्यमातून सोडविले इत्यादी मुलभूत गरजांची पूर्तता ग्रामांमध्ये करण्यावर भर दिला आहे. गांधीजी म्हणाले होते की, दिल्ली भारत नाही, तर भारत गावांमध्ये बसलेला आहे. त्यामुळे भारताचा विकास करावयाचा असेल तर ग्रामनावांचा विकास करावा लागेल. त्यांनी 'खेड्यांकडे परत चला' या नारा दिला होता. 'भारत खेड्यांचा देश असल्यामुळे खेड्यांच्या विकासावर देशाचा विकास अवलंबून आहे. घाची गांधीजींना जाणीव होती. त्यामुळे भारताच्या विकासाच्या संकल्पनेत ग्रामांच्या विकासावर भर दिला.

महत्त्वा गांधीजींचा कृतिवृत्त कार्यक्रम

गांधीजींनी भारतातील खेड्यांच्या विकासाची संकल्पना मंडली. त्या संकल्पनेनुसार कृतिवृत्त कार्यक्रम तयार करून प्रत्यक्ष कार्य केले. गांधीजींच्या ग्रामविकास कृतिवृत्त कार्यक्रमात ग्राम उद्योग संघ, तालमी संघ, गो रक्षा संघ इत्यादींचा समावेश होता. या संस्था स्थापन करून खेड्यात शिक्षण, रोजगार, मातृभाषा, सामाजिक समता, संस्कृती संवर्धन इत्यादींचा विकास करण्यासाठी कार्य केले.

तालमी संघ (Basic Education Society)

इ.स. १९३६ मध्ये गांधीजी महाराष्ट्र राज्याच्या वर्धा जिल्ह्यातील सेवाग्राम येथे वास्तव्याला आले. त्याचवर्षी खेड्यांच्या विकासासाठी मूल्य आणि रोजगार निर्माण करणारे कौमन्यावर आधारित शिक्षण खेड्यातील मुला-मुनींना देण्यासाठी 'नई तालीम' शिक्षणपद्धती सुरू केली. त्यानुसार खेड्यातील सात वर्षांच्यातील मुला-मुनींना मोफत शिक्षण मातृभाषेनुसार देण्यात यावे. विद्यार्थ्यांच्या परंपरागत व्यवसायाला कोणतीही बाधा निर्माण होऊ न देता उत्पादन, धर्म व

हस्तकलाच्यावर आधारित शिक्षण देण्यावर भर होता. या योजनेला राबविण्यासाठी 'गावठी संघ' स्थापन करण्यात आला. गांधीजींची ही शिक्षणपद्धती खेड्यातील परंपरागत व्यवसायाला प्रोत्साहन देणारी होती. धन व हुस्नकीलन्यावर आधारित शिक्षण ग्रामीण भागातील विद्यार्थ्यांना महानयनापासून दिव्यास परंपरेने वाचवत आलेल्या हुस्नकीलन्याचे ज्ञान विद्यार्थ्यांना मिळेल ज्यामुळे खेड्यात रोजगार निर्माण होतील. गांधीजींनी ग्रामीण भागातील विद्यार्थ्यांना मातृभाषेतून वैयक्तिक ज्ञान चांगले संपादन करता येईल. असे गांधीजींचे मत होते. खेड्यामध्ये रोजगाराची उपलब्धता कमी असल्यामुळे खेड्यातील लोक आर्थिकदृष्ट्या दुर्बल असतात. त्यामुळे खेड्यातील सात वर्षांच्यातील मुला-मुलींना मोठे शिक्षण देण्यात आर्थिक समस्या इत्यादींची जागृती विद्यार्थ्यांमध्ये मिळणावून निर्माण झाली पाहिजे. अशा पद्धतीचे ग्रामीण भागातील जागृतीनिर्भर व आदर्श बनतील.

ग्राम उद्योग संघ (Village Industries Association)

ग्रामीण क्षेत्रातील सेवाग्राम येथे वास्तव्याला असताना ग्रामीण भागात रोजगाराभिमुख बनविण्यासाठी गांधीजींनी ग्राम उद्योग संघ स्थापन केला. खेड्यातील लोकांच्या आर्थिक गरजा ग्रामांमध्येच पूर्ण करण्यासाठी खेड्यातील लोकांच्या हुस्नकला कौशल्येचा विकास करणे, शेतीतून उत्पादन देण्यासाठी शेतकऱ्यांना प्रोत्साहित करणे, गावांमध्ये पशुपालना, फळे इत्यादींचे उत्पादन आणणे पाहिजे. ग्रामातील ग्राम उद्योग संपाने कार्य केले. इ.स. १९३४ मध्ये स्वातंत्र्य लढाऊातील इतर नेत्यांसोबत फारकट झाल्यानंतर भारतीय राजकारणापासून काहीकाळ अलिंगित झाल्यानंतर गांधीजींनी विषय सामाजिक व आर्थिक गटात समानता निर्माण करण्यासाठी इ.स. १९३९ पासून ग्राम उद्योग संपाने कार्य करायला सुरुवात केली.^१ खेड्यातील लोकांना गाम वृक्ष व मुठापासून निरा बनविणे, सुतार काम, कुंभार काम, हातमागावर कापड तयार करणे, मधमाशी पालन, चांबड्याच्या वस्तू बनविणे, साकूट-बांबू पासून कनातुसरीच्या वस्तू बनविणे, तेल काढणे इत्यादींचे प्रशिक्षण ग्राम उद्योग संपानेच्या केंद्रावरून देण्यात येत होते. भारतातील खेड्यांच्या विकासात्मक कार्याला गती मिळण्यासाठी अखिल भारतीय स्थिरते असोसिएशनचे मुख्यालय गांधीजींनी सेवाग्राम येथे हलविले. गावात रोजगार निर्माण करण्यावर रोबरच आदर्श गाव निर्माण करण्यासाठी गावात पिण्याच्या पाण्याची व्यवस्था, चांगले रस्ते, स्वच्छता, रुग्णालय इत्यादी ग्राम उद्योग संपानेच्या माध्यमाने निर्माण करण्यासाठी कार्य व जनजागृती केली.

गो रक्षा संघ

गांधीजींनी गावीच्या संरक्षणासाठी गो रक्षा संघ स्थापन केला. या संघाच्या माध्यमाने समाजामध्ये गावीच्या संरक्षणासाठी जनजागृती निर्माण केली. भारतीय परंपरेत गाय पवित्र आहे. शेतीसाठी आवश्यक असलेले बैल गावीपासून मिळतात. गावीपासून दुध, शेंणखत मिळते. दुध उत्पादनामुळे गावातील लोकांना पुरक व्यवसाय निर्माण होतो. शेंणखतामुळे शेतीतून उत्पादन चांगले येते. त्यामुळे गांधीजींनी ग्राम विकासासाठी गावीची सुरक्षितताही महत्वाची मानली.

गुरुनाथ

महात्मा गांधीजींची ग्राम विकासाची संकल्पना व त्यांनी ग्राम विकासासाठी केलेले कार्य खेड्यांना आत्मनिर्भर व स्वतंत्र गाव निर्माण करणारी आहे. गांधीजींची ग्राम विकासाच्या संकल्पनेत खेड्यातून रोजगार निर्मिती करण्यावर भर दिला. गावात शाळा, चांगले रस्ते, स्वच्छतागृह, पिण्याच्या पाण्याच्या मोई, रुग्णालय, ग्रामपंचायत इत्यादी सोयीसुविधा निर्माण झाल्यास आदर्श खेडी निर्माण होतील. गावात दिल्या जाणाऱ्या शिक्षणात भाषा, संस्कृती संवर्धनाचा अंतर्भाव करावा. त्यामुळे भारतीय भाषा व संस्कृतीचे जतन व संवर्धन होईल. गांधीजींची खेड्यांच्या विकासाची योजना सर्वांगीण

Kisan Shikshan Prasarak Mandal, Hadolti

Karmayogi Tulshiram Pawar Mahavidyalaya, Hadolti.

Tq. Ahmedpur Dist. Latur - 413514 (M.S.)



Department of History, Economics & Philosophy in collaboration with
Swami Ramanand Teerth Marathwada University, Nanded.

One Day Interdisciplinary National Conference on
'Thoughts of Mahatma Gandhi: Yesterday, Today & Tomorrow'

CERTIFICATE

Date: 28 / 10 / 2023

This is to certify that Dr./Prof./Mr./Ms. Pundlik Jaypal Choudhary

of Raje Ramrao Mahavidyalaya, Tath attended One Day Interdisciplinary National Conference on

'Thoughts of Mahatma Gandhi: Yesterday, Today and Tomorrow' organized by Department of History, Economics and Philosophy, Karmayogi Tulshiram Pawar

Mahavidyalaya, Hadolti in collaboration with Swami Ramanand Teerth Marathwada University, Nanded on 28th October 2023. He/She has also shared announced as

Resource Person/presented a paper entitled.....

महाना गांधीजींची सामाजिक संकल्पना व कार्य

Dr. Ramesh Gangobade
Organizer & Co-Convenor

Dr. Ramabehn Ingole
Organizer & Co-Convenor

Dr. Sushama Tenkale
Organizer & Co-Convenor

Dr. Deepak Bachevar
Principal & Convenor

Table of Content

Sr. no.	Title of the paper	Page no.
1	महात्मा गांधीजी वई जीवन, एक संक्षिप्त विवेचन - इरफे राशिडी किरडिरे	821 - 826
2	महात्मा गांधीजीच्या आर्थिक विचारांच्या परामर्श - डा. डॉ. अशित शिखर शारका	827 - 831
3	महात्मा गांधी यांचे सात्वाग्रहाचे विचार - डा. डॉ. विजया बाघी	834 - 840
4	गांधीविचारांची वर्तमानकाळातील प्रामाणिकता - डा. डॉ. बालाजी कृष्णराव चवले	841 - 844
5	वेळ्याकडे येना - महात्मा गांधी - डा. डॉ. कलका बालागज सोववडी	845 - 849
6	महात्मा गांधीजींची साध्यावराज्य संकल्पना - डा. डॉ. संजय एम. बाकुलगाडे	850 - 854
7	महात्मा गांधी यांच्या शिक्षण विषयक विचारांची प्रामाणिकता - डा. डॉ. श्री ए. पद्मके आणि डा. डॉ. एम. के. जेधने	855 - 859
8	गांधीजींच्या मूल्य व अधिािकी प्रामाणिकता - डॉ. सुखदे इतुपान	860 - 863
9	महात्मा गांधी यांचे सात्वाग्रहासंबंधी विचार - डॉ. सुख चोखळे	864 - 867
10	महात्मा गांधीजी आणि स्वातंत्र्यनंदनाम - सुने सोववडी बाळबराज	868 - 873
11	महात्मा गांधीजींची 3H (Head, Hand, Heart) संकल्पना. - अरसुळे अशेल नकनार	874 - 879
12	महात्मा गांधीजी आणि त्यांचे स्वातंत्र्य संकल्पना - डॉ. भरत बाळबराज सुखबारा	880 - 883
13	महात्मा गांधीजींचे महिलाविषयक विचार - डा. डॉ. राजनी अरनाराज बीरते	886 - 890
14	Mahatma Gandhi's Views on the Indian Economy. A Path to Self-Reliance and Social Justice - Dr. S. B. Shaikh	891 - 893
15	‘एकदश ब्रत’ : गांधीजींची नैतिक जीवन पद्धती - डॉ. मिलन देवळे	894 - 899

44	महात्मा गांधी व दांडी यात्रा - डा. बसोदे जी. शम.	1039 - 1041
45	महात्मा गांधीजींचे धार्मिक विचार : एक अभ्यास - डा. डॉ. अश्विन जी. हावत	1042 - 1044
46	संघ संरचनातील महात्मा गांधीजींचे योगदान - डा. डॉ. पिसा अरुण	1045 - 1048
47	महात्मा गांधींचे "शिक्षण पद्धती" विषयी विचार - डा. पाटील अश्वय मधुरात्म	1049 - 1054
48	महात्मा गांधींचे पर्यावरण विषयी विचार - डा. पांडुरंग विरी	1055 - 1057
49	Reflection of 'Subaltern' in Mahatma Gandhi's Autobiography: The Story of My Experiments with Truth (1927) - Dr. Prashant U. Gambhire	1058 - 1060
50	राष्ट्रविता महात्मा गांधी यांच्या शिक्षण पद्धतीचे स्वरूप आणि शैक्षणिक तत्वज्ञान - डा. डॉ. प्रशांत राजारामाहेर अच्युत	1061 - 1065
51	महात्मा गांधीजींचे सत्याग्रही विचार आणि मराठी साहित्य - डा. डॉ. केदार अणपुले	1066 - 1070
52	Mahatma Gandhi and Non Violence - Dr. Patil Shyam Pusdikrao	1071 - 1075
53	महात्मागांधी व सर्वोदय समाज - डा. डॉ. कल्पना तापवारे	1076 - 1080
54	महात्मा गांधीजींच्या धर्मविषयक विचारांची प्रामाणिकता - डा. अविश रामकिशन मोनकावडे	1081 - 1084
55	महात्मा गांधीजींची ग्रामविकास संकल्पना व कार्ये - सी. जे. चौधरी	1085 - 1088
56	Religion Philosophy of Mahatma Gandhi - Dr. Narendra Deshmukh	1089 - 1095
57	Literary Explorations of Gandhi's Ideals - Dr. Umakant D. Padamwar	1096 - 1097



**ONE DAY INTERDISCIPLINARY NATIONAL CONFERENCE
ON
'THOUGHTS OF MAHATMA GANDHI : YESTERDAY,
TODAY & TOMORROW'**

Organized by

Swami Ramanand Teerth Marathwada University, Nanded

&

Department of History, Economics & Philosophy

KARMAYOGI TULSHIRAM PAWAR MAHAVIDYALAYA, HADOLTI

Tq. Ahmedpur Dist. Latur (M.S.)

NAAC Accredited With 'B' Grade

Saturday 28th October 2023



Impact Factor : 7.9 (2022)

उदयगिरी बहुभाषिक इतिहास संशोधन पत्रिका

ISSN - 2243-4403 (Printed)
<http://www.karmayogi.org>

A Bimonthly, Refereed, & Peer Reviewed Journal of History, September - October - 2023 (ISSUE No : 04)

Chief Editor

Dr. Anant N. Shinde

Udayagiri Bahubhashik Itihas
Sanskhodhan Patrika

Executive Editor

Dr. Deepak Bachewar

Principal
Karmayogi Tulshiram Pawar Mahavidyalaya,
Hadolti Tq. Ahmedpur Dist. Latur

Editors

Dr. Ramesh Gangthade

Dr. Rasoahab Ingle
Dr. Suvarna Tenkale

See discussions, stats, and author profiles for this publication at: <https://www.researchgate.net/publication/385273551>

ORYZA SATIVA HUSK AS A SUSTAINABLE SOURCE OF SILICON A REVIEW

Article · October 2024

CITATIONS

0

READS

4

1 author:



Rajendra Lavate

Shikshanmaharshi Dr. Bapuji Salunkhe College Miraj

38 PUBLICATIONS 106 CITATIONS

SEE PROFILE

ORYZA SATIVA HUSK AS A SUSTAINABLE SOURCE OF SILICON: A REVIEW

Rajendra Lavate, Sohan Thombare*, Shankar Soudagar and Appasaheb Bhosale

Department of Botany and Physics, Raje Ramrao College, Jath,
(Affiliated to Shivaji University) Kolhapur Sangli-416404, India.

*Department of Medical Physics, Centre for Interdisciplinary, Research, D. Y. Patil Education Society (Deemed to Be University), Kolhapur-416006, India.

ABSTRACT

This review focuses on utilisation of *Oryza sativa* Husk as a source for silicon nanoparticles (Si NPs) that are created via magnesiothermic reduction and used in composite anodes for lithium-ion batteries (LIBs). The production of silicon nanoparticles (Si NPs) has been explained and, their electrochemical characteristics, and possibility for activated carbon-decorated silicon nanocrystals (AC@nc-Si@AC) to serve as high-capacity anode materials have been discussed. The study emphasises cost-effective, synthesis techniques for creating environmentally acceptable energy storage technologies with the use of biomass.

Introduction:

The majority of people in the world consume rice (*Oryza sativa*) regularly. To fulfil the demands of the expanding population, it is crucial to cultivate *Oryza sativa* sustainably. In recent years, the world has consumed about 470 million metric tons of *Oryza sativa* (Wong, *et al.*, 2014). Millions of tonnes of *Oryza sativa* husk is produced during the manufacturing of rice. Although *Oryza sativa* husk can be utilised to make fuel, fertiliser, and building materials, it is frequently considered a waste product (Rodríguez de Sensale, 2006; Kamenidou *et al.*, 2010; Duan *et al.*, 2013; Fang *et al.*, 2004). Even though *Oryza sativa* husk decomposes naturally, the readily available quantity may convert it as a resource for novel technologies for the benefit of mankind.

Oryza sativa husk contains a high proportion of Silicon dioxide (SiO₂), Depending on the type of soil used to cultivate *Oryza sativa*, the SiO₂ content in its husk ranges from 10 to 20 % (Chandrasekhar *et al.*, 2003). The *Oryza sativa* husk can be pre-treated with various acids before being pyrolyzed to recover SiO₂ from it (Yalcin and Sevinc, 2001; Kalapathy, *et al.*, 2002; Liou, 2004; Adam, *et*

al., 2012). The characteristics of silicon dioxide recovered from husk vary with the source or raw material. Even the amount of SiO₂ differs across *Oryza sativa* husks from different geographical areas. This may have an impact on the SiO₂ extraction characteristics, including purity, particle size, and shape (Carmona, *et al.*, 2013; Le, *et al.*, 2013). The SiO₂ obtained from the *Oryza sativa* has a nanoscale shape. SiO₂ can be converted into silicon (Si) by employing magnesiothermic reduction method, wherein magnesium (Mg) powder and SiO₂ are heated in a furnace until they react. Pure Si is left behind when the SiO₂ and magnesium react with the oxygen to generate magnesium oxide (MgO) (Banerjee *et al.*, 1982). In this way, SiO₂ can be converted to Si in its original shape via magnesiothermic reduction method. Since the reaction is carried out at a temperature of 600 °C the silicon nanoparticles (Si NPs) can be subjected to sintering into a bulk substance. During sintering, the particles come together to create a solid mass. It takes less time for the particles to sinter together when the reaction is carried out at a low temperature, resulting in smaller, more homogeneous Si NPs. Thus it is possible to use silicon dioxide nanoparticles (SiO₂ NPs) as a raw material to create Si NPs. This might

result in the creation of innovative and effective processes for Si NPs synthesis (Sun and Gong, 2001). This process enables the possibility of using low-cost Si NPs in lithium-ion battery systems. This might result in the creation of lithium-ion batteries (LIBs) that are more cost-effective and environmentally friendly (Xing, *et. al*, 2013; Liu, *et. al.*, 2013; Junget. *et. al.*, 2013).

In upcoming LIBs, Si NPs will be a potential anode material. This is due to enormous capacity of Si to store a large amount of energy (Kasavajjula *et. al.*, 2007). Furthermore, Si NPs have a large surface area, which increases their reactivity with lithium ions. This may result in quicker charging and discharging times as well as increased battery performance. Theoretically, Si is the alloying material that can react with lithium ions. The capacity of producing 4200 mAh/g during this reaction, at room temperature, is 10-12 times larger than the specific capacity of conventional graphite based anodes. LIBs, made with the help of Si-based materials have an issue with volume expansion during the charge-discharge cycle. This is due to the many alloy formation stages that Si goes through during the charge-discharge cycle, which causes it to expand and contract. The Si anode may break as a result of this growth in the volume, which could affect the battery performance and lifespan (Boukamp, 1981). A similar issue that can be experienced with Si-based materials is their inherently low conductivity. This indicates that Si is a poor conductor of electricity, which may reduce the battery capacity (Lee, *et al.*, 2010; Magasinski, *et. al.*, 2010). In addition to its low working voltage, abundance on Earth, and low toxicity, Si has several further advantages as an anode material for LIBs (Entwistle, *et. al.*, 2018).

Lithium ions are injected into the material in a process known as intercalation that produces lithiation in conventional electrode materials. The intercalation method results in very few structural changes and with high retention capacity. On the other hand, Si and lithium combine to form an alloy that requires periodic cycles of contravention and re-establishing chemical connections with the

host structure. Low conductivity and the possibility of volume increase are the main drawbacks of adopting Si as an anode material for LIBs. The Si can swell by as much as 280% when a lot of lithium ions are injected into it. The Si anode may fracture and break as a result of the volume increase, which could result in a decrease in battery performance and life. The composite electrode may sustain structural degradation due to the dimensions increase of Si during cycling, which isolates the active component and reduces capacity. This poses a significant obstacle to the creation of Si anodes with large capacities and long cycle lives (Entwistle, *et. al.*, 2018).

The synthesis of SiO₂ and Si materials for LIBs from the husk of *Oryza sativa*, using various extraction methods and magnesiothermic reduction, have been discussed in this communication.

Synthesis:

Ratsameetammajak *et al.* (2022) described the process of preparing silica from the husk of *Oryza sativa* (rice). Rice husks are taken from farms and washed in water. They are then completely dried at 100 °C. To get rid of any metallic impurities, rice husks are soaked in an aqueous solution of hydrochloric acid (HCl) overnight. In order to achieve the pH value of pH of 7, rice husks are thoroughly rinsed in water. Then the rice husks are dried at 100 °C, and subsequently burnt in a muffle furnace at 700 °C for two hours. The burning process is repeated once again to ensure the perfect removal of organic matter and the creation of rice husk ash, an ample source of silica. Where the silica comes from. Below is a summary of the process used to create reduced graphene oxide (rGO): An adaptation of the Hummers process is used to create graphite oxide (GO) from graphite powder. In a non-reactive atmosphere for 5 hours, reduce the GO in a tube furnace at 800 °C (Autthawong *et. al.*, 2020)

The process of creating the composite material made of SiO₂@rGO with a proportion of 30:70 can be summed up as follows: Prepare recently generated SiO₂ by precipitating it for 2 hours at 120 °C in a NaOH solution. In the suspension, distribute rGO by

utilising a hydrochloric acid solution.

Graphene oxide (GO) is a unique material that can be viewed as a single monomolecular layer of graphite with various oxygen-containing functionalities such as epoxide, carbonyl, carboxyl, and hydroxyl groups. Reduced graphene oxide (RGO) is the form of GO that is processed by chemical, thermal and other methods to reduce the oxygen content. As graphite oxide is a material produced by oxidation of graphite, it leads to increased interlayer spacing and functionalization of the basal planes of graphite.

Raise the pH of the mixture to 7. Keep aside overnight at room temperature, and then stir the mixture. Rinse the mixture with deionized (DI) H₂O and ethyl alcohol (CH₃CH₂OH) and then centrifug. Dry the sample thus obtained in a hot air oven at 60 °C as described by Ratsameetammajak et. al., (2022).

The creation of the composite material (SiO₂@rGO and Polyaniline) including SiO₂ / rGO and Polyaniline (PANI) can be summed up as follows: In a mixture of 10 mL ethanol, 5 ml deionized water, and 5 ml H₂SO₄, make a suspension of SiO₂@rGO. To produce a consistent dispersion, sonicate the suspension. While agitating ferociously in an ice bath, dropwise add the aniline monomer to the solution. Stir the solution for 6 hours in an ice bath while adding Ammonium Persulfate ((NH₄)₂S₂O₈). When polymerization takes place leading to the formation of polyaniline emeraldine salt, the solution will turn dark green. To achieve a clear solution, repeatedly wash the suspension in H₂O and CH₃CH₂OH.

The electrochemical behaviour of the PANI-SiO₂@rGO composite was further studied in a coin-type cell utilising lithium foil as

the reference and counter electrodes. A composite anode made of SiO₂ and rGO was used in parallel tests to compare the results. The initial three lithiation-delithiation curves of the SiO₂@rGO and PANI-SiO₂@rGO electrodes at a potential range of 0.01-3.00 V (vs. Li/Li⁺) at a current density of 0.4 A g⁻¹ are shown in Figures 1b and 1c, respectively.

The SiO₂@rGO composite electrode's initial lithiation and delithiation specific capacities were 1012 and 300 mAh/g, respectively, however, it had a poor coulombic efficiency (CE) of 29.6%. The PANI-SiO₂@rGO composite electrode initial lithiation/delithiation specific capacities, on the other hand, were 1508 and 647 mAh/g, respectively, with a CE of 42.9%. The reduction of silica in SiO₂@rGO and PANI-SiO₂@rGO composites, results in lithium loss, causing initial low CE. The potential gradient plateaus on both electrodes, which range from 1.5 to 0.5 V, clearly show the formation of a solid electrolyte interphase (SEI) layer (Ratsameetammajak et. al., 2022).

The existence of stable plateaus during early cycles is an evidence of this reaction (Figure 1d). The subsequent cycles show that the SEI layer is only formed in the initial cycle, as the slopes gradually become sharper and the hills gradually get smaller. The charge voltage profiles become noticeably steeper rather than staying flat at potentials higher than 1.5 V. This invention can be attributed to solvent degradation processes occurring on the oxide electrode surface, which produced the SEI coating (Ratsameetammajak et. al., 2022).

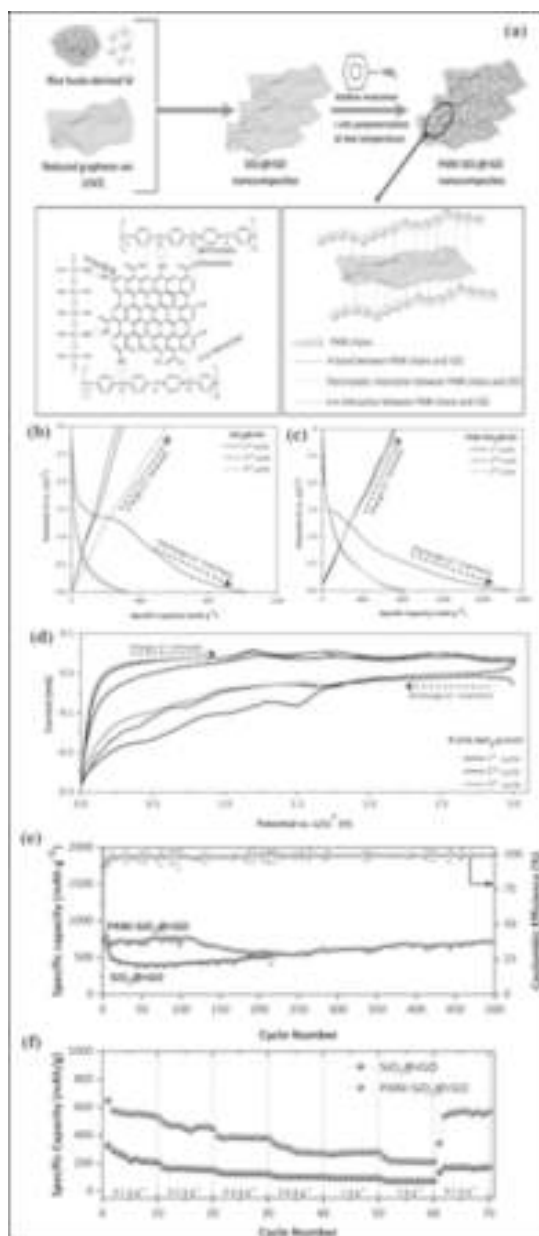


Figure 1(a-f) (a) the synthetic pathway for the preparation of the PANI-SiO₂@rGO composite, lithiation-delithiation profiles for the composites PANI-SiO₂@rGO and SiO₂@rGO measured at 400 mA g⁻¹ in current density (b) and (c), during the first three cycles, cyclic voltammograms (CV) of the PANI-SiO₂@rGO electrode were

recorded at a scan rate of 0.1 mV s⁻¹ and are displayed in (d), SiO₂@rGO and PANI-SiO₂@rGO composites long-term cycling stability and Coulombic efficiency comparison at 400 mA g⁻¹ are depicted in (e). SiO₂@rGO and PANI-SiO₂@rGO composites rate performance evaluation is depicted in (f).

During the initial cycle of delithiation and lithiation, a layer on the surface of anode known as the SEI film develops. It is produced by the interaction of the electrode material and the electrolyte at the solid-liquid interface. It is thought that the partial breakdown of the SEI coating was mostly due to the initial poor CE. The initial coulombic efficiency of PANI-SiO₂@rGO electrode is greater than that of SiO₂@rGO composite electrode. This is because the PANI covering shell prevents the electrolyte at SiO₂@rGO surface from decomposing.

Figure 1e compares the long-term cycling stability of SiO₂@rGO nanocomposite (NC) electrode with the PANI-SiO₂@rGO composite electrode. The PANI-SiO₂@rGO NC anode has outstanding long-term cycling performance at 0.4 A g⁻¹ and maintains a high reversible capacity of 680 mAh/g after 400 cycles, which is about twice as much capacity as standard graphite anodes. In comparison, after 215 cycles, SiO₂@rGO NC electrode can only discharge 414 mAh/g. This shows that only mild pulverisation of SiO₂ in the PANI-SiO₂@rGO NC occurred. The PANI coating efficiently slows down electrolyte degradation on the surface of SiO₂ and serves as a flexible protective layer to absorb SiO₂ volumetric changes.

The results presented above make it clear that the PANI shell outstanding mechanical qualities may prevent SiO₂ nanoparticle volumetric alterations. This capability guarantees that the working electrode structural integrity is maintained throughout discharge and charge cycles, greatly enhancing the electrode sustained stability over time.

The rate performance of PANI-SiO₂@rGO and SiO₂@rGO NC electrodes was evaluated at different current densities ranging

from 0.1 to 2.0 A g⁻¹, as shown in Figure 1f. At the corresponding current densities of 0.1 to 2 A g⁻¹, the PANI-SiO₂@rGO NC electrode displayed discharge capacities ranging from 563.6 to 217.1 mAh/g. After cycling at 2 A g⁻¹, the electrode maintained a discharge capacity of 539.4 mAh/g when cycled back to 0.1 A g⁻¹, illustrating its excellent rate performance. These results show that using PANI-SiO₂@rGO NC is an effective way to improve the electrochemical properties of SiO₂@rGO (Ratsameetammajak *et al.*, 2022).

N-doped carbon coated PANI-SiO₂@rGO NC has superior lithium storage capacity. Which can be attributed to their distinctive structure. SiO₂ nanoscale properties shorten the lithium ion diffusion path, which enhances lithium-ion diffusion and electronic transport. however, the rate capability may suffer. The encircling rGO sheets on the SiO₂ surface have generated a continuous conductive channel that connects the SiO₂ nanoparticles, considerably improving the conductivity of PANI-SiO₂@rGO NC electrode. SiO₂ pulverisation is avoided because the PANI materials elasticity effectively adapts to the NC volume variations during the Li-alloying and dealloying operations (Ratsameetammajak *et al.*, 2022; (Liao, *et al.* 2020; Charlton, *et al.*, 2020, Chen, 2019). In conclusion, PANI-SiO₂@rGO NC had an improved initial CE of 42.9% and a high specific capacity of 680 mAh/g at 400 mA/g after 215 cycles (Ratsameetammajak *et al.*, 2022).

Synthesis of silicon nanoparticles:

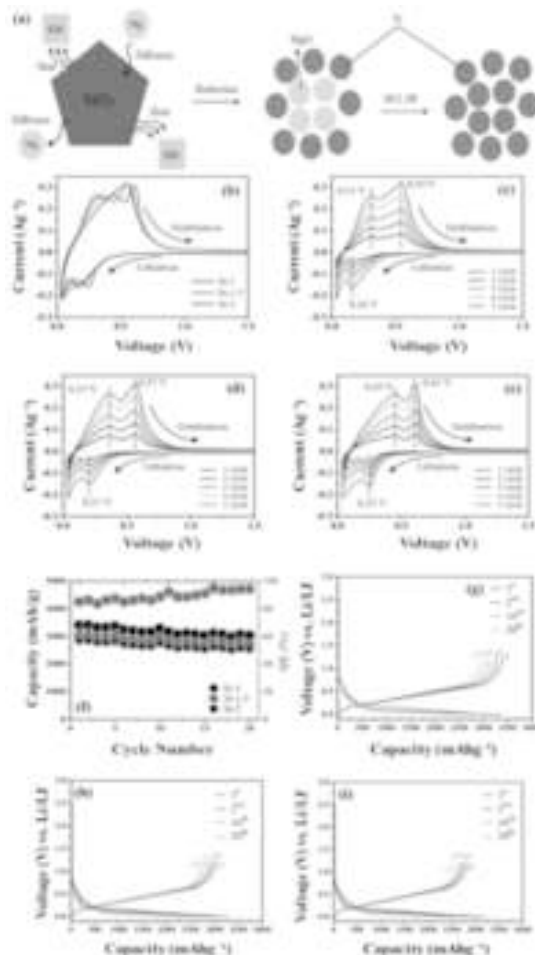
Daulay *et al.* (2022) heated *Oryza sativa* husk at 600°C for 5 hours to produce ash. Thereafter the ash and NaOH were combined and stirred for three hours at 240 rpm and 100°C. The mixture was filtered, and HCl was added until a pH reached 7.0, The precipitate was filtered out and residual solution was heated at 100°C for three hours again for precipitation, which was again removed by filtration. After several rounds of washing with distilled water and drying, SiO₂ was produced in the form of powder. It was then mixed with KBr with a ratio of 1:10,

deionized water was added, and stirring was carried out for three hours. The combination was subjected to ultrasonication for six hours. The residue produced after ultrasonication was separated by decantation, and the filtrate was allowed to dry for 12 hours. The dry powder was mixed with Mg powder in various ratios (1:1.0, 1:1.5, 1:2.0). The next calcination procedure was undertaken at 800°C for 8 hours. During the first purification stage, 150 mL of deionized water and 15 mL of ethanol were added. After that, there was 3 hours of agitation. Centrifugation of the mixture was done for 30 minutes at a speed of 4000 rpm. After being regularly cleaned with deionized water, it was dried for six hours at 80 °C. The second stage involved addition of 150 ml, 5 N HCl and a 12-hour rest period. The sample was dried at 80 °C for 6 hours, washed with deionized water, and then centrifuged once again for 30 minutes at 4000 rpm. Then 150 mL of 10% hydrogen fluoride (HF) was added as the last stage, and the mixture was allowed to settle for 15 minutes. The mixture was first dried, followed by several washes in deionized water, and a second drying step was six hours at 80 °C. Si-1, Si-1.5, and Si-2 thus produced were labelled. (Daulay, *et al.*, 2022).

Figure 2b displays cyclic voltammetry profiles for Si NPs. The data demonstrated that as the ratio of SiO₂ and Mg increases during reduction, the magnesiothermic reduction causes a higher reduction peak associated with the production of delithiation as well as oxidation peaks, associated with the lithiation to Si. Cyclic voltammetry (CV) was used to measure the activation process for Si-1, Si-1.5, and Si-2 electrodes with a voltage range of 0.01 to 1 V (against Li^{+/}Li) and a scan rate of 0.2 mVs⁻¹. The CV analysis of Si-1 (Figure 2c) revealed lithiation-related reduction peaks (0.16 V) as well as the delithiation-related oxidation peaks (0.31 V and 0.54 V). Figure 2d depicts the lithiation of Si-1.5 at 0.21 V and its delithiation at 0.37 V and 0.57 V. In Figure 2e, the lithiation (0.25 V) and delithiation (0.45 V and 0.61 V) peaks for Si-2 are displayed. These peak intensities increase during the cycles, suggesting that more lithium ions are possibly

moving between the electrode and electrolyte. This indicated gradual activation of substances. Compared to Si-1.5 and Si-2, Si-1 showed less significant peaks in both lithiation and delithiation. More efficient transport of lithium ions from the cathode to the anode and vice versa is shown by smaller lithiation and delithiation peaks in CV (Daulay *et al.*, 2022).

The rate capability study for the Si-1, Si-1.5, and Si-2 electrodes is shown in Figure 2f. The first cycle is performed to ensure that Si is adequately activated, as shown by cyclic voltammetry, which aids in the creation of a stable solid electrolyte interphase (SEI) layer (Liu *et al.*, 2006). Si-1, Si-1.5, and Si-2 electrodes, respectively, had initial discharge capacities of 3416, 3037, and 2847 mAh/g. 54.9, 85.4, and 85.6 % are the comparable *Conformite Europeenne* (CE). The silicon lithiation potential range (0.01 V to 0.50 V) is higher than the carbonate-based lowest unoccupied molecular orbital (LUMO) electrolyte. When a voltage is applied, Si is lithiated, resulting in the formation of an amorphous solid electrolyte interface (SEI). By reductively destroying the electrolyte, this SEI is created. The native oxide layer on the Si surface is damaged during the initial lithiation process, which causes an inner SEI predominantly made of lithium ethylene dicarbonate (LEDC) and Li_xSiO_y to develop. While the continuing discharge causes LiF to be produced, a significant amount of outer SEI is predominantly made up of LEDC. Within the defined potential range, these SEI components containing lithium remain stable. Because of this, the lithium that is used during delithiation cannot be completely recovered from the created SEI constituents, which results in permanent capacity loss and reduced coulombic efficiency during the initial cycle (Schroder, *et al.*, 2015). Si-1 improved electrochemical compatibility with Si and LiPF_6 electrolytes were highlighted by the slightly higher initial charge-discharge coulombic efficiency seen in Si-1 compared to Si-1.5 and Si-2.



This suggests that the anodes have the following rate capabilities: Si-1 > Si-1.5 > Si-2. Examining these electrode typical charge-discharge curves at particular rates lends credence to this claim. The electrode is more stable during discharge because the voltage hysteresis is reduced. The higher capacity of Si-1 electrode compared to Si-1.5 and Si-2 anodes demonstrates superior adaptability of Si-1 and endurance as a protective shell for absorbing significant volume variations. As seen by Si-1 more stable behaviour, this improves cyclability. Because of their greater ability to transport electrons and ions more quickly, Si NPs operate more quickly than nonconductive binder (PAA). The better electrical conductivity and superior specific

capacities at high current densities of Si-1, as compared to Si-1.5 and Si-2, are evidence of its improved physical encapsulation of silicon.

These variations imply that Si-1 performs better in LIBs than Si-1.5 and Si-2, suggesting that Si-1 has an advantage over other materials as an anode material. In conclusion, using the magnesiothermic process and KBr as a scavenger, Si NPs were created from *Oryza sativa* husk. Three different Si NPs kinds were produced using this ecologically friendly method (Salah, *et. al.*, 2019). As LIB anodes, all three varieties of Si NPs demonstrated excellent performance. Si-1, Si-1.5, and Si-2 had specific capacities of 3416, 3037, and 2847 mAh/g, respectively. Si-1, Si-1.5, and Si-2 had lithiation potentials and delithiation potentials of 0.16, 0.21, and 0.25 V, respectively (Daulay *et. al.*, 2022).

Synthesis of activated carbon-decorated nanocrystals-silicon:

Sekar *et al.* (2019) heated brown *Oryza sativa* Husks in an air atmosphere for 120 minutes at 500 °C to collect the ash. After that, 1.0 g of ash and 0.2 g of magnesium (Mg) powder were mixed. This mixture was put in an alumina crucible and annealed for 120 minutes at 700 °C in an argon (Ar) environment. Magnesiothermic reduction took place throughout this procedure. The annealed mixtures underwent a 6-hour stirring procedure in 1 M hydrochloric acid (HCl) to isolate acicular nc-Si-enriched activated carbon nanocomposites and remove magnesium silicide (Mg_2Si) precipitates, magnesium oxide (MgO) residues, and native silicon dioxide (SiO_2) impurities. The next step involved 1-hour reaction with 5% hydrofluoric acid (HF). The wet activated-carbon-decorated silicon nanocrystal products were then collected from the resultant solution, filtered, and washed with deionized water before being dried under vacuum for 10 hours at 80 °C. The *Brown Oryza sativa* Husks was used to create the activated-carbon-decorated silicon nanocrystal nanocomposites utilising the magnesiothermic reduction technique (Figure 3a) (Sekar *et. al.*, 2019).

In addition, by integrating the benefits

of both *nanocrystals-silicon* and activated carbon, the novel nanocomposite structure known as activated-carbon-decorated silicon nanocrystal, which consists of activated carbon embellished with nanostructured silicon (nc-Si), is predicted to enhance the electrochemical performance of LIBs. Building LIB anode combinations utilising *nanocrystals-silicon*, activated carbon, and activated-carbon-decorated silicon nanocrystal allowed researchers to test this idea by evaluating the electrochemical characteristics of materials. Initially, cyclic voltammetry (CV) profiles covering the voltage range of 0 to 3.0 V (vs. Li/Li^+) were captured for the prepared anodes using a scan rate of 0.1 mV/s. Different anodic peaks were visible in the LIB configuration with the *nanocrystals-silicon* anode (Figure 3b), which correspond to the incorporation of lithium ions into the nanocrystals-silicon. A cathodic peak at 0.66 V also formed during the first CV cycle and was brought on by the electrode surface developing a solid electrolyte interphase (SEI) layer as well as electrolyte breakdown. The subsequent stabilisation of CV curves from the second to fifth cycles is proof that the SEI layer prevents further electrolyte breakdown and improves LIB stability. The interaction of Li ions with the native SiO_2 present on the nanocrystals-silicon surface is most likely what caused a wider cathodic peak to form at 1.65 V (Sekar, *et. al.*, 2019; Sun, *et. al.*, 2014, 2015).

During the first CV cycle, the activated carbon anode (Figure 3c) had a pronounced cathodic peak at 0.2 V, which was followed by stable following curves. This was most likely caused by the formation of an SEI layer on the activated carbon surface. In a similar manner, when using activated-carbon-decorated silicon nanocrystal as the anode. Although the nanocomposites included minute amounts of MgO residue, the device did not show any MgO-related peaks. The activated-carbon-decorated silicon nanocrystal nanocomposites showed noticeably more powerful anodic responses than the nanocrystals-silicon instance. This shows that the highly conductive activated carbon nanosheets inside the activated-carbon-silicon

nanocomposite system caused the activated-carbon-decorated silicon nanocrystal to suffer faster electrochemical reactions (Sekar, et. al., 2019).

GCD measurements were used to assess the samples electrochemical properties. The initial lithiation and delithiations capacities for the nanocrystals-silicon sample during the first cycle were 336 and 75 mAh/g, respectively (Figure 3e). Due to the intrinsic oxide tendency to lithiate, the initial coulombic efficiency was thus only about 22%. The 1st discharge curve of the nanocrystals-silicon sample (Figure 3e) exhibits a large plateau at about 0.09 V, which denotes the development of SEI layers and Li-Si alloys on the anode material surface. Due to limitations in electronic conductivity, sluggish chemical reactions, and a reduction in surface area, the GCD performance drastically declined in the second cycle (Sekar, et. al., 2019). The charge and discharge capacities for the activated carbon sample, which is depicted in Figure 3f, were 295 and 545 mAh/g, respectively. This resulted in a coulombic efficiency of 54%. The initial discharge curve suggested that the formation of the SEI layer might lead to a plateau at 0.8 V. After multiple charge-discharge cycles, this plateau disappeared because of the stability of the carbon-based LIB anode (Sekar, et. al., 2019).

When the activated-carbon-decorated silicon nanocrystal anode was employed, the LIB device displayed greater charge (510 mAh/g) and discharge (716 mAh/g) capabilities than the other samples (Figure 3g). The enhanced coulombic efficiency of activated-carbon-decorated silicon nanocrystal anode was 71% as a result. This increased efficiency can be related to the structure of activated carbon-coated nanocrystals-silicon nanocomposite, which efficiently reduces unfavourable processes (such Li-Si alloying on the nanocrystals-silicon surface) and encourages electron diffusion because mesoporous nanocrystals-silicon is present. The 1st discharge cycle showed three potential plateaus (0.3, 0.5, and 0.8 V) as a result of the formation of the SEI layer and the lithiation of amorphous Li_xSi and Si (Sekar, et.

al., 2019).

The rate capability and cycle stability of LIBs with activated carbon and silicon nanocrystal anodes coated with activated carbon were then evaluated. The LIB device with the nanocrystal-silicon anode was excluded due to its poor electrical conductivity, as was already indicated. (Sekar, et. al., 2019).

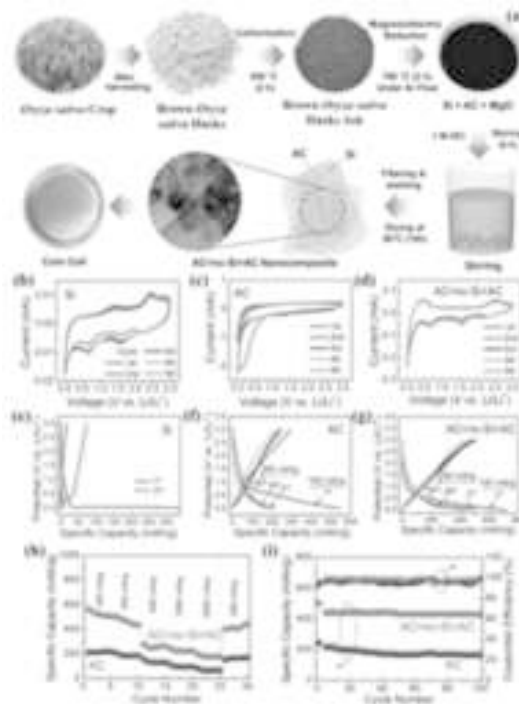


Figure 3: The experimental methods for simultaneously obtaining silicon nanocrystal nanocomposites adorned with activated carbon from the biomass resource known as Brown Oryza sativa Husks (BOSHs), lithium-ion battery (LIB) device cyclic voltammetry (CV) curves using anode materials made of (b) nc-Si, (c) AC, and (d) AC@nc-Si@AC nanocomposites, the scanning rate used for all of the CV measurements was 0.1 mV/s. Galvanostatic charge-discharge (GCD) curves of LIB devices using (e) nc-Si, (f) AC, and (g) activated-carbon-decorated silicon nanocrystal nanocomposites as anode materials, A current density of 100 mA/g was used for

the first GCD cycle, and a current density of 200 mA/g was used for the subsequent cycles, (h) Rate performance for the LIB devices using the anode materials of AC nanosheets and activated-carbon-decorated silicon nanocrystal nanocomposites at different current densities and (i) Cycling performance and coulombic efficiency determined for LIB devices using AC@nc-Si@AC as anode materials under an applied current density of 200 mA/g.

Figure 3h shows the rate performance of the LIBs based on the applied current density. The LIB with the activated carbon anode displayed reversible discharge capacities ranging from 214 to 83 mAh/g at applied current densities of 100 to 2000 mA/g. The silicon nanocrystal activated-carbon decorated anode of the LIB demonstrated reversible discharge capacities ranging from 561 to 199 mAh/g at applied current densities of 100 to 2000 mA/g, respectively. Both times, when the applied current density was lowered to 200 mA/g after 25 cycles, the discharge capacity fully recovered, indicating good reversibility. However, the initial specific capacity (during the first cycle at 100 mA/g) and the specific capacity window (the variance of specific capacity with varying applied current density) were approximately 2.6 times and 1.5 times, respectively (Sekar, et. al., 2019).

The silicon nanocrystal anode coated with activated carbon also showed excellent cycle performance and a good CE. As shown in Figure 3i, the activated carbon anode had a noticeably lower discharge capacity of 166 mAh/g, which is only 0.38 times that of the activated carbon-decorated silicon nanocrystal anode, while the activated carbon anode maintained a high discharge capacity of 429 mAh/g over 100 cycles. Additionally, the silicon nanocrystal anode-equipped LIB maintained a rather high CE of around 97.5% throughout 100 charge-discharge cycles.

The discharge capacity observed here was enhanced by around 1.2 times in comparison to commercial graphite (372 mAh/g), owing to the greater specific capacity

of Si in activated-carbon-decorated silicon nanocrystal nanocomposites. The two-dimensional shape and superior electronic conductivity of the activated carbon nanosheets in the silicon nanocrystal coated with activated carbon may improve ion diffusion and storage in LIBs.

The strong structural stability of activated-carbon-decorated silicon nanocrystal nanocomposites is responsible for these exceptional rate and cyclic performances. In essence, the *activated carbon* nanosheets served as a protective coating or shell for the Si nanocrystals, minimising the volumetric changes in those crystals. The Li interaction with *nanocrystals-silicon* was considerably hampered throughout the whole solid-state system of the activated-carbon-decorated silicon nanocrystal nanocomposite because the *activated carbon* shell allowed plenty of room for Li-ion diffusion during charge-discharge operations.

The initial capacity of fully biomass-derived activated carbon could still be raised, even though adding nanocrystals-silicon and highly conductive nanomaterials (like graphene, carbon nanotubes, conducting polymers, etc.) could be the next steps to improve the electrical conductivity and porosity of the entire composite material system, leading to further improvements in its electrochemical performance.

Finally, activated carbon made from brown *Oryza sativa* husks and silicon nanocrystals Activated carbon nanocomposites have a high initial discharge capacity, reversible specific capacity, rate performance, cyclic stability, and coulombic efficiency. These nanocomposites have the potential to serve as high-performing anode materials for LIB devices (Sekar, et. al., 2019).

Synthesis of nano-silicon:

Husks of *Oryza sativa* were calcined for 5 hours at 600 °C following Sudarman et al. *Oryza sativa* husk ash and a 10% sodium hydroxide (NaOH) solution were mixed for three hours at a temperature of 100°C and a rotational speed of 240 rpm. After being

filtered, the filtrate from the stirring procedure was gradually combined with 37% hydrochloric acid (HCl) until the pH reached to 7.0, which led to the precipitation of a precipitate. Silica (SiO_2) gel was created after extensively filtering and washing the precipitate with deionized water. The next step was to combine SiO_2 gel with 98% magnesium powder in a weight-to-ratio of (1: 0.5, 1: 0.6, or 1: 0.7). The last combination was sealed entirely in an autoclave made of stainless steel. The autoclave was then heated in a microwave for 10 hours at 180°C before being cooled for 12 hours at room temperature. The powder obtained was put through a purifying process. The purification procedure began with the addition of a 5 N hydrochloric acid (HCl) solution for 12 hours. The mixture was rinsed three times with deionized water, and then the silicon was removed by centrifuging the mixture at 4000 rpm for 30 minutes. Adding a 10% hydrofluoric acid (HF) solution for 15 minutes was the second step in the purification process. Three rounds of washing with deionized water were followed by a 30-minute centrifugation at 4000 rpm to remove unreacted SiO_2 and other impurities produced. Three samples were given the designations Si-0.5, Si-0.6, and Si-0.7, with the numbers 0.5, 0.6, and 0.7 designating the amounts of magnesium (Mg) powder used in each sample. Using a hydrothermal process, silicon (Si) with a diameter of only a few nm was produced in an aqueous solution. This required the SiO_2 to be reduced using a mixture of *Oryza sativa* husk SiO_2 gel and Mg powder. SiO_2 gel and Mg powder reacted to form Si and magnesium oxide (MgO). The hydrothermal procedure, which comprises lowering SiO_2 at a temperature of 180°C for 10 hours, results in a mixture of Si and MgO. High-purity nano-Si is produced through further purification procedures. To remove Mg, magnesium silicide (Mg_2Si), and MgO from the mixture,

hydrochloric acid (HCl) is added in the first purification stage. HF is added during the second purification stage to efficiently remove SiO_2 . In Figure 4a, the hydrothermal technique for synthesising nano-Si is shown graphically (Sudarman *et al.*, 2023).

Additionally, cyclic voltammetry (CV) on Si-0.5, Si-0.6, and Si-0.7 was carried out at a scan rate of 0.2 mV s^{-1} throughout a voltage range of 0.01 to 1.5 V. In Figure 4b, the CV of Si-0.5 shows two reduction peaks at 0.38 V and 0.58 V, which are associated with the extraction of Li^+ ions, and one oxidation peak at 0.16 V, which is associated with the insertion of Li^+ ions. Li^+ extraction at 0.38 V, 0.56 V, and Li^+ insertion at 0.16 V are all shown for Si-0.6 CV in Figure 4c. The cyclic voltammetry of Si-0.7 (Figure 4d), which displays Li^+ extraction at 0.38 V and 0.59 V and Li^+ insertion at 0.17 V, demonstrates similar results. The cathodic peak below 0.3 V, which is supported by the huge anodic peak in the CV curve, points to a single mechanism that converts nano-Si into amorphous Li_xSi ($x = 3.75$). However, the electrochemical procedure for producing $\text{Li}_{3.75}\text{Si}$ at room temperature is not very advanced. Regarding the extraction of Li^+ from nano-Si, it is clear that Si-0.6 has the lowest value, demonstrating its superiority to Si-0.5 and Si-0.7. Si-0.6 has pores that are larger than those of Si-0.5 and smaller than those of Si-0.7, which accounts for the disparity. Si-0.7, which has the smallest pore size in comparison to Si-0.5 and Si-0.6, demonstrates greater Li^+ extraction as a result (Sudarman *et al.*, 2023).

Figure 4e shows how well nano-Si electrode cycled over 200 times. During the first cycle, Si-0.5, Si-0.6, and Si-0.7 exhibit capacities of 1575, 1757, and 1525 mAh/g, respectively. Notably, Si-0.6 is more capacious than Si-0.5 and Si-0.7, although Si-0.7 has less capacity than the other two (Sudarman *et al.*, 2023).

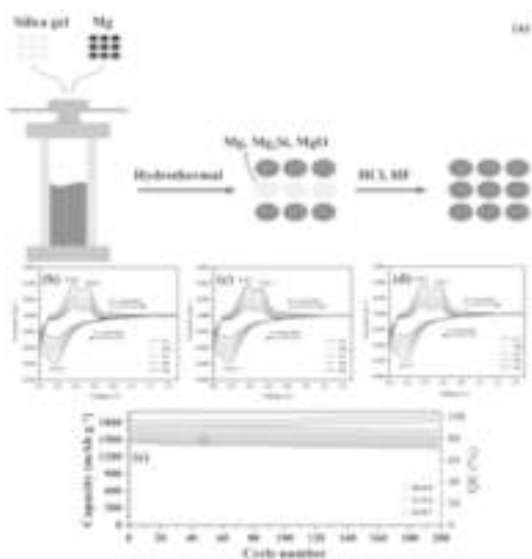


Fig. 4 The cycling performance of a nano-silicon electrode over 200 cycles using the cyclic voltammetry (CV) of Si-0.5, Si-0.6, and Si-0.7 (Sudarman et al., 2023)

This finding emphasises how important pore size is for Li^+ extraction and capacity. The increased capacity of Si-0.6 is a result of its bigger pore size, whereas Si-0.7 has the lowest capacity due to its smaller pore size. As a result, the pore size has a significant impact on lithium-ion battery capacity, favouring larger pore sizes for greater performance. The considerable volume changes that take place throughout the Li^+ extraction and insertion cycles make Si employment as a LIB anode material challenging. Electrode cracking and capacity loss are frequent consequences of these volume fluctuations. Since Si NPs are naturally resistant to fractures, they are employed to reduce cracking. In addition to improving fracture resistance, the nanoscale structure capacity to accept strain from Li^+ extraction and insertion through plastic deformation lowers stresses during volume changes. Therefore, this study focuses on producing porous nanostructured Si in addition to employing Si with nanoparticle-sized Si. Due to the increased capacity that nanostructured Si offers compared to other anode materials, this strategy is essential. With a possibility for further improvement, the

discharge capacity of 1757 mAh/g over 200 cycles demonstrates the exceptional performance of nanostructured Si as a LIB anode, outperforming commercial batteries, graphite, and graphene (Sudarman et al., 2023)

Thus the improved lithium-ion battery performance was made possible by novel synthesis techniques for advanced anode materials, including PANI-SiO₂@rGO nanocomposites, scalable silicon nanoparticles from rice husk, nano-silica by hydrothermal processing, and AC@nc-Si@AC nanocomposites. These methods provide increased stability, conductivity, and capacity, indicating a viable route to the creation of practical and affordable LIB devices.

Acknowledgements:

The authors are thankful to the Department of Botany and Physics, Rajee Ramrao College, Jath and Department of Medical Physics, Centre for Interdisciplinary, Research, D. Y. Patil Education Society (Deemed to Be University), Kolhapur.

References:

- Adam, F. Appaturi, J. N. and Iqbal, A. (2012) *Catal. Today*. **190**:2.
- Autthawong, T. Chimupala, Y Haruta, M. Kurata, H Kiyomura, T. Yu, A. Chairuangstri, T and Sarakonsri, T. (2020) *RSC Adv.* **10**:43811.
- Banerjee, H. D. Sen. S. and Acharya, H. N. (1982) *Mater. Sci. Eng.* **52**:173.
- Boukamp, B. A. (1981) *J. Electrochem. Soc.* **128**:725.
- Carmona, V. B. Oliveira, R. M. Silva, M. W. T. Mattoso, L. H. C and Marconcini, J. M. (2013) *Ind. Crops Prod.* **43**:291.
- Chandrasekhar, S. Satyanarayana, K. G. Pramada, P. N. Raghavan, P and Gupta, T. N. (2003) *J. Mater. Sci.* **38**:3159.
- Charlton, Hatchard, M. T. D. and Obrovac, M. N. (2020) *J. Electrochem. Soc.* **167**:80501.

- Chen, Y. (2019) *IOP Conf. Ser. Mater. Sci. Eng.* **677**:022115.
- Daulay, A. Andriavani and Marpongahtun, Gea, S. (2022) **6**:100256.
- Duan, F. Chyang, C-S. Lin C-W. and Tso, J. (2013) *Bioresour. Technol.* **134**:204.
- Entwistle, J. Rennie, A. and Patwardhan, S. (2018) *J. Mater. Chem. A.* **6**:18344.
- Fang, M. Yang, L. Chen, G. Shi, Z. Luo, Z. and Cen, K. (2004) *Fuel Process. Technol.* **85**:1273.
- Jung, D. Ryou, M. Sung, Y. Park, S and Choi, (2013) *J Proc. Natl. Acad. Sci. U. S. A.* **110**:12229.
- Kalapathy, U. Proctor, A. and J. Shultz, J. (2002) *Bioresour. Technol.* **85**:285.
- Kamenidou, S. Cavins, T. J. and Marek, S. (2010) *Sci. Hortic.* **123**:390.
- Kasavajjula, U. Wang, C and Appleby, A. J. (2007) *J. Power Sources* **163**:1003.
- Le, V. H. Thuc, C. N. H and Thuc, H. H. (2013) *Nanoscale Res. Lett.* **8**:58.
- Lee, J. K. Smith, K. B. Hayner, C. M. and Kung, H. H. (2010) *Chem. Commun.* **46**:2025.
- Liao, Y. Liang, K Ren, Y. and Huang, X. (2020) *Front. Chem.* **8**:96.
- Liou, T-H. (2004) *Mater. Sci. Eng., A*, **364**:313.
- Liu, C. Li, C. Ahmed, K. Wang, W. Lee, I. Zaera, F Ozkan, C. S. and Ozkan, M. (2006) *RSC Adv.* **6**:81712.
- Liu, N. Huo, K. McDowell, M. Zhao, J and Cui, Y. (2013) *Sci. Rep.* **3**:1919.
- Magasinski, A. Dixon, P. Hertzberg, B. Kvit, A. Ayala, J. and Yushin, G. (2010) *Nat. Mater.* **9**:353.
- Ratsameetammajak, N. Autthawong, T, Chairuang Sri, T. Kurata, H. Yu, A-S. and Sarakonsri, T. (2022) *RSC Adv.* **12**:14621.
- Rodríguez de Sensale, G. (2006) *Cem. Concr. Compos.* **28**:158.
- Salah, M. Murphy, P Hall, C. Francis, C. Kerr, R. and Fabretto, (2019) *M. J. Power Sources.* **414**:48.
- Schroder, K. Alvarado, K. J. J Yersak, J. T. A. Li, T. A. J. Dudney, N Webb, L. J. Meng, Y. S. and Stevenson, K. J. (2015) *Chem. Mater.* **27**:5531.
- Sekar, S. Ahmed, A. T. A. A, Inamdar, A. I. Lee, Y. Im, H, Kim, D. Y. and Lee, S (2019) *Nanomaterials.* **9**:1055.
- Sudarman, S. Andriayani, and Tamrin, Taufik, M. (2023) *Materials Science for Energy Technologies.* **1**:8
- Sun, L and Gong, K (2001) *Ind. Eng. Chem. Res.* **40**:5861.
- Sun, Z. Song, X. Zhang, P. and Gao, L. (2014) *RSC Adv.* **4**:20814.
- Sun, Z. Tao, S. Song, X. Zhang, and P. Gao, L. (2015) *J. Electrochem. Soc.* **162**:A1530.
- Wong, D. P. Suriyaprabha, R. Yuvakumar, R. Rajendran, V. Chen, Y-T. Hwang, B-J. Chen, L-C. and Chen, K-H. (2014) *J. Mater. Chem. A*, **2**:13437.
- Xing, A. Tian, S. Tang, H. Losic, D and Bao, Z (2013) *RSC Adv.* **3**:10145.
- Yalcin, N. and Sevinc, V. (2001) *Ceram. Int.* **27**:219.

WATER LOVING, WATER HATING AND WATER REPELLENCE PROPERTIES OF SOME PLANTS

Rajendra Lavate, Sohan Thombare*, Shankar Soudagar, Rajesh Sawant and Appasaheb Bhosale

Department of Botany, Chemistry and Physics, Raje Ramrao College, Jath, (Affiliated to Shivaji University Kolhapur) Sangli-416404, India.

Department of Medical Physics, Centre for Interdisciplinary, Research, D. Y. Patil Education Society (Deemed to Be University), Kolhapur-416006, India.

ABSTRACT

Hydrophilic surfaces, which have an affinity for water molecules, are those that prefer water. Water molecules are attracted to hydrophobic surfaces because they reject water molecules. Surfaces that are particularly water-repellent are known as superhydrophobic surfaces. Because of their great surface roughness and low surface energy, superhydrophobic surfaces allow water droplets to easily bead up and slide off. During the present investigation, beautiful materials found in nature have been explored to examine their water-loving, water-hating, and superhydrophobic characteristics. *Aloe vera*, rose petals, gerbera blossoms, *Aloe barbadensis*, miller leaves, and anthurium flowers are some of the botanical blooms that have been included for present study. All naturally occurring substances possess a reduced surface tension. Water has lower surface tension than most other naturally occurring substances. It was observed that the contact angles of the water droplets on the rose petals altered at three different time points: 120 minutes, 240 minutes, and 360 minutes.

Keywords: Anthurium, *Aloe Vera*, *Colocasia*, *Gerbera* Flower, Rose Petal

Introduction:

Many natural surfaces exhibit characteristics of water affinity, water aversion, and water repellency (Darmanin, and Guittard, 2014; Darmanin, *et. al.*, 2013) Nature has produced insects, animals, and plants for millennia. The Cassie-Baxter and Wenzel models explain how the topography and shape of surfaces greatly influence their water-hating characteristics (Wenzel, 1936; Cassie and Baxter, (1944). The existence of microscopic hairs on leaves is thought to be responsible for their superhydrophobic qualities, which have been documented in the literature. Vertical hairs are found on lady's mantle (Brewer and Willis, 2008) while horizontal hairs are being

observed on poplar leaves and ragwort (Gua *et. al.*, 2005; Ye, *et. al.* 2011). Animals with water-repellent qualities include geckos, butterflies, and water-walking arthropods. Animals and birds, like cicada, translucent butterfly wings, water-walking arthropods, and gecko foot, have some of the most well-known naturally water-repellent surfaces in the universe. Cactus spines, the skin of the filefish *Navodon septentrionlis*, shark skin (Cai, *et al.*, 2014), leafhoppers (Rakitov and Gorb, 2013), and springtail surfaces all exhibit underwater superhydrophobic qualities (Nickerl, *et. al.*, 2013 It is crucial for water repellence qualities to remain stable even after pressure that accounts for the dual action of rainfall (Nosonovsky and Bhushan, 2008).

Super hydrophobicity:

Young's State: The Young equation relates the three surface tensions of liquid-vapor, solid-vapor, and liquid-solid and predicts the contact angle between a liquid droplet and a solid surface. This prediction holds true independent of the surface chemistry (Young,1805). The Young equation explains the liquid's contact angle with a perfectly smooth, chemically homogeneous solid surface as shown in Figure 1a and explained in

$$\cos \theta = (\gamma_{sv} - \gamma_{sl}) / \gamma_{lv}$$

the following equation.

Where γ_{lv} , γ_{sv} and γ_{sl} represent the surface tensions at the interfaces between solids and liquids, respectively. A contact angle (θ) is created when a single drop of fluid (oil or water) is deposited on a solid surface. The Young equation only holds true for smooth surfaces; hence it cannot be used to describe textured surfaces. A liquid contact angle (θ) with a rough surface will be different from that of a liquid with a smooth surface since wetting surfaces are chemically diverse, they are more complicated and rougher. The effect of surface roughness on contact angle can be studied in two modes or states.

Wenzel's State: Figure 2b illustrates the contact angle model that created by Wenzel for rough surfaces, which allows liquid to completely permeate into the rough grooves (Wenzel, 1936). Due to the increase in the solid-liquid interface in the rough grooves, air bubbles may become trapped there, but only if the height of the asperities (H) is high enough. In this instance, a liquid droplet (oil or water) is present on a composite surface, and the Cassie-Baxter model is used to characterise the wetting nature as:

$$\cos \theta_w = r \cos \theta$$

$$i.e. \cos \theta_w = r (\gamma_{sv} - \gamma_{sl}) / \gamma_{lv}$$

Where the Young's contact angle (θ) is and r is the roughness ratio. The ratio of the anticipated surface area to the actual surface area is known as the roughness parameter, or r. When a surface is completely smooth, $r = 1$, and when a surface is rough, $r > 1$. The Wenzel state states that for materials having a contact angle larger than 90° (intrinsically water-hating materials), wetting is minimized by roughness.

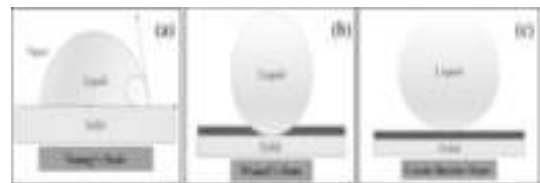


Figure 1: The wetting behaviour of a liquid droplet on a rough solid surface under three different states: a) Young's state, b) Wenzel's state, and c) Cassie-Baxter state.

Cassie- Baxter's State:

The heterogeneous state or composite state are other names for the Cassie-Baxter state. The Cassie-Baxter condition of wetting is seen in Figure 1c, where the grooves beneath the droplet are filled with vapour rather than liquid (Cassie, and Baxter, 1944). The most crucial characteristic of a coating designed to repel water is robustness. Even after being released, the substance retains its high-pressure qualities. The rise in the solid-vapor barrier at low H makes the Cassie-Baxter state a good predictor of water-repellence qualities. It also has anti-icing (heat transfer), anti-corrosion (batteries, water desalination, and ion penetration), and anti-corrosion (ion penetration) capabilities. In spite of a rise in surface roughness, the material's inherent characteristics get better. There are two phases that make up the liquid surface interface: the liquid-vapor interface and the liquid-solid interface.

$$\cos \theta_w = \phi_1 \cos \theta_1 + \phi_2 \cos \theta_2$$

The contributions of the various phases are combined to generate the apparent contact angle, where w is the apparent contact angle and 1 and 2 are the surface fractions of phases 1 and 2, respectively. Phase 1 and Phase 2's respective contact angles are 1 and 2, respectively. The solid fraction, symbolised by the Greek letter, refers to the area of a solid surface that has been moistened by a liquid when one of the surfaces is the air-liquid interface. $(1-\phi)$ represents the air fraction. Because it included the air component, in the denominator, the original equation was wrong. The air percentage should be in the numerator since it represents the portion of the surface that is not moistened by liquid.

$$\phi \cos \theta + (1 - \phi) \cos 180^\circ = \phi \cos \theta + (\phi - 1) = \cos \theta_w$$

When the surface reaches unity (1), the liquid droplet will expand out to cover the entire area. The liquid droplet will not even come close to the surface when surface = 0. For a flat surface, the solid fraction varies from 0 to 1. In this condition, the droplet can readily roll over the solid surface due to the narrow contact area between them.

Contact angle: When a surface is superhydrophobic, it displays high water contact angle ($WCA > 150^\circ$) and low water contact angle hysteresis (CSH 10°). This surface is not only self-cleaning, but also water-repellent (Su, *et al.*, 2010; Bhushan, and Her, 2010; Bormashenko, *et. al.*, 2006) Contact angle hysteresis (CHA) is the distinction between advancing and receding contact angles (Ferrari and Ravera, 2010; Nosonovsky, and Bhushan, 2008). When water droplets form on a superhydrophobic surface, they take on a nearly spherical shape and readily move when subjected to low tilting angles.

Hydrophilic Nature:

Hydrophilic compounds readily dissolve

in water and have a great attraction for it. Water-loving is the opposite of water-repelling. There are numerous uses for surfaces that attract or repel water. Figure 2a illustrates water-loving compounds that can corrode metal surfaces and alloys. Polar molecules are also described as molecules that love water. Because it can form hydrogen bonds and is frequently polar, a molecule's water-loving component can dissolve in water more quickly than its oil- or other water-hating solvent-loving counterpart. It may appear as though water molecules in the air are drawn to substances that love water. In settings with considerable condensation and for shielding exchangers from water's corrosive effects, hydrophilic coatings are very useful. Additionally, hydrophilic coatings do exceptionally well at keeping out water in hot and salty situations.

Hydrophobic Nature:

Figure 2b illustrates how the words "water-hating" and "hating water" have Greek roots that imply "phobia" and "hydrophobia," respectively. Scientists refer to nonpolar substances as being "hydrophobic" because they do not combine with water molecules. Examine that definition in more detail. Since its atoms carry a partial charge, hydro is a polar molecule. The most electronegative atom is oxygen, whose core electrons in each bond are extremely close to one another. Any charged substance will interact with hydro molecules to dissolve, whether it has a positive or negative charge. In essence, molecules that dislike water are non-polar, which means they don't have a net charge. These molecules lack any connections between charges that would enable them to interact with hydro while not having any charges. Water Hating substances frequently insoluble in water or any other solution with a predominately watery environment. In many areas of biology, including the structure of animals, cellular function, and molecular interactions, the traits of being water-hating or non-polar are crucial.



Figure 2: three different surface types: a) hydrophilic, b) hydrophobic, and 3) superhydrophobic.

Water Repellence:

Super-hydrophobic surfaces are very water-repellent, making it very difficult to wet them. On a superhydrophobic surface, a water droplet's contact angle is greater than 150° , and the difference between its advancing and receding contact angles is less than 10° . A droplet can entirely bounce after colliding with a superhydrophobic surface, much like an elastic sphere. This is also referred to as the lotus effect, after the self-cleaning properties of the leaves of the lotus plant.

Experimental Details and Results: Rosaceae Petals:

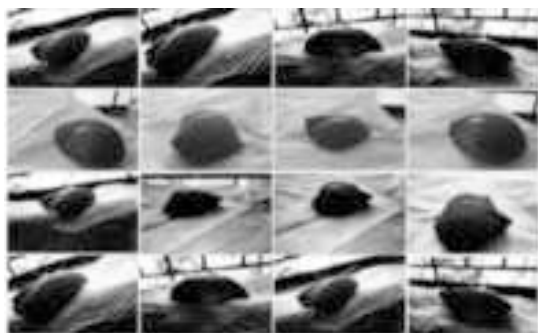


Figure 3: Images of Rosaceae petals at different times, illustrating their water-hating and water-repellence properties.

Rosaceae and the genus *Rosa* contain the most well-known flower in all of nature. The petals of Rose (*Rosa damascene*) of the family Rosaceae, are amphiphilic, meaning they have both a love of and a dislike of water. Even with the petal turned upside down, a water droplet that is small enough will slide off. High sticky forces are incompatible with water repellence. Chinese researchers have established that rose petals and water have an unusual bond that is not shared by other

plants. The micro-nanoscale topography of a rose petal comprises hills and valleys. The large valleys allow a small amount of water to soak in, creating a sticky surface on which smaller droplets can condense and stick to the petal. Since the surface of the rose petals is amphiphilic, it has both water-loving and water-hating characteristics. While the water-hating portions of the petals vigorously oppose water, the water-loving sections have a great attraction for it. The irregular topography of small valleys. Rose petals' micro-papillae produce two reactions in response to water. Larger droplets are repelled by the micro-papillae and tiny valleys. Water-hating and water-repellence are two characteristics displayed by rose petals. Following a few minutes, after 120 minutes, after 240 minutes, and after 360 minutes, it was noted that the contact angles altered during the course of the current investigation.

Asteraceae Flower:

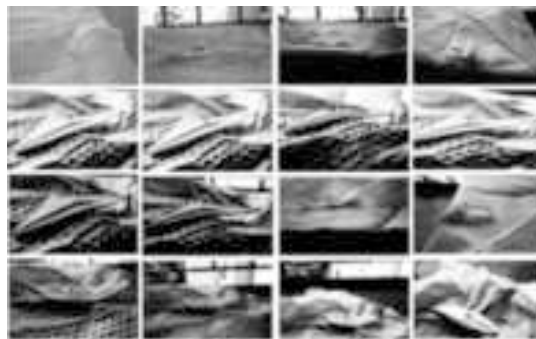


Figure 4: Images of Gerbera petals at different times, illustrating their water-loving, water-hating, and water-repellent properties.

The *Asteraceae* family's Gerbera flower is well-known. The gerbera flower is three-lobed, strap-shaped, and the individual flowers are found in the heads (Barthlott, and Neinhuis, 1997). Its aversion to water is one of its most significant characteristics. The micro-nanoscale surface area of gerbera flowers gives them the ability to both love and hate water. In the current investigation, it has been shown that the contact angles change over the first few minutes, following 120, 240 and 360 minutes.

Colocasía:

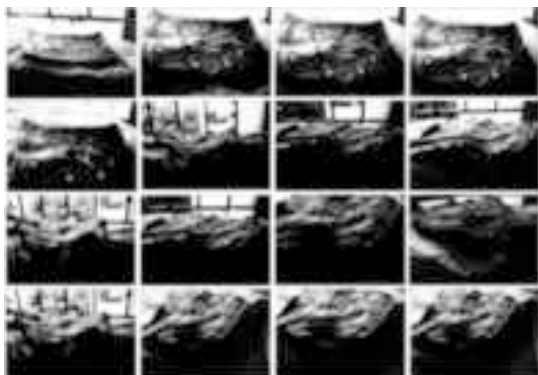


Figure 6: Images of *Colocasía* (*Araceae*) leaves at different times, illustrating their water-loving and water-repelling properties.

The elephant ears, often referred to as *Colocasía*, are the most well-known leaves in the world. Elephant ears belong to the *Araceae* family and the *Colocasía* genus. *Colocasía* leaves exhibit water-loving, water-hating, and water-repellent surface characteristics. In current investigation, it was found that the contact angles altered after a few minutes, after 120 minutes, and after 240 and 360 minutes.

Anthurium:

The genus *Anthurium* includes perennial evergreen plants that are part of the *Araceae* family. *Anthurium* plants have subterranean rhizomes and adventitious roots. *Anthurium* plants create a long-lasting, vivid spathe that comes in a variety of colours, including cream, pink, red, light red, white, dark red, green, lavender, and salmon pink. Most of the time, it is planted as a crop for cut flowers because of its spadix, which is prized for its colorful, long-lasting spathe. *Anthurium* plants are famous for their variety of colors, massive effect, and elegance.

The surface characteristics of *Anthurium* flowers in this study demonstrated both water-loving and water-repelling characteristics. The contact angles were seen to fluctuate throughout the course of the investigation at the following intervals: i.e., after 120, 240, and 360 minutes.

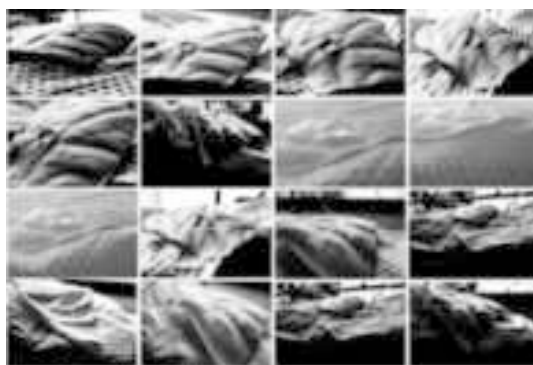


Figure 7 Images of the *Anthurium* flower (*Araceae*) are shows water loving and water hating properties at different time.

***Aloe barbadensis*:**

Aloe vera belongs to the family *Asphodelaceae* and genus *Aloe*. *Aloe barbadensis* leaves have microstructures with tiny height and high pitch values, which change the contact angle between a surface and a water droplet (Bhushan and Her, 2010). The wetting state may be reached if water impregnates between microstructures (Bormashenko, *et al.*, 2006). The hydrophobic liquid's contact area with the surface is less than in the Wenzel state but greater than in the intermediate wetting state. *Aloe barbadensis* leaves are water-loving due to their wide surface area. *Aloe barbadensis* leaves exhibit all three water-loving, water-hating, and water-repellency properties. The contact angles were seen to fluctuate throughout the course of the investigation after a few, 120, 240 and 360 minutes.

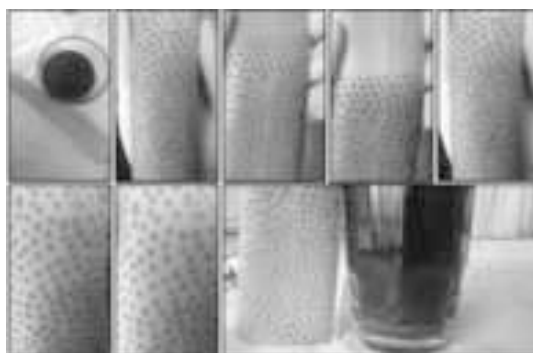


Figure 8: Asphodelaceae that simultaneously display their water-loving characteristics.

During present investigation, the water-loving, water-hating, and water-repellency qualities in Nature's exquisite materials were investigated. The rose petals were water-hating and water-repellent in nature. High adhesive forces were not always associated with water repellence. The petals of a red rose had curious relationship with water, but not for other liquids. Rose petals have a water-loving surface that strongly attracts water while water-hating surfaces strongly repel water. Rose petals had water-hating and water-repellent characteristics, but the latter is the more significant one. A surface's ability to self-clean entails that it can eliminate dirt and debris by dispersing water droplets. The leaves of *Colocasia* leaves had characteristics that attract, resist and love water. *Aloe Vera* leaf surface area demonstrated its affinity for water. Water-loving, water-hating, and water-repellent qualities were found to be present in every flower, petal and leaf. It has been shown that the contact angles change over the first few minutes, the following 120, 240 and 360 minutes.

Acknowledgements:

The authors are thankful to the Department of Botany and Physics Rajee Ramrao College, Jath.

References:

- Barthlott, W. and Neinhuis, C. (1997) *Planta* **202**:1.
- Bhushan, B. and Her, E-K. (2010) *Langmuir* **21**:8207.
- Bormashenko, E. Stein, T. Whyman, G. Bormashenko, Y and Pogreb, R. (2006) *Langmuir* **22**:9982.
- Brewer, S. A. and Willis, C. R. (2008) *Appl. Surf. Sci.* **254**:6450.
- Cai, Y. Lin, L. Xue, Z. Liu, M. Wang, S. and Jiang, L. (2014) *Adv. Funct. Mater.* **24**:809.
- Cassie, A. B. D. and Baxter, S. (1944) *Trans. Faraday Soc.* **40**:546.
- Darmanin, T. and Guittard, F. (2014) *Prog. Polym. Sci.* **39** (4): 656.
- Darmanin, T. Givenchy, E. T. D. Amigoni, S. and Guittard, F (2013) *Adv. Mater.* **25**:1378.
- Ferrari, M and Ravera, F. (2010) *Adv. Colloid Interface Sci.* **161**: 22.
- Gua, Z-Z. Wei, H-M. Zhang, R-Q, Han, G-Z. Pan, C. Zhang, H. Tian, X-J. and Chen, Z-M. (2005) *Appl. Phys. Lett.* **86**:201915.
- Nickerl, J. Helbig, R. Schulz, H-J. Werner, C. and Neinhuis, C. (2013) *Zoomorphology* **132**:183.
- Nosonovsky, M. and Bhushan, B. (2008) *Adv. Funct. Mater.* **18**:843.
- Rakitov, R. and Gorb, S. N. (2013) *Proc. R. Soc. B* **280**:20122391.
- Su, Y. Ji, B. Zhang, K. Gao, H. Huang, Y. and Hwang, K. (2010) *Langmuir* **26**:4984.
- Wenzel, R. N. (1936) *Ind. Eng. Chem.* **28**:988.
- Ye, C. Li, M. Hu, J. Cheng, Q. Jiang, L. and Song, Y. (2011) *Energy Environ. Sci.* **4**:3364.
- Young, T. (1805) *Philos. Trans. R. Soc. Lond.* **95**:65.

See discussions, stats, and author profiles for this publication at: <https://www.researchgate.net/publication/385273551>

ORYZA SATIVA HUSK AS A SUSTAINABLE SOURCE OF SILICON A REVIEW

Article · October 2024

CITATIONS

0

READS

4

1 author:



[Rajendra Lavate](#)

Shikshanmaharshi Dr. Bapuji Salunkhe College Miraj

38 PUBLICATIONS 106 CITATIONS

SEE PROFILE

ORYZA SATIVA HUSK AS A SUSTAINABLE SOURCE OF SILICON: A REVIEW

Rajendra Lavate, Sohan Thombare*, Shankar Soudagar and Appasaheb Bhosale

Department of Botany and Physics, Raje Ramrao College, Jath,
(Affiliated to Shivaji University) Kolhapur Sangli-416404, India.

*Department of Medical Physics, Centre for Interdisciplinary, Research, D. Y. Patil Education Society (Deemed to Be University), Kolhapur-416006, India.

ABSTRACT

This review focuses on utilisation of *Oryza sativa* Husk as a source for silicon nanoparticles (Si NPs) that are created via magnesiothermic reduction and used in composite anodes for lithium-ion batteries (LIBs). The production of silicon nanoparticles (Si NPs) has been explained and, their electrochemical characteristics, and possibility for activated carbon-decorated silicon nanocrystals (AC@nc-Si@AC) to serve as high-capacity anode materials have been discussed. The study emphasises cost-effective, synthesis techniques for creating environmentally acceptable energy storage technologies with the use of biomass.

Introduction:

The majority of people in the world consume rice (*Oryza sativa*) regularly. To fulfil the demands of the expanding population, it is crucial to cultivate *Oryza sativa* sustainably. In recent years, the world has consumed about 470 million metric tons of *Oryza sativa* (Wong, *et al.*, 2014). Millions of tonnes of *Oryza sativa* husk is produced during the manufacturing of rice. Although *Oryza sativa* husk can be utilised to make fuel, fertiliser, and building materials, it is frequently considered a waste product (Rodríguez de Sensale, 2006; Kamenidou *et al.*, 2010; Duan *et al.*, 2013; Fang *et al.*, 2004). Even though *Oryza sativa* husk decomposes naturally, the readily available quantity may convert it as a resource for novel technologies for the benefit of mankind.

Oryza sativa husk contains a high proportion of Silicon dioxide (SiO₂), Depending on the type of soil used to cultivate *Oryza sativa*, the SiO₂ content in its husk ranges from 10 to 20 % (Chandrasekhar *et al.*, 2003). The *Oryza sativa* husk can be pre-treated with various acids before being pyrolyzed to recover SiO₂ from it (Yalcin and Sevinc, 2001; Kalapathy, *et al.*, 2002; Liou, 2004; Adam, *et*

al., 2012). The characteristics of silicon dioxide recovered from husk vary with the source or raw material. Even the amount of SiO₂ differs across *Oryza sativa* husks from different geographical areas. This may have an impact on the SiO₂ extraction characteristics, including purity, particle size, and shape (Carmona, *et al.*, 2013; Le, *et al.*, 2013). The SiO₂ obtained from the *Oryza sativa* has a nanoscale shape. SiO₂ can be converted into silicon (Si) by employing magnesiothermic reduction method, wherein magnesium (Mg) powder and SiO₂ are heated in a furnace until they react. Pure Si is left behind when the SiO₂ and magnesium react with the oxygen to generate magnesium oxide (MgO) (Banerjee *et al.*, 1982). In this way, SiO₂ can be converted to Si in its original shape via magnesiothermic reduction method. Since the reaction is carried out at a temperature of 600 °C the silicon nanoparticles (Si NPs) can be subjected to sintering into a bulk substance. During sintering, the particles come together to create a solid mass. It takes less time for the particles to sinter together when the reaction is carried out at a low temperature, resulting in smaller, more homogeneous Si NPs. Thus it is possible to use silicon dioxide nanoparticles (SiO₂ NPs) as a raw material to create Si NPs. This might

result in the creation of innovative and effective processes for Si NPs synthesis (Sun and Gong, 2001). This process enables the possibility of using low-cost Si NPs in lithium-ion battery systems. This might result in the creation of lithium-ion batteries (LIBs) that are more cost-effective and environmentally friendly (Xing, *et. al*, 2013; Liu, *et. al.*, 2013; Junget. *et. al.*, 2013).

In upcoming LIBs, Si NPs will be a potential anode material. This is due to enormous capacity of Si to store a large amount of energy (Kasavajjula *et. al.*, 2007). Furthermore, Si NPs have a large surface area, which increases their reactivity with lithium ions. This may result in quicker charging and discharging times as well as increased battery performance. Theoretically, Si is the alloying material that can react with lithium ions. The capacity of producing 4200 mAh/g during this reaction, at room temperature, is 10-12 times larger than the specific capacity of conventional graphite based anodes. LIBs, made with the help of Si-based materials have an issue with volume expansion during the charge-discharge cycle. This is due to the many alloy formation stages that Si goes through during the charge-discharge cycle, which causes it to expand and contract. The Si anode may break as a result of this growth in the volume, which could affect the battery performance and lifespan (Boukamp, 1981). A similar issue that can be experienced with Si-based materials is their inherently low conductivity. This indicates that Si is a poor conductor of electricity, which may reduce the battery capacity (Lee, *et al.*, 2010; Magasinski, *et. al.*, 2010). In addition to its low working voltage, abundance on Earth, and low toxicity, Si has several further advantages as an anode material for LIBs (Entwistle, *et. al.*, 2018).

Lithium ions are injected into the material in a process known as intercalation that produces lithiation in conventional electrode materials. The intercalation method results in very few structural changes and with high retention capacity. On the other hand, Si and lithium combine to form an alloy that requires periodic cycles of contravention and re-establishing chemical connections with the

host structure. Low conductivity and the possibility of volume increase are the main drawbacks of adopting Si as an anode material for LIBs. The Si can swell by as much as 280% when a lot of lithium ions are injected into it. The Si anode may fracture and break as a result of the volume increase, which could result in a decrease in battery performance and life. The composite electrode may sustain structural degradation due to the dimensions increase of Si during cycling, which isolates the active component and reduces capacity. This poses a significant obstacle to the creation of Si anodes with large capacities and long cycle lives (Entwistle, *et. al.*, 2018).

The synthesis of SiO₂ and Si materials for LIBs from the husk of *Oryza sativa*, using various extraction methods and magnesiothermic reduction, have been discussed in this communication.

Synthesis:

Ratsameetammajak *et al.* (2022) described the process of preparing silica from the husk of *Oryza sativa* (rice). Rice husks are taken from farms and washed in water. They are then completely dried at 100 °C. To get rid of any metallic impurities, rice husks are soaked in an aqueous solution of hydrochloric acid (HCl) overnight. In order to achieve the pH value of pH of 7, rice husks are thoroughly rinsed in water. Then the rice husks are dried at 100 °C, and subsequently burnt in a muffle furnace at 700 °C for two hours. The burning process is repeated once again to ensure the perfect removal of organic matter and the creation of rice husk ash, an ample source of silica. Where the silica comes from. Below is a summary of the process used to create reduced graphene oxide (rGO): An adaptation of the Hummers process is used to create graphite oxide (GO) from graphite powder. In a non-reactive atmosphere for 5 hours, reduce the GO in a tube furnace at 800 °C (Autthawong *et. al.*, 2020)

The process of creating the composite material made of SiO₂@rGO with a proportion of 30:70 can be summed up as follows: Prepare recently generated SiO₂ by precipitating it for 2 hours at 120 °C in a NaOH solution. In the suspension, distribute rGO by

utilising a hydrochloric acid solution.

Graphene oxide (GO) is a unique material that can be viewed as a single monomolecular layer of graphite with various oxygen-containing functionalities such as epoxide, carbonyl, carboxyl, and hydroxyl groups. Reduced graphene oxide (RGO) is the form of GO that is processed by chemical, thermal and other methods to reduce the oxygen content. As graphite oxide is a material produced by oxidation of graphite, it leads to increased interlayer spacing and functionalization of the basal planes of graphite.

Raise the pH of the mixture to 7. Keep aside overnight at room temperature, and then stir the mixture. Rinse the mixture with deionized (DI) H₂O and ethyl alcohol (CH₃CH₂OH) and then centrifug. Dry the sample thus obtained in a hot air oven at 60 °C as described by Ratsameetammajak et. al., (2022).

The creation of the composite material (SiO₂@rGO and Polyaniline) including SiO₂ / rGO and Polyaniline (PANI) can be summed up as follows: In a mixture of 10 mL ethanol, 5 ml deionized water, and 5 ml H₂SO₄, make a suspension of SiO₂@rGO. To produce a consistent dispersion, sonicate the suspension. While agitating ferociously in an ice bath, dropwise add the aniline monomer to the solution. Stir the solution for 6 hours in an ice bath while adding Ammonium Persulfate ((NH₄)₂S₂O₈). When polymerization takes place leading to the formation of polyaniline emeraldine salt, the solution will turn dark green. To achieve a clear solution, repeatedly wash the suspension in H₂O and CH₃CH₂OH.

The electrochemical behaviour of the PANI-SiO₂@rGO composite was further studied in a coin-type cell utilising lithium foil as

the reference and counter electrodes. A composite anode made of SiO₂ and rGO was used in parallel tests to compare the results. The initial three lithiation-delithiation curves of the SiO₂@rGO and PANI-SiO₂@rGO electrodes at a potential range of 0.01-3.00 V (vs. Li/Li⁺) at a current density of 0.4 A g⁻¹ are shown in Figures 1b and 1c, respectively.

The SiO₂@rGO composite electrode's initial lithiation and delithiation specific capacities were 1012 and 300 mAh/g, respectively, however, it had a poor coulombic efficiency (CE) of 29.6%. The PANI-SiO₂@rGO composite electrode initial lithiation/delithiation specific capacities, on the other hand, were 1508 and 647 mAh/g, respectively, with a CE of 42.9%. The reduction of silica in SiO₂@rGO and PANI-SiO₂@rGO composites, results in lithium loss, causing initial low CE. The potential gradient plateaus on both electrodes, which range from 1.5 to 0.5 V, clearly show the formation of a solid electrolyte interphase (SEI) layer (Ratsameetammajak et. al., 2022).

The existence of stable plateaus during early cycles is an evidence of this reaction (Figure 1d). The subsequent cycles show that the SEI layer is only formed in the initial cycle, as the slopes gradually become sharper and the hills gradually get smaller. The charge voltage profiles become noticeably steeper rather than staying flat at potentials higher than 1.5 V. This invention can be attributed to solvent degradation processes occurring on the oxide electrode surface, which produced the SEI coating (Ratsameetammajak et. al., 2022).

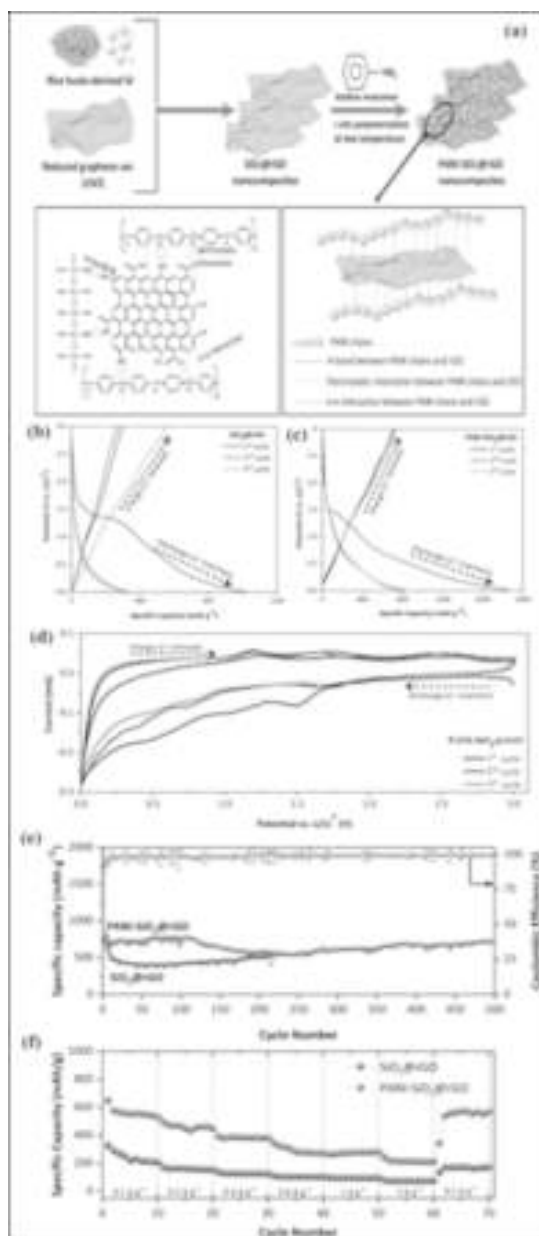


Figure 1(a-f) (a) the synthetic pathway for the preparation of the PANI-SiO₂@rGO composite, lithiation-delithiation profiles for the composites PANI-SiO₂@rGO and SiO₂@rGO measured at 400 mA g⁻¹ in current density (b) and (c), during the first three cycles, cyclic voltammograms (CV) of the PANI-SiO₂@rGO electrode were

recorded at a scan rate of 0.1 mV s⁻¹ and are displayed in (d), SiO₂@rGO and PANI-SiO₂@rGO composites long-term cycling stability and Coulombic efficiency comparison at 400 mA g⁻¹ are depicted in (e). SiO₂@rGO and PANI-SiO₂@rGO composites rate performance evaluation is depicted in (f).

During the initial cycle of delithiation and lithiation, a layer on the surface of anode known as the SEI film develops. It is produced by the interaction of the electrode material and the electrolyte at the solid-liquid interface. It is thought that the partial breakdown of the SEI coating was mostly due to the initial poor CE. The initial coulombic efficiency of PANI-SiO₂@rGO electrode is greater than that of SiO₂@rGO composite electrode. This is because the PANI covering shell prevents the electrolyte at SiO₂@rGO surface from decomposing.

Figure 1e compares the long-term cycling stability of SiO₂@rGO nanocomposite (NC) electrode with the PANI-SiO₂@rGO composite electrode. The PANI-SiO₂@rGO NC anode has outstanding long-term cycling performance at 0.4 A g⁻¹ and maintains a high reversible capacity of 680 mAh/g after 400 cycles, which is about twice as much capacity as standard graphite anodes. In comparison, after 215 cycles, SiO₂@rGO NC electrode can only discharge 414 mAh/g. This shows that only mild pulverisation of SiO₂ in the PANI-SiO₂@rGO NC occurred. The PANI coating efficiently slows down electrolyte degradation on the surface of SiO₂ and serves as a flexible protective layer to absorb SiO₂ volumetric changes.

The results presented above make it clear that the PANI shell outstanding mechanical qualities may prevent SiO₂ nanoparticle volumetric alterations. This capability guarantees that the working electrode structural integrity is maintained throughout discharge and charge cycles, greatly enhancing the electrode sustained stability over time.

The rate performance of PANI-SiO₂@rGO and SiO₂@rGO NC electrodes was evaluated at different current densities ranging

from 0.1 to 2.0 A g⁻¹, as shown in Figure 1f. At the corresponding current densities of 0.1 to 2 A g⁻¹, the PANI-SiO₂@rGO NC electrode displayed discharge capacities ranging from 563.6 to 217.1 mAh/g. After cycling at 2 A g⁻¹, the electrode maintained a discharge capacity of 539.4 mAh/g when cycled back to 0.1 A g⁻¹, illustrating its excellent rate performance. These results show that using PANI-SiO₂@rGO NC is an effective way to improve the electrochemical properties of SiO₂@rGO (Ratsameetammajak *et al.*, 2022).

N-doped carbon coated PANI-SiO₂@rGO NC has superior lithium storage capacity. Which can be attributed to their distinctive structure. SiO₂ nanoscale properties shorten the lithium ion diffusion path, which enhances lithium-ion diffusion and electronic transport. however, the rate capability may suffer. The encircling rGO sheets on the SiO₂ surface have generated a continuous conductive channel that connects the SiO₂ nanoparticles, considerably improving the conductivity of PANI-SiO₂@rGO NC electrode. SiO₂ pulverisation is avoided because the PANI materials elasticity effectively adapts to the NC volume variations during the Li-alloying and dealloying operations (Ratsameetammajak *et al.*, 2022; (Liao, *et al.* 2020; Charlton, *et al.*, 2020, Chen, 2019). In conclusion, PANI-SiO₂@rGO NC had an improved initial CE of 42.9% and a high specific capacity of 680 mAh/g at 400 mA/g after 215 cycles (Ratsameetammajak *et al.*, 2022).

Synthesis of silicon nanoparticles:

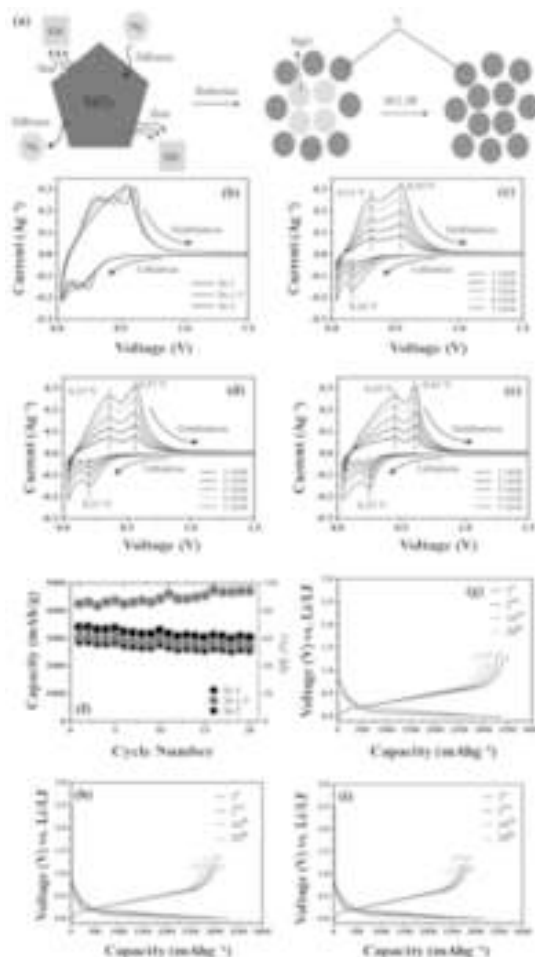
Daulay *et al.* (2022) heated *Oryza sativa* husk at 600°C for 5 hours to produce ash. Thereafter the ash and NaOH were combined and stirred for three hours at 240 rpm and 100°C. The mixture was filtered, and HCl was added until a pH reached 7.0, The precipitate was filtered out and residual solution was heated at 100°C for three hours again for precipitation, which was again removed by filtration. After several rounds of washing with distilled water and drying, SiO₂ was produced in the form of powder. It was then mixed with KBr with a ratio of 1:10,

deionized water was added, and stirring was carried out for three hours. The combination was subjected to ultrasonication for six hours. The residue produced after ultrasonication was separated by decantation, and the filtrate was allowed to dry for 12 hours. The dry powder was mixed with Mg powder in various ratios (1:1.0, 1:1.5, 1:2.0). The next calcination procedure was undertaken at 800°C for 8 hours. During the first purification stage, 150 mL of deionized water and 15 mL of ethanol were added. After that, there was 3 hours of agitation. Centrifugation of the mixture was done for 30 minutes at a speed of 4000 rpm. After being regularly cleaned with deionized water, it was dried for six hours at 80 °C. The second stage involved addition of 150 ml, 5 N HCl and a 12-hour rest period. The sample was dried at 80 °C for 6 hours, washed with deionized water, and then centrifuged once again for 30 minutes at 4000 rpm. Then 150 mL of 10% hydrogen fluoride (HF) was added as the last stage, and the mixture was allowed to settle for 15 minutes. The mixture was first dried, followed by several washes in deionized water, and a second drying step was six hours at 80 °C. Si-1, Si-1.5, and Si-2 thus produced were labelled. (Daulay, *et al.*, 2022).

Figure 2b displays cyclic voltammetry profiles for Si NPs. The data demonstrated that as the ratio of SiO₂ and Mg increases during reduction, the magnesiothermic reduction causes a higher reduction peak associated with the production of delithiation as well as oxidation peaks, associated with the lithiation to Si. Cyclic voltammetry (CV) was used to measure the activation process for Si-1, Si-1.5, and Si-2 electrodes with a voltage range of 0.01 to 1 V (against Li⁺/Li) and a scan rate of 0.2 mVs⁻¹. The CV analysis of Si-1 (Figure 2c) revealed lithiation-related reduction peaks (0.16 V) as well as the delithiation-related oxidation peaks (0.31 V and 0.54 V). Figure 2d depicts the lithiation of Si-1.5 at 0.21 V and its delithiation at 0.37 V and 0.57 V. In Figure 2e, the lithiation (0.25 V) and delithiation (0.45 V and 0.61 V) peaks for Si-2 are displayed. These peak intensities increase during the cycles, suggesting that more lithium ions are possibly

moving between the electrode and electrolyte. This indicated gradual activation of substances. Compared to Si-1.5 and Si-2, Si-1 showed less significant peaks in both lithiation and delithiation. More efficient transport of lithium ions from the cathode to the anode and vice versa is shown by smaller lithiation and delithiation peaks in CV (Daulay *et al.*, 2022).

The rate capability study for the Si-1, Si-1.5, and Si-2 electrodes is shown in Figure 2f. The first cycle is performed to ensure that Si is adequately activated, as shown by cyclic voltammetry, which aids in the creation of a stable solid electrolyte interphase (SEI) layer (Liu *et al.*, 2006). Si-1, Si-1.5, and Si-2 electrodes, respectively, had initial discharge capacities of 3416, 3037, and 2847 mAh/g. 54.9, 85.4, and 85.6 % are the comparable *Conformite Europeenne* (CE). The silicon lithiation potential range (0.01 V to 0.50 V) is higher than the carbonate-based lowest unoccupied molecular orbital (LUMO) electrolyte. When a voltage is applied, Si is lithiated, resulting in the formation of an amorphous solid electrolyte interface (SEI). By reductively destroying the electrolyte, this SEI is created. The native oxide layer on the Si surface is damaged during the initial lithiation process, which causes an inner SEI predominantly made of lithium ethylene dicarbonate (LEDC) and Li_xSiO_y to develop. While the continuing discharge causes LiF to be produced, a significant amount of outer SEI is predominantly made up of LEDC. Within the defined potential range, these SEI components containing lithium remain stable. Because of this, the lithium that is used during delithiation cannot be completely recovered from the created SEI constituents, which results in permanent capacity loss and reduced coulombic efficiency during the initial cycle (Schroder, *et al.*, 2015). Si-1 improved electrochemical compatibility with Si and LiPF_6 electrolytes were highlighted by the slightly higher initial charge-discharge coulombic efficiency seen in Si-1 compared to Si-1.5 and Si-2.



This suggests that the anodes have the following rate capabilities: Si-1 > Si-1.5 > Si-2. Examining these electrode typical charge-discharge curves at particular rates lends credence to this claim. The electrode is more stable during discharge because the voltage hysteresis is reduced. The higher capacity of Si-1 electrode compared to Si-1.5 and Si-2 anodes demonstrates superior adaptability of Si-1 and endurance as a protective shell for absorbing significant volume variations. As seen by Si-1 more stable behaviour, this improves cyclability. Because of their greater ability to transport electrons and ions more quickly, Si NPs operate more quickly than nonconductive binder (PAA). The better electrical conductivity and superior specific

capacities at high current densities of Si-1, as compared to Si-1.5 and Si-2, are evidence of its improved physical encapsulation of silicon.

These variations imply that Si-1 performs better in LIBs than Si-1.5 and Si-2, suggesting that Si-1 has an advantage over other materials as an anode material. In conclusion, using the magnesiothermic process and KBr as a scavenger, Si NPs were created from *Oryza sativa* husk. Three different Si NPs kinds were produced using this ecologically friendly method (Salah, *et. al.*, 2019). As LIB anodes, all three varieties of Si NPs demonstrated excellent performance. Si-1, Si-1.5, and Si-2 had specific capacities of 3416, 3037, and 2847 mAh/g, respectively. Si-1, Si-1.5, and Si-2 had lithiation potentials and delithiation potentials of 0.16, 0.21, and 0.25 V, respectively (Daulay *et. al.*, 2022).

Synthesis of activated carbon-decorated nanocrystals-silicon:

Sekar *et al.* (2019) heated brown *Oryza sativa* Husks in an air atmosphere for 120 minutes at 500 °C to collect the ash. After that, 1.0 g of ash and 0.2 g of magnesium (Mg) powder were mixed. This mixture was put in an alumina crucible and annealed for 120 minutes at 700 °C in an argon (Ar) environment. Magnesiothermic reduction took place throughout this procedure. The annealed mixtures underwent a 6-hour stirring procedure in 1 M hydrochloric acid (HCl) to isolate acicular nc-Si-enriched activated carbon nanocomposites and remove magnesium silicide (Mg_2Si) precipitates, magnesium oxide (MgO) residues, and native silicon dioxide (SiO_2) impurities. The next step involved 1-hour reaction with 5% hydrofluoric acid (HF). The wet activated-carbon-decorated silicon nanocrystal products were then collected from the resultant solution, filtered, and washed with deionized water before being dried under vacuum for 10 hours at 80 °C. The *Brown Oryza sativa Husks* was used to create the activated-carbon-decorated silicon nanocrystal nanocomposites utilising the magnesiothermic reduction technique (Figure 3a) (Sekar *et. al.*, 2019).

In addition, by integrating the benefits

of both *nanocrystals-silicon* and activated carbon, the novel nanocomposite structure known as activated-carbon-decorated silicon nanocrystal, which consists of activated carbon embellished with nanostructured silicon (nc-Si), is predicted to enhance the electrochemical performance of LIBs. Building LIB anode combinations utilising *nanocrystals-silicon*, activated carbon, and activated-carbon-decorated silicon nanocrystal allowed researchers to test this idea by evaluating the electrochemical characteristics of materials. Initially, cyclic voltammetry (CV) profiles covering the voltage range of 0 to 3.0 V (vs. Li/Li^+) were captured for the prepared anodes using a scan rate of 0.1 mV/s. Different anodic peaks were visible in the LIB configuration with the *nanocrystals-silicon* anode (Figure 3b), which correspond to the incorporation of lithium ions into the nanocrystals-silicon. A cathodic peak at 0.66 V also formed during the first CV cycle and was brought on by the electrode surface developing a solid electrolyte interphase (SEI) layer as well as electrolyte breakdown. The subsequent stabilisation of CV curves from the second to fifth cycles is proof that the SEI layer prevents further electrolyte breakdown and improves LIB stability. The interaction of Li ions with the native SiO_2 present on the nanocrystals-silicon surface is most likely what caused a wider cathodic peak to form at 1.65 V (Sekar, *et. al.*, 2019; Sun, *et. al.*, 2014, 2015).

During the first CV cycle, the activated carbon anode (Figure 3c) had a pronounced cathodic peak at 0.2 V, which was followed by stable following curves. This was most likely caused by the formation of an SEI layer on the activated carbon surface. In a similar manner, when using activated-carbon-decorated silicon nanocrystal as the anode. Although the nanocomposites included minute amounts of MgO residue, the device did not show any MgO-related peaks. The activated-carbon-decorated silicon nanocrystal nanocomposites showed noticeably more powerful anodic responses than the nanocrystals-silicon instance. This shows that the highly conductive activated carbon nanosheets inside the activated-carbon-silicon

nanocomposite system caused the activated-carbon-decorated silicon nanocrystal to suffer faster electrochemical reactions (Sekar, et. al., 2019).

GCD measurements were used to assess the samples electrochemical properties. The initial lithiation and delithiations capacities for the nanocrystals-silicon sample during the first cycle were 336 and 75 mAh/g, respectively (Figure 3e). Due to the intrinsic oxide tendency to lithiate, the initial coulombic efficiency was thus only about 22%. The 1st discharge curve of the nanocrystals-silicon sample (Figure 3e) exhibits a large plateau at about 0.09 V, which denotes the development of SEI layers and Li-Si alloys on the anode material surface. Due to limitations in electronic conductivity, sluggish chemical reactions, and a reduction in surface area, the GCD performance drastically declined in the second cycle (Sekar, et. al., 2019). The charge and discharge capacities for the activated carbon sample, which is depicted in Figure 3f, were 295 and 545 mAh/g, respectively. This resulted in a coulombic efficiency of 54%. The initial discharge curve suggested that the formation of the SEI layer might lead to a plateau at 0.8 V. After multiple charge-discharge cycles, this plateau disappeared because of the stability of the carbon-based LIB anode (Sekar, et. al., 2019).

When the activated-carbon-decorated silicon nanocrystal anode was employed, the LIB device displayed greater charge (510 mAh/g) and discharge (716 mAh/g) capabilities than the other samples (Figure 3g). The enhanced coulombic efficiency of activated-carbon-decorated silicon nanocrystal anode was 71% as a result. This increased efficiency can be related to the structure of activated carbon-coated nanocrystals-silicon nanocomposite, which efficiently reduces unfavourable processes (such Li-Si alloying on the nanocrystals-silicon surface) and encourages electron diffusion because mesoporous nanocrystals-silicon is present. The 1st discharge cycle showed three potential plateaus (0.3, 0.5, and 0.8 V) as a result of the formation of the SEI layer and the lithiation of amorphous Li_xSi and Si (Sekar, et.

al., 2019).

The rate capability and cycle stability of LIBs with activated carbon and silicon nanocrystal anodes coated with activated carbon were then evaluated. The LIB device with the nanocrystal-silicon anode was excluded due to its poor electrical conductivity, as was already indicated. (Sekar, et. al., 2019).

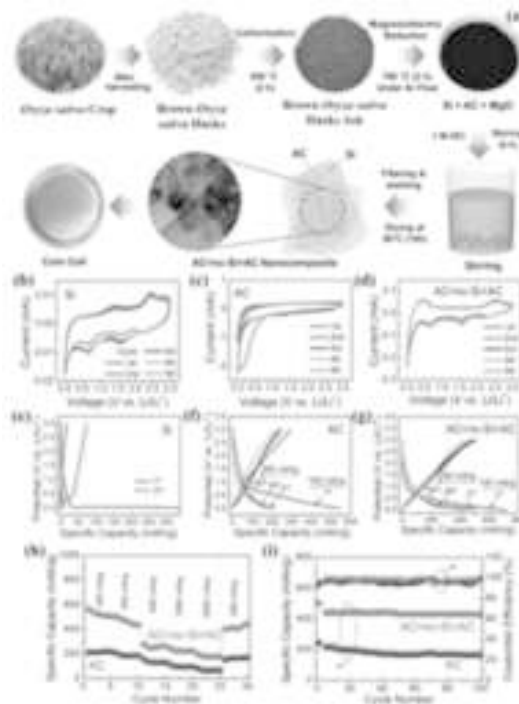


Figure 3: The experimental methods for simultaneously obtaining silicon nanocrystal nanocomposites adorned with activated carbon from the biomass resource known as Brown Oryza sativa Husks (BOSHs), lithium-ion battery (LIB) device cyclic voltammetry (CV) curves using anode materials made of (b) nc-Si, (c) AC, and (d) AC@nc-Si@AC nanocomposites, the scanning rate used for all of the CV measurements was 0.1 mV/s. Galvanostatic charge-discharge (GCD) curves of LIB devices using (e) nc-Si, (f) AC, and (g) activated-carbon-decorated silicon nanocrystal nanocomposites as anode materials, A current density of 100 mA/g was used for

the first GCD cycle, and a current density of 200 mA/g was used for the subsequent cycles, (h) Rate performance for the LIB devices using the anode materials of AC nanosheets and activated-carbon-decorated silicon nanocrystal nanocomposites at different current densities and (i) Cycling performance and coulombic efficiency determined for LIB devices using AC@nc-Si@AC as anode materials under an applied current density of 200 mA/g.

Figure 3h shows the rate performance of the LIBs based on the applied current density. The LIB with the activated carbon anode displayed reversible discharge capacities ranging from 214 to 83 mAh/g at applied current densities of 100 to 2000 mA/g. The silicon nanocrystal activated-carbon decorated anode of the LIB demonstrated reversible discharge capacities ranging from 561 to 199 mAh/g at applied current densities of 100 to 2000 mA/g, respectively. Both times, when the applied current density was lowered to 200 mA/g after 25 cycles, the discharge capacity fully recovered, indicating good reversibility. However, the initial specific capacity (during the first cycle at 100 mA/g) and the specific capacity window (the variance of specific capacity with varying applied current density) were approximately 2.6 times and 1.5 times, respectively (Sekar, et. al., 2019).

The silicon nanocrystal anode coated with activated carbon also showed excellent cycle performance and a good CE. As shown in Figure 3i, the activated carbon anode had a noticeably lower discharge capacity of 166 mAh/g, which is only 0.38 times that of the activated carbon-decorated silicon nanocrystal anode, while the activated carbon anode maintained a high discharge capacity of 429 mAh/g over 100 cycles. Additionally, the silicon nanocrystal anode-equipped LIB maintained a rather high CE of around 97.5% throughout 100 charge-discharge cycles.

The discharge capacity observed here was enhanced by around 1.2 times in comparison to commercial graphite (372 mAh/g), owing to the greater specific capacity

of Si in activated-carbon-decorated silicon nanocrystal nanocomposites. The two-dimensional shape and superior electronic conductivity of the activated carbon nanosheets in the silicon nanocrystal coated with activated carbon may improve ion diffusion and storage in LIBs.

The strong structural stability of activated-carbon-decorated silicon nanocrystal nanocomposites is responsible for these exceptional rate and cyclic performances. In essence, the *activated carbon* nanosheets served as a protective coating or shell for the Si nanocrystals, minimising the volumetric changes in those crystals. The Li interaction with *nanocrystals-silicon* was considerably hampered throughout the whole solid-state system of the activated-carbon-decorated silicon nanocrystal nanocomposite because the *activated carbon* shell allowed plenty of room for Li-ion diffusion during charge-discharge operations.

The initial capacity of fully biomass-derived activated carbon could still be raised, even though adding nanocrystals-silicon and highly conductive nanomaterials (like graphene, carbon nanotubes, conducting polymers, etc.) could be the next steps to improve the electrical conductivity and porosity of the entire composite material system, leading to further improvements in its electrochemical performance.

Finally, activated carbon made from brown *Oryza sativa* husks and silicon nanocrystals Activated carbon nanocomposites have a high initial discharge capacity, reversible specific capacity, rate performance, cyclic stability, and coulombic efficiency. These nanocomposites have the potential to serve as high-performing anode materials for LIB devices (Sekar, et. al., 2019).

Synthesis of nano-silicon:

Husks of *Oryza sativa* were calcined for 5 hours at 600 °C following Sudarman et al. *Oryza sativa* husk ash and a 10% sodium hydroxide (NaOH) solution were mixed for three hours at a temperature of 100°C and a rotational speed of 240 rpm. After being

filtered, the filtrate from the stirring procedure was gradually combined with 37% hydrochloric acid (HCl) until the pH reached to 7.0, which led to the precipitation of a precipitate. Silica (SiO_2) gel was created after extensively filtering and washing the precipitate with deionized water. The next step was to combine SiO_2 gel with 98% magnesium powder in a weight-to-ratio of (1: 0.5, 1: 0.6, or 1: 0.7). The last combination was sealed entirely in an autoclave made of stainless steel. The autoclave was then heated in a microwave for 10 hours at 180°C before being cooled for 12 hours at room temperature. The powder obtained was put through a purifying process. The purification procedure began with the addition of a 5 N hydrochloric acid (HCl) solution for 12 hours. The mixture was rinsed three times with deionized water, and then the silicon was removed by centrifuging the mixture at 4000 rpm for 30 minutes. Adding a 10% hydrofluoric acid (HF) solution for 15 minutes was the second step in the purification process. Three rounds of washing with deionized water were followed by a 30-minute centrifugation at 4000 rpm to remove unreacted SiO_2 and other impurities produced. Three samples were given the designations Si-0.5, Si-0.6, and Si-0.7, with the numbers 0.5, 0.6, and 0.7 designating the amounts of magnesium (Mg) powder used in each sample. Using a hydrothermal process, silicon (Si) with a diameter of only a few nm was produced in an aqueous solution. This required the SiO_2 to be reduced using a mixture of *Oryza sativa* husk SiO_2 gel and Mg powder. SiO_2 gel and Mg powder reacted to form Si and magnesium oxide (MgO). The hydrothermal procedure, which comprises lowering SiO_2 at a temperature of 180°C for 10 hours, results in a mixture of Si and MgO. High-purity nano-Si is produced through further purification procedures. To remove Mg, magnesium silicide (Mg_2Si), and MgO from the mixture,

hydrochloric acid (HCl) is added in the first purification stage. HF is added during the second purification stage to efficiently remove SiO_2 . In Figure 4a, the hydrothermal technique for synthesising nano-Si is shown graphically (Sudarman *et al.*, 2023).

Additionally, cyclic voltammetry (CV) on Si-0.5, Si-0.6, and Si-0.7 was carried out at a scan rate of 0.2 mV s^{-1} throughout a voltage range of 0.01 to 1.5 V. In Figure 4b, the CV of Si-0.5 shows two reduction peaks at 0.38 V and 0.58 V, which are associated with the extraction of Li^+ ions, and one oxidation peak at 0.16 V, which is associated with the insertion of Li^+ ions. Li^+ extraction at 0.38 V, 0.56 V, and Li^+ insertion at 0.16 V are all shown for Si-0.6 CV in Figure 4c. The cyclic voltammetry of Si-0.7 (Figure 4d), which displays Li^+ extraction at 0.38 V and 0.59 V and Li^+ insertion at 0.17 V, demonstrates similar results. The cathodic peak below 0.3 V, which is supported by the huge anodic peak in the CV curve, points to a single mechanism that converts nano-Si into amorphous Li_xSi ($x = 3.75$). However, the electrochemical procedure for producing $\text{Li}_{3.75}\text{Si}$ at room temperature is not very advanced. Regarding the extraction of Li^+ from nano-Si, it is clear that Si-0.6 has the lowest value, demonstrating its superiority to Si-0.5 and Si-0.7. Si-0.6 has pores that are larger than those of Si-0.5 and smaller than those of Si-0.7, which accounts for the disparity. Si-0.7, which has the smallest pore size in comparison to Si-0.5 and Si-0.6, demonstrates greater Li^+ extraction as a result (Sudarman *et al.*, 2023).

Figure 4e shows how well nano-Si electrode cycled over 200 times. During the first cycle, Si-0.5, Si-0.6, and Si-0.7 exhibit capacities of 1575, 1757, and 1525 mAh/g, respectively. Notably, Si-0.6 is more capacious than Si-0.5 and Si-0.7, although Si-0.7 has less capacity than the other two (Sudarman *et al.*, 2023).

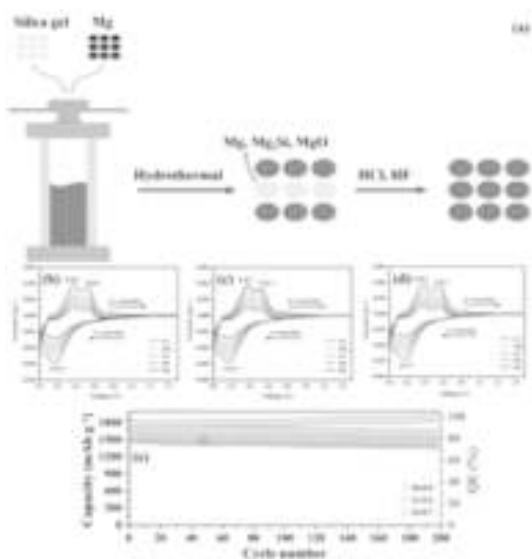


Fig. 4 The cycling performance of a nano-silicon electrode over 200 cycles using the cyclic voltammetry (CV) of Si-0.5, Si-0.6, and Si-0.7 (Sudarman et al., 2023)

This finding emphasises how important pore size is for Li^+ extraction and capacity. The increased capacity of Si-0.6 is a result of its bigger pore size, whereas Si-0.7 has the lowest capacity due to its smaller pore size. As a result, the pore size has a significant impact on lithium-ion battery capacity, favouring larger pore sizes for greater performance. The considerable volume changes that take place throughout the Li^+ extraction and insertion cycles make Si employment as a LIB anode material challenging. Electrode cracking and capacity loss are frequent consequences of these volume fluctuations. Since Si NPs are naturally resistant to fractures, they are employed to reduce cracking. In addition to improving fracture resistance, the nanoscale structure capacity to accept strain from Li^+ extraction and insertion through plastic deformation lowers stresses during volume changes. Therefore, this study focuses on producing porous nanostructured Si in addition to employing Si with nanoparticle-sized Si. Due to the increased capacity that nanostructured Si offers compared to other anode materials, this strategy is essential. With a possibility for further improvement, the

discharge capacity of 1757 mAh/g over 200 cycles demonstrates the exceptional performance of nanostructured Si as a LIB anode, outperforming commercial batteries, graphite, and graphene (Sudarman et al., 2023)

Thus the improved lithium-ion battery performance was made possible by novel synthesis techniques for advanced anode materials, including PANI-SiO₂@rGO nanocomposites, scalable silicon nanoparticles from rice husk, nano-silica by hydrothermal processing, and AC@nc-Si@AC nanocomposites. These methods provide increased stability, conductivity, and capacity, indicating a viable route to the creation of practical and affordable LIB devices.

Acknowledgements:

The authors are thankful to the Department of Botany and Physics, Raje Ramrao College, Jath and Department of Medical Physics, Centre for Interdisciplinary, Research, D. Y. Patil Education Society (Deemed to Be University), Kolhapur.

References:

- Adam, F. Appaturi, J. N. and Iqbal, A. (2012) *Catal. Today*. **190**:2.
- Autthawong, T. Chimupala, Y Haruta, M. Kurata, H Kiyomura, T. Yu, A. Chairuangstri, T and Sarakonsri, T. (2020) *RSC Adv.* **10**:43811.
- Banerjee, H. D. Sen. S. and Acharya, H. N. (1982) *Mater. Sci. Eng.* **52**:173.
- Boukamp, B. A. (1981) *J. Electrochem. Soc.* **128**:725.
- Carmona, V. B. Oliveira, R. M. Silva, M. W. T. Mattoso, L. H. C and Marconcini, J. M. (2013) *Ind. Crops Prod.* **43**:291.
- Chandrasekhar, S. Satyanarayana, K. G. Pramada, P. N. Raghavan, P and Gupta, T. N. (2003) *J. Mater. Sci.* **38**:3159.
- Charlton, Hatchard, M. T. D. and Obrovac, M. N. (2020) *J. Electrochem. Soc.* **167**:80501.

- Chen, Y. (2019) *IOP Conf. Ser. Mater. Sci. Eng.* **677**:022115.
- Daulay, A. Andriavani and Marpongahtun, Gea, S. (2022) **6**:100256.
- Duan, F. Chyang, C-S. Lin C-W. and Tso, J. (2013) *Bioresour. Technol.* **134**:204.
- Entwistle, J. Rennie, A. and Patwardhan, S. (2018) *J. Mater. Chem. A.* **6**:18344.
- Fang, M. Yang, L. Chen, G. Shi, Z. Luo, Z. and Cen, K. (2004) *Fuel Process. Technol.* **85**:1273.
- Jung, D. Ryou, M. Sung, Y. Park, S and Choi, (2013) *J Proc. Natl. Acad. Sci. U. S. A.* **110**:12229.
- Kalapathy, U. Proctor, A. and J. Shultz, J. (2002) *Bioresour. Technol.* **85**:285.
- Kamenidou, S. Cavins, T. J. and Marek, S. (2010) *Sci. Hortic.* **123**:390.
- Kasavajjula, U. Wang, C and Appleby, A. J. (2007) *J. Power Sources* **163**:1003.
- Le, V. H. Thuc, C. N. H and Thuc, H. H. (2013) *Nanoscale Res. Lett.* **8**:58.
- Lee, J. K. Smith, K. B. Hayner, C. M. and Kung, H. H. (2010) *Chem. Commun.* **46**:2025.
- Liao, Y. Liang, K Ren, Y. and Huang, X. (2020) *Front. Chem.* **8**:96.
- Liou, T-H. (2004) *Mater. Sci. Eng., A*, **364**:313.
- Liu, C. Li, C. Ahmed, K. Wang, W. Lee, I. Zaera, F Ozkan, C. S. and Ozkan, M. (2006) *RSC Adv.* **6**:81712.
- Liu, N. Huo, K. McDowell, M. Zhao, J and Cui, Y. (2013) *Sci. Rep.* **3**:1919.
- Magasinski, A. Dixon, P. Hertzberg, B. Kvit, A. Ayala, J. and Yushin, G. (2010) *Nat. Mater.* **9**:353.
- Ratsameetammajak, N. Autthawong, T, Chairuangsri, T. Kurata, H. Yu, A-S. and Sarakonsri, T. (2022) *RSC Adv.* **12**:14621.
- Rodríguez de Sensale, G. (2006) *Cem. Concr. Compos.* **28**:158.
- Salah, M. Murphy, P Hall, C. Francis, C. Kerr, R. and Fabretto, (2019) *M. J. Power Sources.* **414**:48.
- Schroder, K. Alvarado, K. J. J Yersak, J. T. A. Li, T. A. J. Dudney, N Webb, L. J. Meng, Y. S. and Stevenson, K. J. (2015) *Chem. Mater.* **27**:5531.
- Sekar, S. Ahmed, A. T. A. A, Inamdar, A. I. Lee, Y. Im, H, Kim, D. Y. and Lee, S (2019) *Nanomaterials.* **9**:1055.
- Sudarman, S. Andriayani, and Tamrin, Taufik, M. (2023) *Materials Science for Energy Technologies.* **1**:8
- Sun, L and Gong, K (2001) *Ind. Eng. Chem. Res.* **40**:5861.
- Sun, Z. Song, X. Zhang, P. and Gao, L. (2014) *RSC Adv.* **4**:20814.
- Sun, Z. Tao, S. Song, X. Zhang, and P. Gao, L. (2015) *J. Electrochem. Soc.* **162**:A1530.
- Wong, D. P. Suriyaprabha, R. Yuvakumar, R. Rajendran, V. Chen, Y-T. Hwang, B-J. Chen, L-C. and Chen, K-H. (2014) *J. Mater. Chem. A*, **2**:13437.
- Xing, A. Tian, S. Tang, H. Losic, D and Bao, Z (2013) *RSC Adv.* **3**:10145.
- Yalcin, N. and Sevinc, V. (2001) *Ceram. Int.* **27**:219.

WATER LOVING, WATER HATING AND WATER REPELLENCE PROPERTIES OF SOME PLANTS

Rajendra Lavate, Sohan Thombare*, Shankar Soudagar, Rajesh Sawant and Appasaheb Bhosale

Department of Botany, Chemistry and Physics, Raje Ramrao College, Jath, (Affiliated to Shivaji University Kolhapur) Sangli-416404, India.

Department of Medical Physics, Centre for Interdisciplinary, Research, D. Y. Patil Education Society (Deemed to Be University), Kolhapur-416006, India.

ABSTRACT

Hydrophilic surfaces, which have an affinity for water molecules, are those that prefer water. Water molecules are attracted to hydrophobic surfaces because they reject water molecules. Surfaces that are particularly water-repellent are known as superhydrophobic surfaces. Because of their great surface roughness and low surface energy, superhydrophobic surfaces allow water droplets to easily bead up and slide off. During the present investigation, beautiful materials found in nature have been explored to examine their water-loving, water-hating, and superhydrophobic characteristics. *Aloe vera*, rose petals, gerbera blossoms, *Aloe barbadensis*, miller leaves, and anthurium flowers are some of the botanical blooms that have been included for present study. All naturally occurring substances possess a reduced surface tension. Water has lower surface tension than most other naturally occurring substances. It was observed that the contact angles of the water droplets on the rose petals altered at three different time points: 120 minutes, 240 minutes, and 360 minutes.

Keywords: Anthurium, *Aloe Vera*, *Colocasia*, *Gerbera* Flower, Rose Petal

Introduction:

Many natural surfaces exhibit characteristics of water affinity, water aversion, and water repellency (Darmanin, and Guittard, 2014; Darmanin, *et. al.*, 2013) Nature has produced insects, animals, and plants for millennia. The Cassie-Baxter and Wenzel models explain how the topography and shape of surfaces greatly influence their water-hating characteristics (Wenzel, 1936; Cassie and Baxter, (1944). The existence of microscopic hairs on leaves is thought to be responsible for their superhydrophobic qualities, which have been documented in the literature. Vertical hairs are found on lady's mantle (Brewer and Willis, 2008) while horizontal hairs are being

observed on poplar leaves and ragwort (Gua *et. al.*, 2005; Ye, *et. al.* 2011). Animals with water-repellent qualities include geckos, butterflies, and water-walking arthropods. Animals and birds, like cicada, translucent butterfly wings, water-walking arthropods, and gecko foot, have some of the most well-known naturally water-repellent surfaces in the universe. Cactus spines, the skin of the filefish *Navodon septentrionalis*, shark skin (Cai, *et al.*, 2014), leafhoppers (Rakitov and Gorb, 2013), and springtail surfaces all exhibit underwater superhydrophobic qualities (Nickerl, *et. al.*, 2013 It is crucial for water repellence qualities to remain stable even after pressure that accounts for the dual action of rainfall (Nosonovsky and Bhushan, 2008).

Super hydrophobicity:

Young's State: The Young equation relates the three surface tensions of liquid-vapor, solid-vapor, and liquid-solid and predicts the contact angle between a liquid droplet and a solid surface. This prediction holds true independent of the surface chemistry (Young,1805). The Young equation explains the liquid's contact angle with a perfectly smooth, chemically homogeneous solid surface as shown in Figure 1a and explained in

$$\cos \theta = (\gamma_{sv} - \gamma_{sl}) / \gamma_{lv}$$

the following equation.

Where γ_{lv} , γ_{sv} and γ_{sl} represent the surface tensions at the interfaces between solids and liquids, respectively. A contact angle (θ) is created when a single drop of fluid (oil or water) is deposited on a solid surface. The Young equation only holds true for smooth surfaces; hence it cannot be used to describe textured surfaces. A liquid contact angle (θ) with a rough surface will be different from that of a liquid with a smooth surface since wetting surfaces are chemically diverse, they are more complicated and rougher. The effect of surface roughness on contact angle can be studied in two modes or states.

Wenzel's State: Figure 2b illustrates the contact angle model that created by Wenzel for rough surfaces, which allows liquid to completely permeate into the rough grooves (Wenzel, 1936). Due to the increase in the solid-liquid interface in the rough grooves, air bubbles may become trapped there, but only if the height of the asperities (H) is high enough. In this instance, a liquid droplet (oil or water) is present on a composite surface, and the Cassie-Baxter model is used to characterise the wetting nature as:

$$\cos \theta_w = r \cos \theta$$

$$i.e. \cos \theta_w = r (\gamma_{sv} - \gamma_{sl}) / \gamma_{lv}$$

Where the Young's contact angle (θ) is and r is the roughness ratio. The ratio of the anticipated surface area to the actual surface area is known as the roughness parameter, or r. When a surface is completely smooth, $r = 1$, and when a surface is rough, $r > 1$. The Wenzel state states that for materials having a contact angle larger than 90° (intrinsically water-hating materials), wetting is minimized by roughness.

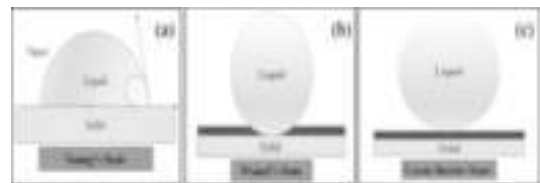


Figure 1: The wetting behaviour of a liquid droplet on a rough solid surface under three different states: a) Young's state, b) Wenzel's state, and c) Cassie-Baxter state.

Cassie- Baxter's State:

The heterogeneous state or composite state are other names for the Cassie-Baxter state. The Cassie-Baxter condition of wetting is seen in Figure 1c, where the grooves beneath the droplet are filled with vapour rather than liquid (Cassie, and Baxter, 1944). The most crucial characteristic of a coating designed to repel water is robustness. Even after being released, the substance retains its high-pressure qualities. The rise in the solid-vapor barrier at low H makes the Cassie-Baxter state a good predictor of water-repellence qualities. It also has anti-icing (heat transfer), anti-corrosion (batteries, water desalination, and ion penetration), and anti-corrosion (ion penetration) capabilities. In spite of a rise in surface roughness, the material's inherent characteristics get better. There are two phases that make up the liquid surface interface: the liquid-vapor interface and the liquid-solid interface.

$$\cos \theta_w = \phi_1 \cos \theta_1 + \phi_2 \cos \theta_2$$

The contributions of the various phases are combined to generate the apparent contact angle, where w is the apparent contact angle and 1 and 2 are the surface fractions of phases 1 and 2, respectively. Phase 1 and Phase 2's respective contact angles are 1 and 2, respectively. The solid fraction, symbolised by the Greek letter, refers to the area of a solid surface that has been moistened by a liquid when one of the surfaces is the air-liquid interface. $(1-\phi)$ represents the air fraction. Because it included the air component, in the denominator, the original equation was wrong. The air percentage should be in the numerator since it represents the portion of the surface that is not moistened by liquid.

$$\phi \cos \theta + (1 - \phi) \cos 180^\circ = \phi \cos \theta + (\phi - 1) = \cos \theta_w$$

When the surface reaches unity (1), the liquid droplet will expand out to cover the entire area. The liquid droplet will not even come close to the surface when surface = 0. For a flat surface, the solid fraction varies from 0 to 1. In this condition, the droplet can readily roll over the solid surface due to the narrow contact area between them.

Contact angle: When a surface is superhydrophobic, it displays high water contact angle ($WCA > 150^\circ$) and low water contact angle hysteresis (CSH 10°). This surface is not only self-cleaning, but also water-repellent (Su, *et al.*, 2010; Bhushan, and Her, 2010; Bormashenko, *et. al.*, 2006) Contact angle hysteresis (CHA) is the distinction between advancing and receding contact angles (Ferrari and Ravera, 2010; Nosonovsky, and Bhushan, 2008). When water droplets form on a superhydrophobic surface, they take on a nearly spherical shape and readily move when subjected to low tilting angles.

Hydrophilic Nature:

Hydrophilic compounds readily dissolve

in water and have a great attraction for it. Water-loving is the opposite of water-repelling. There are numerous uses for surfaces that attract or repel water. Figure 2a illustrates water-loving compounds that can corrode metal surfaces and alloys. Polar molecules are also described as molecules that love water. Because it can form hydrogen bonds and is frequently polar, a molecule's water-loving component can dissolve in water more quickly than its oil- or other water-hating solvent-loving counterpart. It may appear as though water molecules in the air are drawn to substances that love water. In settings with considerable condensation and for shielding exchangers from water's corrosive effects, hydrophilic coatings are very useful. Additionally, hydrophilic coatings do exceptionally well at keeping out water in hot and salty situations.

Hydrophobic Nature:

Figure 2b illustrates how the words "water-hating" and "hating water" have Greek roots that imply "phobia" and "hydrophobia," respectively. Scientists refer to nonpolar substances as being "hydrophobic" because they do not combine with water molecules. Examine that definition in more detail. Since its atoms carry a partial charge, hydro is a polar molecule. The most electronegative atom is oxygen, whose core electrons in each bond are extremely close to one another. Any charged substance will interact with hydro molecules to dissolve, whether it has a positive or negative charge. In essence, molecules that dislike water are non-polar, which means they don't have a net charge. These molecules lack any connections between charges that would enable them to interact with hydro while not having any charges. Water Hating substances frequently insoluble in water or any other solution with a predominately watery environment. In many areas of biology, including the structure of animals, cellular function, and molecular interactions, the traits of being water-hating or non-polar are crucial.



Figure 2: three different surface types: a) hydrophilic, b) hydrophobic, and 3) superhydrophobic.

Water Repellence:

Super-hydrophobic surfaces are very water-repellent, making it very difficult to wet them. On a superhydrophobic surface, a water droplet's contact angle is greater than 150° , and the difference between its advancing and receding contact angles is less than 10° . A droplet can entirely bounce after colliding with a superhydrophobic surface, much like an elastic sphere. This is also referred to as the lotus effect, after the self-cleaning properties of the leaves of the lotus plant.

Experimental Details and Results: Rosaceae Petals:

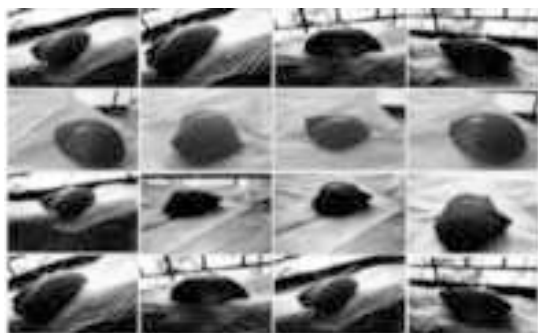


Figure 3: Images of Rosaceae petals at different times, illustrating their water-hating and water-repellence properties.

Rosaceae and the genus *Rosa* contain the most well-known flower in all of nature. The petals of Rose (*Rosa damascene*) of the family Rosaceae, are amphiphilic, meaning they have both a love of and a dislike of water. Even with the petal turned upside down, a water droplet that is small enough will slide off. High sticky forces are incompatible with water repellence. Chinese researchers have established that rose petals and water have an unusual bond that is not shared by other

plants. The micro-nanoscale topography of a rose petal comprises hills and valleys. The large valleys allow a small amount of water to soak in, creating a sticky surface on which smaller droplets can condense and stick to the petal. Since the surface of the rose petals is amphiphilic, it has both water-loving and water-hating characteristics. While the water-hating portions of the petals vigorously oppose water, the water-loving sections have a great attraction for it. The irregular topography of small valleys. Rose petals' micro-papillae produce two reactions in response to water. Larger droplets are repelled by the micro-papillae and tiny valleys. Water-hating and water-repellence are two characteristics displayed by rose petals. Following a few minutes, after 120 minutes, after 240 minutes, and after 360 minutes, it was noted that the contact angles altered during the course of the current investigation.

Asteraceae Flower:

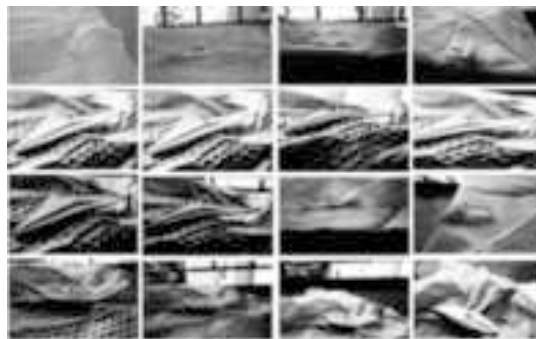


Figure 4: Images of Gerbera petals at different times, illustrating their water-loving, water-hating, and water-repellent properties.

The *Asteraceae* family's Gerbera flower is well-known. The gerbera flower is three-lobed, strap-shaped, and the individual flowers are found in the heads (Barthlott, and Neinhuis, 1997). Its aversion to water is one of its most significant characteristics. The micro-nanoscale surface area of gerbera flowers gives them the ability to both love and hate water. In the current investigation, it has been shown that the contact angles change over the first few minutes, following 120, 240 and 360 minutes.

Colocasía:

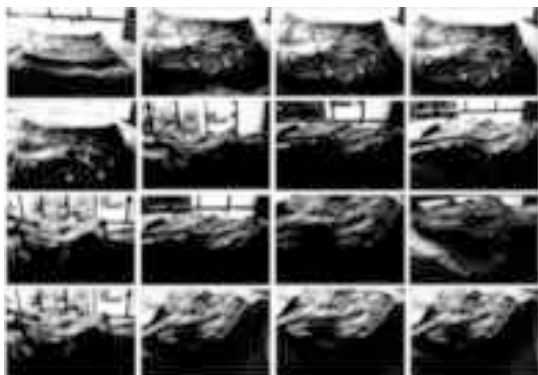


Figure 6: Images of *Colocasía* (*Araceae*) leaves at different times, illustrating their water-loving and water-repelling properties.

The elephant ears, often referred to as *Colocasía*, are the most well-known leaves in the world. Elephant ears belong to the *Araceae* family and the *Colocasía* genus. *Colocasía* leaves exhibit water-loving, water-hating, and water-repellent surface characteristics. In current investigation, it was found that the contact angles altered after a few minutes, after 120 minutes, and after 240 and 360 minutes.

Anthurium:

The genus *Anthurium* includes perennial evergreen plants that are part of the *Araceae* family. *Anthurium* plants have subterranean rhizomes and adventitious roots. *Anthurium* plants create a long-lasting, vivid spathe that comes in a variety of colours, including cream, pink, red, light red, white, dark red, green, lavender, and salmon pink. Most of the time, it is planted as a crop for cut flowers because of its spadix, which is prized for its colorful, long-lasting spathe. *Anthurium* plants are famous for their variety of colors, massive effect, and elegance.

The surface characteristics of *Anthurium* flowers in this study demonstrated both water-loving and water-repelling characteristics. The contact angles were seen to fluctuate throughout the course of the investigation at the following intervals: i.e., after 120, 240, and 360 minutes.

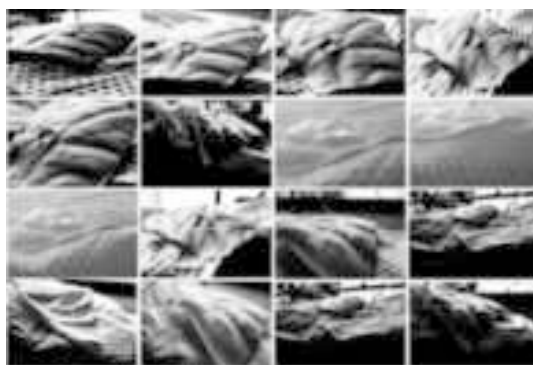


Figure 7 Images of the *Anthurium* flower (*Araceae*) are shows water loving and water hating properties at different time.

***Aloe barbadensis*:**

Aloe vera belongs to the family *Asphodelaceae* and genus *Aloe*. *Aloe barbadensis* leaves have microstructures with tiny height and high pitch values, which change the contact angle between a surface and a water droplet (Bhushan and Her, 2010). The wetting state may be reached if water impregnates between microstructures (Bormashenko, *et al.*, 2006). The hydrophobic liquid's contact area with the surface is less than in the Wenzel state but greater than in the intermediate wetting state. *Aloe barbadensis* leaves are water-loving due to their wide surface area. *Aloe barbadensis* leaves exhibit all three water-loving, water-hating, and water-repellency properties. The contact angles were seen to fluctuate throughout the course of the investigation after a few, 120, 240 and 360 minutes.

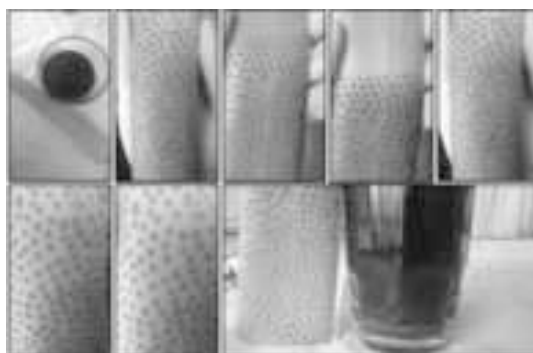


Figure 8: Asphodelaceae that simultaneously display their water-loving characteristics.

During present investigation, the water-loving, water-hating, and water-repellency qualities in Nature's exquisite materials were investigated. The rose petals were water-hating and water-repellent in nature. High adhesive forces were not always associated with water repellence. The petals of a red rose had curious relationship with water, but not for other liquids. Rose petals have a water-loving surface that strongly attracts water while water-hating surfaces strongly repel water. Rose petals had water-hating and water-repellent characteristics, but the latter is the more significant one. A surface's ability to self-clean entails that it can eliminate dirt and debris by dispersing water droplets. The leaves of *Colocasia* leaves had characteristics that attract, resist and love water. *Aloe Vera* leaf surface area demonstrated its affinity for water. Water-loving, water-hating, and water-repellent qualities were found to be present in every flower, petal and leaf. It has been shown that the contact angles change over the first few minutes, the following 120, 240 and 360 minutes.

Acknowledgements:

The authors are thankful to the Department of Botany and Physics Rajee Ramrao College, Jath.

References:

- Barthlott, W. and Neinhuis, C. (1997) *Planta* **202**:1.
- Bhushan, B. and Her, E-K. (2010) *Langmuir* **21**:8207.
- Bormashenko, E. Stein, T. Whyman, G. Bormashenko, Y and Pogreb, R. (2006) *Langmuir* **22**:9982.
- Brewer, S. A. and Willis, C. R. (2008) *Appl. Surf. Sci.* **254**:6450.
- Cai, Y. Lin, L. Xue, Z. Liu, M. Wang, S. and Jiang, L. (2014) *Adv. Funct. Mater.* **24**:809.
- Cassie, A. B. D. and Baxter, S. (1944) *Trans. Faraday Soc.* **40**:546.
- Darmanin, T. and Guittard, F. (2014) *Prog. Polym. Sci.* **39** (4): 656.
- Darmanin, T. Givenchy, E. T. D. Amigoni, S. and Guittard, F (2013) *Adv. Mater.* **25**:1378.
- Ferrari, M and Ravera, F. (2010) *Adv. Colloid Interface Sci.* **161**: 22.
- Gua, Z-Z. Wei, H-M. Zhang, R-Q, Han, G-Z. Pan, C. Zhang, H. Tian, X-J. and Chen, Z-M. (2005) *Appl. Phys. Lett.* **86**:201915.
- Nickerl, J. Helbig, R. Schulz, H-J. Werner, C. and Neinhuis, C. (2013) *Zoomorphology* **132**:183.
- Nosonovsky, M. and Bhushan, B. (2008) *Adv. Funct. Mater.* **18**:843.
- Rakitov, R. and Gorb, S. N. (2013) *Proc. R. Soc. B* **280**:20122391.
- Su, Y. Ji, B. Zhang, K. Gao, H. Huang, Y. and Hwang, K. (2010) *Langmuir* **26**:4984.
- Wenzel, R. N. (1936) *Ind. Eng. Chem.* **28**:988.
- Ye, C. Li, M. Hu, J. Cheng, Q. Jiang, L. and Song, Y. (2011) *Energy Environ. Sci.* **4**:3364.
- Young, T. (1805) *Philos. Trans. R. Soc. Lond.* **95**:65.

See discussions, stats, and author profiles for this publication at: <https://www.researchgate.net/publication/385273551>

ORYZA SATIVA HUSK AS A SUSTAINABLE SOURCE OF SILICON A REVIEW

Article · October 2024

CITATIONS

0

READS

4

1 author:



[Rajendra Lavate](#)

Shikshanmaharshi Dr. Bapuji Salunkhe College Miraj

38 PUBLICATIONS 106 CITATIONS

SEE PROFILE

ORYZA SATIVA HUSK AS A SUSTAINABLE SOURCE OF SILICON: A REVIEW

Rajendra Lavate, Sohan Thombare*, Shankar Soudagar and Appasaheb Bhosale

Department of Botany and Physics, Raje Ramrao College, Jath,
(Affiliated to Shivaji University) Kolhapur Sangli-416404, India.

*Department of Medical Physics, Centre for Interdisciplinary, Research, D. Y. Patil Education Society (Deemed to Be University), Kolhapur-416006, India.

ABSTRACT

This review focuses on utilisation of *Oryza sativa* Husk as a source for silicon nanoparticles (Si NPs) that are created via magnesiothermic reduction and used in composite anodes for lithium-ion batteries (LIBs). The production of silicon nanoparticles (Si NPs) has been explained and, their electrochemical characteristics, and possibility for activated carbon-decorated silicon nanocrystals (AC@nc-Si@AC) to serve as high-capacity anode materials have been discussed. The study emphasises cost-effective, synthesis techniques for creating environmentally acceptable energy storage technologies with the use of biomass.

Introduction:

The majority of people in the world consume rice (*Oryza sativa*) regularly. To fulfil the demands of the expanding population, it is crucial to cultivate *Oryza sativa* sustainably. In recent years, the world has consumed about 470 million metric tons of *Oryza sativa* (Wong, *et. al.*, 2014). Millions of tonnes of *Oryza sativa* husk is produced during the manufacturing of rice. Although *Oryza sativa* husk can be utilised to make fuel, fertiliser, and building materials, it is frequently considered a waste product (Rodríguez de Sensale, 2006; Kamenidou *et. al.*, 2010; Duan *et. al.*, 2013; Fang *et. al.*, 2004). Even though *Oryza sativa* husk decomposes naturally, the readily available quantity may convert it as a resource for novel technologies for the benefit of mankind.

Oryza sativa husk contains a high proportion of Silicon dioxide (SiO₂), Depending on the type of soil used to cultivate *Oryza sativa*, the SiO₂ content in its husk ranges from 10 to 20 % (Chandrasekhar *et. al.*, 2003). The *Oryza sativa* husk can be pre-treated with various acids before being pyrolyzed to recover SiO₂ from it (Yalcin and Sevinc, 2001; Kalapathy, *et. al.*, 2002; Liou, 2004; Adam, *et.*

al., 2012). The characteristics of silicon dioxide recovered from husk vary with the source or raw material. Even the amount of SiO₂ differs across *Oryza sativa* husks from different geographical areas. This may have an impact on the SiO₂ extraction characteristics, including purity, particle size, and shape (Carmona, *et. al.*, 2013; Le, *et. al.*, 2013). The SiO₂ obtained from the *Oryza sativa* has a nanoscale shape. SiO₂ can be converted into silicon (Si) by employing magnesiothermic reduction method, wherein magnesium (Mg) powder and SiO₂ are heated in a furnace until they react. Pure Si is left behind when the SiO₂ and magnesium react with the oxygen to generate magnesium oxide (MgO) (Banerjee *et. al.*, 1982). In this way, SiO₂ can be converted to Si in its original shape via magnesiothermic reduction method. Since the reaction is carried out at a temperature of 600 °C the silicon nanoparticles (Si NPs) can be subjected to sintering into a bulk substance. During sintering, the particles come together to create a solid mass. It takes less time for the particles to sinter together when the reaction is carried out at a low temperature, resulting in smaller, more homogeneous Si NPs. Thus it is possible to use silicon dioxide nanoparticles (SiO₂ NPs) as a raw material to create Si NPs. This might

result in the creation of innovative and effective processes for Si NPs synthesis (Sun and Gong, 2001). This process enables the possibility of using low-cost Si NPs in lithium-ion battery systems. This might result in the creation of lithium-ion batteries (LIBs) that are more cost-effective and environmentally friendly (Xing, *et. al*, 2013; Liu, *et. al.*, 2013; Junget. *et. al.*, 2013).

In upcoming LIBs, Si NPs will be a potential anode material. This is due to enormous capacity of Si to store a large amount of energy (Kasavajjula *et. al.*, 2007). Furthermore, Si NPs have a large surface area, which increases their reactivity with lithium ions. This may result in quicker charging and discharging times as well as increased battery performance. Theoretically, Si is the alloying material that can react with lithium ions. The capacity of producing 4200 mAh/g during this reaction, at room temperature, is 10-12 times larger than the specific capacity of conventional graphite based anodes. LIBs, made with the help of Si-based materials have an issue with volume expansion during the charge-discharge cycle. This is due to the many alloy formation stages that Si goes through during the charge-discharge cycle, which causes it to expand and contract. The Si anode may break as a result of this growth in the volume, which could affect the battery performance and lifespan (Boukamp, 1981). A similar issue that can be experienced with Si-based materials is their inherently low conductivity. This indicates that Si is a poor conductor of electricity, which may reduce the battery capacity (Lee, *et al.*, 2010; Magasinski, *et. al.*, 2010). In addition to its low working voltage, abundance on Earth, and low toxicity, Si has several further advantages as an anode material for LIBs (Entwistle, *et. al.*, 2018).

Lithium ions are injected into the material in a process known as intercalation that produces lithiation in conventional electrode materials. The intercalation method results in very few structural changes and with high retention capacity. On the other hand, Si and lithium combine to form an alloy that requires periodic cycles of contravention and re-establishing chemical connections with the

host structure. Low conductivity and the possibility of volume increase are the main drawbacks of adopting Si as an anode material for LIBs. The Si can swell by as much as 280% when a lot of lithium ions are injected into it. The Si anode may fracture and break as a result of the volume increase, which could result in a decrease in battery performance and life. The composite electrode may sustain structural degradation due to the dimensions increase of Si during cycling, which isolates the active component and reduces capacity. This poses a significant obstacle to the creation of Si anodes with large capacities and long cycle lives (Entwistle, *et. al.*, 2018).

The synthesis of SiO₂ and Si materials for LIBs from the husk of *Oryza sativa*, using various extraction methods and magnesiothermic reduction, have been discussed in this communication.

Synthesis:

Ratsameetammajak *et al.* (2022) described the process of preparing silica from the husk of *Oryza sativa* (rice). Rice husks are taken from farms and washed in water. They are then completely dried at 100 °C. To get rid of any metallic impurities, rice husks are soaked in an aqueous solution of hydrochloric acid (HCl) overnight. In order to achieve the pH value of pH of 7, rice husks are thoroughly rinsed in water. Then the rice husks are dried at 100 °C, and subsequently burnt in a muffle furnace at 700 °C for two hours. The burning process is repeated once again to ensure the perfect removal of organic matter and the creation of rice husk ash, an ample source of silica. Where the silica comes from. Below is a summary of the process used to create reduced graphene oxide (rGO): An adaptation of the Hummers process is used to create graphite oxide (GO) from graphite powder. In a non-reactive atmosphere for 5 hours, reduce the GO in a tube furnace at 800 °C (Autthawong *et. al.*, 2020)

The process of creating the composite material made of SiO₂@rGO with a proportion of 30:70 can be summed up as follows: Prepare recently generated SiO₂ by precipitating it for 2 hours at 120 °C in a NaOH solution. In the suspension, distribute rGO by

utilising a hydrochloric acid solution.

Graphene oxide (GO) is a unique material that can be viewed as a single monomolecular layer of graphite with various oxygen-containing functionalities such as epoxide, carbonyl, carboxyl, and hydroxyl groups. Reduced graphene oxide (RGO) is the form of GO that is processed by chemical, thermal and other methods to reduce the oxygen content. As graphite oxide is a material produced by oxidation of graphite, it leads to increased interlayer spacing and functionalization of the basal planes of graphite.

Raise the pH of the mixture to 7. Keep aside overnight at room temperature, and then stir the mixture. Rinse the mixture with deionized (DI) H₂O and ethyl alcohol (CH₃CH₂OH) and then centrifug. Dry the sample thus obtained in a hot air oven at 60 °C as described by Ratsameetammajak et. al., (2022).

The creation of the composite material (SiO₂@rGO and Polyaniline) including SiO₂ / rGO and Polyaniline (PANI) can be summed up as follows: In a mixture of 10 mL ethanol, 5 ml deionized water, and 5 ml H₂SO₄, make a suspension of SiO₂@rGO. To produce a consistent dispersion, sonicate the suspension. While agitating ferociously in an ice bath, dropwise add the aniline monomer to the solution. Stir the solution for 6 hours in an ice bath while adding Ammonium Persulfate ((NH₄)₂S₂O₈). When polymerization takes place leading to the formation of polyaniline emeraldine salt, the solution will turn dark green. To achieve a clear solution, repeatedly wash the suspension in H₂O and CH₃CH₂OH.

The electrochemical behaviour of the PANI-SiO₂@rGO composite was further studied in a coin-type cell utilising lithium foil as

the reference and counter electrodes. A composite anode made of SiO₂ and rGO was used in parallel tests to compare the results. The initial three lithiation-delithiation curves of the SiO₂@rGO and PANI-SiO₂@rGO electrodes at a potential range of 0.01-3.00 V (vs. Li/Li⁺) at a current density of 0.4 A g⁻¹ are shown in Figures 1b and 1c, respectively.

The SiO₂@rGO composite electrode's initial lithiation and delithiation specific capacities were 1012 and 300 mAh/g, respectively, however, it had a poor coulombic efficiency (CE) of 29.6%. The PANI-SiO₂@rGO composite electrode initial lithiation/delithiation specific capacities, on the other hand, were 1508 and 647 mAh/g, respectively, with a CE of 42.9%. The reduction of silica in SiO₂@rGO and PANI-SiO₂@rGO composites, results in lithium loss, causing initial low CE. The potential gradient plateaus on both electrodes, which range from 1.5 to 0.5 V, clearly show the formation of a solid electrolyte interphase (SEI) layer (Ratsameetammajak et. al., 2022).

The existence of stable plateaus during early cycles is an evidence of this reaction (Figure 1d). The subsequent cycles show that the SEI layer is only formed in the initial cycle, as the slopes gradually become sharper and the hills gradually get smaller. The charge voltage profiles become noticeably steeper rather than staying flat at potentials higher than 1.5 V. This invention can be attributed to solvent degradation processes occurring on the oxide electrode surface, which produced the SEI coating (Ratsameetammajak et. al., 2022).

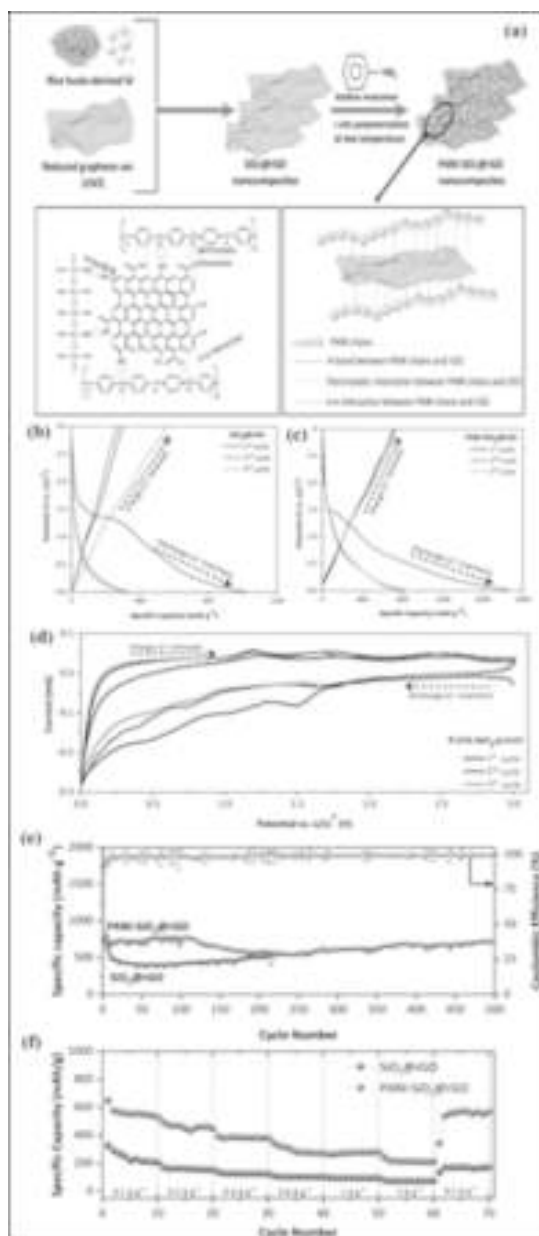


Figure 1(a-f) (a) the synthetic pathway for the preparation of the PANI-SiO₂@rGO composite, lithiation-delithiation profiles for the composites PANI-SiO₂@rGO and SiO₂@rGO measured at 400 mA g⁻¹ in current density (b) and (c), during the first three cycles, cyclic voltammograms (CV) of the PANI-SiO₂@rGO electrode were

recorded at a scan rate of 0.1 mV s⁻¹ and are displayed in (d), SiO₂@rGO and PANI-SiO₂@rGO composites long-term cycling stability and Coulombic efficiency comparison at 400 mA g⁻¹ are depicted in (e). SiO₂@rGO and PANI-SiO₂@rGO composites rate performance evaluation is depicted in (f).

During the initial cycle of delithiation and lithiation, a layer on the surface of anode known as the SEI film develops. It is produced by the interaction of the electrode material and the electrolyte at the solid-liquid interface. It is thought that the partial breakdown of the SEI coating was mostly due to the initial poor CE. The initial coulombic efficiency of PANI-SiO₂@rGO electrode is greater than that of SiO₂@rGO composite electrode. This is because the PANI covering shell prevents the electrolyte at SiO₂@rGO surface from decomposing.

Figure 1e compares the long-term cycling stability of SiO₂@rGO nanocomposite (NC) electrode with the PANI-SiO₂@rGO composite electrode. The PANI-SiO₂@rGO NC anode has outstanding long-term cycling performance at 0.4 A g⁻¹ and maintains a high reversible capacity of 680 mAh/g after 400 cycles, which is about twice as much capacity as standard graphite anodes. In comparison, after 215 cycles, SiO₂@rGO NC electrode can only discharge 414 mAh/g. This shows that only mild pulverisation of SiO₂ in the PANI-SiO₂@rGO NC occurred. The PANI coating efficiently slows down electrolyte degradation on the surface of SiO₂ and serves as a flexible protective layer to absorb SiO₂ volumetric changes.

The results presented above make it clear that the PANI shell outstanding mechanical qualities may prevent SiO₂ nanoparticle volumetric alterations. This capability guarantees that the working electrode structural integrity is maintained throughout discharge and charge cycles, greatly enhancing the electrode sustained stability over time.

The rate performance of PANI-SiO₂@rGO and SiO₂@rGO NC electrodes was evaluated at different current densities ranging

from 0.1 to 2.0 A g⁻¹, as shown in Figure 1f. At the corresponding current densities of 0.1 to 2 A g⁻¹, the PANI-SiO₂@rGO NC electrode displayed discharge capacities ranging from 563.6 to 217.1 mAh/g. After cycling at 2 A g⁻¹, the electrode maintained a discharge capacity of 539.4 mAh/g when cycled back to 0.1 A g⁻¹, illustrating its excellent rate performance. These results show that using PANI-SiO₂@rGO NC is an effective way to improve the electrochemical properties of SiO₂@rGO (Ratsameetammajak *et al.*, 2022).

N-doped carbon coated PANI-SiO₂@rGO NC has superior lithium storage capacity. Which can be attributed to their distinctive structure. SiO₂ nanoscale properties shorten the lithium ion diffusion path, which enhances lithium-ion diffusion and electronic transport. however, the rate capability may suffer. The encircling rGO sheets on the SiO₂ surface have generated a continuous conductive channel that connects the SiO₂ nanoparticles, considerably improving the conductivity of PANI-SiO₂@rGO NC electrode. SiO₂ pulverisation is avoided because the PANI materials elasticity effectively adapts to the NC volume variations during the Li-alloying and dealloying operations (Ratsameetammajak *et al.*, 2022; (Liao, *et al.* 2020; Charlton, *et al.*, 2020, Chen, 2019). In conclusion, PANI-SiO₂@rGO NC had an improved initial CE of 42.9% and a high specific capacity of 680 mAh/g at 400 mA/g after 215 cycles (Ratsameetammajak *et al.*, 2022).

Synthesis of silicon nanoparticles:

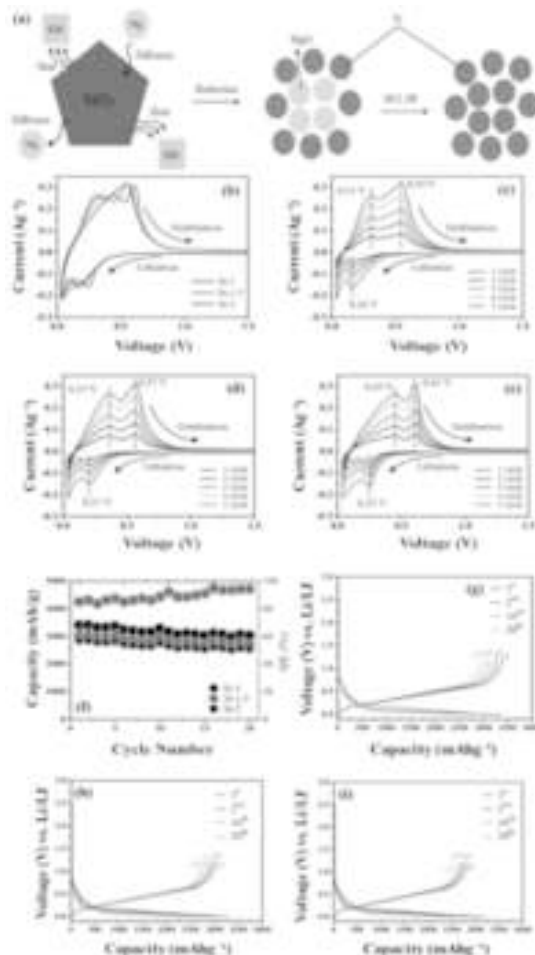
Daulay *et al.* (2022) heated *Oryza sativa* husk at 600°C for 5 hours to produce ash. Thereafter the ash and NaOH were combined and stirred for three hours at 240 rpm and 100°C. The mixture was filtered, and HCl was added until a pH reached 7.0, The precipitate was filtered out and residual solution was heated at 100°C for three hours again for precipitation, which was again removed by filtration. After several rounds of washing with distilled water and drying, SiO₂ was produced in the form of powder. It was then mixed with KBr with a ratio of 1:10,

deionized water was added, and stirring was carried out for three hours. The combination was subjected to ultrasonication for six hours. The residue produced after ultrasonication was separated by decantation, and the filtrate was allowed to dry for 12 hours. The dry powder was mixed with Mg powder in various ratios (1:1.0, 1:1.5, 1:2.0). The next calcination procedure was undertaken at 800°C for 8 hours. During the first purification stage, 150 mL of deionized water and 15 mL of ethanol were added. After that, there was 3 hours of agitation. Centrifugation of the mixture was done for 30 minutes at a speed of 4000 rpm. After being regularly cleaned with deionized water, it was dried for six hours at 80 °C. The second stage involved addition of 150 ml, 5 N HCl and a 12-hour rest period. The sample was dried at 80 °C for 6 hours, washed with deionized water, and then centrifuged once again for 30 minutes at 4000 rpm. Then 150 mL of 10% hydrogen fluoride (HF) was added as the last stage, and the mixture was allowed to settle for 15 minutes. The mixture was first dried, followed by several washes in deionized water, and a second drying step was six hours at 80 °C. Si-1, Si-1.5, and Si-2 thus produced were labelled. (Daulay, *et al.*, 2022).

Figure 2b displays cyclic voltammetry profiles for Si NPs. The data demonstrated that as the ratio of SiO₂ and Mg increases during reduction, the magnesiothermic reduction causes a higher reduction peak associated with the production of delithiation as well as oxidation peaks, associated with the lithiation to Si. Cyclic voltammetry (CV) was used to measure the activation process for Si-1, Si-1.5, and Si-2 electrodes with a voltage range of 0.01 to 1 V (against Li^{+/}Li) and a scan rate of 0.2 mVs⁻¹. The CV analysis of Si-1 (Figure 2c) revealed lithiation-related reduction peaks (0.16 V) as well as the delithiation-related oxidation peaks (0.31 V and 0.54 V). Figure 2d depicts the lithiation of Si-1.5 at 0.21 V and its delithiation at 0.37 V and 0.57 V. In Figure 2e, the lithiation (0.25 V) and delithiation (0.45 V and 0.61 V) peaks for Si-2 are displayed. These peak intensities increase during the cycles, suggesting that more lithium ions are possibly

moving between the electrode and electrolyte. This indicated gradual activation of substances. Compared to Si-1.5 and Si-2, Si-1 showed less significant peaks in both lithiation and delithiation. More efficient transport of lithium ions from the cathode to the anode and vice versa is shown by smaller lithiation and delithiation peaks in CV (Daulay *et al.*, 2022).

The rate capability study for the Si-1, Si-1.5, and Si-2 electrodes is shown in Figure 2f. The first cycle is performed to ensure that Si is adequately activated, as shown by cyclic voltammetry, which aids in the creation of a stable solid electrolyte interphase (SEI) layer (Liu *et al.*, 2006). Si-1, Si-1.5, and Si-2 electrodes, respectively, had initial discharge capacities of 3416, 3037, and 2847 mAh/g. 54.9, 85.4, and 85.6 % are the comparable *Conformite Europeenne* (CE). The silicon lithiation potential range (0.01 V to 0.50 V) is higher than the carbonate-based lowest unoccupied molecular orbital (LUMO) electrolyte. When a voltage is applied, Si is lithiated, resulting in the formation of an amorphous solid electrolyte interface (SEI). By reductively destroying the electrolyte, this SEI is created. The native oxide layer on the Si surface is damaged during the initial lithiation process, which causes an inner SEI predominantly made of lithium ethylene dicarbonate (LEDC) and Li_xSiO_y to develop. While the continuing discharge causes LiF to be produced, a significant amount of outer SEI is predominantly made up of LEDC. Within the defined potential range, these SEI components containing lithium remain stable. Because of this, the lithium that is used during delithiation cannot be completely recovered from the created SEI constituents, which results in permanent capacity loss and reduced coulombic efficiency during the initial cycle (Schroder, *et al.*, 2015). Si-1 improved electrochemical compatibility with Si and LiPF_6 electrolytes were highlighted by the slightly higher initial charge-discharge coulombic efficiency seen in Si-1 compared to Si-1.5 and Si-2.



This suggests that the anodes have the following rate capabilities: Si-1 > Si-1.5 > Si-2. Examining these electrode typical charge-discharge curves at particular rates lends credence to this claim. The electrode is more stable during discharge because the voltage hysteresis is reduced. The higher capacity of Si-1 electrode compared to Si-1.5 and Si-2 anodes demonstrates superior adaptability of Si-1 and endurance as a protective shell for absorbing significant volume variations. As seen by Si-1 more stable behaviour, this improves cyclability. Because of their greater ability to transport electrons and ions more quickly, Si NPs operate more quickly than nonconductive binder (PAA). The better electrical conductivity and superior specific

capacities at high current densities of Si-1, as compared to Si-1.5 and Si-2, are evidence of its improved physical encapsulation of silicon.

These variations imply that Si-1 performs better in LIBs than Si-1.5 and Si-2, suggesting that Si-1 has an advantage over other materials as an anode material. In conclusion, using the magnesiothermic process and KBr as a scavenger, Si NPs were created from *Oryza sativa* husk. Three different Si NPs kinds were produced using this ecologically friendly method (Salah, *et. al.*, 2019). As LIB anodes, all three varieties of Si NPs demonstrated excellent performance. Si-1, Si-1.5, and Si-2 had specific capacities of 3416, 3037, and 2847 mAh/g, respectively. Si-1, Si-1.5, and Si-2 had lithiation potentials and delithiation potentials of 0.16, 0.21, and 0.25 V, respectively (Daulay *et. al.*, 2022).

Synthesis of activated carbon-decorated nanocrystals-silicon:

Sekar *et al.* (2019) heated brown *Oryza sativa* Husks in an air atmosphere for 120 minutes at 500 °C to collect the ash. After that, 1.0 g of ash and 0.2 g of magnesium (Mg) powder were mixed. This mixture was put in an alumina crucible and annealed for 120 minutes at 700 °C in an argon (Ar) environment. Magnesiothermic reduction took place throughout this procedure. The annealed mixtures underwent a 6-hour stirring procedure in 1 M hydrochloric acid (HCl) to isolate acicular nc-Si-enriched activated carbon nanocomposites and remove magnesium silicide (Mg_2Si) precipitates, magnesium oxide (MgO) residues, and native silicon dioxide (SiO_2) impurities. The next step involved 1-hour reaction with 5% hydrofluoric acid (HF). The wet activated-carbon-decorated silicon nanocrystal products were then collected from the resultant solution, filtered, and washed with deionized water before being dried under vacuum for 10 hours at 80 °C. The *Brown Oryza sativa* Husks was used to create the activated-carbon-decorated silicon nanocrystal nanocomposites utilising the magnesiothermic reduction technique (Figure 3a) (Sekar *et. al.*, 2019).

In addition, by integrating the benefits

of both *nanocrystals-silicon* and activated carbon, the novel nanocomposite structure known as activated-carbon-decorated silicon nanocrystal, which consists of activated carbon embellished with nanostructured silicon (nc-Si), is predicted to enhance the electrochemical performance of LIBs. Building LIB anode combinations utilising *nanocrystals-silicon*, activated carbon, and activated-carbon-decorated silicon nanocrystal allowed researchers to test this idea by evaluating the electrochemical characteristics of materials. Initially, cyclic voltammetry (CV) profiles covering the voltage range of 0 to 3.0 V (vs. Li/Li^+) were captured for the prepared anodes using a scan rate of 0.1 mV/s. Different anodic peaks were visible in the LIB configuration with the *nanocrystals-silicon* anode (Figure 3b), which correspond to the incorporation of lithium ions into the nanocrystals-silicon. A cathodic peak at 0.66 V also formed during the first CV cycle and was brought on by the electrode surface developing a solid electrolyte interphase (SEI) layer as well as electrolyte breakdown. The subsequent stabilisation of CV curves from the second to fifth cycles is proof that the SEI layer prevents further electrolyte breakdown and improves LIB stability. The interaction of Li ions with the native SiO_2 present on the nanocrystals-silicon surface is most likely what caused a wider cathodic peak to form at 1.65 V (Sekar, *et. al.*, 2019; Sun, *et. al.*, 2014, 2015).

During the first CV cycle, the activated carbon anode (Figure 3c) had a pronounced cathodic peak at 0.2 V, which was followed by stable following curves. This was most likely caused by the formation of an SEI layer on the activated carbon surface. In a similar manner, when using activated-carbon-decorated silicon nanocrystal as the anode. Although the nanocomposites included minute amounts of MgO residue, the device did not show any MgO-related peaks. The activated-carbon-decorated silicon nanocrystal nanocomposites showed noticeably more powerful anodic responses than the nanocrystals-silicon instance. This shows that the highly conductive activated carbon nanosheets inside the activated-carbon-silicon

nanocomposite system caused the activated-carbon-decorated silicon nanocrystal to suffer faster electrochemical reactions (Sekar, et. al., 2019).

GCD measurements were used to assess the samples electrochemical properties. The initial lithiation and delithiations capacities for the nanocrystals-silicon sample during the first cycle were 336 and 75 mAh/g, respectively (Figure 3e). Due to the intrinsic oxide tendency to lithiate, the initial coulombic efficiency was thus only about 22%. The 1st discharge curve of the nanocrystals-silicon sample (Figure 3e) exhibits a large plateau at about 0.09 V, which denotes the development of SEI layers and Li-Si alloys on the anode material surface. Due to limitations in electronic conductivity, sluggish chemical reactions, and a reduction in surface area, the GCD performance drastically declined in the second cycle (Sekar, et. al., 2019). The charge and discharge capacities for the activated carbon sample, which is depicted in Figure 3f, were 295 and 545 mAh/g, respectively. This resulted in a coulombic efficiency of 54%. The initial discharge curve suggested that the formation of the SEI layer might lead to a plateau at 0.8 V. After multiple charge-discharge cycles, this plateau disappeared because of the stability of the carbon-based LIB anode (Sekar, et. al., 2019).

When the activated-carbon-decorated silicon nanocrystal anode was employed, the LIB device displayed greater charge (510 mAh/g) and discharge (716 mAh/g) capabilities than the other samples (Figure 3g). The enhanced coulombic efficiency of activated-carbon-decorated silicon nanocrystal anode was 71% as a result. This increased efficiency can be related to the structure of activated carbon-coated nanocrystals-silicon nanocomposite, which efficiently reduces unfavourable processes (such Li-Si alloying on the nanocrystals-silicon surface) and encourages electron diffusion because mesoporous nanocrystals-silicon is present. The 1st discharge cycle showed three potential plateaus (0.3, 0.5, and 0.8 V) as a result of the formation of the SEI layer and the lithiation of amorphous Li_xSi and Si (Sekar, et.

al., 2019).

The rate capability and cycle stability of LIBs with activated carbon and silicon nanocrystal anodes coated with activated carbon were then evaluated. The LIB device with the nanocrystal-silicon anode was excluded due to its poor electrical conductivity, as was already indicated. (Sekar, et. al., 2019).

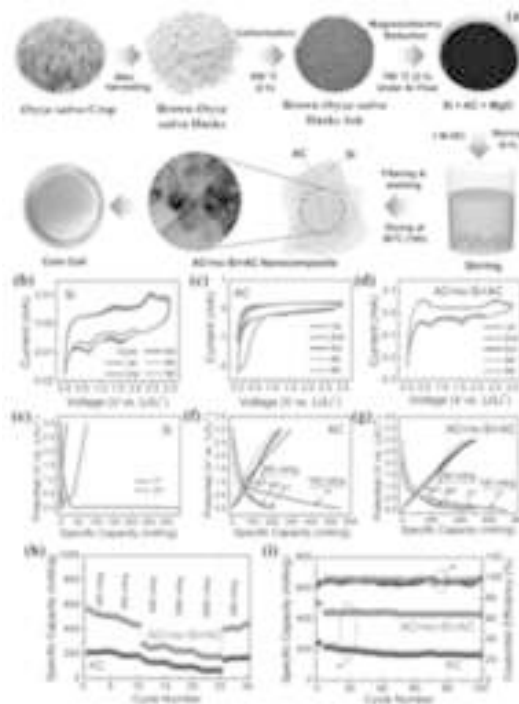


Figure 3: The experimental methods for simultaneously obtaining silicon nanocrystal nanocomposites adorned with activated carbon from the biomass resource known as Brown Oryza sativa Husks (BOSHs), lithium-ion battery (LIB) device cyclic voltammetry (CV) curves using anode materials made of (b) nc-Si, (c) AC, and (d) AC@nc-Si@AC nanocomposites, the scanning rate used for all of the CV measurements was 0.1 mV/s. Galvanostatic charge-discharge (GCD) curves of LIB devices using (e) nc-Si, (f) AC, and (g) activated-carbon-decorated silicon nanocrystal nanocomposites as anode materials, A current density of 100 mA/g was used for

the first GCD cycle, and a current density of 200 mA/g was used for the subsequent cycles, (h) Rate performance for the LIB devices using the anode materials of AC nanosheets and activated-carbon-decorated silicon nanocrystal nanocomposites at different current densities and (i) Cycling performance and coulombic efficiency determined for LIB devices using AC@nc-Si@AC as anode materials under an applied current density of 200 mA/g.

Figure 3h shows the rate performance of the LIBs based on the applied current density. The LIB with the activated carbon anode displayed reversible discharge capacities ranging from 214 to 83 mAh/g at applied current densities of 100 to 2000 mA/g. The silicon nanocrystal activated-carbon decorated anode of the LIB demonstrated reversible discharge capacities ranging from 561 to 199 mAh/g at applied current densities of 100 to 2000 mA/g, respectively. Both times, when the applied current density was lowered to 200 mA/g after 25 cycles, the discharge capacity fully recovered, indicating good reversibility. However, the initial specific capacity (during the first cycle at 100 mA/g) and the specific capacity window (the variance of specific capacity with varying applied current density) were approximately 2.6 times and 1.5 times, respectively (Sekar, et. al., 2019).

The silicon nanocrystal anode coated with activated carbon also showed excellent cycle performance and a good CE. As shown in Figure 3i, the activated carbon anode had a noticeably lower discharge capacity of 166 mAh/g, which is only 0.38 times that of the activated carbon-decorated silicon nanocrystal anode, while the activated carbon anode maintained a high discharge capacity of 429 mAh/g over 100 cycles. Additionally, the silicon nanocrystal anode-equipped LIB maintained a rather high CE of around 97.5% throughout 100 charge-discharge cycles.

The discharge capacity observed here was enhanced by around 1.2 times in comparison to commercial graphite (372 mAh/g), owing to the greater specific capacity

of Si in activated-carbon-decorated silicon nanocrystal nanocomposites. The two-dimensional shape and superior electronic conductivity of the activated carbon nanosheets in the silicon nanocrystal coated with activated carbon may improve ion diffusion and storage in LIBs.

The strong structural stability of activated-carbon-decorated silicon nanocrystal nanocomposites is responsible for these exceptional rate and cyclic performances. In essence, the *activated carbon* nanosheets served as a protective coating or shell for the Si nanocrystals, minimising the volumetric changes in those crystals. The Li interaction with *nanocrystals-silicon* was considerably hampered throughout the whole solid-state system of the activated-carbon-decorated silicon nanocrystal nanocomposite because the *activated carbon* shell allowed plenty of room for Li-ion diffusion during charge-discharge operations.

The initial capacity of fully biomass-derived activated carbon could still be raised, even though adding nanocrystals-silicon and highly conductive nanomaterials (like graphene, carbon nanotubes, conducting polymers, etc.) could be the next steps to improve the electrical conductivity and porosity of the entire composite material system, leading to further improvements in its electrochemical performance.

Finally, activated carbon made from brown *Oryza sativa* husks and silicon nanocrystals Activated carbon nanocomposites have a high initial discharge capacity, reversible specific capacity, rate performance, cyclic stability, and coulombic efficiency. These nanocomposites have the potential to serve as high-performing anode materials for LIB devices (Sekar, et. al., 2019).

Synthesis of nano-silicon:

Husks of *Oryza sativa* were calcined for 5 hours at 600 °C following Sudarman et al. *Oryza sativa* husk ash and a 10% sodium hydroxide (NaOH) solution were mixed for three hours at a temperature of 100°C and a rotational speed of 240 rpm. After being

filtered, the filtrate from the stirring procedure was gradually combined with 37% hydrochloric acid (HCl) until the pH reached to 7.0, which led to the precipitation of a precipitate. Silica (SiO_2) gel was created after extensively filtering and washing the precipitate with deionized water. The next step was to combine SiO_2 gel with 98% magnesium powder in a weight-to-ratio of (1: 0.5, 1: 0.6, or 1: 0.7). The last combination was sealed entirely in an autoclave made of stainless steel. The autoclave was then heated in a microwave for 10 hours at 180°C before being cooled for 12 hours at room temperature. The powder obtained was put through a purifying process. The purification procedure began with the addition of a 5 N hydrochloric acid (HCl) solution for 12 hours. The mixture was rinsed three times with deionized water, and then the silicon was removed by centrifuging the mixture at 4000 rpm for 30 minutes. Adding a 10% hydrofluoric acid (HF) solution for 15 minutes was the second step in the purification process. Three rounds of washing with deionized water were followed by a 30-minute centrifugation at 4000 rpm to remove unreacted SiO_2 and other impurities produced. Three samples were given the designations Si-0.5, Si-0.6, and Si-0.7, with the numbers 0.5, 0.6, and 0.7 designating the amounts of magnesium (Mg) powder used in each sample. Using a hydrothermal process, silicon (Si) with a diameter of only a few nm was produced in an aqueous solution. This required the SiO_2 to be reduced using a mixture of *Oryza sativa* husk SiO_2 gel and Mg powder. SiO_2 gel and Mg powder reacted to form Si and magnesium oxide (MgO). The hydrothermal procedure, which comprises lowering SiO_2 at a temperature of 180°C for 10 hours, results in a mixture of Si and MgO. High-purity nano-Si is produced through further purification procedures. To remove Mg, magnesium silicide (Mg_2Si), and MgO from the mixture,

hydrochloric acid (HCl) is added in the first purification stage. HF is added during the second purification stage to efficiently remove SiO_2 . In Figure 4a, the hydrothermal technique for synthesising nano-Si is shown graphically (Sudarman *et al.*, 2023).

Additionally, cyclic voltammetry (CV) on Si-0.5, Si-0.6, and Si-0.7 was carried out at a scan rate of 0.2 mV s^{-1} throughout a voltage range of 0.01 to 1.5 V. In Figure 4b, the CV of Si-0.5 shows two reduction peaks at 0.38 V and 0.58 V, which are associated with the extraction of Li^+ ions, and one oxidation peak at 0.16 V, which is associated with the insertion of Li^+ ions. Li^+ extraction at 0.38 V, 0.56 V, and Li^+ insertion at 0.16 V are all shown for Si-0.6 CV in Figure 4c. The cyclic voltammetry of Si-0.7 (Figure 4d), which displays Li^+ extraction at 0.38 V and 0.59 V and Li^+ insertion at 0.17 V, demonstrates similar results. The cathodic peak below 0.3 V, which is supported by the huge anodic peak in the CV curve, points to a single mechanism that converts nano-Si into amorphous Li_xSi ($x = 3.75$). However, the electrochemical procedure for producing $\text{Li}_{3.75}\text{Si}$ at room temperature is not very advanced. Regarding the extraction of Li^+ from nano-Si, it is clear that Si-0.6 has the lowest value, demonstrating its superiority to Si-0.5 and Si-0.7. Si-0.6 has pores that are larger than those of Si-0.5 and smaller than those of Si-0.7, which accounts for the disparity. Si-0.7, which has the smallest pore size in comparison to Si-0.5 and Si-0.6, demonstrates greater Li^+ extraction as a result (Sudarman *et al.*, 2023).

Figure 4e shows how well nano-Si electrode cycled over 200 times. During the first cycle, Si-0.5, Si-0.6, and Si-0.7 exhibit capacities of 1575, 1757, and 1525 mAh/g, respectively. Notably, Si-0.6 is more capacious than Si-0.5 and Si-0.7, although Si-0.7 has less capacity than the other two (Sudarman *et al.*, 2023).

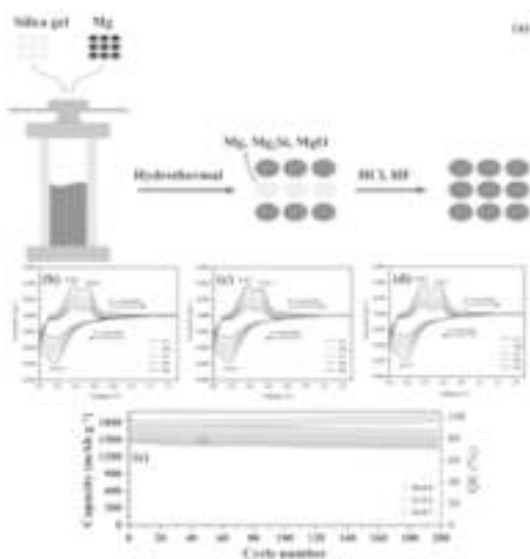


Fig. 4 The cycling performance of a nano-silicon electrode over 200 cycles using the cyclic voltammetry (CV) of Si-0.5, Si-0.6, and Si-0.7 (Sudarman et al., 2023)

This finding emphasises how important pore size is for Li^+ extraction and capacity. The increased capacity of Si-0.6 is a result of its bigger pore size, whereas Si-0.7 has the lowest capacity due to its smaller pore size. As a result, the pore size has a significant impact on lithium-ion battery capacity, favouring larger pore sizes for greater performance. The considerable volume changes that take place throughout the Li^+ extraction and insertion cycles make Si employment as a LIB anode material challenging. Electrode cracking and capacity loss are frequent consequences of these volume fluctuations. Since Si NPs are naturally resistant to fractures, they are employed to reduce cracking. In addition to improving fracture resistance, the nanoscale structure capacity to accept strain from Li^+ extraction and insertion through plastic deformation lowers stresses during volume changes. Therefore, this study focuses on producing porous nanostructured Si in addition to employing Si with nanoparticle-sized Si. Due to the increased capacity that nanostructured Si offers compared to other anode materials, this strategy is essential. With a possibility for further improvement, the

discharge capacity of 1757 mAh/g over 200 cycles demonstrates the exceptional performance of nanostructured Si as a LIB anode, outperforming commercial batteries, graphite, and graphene (Sudarman et al., 2023)

Thus the improved lithium-ion battery performance was made possible by novel synthesis techniques for advanced anode materials, including PANI-SiO₂@rGO nanocomposites, scalable silicon nanoparticles from rice husk, nano-silica by hydrothermal processing, and AC@nc-Si@AC nanocomposites. These methods provide increased stability, conductivity, and capacity, indicating a viable route to the creation of practical and affordable LIB devices.

Acknowledgements:

The authors are thankful to the Department of Botany and Physics, Rajee Ramrao College, Jath and Department of Medical Physics, Centre for Interdisciplinary, Research, D. Y. Patil Education Society (Deemed to Be University), Kolhapur.

References:

- Adam, F. Appaturi, J. N. and Iqbal, A. (2012) *Catal. Today*. **190**:2.
- Autthawong, T. Chimupala, Y Haruta, M. Kurata, H Kiyomura, T. Yu, A. Chairuangstri, T and Sarakonsri, T. (2020) *RSC Adv.* **10**:43811.
- Banerjee, H. D. Sen. S. and Acharya, H. N. (1982) *Mater. Sci. Eng.* **52**:173.
- Boukamp, B. A. (1981) *J. Electrochem. Soc.* **128**:725.
- Carmona, V. B. Oliveira, R. M. Silva, M. W. T. Mattoso, L. H. C and Marconcini, J. M. (2013) *Ind. Crops Prod.* **43**:291.
- Chandrasekhar, S. Satyanarayana, K. G. Pramada, P. N. Raghavan, P and Gupta, T. N. (2003) *J. Mater. Sci.* **38**:3159.
- Charlton, Hatchard, M. T. D. and Obrovac, M. N. (2020) *J. Electrochem. Soc.* **167**:80501.

- Chen, Y. (2019) *IOP Conf. Ser. Mater. Sci. Eng.* **677**:022115.
- Daulay, A. Andriavani and Marpongahtun, Gea, S. (2022) **6**:100256.
- Duan, F. Chyang, C-S. Lin C-W. and Tso, J. (2013) *Bioresour. Technol.* **134**:204.
- Entwistle, J. Rennie, A. and Patwardhan, S. (2018) *J. Mater. Chem. A.* **6**:18344.
- Fang, M. Yang, L. Chen, G. Shi, Z. Luo, Z. and Cen, K. (2004) *Fuel Process. Technol.* **85**:1273.
- Jung, D. Ryou, M. Sung, Y. Park, S and Choi, (2013) *J Proc. Natl. Acad. Sci. U. S. A.* **110**:12229.
- Kalapathy, U. Proctor, A. and J. Shultz, J. (2002) *Bioresour. Technol.* **85**:285.
- Kamenidou, S. Cavins, T. J. and Marek, S. (2010) *Sci. Hortic.* **123**:390.
- Kasavajjula, U. Wang, C and Appleby, A. J. (2007) *J. Power Sources* **163**:1003.
- Le, V. H. Thuc, C. N. H and Thuc, H. H. (2013) *Nanoscale Res. Lett.* **8**:58.
- Lee, J. K. Smith, K. B. Hayner, C. M. and Kung, H. H. (2010) *Chem. Commun.* **46**:2025.
- Liao, Y. Liang, K Ren, Y. and Huang, X. (2020) *Front. Chem.* **8**:96.
- Liou, T-H. (2004) *Mater. Sci. Eng., A*, **364**:313.
- Liu, C. Li, C. Ahmed, K. Wang, W. Lee, I. Zaera, F Ozkan, C. S. and Ozkan, M. (2006) *RSC Adv.* **6**:81712.
- Liu, N. Huo, K. McDowell, M. Zhao, J and Cui, Y. (2013) *Sci. Rep.* **3**:1919.
- Magasinski, A. Dixon, P. Hertzberg, B. Kvit, A. Ayala, J. and Yushin, G. (2010) *Nat. Mater.* **9**:353.
- Ratsameetammajak, N. Autthawong, T, Chairuang Sri, T. Kurata, H. Yu, A-S. and Sarakonsri, T. (2022) *RSC Adv.* **12**:14621.
- Rodríguez de Sensale, G. (2006) *Cem. Concr. Compos.* **28**:158.
- Salah, M. Murphy, P Hall, C. Francis, C. Kerr, R. and Fabretto, (2019) *M. J. Power Sources.* **414**:48.
- Schroder, K. Alvarado, K. J. J Yersak, J. T. A. Li, T. A. J. Dudney, N Webb, L. J. Meng, Y. S. and Stevenson, K. J. (2015) *Chem. Mater.* **27**:5531.
- Sekar, S. Ahmed, A. T. A. A, Inamdar, A. I. Lee, Y. Im, H, Kim, D. Y. and Lee, S (2019) *Nanomaterials.* **9**:1055.
- Sudarman, S. Andriayani, and Tamrin, Taufik, M. (2023) *Materials Science for Energy Technologies.* **1**:8
- Sun, L and Gong, K (2001) *Ind. Eng. Chem. Res.* **40**:5861.
- Sun, Z. Song, X. Zhang, P. and Gao, L. (2014) *RSC Adv.* **4**:20814.
- Sun, Z. Tao, S. Song, X. Zhang, and P. Gao, L. (2015) *J. Electrochem. Soc.* **162**:A1530.
- Wong, D. P. Suriyaprabha, R. Yuvakumar, R. Rajendran, V. Chen, Y-T. Hwang, B-J. Chen, L-C. and Chen, K-H. (2014) *J. Mater. Chem. A*, **2**:13437.
- Xing, A. Tian, S. Tang, H. Losic, D and Bao, Z (2013) *RSC Adv.* **3**:10145.
- Yalcin, N. and Sevinc, V. (2001) *Ceram. Int.* **27**:219.

WATER LOVING, WATER HATING AND WATER REPELLENCE PROPERTIES OF SOME PLANTS

Rajendra Lavate, Sohan Thombare*, Shankar Soudagar, Rajesh Sawant and Appasaheb Bhosale

Department of Botany, Chemistry and Physics, Raje Ramrao College, Jath, (Affiliated to Shivaji University Kolhapur) Sangli-416404, India.

Department of Medical Physics, Centre for Interdisciplinary, Research, D. Y. Patil Education Society (Deemed to Be University), Kolhapur-416006, India.

ABSTRACT

Hydrophilic surfaces, which have an affinity for water molecules, are those that prefer water. Water molecules are attracted to hydrophobic surfaces because they reject water molecules. Surfaces that are particularly water-repellent are known as superhydrophobic surfaces. Because of their great surface roughness and low surface energy, superhydrophobic surfaces allow water droplets to easily bead up and slide off. During the present investigation, beautiful materials found in nature have been explored to examine their water-loving, water-hating, and superhydrophobic characteristics. *Aloe vera*, rose petals, gerbera blossoms, *Aloe barbadensis*, miller leaves, and anthurium flowers are some of the botanical blooms that have been included for present study. All naturally occurring substances possess a reduced surface tension. Water has lower surface tension than most other naturally occurring substances. It was observed that the contact angles of the water droplets on the rose petals altered at three different time points: 120 minutes, 240 minutes, and 360 minutes.

Keywords: Anthurium, *Aloe Vera*, *Colocasia*, *Gerbera* Flower, Rose Petal

Introduction:

Many natural surfaces exhibit characteristics of water affinity, water aversion, and water repellency (Darmanin, and Guittard, 2014; Darmanin, *et. al.*, 2013) Nature has produced insects, animals, and plants for millennia. The Cassie-Baxter and Wenzel models explain how the topography and shape of surfaces greatly influence their water-hating characteristics (Wenzel, 1936; Cassie and Baxter, (1944). The existence of microscopic hairs on leaves is thought to be responsible for their superhydrophobic qualities, which have been documented in the literature. Vertical hairs are found on lady's mantle (Brewer and Willis, 2008) while horizontal hairs are being

observed on poplar leaves and ragwort (Gua *et. al.*, 2005; Ye, *et. al.* 2011). Animals with water-repellent qualities include geckos, butterflies, and water-walking arthropods. Animals and birds, like cicada, translucent butterfly wings, water-walking arthropods, and gecko foot, have some of the most well-known naturally water-repellent surfaces in the universe. Cactus spines, the skin of the filefish *Navodon septentrionalis*, shark skin (Cai, *et al.*, 2014), leafhoppers (Rakitov and Gorb, 2013), and springtail surfaces all exhibit underwater superhydrophobic qualities (Nickerl, *et. al.*, 2013 It is crucial for water repellence qualities to remain stable even after pressure that accounts for the dual action of rainfall (Nosonovsky and Bhushan, 2008).

Super hydrophobicity:

Young's State: The Young equation relates the three surface tensions of liquid-vapor, solid-vapor, and liquid-solid and predicts the contact angle between a liquid droplet and a solid surface. This prediction holds true independent of the surface chemistry (Young,1805). The Young equation explains the liquid's contact angle with a perfectly smooth, chemically homogeneous solid surface as shown in Figure 1a and explained in

$$\cos \theta = (\gamma_{sv} - \gamma_{sl}) / \gamma_{lv}$$

the following equation.

Where γ_{lv} , γ_{sv} and γ_{sl} represent the surface tensions at the interfaces between solids and liquids, respectively. A contact angle (θ) is created when a single drop of fluid (oil or water) is deposited on a solid surface. The Young equation only holds true for smooth surfaces; hence it cannot be used to describe textured surfaces. A liquid contact angle (θ) with a rough surface will be different from that of a liquid with a smooth surface since wetting surfaces are chemically diverse, they are more complicated and rougher. The effect of surface roughness on contact angle can be studied in two modes or states.

Wenzel's State: Figure 2b illustrates the contact angle model that created by Wenzel for rough surfaces, which allows liquid to completely permeate into the rough grooves (Wenzel, 1936). Due to the increase in the solid-liquid interface in the rough grooves, air bubbles may become trapped there, but only if the height of the asperities (H) is high enough. In this instance, a liquid droplet (oil or water) is present on a composite surface, and the Cassie-Baxter model is used to characterise the wetting nature as:

$$\cos \theta_w = r \cos \theta$$

$$i.e. \cos \theta_w = r (\gamma_{sv} - \gamma_{sl}) / \gamma_{lv}$$

Where the Young's contact angle (θ) is and r is the roughness ratio. The ratio of the anticipated surface area to the actual surface area is known as the roughness parameter, or r. When a surface is completely smooth, $r = 1$, and when a surface is rough, $r > 1$. The Wenzel state states that for materials having a contact angle larger than 90° (intrinsically water-hating materials), wetting is minimized by roughness.

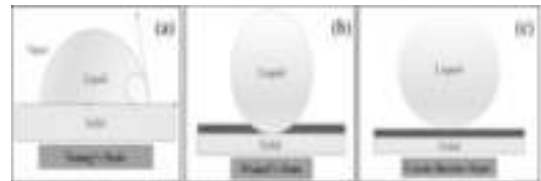


Figure 1: The wetting behaviour of a liquid droplet on a rough solid surface under three different states: a) Young's state, b) Wenzel's state, and c) Cassie-Baxter state.

Cassie- Baxter's State:

The heterogeneous state or composite state are other names for the Cassie-Baxter state. The Cassie-Baxter condition of wetting is seen in Figure 1c, where the grooves beneath the droplet are filled with vapour rather than liquid (Cassie, and Baxter, 1944). The most crucial characteristic of a coating designed to repel water is robustness. Even after being released, the substance retains its high-pressure qualities. The rise in the solid-vapor barrier at low H makes the Cassie-Baxter state a good predictor of water-repellence qualities. It also has anti-icing (heat transfer), anti-corrosion (batteries, water desalination, and ion penetration), and anti-corrosion (ion penetration) capabilities. In spite of a rise in surface roughness, the material's inherent characteristics get better. There are two phases that make up the liquid surface interface: the liquid-vapor interface and the liquid-solid interface.

$$\cos \theta_w = \phi_1 \cos \theta_1 + \phi_2 \cos \theta_2$$

The contributions of the various phases are combined to generate the apparent contact angle, where w is the apparent contact angle and 1 and 2 are the surface fractions of phases 1 and 2, respectively. Phase 1 and Phase 2's respective contact angles are θ_1 and θ_2 , respectively. The solid fraction, symbolised by the Greek letter ϕ , refers to the area of a solid surface that has been moistened by a liquid when one of the surfaces is the air-liquid interface. $(1-\phi)$ represents the air fraction. Because it included the air component, in the denominator, the original equation was wrong. The air percentage should be in the numerator since it represents the portion of the surface that is not moistened by liquid.

$$\phi \cos \theta + (1 - \phi) \cos 180^\circ = \phi \cos \theta + (\phi - 1) = \cos \theta_w$$

When the surface reaches unity (1), the liquid droplet will expand out to cover the entire area. The liquid droplet will not even come close to the surface when surface = 0. For a flat surface, the solid fraction varies from 0 to 1. In this condition, the droplet can readily roll over the solid surface due to the narrow contact area between them.

Contact angle: When a surface is superhydrophobic, it displays high water contact angle ($WCA > 150^\circ$) and low water contact angle hysteresis (CSH 10°). This surface is not only self-cleaning, but also water-repellent (Su, *et al.*, 2010; Bhushan, and Her, 2010; Bormashenko, *et. al.*, 2006) Contact angle hysteresis (CHA) is the distinction between advancing and receding contact angles (Ferrari and Ravera, 2010; Nosonovsky, and Bhushan, 2008). When water droplets form on a superhydrophobic surface, they take on a nearly spherical shape and readily move when subjected to low tilting angles.

Hydrophilic Nature:

Hydrophilic compounds readily dissolve

in water and have a great attraction for it. Water-loving is the opposite of water-repelling. There are numerous uses for surfaces that attract or repel water. Figure 2a illustrates water-loving compounds that can corrode metal surfaces and alloys. Polar molecules are also described as molecules that love water. Because it can form hydrogen bonds and is frequently polar, a molecule's water-loving component can dissolve in water more quickly than its oil- or other water-hating solvent-loving counterpart. It may appear as though water molecules in the air are drawn to substances that love water. In settings with considerable condensation and for shielding exchangers from water's corrosive effects, hydrophilic coatings are very useful. Additionally, hydrophilic coatings do exceptionally well at keeping out water in hot and salty situations.

Hydrophobic Nature:

Figure 2b illustrates how the words "water-hating" and "hating water" have Greek roots that imply "phobia" and "hydrophobia," respectively. Scientists refer to nonpolar substances as being "hydrophobic" because they do not combine with water molecules. Examine that definition in more detail. Since its atoms carry a partial charge, hydro is a polar molecule. The most electronegative atom is oxygen, whose core electrons in each bond are extremely close to one another. Any charged substance will interact with hydro molecules to dissolve, whether it has a positive or negative charge. In essence, molecules that dislike water are non-polar, which means they don't have a net charge. These molecules lack any connections between charges that would enable them to interact with hydro while not having any charges. Water Hating substances frequently insoluble in water or any other solution with a predominately watery environment. In many areas of biology, including the structure of animals, cellular function, and molecular interactions, the traits of being water-hating or non-polar are crucial.



Figure 2: three different surface types: a) hydrophilic, b) hydrophobic, and 3) superhydrophobic.

Water Repellence:

Super-hydrophobic surfaces are very water-repellent, making it very difficult to wet them. On a superhydrophobic surface, a water droplet's contact angle is greater than 150° , and the difference between its advancing and receding contact angles is less than 10° . A droplet can entirely bounce after colliding with a superhydrophobic surface, much like an elastic sphere. This is also referred to as the lotus effect, after the self-cleaning properties of the leaves of the lotus plant.

Experimental Details and Results: Rosaceae Petals:

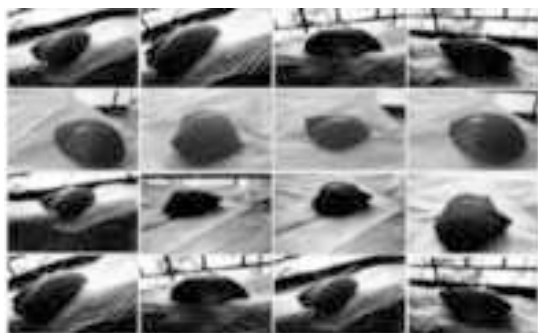


Figure 3: Images of Rosaceae petals at different times, illustrating their water-hating and water-repellence properties.

Rosaceae and the genus *Rosa* contain the most well-known flower in all of nature. The petals of Rose (*Rosa damascene*) of the family Rosaceae, are amphiphilic, meaning they have both a love of and a dislike of water. Even with the petal turned upside down, a water droplet that is small enough will slide off. High sticky forces are incompatible with water repellence. Chinese researchers have established that rose petals and water have an unusual bond that is not shared by other

plants. The micro-nanoscale topography of a rose petal comprises hills and valleys. The large valleys allow a small amount of water to soak in, creating a sticky surface on which smaller droplets can condense and stick to the petal. Since the surface of the rose petals is amphiphilic, it has both water-loving and water-hating characteristics. While the water-hating portions of the petals vigorously oppose water, the water-loving sections have a great attraction for it. The irregular topography of small valleys. Rose petals' micro-papillae produce two reactions in response to water. Larger droplets are repelled by the micro-papillae and tiny valleys. Water-hating and water-repellence are two characteristics displayed by rose petals. Following a few minutes, after 120 minutes, after 240 minutes, and after 360 minutes, it was noted that the contact angles altered during the course of the current investigation.

Asteraceae Flower:

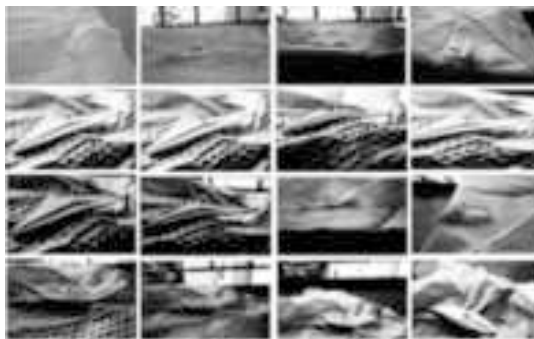


Figure 4: Images of Gerbera petals at different times, illustrating their water-loving, water-hating, and water-repellent properties.

The *Asteraceae* family's Gerbera flower is well-known. The gerbera flower is three-lobed, strap-shaped, and the individual flowers are found in the heads (Barthlott, and Neinhuis, 1997). Its aversion to water is one of its most significant characteristics. The micro-nanoscale surface area of gerbera flowers gives them the ability to both love and hate water. In the current investigation, it has been shown that the contact angles change over the first few minutes, following 120, 240 and 360 minutes.

Colocasía:

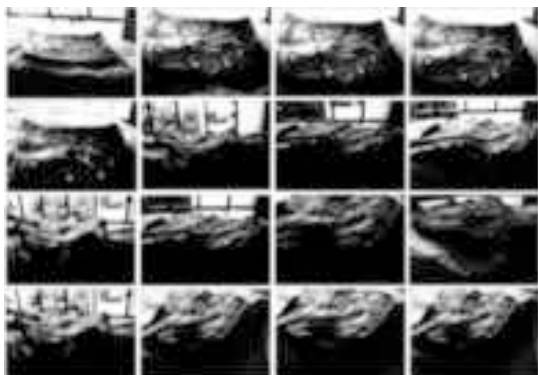


Figure 6: Images of *Colocasía* (*Araceae*) leaves at different times, illustrating their water-loving and water-repelling properties.

The elephant ears, often referred to as *Colocasía*, are the most well-known leaves in the world. Elephant ears belong to the *Araceae* family and the *Colocasía* genus. *Colocasía* leaves exhibit water-loving, water-hating, and water-repellent surface characteristics. In current investigation, it was found that the contact angles altered after a few minutes, after 120 minutes, and after 240 and 360 minutes.

Anthurium:

The genus *Anthurium* includes perennial evergreen plants that are part of the *Araceae* family. *Anthurium* plants have subterranean rhizomes and adventitious roots. *Anthurium* plants create a long-lasting, vivid spathe that comes in a variety of colours, including cream, pink, red, light red, white, dark red, green, lavender, and salmon pink. Most of the time, it is planted as a crop for cut flowers because of its spadix, which is prized for its colorful, long-lasting spathe. *Anthurium* plants are famous for their variety of colors, massive effect, and elegance.

The surface characteristics of *Anthurium* flowers in this study demonstrated both water-loving and water-repelling characteristics. The contact angles were seen to fluctuate throughout the course of the investigation at the following intervals: i.e., after 120, 240, and 360 minutes.

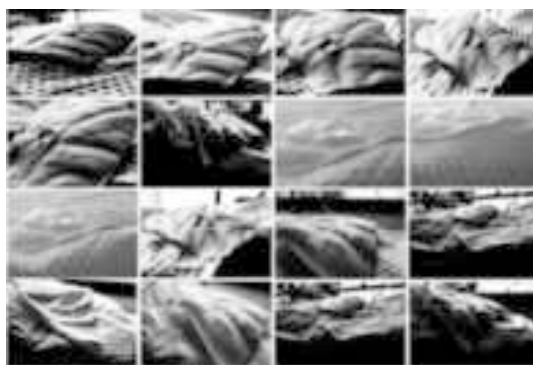


Figure 7 Images of the *Anthurium* flower (*Araceae*) are shows water loving and water hating properties at different time.

***Aloe barbadensis*:**

Aloe vera belongs to the family *Asphodelaceae* and genus *Aloe*. *Aloe barbadensis* leaves have microstructures with tiny height and high pitch values, which change the contact angle between a surface and a water droplet (Bhushan and Her, 2010). The wetting state may be reached if water impregnates between microstructures (Bormashenko, *et al.*, 2006). The hydrophobic liquid's contact area with the surface is less than in the Wenzel state but greater than in the intermediate wetting state. *Aloe barbadensis* leaves are water-loving due to their wide surface area. *Aloe barbadensis* leaves exhibit all three water-loving, water-hating, and water-repellency properties. The contact angles were seen to fluctuate throughout the course of the investigation after a few, 120, 240 and 360 minutes.

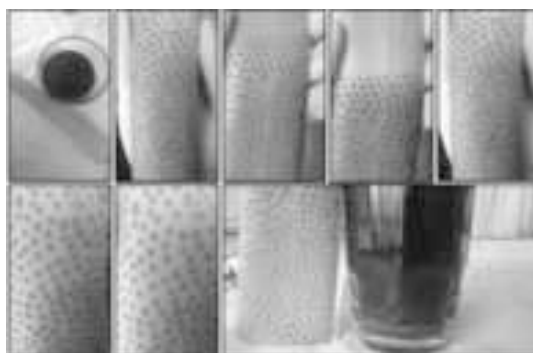


Figure 8: Asphodelaceae that simultaneously display their water-loving characteristics.

During present investigation, the water-loving, water-hating, and water-repellency qualities in Nature's exquisite materials were investigated. The rose petals were water-hating and water-repellent in nature. High adhesive forces were not always associated with water repellence. The petals of a red rose had curious relationship with water, but not for other liquids. Rose petals have a water-loving surface that strongly attracts water while water-hating surfaces strongly repel water. Rose petals had water-hating and water-repellent characteristics, but the latter is the more significant one. A surface's ability to self-clean entails that it can eliminate dirt and debris by dispersing water droplets. The leaves of *Colocasia* leaves had characteristics that attract, resist and love water. *Aloe Vera* leaf surface area demonstrated its affinity for water. Water-loving, water-hating, and water-repellent qualities were found to be present in every flower, petal and leaf. It has been shown that the contact angles change over the first few minutes, the following 120, 240 and 360 minutes.

Acknowledgements:

The authors are thankful to the Department of Botany and Physics Rajee Ramrao College, Jath.

References:

- Barthlott, W. and Neinhuis, C. (1997) *Planta* **202**:1.
- Bhushan, B. and Her, E-K. (2010) *Langmuir* **21**:8207.
- Bormashenko, E. Stein, T. Whyman, G., Bormashenko, Y and Pogreb, R. (2006) *Langmuir* **22**:9982.
- Brewer, S. A. and Willis, C. R. (2008) *Appl. Surf. Sci.* **254**:6450.
- Cai, Y. Lin, L. Xue, Z. Liu, M. Wang, S. and Jiang, L. (2014) *Adv. Funct. Mater.* **24**:809.
- Cassie, A. B. D. and Baxter, S. (1944) *Trans. Faraday Soc.* **40**:546.
- Darmanin, T. and Guittard, F. (2014) *Prog. Polym. Sci.* **39** (4): 656.
- Darmanin, T. Givenchy, E. T. D. Amigoni, S. and Guittard, F (2013) *Adv. Mater.* **25**:1378.
- Ferrari, M and Ravera, F. (2010) *Adv. Colloid Interface Sci.* **161**: 22.
- Gua, Z-Z. Wei, H-M. Zhang, R-Q, Han, G-Z. Pan, C. Zhang, H. Tian, X-J. and Chen, Z-M. (2005) *Appl. Phys. Lett.* **86**:201915.
- Nickerl, J. Helbig, R. Schulz, H-J. Werner, C. and Neinhuis, C. (2013) *Zoomorphology* **132**:183.
- Nosonovsky, M. and Bhushan, B. (2008) *Adv. Funct. Mater.* **18**:843.
- Rakitov, R. and Gorb, S. N. (2013) *Proc. R. Soc. B* **280**:20122391.
- Su, Y. Ji, B. Zhang, K. Gao, H. Huang, Y. and Hwang, K. (2010) *Langmuir* **26**:4984.
- Wenzel, R. N. (1936) *Ind. Eng. Chem.* **28**:988.
- Ye, C. Li, M. Hu, J. Cheng, Q. Jiang, L. and Song, Y. (2011) *Energy Environ. Sci.* **4**:3364.
- Young, T. (1805) *Philos. Trans. R. Soc. Lond.* **95**:65.

See discussions, stats, and author profiles for this publication at: <https://www.researchgate.net/publication/385273551>

ORYZA SATIVA HUSK AS A SUSTAINABLE SOURCE OF SILICON A REVIEW

Article · October 2024

CITATIONS

0

READS

4

1 author:



[Rajendra Lavate](#)

Shikshanmaharshi Dr. Bapuji Salunkhe College Miraj

38 PUBLICATIONS 106 CITATIONS

SEE PROFILE

ORYZA SATIVA HUSK AS A SUSTAINABLE SOURCE OF SILICON: A REVIEW

Rajendra Lavate, Sohan Thombare*, Shankar Soudagar and Appasaheb Bhosale

Department of Botany and Physics, Raje Ramrao College, Jath,
(Affiliated to Shivaji University) Kolhapur Sangli-416404, India.

*Department of Medical Physics, Centre for Interdisciplinary, Research, D. Y. Patil Education Society (Deemed to Be University), Kolhapur-416006, India.

ABSTRACT

This review focuses on utilisation of *Oryza sativa* Husk as a source for silicon nanoparticles (Si NPs) that are created via magnesiothermic reduction and used in composite anodes for lithium-ion batteries (LIBs). The production of silicon nanoparticles (Si NPs) has been explained and, their electrochemical characteristics, and possibility for activated carbon-decorated silicon nanocrystals (AC@nc-Si@AC) to serve as high-capacity anode materials have been discussed. The study emphasises cost-effective, synthesis techniques for creating environmentally acceptable energy storage technologies with the use of biomass.

Introduction:

The majority of people in the world consume rice (*Oryza sativa*) regularly. To fulfil the demands of the expanding population, it is crucial to cultivate *Oryza sativa* sustainably. In recent years, the world has consumed about 470 million metric tons of *Oryza sativa* (Wong, *et. al.*, 2014). Millions of tonnes of *Oryza sativa* husk is produced during the manufacturing of rice. Although *Oryza sativa* husk can be utilised to make fuel, fertiliser, and building materials, it is frequently considered a waste product (Rodríguez de Sensale, 2006; Kamenidou *et. al.*, 2010; Duan *et. al.*, 2013; Fang *et. al.*, 2004). Even though *Oryza sativa* husk decomposes naturally, the readily available quantity may convert it as a resource for novel technologies for the benefit of mankind.

Oryza sativa husk contains a high proportion of Silicon dioxide (SiO₂), Depending on the type of soil used to cultivate *Oryza sativa*, the SiO₂ content in its husk ranges from 10 to 20 % (Chandrasekhar *et. al.*, 2003). The *Oryza sativa* husk can be pre-treated with various acids before being pyrolyzed to recover SiO₂ from it (Yalcin and Sevinc, 2001; Kalapathy, *et. al.*, 2002; Liou, 2004; Adam, *et.*

al., 2012). The characteristics of silicon dioxide recovered from husk vary with the source or raw material. Even the amount of SiO₂ differs across *Oryza sativa* husks from different geographical areas. This may have an impact on the SiO₂ extraction characteristics, including purity, particle size, and shape (Carmona, *et. al.*, 2013; Le, *et. al.*, 2013). The SiO₂ obtained from the *Oryza sativa* has a nanoscale shape. SiO₂ can be converted into silicon (Si) by employing magnesiothermic reduction method, wherein magnesium (Mg) powder and SiO₂ are heated in a furnace until they react. Pure Si is left behind when the SiO₂ and magnesium react with the oxygen to generate magnesium oxide (MgO) (Banerjee *et. al.*, 1982). In this way, SiO₂ can be converted to Si in its original shape via magnesiothermic reduction method. Since the reaction is carried out at a temperature of 600 °C the silicon nanoparticles (Si NPs) can be subjected to sintering into a bulk substance. During sintering, the particles come together to create a solid mass. It takes less time for the particles to sinter together when the reaction is carried out at a low temperature, resulting in smaller, more homogeneous Si NPs. Thus it is possible to use silicon dioxide nanoparticles (SiO₂ NPs) as a raw material to create Si NPs. This might

result in the creation of innovative and effective processes for Si NPs synthesis (Sun and Gong, 2001). This process enables the possibility of using low-cost Si NPs in lithium-ion battery systems. This might result in the creation of lithium-ion batteries (LIBs) that are more cost-effective and environmentally friendly (Xing, *et. al*, 2013; Liu, *et. al.*, 2013; Junget. *et. al.*, 2013).

In upcoming LIBs, Si NPs will be a potential anode material. This is due to enormous capacity of Si to store a large amount of energy (Kasavajjula *et. al.*, 2007). Furthermore, Si NPs have a large surface area, which increases their reactivity with lithium ions. This may result in quicker charging and discharging times as well as increased battery performance. Theoretically, Si is the alloying material that can react with lithium ions. The capacity of producing 4200 mAh/g during this reaction, at room temperature, is 10-12 times larger than the specific capacity of conventional graphite based anodes. LIBs, made with the help of Si-based materials have an issue with volume expansion during the charge-discharge cycle. This is due to the many alloy formation stages that Si goes through during the charge-discharge cycle, which causes it to expand and contract. The Si anode may break as a result of this growth in the volume, which could affect the battery performance and lifespan (Boukamp, 1981). A similar issue that can be experienced with Si-based materials is their inherently low conductivity. This indicates that Si is a poor conductor of electricity, which may reduce the battery capacity (Lee, *et al.*, 2010; Magasinski, *et. al.*, 2010). In addition to its low working voltage, abundance on Earth, and low toxicity, Si has several further advantages as an anode material for LIBs (Entwistle, *et. al.*, 2018).

Lithium ions are injected into the material in a process known as intercalation that produces lithiation in conventional electrode materials. The intercalation method results in very few structural changes and with high retention capacity. On the other hand, Si and lithium combine to form an alloy that requires periodic cycles of contravention and re-establishing chemical connections with the

host structure. Low conductivity and the possibility of volume increase are the main drawbacks of adopting Si as an anode material for LIBs. The Si can swell by as much as 280% when a lot of lithium ions are injected into it. The Si anode may fracture and break as a result of the volume increase, which could result in a decrease in battery performance and life. The composite electrode may sustain structural degradation due to the dimensions increase of Si during cycling, which isolates the active component and reduces capacity. This poses a significant obstacle to the creation of Si anodes with large capacities and long cycle lives (Entwistle, *et. al.*, 2018).

The synthesis of SiO₂ and Si materials for LIBs from the husk of *Oryza sativa*, using various extraction methods and magnesiothermic reduction, have been discussed in this communication.

Synthesis:

Ratsameetammajak *et al.* (2022) described the process of preparing silica from the husk of *Oryza sativa* (rice). Rice husks are taken from farms and washed in water. They are then completely dried at 100 °C. To get rid of any metallic impurities, rice husks are soaked in an aqueous solution of hydrochloric acid (HCl) overnight. In order to achieve the pH value of pH of 7, rice husks are thoroughly rinsed in water. Then the rice husks are dried at 100 °C, and subsequently burnt in a muffle furnace at 700 °C for two hours. The burning process is repeated once again to ensure the perfect removal of organic matter and the creation of rice husk ash, an ample source of silica. Where the silica comes from. Below is a summary of the process used to create reduced graphene oxide (rGO): An adaptation of the Hummers process is used to create graphite oxide (GO) from graphite powder. In a non-reactive atmosphere for 5 hours, reduce the GO in a tube furnace at 800 °C (Autthawong *et. al.*, 2020)

The process of creating the composite material made of SiO₂@rGO with a proportion of 30:70 can be summed up as follows: Prepare recently generated SiO₂ by precipitating it for 2 hours at 120 °C in a NaOH solution. In the suspension, distribute rGO by

utilising a hydrochloric acid solution.

Graphene oxide (GO) is a unique material that can be viewed as a single monomolecular layer of graphite with various oxygen-containing functionalities such as epoxide, carbonyl, carboxyl, and hydroxyl groups. Reduced graphene oxide (RGO) is the form of GO that is processed by chemical, thermal and other methods to reduce the oxygen content. As graphite oxide is a material produced by oxidation of graphite, it leads to increased interlayer spacing and functionalization of the basal planes of graphite.

Raise the pH of the mixture to 7. Keep aside overnight at room temperature, and then stir the mixture. Rinse the mixture with deionized (DI) H₂O and ethyl alcohol (CH₃CH₂OH) and then centrifug. Dry the sample thus obtained in a hot air oven at 60 °C as described by Ratsameetammajak et. al., (2022).

The creation of the composite material (SiO₂@rGO and Polyaniline) including SiO₂ / rGO and Polyaniline (PANI) can be summed up as follows: In a mixture of 10 mL ethanol, 5 ml deionized water, and 5 ml H₂SO₄, make a suspension of SiO₂@rGO. To produce a consistent dispersion, sonicate the suspension. While agitating ferociously in an ice bath, dropwise add the aniline monomer to the solution. Stir the solution for 6 hours in an ice bath while adding Ammonium Persulfate ((NH₄)₂S₂O₈). When polymerization takes place leading to the formation of polyaniline emeraldine salt, the solution will turn dark green. To achieve a clear solution, repeatedly wash the suspension in H₂O and CH₃CH₂OH.

The electrochemical behaviour of the PANI-SiO₂@rGO composite was further studied in a coin-type cell utilising lithium foil as

the reference and counter electrodes. A composite anode made of SiO₂ and rGO was used in parallel tests to compare the results. The initial three lithiation-delithiation curves of the SiO₂@rGO and PANI-SiO₂@rGO electrodes at a potential range of 0.01-3.00 V (vs. Li/Li⁺) at a current density of 0.4 A g⁻¹ are shown in Figures 1b and 1c, respectively.

The SiO₂@rGO composite electrode's initial lithiation and delithiation specific capacities were 1012 and 300 mAh/g, respectively, however, it had a poor coulombic efficiency (CE) of 29.6%. The PANI-SiO₂@rGO composite electrode initial lithiation/delithiation specific capacities, on the other hand, were 1508 and 647 mAh/g, respectively, with a CE of 42.9%. The reduction of silica in SiO₂@rGO and PANI-SiO₂@rGO composites, results in lithium loss, causing initial low CE. The potential gradient plateaus on both electrodes, which range from 1.5 to 0.5 V, clearly show the formation of a solid electrolyte interphase (SEI) layer (Ratsameetammajak et. al., 2022).

The existence of stable plateaus during early cycles is an evidence of this reaction (Figure 1d). The subsequent cycles show that the SEI layer is only formed in the initial cycle, as the slopes gradually become sharper and the hills gradually get smaller. The charge voltage profiles become noticeably steeper rather than staying flat at potentials higher than 1.5 V. This invention can be attributed to solvent degradation processes occurring on the oxide electrode surface, which produced the SEI coating (Ratsameetammajak et. al., 2022).

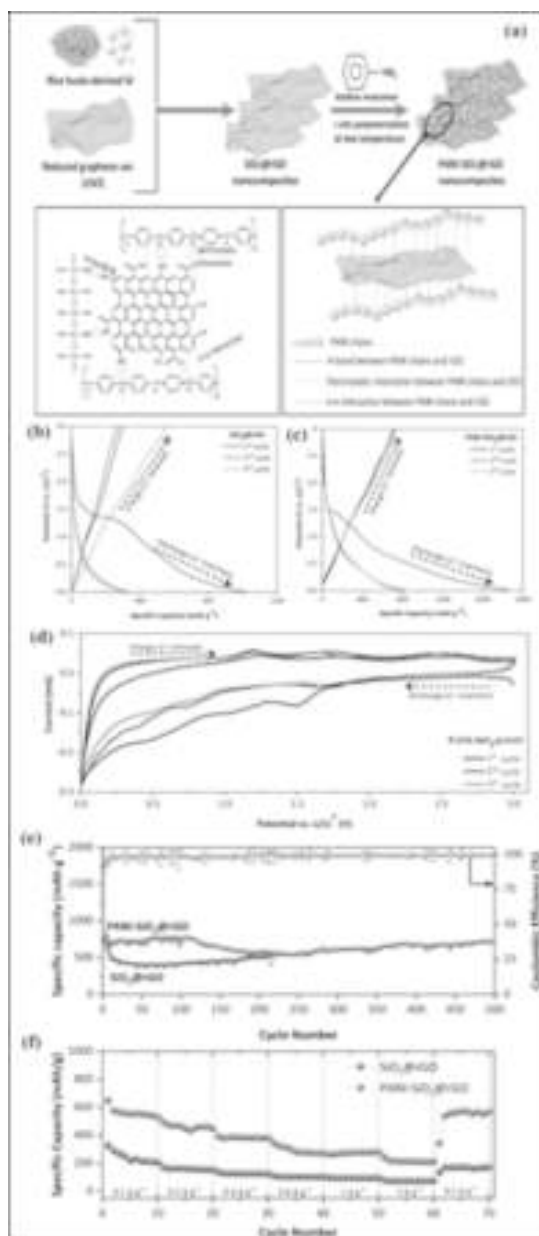


Figure 1(a-f) (a) the synthetic pathway for the preparation of the PANI-SiO₂@rGO composite, lithiation-delithiation profiles for the composites PANI-SiO₂@rGO and SiO₂@rGO measured at 400 mA g⁻¹ in current density (b) and (c), during the first three cycles, cyclic voltammograms (CV) of the PANI-SiO₂@rGO electrode were

recorded at a scan rate of 0.1 mV s⁻¹ and are displayed in (d), SiO₂@rGO and PANI-SiO₂@rGO composites long-term cycling stability and Coulombic efficiency comparison at 400 mA g⁻¹ are depicted in (e). SiO₂@rGO and PANI-SiO₂@rGO composites rate performance evaluation is depicted in (f).

During the initial cycle of delithiation and lithiation, a layer on the surface of anode known as the SEI film develops. It is produced by the interaction of the electrode material and the electrolyte at the solid-liquid interface. It is thought that the partial breakdown of the SEI coating was mostly due to the initial poor CE. The initial coulombic efficiency of PANI-SiO₂@rGO electrode is greater than that of SiO₂@rGO composite electrode. This is because the PANI covering shell prevents the electrolyte at SiO₂@rGO surface from decomposing.

Figure 1e compares the long-term cycling stability of SiO₂@rGO nanocomposite (NC) electrode with the PANI-SiO₂@rGO composite electrode. The PANI-SiO₂@rGO NC anode has outstanding long-term cycling performance at 0.4 A g⁻¹ and maintains a high reversible capacity of 680 mAh/g after 400 cycles, which is about twice as much capacity as standard graphite anodes. In comparison, after 215 cycles, SiO₂@rGO NC electrode can only discharge 414 mAh/g. This shows that only mild pulverisation of SiO₂ in the PANI-SiO₂@rGO NC occurred. The PANI coating efficiently slows down electrolyte degradation on the surface of SiO₂ and serves as a flexible protective layer to absorb SiO₂ volumetric changes.

The results presented above make it clear that the PANI shell outstanding mechanical qualities may prevent SiO₂ nanoparticle volumetric alterations. This capability guarantees that the working electrode structural integrity is maintained throughout discharge and charge cycles, greatly enhancing the electrode sustained stability over time.

The rate performance of PANI-SiO₂@rGO and SiO₂@rGO NC electrodes was evaluated at different current densities ranging

from 0.1 to 2.0 A g⁻¹, as shown in Figure 1f. At the corresponding current densities of 0.1 to 2 A g⁻¹, the PANI-SiO₂@rGO NC electrode displayed discharge capacities ranging from 563.6 to 217.1 mAh/g. After cycling at 2 A g⁻¹, the electrode maintained a discharge capacity of 539.4 mAh/g when cycled back to 0.1 A g⁻¹, illustrating its excellent rate performance. These results show that using PANI-SiO₂@rGO NC is an effective way to improve the electrochemical properties of SiO₂@rGO (Ratsameetammajak *et al.*, 2022).

N-doped carbon coated PANI-SiO₂@rGO NC has superior lithium storage capacity. Which can be attributed to their distinctive structure. SiO₂ nanoscale properties shorten the lithium ion diffusion path, which enhances lithium-ion diffusion and electronic transport. however, the rate capability may suffer. The encircling rGO sheets on the SiO₂ surface have generated a continuous conductive channel that connects the SiO₂ nanoparticles, considerably improving the conductivity of PANI-SiO₂@rGO NC electrode. SiO₂ pulverisation is avoided because the PANI materials elasticity effectively adapts to the NC volume variations during the Li-alloying and dealloying operations (Ratsameetammajak *et al.*, 2022; (Liao, *et al.* 2020; Charlton, *et al.*, 2020, Chen, 2019). In conclusion, PANI-SiO₂@rGO NC had an improved initial CE of 42.9% and a high specific capacity of 680 mAh/g at 400 mA/g after 215 cycles (Ratsameetammajak *et al.*, 2022).

Synthesis of silicon nanoparticles:

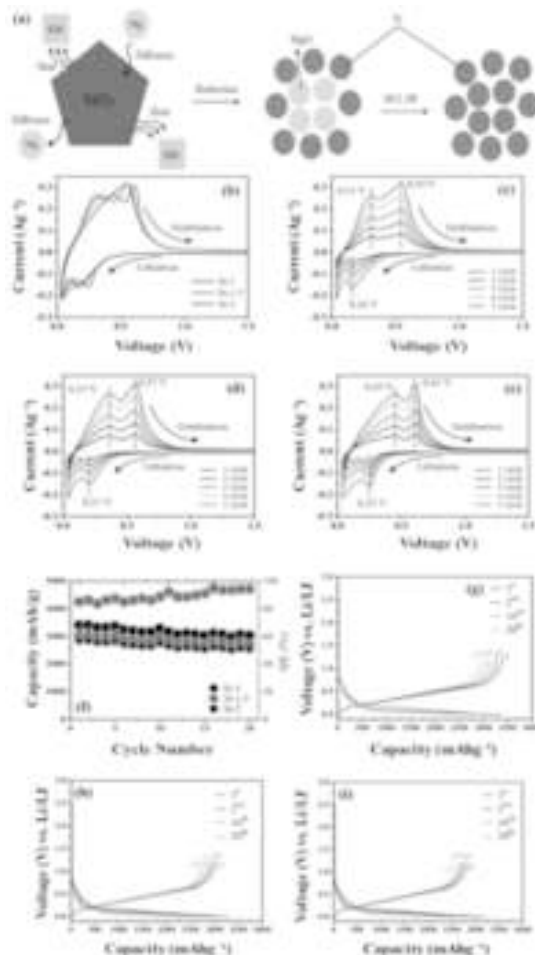
Daulay *et al.* (2022) heated *Oryza sativa* husk at 600°C for 5 hours to produce ash. Thereafter the ash and NaOH were combined and stirred for three hours at 240 rpm and 100°C. The mixture was filtered, and HCl was added until a pH reached 7.0, The precipitate was filtered out and residual solution was heated at 100°C for three hours again for precipitation, which was again removed by filtration. After several rounds of washing with distilled water and drying, SiO₂ was produced in the form of powder. It was then mixed with KBr with a ratio of 1:10,

deionized water was added, and stirring was carried out for three hours. The combination was subjected to ultrasonication for six hours. The residue produced after ultrasonication was separated by decantation, and the filtrate was allowed to dry for 12 hours. The dry powder was mixed with Mg powder in various ratios (1:1.0, 1:1.5, 1:2.0). The next calcination procedure was undertaken at 800°C for 8 hours. During the first purification stage, 150 mL of deionized water and 15 mL of ethanol were added. After that, there was 3 hours of agitation. Centrifugation of the mixture was done for 30 minutes at a speed of 4000 rpm. After being regularly cleaned with deionized water, it was dried for six hours at 80 °C. The second stage involved addition of 150 ml, 5 N HCl and a 12-hour rest period. The sample was dried at 80 °C for 6 hours, washed with deionized water, and then centrifuged once again for 30 minutes at 4000 rpm. Then 150 mL of 10% hydrogen fluoride (HF) was added as the last stage, and the mixture was allowed to settle for 15 minutes. The mixture was first dried, followed by several washes in deionized water, and a second drying step was six hours at 80 °C. Si-1, Si-1.5, and Si-2 thus produced were labelled. (Daulay, *et al.*, 2022).

Figure 2b displays cyclic voltammetry profiles for Si NPs. The data demonstrated that as the ratio of SiO₂ and Mg increases during reduction, the magnesiothermic reduction causes a higher reduction peak associated with the production of delithiation as well as oxidation peaks, associated with the lithiation to Si. Cyclic voltammetry (CV) was used to measure the activation process for Si-1, Si-1.5, and Si-2 electrodes with a voltage range of 0.01 to 1 V (against Li^{+/}Li) and a scan rate of 0.2 mVs⁻¹. The CV analysis of Si-1 (Figure 2c) revealed lithiation-related reduction peaks (0.16 V) as well as the delithiation-related oxidation peaks (0.31 V and 0.54 V). Figure 2d depicts the lithiation of Si-1.5 at 0.21 V and its delithiation at 0.37 V and 0.57 V. In Figure 2e, the lithiation (0.25 V) and delithiation (0.45 V and 0.61 V) peaks for Si-2 are displayed. These peak intensities increase during the cycles, suggesting that more lithium ions are possibly

moving between the electrode and electrolyte. This indicated gradual activation of substances. Compared to Si-1.5 and Si-2, Si-1 showed less significant peaks in both lithiation and delithiation. More efficient transport of lithium ions from the cathode to the anode and vice versa is shown by smaller lithiation and delithiation peaks in CV (Daulay *et al.*, 2022).

The rate capability study for the Si-1, Si-1.5, and Si-2 electrodes is shown in Figure 2f. The first cycle is performed to ensure that Si is adequately activated, as shown by cyclic voltammetry, which aids in the creation of a stable solid electrolyte interphase (SEI) layer (Liu *et al.*, 2006). Si-1, Si-1.5, and Si-2 electrodes, respectively, had initial discharge capacities of 3416, 3037, and 2847 mAh/g. 54.9, 85.4, and 85.6 % are the comparable *Conformite Europeenne* (CE). The silicon lithiation potential range (0.01 V to 0.50 V) is higher than the carbonate-based lowest unoccupied molecular orbital (LUMO) electrolyte. When a voltage is applied, Si is lithiated, resulting in the formation of an amorphous solid electrolyte interface (SEI). By reductively destroying the electrolyte, this SEI is created. The native oxide layer on the Si surface is damaged during the initial lithiation process, which causes an inner SEI predominantly made of lithium ethylene dicarbonate (LEDC) and Li_xSiO_y to develop. While the continuing discharge causes LiF to be produced, a significant amount of outer SEI is predominantly made up of LEDC. Within the defined potential range, these SEI components containing lithium remain stable. Because of this, the lithium that is used during delithiation cannot be completely recovered from the created SEI constituents, which results in permanent capacity loss and reduced coulombic efficiency during the initial cycle (Schroder, *et al.*, 2015). Si-1 improved electrochemical compatibility with Si and LiPF_6 electrolytes were highlighted by the slightly higher initial charge-discharge coulombic efficiency seen in Si-1 compared to Si-1.5 and Si-2.



This suggests that the anodes have the following rate capabilities: Si-1 > Si-1.5 > Si-2. Examining these electrode typical charge-discharge curves at particular rates lends credence to this claim. The electrode is more stable during discharge because the voltage hysteresis is reduced. The higher capacity of Si-1 electrode compared to Si-1.5 and Si-2 anodes demonstrates superior adaptability of Si-1 and endurance as a protective shell for absorbing significant volume variations. As seen by Si-1 more stable behaviour, this improves cyclability. Because of their greater ability to transport electrons and ions more quickly, Si NPs operate more quickly than nonconductive binder (PAA). The better electrical conductivity and superior specific

capacities at high current densities of Si-1, as compared to Si-1.5 and Si-2, are evidence of its improved physical encapsulation of silicon.

These variations imply that Si-1 performs better in LIBs than Si-1.5 and Si-2, suggesting that Si-1 has an advantage over other materials as an anode material. In conclusion, using the magnesiothermic process and KBr as a scavenger, Si NPs were created from *Oryza sativa* husk. Three different Si NPs kinds were produced using this ecologically friendly method (Salah, *et. al.*, 2019). As LIB anodes, all three varieties of Si NPs demonstrated excellent performance. Si-1, Si-1.5, and Si-2 had specific capacities of 3416, 3037, and 2847 mAh/g, respectively. Si-1, Si-1.5, and Si-2 had lithiation potentials and delithiation potentials of 0.16, 0.21, and 0.25 V, respectively (Daulay *et. al.*, 2022).

Synthesis of activated carbon-decorated nanocrystals-silicon:

Sekar *et al.* (2019) heated brown *Oryza sativa* Husks in an air atmosphere for 120 minutes at 500 °C to collect the ash. After that, 1.0 g of ash and 0.2 g of magnesium (Mg) powder were mixed. This mixture was put in an alumina crucible and annealed for 120 minutes at 700 °C in an argon (Ar) environment. Magnesiothermic reduction took place throughout this procedure. The annealed mixtures underwent a 6-hour stirring procedure in 1 M hydrochloric acid (HCl) to isolate acicular nc-Si-enriched activated carbon nanocomposites and remove magnesium silicide (Mg_2Si) precipitates, magnesium oxide (MgO) residues, and native silicon dioxide (SiO_2) impurities. The next step involved 1-hour reaction with 5% hydrofluoric acid (HF). The wet activated-carbon-decorated silicon nanocrystal products were then collected from the resultant solution, filtered, and washed with deionized water before being dried under vacuum for 10 hours at 80 °C. The *Brown Oryza sativa* Husks was used to create the activated-carbon-decorated silicon nanocrystal nanocomposites utilising the magnesiothermic reduction technique (Figure 3a) (Sekar *et. al.*, 2019).

In addition, by integrating the benefits

of both *nanocrystals-silicon* and activated carbon, the novel nanocomposite structure known as activated-carbon-decorated silicon nanocrystal, which consists of activated carbon embellished with nanostructured silicon (nc-Si), is predicted to enhance the electrochemical performance of LIBs. Building LIB anode combinations utilising *nanocrystals-silicon*, activated carbon, and activated-carbon-decorated silicon nanocrystal allowed researchers to test this idea by evaluating the electrochemical characteristics of materials. Initially, cyclic voltammetry (CV) profiles covering the voltage range of 0 to 3.0 V (vs. Li/Li^+) were captured for the prepared anodes using a scan rate of 0.1 mV/s. Different anodic peaks were visible in the LIB configuration with the *nanocrystals-silicon* anode (Figure 3b), which correspond to the incorporation of lithium ions into the nanocrystals-silicon. A cathodic peak at 0.66 V also formed during the first CV cycle and was brought on by the electrode surface developing a solid electrolyte interphase (SEI) layer as well as electrolyte breakdown. The subsequent stabilisation of CV curves from the second to fifth cycles is proof that the SEI layer prevents further electrolyte breakdown and improves LIB stability. The interaction of Li ions with the native SiO_2 present on the nanocrystals-silicon surface is most likely what caused a wider cathodic peak to form at 1.65 V (Sekar, *et. al.*, 2019; Sun, *et. al.*, 2014, 2015).

During the first CV cycle, the activated carbon anode (Figure 3c) had a pronounced cathodic peak at 0.2 V, which was followed by stable following curves. This was most likely caused by the formation of an SEI layer on the activated carbon surface. In a similar manner, when using activated-carbon-decorated silicon nanocrystal as the anode. Although the nanocomposites included minute amounts of MgO residue, the device did not show any MgO-related peaks. The activated-carbon-decorated silicon nanocrystal nanocomposites showed noticeably more powerful anodic responses than the nanocrystals-silicon instance. This shows that the highly conductive activated carbon nanosheets inside the activated-carbon-silicon

nanocomposite system caused the activated-carbon-decorated silicon nanocrystal to suffer faster electrochemical reactions (Sekar, et. al., 2019).

GCD measurements were used to assess the samples electrochemical properties. The initial lithiation and delithiations capacities for the nanocrystals-silicon sample during the first cycle were 336 and 75 mAh/g, respectively (Figure 3e). Due to the intrinsic oxide tendency to lithiate, the initial coulombic efficiency was thus only about 22%. The 1st discharge curve of the nanocrystals-silicon sample (Figure 3e) exhibits a large plateau at about 0.09 V, which denotes the development of SEI layers and Li-Si alloys on the anode material surface. Due to limitations in electronic conductivity, sluggish chemical reactions, and a reduction in surface area, the GCD performance drastically declined in the second cycle (Sekar, et. al., 2019). The charge and discharge capacities for the activated carbon sample, which is depicted in Figure 3f, were 295 and 545 mAh/g, respectively. This resulted in a coulombic efficiency of 54%. The initial discharge curve suggested that the formation of the SEI layer might lead to a plateau at 0.8 V. After multiple charge-discharge cycles, this plateau disappeared because of the stability of the carbon-based LIB anode (Sekar, et. al., 2019).

When the activated-carbon-decorated silicon nanocrystal anode was employed, the LIB device displayed greater charge (510 mAh/g) and discharge (716 mAh/g) capabilities than the other samples (Figure 3g). The enhanced coulombic efficiency of activated-carbon-decorated silicon nanocrystal anode was 71% as a result. This increased efficiency can be related to the structure of activated carbon-coated nanocrystals-silicon nanocomposite, which efficiently reduces unfavourable processes (such Li-Si alloying on the nanocrystals-silicon surface) and encourages electron diffusion because mesoporous nanocrystals-silicon is present. The 1st discharge cycle showed three potential plateaus (0.3, 0.5, and 0.8 V) as a result of the formation of the SEI layer and the lithiation of amorphous Li_xSi and Si (Sekar, et.

al., 2019).

The rate capability and cycle stability of LIBs with activated carbon and silicon nanocrystal anodes coated with activated carbon were then evaluated. The LIB device with the nanocrystal-silicon anode was excluded due to its poor electrical conductivity, as was already indicated. (Sekar, et. al., 2019).

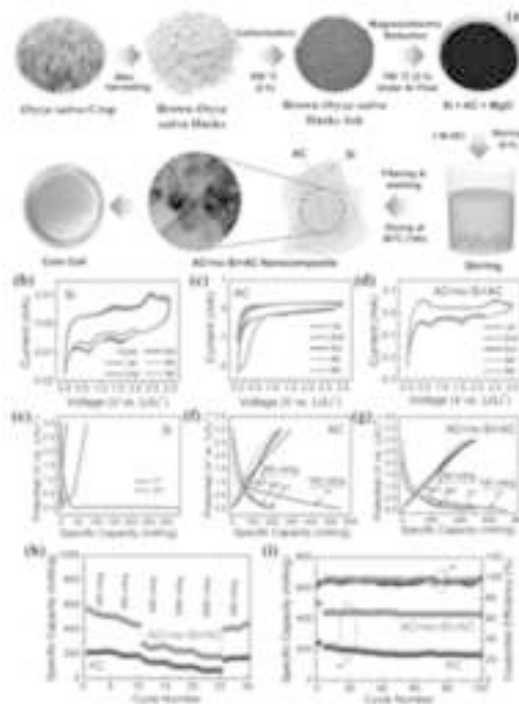


Figure 3: The experimental methods for simultaneously obtaining silicon nanocrystal nanocomposites adorned with activated carbon from the biomass resource known as Brown Oryza sativa Husks (BOSHs), lithium-ion battery (LIB) device cyclic voltammetry (CV) curves using anode materials made of (b) nc-Si, (c) AC, and (d) AC@nc-Si@AC nanocomposites, the scanning rate used for all of the CV measurements was 0.1 mV/s. Galvanostatic charge-discharge (GCD) curves of LIB devices using (e) nc-Si, (f) AC, and (g) activated-carbon-decorated silicon nanocrystal nanocomposites as anode materials, A current density of 100 mA/g was used for

the first GCD cycle, and a current density of 200 mA/g was used for the subsequent cycles, (h) Rate performance for the LIB devices using the anode materials of AC nanosheets and activated-carbon-decorated silicon nanocrystal nanocomposites at different current densities and (i) Cycling performance and coulombic efficiency determined for LIB devices using AC@nc-Si@AC as anode materials under an applied current density of 200 mA/g.

Figure 3h shows the rate performance of the LIBs based on the applied current density. The LIB with the activated carbon anode displayed reversible discharge capacities ranging from 214 to 83 mAh/g at applied current densities of 100 to 2000 mA/g. The silicon nanocrystal activated-carbon decorated anode of the LIB demonstrated reversible discharge capacities ranging from 561 to 199 mAh/g at applied current densities of 100 to 2000 mA/g, respectively. Both times, when the applied current density was lowered to 200 mA/g after 25 cycles, the discharge capacity fully recovered, indicating good reversibility. However, the initial specific capacity (during the first cycle at 100 mA/g) and the specific capacity window (the variance of specific capacity with varying applied current density) were approximately 2.6 times and 1.5 times, respectively (Sekar, et. al., 2019).

The silicon nanocrystal anode coated with activated carbon also showed excellent cycle performance and a good CE. As shown in Figure 3i, the activated carbon anode had a noticeably lower discharge capacity of 166 mAh/g, which is only 0.38 times that of the activated carbon-decorated silicon nanocrystal anode, while the activated carbon anode maintained a high discharge capacity of 429 mAh/g over 100 cycles. Additionally, the silicon nanocrystal anode-equipped LIB maintained a rather high CE of around 97.5% throughout 100 charge-discharge cycles.

The discharge capacity observed here was enhanced by around 1.2 times in comparison to commercial graphite (372 mAh/g), owing to the greater specific capacity

of Si in activated-carbon-decorated silicon nanocrystal nanocomposites. The two-dimensional shape and superior electronic conductivity of the activated carbon nanosheets in the silicon nanocrystal coated with activated carbon may improve ion diffusion and storage in LIBs.

The strong structural stability of activated-carbon-decorated silicon nanocrystal nanocomposites is responsible for these exceptional rate and cyclic performances. In essence, the *activated carbon* nanosheets served as a protective coating or shell for the Si nanocrystals, minimising the volumetric changes in those crystals. The Li interaction with *nanocrystals-silicon* was considerably hampered throughout the whole solid-state system of the activated-carbon-decorated silicon nanocrystal nanocomposite because the *activated carbon* shell allowed plenty of room for Li-ion diffusion during charge-discharge operations.

The initial capacity of fully biomass-derived activated carbon could still be raised, even though adding nanocrystals-silicon and highly conductive nanomaterials (like graphene, carbon nanotubes, conducting polymers, etc.) could be the next steps to improve the electrical conductivity and porosity of the entire composite material system, leading to further improvements in its electrochemical performance.

Finally, activated carbon made from brown *Oryza sativa* husks and silicon nanocrystals Activated carbon nanocomposites have a high initial discharge capacity, reversible specific capacity, rate performance, cyclic stability, and coulombic efficiency. These nanocomposites have the potential to serve as high-performing anode materials for LIB devices (Sekar, et. al., 2019).

Synthesis of nano-silicon:

Husks of *Oryza sativa* were calcined for 5 hours at 600 °C following Sudarman et al. *Oryza sativa* husk ash and a 10% sodium hydroxide (NaOH) solution were mixed for three hours at a temperature of 100°C and a rotational speed of 240 rpm. After being

filtered, the filtrate from the stirring procedure was gradually combined with 37% hydrochloric acid (HCl) until the pH reached to 7.0, which led to the precipitation of a precipitate. Silica (SiO_2) gel was created after extensively filtering and washing the precipitate with deionized water. The next step was to combine SiO_2 gel with 98% magnesium powder in a weight-to-ratio of (1: 0.5, 1: 0.6, or 1: 0.7). The last combination was sealed entirely in an autoclave made of stainless steel. The autoclave was then heated in a microwave for 10 hours at 180°C before being cooled for 12 hours at room temperature. The powder obtained was put through a purifying process. The purification procedure began with the addition of a 5 N hydrochloric acid (HCl) solution for 12 hours. The mixture was rinsed three times with deionized water, and then the silicon was removed by centrifuging the mixture at 4000 rpm for 30 minutes. Adding a 10% hydrofluoric acid (HF) solution for 15 minutes was the second step in the purification process. Three rounds of washing with deionized water were followed by a 30-minute centrifugation at 4000 rpm to remove unreacted SiO_2 and other impurities produced. Three samples were given the designations Si-0.5, Si-0.6, and Si-0.7, with the numbers 0.5, 0.6, and 0.7 designating the amounts of magnesium (Mg) powder used in each sample. Using a hydrothermal process, silicon (Si) with a diameter of only a few nm was produced in an aqueous solution. This required the SiO_2 to be reduced using a mixture of *Oryza sativa* husk SiO_2 gel and Mg powder. SiO_2 gel and Mg powder reacted to form Si and magnesium oxide (MgO). The hydrothermal procedure, which comprises lowering SiO_2 at a temperature of 180°C for 10 hours, results in a mixture of Si and MgO. High-purity nano-Si is produced through further purification procedures. To remove Mg, magnesium silicide (Mg_2Si), and MgO from the mixture,

hydrochloric acid (HCl) is added in the first purification stage. HF is added during the second purification stage to efficiently remove SiO_2 . In Figure 4a, the hydrothermal technique for synthesising nano-Si is shown graphically (Sudarman *et al.*, 2023).

Additionally, cyclic voltammetry (CV) on Si-0.5, Si-0.6, and Si-0.7 was carried out at a scan rate of 0.2 mV s^{-1} throughout a voltage range of 0.01 to 1.5 V. In Figure 4b, the CV of Si-0.5 shows two reduction peaks at 0.38 V and 0.58 V, which are associated with the extraction of Li^+ ions, and one oxidation peak at 0.16 V, which is associated with the insertion of Li^+ ions. Li^+ extraction at 0.38 V, 0.56 V, and Li^+ insertion at 0.16 V are all shown for Si-0.6 CV in Figure 4c. The cyclic voltammetry of Si-0.7 (Figure 4d), which displays Li^+ extraction at 0.38 V and 0.59 V and Li^+ insertion at 0.17 V, demonstrates similar results. The cathodic peak below 0.3 V, which is supported by the huge anodic peak in the CV curve, points to a single mechanism that converts nano-Si into amorphous Li_xSi ($x = 3.75$). However, the electrochemical procedure for producing $\text{Li}_{3.75}\text{Si}$ at room temperature is not very advanced. Regarding the extraction of Li^+ from nano-Si, it is clear that Si-0.6 has the lowest value, demonstrating its superiority to Si-0.5 and Si-0.7. Si-0.6 has pores that are larger than those of Si-0.5 and smaller than those of Si-0.7, which accounts for the disparity. Si-0.7, which has the smallest pore size in comparison to Si-0.5 and Si-0.6, demonstrates greater Li^+ extraction as a result (Sudarman *et al.*, 2023).

Figure 4e shows how well nano-Si electrode cycled over 200 times. During the first cycle, Si-0.5, Si-0.6, and Si-0.7 exhibit capacities of 1575, 1757, and 1525 mAh/g, respectively. Notably, Si-0.6 is more capacious than Si-0.5 and Si-0.7, although Si-0.7 has less capacity than the other two (Sudarman *et al.*, 2023).

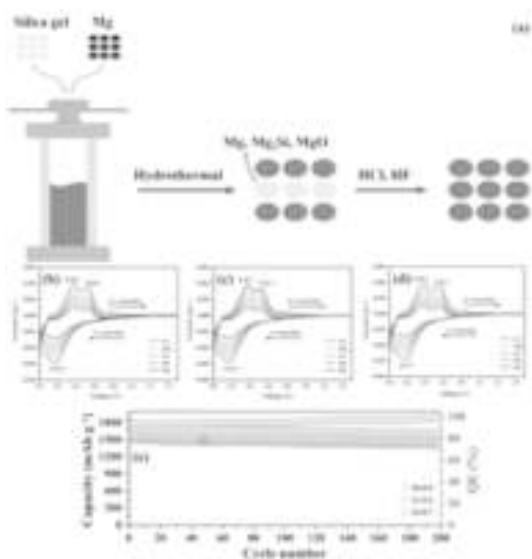


Fig. 4 The cycling performance of a nano-silicon electrode over 200 cycles using the cyclic voltammetry (CV) of Si-0.5, Si-0.6, and Si-0.7 (Sudarman et al., 2023)

This finding emphasises how important pore size is for Li^+ extraction and capacity. The increased capacity of Si-0.6 is a result of its bigger pore size, whereas Si-0.7 has the lowest capacity due to its smaller pore size. As a result, the pore size has a significant impact on lithium-ion battery capacity, favouring larger pore sizes for greater performance. The considerable volume changes that take place throughout the Li^+ extraction and insertion cycles make Si employment as a LIB anode material challenging. Electrode cracking and capacity loss are frequent consequences of these volume fluctuations. Since Si NPs are naturally resistant to fractures, they are employed to reduce cracking. In addition to improving fracture resistance, the nanoscale structure capacity to accept strain from Li^+ extraction and insertion through plastic deformation lowers stresses during volume changes. Therefore, this study focuses on producing porous nanostructured Si in addition to employing Si with nanoparticle-sized Si. Due to the increased capacity that nanostructured Si offers compared to other anode materials, this strategy is essential. With a possibility for further improvement, the

discharge capacity of 1757 mAh/g over 200 cycles demonstrates the exceptional performance of nanostructured Si as a LIB anode, outperforming commercial batteries, graphite, and graphene (Sudarman et al., 2023)

Thus the improved lithium-ion battery performance was made possible by novel synthesis techniques for advanced anode materials, including PANI-SiO₂@rGO nanocomposites, scalable silicon nanoparticles from rice husk, nano-silica by hydrothermal processing, and AC@nc-Si@AC nanocomposites. These methods provide increased stability, conductivity, and capacity, indicating a viable route to the creation of practical and affordable LIB devices.

Acknowledgements:

The authors are thankful to the Department of Botany and Physics, Rajee Ramrao College, Jath and Department of Medical Physics, Centre for Interdisciplinary, Research, D. Y. Patil Education Society (Deemed to Be University), Kolhapur.

References:

- Adam, F. Appaturi, J. N. and Iqbal, A. (2012) *Catal. Today*. **190**:2.
- Autthawong, T. Chimupala, Y Haruta, M. Kurata, H Kiyomura, T. Yu, A. Chairuangstri, T and Sarakonsri, T. (2020) *RSC Adv.* **10**:43811.
- Banerjee, H. D. Sen. S. and Acharya, H. N. (1982) *Mater. Sci. Eng.* **52**:173.
- Boukamp, B. A. (1981) *J. Electrochem. Soc.* **128**:725.
- Carmona, V. B. Oliveira, R. M. Silva, M. W. T. Mattoso, L. H. C and Marconcini, J. M. (2013) *Ind. Crops Prod.* **43**:291.
- Chandrasekhar, S. Satyanarayana, K. G. Pramada, P. N. Raghavan, P and Gupta, T. N. (2003) *J. Mater. Sci.* **38**:3159.
- Charlton, Hatchard, M. T. D. and Obrovac, M. N. (2020) *J. Electrochem. Soc.* **167**:80501.

- Chen, Y. (2019) *IOP Conf. Ser. Mater. Sci. Eng.* **677**:022115.
- Daulay, A. Andriavani and Marpongahtun, Gea, S. (2022) **6**:100256.
- Duan, F. Chyang, C-S. Lin C-W. and Tso, J. (2013) *Bioresour. Technol.* **134**:204.
- Entwistle, J. Rennie, A. and Patwardhan, S. (2018) *J. Mater. Chem. A.* **6**:18344.
- Fang, M. Yang, L. Chen, G. Shi, Z. Luo, Z. and Cen, K. (2004) *Fuel Process. Technol.* **85**:1273.
- Jung, D. Ryou, M. Sung, Y. Park, S and Choi, (2013) *J Proc. Natl. Acad. Sci. U. S. A.* **110**:12229.
- Kalapathy, U. Proctor, A. and J. Shultz, J. (2002) *Bioresour. Technol.* **85**:285.
- Kamenidou, S. Cavins, T. J. and Marek, S. (2010) *Sci. Hortic.* **123**:390.
- Kasavajjula, U. Wang, C and Appleby, A. J. (2007) *J. Power Sources* **163**:1003.
- Le, V. H. Thuc, C. N. H and Thuc, H. H. (2013) *Nanoscale Res. Lett.* **8**:58.
- Lee, J. K. Smith, K. B. Hayner, C. M. and Kung, H. H. (2010) *Chem. Commun.* **46**:2025.
- Liao, Y. Liang, K Ren, Y. and Huang, X. (2020) *Front. Chem.* **8**:96.
- Liou, T-H. (2004) *Mater. Sci. Eng., A*, **364**:313.
- Liu, C. Li, C. Ahmed, K. Wang, W. Lee, I. Zaera, F Ozkan, C. S. and Ozkan, M. (2006) *RSC Adv.* **6**:81712.
- Liu, N. Huo, K. McDowell, M. Zhao, J and Cui, Y. (2013) *Sci. Rep.* **3**:1919.
- Magasinski, A. Dixon, P. Hertzberg, B. Kvit, A. Ayala, J. and Yushin, G. (2010) *Nat. Mater.* **9**:353.
- Ratsameetammajak, N. Autthawong, T, Chairuang Sri, T. Kurata, H. Yu, A-S. and Sarakonsri, T. (2022) *RSC Adv.* **12**:14621.
- Rodríguez de Sensale, G. (2006) *Cem. Concr. Compos.* **28**:158.
- Salah, M. Murphy, P Hall, C. Francis, C. Kerr, R. and Fabretto, (2019) *M. J. Power Sources.* **414**:48.
- Schroder, K. Alvarado, K. J. J Yersak, J. T. A. Li, T. A. J. Dudney, N Webb, L. J. Meng, Y. S. and Stevenson, K. J. (2015) *Chem. Mater.* **27**:5531.
- Sekar, S. Ahmed, A. T. A. A, Inamdar, A. I. Lee, Y. Im, H, Kim, D. Y. and Lee, S (2019) *Nanomaterials.* **9**:1055.
- Sudarman, S. Andriayani, and Tamrin, Taufik, M. (2023) *Materials Science for Energy Technologies.* **1**:8
- Sun, L and Gong, K (2001) *Ind. Eng. Chem. Res.* **40**:5861.
- Sun, Z. Song, X. Zhang, P. and Gao, L. (2014) *RSC Adv.* **4**:20814.
- Sun, Z. Tao, S. Song, X. Zhang, and P. Gao, L. (2015) *J. Electrochem. Soc.* **162**:A1530.
- Wong, D. P. Suriyaprabha, R. Yuvakumar, R. Rajendran, V. Chen, Y-T. Hwang, B-J. Chen, L-C. and Chen, K-H. (2014) *J. Mater. Chem. A*, **2**:13437.
- Xing, A. Tian, S. Tang, H. Losic, D and Bao, Z (2013) *RSC Adv.* **3**:10145.
- Yalcin, N. and Sevinc, V. (2001) *Ceram. Int.* **27**:219.

WATER LOVING, WATER HATING AND WATER REPELLENCE PROPERTIES OF SOME PLANTS

Rajendra Lavate, Sohan Thombare*, Shankar Soudagar, Rajesh Sawant and Appasaheb Bhosale

Department of Botany, Chemistry and Physics, Raje Ramrao College, Jath, (Affiliated to Shivaji University Kolhapur) Sangli-416404, India.

Department of Medical Physics, Centre for Interdisciplinary, Research, D. Y. Patil Education Society (Deemed to Be University), Kolhapur-416006, India.

ABSTRACT

Hydrophilic surfaces, which have an affinity for water molecules, are those that prefer water. Water molecules are attracted to hydrophobic surfaces because they reject water molecules. Surfaces that are particularly water-repellent are known as superhydrophobic surfaces. Because of their great surface roughness and low surface energy, superhydrophobic surfaces allow water droplets to easily bead up and slide off. During the present investigation, beautiful materials found in nature have been explored to examine their water-loving, water-hating, and superhydrophobic characteristics. *Aloe vera*, rose petals, gerbera blossoms, *Aloe barbadensis*, miller leaves, and anthurium flowers are some of the botanical blooms that have been included for present study. All naturally occurring substances possess a reduced surface tension. Water has lower surface tension than most other naturally occurring substances. It was observed that the contact angles of the water droplets on the rose petals altered at three different time points: 120 minutes, 240 minutes, and 360 minutes.

Keywords: Anthurium, *Aloe Vera*, *Colocasia*, *Gerbera* Flower, Rose Petal

Introduction:

Many natural surfaces exhibit characteristics of water affinity, water aversion, and water repellency (Darmanin, and Guittard, 2014; Darmanin, *et. al.*, 2013) Nature has produced insects, animals, and plants for millennia. The Cassie-Baxter and Wenzel models explain how the topography and shape of surfaces greatly influence their water-hating characteristics (Wenzel, 1936; Cassie and Baxter, (1944). The existence of microscopic hairs on leaves is thought to be responsible for their superhydrophobic qualities, which have been documented in the literature. Vertical hairs are found on lady's mantle (Brewer and Willis, 2008) while horizontal hairs are being

observed on poplar leaves and ragwort (Gua *et. al.*, 2005; Ye, *et. al.* 2011). Animals with water-repellent qualities include geckos, butterflies, and water-walking arthropods. Animals and birds, like cicada, translucent butterfly wings, water-walking arthropods, and gecko foot, have some of the most well-known naturally water-repellent surfaces in the universe. Cactus spines, the skin of the filefish *Navodon septentrionalis*, shark skin (Cai, *et al.*, 2014), leafhoppers (Rakitov and Gorb, 2013), and springtail surfaces all exhibit underwater superhydrophobic qualities (Nickerl, *et. al.*, 2013 It is crucial for water repellence qualities to remain stable even after pressure that accounts for the dual action of rainfall (Nosonovsky and Bhushan, 2008).

Super hydrophobicity:

Young's State: The Young equation relates the three surface tensions of liquid-vapor, solid-vapor, and liquid-solid and predicts the contact angle between a liquid droplet and a solid surface. This prediction holds true independent of the surface chemistry (Young,1805). The Young equation explains the liquid's contact angle with a perfectly smooth, chemically homogeneous solid surface as shown in Figure 1a and explained in

$$\cos \theta = (\gamma_{sv} - \gamma_{sl}) / \gamma_{lv}$$

the following equation.

Where γ_{lv} , γ_{sv} and γ_{sl} represent the surface tensions at the interfaces between solids and liquids, respectively. A contact angle (θ) is created when a single drop of fluid (oil or water) is deposited on a solid surface. The Young equation only holds true for smooth surfaces; hence it cannot be used to describe textured surfaces. A liquid contact angle (θ) with a rough surface will be different from that of a liquid with a smooth surface since wetting surfaces are chemically diverse, they are more complicated and rougher. The effect of surface roughness on contact angle can be studied in two modes or states.

Wenzel's State: Figure 2b illustrates the contact angle model that created by Wenzel for rough surfaces, which allows liquid to completely permeate into the rough grooves (Wenzel, 1936). Due to the increase in the solid-liquid interface in the rough grooves, air bubbles may become trapped there, but only if the height of the asperities (H) is high enough. In this instance, a liquid droplet (oil or water) is present on a composite surface, and the Cassie-Baxter model is used to characterise the wetting nature as:

$$\cos \theta_w = r \cos \theta$$

$$i.e. \cos \theta_w = r (\gamma_{sv} - \gamma_{sl}) / \gamma_{lv}$$

Where the Young's contact angle (θ) is and r is the roughness ratio. The ratio of the anticipated surface area to the actual surface area is known as the roughness parameter, or r. When a surface is completely smooth, $r = 1$, and when a surface is rough, $r > 1$. The Wenzel state states that for materials having a contact angle larger than 90° (intrinsically water-hating materials), wetting is minimized by roughness.

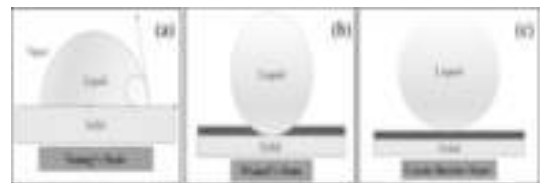


Figure 1: The wetting behaviour of a liquid droplet on a rough solid surface under three different states: a) Young's state, b) Wenzel's state, and c) Cassie-Baxter state.

Cassie- Baxter's State:

The heterogeneous state or composite state are other names for the Cassie-Baxter state. The Cassie-Baxter condition of wetting is seen in Figure 1c, where the grooves beneath the droplet are filled with vapour rather than liquid (Cassie, and Baxter, 1944). The most crucial characteristic of a coating designed to repel water is robustness. Even after being released, the substance retains its high-pressure qualities. The rise in the solid-vapor barrier at low H makes the Cassie-Baxter state a good predictor of water-repellence qualities. It also has anti-icing (heat transfer), anti-corrosion (batteries, water desalination, and ion penetration), and anti-corrosion (ion penetration) capabilities. In spite of a rise in surface roughness, the material's inherent characteristics get better. There are two phases that make up the liquid surface interface: the liquid-vapor interface and the liquid-solid interface.

$$\cos \theta_w = \phi_1 \cos \theta_1 + \phi_2 \cos \theta_2$$

The contributions of the various phases are combined to generate the apparent contact angle, where w is the apparent contact angle and 1 and 2 are the surface fractions of phases 1 and 2, respectively. Phase 1 and Phase 2's respective contact angles are 1 and 2, respectively. The solid fraction, symbolised by the Greek letter, refers to the area of a solid surface that has been moistened by a liquid when one of the surfaces is the air-liquid interface. $(1-\phi)$ represents the air fraction. Because it included the air component, in the denominator, the original equation was wrong. The air percentage should be in the numerator since it represents the portion of the surface that is not moistened by liquid.

$$\phi \cos \theta + (1 - \phi) \cos 180^\circ = \phi \cos \theta + (\phi - 1) = \cos \theta_w$$

When the surface reaches unity (1), the liquid droplet will expand out to cover the entire area. The liquid droplet will not even come close to the surface when surface = 0. For a flat surface, the solid fraction varies from 0 to 1. In this condition, the droplet can readily roll over the solid surface due to the narrow contact area between them.

Contact angle: When a surface is superhydrophobic, it displays high water contact angle ($WCA > 150^\circ$) and low water contact angle hysteresis (CSH 10°). This surface is not only self-cleaning, but also water-repellent (Su, *et al.*, 2010; Bhushan, and Her, 2010; Bormashenko, *et. al.*, 2006) Contact angle hysteresis (CHA) is the distinction between advancing and receding contact angles (Ferrari and Ravera, 2010; Nosonovsky, and Bhushan, 2008). When water droplets form on a superhydrophobic surface, they take on a nearly spherical shape and readily move when subjected to low tilting angles.

Hydrophilic Nature:

Hydrophilic compounds readily dissolve

in water and have a great attraction for it. Water-loving is the opposite of water-repelling. There are numerous uses for surfaces that attract or repel water. Figure 2a illustrates water-loving compounds that can corrode metal surfaces and alloys. Polar molecules are also described as molecules that love water. Because it can form hydrogen bonds and is frequently polar, a molecule's water-loving component can dissolve in water more quickly than its oil- or other water-hating solvent-loving counterpart. It may appear as though water molecules in the air are drawn to substances that love water. In settings with considerable condensation and for shielding exchangers from water's corrosive effects, hydrophilic coatings are very useful. Additionally, hydrophilic coatings do exceptionally well at keeping out water in hot and salty situations.

Hydrophobic Nature:

Figure 2b illustrates how the words "water-hating" and "hating water" have Greek roots that imply "phobia" and "hydrophobia," respectively. Scientists refer to nonpolar substances as being "hydrophobic" because they do not combine with water molecules. Examine that definition in more detail. Since its atoms carry a partial charge, hydro is a polar molecule. The most electronegative atom is oxygen, whose core electrons in each bond are extremely close to one another. Any charged substance will interact with hydro molecules to dissolve, whether it has a positive or negative charge. In essence, molecules that dislike water are non-polar, which means they don't have a net charge. These molecules lack any connections between charges that would enable them to interact with hydro while not having any charges. Water Hating substances frequently insoluble in water or any other solution with a predominately watery environment. In many areas of biology, including the structure of animals, cellular function, and molecular interactions, the traits of being water-hating or non-polar are crucial.



Figure 2: three different surface types: a) hydrophilic, b) hydrophobic, and 3) superhydrophobic.

Water Repellence:

Super-hydrophobic surfaces are very water-repellent, making it very difficult to wet them. On a superhydrophobic surface, a water droplet's contact angle is greater than 150° , and the difference between its advancing and receding contact angles is less than 10° . A droplet can entirely bounce after colliding with a superhydrophobic surface, much like an elastic sphere. This is also referred to as the lotus effect, after the self-cleaning properties of the leaves of the lotus plant.

Experimental Details and Results: Rosaceae Petals:

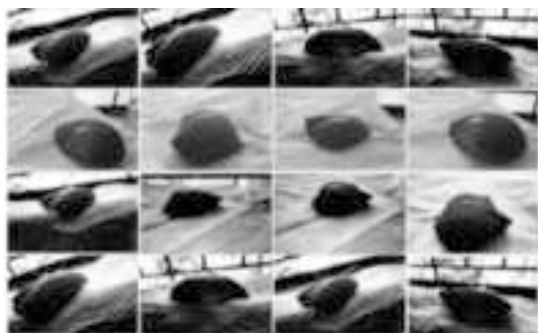


Figure 3: Images of Rosaceae petals at different times, illustrating their water-hating and water-repellence properties.

Rosaceae and the genus *Rosa* contain the most well-known flower in all of nature. The petals of Rose (*Rosa damascene*) of the family Rosaceae, are amphiphilic, meaning they have both a love of and a dislike of water. Even with the petal turned upside down, a water droplet that is small enough will slide off. High sticky forces are incompatible with water repellence. Chinese researchers have established that rose petals and water have an unusual bond that is not shared by other

plants. The micro-nanoscale topography of a rose petal comprises hills and valleys. The large valleys allow a small amount of water to soak in, creating a sticky surface on which smaller droplets can condense and stick to the petal. Since the surface of the rose petals is amphiphilic, it has both water-loving and water-hating characteristics. While the water-hating portions of the petals vigorously oppose water, the water-loving sections have a great attraction for it. The irregular topography of small valleys. Rose petals' micro-papillae produce two reactions in response to water. Larger droplets are repelled by the micro-papillae and tiny valleys. Water-hating and water-repellence are two characteristics displayed by rose petals. Following a few minutes, after 120 minutes, after 240 minutes, and after 360 minutes, it was noted that the contact angles altered during the course of the current investigation.

Asteraceae Flower:

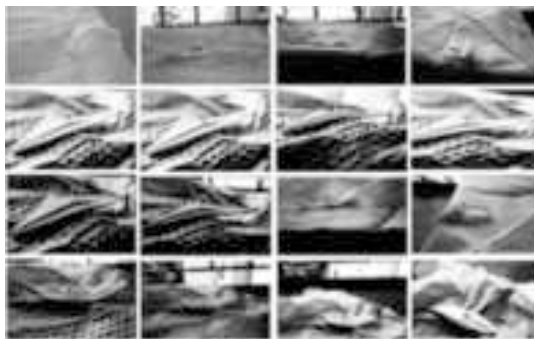


Figure 4: Images of Gerbera petals at different times, illustrating their water-loving, water-hating, and water-repellent properties.

The *Asteraceae* family's Gerbera flower is well-known. The gerbera flower is three-lobed, strap-shaped, and the individual flowers are found in the heads (Barthlott, and Neinhuis, 1997). Its aversion to water is one of its most significant characteristics. The micro-nanoscale surface area of gerbera flowers gives them the ability to both love and hate water. In the current investigation, it has been shown that the contact angles change over the first few minutes, following 120, 240 and 360 minutes.

Colocasía:

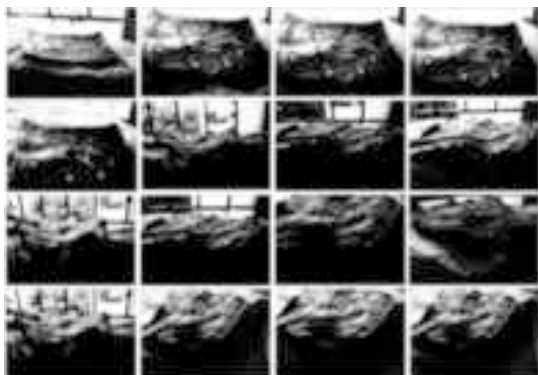


Figure 6: Images of *Colocasía* (*Araceae*) leaves at different times, illustrating their water-loving and water-repelling properties.

The elephant ears, often referred to as *Colocasía*, are the most well-known leaves in the world. Elephant ears belong to the *Araceae* family and the *Colocasía* genus. *Colocasía* leaves exhibit water-loving, water-hating, and water-repellent surface characteristics. In current investigation, it was found that the contact angles altered after a few minutes, after 120 minutes, and after 240 and 360 minutes.

Anthurium:

The genus *Anthurium* includes perennial evergreen plants that are part of the *Araceae* family. *Anthurium* plants have subterranean rhizomes and adventitious roots. *Anthurium* plants create a long-lasting, vivid spathe that comes in a variety of colours, including cream, pink, red, light red, white, dark red, green, lavender, and salmon pink. Most of the time, it is planted as a crop for cut flowers because of its spadix, which is prized for its colorful, long-lasting spathe. *Anthurium* plants are famous for their variety of colors, massive effect, and elegance.

The surface characteristics of *Anthurium* flowers in this study demonstrated both water-loving and water-repelling characteristics. The contact angles were seen to fluctuate throughout the course of the investigation at the following intervals: i.e., after 120, 240, and 360 minutes.

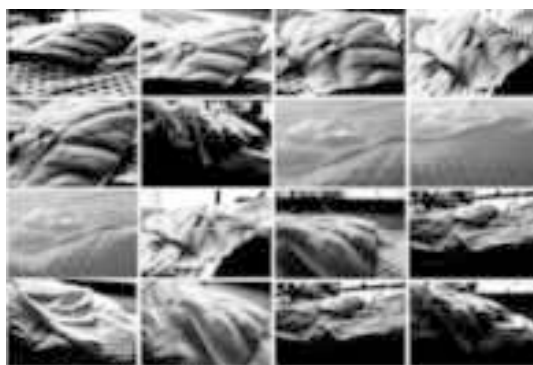


Figure 7 Images of the *Anthurium* flower (*Araceae*) are shows water loving and water hating properties at different time.

***Aloe barbadensis*:**

Aloe vera belongs to the family *Asphodelaceae* and genus *Aloe*. *Aloe barbadensis* leaves have microstructures with tiny height and high pitch values, which change the contact angle between a surface and a water droplet (Bhushan and Her, 2010). The wetting state may be reached if water impregnates between microstructures (Bormashenko, *et al.*, 2006). The hydrophobic liquid's contact area with the surface is less than in the Wenzel state but greater than in the intermediate wetting state. *Aloe barbadensis* leaves are water-loving due to their wide surface area. *Aloe barbadensis* leaves exhibit all three water-loving, water-hating, and water-repellency properties. The contact angles were seen to fluctuate throughout the course of the investigation after a few, 120, 240 and 360 minutes.

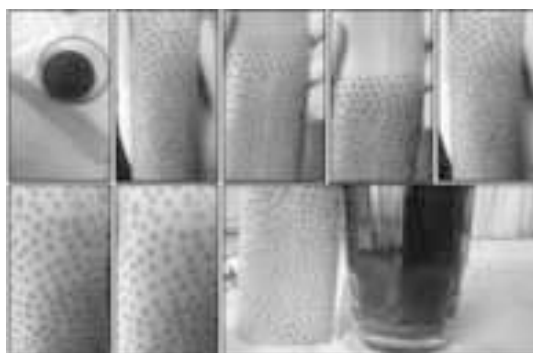


Figure 8: Asphodelaceae that simultaneously display their water-loving characteristics.

During present investigation, the water-loving, water-hating, and water-repellency qualities in Nature's exquisite materials were investigated. The rose petals were water-hating and water-repellent in nature. High adhesive forces were not always associated with water repellence. The petals of a red rose had curious relationship with water, but not for other liquids. Rose petals have a water-loving surface that strongly attracts water while water-hating surfaces strongly repel water. Rose petals had water-hating and water-repellent characteristics, but the latter is the more significant one. A surface's ability to self-clean entails that it can eliminate dirt and debris by dispersing water droplets. The leaves of *Colocasia* leaves had characteristics that attract, resist and love water. *Aloe Vera* leaf surface area demonstrated its affinity for water. Water-loving, water-hating, and water-repellent qualities were found to be present in every flower, petal and leaf. It has been shown that the contact angles change over the first few minutes, the following 120, 240 and 360 minutes.

Acknowledgements:

The authors are thankful to the Department of Botany and Physics Rajee Ramrao College, Jath.

References:

- Barthlott, W. and Neinhuis, C. (1997) *Planta* **202**:1.
- Bhushan, B. and Her, E-K. (2010) *Langmuir* **21**:8207.
- Bormashenko, E. Stein, T. Whyman, G. Bormashenko, Y and Pogreb, R. (2006) *Langmuir* **22**:9982.
- Brewer, S. A. and Willis, C. R. (2008) *Appl. Surf. Sci.* **254**:6450.
- Cai, Y. Lin, L. Xue, Z. Liu, M. Wang, S. and Jiang, L. (2014) *Adv. Funct. Mater.* **24**:809.
- Cassie, A. B. D. and Baxter, S. (1944) *Trans. Faraday Soc.* **40**:546.
- Darmanin, T. and Guittard, F. (2014) *Prog. Polym. Sci.* **39** (4): 656.
- Darmanin, T. Givenchy, E. T. D. Amigoni, S. and Guittard, F (2013) *Adv. Mater.* **25**:1378.
- Ferrari, M and Ravera, F. (2010) *Adv. Colloid Interface Sci.* **161**: 22.
- Gua, Z-Z. Wei, H-M. Zhang, R-Q, Han, G-Z. Pan, C. Zhang, H. Tian, X-J. and Chen, Z-M. (2005) *Appl. Phys. Lett.* **86**:201915.
- Nickerl, J. Helbig, R. Schulz, H-J. Werner, C. and Neinhuis, C. (2013) *Zoomorphology* **132**:183.
- Nosonovsky, M. and Bhushan, B. (2008) *Adv. Funct. Mater.* **18**:843.
- Rakitov, R. and Gorb, S. N. (2013) *Proc. R. Soc. B* **280**:20122391.
- Su, Y. Ji, B. Zhang, K. Gao, H. Huang, Y. and Hwang, K. (2010) *Langmuir* **26**:4984.
- Wenzel, R. N. (1936) *Ind. Eng. Chem.* **28**:988.
- Ye, C. Li, M. Hu, J. Cheng, Q. Jiang, L. and Song, Y. (2011) *Energy Environ. Sci.* **4**:3364.
- Young, T. (1805) *Philos. Trans. R. Soc. Lond.* **95**:65.



International Journal of Advance Studies and Growth Evaluation

Recent Progress in Fabrication of Candle Soot Modified Superhydrophobic/Superoleophilic Surfaces for Oil-Water Separation

¹ Mehejbin R Mujawar, ² Rajesh B Sawant, ³ Deepak A Kumbhar, ⁴ Sanjay S Latthe, ⁵ Ankush M Sargar and ^{*6} Shivaji R Kulal

^{1,2} Research Scholar, Department of Chemistry, Raje Ramrao Mahavidyalaya, Jath, Sangli, Maharashtra, India.

³ Assistant Professor, Department of Chemistry, Dattajirao Kadam Arts, Science and Commerce College, Ichalkarnji, Kolhapur, Maharashtra, India.

⁴ Assistant Professor, Research Laboratory, Department of Physics, Vivekanand College (Autonomous), Kolhapur, Kolhapur, Maharashtra, India.

⁵ Assistant Professor, Department of Chemistry, Bharati Vidyapeeth's Dr. Patangrao Kadam Mahavidyalaya, Sangli, Sangli, Maharashtra, India.

^{*6} Assistant Professor, Department of Chemistry, Raje Ramrao Mahavidyalaya, Jath, Sangli, Maharashtra, India.

Article Info.

E-ISSN: 2583-6528

Impact Factor (SJIF): 5.231

Peer Reviewed Journal

Available online:

www.alladvancejournal.com

Received: 12/Feb/2024

Accepted: 15/Mar/2024

Abstract

Continually occurred the oceanic oil spill accidents and discharging huge amount of industrial oily wastewater cause a serious threat to the environment. Oil and organic pollutants in water has a severe problem for aquatic life and human being. There is a need to develop technology for oil-water separation. Recently, superhydrophobic/superoleophilic sponges, metal meshes, membranes and porous materials plays crucial role to separate oil from oil-water mixture. The micro and nanopores of substrate facilitate to enter liquid into it and superhydrophobic/superoleophilic property of substrate surface resist water and allows oil to enter into the porous substrate. Carbon soot nanoparticles are hydrophobic (water repellent) in nature and has the advantages of cost-effectiveness and production scalability over other carbons like graphene, carbon nanotubes (CNTs), carbon nanodots (CNDs), etc., in their synthesis. Carbon soot based superhydrophobic/superoleophilic surfaces have outstanding water repulsion and oil absorption capacity, highly selectivity, chemical inertness and excellent recyclability. In this paper, we discussed recent progress of carbon soot based superhydrophobic/superoleophilic sponges and meshes for oil-water separation.

*Corresponding Author

Shivaji R Kulal

Assistant Professor, Department of Chemistry, Raje Ramrao Mahavidyalaya, Jath, Sangli, Maharashtra, India.

Keywords: Carbon soot, oil-water separation, sponge, stainless steel mesh and superhydrophobic.

Introduction

The oil spillage and industrial pollutants has emerged as critical issue to an ecosystem, human health, economic growth, etc. To address this challenge, several efforts have been done to separate oil and organic solvents from oil contaminated water [1-2]. The various methods such as spray coating, dip-coating, hydrothermal method, chemical vapour deposition, surface etching, solvothermal method, layer-by-layer assembly and electrochemical treatment have been used to prepare superhydrophobic/superoleophilic coating on sponge and mesh surface [3]. The ideal superhydrophobic/superoleophilic meshes and sponges must have following characteristics, such as fine selectivity toward various oils, high separation efficiency, reusability and along with high mechanical, chemical, and thermal stability [4].

The superhydrophobic/superoleophilic surfaces have shown water contact angle (WCA) over 150°, sliding angle < 10° and oil contact angle < 5° [5]. The traditional technologies, including in situ burning, bioremediation, chemical dispersant methods, skimming, and sorbents are used for oil-water separation. However, many of these technologies involve energy intensive and slow processes, have low oil-water separation capacities or create secondary pollution during the oil-water separation process, restricting their widespread practical applications [6-8]. Different strategies used for formation of hierarchical structures such as sol-gel coating, chemical vapor deposition, plasma etching, template processing, lithographic patterning, etc. have been adopted [9-10].

Carbon soot (CS) generated from incomplete combustion of paraffin wax has demonstrated the advantages of cost effectiveness and production scalability over carbon nanotubes (CNTs), graphene and activated carbons in their synthesis. Hence, the carbon soot coated superhydrophobic/superoleophilic surfaces shows excellent oil-water separation ability rather than carbon nanotubes, carbon nanodots and graphene [11].

Song *et al.* [12] have fabricated carbon soot (CS) coated mesh using dip-coating method. The cleaned stainless-steel mesh (SSM) was subsequently dipped in the glue solution for 10 min and CS-dispersion, finally dried at 80°C to obtain the CS-glue coated mesh. The CS coating is close packed because of using superglue (EVO-STIK Serious Glue) as a binder. The CS-glue coated mesh revealed the separation efficiency higher than 99.95%. Even after 20 cycle separation tests, it was shown excellent reusability and durability. The different chemical methods are used for the fabrication of the superhydrophobic/superoleophilic meshes/sponges for efficient oil-water separation. As the carbon nanotubes are hydrophobic in nature and it shows strong affinity toward oil, Lee *et al.* [13] adopted chemical vapor deposition (CVD) technique to deposit vertically aligned CNTs on stainless steel (SS) mesh. The as-prepared SS-CNT mesh effectively separates oil from water-in-oil emulsions with efficiency higher than 80%. Gu *et al.* [14] prepared polystyrene (PS) and carbon nanotubes coated superhydrophobic/superoleophilic membrane. The as-prepared superhydrophobic/superoleophilic membrane shows mechanically robust PS-CNT surface shows excellent oil separation from oil-water mixture with good repeatability and separation efficiency of more than 99%. Electrospinning technique can be effectively used to form superhydrophobic/superoleophilic surfaces. Wang *et al.* [15] prepared the polyurethane (PU) sponge from hydrophilic to superhydrophobic by dip coating it from the nanocomposite of CNT/poly-(dimethyl siloxane) (PDMS). The as-prepared superhydrophobic/superoleophilic sponge shows the continuous removal of various oils such as Soybean oil, motor oil, diesel, n-hexadecane, gasoline, and n-hexane from the surface of the water with high separation efficiency.

In this article, we will discuss on the simple, low-cost, rapid and innovative methods for the fabrication of superhydrophobic/superoleophilic carbon soot nanoparticle coated sponges and meshes for efficient oil-water separation application.

Recent Developments for Effective Oil-Water Separation Superhydrophobic-Superoleophilic Sponge

Hydrophobic candle soot (CS) particles can be collected easily and cost effectively from the candle flame. Li *et al.* [16] obtained the hydrophobic CS particles by incomplete combustion of hydrocarbons from the mid-candle flame. The polyurethane sponge immersed in the mixture of CS, hydrophobic silica nanoparticles, and PU resin to achieve stable superhydrophobicity. The CS-SiO₂-PU sponge showed excellent oil separation capacity from hot water and acidic, alkaline, and salt solutions. The CS-SiO₂-PU sponges could absorb a various oil efficiently and selectively, and show high absorption capacity that is up to 65 times of its own weight. Furthermore, the CS-SiO₂-PU sponge possesses stable superhydrophobicity and excellent ability of selective absorption to oil even at various harsh conditions, including acid (1M HCl) and alkali (1M NaOH), and salt (1M NaCl) aqueous solutions at mechanical agitation condition, hot water and ice/water mixtures. The CS-SiO₂-PU sponge combination

with a vacuum system could continuously absorb and remove oil from water surface. As shown in (Fig. 1a), the contact angle of coloured water droplet on the PU sponge is nearly 100° and the coloured kerosene droplet contact angle is about 0°. However, the CS-SiO₂-PU sponge shows superhydrophobicity and superoleophobicity simultaneously (Fig. 1b). The kerosene droplet was absorbed by the CS-SiO₂-PU sponge immediately when it was dropped on the surface of sponge, while the water droplet stayed on the surface of as-prepared sponge and kept its spherical shape. As shown in (Fig. 1c and d), the water contact angle on the CS-SiO₂-PU sponge is up to 155° and the SA is as low as 7°. Therefore, the water was repelled by the as-prepared sponge, whereas the oil absorbed through the sponge quickly.

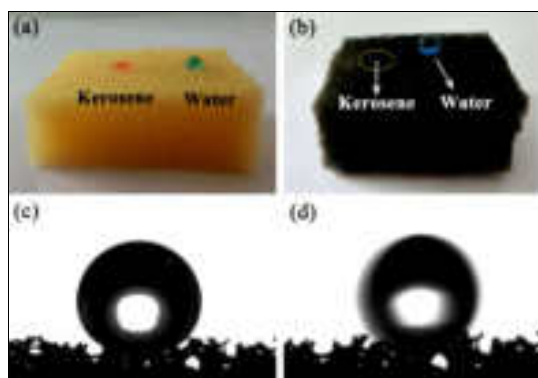


Fig 1: (a and b) Schematic illustration of the fabrication the wettability of the pristine PU sponge and the CS-SiO₂-PU sponge to water and oil droplets, respectively. (c and d) The CA and SA of water on the CS-SiO₂-PU sponge, respectively [16], with permission from J. Sol-Gel Sci Technol., Copyright 2017.

Beshkar *et al.* [17] prepared durable magnetic superhydrophobic PU sponge by immersing it in the colloidal solution of straw candle soot (carbon nanoparticles) and further modification was done by Fe₂O₄ nanoparticles and PDMS. The waste oil was easily collected from the surface of water through guiding the magnetic superhydrophobic polyurethane (PU) sponge by a bar magnet. The wettability of sponge remained unchanged even after 30 absorption/desorption cycles. The oil-water separation experiments were performed using the as-prepared optimized superhydrophobic sponge to absorbing of waste oil. The schematic of experimental protocol for preparation and operation superhydrophobic/superoleophilic magnetic straw soot sponge is shown in Fig. 2. It was indicated that the superhydrophobic sponge is taken by a magnet bar and absorbs waste oil completely from the oil-water mixture within 10 seconds.

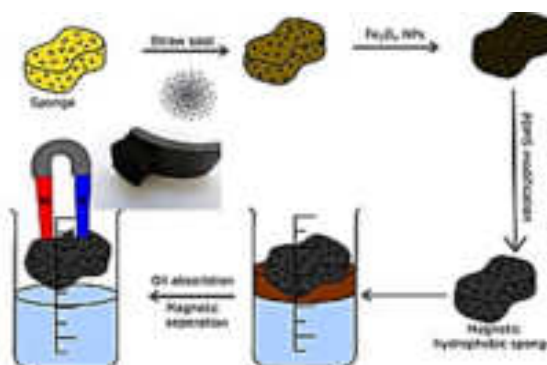


Fig 2: Schematic illustration of preparation of modified polyurethane sponge and oil separation process. Images reprinted from [17], with permission from Elsevier, Copyright 2017.

Gao *et al.* [18] obtained the candle soot (CS) particles from combustion flame and dispersed it in 1,2-dichloroethane (DCE). The superhydrophobic/superoleophilic melamine sponge prepared by a uniform coating of as-grown CS-DCE solution using dip-coating method. The CS-modified sponge exhibited strong water repellency and oil absorbency without further chemical modification (Fig. 3. a and b). An easy and fast recovery of engine oil floating on the water surface by CS-modified sponge confirms its high oil-water separation efficiency (Fig. 3. c-e). The CS-modified sponge could absorb numerous oils and organic solvents with an absorption capacity of 25-80 times of its own weight. Oil can be recycled for more than 10 times with absolutely no change in an oil absorption capacity and wettability of the CS-modified sponge.

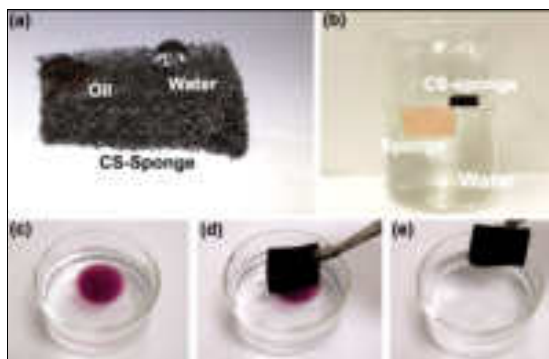


Fig 3: Schematic showing (a) Photograph of water and oil droplets on the surface of a CS-sponge. (b) Photograph of pure and CS-sponges placed on water. (c-e) Photographs demonstrating the removal of an oil droplet from water using a CS-sponge [18], with permission from American Chemical Society, Copyright 2014.

Yue *et al.* [19] the superhydrophobic surface was fabricated by using PVDF and candle soot via sugar template method. It was shown the water contact angle of 158° and roll-on angle of $<6^\circ$. The oil quickly absorbed by superhydrophobic sponge shows the superoleophilic property. The sponge shows excellent oil-water separation property even after 25 cycles. The strong elasticity, high stretching resistance confirms that the modified superhydrophobic surface is highly mechanical durable. The modified sponge maintains the 89% of recovery rate even after 10 cycles. The absorption capability recovered up to 96% without obvious change of morphology of the sponge surface. This method was used to prepare a photothermal, porous PVDF/CS sponge with structural, chemical and mechanical property [19]. Fig. 4 shows that the preparation process of the porous PVDF/candle soot sponge. In short, sugar particles were placed into a mixture of PVDF/DMF/CS solution, followed by removing sugar templates via the water dissolving. It is important to note that a simple sugar-templating process was used for formation of superhydrophobic sponge, it requires only a simple as well as eco-friendly preparation process.

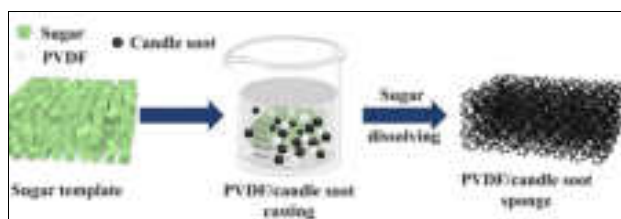


Fig 4: Schematic illustration of the fabrication of porous PVDF/candle soot sponge using sugar template. Images reprinted from [19], with permission from Elsevier, Copyright 2021.

Superhydrophobic/Superoleophilic Mesh

Li *et al.* [20] deposited hydrophobic CS particles on a SS mesh by holding it in the mid-flame of paraffin candle and then spray coated the hydrophobic silica nanoparticles (50 nm) on it. The as-prepared carbon soot/silica nanoparticles (CS/SiO₂) hybrid mesh revealed strong repellence toward pure water and droplets of pH ranging from 1 to 14, whereas the oil drops quickly spread on the surface. The hybrid mesh revealed strong ability to separate various oils and organic liquids mixed in pure water, hot water (92°C), and strong corrosive solutions (1M HCl, NaOH, and NaCl) with more than 98% of separation efficiency. The oil/water separation was performed as shown in Fig. 5. Because of the excellent mechanical flexibility of the stainless-steel mesh, the mesh was folded into a three-dimensional structure, then coated with CS and hydrophobic silica for oil/water separation. The coated mesh was placed on beaker and mixture of kerosene and water was poured onto the three-dimensional superhydrophobic mesh, as shown in Fig. 5a-c. Kerosene was dropped into the beaker, while water was repelled and retained above the mesh. Fig. 5d exhibited that there are no oily droplets were present in the water. After the separation, nearly equal amount of water and kerosene were collected, which was suggested that extremely high separation efficiency of the coated mesh as shown in Fig. 5e.

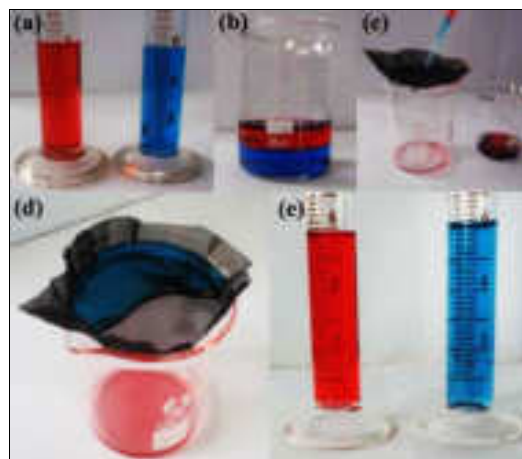


Fig 5: Schematic illustration of the separation process of oil (kerosene)/water mixture based on the CS and silica overlap coated mesh. (a-b) water is dyed with methylene blue and oil is dyed with Oil Red O and then they are mixed before separation. (c-d) the separation process of the oil/water mixture using the overlap coated mesh. (e) The water and oil volume keep nearly the same after separation [20], with permission from RSC Nanoscale, Copyright 2016.

Cao *et al.* [21] used the electrodeposition technique for the formation of superhydrophobic/superoleophilic copper meshes and then held it above candle flame to deposit carbon soot (CS) nanoparticles. The agglomerated CS nanoparticles formed a chain like rough hierarchical structure on which water drop exhibited contact angle higher than 153° . The CS deposited copper mesh quickly separated various oils such as silicone oil, cyclohexane, n-hexane, n-heptane, petroleum ether, and liquid paraffin from oil-water mixtures with oil separation efficiency greater than 90% even after 30 separation cycles. The rough mesh was placed on 1.5 cm height of flame of burning candle for deposition for 5 minutes, the whole preparation process is shown in the fig. 6, the superhydrophobic mesh surface was formed by using candle soot.

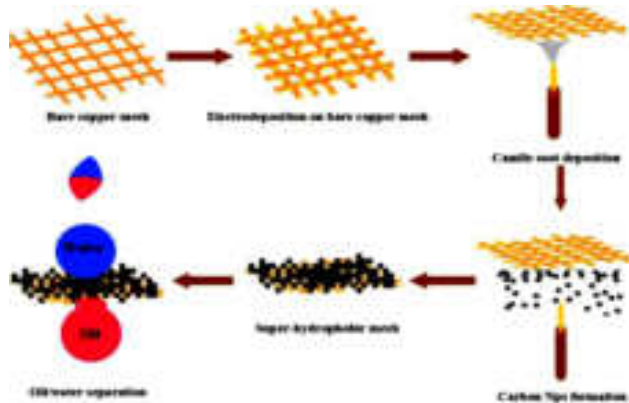


Fig 6: Schematic illustration of the preparation process of superhydrophobic and super-oleophilic copper mesh, and the application in oil-water separation [21], with permission from Colloids and Surfaces A: Physicochem. Eng. Aspects, Copyright 2017.

Zulfiquar *et al.* [22] deposited cheaply available sawdust on polychloroprene adhesive-coated SS mesh with subsequent deposition of silicone polymer by dip coating. Thereafter, a thin layer of CS particles was applied on the as-prepared mesh by holding above a candle flame. The carbon soot (CS) nanoparticles uniformly deposited on silicone covered SD exhibited highly rough and porous morphology required for superhydrophobicity and superoleophobicity. As depicted in Fig. 7, a superhydrophobic SS mesh easily and rapidly separated oil-water mixture. No trace of water was observed in separated oil confirming its potential in oil-water separation capability. Apart from excellent oil-water separation efficiency (>95%), the superhydrophobic SS mesh exhibited good recyclability, reusability, and mechanical stability. The potential of these coatings for oil/water separation is shown in Fig. 7. The figure typically shows a mesh coated with superhydrophobic material holding water without any leakage. The superhydrophobic mesh was used for the separation of oil from oil-water mixtures as shown in Fig. 7. The mesh readily separated the oil while blocking the flow of water through its pores. The water content was not found in the separated oil, which confirms the excellent superhydrophobic/superoleophilic property. The steel mesh with excellent mechanical stability modified with durable superhydrophobic coating can be used as a medium for oil/water separation.

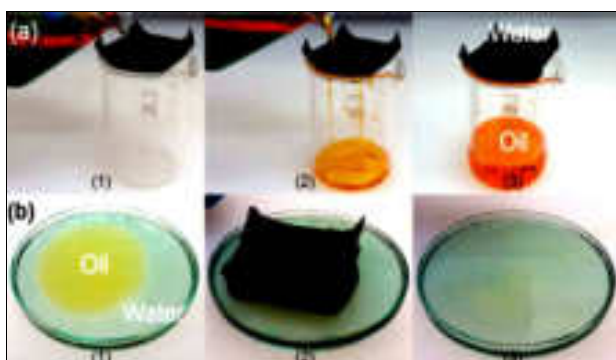


Fig 7: Schematic illustration of a superhydrophobic mesh demonstrating (a) the separation of oil/water mixture and (b) collection of oil from oil/water mixture [22], with permission from Colloids and Surfaces A: Physicochem. Eng. Aspects, Copyright 2017.

Chen *et al.* [23] synthesized a superhydrophobic surfaces by simply placing the stainless steel (SS) on the middle of candle flame for deposition of carbon soot (CS) on the SS mesh. The

candle soot coated substrate together with SiCl₄ was placed in a drier for chemical vapour deposition. Then, though calcination at 600°C for half in air, CS composed NPs thermally degraded and diffused through the silica shell gradually. It was shows excellent oil-water separation efficiency even after 30 times recycling use of modified superhydrophobic surfaces. The superhydrophobic coating revealed excellent separation efficiency even after 6 times reuses of same superhydrophobic surface. It could be potentially used in optical and visual application scenarios were in harsh, oily environments, like goggles, building façade, visual oil-water separation device, touch screen, etc. As shown in Fig. 8, the cheap and accessible candle soot were used for formation of a rough surface template to directly deposition on the substrate. The candle soot was formed carbon nanoparticles forming by incompletely burned paraffin, which loosely bounded on the substrate and formed a rough surface. Finally, a hard and porous silica shell was deposited on the candle soot template through chemical vapor deposition of SiCl₄ like Stober reaction, which completely formed the roughness of the template and a robust rough surface.

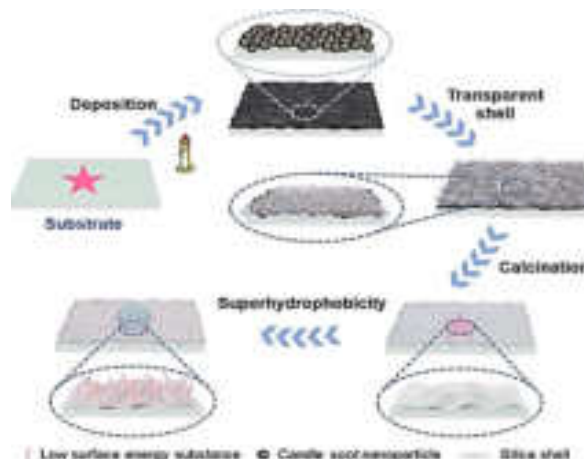


Fig 8: Schematic of preparation and properties of the transparent and robust superhydrophobic coating and oil-water separation. Images reprinted from [23], with permission from Nature, Copyright 2022.

Conclusion

As this review highlights, carbon soot nanoparticles are unique in that, their fabrication requires little control of external parameters. It is beneficial economically, facile and straightforward to synthesize. The carbon soot nanoparticles coated sponges and mesh has been developed by using carbon soot nanoparticles and different polymers. The absorption/separation investigation demonstrates that, the carbon soot surface is highly efficient and stable in absorbing a wide range of oil and organic solvents. It can be believed that, the carbon soot coated superhydrophobic materials are very useful for oil-water separation. The carbon soot synthesis, carbon soot coated sponge/mesh preparation, procedures are simple, cost-effective and scalable. The absorption/separation investigation demonstrates that, the carbon soot sponge/mesh is highly efficient and stable in absorbing a wide range of oil and organic solvents. It can be believed that, the carbon soot coated superhydrophobic surfaces are very useful for oil-water separation. It shows various tremendous results with carbon soot-polymer composite in various mechanical conditions. A carbon soot nanoparticle shows significant surface area to volume ratio, high electronic and ionic conductivity. Carbon soot is

produced by simply burning of candles and hence, it is ecofriendly, economical and useful. Carbon soot coated sponge and mesh can show stability, durability, reusability and reproducibility. Hence, this review is helpful to upcoming researchers to develop highly scalable superhydrophobic surfaces for efficient oil-water separation applications.

Acknowledgement

One of the authors R. B. Sawant is grateful to Chhatrapati Shahu Maharaj Research, Training and Human Development Institute (SARTHI) Fellowship, Govt. of Maharashtra, India.

References

- Alaaeddin A, Brian JS, Leilei X, Yuhan L, Damian EH, William RD. Rapid removal of organic micropollutants from water by a porous β -cyclodextrin polymer. *Nature*. 2016; 529:190-194.
- Yong L, Zhaozhu Z, Bo G, Xuehu M, Qunji X. One-pot, template-free synthesis of robust superhydrophobic polymer monolith with adjustable hierarchical porous structure. *Green Chem*. 2016; 18:5266-5272.
- Qinglang M, Hongfei C, Anthony GF, Rong W, Hua Z. Recent Development of Advanced Materials with Special Wettability for Selective Oil/Water Separation. *Small*. 2016; 12:2186-2202.
- Lingxiao L, Bucheng L, Jie D, Junping Z. Roles of silanes and silicones in forming superhydrophobic and superoleophobic materials. *J. Mater. Chem. A*. 2016; 4:13677-13725.
- Jianan S, Haiyang W, Ziwei L, Yuanzheng L, Zhenglian L, Haolun W, Xiaoyan L, Minghao F, Bo L, Hui W. Large-scale blow spinning of carbon microfiber sponge as efficient and recyclable oil sorbent. *Chemical Engineering Journal*. 2018; 343:638-644.
- Zhenxing W, Yanchao X, Yuyan Li, Lu S. A Novel Mussel-Inspired Strategy toward Superhydrophobic Surface for Self-Driven Crude Oil Spill Cleanup. *J. Mater. Chem. A*. 2015; 3:266-273.
- Jin J L, Li T Z, Zheng HL. Electrospun fibrous membrane with enhanced switchable oil/water wettability for oily water separation. *Chem. Eng. J*. 2016; 287:474-481.
- Alireza K, Hamid Z, Amir A, Ahmad A. Enhancing oil removal from water by immobilizing multi-wall carbon nanotubes on the surface of polyurethane foam. *Journal of Environ. Management*. 2015; 157:279-286.
- Guina R, Yuanming S, Xiangming L, Yanli Z, Zhaozhu Z, Xiaotao Z. A superhydrophobic copper mesh as an advanced platform for oil-water separation. *Applied Surface Science*. 2018; 428:520-525.
- Ebenezer KS, Daniel KS, Xiaomeng L, Botao L, Xinxin X, Shanhe G. *et al.* Recent development in the fabrication of self-healing superhydrophobic surfaces. *Chemical Engineering Journal*. 2019; 19:3012-3018.
- Kwangseok S, Minyoung K, Do HK. Candle-based process for creating a stable superhydrophobic surface. *CARBON*. 2014; 68:583-596.
- Jiajia S, Na L, Jiakai L, Yingze C, Haijie C. Facile Fabrication of Highly Hydrophobic Onion-Like Candle Soot-Coated Mesh for Durable Oil/Water Separation. *Nanomaterials*. 2022; 12:761-772.
- Chee HL, Nick J, Jaroslaw D, Yoke KY. The performance of superhydrophobic and superoleophilic carbon nanotube meshes in water-oil filtration. *CARBON*. 2011; 49:669-676.
- Jincui G, Peng X, Jing C, Fu L, Youju H, Gaiye L, Jiawei Z, Tao C. Robust preparation of superhydrophobic polymer/ carbon nanotube hybrid membranes for highly effective removal of oils and separation of water-in-oil emulsions. *J. Mater. Chem. A*. 2014; 2:15268-15272.
- Chih FW, Sheng JL. Robust Superhydrophobic/Superoleophilic Sponge for Effective Continuous Absorption and Expulsion of Oil Pollutants from Water. *ACS Appl. Mater. Interfaces*. 2013; 5:8861-8864.
- Jian L, Zhihong Z, Ruimei K, Yan Z, Weizhong L, Mouji L, Runan J, Liangjie L. Robust superhydrophobic candle soot and silica composite sponges for efficient oil/water separation in corrosive and hot water. *J. Sol-Gel Sci. Technol*. 2017; 3:817-826.
- Farshad B, Hossein K, Masoud SN. Recyclable Magnetic Superhydrophobic Straw Soot Sponge for Highly Efficient Oil/water Separation. *J. Colloid Interface Sci*. 2017; 497:57-65.
- Yang G, Yun SZ, Wei X, Mengmeng W, Lisha F, Hossein RG. *et al.* Highly Efficient and Recyclable Carbon Soot Sponge for Oil Cleanup. *ACS Appl. Mater. Interfaces*. 2014; 6:5924-5929.
- Xuejie Y, Ziqi Z, Tao Z, Dongya Y, Jicheng X, Fengxian Q. Simply realizing durable PVDF/candle soot foam with excellent solar absorption for solar-assisted recovery of heavy oil spill. *Elsevier*. 2021; 7:1-7.
- Jian L, Ruimei K, Xiaohua T, Houde S, Yaoxia Y, Fei Z. Superhydrophobic meshes that can repel hot water and strong corrosive liquids used for efficient gravity-driven oil/water separation. *Nanoscale*. 2016; 8:7638-7645.
- Huaijie C, Jingyuan F, Ying L, Shougang C. Facile Design of Superhydrophobic and Superoleophilic Copper Mesh Assisted by Candle Soot for Oil Water Separation. *Colloids Surf. A Physicochem. Eng. Asp*. 2018; 537:294-302.
- Usama Z, Syed ZH, Tayyab S, Irshad H, Habib R. Mechanically robust superhydrophobic coating from sawdust particles and carbon soot for oil/water separation. *Colloids Surf. A Physicochem. Eng. Asp*. 2018; 539:391-398.
- Baiyi C, Rongrong Z, Hexuan F, Jiadai X, Yuan J, Guohe X, Bin W, Xu H. Efficient oil-water separation coating with robust superhydrophobicity and high transparency. *Scientific Reports*. 2022; 8:1-9.



International Journal of Advance Studies and Growth Evaluation

Recent Progress in Fabrication of Candle Soot Modified Superhydrophobic/Superoleophilic Surfaces for Oil-Water Separation

¹ Mehejbin R Mujawar, ² Rajesh B Sawant, ³ Deepak A Kumbhar, ⁴ Sanjay S Latthe, ⁵ Ankush M Sargar and ^{*6} Shivaji R Kulal

^{1,2} Research Scholar, Department of Chemistry, Raje Ramrao Mahavidyalaya, Jath, Sangli, Maharashtra, India.

³ Assistant Professor, Department of Chemistry, Dattajirao Kadam Arts, Science and Commerce College, Ichalkarnji, Kolhapur, Maharashtra, India.

⁴ Assistant Professor, Research Laboratory, Department of Physics, Vivekanand College (Autonomous), Kolhapur, Kolhapur, Maharashtra, India.

⁵ Assistant Professor, Department of Chemistry, Bharati Vidyapeeth's Dr. Patangrao Kadam Mahavidyalaya, Sangli, Sangli, Maharashtra, India.

^{*6} Assistant Professor, Department of Chemistry, Raje Ramrao Mahavidyalaya, Jath, Sangli, Maharashtra, India.

Article Info.

E-ISSN: 2583-6528

Impact Factor (SJIF): 5.231

Peer Reviewed Journal

Available online:

www.alladvancejournal.com

Received: 12/Feb/2024

Accepted: 15/Mar/2024

Abstract

Continually occurred the oceanic oil spill accidents and discharging huge amount of industrial oily wastewater cause a serious threat to the environment. Oil and organic pollutants in water has a severe problem for aquatic life and human being. There is a need to develop technology for oil-water separation. Recently, superhydrophobic/superoleophilic sponges, metal meshes, membranes and porous materials plays crucial role to separate oil from oil-water mixture. The micro and nanopores of substrate facilitate to enter liquid into it and superhydrophobic/superoleophilic property of substrate surface resist water and allows oil to enter into the porous substrate. Carbon soot nanoparticles are hydrophobic (water repellent) in nature and has the advantages of cost-effectiveness and production scalability over other carbons like graphene, carbon nanotubes (CNTs), carbon nanodots (CNDs), etc., in their synthesis. Carbon soot based superhydrophobic/superoleophilic surfaces have outstanding water repulsion and oil absorption capacity, highly selectivity, chemical inertness and excellent recyclability. In this paper, we discussed recent progress of carbon soot based superhydrophobic/superoleophilic sponges and meshes for oil-water separation.

*Corresponding Author

Shivaji R Kulal

Assistant Professor, Department of Chemistry, Raje Ramrao Mahavidyalaya, Jath, Sangli, Maharashtra, India.

Keywords: Carbon soot, oil-water separation, sponge, stainless steel mesh and superhydrophobic.

Introduction

The oil spillage and industrial pollutants has emerged as critical issue to an ecosystem, human health, economic growth, etc. To address this challenge, several efforts have been done to separate oil and organic solvents from oil contaminated water [1-2]. The various methods such as spray coating, dip-coating, hydrothermal method, chemical vapour deposition, surface etching, solvothermal method, layer-by-layer assembly and electrochemical treatment have been used to prepare superhydrophobic/superoleophilic coating on sponge and mesh surface [3]. The ideal superhydrophobic/superoleophilic meshes and sponges must have following characteristics, such as fine selectivity toward various oils, high separation efficiency, reusability and along with high mechanical, chemical, and thermal stability [4].

The superhydrophobic/superoleophilic surfaces have shown water contact angle (WCA) over 150°, sliding angle < 10° and oil contact angle < 5° [5]. The traditional technologies, including in situ burning, bioremediation, chemical dispersant methods, skimming, and sorbents are used for oil-water separation. However, many of these technologies involve energy intensive and slow processes, have low oil-water separation capacities or create secondary pollution during the oil-water separation process, restricting their widespread practical applications [6-8]. Different strategies used for formation of hierarchical structures such as sol-gel coating, chemical vapor deposition, plasma etching, template processing, lithographic patterning, etc. have been adopted [9-10].

Carbon soot (CS) generated from incomplete combustion of paraffin wax has demonstrated the advantages of cost effectiveness and production scalability over carbon nanotubes (CNTs), graphene and activated carbons in their synthesis. Hence, the carbon soot coated superhydrophobic/superoleophilic surfaces shows excellent oil-water separation ability rather than carbon nanotubes, carbon nanodots and graphene [11].

Song *et al.* [12] have fabricated carbon soot (CS) coated mesh using dip-coating method. The cleaned stainless-steel mesh (SSM) was subsequently dipped in the glue solution for 10 min and CS-dispersion, finally dried at 80°C to obtain the CS-glue coated mesh. The CS coating is close packed because of using superglue (EVO-STIK Serious Glue) as a binder. The CS-glue coated mesh revealed the separation efficiency higher than 99.95%. Even after 20 cycle separation tests, it was shown excellent reusability and durability. The different chemical methods are used for the fabrication of the superhydrophobic/superoleophilic meshes/sponges for efficient oil-water separation. As the carbon nanotubes are hydrophobic in nature and it shows strong affinity toward oil, Lee *et al.* [13] adopted chemical vapor deposition (CVD) technique to deposit vertically aligned CNTs on stainless steel (SS) mesh. The as-prepared SS-CNT mesh effectively separates oil from water-in-oil emulsions with efficiency higher than 80%. Gu *et al.* [14] prepared polystyrene (PS) and carbon nanotubes coated superhydrophobic/superoleophilic membrane. The as-prepared superhydrophobic/superoleophilic membrane shows mechanically robust PS-CNT surface shows excellent oil separation from oil-water mixture with good repeatability and separation efficiency of more than 99%. Electrospinning technique can be effectively used to form superhydrophobic/superoleophilic surfaces. Wang *et al.* [15] prepared the polyurethane (PU) sponge from hydrophilic to superhydrophobic by dip coating it from the nanocomposite of CNT/poly-(dimethyl siloxane) (PDMS). The as-prepared superhydrophobic/superoleophilic sponge shows the continuous removal of various oils such as Soybean oil, motor oil, diesel, n-hexadecane, gasoline, and n-hexane from the surface of the water with high separation efficiency.

In this article, we will discuss on the simple, low-cost, rapid and innovative methods for the fabrication of superhydrophobic/superoleophilic carbon soot nanoparticle coated sponges and meshes for efficient oil-water separation application.

Recent Developments for Effective Oil-Water Separation Superhydrophobic-Superoleophilic Sponge

Hydrophobic candle soot (CS) particles can be collected easily and cost effectively from the candle flame. Li *et al.* [16] obtained the hydrophobic CS particles by incomplete combustion of hydrocarbons from the mid-candle flame. The polyurethane sponge immersed in the mixture of CS, hydrophobic silica nanoparticles, and PU resin to achieve stable superhydrophobicity. The CS-SiO₂-PU sponge showed excellent oil separation capacity from hot water and acidic, alkaline, and salt solutions. The CS-SiO₂-PU sponges could absorb a various oil efficiently and selectively, and show high absorption capacity that is up to 65 times of its own weight. Furthermore, the CS-SiO₂-PU sponge possesses stable superhydrophobicity and excellent ability of selective absorption to oil even at various harsh conditions, including acid (1M HCl) and alkali (1M NaOH), and salt (1M NaCl) aqueous solutions at mechanical agitation condition, hot water and ice/water mixtures. The CS-SiO₂-PU sponge combination

with a vacuum system could continuously absorb and remove oil from water surface. As shown in (Fig. 1a), the contact angle of coloured water droplet on the PU sponge is nearly 100° and the coloured kerosene droplet contact angle is about 0°. However, the CS-SiO₂-PU sponge shows superhydrophobicity and superoleophobicity simultaneously (Fig. 1b). The kerosene droplet was absorbed by the CS-SiO₂-PU sponge immediately when it was dropped on the surface of sponge, while the water droplet stayed on the surface of as-prepared sponge and kept its spherical shape. As shown in (Fig. 1c and d), the water contact angle on the CS-SiO₂-PU sponge is up to 155° and the SA is as low as 7°. Therefore, the water was repelled by the as-prepared sponge, whereas the oil absorbed through the sponge quickly.

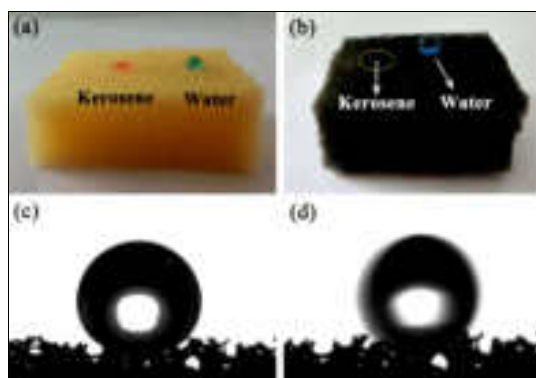


Fig 1: (a and b) Schematic illustration of the fabrication the wettability of the pristine PU sponge and the CS-SiO₂-PU sponge to water and oil droplets, respectively. (c and d) The CA and SA of water on the CS-SiO₂-PU sponge, respectively [16], with permission from J. Sol-Gel Sci Technol., Copyright 2017.

Beshkar *et al.* [17] prepared durable magnetic superhydrophobic PU sponge by immersing it in the colloidal solution of straw candle soot (carbon nanoparticles) and further modification was done by Fe₂O₄ nanoparticles and PDMS. The waste oil was easily collected from the surface of water through guiding the magnetic superhydrophobic polyurethane (PU) sponge by a bar magnet. The wettability of sponge remained unchanged even after 30 absorption/desorption cycles. The oil-water separation experiments were performed using the as-prepared optimized superhydrophobic sponge to absorbing of waste oil. The schematic of experimental protocol for preparation and operation superhydrophobic/superoleophilic magnetic straw soot sponge is shown in Fig. 2. It was indicated that the superhydrophobic sponge is taken by a magnet bar and absorbs waste oil completely from the oil-water mixture within 10 seconds.

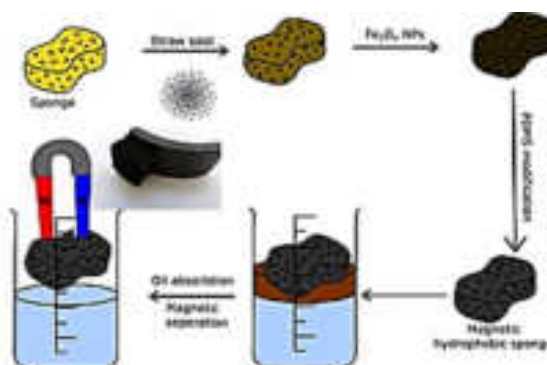


Fig 2: Schematic illustration of preparation of modified polyurethane sponge and oil separation process. Images reprinted from [17], with permission from Elsevier, Copyright 2017.

Gao *et al.* [18] obtained the candle soot (CS) particles from combustion flame and dispersed it in 1,2-dichloroethane (DCE). The superhydrophobic/superoleophilic melamine sponge prepared by a uniform coating of as-grown CS-DCE solution using dip-coating method. The CS-modified sponge exhibited strong water repellency and oil absorbency without further chemical modification (Fig. 3. a and b). An easy and fast recovery of engine oil floating on the water surface by CS-modified sponge confirms its high oil-water separation efficiency (Fig. 3. c-e). The CS-modified sponge could absorb numerous oils and organic solvents with an absorption capacity of 25-80 times of its own weight. Oil can be recycled for more than 10 times with absolutely no change in an oil absorption capacity and wettability of the CS-modified sponge.

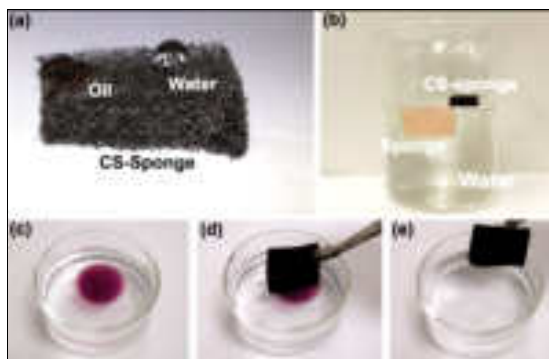


Fig 3: Schematic showing (a) Photograph of water and oil droplets on the surface of a CS-sponge. (b) Photograph of pure and CS-sponges placed on water. (c-e) Photographs demonstrating the removal of an oil droplet from water using a CS-sponge [18], with permission from American Chemical Society, Copyright 2014.

Yue *et al.* [19] the superhydrophobic surface was fabricated by using PVDF and candle soot via sugar template method. It was shown the water contact angle of 158° and roll-on angle of $<6^\circ$. The oil quickly absorbed by superhydrophobic sponge shows the superoleophilic property. The sponge shows excellent oil-water separation property even after 25 cycles. The strong elasticity, high stretching resistance confirms that the modified superhydrophobic surface is highly mechanical durable. The modified sponge maintains the 89% of recovery rate even after 10 cycles. The absorption capability recovered up to 96% without obvious change of morphology of the sponge surface. This method was used to prepare a photothermal, porous PVDF/CS sponge with structural, chemical and mechanical property [19]. Fig. 4 shows that the preparation process of the porous PVDF/candle soot sponge. In short, sugar particles were placed into a mixture of PVDF/DMF/CS solution, followed by removing sugar templates via the water dissolving. It is important to note that a simple sugar-templating process was used for formation of superhydrophobic sponge, it requires only a simple as well as eco-friendly preparation process.

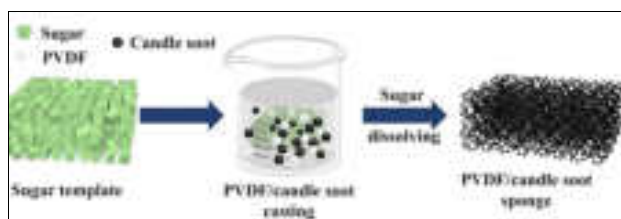


Fig 4: Schematic illustration of the fabrication of porous PVDF/candle soot sponge using sugar template. Images reprinted from [19], with permission from Elsevier, Copyright 2021.

Superhydrophobic/Superoleophilic Mesh

Li *et al.* [20] deposited hydrophobic CS particles on a SS mesh by holding it in the mid-flame of paraffin candle and then spray coated the hydrophobic silica nanoparticles (50 nm) on it. The as-prepared carbon soot/silica nanoparticles (CS/SiO₂) hybrid mesh revealed strong repellence toward pure water and droplets of pH ranging from 1 to 14, whereas the oil drops quickly spread on the surface. The hybrid mesh revealed strong ability to separate various oils and organic liquids mixed in pure water, hot water (92°C), and strong corrosive solutions (1M HCl, NaOH, and NaCl) with more than 98% of separation efficiency. The oil/water separation was performed as shown in Fig. 5. Because of the excellent mechanical flexibility of the stainless-steel mesh, the mesh was folded into a three-dimensional structure, then coated with CS and hydrophobic silica for oil/water separation. The coated mesh was placed on beaker and mixture of kerosene and water was poured onto the three-dimensional superhydrophobic mesh, as shown in Fig. 5a-c. Kerosene was dropped into the beaker, while water was repelled and retained above the mesh. Fig. 5d exhibited that there are no oily droplets were present in the water. After the separation, nearly equal amount of water and kerosene were collected, which was suggested that extremely high separation efficiency of the coated mesh as shown in Fig. 5e.

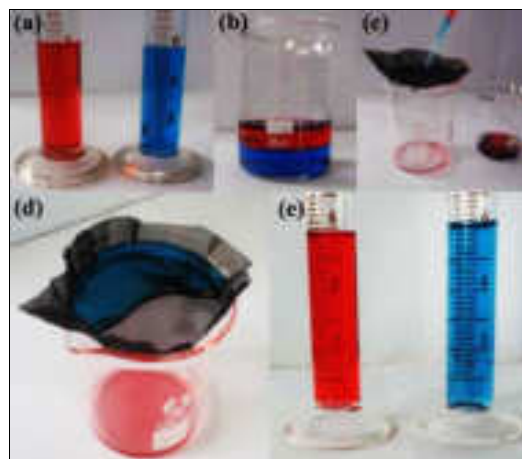


Fig 5: Schematic illustration of the separation process of oil (kerosene)/water mixture based on the CS and silica overlap coated mesh. (a-b) water is dyed with methylene blue and oil is dyed with Oil Red O and then they are mixed before separation. (c-d) the separation process of the oil/water mixture using the overlap coated mesh. (e) The water and oil volume keep nearly the same after separation [20], with permission from RSC Nanoscale, Copyright 2016.

Cao *et al.* [21] used the electrodeposition technique for the formation of superhydrophobic/superoleophilic copper meshes and then held it above candle flame to deposit carbon soot (CS) nanoparticles. The agglomerated CS nanoparticles formed a chain like rough hierarchical structure on which water drop exhibited contact angle higher than 153° . The CS deposited copper mesh quickly separated various oils such as silicone oil, cyclohexane, n-hexane, n-heptane, petroleum ether, and liquid paraffin from oil-water mixtures with oil separation efficiency greater than 90% even after 30 separation cycles. The rough mesh was placed on 1.5 cm height of flame of burning candle for deposition for 5 minutes, the whole preparation process is shown in the fig. 6, the superhydrophobic mesh surface was formed by using candle soot.

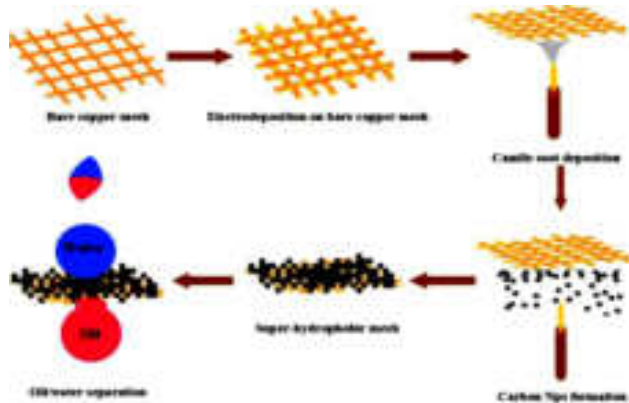


Fig 6: Schematic illustration of the preparation process of superhydrophobic and super-oleophilic copper mesh, and the application in oil-water separation [21], with permission from Colloids and Surfaces A: Physicochem. Eng. Aspects, Copyright 2017.

Zulficar *et al.* [22] deposited cheaply available sawdust on polychloroprene adhesive-coated SS mesh with subsequent deposition of silicone polymer by dip coating. Thereafter, a thin layer of CS particles was applied on the as-prepared mesh by holding above a candle flame. The carbon soot (CS) nanoparticles uniformly deposited on silicone covered SD exhibited highly rough and porous morphology required for superhydrophobicity and superoleophobicity. As depicted in Fig. 7, a superhydrophobic SS mesh easily and rapidly separated oil-water mixture. No trace of water was observed in separated oil confirming its potential in oil-water separation capability. Apart from excellent oil-water separation efficiency (>95%), the superhydrophobic SS mesh exhibited good recyclability, reusability, and mechanical stability. The potential of these coatings for oil/water separation is shown in Fig. 7. The figure typically shows a mesh coated with superhydrophobic material holding water without any leakage. The superhydrophobic mesh was used for the separation of oil from oil-water mixtures as shown in Fig. 7. The mesh readily separated the oil while blocking the flow of water through its pores. The water content was not found in the separated oil, which confirms the excellent superhydrophobic/superoleophilic property. The steel mesh with excellent mechanical stability modified with durable superhydrophobic coating can be used as a medium for oil/water separation.

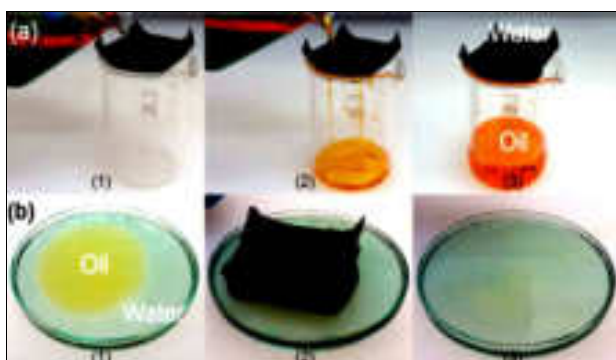


Fig 7: Schematic illustration of a superhydrophobic mesh demonstrating (a) the separation of oil/water mixture and (b) collection of oil from oil/water mixture [22], with permission from Colloids and Surfaces A: Physicochem. Eng. Aspects, Copyright 2017.

Chen *et al.* [23] synthesized a superhydrophobic surfaces by simply placing the stainless steel (SS) on the middle of candle flame for deposition of carbon soot (CS) on the SS mesh. The

candle soot coated substrate together with SiCl₄ was placed in a drier for chemical vapour deposition. Then, though calcination at 600°C for half in air, CS composed NPs thermally degraded and diffused through the silica shell gradually. It was shows excellent oil-water separation efficiency even after 30 times recycling use of modified superhydrophobic surfaces. The superhydrophobic coating revealed excellent separation efficiency even after 6 times reuses of same superhydrophobic surface. It could be potentially used in optical and visual application scenarios were in harsh, oily environments, like goggles, building façade, visual oil-water separation device, touch screen, etc. As shown in Fig. 8, the cheap and accessible candle soot were used for formation of a rough surface template to directly deposition on the substrate. The candle soot was formed carbon nanoparticles forming by incompletely burned paraffin, which loosely bounded on the substrate and formed a rough surface. Finally, a hard and porous silica shell was deposited on the candle soot template through chemical vapor deposition of SiCl₄ like Stober reaction, which completely formed the roughness of the template and a robust rough surface.

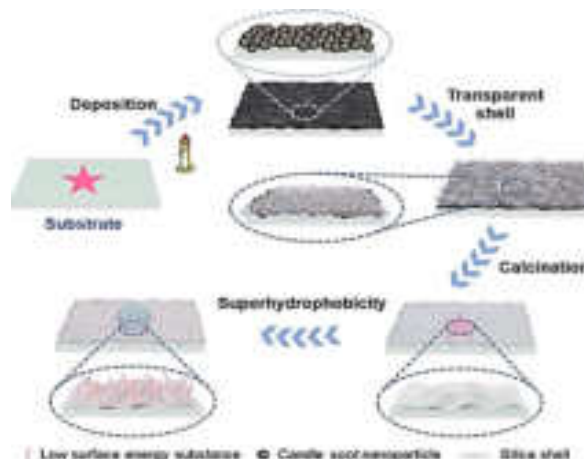


Fig 8: Schematic of preparation and properties of the transparent and robust superhydrophobic coating and oil-water separation. Images reprinted from [23], with permission from Nature, Copyright 2022.

Conclusion

As this review highlights, carbon soot nanoparticles are unique in that, their fabrication requires little control of external parameters. It is beneficial economically, facile and straightforward to synthesize. The carbon soot nanoparticles coated sponges and mesh has been developed by using carbon soot nanoparticles and different polymers. The absorption/separation investigation demonstrates that, the carbon soot surface is highly efficient and stable in absorbing a wide range of oil and organic solvents. It can be believed that, the carbon soot coated superhydrophobic materials are very useful for oil-water separation. The carbon soot synthesis, carbon soot coated sponge/mesh preparation, procedures are simple, cost-effective and scalable. The absorption/separation investigation demonstrates that, the carbon soot sponge/mesh is highly efficient and stable in absorbing a wide range of oil and organic solvents. It can be believed that, the carbon soot coated superhydrophobic surfaces are very useful for oil-water separation. It shows various tremendous results with carbon soot-polymer composite in various mechanical conditions. A carbon soot nanoparticle shows significant surface area to volume ratio, high electronic and ionic conductivity. Carbon soot is

produced by simply burning of candles and hence, it is ecofriendly, economical and useful. Carbon soot coated sponge and mesh can show stability, durability, reusability and reproducibility. Hence, this review is helpful to upcoming researchers to develop highly scalable superhydrophobic surfaces for efficient oil-water separation applications.

Acknowledgement

One of the authors R. B. Sawant is grateful to Chhatrapati Shahu Maharaj Research, Training and Human Development Institute (SARTHI) Fellowship, Govt. of Maharashtra, India.

References

- Alaaeddin A, Brian JS, Leilei X, Yuhan L, Damian EH, William RD. Rapid removal of organic micropollutants from water by a porous β -cyclodextrin polymer. *Nature*. 2016; 529:190-194.
- Yong L, Zhaozhu Z, Bo G, Xuehu M, Qunji X. One-pot, template-free synthesis of robust superhydrophobic polymer monolith with adjustable hierarchical porous structure. *Green Chem*. 2016; 18:5266-5272.
- Qinglang M, Hongfei C, Anthony GF, Rong W, Hua Z. Recent Development of Advanced Materials with Special Wettability for Selective Oil/Water Separation. *Small*. 2016; 12:2186-2202.
- Lingxiao L, Bucheng L, Jie D, Junping Z. Roles of silanes and silicones in forming superhydrophobic and superoleophobic materials. *J. Mater. Chem. A*. 2016; 4:13677-13725.
- Jianan S, Haiyang W, Ziwei L, Yuanzheng L, Zhenglian L, Haolun W, Xiaoyan L, Minghao F, Bo L, Hui W. Large-scale blow spinning of carbon microfiber sponge as efficient and recyclable oil sorbent. *Chemical Engineering Journal*. 2018; 343:638-644.
- Zhenxing W, Yanchao X, Yuyan Li, Lu S. A Novel Mussel-Inspired Strategy toward Superhydrophobic Surface for Self-Driven Crude Oil Spill Cleanup. *J. Mater. Chem. A*. 2015; 3:266-273.
- Jin J L, Li T Z, Zheng HL. Electrospun fibrous membrane with enhanced switchable oil/water wettability for oily water separation. *Chem. Eng. J*. 2016; 287:474-481.
- Alireza K, Hamid Z, Amir A, Ahmad A. Enhancing oil removal from water by immobilizing multi-wall carbon nanotubes on the surface of polyurethane foam. *Journal of Environ. Management*. 2015; 157:279-286.
- Guina R, Yuanming S, Xiangming L, Yanli Z, Zhaozhu Z, Xiaotao Z. A superhydrophobic copper mesh as an advanced platform for oil-water separation. *Applied Surface Science*. 2018; 428:520-525.
- Ebenezer KS, Daniel KS, Xiaomeng L, Botao L, Xinxin X, Shanhe G. *et al.* Recent development in the fabrication of self-healing superhydrophobic surfaces. *Chemical Engineering Journal*. 2019; 19:3012-3018.
- Kwangseok S, Minyoung K, Do HK. Candle-based process for creating a stable superhydrophobic surface. *CARBON*. 2014; 68:583-596.
- Jiajia S, Na L, Jiakai L, Yingze C, Haijie C. Facile Fabrication of Highly Hydrophobic Onion-Like Candle Soot-Coated Mesh for Durable Oil/Water Separation. *Nanomaterials*. 2022; 12:761-772.
- Chee HL, Nick J, Jaroslaw D, Yoke KY. The performance of superhydrophobic and superoleophilic carbon nanotube meshes in water-oil filtration. *CARBON*. 2011; 49:669-676.
- Jincui G, Peng X, Jing C, Fu L, Youju H, Gaiye L, Jiawei Z, Tao C. Robust preparation of superhydrophobic polymer/ carbon nanotube hybrid membranes for highly effective removal of oils and separation of water-in-oil emulsions. *J. Mater. Chem. A*. 2014; 2:15268-15272.
- Chih FW, Sheng JL. Robust Superhydrophobic/Superoleophilic Sponge for Effective Continuous Absorption and Expulsion of Oil Pollutants from Water. *ACS Appl. Mater. Interfaces*. 2013; 5:8861-8864.
- Jian L, Zhihong Z, Ruimei K, Yan Z, Weizhong L, Mouji L, Runan J, Liangjie L. Robust superhydrophobic candle soot and silica composite sponges for efficient oil/water separation in corrosive and hot water. *J. Sol-Gel Sci. Technol*. 2017; 3:817-826.
- Farshad B, Hossein K, Masoud SN. Recyclable Magnetic Superhydrophobic Straw Soot Sponge for Highly Efficient Oil/water Separation. *J. Colloid Interface Sci*. 2017; 497:57-65.
- Yang G, Yun SZ, Wei X, Mengmeng W, Lisha F, Hossein RG. *et al.* Highly Efficient and Recyclable Carbon Soot Sponge for Oil Cleanup. *ACS Appl. Mater. Interfaces*. 2014; 6:5924-5929.
- Xuejie Y, Ziqi Z, Tao Z, Dongya Y, Jicheng X, Fengxian Q. Simply realizing durable PVDF/candle soot foam with excellent solar absorption for solar-assisted recovery of heavy oil spill. *Elsevier*. 2021; 7:1-7.
- Jian L, Ruimei K, Xiaohua T, Houde S, Yaoxia Y, Fei Z. Superhydrophobic meshes that can repel hot water and strong corrosive liquids used for efficient gravity-driven oil/water separation. *Nanoscale*. 2016; 8:7638-7645.
- Huaijie C, Jingyuan F, Ying L, Shougang C. Facile Design of Superhydrophobic and Superoleophilic Copper Mesh Assisted by Candle Soot for Oil Water Separation. *Colloids Surf. A Physicochem. Eng. Asp*. 2018; 537:294-302.
- Usama Z, Syed ZH, Tayyab S, Irshad H, Habib R. Mechanically robust superhydrophobic coating from sawdust particles and carbon soot for oil/water separation. *Colloids Surf. A Physicochem. Eng. Asp*. 2018; 539:391-398.
- Baiyi C, Rongrong Z, Hexuan F, Jiadai X, Yuan J, Guohe X, Bin W, Xu H. Efficient oil-water separation coating with robust superhydrophobicity and high transparency. *Scientific Reports*. 2022; 8:1-9.



International Journal of Advance Studies and Growth Evaluation

Recent Progress in Fabrication of Candle Soot Modified Superhydrophobic/Superoleophilic Surfaces for Oil-Water Separation

¹ Mehejbin R Mujawar, ² Rajesh B Sawant, ³ Deepak A Kumbhar, ⁴ Sanjay S Latthe, ⁵ Ankush M Sargar and ^{*6} Shivaji R Kulal

^{1,2} Research Scholar, Department of Chemistry, Raje Ramrao Mahavidyalaya, Jath, Sangli, Maharashtra, India.

³ Assistant Professor, Department of Chemistry, Dattajirao Kadam Arts, Science and Commerce College, Ichalkarnji, Kolhapur, Maharashtra, India.

⁴ Assistant Professor, Research Laboratory, Department of Physics, Vivekanand College (Autonomous), Kolhapur, Kolhapur, Maharashtra, India.

⁵ Assistant Professor, Department of Chemistry, Bharati Vidyapeeth's Dr. Patangrao Kadam Mahavidyalaya, Sangli, Sangli, Maharashtra, India.

^{*6} Assistant Professor, Department of Chemistry, Raje Ramrao Mahavidyalaya, Jath, Sangli, Maharashtra, India.

Article Info.

E-ISSN: 2583-6528

Impact Factor (SJIF): 5.231

Peer Reviewed Journal

Available online:

www.alladvancejournal.com

Received: 12/Feb/2024

Accepted: 15/Mar/2024

Abstract

Continually occurred the oceanic oil spill accidents and discharging huge amount of industrial oily wastewater cause a serious threat to the environment. Oil and organic pollutants in water has a severe problem for aquatic life and human being. There is a need to develop technology for oil-water separation. Recently, superhydrophobic/superoleophilic sponges, metal meshes, membranes and porous materials plays crucial role to separate oil from oil-water mixture. The micro and nanopores of substrate facilitate to enter liquid into it and superhydrophobic/superoleophilic property of substrate surface resist water and allows oil to enter into the porous substrate. Carbon soot nanoparticles are hydrophobic (water repellent) in nature and has the advantages of cost-effectiveness and production scalability over other carbons like graphene, carbon nanotubes (CNTs), carbon nanodots (CNDs), etc., in their synthesis. Carbon soot based superhydrophobic/superoleophilic surfaces have outstanding water repulsion and oil absorption capacity, highly selectivity, chemical inertness and excellent recyclability. In this paper, we discussed recent progress of carbon soot based superhydrophobic/superoleophilic sponges and meshes for oil-water separation.

*Corresponding Author

Shivaji R Kulal

Assistant Professor, Department of Chemistry, Raje Ramrao Mahavidyalaya, Jath, Sangli, Maharashtra, India.

Keywords: Carbon soot, oil-water separation, sponge, stainless steel mesh and superhydrophobic.

Introduction

The oil spillage and industrial pollutants has emerged as critical issue to an ecosystem, human health, economic growth, etc. To address this challenge, several efforts have been done to separate oil and organic solvents from oil contaminated water [1-2]. The various methods such as spray coating, dip-coating, hydrothermal method, chemical vapour deposition, surface etching, solvothermal method, layer-by-layer assembly and electrochemical treatment have been used to prepare superhydrophobic/superoleophilic coating on sponge and mesh surface [3]. The ideal superhydrophobic/superoleophilic meshes and sponges must have following characteristics, such as fine selectivity toward various oils, high separation efficiency, reusability and along with high mechanical, chemical, and thermal stability [4].

The superhydrophobic/superoleophilic surfaces have shown water contact angle (WCA) over 150°, sliding angle < 10° and oil contact angle < 5° [5]. The traditional technologies, including in situ burning, bioremediation, chemical dispersant methods, skimming, and sorbents are used for oil-water separation. However, many of these technologies involve energy intensive and slow processes, have low oil-water separation capacities or create secondary pollution during the oil-water separation process, restricting their widespread practical applications [6-8]. Different strategies used for formation of hierarchical structures such as sol-gel coating, chemical vapor deposition, plasma etching, template processing, lithographic patterning, etc. have been adopted [9-10].

Carbon soot (CS) generated from incomplete combustion of paraffin wax has demonstrated the advantages of cost effectiveness and production scalability over carbon nanotubes (CNTs), graphene and activated carbons in their synthesis. Hence, the carbon soot coated superhydrophobic/superoleophilic surfaces shows excellent oil-water separation ability rather than carbon nanotubes, carbon nanodots and graphene [11].

Song *et al.* [12] have fabricated carbon soot (CS) coated mesh using dip-coating method. The cleaned stainless-steel mesh (SSM) was subsequently dipped in the glue solution for 10 min and CS-dispersion, finally dried at 80°C to obtain the CS-glue coated mesh. The CS coating is close packed because of using superglue (EVO-STIK Serious Glue) as a binder. The CS-glue coated mesh revealed the separation efficiency higher than 99.95%. Even after 20 cycle separation tests, it was shown excellent reusability and durability. The different chemical methods are used for the fabrication of the superhydrophobic/superoleophilic meshes/sponges for efficient oil-water separation. As the carbon nanotubes are hydrophobic in nature and it shows strong affinity toward oil, Lee *et al.* [13] adopted chemical vapor deposition (CVD) technique to deposit vertically aligned CNTs on stainless steel (SS) mesh. The as-prepared SS-CNT mesh effectively separates oil from water-in-oil emulsions with efficiency higher than 80%. Gu *et al.* [14] prepared polystyrene (PS) and carbon nanotubes coated superhydrophobic/superoleophilic membrane. The as-prepared superhydrophobic/superoleophilic membrane shows mechanically robust PS-CNT surface shows excellent oil separation from oil-water mixture with good repeatability and separation efficiency of more than 99%. Electrospinning technique can be effectively used to form superhydrophobic/superoleophilic surfaces. Wang *et al.* [15] prepared the polyurethane (PU) sponge from hydrophilic to superhydrophobic by dip coating it from the nanocomposite of CNT/poly-(dimethyl siloxane) (PDMS). The as-prepared superhydrophobic/superoleophilic sponge shows the continuous removal of various oils such as Soybean oil, motor oil, diesel, n-hexadecane, gasoline, and n-hexane from the surface of the water with high separation efficiency.

In this article, we will discuss on the simple, low-cost, rapid and innovative methods for the fabrication of superhydrophobic/superoleophilic carbon soot nanoparticle coated sponges and meshes for efficient oil-water separation application.

Recent Developments for Effective Oil-Water Separation Superhydrophobic-Superoleophilic Sponge

Hydrophobic candle soot (CS) particles can be collected easily and cost effectively from the candle flame. Li *et al.* [16] obtained the hydrophobic CS particles by incomplete combustion of hydrocarbons from the mid-candle flame. The polyurethane sponge immersed in the mixture of CS, hydrophobic silica nanoparticles, and PU resin to achieve stable superhydrophobicity. The CS-SiO₂-PU sponge showed excellent oil separation capacity from hot water and acidic, alkaline, and salt solutions. The CS-SiO₂-PU sponges could absorb a various oil efficiently and selectively, and show high absorption capacity that is up to 65 times of its own weight. Furthermore, the CS-SiO₂-PU sponge possesses stable superhydrophobicity and excellent ability of selective absorption to oil even at various harsh conditions, including acid (1M HCl) and alkali (1M NaOH), and salt (1M NaCl) aqueous solutions at mechanical agitation condition, hot water and ice/water mixtures. The CS-SiO₂-PU sponge combination

with a vacuum system could continuously absorb and remove oil from water surface. As shown in (Fig. 1a), the contact angle of coloured water droplet on the PU sponge is nearly 100° and the coloured kerosene droplet contact angle is about 0°. However, the CS-SiO₂-PU sponge shows superhydrophobicity and superoleophobicity simultaneously (Fig. 1b). The kerosene droplet was absorbed by the CS-SiO₂-PU sponge immediately when it was dropped on the surface of sponge, while the water droplet stayed on the surface of as-prepared sponge and kept its spherical shape. As shown in (Fig. 1c and d), the water contact angle on the CS-SiO₂-PU sponge is up to 155° and the SA is as low as 7°. Therefore, the water was repelled by the as-prepared sponge, whereas the oil absorbed through the sponge quickly.

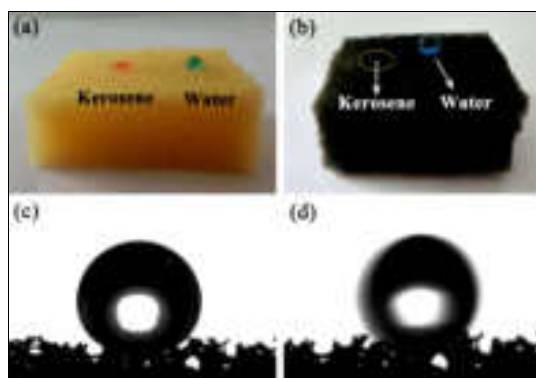


Fig 1: (a and b) Schematic illustration of the fabrication the wettability of the pristine PU sponge and the CS-SiO₂-PU sponge to water and oil droplets, respectively. (c and d) The CA and SA of water on the CS-SiO₂-PU sponge, respectively [16], with permission from J. Sol-Gel Sci Technol., Copyright 2017.

Beshkar *et al.* [17] prepared durable magnetic superhydrophobic PU sponge by immersing it in the colloidal solution of straw candle soot (carbon nanoparticles) and further modification was done by Fe₂O₄ nanoparticles and PDMS. The waste oil was easily collected from the surface of water through guiding the magnetic superhydrophobic polyurethane (PU) sponge by a bar magnet. The wettability of sponge remained unchanged even after 30 absorption/desorption cycles. The oil-water separation experiments were performed using the as-prepared optimized superhydrophobic sponge to absorbing of waste oil. The schematic of experimental protocol for preparation and operation superhydrophobic/superoleophilic magnetic straw soot sponge is shown in Fig. 2. It was indicated that the superhydrophobic sponge is taken by a magnet bar and absorbs waste oil completely from the oil-water mixture within 10 seconds.

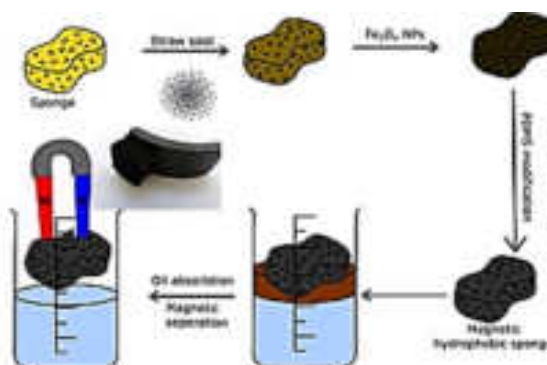


Fig 2: Schematic illustration of preparation of modified polyurethane sponge and oil separation process. Images reprinted from [17], with permission from Elsevier, Copyright 2017.

Gao *et al.* [18] obtained the candle soot (CS) particles from combustion flame and dispersed it in 1,2-dichloroethane (DCE). The superhydrophobic/superoleophilic melamine sponge prepared by a uniform coating of as-grown CS-DCE solution using dip-coating method. The CS-modified sponge exhibited strong water repellency and oil absorbency without further chemical modification (Fig. 3. a and b). An easy and fast recovery of engine oil floating on the water surface by CS-modified sponge confirms its high oil-water separation efficiency (Fig. 3. c-e). The CS-modified sponge could absorb numerous oils and organic solvents with an absorption capacity of 25-80 times of its own weight. Oil can be recycled for more than 10 times with absolutely no change in an oil absorption capacity and wettability of the CS-modified sponge.

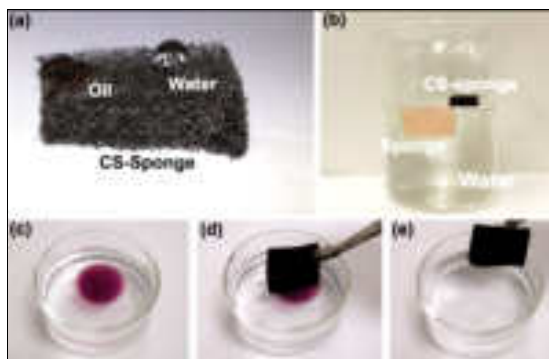


Fig 3: Schematic showing (a) Photograph of water and oil droplets on the surface of a CS-sponge. (b) Photograph of pure and CS-sponges placed on water. (c-e) Photographs demonstrating the removal of an oil droplet from water using a CS-sponge [18], with permission from American Chemical Society, Copyright 2014.

Yue *et al.* [19] the superhydrophobic surface was fabricated by using PVDF and candle soot via sugar template method. It was shown the water contact angle of 158° and roll-on angle of $<6^\circ$. The oil quickly absorbed by superhydrophobic sponge shows the superoleophilic property. The sponge shows excellent oil-water separation property even after 25 cycles. The strong elasticity, high stretching resistance confirms that the modified superhydrophobic surface is highly mechanical durable. The modified sponge maintains the 89% of recovery rate even after 10 cycles. The absorption capability recovered up to 96% without obvious change of morphology of the sponge surface. This method was used to prepare a photothermal, porous PVDF/CS sponge with structural, chemical and mechanical property [19]. Fig. 4 shows that the preparation process of the porous PVDF/candle soot sponge. In short, sugar particles were placed into a mixture of PVDF/DMF/CS solution, followed by removing sugar templates via the water dissolving. It is important to note that a simple sugar-templating process was used for formation of superhydrophobic sponge, it requires only a simple as well as eco-friendly preparation process.

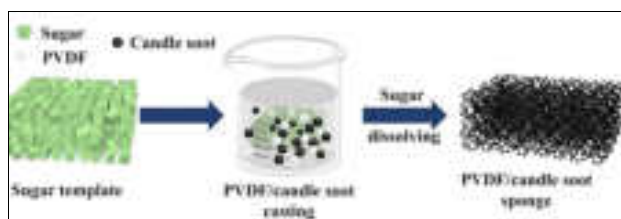


Fig 4: Schematic illustration of the fabrication of porous PVDF/candle soot sponge using sugar template. Images reprinted from [19], with permission from Elsevier, Copyright 2021.

Superhydrophobic/Superoleophilic Mesh

Li *et al.* [20] deposited hydrophobic CS particles on a SS mesh by holding it in the mid-flame of paraffin candle and then spray coated the hydrophobic silica nanoparticles (50 nm) on it. The as-prepared carbon soot/silica nanoparticles (CS/SiO₂) hybrid mesh revealed strong repellence toward pure water and droplets of pH ranging from 1 to 14, whereas the oil drops quickly spread on the surface. The hybrid mesh revealed strong ability to separate various oils and organic liquids mixed in pure water, hot water (92°C), and strong corrosive solutions (1M HCl, NaOH, and NaCl) with more than 98% of separation efficiency. The oil/water separation was performed as shown in Fig. 5. Because of the excellent mechanical flexibility of the stainless-steel mesh, the mesh was folded into a three-dimensional structure, then coated with CS and hydrophobic silica for oil/water separation. The coated mesh was placed on beaker and mixture of kerosene and water was poured onto the three-dimensional superhydrophobic mesh, as shown in Fig. 5a-c. Kerosene was dropped into the beaker, while water was repelled and retained above the mesh. Fig. 5d exhibited that there are no oily droplets were present in the water. After the separation, nearly equal amount of water and kerosene were collected, which was suggested that extremely high separation efficiency of the coated mesh as shown in Fig. 5e.

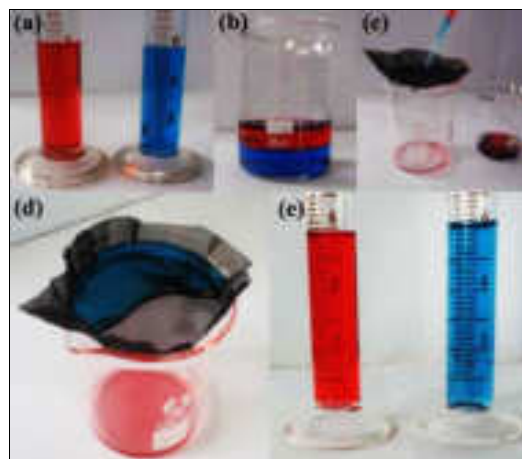


Fig 5: Schematic illustration of the separation process of oil (kerosene)/water mixture based on the CS and silica overlap coated mesh. (a-b) water is dyed with methylene blue and oil is dyed with Oil Red O and then they are mixed before separation. (c-d) the separation process of the oil/water mixture using the overlap coated mesh. (e) The water and oil volume keep nearly the same after separation [20], with permission from RSC Nanoscale, Copyright 2016.

Cao *et al.* [21] used the electrodeposition technique for the formation of superhydrophobic/superoleophilic copper meshes and then held it above candle flame to deposit carbon soot (CS) nanoparticles. The agglomerated CS nanoparticles formed a chain like rough hierarchical structure on which water drop exhibited contact angle higher than 153° . The CS deposited copper mesh quickly separated various oils such as silicone oil, cyclohexane, n-hexane, n-heptane, petroleum ether, and liquid paraffin from oil-water mixtures with oil separation efficiency greater than 90% even after 30 separation cycles. The rough mesh was placed on 1.5 cm height of flame of burning candle for deposition for 5 minutes, the whole preparation process is shown in the fig. 6, the superhydrophobic mesh surface was formed by using candle soot.

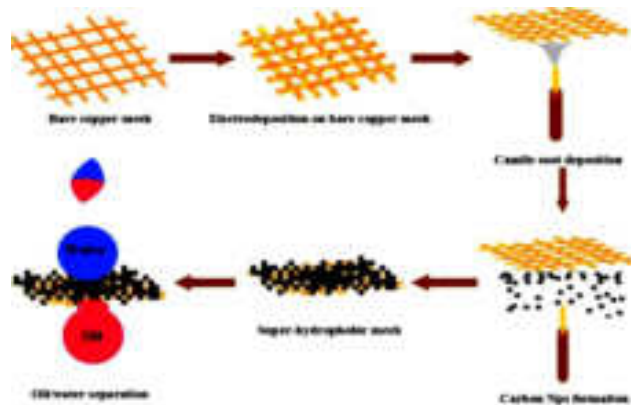


Fig 6: Schematic illustration of the preparation process of superhydrophobic and super-oleophilic copper mesh, and the application in oil-water separation [21], with permission from Colloids and Surfaces A: Physicochem. Eng. Aspects, Copyright 2017.

Zulfiqar *et al.* [22] deposited cheaply available sawdust on polychloroprene adhesive-coated SS mesh with subsequent deposition of silicone polymer by dip coating. Thereafter, a thin layer of CS particles was applied on the as-prepared mesh by holding above a candle flame. The carbon soot (CS) nanoparticles uniformly deposited on silicone covered SD exhibited highly rough and porous morphology required for superhydrophobicity and superoleophobicity. As depicted in Fig. 7, a superhydrophobic SS mesh easily and rapidly separated oil-water mixture. No trace of water was observed in separated oil confirming its potential in oil-water separation capability. Apart from excellent oil-water separation efficiency (>95%), the superhydrophobic SS mesh exhibited good recyclability, reusability, and mechanical stability. The potential of these coatings for oil/water separation is shown in Fig. 7. The figure typically shows a mesh coated with superhydrophobic material holding water without any leakage. The superhydrophobic mesh was used for the separation of oil from oil-water mixtures as shown in Fig. 7. The mesh readily separated the oil while blocking the flow of water through its pores. The water content was not found in the separated oil, which confirms the excellent superhydrophobic/superoleophilic property. The steel mesh with excellent mechanical stability modified with durable superhydrophobic coating can be used as a medium for oil/water separation.

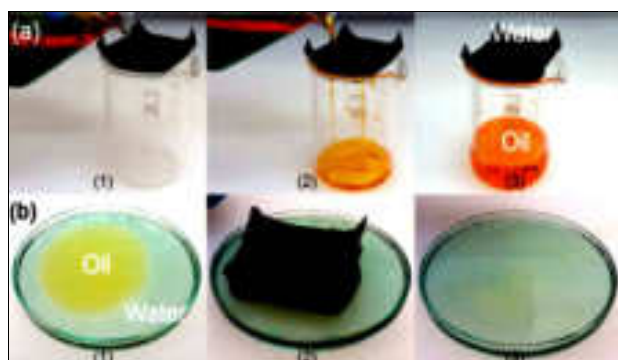


Fig 7: Schematic illustration of a superhydrophobic mesh demonstrating (a) the separation of oil/water mixture and (b) collection of oil from oil/water mixture [22], with permission from Colloids and Surfaces A: Physicochem. Eng. Aspects, Copyright 2017.

Chen *et al.* [23] synthesized a superhydrophobic surfaces by simply placing the stainless steel (SS) on the middle of candle flame for deposition of carbon soot (CS) on the SS mesh. The

candle soot coated substrate together with SiCl_4 was placed in a drier for chemical vapour deposition. Then, though calcination at 600°C for half in air, CS composed NPs thermally degraded and diffused through the silica shell gradually. It was shows excellent oil-water separation efficiency even after 30 times recycling use of modified superhydrophobic surfaces. The superhydrophobic coating revealed excellent separation efficiency even after 6 times reuses of same superhydrophobic surface. It could be potentially used in optical and visual application scenarios were in harsh, oily environments, like goggles, building façade, visual oil-water separation device, touch screen, etc. As shown in Fig. 8, the cheap and accessible candle soot were used for formation of a rough surface template to directly deposition on the substrate. The candle soot was formed carbon nanoparticles forming by incompletely burned paraffin, which loosely bounded on the substrate and formed a rough surface. Finally, a hard and porous silica shell was deposited on the candle soot template through chemical vapor deposition of SiCl_4 like Stober reaction, which completely formed the roughness of the template and a robust rough surface.

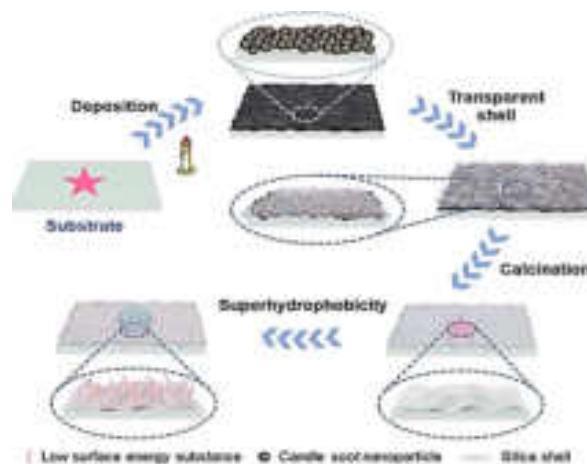


Fig 8: Schematic of preparation and properties of the transparent and robust superhydrophobic coating and oil-water separation. Images reprinted from [23], with permission from Nature, Copyright 2022.

Conclusion

As this review highlights, carbon soot nanoparticles are unique in that, their fabrication requires little control of external parameters. It is beneficial economically, facile and straightforward to synthesize. The carbon soot nanoparticles coated sponges and mesh has been developed by using carbon soot nanoparticles and different polymers. The absorption/separation investigation demonstrates that, the carbon soot surface is highly efficient and stable in absorbing a wide range of oil and organic solvents. It can be believed that, the carbon soot coated superhydrophobic materials are very useful for oil-water separation. The carbon soot synthesis, carbon soot coated sponge/mesh preparation, procedures are simple, cost-effective and scalable. The absorption/separation investigation demonstrates that, the carbon soot sponge/mesh is highly efficient and stable in absorbing a wide range of oil and organic solvents. It can be believed that, the carbon soot coated superhydrophobic surfaces are very useful for oil-water separation. It shows various tremendous results with carbon soot-polymer composite in various mechanical conditions. A carbon soot nanoparticle shows significant surface area to volume ratio, high electronic and ionic conductivity. Carbon soot is

produced by simply burning of candles and hence, it is ecofriendly, economical and useful. Carbon soot coated sponge and mesh can show stability, durability, reusability and reproducibility. Hence, this review is helpful to upcoming researchers to develop highly scalable superhydrophobic surfaces for efficient oil-water separation applications.

Acknowledgement

One of the authors R. B. Sawant is grateful to Chhatrapati Shahu Maharaj Research, Training and Human Development Institute (SARTHI) Fellowship, Govt. of Maharashtra, India.

References

- Alaaeddin A, Brian JS, Leilei X, Yuhan L, Damian EH, William RD. Rapid removal of organic micropollutants from water by a porous β -cyclodextrin polymer. *Nature*. 2016; 529:190-194.
- Yong L, Zhaozhu Z, Bo G, Xuehu M, Qunji X. One-pot, template-free synthesis of robust superhydrophobic polymer monolith with adjustable hierarchical porous structure. *Green Chem*. 2016; 18:5266-5272.
- Qinglang M, Hongfei C, Anthony GF, Rong W, Hua Z. Recent Development of Advanced Materials with Special Wettability for Selective Oil/Water Separation. *Small*. 2016; 12:2186-2202.
- Lingxiao L, Bucheng L, Jie D, Junping Z. Roles of silanes and silicones in forming superhydrophobic and superoleophobic materials. *J. Mater. Chem. A*. 2016; 4:13677-13725.
- Jianan S, Haiyang W, Ziwei L, Yuanzheng L, Zhenglian L, Haolun W, Xiaoyan L, Minghao F, Bo L, Hui W. Large-scale blow spinning of carbon microfiber sponge as efficient and recyclable oil sorbent. *Chemical Engineering Journal*. 2018; 343:638-644.
- Zhenxing W, Yanchao X, Yuyan Li, Lu S. A Novel Mussel-Inspired Strategy toward Superhydrophobic Surface for Self-Driven Crude Oil Spill Cleanup. *J. Mater. Chem. A*. 2015; 3:266-273.
- Jin J L, Li T Z, Zheng HL. Electrospun fibrous membrane with enhanced switchable oil/water wettability for oily water separation. *Chem. Eng. J*. 2016; 287:474-481.
- Alireza K, Hamid Z, Amir A, Ahmad A. Enhancing oil removal from water by immobilizing multi-wall carbon nanotubes on the surface of polyurethane foam. *Journal of Environ. Management*. 2015; 157:279-286.
- Guina R, Yuanming S, Xiangming L, Yanli Z, Zhaozhu Z, Xiaotao Z. A superhydrophobic copper mesh as an advanced platform for oil-water separation. *Applied Surface Science*. 2018; 428:520-525.
- Ebenezer KS, Daniel KS, Xiaomeng L, Botao L, Xinxin X, Shanhe G. *et al.* Recent development in the fabrication of self-healing superhydrophobic surfaces. *Chemical Engineering Journal*. 2019; 19:3012-3018.
- Kwangseok S, Minyoung K, Do HK. Candle-based process for creating a stable superhydrophobic surface. *CARBON*. 2014; 68:583-596.
- Jiajia S, Na L, Jiakai L, Yingze C, Haijie C. Facile Fabrication of Highly Hydrophobic Onion-Like Candle Soot-Coated Mesh for Durable Oil/Water Separation. *Nanomaterials*. 2022; 12:761-772.
- Chee HL, Nick J, Jaroslaw D, Yoke KY. The performance of superhydrophobic and superoleophilic carbon nanotube meshes in water-oil filtration. *CARBON*. 2011; 49:669-676.
- Jincui G, Peng X, Jing C, Fu L, Youju H, Gaiye L, Jiawei Z, Tao C. Robust preparation of superhydrophobic polymer/ carbon nanotube hybrid membranes for highly effective removal of oils and separation of water-in-oil emulsions. *J. Mater. Chem. A*. 2014; 2:15268-15272.
- Chih FW, Sheng JL. Robust Superhydrophobic/Superoleophilic Sponge for Effective Continuous Absorption and Expulsion of Oil Pollutants from Water. *ACS Appl. Mater. Interfaces*. 2013; 5:8861-8864.
- Jian L, Zhihong Z, Ruimei K, Yan Z, Weizhong L, Mouji L, Runan J, Liangjie L. Robust superhydrophobic candle soot and silica composite sponges for efficient oil/water separation in corrosive and hot water. *J. Sol-Gel Sci. Technol*. 2017; 3:817-826.
- Farshad B, Hossein K, Masoud SN. Recyclable Magnetic Superhydrophobic Straw Soot Sponge for Highly Efficient Oil/water Separation. *J. Colloid Interface Sci*. 2017; 497:57-65.
- Yang G, Yun SZ, Wei X, Mengmeng W, Lisha F, Hossein RG. *et al.* Highly Efficient and Recyclable Carbon Soot Sponge for Oil Cleanup. *ACS Appl. Mater. Interfaces*. 2014; 6:5924-5929.
- Xuejie Y, Ziqi Z, Tao Z, Dongya Y, Jicheng X, Fengxian Q. Simply realizing durable PVDF/candle soot foam with excellent solar absorption for solar-assisted recovery of heavy oil spill. *Elsevier*. 2021; 7:1-7.
- Jian L, Ruimei K, Xiaohua T, Houde S, Yaoxia Y, Fei Z. Superhydrophobic meshes that can repel hot water and strong corrosive liquids used for efficient gravity-driven oil/water separation. *Nanoscale*. 2016; 8:7638-7645.
- Huaijie C, Jingyuan F, Ying L, Shougang C. Facile Design of Superhydrophobic and Superoleophilic Copper Mesh Assisted by Candle Soot for Oil Water Separation. *Colloids Surf. A Physicochem. Eng. Asp*. 2018; 537:294-302.
- Usama Z, Syed ZH, Tayyab S, Irshad H, Habib R. Mechanically robust superhydrophobic coating from sawdust particles and carbon soot for oil/water separation. *Colloids Surf. A Physicochem. Eng. Asp*. 2018; 539:391-398.
- Baiyi C, Rongrong Z, Hexuan F, Jiadai X, Yuan J, Guohe X, Bin W, Xu H. Efficient oil-water separation coating with robust superhydrophobicity and high transparency. *Scientific Reports*. 2022; 8:1-9.

अनुक्रमिका

श.न.	संज्ञा	ज्ञापनपत्रांतर्गत	पृ. न.
- शास्त्रिक विभाग -			
१	प्रा. डॉ. डोंगरदिवे वि. एम.	सुरेन्द्रनाथ बॅनर्जी यांच्या राजकीय क्षेत्रातील नैतिक मूल्यांचा अभ्यास	२-७
२	गणेश रेवणसिद्ध वाघमारे	फलटण संस्थानाधिपती मुधोजीराजे नाईक निवाळकर (४थे) यांचे शिक्षण क्षेत्रातील योगदान	८-१६
३	श्री. सुनील श्रावण	आधुनिक इतिहासाची भूमिका आणि नवीन प्रवाह : एक अभ्यास	१७-२५
४	प्रा.डॉ.गोकुळ निंबा पाटील	भारतीय संविधान समितीच्या कार्याचा ऐतिहासिक आढावा	२६-३०
५	डॉ. संजय गायकवाड	क्रांतिकारक व कृतिशील संत गाडगे महाराज	३१-३७
६	भरत केवळ आहेर	महाराजा सयाजीराव गायकवाड यांचे स्त्री शिक्षण विषयक कार्य	३८-४३
७	प्रा.डॉ.बोत्रे अमोल पोपट	मणिभाई देसाई आणि उरुळी कांचन गृहक्षक दल	४४-४८
८	प्रा. सतीश सावता फुले	आधुनिक कालखंडातील माणदेशाचा ऐतिहासिक दृष्टिकोनातून सामाजिक अभ्यास	४९-५५
९	डॉ.यशवंत चेमा गावीत	सरदार पटेल व पश्चिम खानदेशातील जनजागृती - एक अभ्यास	५६-५९
१०	श्री. सुनील श्रावण	भारतीय स्वातंत्र्य लढ्यात खानदेशातील स्त्रियांचे योगदान	६०-६६
११	प्रा. डॉ. सुभाष श्रावण धनगर	भारतीय स्वातंत्र्य लढ्यात खानदेशातील स्त्रियांचे योगदान	६७-७३
१२	डॉ.राजाराम सोनवणे	सहकार व ग्राम विकासाचे शिल्पकार डॉ.बाबुराव बापूजी तनपुरे (दादासाहेब)	७४-७८
१३	प्रा.डॉ. भामरे नानाजी दगा	स्वामी विवेकानंदाचे शिक्षणविषयक तत्वज्ञान	७९-८७
१४	प्रा. डॉ. सौ. अरुणा रविंद्र वाघोले	२१ व्या शतकातीलभिडेवाडा स्मारक दीपस्तंभ उरणारी-क्रांतीज्योती सावित्रीबाई फुले	८८-९६
१५	प्राचार्य डॉ. प्रशांत पी. कोठे	डॉ. पंजराबव देशमुख आणि भारत कृषक समाज	९७-१००
१६	प्रमोद रमेश हंचाटे	इंद्रभुवन स्थापत्य कलेचा उत्कृष्ट नमुना	१०१-१०४
१७	प्रा.सुनील लक्ष्मण परदेशी	महात्मा गांधी यांचे विचार	१०५-१०९
१८	मनिषा शरद इंगळे	भारतीय स्वातंत्र्य चळवळीतील महात्मा गांधींचे योगदान	११०-११२
१९	मनिषा शरद इंगळे	महाराष्ट्राचा सांस्कृतिक ठेवा -लावणी	११३-११७
२०	प्रा. सरला ब्रम्हेदेव चव्हाण	क्रांतीज्योती सावित्रीबाई फुले यांचे कार्य	११८-१२८
२१	गणेश पुनमचंद बिरुटे	साने गुरुजींवर महात्मा गांधींजींचा पडलेला प्रभाव	१२९-१३२
२२	प्रा. डॉ. शितल अरविंद धरम	अहमदनगर जिल्ह्यातील कम्युनिस्ट कार्यकर्त्यांची संयुक्त महाराष्ट्र चळवळीतील भूमिका	१३३-१३६
२३	डॉ. भूषण गोविंद फडतरे	शोधनिबंध विषय: स्थानिक इतिहासाच्या दृष्टीने हुतात्मा स्मारकांचे महत्त्व	१३७-१४३
२४	प्रा. प्रणय जाधव	भारतीय राज्यघटनेच्या सरनाम्याचे चिकित्सक समालोचन	१४४-१४६
२५	प्रमोद मारुती जाधव	म. न. वि. विद्यापीठ - न. वि. वि. विद्यापीठ - न. वि. वि. विद्यापीठ	१४७-१५२
२६	प्रतिक बाबासाहेब सुरसे	विसाव्या शतकात महाराष्ट्रातील भिल्ल चळवळीचे योगदान	१५३-१५७
२७	किशोर नगनाथ जोगदं	उपेक्षिताचे नायक : रघुनाथ नामदेव राऊळ उर्फ भाई राऊळ	१५८-१६४
२८	मरकड श्रीराम विलास	शिक्षणमहर्षी मारुतराव फुले यांचे शिक्षणविषयक विचार व कार्य	१६५-१७२
२९	प्रा. अर्चना राजेंद्र गायकवाड	महिला सशक्तीकरणातील डॉ.बाबासाहेब आंबेडकर यांची भूमिका	१७३-१७६

३०	प्रा. डॉ. रघुराज मुगुराव कुरूमकर	डॉ. बाबासाहेब आंबेडकर यांचे शैक्षणिक विचार	१७७-१८१
३१	अनिल तानाजी जाधवर	मुंबई प्रांतातील शैक्षणिक सुधारणा एक अभ्यास (इ.स. १८१८ ते इ.स. १९४७)	१८२-१९३
३२	डॉ. संदीप मनोहराव राऊत	संत गाडगेबाबांचे आर्थिक नियोजन कौशल्य	१९४-२०२
३३	डॉ. प्रतिक्षा ब्रम्हदेव देशमुख	भारतीय स्वातंत्र्य आंदोलनातील एक विस्मरित चरित्र – अवतिकाबाई गोखले	२०३-२०६
३४	श्री. पारधी रवींद्र पुनाजी	स्वातंत्र्यपूर्व काळातील वृत्तपत्रांचे योगदान	२०७-२११
३५	बेबी केशव खोरणे	विदर्भातील धनगर समाज, संस्कृती, लोकगीत व परंपरांचा अभ्यास	२१२-२१७
३६	डॉ. गहिनीनाथ लिंबराज शेळके	वसाहतवाद आणि भारतीय स्त्रियांचे अधिकार	२१८-२२२
३७	श्री. अनिल पोपट लोखंडे	डॉ. बाबासाहेब आंबेडकर यांच्या वतनपरिषदा आणि सामाजिक बदलाची भूमिका	२२३-२२८
३८	मस्के प्रविण एकनाथ	महाराष्ट्रातील दलित नेतृत्वाचे राजकारण आणि सद्यःस्थिती	२२९-२३५
३९	वर्षा नारायण पवार	कसमादे परिसरात ईस्ट इंडिया कंपनीच्या काळात पडलेले दुष्काळ एक आढावा	२३६-२४०
४०	मंगल क्षत्रीकृपा: गटोड	गंगानदी व खोसरा एफ पत्रिका	२४१-२४४
४१	ग. अश्विनी नरेंद्र पारने	मंगल नदी व खोसरा वहाण्याचे विषय: साहित्यीक प्रगती	२४५-२५२
४२	प्रा.डॉ.अश्विनकुमार र.राठोड	ब्रिटीश वसाहतवाद व भारतीय पुरातत्व	२५३-२५९
४३	श्री.गणेश त्रिंबक राजदेव	भारतीय स्वातंत्र्य आंदोलनातील संगमनेर शहराचे योगदान	२६०-२६६
४४	जान्हवी प्रफुल्ल नाईक	स्त्री मुक्ती संघटनेच्या कलापथकाचे कार्य	२६७-२७७
४५	प्रा. अर्चना वालचंद बच्छाव	भारतीय स्वातंत्र्य आंदोलनात नासिक जिल्ह्यातील स्त्रियांचा सहभाग	२७८-२८३
४६	कु. सानिया सर्फराजखान पठाण	अहमदनगर जिल्ह्यातील कामगार चळवळीतील निवडक व्यक्तींचे कार्य	२८४-२९२
४७	प्रा. डॉ. ओलेकर प्रमोदकुमार अंकुश	भारतातील लोकशाहीच्या प्रारंभाची घटनात्मक आणि संस्थात्मक ऐतिहासिक गाथा	२९३-२९९
४८	डॉ. अनंत दादाराव मरकाळे	श्रीनिवास व्यंकटराव खोत आणि हैद्राबाद स्वातंत्र्य संग्राम	३००-३०२
४९	प्रज्ञा निवृत्ती साळवे	महाराजा सयाजीराव गायकवाड: सामाजिक कार्य	३०३-३०६
५०	डॉ. सुग्रीव बाबुराव आंधळे	ठाणे जिल्ह्यातील वेठबिगार मुक्तीसाठी श्रमजीवी संघटनेने केलेले कार्य	३०७-३१२
५१	गव्हादे रवि शामराव	डॉ. बाबासाहेब आंबेडकर यांचा खोतशाही विरोधातील लढा	३१३-३२९
५२	प्रा. डॉ. गोविंद तिरमनवार	हुतात्मा ज्ञानेश्वर देशपांडे यांचे स्वातंत्र्य लढ्यातील योगदान	३३०-३३५
५३	प्रा. सचिन अशोक धेंडे	स्वातंत्र्यपूर्व काळातील अहमदनगर जिल्ह्यातील दलित संघटन व राजकारण : एक चिकित्सा	३३६-३४३
५४	प्रा.डॉ. रावसाहेब पवार	आधुनिक काळातील आदिवासी संस्कृतीचे संरक्षक	३४४-३४८
५५	गंगुळी विधान संघटने	गंगुळी नदी व खोसरा वहाण्याचे विषय: साहित्यीक प्रगती	३४९-३५४
५६	प्रा. राजरत्न कि. दवणे	१९५६ चे धर्मांतर नव्या ऐतिहासिक पर्वाचा आरंभ	३५५-३६२
५७	विष्णू रघू गैर हेलूड	भारतीय स्वातंत्र्य चळवळीत जे.बी.कृपलानी यांचे योगदान (इ.स.१९८८ ते १९८२)	३६३-३६५
५८	डॉ.सोमनाथ दत्तात्रय कदम	गुरुवर्य कृष्णराव अर्जुन केळूसकर यांचे लेख व त्यांचा सुधारणावादी दृष्टिकोन	३६६-३७०
५९	प्रा. डॉ. दयानंद प्रभू गायकवाड	स्त्री उद्धारक सावित्रीबाई फुले	३७१-३७४
६०	प्रा.डॉ.ज्ञानोबा तुकाराम कदम	डॉ. बाबासाहेब आंबेडकरांची पत्रकारीता	३७५-३७७
६१	डॉ. प्रभाकर गणपत गावंड	ब्रिटिशकालीन स्वातंत्र्य चळवळीमधील वैयक्तिक सत्याग्रहात पेण	३७८-३८२

डॉ. बाबासाहेब आंबेडकर यांच्या वतनपरिषदा आणि सामाजिक बदलाची भूमिका

श्री. अनिल पोपट लोखंडे

संशोधक विद्यार्थी

मो. नं. ९९६०७९७४४४

ई- मेल - lokhandeanil143@gmail.com

* प्रस्तावना :-

महाराष्ट्राला सामाजिक सुधारणेच्या इतिहासाची, परिवर्तनाच्या /क्रांतीच्या लढ्यांची महान परंपरा लाभलेली आहे. सामाजिक सुधारणेच्या योगदानात सुधारकांच्या यादीमध्ये अग्रगण्य असलेले नाव म्हणजे डॉ. बाबासाहेब आंबेडकर होय. सामाजिक परिवर्तनास चालना देण्यासाठी सत्याग्रह, मंदिर प्रवेश चळवळ, सभा आणि परिषदा यांच्या माध्यमातून समाजाच्या उन्नतीसाठी लढा उभारून न्याय मिळवून देण्याचे उल्लेखनीय कार्य केले. अस्पृश्य, बहिष्कृत, शेतकरी, कामगार, महिला, वतन, शैक्षणिक, धर्म, गोलमेज परिषदा यामधील वतन परिषदा या ही तितक्याच महत्वाच्या आहेत. वतन परिषदा मध्ये महार वतन परिषदा, मांग/मातंग परिषदा, महार- मांग वतन परिषदा(संयुक्त) अशा वेगवेगळ्या प्रकारच्या वतन परिषदा घेतल्या गेल्या आहेत. परिषदांच्या माध्यमातून ' वतने खालसा ' करून आपला आत्मसन्मान जागृत ठेवण्याचा मौलिक सल्ला डॉ.आंबेडकर यांनी दिला. त्यामुळे अस्पृश्य समजल्या जाणाऱ्या महार - मांग समाजात आत्मभान जागृत झाले. त्यांनी पिढ्यानपिढ्या लादलेली बंधने झुगारून दिली. वतन परिषदाच्या वेळी झालेले ठराव हेही तितकेच बळ देणारे आणि चळवळीला गती देणारे ठरले. त्यामुळे सामाजिक स्थितंतर झाल्याने समाज बदलाची प्रक्रिया गतिमान झाली. ती ही सामाजिक,सांस्कृतिक,राजकीय,मानसिक,शैक्षणिक आणि धार्मिक या घटकांच्या बदलाच्या अंगाने झाली.म्हणूनच प्रस्तुत शोध निबंधामध्ये 'डॉ. बाबासाहेब आंबेडकर यांच्या वतनपरिषदा आणि सामाजिक बदलाची भूमिका' या अनुषंगाने संशोधन करण्यात आलेले आहे.

* संशोधनाची उद्दिष्ट्ये:-

- १) वतन, वतनदार त्यांची कार्ये याचा अभ्यास करणे.
- २) वतन परिषदा कालीन सामाजिक आर्थिक परिस्थितीचा आढावा घेणे.
- ३) सामाजिक क्रांतीचा पाया म्हणून वतन परिषदांचे आयोजन सहसंबंध अभ्यासणे.
- ४) डॉ. बाबासाहेब आंबेडकर यांच्या मार्गदर्शनाखालील / नेतृत्वाखालील वतनपरिषदांच्या माध्यमातून झालेल्या सामाजिक बदलाची भूमिका अभ्यास करणे.

*** वतन व वतनदार व त्यांची कार्ये :-**

वतन हा शब्द अरबी भाषेतील असून त्याचा मूळ अर्थ आपला देश, आपली जमीन असा आहे. इस्लामी राजवटीत हा शब्द आपल्या मराठी भाषेत रूढ झाला. सरकारकडून गावच्या अधिकाऱ्याला अथवा सेवकाला त्याच्या चाकरीच्या मोबदल्यात जी जमिनीची देणगी मिळेल तिला 'वतन' ही संज्ञा प्राप्त झाली. ही देणगी (म्हणजे वतनी जमिनीची देणगी) वंशपरंपरेने त्या कुटुंबात राहत असे. वतन ही मध्ययुगीन काळासह शिवकालीन कालखंडात गावगाड्यामध्ये पाटील, कुलकर्णी, चौगुले, शेते - महाजन, देशमुख - देशपांडे हे गावातील प्रमुख वतनदार लोक होते. वतनदार एक प्रकारचे ग्रामआधिकारीच होते. गावचा कारभार कार्यक्षमपणे चालवण्यासाठी त्यांची निर्मिती केली गेली. शिवकालीन समाज जीवनात 'वतनास' मोठी प्रतिष्ठा होती. इतिहासाच्या संदर्भात 'वतन' ही संज्ञा एखाद्या गावच्या कायमच्या रहिवाशाला त्याने ग्रामसेवा करावी या उद्देशाने त्याच्या घराण्याला सरकारी सारा माफ, जमीन वंशपरंपरागत एका सरकारी सनदे द्वारे बहाल केली जात तेव्हा त्यास वतन म्हणत. सर्वप्रथम इतिहासाच्या दृष्टिकोनातून 'वतन' याचा अर्थ समजून घेतला पाहिजे. शिवकालीन समाजव्यवस्था / वतनव्यवस्था यामध्ये आढळणारा मिरासदार / जमीनदार यांच्या शेतावर राबणारा वर्ग अशी ज्यांची गणना होत असे तो बलुतेदार वर्ग. मध्ययुगीन महाराष्ट्रातील समाजव्यवस्थेचा बलुता हा एक प्रकारे अविभाज्य घटक होता. तत्कालिन वतनसंस्थेत / समाज व्यवस्थेत बलुतेदार याची संख्या १२ असलेली पाहायला मिळते. वतन संस्थेमधील बलुतेदार वर्ग यामधील प्रमुख जाती महार - मांग यांसह इतरही होत्या. मध्ययुगीन काळात सुरू झालेली ही व्यवस्था आधुनिक काळातही अस्तित्वात होती.

वतनदारास (बलुतेदार) सरकारी व खाजगी कामे करावी लागत होती. दररोज पाटील, कुलकर्णी यांची विविध कामे करावी लागत असत. गावातील मेलेली जनावरे गावाबाहेर ओढून नेऊन टाकणे. प्रेतांची लाकडे टाकणे, जनावरे राखणे, गावची राखण करणे, गावाची साफसफाई करणे, लाकडे फोडणे इत्यादी कामे कमी मोबदल्यात करावी लागत होती.

वेळप्रसंगी वतनदाराकडून विनावेतन काम करून घेतल्यामुळे त्यांना हलाखीचे जीवन जगावे लागे. हिंदू समाजाने वतनापोटी लादलेल्या गुलामगिरीतून त्यांची मुक्तता करून केवळ बंधनातून मुक्तच केले नाही तर इतर समाज उपभोगीत असलेले सर्व मानवी हक्क त्यांना बहाल केले. सप्टेंबर १९१८ मध्ये महार वतन रद्दबातल केले. अशा प्रकारे समाज व्यवस्थेला धक्का देण्याचा पहिला प्रयत्न छ. शाहू महाराज यांनी कोल्हापूर संस्थानात केला. छ. शाहू महाराजांचा सामाजिक न्यायाचा वारसा बाबासाहेबांनी पुढे चालू ठेवला. बाबासाहेबांच्या मते वतन हे या समाजातील लोकांच्या प्रगतीला अडथळा ठरत आहे.

* डॉ. बाबासाहेब आंबेडकर यांच्या वतन परिषदा

महाराष्ट्रात काही जाती व जमातींना वतनदारी प्राप्त झालेली होती त्यात महार समाजाला वतन जास्त प्रमाणात ठिकठिकाणी मिळालेले होते हे सर्वश्रुतच आहे. तसेच काही मांग कुटुंबियांना सुद्धा अशी वतने मिळालेली होती.

१) महार वतनपरिषदा

बाबासाहेबांच्या वतनपरिषदा मधील महत्त्वपूर्ण भाग म्हणजे महार वतन परिषदा होय. बाबासाहेब आंबेडकर विविध परिषदा आणि कार्यक्रमाच्या निमित्ताने सोलापूर शहर आणि जिल्ह्यात आले होते. त्यांच्या अध्यक्षतेखाली सोलापूर शहरातील आताचे मिलिंद नगर आणि तत्कालीन थोरल्या राजवाड्यातील पंचाच्या चावडीत २६ व २७ नोव्हेंबर १९२७ रोजी वतनदार महार परिषद संपन्न झाली होती. अशा अनेक महार वतन परिषदा बाबासाहेबांच्या मार्गदर्शनाखाली कधी अध्यक्षतेखाली महाराष्ट्रभर झाल्या होत्या. त्याची आकडेवारी निश्चित सांगता येत नाही. मात्र ज्या वतन परिषदांची माहिती उपलब्ध आहे. त्यापैकी उदाहरण दाखल सोलापूर येथील २६ व २७ नोव्हेंबर १९२७ ची परिषद हिचे स्वागताध्यक्ष जिवाप्पा सुभानरव ऐदाळे होते. सोलापूरची ही परिषद ऐतिहासिक आणि क्रांतिकारी मानली जाते. या परिषदेसाठी शहर आणि जिल्ह्यातून साधारणता पाच हजार पेक्षा जास्त जनसमुदाय उपस्थित होता. या परिषदेत अध्यक्षीय भाषणात डॉ. बाबासाहेब आंबेडकर यांनी अस्पृश्य बांधवांना 'महार वतन' सोडा असा मौलिक सल्ला दिला होता. अस्पृश्य बांधवांनी आपली गावे सोडून स्वतःची स्वतंत्र वसाहत निर्माण करून राहिला शिकलं पाहिजे. स्वतःच्या आर्थिक उन्नतीचा पाया स्वतःच रचला पाहिजे. स्वावलंबी झालं पाहिजे. त्यासाठी बाबासाहेबांनी खादी विणा असा एक स्वतंत्र व्यवसाय सुचवला होता. अस्पृश्य समाजातील प्रत्येकाने खादीचे कपडे घेतल्यास तो रोजगार आपल्या अस्पृश्य बांधवांना खादीतून मिळू शकतो. असा अनमोल असा सल्ला बाबासाहेबांनी दिला होता.

या परिषदेत महत्त्वपूर्ण आठ ठराव करण्यात आले होते. त्यास उपस्थित सर्वांनी टाळ्यांच्या कडकडात अस्पृश्य जनतेच्या वतीने आठही ठरावांना मंजूरी दिली होती. त्यापैकी एक अतिशय महत्त्वाचा ठराव म्हणजे हिंदू समाजातील समाज बांधवांनी चातुर्वर्ण पद्धती बंद करून सर्वांसाठी एकच वर्ण कसा करता येईल. यावर कृतीशील अंमलबजावणी तातडीने करावी. त्यास जर विलंब झाला तर अस्पृश्य जनतेला धर्मातरासारखा वेगळा विचार करावा लागेल असा महत्त्वपूर्ण ठराव करून धमकीवजा इशारा त्यावेळी परिषदेच्या माध्यमातून बाबासाहेबांनी दिला होता.

२) मांग/ मातंग वतनपरिषदा

बाबासाहेब आंबेडकर यांनी ज्या प्रकारे महार समाजाला वतन परिषदा घेऊन वतनातून मुक्त होण्यास प्रवृत्त केले. बाबासाहेबांच्या मार्गदर्शनाखाली, अध्यक्षतेखाली मातंग समाजासाठीही स्वतंत्र अशा १४ परिषदांचे आयोजन करण्यात आले होते. यातील काही मोजक्याच परिषदांची माहिती आज उपलब्ध आहे. उदा. मुंबई, दोंड, सोलापूर, नाशिक, काटोल, अकोला अशा अनेक ठिकाणी परिषदा संपन्न झाल्या आहेत. मातंग समाजातील अनेक तत्कालिन पुढाऱ्यांनी मोठ्या हिरहिरिने या परिषदांचे आयोजन करून बाबासाहेबांच्या मार्गदर्शनाखाली आपल्या हक्क आणि अधिकार यांची जाणिव करून देण्याचे काम केले. मातंग समाजातील लोकांचा प्रतिसाद हा दिवसेंदिवस वाढत होता. मातंग समाज परिषदांपैकी ७ डिसेंबर १९२७ साली मातंग समाज परिषद, मुंबई येथे भरली होती. या परिषदेचे मार्गदर्शक स्वतः बाबासाहेब तर अध्यक्ष बाबासाहेबांचे विश्वासू सहकारी कोंडाजी रामाजी मास्तर मांग होते. या परिषदेत बाबासाहेबांनी मातंग समाजाच्या डोळ्यात झणझणीत अंजन घालणारे मार्गदर्शन केले. याप्रसंगी बोलताना बाबासाहेब म्हणाली की, " मातंग समाजाने बघ्याची भूमिका न घेता उन्नतीच्या या चळवळीत सामील व्हावे आणि अशा समाजकार्याला सहयोग द्यावा ." या बाबासाहेबांच्या विचाराने व कार्याने मातंग समाज भारावून गेला. या परिषदेला सुमारे २०० मातंग स्त्री - पुरुष उपस्थित होते. याप्रसंगी बाबासाहेब आपल्या भाषणात पुढे म्हणतात, " मला असे वाटते की जोपर्यंत मातंग समाजाला शिळे तुकडे खायला मिळत आहेत. तोपर्यंत मातंग समाजाची हीच स्थिती राहणार आहे. मातंग समाजात हिंदू धर्माने ठरवून दिलेला जुना मार्ग जोपर्यंत चालू आहे. तोपर्यंत नव्या मार्गाने जाण्यास कोणीही मातंग कार्यकर्ता निघणार नाही. हिंदू धर्माने दाखवून दिलेल्या जुन्या मार्गाचा अवलंब करून मातंग आज माणुसकीला दुरावला आहे." या परिषदेत काही महत्त्वाचे ठराव मांडले, मंजूर करून जाहीर केले ते खालील प्रमाणे.

१) डॉ. बाबासाहेब आंबेडकर यांच्या नेतृत्वाखालील महाड येथील सत्याग्रहाला मातंग समाजाने पाठिंबा द्यावा

२) म्युनिसिपल स्कूल मुंबई येथे अस्पृश्य व मांग मुलांना एकत्र बसण्यास व पाणी पिण्यास मज्जाव केला जातो. या कृतीचा आम्ही जाहीर निषेध करतो.

३) चातुर्वर्ण्य पद्धती ऐवजी एकवर्ण पद्धती अस्तित्वात आणली नाही तर परधर्मात जाण्याचा विचार बाबासाहेबांनी परिषदेत मांडला. परिषदेने या विचाराला जाहीर पाठिंबा घोषित केला.

३) महार- मांग वतनपरिषदा(संयुक्त)

महार - मांग वतनदार परिषद ,कसबे तडवळे (ढोकी) २३ फेब्रुवारी १९४१ -

सन १९४१ च्या निजाम काळात अस्पृश्यांच्या प्रश्नावर, त्यांच्या शोषणमुक्तीच्या प्रश्नावर त्यांना जागृत करणे तसेच महार - मांग समाजात जागृती करण्यासाठी, त्यांचे संघटन करण्यासाठी आणि त्यांच्यामध्ये

शिक्षणाची गोडी निर्माण व्हावी यासाठी बाबासाहेबांना ही परिषद आवश्यक होती. म्हणून त्याकाळात बाबासाहेबांना या जनजागृतीसाठी मराठवाड्यातील निजाम राज्यामध्ये कोणत्याही गावात महार - मांग अस्पृश्यांची परिषद घ्यायची होती. मात्र निजामाने ही परिषद घेण्यास मनाई केल्याने बाबासाहेबांनी इंग्रज सरकारकडे परवानगी मागितली परवानगी घेताना कसबे तडवळे हे गाव जाणीवपूर्वक निवडले कारण या गावाच्या तिन्ही बाजूला हैद्राबादच्या निजामाचे राज्य म्हणजेच हे गाव आंग्लाई आणि मोगलाई च्या सरहद्दीवर वसलेले असल्याने हे ठिकाण परिषदेस योग्य होते, कारण बाबासाहेबांना व इतर पुढाऱ्यांना मोगलाईत भाषण बंद होती. हे लक्षात घेता सरहद्दीवरील गावात परिषद घ्यायची असा हेतू संयोजकांचा असावा. त्या अर्थी कसबे तडवळे(ढोकी) हे गाव बाबासाहेबांना परिषदेस सोयीस्कर वाटले.

ठरल्याप्रमाणे दि.२२ फेब्रुवारी रोजी बाबासाहेब रेल्वेने परिषदेच्या ठिकाणी उपस्थित राहण्यासाठी सकाळी दहा वाजता रेल्वेचा शेवटचा थांबा असलेल्या कसबे तडवळे येथे पोहोचले. बाबासाहेबांची मिरवणूक तुतारी, नगारे, सनई, ढोल लेझीम, इत्यादीच्या जयघोषात बैलगाडीतून काढण्यात आली. दुसऱ्या दिवशी २३ फेब्रुवारी सभेला संबोधित करत असताना बाबासाहेब म्हणाले, गांधीजींना हिंदू गव्हर्नर पाहिजे, कलेक्टर पाहिजे, मग अस्पृश्य का नको? निजाम हद्दीतच काय? कुठेही जावा महारांची स्थिती सर्वत्र सारखीच अशी खंत व्यक्त केली. अजुन त्यांच्या पोटाचा प्रश्न सुटला नाही, शिक्षणाची ही सोय झालेली नाही, लाखो एकर जमीन गायरान पडलेली असून अस्पृश्यांची उपासमार होते. यासाठी संघटन करावे. मृत प्राण्यांची मांस खाऊ नका, शिका, स्वच्छ रहा, स्वाभिमान बाळगा वगैरे विषयांवर या परिषदेत विस्तृत मार्गदर्शन केले. बाबासाहेबांनी म्हणाले निजाम संस्थानातील महार व मांग वतनदाराची स्थिती सारखीच होती भारतातील अनेक संस्थांना पैकी निजामाचे राज्य सर्वांत मोठे होते. त्यामानाने बडोदा राज्य फार लहान आहे. परंतु या संस्थानाने अस्पृश्यांच्या शिक्षणाची सोय केली. तर म्हैसूर संस्थानामध्ये अस्पृश्यांना जमिनी मिळाल्या. त्या संस्थानात त्यांच्या हिताकडे विशेष लक्ष दिल्याचे दिसून येते. मात्र तशी हैदराबाद संस्थानात सोय झाली नाही. बाबासाहेबांनी कसबे तडवळे महार - मांग वतनदार परिषदेमध्ये त्यांच्यावर होणारे अन्यायाला निश्चितच वाचा फोडली होती. जातीव्यवस्था, अस्पृश्यता याविषयी चिंता व्यक्त करून मार्गदर्शन केले. असे त्यावेळेस त्यांनी मार्गदर्शनपर उपाय सांगितले. वतनदार परिषदेमध्ये बाबासाहेबांचे भाषण झाल्यावर तीन ठराव मांडून पास करून घेण्यात आले होते. ते खालीलप्रमाणे....

- १) निजाम सरकारच्या हद्दीतील वतनदार महार - मांग लोकांना करावी लागणारी कामे लक्षात घेता त्यांना सरकारकडून योग्य मोबदला मिळत नाही. तरी सरकारी जंगलांच्या जमिनी देऊन त्यांच्या पोटाचा प्रश्न मिटवावा.

- २) निजाम हद्दीत राहणाच्या अस्पृश्य लोकांची हेळसांड होत आहे. तरी सरकार तर्फे त्यांच्या प्राथमिक शिक्षणाची सोय त्वरित करण्यात यावी.
- ३) नवीन होणाऱ्या राज्यघटनेत निजाम हद्दीतील अस्पृश्य जनतेला त्यांच्या लोकसंख्येच्या प्रमाणात प्रतिनिधी मिळावे

सारांश / निष्कर्ष :-


स्वातंत्र्यपूर्व व स्वातंत्र्योत्तर काळात डॉ. बाबासाहेब आंबेडकर यांच्या मार्गदर्शनाखाली व अध्यक्षतेखाली घेण्यात आलेल्या वतन परिषदा ह्या अस्पृश्यांच्या सामाजिक, सांस्कृतिक, राजकीय, मानसिक, शैक्षणिक आणि धार्मिक जीवनात अमुलाग्र बदल करण्याच्या कार्यात मैलाच्या दगड ठरल्या आहेत. वतन परिषदांमध्ये मांडण्यात आलेले ठराव आणि त्यास एकमुखाने मिळणारी मंजूरी व पाठिंबा हा देखील इथल्या व्यवस्थेला सुरंग लावणारी क्रांतिकारी गोष्ट होती. जनसमुदायाच्या मानवमुक्तीच्या लढ्यात वाढता सहभाग हे झालेल्या वतन परिषदांचे फलित होते. अनेक परिषदा या अस्पृश्यांच्यासाठी आयोजित केल्या होत्या त्यामध्ये अस्पृश्यांनी सहभाग घेतला होता म्हणजेच सामाजिक बदलासाठी अस्पृश्य- अस्पृश्य लोकांनी एकत्रितपणे सहभाग घेतला हे वतन परिषदेचे यश आहे.

संदर्भ साधने :-

- १) डॉ. जयसिंगराव पवार, डॉ. मंजुश्री पवार मराठ्यांची राज्यव्यवस्था, समाज व्यवस्था आणि अर्थव्यवस्था, फडके प्रकाशन, कोल्हापूर, जून २०१९, पृष्ठ - ६९, ७४
- २) डॉ. सोमनाथ कदम, आंबेडकरी चळवळीतील मातंग समाज, लोकवाड: मय गृह, मुंबई, ई-आवृत्ती, जुलै २०२१, पृष्ठ - ९१, ९२, ९३, ९४, ९५
- ३) डॉ. बाबासाहेब आंबेडकर यांची भाषणे भाग -१, डॉ. बाबासाहेब आंबेडकर चरित्र - साधने प्रकाशन समिती, उच्च आणि तंत्रशिक्षण विभाग, महाराष्ट्र शासन, मुंबई प्रथमावृत्ती, १५ ऑक्टोबर २००२, पृष्ठ - ८५, ९७, ९८, ९९
- ४) डॉ. बाबासाहेब आंबेडकर यांची भाषणे भाग -२, डॉ. बाबासाहेब आंबेडकर चरित्र - साधने प्रकाशन समिती, उच्च आणि तंत्रशिक्षण विभाग, महाराष्ट्र शासन, मुंबई प्रथमावृत्ती, १५ ऑक्टोबर २००२, पृष्ठ - ३६६, ३६८, ३६९, ३७०



Exploring silicon nanoparticles and nanographite-based anodes for lithium-ion batteries

Sohan Thombare¹ , Rohan Patil², Ranjit Humane³, Bharat Kale^{3,4}, Ramchandra Kalubarme³, Dhanaji Malavekar⁵, Manisha Phadatare^{2,*}, and Chandrakant Lokhande^{1,*}

¹ Center for Interdisciplinary Research, D. Y. Patil Education Society (Deemed To Be University), Kolhapur, Maharashtra 416006, India

² Departments of Engineering, Mathematics and Subject Didactics (IMD), Mid Sweden University, Sundsvall, SE 85170, Sweden

³ Center for Materials for Electronics Technology (C-MET), Government of India, Panchawati, Off. Pashan Road, Pune 411008, India

⁴ Materials Science (COE) Research and Development, MIT World Peace University (MIT-WPU), Kothrud, Pune 411038, Maharashtra, India

⁵ Optoelectronics Convergence Research Center, Department of Materials Science and Engineering, Chonnam National University, Gwangju 61186, South Korea

Received: 20 January 2024

Accepted: 30 June 2024

Published online:
25 July 2024

© The Author(s), 2024

ABSTRACT

This study investigates the performance of silicon nanoparticles (Si NPs) and silicon nanographite (SiNG) composite-based anodes for lithium-ion batteries (LiBs). Si offers a promising alternative to traditional graphite anodes due to its higher theoretical capacity, despite encountering challenges such as volume expansion, pulverization, and the formation of a solid electrolyte interface (SEI) during lithiation. SiNPs anode exhibited initial specific capacities of 1568.9 mAh/g, decreasing to 1137.6 mAh/g after 100th cycles, with stable Li–Si alloy phases and high Coulombic efficiency (100.48%). It also showed good rate capability, retaining 1191.3 mAh/g at 8400 mA g⁻¹ (2.82C), attributed to its carbon matrix structure. EIS indicated charge transfer with R_B of 3.9 Ω/cm^{-2} and R_{CT} of 11.4 Ω/cm^{-2} . Contrastingly, SiNG composite anode had an initial capacity of 1780.7 mAh/g, decreasing to 1297.5 mAh/g after 100 cycles. Its composite structure provided cycling stability, with relatively stable capacities after 50 cycles. It exhibited good rate capability (1191.3 mAh/g at 8399.9 mA g⁻¹), attributed to its carbon matrix structure. Electrochemical impedance spectroscopy showed higher resistances for R_B of 4.2 Ω/cm^{-2} and R_{CT} of 15.6 Ω/cm^{-2} compared to SiNPs anode. These findings suggest avenues for improving energy storage devices by selecting and designing suitable anode materials.

Address correspondence to E-mail: Manisha.Phadatare@miun.se; l_chandrakant@yahoo.com

1 Introduction

Li-ion batteries (LiBs) are up-and-coming electrochemical energy storage gadgets [1]. Nowadays, a silicon (Si) element is naturally available in the Earth's womb. Its theoretical capacity as a discharging anode element in LiBs is ten times greater than that of a natural graphite anode. Due to its high theoretical capacity (4200 mAh/g), it is considered an attractive candidate for a high-energy-density anode for the next-generation [1]. However, Si is hindered by significant limitations that have thus far restricted its widespread commercial adoption. The most significant concerns involve the pulverization of Si particles, structural failure of composite electrode (such as the mechanical detachment of Si particles), and the ongoing degradation resulting from the continuous breakdown and regeneration of solid electrolyte interphase (SEI) layer, as observed in other alloy materials [2]. These difficulties stem from the persistent changes in volume experienced by Si during the processes of lithiation and delithiation, leading to continual active lithium loss and irreversible electrolyte consumption, consequently leading to notable capacity degradation [2]. Numerous endeavors have been undertaken to mitigate the issue of Si particle cracking, including strategies such as coating or employing advanced particle designs [3]. Typically, decreasing the particle size diminishes cracking and consequently reduces electrode pulverization. The critical size threshold has been identified at approximately 150 nm; however, further reduction in particle size alters the electrochemical characteristics due to a significant increase in specific surface area [4]. Moreover, the rise in surface area also results in an elevated irreversible capacity and active lithium loss during the initial cycle, thereby manifesting as a reduced Coulombic efficiency [5]. Si/C composites, where Si nanostructures are distributed on a carbon support, have emerged as a viable option for commercial use. A range of carbon materials, including amorphous carbon, carbon nanotubes, graphite, and graphene, have been employed as matrices. Notably, graphite and graphene are favored due to their substantial specific surface area and excellent electrical conductivity. Nonetheless, stabilizing Si nanoparticles on the surfaces of graphite and graphene presents a significant challenge due to the weak interaction between basal plane sp^2 carbon atoms and Si NPs [6].

In this study, pre-made nanoparticles were selected to design Si NPs and nanographite (NG) anode

electrodes. Si offers a significantly higher theoretical capacity for lithium-ion storage compared to traditional graphite anodes. Si NPs can store more lithium ions per unit mass, thereby increasing the energy density of LiBs. Meanwhile, NG, with its nanoscale dimensions, enhances the electrical conductivity of composite anode material. This improves electron transport during delithiation and lithiation cycles, leading to enhanced battery performance. Si NPs possess excellent electrical conductivity, crucial for ensuring efficient electron transport during charge and discharge cycles in the battery. This characteristic aids in maintaining high-power output and reducing internal resistance, thus enhancing the overall battery performance. Si NPs offer the advantage of being readily scalable for industrial production, making them a viable candidate for large-scale battery manufacturing. Their synthesis can be achieved through various cost-effective methods, ensuring feasibility for commercialization. Combining Si NPs with NG in a composite anode can result in synergistic effects. The unique properties of each component, including the high lithium storage capacity of Si NPs and the excellent conductivity of NG, complement each other, contributing to overall LiBs performance improvement. Additionally, Si NPs often undergo significant volume changes during lithium-ion insertion and extraction, leading to electrode pulverization and capacity fading. The inclusion of NG mitigates these issues by providing mechanical support and enhancing the structural stability of composite anode. Both Si NPs and SiNG can be surface-functionalized to tailor their properties, improving compatibility with the electrolyte and other battery components. This enhances interfacial interactions and electrochemical performance. The Si NPs and SiNG flakes, developed as spherical clustered-type anodes for lithium-ion batteries (LiBs), form an effective electronic conductive network in the composite material. Various physicochemical methods, including X-ray diffraction (XRD), Fourier transform infrared spectroscopy (FTIR), surface area analysis, field emission scanning electron microscopy (FE-SEM), and Raman spectroscopy, were employed for structural and chemical bonding analysis, as well as contact angle analysis. Electrochemical characterization of Si-NG-based anodes in half-coin cell devices was performed using techniques such as differential derivative capacity, galvanostatic charge-discharge (GCD), and electrochemical impedance spectroscopy (EIS), followed by post-mortem physicochemical

study. These findings demonstrate the potential of Si-NG-based anodes for high-performance LiBs, marking a step forward in sustainable energy storage technology.

2 Experimental details

2.1 Materials

For silicon nanoparticles (Si NPs) and silicon nanographite (SiNG)-based electrodes, Si NPs with a particle size of 100 nm or less and a base metal content of 98% were purchased from Sigma-Aldrich. NG powder with particle sizes under 500 nm (battery grade) was purchased from Xiamen Tob New Energy Technology Co., Ltd., China. N-methyl-2-pyrrolidone (NMP), activated charcoal (AC), polyvinylidene fluoride (PVDF) were purchased from Sigma-Aldrich.

For Si NPs and SiNG composite anode half-coin cell fabrication, A type lithium battery CR2032 3 V coin cell were purchased from Sigma-Aldrich, 1 M Lithium hexafluorophosphate (LiPF_6) is a solution of (dimethyl carbonate (DMC), ethylene carbonate (EC), and diethyl carbonate) were purchased from Sigma-Aldrich, Lithium metal foil of thickness 0.6 mm was purchased from Sigma-Aldrich, and Whatman™ filter paper was purchased from Sigma-Aldrich. All chemicals were used without additional purification. For post-mortem analysis, the half-coin cells were fully lithiated. The disassembly procedure was conducted in an argon-filled glove box ($\text{H}_2\text{O} < 0.1$ ppm and $\text{O}_2 < 0.1$ ppm). Using stainless steel scissors, samples from most of electrode material were carefully cut after Si NPs and SiNG composite electrodes. The samples were carefully handled with tweezers, grasping them only by the edges, and were kept separately in individual plastic bags.

2.2 Preparation of Si NPs and SiNG anode and device fabrication

In N-methyl-2-pyrrolidone (NMP), a mixture of Si NPs, activated charcoal (AC), black sucrose powder (BSP), and polyvinylidene fluoride (PVDF) was mixed in a weight ratio of 70:10:10:10. The PVDF was used as a binding agent, and NMP was selected as the solvent in the formulation. BSP was added to increase the anode porosity, and activated charcoal was used as a conductive additive. The components were placed on

a magnetic stirrer to prepare the mixture and mixed thoroughly for 36 h at 1000 revolutions per minute. This process resulted in a uniform, thick, and sticky slurry texture. Subsequently, the slurry was applied to a copper foil using a doctor blade method, ensuring an even coating. The coated foil was then dried for 12 h at 100 °C in a vacuum oven to remove the solvent and achieve a solid film. After drying, the anode was cut into round disc-shaped with a diameter of 16 mm. The weight was recorded as 4.87 mg (2.01 mg cm^{-2}).

Additionally, a SiNG composite anode was formed by combining two distinct anode materials: nanographite (NG) and Si NPs. The components used in the composite anode were Si NPs, NG, AC, BSP, and PVDF, which were mixed in N-methyl-2-pyrrolidone at a weight ratio of 50:20:10:10:10. To prepare the anode, the slurry was applied to a copper metal foil substrate using a doctor blade, ensuring a thin and uniform coating. The coated substrate was then heated for 12 h at 100 °C, which assisted in solidifying the slurry and evaporating the solvent. After the heating process, the anode was dried and sliced into circular discs with a diameter of 16 mm. The weight measurement of anode was 4.32 mg (2.01 mg cm^{-2}).

The half-coin cell was assembled using the following components: the reference and counter electrodes were constructed from lithium metal foil with a thickness of 0.6 mm. A 1 M LiPF_6 solution was employed as the electrolyte in a 1:1 weight ratio of ethylene carbonate (EC) and diethyl carbonate (DEC). Filter paper (Whatman™) was used as a separator. The electrolyte solution served as the cells ion transport medium. The entire cell assembly process was conducted inside a glove box filled with argon gas ($\text{H}_2\text{O} < 0.1$ ppm and $\text{O}_2 < 0.1$ ppm) to ensure an inert environment to prevent unwanted reactions or contamination.

2.3 Material characterization

The sample crystallinity was analyzed via X-ray diffraction by a Rigaku mini flex-600 instrument that utilized $\text{CuK}\alpha$ ($\lambda = 1.54184 \text{ \AA}$) over a 2θ range of 10° – 90° . The surface studies were performed on a JASCO FTIR 6100 apparatus. The specific surface area and pore size distribution details were collected by surface area analysis and surface area analysis model using Quantachrome Instruments v3.01. Raman spectra were acquired over the spectral range of 50 – 1000 cm^{-1} using a Renishaw inVia™ Raman microscope by laser stimulation at 532 nm. Sample morphology, crystallite size,

and elemental composition were studied using field emission scanning electron microscopy (FE-SEM) and energy-dispersive X-ray spectroscopy (EDX) using the NOVA NANOSEM 450 instrument. The contact angles of both Si nanoparticles (NPs) and SiNG composite were determined utilizing a contact angle meter (HO-IADCAM-01, Holmarc OptoMechatronics Pvt. Ltd., India).

The post-mortem physico-chemical characterization study, the sample crystallinity, alloy formation phases was analyzed via post-mortem X-ray diffraction by a Rigaku mini flex-600 instrument that utilized $\text{CuK}\alpha$ ($\lambda = 1.54184 \text{ \AA}$) over a 2θ range of 10° – 80° . Also, sample morphology like solid electrolyte interphase layer, cracking of electrode were studied using post-mortem field emission scanning electron microscopy (FE-SEM) using the NOVA NANOSEM 450 instrument.

3 Results and discussion

3.1 Structural analysis

Figure 1a illustrates the XRD pattern of Si NPs, showing prominent peaks at approximately 28.7° , 47.7° , 56.5° , 69.6° , and 76.6° , corresponding to the diffraction planes of (111), (220), (311), (400), and (331) of Si [JCPDS no. 27-1402], respectively [7]. Figure 1b depicts the XRD pattern of SiNG composite anode, revealing diffraction peaks at $2\theta = 26.4^\circ$, 28.5° , 47.3° , and 54.67° , assignable to the (002), (111), (220), and (004) planes of SiNG composite anode. The presence of graphite is confirmed in this SiNG composite anode [JCPDS no. 41-1487] [6]. The higher intensity of (111) peak in Si NPs anode suggests that it is more crystalline compared to SiNG composite anode. These findings offer valuable insights into the structure and composition of Si NPs and SiNG composite anodes. The reduction in prominent peaks associated with Si and NG in the XRD pattern of SiNG composite can be attributed to the presence of non-crystalline substances enveloping the structure. These substances hinder X-ray penetration towards the crystalline Si particles and NG flakes, resulting in decreased peak intensity. This suggests that the crystalline structure of Si NPs anode is more pronounced or ordered compared to that of SiNG composite anode. In XRD analysis, peak intensity reflects the crystalline quality or degree of ordering in the crystal lattice [8]. A higher intensity peak indicates a greater abundance of corresponding

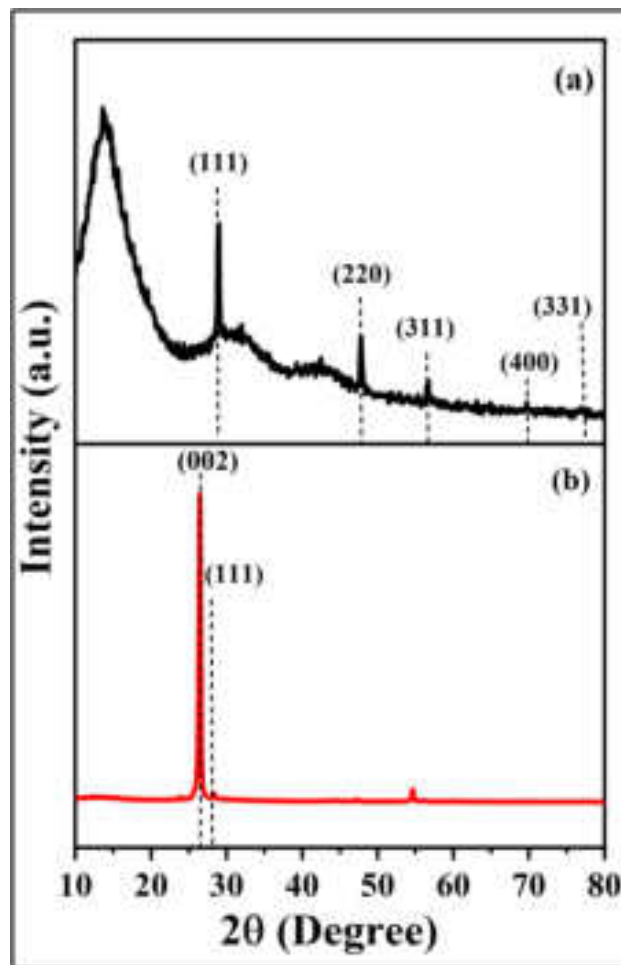


Fig. 1 The X-ray diffraction patterns of **a** Si NPs and **b** SiNG composite

crystallographic plane in the sample, often correlating with higher crystallinity [9]. Therefore, the observed higher intensity peak in Si NPs anode implies a more well-defined crystalline structure, potentially indicating better structural integrity or a more ordered arrangement of Si NPs compared to SiNG composite anode. Introducing NG to Si NPs may enhance the electrical conductivity of composite material, thereby improving electron transfer kinetics during charge and discharge cycles. Additionally, SiNG might contribute to the structural stability of composite anode, potentially alleviating volume expansion and contraction issues associated with the lithiation and delithiation processes in LiBs. Here oxide feature is absent because the source of oxygen in the electrode could be attributed to surface oxidation of Si NPs or NG during synthesis, handling, or exposure to air. However, this surface oxidation may not result in the formation

of detectable crystalline oxides, especially if the oxidation is superficial [10]. In the XRD spectrum spanning 10° – 80° , a discernible bump indicative of SiNPs transitioning to SiO_2 is evident, typically within the 17° – 25° . This phenomenon is observed in the anode. Notably, in the corresponding bump within the SiNG composite electrode, the intensity associated with SiO_2 is noticeably diminished [JCPDS File No. 029-0085].

3.2 Fourier transform infrared spectroscopy

Fourier transform infrared spectroscopy (FTIR) analysis was carried out to identify the organic, inorganic, and polymeric materials in Si NPs and the mixture of SiNG composite anode. The FTIR spectra in the 400 – 4000 cm^{-1} wavenumber range are illustrated in Fig. 2a, b. For Si NPs anode, the spectrum showed a signal for Si–O strong bending vibration at 483 cm^{-1} [11–13], indicating the presence of Si–O bonds. Additionally, signals for the asymmetric vibration of Si–O–Si are detected at 873 , 1089 , and 1190 cm^{-1} [11, 12], suggesting the presence of Si–O–Si bonds. The spectrum also shows signals for Si–H stretching modes at 1868 and 2258 cm^{-1} . For SiNG composite anode, the SiNG composite anode displayed distinct signals in the FTIR spectrum. The Si–O strong bending vibration is observed at 498 cm^{-1} , indicating the presence of Si–O bonds [11, 12]. Additionally, signals for the asymmetric vibration of Si–O–Si were detected at 866 , 1125 , and 1233 cm^{-1} , suggesting the presence of Si–O–Si bonds. The spectrum also showed signals for –COOH stretching at 1378 and 1601 cm^{-1} and carboxyl C=O stretching at 1750 cm^{-1} .

In the FTIR analysis shows that both anodes comprise of Si–O and Si–O–Si bonds. The SiNG composite anode also contains –COOH and carboxyl C=O functional groups. The bonding density of Si–OH and Si–O–Si is higher in SiNG composite anode than in Si NPs anode. This suggests that adding NG to Si NPs improves the bonding between Si and oxygen atoms, which may be beneficial for the electrochemical performance of anode.

The observed shifts in the FTIR signals for Si–O and other bonding features between Si NPs and SiNG can be attributed to several factors. Firstly, Si NPs and SiNG may possess distinct surface chemistries or compositions, leading to differences in the types and positions of observed bonding features in the FTIR spectra. Additionally, the incorporation of NG in the SiNG composite could induce surface functionalization or

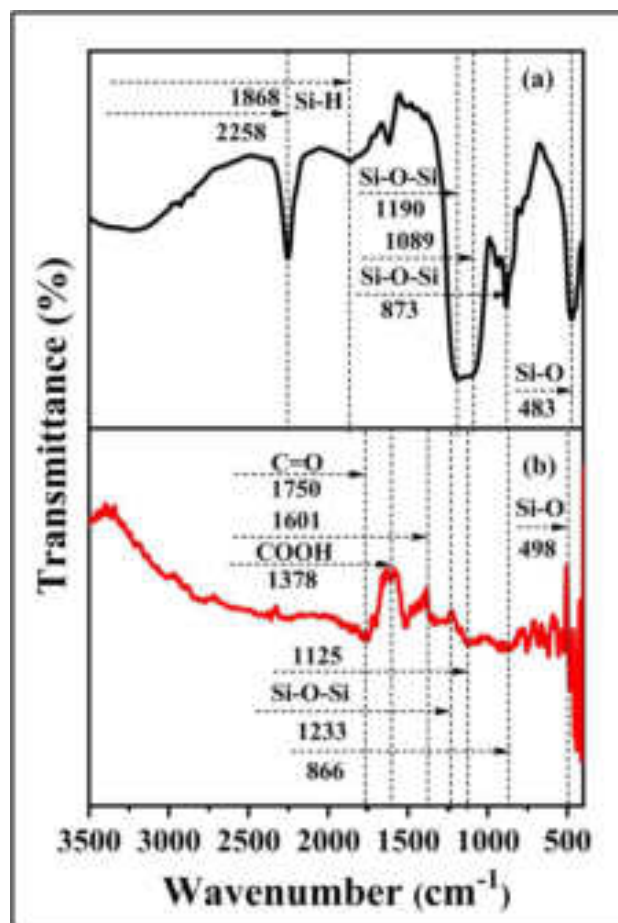


Fig. 2 The Fourier transform infrared spectroscopy of **a** Si NPs and **b** SiNG composite

chemical interactions, altering the bonding environment of Si NPs and resulting in shifts in the positions of Si–O and other bonding peaks in the FTIR spectra. Moreover, variations in the oxidation state or degree of surface oxidation between Si NPs and SiNG may also influence the FTIR spectra, contributing to differences in the observed bonding features [14].

3.3 Surface area analysis

The Brunauer–Emmett–Teller (BET) isotherm, specifically type III and IV, is a well-known model in surface chemistry and materials research. It characterizes the relationship between gas adsorption on a solid surface and relative pressure (P/P_0), where P_0 denotes the saturation vapor pressure of adsorbate at a specific temperature.

For Si NPs anode Fig. 3a, b BET type III isotherms typically exhibit a sharp rise at low relative pressures,

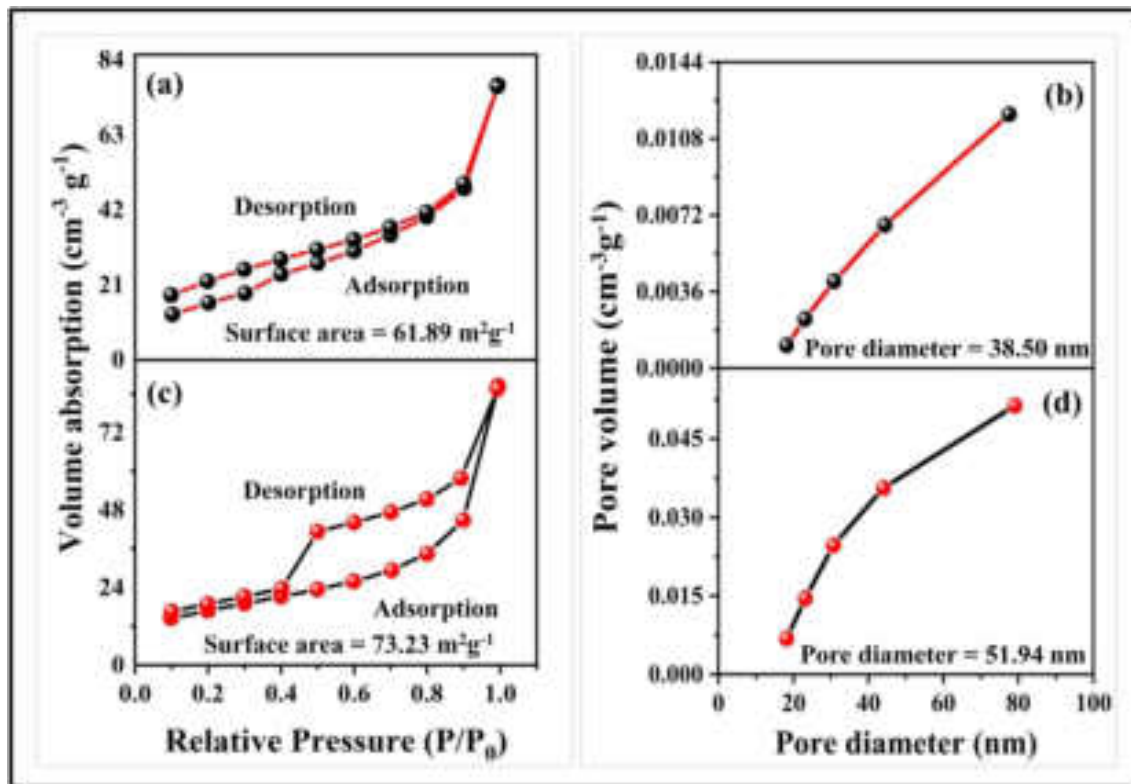


Fig. 3 Nitrogen adsorption–desorption isotherms of **a** Si NPs and **c** SiNG composite, and pore size distribution curves of **b** Si NPs and **d** SiNG composite

indicating monolayer formation on the solid surface. An inflection point marks the transition from monolayer to multilayer adsorption, reaching a plateau to represent surface saturation. Hysteresis during desorption is common, indicating non-ideal porous structures. The specific surface area of Si NPs is $61.89 \text{ m}^2 \text{ g}^{-1}$, with an average pore diameter of 38.50 nm.

For SiNG composite anode Fig. 3c, d, BET type IV isotherms also start with a rapid increase at low relative pressures, forming a monolayer. Pronounced hysteresis loops during desorption suggest capillary condensation within pores. The total adsorption capacity is typically higher than type III, reflecting a more extensive adsorption capability. The specific surface area of SiNG composite anode is $73.23 \text{ m}^2 \text{ g}^{-1}$, with a mean pore size of 51.94 nm, indicating a mesoporous structure.

The Barrett–Joyner–Halenda (BJH) analysis is a technique utilized for determining the pore size distribution in porous materials, such as catalysts, adsorbents, and membranes. Named after the scientists who developed it Barrett, Joyner, and Halenda the method relies on analyzing the adsorption or

desorption isotherms obtained from gas adsorption experiments, typically utilizing nitrogen as the adsorbate. This approach is widely applied in characterizing porous materials through gas adsorption techniques, notably nitrogen adsorption/desorption isotherms conducted at cryogenic temperatures [15].

The morphology of SiNG composite anode reveals the presence of smaller NG flakes within the pores, alongside large flakes and spherical clusters. The high surface energy and free hydroxyl (OH) groups on Si NPs likely contribute to the aggregation and growth of flakes, creating a heterogeneous microstructure that may impact electrochemical performance [16].

The discrepancy between the beginning and end points of desorption and adsorption in gas adsorption isotherms is common and can stem from hysteresis caused by capillary condensation, pore blocking, or differences in pore sizes and surface properties. These factors can lead to non-coinciding curves due to variations in adsorption and desorption behaviors [17].

3.4 Raman spectrum analysis

Raman spectroscopy was used to investigate the chemical bonding characteristics of Si NPs and SiNG composite anode. The Raman spectra of (a) Si NPs and (b) SiNG are shown in Fig. 4. For Si NPs anode the Raman spectrum of Si NPs anode shows a peak centered at 523 cm^{-1} , which is associated with crystalline silicon (C-Si) [7]. This indicates that Si NPs do not undergo a phase transition during the preparation of anode. The Raman spectrum of SiNG composite anode shows two peaks at 1346 and 1579 cm^{-1} , associated with graphite. These peaks correspond to *D* and *G* bands [7]. These peaks indicate that SiNG composite anode contains graphite. The 2D band is defect-related and typically observed in highly disordered graphite. The fact that 2D band in the Raman spectrum of SiNG composite anode suggests that graphite in the composite is highly disordered. This may be due to the interaction between graphite and Si NPs. The presence of graphite in SiNG composite anode may also improve the cycling stability of anode. Graphite is a hard material

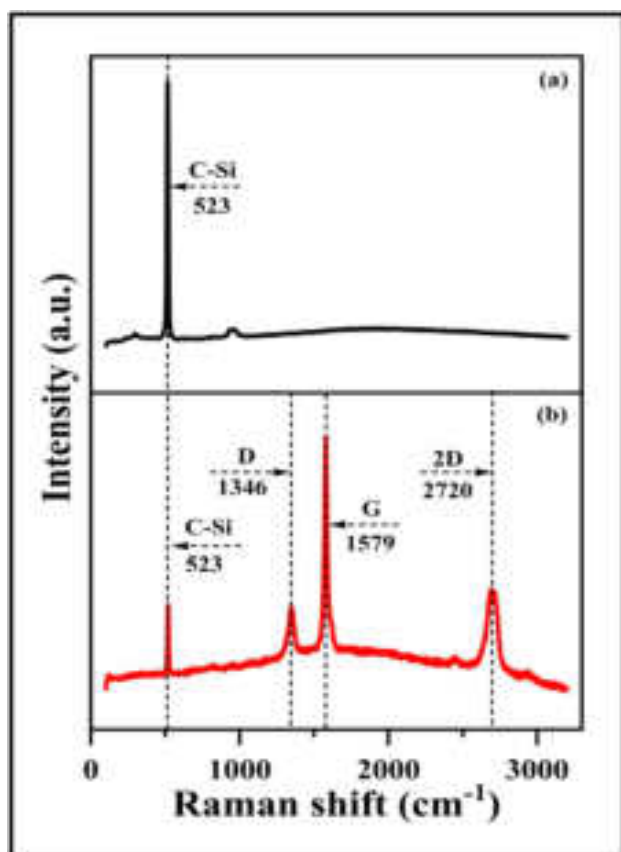


Fig. 4 The Raman spectra of **a** Si NPs and **b** SiNG composite

that is less likely to undergo volume expansion during cycling. This may help to prevent the anode from cracking or delaminating, which can lead to a loss of capacity. Raman analysis shows that Si NPs anode has crystalline Si, while SiNG composite anode has both crystalline Si and NG. The presence of NG in SiNG composite anode enhances the electrochemical performance of anode as a good electron conductor.

3.5 Morphological analysis

Field emission scanning electron microscopy (FE-SEM) was used to investigate the size and morphology of Si NPs and SiNG composite anodes. Figure 5a, b show FE-SEM images of Si NPs anode, while Fig. 5d, e show FE-SEM images of SiNG composite anode. The FE-SEM image of Si NPs anode shows porous spherical clusters composed of aggregated particles ranging in size from 48 to 124 nm.

The FE-SEM image of SiNG composite anode shows a combination of small and large pores. Additionally, NG flakes can be observed. The morphology of SiNG composite anode is a mix of large flakes and spherical clusters. The large flakes are likely due to the high surface energy and free OH groups on the surface of Si NPs. These groups interact with NG flakes, causing them to adhere to Si NPs. The spherical clusters are formed by the aggregation of smaller Si NPs. This may help to prevent the anode from cracking or delaminating, which leads to a loss of capacity. The results of FE-SEM show that Si NPs anode porous spherical clusters, and SiNG anode has porous spherical clusters with NG flakes. Porous structure benefits ion and electron transport, while NG flakes may enhance mechanical stability and electrochemical performance [18].

3.6 Energy-dispersive X-ray spectroscopy

Figure 5 shows the chemical composition of (c) Si NPs and (f) SiNG composite anode as determined by EDX. The EDX spectra confirm the absence of other impurities and show the presence of Si and C elements. In Si NPs the atomic percentages are Si as 56.20%, O as 43.80%.

Figure 5f displays SiNG composite anode EDX spectra. The Si, C, O atomic percentages are shown in the inset of each range, confirming the anode composite origin of carbon. The atomic percentages are Si as 42.68%, O as 41.90%, and C as 15.43%. Gold (Au) was detected due to coating used to enhance conductivity.

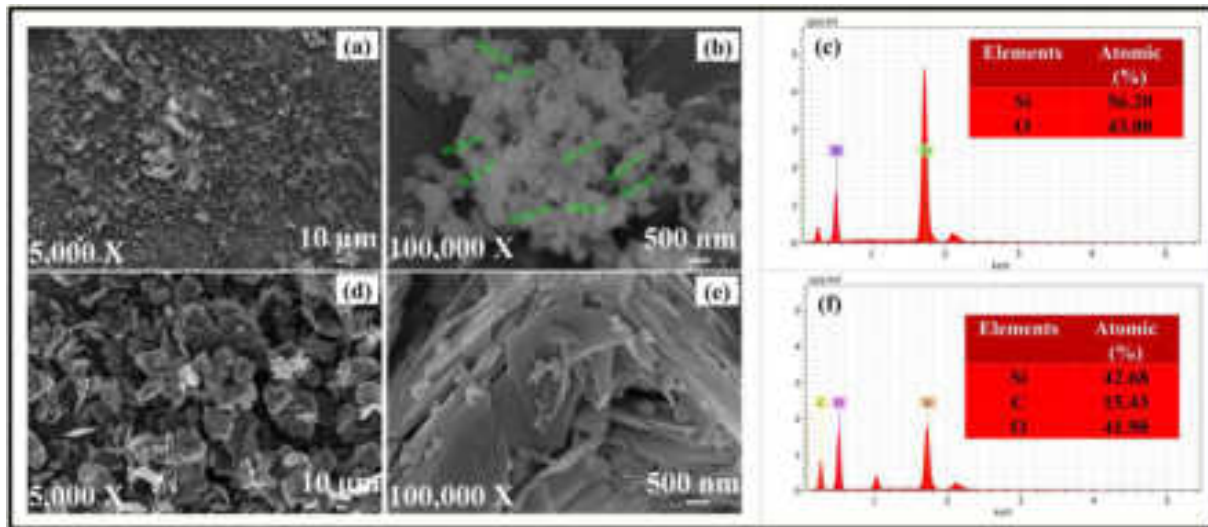


Fig. 5 FE-SEM images of Si NPs anode: **a** 5 k, **b** 100 kX, **c** EDX spectrum (Insets show atomic percentages of elements). For SiNG composite anode: **d** 5 k, **e** 100 kX, and **f** EDX spectrum (Insets show atomic percentages of elements)

3.7 Contact angle measurement

The surface structure of solid anode electrodes plays a crucial role in their interaction with water-based electrolytes, significantly impacting electrochemical performance. Reduced contact angles and increased surface energy enhance the electrodes electrochemical performance. Contact angle values are influenced by factors such as particle size, shape, purity, surface roughness, cleanliness, and heterogeneity [19, 20]. In LiBs application, hydrophilic and super-hydrophilic characteristics are beneficial as they increase the surface area for electrolyte-ion interaction with the active electrode. Figure 6 illustrates water contact angle

images of (a) Si NPs and (b) SiNG composite anodes. Figure 6a highlights the superior super-hydrophilic surface properties of Si NPs surfaces.

The super-hydrophilicity of Si NPs electrode surfaces is evidenced by water droplets completely dispersing and forming a thin, homogeneous coating with a zero-degree water contact angle, firmly adhering to the electrode surface. This unique property arises from the surface chemistry and structure of Si NPs. The water contact angle of SiNG composite anodes is 40.10° , as shown in Fig. 6b. The lower water contact angle benefits the porous surface of SiNG composite anode, enhancing the hydrophilic property and potentially reducing resistance by establishing close

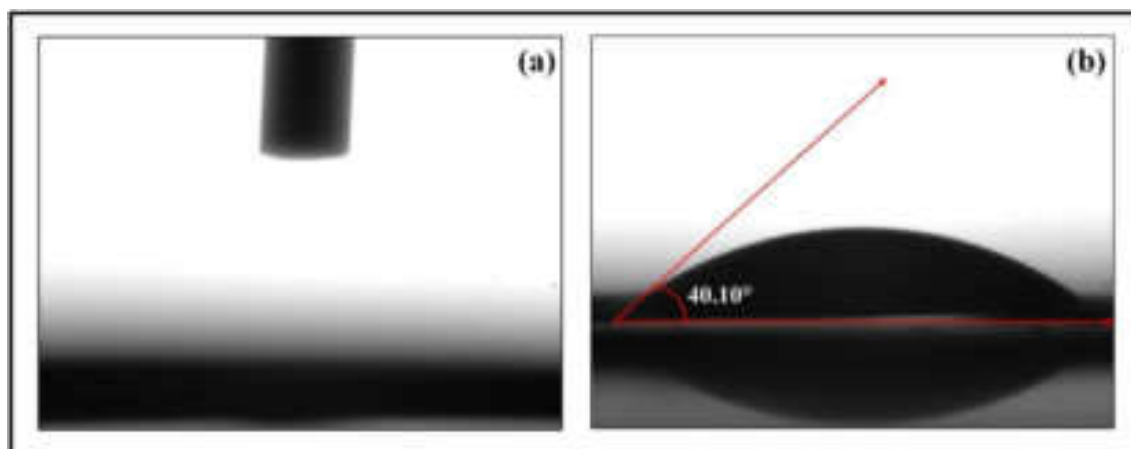


Fig. 6 Water contact angle photographs of **a** Si NPs and **b** SiNG composite electrode

contact with the water-based electrolyte. Improving the surface characteristics of solid anode electrodes, such as achieving super-hydrophilicity with zero contact angles or hydrophilicity with decreasing water contact angles, can enhance the performance of electrochemical devices like LiBs [21]. To transform superhydrophobic Si NPs into a hydrophilic state, a coating of PVDF hydrophilic polymers can be applied onto their surface. This coating effectively shields the inherent hydrophobicity of Si NPs, rendering them compatible with aqueous environments [22]. Additionally, adjusting the surface charge of Si NPs can further enhance their hydrophilicity. This can be accomplished by introducing charged molecules or polymers onto the surface [23].

3.8 Electrochemical characterizations

3.8.1 Differential derivative capacity

The electrochemical measurement of Si NPs-NG-based anodes in LiBs was performed with a half-coin cell formation in 1 M LiPF₆ electrolyte solution. In this Si NPs-NG-based anode setup, lithium metal chip acts as the counter and reference electrode. This half-coin cell device is illustrated in Fig. 7.

The GCD measurements were performed within the 0 to 1.5 V voltage range vs. Li/Li⁺. The corresponding derivative capacity for one cycle of each anode is illustrated in Fig. 8a, b. For Si NPs anode, the first strong lithiation peak observed in the GCD derivative capacity plot represents solid electrolyte interface (SEI) film formation and transforming crystalline Si into

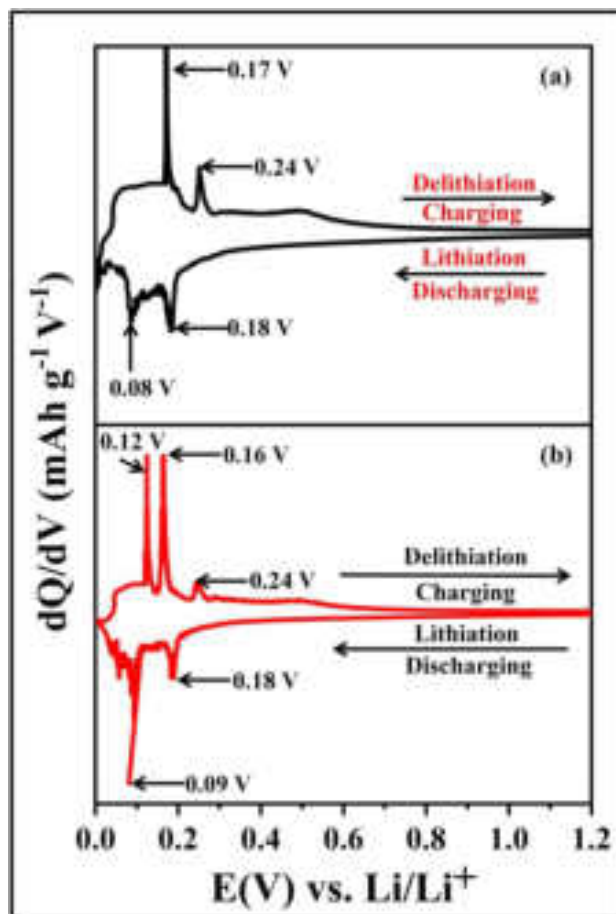
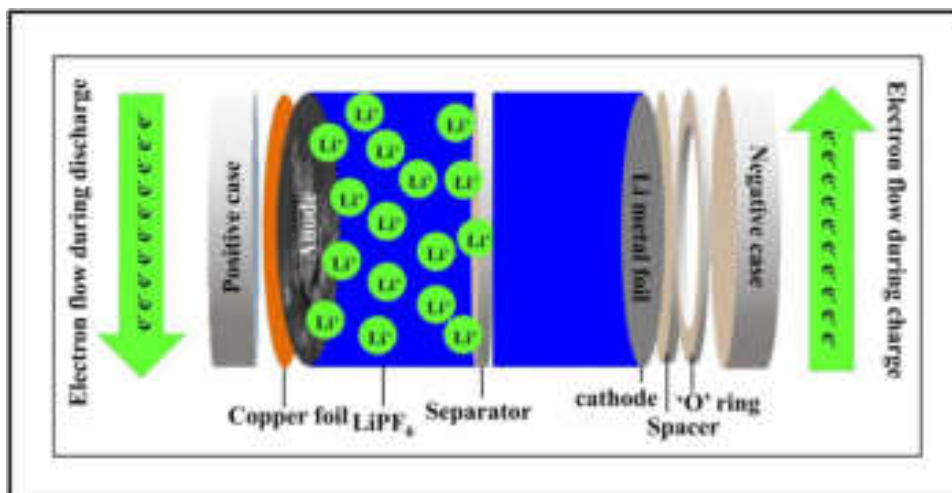


Fig. 8 The galvanostatic charge–discharge (GCD) potential profiles and derivative capacity curve of **a** Si NPs at 0.14C and **b** SiNG composite anode at 0.18C

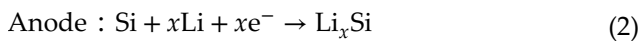
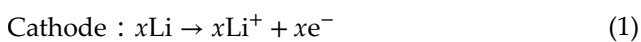
amorphous Si. This peak appears at approximately +0.18 V vs. Li/Li⁺. The subsequent lithiation cycles exhibit lithiation peaks at different voltages, namely

Fig. 7 The schematic representation of Si NPs anode half-coin cell device

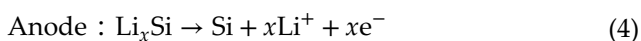
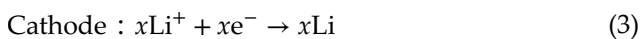


+0.25 V, +0.10 V, and +0.04 V vs. Li/Li⁺, which correspond to the lithiation of amorphous Si to various lithiated states such as Li_xSi phases [24]. For SiNG composite anode, SiNG composite anode exhibits a similar GCD profile to Si NPs anode. The first strong lithiation peaks appear at around +0.18 V and 0.09 V vs. Li/Li⁺. The subsequent lithiation cycles show peaks at different voltages, namely +0.25 V, +0.10 V, and +0.04 V vs. Li/Li⁺. During discharge, the ions return to the cathode. In the case where Si NPs are used as the anode and lithium is used as the cathode, the redox process occurs as follows [25];

During lithiation

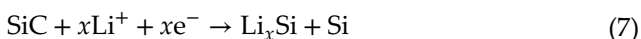
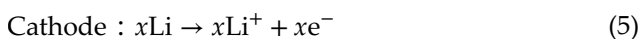


During delithiation

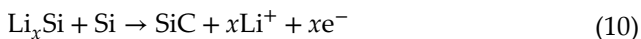
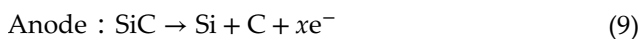
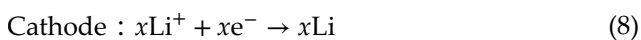


When using a SiNG composite anode and lithium cathode, the redox process occurs as follows;

During lithiation



During delithiation



The differential derivative capacity results show that Si NPs and SiNG composite anodes have a similar profile. In both anodes, the first strong lithiation peak indicates an SEI films formation and crystalline Si transformation into amorphous Si [26]. In both anodes, the subsequent lithiation cycles show lithiation peaks at different voltages, corresponding to the lithiation of amorphous Si to various lithiated states like Li_xSi phases [26]. The differential derivative capacity results offer valuable insights into the electrochemical

performance of Si NPs and SiNG composite anodes. During lithiation, Li ions react with Si and C to form various Li–Si–C alloys. These alloys have larger volumes than the original Si, contributing to volume expansion. As the delithiation process proceeds, these alloys decompose back into Si–C and Li ions.

In this work, a Versastat4 Potentiostat was utilized to conduct Cyclic voltammetry (CV) experiments in the voltage range of 0 to +1.2 V vs. Li/Li⁺ at a scan rate of 0.1 mV s⁻¹. A representative CV of a half-coin cell containing a Si NPs and SiNG composite anode is illustrated in Fig. 9.

The SiNG composite anode shows a slightly higher specific capacity (i.e., 1297.5 mAh/g) than of Si NPs anode specific capacity (i.e., 1137.6 mAh/g) for 100th cycles. This is likely because of porous morphology of SiNG composite anode, which offers a larger surface area for electrochemical reactions. The differential derivative capacity results explain the superior electrochemical performance of Si NPs and SiNG composite anodes.

3.8.2 Galvanostatic charge–discharge

Galvanostatic charge–discharge (GCD) experiments were conducted to evaluate the electrochemical performance of Si NPs anode. The theoretical capacity of electrode is 2977.2 mAh/g (see supplementary information for details). The GCD tests were carried out within the voltage range of 0 to +1.5 V vs. Li/Li⁺, with a C-rate of 0.14C, corresponding to a current density

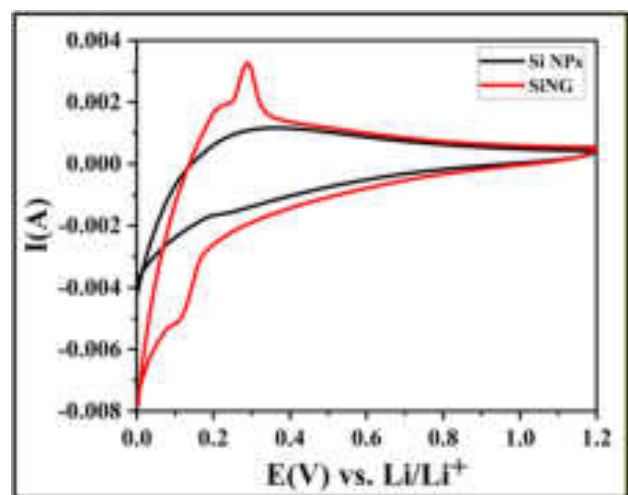


Fig. 9 CV of Si NPs and SiNG composite anode at the scan rate of 0.1 mV s⁻¹

of 420 mA g^{-1} . Figure 10a shows the charge–discharge profiles of Si NPs anode for the 1st, 5th, 25th, 50th, 75th, and 100th cycles.

The scale for specific capacity on the left side of Fig. 10b illustrates the relationship between the number of cycles and the specific capacities of Si NPs anode at a current density of 420 mA g^{-1} (0.14C) throughout 100 cycles. The anode exhibits a high initial specific capacity of 1568.9 mAh/g , gradually decreasing with cycling. However, the anode still retains a specific capacity of 1137.6 mAh/g after 100 cycles, which is significant. An improvement over traditional Si anodes. The results of GCD experiments indicate that Si NPs anode exhibits good electrochemical performance [27]. The anode has a high initial specific capacity and retains significant capacity after 100 cycles [28]. The formation of Li–Si alloy phases is likely responsible for the good electrochemical performance of anode

[29]. The Si NPs anode exhibits good electrochemical performance. The anode has a high initial specific capacity and retains significant capacity after 100th cycles. The formation of Li–Si alloy phases is likely responsible for the good electrochemical performance of anode.

The scale for Coulombic efficiency on the right side of Fig. 10b depicts the cycling performance and corresponding Coulombic efficiency of Si NPs anode at a current density of 420 mA g^{-1} (0.14C). In the first cycle, Si NPs anode demonstrates a Coulombic efficiency of 100.48%, with a discharge capacity of 1568.9 mAh/g and a charge capacity of 1561.3 mAh/g . The discharge capacity gradually decreases to 1137.6 mAh/g throughout the cycling process, while the charge capacity increases to 1132.7 mAh/g . Interestingly, the Coulombic efficiency remains consistent at 100.48% even in the 100th cycle. The results of cycling

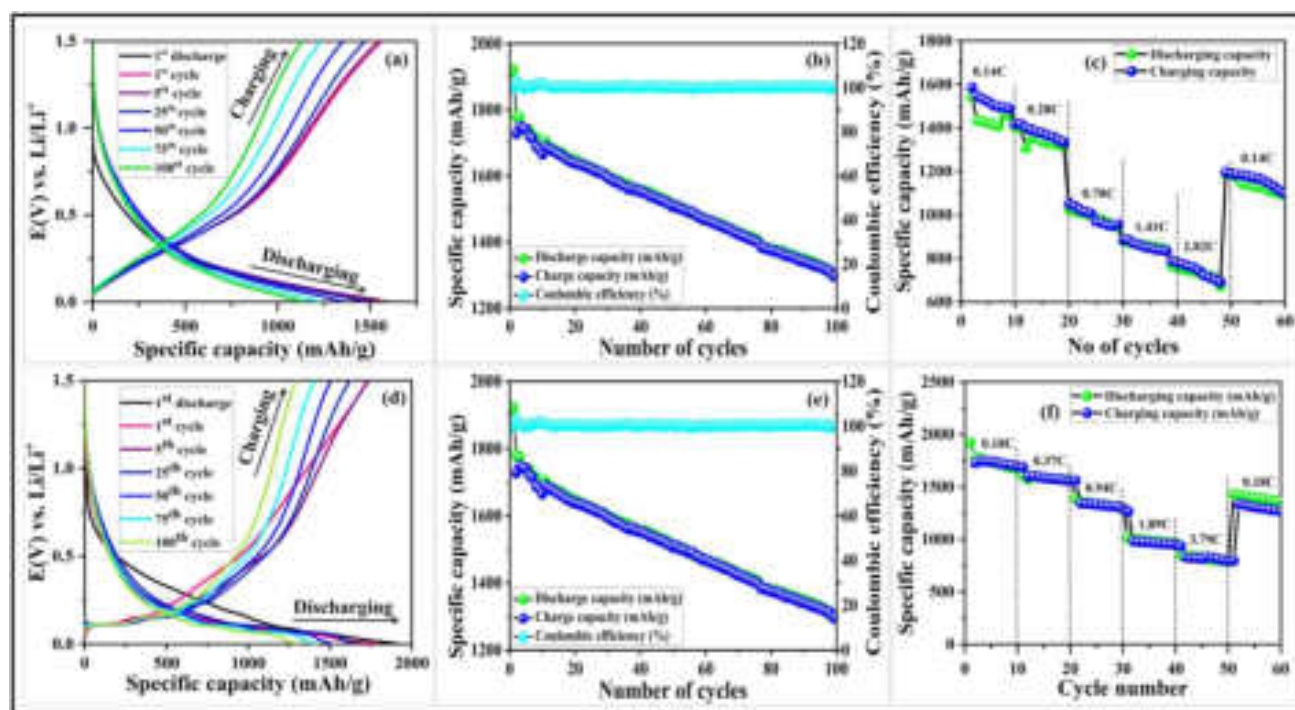


Fig. 10 **a** Galvanostatic charge–discharge profiles of Si NPs anode for the 1st, 5th, 25th, 50th, 75th and 100th cycles at a current density of 420 mA g^{-1} (0.14C), **b** Number of cycles vs. specific capacities and Coulombic efficiency of Si NPs anode at current density of 420 mA g^{-1} (0.14C), with specific capacity scale located on the left side and Coulombic efficiency scale located on the right side, **c** The rate performance of SiNPs anode at different current densities are 420 mA g^{-1} (0.14C), 840 mA g^{-1} (0.28C), 2100 mA g^{-1} (0.70C), 4200 mA g^{-1} (1.41C), and 8400 mA g^{-1} (2.82C), **d** Galvanostatic charge–discharge profiles of SiNG

composite anode for the 1st, 5th, 25th, 50th, 75th and 100th cycles at a current density of 419.98 mA g^{-1} (0.18C), **e** Number of cycles vs. specific capacities and Coulombic efficiency of Si NPs anode at current density of 419.98 mA g^{-1} (0.18C), with specific capacity scale located on left side and Coulombic efficiency scale located on the right side and **f** The rate performance of SiNG composite anode at different current densities are 420.1 mA g^{-1} (0.18C), 839 mA g^{-1} (0.37C), 2099 mA g^{-1} (0.94C), 4199.9 mA g^{-1} (1.89C), and 8399.9 mA g^{-1} (3.79C)

experiments indicate that Si NPs anode exhibits excellent electrochemical performance. The anode has a high initial Coulombic efficiency and retains this efficiency even after 100th cycles. This is likely due to the formation of Li–Si alloy phases, which are stable and have a high electrochemical energy density [30].

Figure 10c illustrates the discharge and charge profiles of Si NPs anode at different current densities, namely 420 mA g^{-1} (0.14C), 840 mA g^{-1} (0.28C), 2100 mA g^{-1} (0.70C), 4200 mA g^{-1} (1.41C), and 8400 mA g^{-1} (2.82C) (see supplementary information for details). The Si NPs exhibit specific discharge capacities ranging from 1585.8 to 1420.1 mAh/g, accompanied by forming Li–Si alloying phases such as $\text{Li}_{21}\text{Si}_5$ and $\text{Li}_{17}\text{Si}_4$. From the 11th to the 50th cycles, the specific capacities range from 1417.6 to 1153.8 mAh/g, consistently involving Li–Si alloying phases of $\text{Li}_{21}\text{Si}_5$ to $\text{Li}_{17}\text{Si}_4$. The results of cycling experiments indicate that Si NPs anode exhibits good electrochemical performance at different current densities [31]. The anode has a high initial specific capacity and retains significant capacity even at high current densities [28]. The formation of Li–Si alloy phases is likely responsible for the good electrochemical performance of anode [29]. The anode can be cycled at high current densities without a significant loss of capacity, which is essential for high-power applications [32].

The GCD experiments were conducted at a current density of 419.98 mA g^{-1} (0.18C) across a voltage range of 0 to +1.5 V vs. Li/Li^+ to evaluate the electrochemical performance of SiNG composite anode. The theoretical capacity of electrode is 2977.2 mAh/g. Figure 10d exhibits the representative charge–discharge profiles of SiNG composite anode for the 1st, 5th, 25th, 50th, 75th, and 100th cycles. The corresponding discharging specific capacities were 1780.7, 1721.3, 1623.3, 1512.1, 1409.9 and 1297.5 mAh/g, respectively. The Li–Si alloy formation phases observed during these cycles were consistently $\text{Li}_{21}\text{Si}_5$, $\text{Li}_{21}\text{Si}_5$, $\text{Li}_{21}\text{Si}_5$, $\text{Li}_{21}\text{Si}_5$, $\text{Li}_{21}\text{Si}_5$, and $\text{Li}_{17}\text{Si}_4$ at the constant current density of 419.98 mA g^{-1} (0.18C). Due to the formation of a SEI layer and the incorporation of lithium into Si lattice, it is common to observe a relatively high initial discharge capacity in the first cycle [33]. However, in the 5th cycle, the specific capacity during discharging decreases to 1721.3 mAh/g. This slight reduction in capacity is likely attributed to the irreversible loss of lithium during the initial cycles [34]. The capacity degradation can be attributed to various factors, including mechanical stress resulting from the volume

expansion and contraction of Si during lithiation and delithiation and the formation of an unstable SEI layer [35]. By the 25th cycle, the specific capacity decreases to 1623.3 mAh/g and 100th cycle, capacity further decreases to 1297.5 mAh/g, the capacity fading is substantial, as expected in Si-based anodes, and the change in the alloy formation phase indicates a significant transformation of anode material [36].

In addition to the below, the scale for specific capacity on the left side of Fig. 10e illustrates the cycling performance of SiNG composite anode at a current density of 419.98 mA g^{-1} (0.18C) for 100 cycles. The specific capacity of SiNG composite anode decreased gradually from 1780.7 mAh/g at the first cycle and to 1297.5 mAh/g at the 100th cycle. However, the specific capacity remained relatively stable after 50 cycles. This suggests that SiNG composite anode has good cycling stability.

The scale for Coulombic efficiency on the right side of Fig. 10e illustrates the cycling performance and corresponding Coulombic efficiency of SiNG composite anode at a current density of 419.98 mA g^{-1} (0.18C). In the first cycle, Si NPs anode has a discharge capacity of 1780.7 mAh/g and a charge capacity of 1728.6 mAh/g with a Coulombic efficiency of 103%. Finally, in the 100th cycle, the discharge capacity decreases to 1297.5 mAh/g and a charge capacity of 1294.9 mAh/g with a Coulombic efficiency of 100.19%. These results suggest that SiNG composite anode has good cycling stability and Coulombic efficiency. The high Coulombic efficiency of SiNG composite anode is likely due to the excellent compatibility between SiNPs and electrolyte. The good cycling stability and Coulombic efficiency of SiNG composite anode are possible due to the carbon matrix porous structure, which helps prevent the formation of SEI and the pulverization of SiNPs [37].

Figure 10f illustrates that SiNG composite anode exhibits good rate capability at various current densities. During the initial cycles, the discharging specific capacities range from 1780.7 to 1665.8 mAh/g, followed by 1469.7 to 1573.8 mAh/g values in the subsequent cycles. As the cycles progress, the specific capacity further decrease and finally 1191.3 mAh/g. These results suggest that SiNG composite anode has good rate capability, retaining a high specific capacity even at high current densities. The specific discharge capacity decreased gradually with increasing current density, but it kept a capacity of 1191.3 mAh/g at a current density of 8399.9 mA g^{-1} (3.79C). The excellent

rate capability of SiNG composite anode is likely due to the carbon matrix porous structure [38].

Table 1 illustrates the utilization of Silicon (Si) in organic electrolytes for charging/discharging capacity

in LiBs. In this investigation, at 420 mA g⁻¹ (0.14C) current density, the Si NPs anode demonstrates stable cycling performance with 100% Coulombic efficiency in the 1st cycle. It maintains 100.48% Coulombic

Table 1 Silicon (Si) in organic electrolyte with charging/discharging capacity for LiB

Sr. No	Anodes for lithium-ion battery (LIB)	Organic electrolyte (OE)	Specific capacity mAh/g (Discharge/charge)	Stability Cycles No with specific capacity (mAh/g)	Refs. No
1	Si NPs + Cellulose	1.3 M LiPF ₆	2022/1594	500 808	[39]
2	Si/CNT/CM + Sucrose	1 M LiPF ₆	2302/3152	100 784	[40]
3	Si@SiO _x @C + Sucrose	1 M LiPF ₆	2560/1972	50–1800 100–2000	[41]
4	3-APTS-EGO/Si@C + Sucrose	1 M LiPF ₆	1201/798	350~750	[42]
5	Nc-Si@HCS + Sucrose	1 M LiPF ₆	3400/1570	938 50	[43]
6	T-SGT/Si@C CGT/Si@C	1 M LiPF ₆	774.5/620.4 781.8/617.4	300–434.1 300–589.8	[44]
7	Si@G	1 M LiPF ₆	1290/1001	850 100	[45]
8	nano-Si/G-1 nano-Si/G-2 nano-Si/G-3	1 M LiPF ₆	596/532 894/813 1284/958	100–451.4 100–592.5 100–763.1	[46]
9	Si@C/G	1 M LiPF ₆	1267/985.6	150 919	[47]
10	Si/C	1 M LiPF ₆	867.6/640.5	40 447.5	[48]
11	G/Si@reGO	1 M LiPF ₆	~770/580	50 420.5	[49]
14	Si-G	1 M LiPF ₆	~1550/-	1300 400	[50]
15	SNGA/NG	1 M LiPF ₆	1400/~1070	200 455	[7]
16	VMoS ₂	1 M NaSO ₃ CF ₃ into DGM	548.1	800 451.6	[51]
17	CoS ₂ /NiS ₂	1 M NaSO ₃ CF ₃ into DGM	906.3/801.5	2000 545.1	[52]
18	MoS ₂ -MS	1 M NaSO ₃ CF ₃ into DGM	498/438	500 412	[53]
19	CoNi@NCNTs/S	1 M LiTFSI	676.8	500 486	[54]
20	Si NPs + Sucrose + CB	1 M LiPF₆	1568.9/1561.3	100 1137.6	Present work
21	SiNG + Sucrose + CB	1 M LiPF₆	1780.7/1728.6	100 1297.5	Present work

Bold values indicate the results of the present work. The table compares these results with those from the literature survey

efficiency even after 100 cycles, with discharge and charge capacities of 1137.6 and 1132.7 mAh/g, respectively. Additionally, the SiNG composite anode shows cycling performance at 419.98 mA g⁻¹ (0.18C), with initial discharge/charge capacities of 1780.7 and 1728.6 mAh/g at 103% Coulombic efficiency. After 100 cycles, it exhibits discharge/charge capacities of 1297.5 and 1294.9 mAh/g with 100.19% Coulombic efficiency is represent in Table 1.

3.8.3 Electrochemical impedance spectroscopy

The Nyquist plot for Si NPs and SiNG composite anodes is shown in Fig. 11. In Electrochemical Impedance Spectroscopy (EIS), two semicircles are commonly observed in the Nyquist plot, representing charge transfer processes. These two semicircles are associated with two distinct electrochemical methods

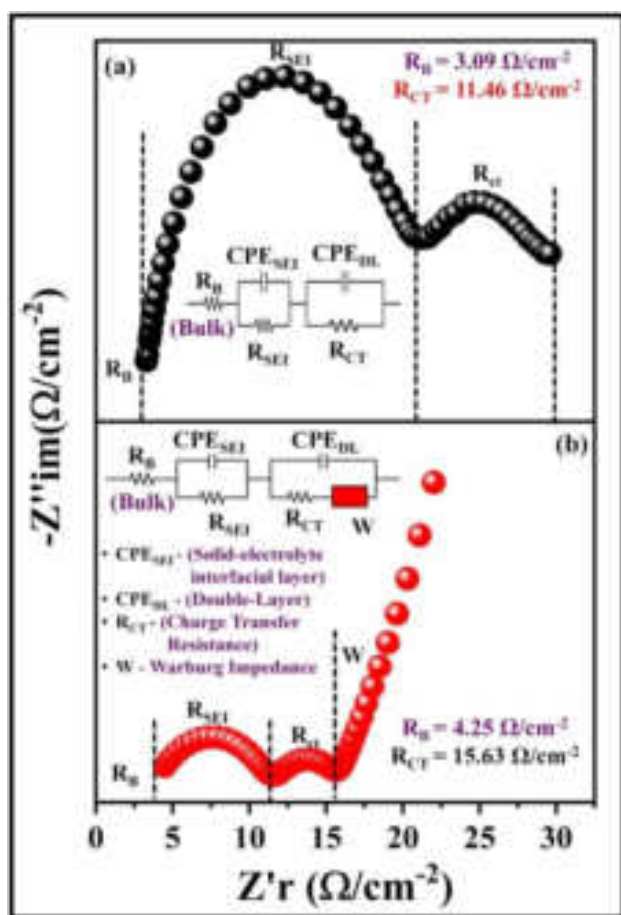


Fig. 11 The electrochemical impedance spectra (EIS) of **a** Si NPs and **b** SiNG composite anode half-coin cells

in Si NPs and SiNG composite anodes of half-coin cell LiBs: charge transfer and diffusion. We determined the bulk resistance (R_B) values to be 3.9 Ω/cm^2 for Si NPs and 4.2 Ω/cm^2 for SiNG composite anodes. During the charge transfer process, Li ions are transferred between the anodes and the electrolyte, represented by the first semicircle. The values of charge transfer resistance (R_{CT}) were 11.4 Ω/cm^2 for Si NPs and 15.6 Ω/cm^2 for SiNG composite anodes.

The equivalent circuit model derived from the EIS data enables the generation of corresponding Nyquist plots, as shown in Fig. 11. The bulk resistance of a half-coin cell (R_B) collectively represents the resistance of electrodes, electrolyte, and separator. This value can be obtained by identifying the initial x-axis intercept on the Nyquist plot [55].

The first semicircle observed in the Nyquist plot corresponds to the resistance (R_{SEI}) and capacitance (CPE_{SEI}) of solid electrolyte interphase (SEI) layer [55]. These parameters are directly associated with forming the interfacial layer on the electrode, particularly the deposition of SEI layer resulting from the decomposition of materials in the electrolyte [56]. The progress of SEI layer formation can be evaluated by analyzing the values of R_{SEI} and CPE_{SEI} [57]. characteristics dependent on temperature and reaction dynamics [18]. The ion diffusion process within the battery is represented by a straight line on the right side of Nyquist plot, known as Warburg impedance (W) [55]. This impedance is associated with the flow of charge at the electrode–electrolyte interface and is linked to ion diffusion within the anode material [19].

The diameter of Warburg impedance affects the charge transfer rate and provides insights into the kinetics of battery charge transfer [58]. It is often represented as a straight line with a 45° slope on the Nyquist plot and offers information about the diffusion coefficient and effective diffusion length of lithium ions within the anode materials. The results suggest that SiNG composite anode has higher R_B and R_{CT} than Si NPs anode, but it also exhibits a more significant Warburg impedance, indicating a faster charge transfer rate. The EIS analysis of Si NPs and SiNG composite anodes offers valuable insights into their electrochemical performance, enhancing Si anode design and synthesis for LiBs. The higher R_B and R_{CT} of SiNG composite anode result from the larger surface area of SiNPs, leading to an increased contact area between anode and electrolyte. The more significant Warburg impedance of SiNG composite anode is due

to the porous structure of carbon matrix, allowing for faster ion diffusion within the anode material. electrochemical performance, enhancing Si anode design and synthesis for LiBs. The higher R_B and R_{CT} of SiNG composite anode result from the larger surface area of Si NPs, leading to an increased contact area between anode and electrolyte [59]. The more significant Warburg impedance of SiNG composite anode is due to the porous structure of carbon matrix, allowing for faster ion diffusion within the anode material [60].

3.9 Post-mortem physico-chemical characterizations

3.9.1 Post-mortem X-ray diffraction

The Si NPs and SiNG composite anode half-coin cells were fully lithiated for post-mortem XRD analysis. The disassembly process occurred within a glove box filled with argon ($H_2O < 0.1$ ppm and $O_2 < 0.1$ ppm). Following the unwinding of Si NPs and SiNG composite electrode (anode), Whatman™ filter paper (separator), and lithium metal chip (cathode), discharged electrodes were precisely excised from the majority of electrode material using stainless steel scissors. These samples were individually stored in separate resealable plastic bags, and meticulous care was exercised in their handling with tweezers, ensuring gripping only at the edges [61].

The Si NPs and SiNG composite discharged electrodes were transferred to a nearby glove box for analysis via a shared antechamber after the electrodes in one glove box were unwound and harvested [62]. During this transfer, the samples were shielded from exposure to air; instead, they were subjected to pressures of approximately 1.0×10^{-4} kPa for 15 min. Subsequently, the electrodes were meticulously placed onto glass slides in a sample holder compatible with the Rigaku MiniFlex 600 instrument, which utilizes $CuK\alpha$ radiation ($\lambda = 1.54184 \text{ \AA}$) over a 2θ range of 10° – 80° for XRD analysis.

The post-XRD patterns of (a) Si nanoparticles (NPs) and (b) SiNG composite anode materials are depicted in Fig. 12. The peak positions in the XRD patterns of Li_xSi compounds can vary due to their specific insertion process, resulting in distinct stages and lattice characteristics known as the Li_xSi composition phases. Here are some typical approximations of 2θ values or hkl planes for Li_xSi phases [63]. The $Li_{21}Si_5$ phase exhibits Bragg reflections from the (100) planes,

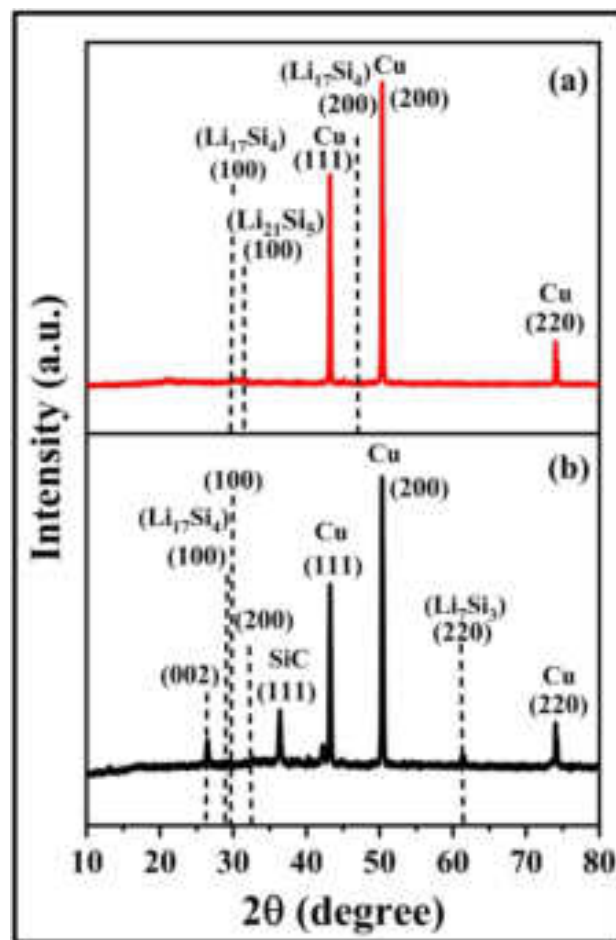


Fig. 12 The post-mortem XRD patterns of **a** Si NPs and **b** SiNG composite-lithiated electrodes

offering a high theoretical capacity, although it can lead to substantial volume expansion during lithiation, causing mechanical stress and electrode deterioration [64]. The $Li_{17}Si_4$ phase displays Bragg reflections from the (100) and (200) planes, also providing a high theoretical capacity but with noticeable volume expansion during lithiation, affecting cycling performance and stability.

The XRD pattern of SiC varies depending on its type and crystallographic phase. The (111) plane for SiC is typically observed at a 2θ of approximately 36.6° and is often the most prominent [65]. Additionally, Cu peaks corresponding to the (111), (200), and (220) planes are observed in the XRD pattern, originating from the Cu substrate of current collector [66]. The appearance of SiC (111) peak in the post-mortem XRD pattern, absent before lithiation, suggests a transformation or reaction occurring in the SiC material during

battery operation. Potential reasons for this observation include. Reaction with Li to form Si–Li alloys during lithiation, introducing new diffraction features in the XRD pattern. Induced structural changes in the SiC material, such as lattice expansion or contraction, phase transitions, or the formation of new crystallographic orientations, manifesting as new peaks or shifts in peak positions [67]. Lithiation-induced volume expansion and contraction introducing lattice strain in the SiC material, affecting diffraction behavior and resulting in the appearance of new peaks or changes in peak intensities [68]. In the field of SiNP anode materials for LiBs, managing issues related to volume expansion and contraction during cycling is crucial for their utilization in real-world applications, despite their high theoretical capacity [4].

3.9.2 Post-mortem field emission scanning electron microscopy

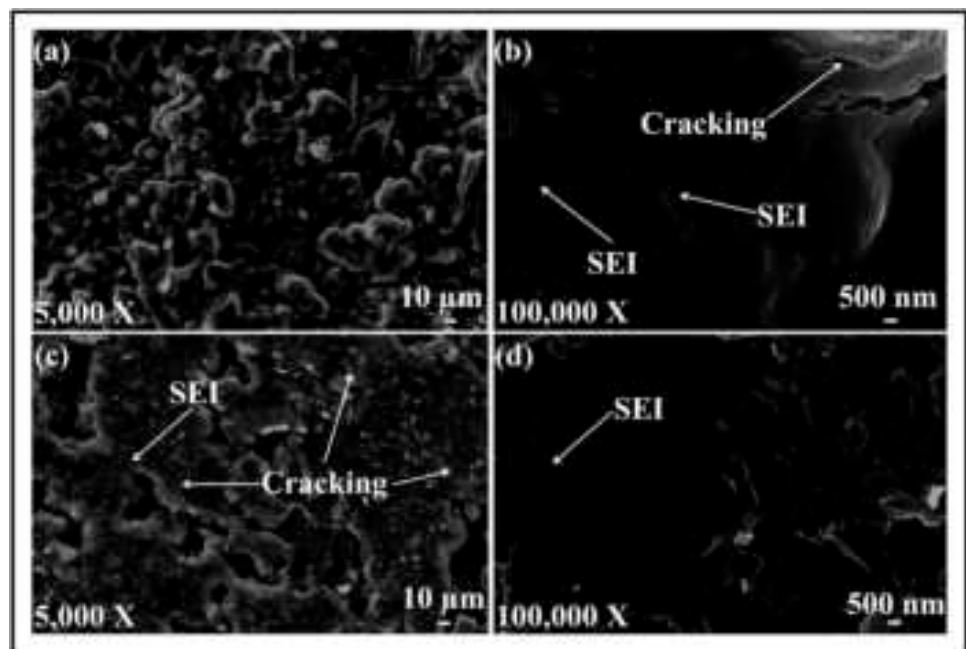
The Si NPs and SiNG composite anode half-coin cells underwent full lithiated for post-mortem FE-SEM analysis. The disassembly process occurred within a glove box filled with argon ($\text{H}_2\text{O} < 0.1$ ppm and $\text{O}_2 < 0.1$ ppm). Subsequent to unwinding the Si NPs and SiNG composite-lithiated electrode (anode), Whatman™ filter paper (separator), and lithium metal chip (cathode), samples were precisely excised from

the predominant electrode material using stainless steel scissors. These samples were individually stored in separate plastic bags, and meticulous care was taken during handling, utilizing tweezers and gripping only at the edges [61].

Post-mortem electrodes were transferred to a nearby glove box for analysis via a shared antechamber following the unwinding and harvesting of electrodes in one glove box [62]. Throughout this transfer, both electrodes remained unexposed to air; instead, they were subjected to pressures of approximately 1.0×10^{-4} kPa for 15 min. The Si NPs and SiNG composite-lithiated electrodes designated for post-mortem FE-SEM analysis were transported to the microscope using a custom airtight sample holder, specifically designed and modified for this purpose. Micrographs were acquired with a secondary electron detector at a working distance of 15 mm and an accelerating voltage of 15 kV using a NOVA NANOSEM 450 instrument FE-SEM.

Figure 13 shows post-mortem FE-SEM pictures of (a) Si NPs and (b) SiNG composite anodes electrodes at 5 kX and 100 kX magnifications. Notably, both electrode types show evidence of creating a SEI layer, emphasizing the importance of this layer in stabilizing the electrode/electrolyte interface during LiBs cycling [69]. Furthermore, the FE-SEM images exhibit a noticeable reduction in the size of Si NPs in the electrode,

Fig. 13 Post FE-SEM images of Si NPs anode lithiated electrode **a** 5 kX, **b** 100 kX and SiNG composite anode lithiated electrode **c** 5 kX, **d** 100 kX



particularly in the 500 nm image. Electrode integrity and cycling stability may suffer due to this pulverization process [70]. Interestingly, SiNG composite anode exhibits a noticeably lower level of pulverization, pointing to the potential advantages of using graphene to address this problem. In post-mortem FE-SEM images, the SEI layer frequently appears darker than the surrounding SiNG material, highlighting differences in electron interaction. Variations in the thickness, consistency, and homogeneity of SEI layer over SiNG surface indicate changes in lithiation and SEI growth dynamics. The SEI layer may also include irregularities and roughness, which show how it behaves dynamically during charge and discharge cycles.

Our findings significantly improve our knowledge of electrochemical behaviour of SiNG anodes in LiBs. They stress how crucial SEI characterization is for gaining a fundamental understanding and evaluating battery performance and long-term stability. These results open the door to more investigation and advancement of cutting-edge electrode materials and battery technology. Composite-lithiated electrodes designated for post-mortem FE-SEM analysis were transported.

4 Conclusions

In conclusions, the study highlights the potential of Si NPs and SiNG composite anodes for high-performance LiBs. Combining Si NPs with NG yields synergistic effects, improving battery performance by addressing issues like electrode pulverization and capacity fading. This integration enhances structural and cycling stability, showcasing a promising avenue for advancing LiBs technology. Electrochemical tests confirm the outstanding performance of both Si NPs and SiNG composite anodes. Despite capacity decline over cycling, they retain substantial capacity, outperforming traditional Si-based anodes. Consistent Coulombic efficiency throughout cycling suggests stable electrochemical behavior. Post-mortem analysis using XRD and FE-SEM reveals structural and morphological changes during battery operation. Observation of Li–Si alloy phases and SEI layer formation underscores the dynamic electrode–electrolyte interactions. The study emphasizes the significance of SEI characterization for battery performance and stability. It offers valuable insights into advanced electrode material design, enabling the

development of next-generation LiBs with improved energy density, cycling stability, and rate capability.

Acknowledgements

We acknowledge funding from the Swedish Energy Agency (project number: 39038-2), the EU Regional Fund, the KK Foundation, STINT (IB-2018 7535) and D. Y. Patil Education Society (Deemed to be University). Also this research is supported by Centre for Materials for Electronics Technology (C-MET), Pune for providing a battery fabrication system and Central Instrumentation Facility, Department of Chemistry and Physics, Savitribai Phule Pune University, Pune for providing a physico-chemical characterizations instruments facility.

Author contributions

Sohan Thombare carried out an investigation and formal analysis, data curation, original draft writing, and formal analysis. Ranjit Humane, Bharat Kale and Ramchandra Kalubarme provided electrochemical analysis facility, Rohan Patil, Ranjit Humane and Manisha Phadatare carried out calculation of battery C-Rate, Dhanaji Malavekar carried out modification and presentations, Rohan Patil, Bharat Kale, Ramchandra Kalubarme, Manisha Phadatare and Chandrakant Lokhande carried out funding acquisition, administration, supervision, and manuscript editing. All persons made substantial contributions to the work reported in the manuscript.

Funding

Open access funding provided by Mid Sweden University. This study was funded by Swedish Energy Agency, the EU Regional Fund, the KK Foundation, STINT and D. Y. Patil Education Society (Deemed to be University) Kolhapur.

Data availability

The data used in this study is part of ongoing research and cannot be provided at this stage. However, it will be made available after the completion of ongoing research on request from corresponding author.

Declarations

Conflict of interest There are no conflicts to declare.

Supplementary Information The online version contains supplementary material available at <https://doi.org/10.1007/s10854-024-13140-z>.

Open Access This article is licensed under a Creative Commons Attribution 4.0 International License, which permits use, sharing, adaptation, distribution and reproduction in any medium or format, as long as you give appropriate credit to the original author(s) and the source, provide a link to the Creative Commons licence, and indicate if changes were made. The images or other third party material in this article are included in the article's Creative Commons licence, unless indicated otherwise in a credit line to the material. If material is not included in the article's Creative Commons licence and your intended use is not permitted by statutory regulation or exceeds the permitted use, you will need to obtain permission directly from the copyright holder. To view a copy of this licence, visit <http://creativecommons.org/licenses/by/4.0/>.

References


- B. Scrosati, J. Hassoun, Y.-K. Sun, *Energy Environ. Sci.* **4**, 3287 (2011)
- Y. Jin, B. Zhu, Z. Lu, N. Liu, J. Zhu, *Adv. Energy Mater.* **7**, 1700715 (2017)
- S. Fan, H. Wang, J. Qian, Y. Cao, H. Yang, X. Ai, F. Zhong, *A.C.S. Appl. Mater. Interfaces* **13**, 16411 (2020)
- F. Tareq, S. Rudra, *Mater. Today Commun.* **39**, 108653 (2024)
- J. Edge, S. O'Kane, R. Prosser, N. Kirkaldy, A. Patel, A. Hales, A. Ghosh, W. Ai, J. Chen, J. Yang, S. Li, M.-C. Pang, L. Diaz, A. Tomaszewska, M. Marzook, K. Radhakrishnan, H. Wang, Y. Patel, B. Wu, G. Offer, *Phys. Chem. Chem. Phys.* **23**, 8200 (2021)
- Y. Zhang, K. Hu, J. Ren, Y. Wu, N. Yu, A. Feng, Z. Huang, Z. Jiach, G. Wu, *Dalton Trans.* **48**, 17683 (2019)
- M. Phadatare, R. Patil, N. Blomquist, S. Forsberg, J. Ortegren, M. Hummelgard, J. Meshram, G. Hernandez, D. Brandell, K. Leifer, S.K.M. Sathyanath, H. Olin, *Sci. Rep.* **9**, 14621 (2019)
- C. Holder, R. Schaak, *ACS Nano* **13**, 7359 (2019)
- A. Bunaciu, E. Tioiub, H. Aboul-Enein, *Crit. Rev. Anal. Chem.* **45**, 289 (2015)
- A. Akbashev, *Curr. Opin. Electrochem.* **35**, 101095 (2022)
- A. Yusof, N. Nizam, N.A.A. Rashid, A. Yusof, N. Nizam, *J. Porous Mater.* **17**, 39 (2009)
- T. Lee, R. Othman, F.-Y. Yeoh, *Biomass Bioenergy* **59**, 380 (2013)
- D. Prasetyoko, Z. Ramli, S. Endud, H. Hamdan, B. Sulikowski, *Waste Mang.* **26**, 1173 (2006)
- M. Mohamed, J. Jaafar, A. Ismail, M.H.D. Othman, M. Rahman, *Membr. Charact.* **3** (2017)
- S. Seifi, D. Levacher, A. Razakamanantsoa, N. Sebaibi, *Appl. Sci.* **13**, 5616 (2023)
- T. Jiang, H. Yang, G. Chen, *Nanoenergy Adv.* **2**, 165 (2022)
- A. Grosman, C. Ortega, *Langmuir* **24**, 3977 (2008)
- H. Wang, Y. Wang, X. Cao, M. Feng, G. Lan, J. Raman Spectrosc. **40**, 1791 (2009)
- Y. Huang, C. Chang, M. Lin, *Phys. Rev. B* **78**, 115422 (2008)
- X. Kong, Z. Xi, L. Wang, Y. Zhou, Y. Liu, L. Wang, S. Li, X. Chen, Z. Wan, *Molecules* **28**, 2079 (2023)
- J. Lee, H. Lee, C. Bak, Y. Hong, D. Joung, J. Ko, Y. Lee, C. Kim, *Nano-Micro Lett.* **15**, 97 (2023)
- J. Efome, M. Baghbanzadeh, D. Rana, T. Matsuura, C. Lan, *Desalination* **373**, 47 (2015)
- S. Ribeiro, R. Meira, D. Correia, C. Tubio, C. Ribeiro, C. Baleizão, S. Lanceros-Méndez, *Compos. B Eng.* **185**, 107786 (2020)
- K. Adpakpang, S.B. Patil, S.M. Oh, J.-H. Kang, M. Lacroix, S.-J. Hwang, *Electrochim. Acta* **204**, 60 (2016)
- R. Patil, Silicon-nanographite aerogel-based anodes for high performance lithium ion batteries, 1 (2019)
- F. Wang, L. Wu, B. Key, X.-Q. Yang, C. Grey, Y. Zhu, J. Graetz, *Adv. Energy Mater.* **3**, 1324 (2013)
- R. Shao, F. Zhu, Z. Cao, Z. Zhang, M. Dou, J. Niu, B. Zhu, F. Wang, *J. Mater. Chem. A* **8**, 18338 (2020)
- Z. Li, Y. Zhang, T. Liu, X. Gao, S. Li, M. Ling, C. Liang, J. Zheng, Z. Lin, *Adv. Energy Mater.* **10**, 1903110 (2020)
- W.-J. Zhang, *J. Power. Sources* **196**, 877 (2011)
- J.-Y. Li, Q. Xu, G. Li, Y.-X. Yin, L.-J. Wan, Y.-G. Guo, *Mater. Chem. Front.* **1**, 1691 (2017)
- C. Fang, Y. Deng, Y. Xie, J. Su, G. Chen, *J. Phys. Chem. C* **119**, 1720 (2015)
- C. Wang, C. Yang, Z. Zheng, *Adv. Sci.* **9**, 21055213 (2022)
- V. Chakrapani, F. Rusli, M. Filler, P. Kohl, *J. Power. Sources* **5**, 433 (2012)

34. Y. Oumellal, N. Delpuech, D. Mazouzi, N. Dupre, J. Gaubicher, P. Moreau, P. Soudan, B. Lestriez, D. Guyomard, *J. Mater. Chem.* **21**, 6201 (2011)
35. X. Su, Q. Wu, J. Li, X. Xiao, A. Lott, W. Lu, B. Sheldon, J. Wu, *Adv. Energy Mater.* **7**, 1300882 (2014)
36. N. Dimov, S. Kuginov, M. Yoshio, *Electrochim. Acta. Acta* **48**, 1579 (2003)
37. Y. Yang, W. Yuan, W. Kang, Y. Ye, Q. Pan, X. Zhang, Y. Ke, Z. Qiu, C. Wang, Y. Tang, *Sustainable. Energy Fuels* **4**, 1577 (2020)
38. X. Li, M. Zhang, S. Yuan, C. Lu, *ChemElectroChem* **2**, 4289 (2020)
39. J. Kim, V. Guccini, K.-W. Seong, J. Oh, G. Salazar-Alvarez, Y. Piao, *Carbon* **118**, 8 (2017)
40. B. Park, J. Jeong, G.-W. Lee, Y.-W. Kim, K. Roh, K.-B. Kim, *J. Power. Sources* **394**, 94 (2018)
41. B. Jiang, S. Zeng, H. Wang, D. Liu, J. Cao, H. Yang, X. Ai, *A.C.S. Appl. Mater. Interfaces* **8**, 31611 (2016)
42. X. Li, X. Tian, T. Yang, W. Wang, Y. Song, Q. Guo, Z. Liu, *J. Power. Sources* **385**, 84 (2018)
43. T. Jaumann, M. Gerwig, J. Balach, S. Oswald, E. Brendler, R. Hauser, B. Kieback, J. Eckert, L. Giebeler, E. Kroke, *J. Mater. Chem. A.* **5**, 9262 (2017)
44. D. Ruan, L. Wu, F. Wang, K. Du, Z. Zhang, K. Zou, X. Wu, G. Hu, *J. Electroanal. Chem. Electroanal. Chem.* **884**, 115073 (2021)
45. M. Cabello, E. Gucciardi, A. Herran, D. Carriazo, A. Villaverde, T. Rojo, *Molecules* **25**, 2494 (2020)
46. A. Sun, H. Zhong, X. Zhou, J. Tang, M. Jia, F. Cheng, Q. Wang, J. Yang, *Appl. Surf. Sci.* **470**, 445 (2019)
47. X. Li, D. Yang, X. Hou, J. Shi, Y. Peng, H. Yang, *J. Alloys Compd.* **728**, 1 (2017)
48. M. Su, Z. Wang, H. Guo, X. Li, S. Huang, L. Gan, *Adv. Powder Technol.* **24**, 921 (2013)
49. L. Gan, H. Guo, Z. Wang, X. Li, W. Peng, J. Wang, S. Huang, M. Su, *Electrochim. Acta. Acta* **104**, 117 (2013)
50. Z. Luo, Q. Xiao, G. Lei, Z. Li, C. Tang, *Carbon* **98**, 373 (2016)
51. X. Yue, J. Wang, A. Patil, X. An, Z. Xie, X. Hao, Z. Jiang, A. Abudula, G. Guan, *J. Chem. Eng.* **417**, 128107 (2021)
52. J. Wang, X. Yue, X. Cao, Z. Liu, A. Patil, J. Wang, X. Hao, A. Abudula, G. Guan, *J. Chem. Eng.* **431**, 134091 (2022)
53. X. Yue, J. Wang, Z. Xie, A. Patil, T. Yu, X. Du, Z. Wang, X. Hao, A. Abudula, G. Guan, *J. Mater. Sci.* **55**, 14389 (2020)
54. J. Wang, X. Yue, Z. Xie, A. Patil, S. Peng, X. Hao, A. Abudula, G. Guan, *J. Alloys Compd.* **874**, 159952 (2021)
55. W. Choi, H.-C. Shin, J. Kim, J.-Y. Choi, W.-S. Yoon, *J. Electrochem. Sci. Technol. Electrochem. Sci. Technol.* **11**, 1 (2020)
56. A. Wang, S. Kadam, H. Li, *npj Comput. Mater.* **4**, 15 (2018)
57. X. Li, A. Colclasure, D. Finegan, D. Ren, Y. Shi, X. Feng, L. Cao, Y. Yang, K. Smith, *Electrochim. Acta. Acta* **297**, 1109 (2019)
58. D. Qu, W. Ji, H. Qu, *Commun Mater.* **3**, 61 (2022)
59. C. Sun, A. Du, G. Deng, X. Zhao, J. Pan, X. Fu, J. Liu, L. Cui, Q. Wang, *Electrochim. Acta. Acta* **450**, 142269 (2023)
60. A. Lazanasand, M. Prodromidis, *A.C.S. Meas. Sci.* **3**, 162 (2023)
61. D. Müller, I. Landa-Medrano, A. Eguia-Barrio, I. Boyano, I. Urdampilleta, I. Meatza, A. Fill, P. Birke, *Electrochim. Acta.* **391**, 138966 (2021)
62. L. Somerville, J. Bareno, S. Trask, P. Jennings, A. McGordon, C. Lyness, I. Bloom, *J. Power. Sources* **335**, 189 (2016)
63. S.-B. Son, J. Trevey, H. Roh, S.-H. Kim, K.-B. Kim, J. Cho, J.-T. Moon, C. DeLuca, K. Maute, M. Dunn, H. Han, K. Oh, S.-H. Lee, *Adv. Energy Mater.* **6**, 1999 (2011)
64. C.-W. Hu, J.-P. Chou, S.-C. Hou, A. Hu, Y.-F. Su, T.-Y. Chen, W.-K. Liew, Y.-F. Liao, J.-L. Huang, J.-M. Chen, C.-C. Chan, *Sci. Rep.* **9**, 1299 (2019)
65. E. Njoroge, T. Hlatshwayo, T. Mokgadi, T. Thabethe, V.A. Skuratov, *Mater. Today Commun.* **36**, 106631 (2023)
66. X. He, Y. Hu, H. Tian, Z. Li, P. Huang, J. Jiang, C. Wang, *J. Materiomics* **6**, 192 (2020)
67. S. Dolabella, A. Borzi, A. Dommann, A. Neels, *Small Methods* **6**, 2100932 (2022)
68. V. Vanpeene, A. Heitz, N. Herkendaal, P. Soucy, T. Douillard, L. Roué, *Battery Energy* **1**, 20220016 (2022)
69. M. Schellenberger, R. Golnak, W. Quevedo Garzon, S. Risse, R. Seidel, *Mater. Today Adv.* **14**, 100215 (2022)
70. P. Nzereogu, A. Omah, F. Ezema, E. Iwuoha, A. Nwanya, *Appl. Surf. Sci. Adv.* **9**, 100233 (2022)

Publisher's Note Springer Nature remains neutral with regard to jurisdictional claims in published maps and institutional affiliations.



Synthesis and characterization of crystalline cristobalite alpha low silicon dioxide nanoparticles: a cost-effective anode for lithium-ion battery

Sohan Thombare¹ , Rohan Patil², Ranjit Humane³, Bharat Kale^{4,6}, Ramchandra Kalubarme³, Dhanaji Malavekar⁵, Sambhaji Khot¹, Manisha Phadatare^{2,*}, and Chandrakant Lokhande^{1,*}

¹ Centre for Interdisciplinary, Research, D. Y. Patil Education Society (Deemed To Be University), Kolhapur 416006, India

² Departments of Engineering, Mathematics and Subject Didactics (IMD), Mid Sweden University, 85170 Sundsvall, SE, Sweden

³ Centre for Materials for Electronics Technology, Panchawati, Off. Pashan Road, Pune 411008, India

⁴ Centre for Materials for Electronics Technology (C-MET), Government of India, Pune, Maharashtra 411007, India

⁵ Optoelectronics Convergence Research Center, Department of Materials Science and Engineering, Chonnam National University, Gwangju 61186, South Korea

⁶ Material Science (COE) Research and Development, MIT World Peace University (MIT-WPU) Kothrud Pune, Pune, Maharashtra 411038, India

Received: 24 January 2024

Accepted: 30 June 2024

Published online:
17 July 2024

© The Author(s), 2024

ABSTRACT

Silicon dioxide (SiO₂ or Silica) is one of the most prevalent substances in the crust of the Earth. The main varieties of crystalline silica are quartz, cristobalite, and tridymite. When applied as a material for energy, it is affordable and eco-friendly. The SiO₂ is considered as electrochemically inactive toward lithium. The SiO₂ exhibits low activity for diffusion and inadequate electrical conductivity. As the particle size of SiO₂ decreases, the diffusion pathway of Li-ions shortens, and the electrochemical activity is promoted. In investigation, Cost-effective synthesis approach was employed to produce crystalline cristobalite alpha low silicon dioxide nanoparticles (CCαL SiO₂ NPs) derived from *Oryza sativa* (rice) husk using a solvent extraction modification technique. The objective was to fabricate an cost-effective future anode nanomaterial that could reduce the significant volume expansion growth, pulverization, and increase electrical conductivity of CCαL SiO₂ NPs anode and develop high specific capacity for Lithium-ion battery (LiB). To study the phase and purity of the SiO₂, a variety of characterization methods, including X-Ray Diffraction, Fourier Infra-Red Spectroscopy, Surface area analysis, Raman Shift analysis, Field Emission Scanning Electron Microscopy and Energy Dispersive X-Ray Spectroscopy, Contact angle measurement, Post-mortem X-ray diffraction, and Post-mortem field emission scanning electron microscopy were employed. This cost-effective synthesis of CCαL SiO₂ NPs anode was first reported in this work.

Address correspondence to E-mail: Manisha.Phadatare@miun.se; l_chandrakant@yahoo.com

1 Introduction

The future of innovative, secure, affordable, and ecologically acceptable substances utilized in the construction of lithium-ion batteries (LiBs) is an integral part of the progress of large-scale grids, consumer devices, common carriers, and personal zero-carbon dioxide (CO₂) cars. To meet the demands for more significant storage, strength, and continuous cycle performance, the necessity to design modern LiBs is growing with a companion to the growth of the global electronics demand. Traditional LiBs with lithium metal oxide cathode and graphite anode have achieved their performance boundary. Hence, an enthusiastic investigation into the practice of electrode materials, i.e., cathodes and anodes with specific energy and specific densities and cycles, is going on. Naturally, an excellent negative element in a battery-type anode requires the following characteristics: (i) high specific capacity to improve the energy density, (ii) easy availability and low expense to confirm the commercial devices, (iii) low discharging potential to raise the working voltage window, (iv) appropriate structural integrity to promote cyclic stability, and (v) electrical conductivity and execute high power density and ideal ionic conductivity to boost quick charge transfer [1].

The high specific capacity and safety features of alloy anodes are well-known. The primary obstacle to the use of alloy anodes is their significant volume change (up to 300%) during the insertion and extraction of lithium, which frequently results in the active alloy particles being ground up and insufficient cycle stability. Furthermore, alloy anodes have a first-cycle irreversible capacity loss that is too high for practical use. Over the past 20 years, a great deal of study has been done to solve these two difficulties, and substantial progress has been made. An important problem with anode materials based on alloying elements such as Si, Sn, Sb, Al, Mg, Bi, In, Zn, Pb, Ag, Pt, Au, Cd, As, Ga, and Ge is volume change. When LiBs go through their charge–discharge cycles, there is a volume shift that can have a number of negative consequences [2]. The alloying anode materials have three major disadvantages. (a) Mechanical Stresses: The anode materials lattice structure expands and contracts when lithium ions are added to (charge) and removed from (discharge). The electrode may experience mechanical stress as a result of this constant expansion and contraction. With time, this tension may result in the anode particles may fracture as a result of the

significant volume shift, reducing the surface area accessible for the insertion of lithium ions and lowering battery capacity. In extreme circumstances, the anode material may pulverize due to extreme tension. A total loss of capacity and the electrical separation of the particles may result from this. (b) Loss of Electrical Contact: The mechanical strains brought on by a change in volume may also cause the anode particles and the current collectors electrical contact to break. This can cause capacity decline and lowers the battery efficiency. (c) Instability of the Solid Electrolyte Interface (SEI): During cycling, the SEI layer forms on the electrodes surface. The significant volume variations have the potential to induce this instability. Lithium consumption may rise as a result, and battery performance may suffer [3].

Certain alloying elements are frequently employed in anodes impacted by volume change. Si, Sn, and Sb elements are especially vulnerable to the issues since they undergo some of the biggest volume increases (> 300%) during lithiation. Although the volume changes of Al and Mg elements are less, they can nevertheless experience mechanical degradation and SEI instability. Zn elements have moderate capabilities, but they also alter in bulk when they cycle. In general, the elements Ge, Pt, and Au have smaller capacities and allowable volume variations. While some of Ga elements on this list may have intriguing qualities, they frequently have negative effects like toxicity or poor cyclability because of volume changes or other issues [4].

Scientists are working hard to find solutions to reduce the problem of volume change in alloy-based anodes. Several strategies that show promise by distributing the stress brought on by a change in volume more fairly, the likelihood of cracking and pulverization is decreased. The volume change can be buffered and cycling stability increased by including the alloying element into a composite electrode made of a more stable material. Adding more components to the anode material might occasionally alter its lattice structure and lessen the volume change that occurs during lithiation. All things considered, volume change is still a significant problem for alloy-based anode materials. Ongoing research, however, is creating viable solutions to this problem and opening the door for more advanced LiBs in the future [5].

Silica nanoparticles (SiO₂ NPs) have been used throughout the globe, mainly with medicinal drug systems, organic visual representation, liquid shells,

catalysts, biomedical, sensing detectors, filler in composite materials, and recently in a combination of devices, together with energy storage devices [6, 7]. A technique for creating single-scatter and round-size SiO₂ NPs by the chemical breakdown of a compound due to reaction with water of tetraethyl orthosilicate (TEOS) [8]. The impact of the percentage of water, alkali, and TEOS precursors to resolve on dimensions of the SiO₂ particles was investigated [9]. The shape and size of SiO₂ NPs depend on the temperature at which they react and the concentration [10]. Sodium silicate solution containing silicon (Si) and oxygen (O) is also used as an alternate affordable price material to derive SiO₂ particles. However, natural waste products such as *Oryza sativa* (rice) husk, *Bambusa vulgaris* leaves (bamboo) leaves, *Zea mays* (corn) husk, *Saccharum officinarum* (Sugar cane) husk, and Shadu clay are also used to synthesize SiO₂ particles.

Oryza sativa, a botanical name, is also called rice and is an initially famous staple meal in almost all countries. *Oryza Sativa* husk contains a large amount of SiO₂ element, which can, in turn, be a beneficial source of Si components. The quantity of stalks in the earth contains approximately 10–20% SiO₂ element. Various techniques are available for extracting SiO₂ from *Oryza sativa* husk, including acid pre-treatment as well as similar methods of pyrolysis [11–17]. Kamath and Proctor [1998] created a that could still be present [18].

In this work, the primary objective is to ascertain an efficient way to incorporate *Oryza sativa* husk into anode constituents to augment their effectiveness [18, 19]. Due to its low cost and simplicity of production, SiO₂ exhibits promise elements for reusable LiBs. Theoretically, this material can store more energy than a graphite anode (1964 mAh g⁻¹). Furthermore, while volume expansion during the lithiation cycle is inevitable, SiO₂ shows less volume change than Si during the delithiation and lithiation [20]. Recently, it was found that SiO₂ is an excellent material to make up for Si getting bigger during cycling. This results in good cycle performance and reversible capacity [21]. Some functional SiO₂ and spongy carbons have been employed to increase cycling stability and rate capability. These materials with porous structure and carbon framework are used to buffer the effects of expansion [22]. Herein, crystalline cristobalite alpha low silicon dioxide (CCaL SiO₂ NPs) derived from *Oryza sativa* was prepared by using solvent extraction modification technique. The structural, Fourier transform infrared spectroscopy, surface area analysis, Raman spectra

morphological, chemical composition and contact angle measurements with post-mortem structural and morphological analysis are discussed. The electrochemical testing of CCaL SiO₂ NPs anode in LiB half-coin cell performance is demonstrated for future zero-CO₂ electric cars.

2 Experimental details

2.1 Materials

For the synthesis of CCaL SiO₂ NPs, the waste material *Oryza sativa* husk used in this investigation was collected from a Rice Mill (Shree Mahalaxmi), Ichalkaranji, District Kolhapur. In addition, sodium hydroxide (NaOH), sulfuric acid (H₂SO₄), WhatmanTM filter paper, and the potential of hydrogen (pH) paper were purchased from Thomas Baker.

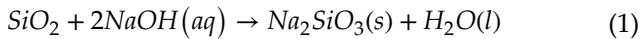
For CCaL SiO₂ NPs half-coin cell fabrication, Battery grade copper foil roll with a thickness of 20 μm were purchased from Trillion Energies, India., Coin cell case CR2032 3 V were purchased from Trillion Energies, India., Lithium hexafluorophosphate (LiPF₆) is a solution of (dimethyl carbonate (DMC), ethylene carbonate (EC), and diethyl carbonate) were purchased from Sigma-Aldrich, Lithium metal chip with a thickness of 0.6 mm were purchased from Sigma-Aldrich, and WhatmanTM filter papers with a thickness of 0.34 mm were purchased from Sigma-Aldrich. All of these chemicals were employed without any further purification.

For post-mortem examination, the half-coin cells were fully lithiated from 0 to 0.5 V. The disassembly process took place within a glove box filled with argon (H₂O < 0.1 ppm and O₂ < 0.1 ppm). Following the unwinding of the CCaL SiO₂ NPs electrode, separator, and lithium metal chip, precise samples were cut from the electrode material using stainless steel scissors. These samples were individually stored in separate plastic bags, and utmost care was exercised in handling them with tweezers, gripping them only by the edges.

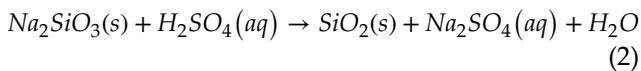
2.2 Synthesis of CCaL SiO₂ NPs

To prepare silicon dioxide nanoparticles (SiO₂ NPs), *Oryza sativa* husk was first heated at 100 °C, and subsequently, the resulting ash underwent treatment with

sodium hydroxide (NaOH) to extract SiO₂ in the form of sodium silicate; the chemical reaction is as (1) [10].



Then, the extracted silicate was separated by filtration, after which concentrated sulfuric acid was added to get pH 7. White precipitate, which was then filtered using filter paper. It was then washed continuously with water, and the chemical reaction is as (2).



Finally, the white precipitate underwent annealing in a muffle furnace at a temperature of 900 °C for a duration of two hours. The flow diagram in Fig. 1a illustrates the process used to extract of SiO₂ NPs from *Oryza sativa* husks in this study.

2.3 Preparation of CCaL SiO₂ NPs electrode and fabrication

A mixture of CCaL SiO₂ NPs, polyvinylidene fluoride (PVDF), black sucrose powder, and activated charcoal was prepared in a mass proportion of 70:10:10:10 in N-methyl-2 pyrrolidone (NMP). NMP was used as a solvent, PVDF acted as a binder, black sucrose powder was added to increase the porosity of the anode, and activated charcoal was used as a conductive additive. The mixture was positioned on a magnetic stirrer at 1000 RPM to create a homogeneous blend, and stirring was continued for 36 h to ensure thorough mixing. The resulting slurry became uniformly thick and adhesive. Employing a doctor blade, the slurry was spread onto a copper metal foil substrate and subjected to heating at 120 °C in vacuum oven for a duration of 12 h. The goal of using vacuum during the 12 h heating process at 120 °C is to avoid surface oxidation of the components, especially SiO₂. The performance of SiO₂ based battery electrodes can be adversely affected by surface oxidation. A non-conductive oxide layer may form on the surface of SiO₂ as a result of oxidation, which may impede the flow of ions and electrons during battery operation. Reduced battery capacity, stability during cycling, and efficiency may result from this. With SiO₂ in particular, the use of water during the 12 h heating process at 120 °C has a specific purpose: it keeps the materials surface from oxidizing.

Electrodes made of SiO₂ that are used in batteries may perform poorly due to surface oxidation. This heating process helped to evaporate the solvent and solidify the slurry, forming a thin, uniform film of the anode material on the copper metal foil substrate. Following the drying process, the anode was precisely sectioned into round, disc-shaped pieces with a diameter of 16 mm. The anode weight was recorded as 0.00432 g or 2.01 mg cm⁻². To assemble the coin cell, a lithium metal chip with a thickness of 0.6 mm was utilized, whereas a Whatman filter paper was employed as the isolating medium, and a 1 M LiPF₆ solution in a blend of dimethyl carbonate (DMC), ethylene carbonate (EC), and diethyl carbonate (DEC) in an equal ratio was utilized the commercial LP30 electrolyte as standard. The objective of this solution was to improve the electrolyte performance by combining the desirable properties of each solvent. The half-coin cell configuration of the coin cell was established within an argon (H₂O < 0.1 ppm and O₂ < 0.1 ppm)-filled glove box during the fabrication process. This half coin cell is 2-electrode cell lithium was used for both the reference and counter electrodes. This half coin cell device is illustrated in Fig. 1b.

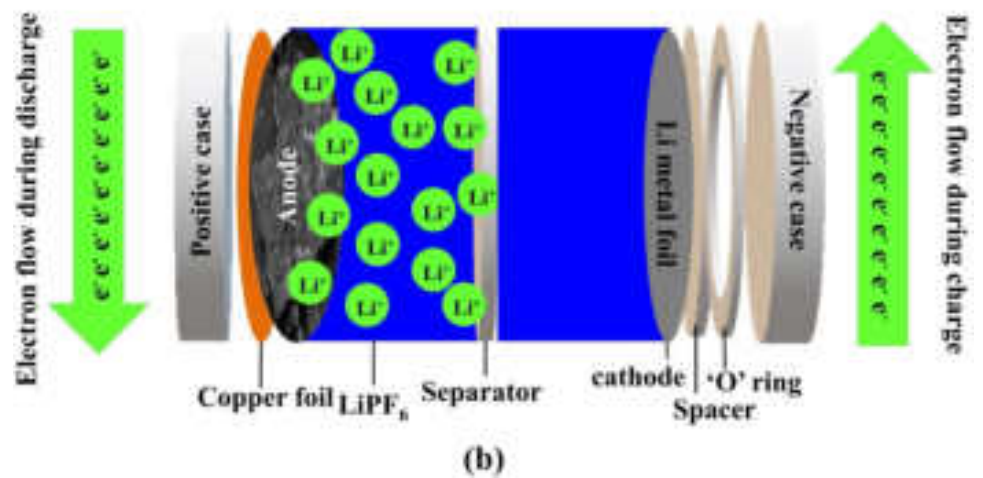
2.4 Physico-chemical characterizations

The sample crystallinity was analyzed via X-ray diffraction by a Rigaku mini flex-600 instrument that utilized CuKα (λ = 1.54184 Å) over a 2θ range of 10°-90°. Surface analyses were conducted using a JASCO FTIR 6100 instrument. The details regarding specific surface area and pore size distribution were acquired through the application of the Brunauer, Emmett, and Teller (BET) analysis model and the Barrett-Joyner-Halenda (BJH) analysis model using Quantachrome Instruments v3.01. Raman spectra were acquired over the spectral range of 50 to 1000 cm⁻¹ using a Renishaw inVia™ Raman microscope by laser stimulation at 532 nm. The morphology of the samples, crystallite size, and elemental composition were examined utilizing field emission scanning electron microscopy (FE-SEM) and energy-dispersive X-ray spectroscopy (EDX) with the NOVA NANOSEM 450 instrument. Additionally, the contact angle of the CCaL SiO₂ NPs anode was determined

Fig. 1 a Flow diagram for the synthesis of crystalline cristobalite alpha low silicon dioxide nanoparticles (CC α L SiO₂ NPs) from *Oryza sativa* husk and **b** Schematic representation of CC α L SiO₂ NPs anode half-coin cell



(a)



(b)

using a contact angle meter (HO-IAD-CAM-01, Holmarc OptoMechatronics Pvt. Ltd., India).

2.5 Electrochemical characterization

To investigate the anode electrochemical performance of CC α LSiO₂ NPs, various tests, including differential derivative capacity (DDC), galvanostatic charge–discharge (GCD), and electrochemical impedance spectroscopy (EIS), were conducted. These measurements were carried out in the voltage range of 0 to 1.5 V vs. Li/Li⁺ using an 8-channel NEWARE battery cyclers system. The DDC

experiments were executed with a current density of 392.7 mA g⁻¹ across a voltage window spanning from 0 to + 1.5 V vs. Li/Li⁺. Simultaneously, EIS analysis was performed using a VersaSTAT 4 Potentiostat.

3 Results and discussion

3.1 Physico-chemical characterizations

3.1.1 X-ray diffraction

Figure 2a illustrates the XRD pattern of CC α L SiO₂ NPs. Where Bragg reflections from (100), (111), (110),

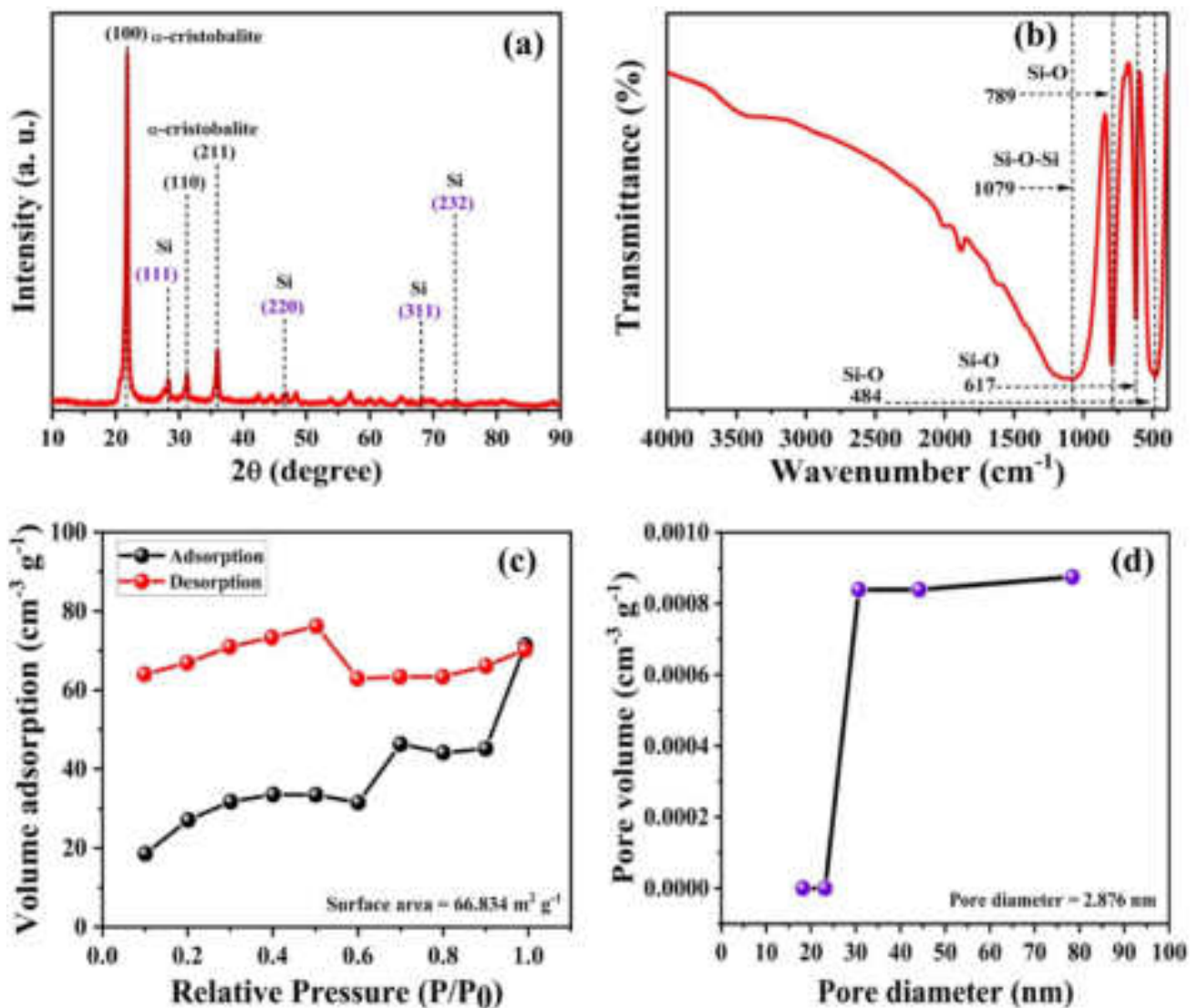


Fig. 2 **a** XRD pattern of CC α L SiO₂ NPs anode, **b** FTIR spectrum of CC α L SiO₂ NPs anode, **c** Nitrogen adsorption–desorption isotherm of CC α L SiO₂ NPs anode and **d** Pore size distribution curves of CC α L SiO₂ NPs anode

(211), (220), (311), and (232) planes of the CCαL SiO₂ phase are observed [JCPDS File No. 98–006-1836] [13, 14]. Scherrer's formula was used to compute the crystallite size "D" of particles [10, 16].

$$D = \frac{0.9\lambda}{\beta \cos\theta} \quad (3)$$

where, 'D' is the crystallite size of CCαL SiO₂ NPs. '0.9' is the Scherrer constant. 'λ' is the wavelength of the X-ray beam. 'β' is the full-width at half maximum (FWHM) of the plane (001). 'θ' is the Bragg's angle.

The calculated crystallite size is 76.70 nm.

The CCαL SiO₂ NPs have a distinct crystalline structure and a sizable grain. The predicted crystallite size offers essential insights into the physical characteristics of the nanomaterial, including its stability, reactivity, and prospective uses. The bigger crystallite size suggests that CCαL SiO₂ NPs have a well-developed crystalline structure with few structural flaws or faults.

3.1.2 Fourier transform infrared spectroscopy

Figure 2b illustrates the FTIR spectrum of the as-prepared CCαL SiO₂ NPs in the 400–4000 cm⁻¹ wavenumber range. The spectrum of CCαL SiO₂ NPs shows the presence of signal associated with Si–O strong bending vibration signal at 484 cm⁻¹, CCαL SiO₂ weak stretching vibration signal at 617 cm⁻¹, SiO₄ tetrahedral symmetric stretching vibration signal at 789 cm⁻¹, and the signal at 1079 cm⁻¹ parallels to Si–O–Si non-symmetric vibration due to more excellent ionic nature of the Si–O bond [23]. The H bond and H₂O molecules are removed when the dispersion of SiO₂ separates from the solid compound called the solvent, forming a Si–O–Si bond [24].

The presence of silicon-oxygen linkages within CCαL SiO₂ NPs is confirmed by the significant bending vibration signal found at 484 cm⁻¹, which indicates the presence of Si–O bonds. Strong confirmation of the precise chemical environment and bonding configuration unique to the NPs is provided by observing a modest stretching vibration signal at 617 cm⁻¹ that corresponds to CCαL SiO₂. The SiO₄ tetrahedral structures are responsible for the symmetric stretching vibration signal at 789 cm⁻¹, further supporting the crystalline character of the CCαL SiO₂ NPs. This conclusion confirms the existence of clearly defined crystal planes inside the NP structure and is perfectly

consistent with the findings of the XRD investigation. Further highlighting the ionic nature of the Si–O bonds found in the CCαL SiO₂ NPs is the discovery of a signal at 1079 cm⁻¹ that is linked to Si–O–Si non-symmetric vibrations. This finding offers convincing insight into the unique, sturdy molecular composition and bonding configuration of the NPs. The as-prepared CCαL SiO₂ NPs thus illuminate their intricate chemical composition, structural arrangement, and bonding interactions.

3.1.3 Surface area analysis

The N₂ adsorption–desorption experiments were executed for the analysis of specific surface area and pore characteristics of CCαL SiO₂ NPs (at 77° K temperature of the liquid nitrogen) and depicted in Fig. 2c. This reveals IV isotherm with H₂ type hysteresis loop of physisorption, according to distribution of International Union of Pure and Applied Chemistry (IUPAC). This curve is detected when capillary condensation is formed. Monolayer formation happens at low pressure followed by multilayer produced by increase in pressure. A material with 2 to 50 nm called multilayer produced by increase in pressure. A material with 2 to 50 nm called mesoporous materials expresses such a type of isotherm. According to the BET equation, the surface areas were calculated as 66.834 m² g⁻¹ of CCαL SiO₂ NPs. The distribution of pore size of CCαL SiO₂ NPs is exhibited in Fig. 2d. An average pore diameter of 2.876 nm of CCαL SiO₂ NPs, respectively. The adsorption and desorption curves exhibit different natures, which means the adsorbed gas molecules are not coming out of the surface of SiO₂ particles. The possible behind this graph feature is that chemical bonds are formed between the gas molecules and the SiO₂ surface. The weak van der Waals forces in physical adsorption are weaker than these bonds. The energy required to break these chemical bonds is higher, which results in a lower desorption rate than adsorption. The desorption curve dips below the adsorption curve, resulting in a hysteresis loop in the isotherm that represents this discrepancy. Moreover, if the SiO₂ particles are porous, it's possible that during adsorption the gas molecules sink deeply into the pores. Diffusion back out is then required after desorption and can take a while depending on the size of the pore and the strength of the adsorption. The desorption curve may lag behind the adsorption curve as a result.

It's possible that changes to the SiO_2 surface during adsorption strengthened the bond between the surface and gas molecules. Reactions with the surrounding environment or the gas itself may be the cause of this alteration. Such modifications would increase the difficulty of desorption.

3.1.4 Raman spectrum

A Raman spectrum was investigated for structural features of CC α L SiO_2 NPs. Figure 3a illustrates the Raman spectrum of CC α L SiO_2 NPs [25]. The CC α L SiO_2 NPs show characteristic peaks at 239 and 416 cm^{-1} corresponding to α -cristobalite peaks, respectively [26]. In conclusion, these distinct peaks appearance provides substantial proof of CC α L SiO_2 NPs crystallinity and the predominance of the α -cristobalite phase. This result supports the NPs clearly defined crystallographic planes, which were discovered using the XRD study.

3.1.5 Field emission scanning electron microscopy

Field emission scanning electron microscopy (FE-SEM) pictures of CC α L SiO_2 NPs anode at 5000 X and 30,000 X are illustrated in Fig. 3b and c, respectively. In Fig. 3b 5000 X magnification, the FE-SEM image offers a thorough perspective of the overall shape of CC α L SiO_2 NPs. It becomes clear that there are agglomerated and spongy granules present. These aggregates are composed of discrete granules grouped to create a porous and interconnected structure. These agglomerates are especially significant because of their enhanced porosity and surface area. In Fig. 3c at 30,000 X magnification, individual features of the clumped spongy granules within CC α L SiO_2 NPs are evident. The connections between individual granules become more apparent, contributing to the overall structural stability of the anode material.

In conclusion, the agglomerated spongy granules within CC α L SiO_2 NPs are significant for their use in lithium-ion battery. Increased porosity and surface area, benefits of the observed microstructure, allow for effective electrolyte interactions, ion transport, and electrochemical reactions. Additionally, the

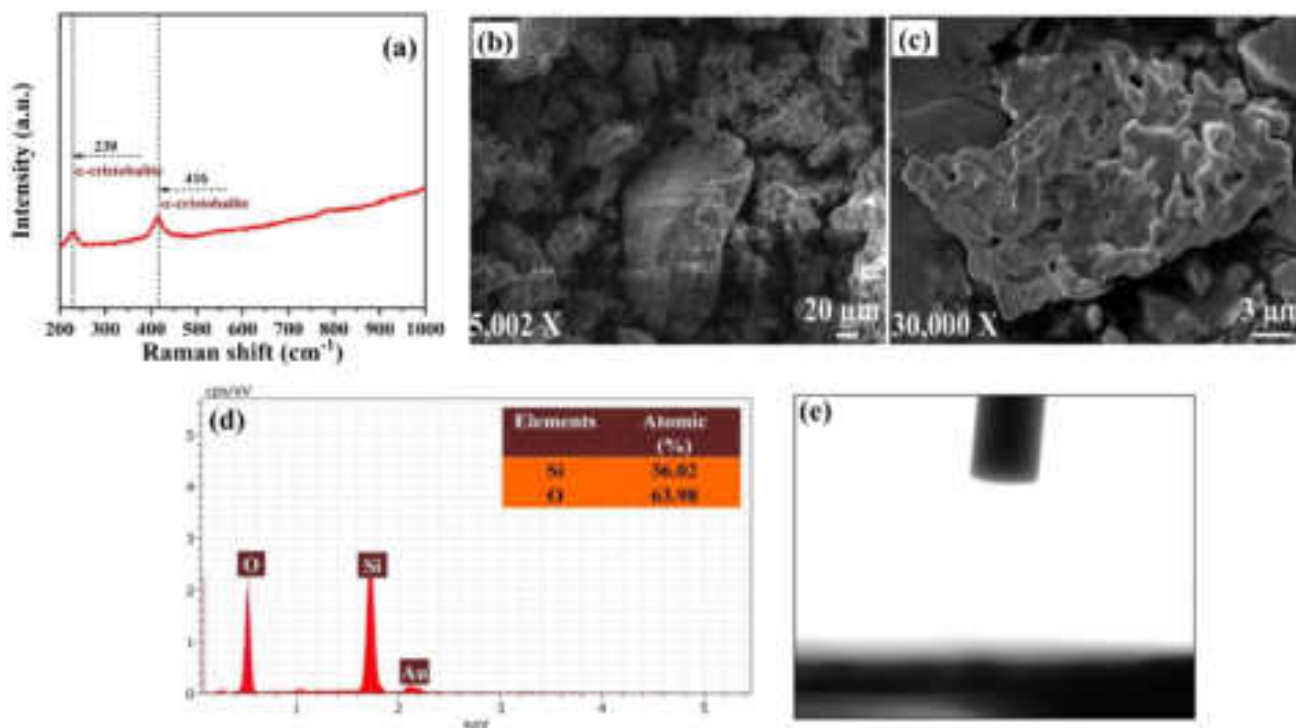


Fig. 3 a The Raman spectrum of CC α L SiO_2 NPs anode, FE-SEM images of CC α L SiO_2 NPs anode at b 5002 X, c 30,000 X magnifications, d EDX spectrum of CC α L SiO_2 NPs (Insets show

atomic percentages of elements) and e water contact angle photograph of CC α L SiO_2 NPs electrode

intergranular bonding guarantees the anode materials structural integrity during cyclic operations.

3.1.6 Energy-dispersive X-ray spectroscopy

Energy-dispersive X-ray spectroscopy (EDX) Fig. 3d displays silicon (Si) and oxygen (O) content, affirming the successful synthesis of SiO₂ NPs. The SiO₂ NPs are observable in the high silicon content (36.02 atomic percentage (%)), and oxygen (63.98%). It indicates a solvent extraction modification method to produce SiO₂ NPs has a high purity. The high degree of purity indicated by this composition confirms that production of SiO₂ NPs utilizing a solvent extraction modification approach was successful. The specificity and purity of produced SiO₂ NPs are further supported by the clear absence of other elements in the EDX spectrum.

3.1.7 Contact angle measurement

We have used a droplet of deionized water to test the wettability of CCαL SiO₂ NPs anode electrode. Figure 3e shows that CCαL SiO₂ NPs has superior super-hydrophilic surface characteristics. Water droplets spread out entirely and create a thin, homogeneous film with a water contact angle of zero degree, which indicates super-hydrophilicity. The surface chemistry and structure of CCαL SiO₂ NPs produce this particular characteristic. It enhances the performance of the applications by offering quick and effective interactions with water-based electrolytes or reactants. This characteristic is beneficial in improving the performance of electrodes, which may eventually result in more effectiveness and durability. The super-hydrophilic properties of CCαL SiO₂ NPs might significantly enhance the success of by facilitating the quick and uniform wetting of the electrode surface.

3.2 Electrochemical characterization

3.2.1 Differential derivative capacity

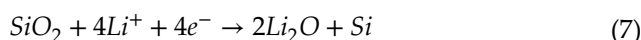
The galvanostatic charge–discharge (GCD) measurements were performed within the voltage range of 0 to 1.5 V vs. Li/Li⁺ corresponding derivative capacity for the 1st, 5th, 25th, and 50th cycles of CCαL SiO₂ NPs anode is illustrated in Fig. 4a. The

transformation from crystalline Si to amorphous Si, along with the formation of a solid electrolyte interface (SEI) film is reflected in the one small low intense lithiation peak at about 0.22 V [26]. The delithiation peaks at 0.28 V vs Li/Li⁺ and 0.45 V vs Li/Li⁺ are attributed to converting amorphous Li_xSi to amorphous Si. The initial capacity loss of CCαL SiO₂ NPs was consistent with the order of their area under the capacity curve derivative, thereby supporting the notion that forming SEI played a role in the observed capacity fading.

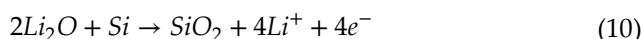
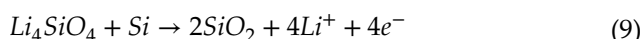
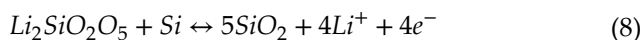
Two electrochemical phases are formed when Li-ions react with SiO₂ during the discharging process. The active phase is Li₂Si₂O₅, while the inactive steps are Li₄SiO₄, Li₂SiO₃, and Li₂O. Additionally, the newly formed Si interacts with Li-ions to create Li_xSi.

However, during the charging process, the inactive phase (Li₄SiO₄, Li₂SiO₃, and Li₂O) leads to a low initial capacity efficiency of SiO₂ [27–29].

During lithiation

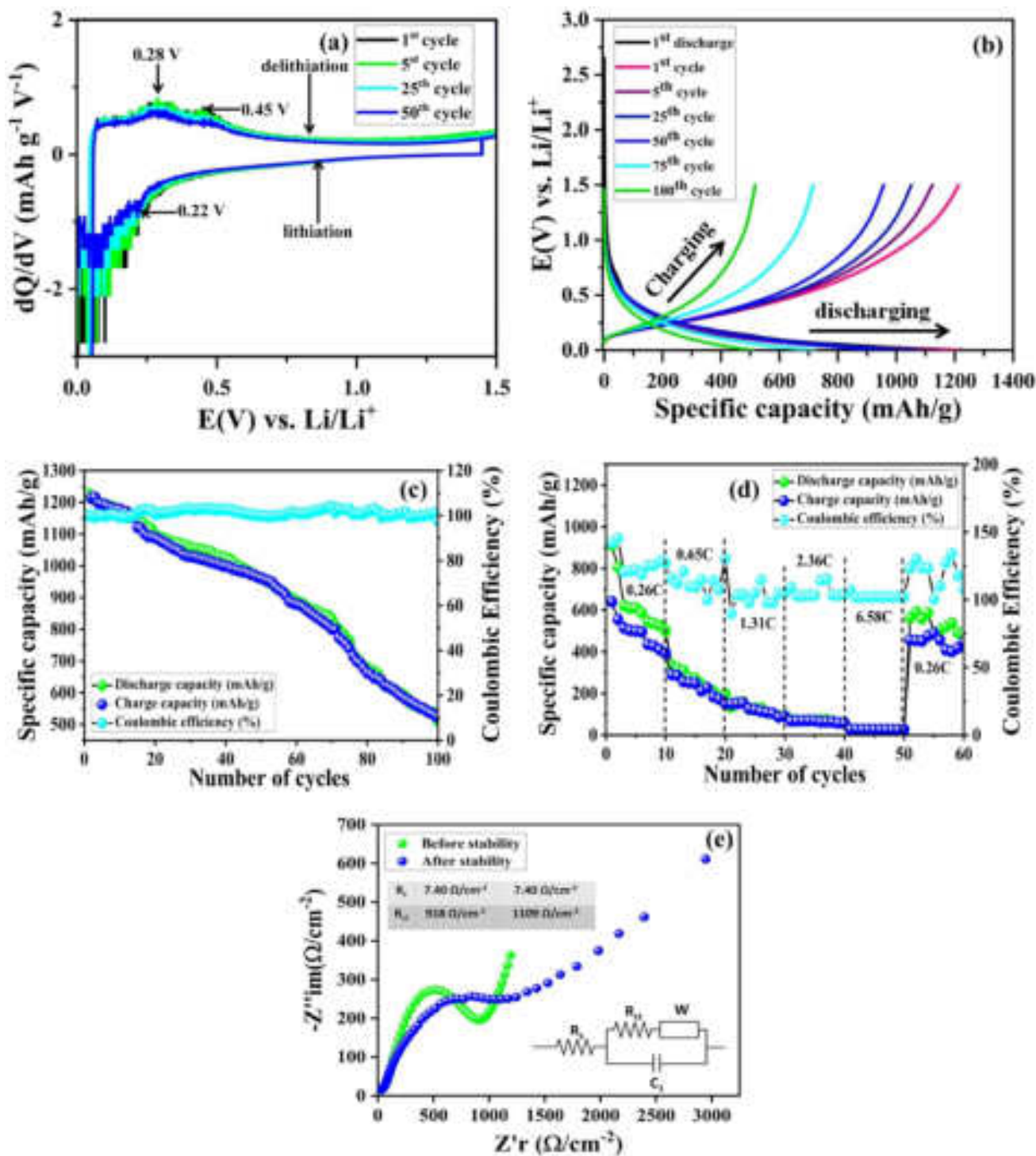


During delithiation



These are all redox reactions, with the production of Li₂SiO₃ and Li₂Si₂O₅ occurring at higher potentials. During the lithiation process, SiO₂ undergoes a more minor change in volume compared to Si, which expands by approximately 300%.

However, the significant volume expansion and contraction can potentially cause damage to the structure of SiO₂ over long cycles. Moreover, the pulverization of the electrode and the formation of a solid electrolyte interphase (SEI) may result in the continual consumption of Li-ions and electrolytes.



The creation of the SEI also impacts the electrical impedance of CCoL SiO₂ NPs, where a thicker SEI increases impedance and hampers the movement of Li⁺ into the CCoL SiO₂ NPs.

3.2.2 Galvanostatic charge–discharge

In this investigation, galvanostatic charge–discharge (GCD) assessments were carried out to analyze the electrochemical properties of CCoL SiO₂ NPs anode.

Fig. 4 a Galvanostatic charge–discharge potential profiles for differential derivative capacity plots of CCαL SiO₂ NPs anode at current density is 392.7 mA g⁻¹, **b** Galvanostatic charge–discharge of CCαL SiO₂ NPs anode for the 1st discharge, 1st, 5th, 25th, 50th, and 100th (current density is 392.7 mA g⁻¹ (0.27C) cycles, **c** Number of cycles vs. specific capacities and Coulombic efficiency of CCαL SiO₂ NPs anode at current density of 392.7 mA g⁻¹ (0.27C), with specific capacity scale located on the left side and Coulombic efficiency scale located on the right side, **d** Rate performance and Coulombic efficiency throughout cycles of CCαL SiO₂ NPs anode at various applied current densities (C-rates): 372.1 mA g⁻¹ (0.26C), 930.3 mA g⁻¹ (0.65C), 1860.6 mA g⁻¹ (1.31C), 3721.25 mA g⁻¹ (2.63C), and 9303.1 mA g⁻¹ (6.58C), with specific capacity scale located on the left side and Coulombic efficiency scale located on the right side and **e** Nyquist plot of CCαL SiO₂ NPs anode (Inset shows the fitted equivalent circuit from the EIS data)

The theoretical capacity of the electrode is 1412 mAh g⁻¹ (see supplementary information for details). The GCD analyses were carried out at a C-rate of 0.27C, corresponding to an applied current density (ACD) of 392.7 mA g⁻¹, within a voltage window spanning from 0 to +1.5 V vs. Li/Li⁺.

Figure 4b shows the GCD profiles of CCαL SiO₂ NPs anode at the 1st discharge, 1st, 5th, 25th, 50th, 75th, and 100th cycles, along with the corresponding discharging specific capacities. The specific discharge capacities for these cycles were found to be 1226.6, 1212.0, 1187.3, 1071.2, 956.8, 720.4, and 511.8 mAh g⁻¹ at an applied current density of 392.7 mA g⁻¹ (0.27C). The higher the specific discharge capacity, the more charge the material can store and deliver. The specific lithiation capacities ranged from 956.8 to 511.8 mAh g⁻¹, indicating differences in the materials performance during the discharge process for different cycles. This suggests that materials capacity to store and deliver charge may vary over time or in response to cycling.

The scale for specific capacity on the left side of Fig. 4c illustrates the relationship between the number of cycles and the specific capacities of CCαL SiO₂ NPs anode at a current density of 392.7 mA g⁻¹ (equivalent to 0.27C) for 100 cycles. As depicted in the figure, an escalation in the number of cycles results in a reduction in the specific capacity. This decrease in capacity can be attributed to two primary factors. Firstly, there is cracking of CCαL SiO₂ NPs anode, which affects its structural integrity and, in turn, its performance. Secondly, the establishment of a solid-electrolyte

interphase (SEI) layer on the anode surface contributes to the decline in capacity. Combining these two factors influences the specific capacity of anode over multiple cycles.

The scale for Coulombic efficiency on the right side of Fig. 4c illustrates the Coulombic efficiency of anode comprising CCαL SiO₂ NPs at an applied current density of 392.7 mA g⁻¹. In the 1st cycle, the CCαL SiO₂ NPs anode demonstrates a lithiation capacity of 1212.2 mAh g⁻¹ and a delithiation capacity of 1213.4 mAh g⁻¹, resulting in a Coulombic efficiency of 99.8%. As the cycling progresses, the lithiation capacity exhibits a gradual decrease to 511.8 mAh g⁻¹, while the delithiation capacity decreases to 524.1 mAh g⁻¹ in the 100th cycle, accompanied by a Coulombic efficiency of 97.6%. These results emphasize the importance of comprehending how the lithiation and delithiation processes interact dynamically inside the anode material. The falling Coulombic efficiency points to possible causes that could affect energy storage and release effectiveness, including electrode deterioration, electrolyte interactions, and modifications in the materials structural integrity. The initial capacity loss of CCαL SiO₂ NPs aligns with the area under the capacity curve derivation, indicating the involvement of the solid-electrolyte interface (SEI) formation in the capacity loss. During the discharging process, the reaction between lithium ions and SiO₂ results in the formation of two electrochemical phases. Upon retesting the coin cell, we observed a Coulombic efficiency that started at 100% and decreased to 97.6% after 100 cycles. Therefore, in Fig. 4c, it is evident that the coulombic efficiency has decreased after 100 cycles.

The scale for specific capacity on the left side of Fig. 4d illustrates the rate capability of CCαL SiO₂ NPs anode in the first 10 cycles, ranging from 911.2 to 500.4 mAh g⁻¹. Similarly, from the 11th to the 30th cycles, the specific discharge capacities decreased gradually up to the 50th cycle. The capacity of a LiB can decrease gradually over cycles due to several factors such as electrode degradation, loss of active material, creation of SEI layer, and alterations in the crystal structure of anode. During cycling, the formation of SEI layer around the anode reduces the availability of active Li-ions for cycling, leading to a decrease in capacity. Moreover, the repetitive insertion and extraction of Li-ions can harm the crystal structure of anode, resulting in decreased overall capacity [25, 29, 30]. The GCD curves of CCαL SiO₂ NPs anode half-coin cell at various current densities exhibited discharge and charge

profiles. The Coulombic efficiency throughout the cycles is represented in the rate capability graph. The scale for Coulombic efficiency is located on the right side of Fig. 4d.

Table 1 represents using *Oryza sativa* husk extract SiO₂ NPs in organic electrolyte with charging/discharging capacity for LiB. The anode material in LiB can be made of SiO₂ powders, which exhibit a changeable 800 mAh g⁻¹ capacity following 200th cycles [29]. The initial cycle of SiO₂/C electrode yielded a discharge capacity of approximately 733 mAh g⁻¹, with a corresponding Coulombic efficiency of 40% [27, 31]. The SN@C/SiO_x electrode demonstrated consistent Li⁺ storage characteristics even after undergoing 1200 cycles at 1.0 A g⁻¹, with a lithiation capacity of 632 mAh g⁻¹ [14]. Similarly, the BM-*Oryza sativa*-SiO₂/NC composites, synthesized through ball milling and thermal processing techniques using biomass *Oryza sativa* husk, exhibited exceptional stability, maintaining a changeable lithiation capacity of 556 mAh g⁻¹ over 1000 cycles [32]. The ZnO/*Oryza sativa* husk-based carbonaceous nanosphere composite showed favorable Li storage characteristics, with a specific charge capacity of 920 mAh g⁻¹ completed over 100 segments at 0.2C [33]. In this investigation, CCαL SiO₂ NPs were employed as the active material in an anode configuration, showing a gradual increase in discharge capacity to 511.8 mAh g⁻¹ after 100 cycles. Enhancing charge

storage capacity and improving electrochemical performance are achieved by activating and optimizing the structure of electrode material, coupled with the formation of a SEI layer on the anode surface.

Vanadium was incorporated into MoS₂ to form VMoS₂, enhancing electronic conductivity and reducing sodium-ion transportation barrier. This resulted in improved electrochemical performance for sodium-ion batteries (SiBs), including high specific capacity, excellent cycling stability, and superb rate performance [32]. For SiBs, a CoS₂/NiS₂ heterostructure made of Co-based metal organic frameworks demonstrates excellent rate performance and high reversible capacity. With exceptional cyclic stability, the anode material provides a capacity of 801.5 mA h g⁻¹ at 0.1 A g⁻¹, continuing to produce 545.1 mA h g⁻¹ even after 2000 cycles at 5 A g⁻¹. CoS₂/NiS₂ has faster reaction kinetics than CoS₂ alone, as evidenced by lower sodium-ion transport barriers found in the compound as determined by in situ X-ray diffraction and density functional theory calculations. The development of additional high-performance anode materials with heterostructures for SiBs appears to be promising with this design idea [34]. High stability and performance are demonstrated by coral reef-like MoS₂ microspheres with a 1 T/2H phase when used as an anode material in SiBs. It exhibits consistent cycling behavior with a specific capacity of 467 at 100 mA g⁻¹ after 100 cycles

Table 1 *Oryza sativa* husk-derived SiO₂ NPs as anodes in organic electrolytes with charging/discharging capacity for Li-ion batteries

Sr. no	Lithium-ion battery	First discharge capacity (mAh g ⁻¹)	First charge capacity (mAh g ⁻¹)	Stability cycles no	Stability capacity	Coulombic efficiency (%)	Furnace Heating Temperature (°C)	References
1	<i>Oryza sativa</i> C/SiO ₂	Near 2100		200th	800	80	–	29
2	<i>Oryza sativa</i> SiO ₂ /C	733	–	50th	176	98	650	32
3	SN@C/SiO _x	Near 2000	Near 1200	1200th	632	70.4	600	14
4	BM-RH-SiO ₂ /NC	1373		100th	780	99	650	33
5	ZnO/rice husk-based hollow carbonaceous nanosphere	1679	1024	100th	920	99.5	500	34
6	<i>Oryza sativa</i> CCαL SiO ₂ NPs	1226.6 C-rate 0.27C OR (392.7 mA g ⁻¹)	1213.4 C-rate 0.27C OR (392.7 mA g ⁻¹)	100th	511.8	97.6	900	This work

and 412 mAh g⁻¹ at 1 A g⁻¹ after 500 cycles. A 100 mAh g⁻¹ capacity is attained even at 20 A g⁻¹. Rapid ion diffusion is made possible by the disordered structure, abundant flaws, and wide interlayer spacing, which all improve electrical conductivity and offer active sites for Na⁺ storage [35]. In lithium-sulfur batteries, CoNi-embedded nitrogen-doped hollow carbon nanotubes (CoNi@NCNTs) function as efficient sulfur hosts. Their capacity of 676.8 mAh g⁻¹ at 1 C in the first cycle is demonstrated by their high Li₂S₆ adsorption ability. They also have outstanding cyclic stability, maintaining 71.8% of their capacity after 500 cycles. The technique of incorporating metal nanoparticles into materials with nanostructured carbon has potential as a high-performing cathode material for lithium-sulfur batteries [36]. An NVP/C core-shell cathode structure is created to improve sodium-ion batteries electrochemical performance. It has exceptional rate capability (85.3 mAh g⁻¹ at 10C), high initial reversible capacity (106.6 mAh g⁻¹ at C/10), and good cycling stability (94.2% retention after 1100 cycles). Phase transitions during cycling are elucidated through operando X-ray diffraction experiments conducted using synchrotron technology. An all-solid-state NVP/C||Na battery reversible capacity of 95 mAh g⁻¹ at C/10 and retention of 78.3% capacity after 1100 cycles are enhanced by the integration of a NASICON solid electrolyte [37]. With a ceramic electrolyte and NASICON-type NaTi₂(PO₄)₃ cathode, these all-solid-state SiBs are promising for large-scale energy storage because of their conductivity and stability. Without changing its structure, the carbon coating on the cathode improves performance. The efficiency of the battery is supported by operando PXRD, which shows reversible structural changes during charge and discharge. This innovation offers a viable route forward for energy storage devices with great performance [38]. With the use of lead (Pb) anode and carbon-coated Na₃V₂(PO₄)₃ (NVP-C) cathode materials, this work presents a promising complete SiB. With a capacity retention of 99.9% after 3500 cycles at a high 5 C rate, the NVP-C cathode exhibits exceptional reversible capacity and stability. Good cyclability and capacity retention are also displayed by the Pb anode. With outstanding rate capability and discharge energy density, the entire cell provides a preliminary reversible capacity of 233 mAh g⁻¹ at C/10 rate. This simple and affordable prototype represents a major advancement toward high-energy, useful SiB applications [39]. The carbon-coated FePO₄ nanoparticles shown in this study serve as a stable cathode for

SiBs, providing a reversible capacity of 103 mAh g⁻¹ along with exceptional rate capability and uniformity. Studies using in situ XRD data show that sodiation involves a biphasic transition. Na₁₅Pb₄ anode complete cell demonstrates 76% capacity retention over 100 cycles at C/10 rate, indicating this technology's potential for use in commercial Na-ion systems [40].

3.2.3 Electrochemical impedance spectroscopy

Figure 4e depicts the electrochemical impedance spectroscopy (EIS) outcomes acquired from the electrode before and following cycling. The impedance spectrum displays a partially circular shape, signifying the impedance linked to charge transfer at the interface between the electrode and electrolyte in the high-frequency region. Additionally, a linear trend is observed, indicating the impedance related to Li diffusion in the low-frequency range. With the increasing delithiation/lithiation cycles, semicircle size in the high-frequency range regime demonstrates a proclivity to enlarge. This phenomenon primarily originates from the volumetric expansion of CCαL SiO₂ NPs anode during the delithiation/lithiation progression, instigating deterioration of SEI film and exposure of CCαL SiO₂ NPs anode surface [41]. Before studying the stability of GCD cycles, we measured the solution resistance (R_s) and charge-transfer resistance (R_{ct}) values to as 7.4 and 918 Ω cm⁻², respectively. After 100 cycles, solution resistance (R_s) remained constant while the charge-transfer resistance (R_{ct}) increased to 1109 Ω cm⁻². The solution resistance is relatively low because electrolyte solution is designed to have good conductivity, allowing for efficient ion transport. The charge transfer resistance is usually higher than the solution resistance because it represents the resistance related to the specific electrochemical reactions at the electrode surface, which is influenced by the organic LiPF₆ electrolyte and affects the speed of electrochemical reaction. As these species accumulate, they can hinder charge transfer and increase the resistance. The subsequent formation of a fresh SEI film consumes electrolytes, thereby elevating the impedance. However, minimal disparity discernible among the curves after 100 cycles, suggest that amplification in interface impedance becomes restricted during cycling. These findings validate the efficacious alleviation of volumetric variations in SiO₂ anode by implementing CCαL structure [41].

3.3 Post-mortem physico-chemical characterizations

3.3.1 Post-mortem X-ray diffraction

The CCαL SiO₂ NPs anode half-coin cells were fully discharged for post-mortem X-ray diffraction (XRD) analysis. The disassembly process occurred within a glove box filled with argon (H₂O < 0.1 ppm and O₂ < 0.1 ppm). After unwinding CCαL SiO₂ NPs electrode, Whatman™ filter paper (separator), and lithium metal chip (cathode), the discharged electrode was accurately cut from the bulk of electrode material using stainless steel scissors. These samples were individually stored in separate plastic bags, and meticulous care was exercised in their handling with tweezers, ensuring gripping only at the edges.

The CCαL SiO₂ NPs discharged anode electrode was transferred to a nearby glove box for analysis via a shared antechamber after the electrodes in one glove box were unwound and harvested. During this transfer, the samples were shielded from exposure to air; instead, they were subjected to pressures of approximately 1.0×10^{-4} kPa for 15 min. Subsequently, the electrodes were meticulously placed onto glass slides in a sample holder compatible with the Rigaku Mini-Flex 600 instrument, which utilizes CuKα radiation ($\lambda = 1.54184$ Å) over a 2θ range of 10°–80° for XRD analysis.

Figure 5a depicts the XRD pattern of CCαL SiO₂ NPs. After lithiation, we observed some changes in the XRD patterns of CCαL SiO₂ NPs. It demonstrated that CCαL SiO₂ NPs have a good crystal structure and are initially crystalline. However, during lithiation, the Si atoms in the SiO₂ lattice react with the Li ions to create SiO₂-Li alloys like Li₂SiO₂O₅, Li₂SiO₃, and Li₄SiO₄ [42]. These transitional periods frequently have an unorganized or amorphous structure. As a result, CCαL SiO₂ NPs anode material exhibits amorphization in the form of a broad, featureless peak or a drop in peak intensity on the XRD pattern. Additionally, we noticed copper peaks that corresponded to the copper planes (111), (200), and (220) [43]. We use the Miller index (hkl) to index well-known copper values for the crystallographic plane. The (111) plane often occurs at two values at 43.3° and is the sharpest. As lithiation progresses, the process creates various lithiated SiO₂ compounds. Among these phases, there is the presence of lithium oxide (Li₂O) [44]. These phases may be recognized and measured because they

have discrete diffraction peaks in the XRD pattern at particular angles. The (111) plane corresponds to the Li₂O peak point at two values between 32° and 34° [45]. The emergence of additional peaks connected to these phases shows that SiO₂ has changed into lithiated compounds. The substantial volume expansion that Si experiences during lithiation causes mechanical strains and fissures in the electrode material. The growth in volume was inferred by analyzing the variations in peak positions and intensities in the XRD pattern. The broadening, which results in structural alterations, might be blamed for variations in peak position or the formation of additional peaks. The lithiation process causes peak broadening in the XRD pattern by introducing microstructural imperfections and disorder into SiO₂ lattice [45].

Broader peaks denote the existence of defects, dislocations, and nanocrystalline domains brought on by lithiation-induced stress and strain [46]. Li insertion into the crystal lattice can cause the XRD peaks connected to SiO₂ to shift to a lower angle [47]. This change indicates that the unit cell has expanded due to lithiation. Crucial markers of copper crystallinity are sharp and intense peaks at two distinctive values. This knowledge is essential for characterizing the structural characteristics of copper foils. Various uses, such as current collectors in LiB and other electronic devices, make it worthwhile for materials research and quality monitoring. When maximizing the design and use of LiB, the performance and stability of SiO₂ NPs-based anodes are crucial.

In conclusion, the XRD examination of CCαL SiO₂ NPs anode following lithiation reveals considerable structural changes in the material. Amorphization, the development of lithiated phases, volume expansion, peak broadening, and peak shifts are some of these modifications. For evaluating the electrochemical, it is essential to comprehend these observations.

3.3.2 Post-mortem field emission scanning electron microscopy

The anode half-coin cell containing CCαL SiO₂ NPs underwent a complete discharge, during which the cell voltage reached 0 V. This discharged state was then utilized for post-mortem field emission scanning electron microscopy (FE-SEM) analysis. The disassembly process occurred within a glove box filled with argon (H₂O < 0.1 and O₂ < 0.1 ppm). After

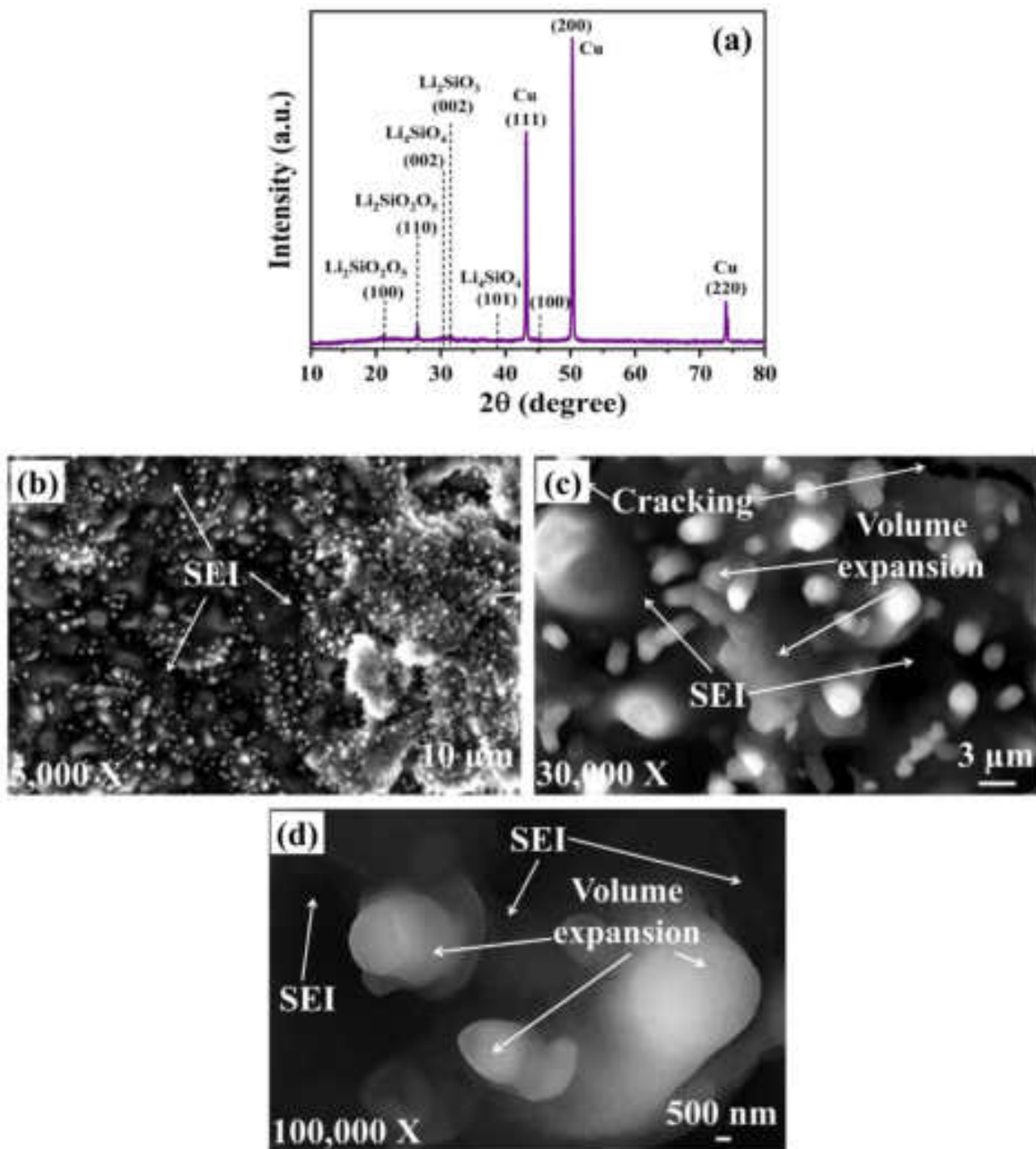


Fig. 5 **a** Post-mortem XRD pattern of CC α L SiO₂ NPs anode lithiated electrode and Post-mortem FE-SEM images of CC α L SiO₂ NPs anode at **b** 5000 X, **c** 30,000 X, and **d** 100,000 X magnifications

carefully unwinding the discharged CC α L SiO₂ NPs electrode along with separator and lithium metal chip, precise samples were cut from the primary electrode material using stainless steel scissors. These samples

were individually stored in separate plastic bags, and meticulous care was taken during handling, utilizing tweezers and gripping only at the edges. In this investigation, post-mortem electrodes were not dissolved

in a solvent (dimethyl carbonate (DMC) or ethylene carbonate (EC) or diethyl carbonate (DEC). Dissolving the electrodes in a solvent solution would result in the removal of Solid Electrolyte Interphase (SEI) layer. Post-mortem electrode was moved to a nearby glove box for analysis via a shared antechamber after the electrodes in one glove box were unwound and harvested. Samples were not exposed to air during this transfer; instead, they were subjected to pressures of about 1.0×10^{-4} kPa for 15 min. Samples for the FE-SEM were brought to the microscope using an airtight sample holder. Micrographs were captured using a secondary electron detector with a working distance of 15 mm and an accelerating voltage of 15 kV on a NOVA NANOSEM 450 FE-SEM instrument.

The CC α L SiO₂ NPs anode is shown in Fig. 5b–d in post-mortem FE-SEM pictures at three different magnifications: (b) 5000 X, (c) 30,000 X, and (d) 100,000 X. In all three magnifications, these photos demonstrate an apparent increase in the size of SiO₂ NPs during the lithiation process. As previously shown by post-structural analysis, during lithiation, Si within the SiO₂ structure experiences a reaction with Li, resulting in the creation of lithiated Si compounds.

This chemical transformation leads to the pulverization and cracking of CC α L SiO₂ NPs anode, ultimately causing a substantial expansion in the volume of anode. The SEI layer, an essential part of LiB systems, stands out for having distinct contrast and brightness properties compared to the underlying electrode material [48]. For instance, the magnification of 5000 X images looks low dark gray in some regions with a black tint because of SEI layer. At a magnification of 30,000 X, the image shows some cracks due to some stress with a combination of dark gray and black portion because of SEI. At magnification of 100,000 X, the image looks dark gray with a black tint due to unique imaging circumstances. The type and density of SEI layer might vary, which is why there is this visual disparity.

The results indicate the formation of a SEI layer on the electrode surface. In contrast to the relatively smooth appearance of electrode material beneath it, the SEI layer exhibits irregularities, coarseness, and fluctuations in thickness [49]. The post-mortem FE-SEM characterization inquiry heavily relies on the presence of SEI layer and the contemporaneous pulverization of electrode material on the surface. These findings have improved the understanding of electrochemical behavior of CC α L SiO₂ NPs anode in LiB application.

It provided insightful information about the structural and morphological changes in the anode during the lithiation process.

Furthermore, the volume changes experienced by the SiO₂ electrode material during the charge and discharge cycles of a LiB are notable. As lithium ions intercalate and deintercalate from the crystal lattice structure, the electrode material undergoes significant alterations. These repeated volume changes induce mechanical stress within the electrode, potentially leading to pulverization. Pulverization occurs when the mechanical stress from volume expansion exceeds the material mechanical strength, resulting in the fracture or breakage of electrode particles. This process reduces the available surface area for lithium-ion interactions, ultimately compromising battery capacity.

4 Conclusion

In conclusions, we have successfully employed the solvent extraction modification technique to create CC α L SiO₂ NPs from *Oryza sativa* husk. This method offers a simple and cost effective strategy for producing these NPs, which can be employed as anode in half-coin cell LiB applications. The CC α L SiO₂ NPs are granules; agglomerated ultrafine particles accommodate the fast diffusion pathway of Li-ion, while spongy granules direct growth in the communication surface area between CC α L SiO₂ NPs and LiPF₆. Agglomerated, porous granules are present in the microstructure as observed, resulting in aggregates with a porous and networked structure. Because of these agglomerates increased porosity and surface area, their distinct shape is very significant. The porous design NPs can be spacious to contribute to volume expansion growth and maintain structural goodness when Li intercalates into Si NPs [50]. A CC α L SiO₂ NPs anode post-mortem after lithiation XRD examination reveals significant structural changes for evaluating its electrochemical performance. In post-mortem analysis of FE-SEM the formation of SEI layer and its distinctive features have improved the understanding of CC α L SiO₂ NPs anode behavior in LiB, particularly regarding structural changes during lithiation.

Acknowledgements

We acknowledge funding from the Swedish Energy Agency (project number: 39038-2), the EU Regional

Fund, the KK Foundation, STINT (IB-2018 7535) and D. Y. Patil Education Society (Deemed to be University). Also this research is supported by Centre for Materials for Electronics Technology (C-MET), Pune for providing a battery fabrication system and Central Instrumentation Facility, Departments of Chemistry and Physics, Savitribai Phule Pune University, Pune for providing a physico-chemical characterizations instruments facility.

Author contributions

Sohan Thombare carried out an investigation and formal analysis, data curation, original draft writing, and formal analysis. Ranjit Humane, Bharat Kale, Ram Kalubarme provided electrochemical analysis facility, Rohan patil, Ranjit Humane, Ramchandra Kalubarme and Manisha Phadatare carried out calculation of battery C-Rate, Dhanaji Malavekar and Sambhaji Khot carried out modification and presentations, Rohan patil, Bharat Kale, Ramchandra Kalubarme, Manisha Phadatare and Chandrakant Lokhande carried out funding acquisition, administration, supervision, and manuscript editing. All persons made substantial contributions to the work reported in the manuscript.

Funding

Open access funding provided by Mid Sweden University. This study was funded by Swedish Energy Agency, the EU Regional Fund, the KK Foundation, STINT and D. Y. Patil Education Society (Deemed to be University) Kolhapur.

Data availability

The data used in this study is part of ongoing research and cannot be provided at this stage. However, it will be made available after the completion of ongoing research on request from corresponding author.

Declarations

Conflict of interest There are no conflicts to declare.

Supplementary Information The online version contains supplementary material available at <https://doi.org/10.1007/s10854-024-13153-8>.

Open Access This article is licensed under a Creative Commons Attribution 4.0 International License, which permits use, sharing, adaptation, distribution and reproduction in any medium or format, as long as you give appropriate credit to the original author(s) and the source, provide a link to the Creative Commons licence, and indicate if changes were made. The images or other third party material in this article are included in the article's Creative Commons licence, unless indicated otherwise in a credit line to the material. If material is not included in the article's Creative Commons licence and your intended use is not permitted by statutory regulation or exceeds the permitted use, you will need to obtain permission directly from the copyright holder. To view a copy of this licence, visit <http://creativecommons.org/licenses/by/4.0/>.

References

1. P. Nadrah, O. Planinšek, M. Gaberšček, *J. Mater. Sci.* **49**, 48 (2014)
2. M. Hossain, M. Chowdhury, N. Hossain, M. Islam, M. Mobarak, *J. Chem. Eng.* **16**, 100569 (2023)
3. M. McDowell, S. Lee, W. Nix, Y. Cui, *Adv. Mater.* **25**, 4966 (2013)
4. S. Imtiaz, I. Amiin, Y. Xu, T. Kennedy, C. Blackman, K. Ryan, *Mater. Today* **48**, 241 (2021)
5. A.-G. Nguyen, R. Verma, P. Didwal, C.-J. Par, *Energy Mater.* **3**, 300030 (2023)
6. K. Gallis, J. Araujo, K. Duff, J. Moore, C. Landry, *Adv. Mater.* **11**, 1452 (1999)
7. E. Wetzels, Y. Lee, R. Egres, K. Kirkwood, J. Kirkwood, N. Wagner, *A.I.P. Conf. Proc.* **712**, 288 (2004)
8. H. Ly, G. Xi, X.Z.H. Sh, G. Xq, J. Wq, C. Zy, *Appl. Surf. Sci.* **252**, 8724 (2006)
9. W. Stöber, A. Fink, E. Bohn, *J. Colloid, Interface Sci.* **26**, 62 (1968)
10. G. Bogush, M. Tracy, C. Zukoski Iv, *J. Non-Cryst. Solids.* **104**, 95 (1988)
11. D. Wong, R. Suriyaprabha, R. Yuvakumar, V. Rajendran, Y.-T. Chen, B.-J. Hwang, L.-C. Chen, K.-H. Chen, *J. Mater. Chem. A.* **2**, 13437 (2014)
12. S. Chandrasekhar, K. Satyanarayana, P. Pramada, P. Raghavan, T. Gupta, *J. Mater. Sci.* **38**, 3159 (2003)

13. T.-H. Liou, *Mater. Sci. Eng. A* **364**, 313 (2004)
14. J. Cui, Y. Qiu, H. Zhang, Z. Yao, W. Zhao, Y. Liu, J. Sun, *Solid State Ion.* **361**, 115548 (2021)
15. A. Yusof, N. Nizam, N.A.A. Rashid, A. Yusof, N. Nizam, *J. Porous Mater.* **17**, 39 (2009)
16. T. Lee, R. Othman, F.-Y. Yeoh, *Biomass Bioenerg.* **59**, 380 (2013)
17. F. Adam, J. Appaturi, A. Iqbal, *Catal. Today* **190**, 2 (2012)
18. A. Agi, R. Junina, M. Jaafar, R. Mohsin, A. Arsad, A. Gbadamosi, C. Fung, J. Gbonhinbor, *J. Mater. Res. Technol.* **9**, 13054 (2020)
19. U. Kalapathy, A. Proctor, J. Shultz, *Bioresour. Technol.* **7**, 257 (2000)
20. T. Autthawong, C. Yodbunork, W. Yodying, R. Boonprachai, O. Namsar, A. Yu, Y. Chimupala, T. Sarakonsri, *ACS Omega* **7**, 1357 (2022)
21. O. Namsar, T. Autthawong, R. Boonprachai, A. Yu, T. Sarakonsri, *J. Mater. Sci. Mater. Electron.* **33**, 6536 (2022)
22. Z. Liu, Q. Yu, Y. Zhao, R. He, M. Xu, S. Feng, S. Li, L. Zhou, L. Mai, *Chem. Soc. Rev.* **48**, 285 (2019)
23. T. Lee, R. Othman, F.-Y. Yeoh, *Biomass Bioenergy* **59**, 380 (2013)
24. W.-S. Chang, C.-M. Park, J.-H. Kim, Y.-U. Kim, G. Jeong, H.-J. Sohn, *Energy Environ. Sci.* **5**, 6895 (2012)
25. M. Mellini, Y. Fuchs, C. Viti, C. Lemaire, J. Linares, *Eur. J. Mineral.* **14**, 97 (2002)
26. V. Ivanov, B. Reyes, E. Fritsch, E. Faulques, *J. Phys. Chem. C* **115**, 11968 (2011)
27. V. Etacheri, R. Marom, R. Elazari, G. Salitra, D. Aurbach, O. Choen, *J. Power. Sources* **254**, 168 (2014)
28. Z. Zhang, Q. Huang, W. Mai, H. Li, *Appl. Surf. Sci.* **538**, 148039 (2021)
29. M. Khan, X. Ding, H. Zhao, Y. Wang, N. Zhang, X. Chen, J. Xu, *J. Electron. Mater.* **51**, 3379 (2022)
30. W.-S. Chang, C.-M. Park, Y.-U. Kim, G. Jeong, H.-J. Sohn, *Energy Environ. Sci.* **5**, 6895 (2012)
31. T. Autthawong, O. Namsar, A. Yu, T. Sarakonsri, *J. Mater. Sci. Mater. Electron.* **31**, 9126 (2020)
32. Y. Feng, L. Liu, X. Liu, Y. Teng, Y. Li, Y. Guo, Y. Zhu, X. Wang, Y. Chao, *Electrochim. Acta* **359**, 136933 (2020)
33. Y. Li, Y. Gao, H. Qi, K. Yu, C. Liang, *RSC Adv.* **8**, 33019 (2018)
34. X. Yue, J. Wang, A. Patil, X. An, Z. Xie, X. Hao, Z. Jiang, A. Abudula, G. Guan, *J. Chem. Eng.* **1**, 128107 (2021)
35. J. Wang, X. Yue, X. Cao, Z. Liu, A. Patil, J. Wang, X. Hao, A. Abudula, G. Guan, *J. Chem. Eng.* **431**, 134091 (2022)
36. X. Yue, J. Wang, Z. Xie, A. Patil, T. Yu, X. Du, Z. Wang, X. Hao, A. Abudula, G. Guan, *J. Mater. Sci.* **55**, 14389 (2020)
37. J. Wang, X. Yue, Z. Xie, A. Patil, S. Penga, X. Hao, A. Abudula, G. Guan **874**, 159952 (2021)
38. B. Pandit, M. Johansen, C. Martinez-Cisneros, J. Naranjo-Balseca, B. Levenfeld, D. Ravnsbaek, A. Varez, *Chem. Mater.* **36**, 2314 (2024)
39. B. Pandit, M. Johansen, B. Andersen, C. Martinez-Cisneros, B. Levenfeld, D. Ravnsbaek, A. Varez, *J. Chem. Eng.* **472**, 144509 (2023)
40. B. Pandit, M. Sougrati, B. Fraisse, L. Monconduit, *Nano Energy* **95**, 107010 (2022)
41. B. Pandit, B. Fraisse, L. Stievana, L. Monconduit, M. Sougrati, *Electrochim. Acta* **409**, 139997 (2022)
42. Al. Jafarawy, M. Hikmah, D. Riyadi, *J. Electron. Mater.* **50**, 6667 (2021)
43. Y.-S. Su, K.-C. Hsiao, P. Sireesha, J.-Y. Huang, *Batteries.* **8**, 2 (2022)
44. X. He, Y. Hu, H. Tian, Z. Li, P. Huang, J. Jiang, C. Wang, *J Materiomics* **6**, 192 (2020)
45. E. Sivonxay, M. Aykol, K. Persson, *Electrochim. Acta* **331**, 135344 (2020)
46. K. Yao, D. Kwabi, R. Quinlan, A. Mansour, A. Grimaud, Y.-L. Lee, Y.-C. Lu, Y. Shao Horn, *J. Electrochem. Soc.* **160**, A824 (2013)
47. C. Arro, A. Mohamed, N. Bensalah, *Mater. Today Commun.* **30**, 103151 (2022)
48. G. Mu, D. Mu, B. Wu, C. Ma, J. Bi, L. Zhang, H. Yang, F. Wu, *Small* **16**, 1905430 (2019)
49. C. Chen, T. Zhou, D. Danilov, L. Gao, S. Benning, N. Schön, S. Tardif, H. Simons, F. Hausen, T. Schüllli, R. Eichel, P. Notten, *Nat. Commun.* **11**, 3283 (2020)
50. K. Guo, R. Kumar, X. Xiao, B. Sheldon, H. Gao, *Nano Energy* **68**, 104357 (2020)

Publisher's Note Springer Nature remains neutral with regard to jurisdictional claims in published maps and institutional affiliations.